

STRATEGIES FOR THE STEREOSELECTIVE SYNTHESIS OF CARBON
QUATERNARY CENTERS VIA TRANSITION METAL-CATALYZED
ALKYLATION OF ENOLATE COMPOUNDS

Thesis by
Corey Michael Reeves

In Partial Fulfillment of the Requirements
for the Degree of
Doctor of Philosophy

CALIFORNIA INSTITUTE OF TECHNOLOGY

Pasadena, California

2015

(Defended May 13, 2015)

© 2015

Corey Michael Reeves

All Rights Reserved

*To Debbie Elaine Ehlers,
My mom.*

ACKNOWLEDGMENTS

All of this started with a car accident. A bad car accident. After spending a week in the hospital, and undergoing a few surgeries, I had a salvaged hand and a tremendous impression of my surgeon, Dr. Michael Mara. I was so impressed, in fact, that I decided to go to college with the intention of one day going to medical school. So, I'd like to start by thanking him.

During his office hour for sophomore organic chemistry, I asked Prof. Tristan Lambert how it was that electrons passed through a nodal plane during an S_N2 displacement if the nodal plane is defined as a space in which there is zero electron density. Years later, Tristan would tell me that at this point he thought, "who is this surfer...is he serious?" For introducing me to organic chemistry, for being my first mentor in chemistry, for taking me into his lab, for always being supportive, for giving me my own project after just a month of tutelage, for teaching me the value inherent in and process of the scientific method, for steering me away from medical school and encouraging me to pursue the graduate education in chemistry that I have now nearly completed, I offer a heartfelt thank you to Tristan. I am also indebted to all of the people who populated the Lambert lab during my tenure there. In particular, Ethan Fisher, my mentor, who is a very talented teacher and chemist, and who was extremely patient with me as I learned the basics of laboratory chemistry. Thank you, as well, to Rocky, Brendan, Julia, Bandar, Elnaz, Tim, and Lisa all of whom were excellent labmates and friends and made the Lambert lab a fun and highly educational place.

Caltech is a truly wonderful place filled with outstanding people. I owe many thanks to Agnes Tong, Lynne Martinez and Anne Penney for their assistance over the years and for always kindly pointing me in the right direction when I had no idea which forms were due or when. Silva Virgil and Vicky Brennan were both so helpful in facilitating teaching assistant responsibilities. Dr. David VanderVelde, although I have had little personal interaction with him, keeps Caltech's NMR facility in first-rate working order and that has been an invaluable asset that I have both taken advantage of and, due to the apparent smoothness of its functioning, taken for granted. Joe Drew is as friendly as they come, helpful to fault and never too shy to say hello in passing. Larrisa Charnsangavej, Dorothy Pan, Beau Pritchett and Swarnima Manohar have all been outstanding co-workers who take pride in what they do as RAs and RLC and show a tremendous amount of character and resilience through difficult times and affairs.

I owe a massive debt of gratitude to Felicia Hunt. Felicia has been an indefatigable source of support to me. I have counted on her in times of personal crisis, poured my heart out to her with no appointment, asked her (repeatedly) for money, and been met with no rebuke upon showing up to meetings with her completely out of it from exhaustion. She does it all, solves all problems, cares tremendously about all of Caltech's students, executes every duty of her position with warmth and a smile, and makes it all look easy. She is much more than the associate dean of students and title IX coordinator at Caltech: she is tirelessly and quietly ensuring that all students here succeed and are as happy as they can possibly be. She is an indispensable pillar of Caltech and she deserves a hug from everyone.

Each member of my thesis committee deserves a hearty thank you. Prof. Linda Hsieh-Wilson has consistently and pleasantly tolerated my last minute scheduling efforts and offered valuable advice and criticisms. She is also an excellent teacher and I sincerely hope that I remember some of what I learned in her class on modern methods in chemical biology as I start my new job. Prof. Peter Dervan was a pleasure to TA for and has done an admirable job in organizing my various meetings, candidacy, proposal defense and thesis defense. More than this, Peter has given me crucial advice and guidance with respect to my career, and has offered me a handful of exceptionally meaningful pieces of support and encouragement. Prof. Sarah Reisman has also been much more than an outstanding committee member to me. Her class, which I both took and TA'd, provided me with an invaluable background in the storied history of chemical research, opened my eyes to the state of the art in synthesis and laid a foundation for mechanistic thinking, stereochemical analysis, synthetic storytelling and scientific writing – tools upon which I have relied throughout my graduate career. Her door is always opened, and I have taken advantage of this on numerous occasions. Sarah has very much been a second advisor to me, as she is to many students in the Stoltz group.

My doctoral advisor, Prof. Brian Stoltz, is truly the best boss one could hope to have and I owe the lion's share of my development as a scientist to him. In research, Brian is unfailingly patient, encouraging, didactic, enthusiastic, and lighthearted. He gave me the freedom to try a bunch of ideas that were longshots at best, the freedom to fail in trying, and the guidance to learn from my failure. He pushed me when I needed to be pushed, and always acted in my best interest. His ability to consolidate the best

interest of the individual and the best interest of the group is truly admirable. I have learned so much from Brian not only in chemistry, but also with respect to being a leader, being a good educator, being a professional colleague, and being a generally good scientist. On a personal level, Brian has been an incredibly understanding and dependable. I've walked into his office on countless occasions and completely blindsided him with an unexpected, non-science conversation to which he has, without fail, stopped what he was doing and listened. And through this all, he has been respectful, supportive and amiable. He has become one of my foremost role models, and with a heavy heart I will leave his lab and try my best to emulate his manner of engaging in science and in my profession life.

Over the years, I have had the privilege of working with and around some of the most talented and entertaining individuals one could hope to encounter. Pioneers of the Reisman lab, Jay Codeli and Roger Nani were particularly helpful to me in my early years at Caltech. Former and current members of the Reisman lab including but not limited to Maddi, Kangway, Alan, Haoxuan, Nat, Lindsay, Raul, Yeoman and Jake are all tremendous chemists and people and it was my pleasure to work across the hall from them. Many thanks to Myles from the Grubbs Lab, Ian and the Sattlers in the Bercaw Lab, and the entirety of the chemistry division at Caltech. All of the students in the CCE neck of campus make the experience here what it is and, for each of their individual contributions, I am appreciative.

Thank you to the members of the Stoltz lab with whom I overlapped during my first, second, third year; in particular, Doug Behenna, Florian Vogt, Chris Henry, Chris Gilmore, Hosea Nelson, Pam Tadross, Allen Hong, Russell Smith, Alex Goldberg,

Jonny Gordon, Hendrik Klare, Jeff Holder, Kathrin Höferl-Prantz, Alex Marziale, Kim Petersen, Hideki Shimizu, Kristy Tran, Max Loewinger and the one and only Nat Sherden, all of whom took myself and the other members of my class in with open arms, patiently taught us basic laboratory technique, at least appeared not to be annoyed by our collective unending stream of questions and provided a vision of what to strive for in our respective graduate careers.

Doug Duquette was my first hoodmate and probably the single biggest personal influence I've had with respect to dance moves. Doug is sincere friend, a terrific chemist and generally bright and interesting person. Our conversations often tended toward the obscure, our music toward loud, and for tolerating that I thank Alex Goldberg, Kristy Tran, Chung Wan Lee, and Doug Behenna, who collectively make up the remaining members of the bogie bay. As well, Christopher Haley, Kelly Kim, Alex Marziale, Yoshitaka Numajiri, Sam Shockley and Max Klatte, who have all been terrific baymates. Neighbors of the bogie bay, Chris Gilmore, Florian Vogt Chris Henry and Maxwell Loewinger rounded out the lab microclimate in the early years, and I learned much from each of them. I feel perhaps most connected in the lab to the other members of my class, them being Rob, Chris Bro, Yiyang, Dougie, and Chung Wan, and I owe them all a sincere thank you and congratulations. I look forward to what the "superclass" gets up to in the future as each goes his own way – expect big things from this very talented bunch.

I owe a huge thanks to Big Doug Behenna. Doug was my mentor and collaborator in the early years in the lab and I learned the majority of my practical laboratory skills from him. Doug is an outstanding scientist and much of the research I

conducted in my time in the Stoltz lab built on discoveries he made years ago. Beyond all of that Big Doug is a great leader and a thoughtful friend.

I have been extremely fortunate to work with a number of talented, motivated and bright collaborators. Doug Behenna is a very difficult act to follow in that regard, but Jimin Kim and Christian Eidamshaus, who initiated and helped finish the cyclobutanones project, respectively, did admirably and I learned a lot from them both. Scott Virgil is a veritable wellspring of useful information, keenly interested in chemistry, runs a first-rate catalysis center and is always available to talk science. Wen-Bo (Boger) Liu is as good a project partner for which one could hope. He is highly motivated, has read and remembers every paper on catalysis ever written, has a ton of great ideas, is thorough, patient and perpetually good-natured. I have no doubt that he will be highly successful as a principal investigator, and very much look forward to reading reports from his lab.

In the spring of 2010, Robert Allen Craig II, and myself beat Sarah Reisman and Roger Nani in a game of beerpong, at which point Sarah was obliged to do a kegstand. And I took a picture of her doing it. This may have been the moment I decided to come to Caltech. Since orientation and the G0 days, Rob Craig has been a great friend and colleague. We went through classes together, TA'd chem1A together and started out in the Stoltz lab together. This series of events that would have been considerably more dull, depressing and challenging, respectively, had it not been for that tall, loveable, goofball that was born Mr. Baby. Tiny Mr. Baby has been an invaluable compatriot and companion throughout graduate school. One who pushed me to work way too late into the evening and was pushed back for years. Who was

always eager to talk chemistry, never too busy to help me with some advanced NMR techniques, or show me how to perform some mindless task. Who kept me endlessly entertained with his terrible country music and one dance move. Who was always ready to wash away the long, hard work-week with a cold beer, a laugh and meal. Rob is a great person and a great friend and he will no doubt be the person to whom I come begging for a job one day.

I have also had the pleasure of forming friendships with younger members of the lab, many of whom have stepped up to take the reigns of the lab as my class departs. Beau Pritchett, Katerina Korch, Nick O'Connor, Kelly Kim and Sam Shockley are all terrific chemists and in their hands the lab will surely continue to flourish. To the newest members of the lab: while you are working hard, don't forget to enjoy yourself.

During the first couple of years of research, in particular, I was quite often a very tired, frustrated version of myself, and I certainly would not have made it to this point without the support of friends and family outside of the lab. To the closest thing the Stoltz lab has to an honorary member, John Steeves, a huge thanks. Sleeve has become a very close friend during the last five years and his patience for my blathering on about chemistry on the way to or from surfing, his patience in painstakingly explaining his own research to me on the way to or from surfing, his companionship during late nights in Sherman Fairchild Library, his enthusiasm for Frisbee golf and generally cheerful comportment have all been indispensable. Sleeve is very much the embodiment of a good-natured Canadian. As a case in point: he didn't complain after getting hit in the face with a surfboard, or when the doctor sewing him back together

from said incident remarked that the inside of his mouth “looked like hamburger meat” for the third time. I have for years been quietly, if slowly, learning to be a more good-natured, thoughtful and considerate person by following his example.

My dad, Brian Reeves, provided me with instrumental encouragement at the beginning of my academic career – words that really set the course of the path I have been on for years, and he has been there ever since, always eager to sit down for breakfast or dinner and to talk. For his encouragement and advice I am grateful. My darling girlfriend, Elizabeth Levin, has been incredibly patient with me, as I have struggled to finish out this degree program. She has seemingly unlimited drive, extremely high standards for herself and talent to spare – all of which make her the perfect person to try to keep pace with. And in doing so, I learn so much from her about the world and about myself. Her love, support, patience and comic relief have made these last months bearable and for that I am very thankful.

My mom, Debbie Ehlers, has been my mom. The best mom. She has been the rock on which I rely no matter what is happening in my life, graduate school related or otherwise. She has been my perpetual cheerleader and is ever ready to tell me what I need to hear to keep going. She has been a constant inspiration, source of love and point of light in my life. Our weekly phone conversations have kept me grounded and she has been unfailingly excited to share in what has been one of the most challenging, exciting, fulfilling, trying and rewarding periods of my life. I am indebted to her for so many things, things that extend well beyond the realm of graduate school and well beyond the scope of these acknowledgements, so to wrap things up I will simply say: thanks, mom, this is for you.

The Stoltz lab really has become like a home to me. I feel at home at my hood, and at home at my desk. That is a pretty amazing thing to be able to say and it stems from the general air about the lab, which arises from the people who show up day after day to populate it. To every member of the Stoltz group past and present who has done so – thank you for making the group the welcoming, exciting, engaging, enlightening, fun place that is. To the very capable younger members of the lab that will carry it into the future, I am confident that you will keep that up. Brian says that his goal is for the Stoltz lab to be the best synthetic chemistry lab in the world: in my opinion, it very much is.

– Corey M. Reeves, April 29th, 2015

ABSTRACT

Notwithstanding advances in modern chemical methods, the selective installation of sterically encumbered carbon stereocenters, in particular all-carbon quaternary centers, remains an unsolved problem in organic chemistry. The prevalence of all-carbon quaternary centers in biologically active natural products and pharmaceutical compounds provides a strong impetus to address current limitations in the state of the art of their generation. This thesis presents four related projects, all of which share in the goal of constructing highly-congested carbon centers in a stereoselective manner, and in the use of transition-metal catalyzed alkylation as a means to address that goal.

The first research described is an extension of allylic alkylation methodology previously developed in the Stoltz group to small, strained rings. This research constitutes the first transition metal-catalyzed enantioselective α -alkylation of cyclobutanones. Under Pd-catalysis, this chemistry affords all-carbon α -quaternary cyclobutanones in good to excellent yields and enantioselectivities.

Next is described our development of a (trimethylsilyl)ethyl β -ketoester class of enolate precursors, and their application in palladium-catalyzed asymmetric allylic alkylation to yield a variety of α -quaternary ketones and lactams. Independent coupling partner synthesis engenders enhanced allyl substrate scope relative to allyl β -ketoester substrates; highly functionalized α -quaternary ketones generated by the union of our fluoride-triggered β -ketoesters and sensitive allylic alkylation coupling partners serve to demonstrate the utility of this method for complex fragment coupling.

Lastly, our development of an Ir-catalyzed asymmetric allylic alkylation of cyclic β -ketoesters to afford highly congested, vicinal stereocenters comprised of tertiary and all-carbon quaternary centers with outstanding regio-, diastereo-, and enantiocontrol is detailed. Implementation of a subsequent Pd-catalyzed alkylation affords dialkylated products with pinpoint stereochemical control of both chiral centers. The chemistry is then extended to include acyclic β -ketoesters and similar levels of selective and functional group tolerance are observed. Critical to the successful development of this method was the employment of iridium catalysis in concert with *N*-aryl-phosphoramidite ligands.

TABLE OF CONTENTS

Dedication	iii
Acknowledgements.....	iv
Abstract	xiii
Table of Contents.....	xiv
List of Figures.....	xxi
List of Schemes	xxiv
List of Tables.....	xxxvi
List of Abbreviations	xxxix

CHAPTER 1

1

Enantioselective Construction of α -Quaternary Cyclobutanones by Catalytic Asymmetric Allylic Alkylation

1.1 Introduction	1
1.1.1 Palladium catalyzed allylic alkylation	1
1.1.2 Palladium catalyzed allylic alkylation of cyclobutanones.....	5
1.2 Preparation of cyclobutanones β -ketoester substrates and reaction optimization.....	7
1.2.1 Cyclobutanones β -ketoester substrates synthesis	7
1.2.2 Optimization of cyclobutanones allylic alkylation	9
1.3 Exploration of the reaction scope.....	11
1.3.1 Reaction scope with respect to enolate α -substitution	11
1.3.2 Reaction scope with respect to allyl substitution	13
1.4 Derivatization of reaction products.....	14
1.5 Concluding remarks	15
1.6 Experimental section	16
1.6.1 Materials and methods.....	16
1.6.2 Representative procedures for the synthesis of 2-oxocyclobutanecarboxylates ..	18
1.6.3 Representative procedures for the synthesis of 2-H-2-oxocyclobutane- carboxylates.....	19
1.6.4 Spectroscopic data for novel cyclobutanone β -ketoester substrates	20
1.6.5 Representative procedure for the asymmetric decarboxylative allylic alkylation of 2-oxocyclobutanecarboxylates.....	31
1.6.6 Spectroscopic data for novel α -quaternary cyclobutanone products.....	32

1.6.7	Procedures for derivatization of α -quaternary cyclobutanones and determination of absolute stereochemical configuration	42
1.6.8	Determination of enantiomeric excess	49
1.7	References and Notes	51

APPENDIX 1 **60**

Spectra Relevant to Chapter 1

CHAPTER 2 **137**

Development of (Trimethylsilyl)Ethyl Ester Protected Enolates and Applications in Palladium-Catalyzed Enantioselective Allylic Alkylation: Intermolecular Cross-Coupling of Functionalized Electrophiles

2.1	Introduction	137
2.1.1	Latent enolates: silyl enol ethers	137
2.1.2	Latent enolates: β -ketoesters	138
2.1.3	Latent enolates: TMSE β -ketoesters	139
2.2	Synthesis of and Reaction Optimization with TMSE β -ketoesters	141
2.2.1	Substrate synthesis	141
2.2.2	TMSE- β -ketoester allylic alkylation optimization	142
2.3	Palladium-Catalyzed Allylic Alkylation with TMSE β -Ketoesters	146
2.3.1	Reaction scope with respect to nucleophile	146
2.3.2	Reaction scope with respect to electrophile	148
2.4	Coupling of TMSE β -Ketoesters with Functionally Complex Electrophilic Partners	149
2.5	Concluding Remarks	152
2.6	Experimental Section	154
2.6.1	Materials and Methods	154
2.6.2	General Procedure for TMSE β -Ketoester Substrate Synthesis	156
2.6.3	Procedures for the syntheses of TMSE β -ketoester intermediate 88 and ketoester 77b	157
2.6.4	Spectroscopic data for TMSE β -ketoester substrates	159
2.6.5	General procedure for allyl carbonate substrate syntheses	164
2.6.6	Spectroscopic data for allyl carbonate substrates	165
2.6.7	Procedure for the synthesis allyl carbonate 82	167

2.6.8	Optimization of reaction parameters.....	169
2.6.9	General procedure for Pd-catalyzed allylic alkylation.....	170
2.6.10	Spectroscopic data for Pd-catalyzed allylic alkylation products.....	172
2.6.11	Determination of enantiomeric excess and optical rotations.....	179
2.7	References and Notes.....	180

APPENDIX 2 **183**

Spectra Related to Chapter 2

CHAPTER 3 **226**

Construction of Vicinal Tertiary and All-Carbon Quaternary Stereocenters via Ir-Catalyzed Regio-, Diastereo-, and Enantioselective Allylic Alkylation and Applications in Sequential Pd-Catalysis

3.1	Introduction.....	226
3.1.1	State of the art in the asymmetric construction of vicinal quaternary and tertiary carbon centers.....	226
3.2	Reaction Optimization and Development.....	228
3.2.1	Discovery and optimization of iridium catalyzed regio-, diastereo- and enantioselective allylic alkylation of cyclic ketones.....	228
3.2.2	Further development of the reaction conditions.....	231
3.3	Survey of Reaction Scope.....	231
3.3.1	Exploration of the reaction scope with respect to allyl electrophile.....	231
3.3.2	Exploration of the reaction scope with respect to ketoester nucleophile.....	232
3.4	Employment of TMSE β -Ketoester to Enable Sequential Catalysis.....	233
3.5	Concluding Remarks.....	236
3.6	Experimental Section.....	237
3.6.1	Materials and Methods.....	237
3.6.2	Optimization of reaction parameters.....	239
3.6.3	General procedure for the Ir-catalyzed asymmetric allylic alkylation of β -ketoesters.....	240
3.6.4	Spectroscopic data for Ir-catalyzed allylic alkylation products.....	242
3.6.5	General procedure for Pd-catalyzed allylic alkylation.....	256
3.6.6	Determination of the relative configuration of compound 106a.....	259
3.6.7	Spectroscopic data for new phosphinooxazoline ligands.....	260

3.6.8	Determination of enantiomeric excess	263
3.7	References and Notes	265

APPENDIX 3 **272**

Spectra Related to Chapter 3

APPENDIX 4 **319**

X-Ray Crystallography Reports Relevant to Appendix 3

CHAPTER 4 **330**

Enantio-, Diastereo- and Regioselective Iridium-Catalyzed Asymmetric Allylic Alkylation of Acyclic β -Ketoesters

4.1	Introduction	330
4.1.1	State of the art in the asymmetric construction of vicinal quaternary and tertiary carbon centers	330
4.2	Development and Optimization of an Iridium-Catalyzed Allylic Alkylation of Linear β -Ketoesters	332
4.3	Exploration of the Reaction Scope and Substituent Effects	334
4.3.1	Exploration of the iridium-catalyzed allylic alkylation of linear β -ketoesters with respect to allyl electrophile	334
4.3.2	Investigation of allyl electrophile substituent effects on reaction selectivity	336
4.3.3	Exploration of the iridium-catalyzed allylic alkylation of linear β -ketoesters with respect to β -ketoester nucleophile	337
4.4	Elaboration of the Allylic Alkylation Products	339
4.5	Concluding Remarks	340
4.6	Experimental Section	341
4.6.1	Materials and Methods	341
4.6.2	Optimization of reaction parameters	343
4.6.3	General procedure for the Ir-catalyzed asymmetric allylic alkylation of acyclic β -ketoesters	345
4.6.4	Spectroscopic data for Ir-catalyzed allylic alkylation products	374

4.6.5	Procedures for derivatization of allylic alkylation products and spectroscopic data of derivatives	373
4.6.6	Determination of the absolute confirmation of compound 112f	376
4.6.7	Determination of enantiomeric excess	378
4.7	References and Notes	382

APPENDIX 5 **384**

Stereochemical Model and Mechanistic Discussion for Iridium Catalyzed Allylic Alkylation

A5.1	Introduction	384
A5.2	Stereochemical Model for Diastereoselectivity in Iridium-Catalyzed Allylic Alkylation	385
A5.3	References and Notes	388

APPENDIX 6 **390**

Spectra Related to Chapter 4

APPENDIX 7 **466**

X-Ray Crystallography Reports Relevant to Chapter 4

APPENDIX 8 **480**

Development of an α -Arylation Reaction of TMSE β -Ketoesters

A8.1	Introduction.....	480
A8.1.1	Background and state of the art in the α -arylation of cyclic ketones	480
A8.1.2	State of the art in the asymmetric α -arylation of cyclic ketones	482
A8.2	Background: Extension of Carboxylate Protected Enolate Cross Coupling Strategy to α -Arylation	484
A8.2.1	Use of allyl β -ketoester protected enolates in non-allylic alkylation processes.	484
A8.2.2	New pathways into catalysis via a carboxylate protected prochiral enolate strategy	487
A8.3	Initial Evaluation of TMSE β -Ketoester in α -Arylation	489
A8.3.1	Symyx assisted reaction development: early experiments.....	489

A8.3.2	Symyx assisted reaction development: beyond the initial experiments	491
A8.4	Optimization of The Palladium catalyzed α -Arylation of TMSE β -Ketoesters	493
A8.5	Outlook and Future Directions for carboxylate protected enolates in α -Arylation.....	499
A8.5.1	Hypotheses that remain to be tested in α -arylation of TMSE β -ketoesters	499
A8.5.2	Deacylative in situ access to prochiral enolates	500
A8.6	Concluding Remarks	502
A8.7	Experimental Section.....	503
A8.7.1	Materials and Methods.....	503
A8.6.2	Procedure for Symyx assisted screening of α -arylation	504
A8.6.3	Procedure for manual screening of α -arylation.....	508
A8.7	References and Notes.....	509

APPENDIX 9

511

Studies Toward the Enantioselective Total Synthesis of (+)-Lingzhiol

A9.1	Introduction.....	511
A9.1.1	Isolation studies of the lingzhiols	511
A9.1.2	Biological studies on and bioactivity profile of lingzhiol	512
A9.2	Retrosynthetic Analysis of (+)-Lingzhiol	513
A9.3	Model Studies to Investigate Key (3+2) Cycloaddition in the Synthesis of (+)-Lingzhiol....	514
A9.3.1	Retrosynthetic plan for lingzhiol model system	514
A9.3.2	Synthesis of lingzhiol model system and testing of key (3+2) cycloaddition	515
A9.4	Revised Model Studies to Investigate Key (3+2) Cycloaddition in the Synthesis of (+)-Lingzhiol	519
A9.4.1	Rationale and revised plan for (+)-lingzhiol model system	519
A9.4.2	Synthesis of the revised model system for (+)-lingzhiol.....	520
A9.5	Revised Strategy for the Synthesis of (+)-Lingzhiol	523
A9.6	Concluding Remarks	525
A9.7	Experimental Section.....	525
A9.7.1	Materials and Methods.....	525
A9.7.2	Procedures for the preparation of and spectroscopic data for compounds in scheme A9.3.2.1	526
A9.7.3	Procedures for the preparation of and spectroscopic data for compounds in scheme A9.3.2.2	528
A9.7.4	Procedures for the preparation of and spectroscopic data for compounds in	

	scheme A9.3.2.3	530
A9.7.5	Procedures for the preparation of and spectroscopic data for compounds in scheme A9.3.2.4	532
A9.7.6	Procedures for the preparation of and spectroscopic data for compounds in scheme A9.4.2.1	533
A9.7.7	Procedures for the preparation of and spectroscopic data for compounds in scheme A9.4.2.2	537
A9.8	References and Notes	541

APPENDIX 10 **544**

Spectra Related to Appendix 9

Comprehensive Bibliography	567
Index	587
About the Author	590

LIST OF FIGURES

CHAPTER 1

Figure 1.1.2.1	(A) Representative cycbutanoid natural products; (B) ring, conformational and torsional strain in cyclobutanone enolates	6
Figure 1.2.1.1	Construction of allyl 1-benzyl-2-oxocyclobutane-carboxylate (36)	9
Figure 1.2.2.1	General initial reaction parameters and select ligands	10
Figure 1.2.2.2	Solvent and temperature optimization of the palladium catalyzed allylic alkylation reaction.....	11
Figure 1.3.1.1	Reaction scope with respect to α -quaternary substitution (R^1).....	13
Figure 1.3.2.1	Reaction scope with respect to allyl substitution (R^2)	14
Figure 1.4.1	Derivatization of α -quaternary cyclobutanones	15

APPENDIX 1

Figure A1.1	^1H NMR (500 MHz, CDCl_3) of compound 48	61
Figure A1.2	Infrared spectrum (thin film/ NaCl) of compound 48	62
Figure A1.3	^{13}C NMR (125 MHz, CDCl_3) of compound 48	62
Figure A1.4	^1H NMR (500 MHz, CDCl_3) of compound 39a	63
Figure A1.5	Infrared spectrum (thin film/ NaCl) of compound 39a	64
Figure A1.6	^{13}C NMR (125 MHz, CDCl_3) of compound 39a	64
Figure A1.7	^1H NMR (500 MHz, CDCl_3) of compound 39b	65
Figure A1.8	Infrared spectrum (thin film/ NaCl) of compound 39b	66
Figure A1.9	^{13}C NMR (125 MHz, CDCl_3) of compound 39b	66
Figure A1.10	^1H NMR (500 MHz, CDCl_3) of compound 39c	67
Figure A1.11	Infrared spectrum (thin film/ NaCl) of compound 39c	68
Figure A1.12	^{13}C NMR (125 MHz, CDCl_3) of compound 39c	68
Figure A1.13	^1H NMR (500 MHz, CDCl_3) of compound 39d	69
Figure A1.14	Infrared spectrum (thin film/ NaCl) of compound 39d	70
Figure A1.15	^{13}C NMR (125 MHz, CDCl_3) of compound 39d	70
Figure A1.16	^1H NMR (500 MHz, CDCl_3) of compound 39e	71
Figure A1.17	Infrared spectrum (thin film/ NaCl) of compound 39e	72
Figure A1.18	^{13}C NMR (125 MHz, CDCl_3) of compound 39e	72
Figure A1.19	^1H NMR (500 MHz, CDCl_3) of compound 39f	73
Figure A1.20	Infrared spectrum (thin film/ NaCl) of compound 39f	74
Figure A1.21	^{13}C NMR (125 MHz, CDCl_3) of compound 39f	74

Figure A1.22	^1H NMR (500 MHz, CDCl_3) of compound 39g	75
Figure A1.23	Infrared spectrum (thin film/ NaCl) of compound 39g	76
Figure A1.24	^{13}C NMR (125 MHz, CDCl_3) of compound 39g	76
Figure A1.25	^1H NMR (500 MHz, CDCl_3) of compound 39h	77
Figure A1.26	Infrared spectrum (thin film/ NaCl) of compound 39h	78
Figure A1.27	^{13}C NMR (125 MHz, CDCl_3) of compound 39h	78
Figure A1.28	^1H NMR (500 MHz, CDCl_3) of compound 41a	79
Figure A1.29	Infrared spectrum (thin film/ NaCl) of compound 41a	80
Figure A1.30	^{13}C NMR (125 MHz, CDCl_3) of compound 41a	80
Figure A1.31	^1H NMR (500 MHz, CDCl_3) of compound 41b	81
Figure A1.32	Infrared spectrum (thin film/ NaCl) of compound 41b	82
Figure A1.33	^{13}C NMR (125 MHz, CDCl_3) of compound 41b	82
Figure A1.34	^1H NMR (500 MHz, CDCl_3) of compound 41c	83
Figure A1.35	Infrared spectrum (thin film/ NaCl) of compound 41c	84
Figure A1.36	^{13}C NMR (125 MHz, CDCl_3) of compound 41c	84
Figure A1.37	^1H NMR (500 MHz, CDCl_3) of compound 36	85
Figure A1.38	Infrared spectrum (thin film/ NaCl) of compound 36	86
Figure A1.39	^{13}C NMR (125 MHz, CDCl_3) of compound 36	86
Figure A1.40	^1H NMR (500 MHz, CDCl_3) of compound 41d	87
Figure A1.41	Infrared spectrum (thin film/ NaCl) of compound 41d	88
Figure A1.42	^{13}C NMR (125 MHz, CDCl_3) of compound 41d	88
Figure A1.43	^1H NMR (500 MHz, CDCl_3) of compound 41e	89
Figure A1.44	Infrared spectrum (thin film/ NaCl) of compound 41e	90
Figure A1.45	^{13}C NMR (125 MHz, CDCl_3) of compound 41e	90
Figure A1.46	^1H NMR (500 MHz, CDCl_3) of compound 41f	91
Figure A1.47	Infrared spectrum (thin film/ NaCl) of compound 41f	92
Figure A1.48	^{13}C NMR (125 MHz, CDCl_3) of compound 41f	92
Figure A1.49	^1H NMR (500 MHz, CDCl_3) of compound 40a	93
Figure A1.50	Infrared spectrum (thin film/ NaCl) of compound 40a	94
Figure A1.51	^{13}C NMR (125 MHz, CDCl_3) of compound 40a	94
Figure A1.52	^1H NMR (500 MHz, CDCl_3) of compound 40b	95
Figure A1.53	Infrared spectrum (thin film/ NaCl) of compound 40b	96
Figure A1.54	^{13}C NMR (125 MHz, CDCl_3) of compound 40b	96
Figure A1.55	^1H NMR (500 MHz, CDCl_3) of compound 40c	97
Figure A1.56	Infrared spectrum (thin film/ NaCl) of compound 40c	97

Figure A1.57	^{13}C NMR (125 MHz, CDCl_3) of compound 40c	98
Figure A1.58	^1H NMR (500 MHz, CDCl_3) of compound 40d	99
Figure A1.59	Infrared spectrum (thin film/ NaCl) of compound 40d	100
Figure A1.60	^{13}C NMR (125 MHz, CDCl_3) of compound 40d	100
Figure A1.61	^1H NMR (500 MHz, CDCl_3) of compound 40e	101
Figure A1.62	Infrared spectrum (thin film/ NaCl) of compound 40e	102
Figure A1.63	^{13}C NMR (125 MHz, CDCl_3) of compound 40e	102
Figure A1.64	^1H NMR (500 MHz, CDCl_3) of compound 40f	103
Figure A1.65	Infrared spectrum (thin film/ NaCl) of compound 40f	104
Figure A1.66	^{13}C NMR (125 MHz, CDCl_3) of compound 40f	104
Figure A1.67	^1H NMR (500 MHz, CDCl_3) of compound 40g	105
Figure A1.68	Infrared spectrum (thin film/ NaCl) of compound 40g	106
Figure A1.69	^{13}C NMR (125 MHz, CDCl_3) of compound 40g	106
Figure A1.70	^1H NMR (500 MHz, CDCl_3) of compound 40h	107
Figure A1.71	Infrared spectrum (thin film/ NaCl) of compound 40h	108
Figure A1.72	^{13}C NMR (125 MHz, CDCl_3) of compound 40h	108
Figure A1.73	^1H NMR (500 MHz, CDCl_3) of compound 42a	109
Figure A1.74	Infrared spectrum (thin film/ NaCl) of compound 42a	110
Figure A1.75	^{13}C NMR (125 MHz, CDCl_3) of compound 42a	110
Figure A1.76	^1H NMR (500 MHz, CDCl_3) of compound 42b	111
Figure A1.77	Infrared spectrum (thin film/ NaCl) of compound 42b	112
Figure A1.78	^{13}C NMR (125 MHz, CDCl_3) of compound 42b	112
Figure A1.79	^1H NMR (500 MHz, CDCl_3) of compound 42c	113
Figure A1.80	Infrared spectrum (thin film/ NaCl) of compound 42c	114
Figure A1.81	^{13}C NMR (125 MHz, CDCl_3) of compound 42c	114
Figure A1.82	^1H NMR (500 MHz, CDCl_3) of compound 38	115
Figure A1.83	Infrared spectrum (thin film/ NaCl) of compound 38	116
Figure A1.84	^{13}C NMR (125 MHz, CDCl_3) of compound 38	116
Figure A1.85	^1H NMR (500 MHz, CDCl_3) of compound 42d	117
Figure A1.86	Infrared spectrum (thin film/ NaCl) of compound 42d	118
Figure A1.87	^{13}C NMR (125 MHz, CDCl_3) of compound 42d	118
Figure A1.88	^1H NMR (500 MHz, CDCl_3) of compound 49	119
Figure A1.89	Infrared spectrum (thin film/ NaCl) of compound 49	120
Figure A1.90	^{13}C NMR (125 MHz, CDCl_3) of compound 49	120
Figure A1.91	^1H NMR (500 MHz, CDCl_3) of compound 42e	121

Figure A1.92	Infrared spectrum (thin film/NaCl) of compound 42e	122
Figure A1.93	¹³ C NMR (125 MHz, CDCl ₃) of compound 42e	122
Figure A1.94	¹ H NMR (500 MHz, CDCl ₃) of compound 42f	123
Figure A1.95	Infrared spectrum (thin film/NaCl) of compound 42f	124
Figure A1.96	¹³ C NMR (125 MHz, CDCl ₃) of compound 42f	124
Figure A1.97	¹ H NMR (500 MHz, CDCl ₃) of compound 44	125
Figure A1.98	Infrared spectrum (thin film/NaCl) of compound 44	126
Figure A1.99	¹³ C NMR (125 MHz, CDCl ₃) of compound 44	126
Figure A1.100	¹ H NMR (500 MHz, CDCl ₃) of compound 45	127
Figure A1.101	Infrared spectrum (thin film/NaCl) of compound 45	128
Figure A1.102	¹³ C NMR (125 MHz, CDCl ₃) of compound 45	128
Figure A1.103	¹ H NMR (500 MHz, CDCl ₃) of compound 46	129
Figure A1.104	Infrared spectrum (thin film/NaCl) of compound 46	130
Figure A1.105	¹³ C NMR (125 MHz, CDCl ₃) of compound 46	130
Figure A1.106	¹ H NMR (500 MHz, CDCl ₃) of compound 47	131
Figure A1.107	Infrared spectrum (thin film/NaCl) of compound 47	132
Figure A1.108	¹³ C NMR (125 MHz, CDCl ₃) of compound 47	132
Figure A1.109	¹ H NMR (500 MHz, CDCl ₃) of compound 51	133
Figure A1.110	Infrared spectrum (thin film/NaCl) of compound 51	134
Figure A1.111	¹³ C NMR (125 MHz, CDCl ₃) of compound 51	134
Figure A1.112	¹ H NMR (500 MHz, CDCl ₃) of compound 52	135
Figure A1.113	Infrared spectrum (thin film/NaCl) of compound 52	136
Figure A1.114	¹³ C NMR (125 MHz, CDCl ₃) of compound 52	136

CHAPTER 2

Figure 2.1.1.1	Drawbacks of silyl enol ether synthesis.....	138
Figure 2.1.2.1	Allyl β-ketoester approach to latent enolate chemistry.....	139
Figure 2.1.3.1	Non-allyl β-ketoester approach to latent enolate chemistry.....	140
Figure 2.1.3.2	TMSE β-ketoester approach to latent enolate chemistry.....	141
Figure 2.3.1.1	Exploration of functional group and scaffold diversity in the fluoride triggered palladium-catalyzed allylic alkylation reaction with respect to nucleophile.	148
Figure 2.3.2.1	Exploration of functional group and scaffold diversity in the fluoride triggered palladium-catalyzed allylic alkylation reaction with respect to electrophile...	14
Figure 2.4.1	Complex allyl architectures.....	150
Figure 2.4.2	Union of complex fragments by asymmetric allylic alkylation.....	153

APPENDIX 2

Figure A2.1	^1H NMR (500 MHz, CDCl_3) of compound 74	184
Figure A2.2	Infrared spectrum (thin film/ NaCl) of compound 74	185
Figure A2.3	^{13}C NMR (125 MHz, CDCl_3) of compound 74	185
Figure A2.4	^1H NMR (500 MHz, CDCl_3) of compound 88	186
Figure A2.5	Infrared spectrum (thin film/ NaCl) of compound 88	187
Figure A2.6	^{13}C NMR (125 MHz, CDCl_3) of compound 88	187
Figure A2.7	^1H NMR (500 MHz, CDCl_3) of compound 77b	188
Figure A2.8	Infrared spectrum (thin film/ NaCl) of compound 77b	189
Figure A2.9	^{13}C NMR (125 MHz, CDCl_3) of compound 77b	189
Figure A2.10	^1H NMR (500 MHz, CDCl_3) of compound 77a	190
Figure A2.11	Infrared spectrum (thin film/ NaCl) of compound 77a	191
Figure A2.12	^{13}C NMR (125 MHz, CDCl_3) of compound 77a	191
Figure A2.13	^1H NMR (500 MHz, CDCl_3) of compound 77c	192
Figure A2.14	Infrared spectrum (thin film/ NaCl) of compound 77c	193
Figure A2.15	^{13}C NMR (125 MHz, CDCl_3) of compound 77c	193
Figure A2.16	^1H NMR (500 MHz, CDCl_3) of compound 77d	194
Figure A2.17	Infrared spectrum (thin film/ NaCl) of compound 77d	195
Figure A2.18	^{13}C NMR (125 MHz, CDCl_3) of compound 77d	195
Figure A2.19	^1H NMR (500 MHz, CDCl_3) of compound 77e	196
Figure A2.20	Infrared spectrum (thin film/ NaCl) of compound 77e	197
Figure A2.21	^{13}C NMR (125 MHz, CDCl_3) of compound 77e	197
Figure A2.22	^1H NMR (500 MHz, CDCl_3) of compound 77f	198
Figure A2.23	Infrared spectrum (thin film/ NaCl) of compound 77f	199
Figure A2.24	^{13}C NMR (125 MHz, CDCl_3) of compound 77f	199
Figure A2.25	^1H NMR (500 MHz, CDCl_3) of compound 77g	200
Figure A2.26	Infrared spectrum (thin film/ NaCl) of compound 77g	201
Figure A2.27	^{13}C NMR (125 MHz, CDCl_3) of compound 77g	201
Figure A2.28	^1H NMR (500 MHz, CDCl_3) of compound 80b	202
Figure A2.29	Infrared spectrum (thin film/ NaCl) of compound 80b	203
Figure A2.30	^{13}C NMR (125 MHz, CDCl_3) of compound 80b	203
Figure A2.31	^1H NMR (500 MHz, CDCl_3) of compound 80d	204
Figure A2.32	Infrared spectrum (thin film/ NaCl) of compound 80d	205
Figure A2.33	^{13}C NMR (125 MHz, CDCl_3) of compound 80d	205
Figure A2.34	^1H NMR (500 MHz, CDCl_3) of compound 83	206

Figure A2.35	Infrared spectrum (thin film/NaCl) of compound 83	206
Figure A2.36	¹³ C NMR (125 MHz, CDCl ₃) of compound 83	206
Figure A2.37	¹ H NMR (500 MHz, CDCl ₃) of compound 92	206
Figure A2.38	Infrared spectrum (thin film/NaCl) of compound 92	207
Figure A2.39	¹³ C NMR (125 MHz, CDCl ₃) of compound 92	207
Figure A2.40	¹ H NMR (500 MHz, CDCl ₃) of compound 82	208
Figure A2.41	Infrared spectrum (thin film/NaCl) of compound 82	209
Figure A2.42	¹³ C NMR (125 MHz, CDCl ₃) of compound 82	209
Figure A2.43	¹ H NMR (500 MHz, CDCl ₃) of compound 81a	210
Figure A2.44	Infrared spectrum (thin film/NaCl) of compound 81a	211
Figure A2.45	¹³ C NMR (125 MHz, CDCl ₃) of compound 81a	211
Figure A2.46	¹ H NMR (500 MHz, CDCl ₃) of compound 79g	212
Figure A2.47	Infrared spectrum (thin film/NaCl) of compound 79g	213
Figure A2.48	¹³ C NMR (125 MHz, CDCl ₃) of compound 79g	213
Figure A2.49	¹ H NMR (500 MHz, CDCl ₃) of compound 81b	214
Figure A2.50	Infrared spectrum (thin film/NaCl) of compound 81b	215
Figure A2.51	¹³ C NMR (125 MHz, CDCl ₃) of compound 81b	215
Figure A2.52	¹ H NMR (500 MHz, CDCl ₃) of compound 81d	216
Figure A2.53	Infrared spectrum (thin film/NaCl) of compound 81d	217
Figure A2.54	¹³ C NMR (125 MHz, CDCl ₃) of compound 81d	217
Figure A2.55	¹ H NMR (500 MHz, CDCl ₃) of compound 84	218
Figure A2.56	Infrared spectrum (thin film/NaCl) of compound 84	219
Figure A2.57	¹³ C NMR (125 MHz, CDCl ₃) of compound 84	219
Figure A2.58	¹ H NMR (500 MHz, CDCl ₃) of compound 85	220
Figure A2.59	Infrared spectrum (thin film/NaCl) of compound 85	221
Figure A2.60	¹³ C NMR (125 MHz, CDCl ₃) of compound 85	221
Figure A2.61	¹ H NMR (500 MHz, CDCl ₃) of compound 86	222
Figure A2.62	Infrared spectrum (thin film/NaCl) of compound 86	223
Figure A2.63	¹³ C NMR (125 MHz, CDCl ₃) of compound 86	223
Figure A2.61	¹ H NMR (500 MHz, CDCl ₃) of compound 87	222
Figure A2.62	Infrared spectrum (thin film/NaCl) of compound 87	223
Figure A2.63	¹³ C NMR (125 MHz, CDCl ₃) of compound 87	223

CHAPTER 3

Figure 3.1.1.1	Ir-catalyzed allylic substitution.....	228
----------------	--	-----

Figure 3.2.1.1	Selected phosphoramidite and PHOX ligands.....	229
Figure 3.3.1.1	Substrate scope of Ir-catalyzed allylic alkylation of β -aetoesters.....	232
Figure 3.3.2.1	Substrate scope of Ir-catalyzed allylic alkylation of β -ketoesters.....	233
Figure 3.4.1	Conceptualization of sequential catalysis.....	234
Figure 3.4.2	Development of Pd-catalyzed diastereoselective decarboxylative allylic alkylation of TMSE- β -ketoesters	236

APPENDIX 3

Figure A3.1	^1H NMR (500 MHz, CDCl_3) of compound 100a	273
Figure A3.2	Infrared spectrum (thin film/ NaCl) of compound 100a	274
Figure A3.3	^{13}C NMR (125 MHz, CDCl_3) of compound 100a	274
Figure A3.4	^1H NMR (500 MHz, CDCl_3) of compound 100b	275
Figure A3.5	Infrared spectrum (thin film/ NaCl) of compound 100b	276
Figure A3.6	^{13}C NMR (125 MHz, CDCl_3) of compound 100b	276
Figure A3.7	^1H NMR (500 MHz, CDCl_3) of compound 100c	277
Figure A3.8	Infrared spectrum (thin film/ NaCl) of compound 100c	278
Figure A3.9	^{13}C NMR (125 MHz, CDCl_3) of compound 100c	278
Figure A3.10	^1H NMR (500 MHz, CDCl_3) of compound 100d	279
Figure A3.11	Infrared spectrum (thin film/ NaCl) of compound 100d	280
Figure A3.12	^{13}C NMR (125 MHz, CDCl_3) of compound 100d	280
Figure A3.13	^1H NMR (500 MHz, CDCl_3) of compound 100e	281
Figure A3.14	Infrared spectrum (thin film/ NaCl) of compound 100e	282
Figure A3.15	^{13}C NMR (125 MHz, CDCl_3) of compound 100e	282
Figure A3.16	^1H NMR (500 MHz, CDCl_3) of compound 100f	283
Figure A3.17	Infrared spectrum (thin film/ NaCl) of compound 100f	284
Figure A3.18	^{13}C NMR (125 MHz, CDCl_3) of compound 100f	284
Figure A3.19	^1H NMR (500 MHz, CDCl_3) of compound 100g	285
Figure A3.20	Infrared spectrum (thin film/ NaCl) of compound 100g	286
Figure A3.21	^{13}C NMR (125 MHz, CDCl_3) of compound 100g	286
Figure A3.22	^1H NMR (500 MHz, CDCl_3) of compound 100h	287
Figure A3.23	Infrared spectrum (thin film/ NaCl) of compound 100h	288
Figure A3.24	^{13}C NMR (125 MHz, CDCl_3) of compound 100h	288
Figure A3.25	^1H NMR (500 MHz, CDCl_3) of compound 100i	289
Figure A3.26	Infrared spectrum (thin film/ NaCl) of compound 100i	290
Figure A3.27	^{13}C NMR (125 MHz, CDCl_3) of compound 100i	290

Figure A3.28	^1H NMR (500 MHz, CDCl_3) of compound 103a	291
Figure A3.29	Infrared spectrum (thin film/ NaCl) of compound 103a	292
Figure A3.30	^{13}C NMR (125 MHz, CDCl_3) of compound 103a	292
Figure A3.31	^1H NMR (500 MHz, CDCl_3) of compound 103b	293
Figure A3.32	Infrared spectrum (thin film/ NaCl) of compound 103b	294
Figure A3.33	^{13}C NMR (125 MHz, CDCl_3) of compound 103b	294
Figure A3.34	^1H NMR (500 MHz, CDCl_3) of compound 103c	295
Figure A3.35	Infrared spectrum (thin film/ NaCl) of compound 103c	296
Figure A3.36	^{13}C NMR (125 MHz, CDCl_3) of compound 103c	296
Figure A3.37	^1H NMR (500 MHz, CDCl_3) of compound 103d	297
Figure A3.38	Infrared spectrum (thin film/ NaCl) of compound 103d	298
Figure A3.39	^{13}C NMR (125 MHz, CDCl_3) of compound 103d	298
Figure A3.40	^1H NMR (500 MHz, CDCl_3) of compound 103e	299
Figure A3.41	Infrared spectrum (thin film/ NaCl) of compound 103e	300
Figure A3.42	^{13}C NMR (125 MHz, CDCl_3) of compound 103e	300
Figure A3.43	^1H NMR (500 MHz, CDCl_3) of compound 103f	301
Figure A3.44	Infrared spectrum (thin film/ NaCl) of compound 103f	302
Figure A3.45	^{13}C NMR (125 MHz, CDCl_3) of compound 103f	302
Figure A3.46	^1H NMR (500 MHz, CDCl_3) of compound 106a and 107a	303
Figure A3.47	Infrared spectrum (thin film/ NaCl) of compound 106a and 107a	304
Figure A3.48	^{13}C NMR (125 MHz, CDCl_3) of compound 106a and 107a	304
Figure A3.49	^1H NMR (500 MHz, CDCl_3) of compound 106b	305
Figure A3.50	Infrared spectrum (thin film/ NaCl) of compound 106b	306
Figure A3.51	^{13}C NMR (125 MHz, CDCl_3) of compound 106b	306
Figure A3.52	^1H NMR (500 MHz, CDCl_3) of compound 106c	307
Figure A3.53	Infrared spectrum (thin film/ NaCl) of compound 106c	308
Figure A3.54	^{13}C NMR (125 MHz, CDCl_3) of compound 106c	308
Figure A3.55	^1H NOESY (600 MHz, CDCl_3) of compound 108	309
Figure A3.56	Infrared spectrum (thin film/ NaCl) of compound 108	310
Figure A3.57	^{13}C NMR (125 MHz, CDCl_3) of compound 108	310
Figure A3.58	^1H NMR (500 MHz, CDCl_3) of compound L14	311
Figure A3.59	Infrared spectrum (thin film/ NaCl) of compound L14	312
Figure A3.60	^{13}C NMR (125 MHz, CDCl_3) of compound L14	312
Figure A3.61	^{19}F NMR (300 MHz, CDCl_3) of compound L14	313
Figure A3.62	^{31}P NMR (500 MHz, CDCl_3) of compound L14	314

Figure A3.63	^1H NMR (500 MHz, CDCl_3) of compound L14	315
Figure A3.64	Infrared spectrum (thin film/ NaCl) of compound L15	316
Figure A3.65	^{13}C NMR (125 MHz, CDCl_3) of compound L15	316
Figure A3.65	^{19}F NMR (300 MHz, CDCl_3) of compound L15	317
Figure A3.67	^{31}P NMR (500 MHz, CDCl_3) of compound L15	318

ADDENDIX 4

Figure A4.1.1.	ORTEP drawing of 100f	320
----------------	------------------------------------	-----

CHAPTER 4

Figure 4.1.1.1	Representative Ir-catalyzed asymmetric allylic alkylation	331
Figure 4.3.2.1	Hammett plot of the log of product ratios (112:113) from Table 2 versus Hammett σ -values	337

APPENDIX 5

Figure A5.2.1	Selected iridium-phosphoramidite complexes: 118 Feringa type; 119 N-arylphosphoramidite (or You) type; 120 (π -allyl)-Ir complex with You type ligand	385
Figure A5.2.2	Approach of the enolate nucleophile in the Ir-catalyzed allylic alkylation ...	387
Figure A5.2.3	Proposed catalytic cycle for iridium-N-arylphosphoramidite complex catalyzed allylic alkylation	388

APPENDIX 6

Figure A6.1	^1H NMR (500 MHz, CDCl_3) of compound 112a	391
Figure A6.2	Infrared spectrum (thin film/ NaCl) of compound 112a	392
Figure A6.3	^{13}C NMR (125 MHz, CDCl_3) of compound 112a	392
Figure A6.4	^1H NMR (500 MHz, CDCl_3) of compound 112b	393
Figure A6.5	Infrared spectrum (thin film/ NaCl) of compound 112b	394
Figure A6.6	^{13}C NMR (125 MHz, CDCl_3) of compound 112b	394
Figure A6.7	^1H NMR (500 MHz, CDCl_3) of compound 112c	395
Figure A6.8	Infrared spectrum (thin film/ NaCl) of compound 112c	396
Figure A6.9	^{13}C NMR (125 MHz, CDCl_3) of compound 112c	396

Figure A6.10	^1H NMR (500 MHz, CDCl_3) of compound 112d	397
Figure A6.11	Infrared spectrum (thin film/ NaCl) of compound 112d	398
Figure A6.12	^{13}C NMR (125 MHz, CDCl_3) of compound 112d	398
Figure A6.13	^1H NMR (500 MHz, CDCl_3) of compound 112e	399
Figure A6.14	Infrared spectrum (thin film/ NaCl) of compound 112e	400
Figure A6.15	^{13}C NMR (125 MHz, CDCl_3) of compound 112e	400
Figure A6.16	^1H NMR (500 MHz, CDCl_3) of compound 112f	401
Figure A6.17	Infrared spectrum (thin film/ NaCl) of compound 112f	402
Figure A6.18	^{13}C NMR (125 MHz, CDCl_3) of compound 112f	402
Figure A6.19	^1H NMR (500 MHz, CDCl_3) of compound 112g	403
Figure A6.20	Infrared spectrum (thin film/ NaCl) of compound 112g	404
Figure A6.21	^{13}C NMR (125 MHz, CDCl_3) of compound 112g	404
Figure A6.22	^1H NMR (500 MHz, CDCl_3) of compound 112h	405
Figure A6.23	Infrared spectrum (thin film/ NaCl) of compound 112h	406
Figure A6.24	^{13}C NMR (125 MHz, CDCl_3) of compound 112h	406
Figure A6.25	^1H NMR (500 MHz, CDCl_3) of compound 113h	407
Figure A6.26	Infrared spectrum (thin film/ NaCl) of compound 113h	408
Figure A6.27	^{13}C NMR (125 MHz, CDCl_3) of compound 113h	408
Figure A6.28	^1H NMR (500 MHz, CDCl_3) of compound 112i	409
Figure A6.29	Infrared spectrum (thin film/ NaCl) of compound 112i	410
Figure A6.30	^{13}C NMR (125 MHz, CDCl_3) of compound 112i	410
Figure A6.31	^1H NMR (500 MHz, CDCl_3) of compound 112j	411
Figure A6.32	Infrared spectrum (thin film/ NaCl) of compound 112j	412
Figure A6.33	^{13}C NMR (125 MHz, CDCl_3) of compound 112j	412
Figure A6.34	^1H NMR (500 MHz, CDCl_3) of compound 112k	413
Figure A6.35	Infrared spectrum (thin film/ NaCl) of compound 112k	414
Figure A6.36	^{13}C NMR (125 MHz, CDCl_3) of compound 112k	414
Figure A6.37	^1H NMR (500 MHz, CDCl_3) of compound 112l	415
Figure A6.38	Infrared spectrum (thin film/ NaCl) of compound 112l	416
Figure A6.39	^{13}C NMR (125 MHz, CDCl_3) of compound 112l	416
Figure A6.40	^1H NMR (500 MHz, CDCl_3) of compound 112m	417
Figure A6.41	Infrared spectrum (thin film/ NaCl) of compound 112m	418
Figure A6.42	^{13}C NMR (125 MHz, CDCl_3) of compound 112m	418
Figure A6.43	^1H NMR (500 MHz, CDCl_3) of compound 112n	419
Figure A6.44	Infrared spectrum (thin film/ NaCl) of compound 112n	420

Figure A6.45	^{13}C NMR (125 MHz, CDCl_3) of compound 112n	420
Figure A6.46	^1H NMR (500 MHz, CDCl_3) of compound 112o	421
Figure A6.47	Infrared spectrum (thin film/ NaCl) of compound 112o	422
Figure A6.48	^{13}C NMR (125 MHz, CDCl_3) of compound 112o	422
Figure A6.49	^1H NMR (500 MHz, CDCl_3) of compound 112p	423
Figure A6.50	Infrared spectrum (thin film/ NaCl) of compound 112p	424
Figure A6.51	^{13}C NMR (125 MHz, CDCl_3) of compound 112p	424
Figure A6.52	^1H NMR (500 MHz, CDCl_3) of compound 112q	425
Figure A6.53	Infrared spectrum (thin film/ NaCl) of compound 112q	426
Figure A6.54	^{13}C NMR (125 MHz, CDCl_3) of compound 112q	426
Figure A6.55	^1H NOESY (600 MHz, CDCl_3) of compound 113q	427
Figure A6.56	Infrared spectrum (thin film/ NaCl) of compound 113q	428
Figure A6.57	^{13}C NMR (125 MHz, CDCl_3) of compound 113q	428
Figure A6.58	^1H NMR (500 MHz, CDCl_3) of compound 112r	429
Figure A6.59	Infrared spectrum (thin film/ NaCl) of compound 112r	430
Figure A6.60	^{13}C NMR (125 MHz, CDCl_3) of compound 112r	430
Figure A6.61	^1H NMR (500 MHz, CDCl_3) of compound 112s	431
Figure A6.61	Infrared spectrum (thin film/ NaCl) of compound 112s	432
Figure A6.63	^{13}C NMR (125 MHz, CDCl_3) of compound 112s	432
Figure A6.64	^1H NMR (500 MHz, CDCl_3) of compound 112t	433
Figure A6.65	Infrared spectrum (thin film/ NaCl) of compound 112t	434
Figure A6.66	^{13}C NMR (125 MHz, CDCl_3) of compound 112t	434
Figure A6.67	^1H NMR (500 MHz, CDCl_3) of compound 112t'	435
Figure A6.68	Infrared spectrum (thin film/ NaCl) of compound 112t'	436
Figure A6.69	^{13}C NMR (125 MHz, CDCl_3) of compound 112t'	436
Figure A6.70	^1H NMR (500 MHz, CDCl_3) of compound 112u	437
Figure A6.71	Infrared spectrum (thin film/ NaCl) of compound 112u	438
Figure A6.72	^{13}C NMR (125 MHz, CDCl_3) of compound 112u	438
Figure A6.73	^1H NMR (500 MHz, CDCl_3) of compound 112v	439
Figure A6.74	Infrared spectrum (thin film/ NaCl) of compound 112v	440
Figure A6.75	^{13}C NMR (125 MHz, CDCl_3) of compound 112v	440
Figure A6.76	^1H NMR (500 MHz, CDCl_3) of compound 112w	441
Figure A6.77	Infrared spectrum (thin film/ NaCl) of compound 112w	442
Figure A6.78	^{13}C NMR (125 MHz, CDCl_3) of compound 112w	442
Figure A6.79	^1H NMR (500 MHz, CDCl_3) of compound 112x	443

Figure A6.80	Infrared spectrum (thin film/NaCl) of compound 112x	444
Figure A6.81	¹³ C NMR (125 MHz, CDCl ₃) of compound 112x	444
Figure A6.82	¹ H NMR (500 MHz, CDCl ₃) of compound 112y	445
Figure A6.83	Infrared spectrum (thin film/NaCl) of compound 112y	446
Figure A6.84	¹³ C NMR (125 MHz, CDCl ₃) of compound 112y	446
Figure A6.85	¹ H NMR (500 MHz, CDCl ₃) of compound 112y'	447
Figure A6.86	Infrared spectrum (thin film/NaCl) of compound 112y'	448
Figure A6.87	¹³ C NMR (125 MHz, CDCl ₃) of compound 112y'	448
Figure A6.88	¹ H NMR (500 MHz, CDCl ₃) of compound 112z	449
Figure A6.89	Infrared spectrum (thin film/NaCl) of compound 112z	450
Figure A6.90	¹³ C NMR (125 MHz, CDCl ₃) of compound 112z	450
Figure A6.91	¹ H NMR (500 MHz, CDCl ₃) of compound 113z	451
Figure A6.92	Infrared spectrum (thin film/NaCl) of compound 113z	452
Figure A6.93	¹³ C NMR (125 MHz, CDCl ₃) of compound 113z	452
Figure A6.94	¹ H NMR (500 MHz, CDCl ₃) of compound 114	453
Figure A6.95	Infrared spectrum (thin film/NaCl) of compound 114	454
Figure A6.96	¹³ C NMR (125 MHz, CDCl ₃) of compound 114	454
Figure A6.97	¹ H NMR (500 MHz, CDCl ₃) of compound 116	455
Figure A6.98	Infrared spectrum (thin film/NaCl) of compound 116	456
Figure A6.99	¹³ C NMR (125 MHz, CDCl ₃) of compound 116	456
Figure A6.100	HSQC NMR (500 MHz, CDCl ₃) of compound 116	457
Figure A6.101	GCOSY NMR (500 MHz, CDCl ₃) of compound 116	458
Figure A6.102	¹ H NOESY NMR (500 MHz, CDCl ₃) of compound 116	459
Figure A6.103	¹ H NMR (500 MHz, CDCl ₃) of compound 115	460
Figure A6.104	Infrared spectrum (thin film/NaCl) of compound 115	461
Figure A6.105	¹³ C NMR (125 MHz, CDCl ₃) of compound 115	461
Figure A6.106	¹ H NMR (500 MHz, CDCl ₃) of compound 117a	462
Figure A6.107	Infrared spectrum (thin film/NaCl) of compound 117a	463
Figure A6.108	¹³ C NMR (125 MHz, CDCl ₃) of compound 117a	463
Figure A6.109	¹ H NMR (500 MHz, CDCl ₃) of compound 117b	464
Figure A6.110	Infrared spectrum (thin film/NaCl) of compound 117b	465
Figure A6.111	¹³ C NMR (125 MHz, CDCl ₃) of compound 117b	465

ADDENDIX 7

Figure A7.1.1. ORTEP drawing of 117	467
--	-----

APPENDIX 8

Figure A8.1.1.1 Natural products containing benzylic quaternary stereocenters	480
Figure A8.2.2.1 Proposed catalytic cycle for the α -arylation of cyclic ketones using in situ generated enolates	488
Figure A8.2.2.2 Proposed catalytic cycle for the α -arylation of cyclic ketones using in situ generated enolates	489
Figure A8.3.1.1 Summarized results of screen 1 at 60 °C	491
Figure A8.3.2.1 Summarized results of screen 2 at 60 °C	493
Figure A8.4.1 Elaborated ligand search	495
Figure A8.4.2 Optimization of fluoride donor, reaction time and temperature	496
Figure A8.4.3 Further optimization of ligand, solvent and temperature	497
Figure A8.4.4 Further optimization of ligand, solvent and temperature	498
Figure A8.4.5 Importance of metal source to ligand ratio	499

APPENDIX 9

Figure A9.1.1.1 The structures of (+)-lingzhiol and (-)-lingzhiol	512
Figure A9.4.1.1 A hypothesis regarding the electronics of exocyclic olefin 182	520

APPENDIX 10

Figure A10.1 ¹ H NMR (500 MHz, CDCl ₃) of compound 181	545
Figure A10.2 ¹³ C NMR (125 MHz, CDCl ₃) of compound 181	546
Figure A10.3 ¹ H NMR (300 MHz, CDCl ₃) of compound 174	547
Figure A10.4 ¹ H NMR (300 MHz, CDCl ₃) of compound 173	548
Figure A10.5 ¹ H NMR (500 MHz, CDCl ₃) of compound 172	549
Figure A10.6 ¹³ C NMR (125 MHz, CDCl ₃) of compound 172	550
Figure A10.7 ¹ H NMR (500 MHz, CDCl ₃) of compound 183	551
Figure A10.8 ¹³ C NMR (125 MHz, CDCl ₃) of compound 183	552
Figure A10.9 ¹ H NMR (300 MHz, CDCl ₃) of compound 187	553

Figure A10.10	¹ H NMR (300 MHz, CDCl ₃) of compound 188'	554
Figure A10.11	¹ H NMR (300 MHz, CDCl ₃) of compound 189	555
Figure A10.12	¹ H NMR (500 MHz, CDCl ₃) of compound 190	556
Figure A10.13	¹ H NMR (500 MHz, CDCl ₃) of compound 191	557
Figure A10.14	¹³ C NMR (125 MHz, CDCl ₃) of compound 191	558
Figure A10.15	¹ H NMR (500 MHz, CDCl ₃) of compound 192	559
Figure A10.16	¹ H NMR (500 MHz, CDCl ₃) of compound 193	560
Figure A10.17	¹³ C NMR (125 MHz, CDCl ₃) of compound 193	561
Figure A10.18	¹ H NMR (500 MHz, CDCl ₃) of compound 194	562
Figure A10.19	¹³ C NMR (125 MHz, CDCl ₃) of compound 194	563
Figure A10.20	¹ H NMR (500 MHz, CDCl ₃) of compound 195	564
Figure A10.21	¹³ C NMR (125 MHz, CDCl ₃) of compound 195	565
Figure A10.22	¹ H NMR (300 MHz, CDCl ₃) of compound 196	566

LIST OF SCHEMES

CHAPTER 1

Scheme 1.1.1.1	Palladium catalyzed allylic alkylation pioneered by Tsuji and coworkers	2
Scheme 1.1.1.2	State of the art in asymmetric alkylation of prochiral enolates, 2003	3
Scheme 1.1.1.3	Stoltz and coworkers approach to asymmetric allylic alkylation	4
Scheme 1.1.1.4	Asymmetric allylic alkylation by Trost (A) and Jacobsen (B)	5
Scheme 1.1.2.1	Selected modern methods for the synthesis of cycbutanoids according to (A) Baudoin, (B) Toste, and (C) Echavarren	7

CHAPTER 2

Scheme 2.2.1.1	TMSE β-ketoester substrate synthesis.....	142
Scheme 2.2.1.2	Fluoride-triggered deprotection of TMSE β-ketoester substrate	142

CHAPTER 4

Scheme 4.4.1	Rapid generation of molecular and stereochemical complexity employing allylic alkylation products.....	340
--------------	--	-----

APPENDIX 8

Scheme A8.1.1.1	Initial Reports of Direct α -Arylation of Ketones by Buchwald (A) and Hartwig (B).....	481
Scheme A8.1.1.2	Improved Catalyst Systems for α -Arylation by Hartwig (A) and Buchwald (B)	482
Scheme A8.1.2.1	Current State of the Art in Catalytic Asymmetric α -Arylation to Form α -Quaternary Ketones.....	484
Scheme A8.2.1.1	Proposed catalytic cycle of asymmetric allylic alkylation.....	486
Scheme A8.2.1.2	A. Asymmetric protonation of allyl β -ketoesters; B. Stereoselective conjugate addition–allylation cascade reaction.....	487
Scheme A8.3.1.1	Initial screens for α -arylation reactivity.....	490
Scheme A8.3.2.1	Revised screens for α -arylation reactivity.....	492
Scheme A8.5.2.1	Conceptual schemes for deacylative enolate formation: A. previous research by Tunge and coworkers; B. proposed allylic alkylation via deacylative pathway; C. proposed α -arylation via deacylative pathway.....	501

APPENDIX 9

Scheme A9.2.1	First-generation retrosynthetic analysis for (+)-lingzhiol.....	514
Scheme A9.3.1.1	First-generation retrosynthetic analysis for (+)-lingzhiol model system.....	515
Scheme A9.3.2.1	A. Foreseeable difficulties in advancing methyl Grignard addition to ketone 176 ; B. Synthesis of olefin 181	516
Scheme A9.3.2.2	Optimization studies for the tandem hydroboration/oxidation elimination of 181	517
Scheme A9.3.2.3	Synthesis of oxime 172 and attempts at (3+2) cycloaddition.....	518

Scheme A9.3.2.4. The intramolecular (3+2) cycloaddition of nitron 182 to form tetracycle 183	519
Scheme A9.4.2.1 Synthesis of revised model for (3+2) cycloaddition studies.....	521
Scheme A9.4.2.2 Synthesis of revised model for (3+2) cycloaddition studies.....	522
Scheme A9.4.2.3 Studies toward the dehydration of tertiary alcohol 196	523
Scheme A9.5.1 Second-generation retrosynthetic analysis toward the synthesis of (+)-lingzhiol.....	524
Scheme A9.5.2 Second-generation retrosynthetic analysis toward the synthesis of (+)-lingzhiol.....	525

LIST OF TABLES

CHAPTER 1

Table 1.2.2.1 Initial optimization of the palladium catalyzed allylic alkylation reaction.....	10
Table 1.6.8.1 Determination of enantiomeric excess.....	149

CHAPTER 2

Table 2.2.2.1 TMSE β -ketoester allylic alkylation initial optimization experiments	144
Table 2.2.2.2 TMSE β -ketoester allylic alkylation solvent effects on reaction yield	145
Table 2.2.2.3 TMSE β -ketoester allylic alkylation solvent effects on reaction selectivity.....	146
Table 2.6.8.1 Optimization of reaction parameters.....	169
Table 2.6.11.1 Determination of enantiomeric excess and optical rotations	179

CHAPTER 3

Table 3.2.1.1 Optimization of reaction parameters.....	230
Table 3.6.2.1 Optimization of reaction parameters.....	239
Table 3.6.8.1 Determination of enantiomeric excess.....	263

APPENDIX 4

Table A4.1	Crystal Data and Structure Analysis Details for allylation ketoester 100f	320
Table A4.2	Atomic coordinates ($\times 10^4$) and equivalent isotropic displacement parameters ($\text{\AA}^2 \times 10^3$) for 100f . $U(\text{eq})$ is defined as one third of the trace of the orthogonalized U^{ij} tensor	322
Table A4.3	Bond lengths [\AA] and angles [$^\circ$] for 100f	323
Table A4.4	Anisotropic displacement parameters ($\text{\AA}^2 \times 10^4$) for 100f . The anisotropic displacement factor exponent takes the form: $-2\pi^2 [h^2 a^*2U_{11} + \dots + 2 h k a^* b^* U_{12}]$	327
Table A4.5	Hydrogen coordinates ($\times 10^3$) and isotropic displacement parameters ($\text{\AA}^2 \times 10^3$) for 100f	328
Table A4.6	Hydrogen bonds for 100f [\AA and $^\circ$].....	328

CHAPTER 4

Table 4.2.1	Optimization of the Ir-catalyzed asymmetric allylic alkylation.....	334
Table 4.3.1.1	Exploration of the reaction scope with respect to allyl electrophile.....	336
Table 4.3.3.1	Exploration of the reaction scope with respect to β -ketoester nucleophile....	339
Table 4.6.2.1	Optimization of reaction parameters.....	343
Table 4.6.7.1	Determination of enantiomeric excess.....	378

APPENDIX 7

Table A7.1	Crystal Data and Structure Analysis Details for diol 117	464
Table A7.2	Atomic coordinates ($\times 10^4$) and equivalent isotropic displacement parameters ($\text{\AA}^2 \times 10^3$) for 117 . $U(\text{eq})$ is defined as one third of the trace of the orthogonalized U^{ij} tensor	469
Table A7.3	Bond lengths [\AA] and angles [$^\circ$] for 117	470
Table A7.4	Anisotropic displacement parameters ($\text{\AA}^2 \times 10^4$) for 117 . The anisotropic displacement factor exponent takes the form: $-2\pi^2 [h^2 a^*2U_{11} + \dots + 2 h k a^* b^* U_{12}]$	474
Table A7.5	Hydrogen coordinates ($\times 10^3$) and isotropic displacement parameters ($\text{\AA}^2 \times 10^3$)	

	103) for 117	475
Table A7.6	Hydrogen bonds for 117 [Å and °].....	476
Table A7.7	Torsion angles [°] for 117 [Å and °].	478

LIST OF ABBREVIATIONS

$[\alpha]_D$	angle of optical rotation of plane-polarized light
Å	angstrom(s)
<i>p</i> -ABSA	<i>para</i> -acetamidobenzenesulfonyl azide
Ac	acetyl
AIBN	azobisisobutyronitrile
APCI	atmospheric pressure chemical ionization
app	apparent
aq	aqueous
Ar	aryl group
At	benztriazolyl
atm	atmosphere(s)
BINAP	2,2'-bis(diphenylphosphino)-1,1'-binaphthyl
Bn	benzyl
Boc	<i>tert</i> -butoxycarbonyl
bp	boiling point
br	broad
Bu	butyl
<i>n</i> -Bu	butyl or <i>norm</i> -butyl
<i>t</i> -Bu	<i>tert</i> -butyl
Bz	benzoyl
<i>c</i>	concentration of sample for measurement of optical rotation

^{13}C	carbon-13 isotope
/C	supported on activated carbon charcoal
$^{\circ}\text{C}$	degrees Celcius
ca.	approximately (Latin: <i>circum</i>)
calc'd	calculated
Cbz	benzyloxycarbonyl
CCDC	Cambridge Crystallographic Data Centre
CDI	1,1'-carbonyldiimidazole
cf.	consult or compare to (Latin: <i>confer</i>)
cm^{-1}	wavenumber(s)
cod	1,5-cyclooctadiene
comp	complex
conc.	concentrated
Cy	cyclohexyl
CSA	camphor sulfonic acid
d	doublet
<i>d</i>	dextrorotatory
DABCO	1,4-diazabicyclo[2.2.2]octane
dba	dibenzylideneacetone
DBU	1,8-diazabicyclo[5.4.0]undec-7-ene
DCE	1,2-dichloroethane
<i>de</i>	diastereomeric excess
DIAD	diisopropyl azodicarboxylate

DIBAL	diisobutyl aluminum hydride
DMAP	4-dimethylaminopyridine
DME	1,2-dimethoxyethane
DMF	<i>N,N</i> -dimethylformamide
DMSO	dimethylsulfoxide
dppb	1,3-bis(diphenylphosphino)butane
dppf	1,3-bis(diphenylphosphino)ferrocene
dppe	1,3-bis(diphenylphosphino)ethane
dppp	1,3-bis(diphenylphosphino)propane
dr	diastereomeric ratio
<i>ee</i>	enantiomeric excess
E	methyl carboxylate (CO ₂ CH ₃)
E ⁺	electrophile
<i>E</i>	trans (entgegen) olefin geometry
e.g.	for example (Latin: <i>exempli gratia</i>)
EI	electron impact
eq	equation
ESI	electrospray ionization
Et	ethyl
<i>et al.</i>	and others (Latin: <i>et alii</i>)
EtOAc	ethyl acetate
FAB	fast atom bombardment
g	gram(s)

h	hour(s)
^1H	proton
$h\nu$	light
HPLC	high performance liquid chromatography
HRMS	high resolution mass spectrometry
Hz	hertz
IBX	2-iodoxybenzoic acid
IC_{50}	half maximal inhibitory concentration (50%)
i.e.	that is (Latin: <i>id est</i>)
iNOS	human-inducible nitric oxide synthase
IR	infrared spectroscopy
J	coupling constant
k	rate constant
kcal	kilocalorie(s)
kg	kilogram(s)
KHMDS	potassium bis(trimethylsilyl)amide
L	liter or neutral ligand
l	levorotatory
LDA	lithium diisopropylamide
LHMDS	lithium bis(trimethylsilyl)amide
LTMP	lithium 2,2,6,6-tetramethylpiperidide
m	multiplet or meter(s)
M	molar or molecular ion

<i>m</i>	meta
μ	micro
<i>m</i> -CPBA	<i>meta</i> -chloroperbenzoic acid
Me	methyl
mg	milligram(s)
MHz	megahertz
min	minute(s)
mL	milliliter(s)
MM	mixed method
mol	mole(s)
MOM	methoxymethyl
mp	melting point
Ms	methanesulfonyl (mesyl)
MS	molecular sieves
<i>m/z</i>	mass-to-charge ratio
N	normal or molar
NBS	<i>N</i> -bromosuccinimide
nm	nanometer(s)
NMR	nuclear magnetic resonance
NOE	nuclear Overhauser effect
NOESY	nuclear Overhauser enhancement spectroscopy
Nu ⁻	nucleophile
<i>o</i>	ortho

[O]	oxidation
OAc	Acetate
<i>p</i>	para
Ph	phenyl
pH	hydrogen ion concentration in aqueous solution
pK_a	acid dissociation constant
PMB	<i>para</i> -methoxybenzyl
ppm	parts per million
Pr	propyl
<i>i</i> -Pr	isopropyl
py	pyridine
q	quartet
R	alkyl group
<i>R</i>	rectus
RCM	ring-closing metathesis
ref	reference
R_f	retention factor
RNA	ribonucleic acid
s	singlet or seconds
<i>S</i>	sinister
sat.	saturated
Selectfluor	1-Chloromethyl-4-fluoro-1,4-diazoniabicyclo[2.2.2]octane bis(tetrafluoroborate)

SFC	supercritical fluid chromatography
t	triplet
TBAF	tetra- <i>n</i> -butylammonium fluoride
TBAT	tetra- <i>n</i> -butylammonium difluorotriphenylsilicate
TBD	1,5,7-triazabicyclo[4.4.0]dec-5-ene
TBHP	<i>tert</i> -butyl hydroperoxide
TBS	<i>tert</i> -butyldimethylsilyl
temp	temperature
Tf	trifluoromethanesulfonyl
t _R	retention time
THF	tetrahydrofuran
TLC	thin layer chromatography
TMP	2,2,6,6-tetramethylpiperidine
TMS	trimethylsilyl
TMSE	2(trimethylsilyl)ethyl
TOF	time-of-flight
tol	tolyl
Ts	<i>para</i> -toluenesulfonyl (tosyl)
UV	ultraviolet
w/v	weight per volume
v/v	volume per volume
X	anionic ligand or halide
Z	cis (zusammen) olefin geometry

CHAPTER 1

Enantioselective Construction of α -Quaternary Cyclobutanones by Catalytic Asymmetric Allylic Alkylation¹

1.1 INTRODUCTION

1.1.1 Palladium catalyzed allylic alkylation

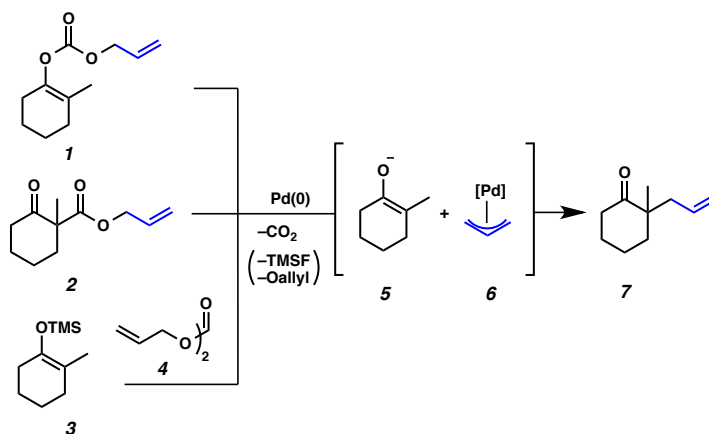
The synthesis of stereogenic all-carbon quaternary centers remains a formidable challenge, notwithstanding the strides made by modern organic chemistry in this regard.¹ Contemporary advances in enolate alkylation have made it a fundamental strategy for the construction of C–C bonds.² Allylic alkylation of tetrasubstituted enolates to give rise to α -quaternary carbonyl compounds has emerged as an efficient solution to this problem.³ The Tsuji research group was among the first to study this class of transformations and pioneering investigations undertaken nearly three decades ago by, which culminated in a series of disclosures describing novel decarboxylative entry into the palladium-catalyzed allylic alkylation of cyclic ketones (Scheme 1.1.1.1).⁴

A simple mechanistic framework for the transformation begins with the oxidative addition of Pd⁰ into the allyl group of an allyl enol carbonate (**1**), allyl β -ketoesters (**2**) or

¹ This work was performed in collaboration with Christian Eidamshaus and Jimin Kim, postdoctoral researchers in the Stoltz group. This work has been published. See: Reeves, C. M, Eidamshaus, C.; Kim, J.; Stoltz, B. M. *Angew. Chem. Int. Ed.* **2013**, 52, 6718.

silyl enol ethers (**3**) in the presence of an allyl source (**4**), and gives a palladium π -allyl species (**6**), and the corresponding free carboxylate species. Spontaneous decarboxylation of the free carboxylate yields a tetrasubstituted enolate (**5**) that may enter into a catalytic cycle and furnish α -quaternary ketones (**7**). This method of enolate formation is particularly attractive in that the so-called “thermodynamic” enolate can be selectively generated *in situ*, in the absence of exogenous base under kinetic control. Furthermore, excellent positional fidelity is observed between the site of enolization and the site of allylic alkylation.

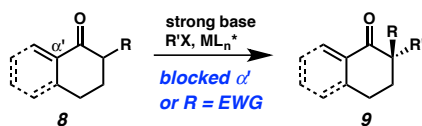
Scheme 1.1.1.1 Palladium catalyzed allylic alkylation pioneered by Tsuji and coworkers



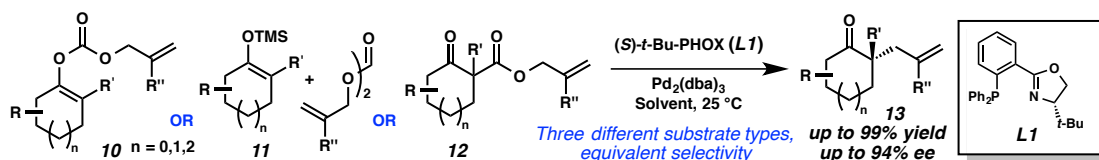
Although methods for the alkylation of a number of enolate types (e.g., ester, ketone, amide, etc.) with a variety of alkylating agents exist, catalytic enantioselective variants of these transformations are relatively rare.⁵ Of the catalytic asymmetric methods available, there have been few examples of general techniques for the asymmetric alkylation of carbocyclic systems, and still fewer that have the capacity to

deliver all-carbon quaternary stereocenters.⁶ While the Merck phase transfer methylation, and Koga alkylation of 2-alkyltetralone-derived silyl enol ethers represent notable exceptions,⁴ the breadth of application and utility of these reactions has been limited. In fact, at the outset of investigations by the Stoltz group in this area, there were no examples of catalytic enantioselective alkylations of monocyclic 2-substituted cycloalkanone enolates in the absence of either α' -blocking groups or α -enolate stabilizing groups (e.g., **8**, R = aryl, ester, etc., Figure 1.1.1.2).

Scheme 1.1.1.2. State of the art in asymmetric alkylation of prochiral enolates, 2003.

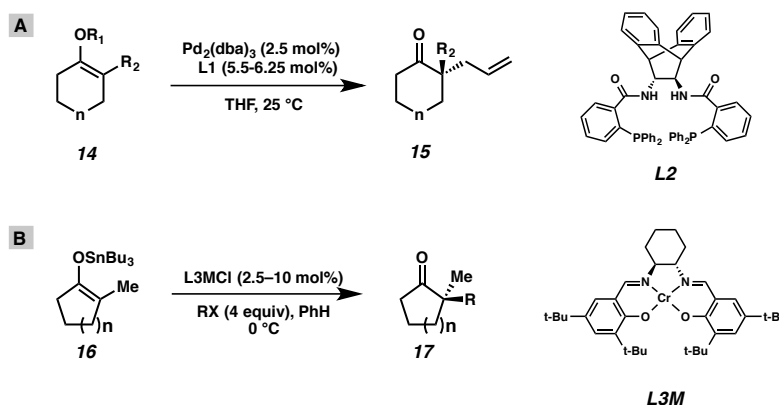


In 2003, we initiated a program for the catalytic enantioselective synthesis of all-carbon quaternary stereocenters by allylic alkylation of prochiral cyclic ketone enolates. We adapted a protocol originally developed by Tsuji⁷ to incorporate a chiral ligand scaffold, and found that the phosphinooxazoline (PHOX) ligands (e.g., **L1**, Scheme 1.1.1.3)⁸ were optimal for both chemical yields and enantioselectivity.⁹ The allylic alkylation protocol developed in the Stoltz laboratory is robust enough to prevail upon several different enolate precursor classes, namely allyl enol carbonates (**10**), enol silanes (**11**), and β -ketoesters (**12**) to deliver the desired α -quaternary cyclic ketone products (**13**) in good to excellent yields and enantioselectivities.^{9,10}

Scheme 1.1.1.3. Stoltz and coworkers' approach to asymmetric allylic alkylation

In addition, the reaction is highly tolerant of a broad range of functionality and substitution on both the enolate precursors and allyl fragments. Enolates derived from cyclic ketones,⁹ enones,¹⁰ vinylogous esters,¹¹ vinylogous thioesters,¹² tetralones,¹⁰ and dioxanones¹³ function with similar levels of selectivity in the catalytic asymmetric chemistry. We have also developed a scale-up protocol employing 2.5 mol % Pd that allows access to >10 g of enantioenriched material in excellent yields.¹⁴

Concurrent to our work in this area,^{10,15} Trost and coworkers have published a series of papers that complement our studies in asymmetric alkylation, and which employ symmetric bidentate C-2 symmetric bisphosphine ligands (**L2**, Scheme 1.1.1.4a).¹⁶ Shortly after this report, Jacobsen and coworkers, as well, have revealed a unique enantioselective method involving the chromium-catalyzed reaction of tin-enolates (**16**) with a variety of non-activated alkyl halides (Scheme 1.1.1.4b).⁶

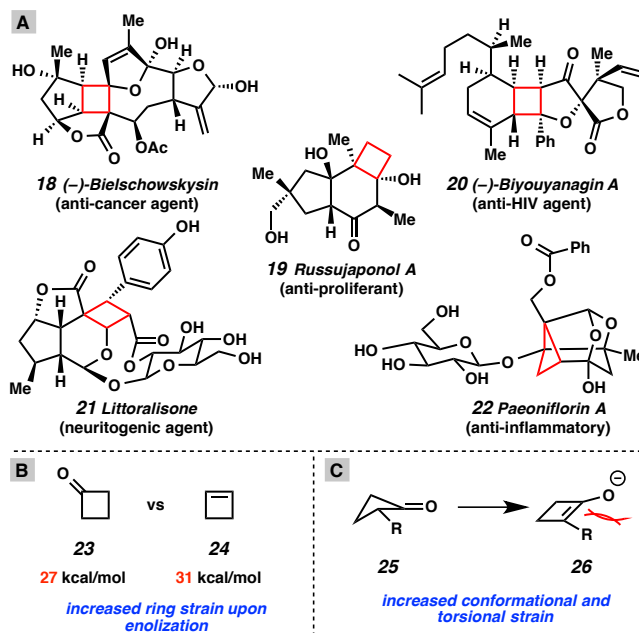
Scheme 1.1.1.4. Asymmetric allylic alkylation by Trost (A) and Jacobsen (B)

1.1.2 Palladium-catalyzed allylic alkylation of cyclobutanones

In the domain of asymmetric allylic alkylation, cyclobutanones have received far less attention relative to their five-, six- and seven-membered congeners, despite the fact that these compounds and their derivatives are prevalent in important biologically-active natural products¹⁷ (**18–22**, Figure 1.1.2.1A). Additionally, cyclobutanones have been shown to serve as highly valuable synthetic intermediates for a variety of transformations.¹⁸ The dearth of reports describing the asymmetric alkylation of cyclobutanones may be attributed to the fact that these compounds possess an estimated 26–28.6 kcal/mol of ring-strain¹⁹ and, in turn, exhibit enhanced carbonyl electrophilicity.²⁰ The propensity of cyclobutanones to alleviate this strain via electrophilic ring opening is often a limiting challenge during their manipulation. Moreover, the energetic requirements for enolization of cyclobutanones (**23**) are compounded by a concomitant increase in ring-strain to 31–34 kcal/mol (calculated for cyclobutene **24**, Figure 1.1.2.1B)¹⁸ as well as enforced deviation from the more favorable puckered conformation (**25**→**26**, Figure 1.1.2.1C).²¹ In the case of α -substituted cyclobutanones, enolization is further impeded

by the development of torsional strain between the putative enolate substituents (**26**, Figure 1.1.2.1C).²²

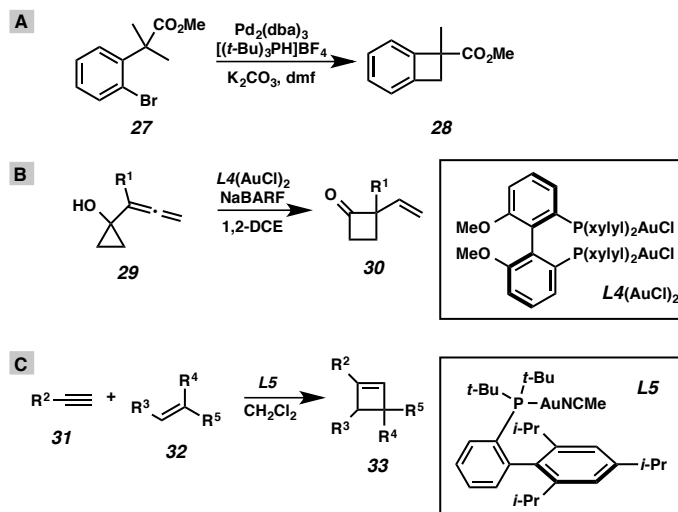
Figure 1.1.2.1. (A) Representative cycbutanoid natural products; (B) ring, conformational and torsional strain in cyclobutanone enolates



Given these data, it is not surprising that previous methods for the preparation of enantioenriched cyclobutanes have relied primarily on either [2+2] cycloaddition reactions²³ or ring expansion from various cyclopropane derivatives.²⁴ Recent reports from Baudoin on annulating C–H activation²⁵ (Scheme 1.1.2.1A) as well as disclosures from Toste²⁶ (Scheme 1.1.2.1B) and Echavarren²⁷ (Scheme 1.1.2.1C) that employ gold(I) catalysis to affect cyclopropanoid rearrangements have emerged as significant new methods for the construction of cyclobutanes, and show the power of transition metals in this regard. Organocatalytic approaches to cyclobutanone synthesis have also gained

traction recently.²⁸ Despite these advances, transformations that produce chiral cyclobutanones remain limited in scope, and very few methods exist for the catalytic construction of chiral cyclobutanones from achiral starting materials.^{9b,29} In order to address these limitations and to further develop the nucleophilic chemistry of these unusually reactive compounds, we report herein the first direct transition metal-catalyzed asymmetric α -alkylation of cyclobutanones to form all-carbon quaternary centers.

Scheme 1.1.2.1. Selected modern methods for the synthesis of cyclobutanoids according to (A) Baudoin, (B) Toste, and (C) Echavarren



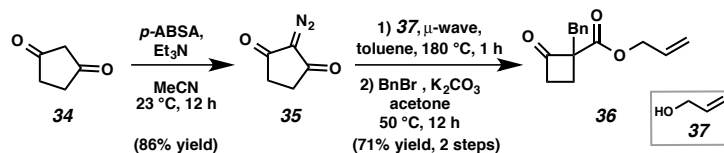
1.2 PREPARATION OF CYCLOBUTANONE β -KETOESTER SUBSTRATES AND REACTION OPTIMIZATION

1.2.1 Cyclobutanone β -ketoester substrate synthesis

A longstanding interest of our research group has been the transition metal-catalyzed asymmetric α -functionalization of carbonyl compounds to form all-carbon

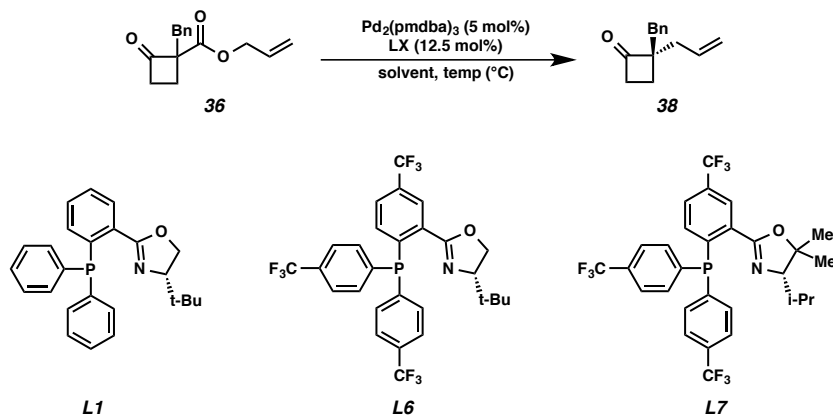
quaternary centers.³⁰ In the course of our studies, we have developed a series of phosphinooxazoline (PHOX) ligands with varied steric and electronic properties that exhibit a range of reactivity and selectivity. We have found that the use of electron deficient ligands (e.g. **L6** and **L7**) often results in superior asymmetric induction in certain cases where electron-rich or electron-neutral ligands perform poorly.³¹ Examination of ligand electronic effects would, therefore, help to inform our development of a method for the asymmetric allylic alkylation of cyclobutanones.

We first established a simple and efficient reaction sequence to access allyl 1-alkyl-2-oxocyclobutanecarboxylate substrates (**36**) (Scheme 1). Diazotization of commercially available 1,3-cyclopentane dione (**34**) with *para*-acetamidobenzenesulfonyl azide (*p*-ABSA)³² delivered the corresponding diazodiketone (**35**) in consistently good yields. Microwave-promoted Wolff rearrangement of diketone **35** in the presence of an allylic alcohol³³ (e.g., allyl alcohol, **37**), followed by alkylation with an alkyl halide (e.g., benzyl bromide) furnished the allyl 1-alkyl-2-oxocyclobutanecarboxylates in good yields over two steps. With a quick and efficient method to access the desired substrates at hand, we next examined reaction parameters to identify optimal conditions for reactivity and enantioselectivity.

Figure 1.2.1.1 Construction of allyl 1-benzyl-2-oxocyclobutane-carboxylate (**36**)

1.2.2 Optimization of cyclobutanone allylic alkylation

Our initial experiments revealed that treatment of allyl 1-benzyl-2-oxocyclobutanecarboxylate (**36**) with catalytic Pd₂(pmdba)₃ in the presence of (*S*)-*t*-BuPHOX (**L1**) in THF delivered the desired α -quaternary (*S*)-2-allyl-2-benzylcyclobutanone (**38**)³⁴ in 90% yield, albeit in moderate enantioselectivity (Figure 1.2.2.1, Table 1.2.2.1, Entry 1). The use of electron-deficient ligands **L6** or **L7** resulted in considerably improved enantioinduction (Table 1.2.2.1, Entries 2 and 5). Although the reaction proceeds well in a number of solvents, toluene was identified as optimal for inducing asymmetry. This solvent effect is likely due to an enhanced binding between the enolate and the electrophilic sigma-allyl-Pd(II) center in the catalytic cycle, which may reinforce a tight ion pair and lead to an inner-sphere mechanism.³⁵ Finally, at temperatures just below ambient, the reaction was found to proceed at a reasonable rate and with high enantioselectivity.

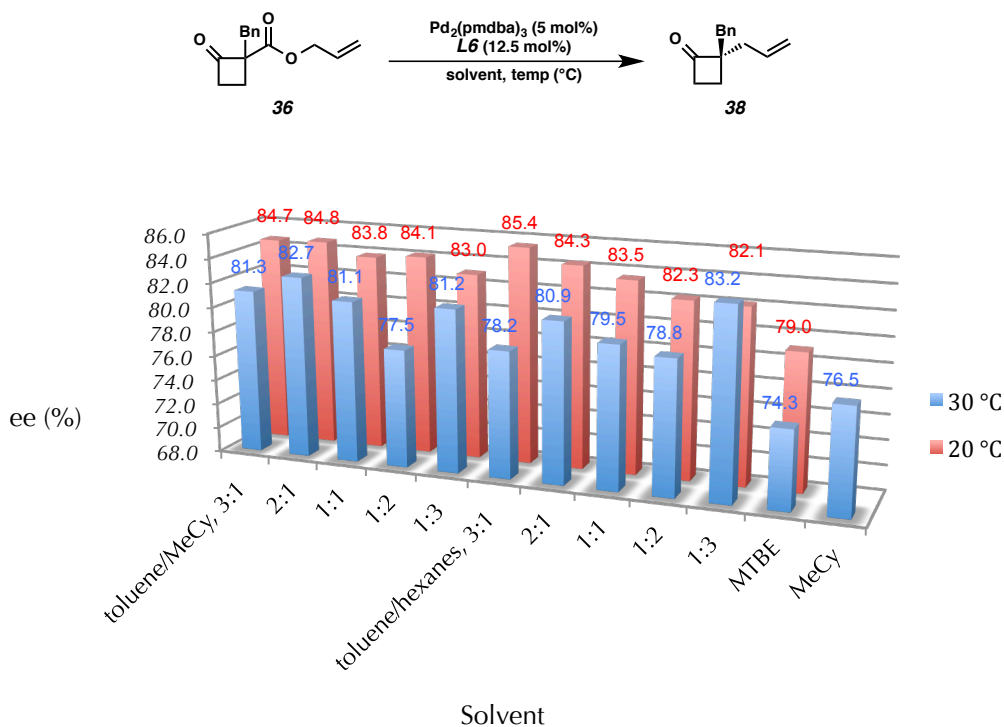
Figure 1.2.2.1. General initial reaction parameters and select ligands**Table 1.2.2.1.** Initial optimization of the palladium-catalyzed allylic alkylation reaction

Entry	Ligand	Solvent	T [$^{\circ}\text{C}$]	ee [%]
1	L1	THF	25	58
2	L6	THF	25	75
3	L6	<i>p</i> -dioxane	25	84
4	L6	benzene	25	84
5	L7	toluene	25	84
6	L6	toluene	25	85

In order to fully explore the effects of solvent on the reactions selectivity, we made use of the reaction automation system in the Caltech Center for Catalysis and Chemical Synthesis. A Symyx systems robot was employed to expedite a panel of experiments that varied solvent and temperature, while holding constant reaction variables that were found to be optimal during preliminary screening (i.e., ligand **L6** and relatively non-polar solvent).³⁶ These studies illustrated that while the reaction was most

selective when carried out in relatively non-polar solvent, a number of different non-polar solvents or solvent combinations could be employed without significant detriment to the reaction selectivity (Figure 1.2.2.2). Finally, these studies revealed that, in most cases, decreasing the temperature at which the reaction was carried out resulted in an increase in selectivity.

Figure 1.2.2.2. Solvent and temperature optimization of the palladium catalyzed allylic alkylation reaction

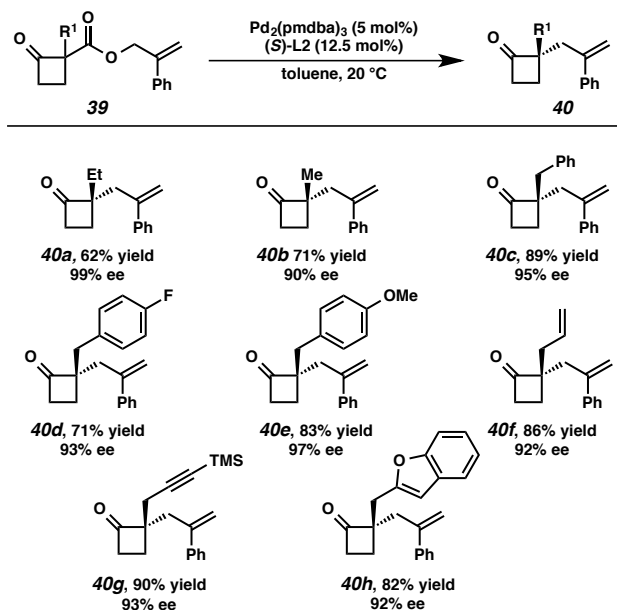


1.3 EXPLORATION OF THE REACTION SCOPE

1.3.1 Reaction scope with respect to enolate α -substitution

With these optimized conditions identified, we next explored the influence of different α -substituents (R^1 , Figure 1.3.1.1) on the efficacy of the allylic alkylation

process. To aid in the isolation of these highly volatile products, we chose coupling fragments of higher molecular weights, bearing substitution at both the α -position and allyl fragment (i.e. 2-phenylallyl and 1-alkyl-2-oxocyclobutanecarboxylate). We were pleased to find that α -alkyl substituents were well tolerated with enantiomeric excess up to 99% (Figure 1.3.1.1, **40a–40b**). α -Benzyl substituents were found to give the respective α -quaternary cyclobutanones with uniformly excellent enantioselectivity regardless of the electronic nature of the benzyl moiety (compounds **40c–40e**). In addition to alkyl- and benzyl- substituents, allyl-, TMS-protected propargyl and heteroaryl substituted 2-carboxyallyl cyclobutanones proved to be eligible substrates in the asymmetric allylic alkylation reaction providing cyclobutanones **40f–40h** in high yields and enantiomeric excess.

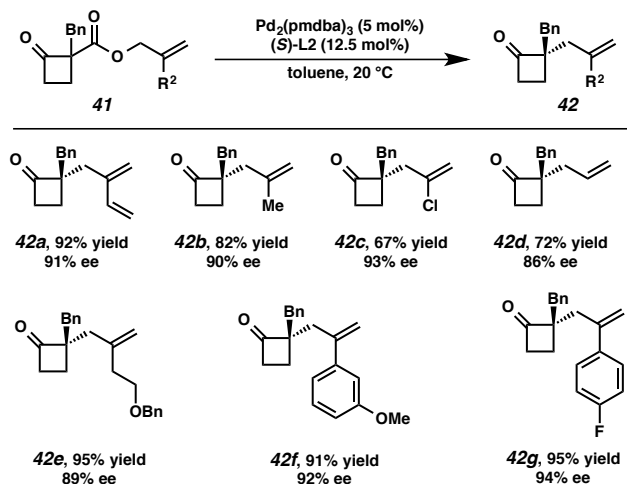
Figure 1.3.1.1. Reaction scope with respect to α -quaternary substitution (R^1)

1.3.2 Reaction scope with respect to allyl coupling partner substitution

Having surveyed the scope of the process with respect to various substituents at the quaternary center, we were poised to investigate the influence of different allyl substitution on the process (R^2 , Figure 1.3.2.1). In accord with previous studies on the palladium-catalyzed asymmetric allylic alkylation, the catalytic system was found to be relatively inactive when terminally-substituted or cyclic allyl fragments were employed.¹⁵ As such, we limited our survey to carboxyallyl fragments bearing substituents at the 2-allyl position. Gratifyingly, diverse substituents were well tolerated (Figure 1.3.2.1). All α -quaternary cyclobutanones were obtained in moderate to high yield and with outstanding enantiopurity. Particularly interesting are compounds **42a**, **42c**, and **42d** featuring a butadiene, a vinyl chloro and a benzyl ether moiety, respectively. Each of these diverse functional groups may potentially serve as handles for various

derivatization reactions (e.g., cycloaddition, annulation or transition metal-catalyzed cross-coupling).

Figure 1.3.2.1. Reaction scope with respect to allyl substitution (R^2)

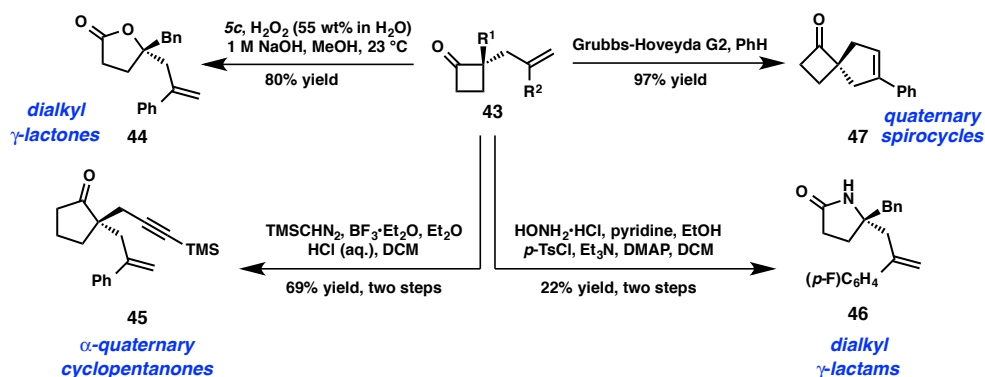


1.4 DERIVATIZATION OF REACTION PRODUCTS

Myriad studies have shown cyclobutanoids to be highly valuable synthetic intermediates, allowing access to enantioenriched oxazepines,³⁷ piperidines,³⁸ tetrahydropyrans,³⁹ α - and β -quaternary cyclopentanones,¹⁷ benzannulated polycycles⁴⁰ as well as β -quaternary linear ketones.¹⁷ Cyclobutanones may participate directly in a variety of robust classical transformations, such as Baeyer-Villiger oxidation and Beckmann rearrangement,¹⁷ as well as transition metal-catalyzed ring expansion,⁴¹ ring contraction⁴² and ring-opening processes.⁴³ To demonstrate the utility of our asymmetric synthesis of cyclobutanones within this domain, we carried out a number of transformations on the chiral cyclobutanones generated in this study. Ring expansion by

Baeyer-Villiger oxidation, treatment with trimethylsilyldiazomethane and Beckmann rearrangement all proceeded smoothly to deliver dialkyl γ -lactone **44**, α -quaternary cyclopentanone **45** and dialkyl γ -lactam **46**, respectively. Additionally, ring-closing metathesis of diallyl-substituted cyclobutanone **40f** cleanly furnished quaternary [4.5]-spirocycle **47**.

Figure 1.4.1. Derivatization of α -quaternary cyclobutanones



1.5 CONCLUDING REMARKS

In summary, we have developed the first transition metal-catalyzed enantioselective α -alkylation of cyclobutanones. This method employs palladium catalysis and an electron-deficient PHOX type ligand to afford α -quaternary cyclobutanones in good to excellent yields and enantioselectivities. A wide variety of substituents are tolerated at both the α -keto and 2-allyl positions. The mild nature of our method is reflected in its compatibility with otherwise highly electrophilic cyclobutanones. We have further demonstrated the utility of chiral cyclobutanones as synthetic building blocks to access a variety of enantioenriched derivative compounds

including dialkyl γ -lactams, dialkyl γ -lactones, α -quaternary cyclopentanones and quaternary [4.5]-spirocycles. We believe that this novel synthetic method will enable the expeditious synthesis of complex bioactive natural products and pharmaceutical components by providing unique access to previously unknown and inaccessible enantioenriched α -quaternary cyclobutanones. Efforts toward this end are currently underway in our laboratory.

1.6 EXPERIMENTAL SECTION

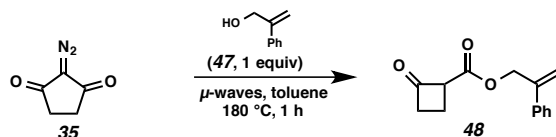
1.6.1 Materials and Methods

Unless otherwise stated, reactions were performed in flame-dried glassware under an inert atmosphere of argon or nitrogen using dry, deoxygenated solvents. Reaction progress was monitored by thin-layer chromatography (TLC). THF, Et₂O, CH₂Cl₂, toluene, benzene, CH₃CN, and dioxane were dried by passage through an activated alumina column under argon. Triethylamine was distilled over CaH₂ prior to use. Brine solutions are saturated aqueous solutions of sodium chloride. 1,3-Cyclopentanedione was purchased from AK Scientific, Inc., reagent grade acetone was purchased from Aldrich and distilled from anhydrous Ca₂SO₄ and stored over molecular sieves (3 Å) under an atmosphere of argon. *para*-Acetamidobenzenesulfonyl azide (*p*-ABSA) was prepared following a procedure by Davies *et al.*⁴⁴ 2-Phenylprop-2-en-1-ol, 2-(4-methoxyphenyl)prop-2-en-1-ol and 2-(3-fluorophenyl)prop-2-en-1-ol were prepared according to the method by Gouverneur and Brown.⁴⁵ 2-Diazocyclopentane-1,3-dione was prepared through diazotization of 1,3-cyclopentanedione with *p*-ABSA following a procedure by Coquerel and Rodriguez.⁴⁶ Phosphinooxazoline (PHOX) ligands were

prepared by methods described in our previous work.^{9, 47} Tris(4,4'-methoxydibenzylideneacetone)dipalladium(0) ($\text{Pd}_2(\text{pmdba})_3$) was prepared according to the method of Ibers⁴⁸ or Fairlamb.⁴⁹ All other reagents were purchased from Sigma-Aldrich, Acros Organics, Strem, or Alfa Aesar and used as received unless otherwise stated. Reaction temperatures were controlled by an IKA Mag temperature modulator unless otherwise indicated. Stirring was accomplished with Teflon® coated magnetic stir bars. Microwave-assisted reactions were performed in a Biotage Initiator 2.5 microwave reactor. Glove box manipulations were performed under a N_2 atmosphere. TLC was performed using E. Merck silica gel 60 F254 precoated glass plates (0.25 mm) and visualized by UV fluorescence quenching, *p*-anisaldehyde, or KMnO_4 staining. Silicycle SiliaFlash P60 Academic Silica gel (particle size 0.040-0.063 mm) was used for flash column chromatography. ^1H NMR spectra were recorded on a Varian Inova 500 MHz spectrometer and are reported relative to residual CHCl_3 (δ 7.26 ppm), C_6H_6 (δ 7.16 ppm), or CH_2Cl_2 (δ 5.32 ppm). ^{13}C NMR spectra were recorded on a Varian Inova 500 MHz (126 MHz) or Varian Mercury 300 MHz (75 MHz) spectrometer and are reported relative to CHCl_3 (δ 77.16 ppm) or C_6H_6 (δ 128.06 ppm). Data for ^1H NMR are reported as follows: chemical shift (δ ppm) (multiplicity, coupling constant (Hz), integration). Multiplicities are reported as follows: s = singlet, d = doublet, t = triplet, q = quartet, p = pentet, h = heptet, m = multiplet, br s = broad singlet, br d = broad doublet, app = apparent. Data for ^{13}C are reported in terms of chemical shifts (δ ppm). IR spectra were obtained using a Perkin Elmer Spectrum BXII spectrometer using thin films deposited on NaCl plates and reported in frequency of absorption (cm^{-1}). Optical rotations were measured with a Jasco P-2000 polarimeter operating on the sodium D-line (589 nm)

using a 100 mm path-length cell and are reported as: $[\alpha]_D^{25}$ (concentration in g/100 mL, solvent, ee). Analytical UHPLC-LCMS was performed with an Agilent 1290 Infinity Series UHPLC/Agilent 6140 Quadrupole LCMS utilizing an Agilent Eclipse Plus C18 RRHD 1.8 μm column (2.1 x 50 mm), part number 959757-902. High-resolution mass spectra (HRMS) were obtained from the Caltech Mass Spectral Facility (EI+ or FAB+) or on an Agilent 6200 Series TOF with an Agilent G1978A Multimode source in electrospray ionization (ESI), atmospheric pressure chemical ionization (APCI), or mixed (MM: ESI-APCI) ionization mode.

1.6.2 Representative procedure for the preparation of 2-oxocyclobutanecarboxylates

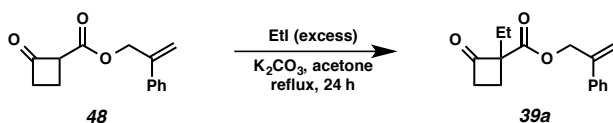


2-Phenylallyl 2-oxocyclobutanecarboxylate. To a 20 mL microwave vial charged with a magnetic stir bar were added 2-diazocyclopentane-1,3-dione (**35**, 500 mg, 4.03 mmol), toluene (13.5 mL) and 2-phenylprop-2-en-1-ol (**47**, 540 mg, 4.03 mmol). The vial was sealed with a microwave crimp cap and heated to 180 °C for one hour using a Biotage Initiator microwave reactor (sensitivity set to low; reaction mixture heated gradually over first 2 min by increasing the temperature in 20 °C increments). After 30 min of stirring, the mixture was cooled to ambient temperature and the pressure was released by puncture of the crimp cap with a needle. The reaction vessel was then subsequently irradiated at 180 °C for an additional 30 min. The vessel was then cooled to ambient temperature, the

vial uncapped and mixture directly loaded onto a silica gel column followed by elution with hexanes to 20% EtOAc in hexanes to afford of **48** (635 mg, 68% yield) as a colorless oil. $R_f = 0.2$ (20% EtOAc in hexanes); $^1\text{H NMR}$ (300 MHz, CDCl_3) δ 7.44–7.30 (m, 5H), 5.57–5.55 (m, 1H), 5.40–5.39 (m, 1H), 5.06–5.05 (m, 2H), 4.26–4.20 (m, 1H), 3.20–3.15 (m, 2H), 2.48–2.34 (m, 1H), 2.29–2.16 (m, 1H); $^{13}\text{C NMR}$ (75 MHz, CDCl_3) δ 199.5, 166.5, 142.0, 137.8, 128.5, 128.1, 126.0, 115.4, 66.5, 64.5, 47.1, 13.6; IR (Neat Film, NaCl) 3448, 3084, 3057, 3024, 2970, 1956, 1790, 1732, 1633, 1600, 1574, 1497, 1445, 1387, 1310, 1177, 1046, 915, 780 cm^{-1} ; HRMS (MM: ESI-APCI) m/z calc'd for $\text{C}_{14}\text{H}_{15}\text{O}_3$ $[\text{M}+\text{H}]^+$: 231.1016; found 231.1018.

With the exception of compound 48, all 2-carboxyallylcyclobutanone derivatives were directly used in the following steps without rigorous characterization due to their instability.

1.6.3 Representative procedure for the alkylation of 2-H-2-oxocyclobutanecarboxylates

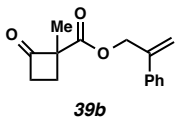


2-Phenylallyl 1-ethyl-2-oxocyclobutanecarboxylate (39a). To a solution of **48** (233 mg, 1.01 mmol) in acetone (14 mL) were added K_2CO_3 (224 mg, 1.62 mmol) and freshly distilled EtI (787 mg, 5.05 mmol). The mixture was heated to reflux until full consumption of the starting material was indicated by TLC analysis (alkylation reaction

times typically ranged from 12 to 24 hours). Upon completion, the mixture was cooled to 25 °C, the solids were removed by filtration through filter paper and the mixture was concentrated *in vacuo*. The crude material was purified by flash column chromatography (SiO₂, hexanes to 10% EtOAc in hexanes to 20% EtOAc in hexanes) to provide **39a** (105 mg, 40% yield) as a colorless oil. $R_f = 0.3$ (20% EtOAc in hexanes); ¹H NMR (300 MHz, CDCl₃) δ 7.42–7.28 (m, 5H), 5.55 (s, 1H), 5.38 (s, 1H), 5.06 (dd, $J = 9.0, 1.0$ Hz, 2H), 2.56–2.17 (m, 3H), 1.88–1.63 (m, 3H), 0.69 (t, $J = 7.5$ Hz, 3H); ¹³C NMR (75 MHz, CDCl₃) δ 209.4, 171.5, 142.2, 137.8, 128.5, 128.1, 126.1, 116.5, 66.5, 63.7, 35.5, 30.4, 27.1, 8.6; IR (Neat Film, NaCl) 3084, 2972, 2880, 1738, 1709, 1460, 1444, 1231, 1207, 1138 cm⁻¹; HRMS (EI+) m/z calc'd for C₁₆H₁₉O₃ [M+H]⁺: 259.1334; found 259.1326.

1.6.4 Spectroscopic data for novel cyclobutanone β -ketoester substrates

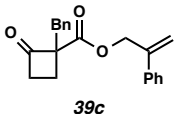
2-Phenylallyl 1-methyl-2-oxocyclobutanecarboxylate (**39b**)



Compound **39b** was isolated by flash column chromatography (SiO₂, hexanes to 10% EtOAc in hexanes) as a colorless oil. 32% yield. $R_f = 0.5$ (20% EtOAc in hexanes); ¹H NMR (500 MHz, CDCl₃) δ 7.40–7.29 (m, 5H), 5.54–5.53 (m, 1H), 5.35–5.34 (m, 1H), 5.06 (dq, $J = 11.2, 1.0$ Hz, 1H), 3.20 (ddd, $J = 18.3, 11.3, 7.6$ Hz, 1H), 3.10 (ddd, $J = 18.3, 9.9, 6.3$ Hz, 1H), 2.53 (td, $J = 11.3, 6.3$ Hz, 1H), 1.84 (ddd, $J = 11.5, 9.9, 7.6$ Hz, 1H), 1.45 (s, 3H); ¹³C NMR (126 MHz, CDCl₃) δ 204.3, 170.0, 142.3, 137.9, 128.5, 128.1, 126.0, 115.2, 69.4, 66.5, 45.3, 23.1, 18.4; IR (Neat Film, NaCl) 2970, 2930, 1788,

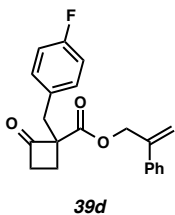
1729, 1452, 1274, 1145, 1049 cm^{-1} ; HRMS (EI+) m/z calc'd for $\text{C}_{15}\text{H}_{16}\text{O}_3$ $[\text{M}]^+$: 244.1100; found 244.1103.

2-Phenylallyl 1-benzyl-2-oxocyclobutanecarboxylate (**39c**)



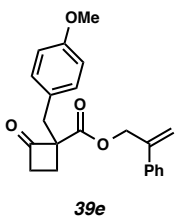
Compound **39c** was isolated by flash column chromatography (SiO_2 , hexanes to 10% EtOAc in hexanes) as a colorless oil. 37% yield. $R_f = 0.4$ (10% EtOAc in hexanes); ^1H NMR (500 MHz, CDCl_3) δ 7.33–7.14 (m, 8H), 7.04–7.02 (m, 2H), 5.47 (s, 1H), 5.28–5.27 (m, 1H), 5.01–4.95 (m, 2H), 3.12, 3.10 (AB system, $J_{\text{AB}} = 14.2$ Hz, 2H), 2.95 (ddd, $J = 18.3, 11.1, 7.3$ Hz, 1H), 2.62 (ddd, $J = 18.3, 10.3, 6.3$ Hz, 1H), 2.39 (ddd, $J = 11.9, 11.1, 6.3$ Hz, 1H), 1.93 (ddd, $J = 11.9, 10.3, 7.3$ Hz, 1H); ^{13}C NMR (126 MHz, CDCl_3) δ 203.7, 168.7, 142.1, 137.8, 135.9, 129.7, 128.51, 128.49, 128.1, 126.9, 126.0, 115.5, 75.0, 66.7, 45.2, 37.9, 19.2; IR (Neat Film, NaCl) 3029, 2924, 1788, 1725, 1496, 1270, 1191, 1046 cm^{-1} ; HRMS (MM: ESI-APCI) m/z calc'd for $\text{C}_{42}\text{H}_{40}\text{NaO}_6$ $[2\text{M}+\text{Na}]^+$: 663.2717; found 663.2692.

2-Phenylallyl 1-(4-fluorobenzyl)-2-oxocyclobutanecarboxylate (39d)



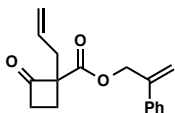
Compound **39d** was isolated by flash column chromatography (SiO₂, 3% EtOAc in hexanes to 6% EtOAc in hexanes) as a colorless oil. 22% yield. $R_f = 0.4$ (20% EtOAc in hexanes); ¹H NMR (500 MHz, CDCl₃) δ 7.40–7.29 (m, 5H), 7.08–7.04 (m, 2H), 6.95–6.91 (m, 2H), 5.54 (s, 1H), 5.34 (d, $J = 0.9$ Hz, 1H), 5.05 (s, 2H), 3.18, 3.16 (AB system, $J_{AB} = 14.3$ Hz, 2H), 3.05 (ddd, $J = 18.4, 11.2, 7.4$ Hz, 1H), 2.73 (ddd, $J = 18.4, 10.2, 6.2$ Hz, 1H), 2.46 (ddd, $J = 11.8, 11.2, 6.2$ Hz, 1H), 1.97 (ddd, $J = 11.8, 10.2, 7.4$ Hz, 1H); ¹³C NMR (126 MHz, CDCl₃) δ 203.4, 168.6, 161.9 (d, $^1J_{CF} = 245.6$ Hz), 142.1, 137.8, 131.6 (d, $^4J_{CF} = 3.7$ Hz), 131.2 (d, $^3J_{CF} = 8.0$ Hz), 128.5, 128.1, 126.0, 115.7, 115.3 (d, $^2J_{CF} = 21.2$ Hz), 75.0, 66.8, 45.2, 37.0, 19.3; IR (Neat Film, NaCl) 3052, 2968, 2928, 1784, 1717, 1506, 1219, 1186, 1042, 912 cm⁻¹; HRMS (MM: ESI-APCI) m/z calc'd for C₂₁H₂₀¹⁹FO₃ [M+H]⁺: 339.1391; found 339.1387.

2-Phenylallyl 1-(4-methoxybenzyl)-2-oxocyclobutanecarboxylate (39e)



To a solution of NaI (1.88 g, 12.54 mmol) in acetone (20 mL) was added 4-methoxybenzyl chloride (1.55 mL, 11.38 mmol). The mixture was stirred at 25 °C for 2 hours before K₂CO₃ (504 mg, 3.65 mmol) and **48** (524 mg, 2.28 mmol) were added. The resulting mixture was heated to reflux for 16 hours until full conversion of the starting material was indicated by TLC analysis. The mixture was cooled to room temperature, the solids removed by filtration and concentrated *in vacuo*. The crude material was purified by flash column chromatography (SiO₂, hexanes to 10% EtOAc in hexanes to 20% EtOAc in hexanes) to provide **39e** (506 mg, 63% yield) as a colorless oil. R_f = 0.5 (20% EtOAc in hexanes); ¹H NMR (500 MHz, CDCl₃) δ 7.41–7.39 (m, 2H), 7.36–7.29 (m, 3H), 7.04–7.01 (m, 2H), 6.80–6.77 (m, 2H), 5.54 (s, 1H), 5.36–5.35 (m, 1H), 5.08–5.02 (m, 2H), 3.77 (s, 3H), 3.13 (s, 2H), 3.00 (ddd, J = 18.3, 11.1, 7.2 Hz, 1H), 2.68 (ddd, J = 18.3, 10.3, 6.4 Hz, 1H), 2.45 (ddd, J = 11.8, 11.1, 6.4 Hz, 1H), 2.00 (ddd, J = 11.8, 10.3, 7.2 Hz, 1H); ¹³C NMR (126 MHz, CDCl₃) δ 203.9, 168.8, 158.5, 142.1, 137.8, 130.7, 128.5, 128.1, 127.8, 126.0, 115.5, 113.9, 75.2, 66.7, 55.2, 45.0, 37.1, 19.1; IR (Neat Film, NaCl) 2957, 2933, 2836, 1788, 1725, 1513, 1248, 1179, 1037 cm⁻¹; HRMS (FAB+) m/z calc'd for C₂₂H₂₃O₄ [M+H]⁺: 351.1596; found 351.1601.

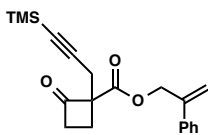
2-Phenylallyl 1-allyl-2-oxocyclobutanecarboxylate (**39f**)



39f

Compound **39f** was isolated by flash column chromatography (SiO₂, 3% EtOAc in hexanes to 4% EtOAc in hexanes) as a colorless oil. 68% yield. $R_f = 0.2$ (10% EtOAc in hexanes); ¹H NMR (500 MHz, CDCl₃) δ 7.49–7.27 (m, 5H), 5.64 (ddt, $J = 17.5, 9.7, 7.1$ Hz, 1H), 5.56 (q, $J = 0.8$ Hz, 1H), 5.38 (q, $J = 1.2$ Hz, 1H), 5.12–5.08 (m, 2H), 5.07 (dd, $J = 1.4, 0.7$ Hz, 2H), 3.14 (ddd, $J = 18.4, 11.0, 7.4$ Hz, 1H), 3.02 (ddd, $J = 18.4, 10.1, 6.4$ Hz, 1H), 2.70 (ddt, $J = 14.3, 7.1, 1.2$ Hz, 1H), 2.59–2.44 (m, 2H), 1.99 (ddd, $J = 11.9, 10.1, 7.4$ Hz, 1H); ¹³C NMR (126 MHz, CDCl₃) δ 203.4, 168.6, 142.3, 137.9, 131.9, 128.5, 128.1, 126.1, 119.2, 115.5, 73.6, 66.6, 45.0, 36.7, 19.5; IR (Neat Film, NaCl) 3072, 2967, 1786, 1725, 1638, 1497, 1440, 1387, 1193, 1142, 1043, 919, 779 cm⁻¹; HRMS (MM: ESI-APCI) m/z calc'd for C₁₇H₁₉O₃ [M+H]⁺: 271.1329; found 271.1330.

2-Phenylallyl 2-oxo-1-(3-(trimethylsilyl)prop-2-yn-1-yl)cyclobutanecarboxylate (**39g**)

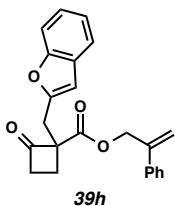


39g

Compound **39g** was isolated by flash column chromatography (SiO₂, 3% EtOAc in hexanes to 7% EtOAc in hexanes) as a colorless oil. 63% yield. $R_f = 0.3$ (10% EtOAc in hexanes); ¹H NMR (500 MHz, CDCl₃) δ 7.42–7.27 (m, 5H), 5.54 (q, $J = 0.7$ Hz, 1H),

5.35 (td, $J = 1.3, 0.7$ Hz, 1H), 5.10–4.98 (m, 2H), 3.18 (ddd, $J = 18.4, 11.0, 7.4$ Hz, 1H), 3.06 (ddd, $J = 18.4, 10.4, 6.5$ Hz, 1H), 2.82 (d, $J = 17.3$ Hz, 1H), 2.69 (d, $J = 17.3$ Hz, 1H), 2.48 (ddd, $J = 11.8, 11.0, 6.5$ Hz, 1H), 2.27 (ddd, $J = 11.8, 10.4, 7.4$ Hz, 1H), 0.13 (s, 9H); ^{13}C NMR (126 MHz, CDCl_3) δ 201.9, 168.1, 142.1, 137.8, 128.5, 128.1, 126.0, 115.4, 100.9, 87.9, 72.1, 66.8, 46.3, 22.8, 19.7, -0.1; IR (Neat Film, NaCl) 3058, 2959, 2177, 1949, 1794, 1732, 1634, 1575, 1496, 1444, 1422, 1315, 1250, 1194, 1161, 1116, 1028, 906, 843, 778, 760, 708 cm^{-1} ; HRMS (APCI) m/z calc'd for $\text{C}_{20}\text{H}_{25}\text{O}_3\text{Si}$ $[\text{M}+\text{H}]^+$: 341.1567; found 341.1582.

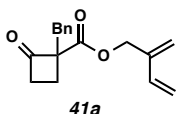
2-Phenylallyl 1-(benzofuran-2-ylmethyl)-2-oxocyclobutanecarboxylate (**39h**)



Compound **39h** was isolated by flash column chromatography (SiO_2 , 5% EtOAc in hexanes to 10% EtOAc in hexanes) as a colorless oil. 27% yield. $R_f = 0.6$ (20% EtOAc in hexanes); ^1H NMR (500 MHz, CDCl_3) δ 7.48–7.46 (m, 1H), 7.40–7.38 (m, 3H), 7.33–7.29 (m, 3H), 7.25–7.18 (m, 2H), 6.37 (d, $J = 0.8$ Hz, 1H), 5.55 (m, 1H), 5.37 (m, 1H), 5.09 (s, 2H), 3.43 (d, $J = 15.6$ Hz, 1H), 3.28 (dd, $J = 15.6, 0.8$ Hz, 1H), 3.18 (ddd, $J = 18.4, 11.2, 7.6$ Hz, 1H), 2.97 (ddd, $J = 18.4, 10.2, 6.1$ Hz, 1H), 2.58 (ddd, $J = 11.9, 11.2, 6.1$ Hz, 1H), 2.11 (ddd, $J = 11.9, 10.2, 7.6$ Hz, 1H); ^{13}C NMR (126 MHz, CDCl_3) δ 202.2, 168.1, 154.8, 153.6, 142.1, 137.7, 128.5, 128.4, 128.1, 126.0, 123.8, 122.7, 120.6, 115.7, 110.9, 104.9, 73.1, 67.0, 45.8, 30.9, 19.9; IR (Neat Film, NaCl) 3582, 3056, 3033,

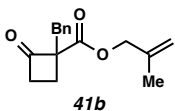
2963, 2928, 1790, 1726, 1601, 1586, 1455, 1253, 1193, 1045 cm^{-1} ; HRMS (MM: ESI-APCI) m/z calc'd for $\text{C}_{23}\text{H}_{21}\text{O}_4$ $[\text{M}+\text{H}]^+$: 361.1434; found 361.1427.

2-Methylenebut-3-en-1-yl 1-benzyl-2-oxocyclobutanecarboxylate (**41a**)



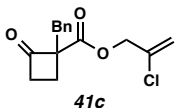
Compound **41a** was isolated by flash column chromatography (SiO_2 , 1% EtOAc in hexanes to 8% EtOAc in hexanes) as a colorless oil. 51% yield. $R_f = 0.4$ (10% EtOAc in hexanes); ^1H NMR (500 MHz, CDCl_3) δ 7.33–7.20 (m, 3H), 7.19–7.05 (m, 2H), 6.36 (ddd, $J = 17.9, 11.1, 0.8$ Hz, 1H), 5.28–5.09 (m, 4H), 4.89–4.78 (m, 2H), 3.24 (dd, $J = 18.6, 14.2$ Hz, 2H), 3.14 (ddd, $J = 18.3, 11.0, 7.2$ Hz, 1H), 2.75 (ddd, $J = 18.3, 10.3, 6.4$ Hz, 1H), 2.58 (ddd, $J = 11.8, 11.0, 6.4$ Hz, 1H), 2.06 (ddd, $J = 11.8, 10.3, 7.2$ Hz, 1H); ^{13}C NMR (126 MHz, CDCl_3) δ 203.7, 168.7, 140.0, 136.0, 135.9, 129.7, 128.5, 127.0, 118.4, 114.8, 75.1, 64.6, 45.2, 38.0, 19.2; IR (Neat Film, NaCl) 3987, 3027, 2929, 1789, 1725, 1598, 1495, 1454, 1393, 1266, 1192, 1044, 909, 743 cm^{-1} ; HRMS (MM: ESI-APCI) m/z calc'd for $\text{C}_{17}\text{H}_{19}\text{O}_3$ $[\text{M}+\text{H}]^+$: 271.1329; found 271.1330.

2-Methylallyl 1-benzyl-2-oxocyclobutanecarboxylate (**41b**)



Compound **41b** was isolated by flash column chromatography (SiO₂, 3% EtOAc in hexanes) as a colorless oil. 44% yield. R_f = 0.4 (10% EtOAc in hexanes); ¹H NMR (500 MHz, CDCl₃) δ 7.32–7.24 (m, 3H), 7.19–7.17 (m, 2H), 4.97 (d, J = 15.1 Hz, 2H), 4.60, 4.56 (AB system, J_{AB} = 13.1 Hz, 2H), 3.28, 3.26 (AB system, J_{AB} = 14.2 Hz, 2H), 3.16 (ddd, J = 18.3, 11.0, 7.2 Hz, 1H), 2.77 (ddd, J = 18.3, 10.4, 6.5 Hz, 1H), 2.61 (ddd, J = 11.8, 11.0, 6.5 Hz, 1H), 2.09 (ddd, J = 11.8, 10.4, 7.2 Hz, 1H) 1.70 (d, J = 0.5 Hz, 3H); ¹³C NMR (126 MHz, CDCl₃) δ 203.9, 168.7, 139.3, 134.0, 129.7, 128.5, 127.0, 113.4, 75.1, 68.7, 45.2, 38.0, 19.4, 19.2; IR (Neat Film, NaCl) 3030, 2974, 2925, 1790, 1727, 1454, 1271, 1193, 1047, 907 cm⁻¹; HRMS (MM: ESI-APCI) m/z calc'd for C₁₈H₁₉O₃ [M+H]⁺ 259.1329; found 259.1340.

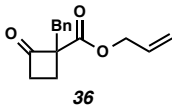
2-Chloroallyl 1-benzyl-2-oxocyclobutanecarboxylate (**41c**)



Compound **41c** was isolated by flash column chromatography (SiO₂, 2% EtOAc in hexanes to 5% EtOAc in hexanes) as a colorless oil. 63% yield. R_f = 0.3 (10% EtOAc in hexanes); ¹H NMR (300 MHz, CDCl₃) δ 7.33–7.24 (m, 3H), 7.18–7.16 (m, 2H), 5.44–5.40 (m, 2H), 4.71 (m, 2H), 3.26 (s, 2H), 3.17 (ddd, J = 18.3, 11.0, 7.2 Hz, 1H),

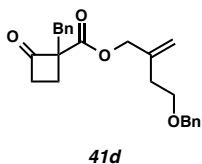
2.77 (ddd, $J = 18.3, 10.3, 6.5$ Hz, 1H), 2.61 (ddd, $J = 11.8, 11.0, 6.5$ Hz, 1H), 2.01 (ddd, $J = 11.8, 10.3, 7.2$ Hz, 1H); ^{13}C NMR (126 MHz, CDCl_3) δ 203.4, 168.2, 135.7, 135.2, 129.7, 128.6, 127.1, 115.3, 74.9, 66.7, 45.3, 38.0, 19.2; IR (Neat Film, NaCl) 3578, 2918, 1792, 1734, 1637, 1439, 1268, 1191, 1045 cm^{-1} ; HRMS (ESI) m/z calc'd for $\text{C}_{15}\text{H}_{15}\text{ClO}_3$ $[\text{M}]^+$: 278.0710; found 278.0714.

Allyl 1-benzyl-2-oxocyclobutanecarboxylate (**36**)



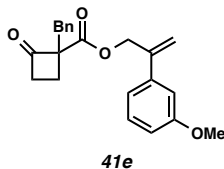
Compound **36** was isolated by flash column chromatography (SiO_2 , 3% EtOAc in hexanes to 6% EtOAc in hexanes) as a colorless oil. 87% yield. $R_f = 0.3$ (10% EtOAc in hexanes); ^1H NMR (500 MHz, CDCl_3) δ 7.30–7.27 (m, 2H), 7.25–7.22 (m, 1H), 7.17–7.14 (m, 2H), 5.88 (ddt, $J = 17.2, 10.5, 5.7$ Hz, 1H), 5.31 (dq, $J = 17.2, 1.4$ Hz, 1H), 5.24 (dq, $J = 10.5, 1.4$ Hz, 1H), 4.64 (dq, $J = 5.7, 1.4$ Hz, 2H), 3.26, 3.22 (AB system, $J_{\text{AB}} = 14.2$ Hz, 2H), 3.14 (ddd, $J = 18.3, 11.0, 7.2$ Hz, 1H), 2.75 (ddd, $J = 18.3, 10.3, 6.5$ Hz, 1H), 2.59 (ddd, $J = 11.8, 11.0, 6.5$ Hz, 1H), 2.07 (ddd, $J = 11.8, 10.3, 7.2$ Hz, 1H); ^{13}C NMR (126 MHz, CDCl_3) δ 203.9, 168.6, 136.0, 131.5, 129.7, 128.5, 127.0, 118.7, 75.1, 66.1, 45.1, 38.1, 19.3; IR (Neat Film, NaCl) 2916, 2848, 1781, 1715, 1438, 1181, 1040 cm^{-1} ; HRMS (MM: ESI-APCI) m/z calc'd for $\text{C}_{15}\text{H}_{17}\text{O}_3$ $[\text{M}+\text{H}]^+$: 245.1172; found 245.1178.

4-(Benzyloxy)-2-methylenebutyl 1-benzyl-2-oxocyclobutanecarboxylate (**41d**)



Compound **41d** was isolated by flash column chromatography (SiO₂, 1% EtOAc in Hexanes to 3% EtOAc in hexanes) as a colorless oil. 51% yield. $R_f = 0.5$ (10% EtOAc in hexanes); ¹H NMR (500 MHz, CDCl₃) δ 7.47–7.12 (m, 10H), 5.11 (q, $J = 1.0$ Hz, 1H), 5.04 (h, $J = 1.1$ Hz, 1H), 4.67, 4.61 (AB system, $J_{AB} = 13.3$ Hz, 2H), 4.53 (s, 2H), 3.60 (t, $J = 6.6$, 2H), 3.26 (s, 2H), 3.14 (ddd, $J = 18.2, 11.0, 7.2$ Hz, 1H), 2.76 (ddd, $J = 18.3, 10.3, 6.4$ Hz, 1H), 2.60 (ddd, $J = 11.8, 11.0, 6.5$ Hz, 1H), 2.42–2.33 (m, 2H), 2.08 (ddd, $J = 11.8, 10.3, 7.2$ Hz, 1H); ¹³C NMR (126 MHz, CDCl₃) δ 203.9, 168.7, 140.7, 138.2, 136.0, 129.7, 128.6, 128.4, 127.7, 127.6, 127.0, 114.4, 75.1, 73.0, 68.5, 68.0, 45.2, 38.1, 33.5, 19.3; IR (Neat Film, NaCl) 3029, 2920, 2849, 1784, 1717, 1495, 1451, 1360, 1268, 1187, 1095, 904, 732 cm⁻¹; HRMS (MM: ESI-APCI) m/z calc'd for C₂₄H₂₇O₄ [M+H]⁺: 379.1904; found 379.1926.

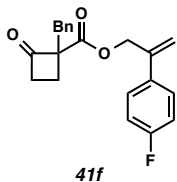
2-(3-Methoxyphenyl)allyl 1-benzyl-2-oxocyclobutanecarboxylate (**41e**)



Compound **41e** was isolated by flash column chromatography (SiO₂, 3% EtOAc in Hexanes to 7% EtOAc in Hexanes) as a colorless oil. 79% yield. $R_f = 0.35$ (10% EtOAc

in hexanes); ^1H NMR (500 MHz, CDCl_3) δ 7.41–7.16 (m, 4H), 7.16–7.09 (m, 2H), 7.05–6.90 (m, 2H), 6.91–6.82 (m, 1H), 5.60–5.53 (m, 1H), 5.37 (q, $J = 1.2$ Hz, 1H), 5.12–5.01 (m, 2H), 3.84 (s, 3H), 3.24, 3.21 (AB system, $J_{\text{AB}} = 14.13$ Hz, 2H), 3.06 (ddd, $J = 18.3, 11.1, 7.3$ Hz, 1H), 2.72 (ddd, $J = 18.3, 10.2, 6.3$ Hz, 1H), 2.51 (ddd, $J = 11.9, 11.1, 6.3$ Hz, 1H), 2.04 (ddd, $J = 11.8, 10.2, 7.3$ Hz, 1H); ^{13}C NMR (126 MHz, CDCl_3) δ 203.7, 168.7, 159.7, 142.1, 139.4, 136.0, 129.7, 129.5, 128.5, 126.9, 118.5, 115.8, 113.6, 111.8, 75.1, 66.8, 55.3, 45.2, 37.9, 19.2; IR (Neat Film, NaCl) 2957, 2833, 1786, 1720, 1575, 1494, 1453, 1387, 1221, 1180, 1039, 783 cm^{-1} ; HRMS (MM: ESI-APCI) m/z calc'd for $\text{C}_{22}\text{H}_{23}\text{O}_4$ $[\text{M}+\text{H}]^+$: 351.1591; found 351.1582.

2-(4-Fluorophenyl)allyl 1-benzyl-2-oxocyclobutanecarboxylate (**41f**)

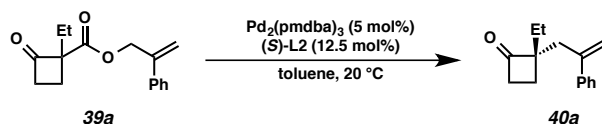


Compound **41f** was isolated by flash column chromatography (SiO_2 , 3% EtOAc in hexanes to 6% EtOAc in hexanes) as a colorless oil. 93% yield. $R_f = 0.3$ (10% EtOAc in hexanes); ^1H NMR (500 MHz, CDCl_3) δ 7.40–7.36 (m, 2H), 7.30–7.23 (m, 3H), 7.14–7.11 (m, 2H), 7.07–7.02 (m, 2H), 5.51 (s, 1H), 5.36 (s, 1H), 5.07–5.01 (m, 2H), 3.23, 3.20 (AB system, $J_{\text{AB}} = 14.2$ Hz, 2H), 3.06 (ddd, $J = 18.3, 11.0, 7.3$ Hz, 1H), 2.74 (ddd, $J = 18.3, 10.3, 6.4$ Hz, 1H), 2.51 (ddd, $J = 11.9, 11.0, 6.4$ Hz, 1H), 2.05 (ddd, $J = 11.9, 10.3, 7.3$ Hz, 1H); ^{13}C NMR (126 MHz, CDCl_3) δ 203.5, 168.6, 162.7 (d, $^1J_{\text{CF}} = 247.5$ Hz), 141.1, 135.9, 133.9 (d, $^4J_{\text{CF}} = 3.9$ Hz), 129.6, 128.5, 127.7 (d, $^3J_{\text{CF}} = 8.6$ Hz), 126.9,

115.7, 115.4 (d, $^2J_{\text{CF}} = 21.4$ Hz), 75.0, 66.7, 45.1, 37.8, 19.2; IR (Neat Film, NaCl) 3060, 3029, 2967, 2928, 1790, 1728, 1634, 1602, 1511, 1454, 1386, 1233, 1193, 1162, 1047, 917, 840, 744 cm^{-1} ; HRMS (MM: ESI-APCI) m/z calc'd for $\text{C}_{21}\text{H}_{20}^{19}\text{FO}_3$ $[\text{M}+\text{H}]^+$: 339.1391; found 339.1397.

1.6.5 Representative procedure for the asymmetric decarboxylative allylic alkylation of 2-oxocyclobutanecarboxylates

(S)-2-Ethyl-2-(2-phenylallyl)cyclobutanone (**40a**)

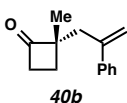


To a 20 mL scintillation vial with a stir bar were added $\text{Pd}_2(\text{pmdba})_3$ (16.4 mg, 0.015 mmol), **L6** (21.9 mg, 0.037 mmol) and toluene (9 mL) in a nitrogen-filled glove box. The dark purple mixture was stirred at ambient glove box temperature (ca. 30 °C) for 35 min at which point the mixture had become red-orange. 2-Carboxyallylcyclobutanone **39a** (80.0 mg, 0.31 mmol) was then added. The resulting yellow-greenish reaction mixture was stirred at 20 °C until full conversion of the starting material was indicated by TLC analysis (reaction times typically ranged from 18 to 36 hours). The vial was removed from the glove box, uncapped and directly purified by flash column chromatography (SiO_2 , pentane to 15% Et_2O in pentane) afforded **40a** (41 mg, 62% yield) as colorless oil. $R_f = 0.3$ (15% Et_2O in pentane); ^1H NMR (300 MHz, CDCl_3) δ 7.46–7.25 (m, 5H), 5.55 (d, $J = 0.9$ Hz, 1H), 5.38 (d, $J = 1.1$ Hz, 1H), 5.16–4.92 (m, 2H), 2.51 (ddd, $J = 14.7$,

10.5, 2.0 Hz, 1H), 2.42–2.30 (m, 1H), 2.29–2.14 (m, 1H), 1.93–1.77 (m, 2H), 1.73–1.59 (m, 1H), 0.69 (t, $J = 7.4$ Hz, 3H); ^{13}C NMR (75 MHz, CDCl_3) δ 215.1, 145.2, 141.9, 128.3, 127.6, 126.5, 116.5, 63.8, 42.8, 40.6, 23.5, 21.6, 8.4; IR (Neat Film, NaCl) 3078, 2966, 1699, 1464, 1443, 905 cm^{-1} ; HRMS (FAB+) m/z calc'd for $\text{C}_{15}\text{H}_{17}\text{O}$ [(M+H)– H_2] $^+$: 213.1279; found 213.1274; $[\alpha]_{\text{D}}^{26.0} +8.50$ (c 1.00, CHCl_3 , 99% ee).

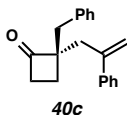
1.6.6 Spectroscopic data for novel α -quaternary cyclobutanone products

(S)-2-Methyl-2-(2-phenylallyl)cyclobutanone (**40b**)



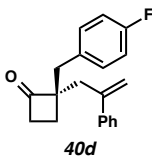
Cyclobutanone **40b** was isolated by flash column chromatography (SiO_2 , 10% Et_2O in pentane) as a colorless oil. 92% yield. $R_f = 0.3$ (10% Et_2O in pentane); ^1H NMR (500 MHz, CDCl_3) δ 7.31–7.19 (m, 5H), 5.25 (d, $J = 1.5$ Hz, 1H), 5.04–5.03 (m, 1H), 2.93–2.66 (m, 3 H), 2.56 (d, $J = 14.1$ Hz, 1H), 1.82 (ddd, $J = 11.4, 10.5, 6.9$ Hz, 1H), 1.47 (ddd, $J = 11.4, 10.2, 6.6$ Hz, 1H), 1.09 (s, 3H); ^{13}C NMR (126 MHz, CDCl_3) δ 215.1, 145.2, 141.9, 128.3, 127.6, 126.5, 116.5, 63.8, 42.8, 40.6, 23.5, 21.6; IR (Neat Film, NaCl) 2080, 2865, 1774, 1443, 1059 cm^{-1} ; HRMS (FAB+) m/z calc'd for $\text{C}_{14}\text{H}_{17}\text{O}$ [M+H] $^+$: 201.1279; found 201.1286; $[\alpha]_{\text{D}}^{26.0} -83.9$ (c 1.00, CHCl_3 , 90% ee).

(R)-2-Benzyl-2-(2-phenylallyl)cyclobutanone (40c)



Cyclobutanone **40c** was isolated by flash column chromatography (SiO₂, 5% Et₂O in petroleum ether) as a colorless oil. 81% yield. $R_f = 0.6$ (10% EtOAc in hexanes); ¹H NMR (500 MHz, CDCl₃) δ 7.36–7.26 (m, 8H), 7.13–7.11 (m, 2H), 5.37 (d, $J = 1.4$ Hz, 1H), 5.15–5.14 (m, 1H), 2.94 (t, $J = 14.9$ Hz, 2H), 2.72 (t, $J = 14.2$ Hz, 2H), 2.61 (ddd, $J = 18.1, 9.6, 7.2$ Hz, 1H), 2.32 (ddd, $J = 18.1, 10.0, 7.5$ Hz, 1H), 1.86–1.77 (m, 2H); ¹³C NMR (126 MHz, CDCl₃) δ 214, 145.0, 141.8, 137.3, 130.0, 128.4, 128.3, 127.7, 126.5, 126.4, 116.9, 68.8, 43.7, 41.2, 39.9, 20.0; IR (Neat Film, NaCl) 3028, 2918, 1770, 1494, 1453, 1074, 905 cm⁻¹; HRMS (EI+) m/z calc'd for C₂₀H₂₁O [M+H]⁺: 277.1587; found 277.1587; $[\alpha]_D^{26.0} -2.91$ (c 1.14, CHCl₃, 95% ee).

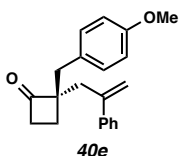
(R)-2-(4-Fluorobenzyl)-2-(2-phenylallyl)cyclobutanone (40d)



Cyclobutanone **40d** was isolated by flash column chromatography (SiO₂, hexanes to 3% Et₂O in hexanes) as a colorless oil. 71% yield. $R_f = 0.3$ (25% EtOAc in hexanes); ¹H NMR (500 MHz, CDCl₃) δ 7.36–7.26 (m, 5H), 7.09–7.05 (m, 2H), 6.97–6.93 (m, 2H), 5.37 (d, $J = 1.4$ Hz, 1H), 5.14 (d, $J = 0.9$ Hz, 1H), 2.93–2.89 (m, 2H), 2.74–2.67 (m, 2H), 2.33 (ddd, $J = 18.1, 10.7, 6.9$ Hz, 1H), 2.62 (ddd, $J = 18.1, 10.4, 6.5$ Hz, 1H), 1.83 (ddd, J

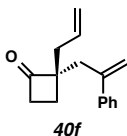
= 11.7, 10.4, 6.9 Hz, 1H), 1.75 (ddd, $J = 11.7, 10.7, 6.5$ Hz, 1H); ^{13}C NMR (126 MHz, CDCl_3) δ 214.7, 161.7 (d, $^1J_{\text{CF}} = 244.8$ Hz), 144.9, 141.8, 132.9 (d, $^4J_{\text{CF}} = 3.8$ Hz), 131.5 (d, $^3J_{\text{CF}} = 8.3$ Hz), 128.8, 127.2, 126.4, 117.0, 115.1 (d, $^2J_{\text{CF}} = 21.1$ Hz), 68.7, 43.7, 40.2, 39.9, 19.9; IR (Neat Film, NaCl) 3047, 2918, 2848, 1772, 1599, 1508, 1221, 1158, 1060 cm^{-1} ; HRMS (MM: ESI-APCI) m/z calc'd for $\text{C}_{20}\text{H}_{20}^{19}\text{FO}$ $[\text{M}+\text{H}]^+$: 294.1420; found 294.1408; $[\alpha]_{\text{D}}^{26.0} -9.9$ (c 0.59, CHCl_3 , 94% ee).

(R)-2-(4-Methoxybenzyl)-2-(2-phenylallyl)cyclobutanone (40e)



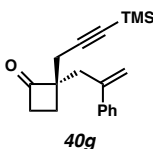
Cyclobutanone **40e** was isolated by flash column chromatography (SiO_2 , 10% EtOAc in hexanes) as a colorless oil. 83% yield. $R_f = 0.3$ (10% EtOAc in hexanes); ^1H NMR (300 MHz, CDCl_3) δ 7.37–7.26 (m, 5H), 7.06–7.01 (m, 2H), 6.83–6.78 (m, 2H), 5.37 (d, $J = 1.2$ Hz, 1H), 5.14 (s, 1H), 3.78 (s, 3H), 2.91 (dd, $J = 14.5, 3.1$ Hz, 2H), 2.69 (dd, $J = 14.5, 1.9$ Hz, 2H), 2.64–2.53 (m, 1H), 2.37–2.26 (m, 1H) 1.78 (ddd, $J = 10.1, 7.2, 2.6$ Hz, 2H); ^{13}C NMR (126 MHz, CDCl_3) δ 215.1, 158.2, 145.0, 141.8, 131.0, 129.2, 128.3, 127.6, 126.4, 116.8, 113.6, 68.9, 55.1, 43.6, 40.3, 39.8; IR (Neat Film, NaCl) 3080, 2913, 2835, 1770, 1611, 1513, 1248, 1179, 1035, 907 cm^{-1} ; HRMS (EI+) m/z calc'd for $\text{C}_{21}\text{H}_{22}\text{O}_2$ $[\text{M}]^+$: 306.1620; found 306.1614; $[\alpha]_{\text{D}}^{26.0} -0.60$ (c 1.00, CHCl_3 , 95% ee).

(R)-2-Allyl-2-(2-phenylallyl)cyclobutanone (40f)



Cyclobutanone **40f** was isolated by flash column chromatography (SiO₂, 3% EtOAc in hexanes to 4% EtOAc in hexanes) as a colorless oil. 86% yield. $R_f = 0.2$ (10% EtOAc in hexanes); ¹H NMR (500 MHz, CDCl₃) δ 7.42–7.25 (m, 5H), 5.84–5.71 (m, 1H), 5.37 (d, $J = 1.5$ Hz, 1H), 5.14 (d, $J = 1.0$ Hz, 1H), 5.15–5.05 (m, 2H), 2.91, 2.70 (AB system, $J_{AB} = 14.4$ Hz, 2H), 2.87–2.65 (m, 2H), 2.36 (ddt, $J = 13.9, 7.1, 1.2$ Hz, 1H), 2.27 (ddt, $J = 13.9, 7.6, 1.1$ Hz, 1H), 1.85 (ddd, $J = 11.7, 10.4, 6.8$ Hz, 1H), 1.77–1.64 (m, 1H); ¹³C NMR (126 MHz, CDCl₃) δ 214.5, 145.1, 141.8, 133.3, 128.3, 128.3, 126.5, 118.7, 116.9, 67.5, 43.3, 39.7, 39.1, 20.3; IR (Neat Film, NaCl) 3078, 2921, 1774, 1625, 1493, 1443, 1387, 1059, 1000, 908, 779 cm⁻¹; HRMS (MM: ESI-APCI) m/z calc'd for C₁₆H₁₉O [M+H]⁺: 227.1430; found 227.1418; $\alpha_D^{25} -13.98$ (c 0.51, CHCl₃, 92% ee).

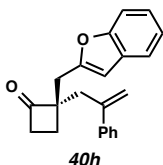
(S)-2-(2-Phenylallyl)-2-[3-(trimethylsilyl)prop-2-yn-1-yl]cyclobutanone (40g)



Cyclobutanone **40g** was isolated by flash column chromatography (SiO₂, 1% EtOAc in hexanes to 3% EtOAc in hexanes) as a colorless oil. 90% yield. $R_f = 0.2$ (10% EtOAc in hexanes); ¹H NMR (500 MHz, CDCl₃) δ 7.51–7.08 (m, 5H), 5.37 (d, $J = 1.4$ Hz, 1H),

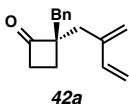
5.13 (d, $J = 1.1$ Hz, 1H), 2.93–2.86 (m, 2H), 2.82–2.75 (m, 2H), 2.42, 2.37 (AB system, $J_{AB} = 17.0$ Hz, 2H), 1.96–1.85 (m, 2H) 0.15 (s, 9H); ^{13}C NMR (126 MHz, CDCl_3) δ 212.6, 144.5, 141.4, 128.4, 127.7, 126.4, 116.9, 102.7, 87.2, 66.6, 43.9, 38.9, 25.8, 20.9, 0.0; IR (Neat Film, NaCl) 2957, 2169, 1776, 1713, 1444, 1249, 1177, 1061, 1031, 834, 760 cm^{-1} ; HRMS (MM: ESI-APCI) m/z calc'd for $\text{C}_{19}\text{H}_{25}\text{OSi}$ $[\text{M}+\text{H}]^+$: 297.1681; found 297.1683; $[\alpha]_{\text{D}}^{25} +10.76$ (c 0.29, CHCl_3 , 93% ee).

(S)-2-(Benzofuran-2-ylmethyl)-2-(2-phenylallyl)cyclobutanone (40h)



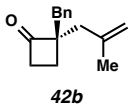
Cyclobutanone **40h** was isolated by flash column chromatography (SiO_2 , hexanes to 10% EtOAc in hexanes) as a colorless oil. 82% yield. $R_f = 0.5$ (10% EtOAc in hexanes); ^1H NMR (500 MHz, CDCl_3) δ 7.50–7.48 (m, 1H), 7.42–7.40 (m, 1H), 7.38–7.36 (m, 2H), 7.33–7.28 (m, 3H), 7.25–7.18 (m, 2H), 6.44 (s, 1H), 5.40 (d, $J = 1.34$ Hz, 1H), 5.17 (m, 1H), 3.07 (d, $J = 15.2$ Hz, 1H), 2.98 (dd, $J = 14.3, 0.9$ Hz, 1H), 2.96 (d, $J = 15.0$ Hz, 1H), 2.82 (d, $J = 14.3$ Hz, 1H), 2.79–2.64 (m, 2H), 1.96–1.86 (m, 2H); ^{13}C NMR (126 MHz, CDCl_3) δ 213.2, 155.0, 154.7, 144.7, 141.6, 128.5, 128.4, 127.8, 126.4, 123.6, 122.6, 120.5, 117.2, 110.9, 105.0, 67.2, 43.8, 39.6, 33.7, 20.9; IR (Neat Film, NaCl) 3054, 2917, 2849, 1770, 1598, 1585, 1453, 1251, 1104, 1061, 905 cm^{-1} ; HRMS (MM ESI-APCI) m/z calc'd for $\text{C}_{22}\text{H}_{21}\text{O}_2$ $[\text{M}+\text{H}]^+$: 317.1536; found 317.1530; $[\alpha]_{\text{D}}^{26} +56.4$ (c 1.00, CHCl_3 , 92% ee).

(S)-2-Benzyl-2-(2-methylenebut-3-en-1-yl)cyclobutanone (42a)



Cyclobutanone **42a** was isolated by flash column chromatography (SiO₂, hexanes to 5% Et₂O in hexanes) as a colorless oil. 92% yield. $R_f = 0.3$ (10% EtOAc in hexanes); ¹H NMR (500 MHz, CDCl₃) δ 7.33–7.27 (m, 3H), 7.25–7.20 (m, 2H), 7.19–7.12 (m, 1H), 6.59–6.19 (m, 1H), 5.24–5.06 (m, 2H), 5.05 (s, 2H), 3.01 (d, $J = 13.6$ Hz, 1H), 2.80 (d, $J = 13.6$ Hz, 1H), 2.68 (ddd, $J = 18.1, 10.3, 6.8$ Hz, 1H), 2.57 (dd, $J = 14.4, 1.0$ Hz, 1H), 2.45 (ddd, $J = 18.1, 10.3, 6.9$ Hz, 1H), 2.40 (d, $J = 14.4$ Hz, 1H), 1.95 (qdd, $J = 11.6, 10.2, 6.8$ Hz, 1H); ¹³C NMR (126 MHz, CDCl₃) δ 215.2, 142.4, 139.4, 137.3, 130.1, 128.3, 126.6, 119.2, 114.5, 68.6, 43.9, 41.4, 35.5, 20.2; IR (Neat Film, NaCl) 3022, 2921, 2843, 1768, 1590, 1493, 1452, 1384, 1065, 989, 898, 755 cm⁻¹; HRMS (MM: ESI-APCI) m/z calc'd for C₁₆H₁₈O [M+H]⁺: 227.1430; found 227.1433; [α]_D²⁵ +0.44 (*c* 1.60, CHCl₃, 91% ee).

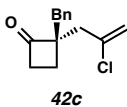
(S)-2-Benzyl-2-(2-methylallyl)cyclobutanone (42b)



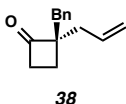
Cyclobutanone **42b** was isolated by flash column chromatography (SiO₂, 2% Et₂O in hexanes to 5% Et₂O in hexanes) as a colorless oil. 82% yield. $R_f = 0.3$ (10% EtOAc in

hexanes); ^1H NMR (300 MHz, CDCl_3) δ 7.41–7.12 (m, 5H), 4.91 (t, $J = 1.7$ Hz, 1H), 4.78 (dd, $J = 2.0$ Hz, 1.0, 1H), 2.88, 2.65 (AB system, $J_{\text{AB}} = 13.7$ Hz, 2H), 2.77 (ddd, $J = 18.1, 9.6, 6.9$ Hz, 1H), 2.43–2.33 (m, 1H), 2.33, 2.22 (AB system, $J_{\text{AB}} = 14.2$ Hz, 2H), 1.97 (ddd, $J = 9.4, 7.2, 3.1$, 2H), 1.80–1.72 (m, 3H); ^{13}C NMR (126 MHz, CDCl_3) δ 215.3, 141.8, 137.4, 130.1, 128.3, 126.5, 114.8, 68.2, 43.6, 43.2, 40.6, 24.0, 20.7; IR (Neat Film, NaCl) 3072, 3027, 2964, 2919, 1772, 1322, 1131, 1062, 894 cm^{-1} ; HRMS (MM: ESI-APCI) m/z calc'd for $\text{C}_{15}\text{H}_{18}\text{O}$ $[\text{M}]^+$: 214.1358, found 214.1346; $[\alpha]_{\text{D}}^{26} -2.4^\circ$ (c 0.48, CHCl_3 , 90% ee).

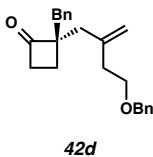
(*R*)-2-Benzyl-2-(2-chloroallyl)cyclobutanone (42c)



Cyclobutanone **42c** was isolated by flash column chromatography (SiO_2 , hexanes to 3% EtOAc in hexanes) as a colorless oil. 67% yield. $R_f = 0.3$ (10% EtOAc in hexanes); ^1H NMR (500 MHz, CDCl_3) δ 7.33–7.21 (m, 3H), 7.18–7.15 (m, 2H), 5.33 (d, $J = 1.3$ Hz, 1H), 5.22–5.21 (m, 1H), 2.97 (d, $J = 13.7$ Hz, 1H), 2.90–2.76 (m, 1H), 2.82 (d, $J = 13.7$ Hz, 1H), 2.74 (dd, $J = 14.7, 1.0$ Hz, 1H), 2.59 (d, $J = 14.7$ Hz, 1H), 2.43 (ddd, $J = 18.1, 10.8, 7.3$ Hz, 1H), 2.19 (ddd, $J = 11.8, 10.2, 7.2$ Hz, 1H), 2.04 (ddd, $J = 11.8, 10.8, 6.1$ Hz, 1H); ^{13}C NMR (126 MHz, CDCl_3) δ 213.7, 138.4, 136.7, 130.1, 128.4, 126.8, 116.4, 67.5, 44.1, 43.8, 40.5, 20.7; IR (Neat Film, NaCl) 3028, 2919, 2848, 1772, 1631, 1494, 1453, 1063, 888 cm^{-1} ; HRMS (MM ESI-APCI) m/z calc'd for $\text{C}_{14}\text{H}_{16}^{35}\text{ClO}$ $[\text{M}+\text{H}]^+$: 235.0884; found 235.0883; $[\alpha]_{\text{D}}^{26} +1.51$ (c 0.56, CHCl_3 , 94% ee).

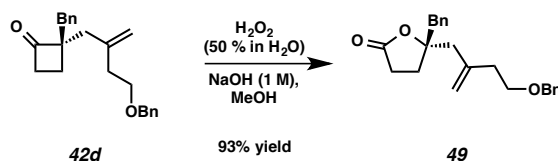
(S)-2-Allyl-2-benzylcyclobutanone (38)

Cyclobutanone **38** was isolated by flash column chromatography (SiO₂, 2% Et₂O in hexanes to 5% Et₂O in hexanes) as a colorless oil. 82% yield. R_f = 0.4 (10% EtOAc in hexanes); ¹H NMR (500 MHz, CDCl₃) δ 7.30–7.27 (m, 2H), 7.24–7.21 (m, 1H), 7.16–7.15 (m, 2H), 5.81 (ddt, *J* = 17.2, 10.0, 7.4 Hz, 1H), 5.16–5.10 (m, 2H), 2.97 (d, *J* = 13.7 Hz, 1H), 2.78 (ddd, *J* = 18.2, 10.3, 6.5 Hz, 1H), 2.72 (d, *J* = 13.7 Hz, 1H), 2.49 (ddd, *J* = 18.2, 10.6, 6.8 Hz, 1H), 2.39 (ddt, *J* = 13.9, 7.4, 1.1 Hz, 1H), 2.67 (ddt, *J* = 13.9, 7.4, 1.1 Hz, 1H), 1.94 (ddd, *J* = 11.5, 10.6, 6.5 Hz, 1H), 1.86 (ddd, *J* = 11.5, 10.3, 6.8 Hz, 1H); ¹³C NMR (126 MHz, CDCl₃) δ 214.9, 137.3, 133.2, 130.0, 128.3, 126.5, 118.7, 68.4, 42.9, 40.3, 39.5, 19.8; IR (Neat Film, NaCl) 3029, 2918, 1771, 1495, 1437, 1454, 1076, 920 cm⁻¹; HRMS (MM: ESI-APCI) *m/z* calc'd for C₁₄H₁₆O [M]⁺: 200.1201; found 200.1199; [α]_D²⁶ +4.69 (*c* 0.55, CHCl₃, 88% ee).

(S)-2-Benzyl-2-[4-(benzyloxy)-2-methylenebutyl]cyclobutanone (42d)

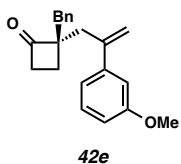
Cyclobutanone **42d** was isolated by flash column chromatography (SiO₂, 1% EtOAc in hexanes to 3% EtOAc in hexanes) as a colorless oil (95% yield). R_f = 0.2 (10% EtOAc in

hexanes); ^1H NMR (500 MHz, CDCl_3) δ 7.41–7.12 (m, 10H), 5.01 (q, $J = 1.4$ Hz, 1H), 4.93–4.92 (m, 1H), 4.54 (s, 2H), 3.59 (td, $J = 6.8, 0.7$, 2H), 2.95, 2.73 (AB system, $J_{\text{AB}} = 13.7$, 2H), 2.83–2.71 (m, 1H), 2.51–2.27 (m, 5H), 2.04–1.92 (m, 2H); ^{13}C NMR (126 MHz, CDCl_3) δ 215.2, 142.6, 138.4, 137.4, 130.1, 128.4, 128.3, 127.7, 127.6, 126.5, 115.1, 72.9, 68.7, 68.3, 43.6, 41.5, 40.6, 37.0, 20.7; IR (Neat Film, NaCl) 3022, 2923, 2853, 1768, 1641, 1494, 1452, 1360, 1099, 899, 735 cm^{-1} ; HRMS (MM: ESI-APCI) m/z calc'd for $\text{C}_{23}\text{H}_{27}\text{O}_2$ $[\text{M}+\text{H}]^+$: 335.2006; found 335.2020;



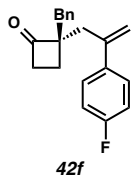
Enantiomeric excess determined for the corresponding Baeyer-Villiger product, which was obtained by the general procedure below. Lactone **49** was isolated by flash column chromatography (SiO_2 , 4% EtOAc in hexanes) as a colorless oil (93% yield). $R_f = 0.2$ (20% EtOAc in hexanes); ^1H NMR (500 MHz, CDCl_3) δ 7.40–7.18 (m, 10H), 5.09 (q, $J = 1.5$ Hz, 1H), 4.98 (dd, $J = 1.7, 0.9$ Hz, 1H), 4.51 (s, 2H), 3.61 (t, $J = 6.5$ Hz, 2H), 3.09 (d, $J = 14.1$ Hz, 1H), 2.75 (d, $J = 14.1$ Hz, 1H), 2.61–2.38 (m, 4H), 2.23 (ddd, $J = 17.6, 9.4, 5.9$ Hz, 1H), 2.17–2.03 (m, 2H), 1.68 (ddd, $J = 17.6, 10.0, 8.6$ Hz, 1H); ^{13}C NMR (126 MHz, CDCl_3) δ 176.9, 141.8, 138.4, 135.5, 130.5, 128.5, 128.3, 127.7, 127.5, 127.1, 117.1, 87.8, 72.8, 68.5, 46.7, 45.6, 37.0, 29.3, 29.2; IR (Neat Film, NaCl) 3524, 3062, 3029, 2919, 2855, 1958, 1770, 1642, 1603, 1495, 1454, 1416, 1361, 1271, 1232, 1177, 1101, 1080, 1029, 932, 741 cm^{-1} ; HRMS (MM: ESI-APCI) m/z calc'd for $\text{C}_{23}\text{H}_{27}\text{O}_3$ $[\text{M}+\text{H}]^+$: 351.1955; found 351.1951; $\alpha_{\text{D}}^{25} +21.17$ (c 0.44, CHCl_3 , 89% ee).

(R)-2-Benzyl-2-(2-[3-methoxyphenyl]allyl)cyclobutanone (42e)



Cyclobutanone **42e** was isolated by flash column chromatography (SiO₂, 1% EtOAc in hexanes to 3% EtOAc in hexanes) as a colorless oil. 91% yield. $R_f = 0.2$ (10% EtOAc in hexanes); ¹H NMR (500 MHz, CDCl₃) δ 7.37–7.19 (m, 4H), 7.19–7.10 (m, 2H), 6.98 (ddd, $J = 7.7, 1.7, 0.9$ Hz, 1H), 6.91 (dd, $J = 2.5, 1.6$ Hz, 1H), 6.85 (ddd, $J = 8.2, 2.6, 0.9$ Hz, 1H), 5.41 (d, $J = 1.4$ Hz, 1H), 5.17 (q, $J = 1.1$ Hz, 1H), 3.83 (s, 3H), 3.03–2.86 (m, 2H), 2.86–2.68 (m, 2H), 2.63 (ddd, $J = 18.1, 9.7, 7.1$ Hz, 1H), 2.35 (ddd, $J = 18.1, 10.1, 7.4$ Hz, 1H), 1.96–1.72 (m, 2H); ¹³C NMR (126 MHz, CDCl₃) δ 215.0, 159.6, 144.9, 143.5, 137.3, 130.1, 129.4, 128.4, 126.6, 119.0, 117.1, 112.9, 112.4, 68.9, 55.3, 43.8, 41.2, 40.0, 20.0; IR (Neat Film, NaCl) 2913, 2829, 1766, 1595, 1572, 1488, 1451, 1286, 1221, 1170, 1039, 898, 873, 779 cm⁻¹; HRMS (MM: ESI-APCI) m/z calc'd for C₂₁H₂₃O₂ [M+H]⁺: 307.1693; found 307.1693; $\alpha_D^{25} -4.78$ (c 0.45, CHCl₃, 92% ee).

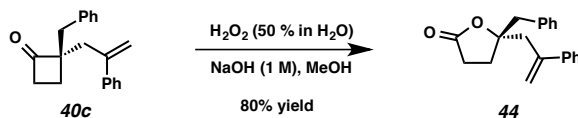
(R)-2-Benzyl-2-(2-(4-fluorophenyl)allyl)cyclobutanone (42f)



Cyclobutanone **42f** was isolated by flash column chromatography (SiO₂, 3% EtOAc in hexanes to 7% EtOAc in hexanes) as a colorless oil. 94% yield. $R_f = 0.3$ (10% EtOAc in

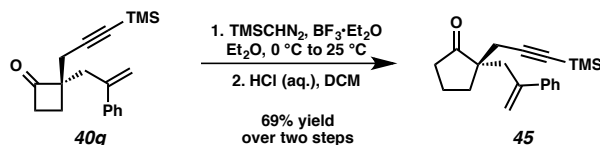
hexanes); ^1H NMR (500 MHz, CDCl_3) δ 7.25–7.12 (m, 5H), 7.05–7.03 (m, 2H), 6.95–6.90 (m, 2H), 5.25 (d, $J = 1.3$ Hz, 1H), 5.05 (s, 1H), 2.88 (d, $J = 13.7$ Hz, 1H), 2.82 (dd, $J = 14.4, 1.0$ Hz, 1H), 2.66 (d, $J = 13.7$ Hz, 1H), 2.59 (d, $J = 14.4$ Hz, 1H), 2.54–2.47 (m, 1H), 2.29–2.22 (m, 1H), 1.73 (t, $J = 8.6$ Hz, 2H); ^{13}C NMR (126 MHz, CDCl_3) δ 214.6, 162.3 (d, $^1J_{\text{CF}} = 246.8$ Hz), 144.0, 137.8 (d, $^4J_{\text{CF}} = 3.3$ Hz), 137.1, 130.0, 128.3, 128.0 (d, $^3J_{\text{CF}} = 7.9$ Hz), 126.6, 116.9, 115.2 (d, $^2J_{\text{CF}} = 21.3$ Hz), 68.6, 43.7, 41.2, 40.5, 20.0; IR (Neat Film, NaCl) 2913, 1766, 1597, 1505, 1219, 1055, 837 cm^{-1} ; HRMS (MM: ESI-APCI) m/z calc'd for $\text{C}_{20}\text{H}_{20}^{19}\text{FO}$ $[\text{M}+\text{H}]^+$: 295.1493; found 295.1502; $[\alpha]_{\text{D}}^{25} +3.53$ (c 0.16, CHCl_3 , 94% ee).

1.6.7 Procedures for derivatization of α -quaternary cyclobutanones and determination of absolute stereochemical configuration



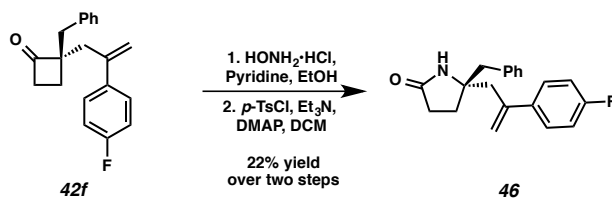
(R)-5-Benzyl-5-(2-phenylallyl)dihydrofuran-2(3H)-one (44). To a stirred solution of cyclobutanone **40c** (43 mg, 0.23 mmol) in MeOH (4.6 mL) was added NaOH (1 M in H_2O , 0.23 μL , 0.23 mmol) followed by H_2O_2 (50 wt% in H_2O , 17 mg, 0.46 mmol). The resulting mixture was stirred at room temperature for 1 h. The reaction mixture was then acidified to pH 7 with 1 N aqueous HCl and extracted with dichloromethane (2 mL x 5). The combined organic layers were dried over MgSO_4 and concentrated *in vacuo*. The crude oil was purified by flash column chromatography (SiO_2 , 15% EtOAc in hexanes) to afford lactone **44** (37 mg, 0.17 mmol, 80% yield) as a colorless oil. $R_f = 0.2$ (20% EtOAc in hexanes); ^1H

NMR (300 MHz, CDCl₃) δ 7.41–7.18 (m, 10H), 5.46 (d, J = 1.4 Hz, 1H), 5.27 (s, 1H), 3.08–2.92 (m, 3H), 2.79 (d, J = 14.1 Hz, 1H), 2.17 (ddd, J = 17.4, 9.8, 6.4 Hz, 1H), 2.04–1.86 (m, 2H), 1.76–1.62 (m, 1H); ¹³C NMR (126 MHz, CDCl₃) δ 176.7, 143.4, 141.7, 135.4, 130.6, 128.6, 128.5, 127.8, 127.0, 126.3, 119.2, 87.7, 46.1, 45.3, 29.3, 28.8; IR (Neat Film, NaCl) 3029, 2918, 1771, 1495, 1437, 1454, 1076, 920 cm⁻¹; HRMS (MM: ESI-APCI) m/z calc'd for C₂₀H₂₁O₂ [M+H]⁺: 293.1536; found 293.1536; [α]_D²⁶ -0.60 (c 1.00, CHCl₃, 89% ee).



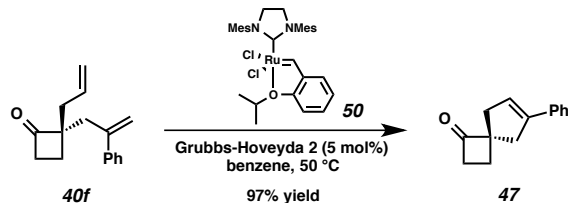
(S)-2-(2-Phenylallyl)-2-(3-(trimethylsilyl)prop-2-yn-1-yl)cyclopentanone (45). To a solution of **40g** (0.1023 g, 0.345 mmol) in Et₂O (3.5 mL), cooled to 0 °C with a water/ice bath, under an atmosphere of N₂, was added BF₃ etherate (0.112 mL, 0.379 mmol) dropwise followed by trimethylsilyldiazomethane (0.345 mL, 2 M solution in hexane) dropwise. The mixture was allowed to warm to 25 °C and stirred for 18 hours, at which point the reaction was determined to be complete by TLC analysis. To the mixture was added 3 mL of saturated aqueous NaHCO₃. After stirring for 30 min, this mixture was extracted with Et₂O (5 mL x 3), dried over MgSO₄ and concentrated *in vacuo*. The crude product was purified by flash column chromatography (SiO₂, 1% EtOAc in hexanes to 5% EtOAc in hexanes) to afford α -trimethylsilylcyclopentanone as a colorless oil. The identity of the α -trimethylsilylcyclopentanone was confirmed by ¹H NMR analysis; the product was taken on without further characterization. R_f = 0.3 (10% EtOAc in hexanes);

To a solution of α -trimethylsilylcyclopentanone (61 mg, 0.159 mmol) in 2 ml dichloromethane was added 2 mL of 1 N aqueous HCl in H₂O at 25 °C. The mixture was stirred for 24 hours at which point the reaction was determined to be complete by TLC analysis. The mixture was diluted with dichloromethane (2 ml) and then extracted with dichloromethane (5 mL x 3). The collected organic layers were then washed with brine (5 mL), dried over MgSO₄, filtered and concentrated *in vacuo*. The crude oil was purified by flash column chromatography (SiO₂, hexanes to 1% EtOAc in hexanes) to afford cyclopentanone **45** (47 mg, 0.153 mmol, 69% yield over two steps) as a colorless oil. $R_f = 0.3$ (10% EtOAc in hexanes); ¹H NMR (500 MHz, CDCl₃) δ 7.58–7.12 (m, 5H), 5.32 (d, $J = 1.6$ Hz, 1H), 5.14–4.97 (m, 1H), 2.83–2.73 (m, 2H), 2.22 (dd, $J = 16.9, 38.9$ Hz, 2H), 2.16–2.08 (m, 1H), 2.03–1.91 (m, 2H), 1.89–1.71 (m, 3H), 0.14 (s, 9H); ¹³C NMR (126 MHz, CDCl₃) δ 221.0, 145.1, 141.6, 128.3, 127.6, 126.5, 117.4, 103.7, 87.1, 52.2, 39.8, 38.4, 31.4, 27.4, 18.7, 0.0; IR (Neat Film, NaCl) 3080, 2958, 1738, 1623, 1494, 1447, 1404, 1308, 1249, 1154, 1046, 1029, 973, 904, 841, 778, 759 cm⁻¹; HRMS (EI+) m/z calc'd for C₂₀H₂₆OSi [M]⁺: 310.1753; found 310.1765; $[\alpha]_D^{25} +4.13$ (*c* 0.50, CHCl₃, 93% ee).

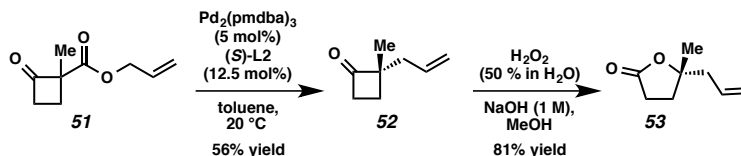


(R)-5-Allyl-5-(2-phenylallyl)pyrrolidin-2-one (46). To a solution of cyclobutanone **42f** (65 mg, 0.221 mmol) in 7 mL absolute ethanol was added hydroxylamine hydrochloride (76 mg, 1.104 mmol), followed by pyridine (0.27 ml, 3.31 mmol) and the mixture was stirred at 25 °C for 24 hours. The crude mixture was concentrated *in vacuo* and loaded

directly onto a flash column. Flash column chromatography (SiO₂, 8% EtOAc in hexanes to 11% EtOAc in hexanes) afforded the corresponding oxime, whose identity was confirmed by ¹H NMR and which was taken on without further characterization; R_f = 0.2 (25% EtOAc in hexanes); To a mixture of 4-toluenesulfonyl chloride (83 mg, 0.43 mmol), triethylamine (0.06 mL, 0.43 mmol) and catalytic 4-dimethylaminopyridine in 2.5 mL of dichloromethane under an atmosphere of N₂ was added dropwise a solution of oxime (54 mg, 0.175 mmol) in 1 mL of dichloromethane. The mixture was stirred at 25 °C for 4 hours. The crude mixture was washed with H₂O (5 mL), washed with brine (5 mL), dried over Na₂SO₄ and concentrated *in vacuo*. The crude oil was purified by flash column chromatography (SiO₂, 3% EtOAc in hexanes to EtOAc) to afford lactam **46** (16 mg, 0.05 mmol, 22% yield over two steps) as a pale yellow oil. R_f = 0.4 (EtOAc); ¹H NMR (500 MHz, CDCl₃) δ 7.34–7.07 (m, 7H), 7.07–6.96 (m, 2H), 5.35 (d, *J* = 1.3 Hz, 1H), 5.26 (s, 1H), 5.15 (q, *J* = 1.0 Hz, 1H), 2.87–2.63 (m, 4H), 2.06–1.85 (m, 3H), 1.69–1.55 (m, 1H); ¹³C NMR (126 MHz, CDCl₃) δ = 176.9, 162.4 (d, ¹J_{CF} = 247.4 Hz), 143.7, 138.0 (d, ⁴J_{CF} = 3.4 Hz), 136.1, 130.3, 128.5, 127.8 (d, ³J_{CF} = 8.0 Hz), 127.0, 118.6, 115.7 (d, ²J_{CF} = 21.4 Hz), 62.0, 47.0, 46.5, 30.9, 30.1; IR (Neat Film, NaCl) 3196, 3081, 2927, 1690, 1601, 1507, 1452, 1260, 1224, 1159, 1087, 906, 842, 750 cm⁻¹; HRMS (EI+) *m/z* calc'd for C₂₀H₂₀ONF [M]⁺: 309.1529; found 309.1517; [α]_D²⁵ +53.19 (*c* 0.08, CHCl₃, 94% ee).



(R)-6-phenylspiro[3.4]oct-6-en-1-one (47). To a flask charged with Grubbs-Hoveyda an atmosphere of argon was added a solution of cyclobutanone **40f** (50 mg, 0.221 mmol) in 5 mL benzene. The reaction mixture was heated to 50 °C and stirred for one hour, at which point the reaction was determined to be complete by TLC analysis. The reaction vessel was cooled to 25 °C and 1 mL of ethyl vinyl ether was added. After 30 min of stirring, the crude mixture was purified directly by flash column chromatography (SiO₂, hexanes to 3% EtOAc in hexanes) to afford spirocycle **9** (43 mg, 0.215 mmol, 97% yield) as a colorless oil. R_f = 0.3 (10% EtOAc in hexanes); ¹H NMR (500 MHz, CDCl₃) δ 7.37–7.31 (m, 2H), 7.32–7.21 (m, 2H), 7.24–7.15 (m, 1H), 5.97 (p, J = 2.4 Hz, 1H), 3.19 (dq, J = 16.0, 2.2 Hz, 1H), 3.04 (t, J = 8.61 Hz, 2H), 3.04–2.97 (m, 1H), 2.81 (dq, J = 16.0, 1.7 Hz, 1H), 2.63 (dtd, J = 17.5, 2.5, 1.4 Hz, 1H), 2.09 (td, J = 8.9, 2.5 Hz, 2H); ¹³C NMR (126 MHz, CDCl₃) δ 214.1, 140.0, 135.6, 128.4, 127.3, 125.6, 122.9, 67.9, 43.6, 43.1, 42.8, 28.3; IR (Neat Film, NaCl) 2890, 2924, 1765, 1595, 1491, 1385, 1298, 1241, 1056, 747 cm⁻¹; HRMS (MM: ESI-APCI) m/z calc'd for C₁₄H₁₅O [M+H]⁺: 199.1117; found 199.1120; $[\alpha]_D^{25}$ –41.23 (c 0.30, CHCl₃, 92% ee).



(S)-5-allyl-5-methyldihydrofuran-2(3H)-one (53). Dihydrofuranone **53** was generated from 2-carboxyallylcyclobutanone **51**, via cyclobutanone **52**, following the general procedures described above (see SI 3, SI 10 and SI 16). When compared with known compound (5*S*)-(+)-5-allyl-5-methyldihydrofuran-2(3*H*)-one, the optical rotation value for **53** was found to be of the same sign and of nearly identical magnitude ($[\alpha]_{\text{D}}^{25} +2.96$ (c 1.5, CH_3OH), literature value: $[\alpha]_{\text{D}}^{17} +3.33$ (c 1.27, CH_3OH)).⁵⁰ The absolute configurations of all other compounds described herein were established by analogy to **52**. Cyclobutanone **51** was isolated by flash column chromatography (SiO_2 , 3% Et_2O in pentane to 7% Et_2O in pentane) as a colorless oil. 84% yield. $R_f = 0.4$ (15% EtOAc in hexanes); $^1\text{H NMR}$ (300 MHz, CDCl_3) δ 5.90 (ddt, $J = 17.2, 10.5, 5.6$ Hz, 1H), 5.38–5.14 (m, 2H), 4.63 (dt, $J = 5.6, 1.4$ Hz, 2H), 3.42–3.06 (m, 2H), 2.65 (td, $J = 11.3, 6.3$ Hz, 1H), 1.88 (ddd, $J = 11.6, 9.9, 7.5$ Hz, 1H), 1.49 (s, 3H); $^{13}\text{C NMR}$ (126 MHz, CDCl_3) δ 204.6, 169.8, 131.6, 118.4, 65.9, 45.2, 23.1, 18.6; IR (Neat Film, NaCl) 2933, 1792, 1730, 1457, 1376, 1274, 1193, 1147, 1050, 983 cm^{-1} ; HRMS (MM: ESI-APCI) m/z calc'd for $\text{C}_9\text{H}_{12}\text{O}_2$ $[\text{M}+\text{H}]^+$: 153.0910; found 153.0905. Cyclobutanone **52** was isolated by flash column chromatography (SiO_2 , 1% Et_2O in pentane to 5% Et_2O in pentane) as a colorless oil. 56% yield. $R_f = 0.3$ (10% EtOAc in hexanes); $^1\text{H NMR}$ (500 MHz, CDCl_3) δ 5.76 (ddt, $J = 16.6, 10.5, 7.3$ Hz, 1H), 5.14–5.05 (m, 2H), 3.08–2.89 (m, 2H), 2.31 (ddt, $J = 13.8, 7.2, 1.2$ Hz, 1H), 2.21 (ddt, $J = 13.8, 7.5, 1.1$ Hz, 1H), 1.98 (ddd, $J = 11.3, 10.3, 6.7$ Hz, 1H), 1.73 (ddd, $J = 11.3, 10.1, 6.9$ Hz, 1H), 1.19 (s, 3H); $^{13}\text{C NMR}$ (126 MHz,

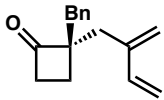
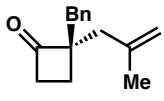
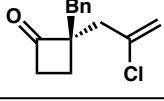
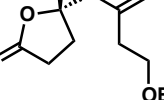
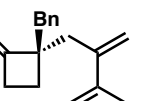
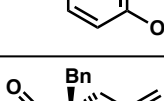
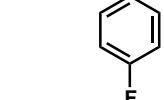
CDCl₃) δ 214.1, 140.0, 135.6, 128.4, 127.3, 125.6, 122.9, 67.9, 43.6, 43.1, 42.8, 28.3; IR (Neat Film, NaCl) 2929, 2854, 1728, 1323, 1261, 1170, 1129, 1060, 1019, 799 cm⁻¹; HRMS (MM: ESI-APCI) m/z calc'd for C₈H₁₂O [M+H]⁺: 125.0961; found 125.0955. Enantiomeric excess was determined for the corresponding Baeyer-Villiger product **53**, which was isolated as by flash column chromatography (SiO₂, 10% Et₂O in pentane) as a colorless oil (81% yield). Spectroscopic and physical data for **53** were identical to those reported in the literature.⁷ ($[\alpha]_D^{25}$ +2.96 (c 1.5, CH₃OH), 83% ee).

1.6.8 Determination of enantiomeric excess

Table 1.6.8 Determination of enantiomeric excess

entry	compound	assay method and conditions	retention time of major isomer (min)	retention time of minor isomer (min)	%ee
1		SFC, 10% MeOH in CO ₂ , 2.5 mL/min, AS-H col.	5.31	6.02	99
2		SFC, 3% MeOH in CO ₂ , 2.5 mL/min, AS-H col.	2.68	3.08	90
3		SFC, 3% MeOH in CO ₂ , 3 mL/min, OJ-H col.	8.91	7.93	95
4		SFC, 2% MeOH in CO ₂ , 3 mL/min, OJ-H col.	10.43	11.45	93
5		SFC, 2% MeOH in CO ₂ , 2.5 mL/min, AS-H col.	8.82	8.38	97
6		SFC, 1% MeOH in CO ₂ , 2.5 mL/min, AS-H col.	3.37	3.15	92
7		SFC, 2% MeOH in CO ₂ , 3.0 mL/min, OJ-H col.	2.68	4.32	93
8		HPLC, 2% <i>i</i> PrOH in hexanes, 0.6 mL/min, AD col.	9.74	8.94	92

Table 1.6.8 Determination of enantiomeric excess (continued)

entry	compound	assay method and conditions	retention time of major isomer (min)	retention time of minor isomer (min)	%ee
9		SFC, 1% MeOH in CO ₂ , 2.5 mL/min, OB-H col.	3.40	2.83	91
10		SFC, 1% MeOH in CO ₂ , 3 mL/min, OB-H col.	2.76	2.53	90
11		GC, 110 °C, isotherm 1 mL/min, GTA col.	10.41	11.34	93
12		SFC, 1% MeOH in CO ₂ , 2.5 mL/min, OB-H col.	3.38	2.93	86
13		SFC, 10% MeOH in CO ₂ , 3.0 mL/min, AD-H col.	6.09	7.29	89
14		SFC, 1% MeOH in CO ₂ , 2.5 mL/min, AS-H col.	16.17	14.84	92
15		SFC, 1% MeOH in CO ₂ , 3 mL/min, AS-H col.	7.29	6.78	94
16		GC, 130 °C, isotherm 1 mL/min, GTA col.	10.15	13.32	83

1.7 REFERENCES AND NOTES

- (1) Carbon-carbon s-bond formation. In *Comprehensive Organic Synthesis*; Trost, B.M., Fleming, I., Eds.; Pergamon Press: New York, 1991; Vol. 3.
- (2) (a) Cain, D. Alkylation and Related Reactions of Ketones and Aldehydes via Metal Enolates. In *Carbon-Carbon Bond Formation*; Augustine, R. L., Ed.; Marcel Dekker: New York, 1979; Vol. 1, pp 85–250. (b) Seebach, D. *Angew. Chem., Int. Ed. Engl.* **1988**, *27*, 1624.
- (3) (a) Trost, B. M. *Chem. Pharm. Bull.* **2002**, *50*, 1. (b) Polet, D.; Alexakis, A. *Chim. Oggi* **2007**, *25*, 31. (c) Mohr, J. T.; Stoltz, B. M. *Chem.–Asian J.* **2007**, *2*, 1476. (d) Falciola, C. A.; Alexakis, A. *Eur. J. Org. Chem.* **2008**, 3765. (e) Trost, B. M. *Org. Process Res. Dev.* **2012**, *16*, 185.
- (4) (a) Shimizu, I.; T. Yamada, J. Tsuji, *Tet. Lett.* **1980**, *21*, 3199. (b) Tsuji, J.; I. Minami, I. Shimizu *Tet. Lett.* **1983**, *24*, 1793. (c) Tsuji, J.; I. Minami, I. Shimizu, *Chem. Lett.* **1983**, 1325.
- (5) (a) Hughes, D. L. Alkylation of Enolates. In *Comprehensive Asymmetric Catalysis*; Jacobsen, E. N., Pfaltz, A., Yamamoto, H., Eds.; Springer: Berlin,

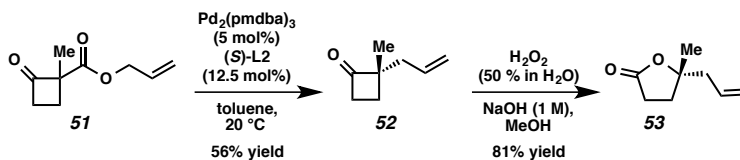
- 1999; Vol. 2, pp 1273–1294. (b) Hughes, D. L. Alkylation of Enolates. In *Comprehensive Asymmetric Catalysis*; Jacobsen, E. N., Pfaltz, A., Yamamoto, H., Eds.; Springer: Berlin, 2004; Supplement 1, pp161.
- (6) (a) Doyle, A. G.; Jacobsen, E. N. *J. Am. Chem. Soc.* **2005**, *127*, 62. (b) Yamashita, Y.; Odashima, K.; Koga, K. *Tetrahedron Lett.* **1999**, *40*, 2803. (c) Dolling, U.-H.; Davis, P.; Grabowski, E. J. J. *J. Am. Chem. Soc.* **1984**, *106*, 446.
- (7) Tsuji, J.; Minami, I. *Acc. Chem. Res.* **1987**, *20*, 140.
- (8) Helmchen, G.; Pfaltz, A. *Acc. Chem. Res.* **2000**, *33*, 336.
- (9) Behenna, D. C.; Stoltz, B. M. *J. Am. Chem. Soc.* **2004**, *126*, 15044.
- (10) Mohr, J. T.; Behenna, D. C.; Harned, A. M.; Stoltz, B. M. *Angew. Chem. Int. Ed.* **2005**, *44*, 6924
- (11) White, D. E.; Stewart, I. C.; Grubbs, R. H.; Stoltz, B. M. *J. Am. Chem. Soc.* **2008**, *130*, 810.
- (12) Levine, S. R.; Krout, M. R.; Stoltz, B. M. *Org. Lett.* **2009**, *11*, 289.
- (13) Seto, M.; Roizen, J. L.; Stoltz, B. M. *Angew. Chem. Int. Ed.* **2008**, *47*, 6873.

- (14) Mohr, J. T.; Krout, M. R.; Stoltz, B. M. *Org. Synth.* **2009**, *86*, 194.
- (15) Behenna, D. C.; J. T. Mohr, N. H. Sherden, S. C. Marinescu, A. M. Harned, K. Tani, M. Seto, S. Ma, Z. Novák, M. R. Krout, R. M. McFadden, J. L. Roizen, J. A. Enquist Jr., D. E. White, S. R. Levine, K. V. Petrova, A. Iwashita, S. C. Virgil, B. M. Stoltz, *Chem.—Eur. J.* **2011**, *17*, 14199.
- (16) (a) Trost, B. M.; Xu, J. *J. Am. Chem. Soc.* **2005**, *127*, 2846. (b) Trost, B. M.; Xu, J. *J. Am. Chem. Soc.* **2005**, *127*, 17180. (c) Trost, B. M.; Bream, R. N.; Xu, J. *Angew. Chem. Int. Ed.* **2006**, *45*, 3109. (d) Trost, B. M.; Xu, J.; Schmidt, T. *J. Am. Chem. Soc.* **2009**, *131*, 18343.
- (17) (a) Belluš, D.; B. Ernst, *Angew. Chem. Int. Ed. Engl.* **1988**, *27*, 797. (b) Sergeiko, A.; V. V. Poroikov, L. O. Hanus, V. M. Dembitsky, *Open Med. Chem. J.* **2008**, *2*, 26. (c) Dembitsky, V. M.; *J. Nat. Med.* **2008**, *62*, 1. (d) Yoshikawa, K.; A. Kaneko, Y. Matsumoto, H. Hama, S. Arihara, *J. Nat. Prod.* **2006**, *69*, 1267. (e) Marrero, J.; A. D. Rodríguez, P. Baran, R. G. Raptis, J. A. Sánchez, E. Ortega-Barria, T. L. Capson, *Org. Lett.* **2004**, *6*, 1661. (f) Li, Y.-S.; K. Matsunaga, M. Ishibashi, Y. Ohizumi, *J. Org. Chem.* **2001**, *66*, 2165. (g) Tanaka, N.; M. Okasaka, Y. Ishimaru, Y. Takaishi, M. Sato, M. Okamoto, T. Oshikawa, S. U. Ahmed, L. M. Consentino, K.-H. Lee, *Org. Lett.* **2005**, *7*, 2997. (h) Jiang, B.; J. Qiao, Y. Yang, Y. Lu, *J. Cell. Biochem.* **2012**, *113*, 2560.

- (18) (a) Seiser, T.; T. Saget, D. N. Tran, N. Cramer, *Angew. Chem.* **2011**, *123*, 7884; *Angew. Chem. Int. Ed.* **2011**, *50*, 7740. (b) Fu, N.-Y.; S.-H. Chan, H. N. C. Wong in *Patai Series: the Chemistry of Functional Groups* (Eds.: Z. Rappoport, J. F. Liebman, S. Patai) John Wiley & Sons, Ltd, Chichester, UK, **2005**. pp. 357–440.
- (19) Bauzá, A.; D. Quiñero, P. M. Deyà, A. Frontera, *Chem. Phys. Lett.* **2012**, *536*, 166.
- (20) Wiberg, K. B. in *Patai Series: the Chemistry of Functional Groups* (Eds.: Z. Rappoport, J. F. Liebman, S. Patai), John Wiley & Sons, Ltd, Chichester, UK, **2005**. pp. 1–15.
- (21) Bauld, N. L.; J. Cessac, R. L. Holloway, *J. Am. Chem. Soc.* **1977**, *99*, 8140.
- (22) Berg, U. in *Patai Series: the Chemistry of Functional Groups* (Eds.: Z. Rappoport, J. F. Liebman, S. Patai) John Wiley & Sons, Ltd, Chichester, UK, **2005**. pp. 83–131.
- (23) (a) Pete, J.-P. *Advances in Photochemistry*, John Wiley & Sons, Inc., Hoboken, NJ, USA, **1996**. (b) Hehn, J. P.; C. Mueller, T. Bach in *Handbook of Synthetic Photochemistry* (Eds.: A. Albini, M. Fagnoni), Wiley-VCH, Weinheim, **2010**, pp. 171–215. (c) N. Hoffmann in *Handbook of Synthetic Photochemistry* (Eds.: A.

- Albini, M. Fagnoni), Wiley-VCH, Weinheim, **2010**, pp. 137–169. (d) Lee-Ruff, E. in *Methods of Organic Chemistry, Vol. E17e* (Ed.: A. De Meijere), Georg Thieme Verlag, Stuttgart, **1997**, pp 179–187.
- (24) (a) Fitjer, L. in *Methods of Organic Chemistry Vol. E17e* (Ed.: A. De Meijere), Georg Thieme Verlag: Stuttgart, **1997**, pp 251-316. (b) Lee-Ruff, E. in *Patai Series: the Chemistry of Functional Groups* (Eds.: Z. Rappoport, J. F. Liebman, S. Patai) John Wiley & Sons, Ltd, Chichester, UK, **2005**, pp. 281–355.
- (25) Chaumontet, M.; R. Piccardi, N. Audic, J. Hitce, J.-L. Peglion, E. Clot, O. Baudoin, *J. Am. Chem. Soc.* **2008**, *130*, 15157.
- (26) (a) Markham, J. P.; S. T. Staben, F. D. Toste, *J. Am. Chem. Soc.* **2005**, *127*, 9708. (b) F. Kleinbeck, F. D. Toste, *J. Am. Chem. Soc.* **2009**, *131*, 9178.
- (27) López-Carrillo, V.; A. M. Echavarren, *J. Am. Chem. Soc.* **2010**, *132*, 9292.
- (28) Mailhol, D.; Duque, M. d. M. S.; Raimondi, W.; Bonne, D.; Constantieux, T.; Coquerel, Y.; Rodriguez, J. *Adv. Synth. & Catal.* **2012**, *354*, 3523.
- (29) (a) Lee-Ruff, E.; G. Mladenova, *Chem. Rev.* **2003**, *103*, 1449. (b) Trost, B. M.; T. Yasukata, *J. Am. Chem. Soc.* **2001**, *123*, 7162. (c) Nemoto, H.; H. Ishibashi, M. Nagamochi, K. Fukumoto, *J. Org. Chem.* **1992**, *57*, 1707.

- (30) See references: 9, 10, 13 and (a) Streuff, J.; D. E. White, S. C. Virgil, B. M. Stoltz, *Nature Chem.* **2010**, 2, 192. (b) Behenna, D. C.; Y. Liu, T. Yurino, J. Kim, D. E. White, S. C. Virgil, B. M. Stoltz, *Nature Chem.* **2012**, 4, 130.
- (31) McDougal, N. T.; Virgil, S. C.; Stoltz, B. M. *Synlett* **2010**, 1712.
- (32) Baum, J. S.; Shook, D. A.; Davies, H. M. L.; Smith, H. D. *Synth. Commun.* **1987**, 14, 1709.
- (33) Presset, M.; Coquerel, Y.; Rodriguez, J. *J. Org. Chem.* **2009**, 74, 415.
- (34) Derivatization of allylic alkylation product 2-allyl-2-methylcyclobutanone **52** to known compound (5*S*)-5-allyl-5-methyldihydrofuran-2(3*H*)-one **53** (below) allowed for comparison of optical rotation data and, by chemical correlation, confirmed (5*S*) absolute configuration (see supporting information). The absolute stereo-configuration of all other products generated in this study were assigned by analogy. These data are consistent with the absolute configurations observed in previous studies on 5-, 6- and 7-membered rings (see ref. 14).



- (35) (a) Sherden, N. H.; D. C. Behenna, S. C. Virgil, B. M. Stoltz, *Angew. Chem. Int. Ed.* **2009**, *48*, 6840. (b) Keith, J. A.; D. C. Behenna, N. Sherden, J. T. Mohr, S. Ma, S. C. Marinescu, R. J. Nielsen, J. Oxgaard, B. M. Stoltz, W. A. Goddard, III. *J. Am. Chem. Soc.* **2012**, *134*, 19050.
- (36) For protocol for the use of Symxy robot, see Appendix 5, vide infra.
- (37) Stevens, S. J.; Bérubé, A.; Wood, J. L. *Tetrahedron* **2011**, *67*, 6479.
- (38) Moustafa, M. M. A. R.; Pagenkopf, B. L. *Org. Lett.* **2010**, *12*, 4732.
- (39) Moustafa, M. M. A. R.; Stevens, A. C.; Machin, B. P.; Pagenkopf, B. L. *Org. Lett.* **2010**, *12*, 4736.
- (40) (a) Nishimura, T.; Ohe, K.; Uemura, S. *J. Am. Chem. Soc.* **1999**, *121*, 2645. (b) Matsuda, T.; Makino, M.; Murakami, M. *Angew. Chem.* **2005**, *117*, 4684; *Angew. Chem. Int. Ed.* **2005**, *44*, 4608. (c) Matsuda, T.; Shigeno, M.; Murakami, M. *J. Am. Chem. Soc.* **2007**, *129*, 12086. (d) Shigeno, M.; Yamamoto, T.; Murakami, M. *Chem.–Eur. J.* **2009**, *15*, 12929.
- (41) O'Brien, J. M.; Kingsbury, J. S. *J. Org. Chem.* **2011**, *76*, 1662.

- (42) Murakami, M.; Amii, H.; Shigeto, K.; Ito, Y. *J. Am. Chem. Soc.* **1996**, *118*, 8285.
- (43) (a) Matsuda, T.; Makino, M.; Murakami, M. *Bull. Chem. Soc. Jpn.* **2005**, *78*, 1528.
(b) Matsuda, T.; Makino, M.; Murakami, M. *Org. Lett.* **2004**, *6*, 1257.
- (44) Davies, H. M. L.; Cantrell, Jr., W. R.; Romines, K. R.; Baum, J. S. *Org. Syn.* **1992**, *70*, 93.
- (45) Hollingworth, C.; Hazari, A.; Hopkinson, M. N.; Tredwell, M.; Benedetto, E.; Huiban, M.; Gee, A. D.; Brown, J. M.; Gouverneur, V. *Angew. Chem. Int. Ed.* **2011**, *50*, 2613.
- (46) Passet, M.; Mailhol, D.; Coquerel, Y.; Rodriguez, J. *Synthesis* **2011**, 2549.
- (47) (a) Tani, K.; Behenna, D. C.; McFadden, R. M.; Stoltz, B. M. *Org. Lett.* **2007**, *9*, 2529. (b) Krout, M. R.; Mohr, J. T.; Stoltz, B. M. *Org. Synth.* **2009**, *86*, 181.
- (48) Ukai, T.; Kawazura, H.; Ishii, Y.; Bonnet, J. J.; Ibers, J. A. *J. Organometallic Chem.* **1999**, *65*, 253.
- (49) Fairlamb, I. J. S.; Kapdi, A. R.; Lee, A. F. *Org. Lett.* **2004**, *6*, 4435.

- (50) Matsuo, K.; Arase, T.; Ishida, S.; Sakaguchi, Y. *Heterocycles*, **1996**, *43*, 1287.

APPENDIX 1

Spectra Relevant to Chapter 1:

Enantioselective Construction of α -Quaternary Cyclobutanones by

Catalytic Asymmetric Allylic Alkylation

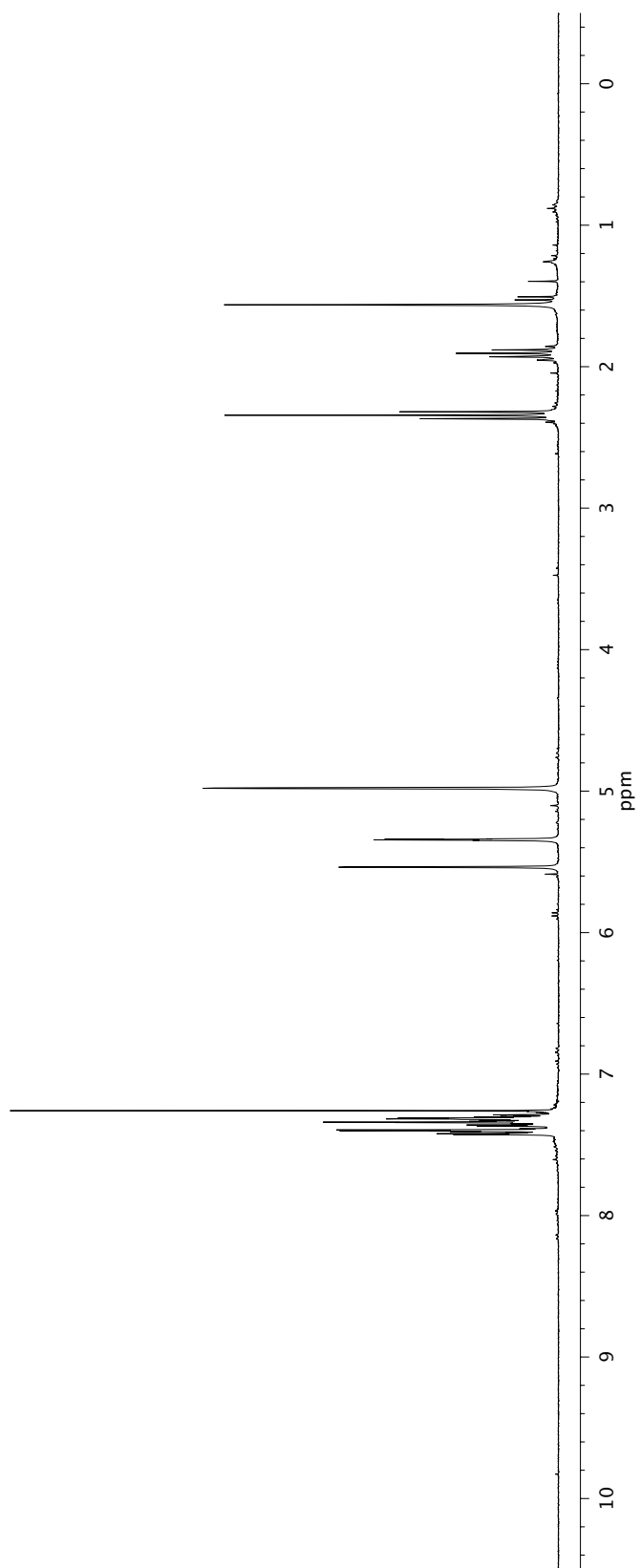
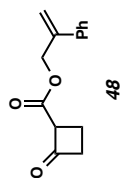


Figure A1.1 $^1\text{H NMR}$ (500 MHz, CDCl_3) of compound 48.

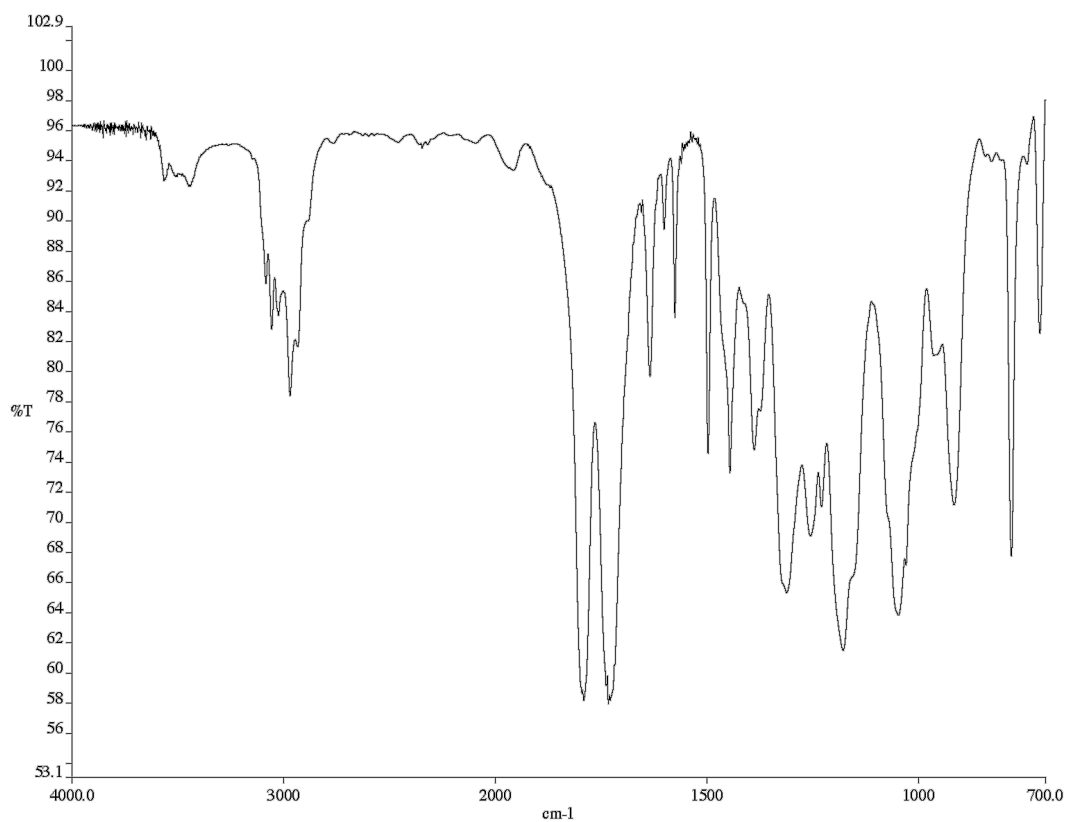


Figure A1.2 Infrared spectrum (thin film/NaCl) of compound **48**

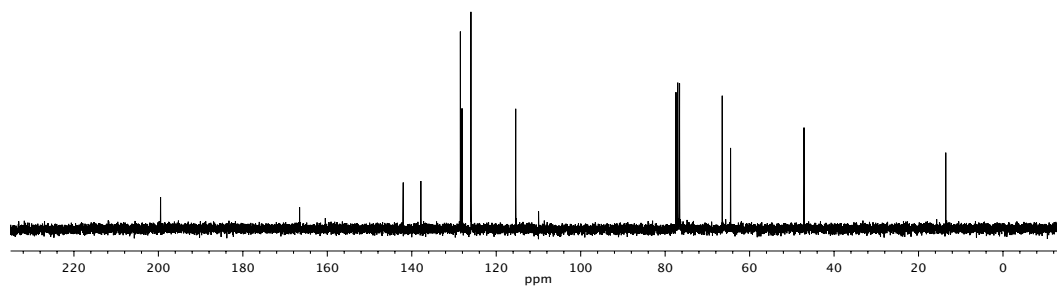


Figure A1.3 ¹³C NMR (75 MHz, CDCl₃) of compound **48**

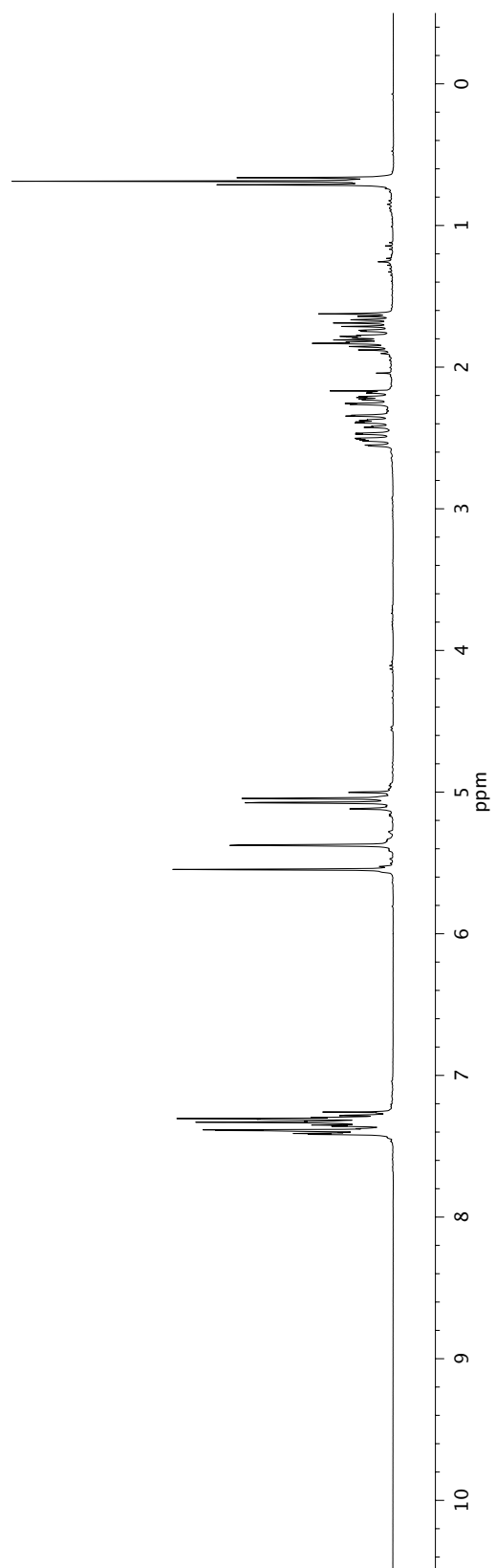
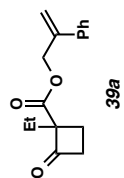


Figure A1.4 ^1H NMR (500 MHz, CDCl_3) of compound **39a**.

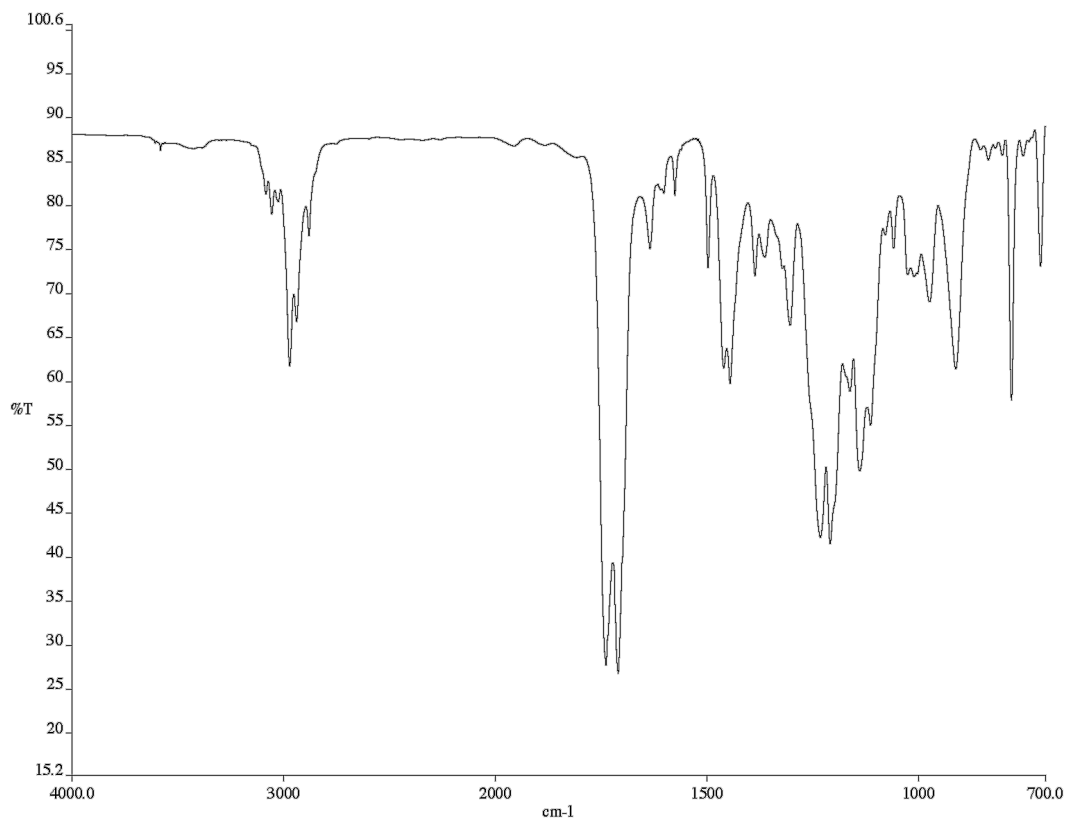


Figure A1.5 Infrared spectrum (thin film/NaCl) of compound **39a**

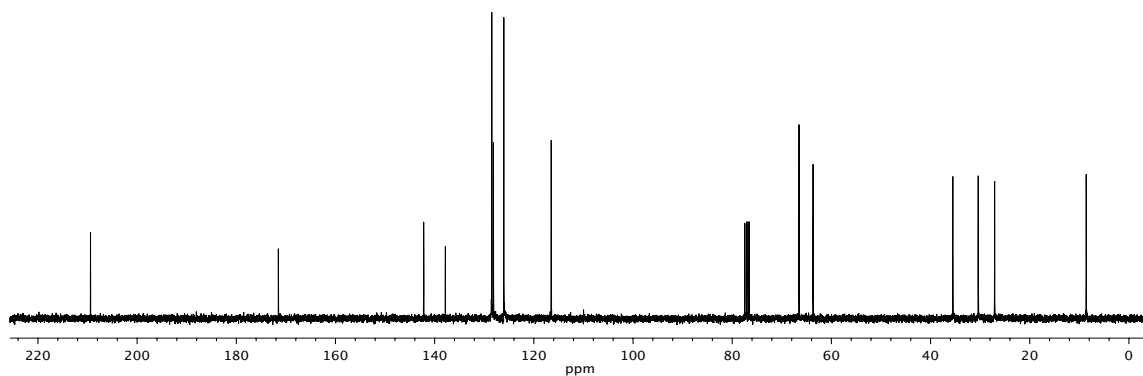


Figure A1.6 ¹³C NMR (125 MHz, CDCl₃) of compound **39a**

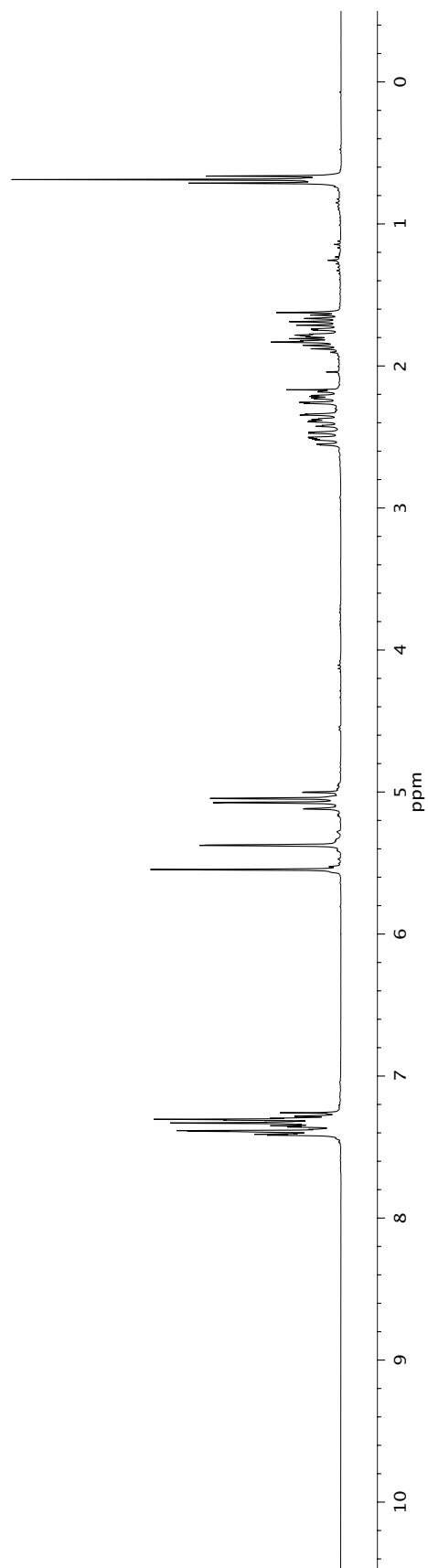
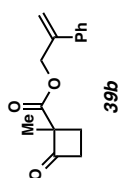


Figure A1.7 ¹H NMR (500 MHz, CDCl₃) of compound **39b**.

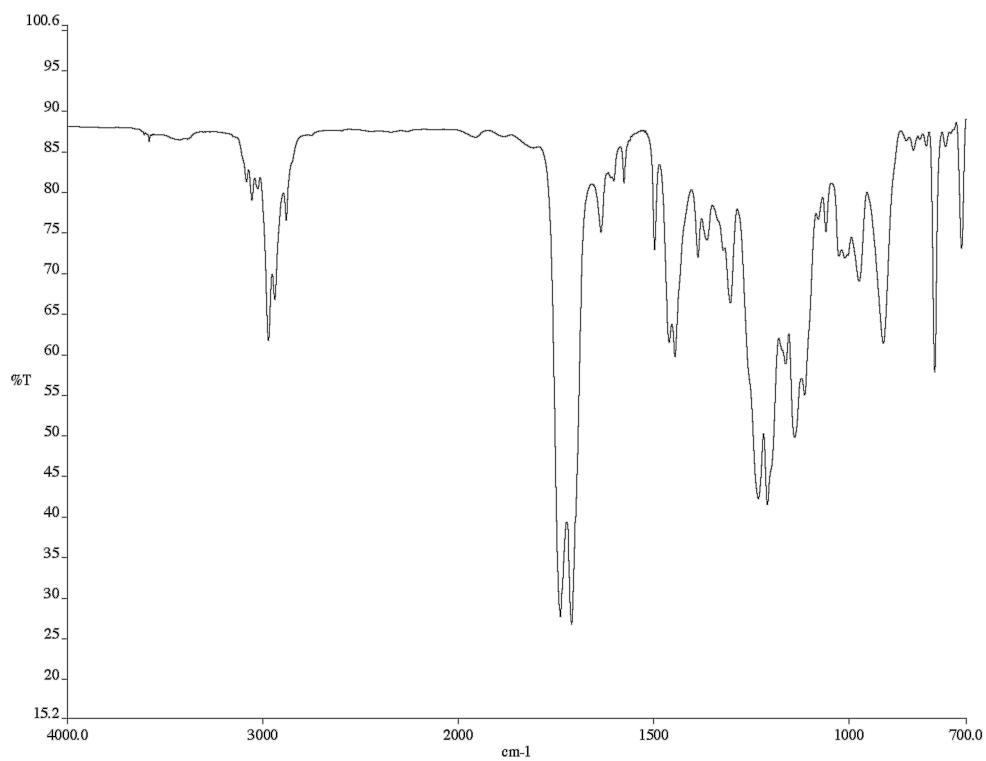


Figure A1.8 Infrared spectrum (thin film/NaCl) of compound **39b**.

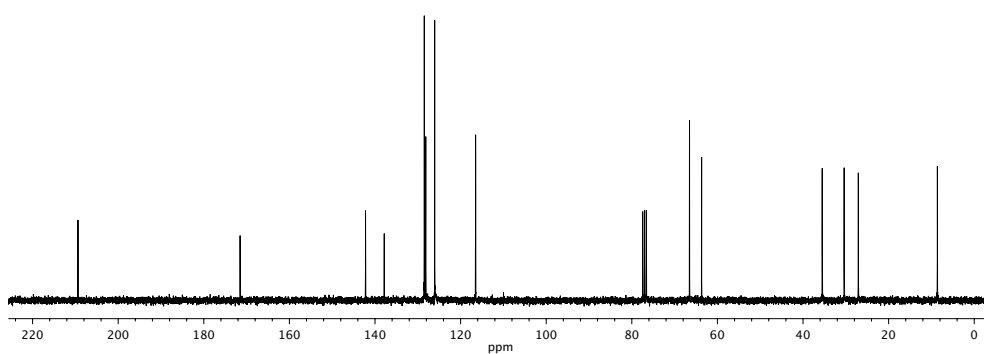


Figure A1.9 ¹³C NMR (125 MHz, CDCl₃) of compound **39b**.

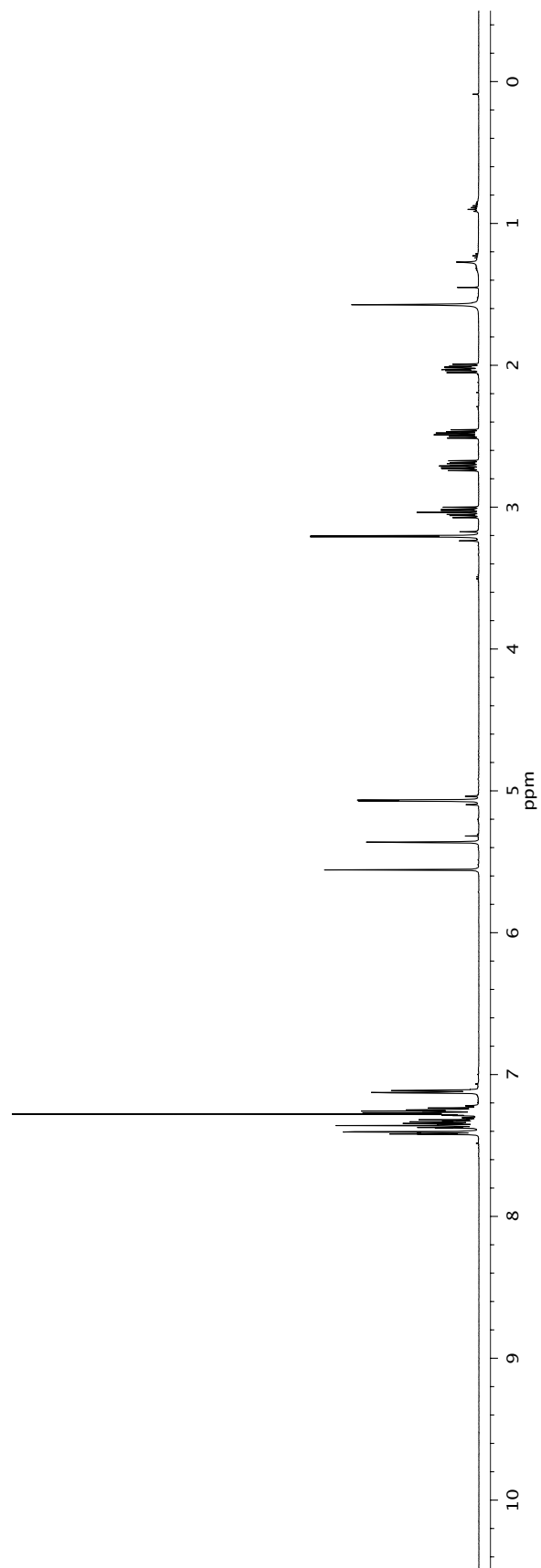
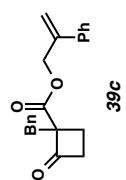


Figure A1.10 ¹H NMR (500 MHz, CDCl₃) of compound **39c**.

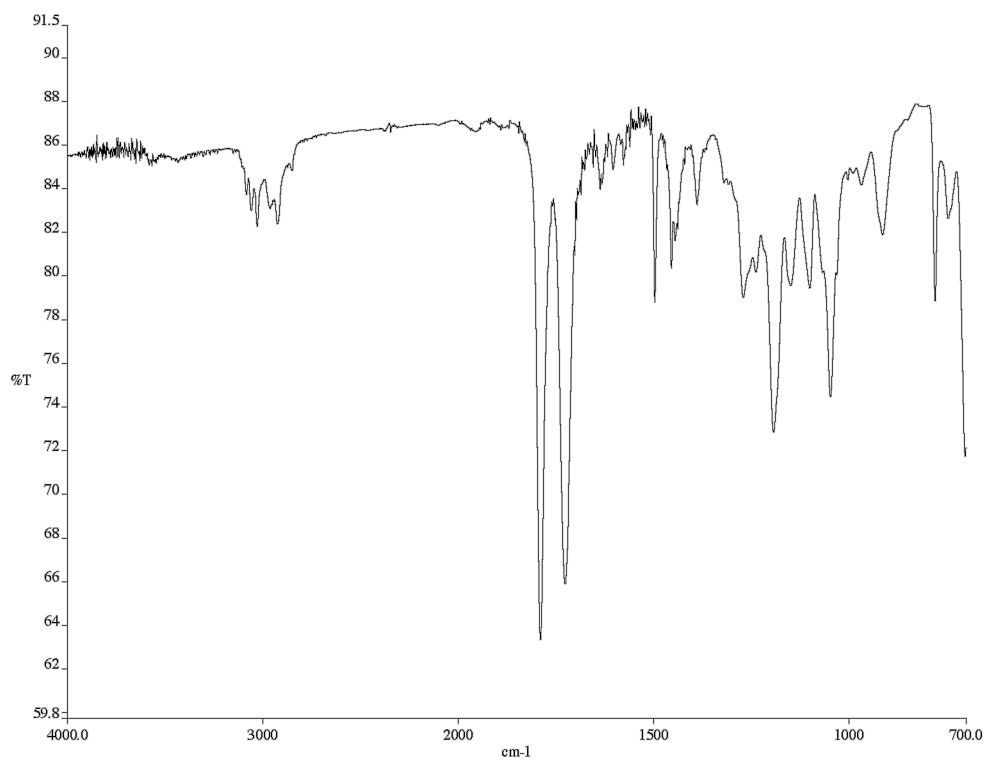


Figure A1.11 Infrared spectrum (thin film/NaCl) of compound **39c**.

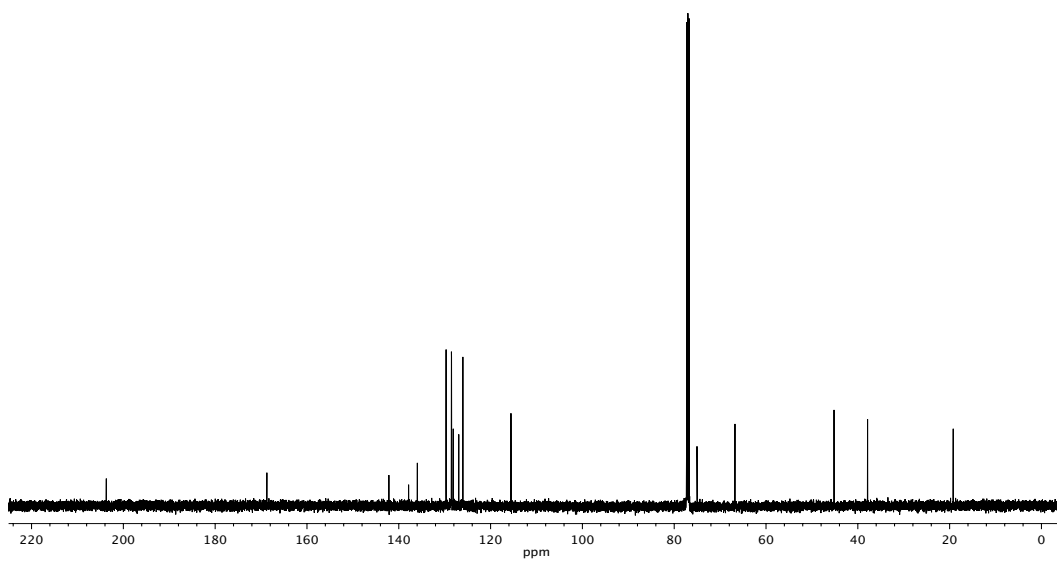


Figure A1.12 ¹³C NMR (125 MHz, CDCl₃) of compound **39c**.

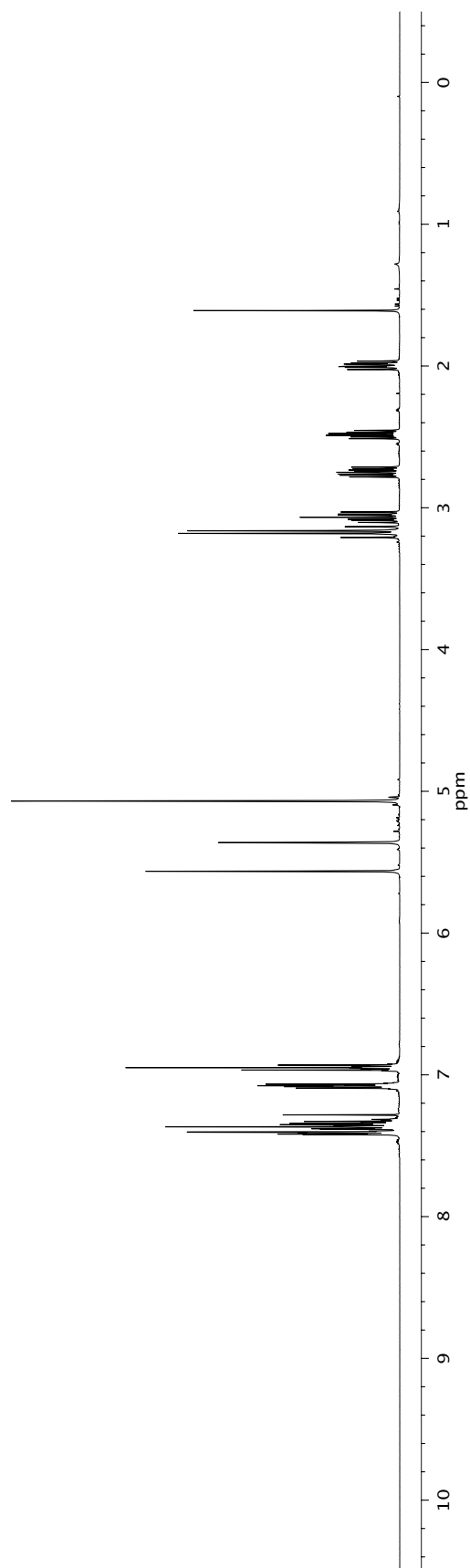
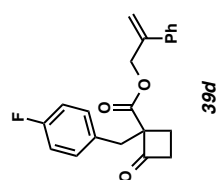


Figure A1.13 ¹H NMR (500 MHz, CDCl₃) of compound **39d**.

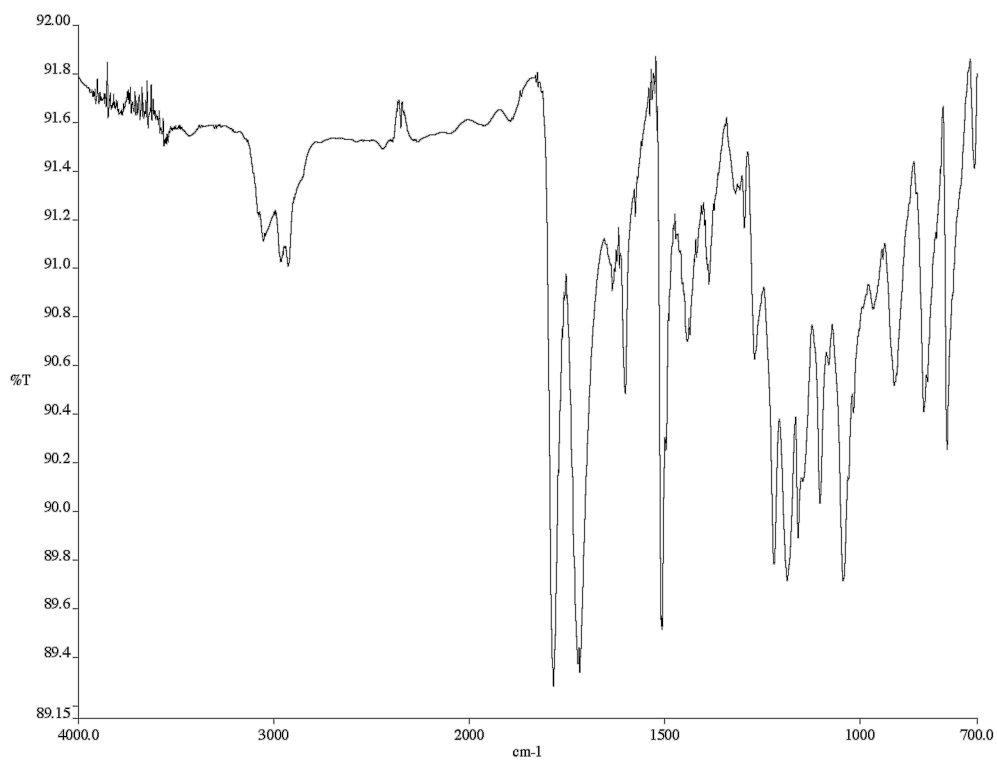


Figure A1.14 Infrared spectrum (thin film/NaCl) of compound **39d**.

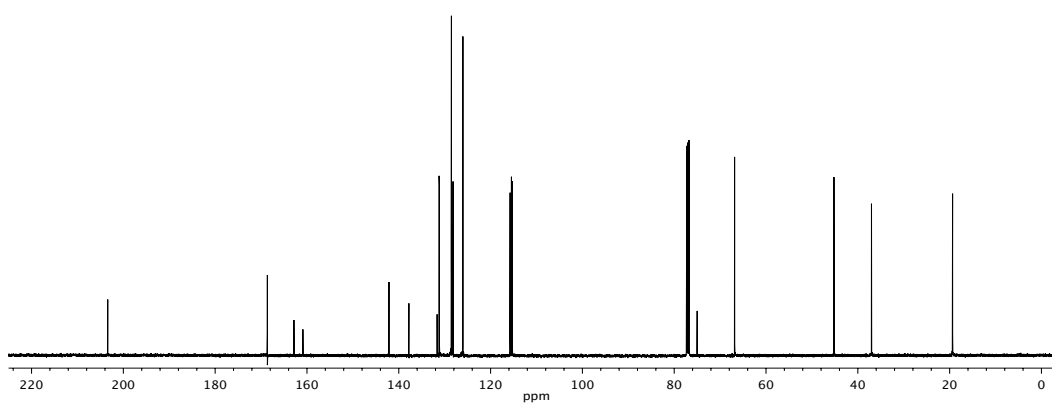


Figure A1.15 ¹³C NMR (125 MHz, CDCl₃) of compound **39d**.

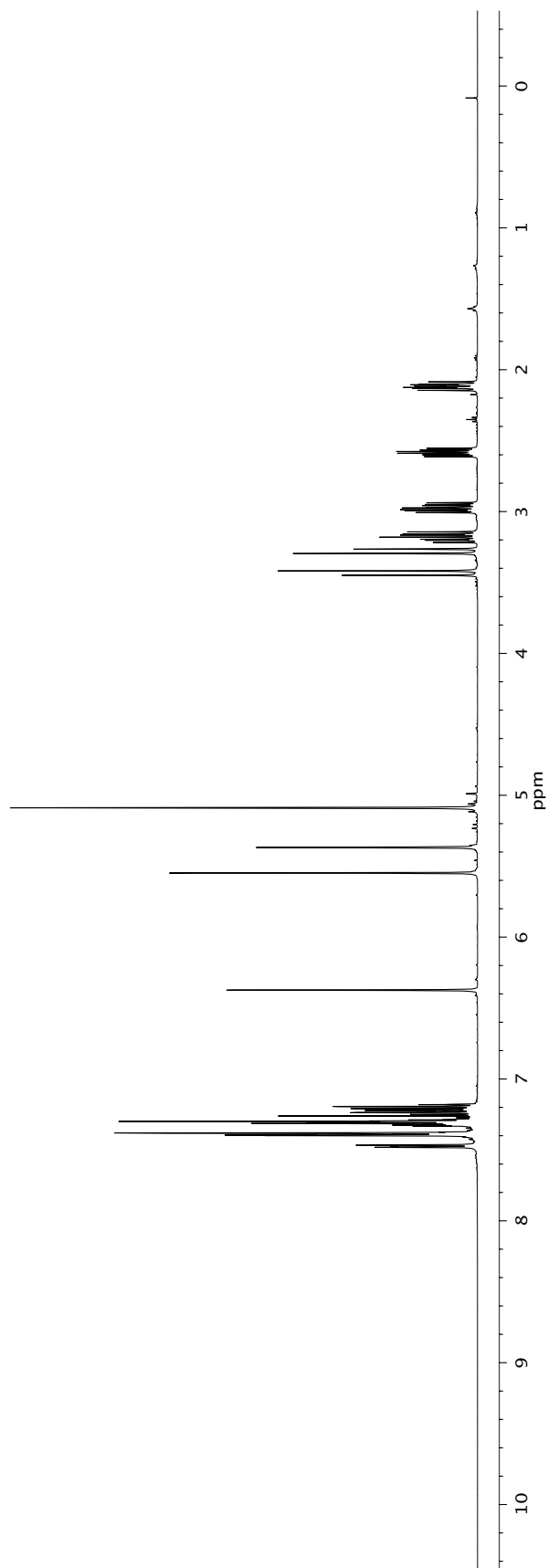
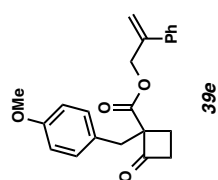


Figure A1.16 ¹H NMR (500 MHz, CDCl₃) of compound **39e**.

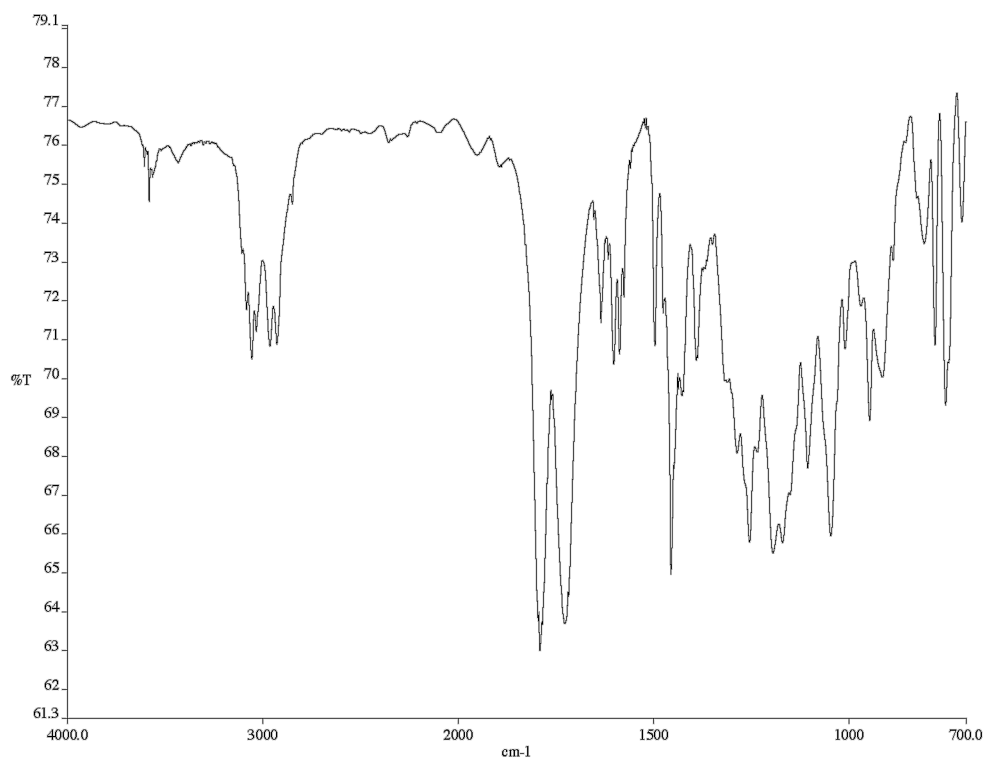


Figure A1.17 Infrared spectrum (thin film/NaCl) of compound **39e**.

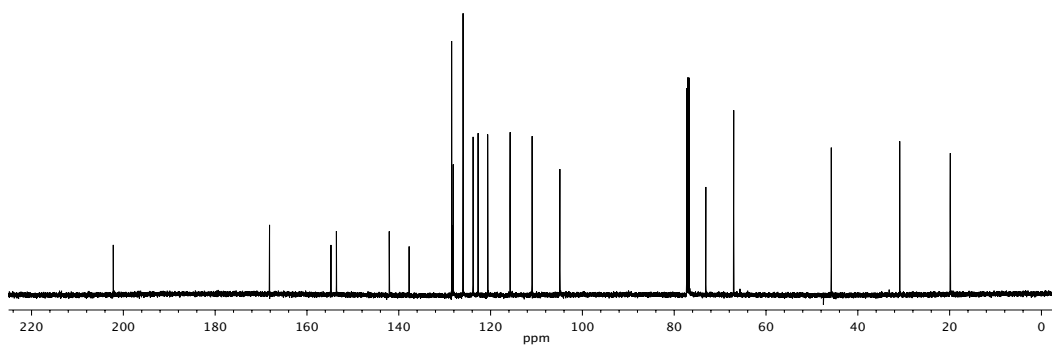


Figure A1.18 ¹³C NMR (125 MHz, CDCl₃) of compound **39e**.

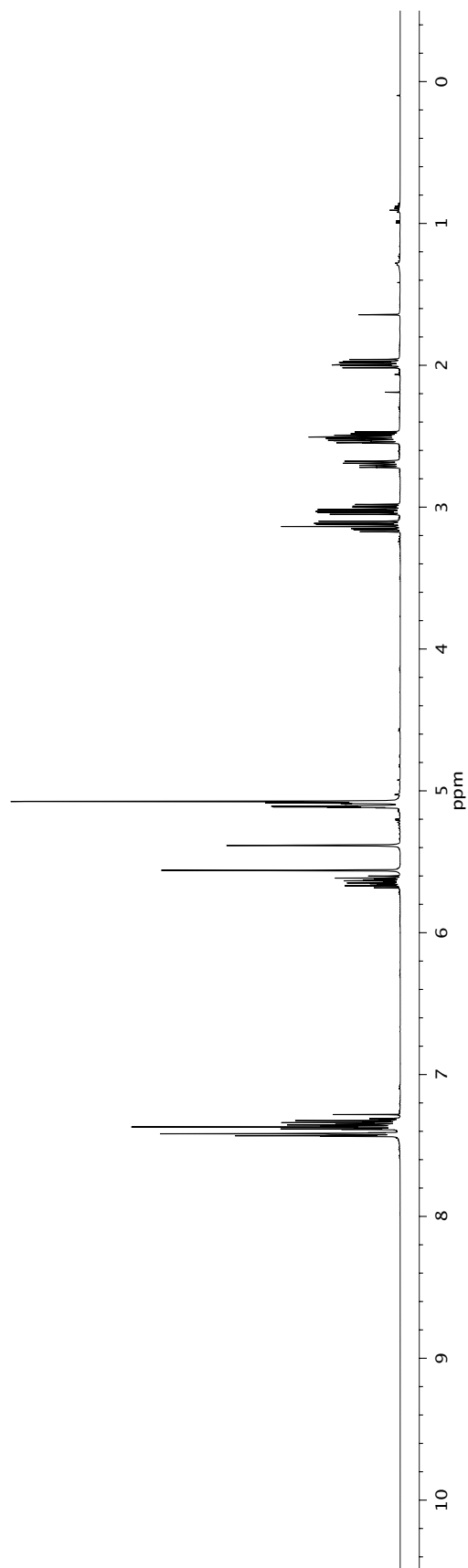
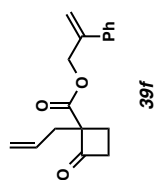


Figure A1.19 ^1H NMR (500 MHz, CDCl_3) of compound **39f**.

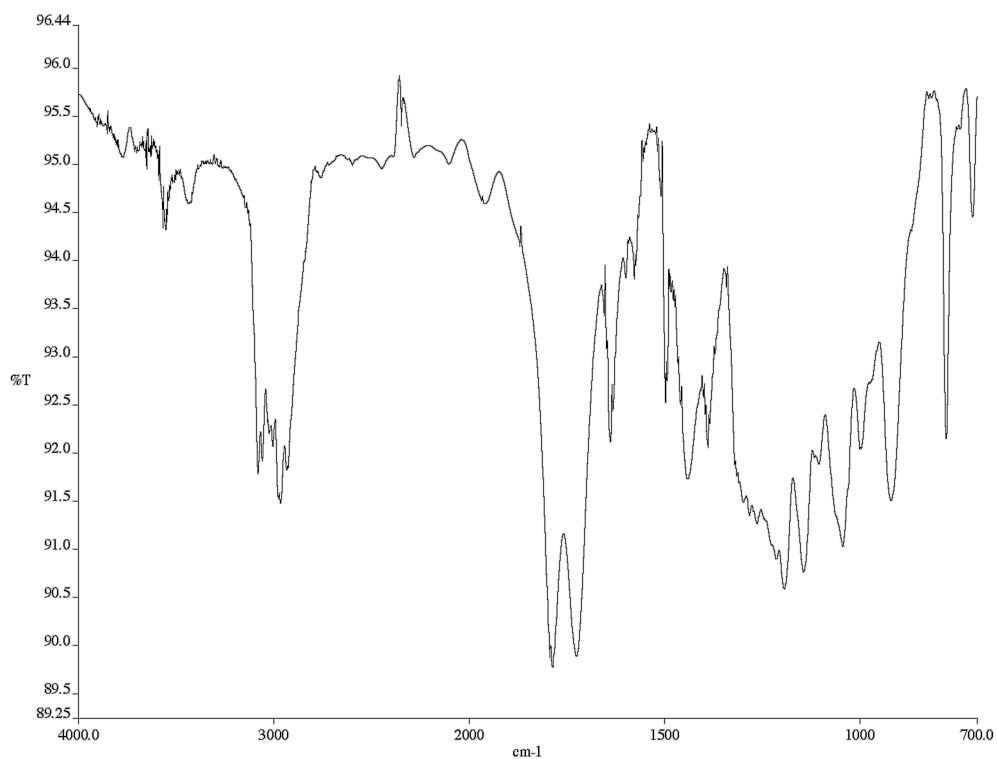


Figure A1.20 Infrared spectrum (thin film/NaCl) of compound **39f**.

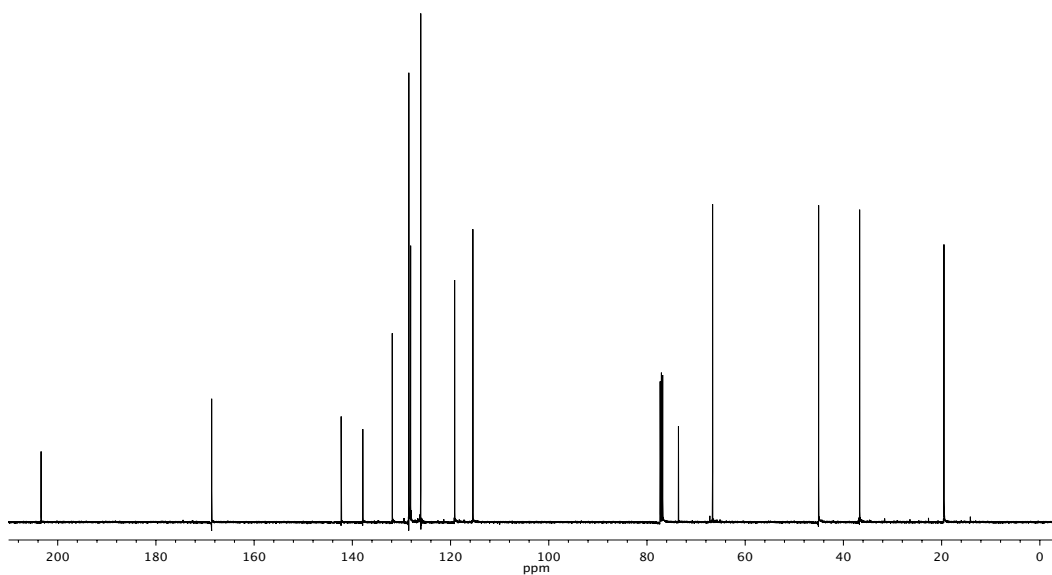


Figure A1.21 ¹³C NMR (125 MHz, CDCl₃) of compound **39f**.

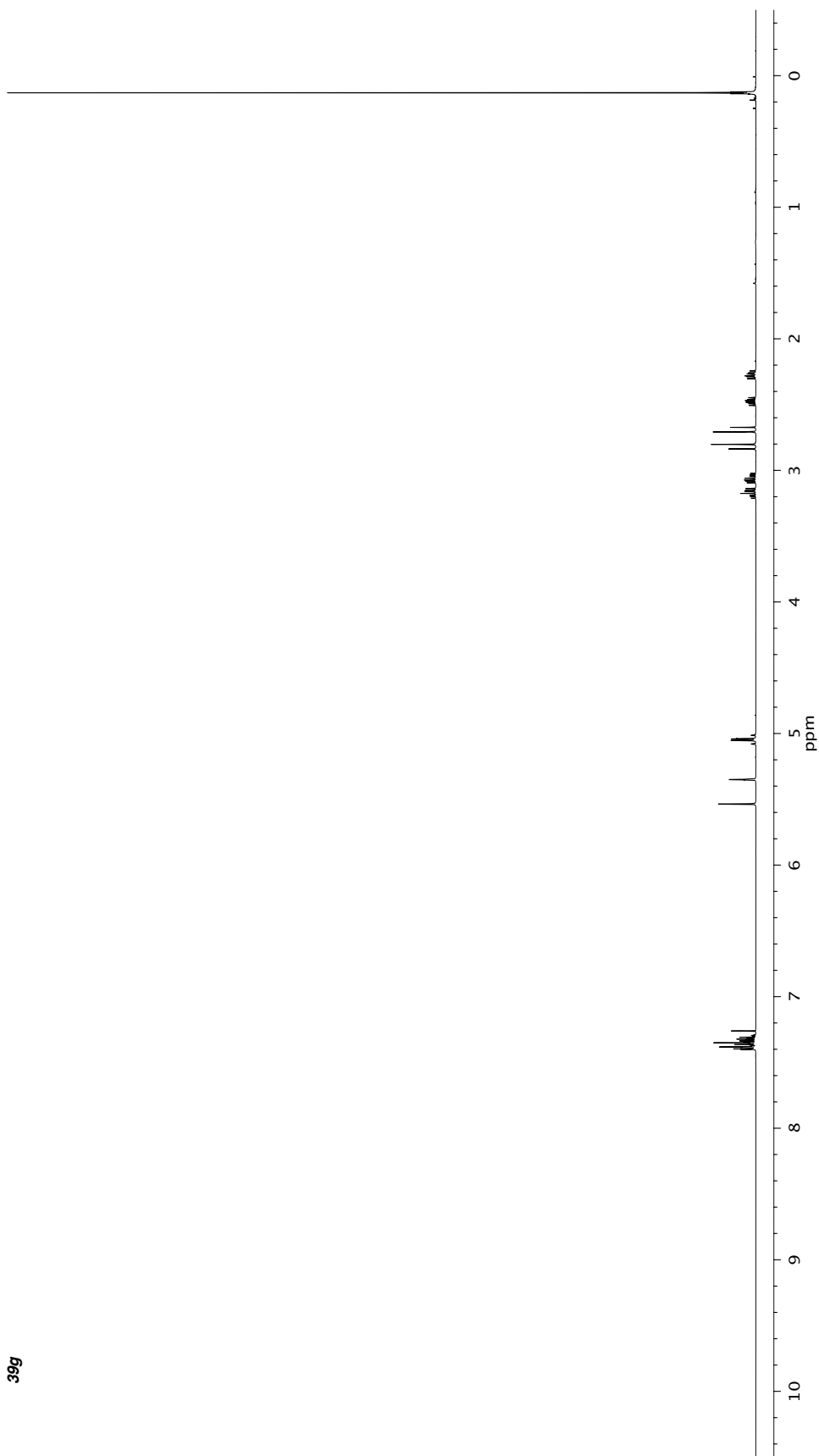
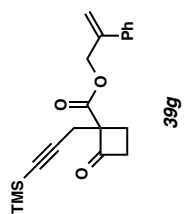


Figure A1.22 ¹H NMR (500 MHz, CDCl₃) of compound **39g**.

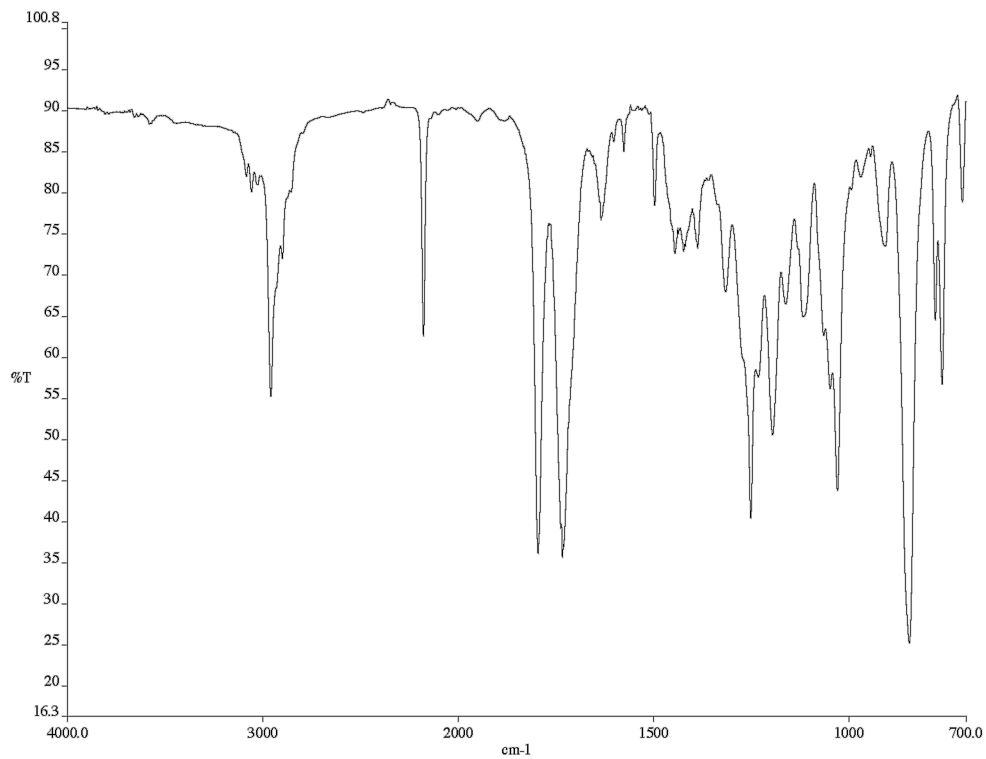


Figure A1.23 Infrared spectrum (thin film/NaCl) of compound **39g**.

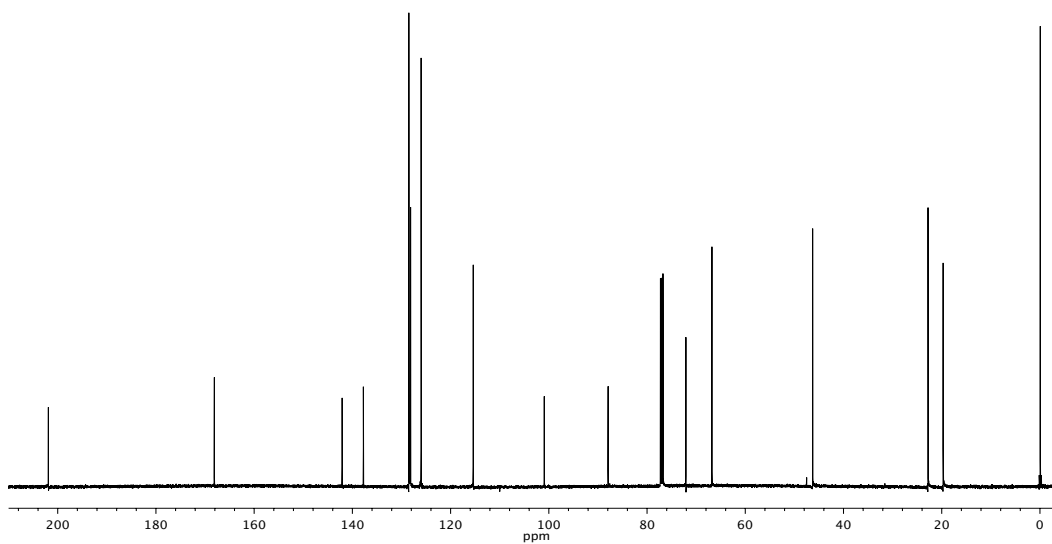


Figure A1.24 ^{13}C NMR (125 MHz, CDCl_3) of compound **39g**.

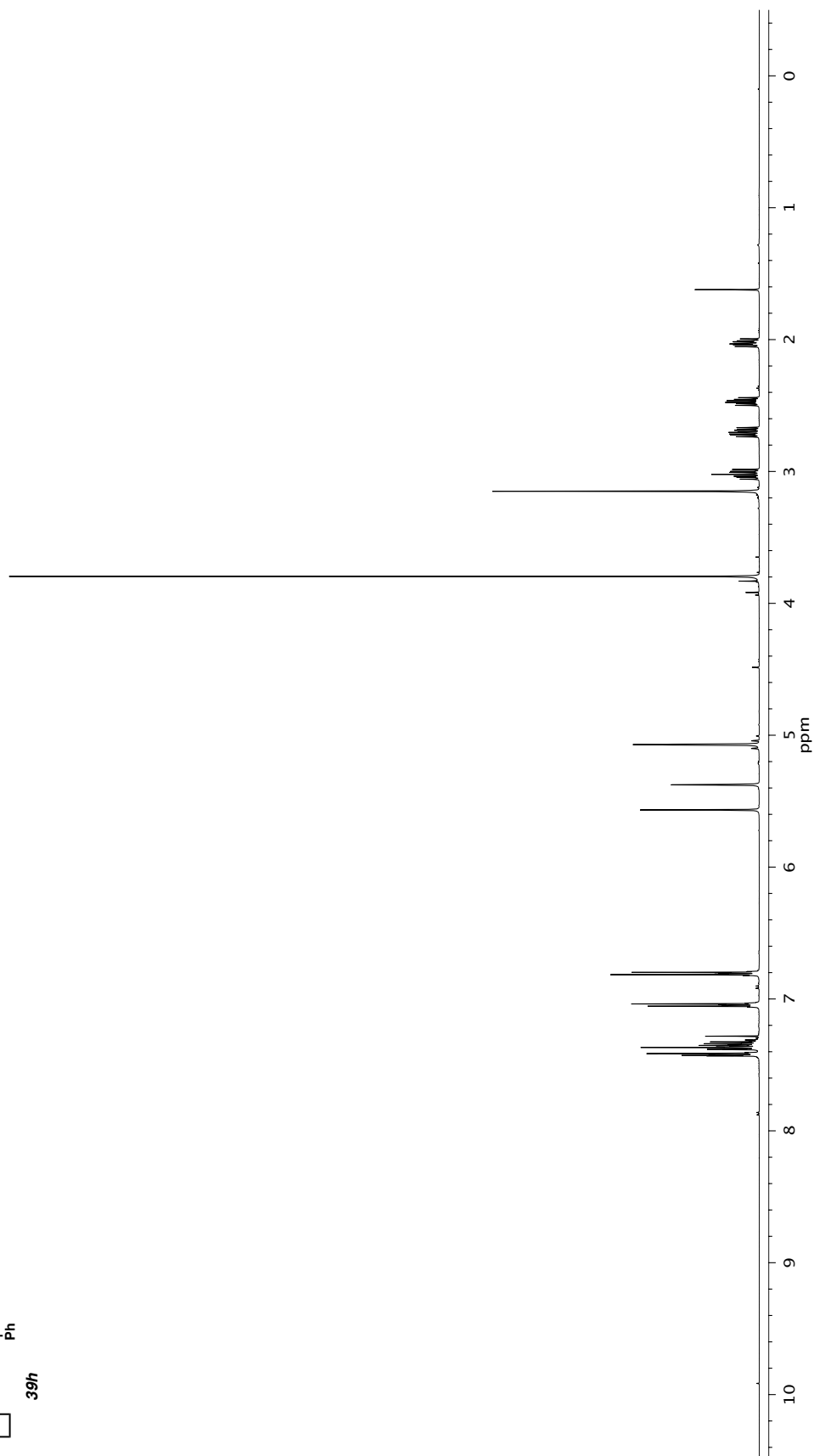
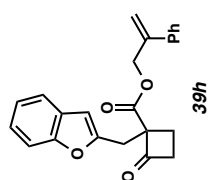


Figure A1.25 $^1\text{H NMR}$ (500 MHz, CDCl_3) of compound **39h**.

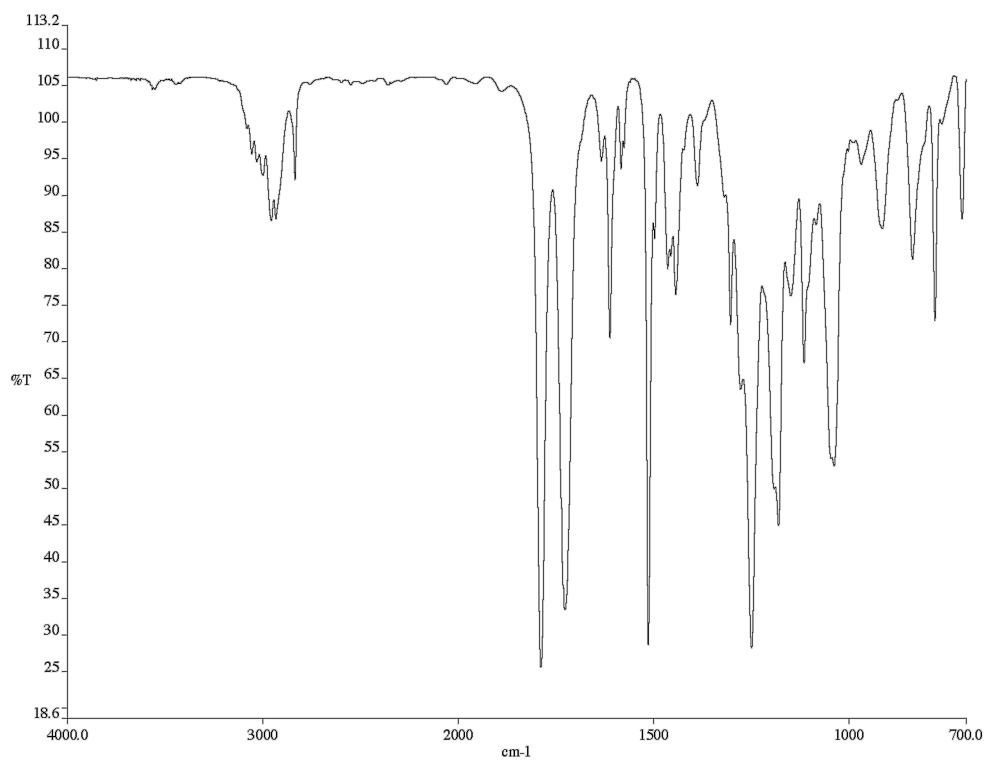


Figure A1.26 Infrared spectrum (thin film/NaCl) of compound **39h**.

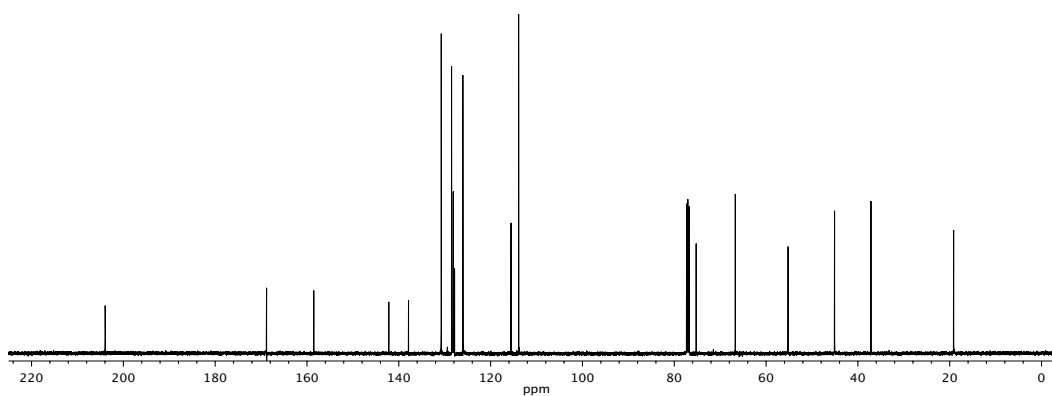
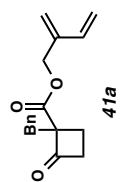
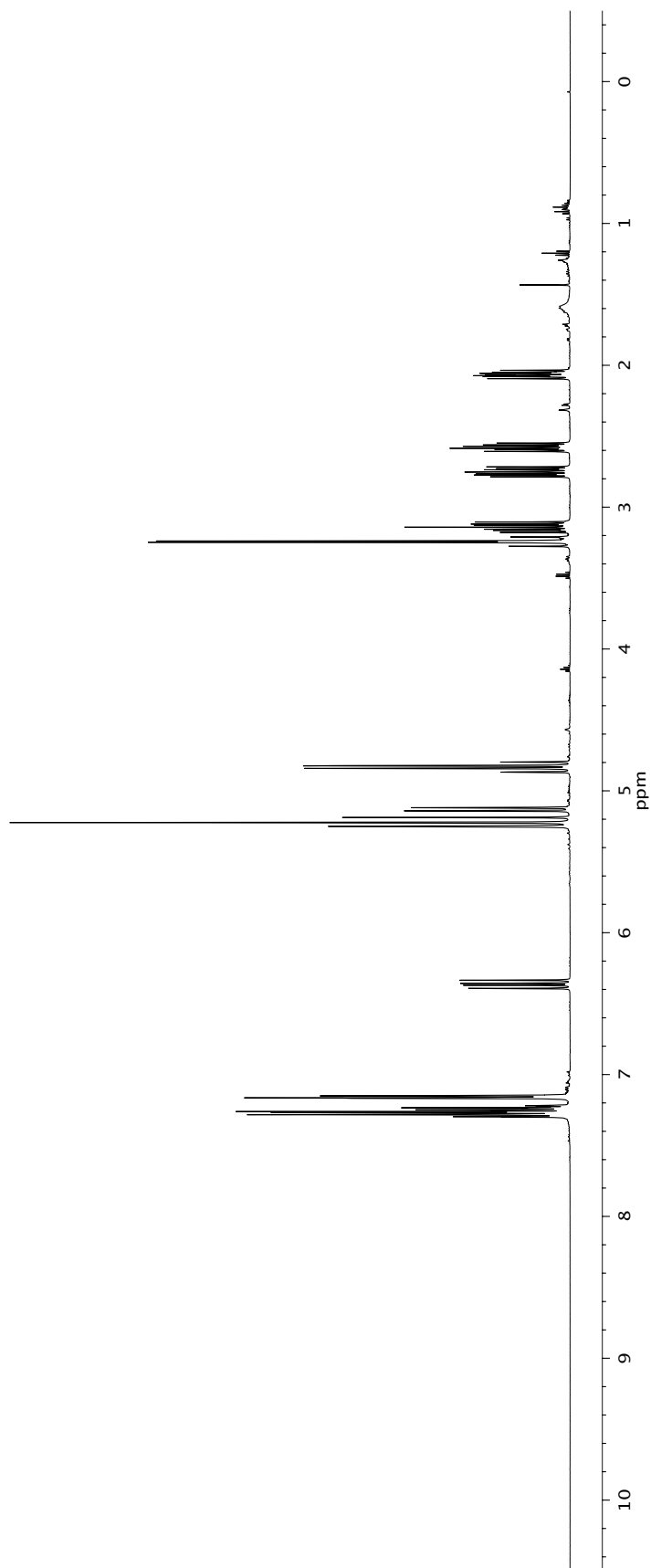


Figure A1.27 ¹³C NMR (125 MHz, CDCl₃) of compound **39h**.



41a

Figure A1.28 ¹H NMR (500 MHz, CDCl₃) of compound 41a.

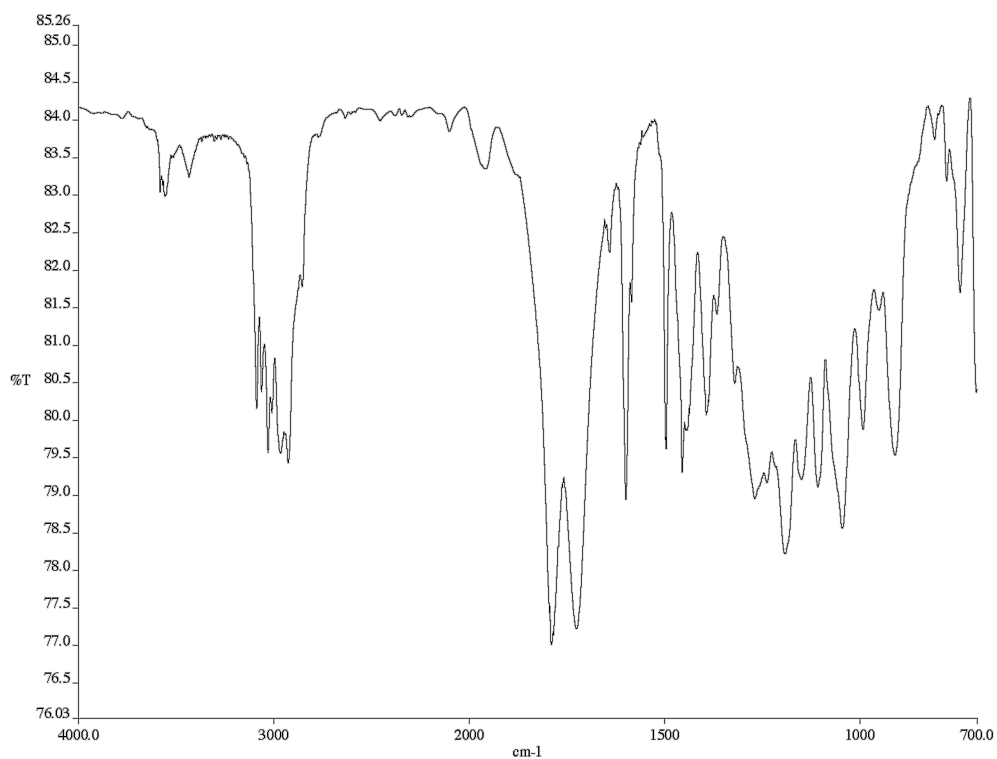


Figure A1.29 Infrared spectrum (thin film/NaCl) of compound **41a**.

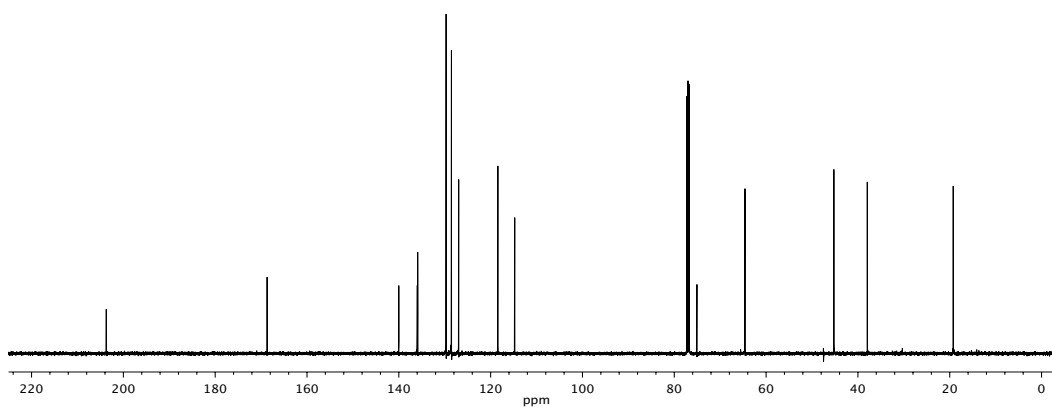


Figure A1.30 ^{13}C NMR (125 MHz, CDCl_3) of compound **41a**.

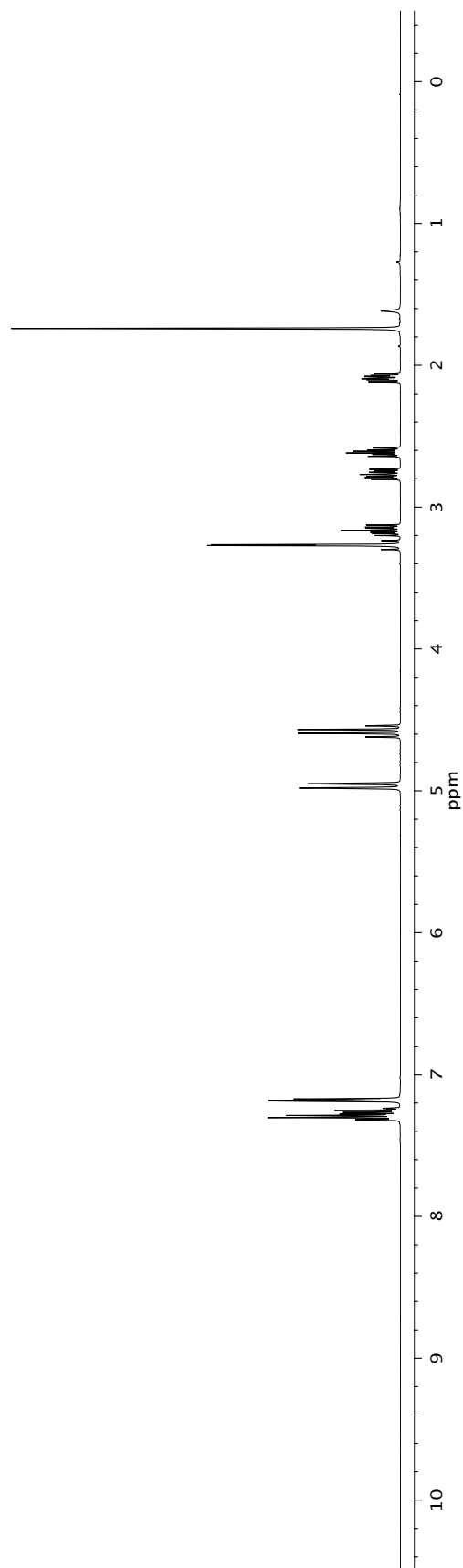
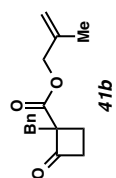


Figure A1.31 ¹H NMR (500 MHz, CDCl₃) of compound **41b**.

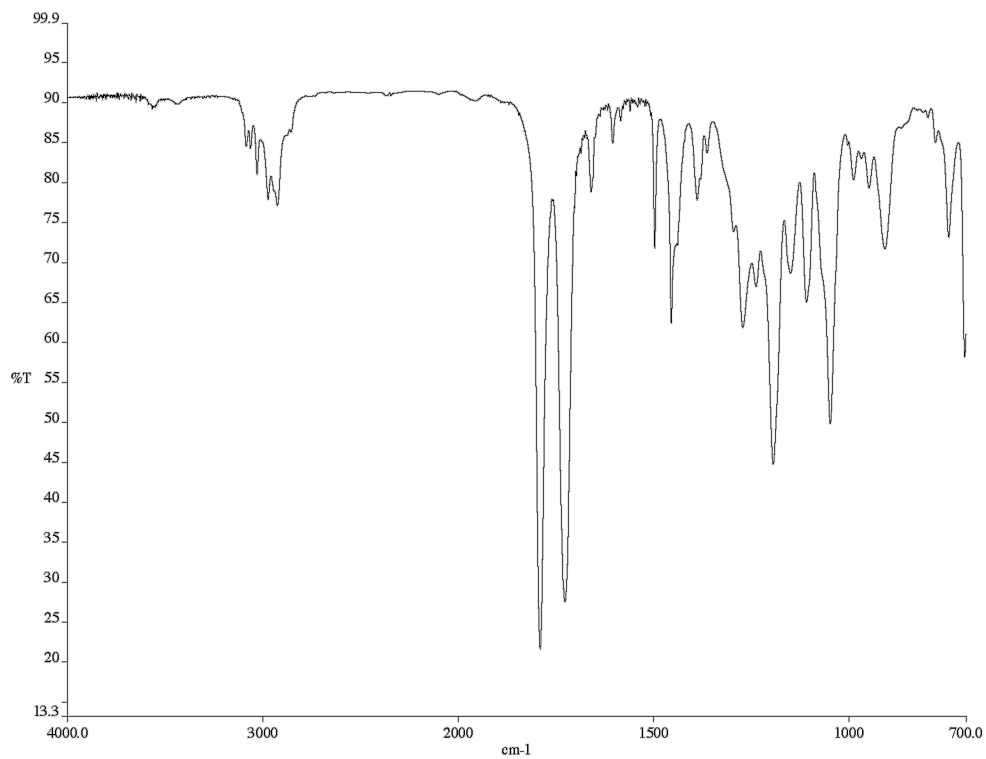


Figure A1.32 Infrared spectrum (thin film/NaCl) of compound **41b**.

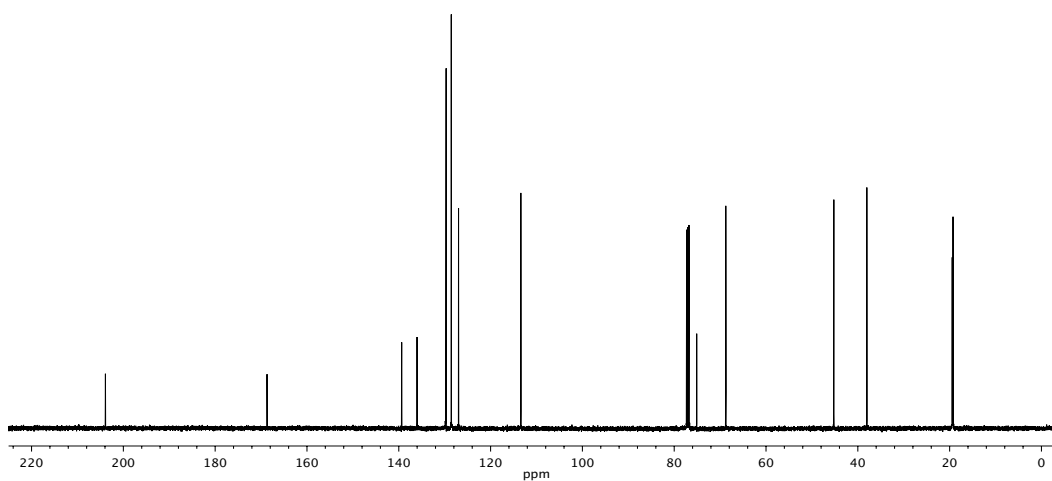


Figure A1.33 ¹³C NMR (125 MHz, CDCl₃) of compound **41b**.

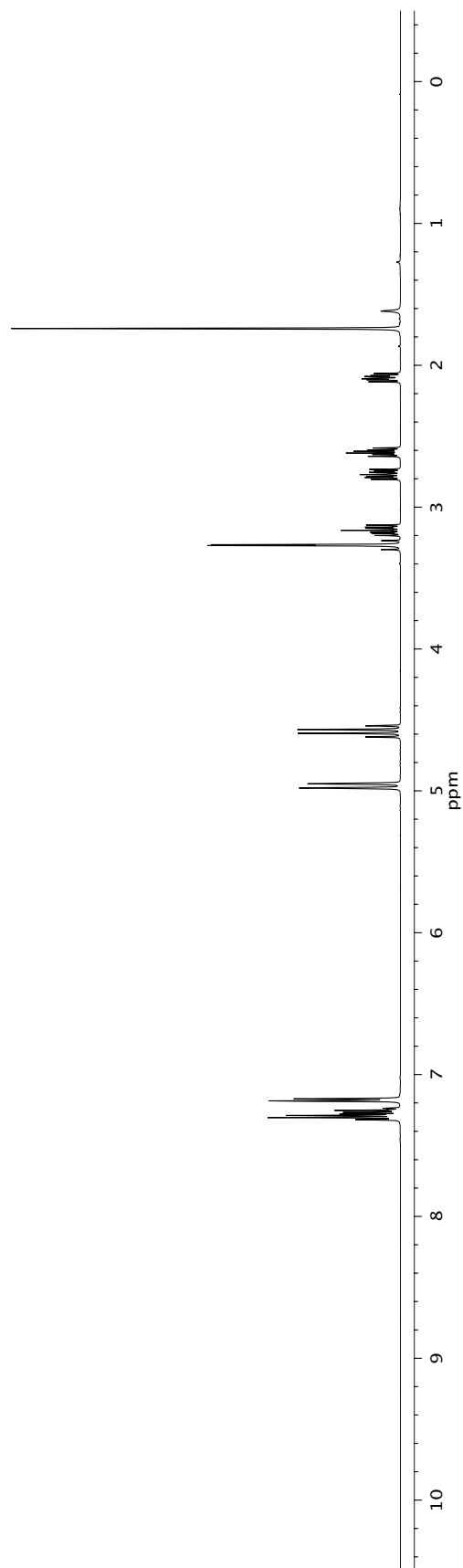
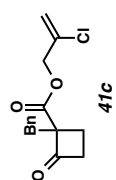


Figure A1.34 ¹H NMR (300 MHz, CDCl₃) of compound 41c.

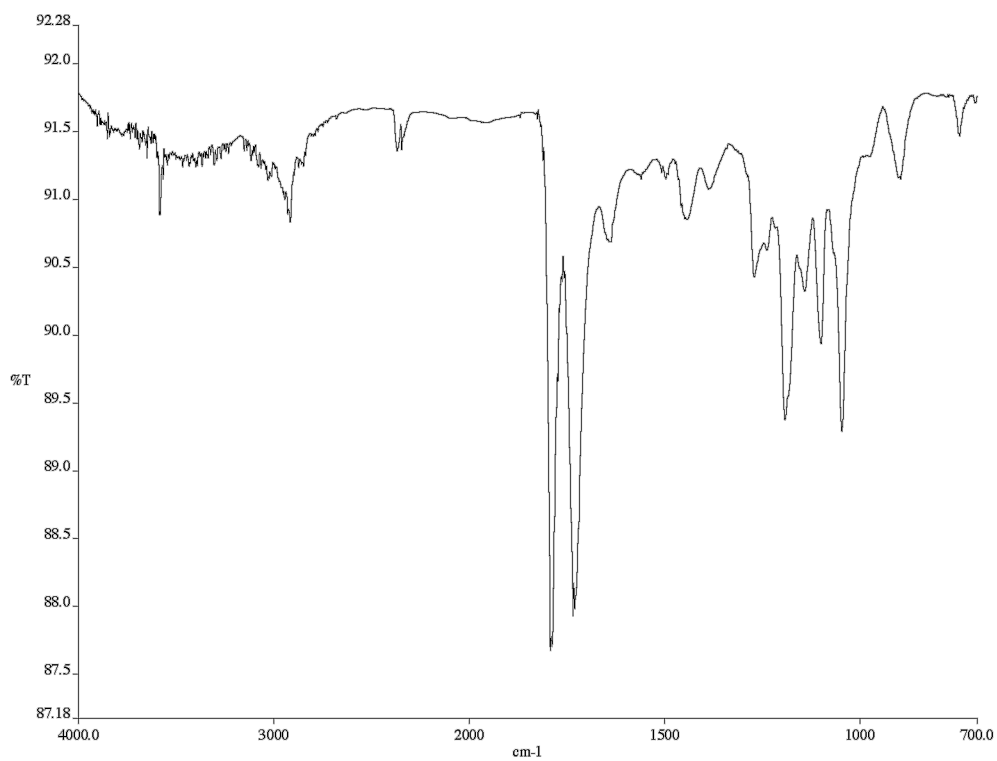


Figure A1.35 Infrared spectrum (thin film/NaCl) of compound **41c**.

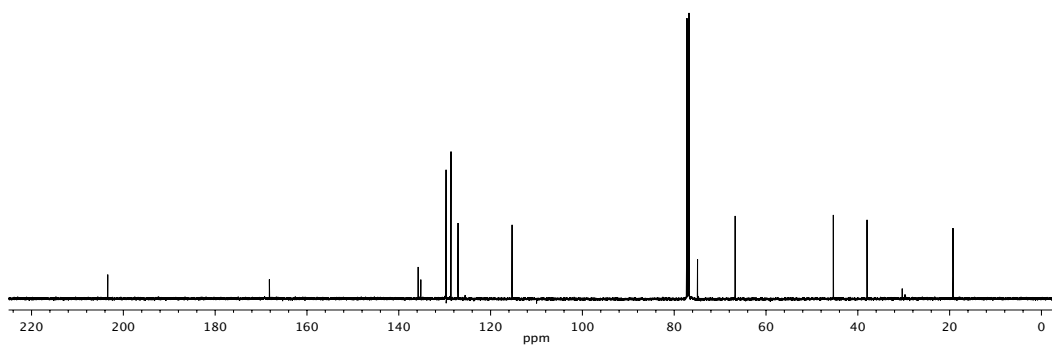


Figure A1.36 ¹³C NMR (125 MHz, CDCl₃) of compound **41c**.

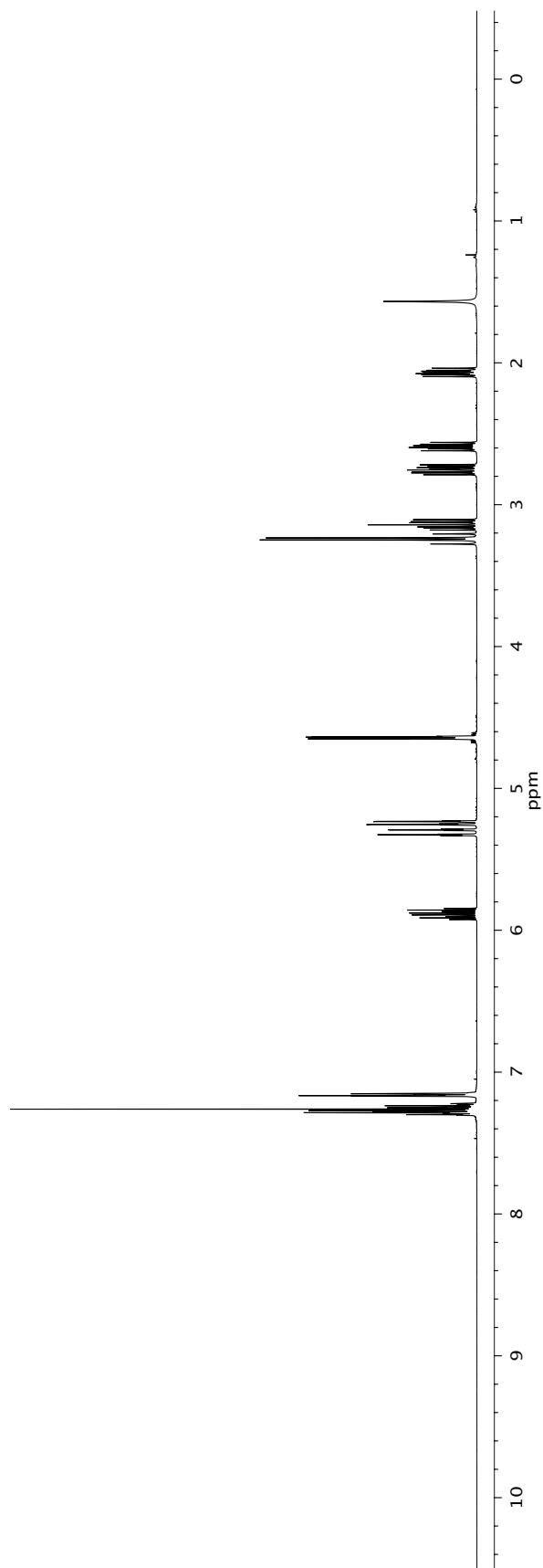
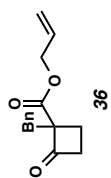


Figure A1.37 $^1\text{H NMR}$ (500 MHz, CDCl_3) of compound **36**.

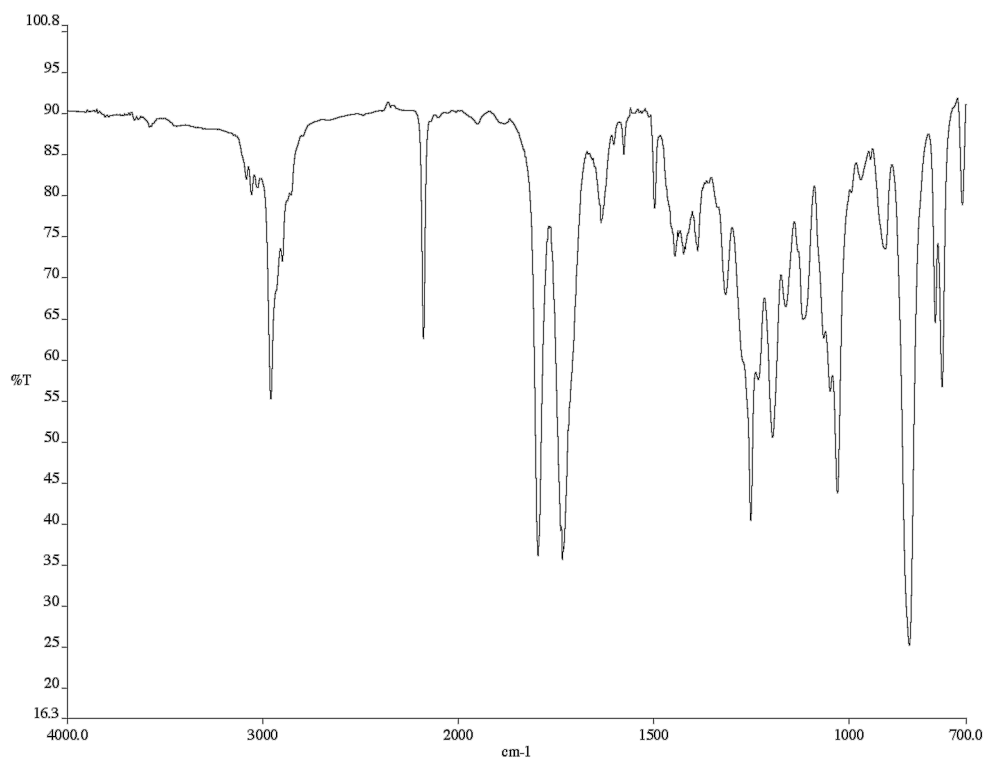


Figure A1.38 Infrared spectrum (thin film/NaCl) of compound 36.

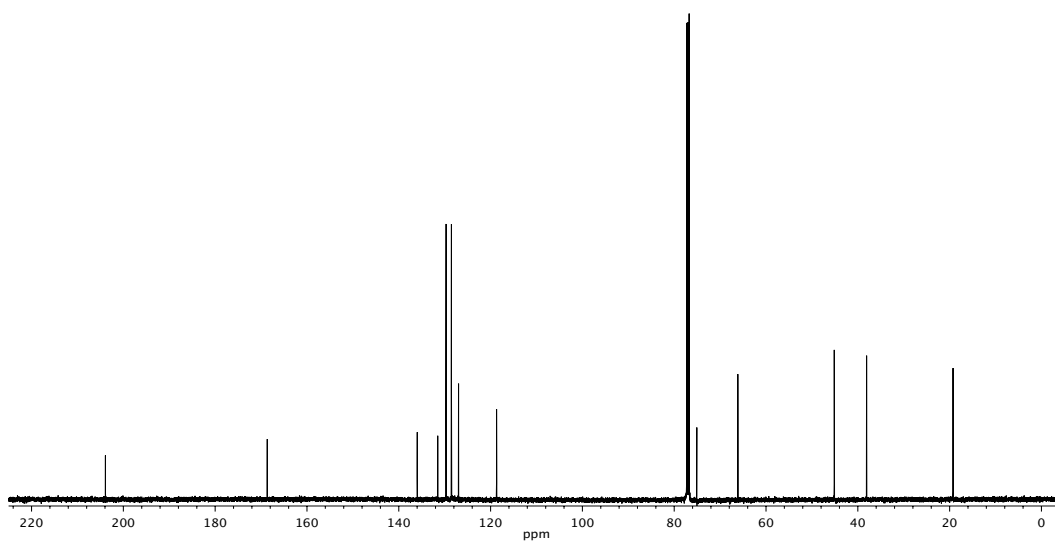


Figure A1.39 ¹³C NMR (125 MHz, CDCl₃) of compound 36.

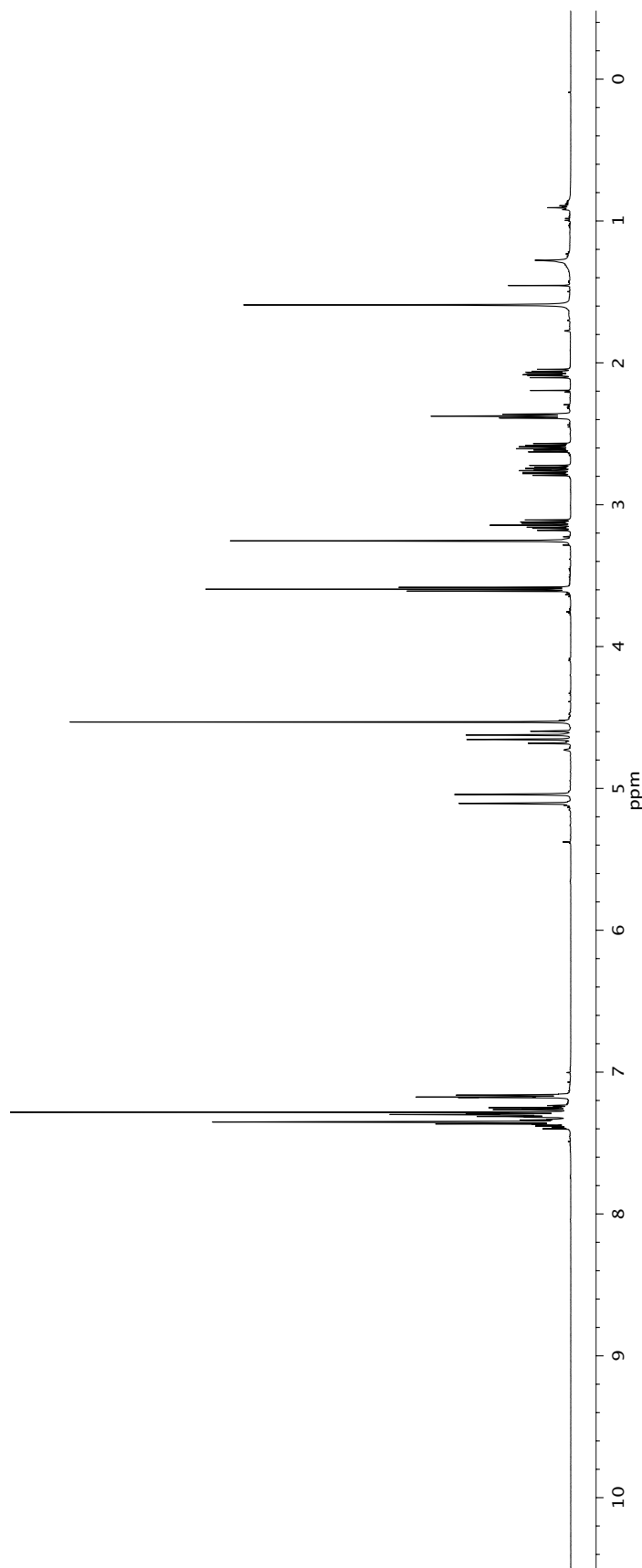
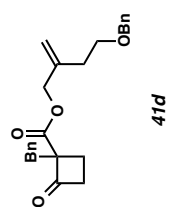


Figure A1.40 ¹H NMR (500 MHz, CDCl₃) of compound 41d.

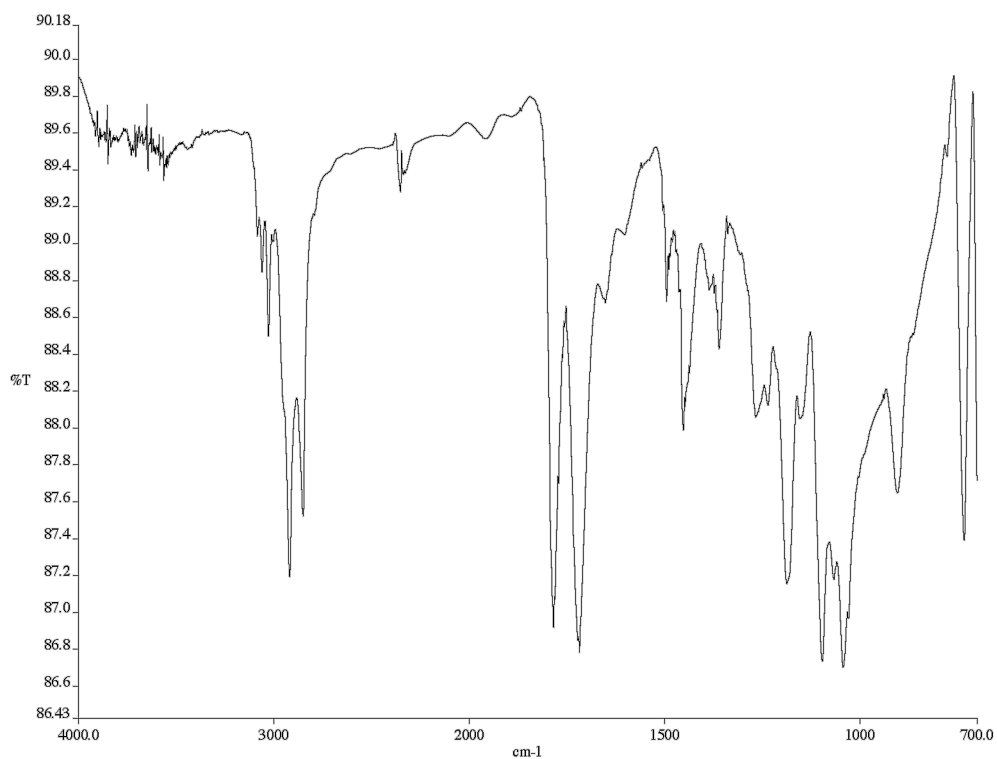


Figure A1.41 Infrared spectrum (thin film/NaCl) of compound **41d**.

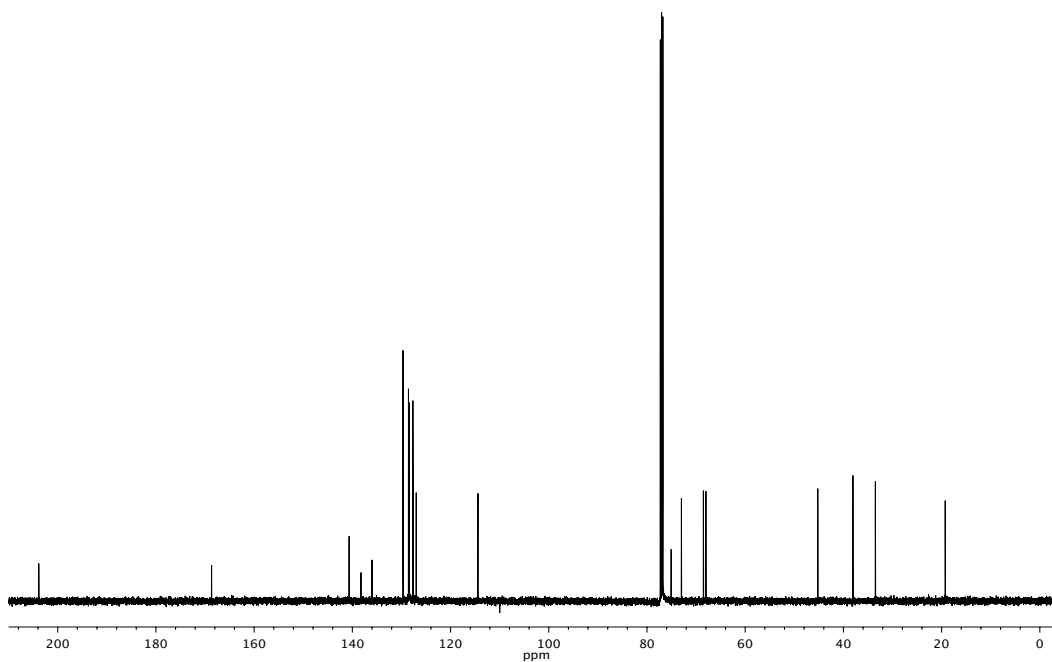


Figure A1.42 ^{13}C NMR (125 MHz, CDCl_3) of compound **41d**.

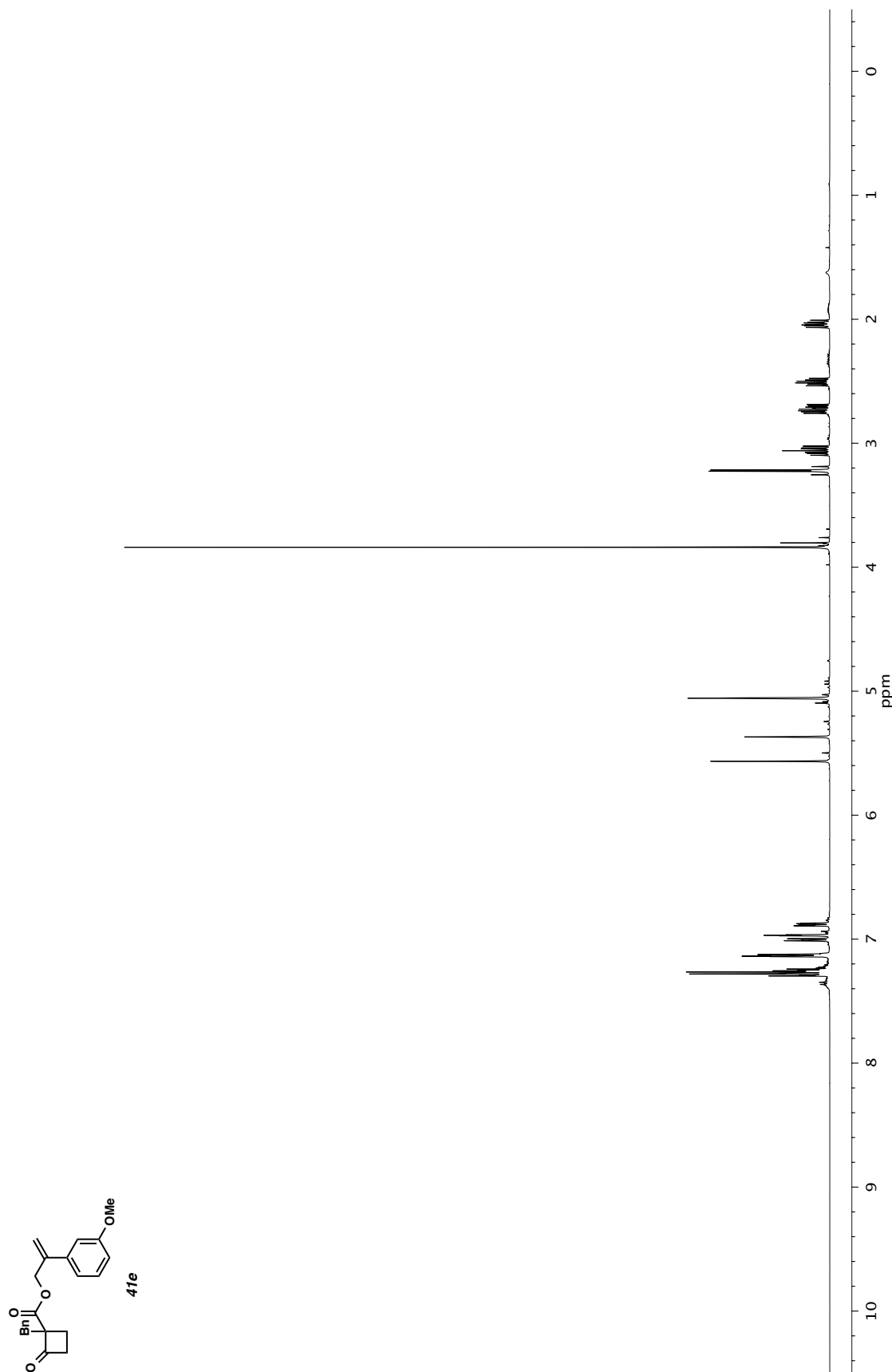


Figure A1.43 ¹H NMR (500 MHz, CDCl₃) of compound **41e**.

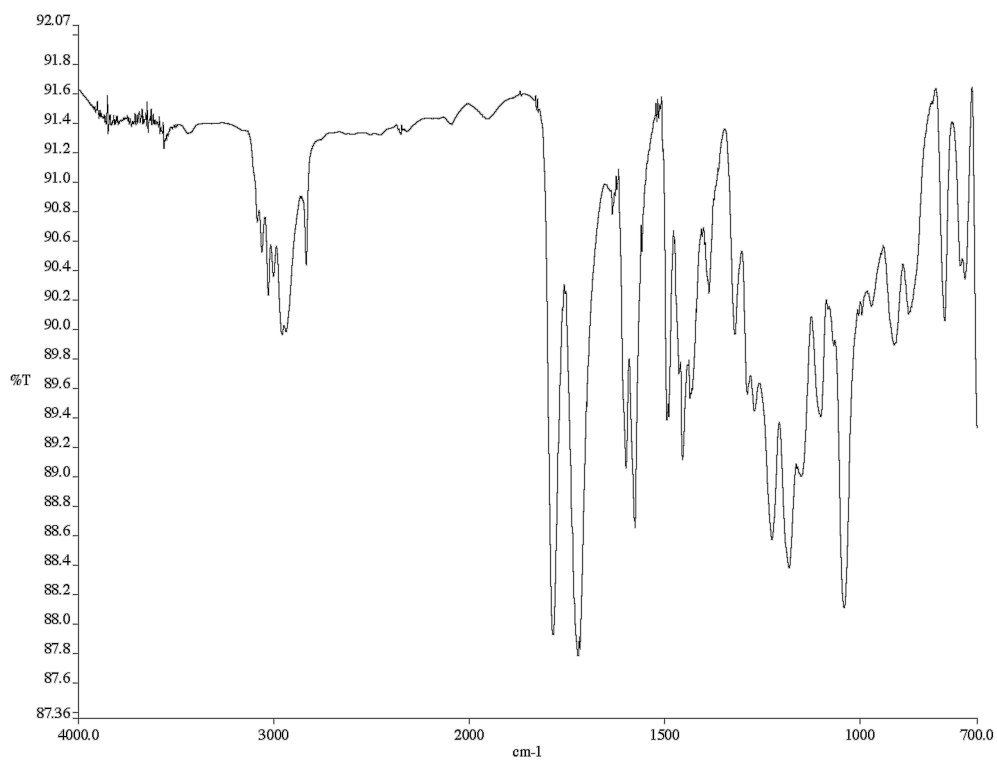


Figure A1.44 Infrared spectrum (thin film/NaCl) of compound **41e**.

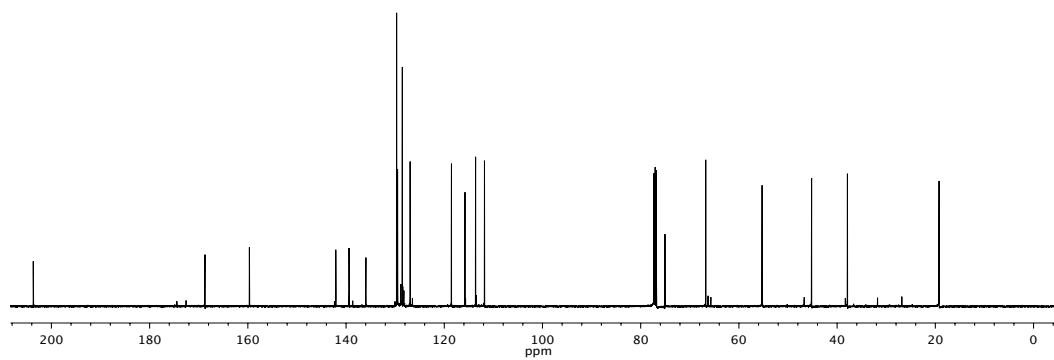


Figure A1.45 ¹³C NMR (125 MHz, CDCl₃) of compound **41e**.

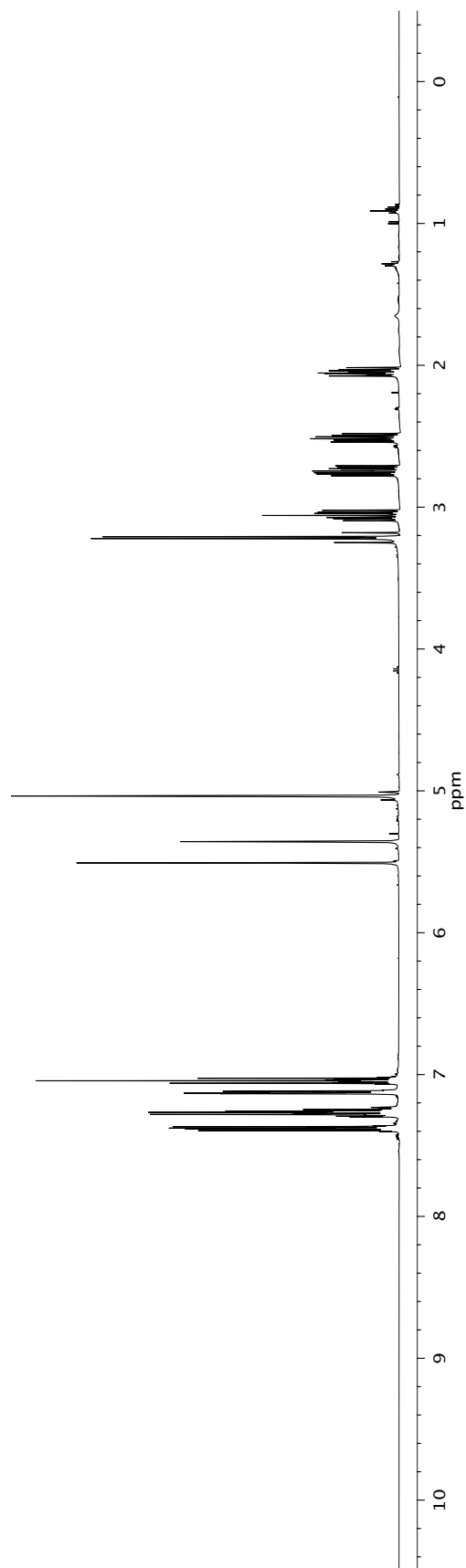
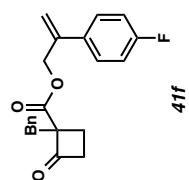


Figure A1.46 ¹H NMR (500 MHz, CDCl₃) of compound **41f**.

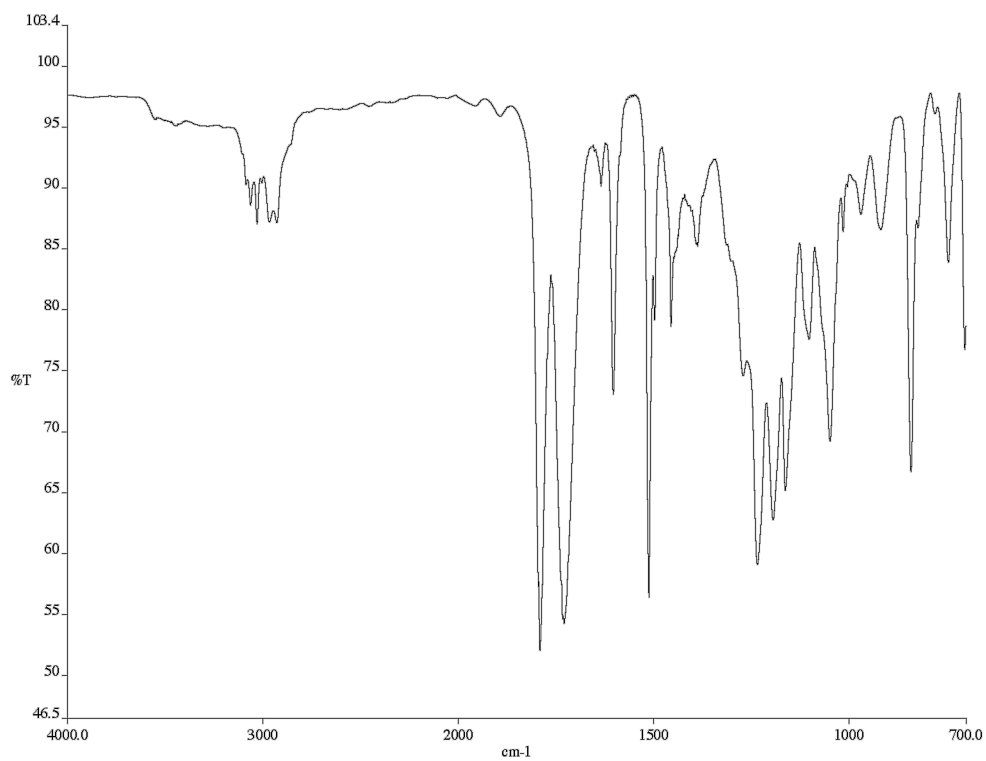


Figure A1.47 Infrared spectrum (thin film/NaCl) of compound **41f**.

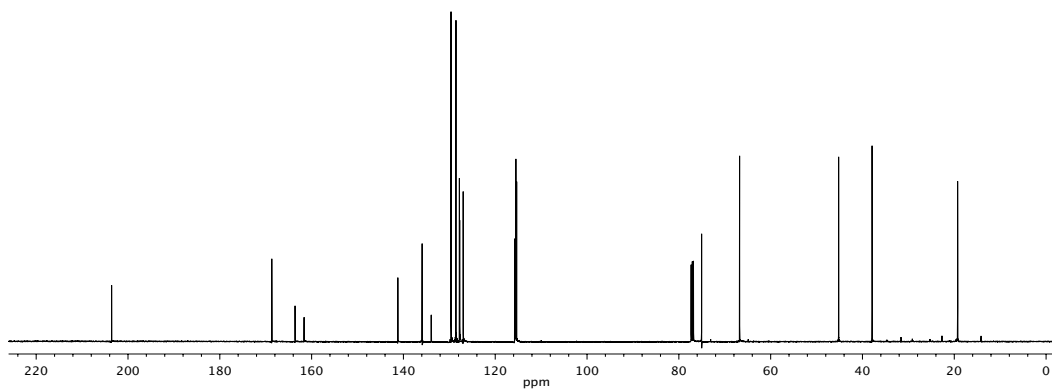


Figure A1.48 ¹³C NMR (125 MHz, CDCl₃) of compound **41f**.

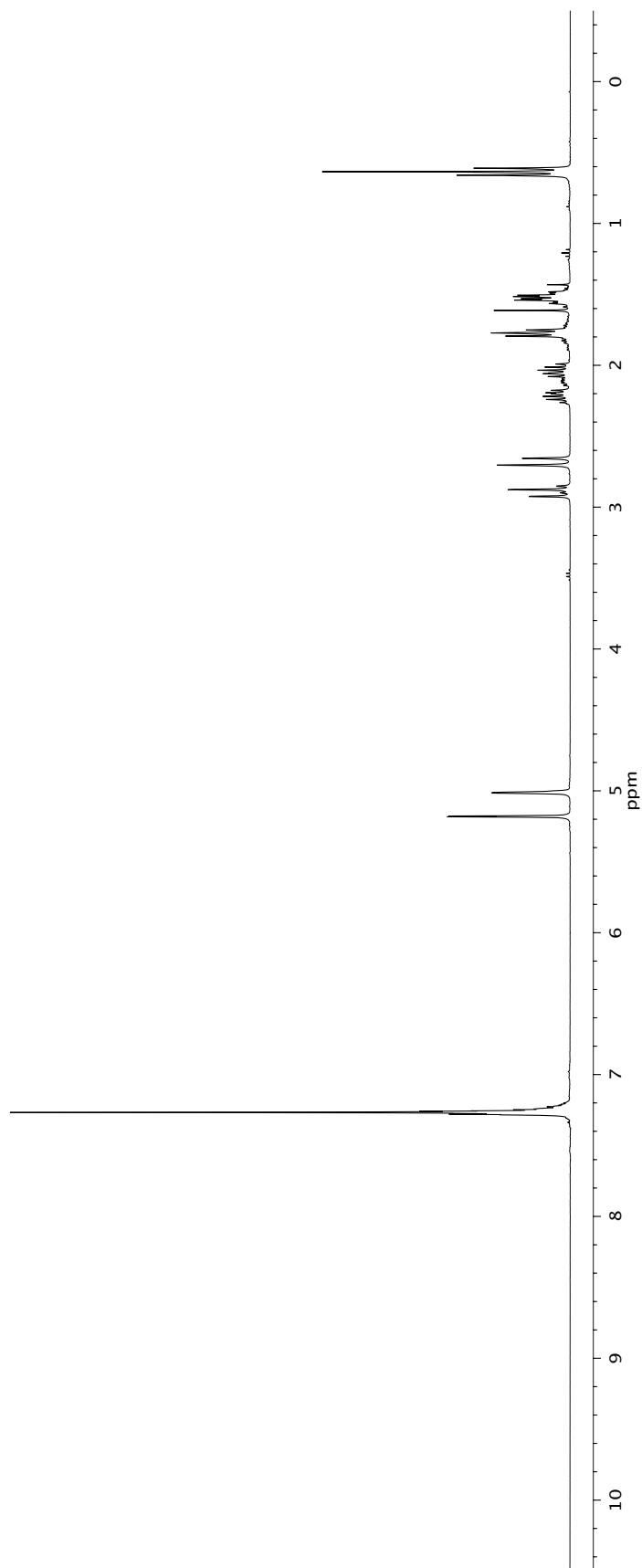
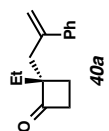


Figure A1.49 ¹H NMR (300 MHz, CDCl₃) of compound **40a**.

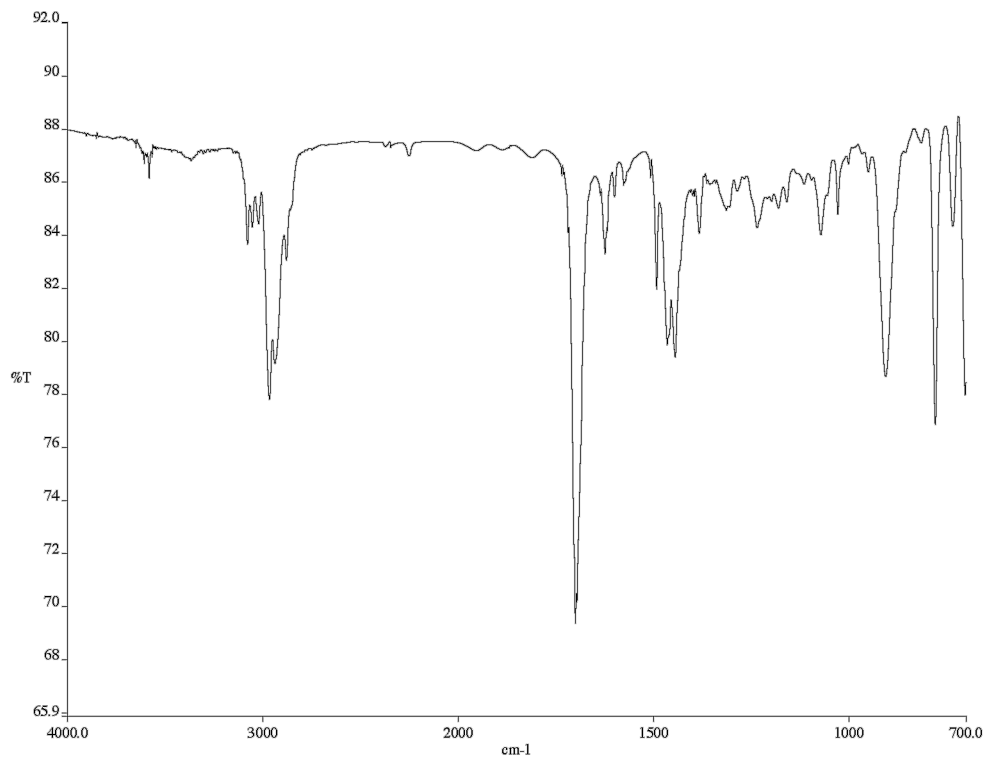


Figure A1.50 Infrared spectrum (thin film/NaCl) of compound **40a**.

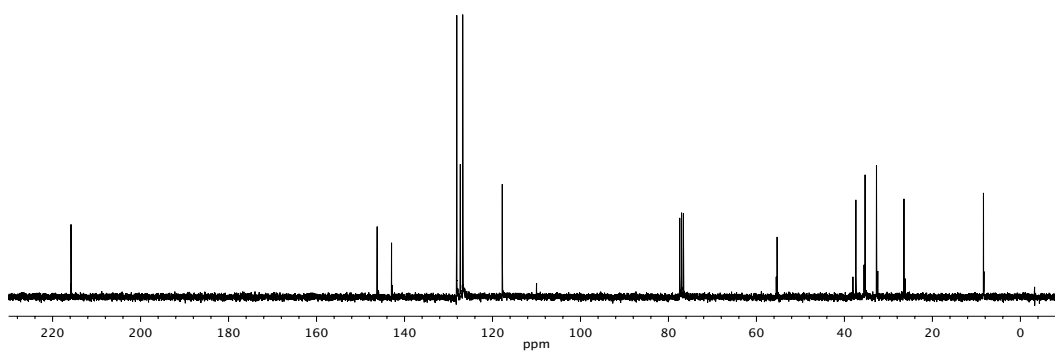


Figure A1.51 ¹³C NMR (75 MHz, CDCl₃) of compound **40a**.

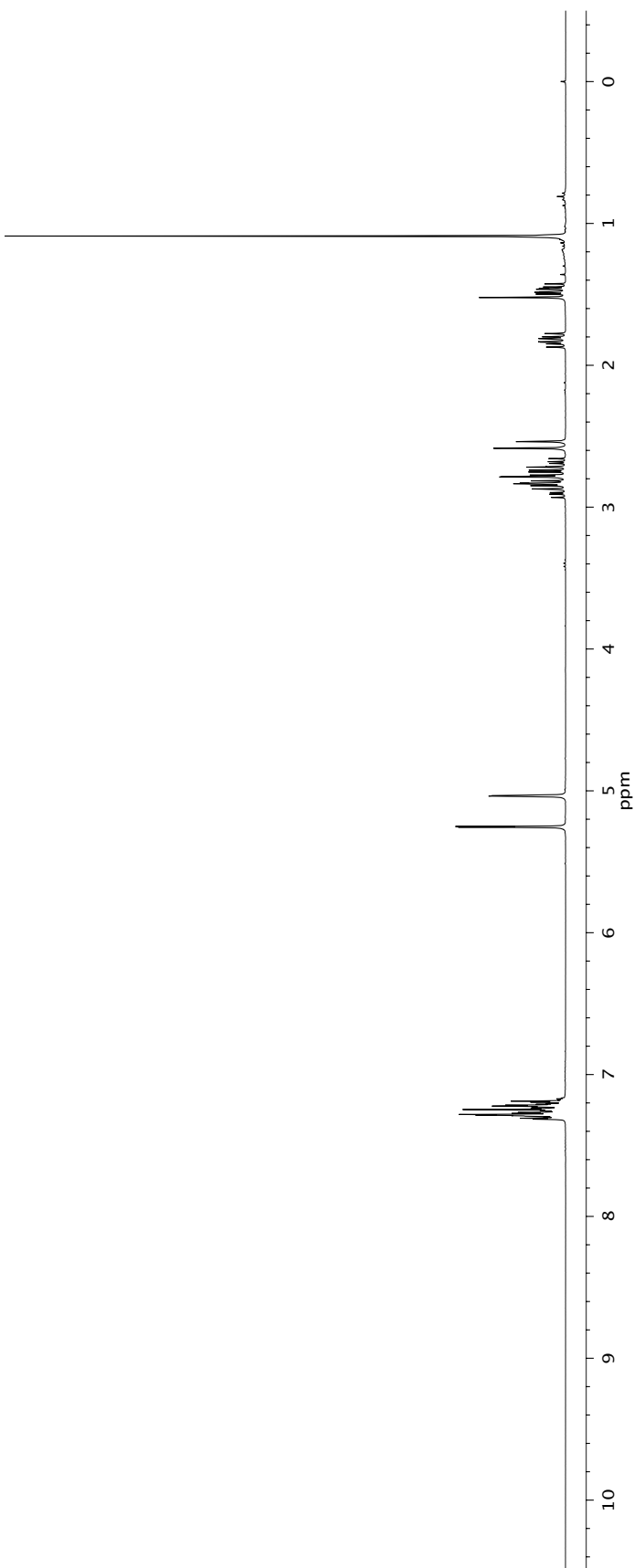
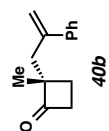


Figure A1.52 $^1\text{H NMR}$ (300 MHz, CDCl_3) of compound 40b.

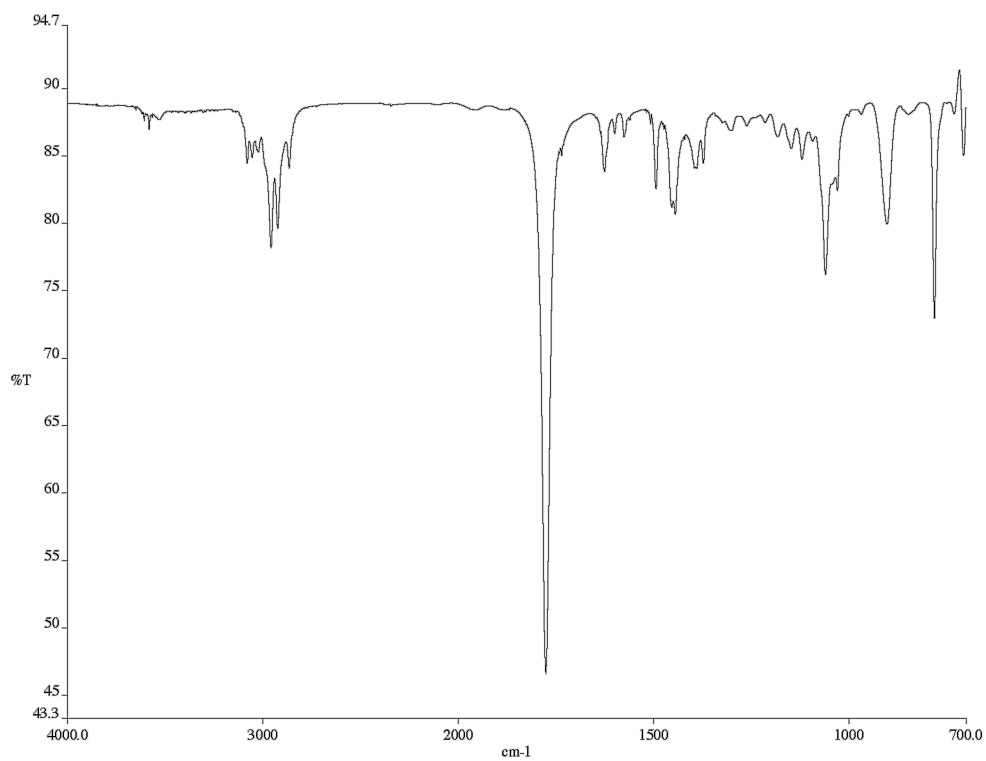


Figure A1.53 Infrared spectrum (thin film/NaCl) of compound **40b**.

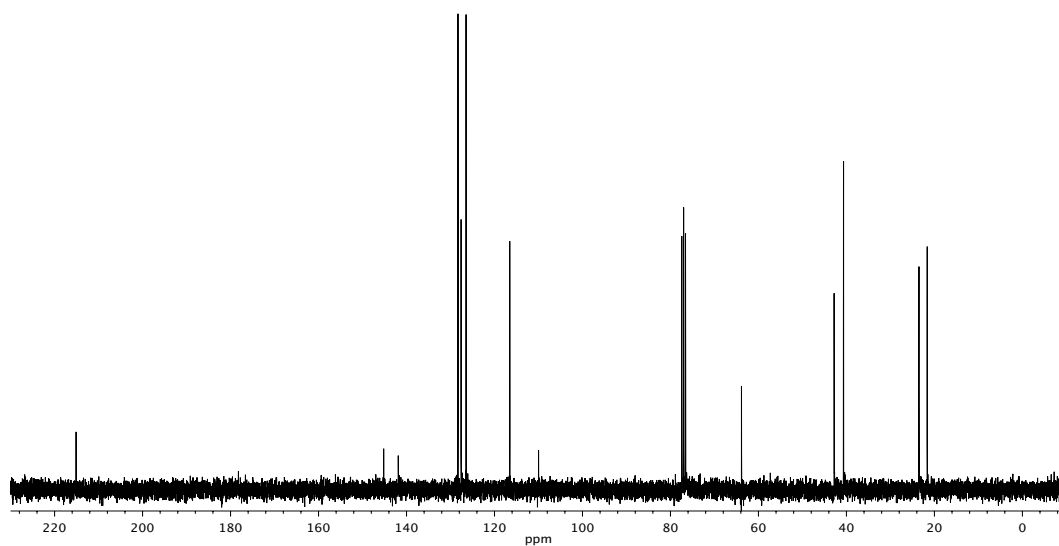


Figure A1.54 ¹³C NMR (125 MHz, CDCl₃) of compound **40b**.

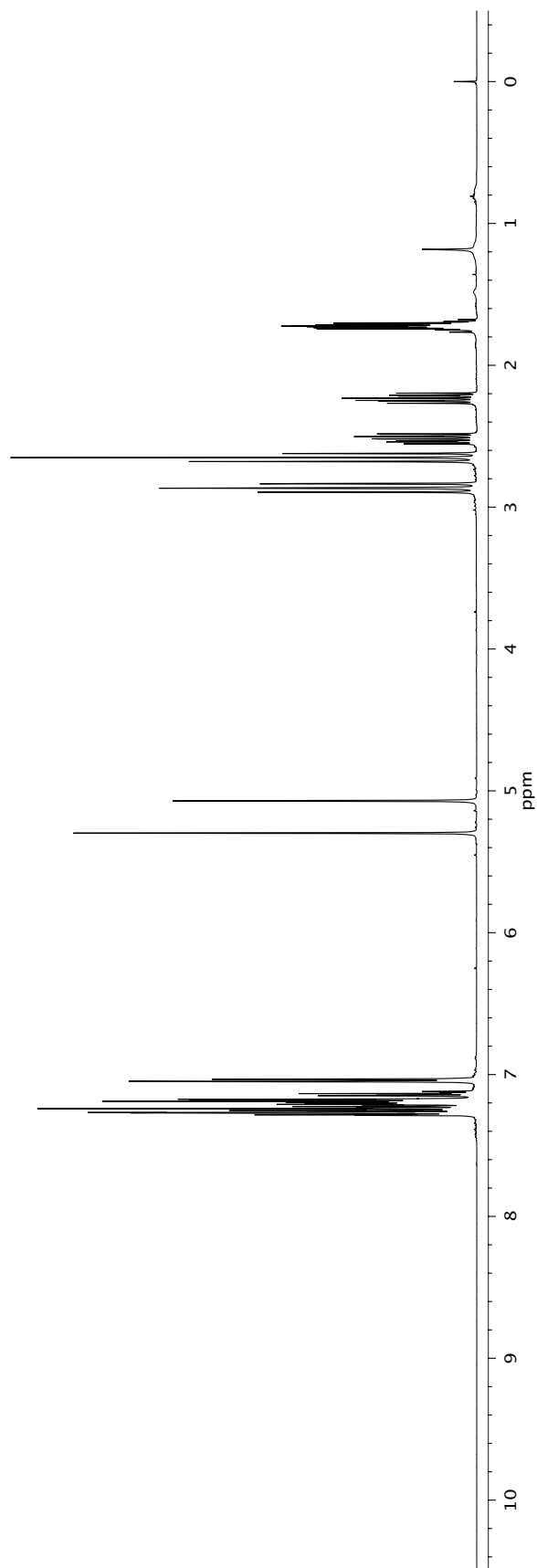
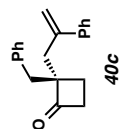


Figure A1.55 ¹H NMR (500 MHz, CDCl₃) of compound **40c**.

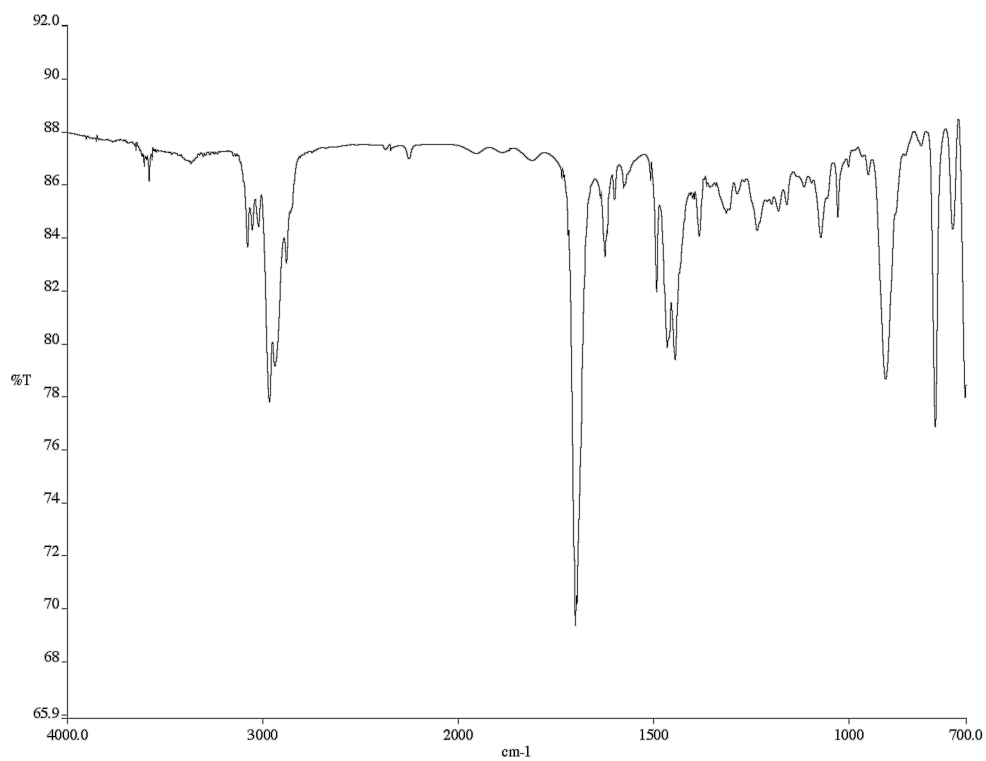


Figure A1.56 Infrared spectrum (thin film/NaCl) of compound **40c**.

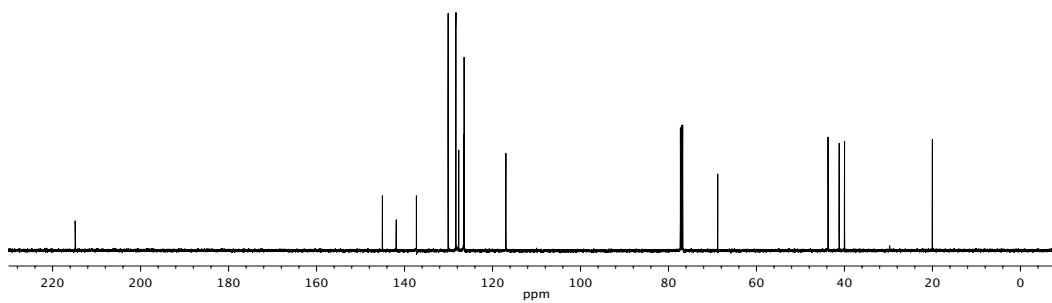


Figure A1.57 ¹³C NMR (125 MHz, CDCl₃) of compound **40c**.

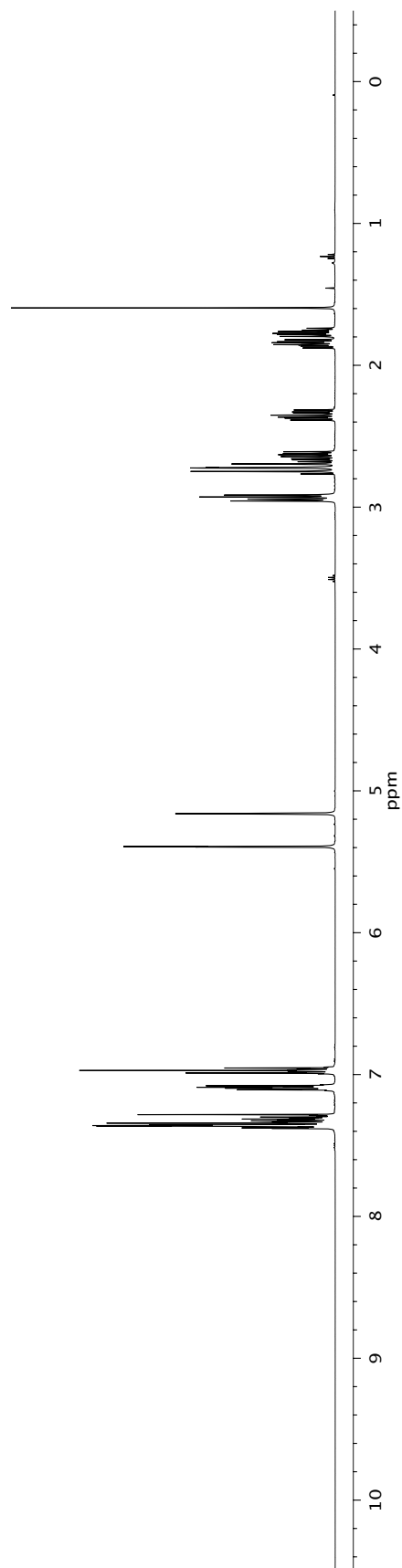
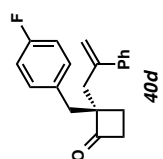


Figure A1.58 ¹H NMR (500 MHz, CDCl₃) of compound **40d**.

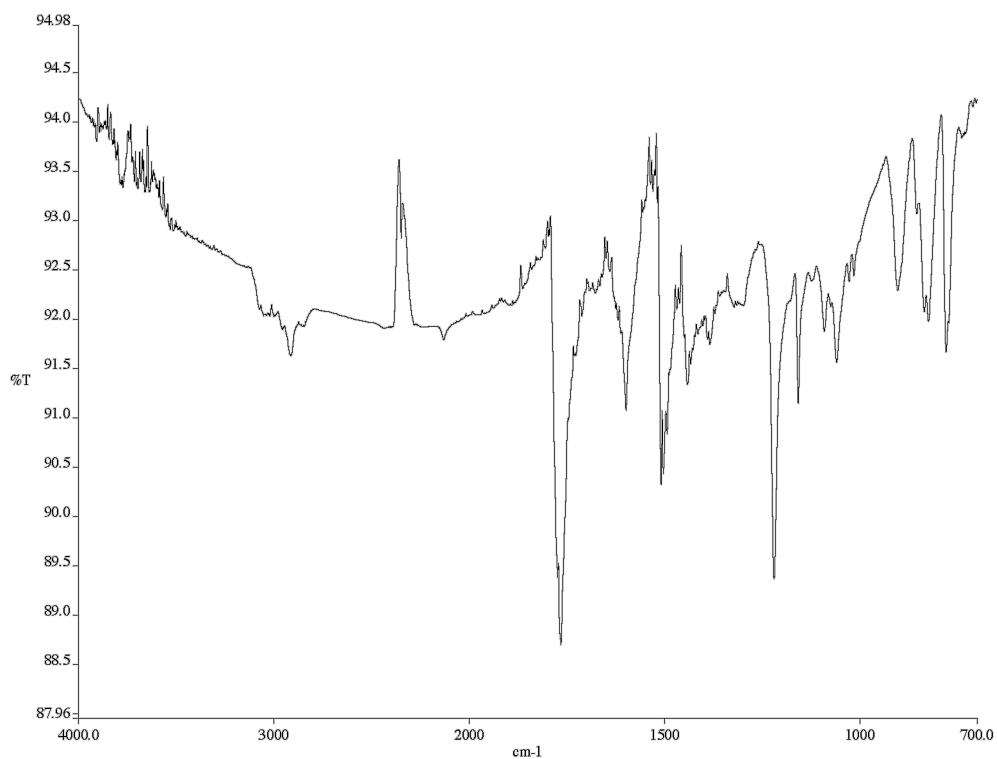


Figure A1.59 Infrared spectrum (thin film/NaCl) of compound **40d**.

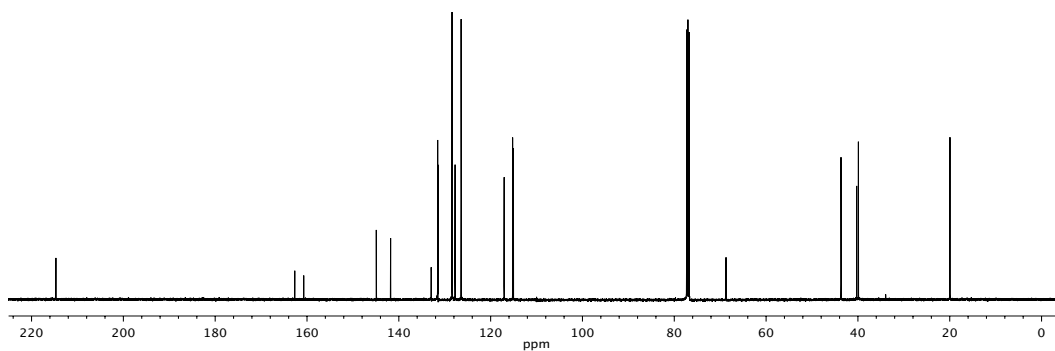
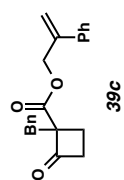
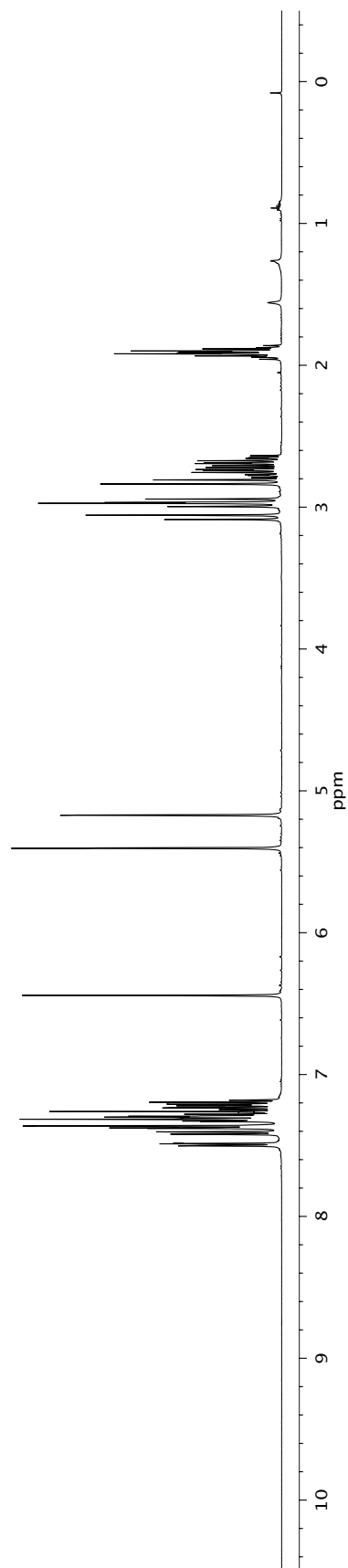


Figure A1.60 ¹³C NMR (125 MHz, CDCl₃) of compound **40d**.



39c

Figure A1.61 ^1H NMR (300 MHz, CDCl_3) of compound 40e.

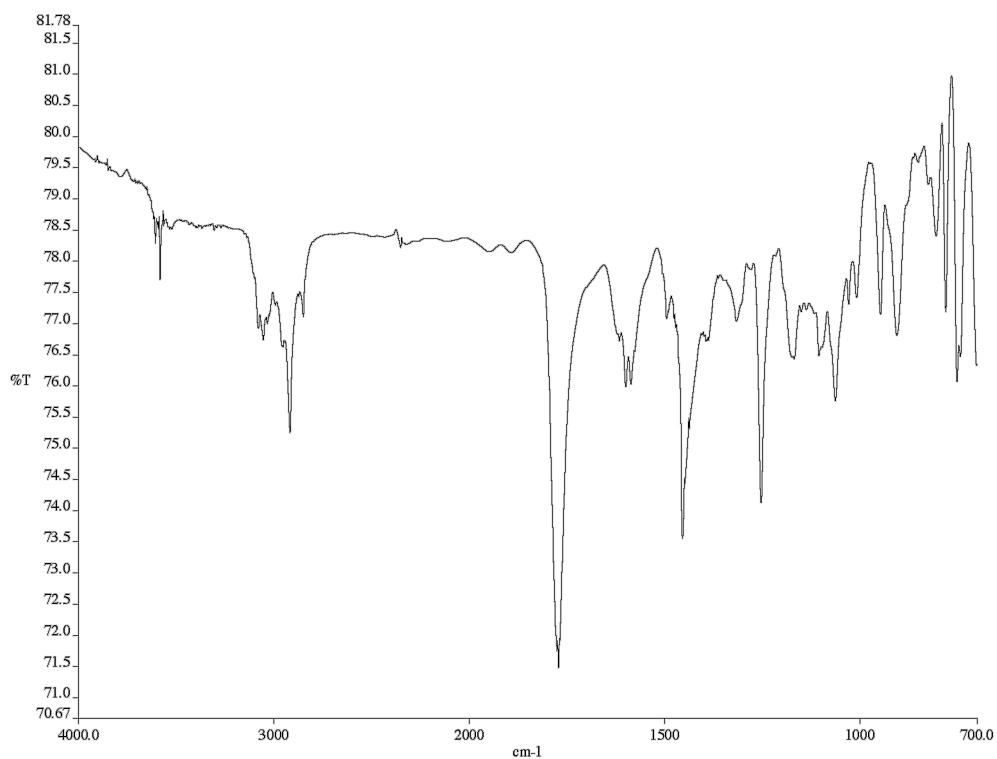


Figure A1.62 Infrared spectrum (thin film/NaCl) of compound **40e**.

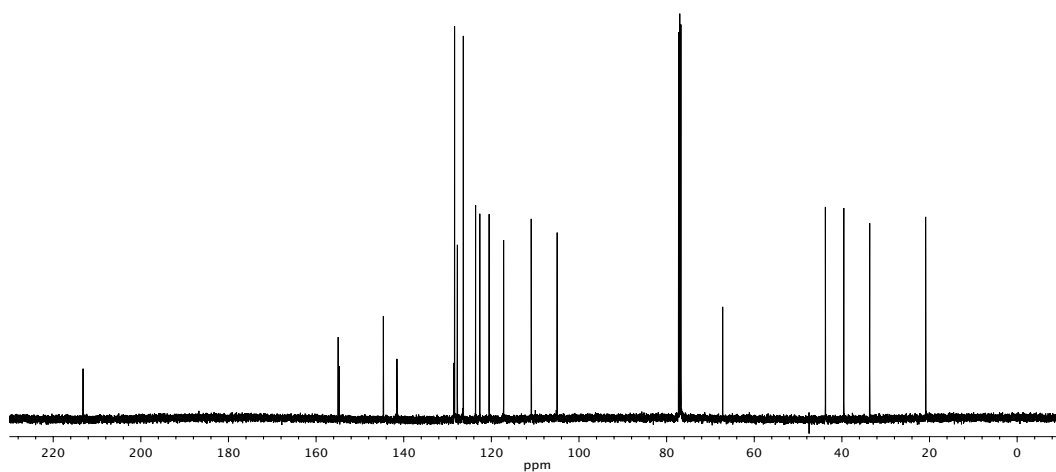


Figure A1.63 ¹³C NMR (125 MHz, CDCl₃) of compound **40e**.

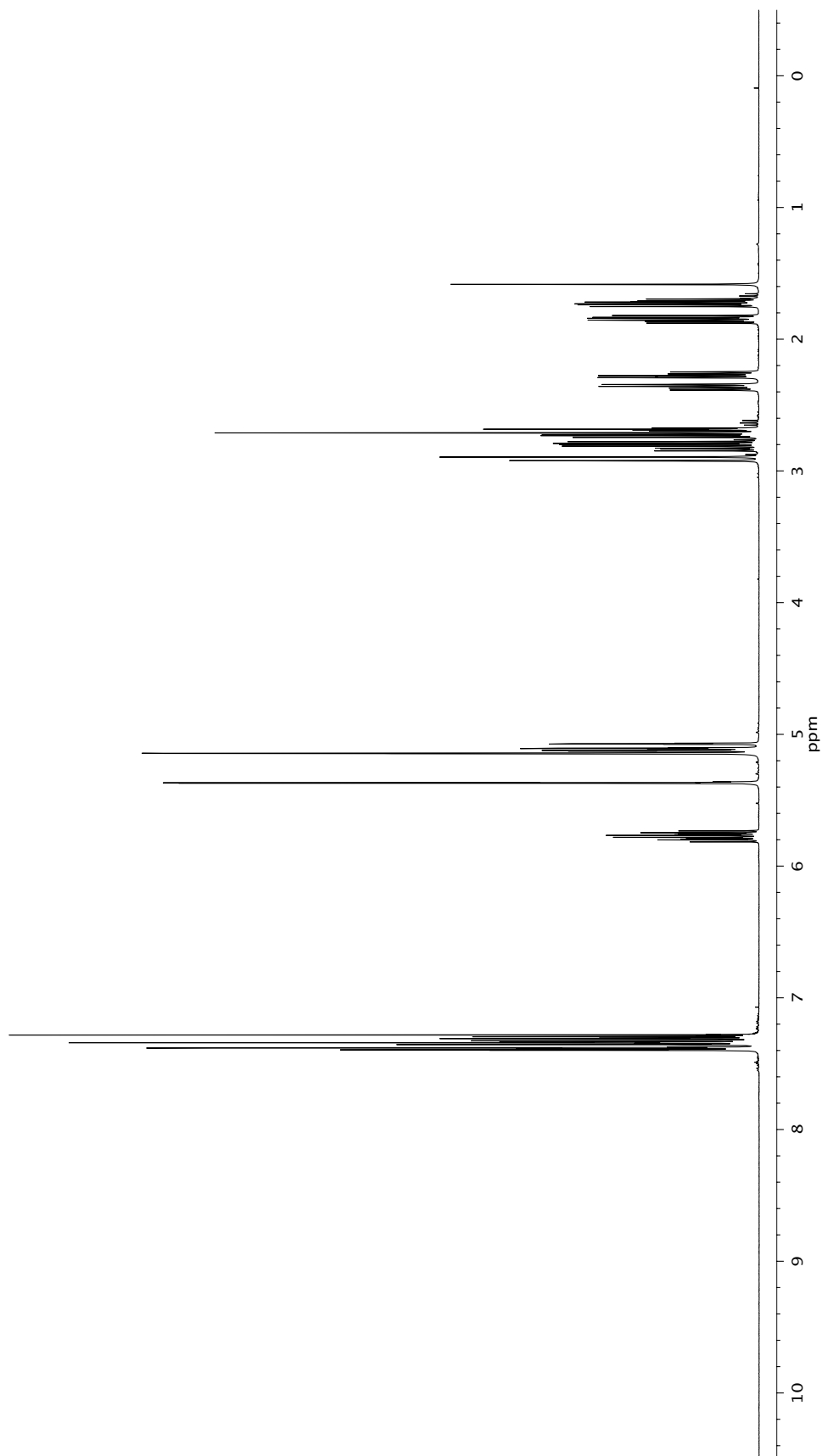
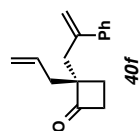


Figure A1.64 ^1H NMR (500 MHz, CDCl_3) of compound 40f.

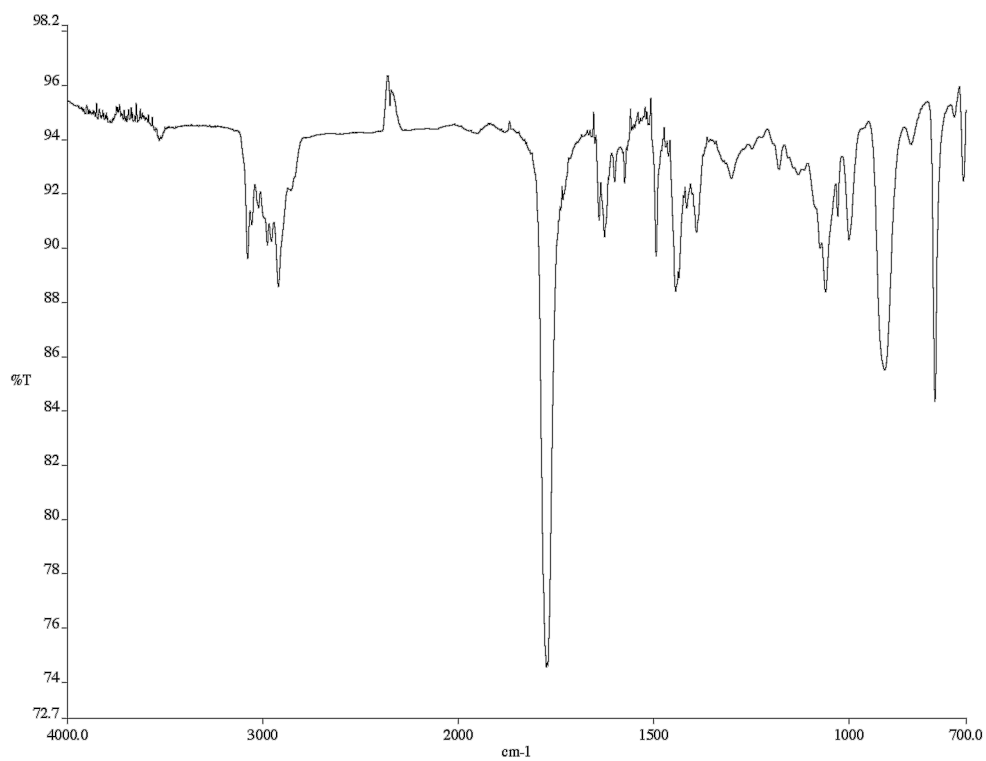


Figure A1.65 Infrared spectrum (thin film/NaCl) of compound **40f**.

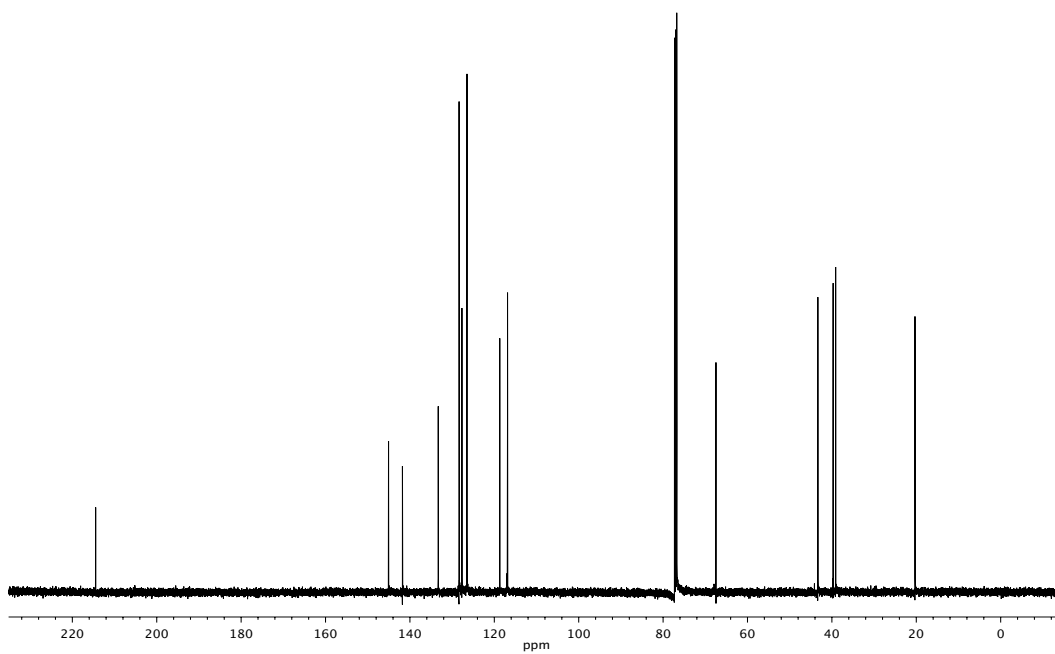


Figure A1.66 ¹³C NMR (125 MHz, CDCl₃) of compound **40f**.

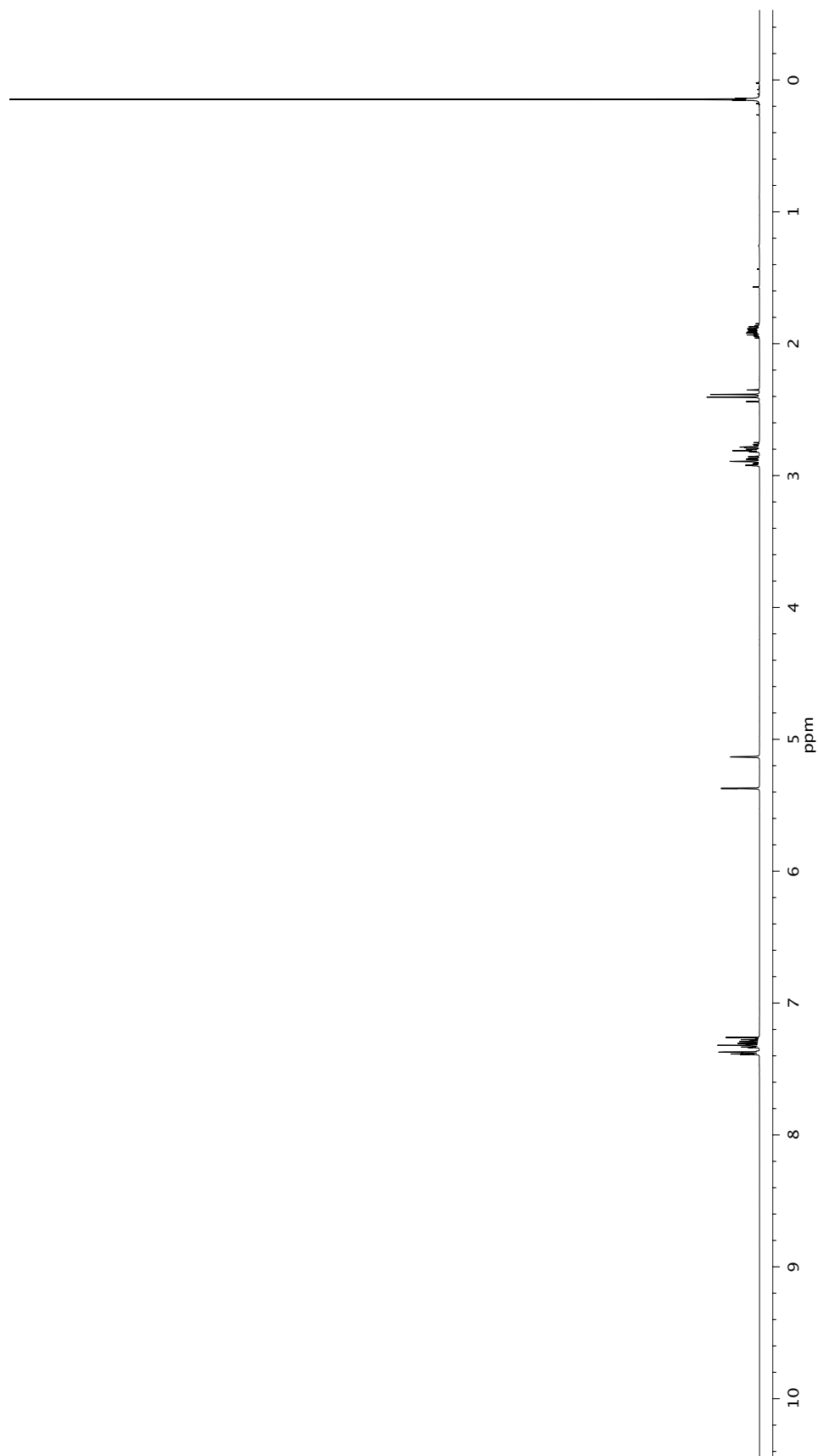
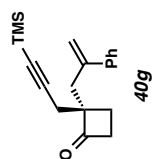


Figure A1.67 ¹H NMR (500 MHz, CDCl₃) of compound 40g.

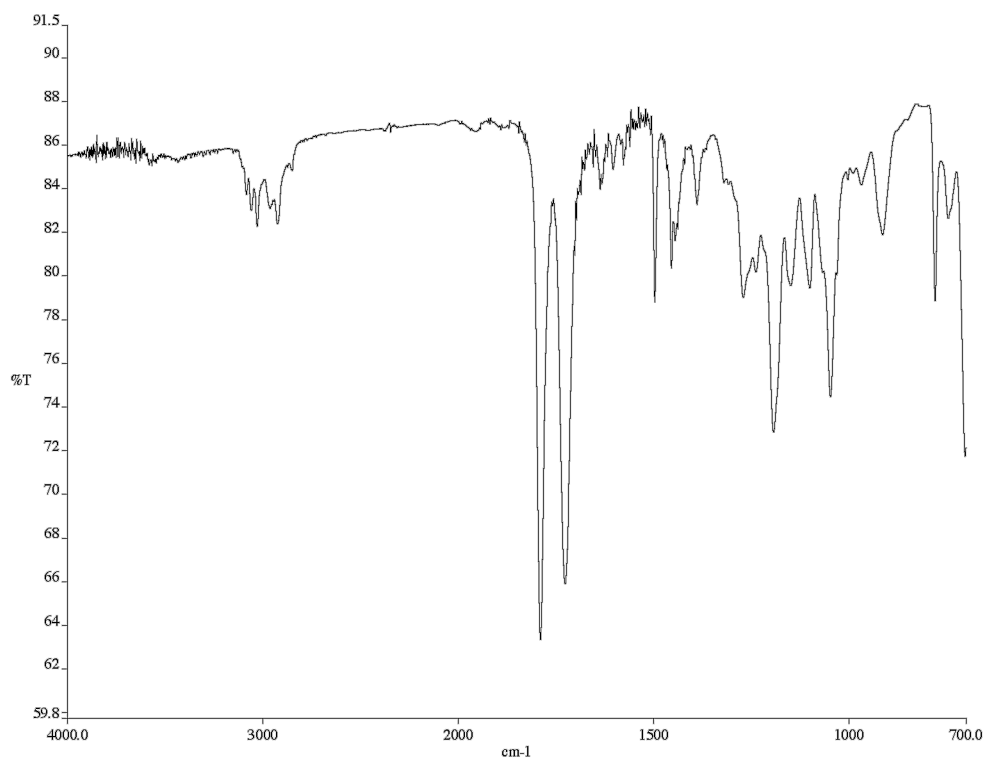


Figure A1.68 Infrared spectrum (thin film/NaCl) of compound **40g**.

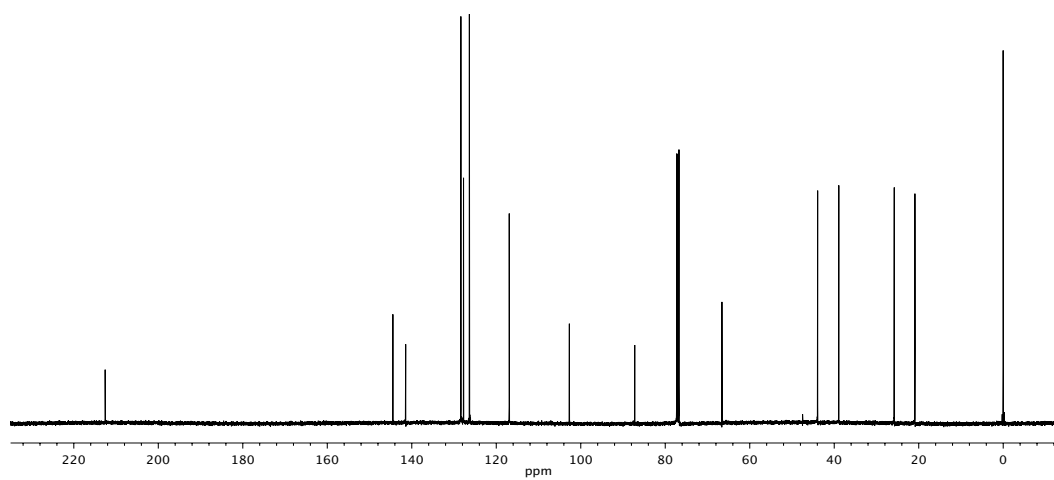


Figure A1.69 ¹³C NMR (125 MHz, CDCl₃) of compound **40g**.

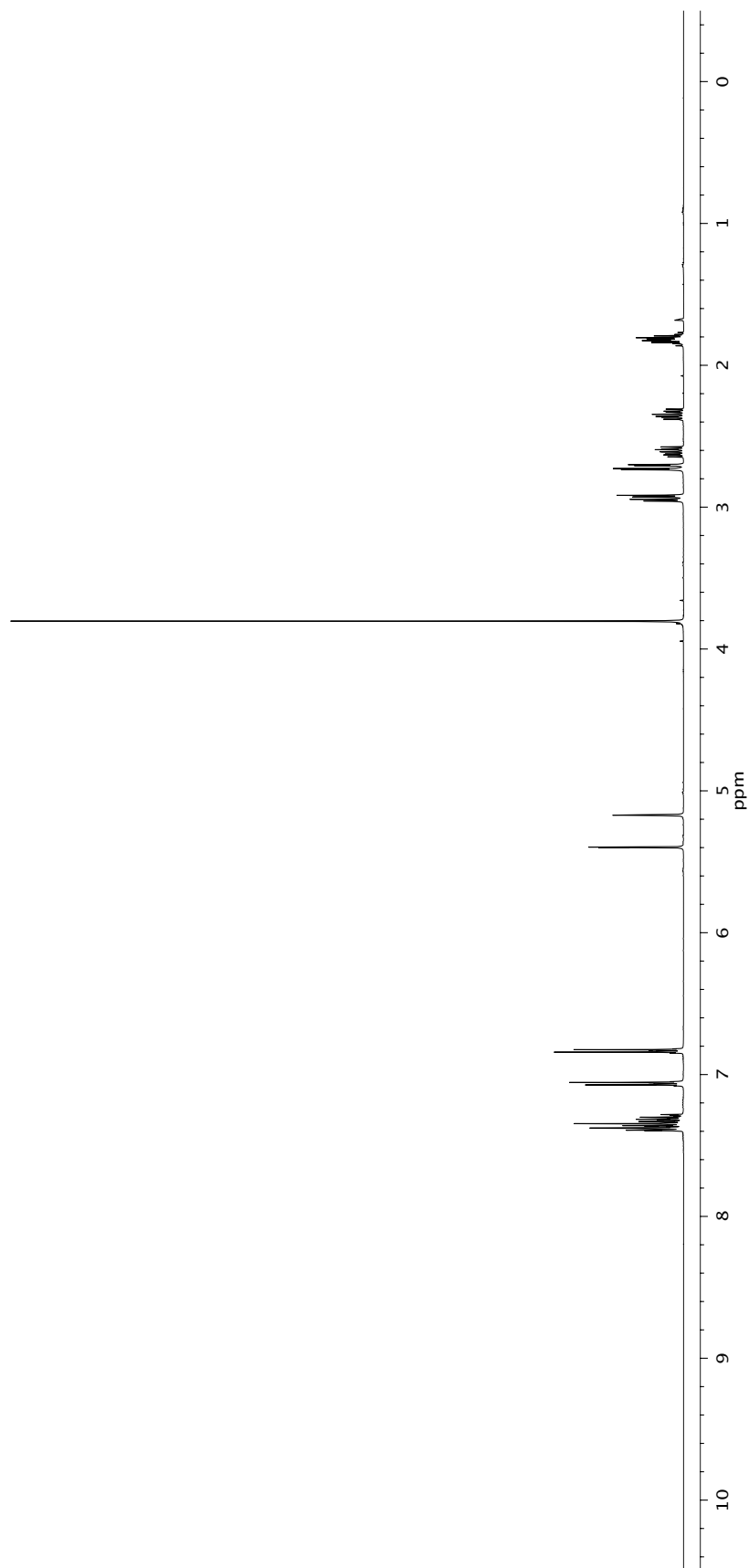
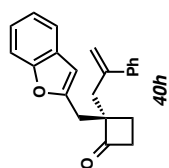


Figure A1.70 ^1H NMR (500 MHz, CDCl_3) of compound 40h.

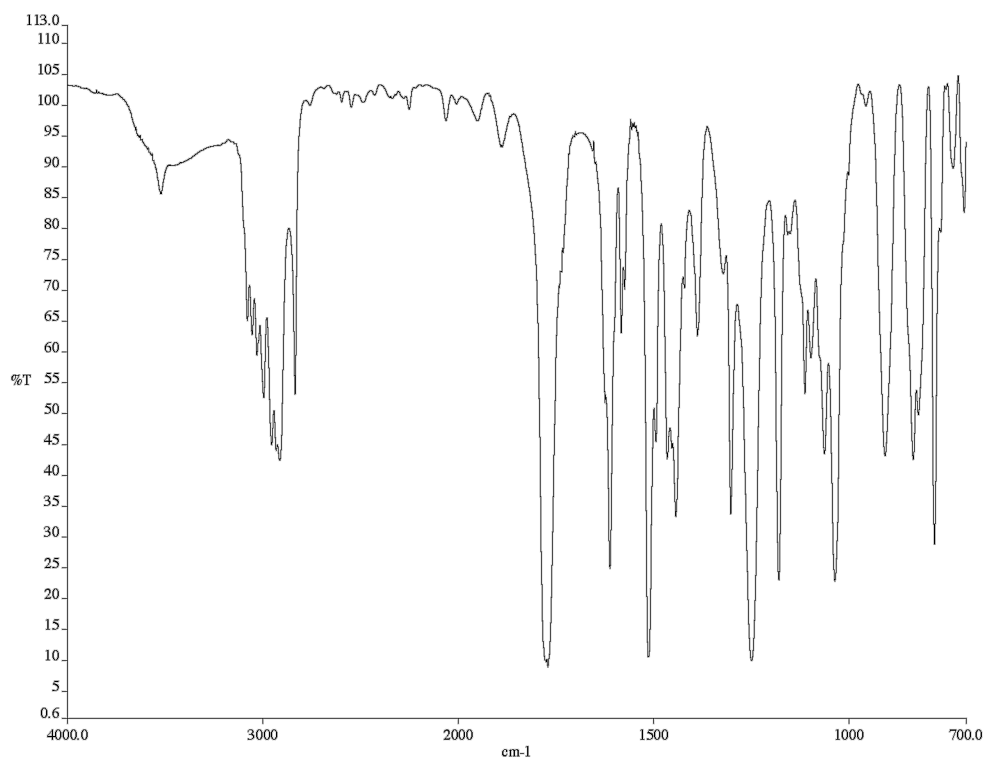


Figure A1.71 Infrared spectrum (thin film/NaCl) of compound **40h**.

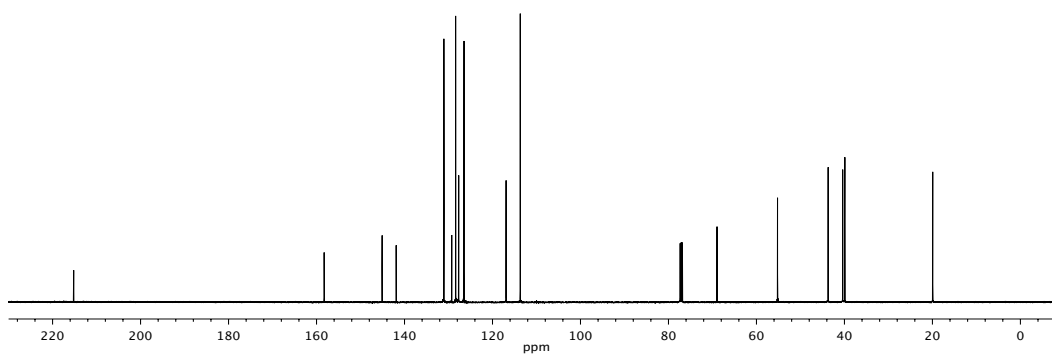


Figure A1.72 ¹³C NMR (125 MHz, CDCl₃) of compound **40h**.

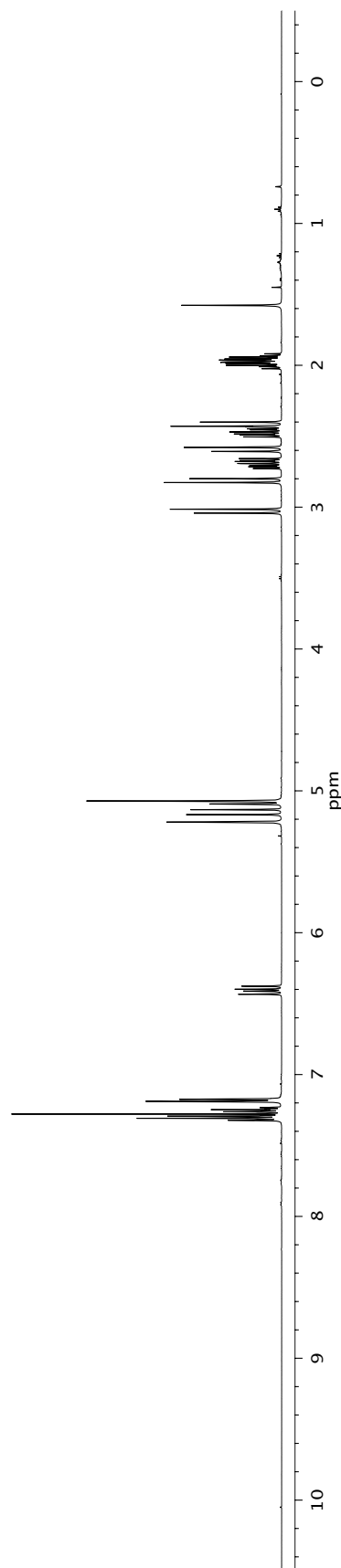
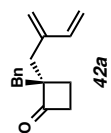


Figure A1.73 ¹H NMR (500 MHz, CDCl₃) of compound 42a.

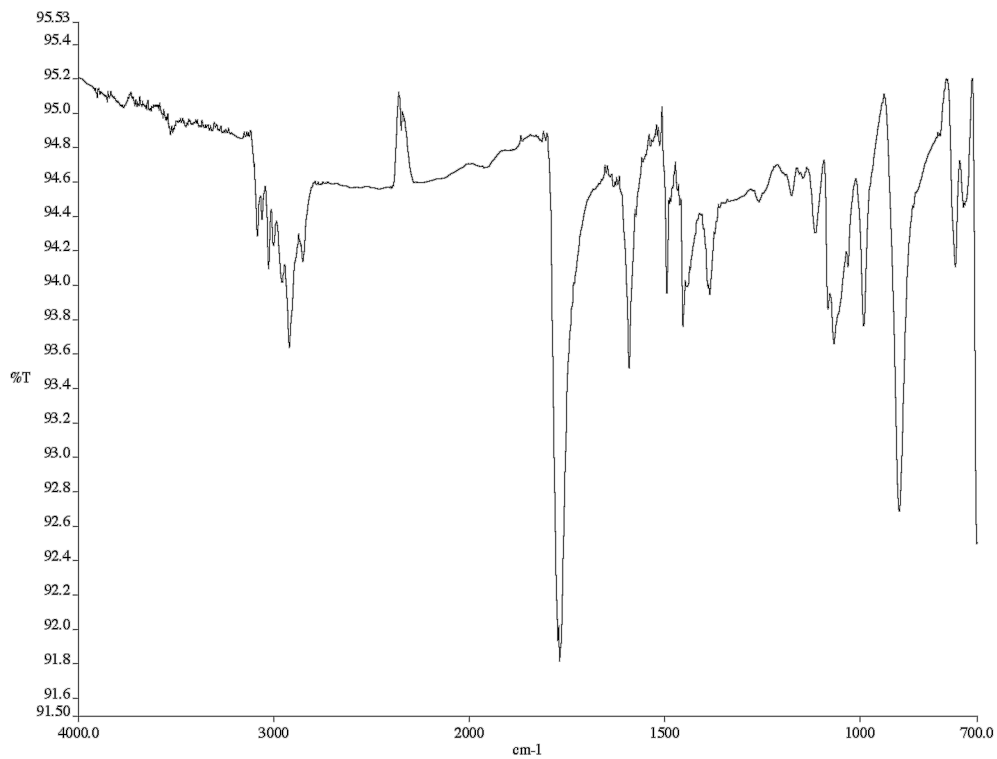


Figure A1.74 Infrared spectrum (thin film/NaCl) of compound **42a**.

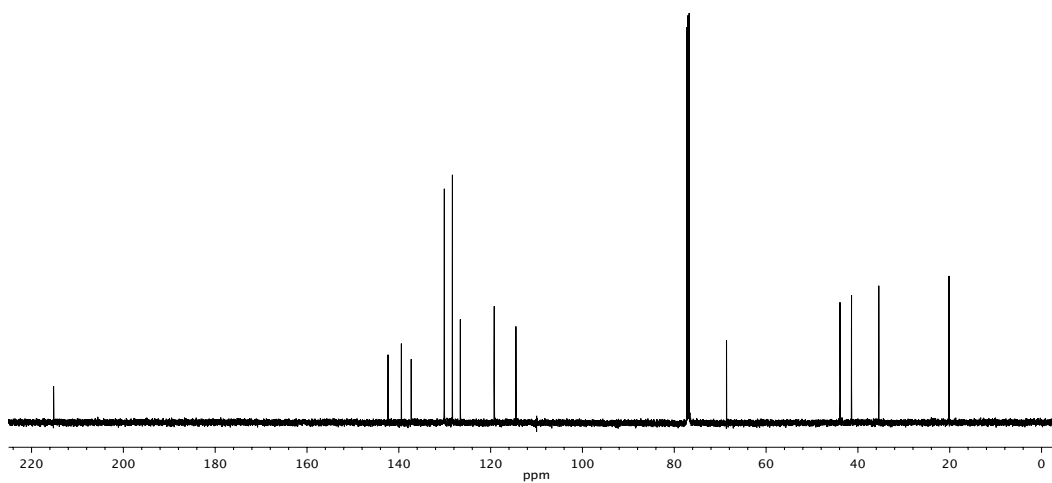


Figure A1.75 ¹³C NMR (125 MHz, CDCl₃) of compound **42a**.

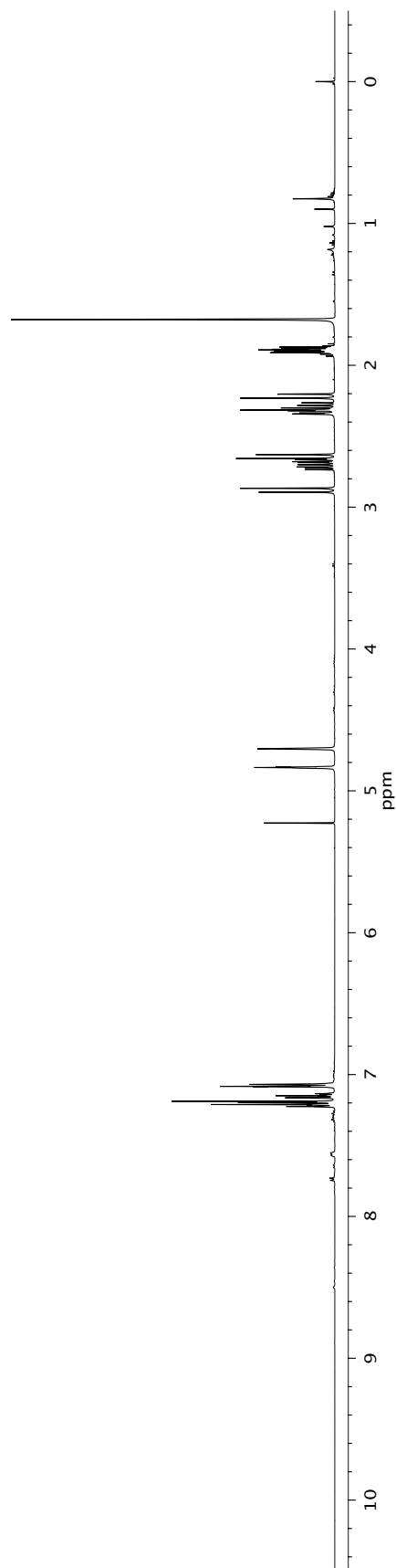
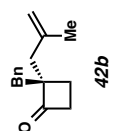


Figure A1.76 ¹H NMR (500 MHz, CDCl₃) of compound 42b.

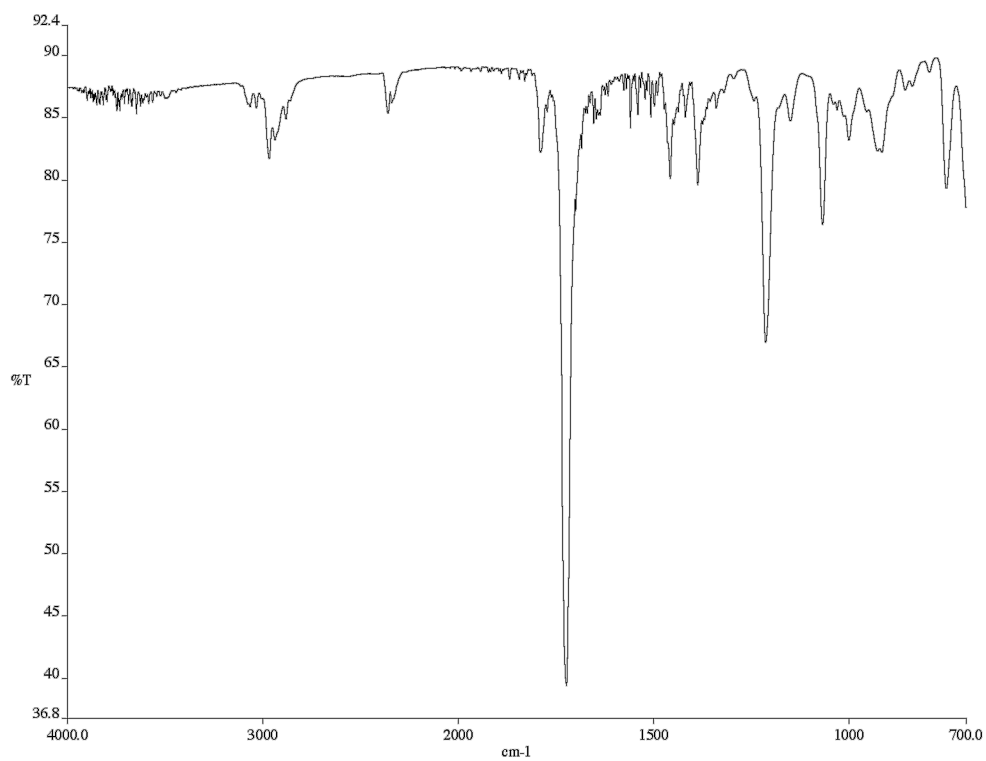


Figure A1.77 Infrared spectrum (thin film/NaCl) of compound **42b**.

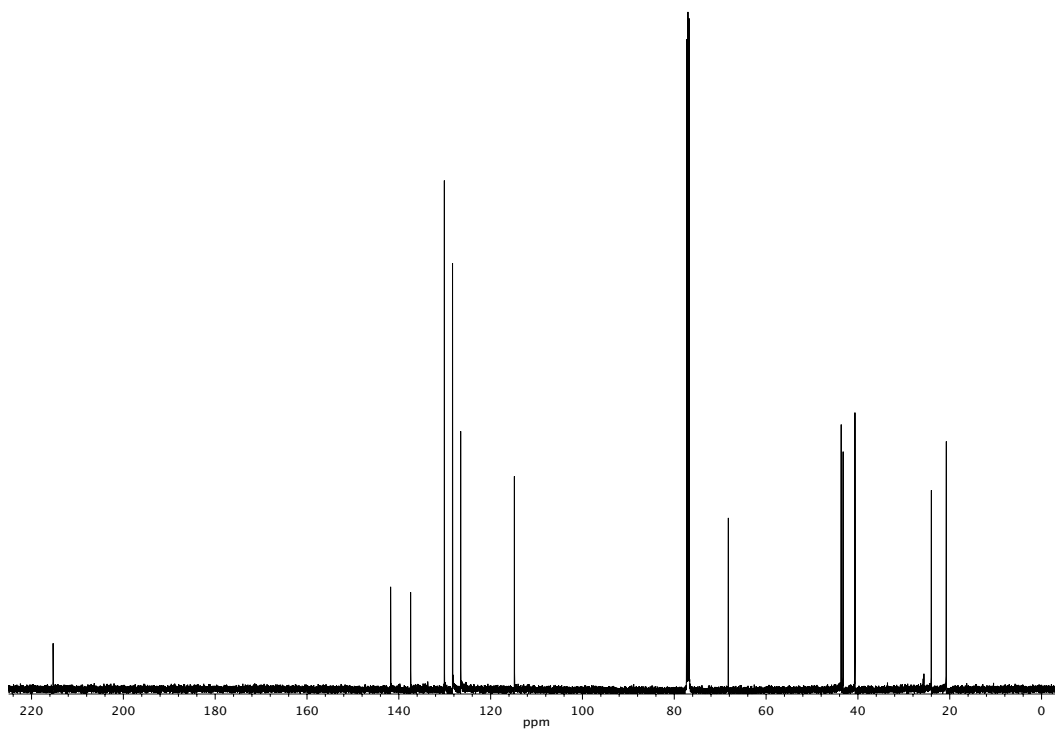


Figure A1.78 ¹³C NMR (125 MHz, CDCl₃) of compound **42b**.

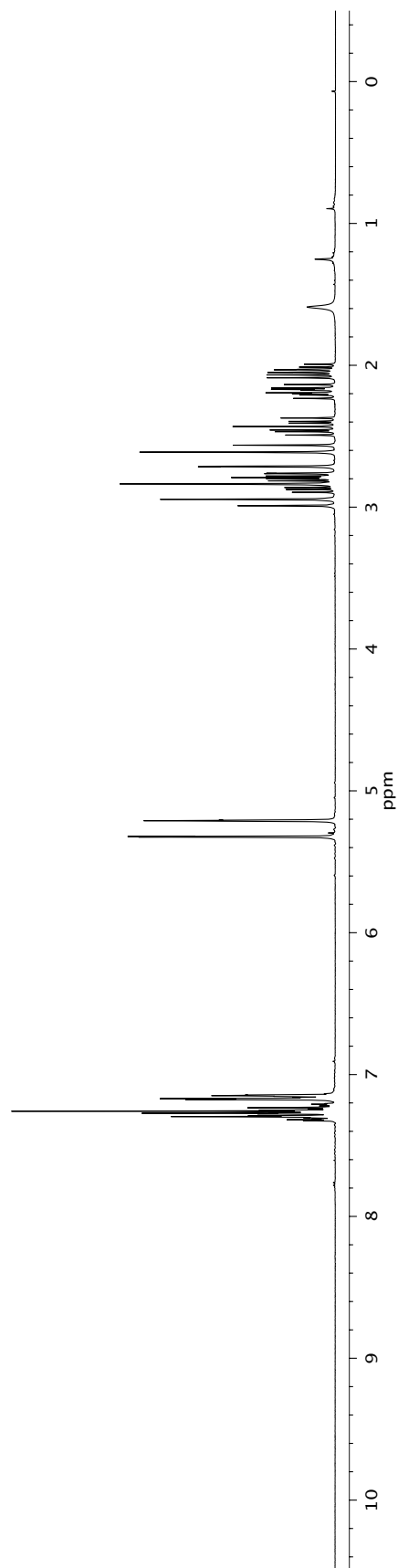
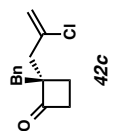


Figure A1.79 ¹H NMR (500 MHz, CDCl₃) of compound **42c**.

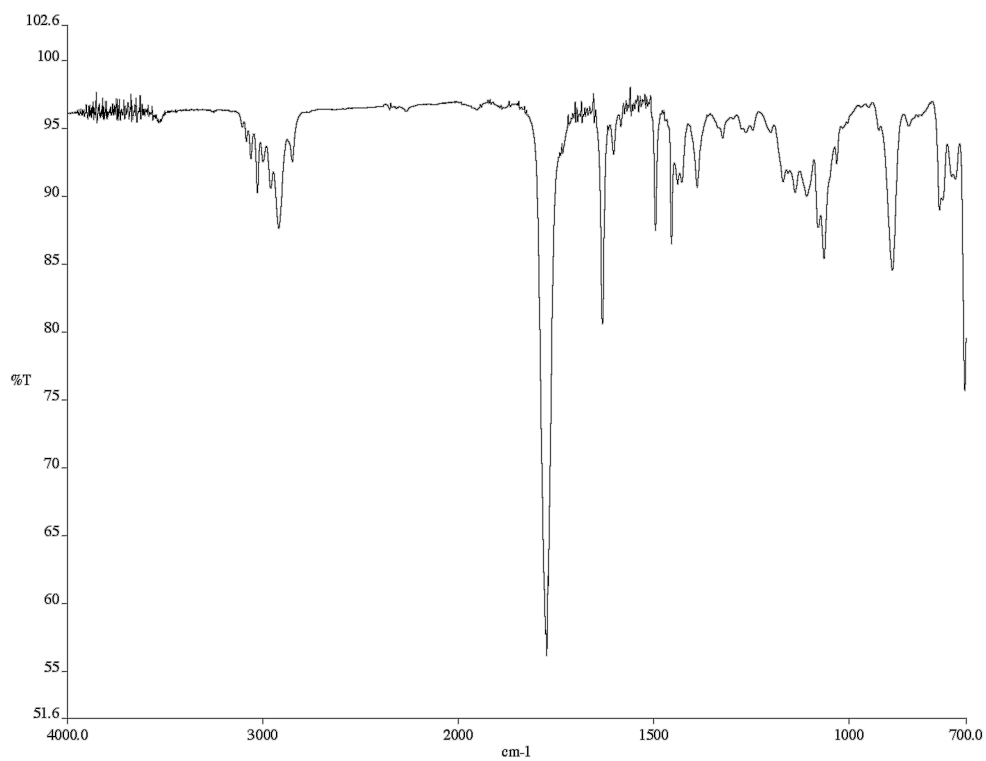


Figure A1.80 Infrared spectrum (thin film/NaCl) of compound **42c**.

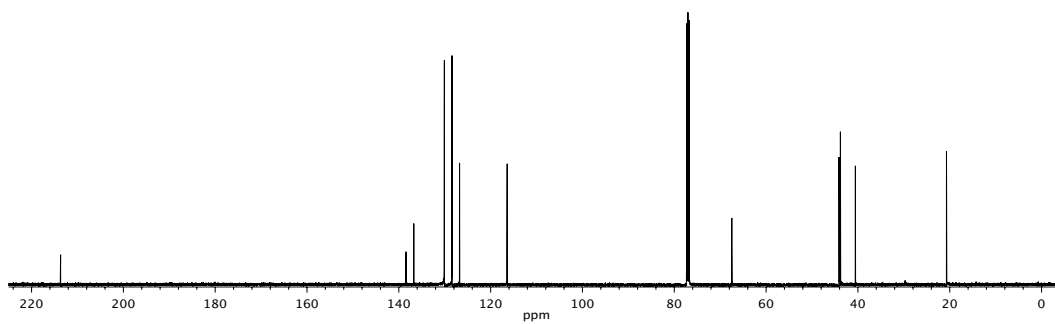


Figure A1.81 ¹³C NMR (125 MHz, CDCl₃) of compound **42c**.

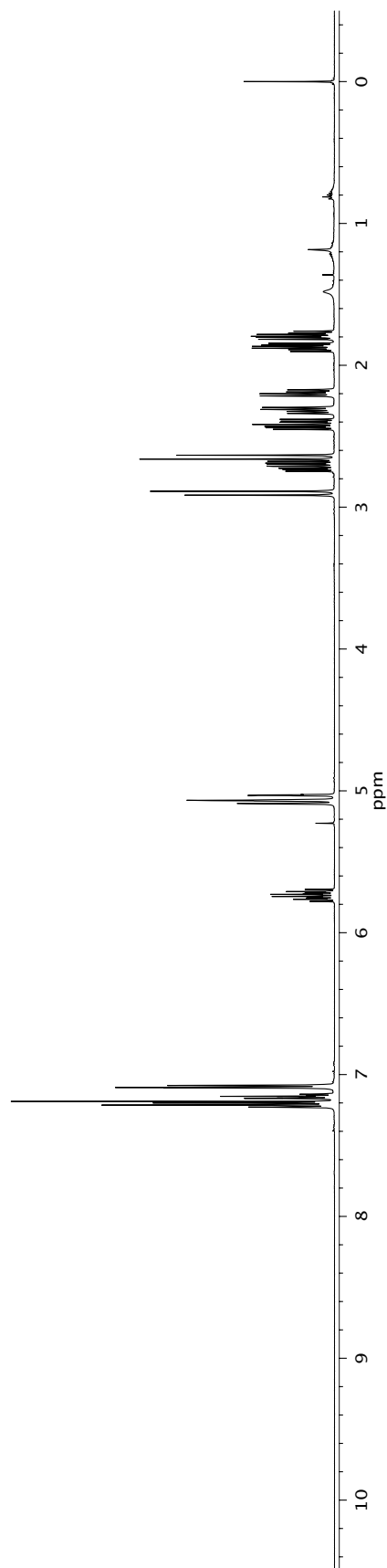
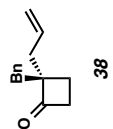


Figure A1.82 ¹H NMR (500 MHz, CDCl₃) of compound **38**.

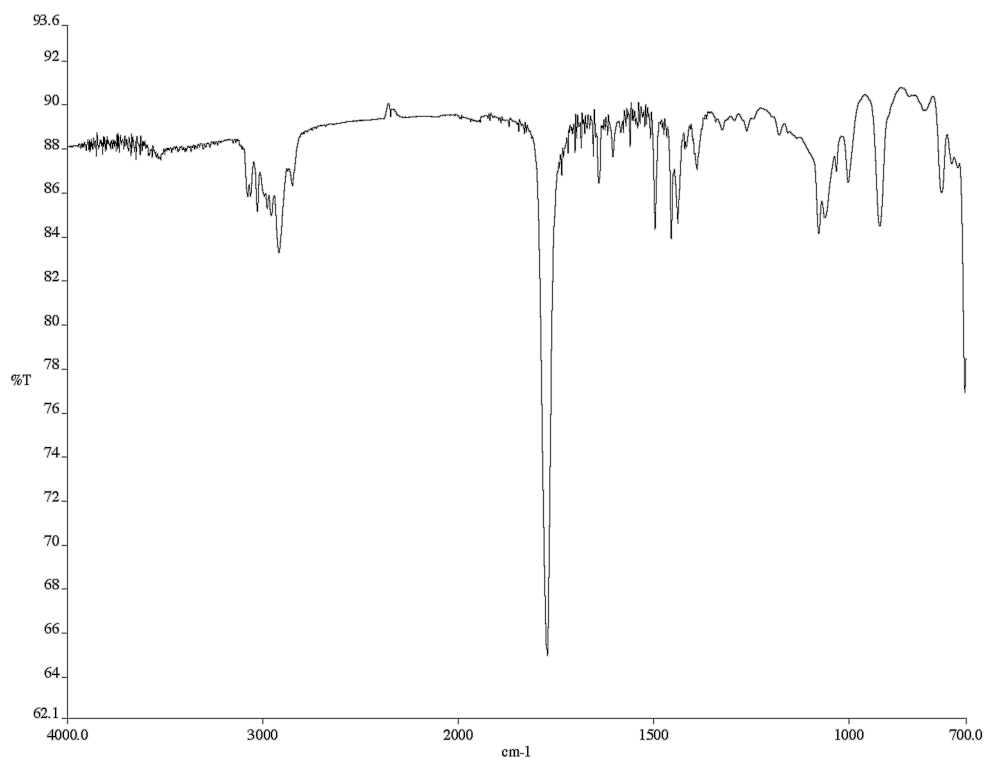


Figure A1.83 Infrared spectrum (thin film/NaCl) of compound **38**.

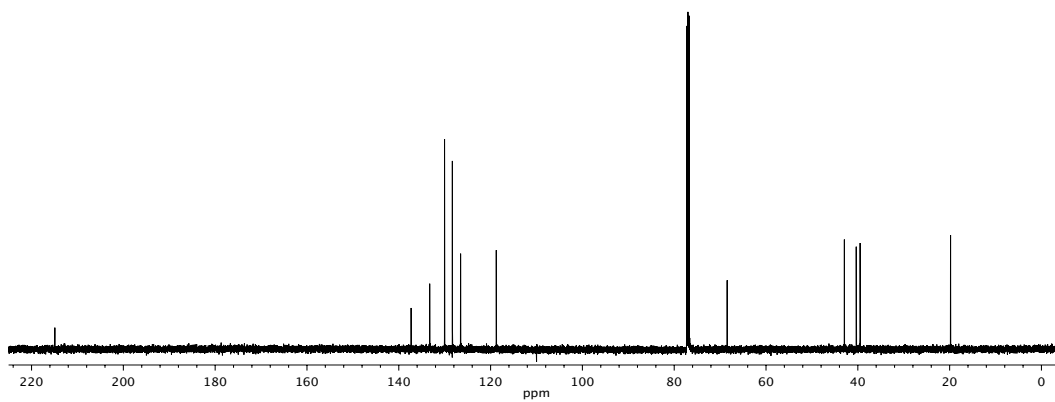


Figure A1.84 ¹³C NMR (125 MHz, CDCl₃) of compound **38**.

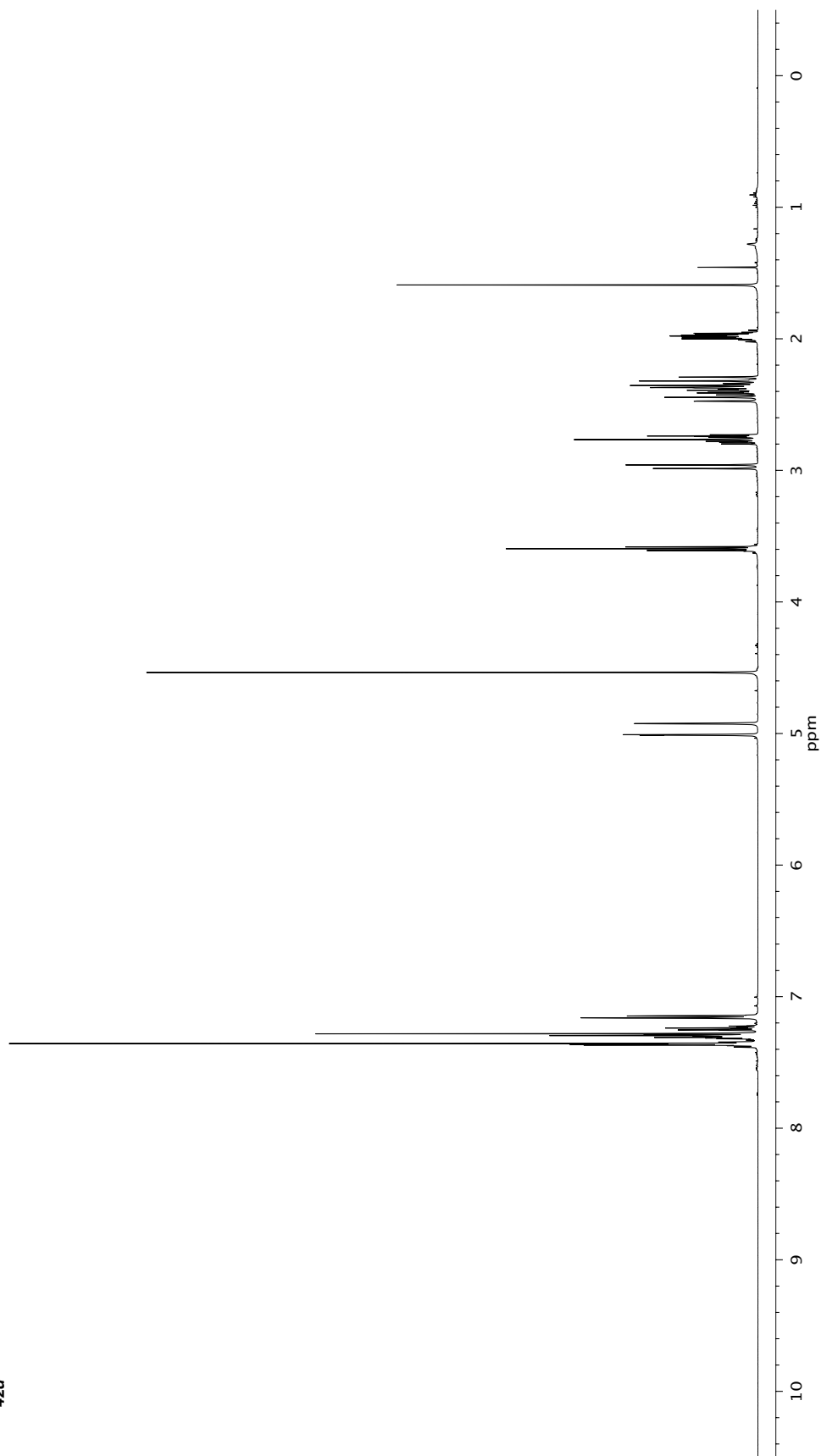
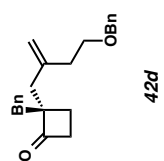


Figure A1.85 ¹H NMR (500 MHz, CDCl₃) of compound 42d.

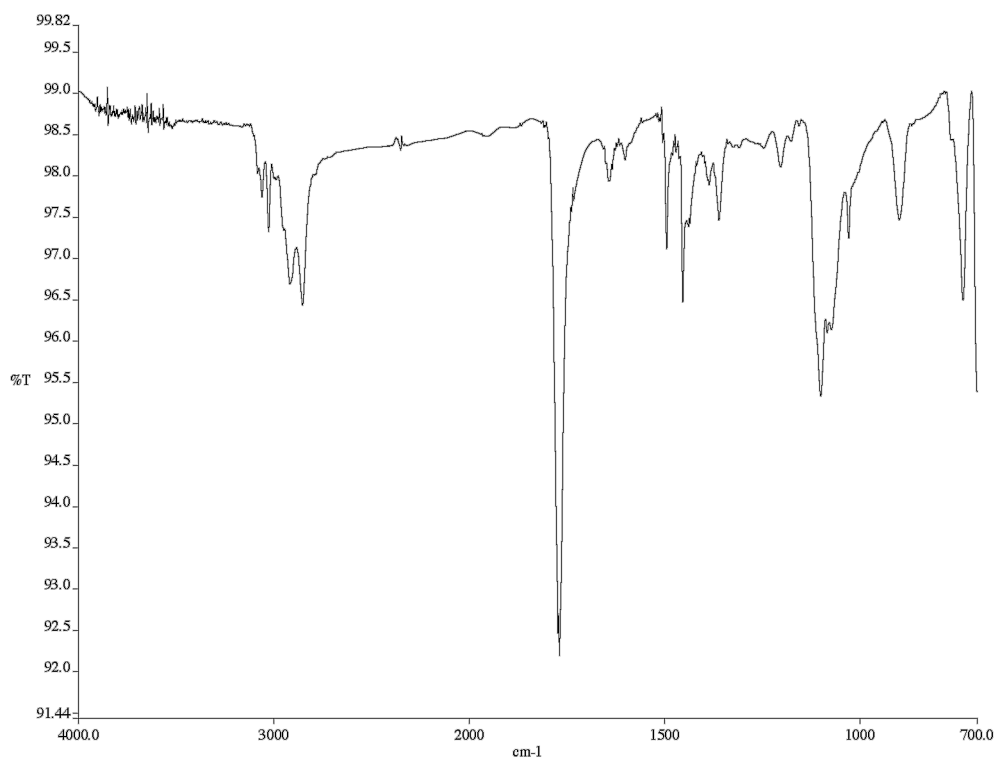


Figure A1.86 Infrared spectrum (thin film/NaCl) of compound **42d**.

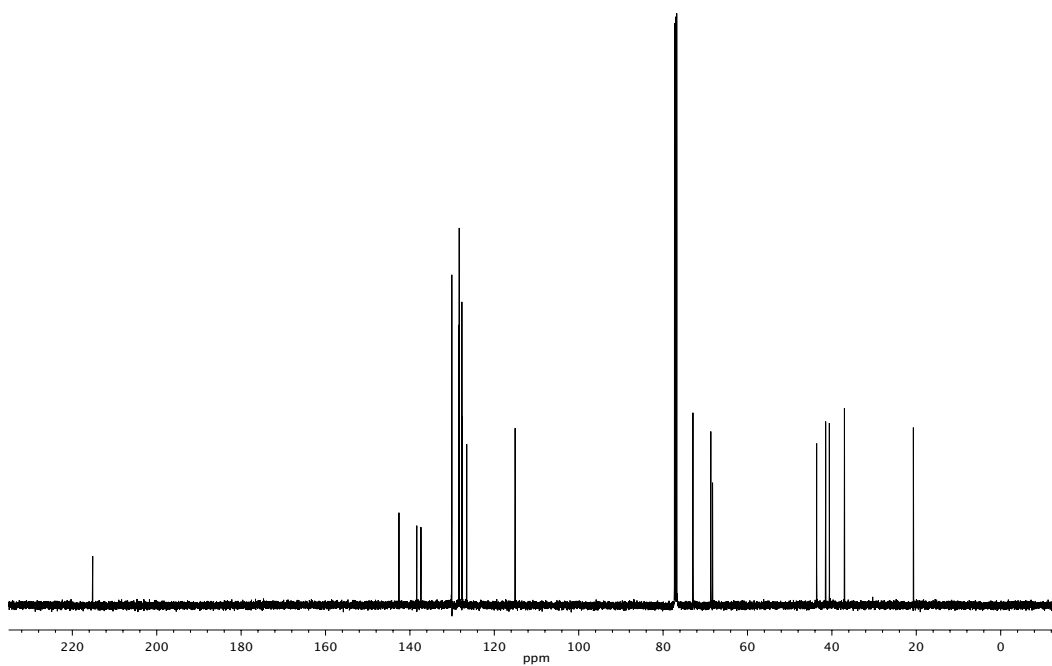
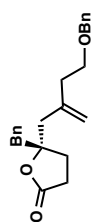
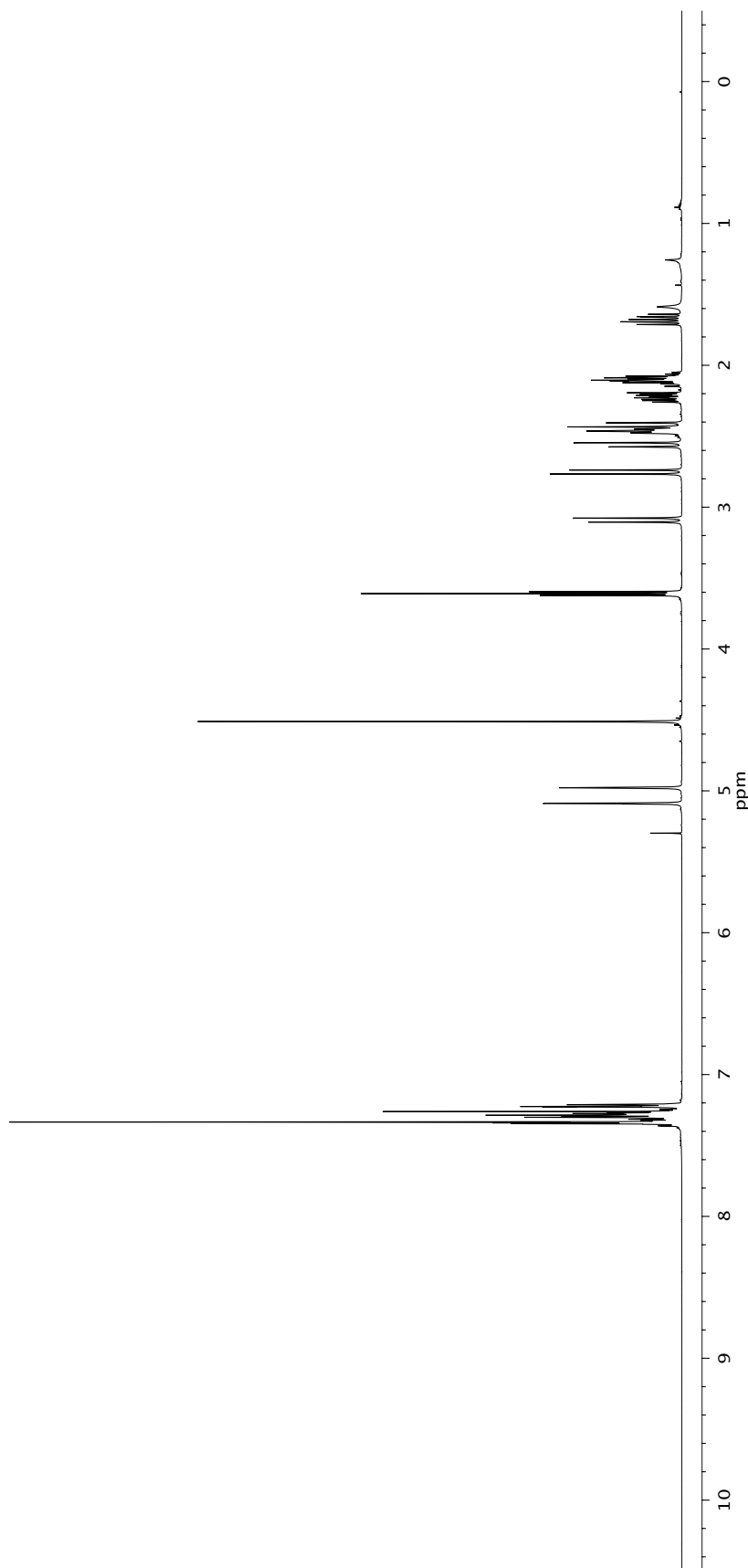


Figure A1.87 ¹³C NMR (125 MHz, CDCl₃) of compound **42d**.



49

Figure A1.88 $^1\text{H NMR}$ (500 MHz, CDCl_3) of compound 49.

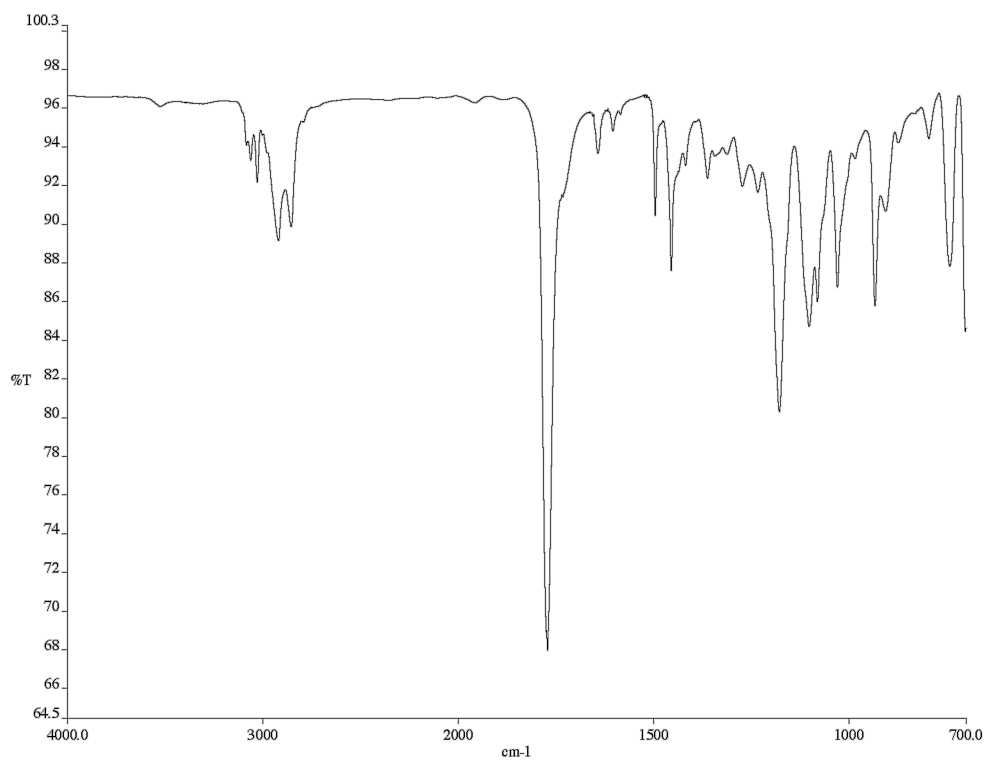


Figure A1.89 Infrared spectrum (thin film/NaCl) of compound 49.

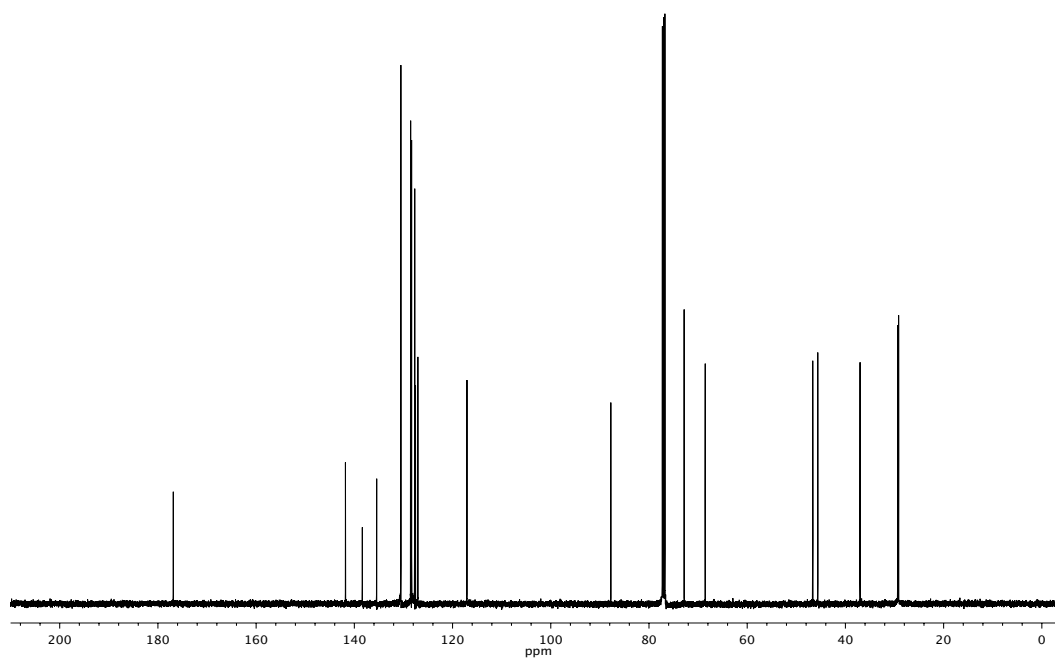


Figure A1.90 ¹³C NMR (125 MHz, CDCl₃) of compound 49.

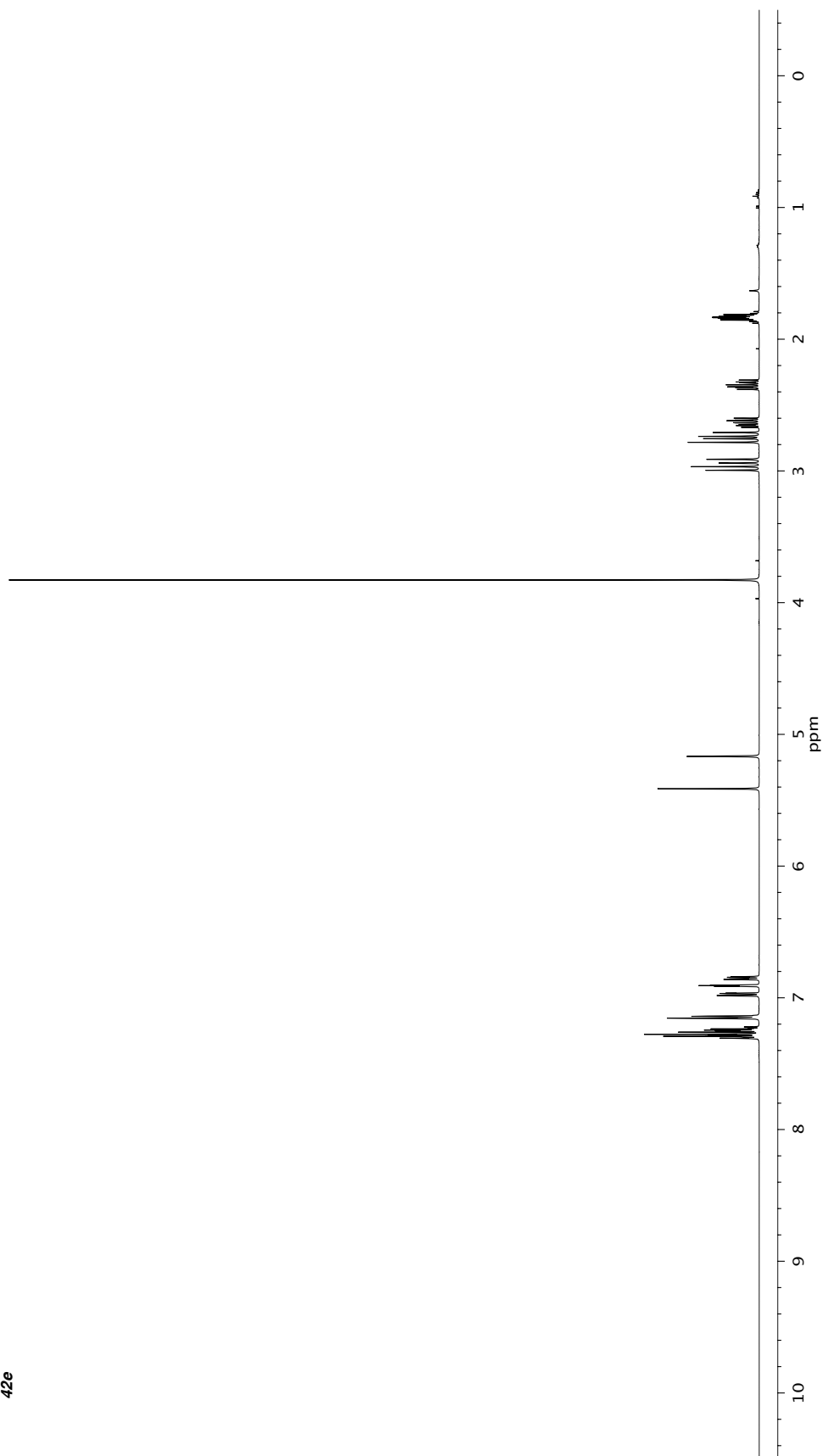
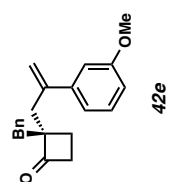


Figure A1.91 ¹H NMR (500 MHz, CDCl₃) of compound 42e.

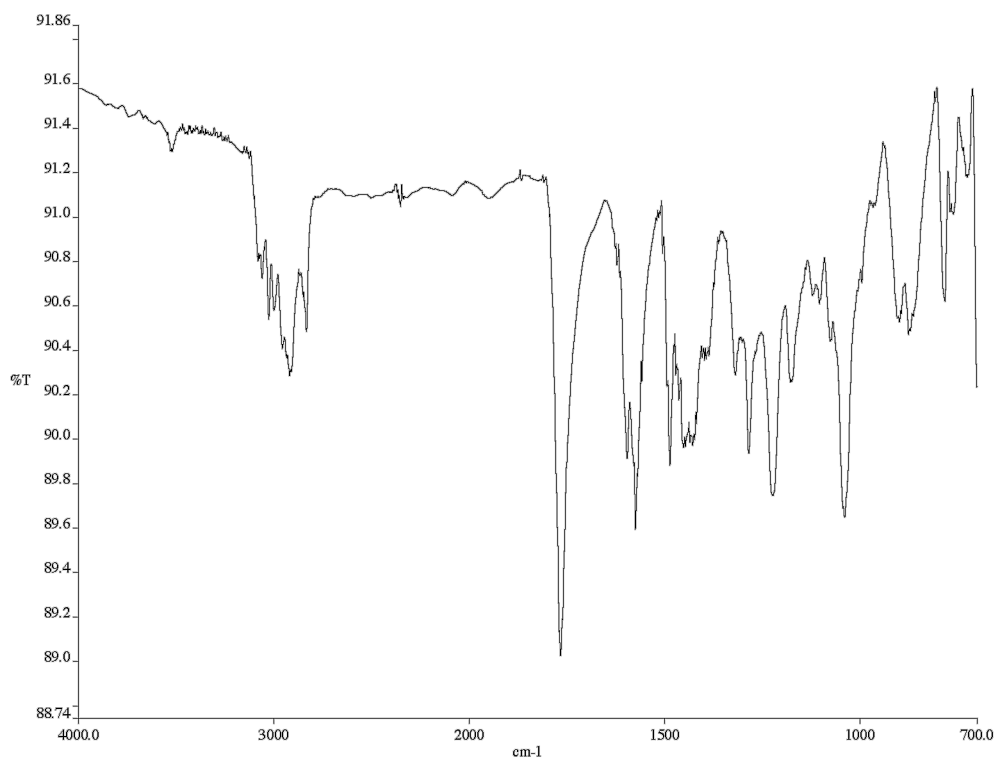


Figure A1.92 Infrared spectrum (thin film/NaCl) of compound **42e**.

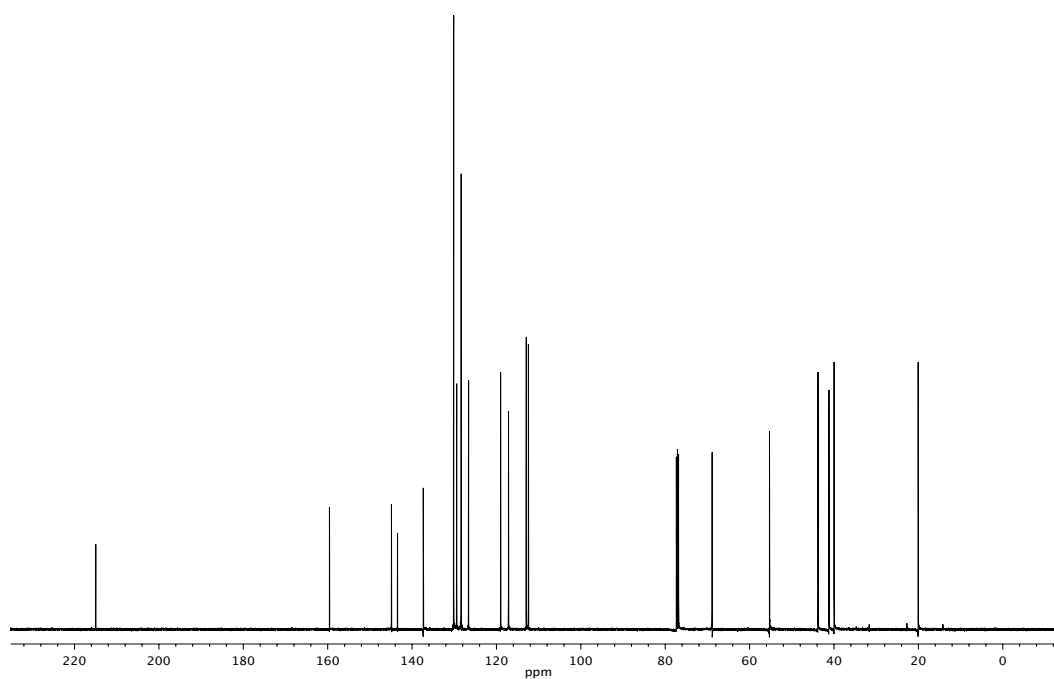


Figure A1.93 ¹³C NMR (125 MHz, CDCl₃) of compound **42e**.

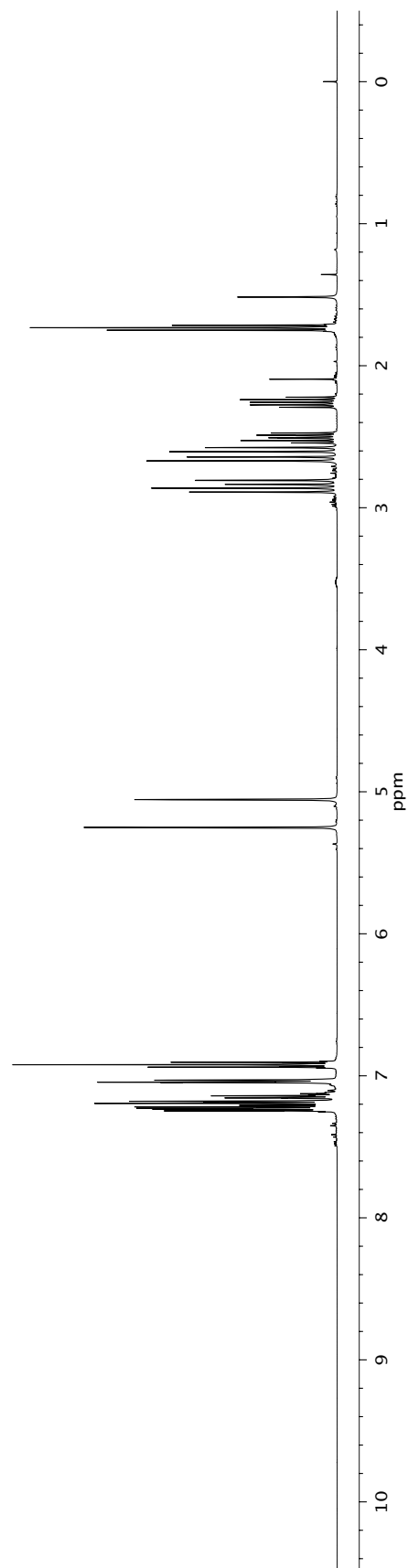
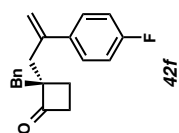


Figure A1.94 ¹H NMR (500 MHz, CDCl₃) of compound 42f.

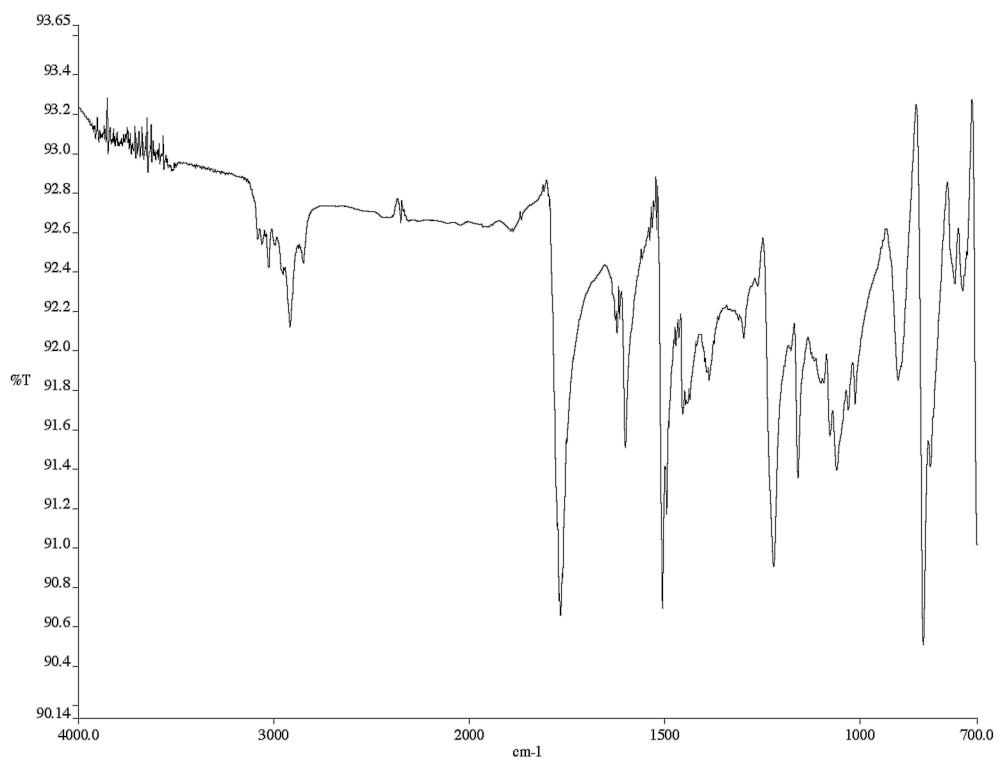


Figure A1.95 Infrared spectrum (thin film/NaCl) of compound **42f**.

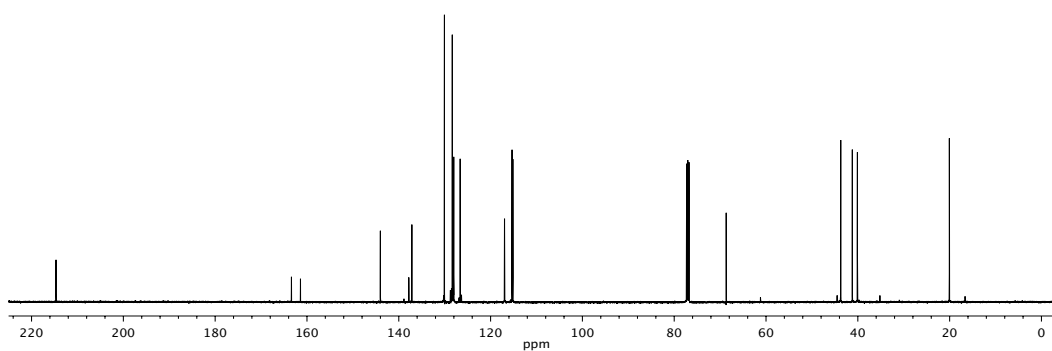


Figure A1.96 ^{13}C NMR (125 MHz, CDCl_3) of compound **42f**.

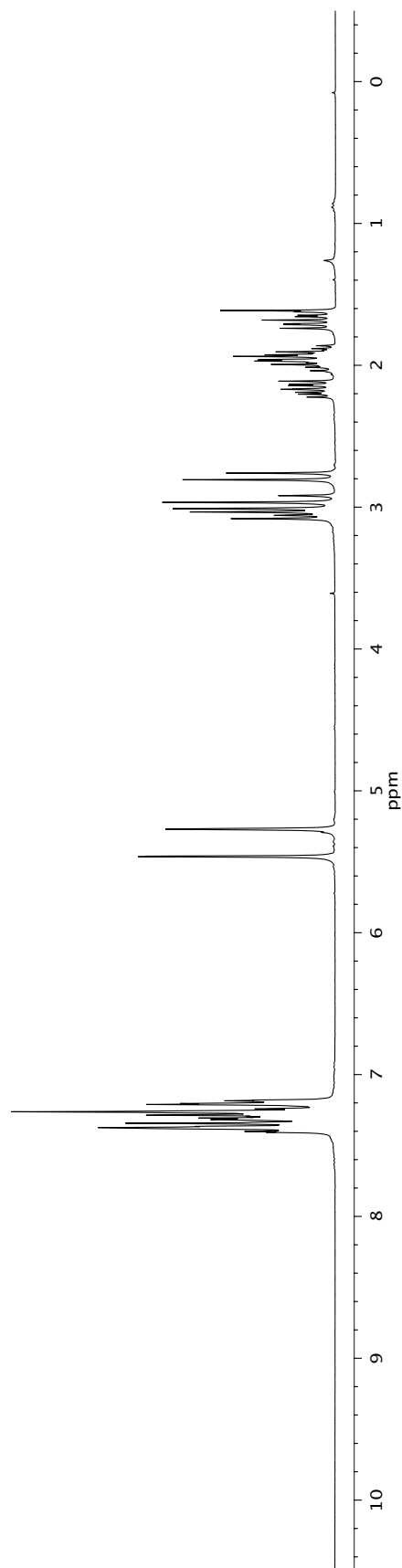
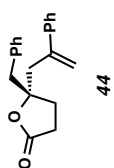


Figure A1.97 ¹H NMR (300 MHz, CDCl₃) of compound 44.

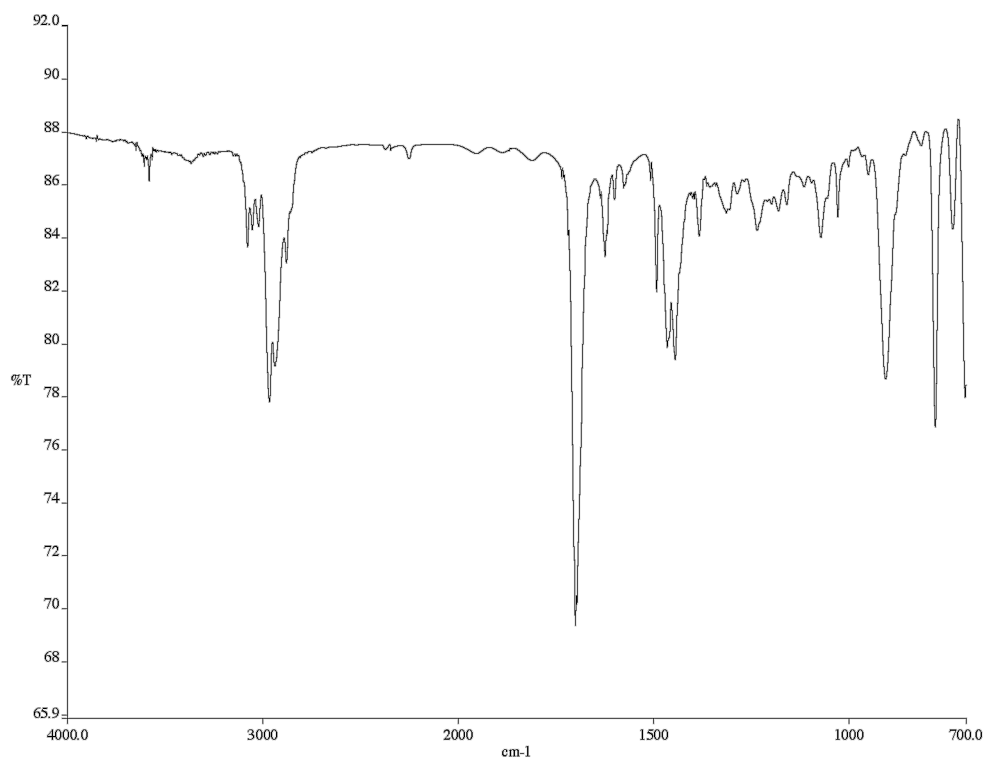


Figure A1.98 Infrared spectrum (thin film/NaCl) of compound 44.

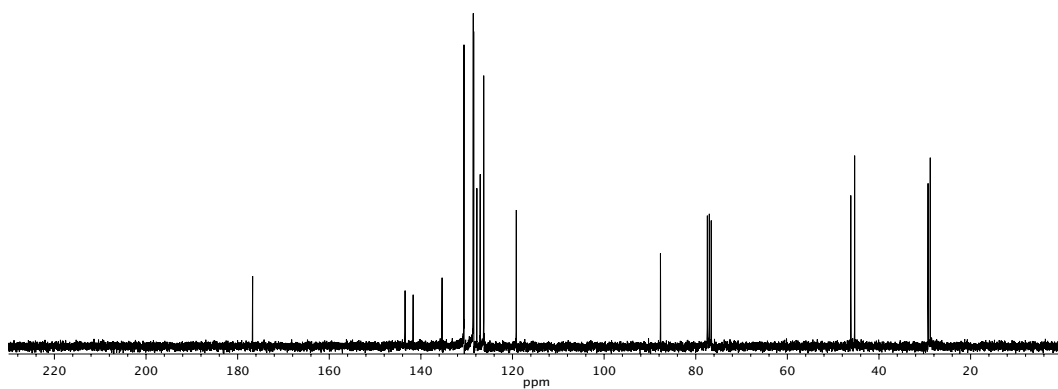


Figure A1.99 ¹³C NMR (125 MHz, CDCl₃) of compound 44.

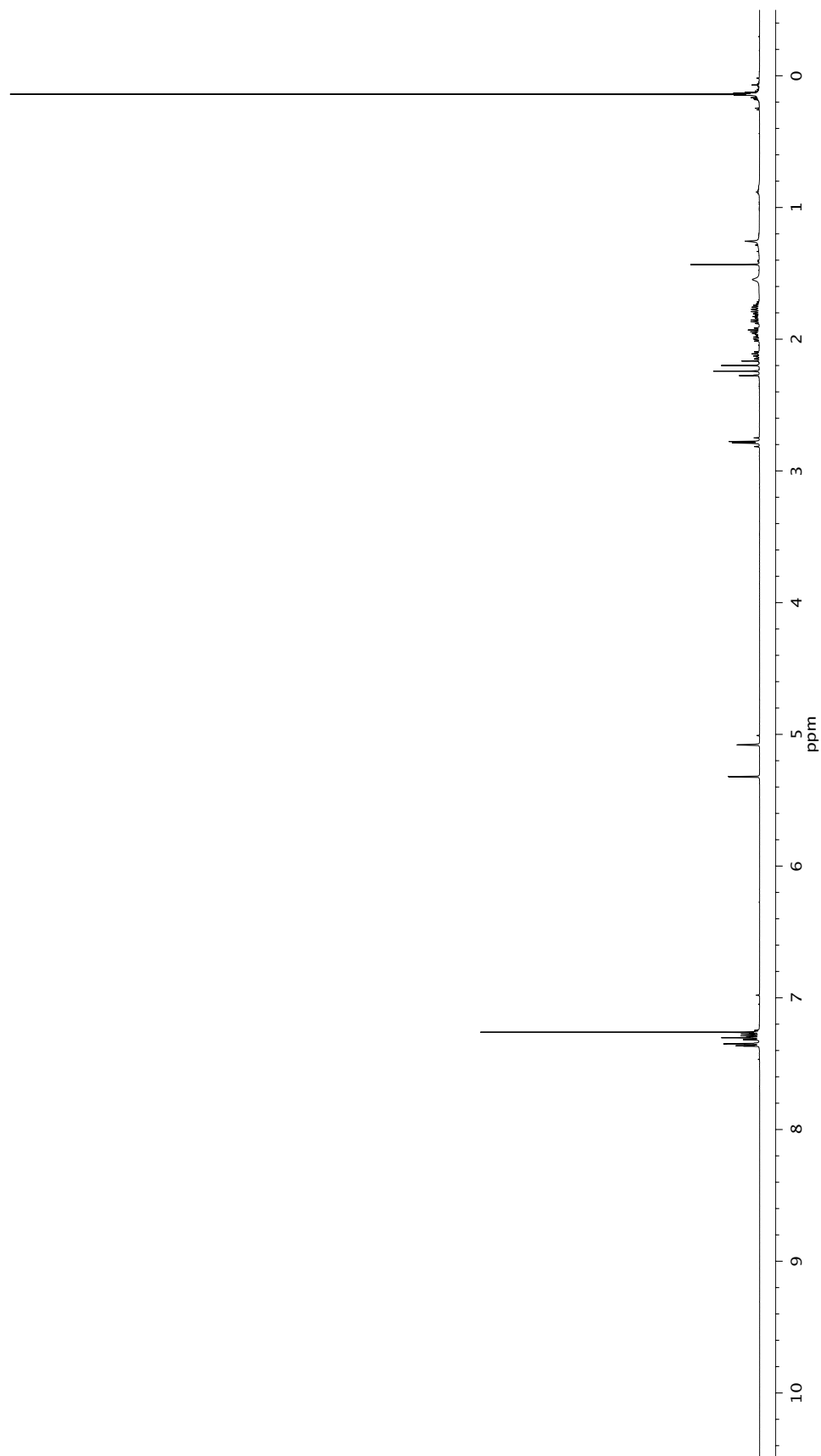
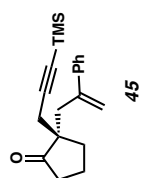


Figure A1.100 ¹H NMR (500 MHz, CDCl₃) of compound 45.

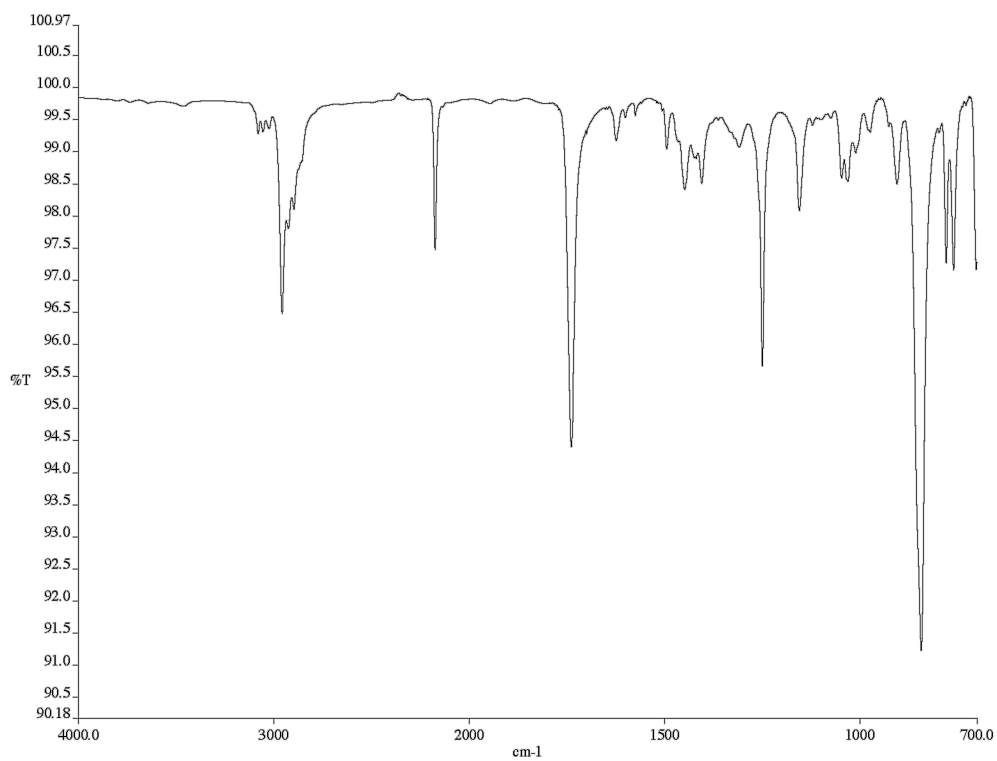


Figure A1.101 Infrared spectrum (thin film/NaCl) of compound **45**.

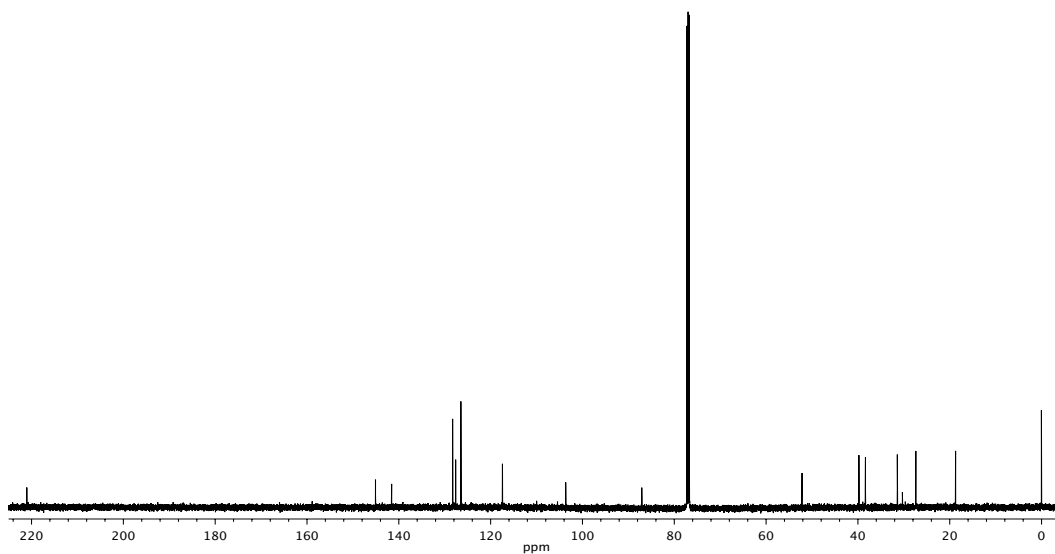
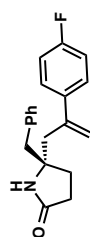


Figure A1.102 ¹³C NMR (125 MHz, CDCl₃) of compound **45**.



46

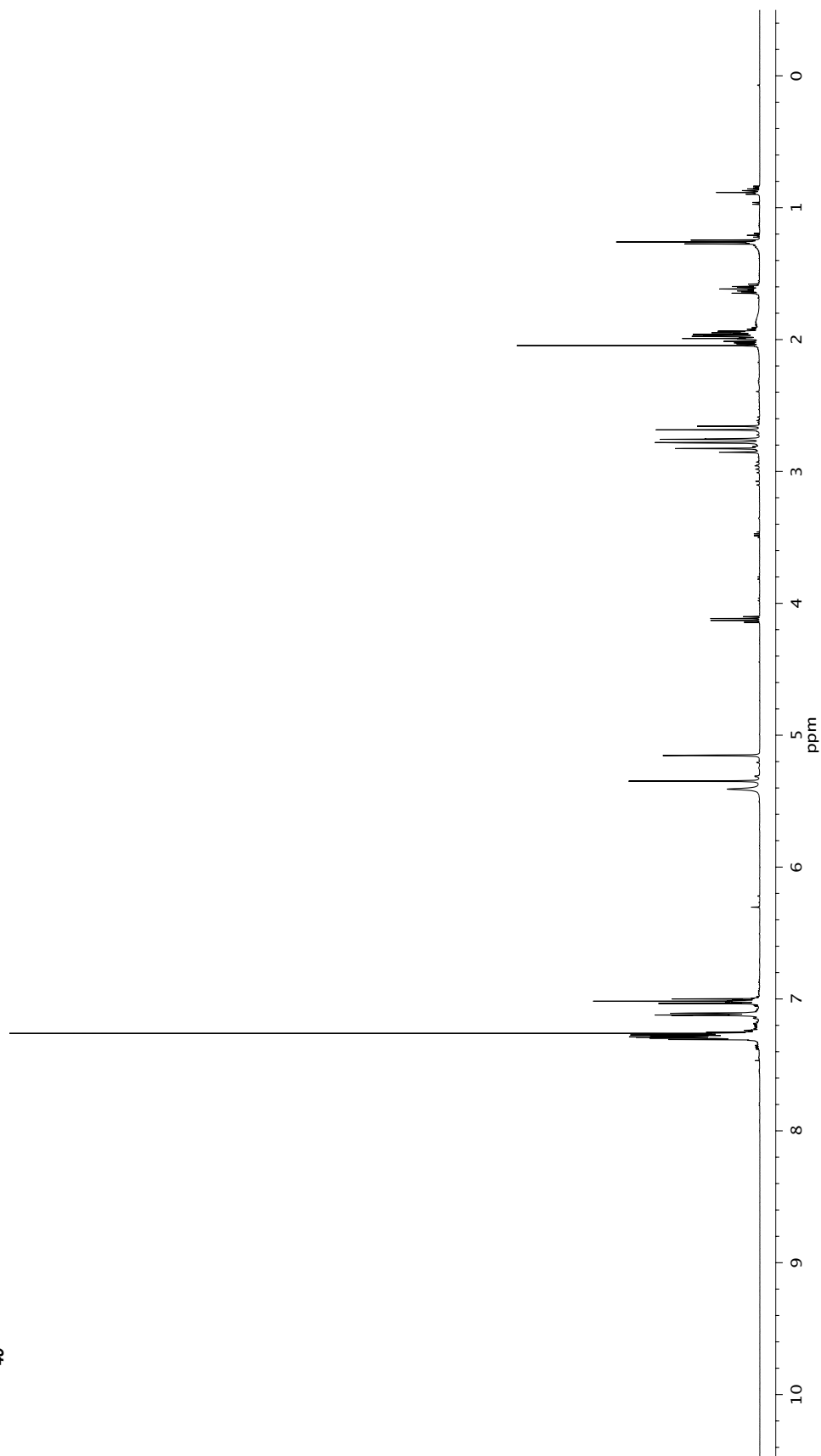


Figure A1.103 ^1H NMR (500 MHz, CDCl_3) of compound **46**.

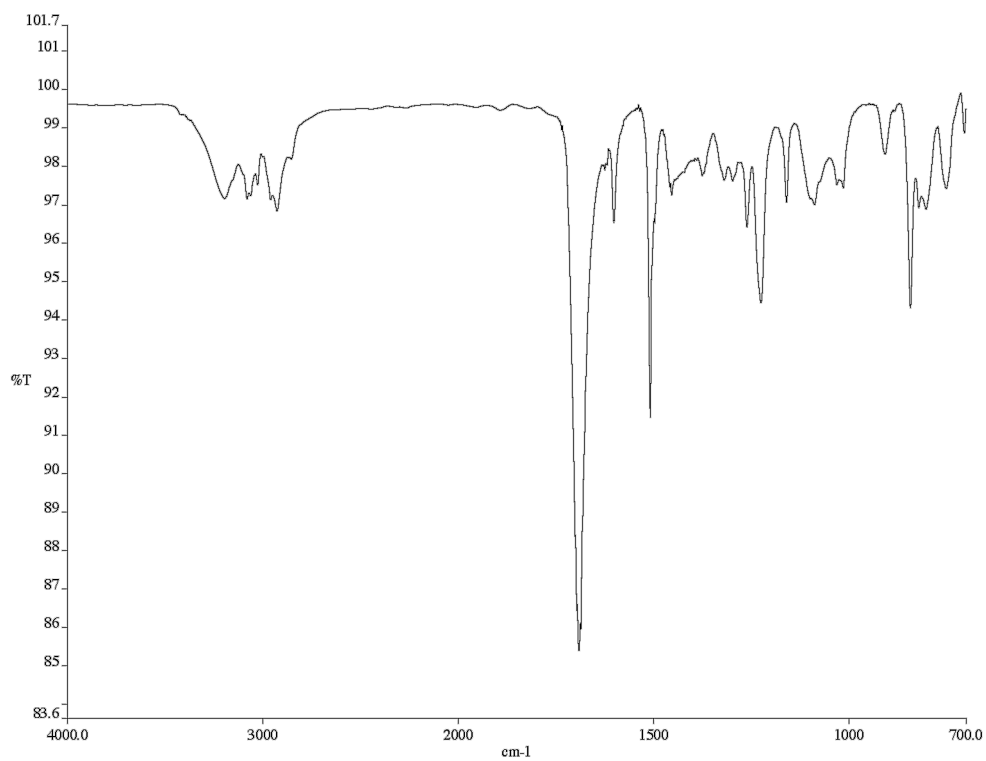


Figure A1.104 Infrared spectrum (thin film/NaCl) of compound **46**.

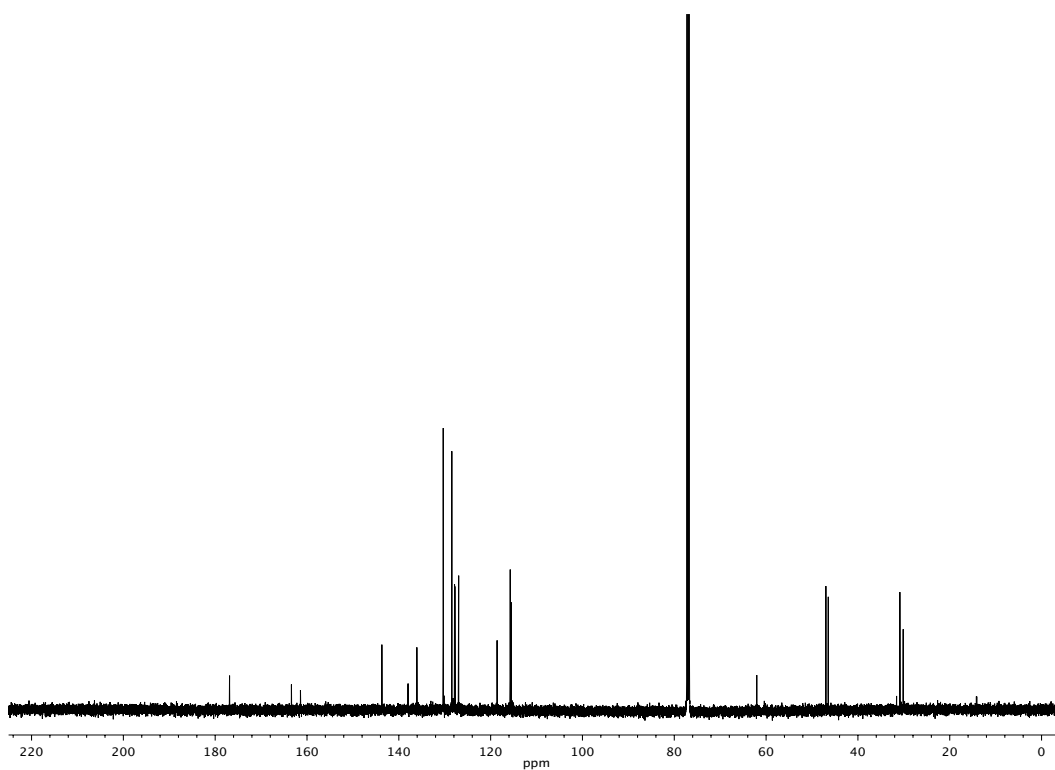


Figure A1.105 ¹³C NMR (125 MHz, CDCl₃) of compound **46**.

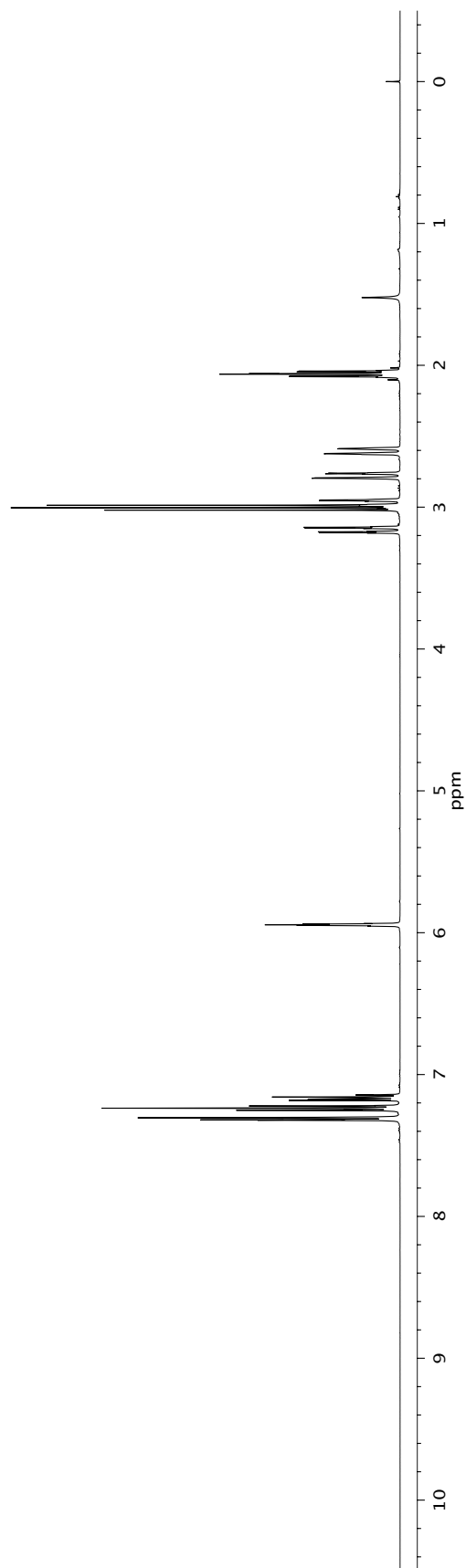
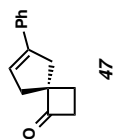


Figure A1.106 ^1H NMR (500 MHz, CDCl_3) of compound 47.

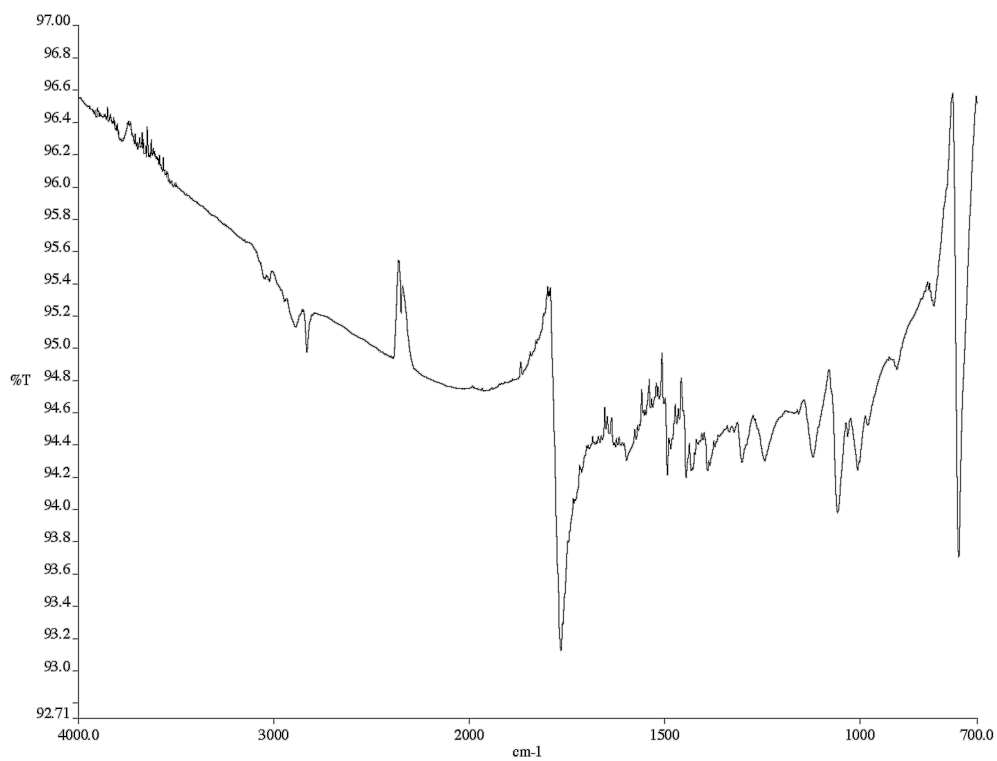


Figure A1.107 Infrared spectrum (thin film/NaCl) of compound **47**.

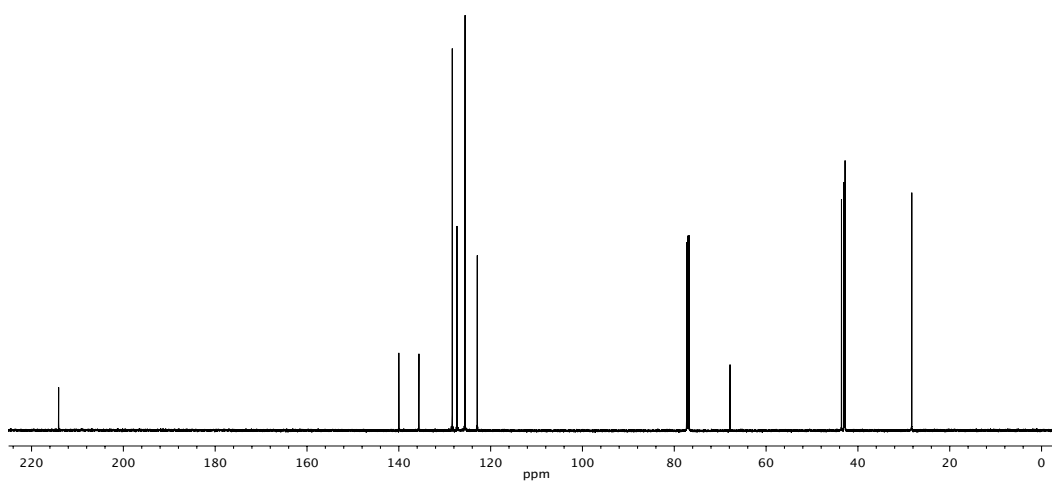


Figure A1.108 ¹³C NMR (125 MHz, CDCl₃) of compound **47**.

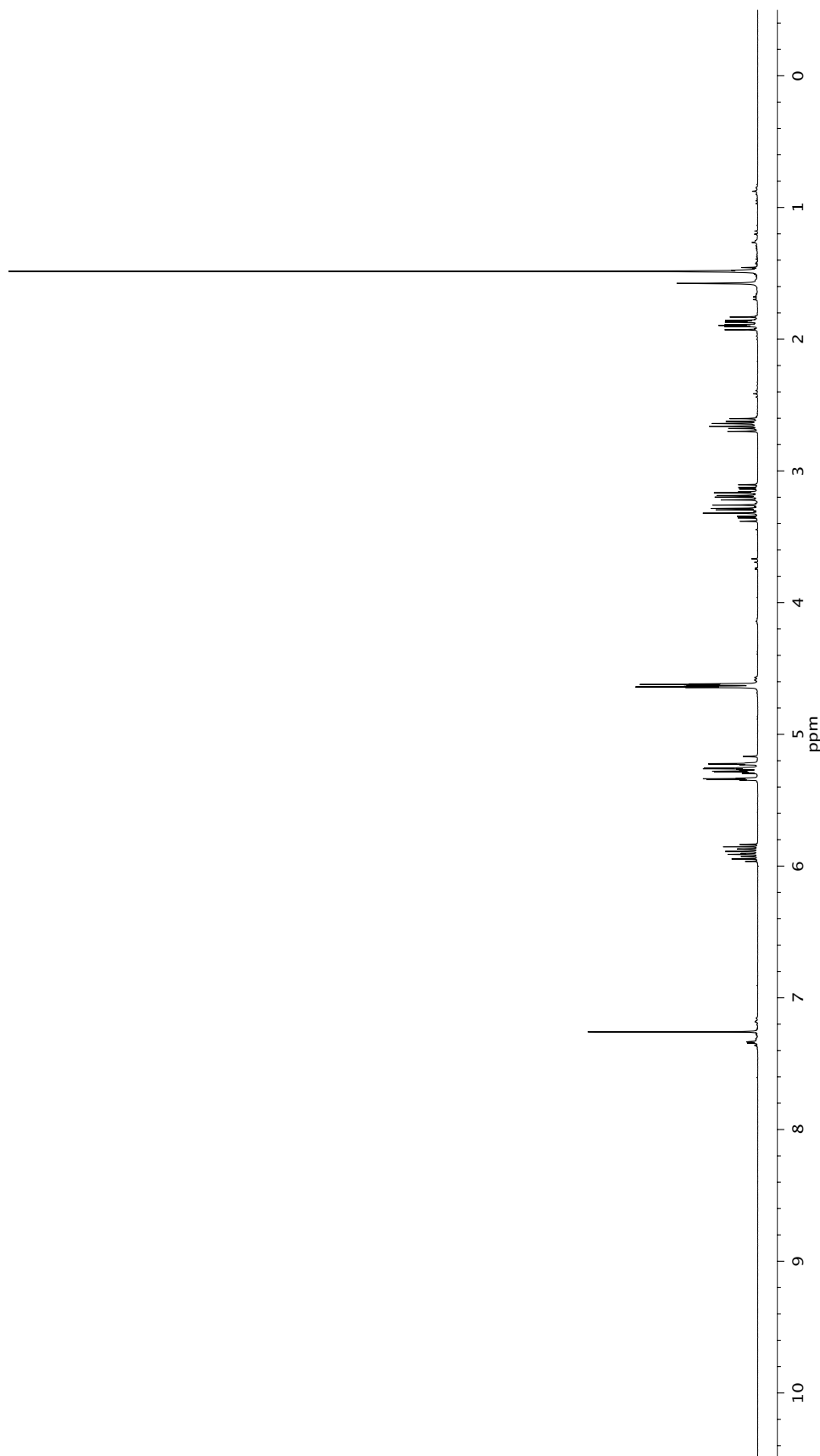
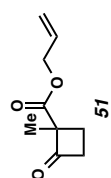


Figure A1.109 ¹H NMR (300 MHz, CDCl₃) of compound 51.

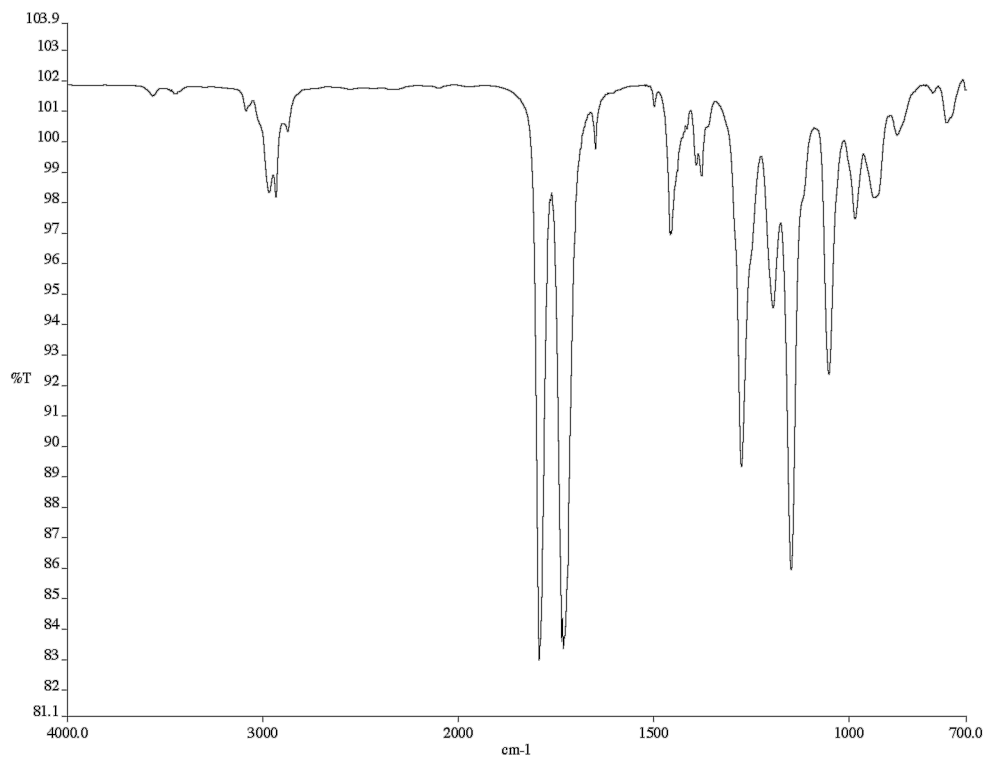


Figure A1.110 Infrared spectrum (thin film/NaCl) of compound **51**.

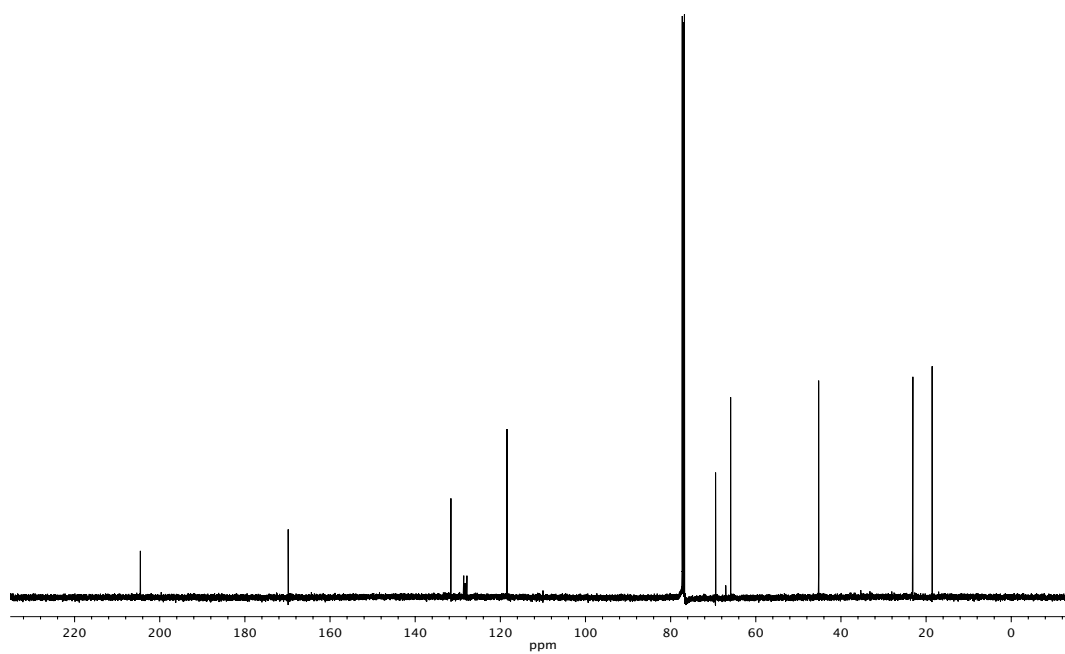


Figure A1.111 ¹³C NMR (125 MHz, CDCl₃) of compound **51**.

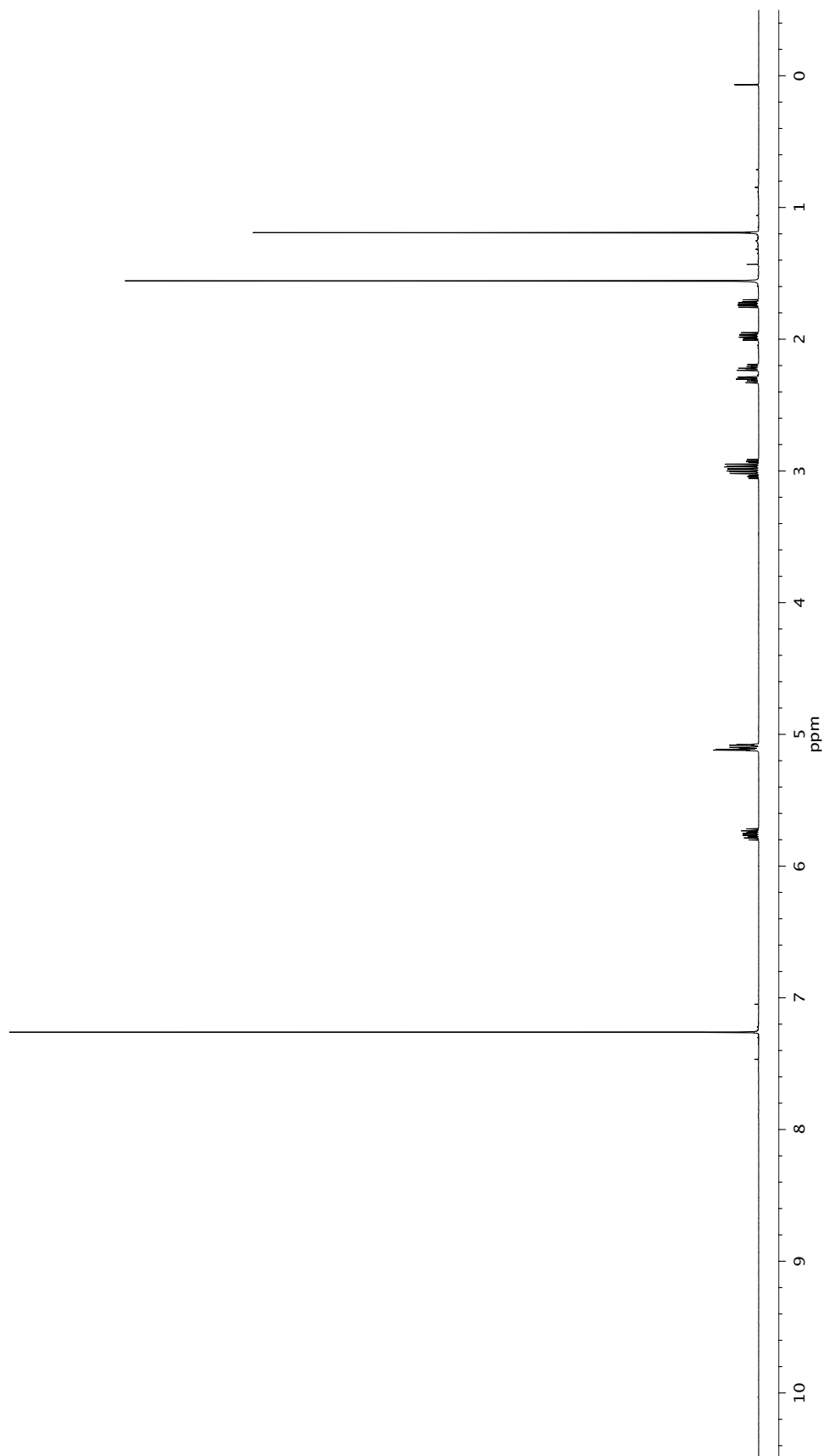
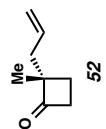


Figure A1.112 ^1H NMR (500 MHz, CDCl_3) of compound 52.

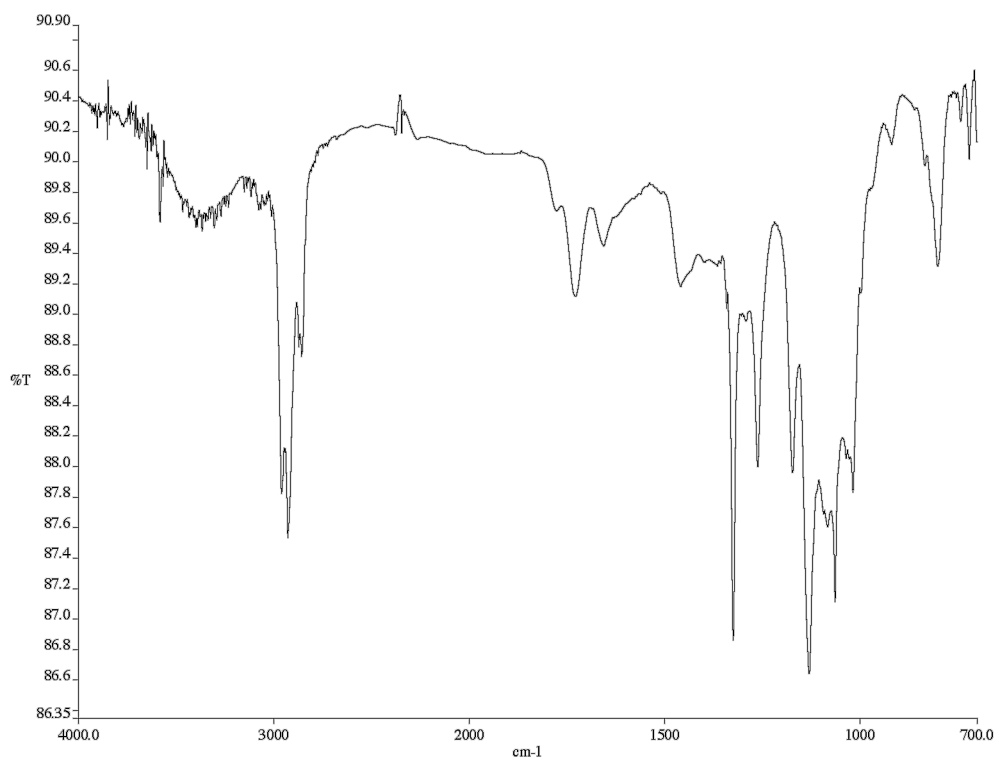


Figure A1.113 Infrared spectrum (thin film/NaCl) of compound **52**.

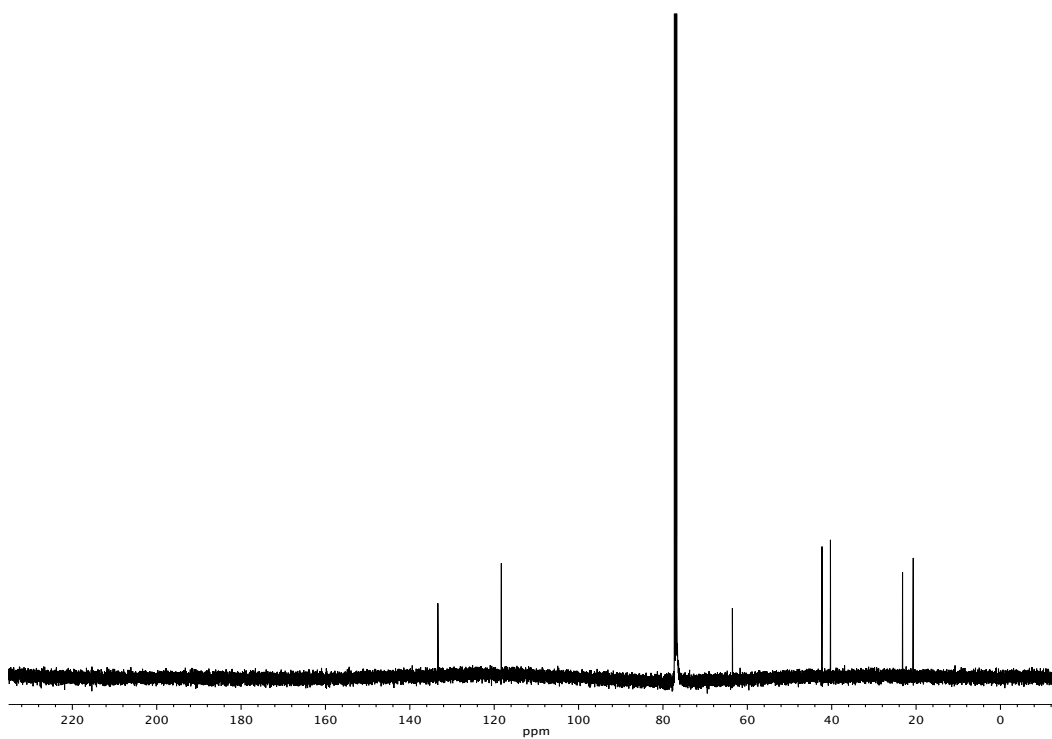


Figure A1.114 ¹³C NMR (125 MHz, CDCl₃) of compound **52**.

CHAPTER 2

Development of (Trimethylsilyl)Ethyl Ester-Protected Enolates and Applications in Palladium–Catalyzed Enantioselective Allylic Alkylation: Intermolecular Cross-Coupling of Functionalized Electrophiles¹

2.1 INTRODUCTION

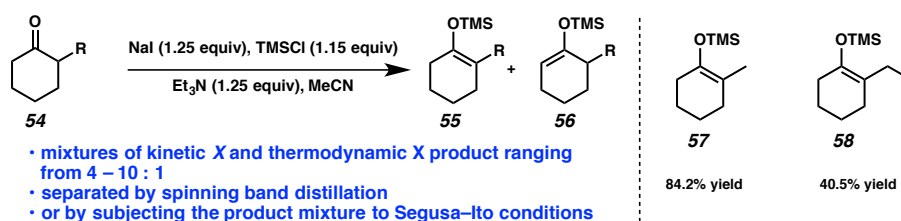
2.1.1 Latent enolates: silyl enol ethers

Latent or protected enolates such as silyl enol ethers, silyl ketene acetals, allyl enol carbonates, allyl β -keto esters and others, have found broad use in organic synthesis owing to their mild release and ease of use.^{51,15} Perhaps the most well studied class of protected enolates employ oxygen-bound protecting groups (i.e. silyl enol ethers). Unfortunately, the utility of this class of compounds is often limited by poor regioselectivity when forming fully substituted enol derivatives.⁵² Although much effort has been devoted to the identification of conditions that allow for selective generation of so-called “thermodynamic” enolate isomers, selectivity often drops precipitously when sterically demanding α -substitution is introduced (Figure 2.1.1.1).⁵³ For example, in previous studies by the Stoltz group, it was found that while formation of the

¹ This work was performed in collaboration with Douglas C. Behenna, staff scientist in the Stoltz group. This work has been published. See: Reeves, C. M.; Behenna, D. C.; Stoltz, B. M. *Org. Lett.* **2014**, *16*, 2314.

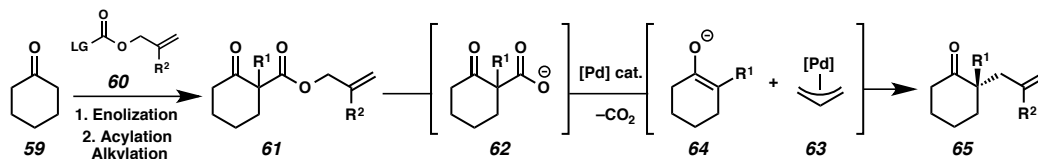
thermodynamic silyl enol ether derived from 2-methyl cyclohexanone (Figure 2.1.1.1, **57**) proceeded in 84% yield, while the corresponding ethyl substituted enol ether (Figure 2.1.1.1, **58**) was formed in only 41% yield.

Figure 2.1.1.1. Drawbacks of silyl enol ether synthesis



2.1.2 Latent enolates: β -ketoesters

The problem of thermodynamic enolate masking would be solved, ideally, by the development of enolate precursors that are readily prepared and, when triggered, release the “thermodynamic” enolate under kinetic control. In the context of allylic alkylation reactions, carboxylate-protected enolates (i.e., allyl β -ketoesters, **61**, Figure 2.1.2.1) represent a significant advance toward such a solution. Allyl β -ketoesters enjoy relatively uncomplicated, selective synthesis⁵⁴ from simple ketones (i.e. **59**) and undergo deprotection upon treatment with a transition metal capable of oxidative addition. Oxidative addition affords a transition metal allyl species, in the case at hand, a palladium π -allyl species **63**, and a free carboxylate **62**. The resulting carboxylate may then spontaneously release CO_2 to give prochiral enolate **64**.⁵⁵ This enolate may then enter into a catalytic cycle and undergo α -functionalization.

Figure 2.1.2.1. Allyl β -ketoester approach to latent enolate chemistry

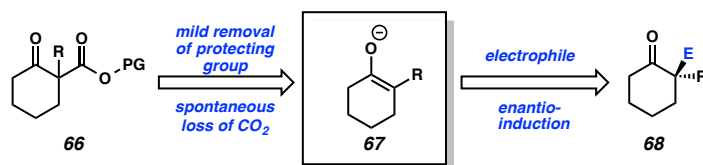
Despite these advantages, allyl β -ketoesters are not without their own limitations. Facile nucleophilic attack of the incipient enolate at the transition metal-allyl species generated during deprotection often precludes applications that do not involve allylic alkylation.⁵⁶ Moreover, with traditional carboxylate-protected enolates, any functionality borne by the allyl fragment (**60**, R^2 , Figure 2.1.2.1) must be compatible with the conditions required for substrate synthesis (i.e. strong base and reactive electrophiles). Tunge and coworkers have demonstrated the utility of acyl-protected enolates, which may undergo deprotection via a retro-Claisen condensation to reveal fully-substituted enolates, that participate in catalysis.⁵⁷ However, these reactions often require the use of elevated temperatures and alkoxide base to proceed.

2.1.3 Latent enolates: TMSE β -ketoesters

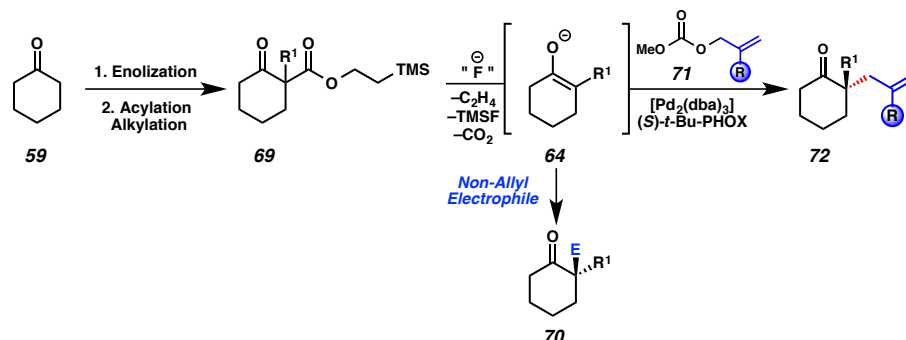
Conceptually, we envisioned a new class of β -ketoester enolate precursors bearing an alkyl ester substituent labile to cleavage (Figure 2.1.3.1, **66**). Ideally, facile deprotection would liberate this alkyl fragment to reveal a free carboxylate species, which, upon spontaneous decarboxylation, would yield the desired tetrasubstituted, prochiral enolate (**67**). Electrophilic trapping of this enolate species in the presence of a

chiral catalyst would, in turn, give rise to enantioenriched α -functionalized carbonyl products (**68**).

Figure 2.1.3.1. Non-allyl β -ketoester approach to latent enolate chemistry



In considering novel carboxylate-protected enolates, our design criteria called for a substrate that could be synthesized efficiently, deprotected under mild conditions and facilitate the convergent union of complex fragments in a synthetic setting. Our approach to this problem was to develop the (trimethylsilyl)ethyl β -ketoester (TMSE β -ketoester)⁵⁸ substrate class (i.e., **69**, Figure 2.1.3.2). These compounds boast similar ease of preparation as compared with allyl β -ketoesters, but are not susceptible to transition metal-mediated deprotection. We hypothesized that use of TMSE β -ketoesters may enhance the breadth of functional group tolerance at the allyl coupling partner in asymmetric allylic alkylations, relative to allyl β -ketoesters, by virtue of the fact that the allyl fragment is not subjected to the conditions of substrate synthesis (Figure 2.1.3.2). We further reasoned that by eliminating allyl from the reaction mixture, we would obviate the problem of competing reaction pathways in non-allyl enolate trapping chemistry, and greatly expand the range of reactions in which carboxylate-protected enolates may participate.

Figure 2.1.3.2. TMSE β -ketoester approach to latent enolate chemistry

In this chapter, we describe the preparation and development of this substrate class and the evaluation thereof in the enantioselective palladium-catalyzed allylic alkylation of 6- and 7-membered ketone and lactam scaffolds. Furthermore, we go on to show how the use of these substrates can enable the union of complex fragments bearing functionality that would be incompatible with incorporation into traditional allyl β -ketoester substrates.

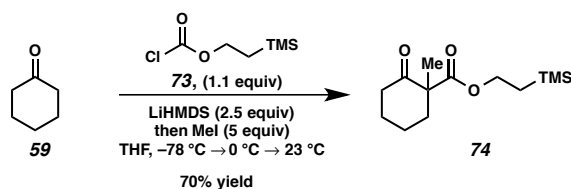
2.2 SYNTHESIS OF AND REACTION OPTIMIZATION WITH TMSE β -KETOESTERS

2.2.1 Substrate synthesis

The initial task pursuant to the goals laid out in Section 2.1.3 was to develop an efficient synthesis of TMSE β -ketoester **69**. We were pleased to find that α -methyl TMSE β -ketoester (**74**) could be prepared in a single synthetic operation from

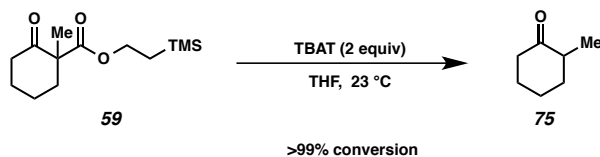
commercially available cyclohexanone (**59**), 2-(trimethylsilyl)ethyl chloroformate (**73**) and methyl iodide (MeI) in good overall yield (Scheme 2.2.1.1).

Scheme 2.2.1.1. TMSE β -ketoester substrate synthesis



In order to evaluate the substrate's capacity to engage in transition metal-mediated catalysis as anticipated, TMSE- β -ketoester **74** was subjected to treatment with tetrabutylammonium difluorotriphenylsilicate (TBAT) in THF at ambient temperature (Scheme 2.2.1.2). The reaction was quenched with saturated aqueous ammonium chloride, and full deprotection to 2-methyl-cyclohexanone **75** was observed after 30 min. This experiment lended proof of principal that our TMSE- β -ketoesters could indeed undergo mild deprotection and encouraged further investigation of the substrate class.

Scheme 2.2.1.2. Fluoride-triggered deprotection of TMSE β -ketoester substrate



2.2.2 TMSE- β -ketoester allylic alkylation optimization

With TMSE β -ketoester **74** in hand, our investigation into this substrate class commenced in the context of Pd-catalyzed allylic alkylation. We were pleased to find that exposure of β -ketoester **74** to allyl bromide, TBAT, [Pd₂(dba)₃] and (*S*)-*t*-Bu-PHOX^{8,59} in toluene at 40 °C generated the desired α -quaternary ketone **7** in modest yield and good enantioselectivity (entry 1, Table 2.2.2.1). We next explored the scope of allyl sources that could be used in the reaction and found that a variety of diverse allyl sources were competent in the chemistry, including allyl sulfonates, allyl acetates and allyl carbonates (entries 2–5). Allyl methyl carbonate proved to be the most efficient, selective and prudent allyl source, in particular, with respect to the number of the allyl equivalents required for optimal reactivity (entry 6). Reaction parameters including relative stoichiometry (entries 7–9), solvent (entries 10–13) and temperature (entry 14) were all subsequently explored and we found that a slight excess of mixed carbonate in THF at 25 °C delivering the desired ketone in 81% yield and 86% enantioselectivity (entry 14).

Table 2.2.2.1. TMSE β -ketoester allylic alkylation initial optimization experiments

entry	X	equiv allyl	sovent	yield (%) ^a	ee (%) ^b
1	Br	1.0	toluene	55	83
2	OTs	1.0	1,4-dioxane	43	77
3	OMs	1.0	1,4-dioxane	45	84
4	OAc	1.0	1,4-dioxane	15	82
5	OCO ₂ Allyl	1.0	1,4-dioxane	78	83
6	OCO ₂ Me	1.0	1,4-dioxane	78	84
7	OCO ₂ Me	0.75	1,4-dioxane	51	82
8	OCO ₂ Me	1.5	1,4-dioxane	74	82
9	OCO ₂ Me	2.0	1,4-dioxane	73	84
10	OCO ₂ Me	1.1	toluene	33	82
11	OCO ₂ Me	1.1	MTBE	65	84
12	OCO ₂ Me	1.1	THF	83	83
13	OCO ₂ Me	1.1	tol/hex	45	93
14 ^c	OCO ₂ Me	1.1	THF	81	86

(a) Yield determined by comparison to tridecane internal standard. (b) % ee Determined by chiral GC analysis of the crude reaction mixture. (c) Reaction performed at 25 °C.

A more rigorous investigation of the solvent effects on the reaction was subsequently conducted. Using preliminarily optimized reaction parameters, we conducted screening experiment wherein the base substrate **74** was treated with TBAT (1.25 equiv), Pd₂(dba)₃ (5 mol%), ligand **L1** (12.5 mol%) and methyl allyl carbonate (1.1 equiv) in a wide variety of solvent combinations. The results of these experiments are shown below in Tables 2.2.2.2 and 2.2.2.3. The results of these experiments show that reaction yield is highly variable based on the solvent employed (Table 2.2.2.2), while reaction selectivity remains relatively uniform (Table 2.2.2.3). With respect to variability

in yield, the primary factor at play in these experiments is hypothesized to be the relative solubility of the fluoride source used, TBAT. In toluene, TBAT is only sparingly soluble, in MTBE still only somewhat soluble, whereas TBAT is completely soluble in THF and *p*-dioxane, even at higher concentrations, thus accounting for lower observed yields in cases where low-dielectric solvents are employed. The majority of mass balance in low-yielding experiments is accounted for in recovered starting material. The fluctuation in enantioselectivity may be rationalized via the working mechanistic hypothesis for this transformation; in particular, that enantioselective allylic alkylation occurs via an inner-sphere pathway,³⁵ and this pathway is reinforced by less polar solvents.

Table 2.2.2.2. TMSE β -ketoester allylic alkylation solvent effects on reaction yield

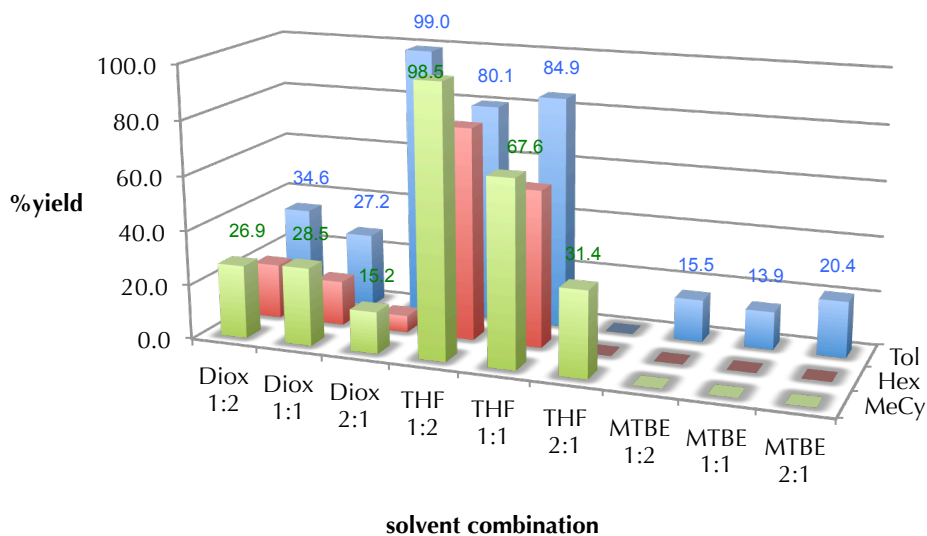
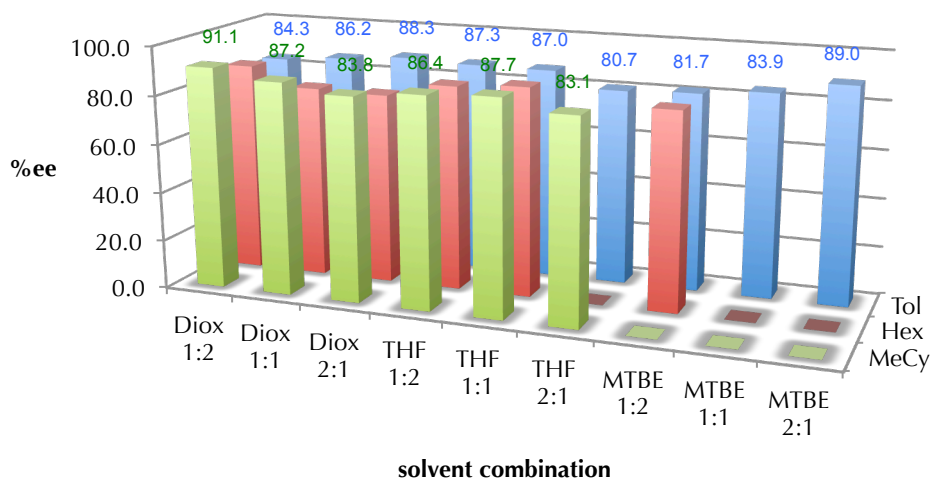


Table 2.2.2.3. TMSE β -ketoester allylic alkylation solvent effects on reaction selectivity

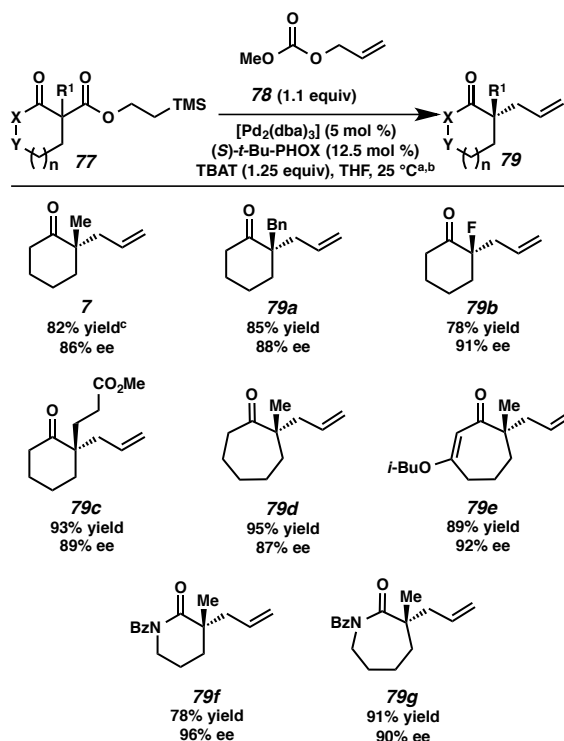
2.3 PALLADIUM-CATALYZED ALLYLIC ALYLATION WITH TMSE- β -KETOESTERS

2.3.1 Reaction scope with respect to nucleophile

Having identified optimal reaction conditions, we turned our attention to exploring reaction scope, beginning with tolerance of variability with respect to the nucleophile's α -substitution, ring size, and carbonyl functionality (Figure 2.3.1.1). Simple α -alkyl substitutions, such as α -benzyl substituted β -ketoester **77a** ($R^1 = \text{Bn}$, $X = \text{CH}_2$, $Y = \text{CH}_2$, $n = 1$, Figure 2), functioned consistently well in the chemistry; the desired benzyl substituted α -quaternary ketone **79a** was obtained in high yield and enantioselectivity. In addition to simple α -alkyl substrates (i.e. compounds **74** and **77a**), heteroatom-substituted substrate **77b** ($R^1 = \text{F}$, $X = Y = \text{CH}_2$, $n = 1$) proved to be a viable coupling partner and provided the corresponding α -fluoro-allylic alkylation product **79b** in good yield and excellent ee. Subjecting methyl ester-bearing substrate **77c** ($R^1 = \text{CH}_2\text{CH}_2\text{CO}_2\text{Me}$, $X = Y = \text{CH}_2$, $n = 1$) to our optimized conditions resulted in an efficient

and selective reaction, furnishing enantioenriched ketone **79c** in 93% yield and 89% ee. Substrates constituted from 7-membered rings, including ketone **77d** ($R^1 = \text{Me}$, $X = Y = \text{CH}_2$, $n = 2$) and vinylogous ester **77e** ($R^1 = \text{Me}$, $X = \text{CH}$, $Y = \text{CO}(i\text{-Bu})$, $n = 2$), were shown to be suitable coupling partners, affording α -quaternary ketone **79d** and α -quaternary vinylogous ester **79e** products in 95% and 89% yield and 87% and 92% ee, respectively. Finally, 6- and 7-membered lactams were investigated. We were pleased to find that under slightly modified reaction conditions (40 °C), the desired α -functionalized lactam products **79f** and **79g** were obtained in good to excellent yields and excellent ee's.

Figure 2.3.1.1. Exploration of functional group and scaffold diversity in the fluoride-triggered palladium-catalyzed allylic alkylation reaction with respect to nucleophile



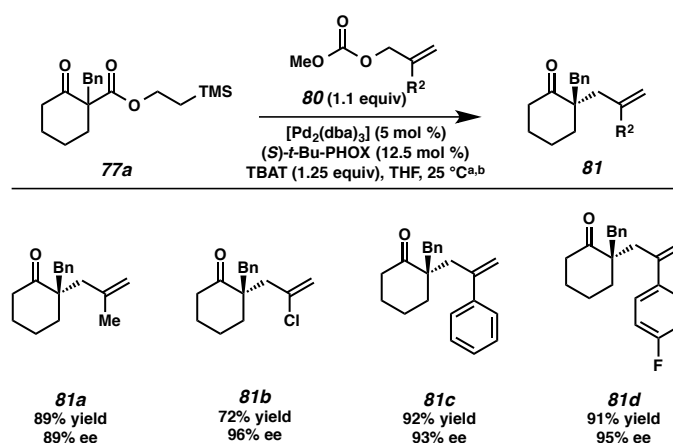
(a) Reaction conditions: **3** (1.0 equiv), **5** (1.1 equiv), $[\text{Pd}_2(\text{dba})_3]$ (5 mol%), (*S*)-*t*-Bu-PHOX (12.5 mol%), TBAT (1.25 equiv) in THF (0.033M) at 25 °C for 12–48 h. (b) Reaction performed on substrates **77f** and **77g** at 40 °C. (c) All reported yields are for isolated products.

2.3.2 Reaction scope with respect to electrophile

Having surveyed the scope of the reaction with respect to nucleophile α -substitution and scaffold type, we next probed the allylic alkylation with respect to substitution at the 2-allyl position. We were pleased to find that a variety of functional groups could be introduced through the use of differentially substituted allyl carbonates (**80**, $\text{R}^2 \neq \text{H}$, Figure 2.3.2.1). Simple alkyl substitution at the internal allyl position was well tolerated as 2-methylallyl ketone **81a** was obtained in 89% yield and 89% ee. 2-

Chloroallyl methyl carbonate (**80**, $R^2 = \text{Cl}$) also participated well in the chemistry, furnishing the corresponding α -quaternary ketone **81b** in 72% yield and 96% ee. Allyl fragments bearing electron-neutral and electron-deficient aryl groups also functioned well in the reaction, delivering the desired allylic alkylation products **81c** and **81d**, respectively, in excellent yields and ee's.

Figure 2.3.2.1. Exploration of functional group and scaffold diversity in the fluoride-triggered palladium-catalyzed allylic alkylation reaction with respect to electrophile



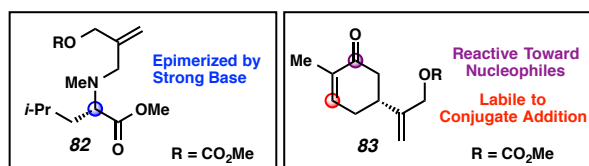
(a) Reaction conditions: **3** (1.0 equiv), **5** (1.1 equiv), $[\text{Pd}_2(\text{dba})_3]$ (5 mol%), (S)-*t*-Bu-PHOX (12.5 mol%), TBAT (1.25 equiv) in THF (0.033M) at 25 °C for 12–48 h. (b) All reported yields are for isolated products.

2.4 COUPLING OF TMSE β -KETOESTERS WITH FUNCTIONALLY COMPLEX ELECTROPHILIC PARTNERS

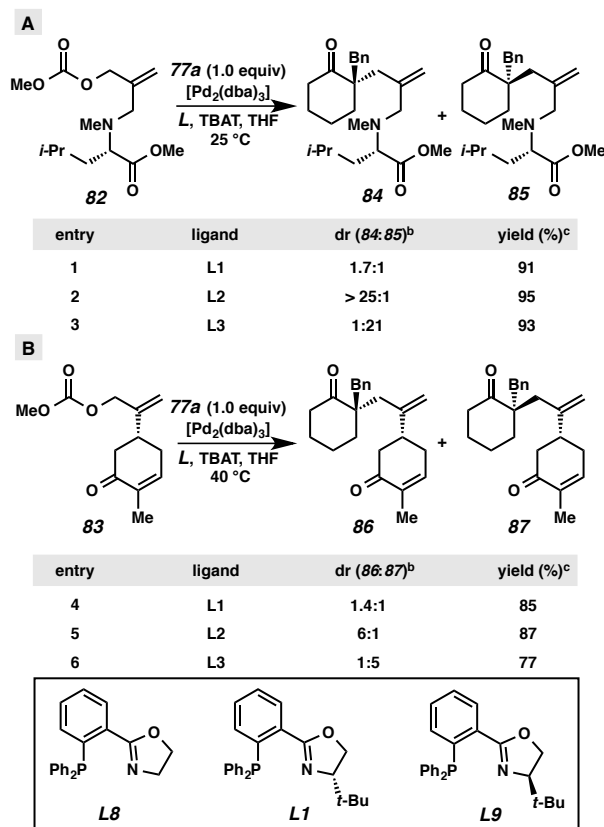
While the new fluoride-triggered chemistry described thus far permits alternative access to structures previously available by allylic alkylation, a distinct advantage offered

by TMSE- β -ketoesters in allylic alkylation chemistry is the ability to introduce allyl-coupling partners that would be unstable to the conditions of allyl β -ketoester substrate synthesis. To illustrate this feature of the new chemistry, we synthesized mixed carbonates **82** and **83** as coupling partners for palladium-catalyzed allylic alkylation (Figure 2.4.1). Allyl carbonate **82**, derived from leucine, bears an epimerizable stereocenter that is racemized upon treatment with strong base.⁶⁰ Since strong base (i.e. LDA, LHMDS, etc.) is typically required for enolization and acylation in the preparation of standard allyl β -ketoesters, employing electrophiles bearing base labile functionality has not previously been possible. Alternatively, allyl carbonate **83**, which was synthesized by allylic oxidation of (*S*)-carvone, also bears functionality that would be unstable to the conditions required for standard allyl β -ketoester substrate synthesis. In particular, we envisioned that attempts to acylate a ketone enolate with an allyl chloro- or allyl cyanoformate bearing enone **83** would be complicated by undesired conjugate addition and enolate chemistries (e.g. Aldol reaction, Michael addition, etc.). In both cases, our new TMSE β -ketoester chemistry allows for the independent preparation and, thus, physical separation of nucleophilic and electrophilic components until the fragment coupling stage.

Figure 2.4.1. Complex allyl architectures



Subjecting allyl carbonate **82** and TMSE β -ketoester **77a** ($R^1 = \text{Bn}$, $X = Y = \text{CH}_2$, $n = 1$, Figure 2.4.2) to our fluoride-modified allylic alkylation conditions with achiral ligand **L8** revealed modest substrate-controlled diastereoselection of 1.7:1 (entry 1, Figure 2.4.2A). Use of (*S*)-*t*-Bu-PHOX (**L1**) resulted in a highly efficient and diastereoselective reaction giving the desired amino ester **84** in 95% yield and greater than 25:1 dr, with no detectable epimerization at the amino ester side chain (entry 2). The inherent diastereoselectivity could be completely reversed under catalyst control by using (*R*)-*t*-Bu-PHOX (**L9**), without significant loss in selectivity or reactivity (entry 3). Likewise, upon exposing carbonate **83** and ketoester **77a** to slightly modified allylic alkylation conditions (40 °C vs. 25 °C) with achiral ligand **L8**, we again observed an efficient reaction and slight inherent diastereoselectivity (entry 4, Figure 2.4.2B). This bias could be enhanced by using ligand **L1** to obtain α -quaternary ketone **86** in 6:1 dr and 87% yield, or overturned by use of **L9** to obtain **87** in 5:1 dr and 77% yield (entries 5 and 6).

Figure 2.4.2. Union of complex fragments by asymmetric allylic alkylation^a

(a) Reaction conditions: **77a** (1.0 equiv), **82** or **83** (1.1 equiv), $[\text{Pd}_2(\text{dba})_3]$ (5 mol%), Ligand (12.5 mol%), TBAT (1.25 equiv) in THF (0.033M) at the indicated temperature for 24–48 h. (b) Diastereoselectivity determined by ^1H NMR analysis of the crude reaction mixture. (c) Yields are reported for combined diastereomeric mixture.

2.5 CONCLUDING REMARKS

In conclusion, we have developed a new class of substrates for enolate alkylation chemistry that benefit from ease of preparation and mild deprotection conditions that are orthogonal to those used for traditional allyl β -ketoesters. We examined the application of these compounds in palladium-catalyzed asymmetric allylic alkylation chemistry and found that a wide range of functional groups and substrate scaffolds are well tolerated,

including 6- and 7-membered ketones and lactams. We have further demonstrated the value of these compounds for uniting complex coupling partners that would be incompatible to preparation via standard allyl β -ketoester based allylic alkylation. We envision that this technology will also enable the convergent cross-coupling of synthetically challenging fragments for complex molecule synthesis. Further studies exploring the application of TMSE β -ketoesters in diverse reaction methodologies and complex natural product synthesis are ongoing in our laboratory.

2.6 EXPERIMENTAL SECTION

2.6.1 Materials and Methods

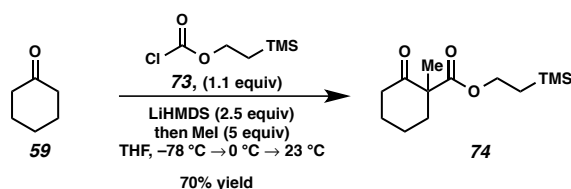
Unless otherwise stated, reactions were performed in flame-dried glassware under an argon or nitrogen atmosphere using dry, deoxygenated solvents. Solvents were dried by passage through an activated alumina column under argon.⁶¹ Reaction progress was monitored by thin-layer chromatography (TLC). TLC was performed using E. Merck silica gel 60 F254 precoated glass plates (0.25 mm) and visualized by UV fluorescence quenching, *p*-anisaldehyde, or KMnO_4 staining. Silicycle SiliaFlash® P60 Academic Silica gel (particle size 40–63 nm) was used for flash chromatography. ^1H NMR spectra were recorded on Varian Inova 300 MHz and 500 MHz spectrometers and are reported relative to residual CHCl_3 (δ 7.26 ppm) or C_6HD_5 (δ 7.16 ppm). ^{13}C NMR spectra were recorded on a Varian Inova 500 MHz spectrometer (125 MHz) and are reported relative to CHCl_3 (δ 77.16 ppm) or C_6HD_5 (δ 128.06 ppm). Data for ^1H NMR are reported as follows: chemical shift (δ ppm) (multiplicity, coupling constant (Hz), integration). Multiplicities are reported as follows: s = singlet, d = doublet, t = triplet, q = quartet, p =

pentet, sept = septuplet, m = multiplet, br s = broad singlet, br d = broad doublet, app = apparent. Data for ^{13}C NMR are reported in terms of chemical shifts (δ ppm). ^{19}F NMR spectra were recorded on a Varian Mercury 300 spectrometer at 282 MHz, and are reported relative to the external standard $\text{F}_3\text{CCO}_2\text{H}$ (δ -76.53 ppm). IR spectra were obtained by use of a Perkin Elmer Spectrum BXII spectrometer or Nicolet 6700 FTIR spectrometer using thin films deposited on NaCl plates and reported in frequency of absorption (cm^{-1}). Optical rotations were measured with a Jasco P-2000 polarimeter operating on the sodium D-line (589 nm), using a 100 mm path-length cell and are reported as: $[\alpha]_{\text{D}}^{\text{T}}$ (concentration in g/100 mL, solvent). Analytical HPLC was performed with an Agilent 1100 Series HPLC utilizing a Chiralpak (AD-H or AS) or Chiralcel (OD-H, OJ-H, or OB-H) columns (4.6 mm x 25 cm) obtained from Daicel Chemical Industries, Ltd. Analytical SFC was performed with a Mettler SFC supercritical CO_2 analytical chromatography system utilizing Chiralpak (AD-H, AS-H or IC) or Chiralcel (OD-H, OJ-H, or OB-H) columns (4.6 mm x 25 cm) obtained from Daicel Chemical Industries, Ltd. Analytical chiral GC analysis was performed with an Agilent 6850 GC utilizing a GTA (30 m x 0.25 mm) column (1.0 mL/min carrier gas flow). High resolution mass spectra (HRMS) were obtained from Agilent 6200 Series TOF with an Agilent G1978A Multimode source in electrospray ionization (ESI+), atmospheric pressure chemical ionization (APCI+), or mixed ionization mode (MM: ESI-APCI+).

Reagents were purchased from Sigma-Aldrich, Gelest, Strem, or Alfa Aesar and used as received unless otherwise stated. 2-(trimethylsilyl)ethyl chloroformate (**78**) was prepared according to a known procedure.⁶² Allyl carbonates **82** and **83** were prepared from methyl chloroformate and the corresponding allyl alcohols by adaptation of a

known procedure.⁶³ β -Ketoesters **74** and **77a–77g** were prepared by adaptation of procedures by Stoltz and co-workers.^{64,15} Data reported herein is for new compounds only.

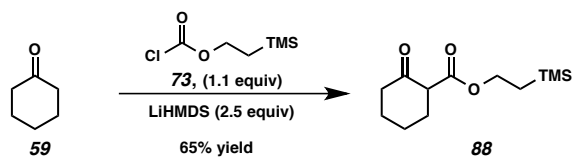
2.6.2 General procedure for TMSE β -ketoester substrate synthesis



2-(Trimethylsilyl)ethyl 1-methyl-2-oxocyclohexane-1-carboxylate (74). A flame-dried 1L round bottom flask was charged with 28.02 g (152.83 mmol, 2.5 equiv) of LiHMDS and a magnetic stirring bar in a nitrogen-filled glove box. The flask was sealed, removed from the glove-box, fitted with a N₂ line, and suspended in a dry ice/acetone bath. 300 mL of THF was added slowly to the flask and allowed to stir until the LiHMDS had completely dissolved. 6.00 g (61.13 mmol, 1.0 equiv) of cyclohexanone **59** in 130 mL of THF was added via cannula over 30 min, and the flask was removed from the cooling bath and allowed to warm to 23 °C while continuing to stir. After 30 min, the flask was suspended in a dry ice/acetone bath and 12.15 g (67.24 mmol, 1.1 equiv) of chloroformate **73** in 130 mL of THF was added over 30 min via cannula. This mixture was allowed to warm to 23 °C and stirred for 6 h. The flask was then suspended in a water/ice bath and 21.69 g (152.83 mmol, 2.5 equiv) of methyl iodide was added dropwise. This mixture was allowed to warm to 23 °C and stirred for 6 h, at which time an additional 21.69 g (152.83 mmol, 2.5 equiv) of methyl iodide was added dropwise.

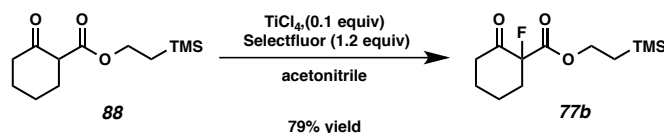
The mixture was then stirred at 23 °C until full consumption of starting material and acylated intermediate was observed by TLC analysis. 300 mL of saturated aqueous NH₄Cl was then added slowly to the mixture and stirring continued for 2 h. The mixture was then extracted with EtOAc (100 mL x 3), the collected organic fractions washed with brine, dried over MgSO₄, filtered and concentrated *in vacuo*. The crude residue was purified by flash column chromatography (SiO₂, hexanes to 3% EtOAc in hexanes) to give 11.05 g (43.08 mmol) of ketoester **74** as a pale yellow oil. 70.1% yield. *R*_f = 0.3 (10% EtOAc in hexanes); ¹H NMR (500 MHz, CDCl₃) δ 4.29–4.12 (m, 2H), 2.57–2.37 (m, 3H), 2.05–1.95 (m, 1H), 1.76–1.57 (m, 3H), 1.48–1.37 (m, 1H), 1.26 (s, 3H), 1.01–0.92 (m, 2H), 0.02 (s, 9H); ¹³C NMR (126 MHz, CDCl₃) δ 208.3, 173.2, 63.6, 57.1, 40.7, 38.2, 27.5, 22.6, 21.2, 17.3, -1.6; IR (Neat Film, NaCl) 3438, 2952, 2897, 2866, 1717, 1452, 1378, 1336, 1251, 1215, 1121, 1084, 1061, 1041, 938, 861, 834, 763 cm⁻¹; HRMS (MM: ESI-APCI+) *m/z* calc'd for C₁₃H₂₅O₃Si [M + H]⁺: 257.1567; found 257.1556.

2.6.3 Procedures for the syntheses of TMSE β-ketoester intermediate **88** and ketoester **77b**



2-(Trimethylsilyl)ethyl 1-H-2-oxocyclohexane-1-carboxylate (88). A flame-dried 500 mL round bottom flask was charged with 4.67 g (25.47 mmol, 1.3 equiv) of LiHMDS and a magnetic stirring bar in a nitrogen-filled glove-box. The flask was sealed, removed

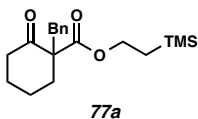
from the glove-box, fitted with a N₂ line, and suspended in a dry ice/acetone bath. 100 mL of THF was added slowly to the flask and allowed to stir until the LiHMDS had been completely dissolved. 2.00 g (20.38 mmol, 1.0 equiv) of cyclohexanone **59** in 50 mL of THF was added via cannula over 30 min, and the flask was removed from the cooling bath and allowed to warm to 23 °C while continuing to stir. After 30 min, the flask was suspended in a dry ice/acetone bath and 4.10 g (22.42 mmol, 1.1 equiv) of chloroformate **73** in 50 mL of THF was added over 30 min via cannula. This mixture was allowed to warm to 23 °C and stirred until full consumption of starting material was observed (ca. 6 h). 100 mL of saturated aqueous NH₄Cl was then added slowly and the mixture stirred for 20 min before being extracted with EtOAc (30 mL x 3). The collected organic fractions were washed with brine, dried over MgSO₄, filtered and concentrated *in vacuo*. The crude residue was purified by flash column chromatography (SiO₂, hexanes to 2% EtOAc in hexanes), to give 3.20 g (43.08 mmol) of ketoester **88** as a colorless oil. 64.6% yield. *R*_f = 0.5 (20% EtOAc in hexanes); ¹H NMR (500 MHz, CDCl₃) δ 12.29 (s, 1H), 4.27–4.21 (m, 2H), 2.23 (dtt, *J* = 24.7, 6.3, 1.6 Hz, 4H), 1.76–1.51 (m, 4H), 1.17–0.86 (m, 2H), 0.04 (s, 9H); ¹³C NMR (126 MHz, CDCl₃) δ 172.9, 171.9, 97.8, 62.4, 29.1, 22.5, 22.4, 21.9, 17.3, -1.5; IR (Neat Film, NaCl) 2952, 2899, 2860, 1742, 1718, 1654, 1618, 1453, 1398, 1360, 1297, 1258, 1219, 1175, 1079, 1060, 936, 859, 837 cm⁻¹; HRMS (MM: ESI-APCI-) *m/z* calc'd for C₁₂H₂₁O₃Si [M – H]⁻: 241.1265; found 241.1270.



2-(Trimethylsilyl)ethyl 1-fluoro-2-oxocyclohexane-1-carboxylate (77b). A flame dried 100 mL round bottom flask was charged with a magnetic stirring bar, 0.35 g **88** (1.44 mmol, 1.0 equiv), 5 mL of acetonitrile and cooled to 0 °C. To this mixture was added 0.027 g TiCl₄ (0.144 mmol, 0.10 equiv) dropwise over 15 min. To this stirring solution was added 0.64 g Selectfluor (1.73 mmol, 1.2 equiv) in 20 mL of acetonitrile over 25 min. The mixture was then allowed to warm to 23 °C and stirred for 8 h. A 1:1 mixture of H₂O/EtOAc (20 mL) was added, and the mixture was extracted with EtOAc (20 mL x 3), dried over MgSO₄ and adsorbed onto 1 g SiO₂ by concentration *in vacuo*. The crude product was isolated by flash column chromatography (SiO₂, 3% Et₂O in pentane to 12% Et₂O in pentane) to give 0.29 g of **77b** as a colorless oil. 79.0% yield. *R_f* = 0.2 (20% EtOAc in hexanes); ¹H NMR (300 MHz, CDCl₃) δ 4.41–4.26 (m, 2H), 2.84–2.36 (m, 3H), 2.21–2.04 (m, 1H), 2.00–1.79 (m, 4H), 1.15–0.97 (m, 2H), 0.04 (s, 9H); ¹³C NMR (75 MHz, CDCl₃) δ 202.0 (d, ⁴*J*_{CF} = 19.5 Hz), 167.0 (d, ²*J*_{CF} = 24.6 Hz), 96.4 (d, ¹*J*_{CF} = 197.0 Hz), 65.0, 39.7, 36.0 (d, ³*J*_{CF} = 21.7 Hz), 26.6, 21.0 (d, ⁵*J*_{CF} = 6.0 Hz), 17.3, -1.6; ¹⁹F NMR (282 MHz, CDCl₃) δ -173.70; IR (Neat Film, NaCl) 2953, 1732, 1452, 1287, 1251, 1223, 1157, 1093, 1051, 860, 838 cm⁻¹; HRMS (MM: ESI-APCI+) *m/z* calc'd for C₁₂H₂₁FO₃SiNa [M + Na]⁺: 283.1136; found 283.1145.

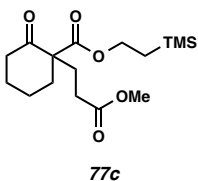
2.6.4 Spectroscopic data for TMSE β-ketoester substrates

2-(Trimethylsilyl)ethyl 1-benzyl-2-oxocyclohexane-1-carboxylate (77a)



Ketoester **77a** was prepared by the general procedure and was isolated by flash column chromatography (SiO₂, hexanes to 5% EtOAc in hexanes) as a colorless oil. 79.4% yield. $R_f = 0.3$ (20% EtOAc in hexanes); ¹H NMR (300 MHz, CDCl₃) δ 7.48–7.04 (m, 5H), 4.16 (td, $J = 9.8, 7.1$ Hz, 2H), 3.13 (dd, $J = 125.3, 13.7$ Hz, 2H), 2.60–2.35 (m, 2H), 2.05 (ddd, $J = 12.4, 6.1, 3.0$ Hz, 1H), 1.83–1.59 (m, 4H), 1.57–1.40 (m, 1H), 0.92 (ddd, $J = 8.9, 7.2, 1.0$ Hz, 2H), 0.07 (s, 9H); ¹³C NMR (75 MHz, CDCl₃) δ 208.9, 172.8, 138.3, 132.0, 129.5, 128.2, 65.2, 63.8, 42.9, 42.0, 37.5, 29.2, 24.1, 18.8, 0.0; IR (Neat Film, NaCl) 3029, 2952, 2856, 1713, 1496, 1453, 1439, 1250, 1221, 1177, 1132, 1086, 1053, 988, 932, 860, 838, 765, 744 cm⁻¹; HRMS (MM: ESI-APCI+) m/z calc'd for C₁₉H₂₉O₃Si [M + H]⁺: 333.1880; found 333.1863.

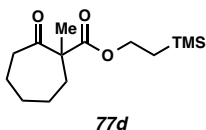
2-(Trimethylsilyl)ethyl 1-(3-methoxy-3-oxopropyl)-2-oxocyclohexane-1-carboxylate (77c)



Ketoester **77c** was prepared according to the general procedure, using methyl acrylate in place of methyl iodide, and isolated by flash column chromatography (SiO₂, 5% EtOAc in hexanes to 10% EtOAc in hexanes) as a colorless oil. 81.2% yield. $R_f = 0.3$ (25%

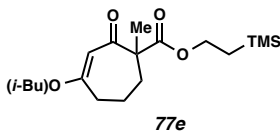
EtOAc in hexanes); ^1H NMR (300 MHz, CDCl_3) δ 4.28–4.08 (m, 2H), 3.62 (s, 3H), 2.41 (dddd, $J = 14.6, 12.9, 6.5, 2.7$ Hz, 4H), 2.27–2.06 (m, 2H), 2.02–1.92 (m, 1H), 1.92–1.84 (m, 1H), 1.76–1.51 (m, 3H), 1.40 (ddd, $J = 13.5, 12.1, 4.2$ Hz, 1H), 1.03–0.91 (m, 2H), 0.00 (s, 9H); ^{13}C NMR (75 MHz, CDCl_3) δ 207.6, 173.5, 171.8, 63.9, 60.0, 51.6, 41.0, 36.3, 29.7, 29.4, 27.5, 22.5, 17.4, -1.6; IR (Neat Film, NaCl) 3432, 2952, 2899, 2866, 1740, 1713, 1437, 1377, 1340, 1308, 1250, 1175, 1137, 1093, 1075, 1062, 1040, 943, 861, 838, 763, 695 cm^{-1} ; HRMS (MM: ESI-APCI+) m/z calc'd for $\text{C}_{16}\text{H}_{28}\text{O}_5\text{SiNa}$ [$\text{M} + \text{Na}$] $^+$: 351.1598; found 351.1602.

2-(Trimethylsilyl)ethyl 1-methyl-2-oxocycloheptane-1-carboxylate (**77d**)



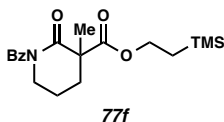
Ketoester **77d** was prepared by the general procedure and purified by flash column chromatography (SiO_2 , hexanes to 5% EtOAc in hexanes) as a colorless oil. 78% yield. $R_f = 0.4$ (20% EtOAc in hexanes); ^1H NMR (500 MHz, CDCl_3) δ 4.25–4.14 (m, 2H), 2.78–2.68 (m, 1H), 2.49 (ddd, $J = 12.2, 8.6, 2.5$ Hz, 1H), 2.19–2.10 (m, 1H), 1.88–1.71 (m, 3H), 1.71–1.48 (m, 3H), 1.43–1.34 (m, 1H), 1.33 (s, 3H), 1.06–0.94 (m, 2H), 0.03 (s, 9H); ^{13}C NMR (126 MHz, CDCl_3) δ 210.5, 173.7, 63.6, 58.8, 42.0, 35.4, 30.1, 25.8, 24.7, 21.5, 17.3, -1.6; IR (Neat Film, NaCl) 2949, 2861, 1736, 1710, 1458, 1378, 1250, 1232, 1152, 1105, 1062, 942, 860, 838 cm^{-1} ; HRMS (EI+) m/z calc'd for $\text{C}_{14}\text{H}_{26}\text{O}_3\text{Si}$ [$\text{M} + \text{Na}$] $^+$: 293.1543; found 293.1543.

2-(Trimethylsilyl)ethyl 4-isobutyl-1-methyl-2-oxocyclohept-3-ene-1-carboxylate (77e)



Vinylogous ester **77e** was prepared by the general procedure, starting from 3-isobutoxycyclohept-2-en-1-one, and purified by flash column chromatography (SiO₂, hexanes to 10% EtOAc in hexanes) as a colorless oil. 85% yield. $R_f = 0.3$ (20% EtOAc in hexanes); ¹H NMR (500 MHz, C₆D₆) δ 5.66–5.53 (m, 1H), 4.32–4.07 (m, 2H), 3.16–3.00 (m, 2H), 2.57 (dddd, $J = 17.7, 10.1, 3.9, 1.2$ Hz, 1H), 2.50–2.37 (m, 1H), 2.20 (ddd, $J = 17.7, 7.0, 3.6$ Hz, 1H), 1.77–1.67 (m, 2H), 1.66 (s, 3H), 1.59–1.41 (m, 2H), 0.88 (ddd, $J = 10.0, 7.0, 2.1$ Hz, 2H), 0.71 (dd, $J = 6.7, 4.2$ Hz, 6H), -0.13 (s, 9H); ¹³C NMR (126 MHz, C₆D₆) δ 197.1, 173.9, 171.7, 105.6, 74.0, 62.9, 58.9, 33.9, 33.7, 27.6, 24.1, 18.7, 18.7, 17.0, -2.1; IR (Neat Film, NaCl) 2951, 1684, 1452, 1386, 1327, 1281, 1251, 1139, 1053, 859, 839, 718, 693, 658 cm⁻¹; HRMS (EI+) m/z calc'd for C₂₈H₃₃O₃Si [M + H]⁺: 341.2143; found 341.2139.

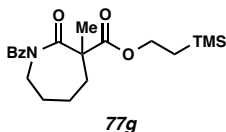
2-(Trimethylsilyl)ethyl 1-benzoyl-3-methyl-2-oxopiperidine-3-carboxylate (77f)



Amide ester **77f** was prepared by the general procedure, starting from *N*-benzoyl-2-piperidone, and purified by flash column chromatography (SiO₂, 5% EtOAc in hexanes

to 25% EtOAc in hexanes) as a colorless oil. 89% yield. $R_f = 0.3$ (35% EtOAc in hexanes); ^1H NMR (500 MHz, CDCl_3) δ 7.76–7.72 (m, 2H), 7.47 (ddt, $J = 8.0, 6.9, 1.3$ Hz, 1H), 7.41–7.36 (m, 2H), 4.38–4.24 (m, 2H), 3.91–3.82 (m, 1H), 3.78 (dtd, $J = 12.9, 5.2, 1.4$ Hz, 1H), 2.47 (dddd, $J = 13.8, 5.7, 4.3, 1.4$ Hz, 1H), 2.06–1.91 (m, 2H), 1.85–1.74 (m, 1H), 1.46 (s, 3H), 1.14–1.05 (m, 2H), 0.07 (s, 9H); ^{13}C NMR (126 MHz, CDCl_3) δ 175.0, 173.1, 173.0, 135.9, 131.6, 129.0, 128.0, 64.4, 52.9, 46.8, 33.7, 22.4, 20.2, 17.5, -1.5; IR (Neat Film, NaCl) 3062, 2953, 2896, 1726, 1703, 1683, 1449, 1389, 1277, 1251, 1192, 1140, 1062, 932, 859, 838, 723, 694 cm^{-1} ; HRMS (MM: ESI-APCI+) m/z calc'd for $\text{C}_{19}\text{H}_{27}\text{NO}_4\text{SiNa}$ $[\text{M} + \text{Na}]^+$: 384.1602; found 384.1611.

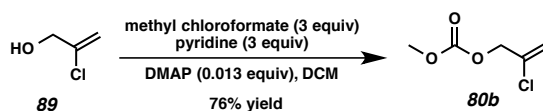
2-(Trimethylsilyl)ethyl 1-benzoyl-3-methyl-2-oxoazepane-3-carboxylate (**77g**)



Amide ester **77g** was prepared by the general procedure, starting from 1-benzoylazepan-2-one, and purified by flash column chromatography (SiO_2 , 5% EtOAc in hexanes to 25% EtOAc in hexanes) as a colorless oil. 77% yield. $R_f = 0.3$ (35% EtOAc in hexanes); ^1H NMR (500 MHz, CDCl_3) δ 7.72–7.68 (m, 2H), 7.50–7.45 (m, 1H), 7.39 (ddt, $J = 8.2, 6.6, 1.1$ Hz, 2H), 4.47–4.39 (m, 1H), 4.38–4.31 (m, 2H), 3.15 (ddd, $J = 15.7, 11.2, 1.2$ Hz, 1H), 2.22 (dtd, $J = 14.8, 3.6, 1.8$ Hz, 1H), 2.01–1.90 (m, 2H), 1.89–1.77 (m, 1H), 1.61 (dddd, $J = 20.7, 12.0, 5.0, 3.2$ Hz, 3H), 1.44 (s, 3H), 1.14–1.06 (m, 2H), 0.08 (s, 9H); ^{13}C NMR (126 MHz, CDCl_3) δ 175.6, 174.9, 173.1, 136.4, 131.5, 128.1, 127.9, 64.3,

55.0, 44.0, 34.4, 27.9, 26.9, 25.0, 17.5, -1.5; IR (Neat Film, NaCl) 2956, 1729, 1661, 1614, 1455, 1383, 1249, 1169, 1115, 860, 838 cm^{-1} ; HRMS (MM: ESI-APCI+) m/z calc'd for $\text{C}_{20}\text{H}_{29}\text{NO}_4\text{SiNa}$ $[\text{M} + \text{Na}]^+$: 398.1758; found 398.1775.

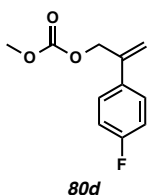
2.6.5 General procedure for allyl carbonate substrate syntheses



2-Chloroallyl methyl carbonate (80b). To a flame-dried 50 mL round bottom flask charged with a magnetic stirring bar, 1.00 g 2-chloroallyl alcohol (**89**) (10.8 mmol, 1.0 equiv), 2.56 g of pyridine (32.4 mmol, 3.0 equiv), 0.016 g of dimethylaminopyridine (0.14 mmol, 0.013 equiv) and 22 mL of DCM at 0 °C, was added 3.06 g of methyl chloroformate (32.43 mmol, 3 equiv), dropwise over 10 min. The solution was allowed to warm to 23 °C and stirred for 12 h. The mixture was then diluted with 40 mL of DCM, washed consecutively with 50 mL H_2O and 50 mL brine before being dried over MgSO_4 and directly subjected to flash column chromatography (SiO_2 , pentane to 5% Et_2O in pentane). 1.23 g of 2-Chloroallyl methyl carbonate was isolated as a colorless oil. 75.6% yield. R_f = 0.6 (20% EtOAc in hexanes); ^1H NMR (500 MHz, CDCl_3) δ 5.49 (dt, J = 2.0, 1.2 Hz, 1H), 5.41 (dt, J = 1.8, 0.9 Hz, 1H), 4.68–4.67 (m, 2H), 3.80 (d, J = 1.2 Hz, 3H); ^{13}C NMR (126 MHz, CDCl_3) δ 155.1, 135.2, 115.2, 69.0, 55.1; IR (Neat Film, NaCl) 3008, 2959, 2255, 1752, 1639, 1444, 1383, 1358, 1265, 1182, 1116, 974,

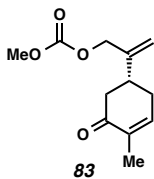
908, 790, 745 cm^{-1} ; HRMS (MM: ESI-APCI+) m/z calc'd for $\text{C}_5\text{H}_8\text{ClO}_3$ $[\text{M} + \text{H}]^+$: 151.0156; found 151.0150.

2.6.6. Spectroscopic data for allyl carbonate substrates



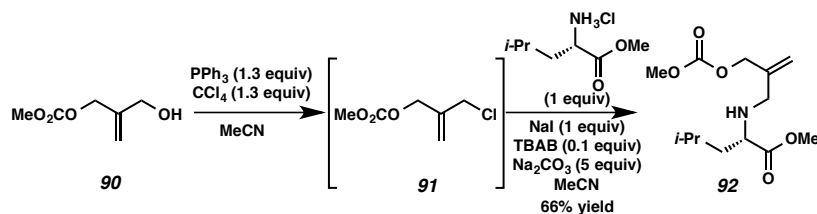
2-(4-Fluorophenyl)allyl methyl carbonate (80d) was prepared by the general procedure from 2-(4-fluorophenyl)allyl alcohol and isolated as a colorless oil by flash column chromatography (SiO_2 , pentane to 5% Et_2O in pentane). 87% yield. $R_f = 0.4$ (20% EtOAc in hexanes); ^1H NMR (500 MHz, CDCl_3) δ 7.44–7.36 (m, 2H), 7.09–6.99 (m, 2H), 5.51 (s, 1H), 5.39 (tt, $J = 1.2, 0.5$ Hz, 1H), 5.00 (dd, $J = 1.3, 0.6$ Hz, 2H), 3.79 (s, 3H); ^{13}C NMR (126 MHz, CDCl_3) δ 162.65 (d, $^1J_{\text{CF}} = 247.0$ Hz), 155.54, 141.1, 133.85, 127.74 (d, $^3J_{\text{CF}} = 7.8$ Hz), 115.85 (d, $^4J_{\text{CF}} = 1.4$ Hz), 115.41 (d, $^2J_{\text{CF}} = 21.9$ Hz), 69.09, 54.89; ^{19}F NMR (282 MHz, CDCl_3) δ -126.95; IR (Neat Film, NaCl) 3007, 2959, 1893, 1750, 1634, 1603, 1511, 1447, 1372, 1260, 1164, 1102, 969, 918, 839, 791, 742 cm^{-1} ; HRMS (MM: ESI-APCI+) m/z calc'd for $\text{C}_{11}\text{H}_{12}\text{FO}_3$ $[\text{M} + \text{H}]^+$: 211.0765; found 211.0772.

(R)-Methyl (2-(4-methyl-5-oxocyclohex-3-en-1-yl)allyl) carbonate (83)



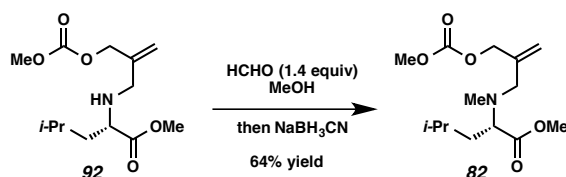
Enone carbonate **83** was prepared by the general method from known allylic alcohol (*R*)-5-(3-hydroxyprop-1-en-2-yl)-2-methylcyclohex-2-en-1-one (i.e. (*R*)-10-hydroxy carvone)⁶⁵ and isolated as a colorless oil by flash column chromatography (SiO₂, 5% EtOAc in hexanes to 20% EtOAc in hexanes). 91% yield. $R_f = 0.2$ (20% EtOAc in hexanes); ¹H NMR (500 MHz, CDCl₃) δ 6.74 (ddd, $J = 5.9, 2.7, 1.4$ Hz, 1H), 5.22 (dt, $J = 1.3, 0.7$ Hz, 1H), 5.07 (dd, $J = 1.4, 0.7$ Hz, 1H), 4.64 (ddt, $J = 3.8, 1.2, 0.5$ Hz, 2H), 3.79 (s, 3H), 2.97–2.74 (m, 1H), 2.63 (ddd, $J = 16.1, 3.8, 1.6$ Hz, 1H), 2.52 (dddt, $J = 18.2, 6.0, 4.5, 1.5$ Hz, 1H), 2.39 (dd, $J = 16.1, 13.2$ Hz, 1H), 2.31 (ddt, $J = 18.2, 10.8, 2.5$ Hz, 1H), 1.78 (dt, $J = 2.6, 1.3$ Hz, 3H); ¹³C NMR (126 MHz, CDCl₃) δ 198.9, 155.5, 144.7, 144.0, 135.6, 114.3, 69.1, 54.9, 42.9, 38.2, 31.3, 15.7; IR (Neat Film, NaCl) 2958, 2928, 2893, 1750, 1671, 1444, 1364, 1266, 1107, 984, 954, 913, 791 cm⁻¹; HRMS (MM: ESI-APCI+) m/z calc'd for C₁₂H₁₇O₄ [M + H]⁺: 225.1121; found 225.1118.

2.6.7 Procedure for the synthesis allyl carbonate 82



Methyl *N*-(2-(((methoxycarbonyl)oxy)methyl)allyl)-*L*-leucinate (92). Known hydroxy carbonate **90**⁶⁶ was prepared by the general method. Following the procedure of Altmann and co-workers,⁶⁷ 0.77 g of **90** (5.27 mmol, 1.0 equiv) was added to flame-dried round bottom flask charged with a magnetic stirring bar and 0.66 mL of acetonitrile. The solution was cooled to 0 °C and 1.80 g of triphenylphosphine (6.83 mmol, 1.3 equiv) and 0.66 mL of carbontetrachloride (6.85 mmol, 1.3 equiv) were added sequentially. The resulting slurry was allowed to warm to 23 °C and stirred for 2 h before being subjected directly to flash column chromatography. The resulting crude oil, **91** was determined to be ca. 95% pure by ¹H NMR analysis and used without further purification (yield not determined). Following a known procedure,⁶⁸ 0.47 g of crude allylic chloride intermediate **91** (2.855 mmol, 1.5 equiv) was combined with 0.28 g of NaI (1.90 mmol, 1.0 equiv), 0.346 g of (*L*)-leucine methyl ester hydrochloride (1.90 mmol, 1.0 equiv), 0.061 g of tetrabutylammonium bromide (0.19 mmol, 0.1 equiv), 1.01 g Na_2CO_3 (9.52 mmol, 5 equiv) and 20 mL acetonitrile in a 50 mL round bottom flask equipped with a magnetic stirring bar. The flask was fitted with a reflux condenser and the mixture stirred at 82 °C for 14 h. The vessel was then cooled to 23 °C and the mixture diluted with 50 mL Et_2O , washed with H_2O (20 mL x 2), dried over MgSO_4 and concentrated *in vacuo*.

The crude oil was purified by flash column chromatography (SiO₂, 5% EtOAc in hexanes to 15% EtOAc in hexanes) to give 0.52 g of amino ester **92** as a colorless oil. 66.1% yield from crude **91**. $R_f = 0.2$ (40% EtOAc in hexanes); ¹H NMR (500 MHz, CDCl₃) δ 5.23–5.08 (m, 2H), 4.66 (t, $J = 1.0$ Hz, 2H), 3.79 (s, 3H), 3.71 (s, 3H), 3.25 (t, $J = 7.3$ Hz, 1H), 3.19 (dd, $J = 80.0, 13.8$ Hz, 1H), 1.74 (dq, $J = 13.5, 6.7$ Hz, 1H), 1.51 (br s, 2H), 1.43 (t, $J = 7.2$ Hz, 2H), 0.89 (dd, $J = 9.2, 6.6$ Hz, 6H); ¹³C NMR (126 MHz, CDCl₃) δ 176.5, 155.7, 141.7, 115.0, 68.9, 59.1, 54.9, 51.7, 50.4, 42.9, 24.9, 22.9, 22.2; IR (Neat Film, NaCl) 2956, 2868, 1750, 1737, 1443, 1368, 1267, 1196, 1151, 980, 943, 792 cm⁻¹; HRMS (MM: ESI-APCI+) m/z calc'd for C₁₃H₂₄NO₅ [M + H]⁺: 274.1649; found 274.1659.



Methyl N-(2-(((methoxycarbonyl)oxy)methyl)allyl)-N-methyl-L-leucinate (82). To a 10 mL round bottom flask containing a magnetic stirring bar and a solution of 0.37 g **92** (1.35 mmol, 1.0 equiv) in 4 mL of methanol was added 0.056 g of formaldehyde (1.88 mmol, 1.4 equiv) as a 37% solution in H₂O. The mixture was stirred at 23 °C for 12 h at which point 0.11 g sodium cyanoborohydride was carefully added. After an additional 12 h of stirring, the mixture was diluted with H₂O (5 mL), extracted with EtOAc (5 mL x 3), dried over MgSO₄, concentrated *in vacuo* and subjected directly to purification by flash column chromatography (SiO₂, 10% EtOAc in hexanes to 25% EtOAc in hexanes) to yield 0.25 g of carbonate **82** as a colorless oil. 63.8% yield. $R_f = 0.5$ (33% EtOAc in hexanes); ¹H NMR (300 MHz, CDCl₃) δ 5.30–5.07 (m, 2H), 4.63 (t, $J = 1.0$ Hz, 2H), 3.79

(s, 3H), 3.69 (s, 3H), 3.34 (dd, $J = 8.3, 7.0$ Hz, 1H), 3.18 (dd, $J = 75.0, 13.8$ Hz, 2H), 2.22 (s, 3H), 1.73–1.61 (m, 1H), 1.61–1.46 (m, 2H), 0.90 (dd, $J = 17.5, 6.6$ Hz, 6H); ^{13}C NMR (126 MHz, CDCl_3) δ 173.3, 155.6, 141.2, 115.4, 68.5, 63.8, 57.3, 54.7, 50.9, 38.4, 37.0, 24.7, 22.9, 21.9; IR (Neat Film, NaCl) 2955, 2870, 2803, 1751, 1658, 1444, 1385, 1368, 1269, 1193, 1157, 1126, 1072, 978, 945, 792 cm^{-1} ; HRMS (MM: ESI-APCI+) m/z calc'd for $\text{C}_{14}\text{H}_{26}\text{NO}_5$ $[\text{M} + \text{H}]^+$: 288.1805; found 288.1795.

2.6.8 Optimization of reaction parameters

Table 2.6.8.1. Optimization of reaction parameters

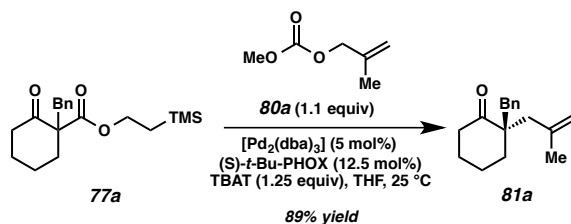
entry	X	equiv allyl	sovent	yield (%) ^a	ee (%) ^b
1	Br	1.0	toluene	55	83
2	OTs	1.0	1,4-dioxane	43	77
3	OMs	1.0	1,4-dioxane	45	84
4	OAc	1.0	1,4-dioxane	15	82
5	OCO ₂ Allyl	1.0	1,4-dioxane	78	83
6	OCO ₂ Me	1.0	1,4-dioxane	78	84
7	OCO ₂ Me	0.75	1,4-dioxane	51	82
8	OCO ₂ Me	1.5	1,4-dioxane	74	82
9	OCO ₂ Me	2.0	1,4-dioxane	73	84
10	OCO ₂ Me	1.1	toluene	33	82
11	OCO ₂ Me	1.1	MTBE	65	84
12	OCO ₂ Me	1.1	THF	83	83
13	OCO ₂ Me	1.1	tol/hex	45	93
14 ^c	OCO ₂ Me	1.1	THF	81	86

General Procedure for Optimization Experiments: Inside a nitrogen-filled glove-box, an oven-dried 0.5 dram vial was charged with a magnetic stirring bar, 0.0046 g

[Pd₂(dba)₃] (0.005 mmol, 0.05 equiv), 0.0047 g (*S*)-*t*-Bu-PHOX (0.0125 mmol, 0.125 equiv), 0.067 g TBAT (0.125 mmol, 1.25 equiv), 0.018 g tridecane (0.10 mmol, 1.0 equiv) and 3.0 mL THF. This mixture was stirred at 25 °C for 30 min at which time 0.026 g of β-ketoester **74** (0.10 mmol, 1.0 equiv) and 0.013 g of allyl methyl carbonate (0.11 mmol, 1.1 equiv) were added, neat. The vial was capped and stirring continued for 12 h at which time the vial was removed from the glove-box, uncapped and the magnetic stirring bar removed. The reaction mixture was diluted with hexanes (2 mL) and passed through a pipette plug (SiO₂) with 4 mL of hexanes followed by 4 mL of Et₂O. From the combined organic fractions, a sample was prepared and the mixture analyzed by GC.

2.6.9 General procedure for Pd-catalyzed allylic alkylation

Please note that the absolute configuration for all products **79** and **81** has been inferred by analogy to previous studies. For isolated yields, see the main text of vide supra. For respective GC, HPLC or SFC conditions, as well as optical rotation data, please refer to Table 2.6.11.

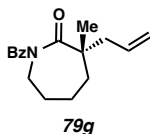


(S)-2-benzyl-2-(2-methylallyl)cyclohexan-1-one (81a). Inside a nitrogen filled glove-box, an oven-dried 20 mL scintillation vial was charged with a magnetic stirring bar, 0.011 g [Pd₂(dba)₃] (0.012 mmol, 0.05 equiv), 0.011 g (*S*)-*t*-Bu-PHOX (0.029 mmol, 0.125 equiv), 0.15 g TBAT (0.28 mmol, 1.25 equiv) and 7 mL THF. This mixture was

stirred at 25 °C for 30 min at which time 0.075 g of β -ketoester **77a** (0.23 mmol, 1.0 equiv) and 0.033 g of allyl methyl carbonate (0.25 mmol, 1.1 equiv) were added, neat. The vial was capped and stirring continued for 16 h at which time the vial was removed from the glove-box, uncapped and magnetic stirring bar removed. The reaction mixture was concentrated *in vacuo*. The resulting crude semisolid was purified by flash column chromatography (SiO₂, hexanes to 2% EtOAc in hexanes) to give ketone **81a** as a colorless oil. 89% yield. 89% ee, $[\alpha]_D^{25}$ -20.1 (*c* 1.2, CHCl₃); R_f = 0.3 (10% EtOAc in hexanes); ¹H NMR (500 MHz, CDCl₃) δ 7.27–7.23 (m, 2H), 7.22–7.17 (m, 1H), 7.15–7.11 (m, 2H), 4.86 (dd, *J* = 2.0, 1.4 Hz, 1H), 4.69 (dd, *J* = 2.0, 1.0 Hz, 1H), 2.93 (dd, *J* = 114.0, 13.7 Hz, 2H), 2.60–2.49 (m, 1H), 2.44–2.38 (m, 1H), 2.37 (s, 3H), 1.92–1.84 (m, 1H), 1.81–1.69 (m, 2H), 1.67 (dd, *J* = 1.5, 0.8 Hz, 3H), 1.64–1.56 (m, 2H); ¹³C NMR (126 MHz, CDCl₃) δ 214.8, 142.2, 137.8, 130.9, 127.9, 126.2, 114.7, 52.5, 43.2, 41.7, 39.7, 35.7, 26.7, 24.6, 20.8; IR (Neat Film, NaCl) 3026, 2935, 2863, 1700, 1448, 1123, 893, 746 cm⁻¹; HRMS (MM: ESI-APCI+) *m/z* calc'd for C₁₇H₂₃O [M + H]⁺: 243.1743, found 243.1745; SFC conditions: 1% MeOH, 2.5 mL/min, Chiralpak OD-H column, λ = 210 nm, *t_r* (min): major = 5.79, minor = 6.48.

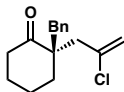
2.6.10 Spectroscopic data for Pd-catalyzed allylic alkylation products

(S)-3-Allyl-1-benzoyl-3-methylazepan-2-one (79g)



Lactam **79g** was prepared by the general procedure and isolated by flash column chromatography (SiO₂, 5% EtOAc in hexanes to 25% EtOAc in hexanes) as a colorless oil. 91% yield. 90% ee, $[\alpha]_D^{25} -35.2$ (*c* 1.7, CHCl₃); $R_f = 0.2$ (30% EtOAc in hexanes); ¹H NMR (500 MHz, CDCl₃) δ 7.52–7.48 (m, 2H), 7.47–7.42 (m, 1H), 7.39–7.35 (m, 2H), 5.72 (dddd, *J* = 17.1, 10.3, 7.6, 7.1 Hz, 1H), 5.13–5.06 (m, 2H), 4.13–4.05 (m, 1H), 3.91 (ddd, *J* = 14.8, 8.8, 2.0 Hz, 1H), 2.40 (dddt, *J* = 71.6, 13.7, 7.6, 1.2 Hz, 2H), 1.91–1.78 (m, 4H), 1.78–1.67 (m, 2H), 1.29 (s, 3H); ¹³C NMR (126 MHz, CDCl₃) δ 182.5, 174.7, 137.0, 133.7, 131.0, 128.1, 127.4, 118.7, 47.7, 44.7, 42.6, 35.1, 28.0, 24.9, 23.3; IR (Neat Film, NaCl) 3072, 2830, 1676, 1448, 1279, 1244, 1224, 1148, 1117, 1096, 971, 951, 919, 790, 726, 695 cm⁻¹; HRMS (MM: ESI-APCI+) *m/z* calc'd for C₁₇H₂₁NO₂ [M + H]⁺: 272.1645, found 272.1660; HPLC conditions: 5% IPA, 1.0 mL/min, Chiralpak OJ–H column, $\lambda = 220$ nm, *t_R* (min): major = 5.60, minor = 5.00.

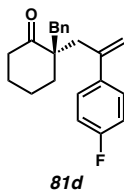
(R)-2-Benzyl-2-(2-chloroallyl)cyclohexan-1-one (81b)



81b

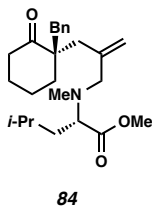
Ketone **81b** was prepared according to the general procedure and isolated by flash column chromatography (SiO₂, 5% EtOAc in hexanes to 10% EtOAc in hexanes) as a colorless oil. 72% yield. 96% ee, $[\alpha]_D^{25} -7.0$ (*c* 1.4, CHCl₃); $R_f = 0.4$ (10% EtOAc in hexanes); ¹H NMR (500 MHz, CDCl₃) δ 7.39–7.16 (m, 2H), 7.20–7.08 (m, 3H), 5.30 (d, *J* = 1.3 Hz, 1H), 5.17 (t, *J* = 1.2 Hz, 1H), 2.99 (dd, *J* = 40.6, 14.1 Hz, 2H), 2.69 (dd, *J* = 56.9, 15.6 Hz, 2H), 2.66–2.34 (m, 2H), 1.97–1.63 (m, 6H); ¹³C NMR (126 MHz, CDCl₃) δ 213.5, 137.0, 130.7, 128.1, 127.7, 126.5, 116.6, 52.5, 43.9, 41.3, 39.7, 35.1, 26.5, 20.9; IR (Neat Film, NaCl) 2939, 2858, 1705, 1631, 1494, 1452, 1429, 1118, 1088, 889, 701 cm⁻¹; HRMS (MM: ESI-APCI+) *m/z* calc'd for C₁₆H₂₀ClO [M + H]⁺: 263.1197, found 263.1199; SFC conditions: 3% MeOH, 2.5 mL/min, Chiralpak OD-H column, λ = 210 nm, *t*_R (min): major = 6.09, minor = 7.04.

(R)-2-Benzyl-2-(2-(4-fluorophenyl)allyl)cyclohexan-1-one (81d)



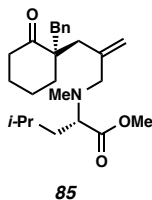
Ketone **81d** was prepared according to the general procedure, and isolated by flash column chromatography (SiO₂, 1% EtOAc in hexanes to 3% EtOAc in hexanes) as a colorless oil. 91% yield. 95% ee, $[\alpha]_D^{25}$ -9.9 (*c* 2.0, CHCl₃); R_f = 0.3 (10% EtOAc in hexanes); ¹H NMR (500 MHz, CDCl₃) δ 7.37–7.12 (m, 5H), 7.11–6.85 (m, 4H), 5.26 (d, *J* = 1.3 Hz, 1H), 5.09 (d, *J* = 1.5 Hz, 1H), 2.86 (dd, *J* = 102.0, 13.7 Hz, 2H), 2.87–2.73 (m, 2H), 2.31 (tt, *J* = 6.2, 2.5 Hz, 2H), 1.83–1.50 (m 6H); ¹³C NMR (126 MHz, CDCl₃) δ 214.3, 162.2 (d, ¹*J*_{CF} = 246.2 Hz), 144.5, 139.2 (d, ⁴*J*_{CF} = 3.3 Hz), 137.8, 130.7, 128.2 (d, ³*J*_{CF} = 7.9 Hz), 127.9, 126.3, 117.6, 115.0 (d, ²*J*_{CF} = 21.3 Hz), 53.3, 41.7, 40.9, 39.7, 35.1, 26.1, 20.8; ¹⁹F NMR (282 MHz, CDCl₃) δ -128.24 ; IR (Neat Film, NaCl) 3027, 2939, 2864, 1703, 1602, 1508, 1453, 1223, 1159, 1126, 905, 841, 750 cm⁻¹; HRMS (MM: ESI-APCI+) *m/z* calc'd for C₂₂H₂₄FO [M + H]⁺: 323.1806, found 323.1809; SFC conditions: 10% MeOH, 2.5 mL/min, Chiralpak OJ-H column, λ = 210 nm, *t_r* (min): major = 8.59, minor = 10.15.

Methyl *N*-(2-(((*R*)-1-benzyl-2-oxocyclohexyl)methyl)allyl)-*N*-methyl-*L*-leucinate (84**)**



Ketone **84** was prepared by the general procedure and isolated by flash column chromatography (SiO₂, 2% EtOAc in hexanes to 5% EtOAc in hexanes) as a colorless oil. 95% yield. >25:1 dr, $[\alpha]_{\text{D}}^{25} -20.57$ (*c* 1.75, CHCl₃); $R_f = 0.5$ (30% EtOAc in hexanes); ¹H NMR (500 MHz, CDCl₃) δ 7.25–7.21 (m, 2H), 7.21–7.16 (m, 1H), 7.15–7.11 (m, 2H), 5.12 (q, *J* = 1.3 Hz, 1H), 4.94–4.88 (m, 1H), 3.67 (s, 3H), 3.33 (t, *J* = 7.6 Hz, 1H), 3.05–2.90 (m, 2H), 2.93 (dd, *J* = 176.8, 13.7 Hz, 2H), 2.67–2.54 (m, 2H), 2.40–2.31 (m, 1H), 2.25 (dd, *J* = 15.1, 1.1 Hz, 1H), 2.20 (s, 3H), 1.90 (ddq, *J* = 8.0, 4.3, 1.9 Hz, 1H), 1.81–1.47 (m, 8H), 0.90 (dd, *J* = 11.9, 6.6 Hz, 6H); ¹³C NMR (126 MHz, CDCl₃) δ 214.9, 173.3, 143.0, 138.1, 130.9, 127.8, 126.1, 116.5, 62.9, 61.8, 52.6, 50.8, 41.2, 39.5, 38.9, 38.4, 36.8, 36.5, 26.9, 24.8, 23.0, 22.2, 20.8; IR (Neat Film, NaCl) 2949, 2868, 1732, 1703, 1641, 1452, 1189, 1152, 1122, 1019, 910, 702 cm⁻¹; HRMS (MM: ESI-APCI+) *m/z* calc'd for C₂₅H₃₇NO₃ [M + H]⁺: 400.2836, found 400.2860.

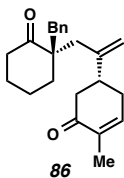
Methyl *N*-(2-(((*S*)-1-benzyl-2-oxocyclohexyl)methyl)allyl)-*N*-methyl-*L*-leucinate (85)



Ketone **85** was prepared by the general procedure, using ligand **L9** instead of **L1**, and isolated by flash column chromatography (SiO₂, 2% EtOAc in hexanes to 5% EtOAc in hexanes) as a colorless oil. 95% yield. 1:21 dr, $[\alpha]_D^{25} +12.94$ (*c* 1.25, CHCl₃); $R_f = 0.5$ (30% EtOAc in hexanes); ¹H NMR (500 MHz, CDCl₃) δ 7.25–7.21 (m, 2H), 7.21–7.16 (m, 1H), 7.16–7.12 (m, 2H), 5.11 (d, *J* = 1.5 Hz, 1H), 4.89 (d, *J* = 1.7 Hz, 1H), 3.68 (s, 3H), 3.29 (dd, *J* = 7.7, 7.0 Hz, 1H), 3.03–2.93 (m, 2H), 2.92 (dd, *J* = 197.9, 13.7 Hz, 2H), 2.68–2.58 (m, 2H), 2.34 (dt, *J* = 13.8, 4.9 Hz, 1H), 2.27–2.21 (m, 1H), 2.19 (s, 3H), 1.91 (d, *J* = 12.8 Hz, 1H), 1.85–1.56 (m, 8H), 0.89 (dd, *J* = 12.4, 6.3 Hz, 6H); ¹³C NMR (126 MHz, CDCl₃) δ 214.8, 173.2, 143.2, 138.2, 131.0, 127.8, 126.1, 116.5, 63.3, 61.6, 52.5, 50.8, 41.1, 39.5, 39.3, 38.2, 36.7, 36.7, 26.9, 24.9, 22.8, 22.5, 20.8; IR (Neat Film, NaCl) 3027, 2950, 2867, 1734, 1702, 1641, 1602, 1495, 1452, 1192, 1154, 1125, 1030, 909, 749, 702 cm⁻¹; HRMS (MM: ESI-APCI+) *m/z* calc'd for C₂₅H₃₇NO₃ [M + H]⁺: 400.2846, found 400.2855.

(R)-5-(3-((S)-1-Benzyl-2-oxocyclohexyl)prop-1-en-2-yl)-2-methylcyclohex-2-en-1-one

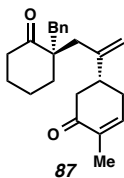
(86)



Ketone **86** was prepared by the general procedure, at 40 °C, and isolated by flash column chromatography (SiO₂, 3% EtOAc in hexanes to 15% EtOAc in hexanes) as a colorless oil. 87% combined yield (**86** and **87**). Characterization data reported for major diastereomer. 6:1 dr, $[\alpha]_D^{25} +49.25$ (*c* 0.25, CHCl₃); $R_f = 0.1$ (30% EtOAc in hexanes); ¹H NMR (500 MHz, CDCl₃) δ 7.25–7.18 (m, 3H), 7.12–7.02 (m, 2H), 6.72 (dq, *J* = 4.2, 1.3 Hz, 1H), 4.97–4.91 (m, 1H), 4.82 (d, *J* = 1.2 Hz, 1H), 3.03–2.83 (m, 2H), 2.64–2.49 (m, 2H), 2.49–2.37 (m, 4H), 2.38–2.09 (m, 3H), 1.85–1.78 (m, 2H), 1.77 (dt, *J* = 2.6, 1.3 Hz, 3H), 1.76–1.61 (m, 4H); ¹³C NMR (126 MHz, CDCl₃) δ 214.7, 199.8, 147.4, 144.7, 137.3, 135.3, 130.6, 128.0, 126.5, 113.1, 52.5, 43.6, 42.2, 41.8, 39.5, 39.4, 35.6, 31.9, 26.7, 20.8, 15.7; IR (Neat Film, NaCl) 2923, 2863, 1702, 1672, 1494, 1450, 1365, 1248, 1109, 901, 750, 703 cm⁻¹; HRMS (MM: ESI-APCI+) *m/z* calc'd for C₂₃H₂₈O₂Na [M + Na]⁺: 359.1982, found 359.1988.

(R)-5-(3-((S)-1-Benzyl-2-oxocyclohexyl)prop-1-en-2-yl)-2-methylcyclohex-2-en-1-one

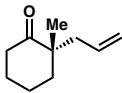
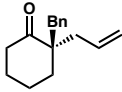
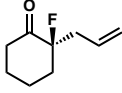
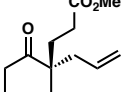
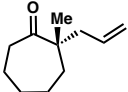
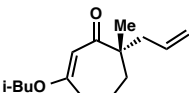
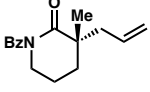
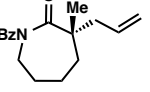
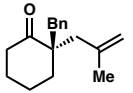
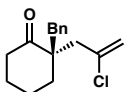
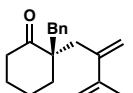
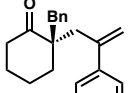
(87)



Ketone **87** was prepared by the general procedure, at 40 °C, and isolated by flash column chromatography (SiO₂, 3% EtOAc in hexanes to 15% EtOAc in hexanes) as a colorless oil. 77% combined yield (**86** and **87**). Characterization data reported for major diastereomer. 6:1 dr, $[\alpha]_D^{25} -10.60$ (*c* 0.50, CHCl₃); $R_f = 0.1$ (30% EtOAc in hexanes); ¹H NMR (500 MHz, CDCl₃) δ 7.25–7.18 (m, 3H), 7.12–7.02 (m, 2H), 6.73 (dq, *J* = 4.2, 1.3 Hz, 1H), 4.98 (s, 1H), 4.84 (s, 1H), 3.01–2.86 (m, 2H), 2.59–2.38 (m, 4H), 2.36–2.11 (m, 3H), 1.88–1.81 (m, 2H), 1.76 (dt, *J* = 2.6, 1.3 Hz, 3H), 1.76–1.61 (m, 4H); ¹³C NMR (126 MHz, CDCl₃) δ 214.6, 199.8, 147.1, 144.5, 137.5, 135.4, 130.6, 128.0, 126.4, 112.7, 52.5, 43.7, 42.6, 41.7, 39.6, 39.2, 35.9, 31.9, 26.8, 20.8, 15.7; IR (Neat Film, NaCl) 2923, 2863, 1702, 1672, 1494, 1450, 1365, 1248, 1109, 901, 750, 703 cm⁻¹; HRMS (MM: ESI-APCI+) *m/z* calc'd for C₂₃H₂₈O₂Na [M + Na]⁺: 359.1982, found 359.1985.

2.6.11 Determination of enantiomeric excess and optical rotations

Table 2.6.11.1. Determination of enantiomeric excess and optical rotations

entry	compound	analytic conditions	ee (%)	polarimetry
1		GC G-TA, 105 °C, isotherm t_R (min): major 7.80, minor 8.24	86	$[\alpha]_D^{25} -11.7$ (c 0.6, CHCl ₃)
2		SFC Chiralpak OJ-H, $\lambda = 210$ nm 3% IPA/CO ₂ , 2.5 mL/min, t_R (min): major 5.74, minor 4.71	88	$[\alpha]_D^{25} -13.6$ (c 1.3, CHCl ₃)
3		GC G-TA, 110 °C, isotherm t_R (min): major 5.039, minor 5.41	91	$[\alpha]_D^{25} -68.74$ (c 1.5, CHCl ₃)
4		GC G-TA, 120 °C, isotherm t_R (min): major 15.3, minor 22.18	89	$[\alpha]_D^{25} 10.51$ (c 1.6, CHCl ₃)
5		GC G-TA, 110 °C, isotherm t_R (min): major 6.45, minor 7.23	87	$[\alpha]_D^{25} -22.13$ (c 1.4, CHCl ₃)
6		HPLC Chiralcel OD-H, $\lambda = 220$ nm 1% IPA/hexanes, 1.0 mL/min t_R (min): major 6.12, minor 7.16	92	$[\alpha]_D^{25} -65.6$ (c 1.0, CHCl ₃)
7		SFC Chiralpak AD-H, $\lambda = 254$ nm 5% MeOH/CO ₂ , 2.5 mL/min, t_R (min): major 5.54, minor 6.23	96	$[\alpha]_D^{25} -76.5$ (c 2.1, CHCl ₃)
8		HPLC Chiralcel OJ-H, $\lambda = 220$ nm 5% IPA/hexanes, 1.0 mL/min t_R (min): major 5.60, minor 5.00	90	$[\alpha]_D^{25} -35.2$ (c 1.7, CHCl ₃)
9		SFC Chiralpak OD-H, $\lambda = 210$ nm 1% MeOH/CO ₂ , 2.5 mL/min, t_R (min): major 5.79, minor 6.48	89	$[\alpha]_D^{25} -20.1$ (c 1.2, CHCl ₃)
10		SFC Chiralpak OD-H, $\lambda = 210$ nm 3% MeOH/CO ₂ , 2.5 mL/min t_R (min): major 6.09, minor 7.04	96	$[\alpha]_D^{25} -7.0$ (c 1.4, CHCl ₃)
11		SFC Chiralpak OJ-H, $\lambda = 210$ nm 4% IPA/CO ₂ , 4.0 mL/min t_R (min): major 7.86, minor 8.66	93	$[\alpha]_D^{25} -10.5$ (c 0.8, CHCl ₃)
12		SFC Chiralcel OJ-H, $\lambda = 210$ nm 10% MeOH/CO ₂ , 2.5 mL/min t_R (min): major 8.59, minor 10.15	95	$[\alpha]_D^{25} -9.9$ (c 2.0, CHCl ₃)

2.7 REFERENCES AND NOTES

- (51) (a) Rasmussen, J. K. *Synthesis* **1977**, 91. (b) Caine, D.; Alkylation of Enols and Enolates. In *Comprehensive Organic Synthesis*, Trost, B. M.; Fleming, I, Eds.; Pergamon Press: Oxford, 1991, Vol. 3, pp. 1-63. (c) Kobayashi, S.; Manabe, K.; Ishitani, H.; Matsuo, J. –I. In *Science of Synthesis, Houben-Weyl Methods of Molecular Transformations*, Bellus, D.; Ley, S. V.; Noyori, R.; Regitz, M.; Schauman, E.; Shinkai, I.; Thomas, E. J.; Trost, B. M. Eds.; Georg Thieme Verlag: Stuttgart, 2002, Vol. 4, pp. 317–369. (d) Lu, Z.; Ma, S. *Angew. Chem.* **2008**, *120*, 264; *Angew. Chem., Int. Ed.* **2008**, *47*, 258. (e) For a recent example in reductive access to enolates, see: Nahra, F.; Macé, Y.; Lambin, D.; Riant, O. *Angew. Chem., Int. Ed.* **2013**, *52*, 3208.
- (52) (a) Cazeau, P.; Duboudin, F.; Moulines, F.; Babot, O.; Dunogues, J. *Tetrahedron* **1987**, *43*, 2075. (b) Cazeau, P.; Duboudin, F.; Moulines, F.; Babot, O.; Dunogues, J. *Tetrahedron*, **1987**, *43*, 2089.
- (53) For examples, see substrate preparation in reference 9 and see: Cheon, H. C.; Yamamoto, H. *J. Am. Chem. Soc.* **2008**, *130*, 9246.
- (54) For a recent example in C-acylation technology, see: Hale, K.J.; Grabski, M.; Flasz, J.T. *Org. Lett.*, **2013**, *15*, 370.

- (55) (a) Tsuji, J.; Takahashi, H.; Morikawa, M. *Tetrahedron Lett.* **1965**, *49*, 4387. (b) Trost, B. M.; Strege, P. E. *J. Am. Chem. Soc.* **1977**, *99*, 1649. (c) Tsuji, J.; Minami, I.; Shimizu, I. *Chem. Lett.* **1983**, 1325. (d) Trost, B. M.; Crawley, M. L. *Chem. Rev.* **2003**, *103*, 2921. (e) Nakamura, M.; Hajra, A.; Endo, K.; Nakamura, E. *Angew. Chem.* **2005**, *117*, 7414; *Angew. Chem., Int. Ed.* **2005**, *44*, 7248. (f) Bélanger, É.; Cantin, K.; Messe, O.; Tremblay, M.; Paquin, J.-F. *J. Am. Chem. Soc.* **2007**, *129*, 1034.
- (56) For example, in previous work on Pd-catalyzed asymmetric protonation multiple equiv of proton source were required to favor protonation. See: (a) Mohr, J. T.; Nishimata, T.; Behenna, D. C.; Stoltz, B. M. *J. Am. Chem. Soc.* **2006**, *128*, 11348.
- (57) (a) Grenning, A. J.; Tunge, J. A. *J. Am. Chem. Soc.* **2011**, *133*, 14785. (b) Grenning, A. J.; Van Allen, C. K.; Maji, T.; Lang, S. B.; Tunge, J. A. *J. Org. Chem.* **2013**, *78*, 7281.
- (58) For select examples of TMSE ester as protecting groups, see: (a) Wood, J. L.; Thompson, B. D.; Yusuff, N.; Pflum, D. A.; Matthäus, M. S. P. *J. Am. Chem. Soc.* **2001**, *123*, 2097. (b) Back, T. G.; Wulff, J. E. *Angew. Chem., Int. Ed.* **2004**, *43*, 6993. (c) Knobloch, E.; Brückner, R. *Synthesis* **2008**, *14*, 2229. (d) Schleicher, K. D.; Jamison, T. F. *Beilstein J. Org. Chem.* **2013**, *9*, 1533.

- (59) For a recent review on P,N-ligands, see: Carroll, M. P.; Guiry, P. J. *Chem. Soc. Rev.* **2014**, *43*, 819.
- (60) Williams, P.; Albericio, F.; Giralt, E. Chemical approaches to the synthesis of peptides and proteins. Boca Raton: CRC Press, 1997, pp.116–119.
- (61) Pangborn, A. M.; Giardello, M. A.; Grubbs, R. H.; Rosen, R. K.; Timmers, F. J. *Organometallics*, **1996**, *15*, 1518.
- (62) Igarashi, J.; Kobayashi, Y. *Tetrahedron Lett.* **2005**, *46*, 6381.
- (63) Dai, Y.; Wu, F.; Zang, Z.; You, H.; Gong, H. *Chem. –Eur. J.* **2012**, *18*, 808.
- (64) Hong, A. Y.; Stoltz, B. M. *Angew. Chem., Int. Ed.* **2012**, *51*, 9674.
- (65) Xuan, M.; Paterson, I.; Dalby, S. M. *Org. Lett.* **2012**, *14*, 5492.
- (66) Flegelová, Z.; Pátek, M. *J. Org. Chem.* **1996**, *61*, 6735.
- (67) Neuhaus, C. M.; Liniger, M.; Stieger, M.; Altmann, K. -H. *Angew. Chem., Int. Ed.* **2013**, *52*, 5866.

(68) Sun, C. -S.; Lin, Y. -S.; Hou, D. -R. *J. Org. Chem.* **2008**, *73*, 6877.

APPENDIX 2

Spectra Related to Chapter 2:

*Development of (Trimethylsilyl)Ethyl Ester Protected Enolates and
Applications in Palladium–Catalyzed Enantioselective Allylic Alkylation:
Intermolecular Cross-Coupling of Functionalized Electrophiles*

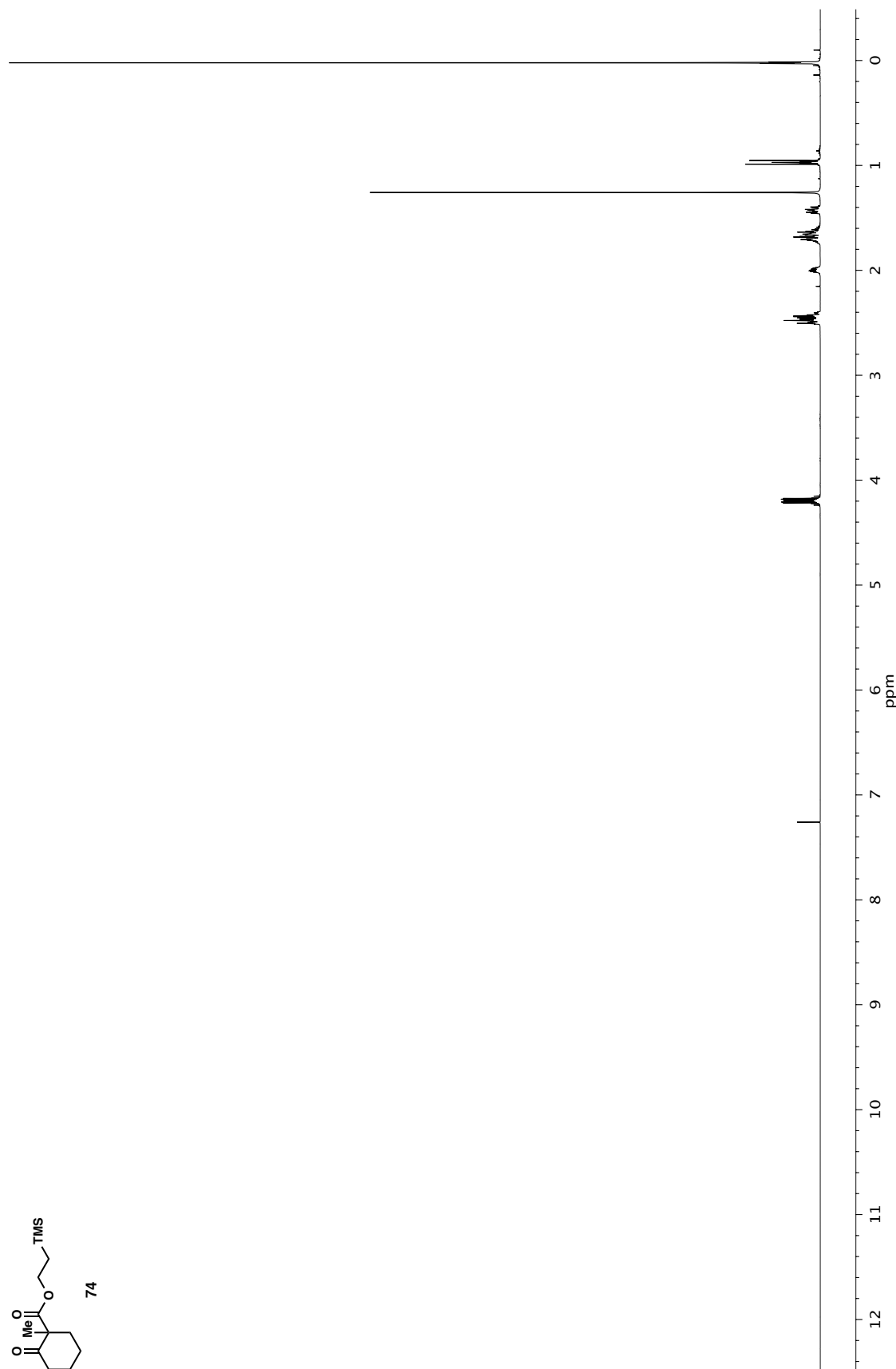
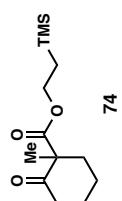


Figure A2.1 ¹H NMR (500 MHz, CDCl₃) of compound 74.

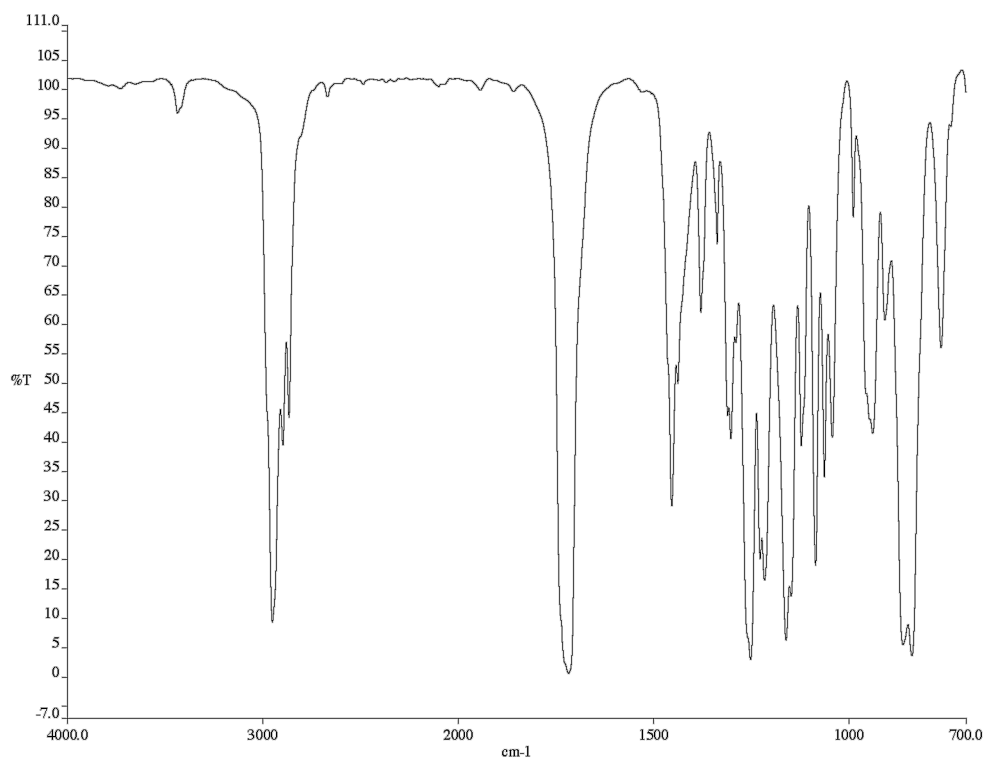


Figure A2.2 Infrared spectrum (thin film/NaCl) of compound **74**.

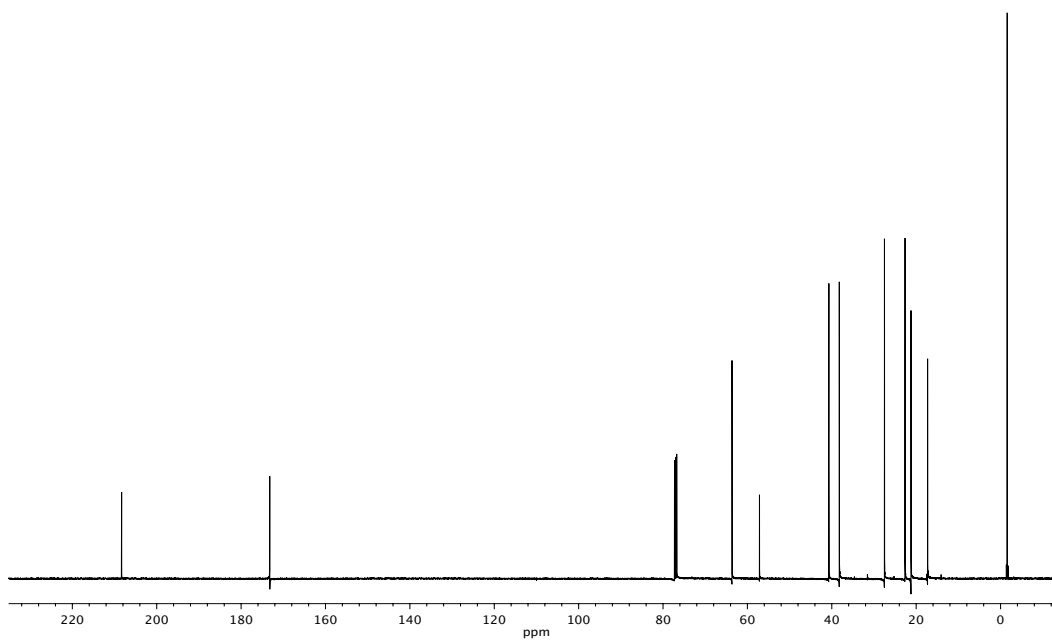


Figure A2.3 ¹³C NMR (125 MHz, CDCl₃) of compound **74**.

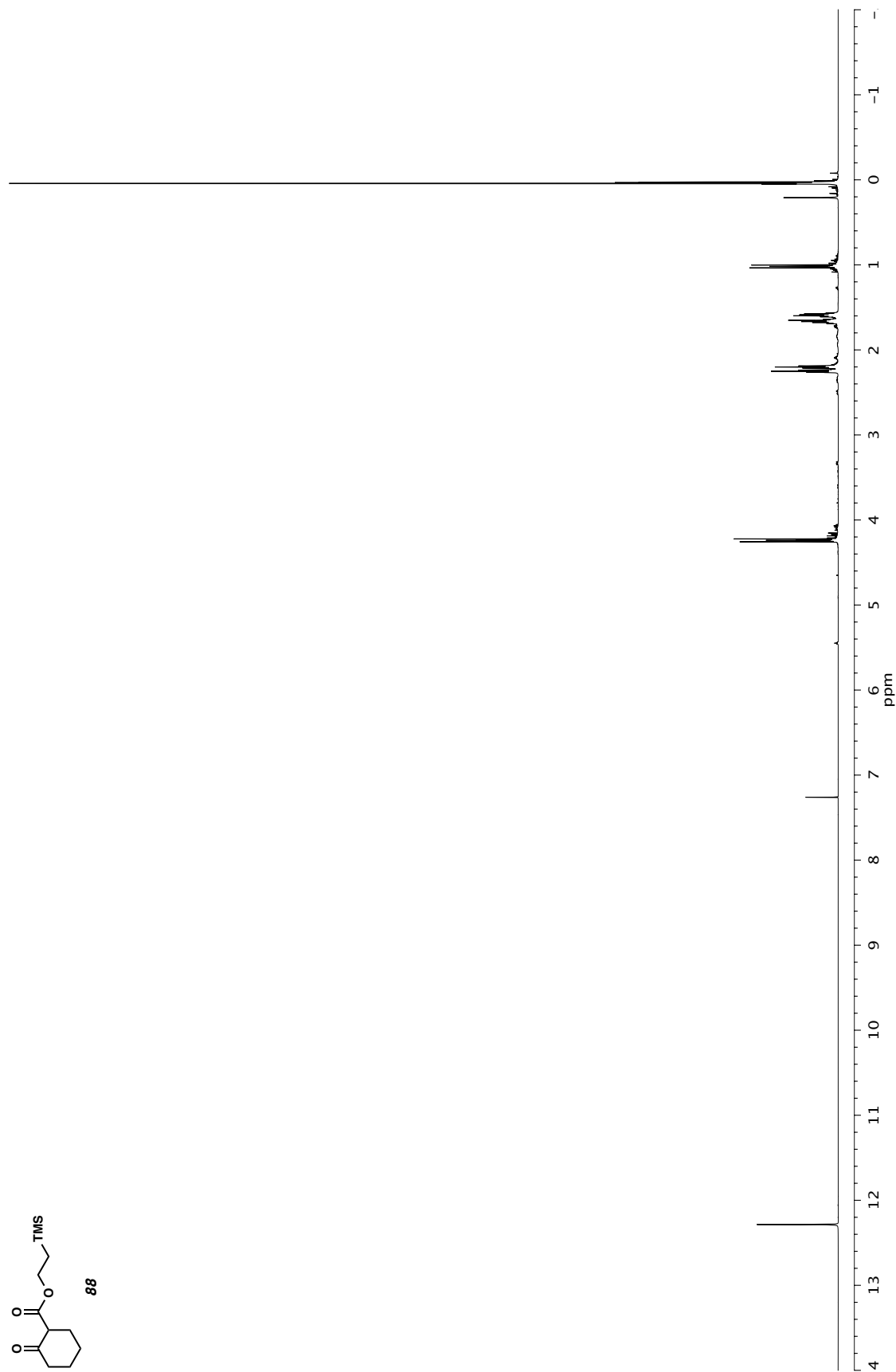
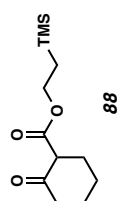


Figure A2.4 ¹H NMR (500 MHz, CDCl₃) of compound **88**.

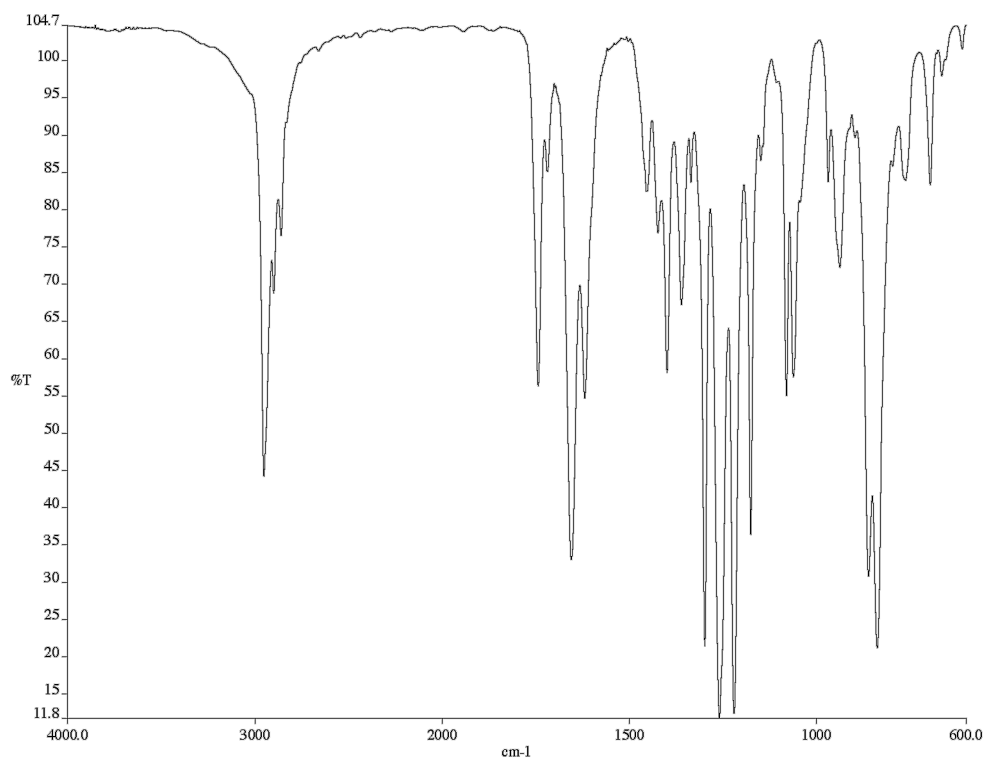


Figure A2.5 Infrared spectrum (thin film/NaCl) of compound **88**.

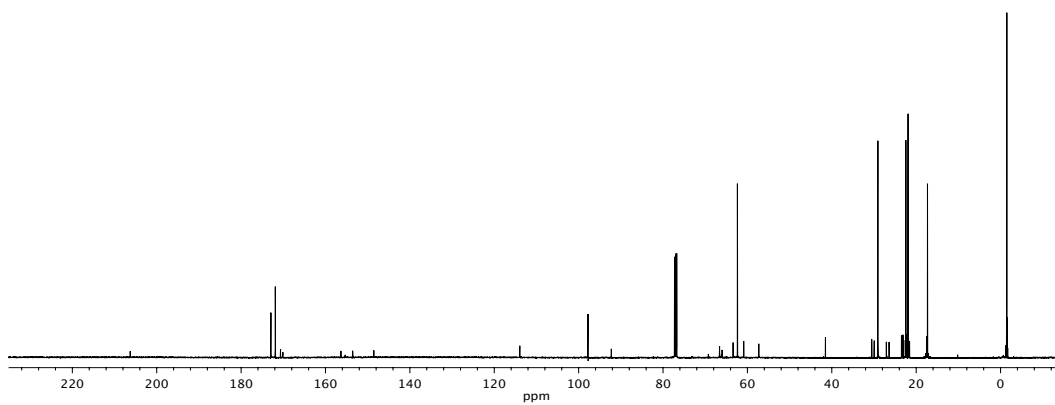


Figure A2.6 ¹³C NMR (125 MHz, CDCl₃) of compound **88**.

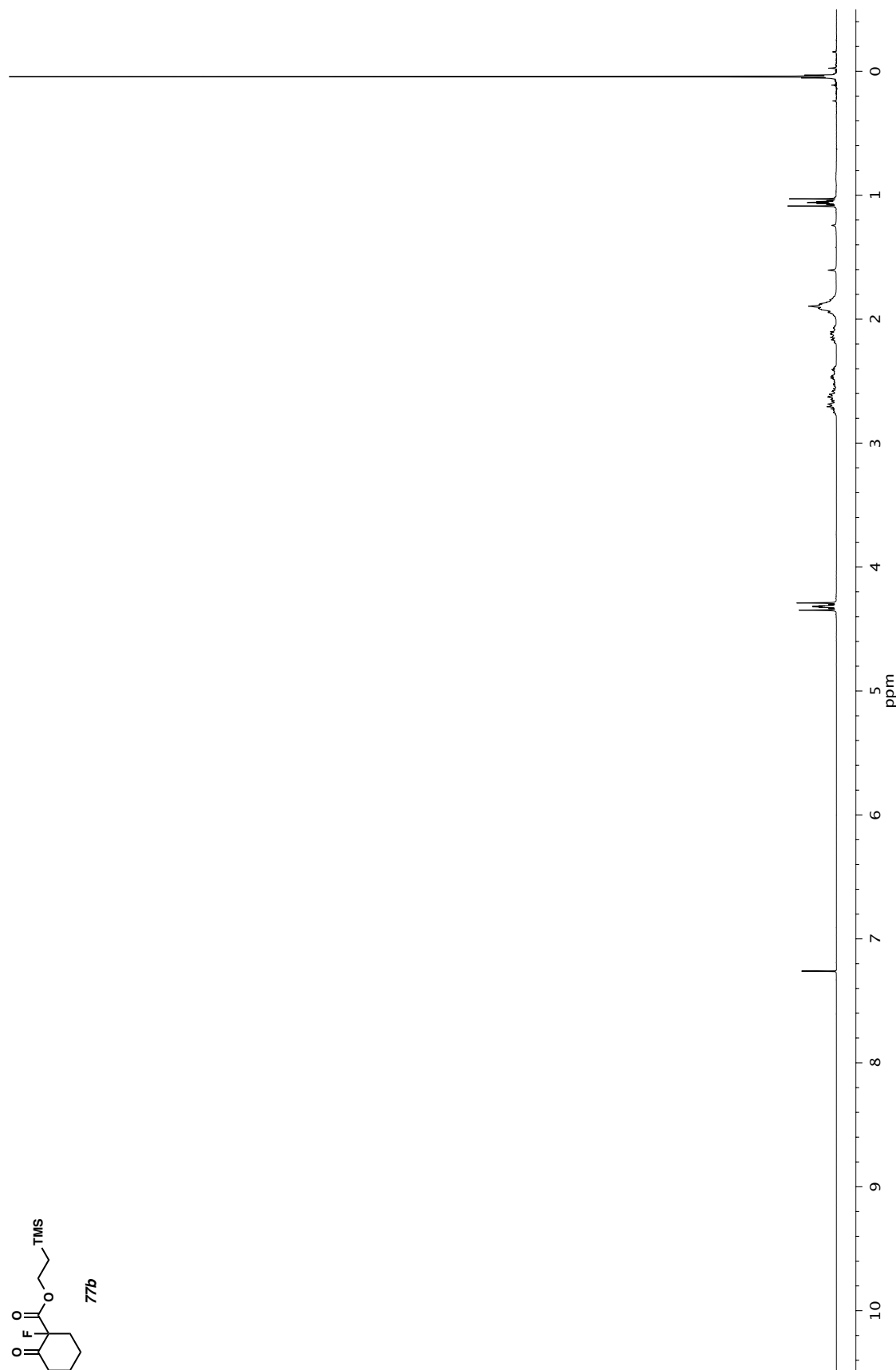
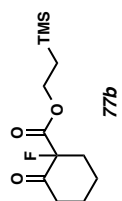


Figure A2.7 ¹H NMR (300 MHz, CDCl₃) of compound 77b.

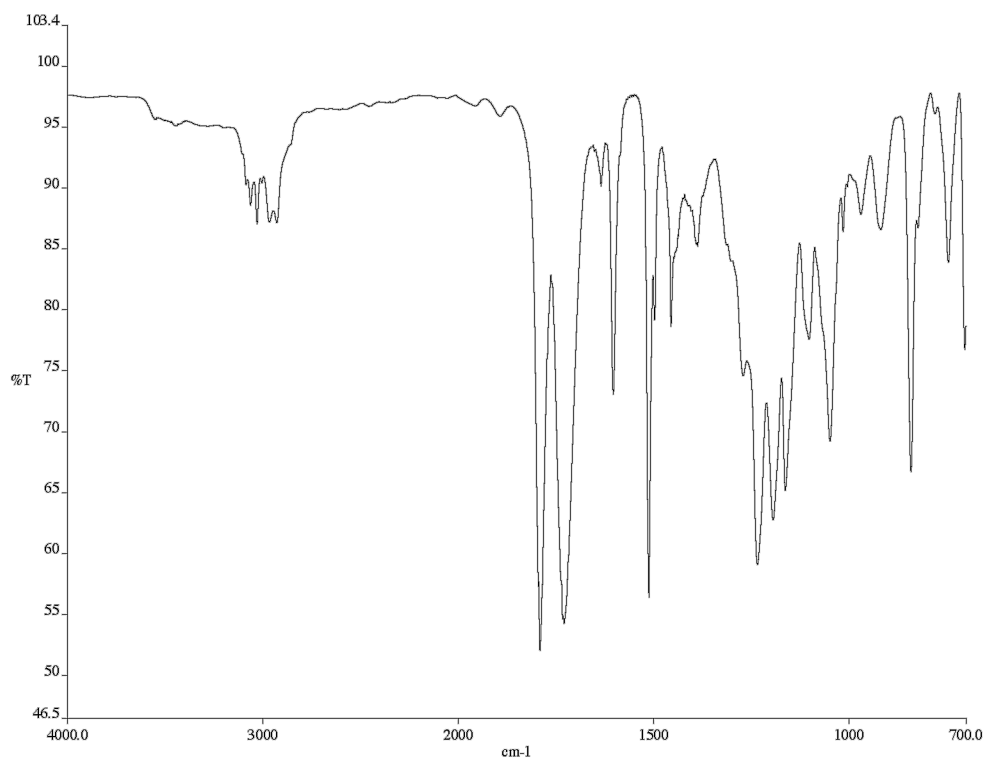


Figure A2.8 Infrared spectrum (thin film/NaCl) of compound **77b**.

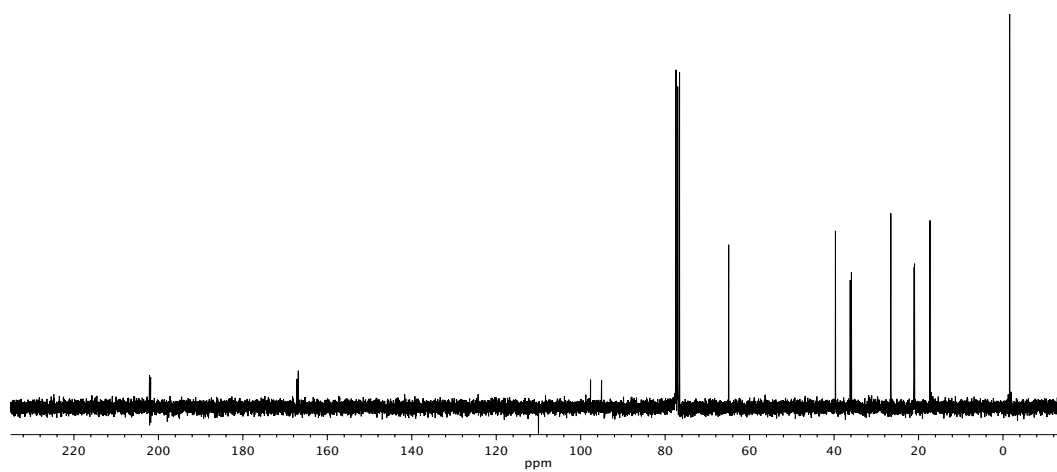


Figure A2.9 ^{13}C NMR (75 MHz, CDCl_3) of compound **77b**.

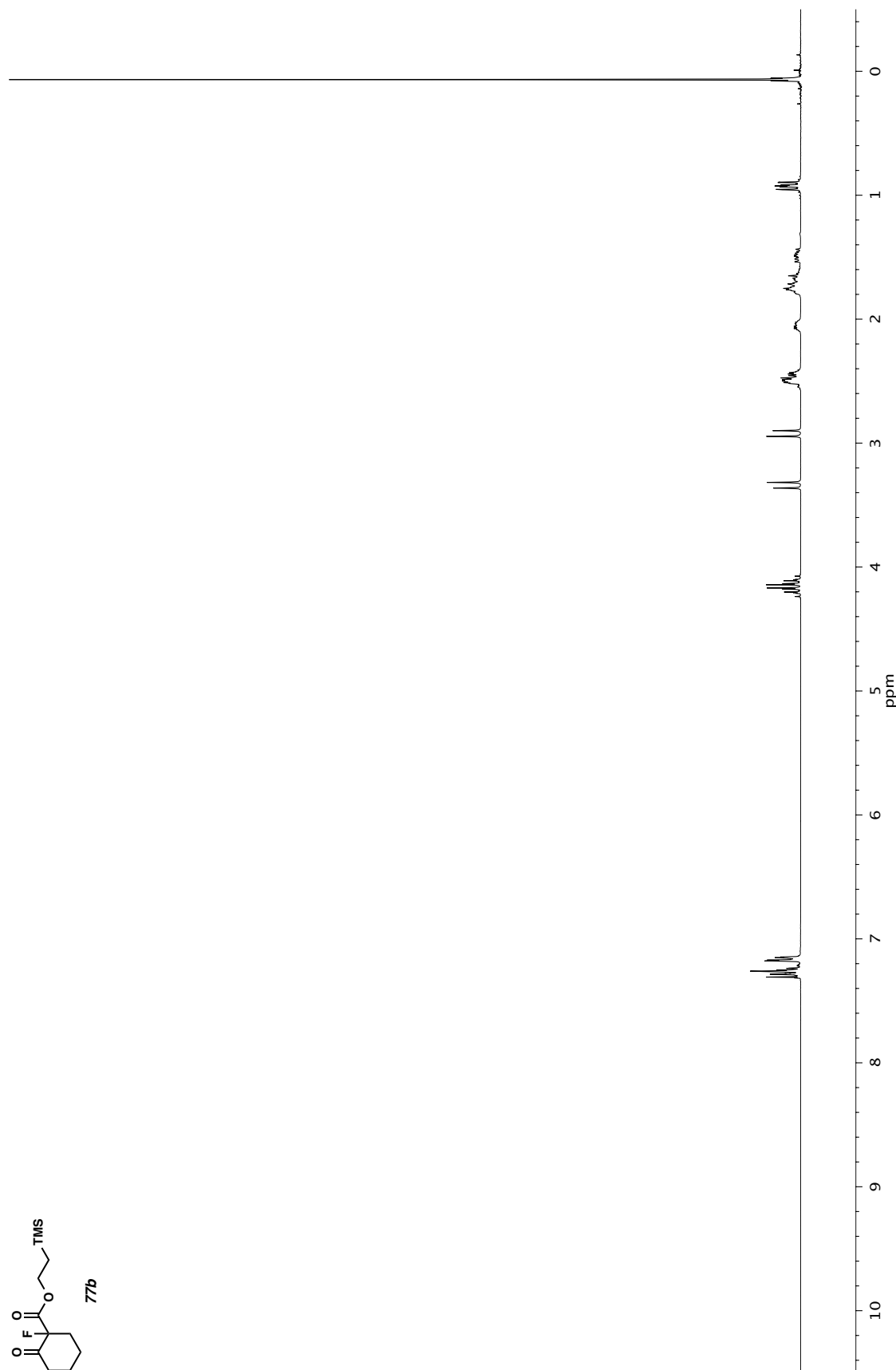
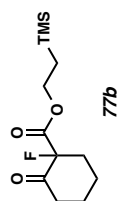


Figure A2.10 ¹H NMR (500 MHz, CDCl₃) of compound 77a.

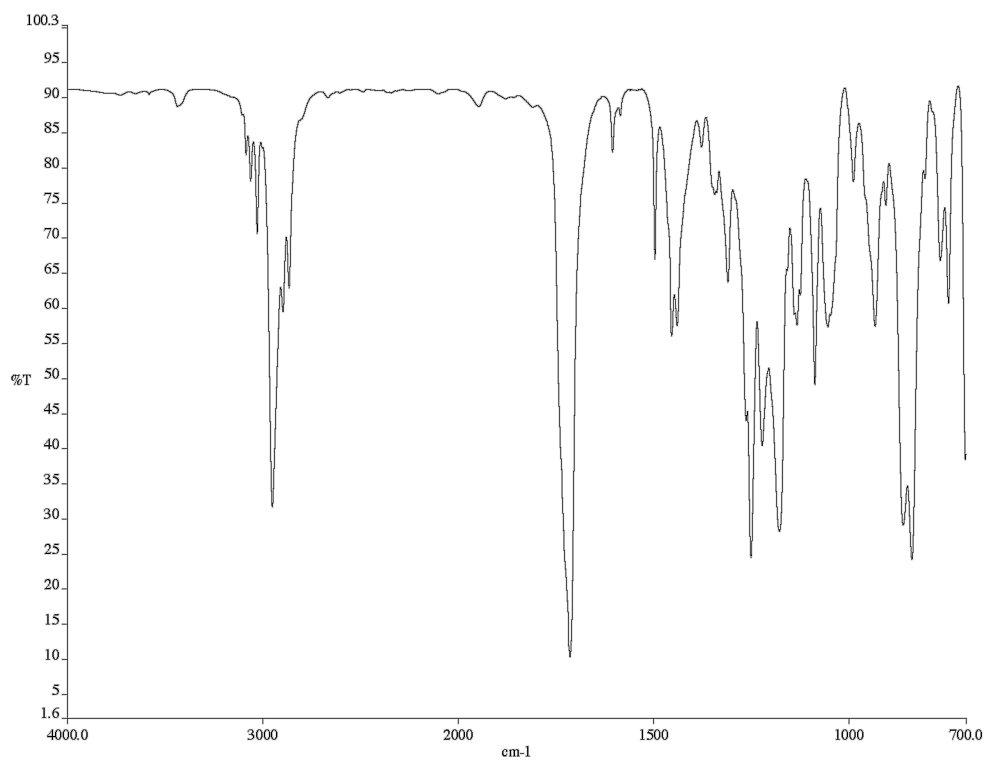


Figure A2.11 Infrared spectrum (thin film/NaCl) of compound **77a**.

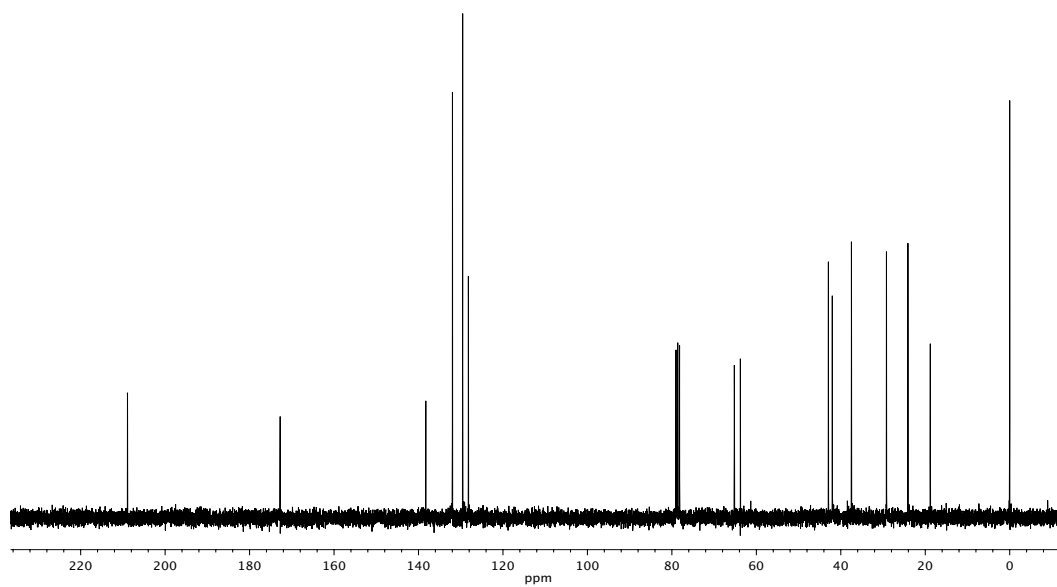


Figure A2.12 ¹³C NMR (125 MHz, CDCl₃) of compound **77a**.

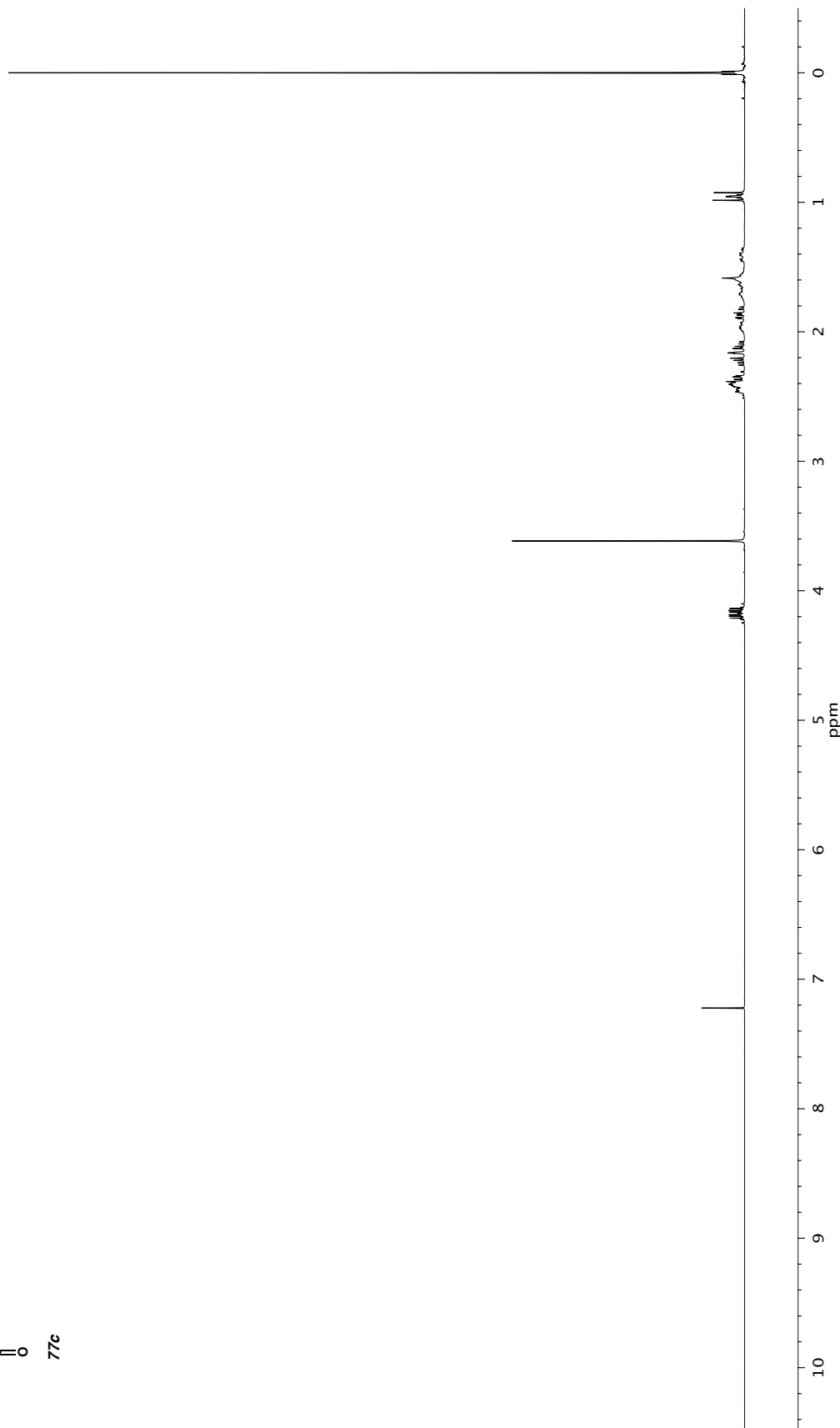
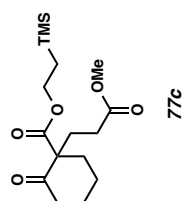


Figure A2.13 ^1H NMR (300 MHz, CDCl_3) of compound 77c.

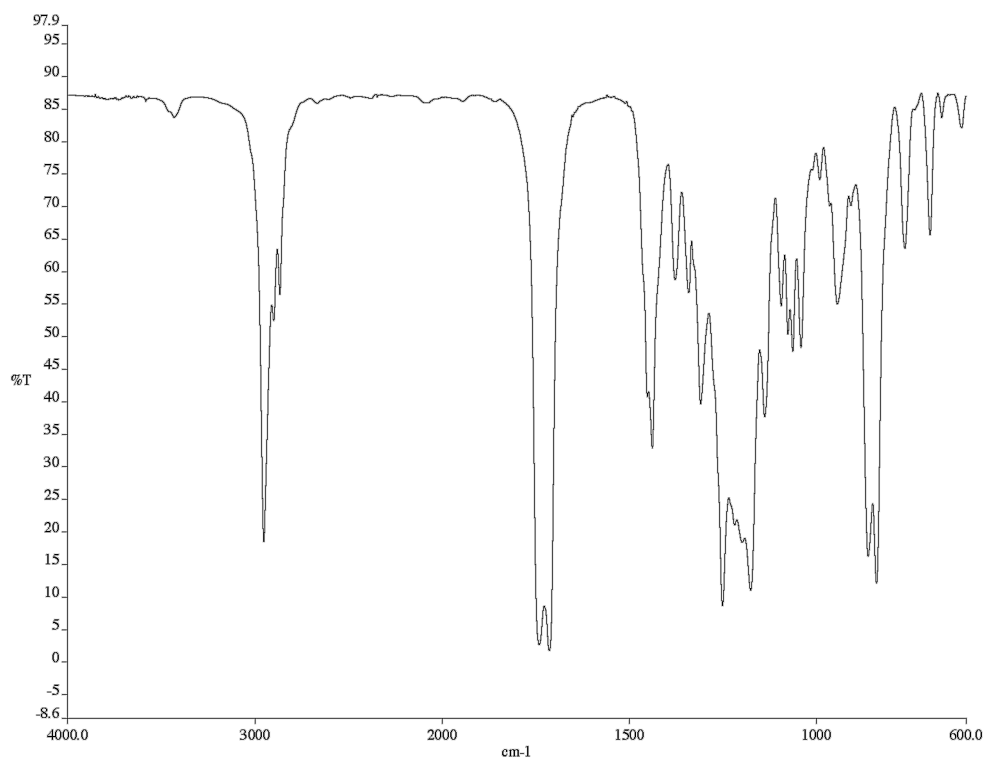


Figure A2.14 Infrared spectrum (thin film/NaCl) of compound 77c.

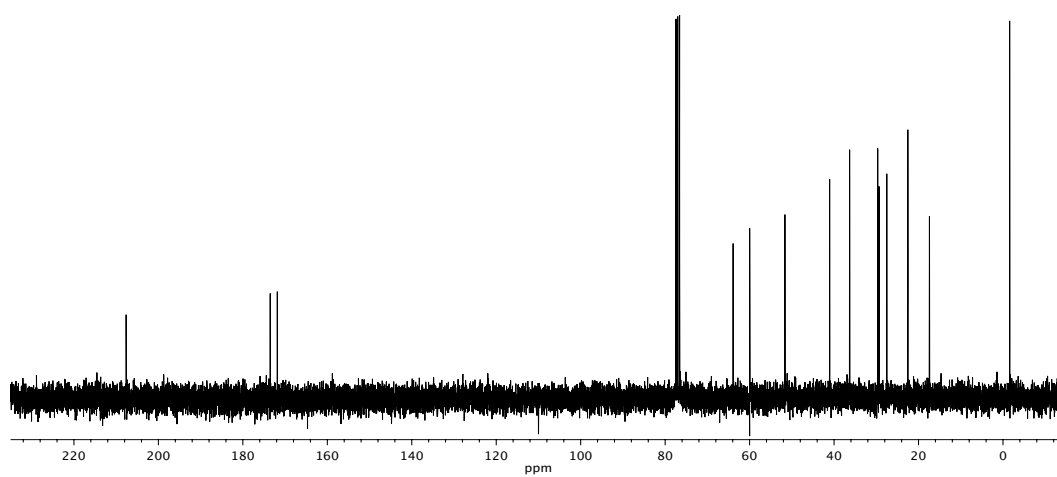


Figure A2.15 ¹³C NMR (75 MHz, CDCl₃) of compound 77c.

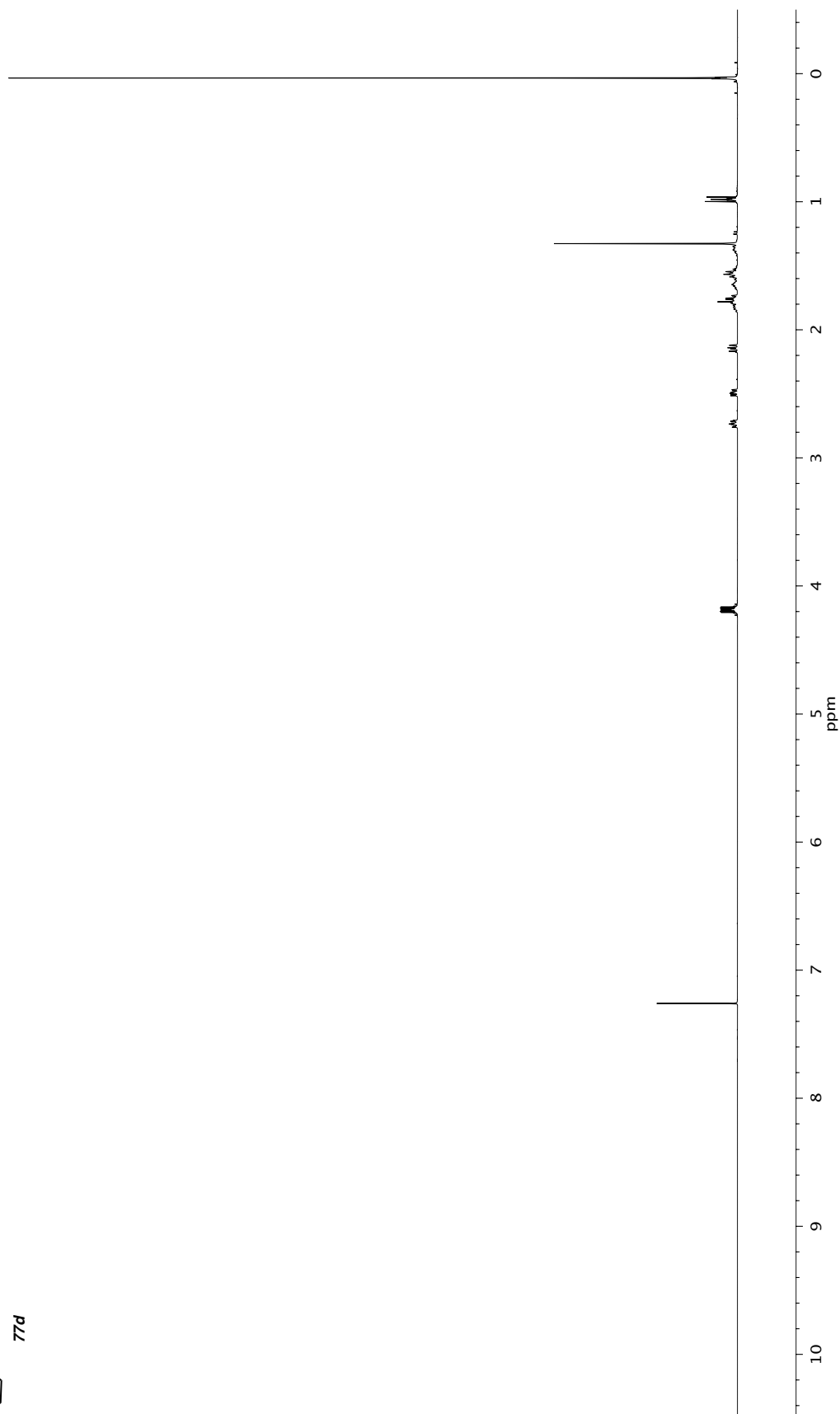
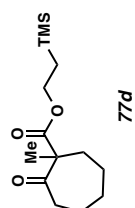


Figure A2.16 ¹H NMR (500 MHz, CDCl₃) of compound **77d**.

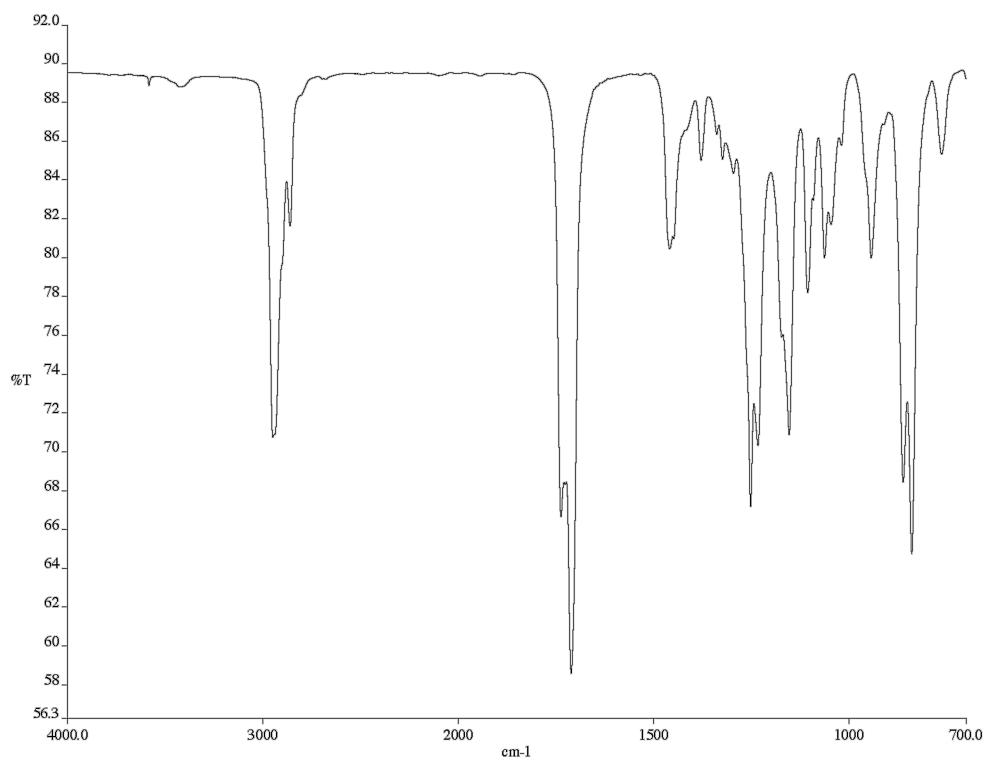


Figure A2.17 Infrared spectrum (thin film/NaCl) of compound **77d**.

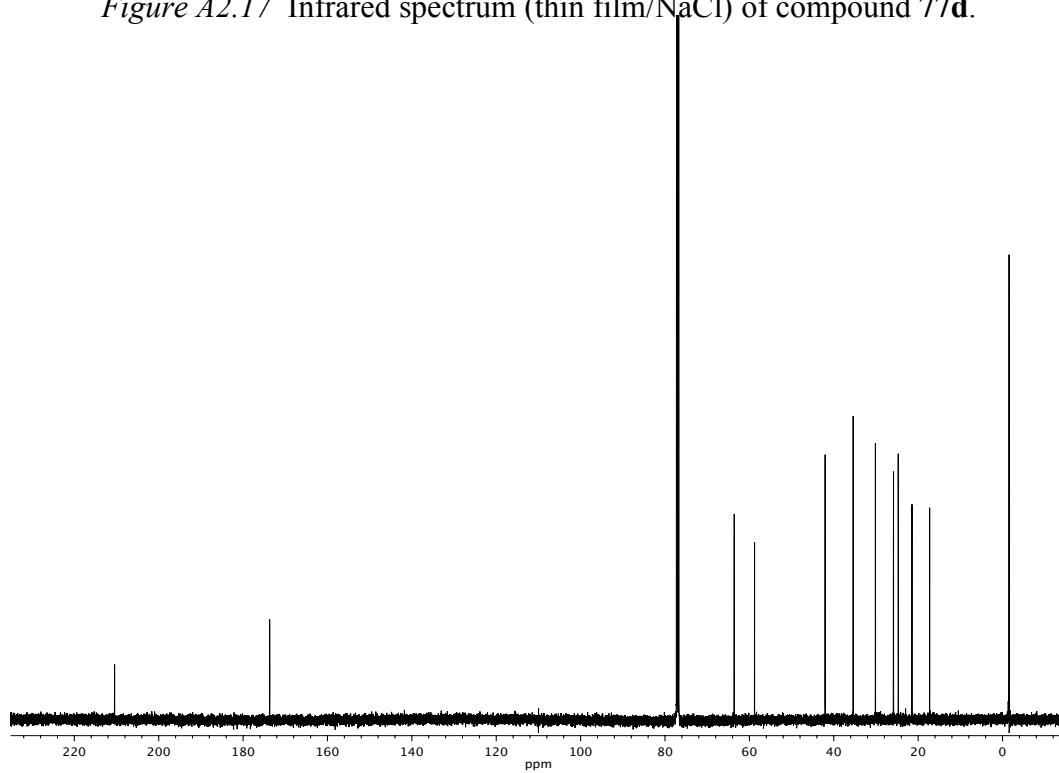


Figure A2.18 ¹³C NMR (125 MHz, CDCl₃) of compound **77d**.

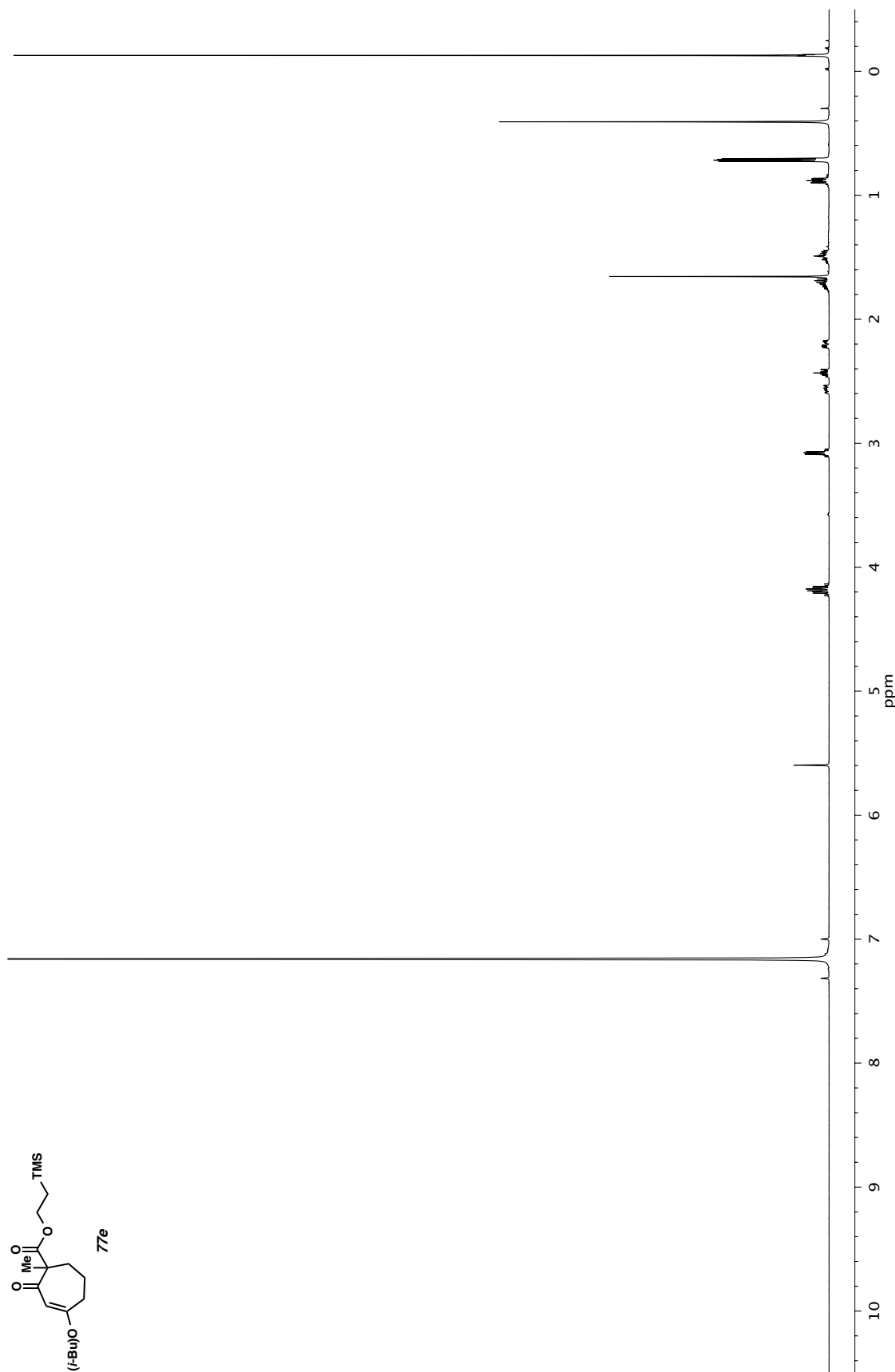


Figure A2.19 ¹H NMR (500 MHz, CDCl₃) of compound 77e.

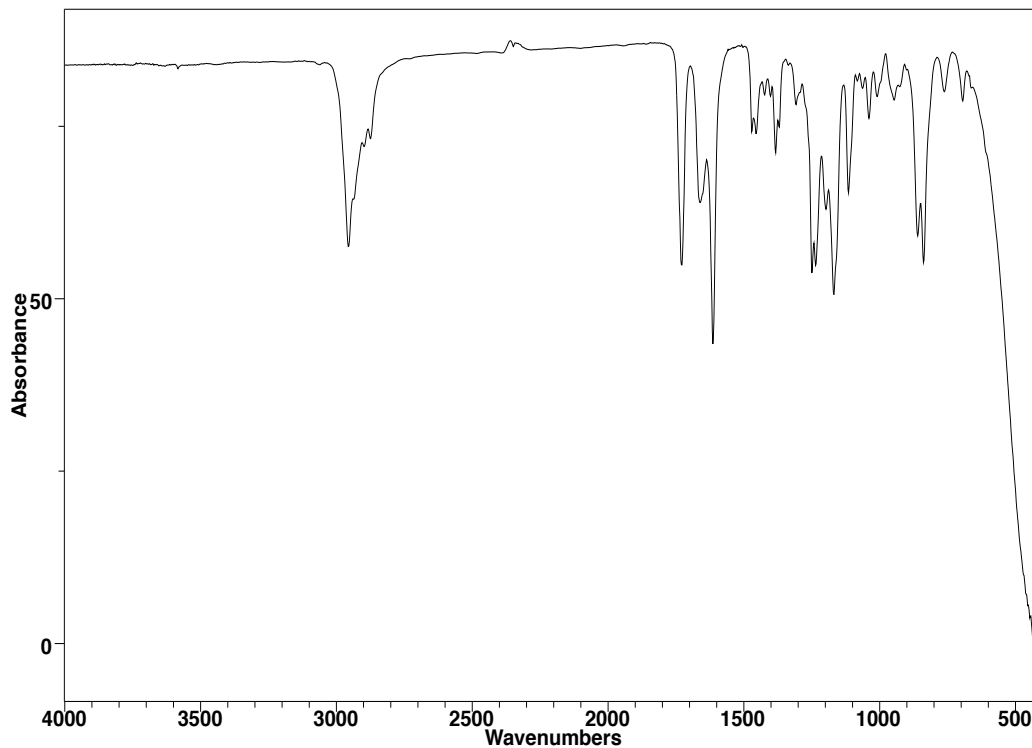


Figure A2.20 Infrared spectrum (thin film/NaCl) of compound 77e.

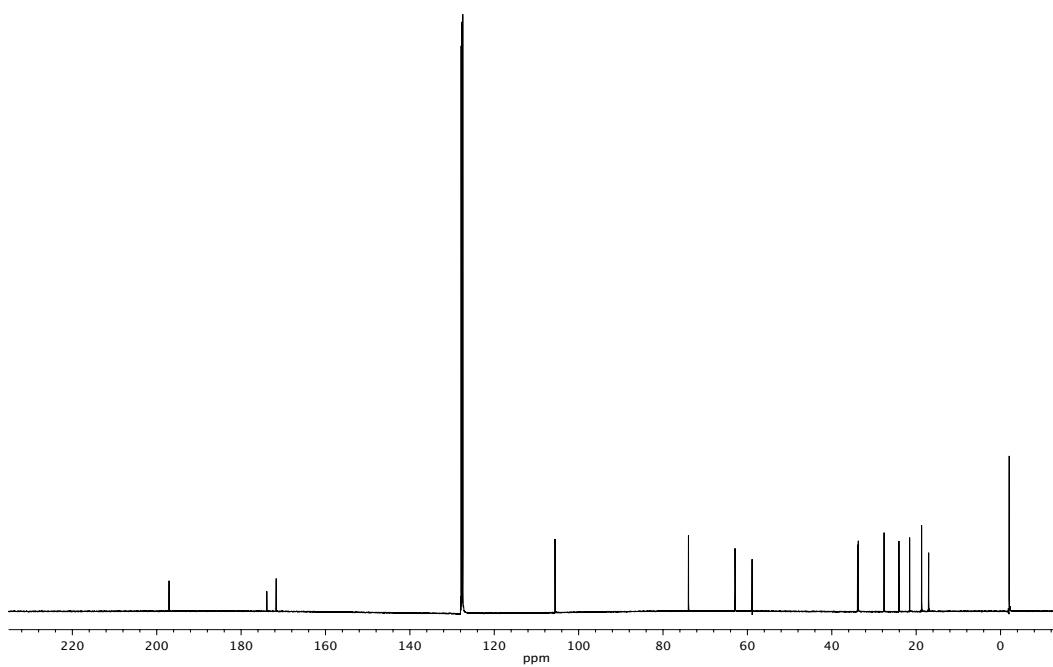


Figure A2.21 ¹³C NMR (125 MHz, CDCl₃) of compound 77e.

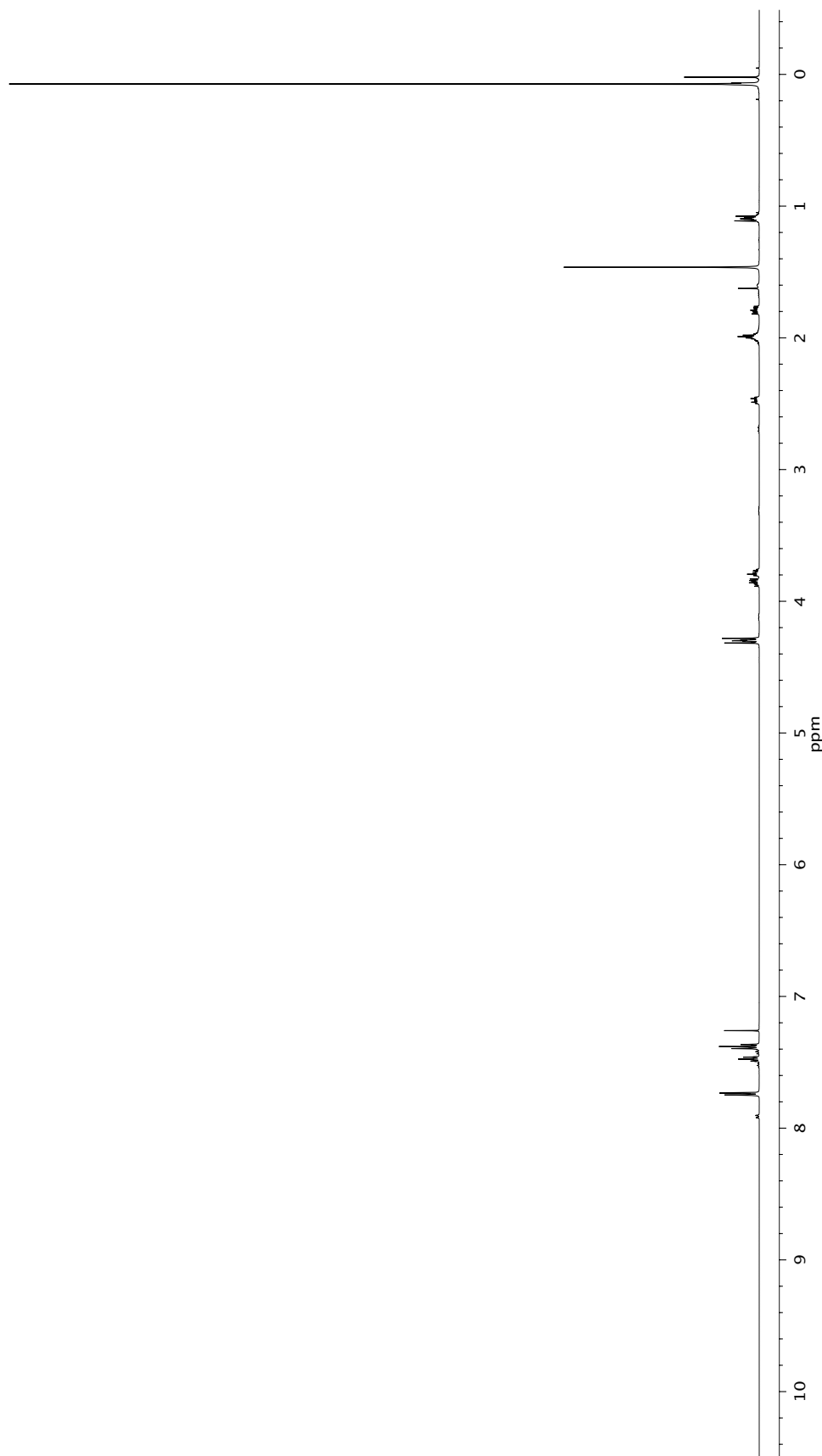
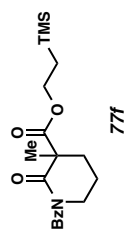


Figure A2.22 ¹H NMR (500 MHz, CDCl₃) of compound 77f.

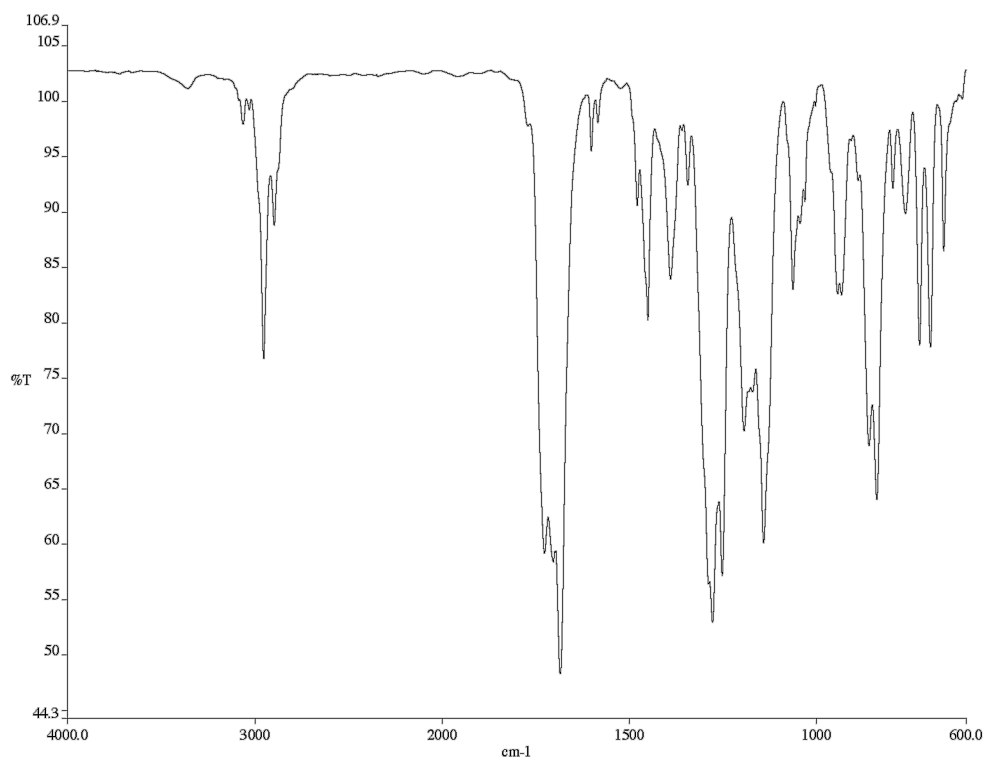


Figure A2.23 Infrared spectrum (thin film/NaCl) of compound **77f**.

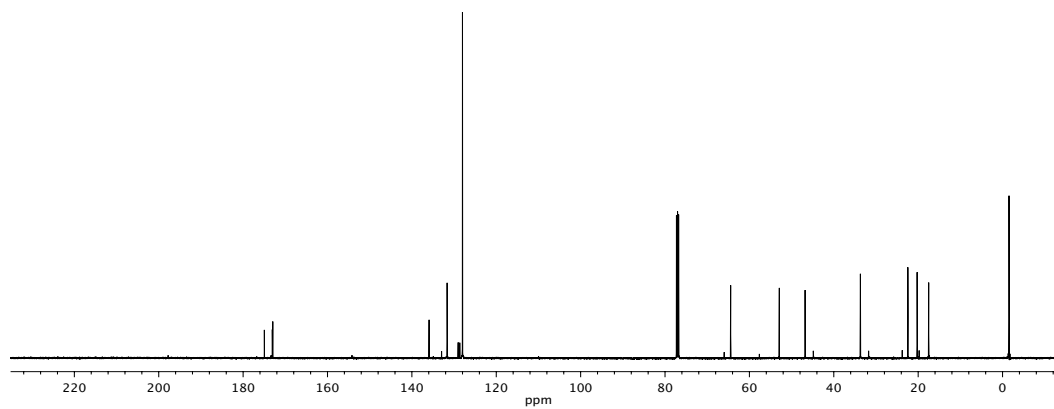


Figure A2.24 ¹³C NMR (125 MHz, CDCl₃) of compound **77f**.

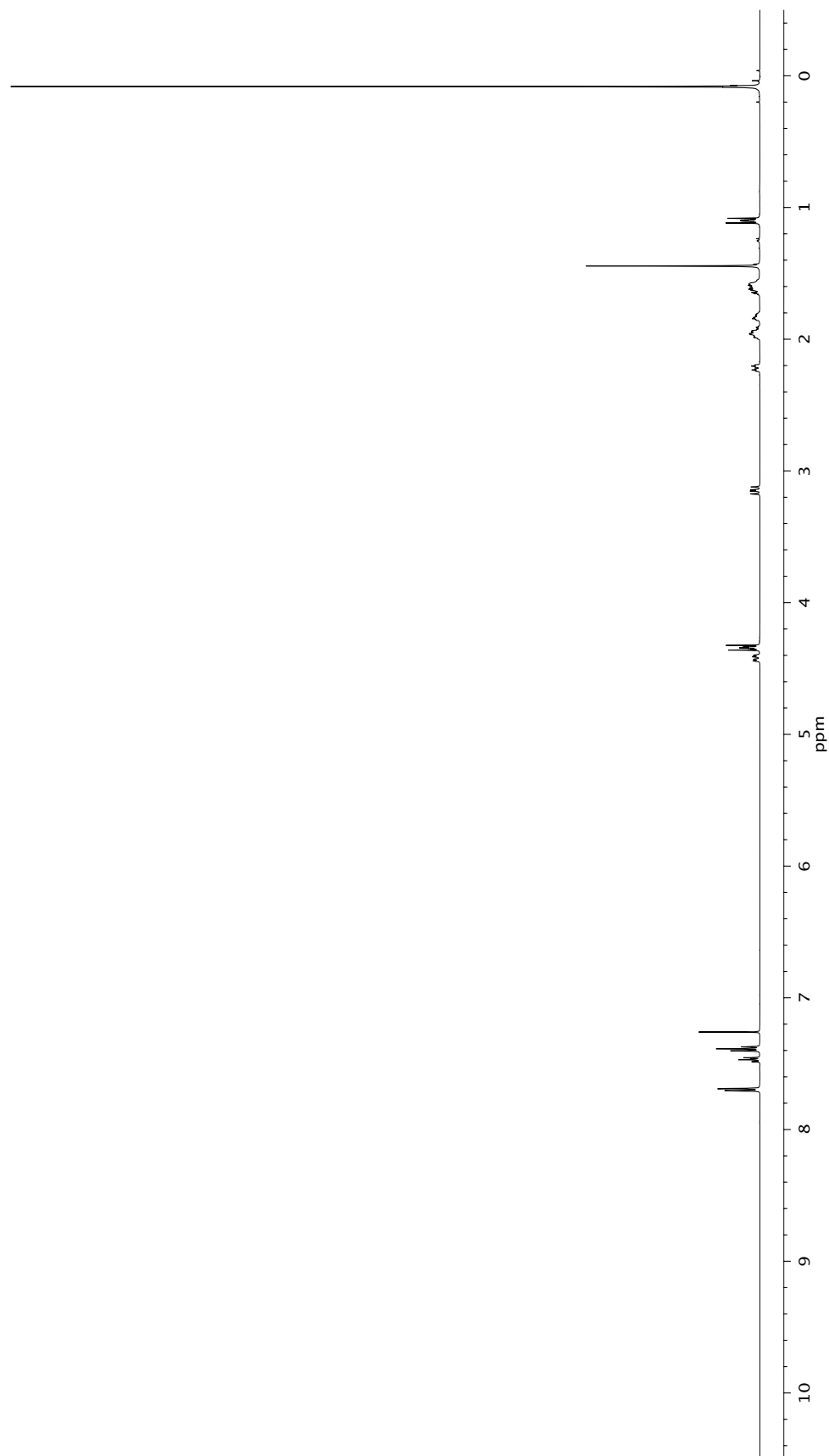
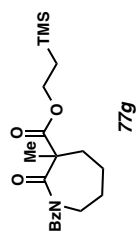


Figure A2.25 ^1H NMR (500 MHz, CDCl_3) of compound 77g.

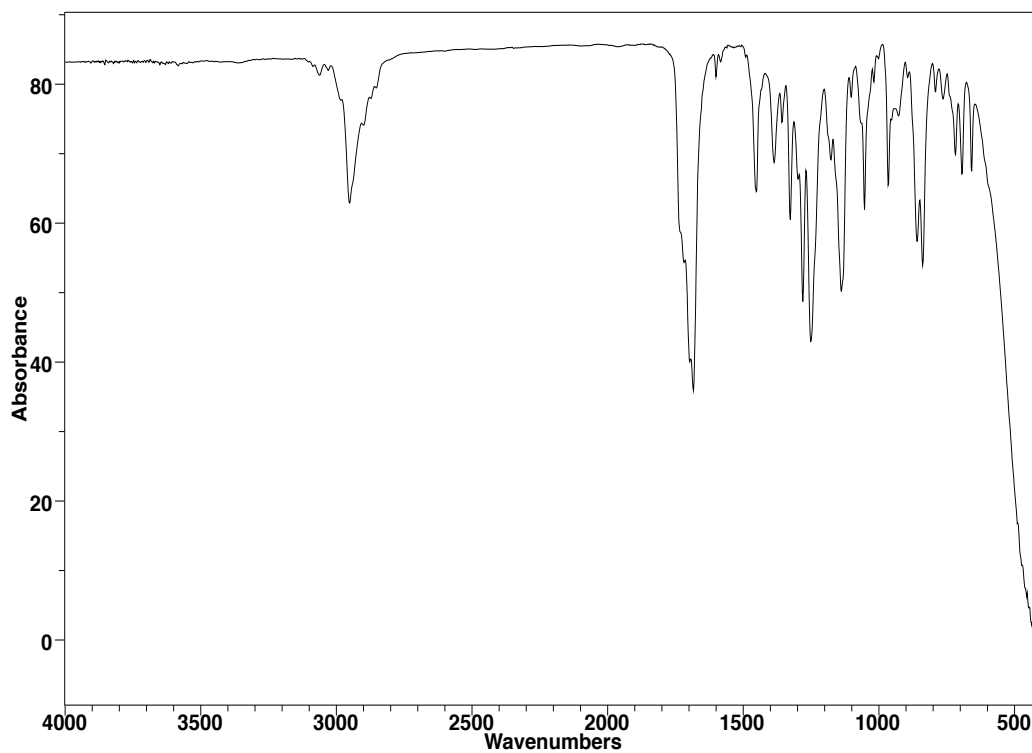


Figure A2.26 Infrared spectrum (thin film/NaCl) of compound **77g**.

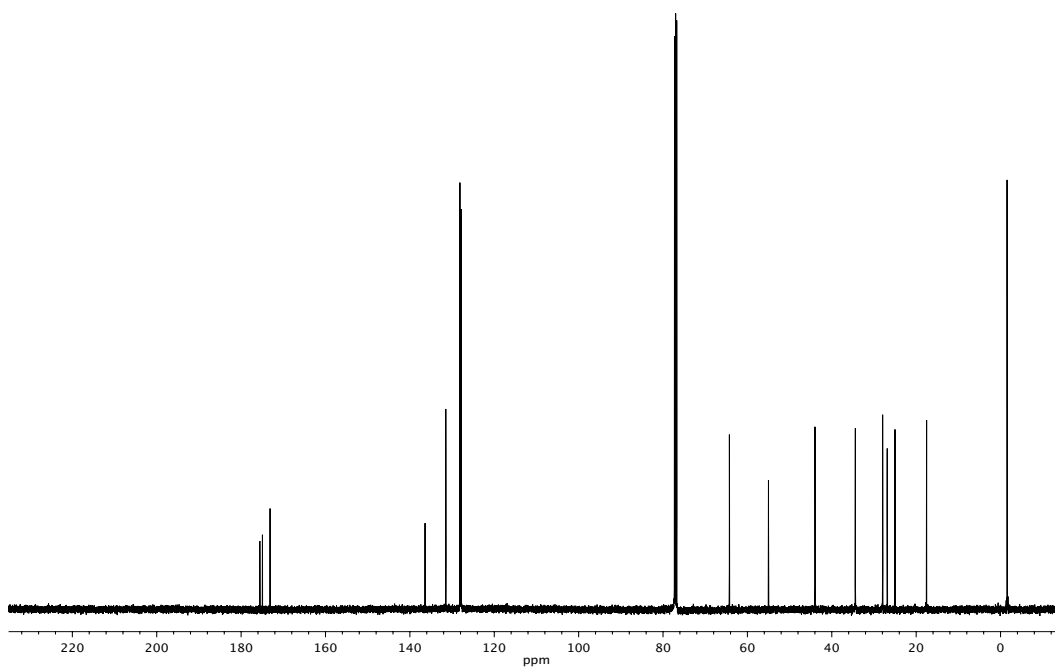


Figure A2.27 ¹³C NMR (125 MHz, CDCl₃) of compound **77g**.

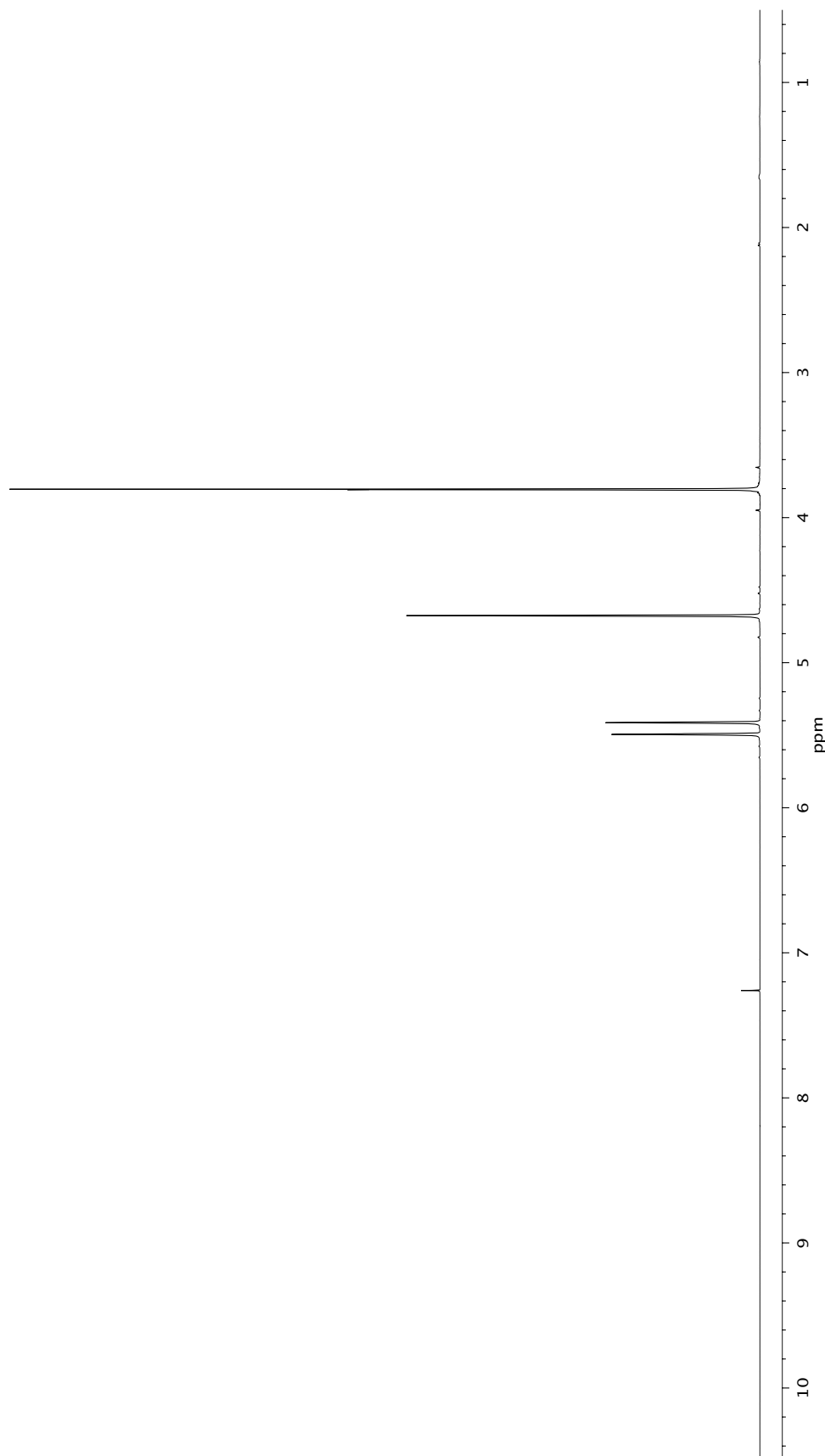
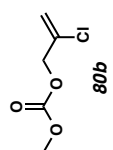


Figure A2.28 ¹H NMR (500 MHz, CDCl₃) of compound 80b.

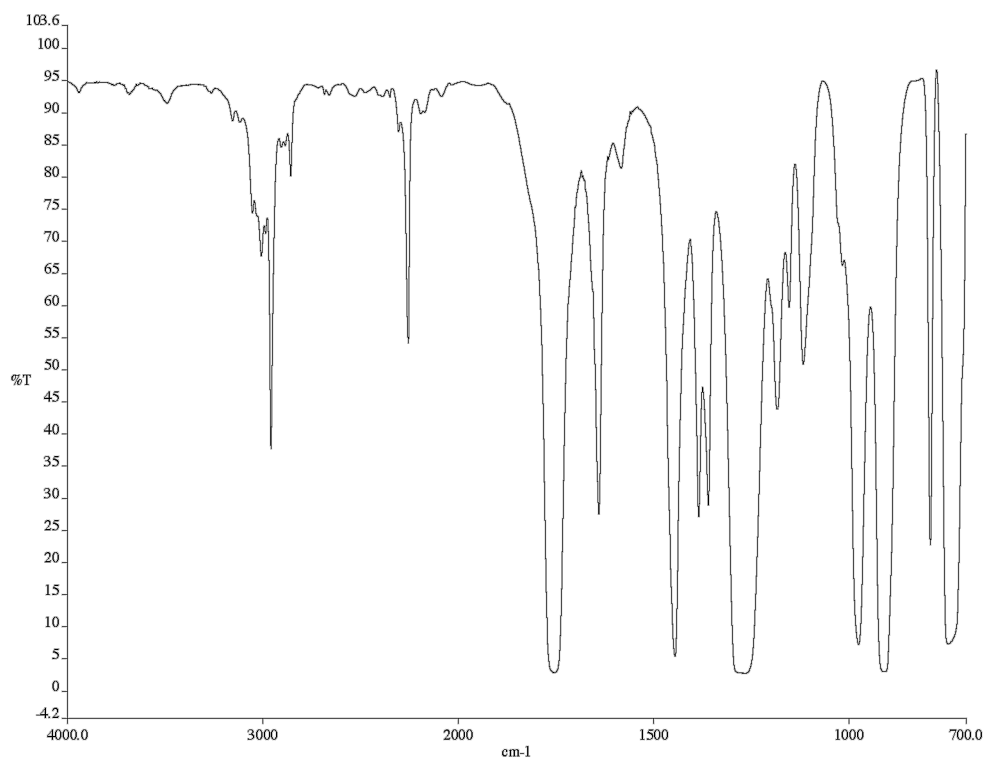


Figure A2.29 Infrared spectrum (thin film/NaCl) of compound **80b**.

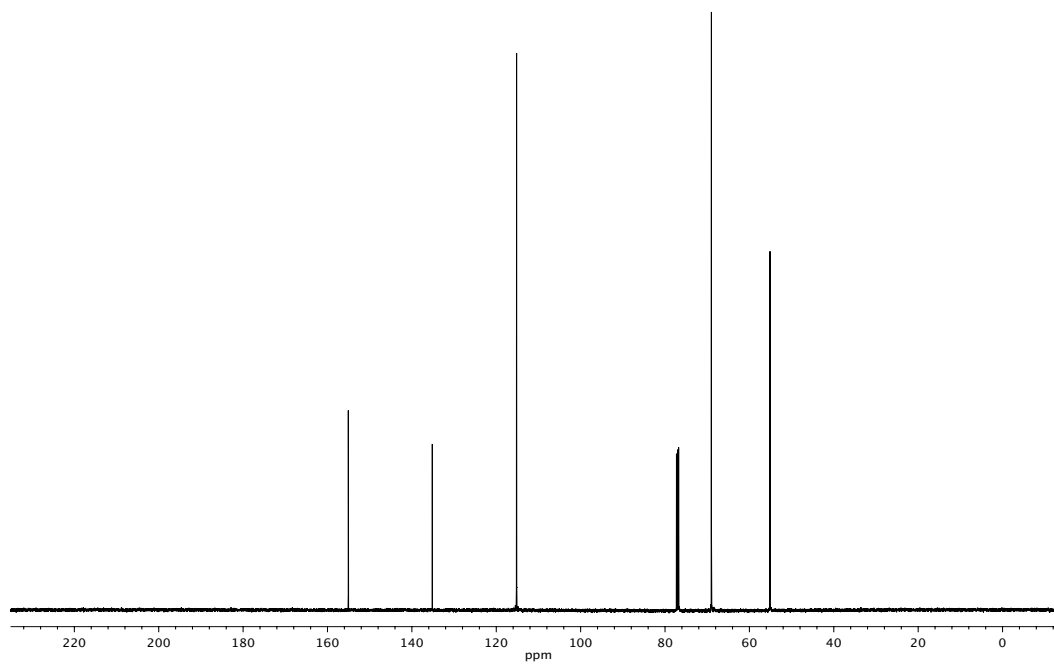


Figure A2.30 ¹³C NMR (125 MHz, CDCl₃) of compound **80b**.

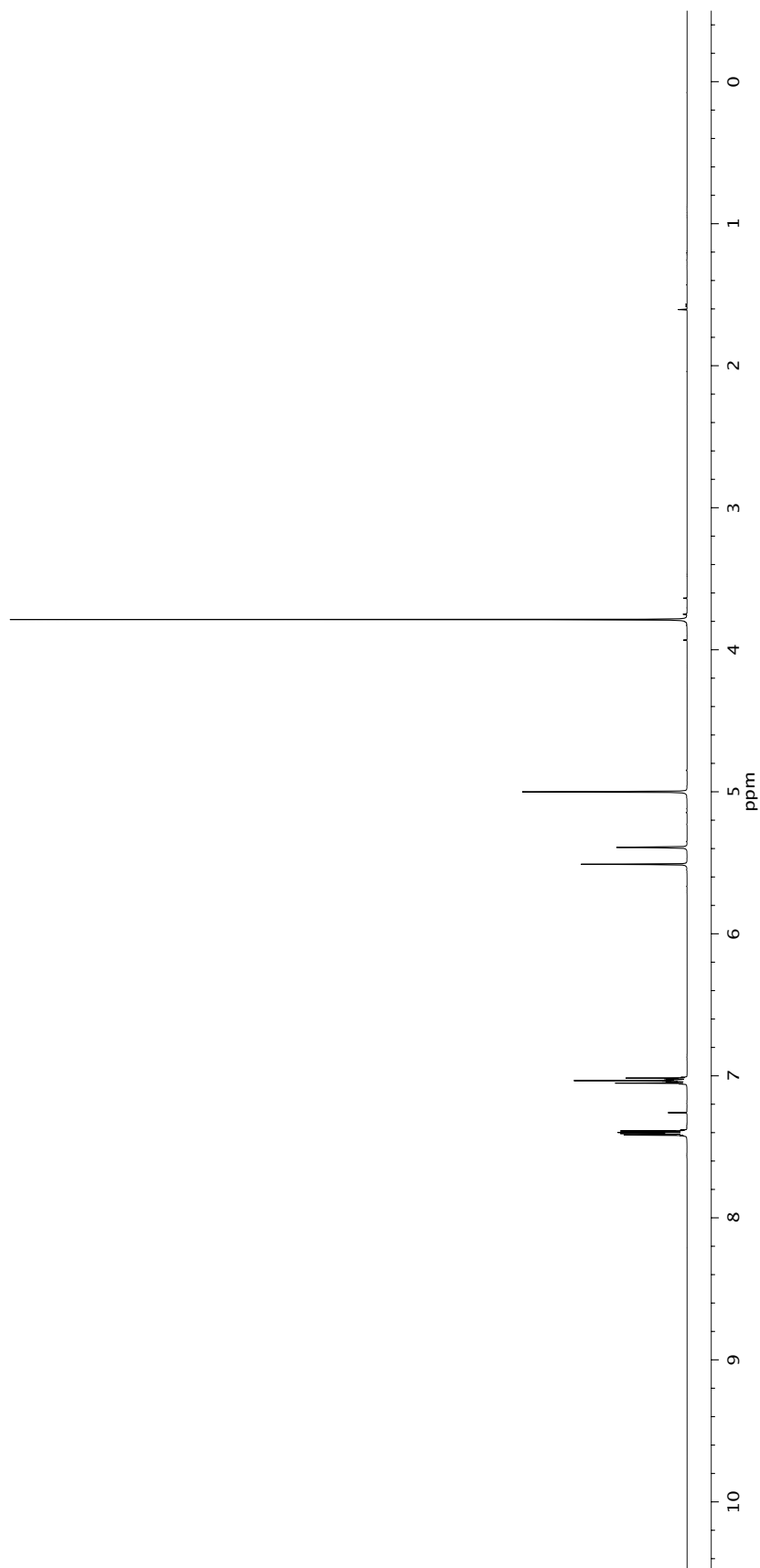
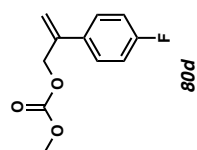


Figure A2.31 ¹H NMR (500 MHz, CDCl₃) of compound **80d**.

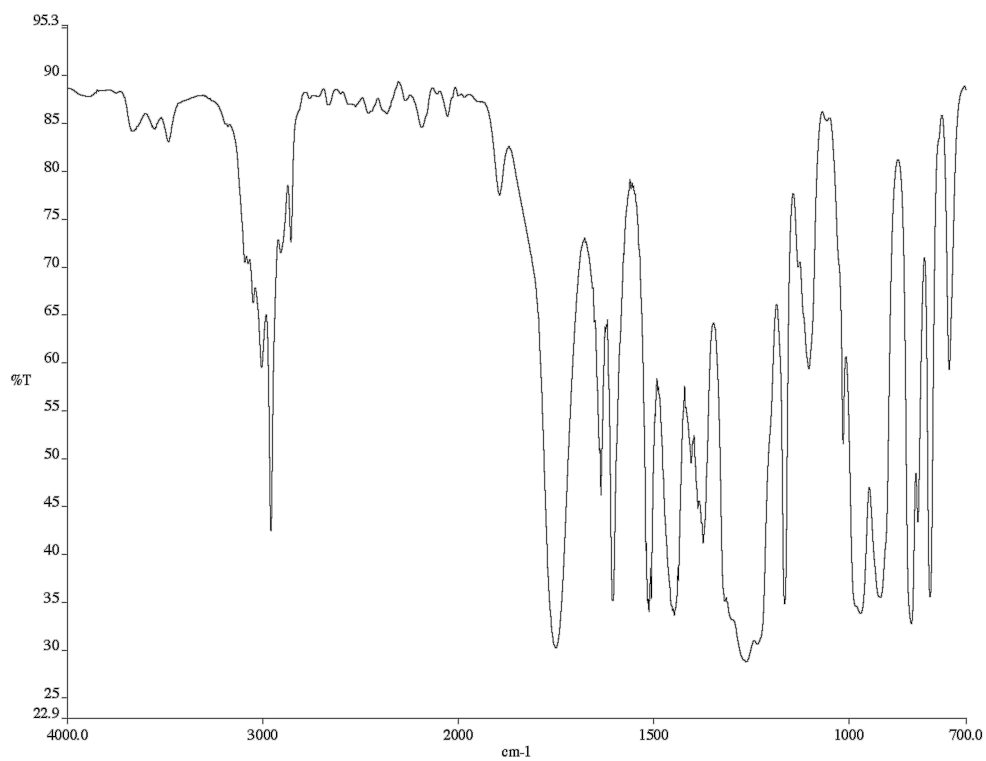


Figure A2.32 Infrared spectrum (thin film/NaCl) of compound **80d**.

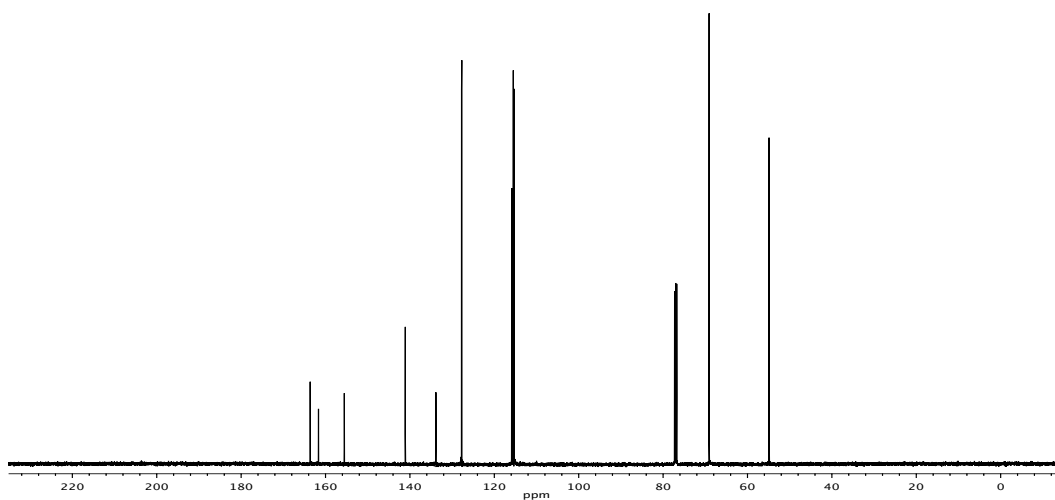


Figure A2.33 ¹³C NMR (125 MHz, CDCl₃) of compound **80d**.

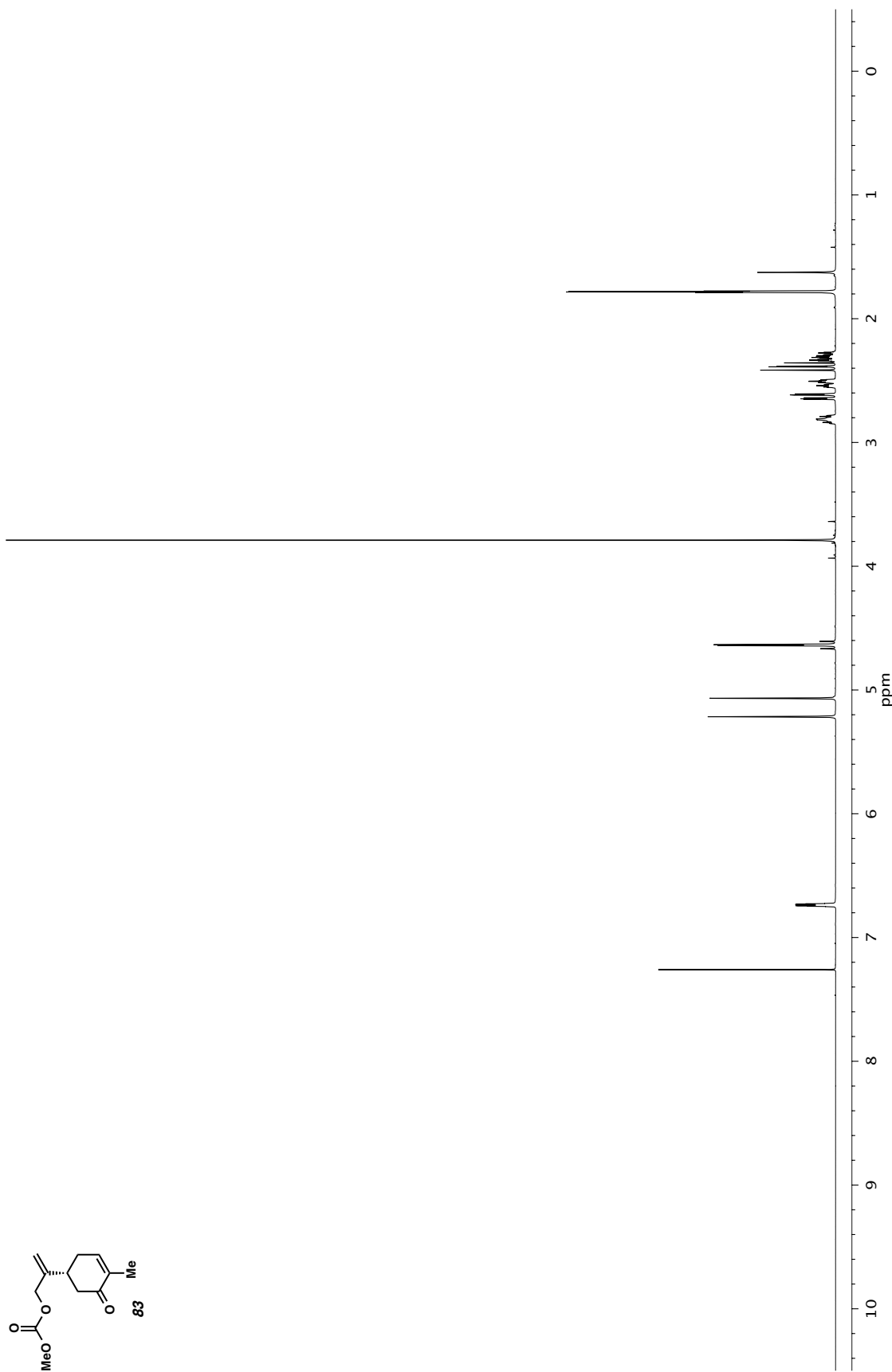


Figure A2.34 ^1H NMR (500 MHz, CDCl_3) of compound **83**.

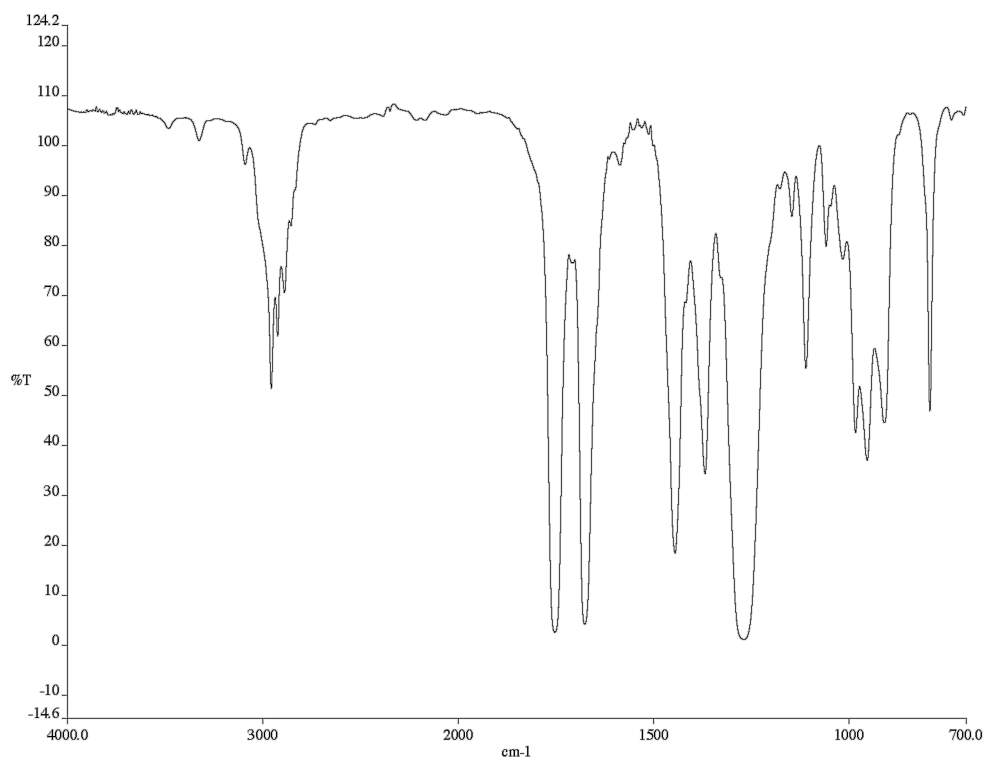


Figure A2.35 Infrared spectrum (thin film/NaCl) of compound **83**.

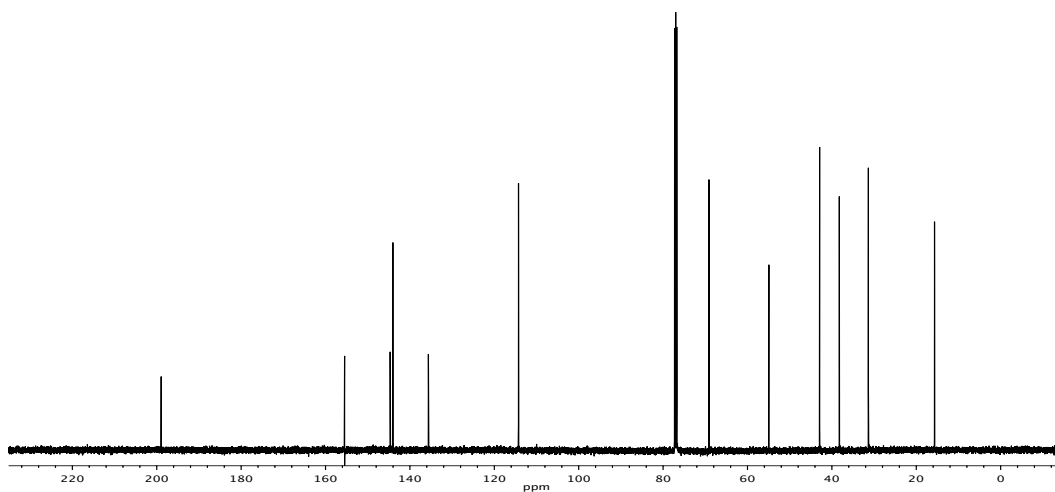


Figure A2.36 ¹³C NMR (125 MHz, CDCl₃) of compound **83**.

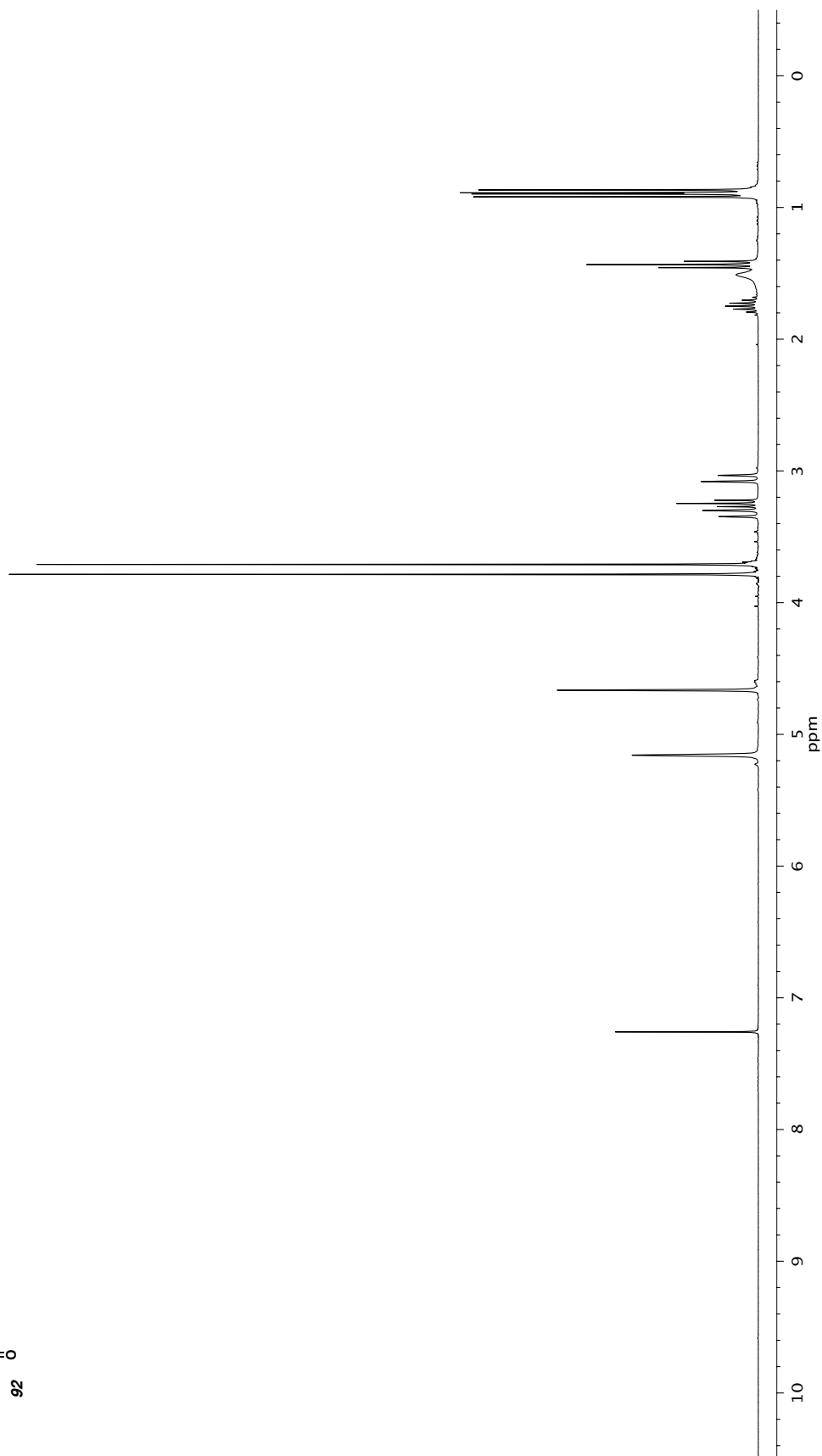
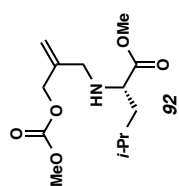


Figure A2.37 ¹H NMR (500 MHz, CDCl₃) of compound **92**.

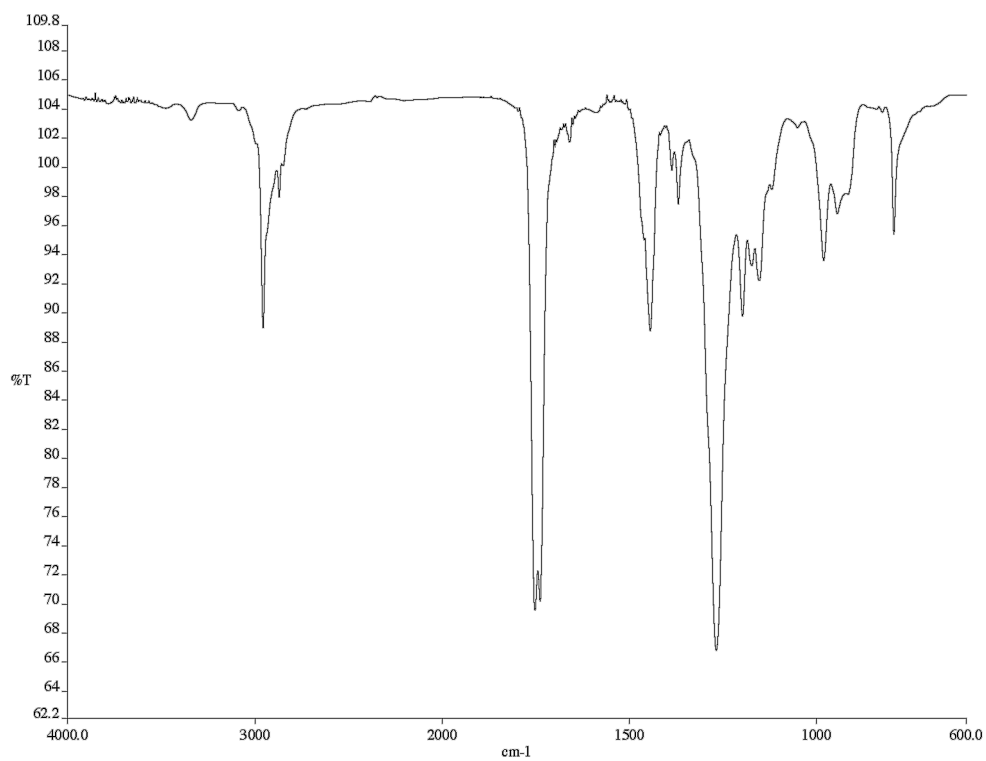


Figure A2.38 Infrared spectrum (thin film/NaCl) of compound **92**.

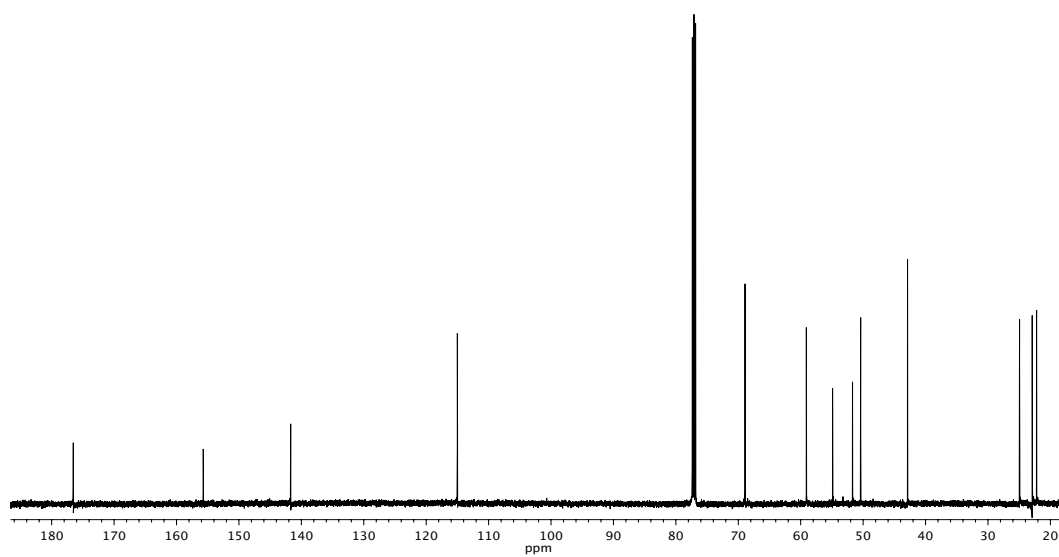


Figure A2.39 ¹³C NMR (125 MHz, CDCl₃) of compound **92**.

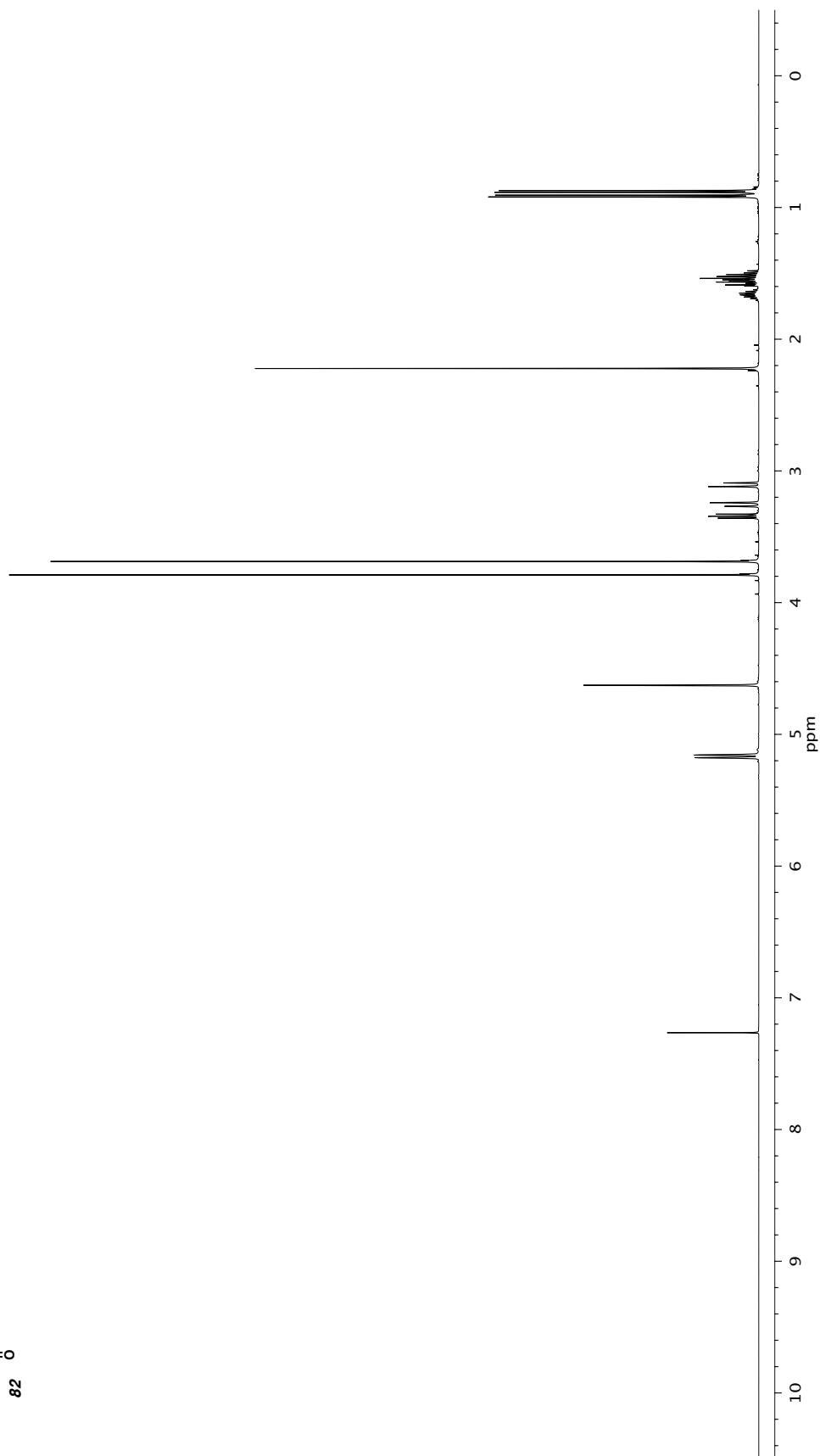
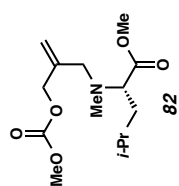


Figure A2.40 ^1H NMR (300 MHz, CDCl_3) of compound **82**.

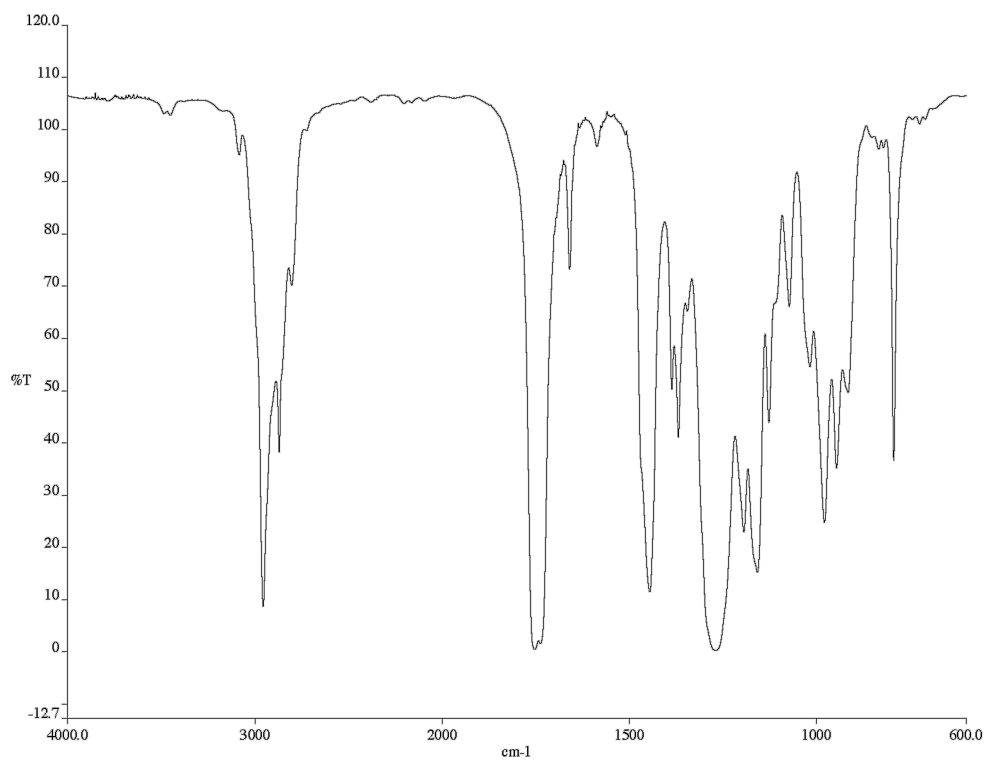


Figure A2.41 Infrared spectrum (thin film/NaCl) of compound **82**.

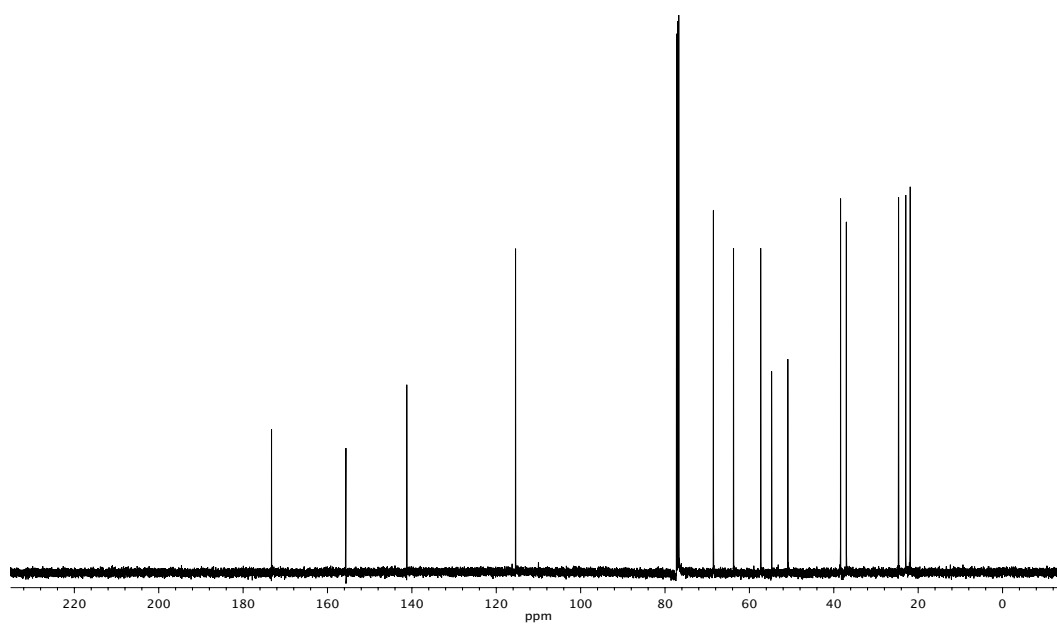


Figure A2.42 ¹³C NMR (125 MHz, CDCl₃) of compound **82**.

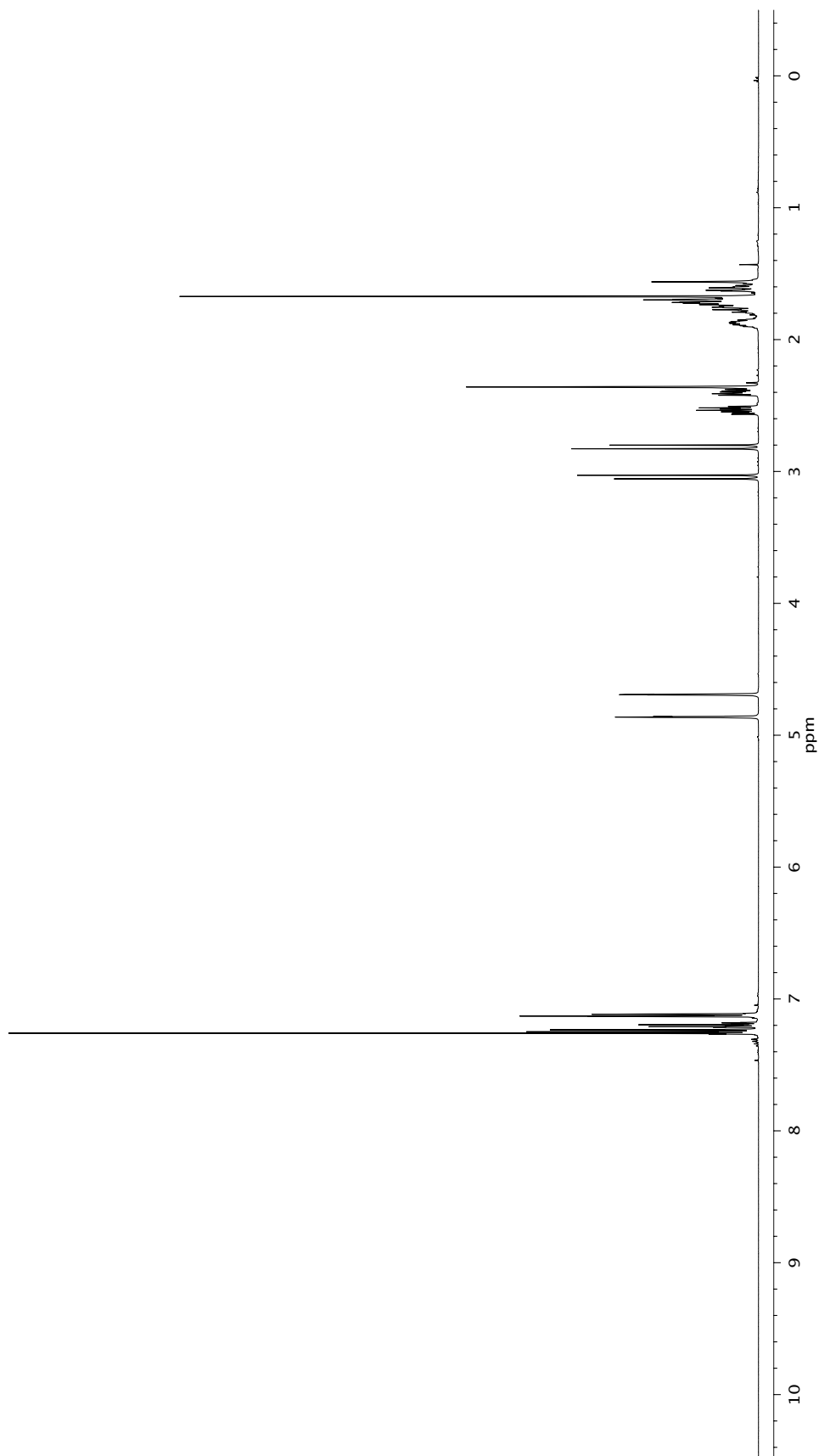
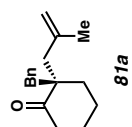


Figure A2.43 ¹H NMR (500 MHz, CDCl₃) of compound **81a**.

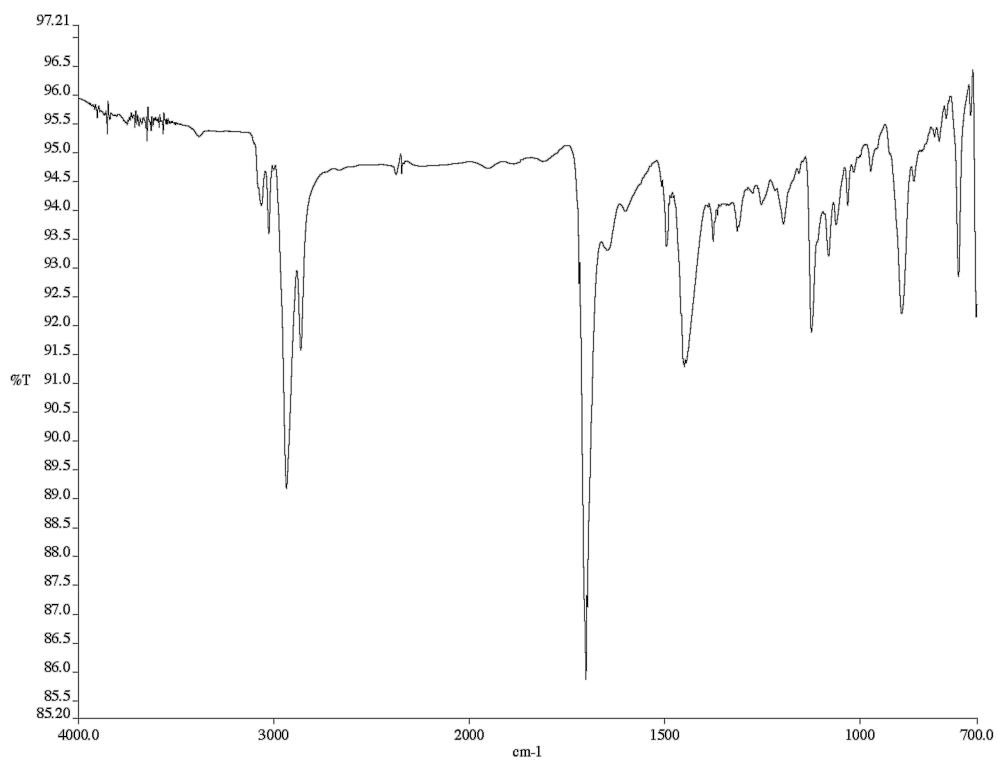


Figure A2.44 Infrared spectrum (thin film/NaCl) of compound **81a**.

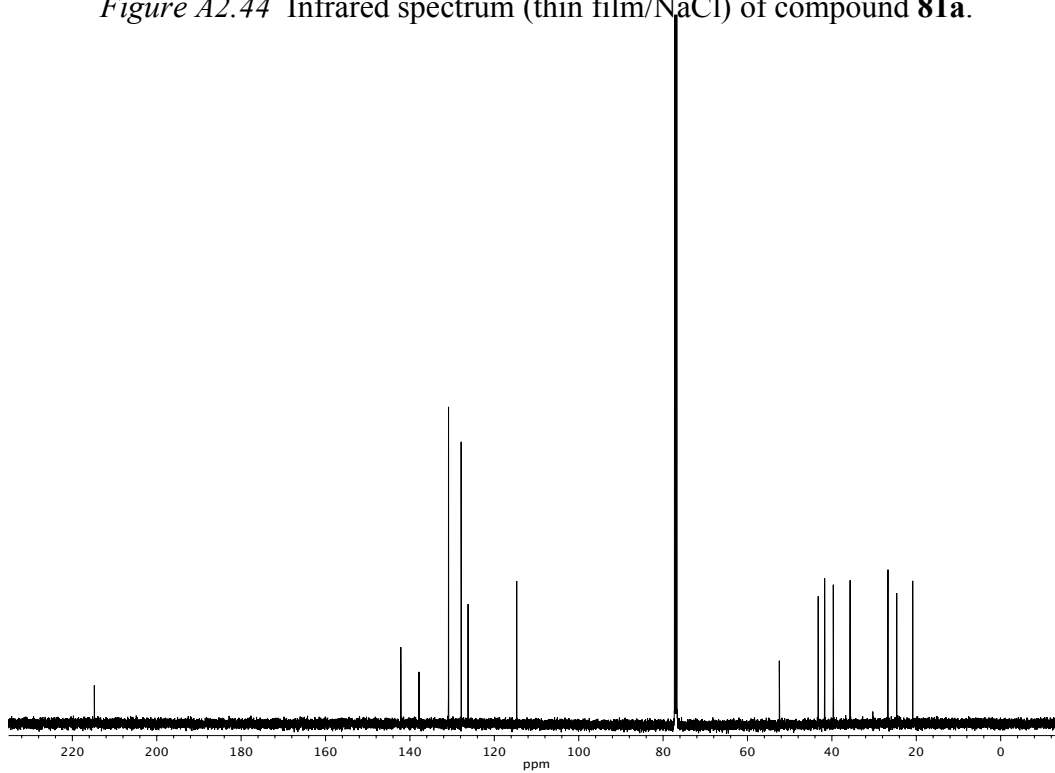


Figure A2.45 ¹³C NMR (125 MHz, CDCl₃) of compound **81a**.

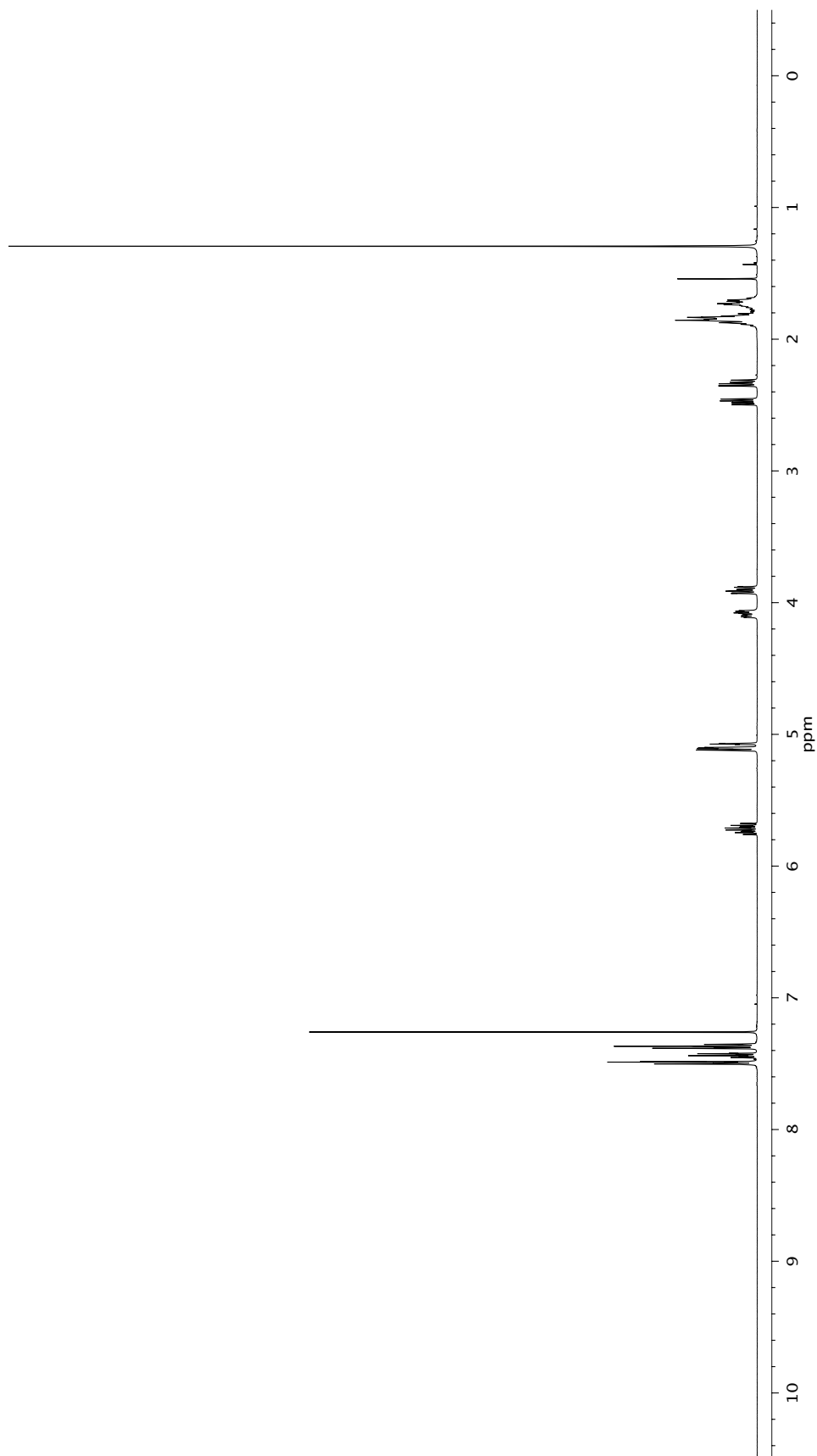
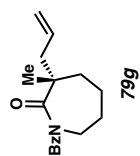


Figure A2.46 ¹H NMR (500 MHz, CDCl₃) of compound 79g.

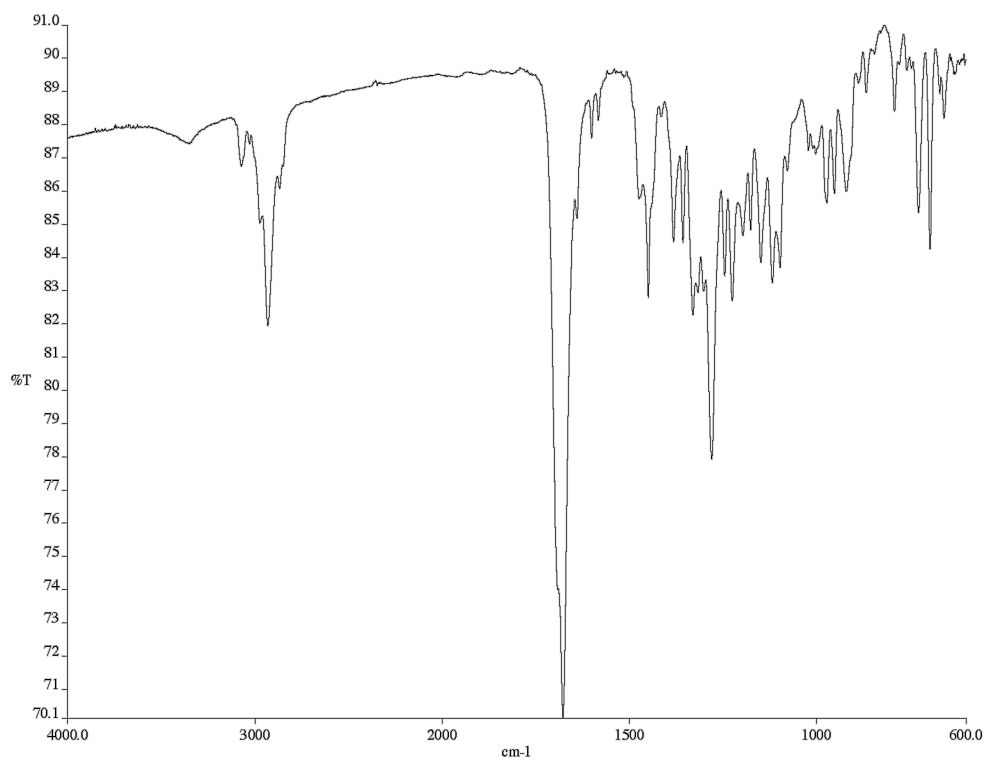


Figure A2.47 Infrared spectrum (thin film/NaCl) of compound **79g**.

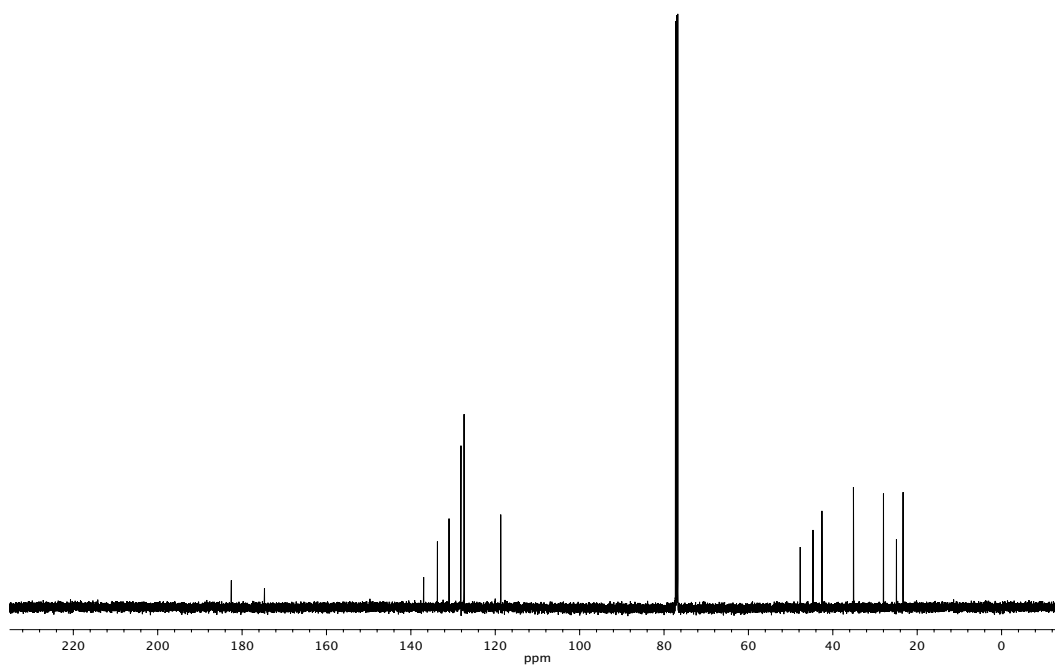
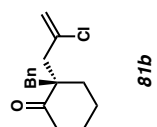
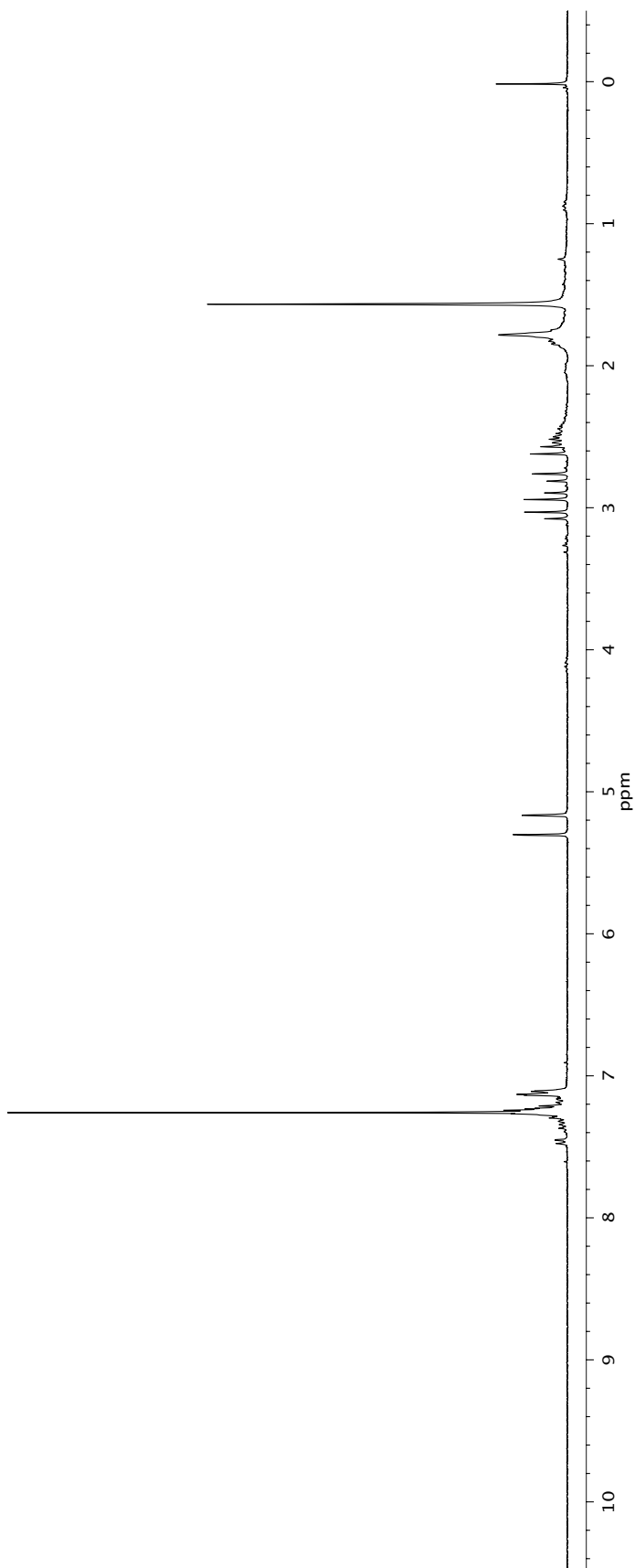


Figure A2.48 ¹³C NMR (125 MHz, CDCl₃) of compound **79g**.

**81b**Figure A2.49 ¹H NMR (500 MHz, CDCl₃) of compound **81b**.

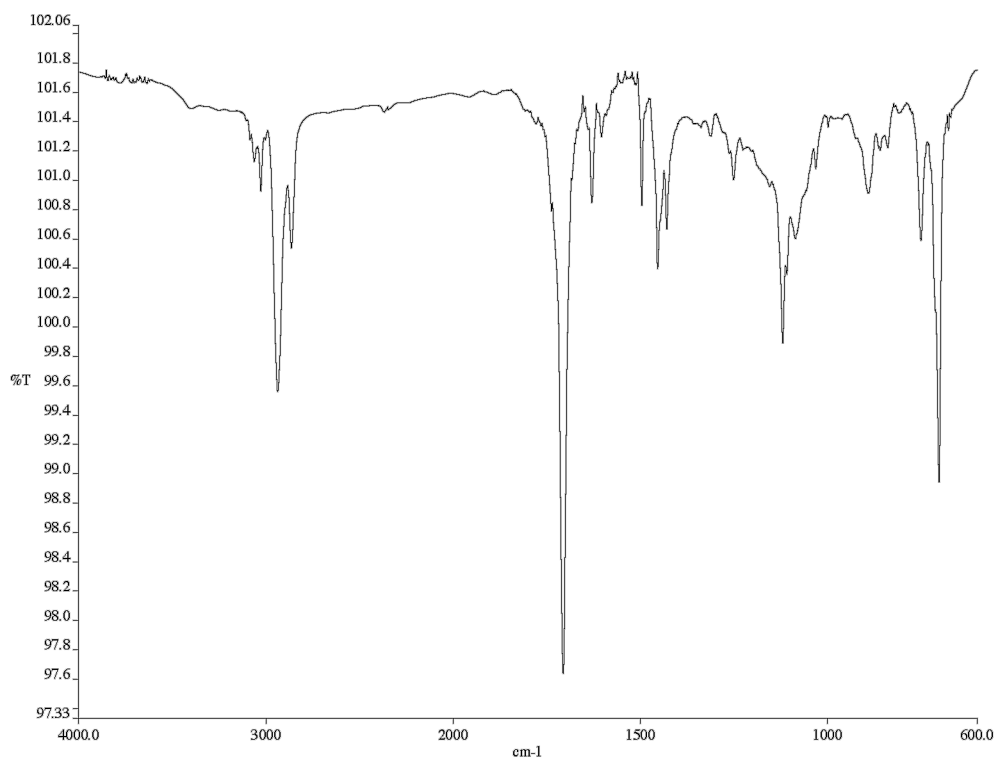


Figure A2.50 Infrared spectrum (thin film/NaCl) of compound **81b**.

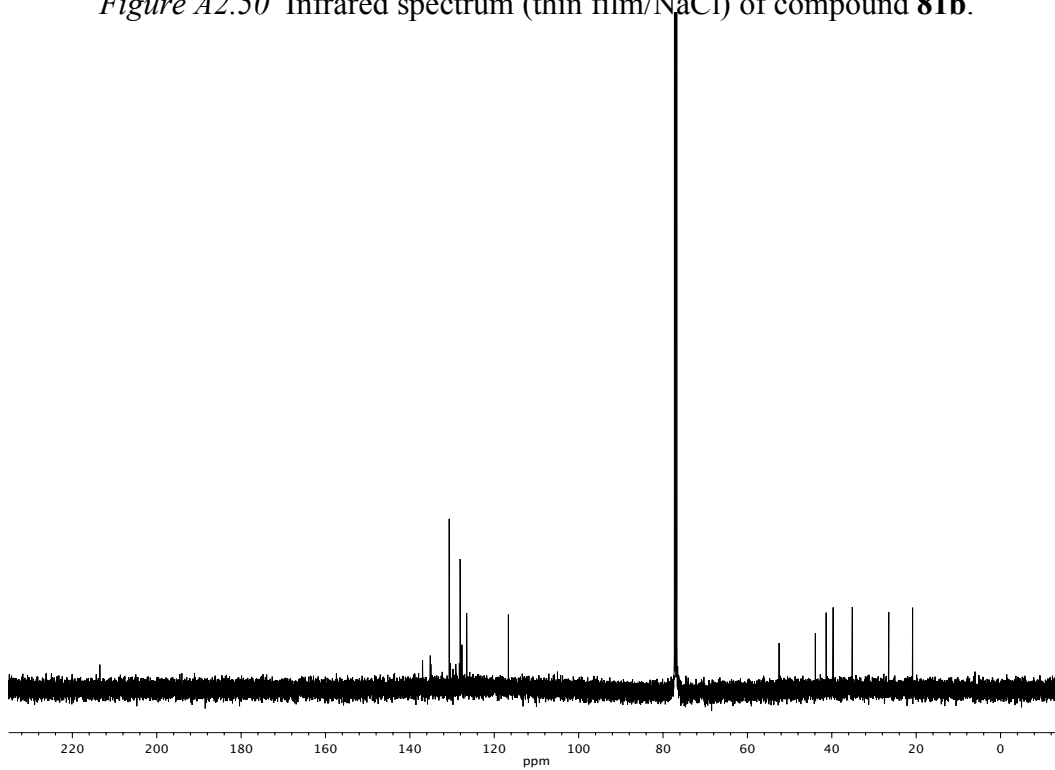


Figure A2.51 ¹³C NMR (125 MHz, CDCl₃) of compound **81b**.

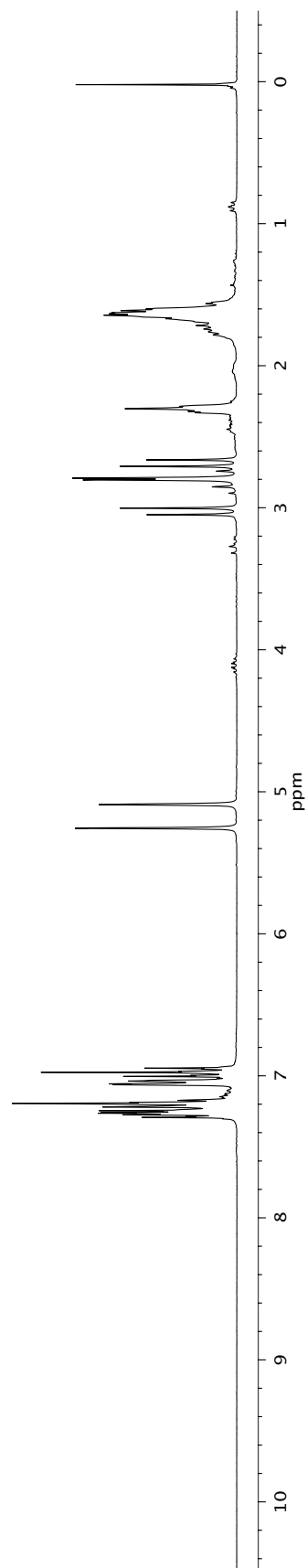
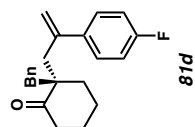


Figure A2.52 ¹H NMR (500 MHz, CDCl₃) of compound **81d**.

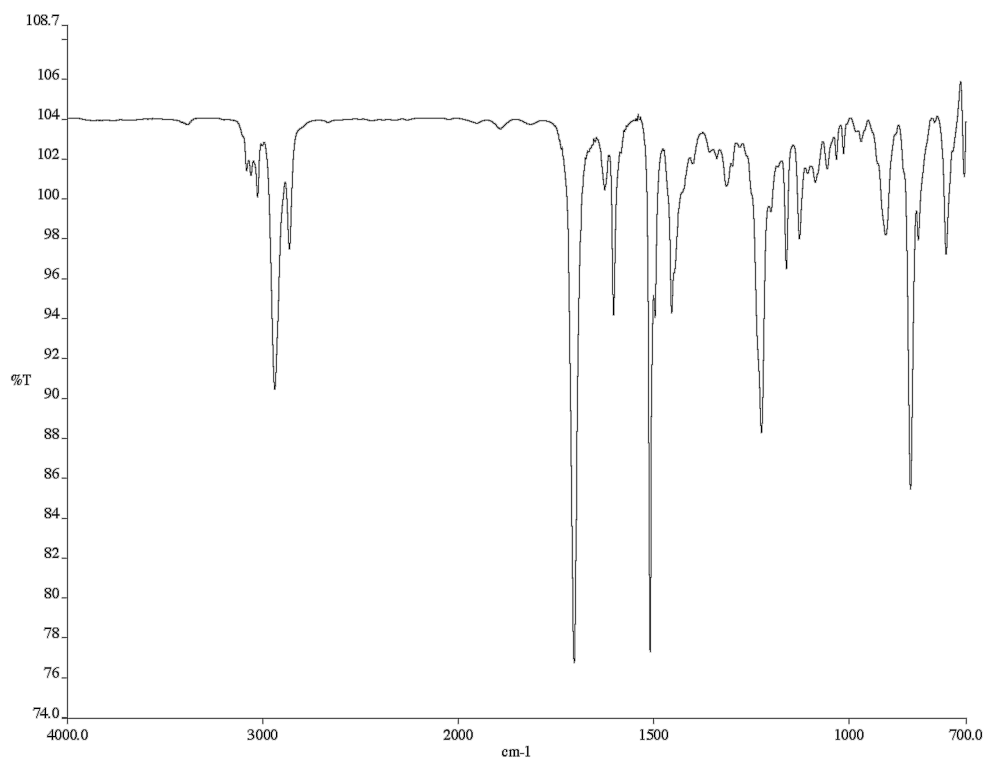


Figure A2.53 Infrared spectrum (thin film/NaCl) of compound **81d**.

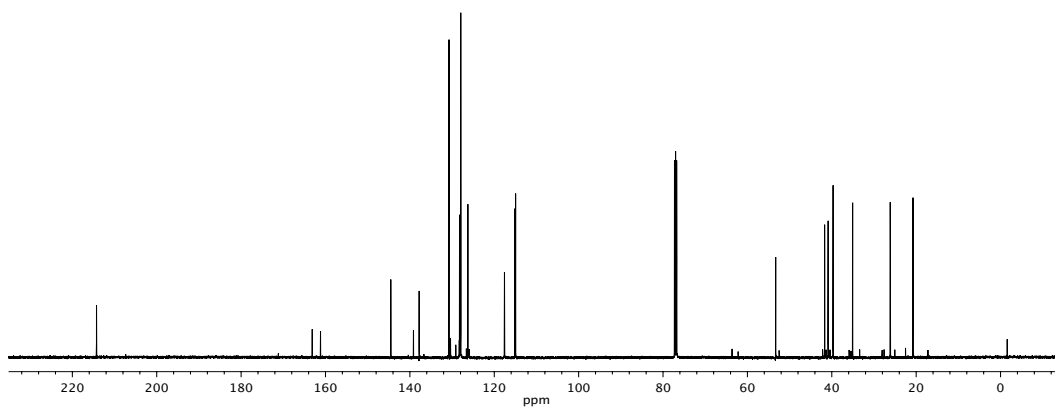


Figure A2.54 ¹³C NMR (125 MHz, CDCl₃) of compound **81d**.

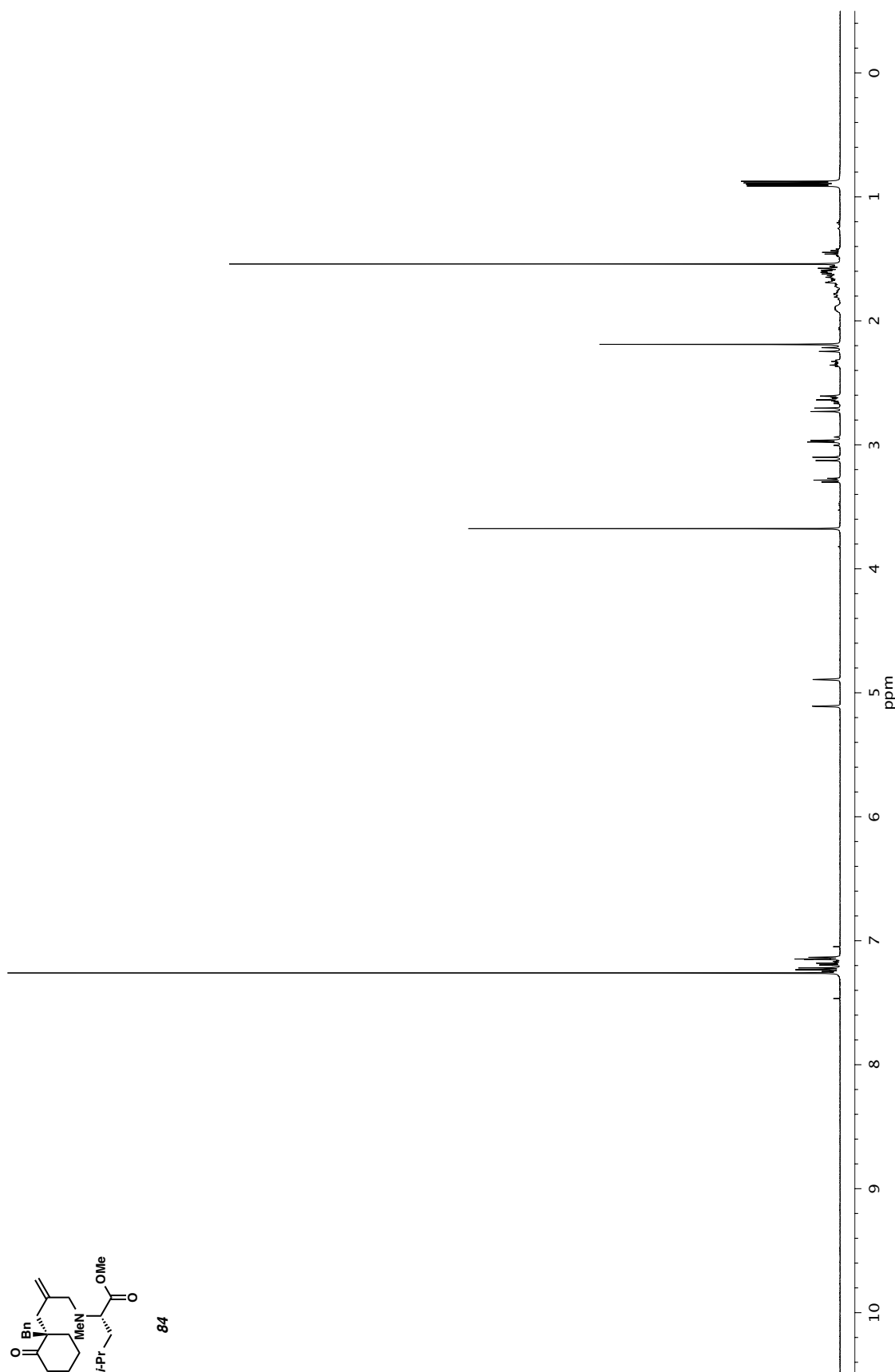


Figure A2.55 ^1H NMR (500 MHz, CDCl_3) of compound **84**.

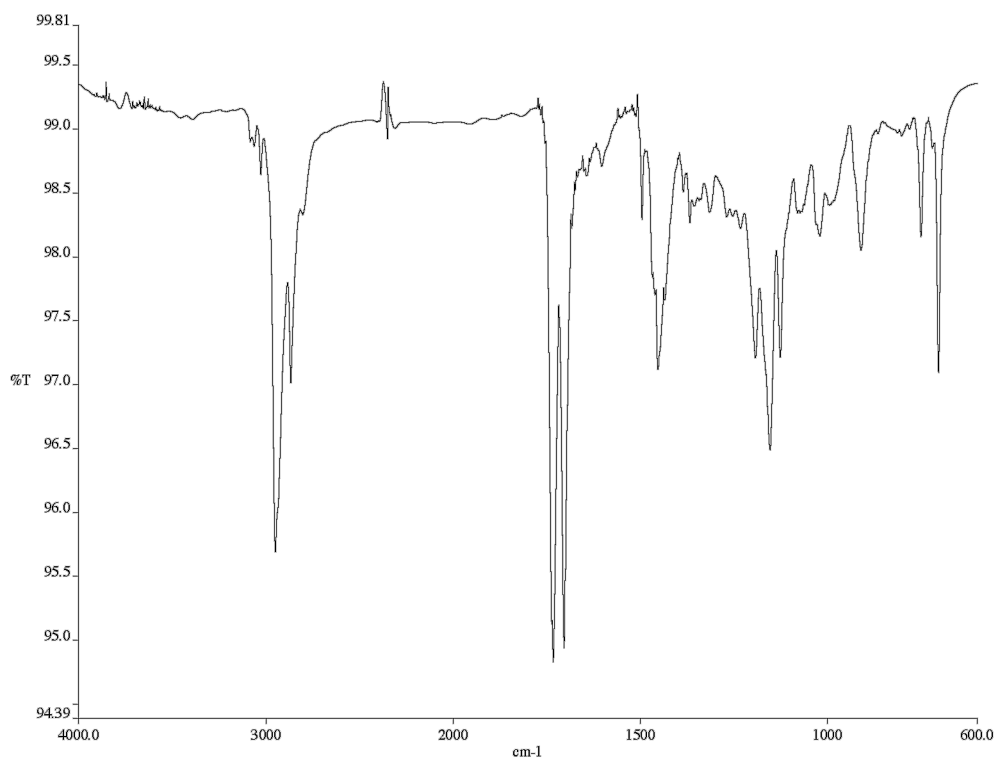


Figure A2.56 Infrared spectrum (thin film/NaCl) of compound **84**.

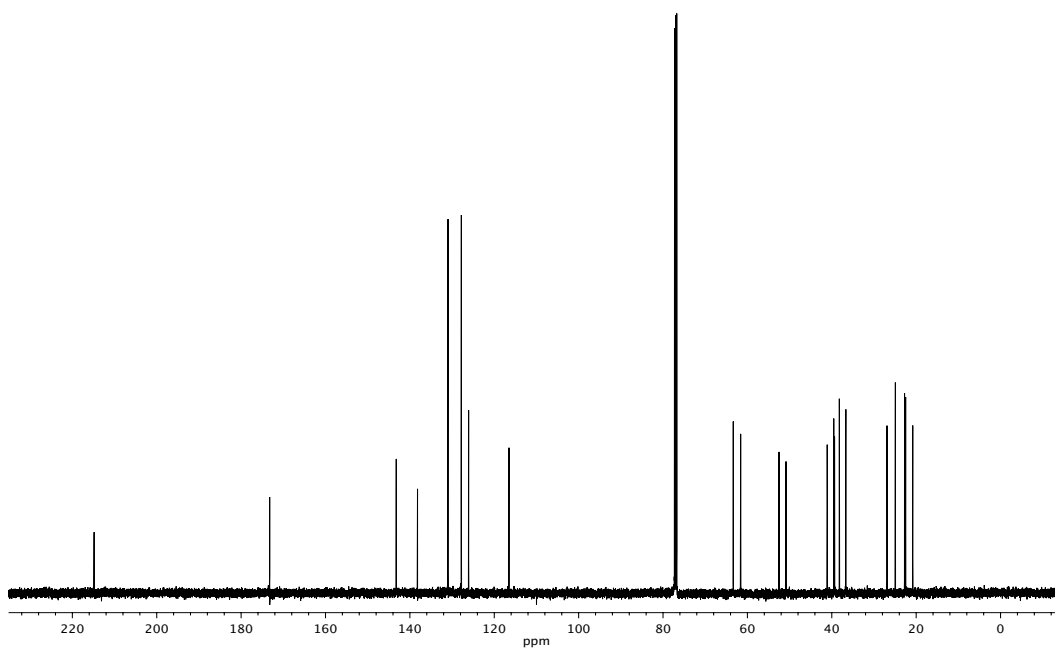
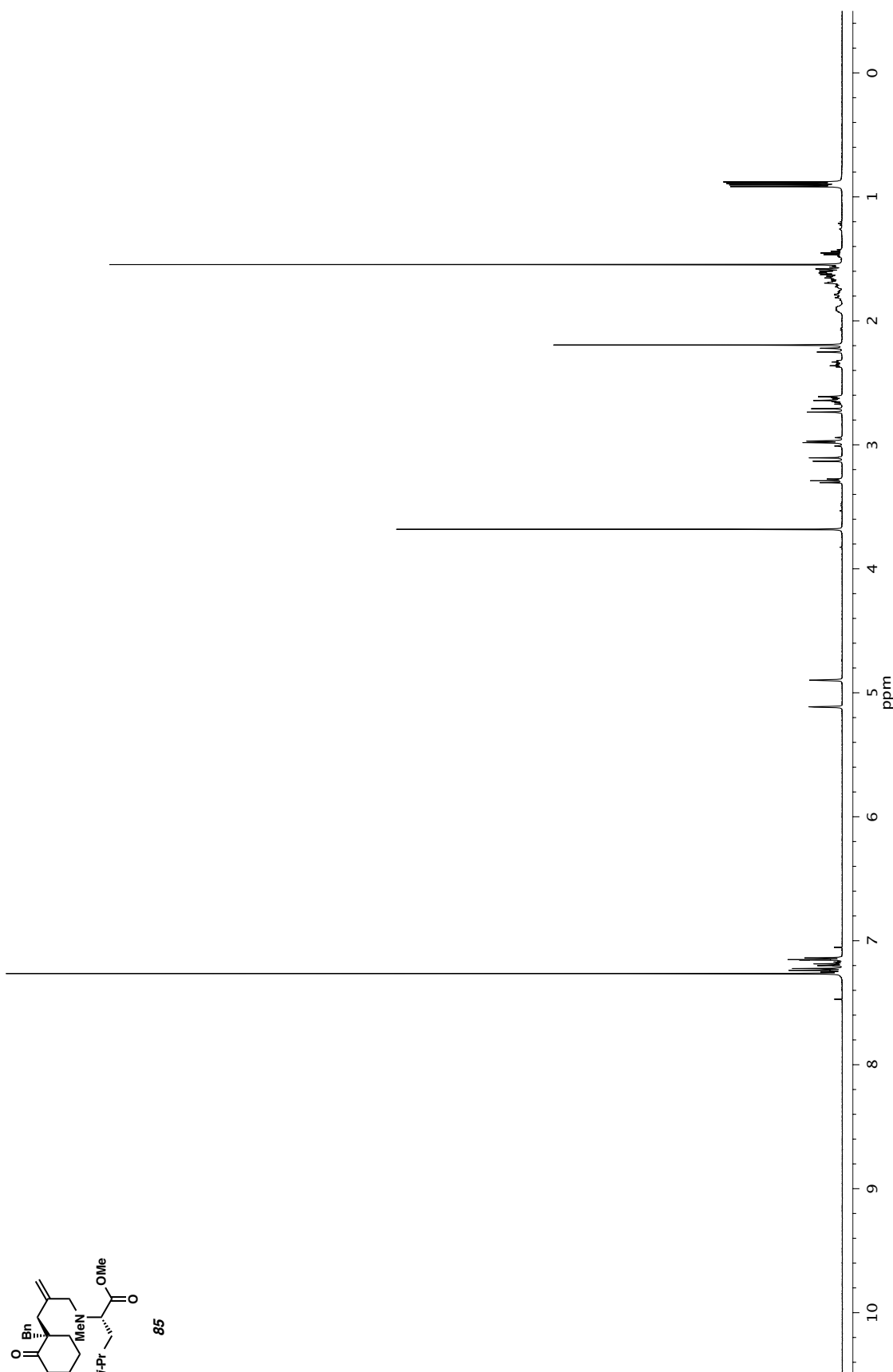


Figure A2.57 ¹³C NMR (125 MHz, CDCl₃) of compound **84**.

Figure A2.58 ^1H NMR (500 MHz, CDCl_3) of compound **85**.

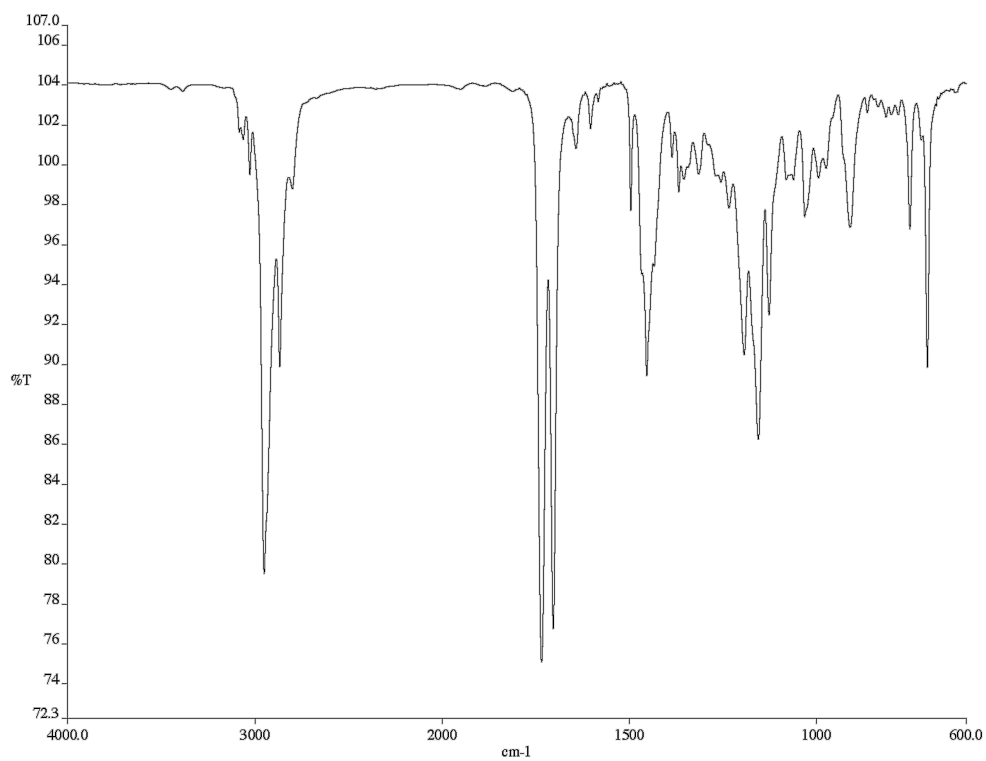


Figure A2.59 Infrared spectrum (thin film/NaCl) of compound **85**.

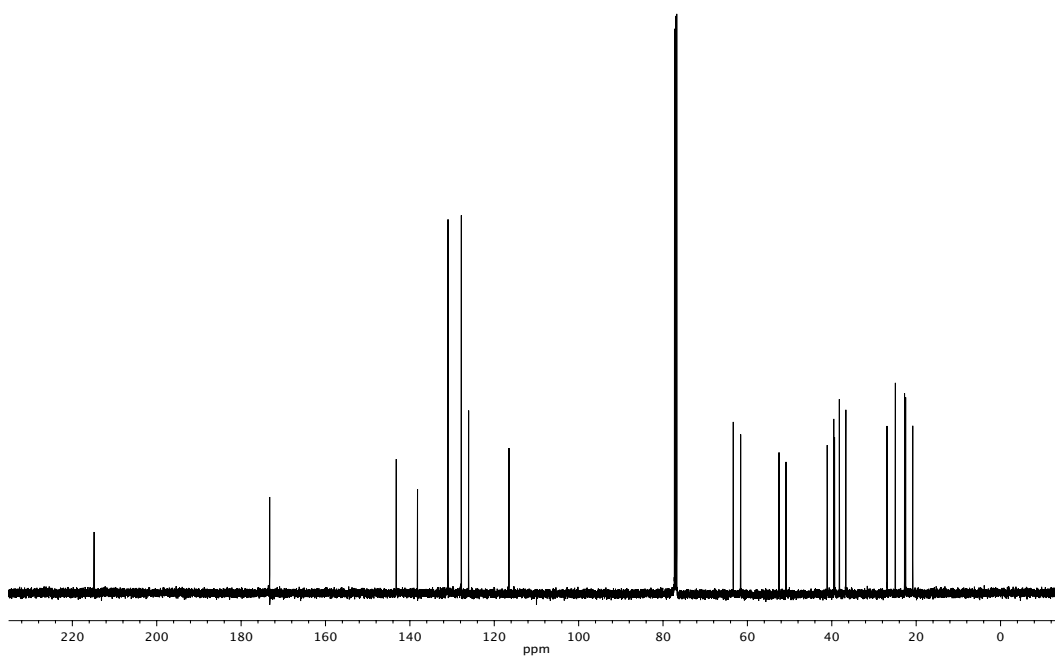


Figure A2.60 ¹³C NMR (125 MHz, CDCl₃) of compound **85**.

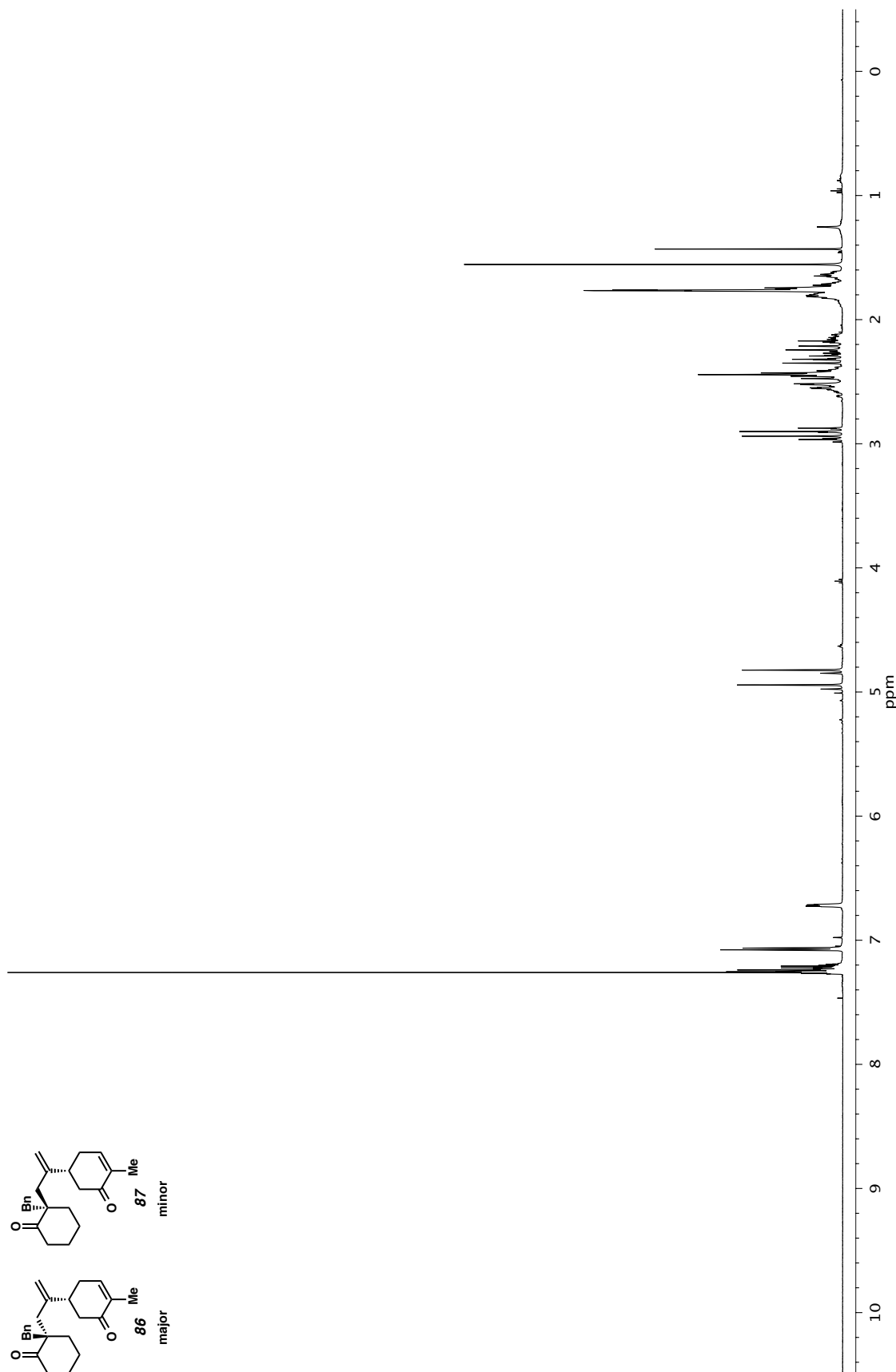


Figure A2.61 ^1H NMR (500 MHz, CDCl_3) of compounds **86** and **87**.

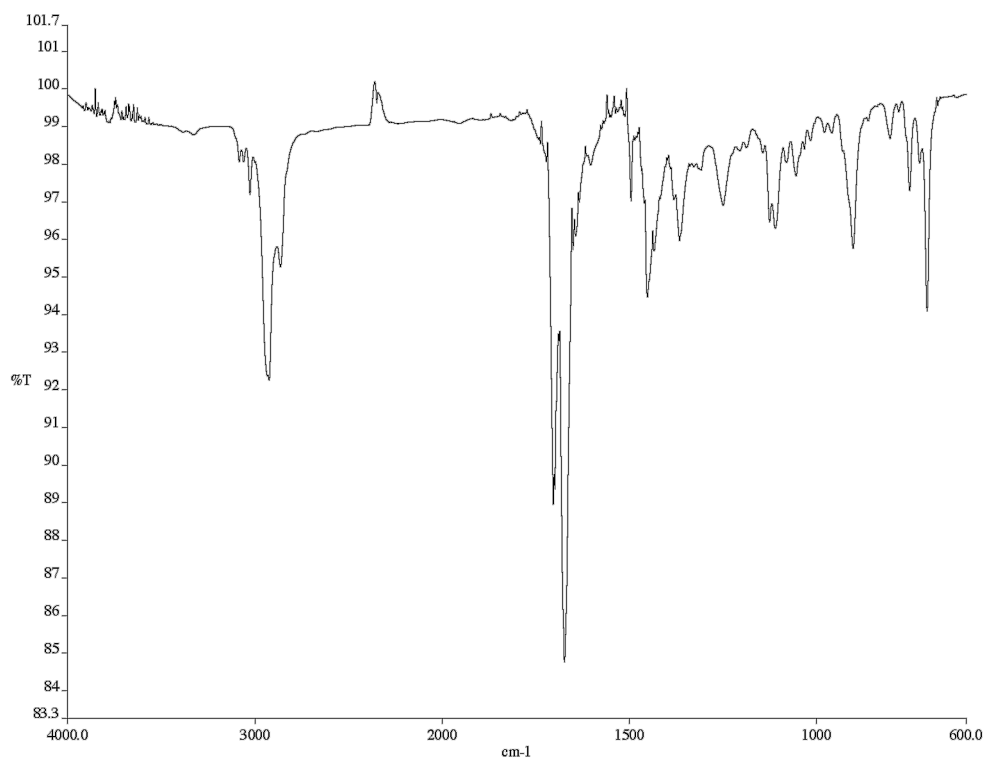


Figure A2.62 Infrared spectrum (thin film/NaCl) of compound **86** and **87**.

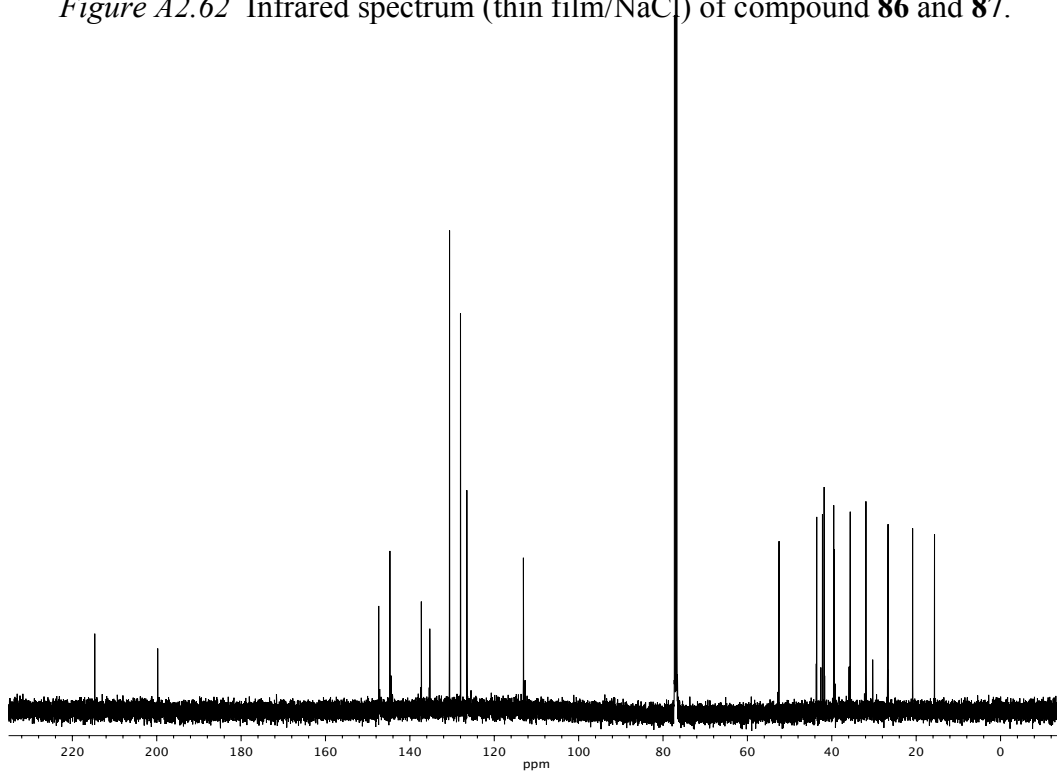


Figure A2.63 ¹³C NMR (125 MHz, CDCl₃) of compound **86** and **87**.

CHAPTER 3

Construction of Vicinal Tertiary and All-Carbon Quaternary Stereocenters via Ir-Catalyzed Regio-, Diastereo-, and Enantioselective Allylic Alkylation and Applications in Sequential Pd-Catalysis¹

3.1 INTRODUCTION

3.1.1 State of the art in the asymmetric construction of vicinal quaternary and tertiary carbon centers

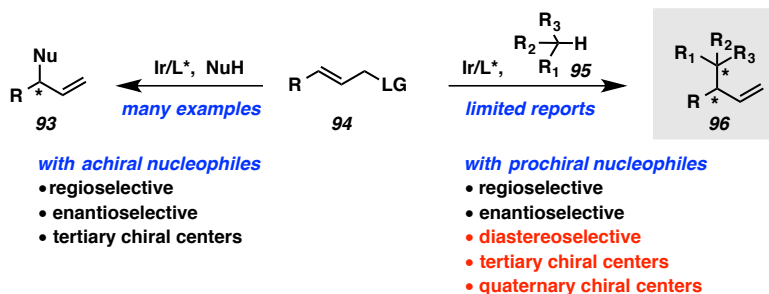
The asymmetric construction of sterically-encumbered, vicinal stereogenic centers is of great interest to synthetic chemists due to the prevalence of such structural arrangements in natural products and bioactive compounds.⁶⁹ The limited number of methods that provide selective access to vicinal tertiary and all-carbon quaternary stereocenters highlights the challenging nature of this task. Enantioselective approaches for accessing this structural dyad have generally relied on asymmetric Michael additions⁷⁰ and Claisen rearrangements.⁷¹ Among the methods available for forging this motif, only a relatively small number have been reported to do so by employing transition metals in a

¹ This work was performed in collaboration with Wen-Bo Lui, postdoctoral researcher in the Stoltz group, and Scott Virgil, manager of the Caltech Center for Catalysis and Chemical Synthesis. This work has been published. See: Liu, W. -B.; Reeves, C. M.; Virgil, S. C.; Stoltz, B. M. *J. Am. Chem. Soc.* **2013**, *135*, 10626.

catalytic, asymmetric fashion.^{72,73} Thus, further investigations into the development of metal-catalyzed methods to directly and selectively generate such stereochemical arrays should prove valuable.

Allylic alkylation chemistry represents a successful strategy for the assembly of highly congested chemical architectures by C–C bond formation⁷⁴ and, within this domain, Ir-catalyzed processes are among the most selective and highest yielding.^{75,76} Initial reports from the Helmchen⁷⁷ and Hartwig⁷⁸ groups demonstrated the utility of Ir-catalyzed allylic substitutions for the synthesis of enantioenriched 3,3-disubstituted (branched) allyl compounds.⁷⁵ As this research area has developed, Ir/phosphoramidite catalysts⁷⁹ have emerged as privileged scaffolds for the regio- and enantioselective allylic alkylation of achiral nucleophiles, such as malonate derivatives and ketone enolates (Figure 3.1.1.1, **94** → **93**).⁸⁰ However, methods for Ir-catalyzed intermolecular allylic alkylation that employ prochiral nucleophiles and display high (1) regio-, (2) diastereo-, and (3) enantioselectivity remain elusive (Figure 3.1.1.1, **94** → **96**).⁸¹ Prior to our investigation, only two reports,⁸² from the laboratories of Takemoto and Hartwig, detailed successful examples in attaining all three of these goals; however, in these accounts, the nucleophiles investigated were limited to amino acid derivatives and azlactones.⁸³

Figure 3.1.1.1. Ir-catalyzed allylic substitution



In this chapter, we detail the development of a highly regio-, diastereo-, and enantioselective Ir-catalyzed α -allylic alkylation of cyclic β -ketoesters that forges vicinal tertiary and all-carbon quaternary centers in one step and in excellent yields. Moreover, we describe the deployment of our novel 2-(trimethylsilyl)ethyl β -ketoester (TMSE β -ketoester) (see Chapter 2), which functions as an oxycarbonyl-protected enolate, enabling sequential catalyst-controlled α -allylic alkylations and, in turn, the ability to select the diastereomer produced within the nascent stereochemical dyad.

3.2 REACTION DEVELOPMENT AND OPTIMIZATION

3.2.1 Discovery and optimization of iridium catalyzed regio-, diastereo- and enantioselective allylic alkylation of cyclic ketones

Our preliminary studies focused on probing the effects of different ligands, bases, additives, and solvents on the efficiency and selectivity of the reaction. Cyclic β -ketoester **97**, cinnamyl carbonate **98**, and [Ir(cod)Cl]₂/phosphoramidite complexes⁸⁴ were chosen as standard reaction components at the outset of our investigations.⁸⁵ Selected

results of these experiments are summarized in Table 3.2.1.1. Our investigations commenced with commonly used phosphoramidite ligand **L10**⁸⁶ and we were pleased to find that the proposed reaction proceeded smoothly under the conditions described (Table 3.2.1.1), delivering α -quaternary β -ketoester **100a** in >95% conversion and in 96% ee. Unfortunately, no diastereoselectivity was observed in this case (Table 3.2.1.1, entry 1). Use of ligand **L11**, a diastereoisomer of **L10**, again produced a high-yielding reaction, but in significantly diminished ee (32%) and modest 1:2 dr (entry 2). Inspired by the You group's use of Ir-*N*-arylphosphoramidite complexes (derived from [Ir(cod)Cl]₂ and **L12**)⁸⁷ to effect the diastereo- and enantioselective intramolecular allylation of indoles and pyrroles,⁸⁸ we envisioned that analogous Ir complexes may prove valuable for the generation of all-carbon quaternary stereocenters. We were delighted to discover that the use of *N*-aryl-phosphoramidite ligand **L12** furnished the desired product in 98% ee, >20:1 dr, and 95:5 branched to linear ratio (entry 3).

Figure 3.2.1.1. Selected phosphoramidite and PHOX ligands

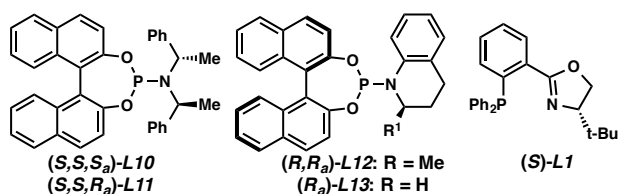


Table 3.2.1.1. Optimization of reaction parameters.^a

entry	L	base or additive (equiv)	100a:101a ^b	dr of 100a ^b	ee of 100a (%) ^c
1	L10	NaH (2)	>95:5	1:1	96 (99) ^d
2	L11	NaH (2)	>95:5	1:2	32 (3) ^e
3	L12	NaH (2)	95:5	>20:1	98
4	L12	-	80:20	11:1	96
5	L12	Et ₃ N (2)	77:23	11:1	97
6	L12	Cs ₂ CO ₃ (2)	63:37	6:1	93
7	L12	K ₃ PO ₄ (2)	63:37	4:1	90
8	L12	LiOt-Bu (2)	95:5	>20:1	99
9	L12	LiCl (1)	88:12	14:1	98
10	L12	LiBr (1)	95:5	>20:1	>99
11	L13	LiBr (1)	80:20	12:1	96
12 ^f	L1	LiBr (1)	12:88	-	-
13 ^g	L12	LiBr (1)	95:5	>20:1	99

^a Reactions performed with 0.1 mmol of **98a**, 0.2 mmol of **97a** at 0.1 M in THF at 20 °C and allowed to proceed to complete consumption of **98a**. ^b Determined by ¹H NMR and UHPLC-MS analysis of the crude mixture. ^c Determined by chiral HPLC analysis of the major diastereomer. ^d (ee) of the alternate diastereomer. ^e (ee) of the major diastereomer. ^f Measured after 60 h at 60% conversion. ^g 1 mol % [Ir(cod)Cl]₂ and 2 mol % L12 were used.

Extensive exploration of various bases, including organic and inorganic bases, revealed that the use of LiOt-Bu afforded the desired product in comparable selectivities as NaH (entries 4–8). Previous reports demonstrating the marked effect of LiCl on the regioselectivity^{79b,80j,81b} in Ir-catalyzed allylic alkylations prompted us to investigate this and related additives. As a result of these efforts (entries 9–10), the combination of LiBr

and THF, at 25 °C, was found to provide **100a** in >20:1 dr, 95:5 branched:linear ratio, and with >99% ee (entry 10).

3.2.2 Further development of the reaction conditions

Under these superior conditions, several more ligands were examined. Use of ligand **L13**^{88b} afforded **100a** in 96% ee and 12:1 dr (entry 11). Employment of *N*-aryl-phosphoramidite scaffolds proved critical to maintaining high diastereoselectivity in the reaction. Phosphinooxazoline (PHOX) type ligands (e.g. **L1**), first used in Ir-catalyzed allylation by Helmchen,⁷⁷ were also examined, but we found these to be poorly suited for our reaction (entry 12). Finally, we found that the catalyst loading could be reduced to 1 mol % (entry 13) without loss of selectivity.

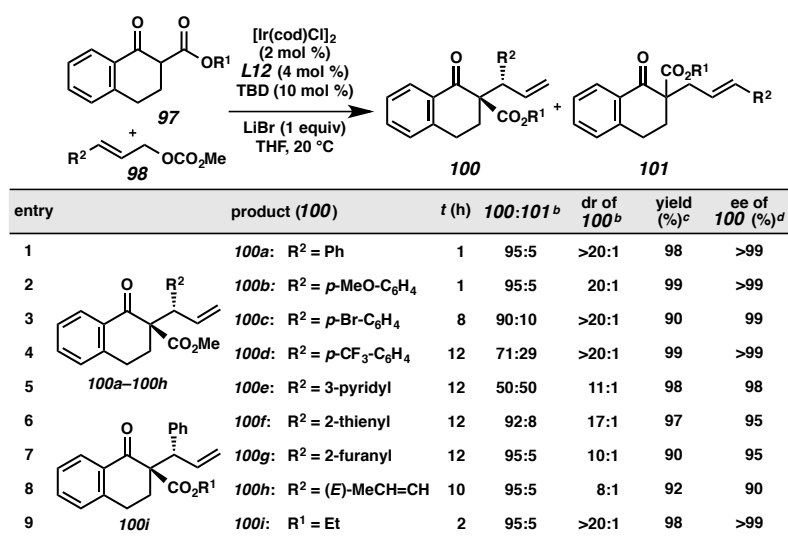
3.3 SURVEY OF REACTION SCOPE

3.3.1 Exploration of the reaction scope with respect to allyl electrophile

With optimized conditions in hand, the scope of substrates tolerated in the reaction was explored. We found that cinnamyl-derived carbonates bearing either electron-donating (–OMe) or electron-withdrawing (–Br, –CF₃) groups on the aromatic ring gave remarkably high dr, ee and yields (99% ee and 20:1 dr, Table 3.3.1.1, entries 1–4). The branched to linear ratio (i.e., **100:101**) tended to decrease as the electron deficiency of the aryl substituents increased (from 95:5 to 71:29, with 4-OMe-C₆H₄ to 4-CF₃-C₆H₄, respectively, entries 2–4). Heteroaryl substituents, such as 3-pyridyl, 2-thienyl and 2-furanyl, were also installed with uniformly excellent enantioselectivities and high diastereoselectivities (95–98% ee and 10:1–17:1 dr, entries 5–7). In addition to aromatic

substituents, methyl sorbyl carbonate was also well tolerated in the chemistry providing diene **100h**, although with a slight decrease in dr and ee (8:1 dr and 90% ee, entry 8).⁸⁹ Moreover, the reaction proceeded smoothly with ethyl β -ketoester **97i**, providing the α -allyl β -ketoester **100i** with excellent yield and selectivity (entry 9).

Figure 3.3.1.1. Substrate scope of Ir-catalyzed allylic alkylation of β -ketoesters^a



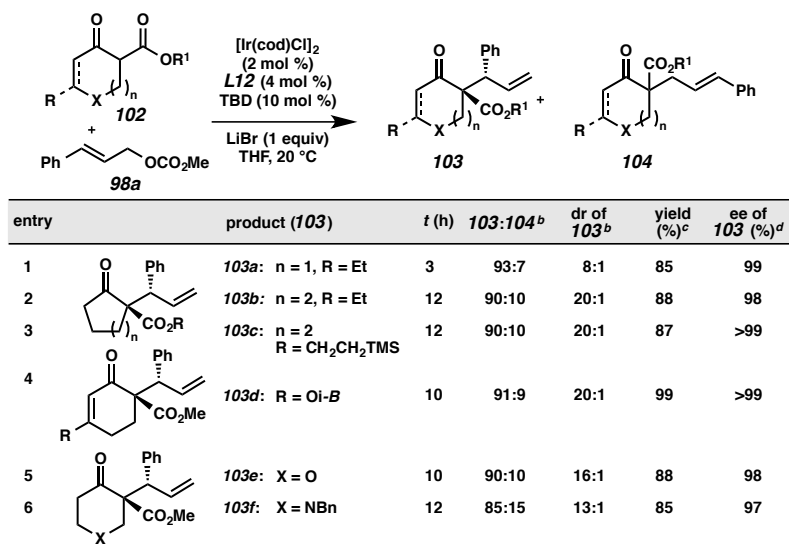
^a Reactions performed under the conditions of Table 1, entry 10. ^b Determined by ¹H NMR analysis of the crude mixture. ^c Isolated yield of **100** and **101**. ^d Determined by chiral HPLC or SFC analysis of the major diastereomer.

3.3.2 Exploration of the reaction scope with respect to ketoester nucleophile

Gratifyingly, aliphatic mono cyclic ketones also proved to be excellent participants in the reaction. Cyclopentanone and cyclohexanone based substrates delivered the products **103a** and **103b** in 98–99% ee and 8:1–20:1 dr, respectively (Figure

3.3.2.1, entries 1–2). Vinylogous ester, tetrahydropyran-4-one, and 4-piperidinone derivatives furnished the corresponding products (**103d–103f**) in high yields (85–99%), good diastereoselectivities (13:1–20:1), and enantioselectivities (97–99%, entries 4–6). The absolute stereochemistry of the product **103f** (>99% ee) was determined as (*R,R*) by single-crystal X-ray analysis.⁹⁰

Figure 3.3.2.1. Substrate scope of Ir-catalyzed allylic alkylation of β -ketoesters

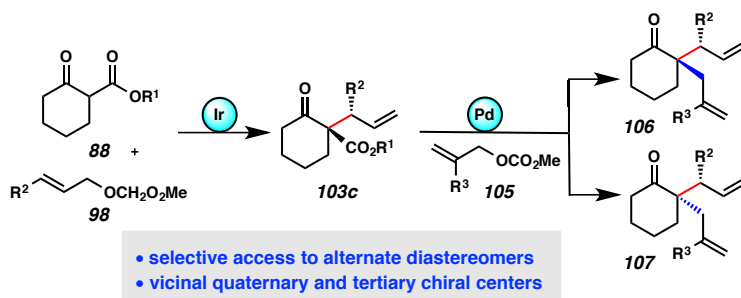


^a Reactions performed under the conditions of Table 1, entry 10. ^b Determined by ¹H NMR analysis of the crude mixture. ^c Isolated yield of **103** and **104**. ^d Determined by chiral HPLC or SFC analysis of the major diastereomer.

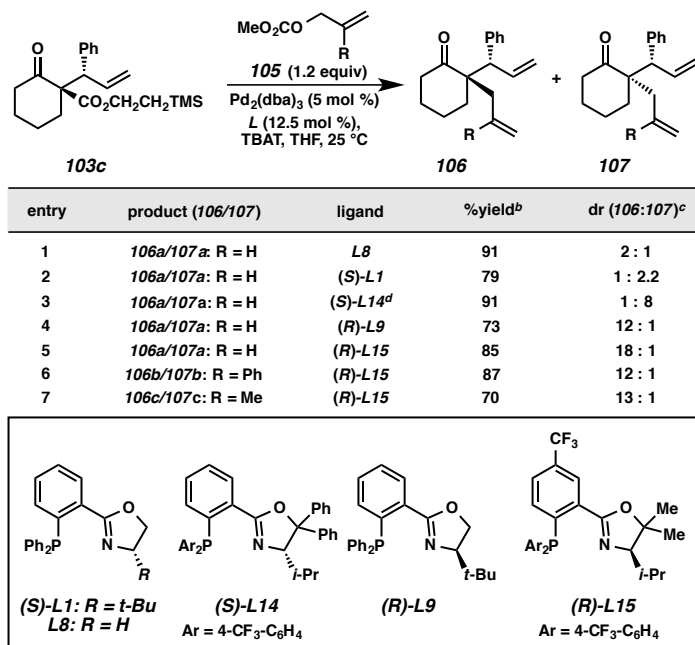
3.4 EMPLOYMENT OF TMSE- β -KETOESTERS TO ENABLE SEQUENTIAL CATALYSIS

During the course of our investigations, we became intrigued by the possibility of developing a sequential allylic alkylation reaction, in which allylation of a dicarbonyl-stabilized enolate would be followed by palladium-catalyzed decarboxylative allylic alkylation and, thus, engender the ability to select among all four possible stereochemical outcomes.^{91,92} In order to realize such a consecutive allylic alkylation, we deployed our novel oxycarbonyl-protected enolate, TMSE β -ketoester **88**, which we hypothesized would successfully undergo Ir-catalyzed allylic alkylation and be poised to subsequently participate in Pd catalysis. Specifically, we envisioned that subsequent to Ir-catalyzed allylic alkylation TMSE β -ketoester **103c** could be triggered with fluoride, and the resulting prochiral enolate then intercepted and engaged in Pd-catalyzed allylic alkylation to deliver α -quaternary ketone **106** or **107** (Figure 3.4.1). In the case at hand, where β -ketoester **103c** contains a chiral branched R group at the α position, we anticipated that with careful choice of catalyst, we could potentially control the newly generated stereocenter independent of the absolute stereochemistry of the side chain.

Figure 3.4.1. Conceptualization of sequential catalysis



We were pleased to find that TMSE β -ketoester **88** is a highly competent substrate for Ir-catalyzed allylic alkylation and, under standard conditions, gave the desired product (**103c**) with excellent yield and selectivity (Figure 3.3.2.1, entry 3). Moreover, exposure of **103c** to catalytic Pd₂(dba)₃/**L8** (Figure 3.4.2) in the presence of allyl methylcarbonate and tetrabutylammonium difluorotriphenylsilicate (TBAT) generated the desired diallylated α -quaternary ketones **106** and **107** in good yield. The use of achiral PHOX ligand **L8** revealed that substrate **103c** displays inherent selectivity under Pd catalysis, furnishing **106a**⁹³ as the major diastereomer in a 2:1 ratio with **107a** (Figure 3.4.2, entry 1). Use of (*S*)-*t*-BuPHOX ligand (*S*)-**L1** resulted in modest reversal of the inherent diastereoselectivity to generate **107a** predominantly (entry 2). Furthermore, we were interested to find that use of ligand (*S*)-**L14**, possessing both an electronically modified phosphine and a smaller *i*-Pr substituent on the oxazoline ring in contrast to the more standard *t*-Bu, produced **107a** with improved diastereoselectivity (**106a:107a**, 1:8 dr) and 91% yield (entry 3). Alternatively, through judicious choice of ligand (e.g., (*R*)-**L15**), the inherent selectivity of the system could be enhanced to afford **106a:107a** with up to 18:1 dr favoring **106a** (entries 4–5). cursory investigation revealed that 2-aryl and 2-alkyl substitutions at the allyl carbonate are well tolerated: allylic alkylation products **106b** and **106c** were obtained in good yields and with excellent diastereoselectivities.

Figure 3.4.2. Development of Pd-catalyzed diastereoselective decarboxylative allylic alkylation of TMSE- β -ketoesters^a

^a Reactions performed with 1.2 equiv of TBAT, and 1.2 equiv of allyl methylcarbonate at 0.03 M.^b Isolated yield of **106** and **107**. ^c Determined by ¹H NMR analysis of the crude mixture and confirmed by GC analysis. ^d 10 mol % ligand was used.

3.5 CONCLUDING REMARKS

In summary, a highly regio-, diastereo-, and enantio-selective method for the synthesis of vicinal tertiary and all-carbon quaternary centers was realized through the use of an [Ir(cod)Cl]₂/*N*-aryl-phosphoramidite (**L12**) catalyst system. Varied substitutions were well tolerated on both the β -ketoester and allyl carbonate fragments. A sequential Ir/Pd-catalyzed dialkylation protocol was also established to deliver bis-allylated α -quaternary ketones with excellent stereoselectivity, while affording access to either product diastereomer with catalyst control. Further studies exploring the

mechanisms of these reactions and exploiting their applications in the total synthesis of complex natural products are underway in our laboratory.

3.6 EXPERIMENTAL SECTION

3.6.1 Materials and Methods

Unless otherwise stated, reactions were performed in flame-dried glassware under an argon or nitrogen atmosphere using dry, deoxygenated solvents. Solvents were dried by passage through an activated alumina column under argon.⁶¹ Reaction progress was monitored by thin-layer chromatography (TLC) or Agilent 1290 UHPLC-LCMS. TLC was performed using E. Merck silica gel 60 F254 precoated glass plates (0.25 mm) and visualized by UV fluorescence quenching, *p*-anisaldehyde, or KMnO₄ staining. Silicycle SiliaFlash® P60 Academic Silica gel (particle size 40–63 nm) was used for flash chromatography. ¹H NMR spectra were recorded on Varian Inova 500 MHz and 600 MHz spectrometers and are reported relative to residual CHCl₃ (δ 7.26 ppm) or C₆HD₅ (δ 7.16 ppm). ¹³C NMR spectra were recorded on a Varian Inova 500 MHz spectrometer (125 MHz) and are reported relative to CHCl₃ (δ 77.16 ppm) or C₆HD₅ (δ 128.06 ppm). ³¹P and ¹⁹F NMR spectra were recorded on a Varian Mercury 300 MHz (at 121 MHz and 282 MHz, respectively). ¹⁹F NMR spectra were reported relative to CFCl₃ (δ 0.0 ppm). ³¹P NMR spectra were reported relative to external H₃PO₄ (δ 0.0 ppm). Data for ¹H NMR are reported as follows: chemical shift (δ ppm) (multiplicity, coupling constant (Hz), integration). Multiplicities are reported as follows: s = singlet, d = doublet, t = triplet, q = quartet, p = pentet, sept = septuplet, m = multiplet, br s = broad singlet, br d = broad doublet, app = apparent. Data for ¹³C NMR are reported in terms of chemical shifts

(δ ppm). IR spectra were obtained by use of a Perkin Elmer Spectrum BXII spectrometer using thin films deposited on NaCl plates and reported in frequency of absorption (cm^{-1}). Optical rotations were measured with a Jasco P-2000 polarimeter operating on the sodium D-line (589 nm), using a 100 mm path-length cell and are reported as: $[\alpha]_{\text{D}}^{\text{T}}$ (concentration in g/100 mL, solvent). Analytical HPLC was performed with an Agilent 1100 Series HPLC utilizing a Chiralpak (AD-H or AS) or Chiralcel (OD-H, OJ-H, or OB-H) columns (4.6 mm x 25 cm) obtained from Daicel Chemical Industries, Ltd. Analytical SFC was performed with a Mettler SFC supercritical CO_2 analytical chromatography system utilizing Chiralpak (AD-H, AS-H or IC) or Chiralcel (OD-H, OJ-H, or OB-H) columns (4.6 mm x 25 cm) obtained from Daicel Chemical Industries, Ltd. High resolution mass spectra (HRMS) were obtained from Agilent 6200 Series TOF with an Agilent G1978A Multimode source in electrospray ionization (ESI+), atmospheric pressure chemical ionization (APCI+), or mixed ionization mode (MM: ESI-APCI+).

Reagents were purchased from Sigma-Aldrich, Acros Organics, Strem, or Alfa Aesar and used as received unless otherwise stated. Ligands **L12–L13**,⁸⁷ ligands **L8–L9** and **L14–L15**,⁹⁴ allyl carbonates,⁹⁵ and β -ketoesters⁹⁶ were prepared by known methods.

3.6.2 Optimization of reaction parameters

Table 3.6.2.1. Optimization of reaction parameters

entry ^a	L	base/additive (equiv)	solvent	t (h)	conv (%) ^b	100a:101a ^b	dr of 100a ^b	ee of 100a (%) ^c
1	L10	NaH (2)	THF	24	>95	>95:5	1:1.4	96 (99) ^d
2	L11	NaH (2)	THF	60	>95	>95:5	1:1.9	32 (3) ^e
3	L12	NaH (2)	THF	12	>95	95:5	>20:1	98
4	L12	—	THF	8	>95	80:20	11:1	96
5	L12	DABCO (2)	THF	8	>95	72:28	5.0:1	96
6	L12	TBD (2)	THF	8	>95	74:26	11:1	95
7	L12	Et ₃ N (2)	THF	8	>95	77:23	11:1	97
8	L12	Cs ₂ CO ₃ (2)	THF	12	>95	63:37	6.3:1	93
9	L12	K ₃ PO ₄ (2)	THF	12	>95	63:37	4.1:1	90
10	L12	NaHMDS (2)	THF	12	>95	75:25	8.3:1	93
11	L12	LiHMDS (2)	THF	12	>95	86:14	13:1	96
12	L12	LiOt-Bu (2)	THF	1	>95	95:5	>20:1	99
13	L12	LiCl (1)	THF	1	>95	88:12	14:1	98
14	L12	LiBr (1)	THF	1	>95 (98)	95:5	>20:1	>99
15	L12	LiI (1)	THF	1	>95	72:28	>20:1	97
16	L10	LiBr (1)	THF	60	<5	nd	nd	nd
17	L11	LiBr (1)	THF	60	<5	nd	nd	nd
18	L13	LiBr (1)	THF	12	>95	80:20	12:1	96
19	L1	LiBr (1)	THF	60	60	12:88	nd	nd
20	L12	LiBr (1)	p-dioxane	1	>95	95:5	>20:1	>99
21	L12	LiBr (1)	Et ₂ O	3	>95	76:24	11:1	96
22	L12	LiBr (1)	CH ₂ Cl ₂	60	55	68:32	9.0:1	66
23	L12	LiBr (1)	toluene	16	>95	>95:5	>20:1	91
24 ^f	L12	LiBr (1)	THF	12	>95	95:5	>20:1	99
25 ^g	L12	LiBr (1)	THF	60	60	92:8	>20:1	94

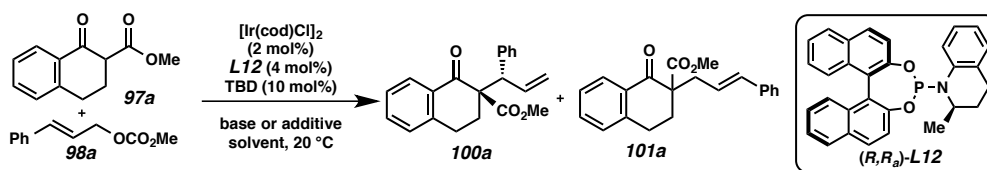
^a Reactions performed with 0.1 mmol of **98a**, 0.2 mmol of **97a** in 1 mL of solvent. ^b Determined by ¹H NMR or UHPLC-MS analysis of the crude reaction mixture. ^d (Ee) of the alternate diastereomer. ^e Measured on the minor isomer and the number in the parenthesis is ee of the major isomer. ^f 1 mol % of [Ir(cod)Cl]₂ and 2 mol % of **L12** were used. ^g 0.5 mol % of [Ir(cod)Cl]₂ and 1 mol % of **L12** were used.

General Procedure for Optimization Reaction (Table 3.6.2.1): All experiments were performed in a nitrogen-filled glove box. [Ir(cod)Cl]₂ (1.4 mg, 0.002 mmol, 2 mol%), ligand (0.004 mmol, 4 mol%), and TBD (1.4 mg, 0.01 mmol, 10 mol%) were

added to a vial equipped with a magnetic stirring bar. The vial was then charged with solvent (0.5 mL) and stirred at 20 °C for 10 min, generating an orange solution. Cinnamyl carbonate **98a** (19.2 mg, 0.1 mmol, 1.0 equiv), β -ketoester **97a** (40.4 mg, 0.2 mmol, 2.0 equiv), base or additive (as indicated below) and another 0.5 mL of solvent were added. The vial was sealed and stirred at 20 °C until allylic carbonate **98a** was fully consumed, as indicated by TLC or UHPLC-MS analysis. The reaction mixture was filtered through a celite pad, rinsed with CH₂Cl₂, and concentrated under reduced pressure. The ratios of constitutional isomers (branched product to linear product: **100a**:**101a**) and diastereomers (dr) were determined by ¹H NMR or UHPLC-MS.

3.6.3. General procedure for the Ir-catalyzed asymmetric allylic alkylation of β -ketoesters

Note: the absolute configuration was determined only for compound **100f** via X-ray analysis (vide infra, Appendix 4). The absolute configuration for all other products **100** has been inferred by analogy. Isolated yields are reported in Figures 3.3.1.1 and 3.3.2.1 (vide infra). For respective HPLC or SFC conditions, please refer to Table 3.6.8.1.



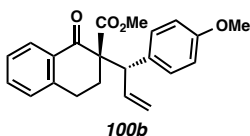
(R)-methyl 1-oxo-2-((S)-1-phenylallyl)-1,2,3,4-tetrahydronaphthalene-2-carboxylate (100a). In a nitrogen-filled glove box, [Ir(cod)Cl]₂ (2.7 mg, 0.004 mmol, 2 mol%), ligand **L12** (3.7 mg, 0.008 mmol, 4 mol%), and TBD (2.8 mg, 0.02 mmol, 10 mol%) were

added to a 2 dram scintillation vial equipped with a magnetic stirring bar. The vial was then charged with THF (1 mL) and stirred at 20 °C for 10 min, generating an orange solution. Cinnamyl carbonate (**98a**) (38.3 mg, 0.2 mmol, 1.0 equiv), LiBr (17.3 mg, 0.2 mmol, 1.0 equiv), β -ketoester **97a** (80.8 mg, 0.4 mmol, 2.0 equiv) and another 1 mL of THF were added. The vial was sealed and stirred at 20 °C until allylic carbonate **98a** was fully consumed, as indicated by TLC or UHPLC-MS analysis. THF was evaporated and the crude mixture was then dissolved in CH₂Cl₂, filtered through a celite pad, rinsed with CH₂Cl₂, and concentrated under reduced pressure. The regioselectivity (branched product to linear product: b:l = 95:5) and diastereoselectivity (dr >20:1) were determined by ¹H NMR or UHPLC-MS. The residue was purified by silica gel flash chromatography (gradient elution, 2→5% EtOAc in hexanes) to afford **100a** and **101a** (62.6 mg, 98% combined yield). Allylation product **100a** was isolated as a white solid by silica gel chromatography (gradient elution, 0→2% EtOAc in hexanes). >99% ee, [α]_D²⁵ +26.3 (*c* 1.11, CHCl₃); R_f = 0.3 (5% EtOAc in hexanes); ¹H NMR (500 MHz, CDCl₃) δ 8.03 (dd, *J* = 7.9, 1.2 Hz, 1H), 7.42–7.39 (m, 3H), 7.28–7.23 (m, 3H), 7.19–7.13 (m, 2H), 6.36 (dt, *J* = 16.8, 10.0 Hz, 1H), 5.21–5.12 (m, 2H), 4.46 (d, *J* = 10.0 Hz, 1H), 3.56 (s, 3H), 3.23 (ddd, *J* = 17.1, 12.1, 4.7 Hz, 1H), 2.88 (ddd, *J* = 17.6, 5.0, 3.0 Hz, 1H), 2.60 (ddd, *J* = 13.7, 4.7, 3.0 Hz, 1H), 2.10 (ddd, *J* = 13.6, 12.1, 5.0 Hz, 1H); ¹³C NMR (126 MHz, CDCl₃) δ 193.2, 170.0, 143.1, 139.8, 136.6, 133.6, 132.5, 130.2, 128.8, 128.4, 128.2, 126.9, 126.7, 117.9, 62.7, 53.9, 52.6, 28.8, 26.4; IR (Neat Film, NaCl) 3066, 3028, 2948, 1731, 1685, 1636, 1599, 1491, 1453, 1433, 1358, 1298, 1283, 1238, 1214, 1169, 1108, 1080, 1032, 1001, 980, 926, 892, 808, 743 cm⁻¹; HRMS (MM: ESI-APCI+) *m/z* calc'd

for C₂₁H₂₁O₃ [M+H]⁺: 321.1485, found 321.1489; HPLC conditions: 2% IPA, 0.6 mL/min, Chiralcel OD-H column, λ = 254 nm, t_R (min): major = 13.80, minor = 17.89.

3.6.4. Spectroscopic data for Ir-catalyzed allylic alkylation products

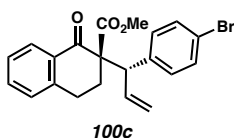
(*R*)-methyl 2-((*S*)-1-(4-methoxyphenyl)allyl)-1-oxo-1,2,3,4-tetrahydronaphthalene-2-carboxylate (**100b**)



Ketoester **100b** was isolated by silica gel chromatography (gradient elution, 0→5% EtOAc in hexanes) as a white solid. >99% ee, [α]_D²⁵ +38.5 (*c* 0.93, CHCl₃); R_f = 0.3 (5% EtOAc in hexanes); ¹H NMR (500 MHz, CDCl₃) δ 8.03 (dd, *J* = 7.9, 1.4 Hz, 1H), 7.41 (td, *J* = 7.5, 1.5 Hz, 1H), 7.37–7.31 (m, 2H), 7.31–7.21 (m, 1H), 7.21–7.12 (m, 1H), 6.86–6.75 (m, 2H), 6.32 (dt, *J* = 16.8, 10.0 Hz, 1H), 5.20–5.09 (m, 2H), 4.41 (d, *J* = 9.9 Hz, 1H), 3.75 (s, 3H), 3.56 (s, 3H), 3.23 (ddd, *J* = 17.1, 12.2, 4.6 Hz, 1H), 2.88 (ddd, *J* = 17.6, 4.9, 2.9 Hz, 1H), 2.58 (ddd, *J* = 13.6, 4.7, 3.0 Hz, 1H), 2.11 (ddd, *J* = 13.6, 12.2, 5.0 Hz, 1H); ¹³C NMR (126 MHz, CDCl₃) δ 193.3, 170.1, 158.4, 143.2, 136.8, 133.6, 132.5, 131.8, 131.2, 128.8, 128.4, 126.7, 117.6, 113.5, 62.8, 55.3, 53.2, 52.6, 28.7, 26.4; IR (Neat Film, NaCl) 3073, 3003, 2950, 2836, 1732, 1687, 1636, 1608, 1601, 1581, 1511, 1454, 1442, 1435, 1357, 1337, 1303, 1242, 1215, 1181, 1114, 1078, 1033, 1000, 981, 923, 893, 834, 808, 749 cm⁻¹; HRMS (ESI+) *m/z* calc'd for fragment C₁₀H₁₁O [M-

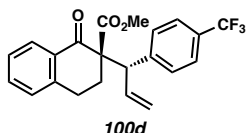
$C_{11}H_{12}O_3+H]^+$: 147.0804, found 147.0807; HPLC conditions: 2% IPA, 0.6 mL/min, Chiralpak AD-H column, $\lambda = 254$ nm, t_R (min): minor = 27.44, major = 37.29.

(R)-methyl 2-((S)-1-(4-bromophenyl)allyl)-1-oxo-1,2,3,4-tetrahydronaphthalene-2-carboxylate (100c)



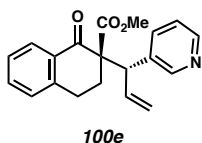
Ketoester **100c** was isolated by silica gel chromatography (gradient elution, 0→3% EtOAc in hexanes) as a colorless oil. 99% ee, $[\alpha]_D^{25} +49.1$ (c 1.18, $CHCl_3$); $R_f = 0.4$ (5% EtOAc in hexanes); 1H NMR (500 MHz, $CDCl_3$) δ 8.02 (dd, $J = 8.0, 1.4$ Hz, 1H), 7.43 (td, $J = 7.5, 1.5$ Hz, 1H), 7.39–7.35 (m, 2H), 7.32–7.27 (m, 2H), 7.27–7.25 (m, 1H), 7.15 (dt, $J = 7.7, 0.9$ Hz, 1H), 6.29 (dt, $J = 16.7, 10.0$ Hz, 1H), 5.32–5.03 (m, 2H), 4.37 (d, $J = 9.9$ Hz, 1H), 3.54 (s, 3H), 3.29–3.15 (m, 1H), 2.88 (ddd, $J = 17.5, 4.9, 2.8$ Hz, 1H), 2.57 (ddd, $J = 13.6, 4.7, 2.9$ Hz, 1H), 2.09 (ddd, $J = 13.5, 12.3, 4.9$ Hz, 1H); ^{13}C NMR (126 MHz, $CDCl_3$) δ 193.2, 169.9, 143.0, 139.0, 136.1, 133.8, 132.4, 132.0, 131.2, 128.8, 128.4, 126.8, 121.0, 118.5, 62.5, 53.7, 52.7, 29.1, 26.4; IR (Neat Film, NaCl) 3074, 3025, 2949, 1732, 1687, 1683, 1633, 1601, 1488, 1454, 1435, 1403, 1357, 1297, 1240, 1215, 1170, 1141, 1112, 1075, 1032, 1010, 981, 925, 892, 831, 808, 750, 741 cm^{-1} ; HRMS (MM: ESI-APCI+) m/z calc'd for $C_{21}H_{20}^{79}BrO_3$ $[M+H]^+$: 399.0590, found 399.0585; HPLC conditions: 2% IPA, 0.6 mL/min, Chiralpak AD-H column, $\lambda = 254$ nm, t_R (min): minor = 19.71, major = 23.59.

(R)-methyl 1-oxo-2-((S)-1-(4-(trifluoromethyl)phenyl)allyl)-1,2,3,4-tetrahydronaphthalene-2-carboxylate (100d)



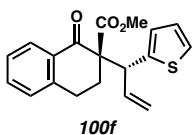
Ketoester **100d** was isolated by silica gel chromatography (gradient elution, 0→5% EtOAc in hexanes) as a colorless oil. $>99\%$ ee, $[\alpha]_D^{25} +32.4$ (c 1.51, CHCl_3); $R_f = 0.3$ (5% EtOAc in hexanes); $^1\text{H NMR}$ (500 MHz, CDCl_3) δ 8.03 (dd, $J = 7.9, 1.4$ Hz, 1H), 7.57 (d, $J = 8.4$ Hz, 2H), 7.52 (d, $J = 8.3$ Hz, 2H), 7.44 (td, $J = 7.5, 1.4$ Hz, 1H), 7.28 (t, $J = 7.5$, 1H), 7.16 (d, $J = 7.7$ Hz, 1H), 6.34 (dt, $J = 16.7, 10.1$ Hz, 1H), 5.33–5.08 (m, 2H), 4.45 (d, $J = 10.0$ Hz, 1H), 3.54 (s, 3H), 3.29–3.16 (m, 1H), 2.90 (ddd, $J = 17.6, 4.9, 2.7$ Hz, 1H), 2.60 (ddd, $J = 13.6, 4.7, 2.8$ Hz, 1H), 2.11 (ddd, $J = 13.5, 12.3, 5.0$ Hz, 1H); $^{13}\text{C NMR}$ (126 MHz, CDCl_3) δ 193.1, 169.9, 144.1, 143.0, 135.8, 133.8, 132.4, 130.6, 129.1 (q, $^2J_{\text{CF}} = 32.4$ Hz), 128.8, 128.4, 126.8, 125.0 (q, $^3J_{\text{CF}} = 3.8$ Hz), 124.3 (q, $^1J_{\text{CF}} = 272.0$ Hz), 118.8, 62.5, 54.1, 52.7, 29.3, 26.4; IR (Neat Film, NaCl) 3074, 2952, 1736, 1733, 1689, 1683, 1616, 1601, 1454, 1435, 1413, 1327, 1241, 1217, 1166, 1123, 1070, 1019, 927, 846, 809, 751, 742 cm^{-1} ; HRMS (MM: ESI-APCI+) m/z calc'd for $\text{C}_{22}\text{H}_{20}^{19}\text{F}_3\text{O}_3$ $[\text{M}+\text{H}]^+$: 389.1359, found 389.1346; SFC conditions: 5% IPA, 4.0 mL/min, Chiralpak AD-H column, $\lambda = 254$ nm, t_R (min): minor = 3.38, major = 3.91.

(R)-methyl 1-oxo-2-((S)-1-(pyridin-3-yl)allyl)-1,2,3,4-tetrahydronaphthalene-2-carboxylate (100e)



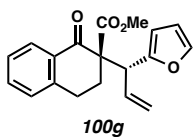
Ketoester **100e** was isolated by silica gel chromatography (gradient elution 20→50% EtOAc in hexanes) as a white solid. 98% ee, $[\alpha]_D^{25} +64.6$ (*c* 0.46, CHCl₃); $R_f = 0.4$ (50% EtOAc in hexanes); ¹H NMR (500 MHz, CDCl₃) δ 8.60 (s, 1H), 8.43 (dd, *J* = 5.0, 1.7 Hz, 1H), 8.02 (dd, *J* = 8.3, 1.3 Hz, 1H), 7.93 (dt, *J* = 8.0, 2.0 Hz, 1H), 7.44 (td, *J* = 7.5, 1.5 Hz, 1H), 7.28 (t, *J* = 7.6 Hz, 1H), 7.23 (dd, *J* = 8.0, 4.8 Hz, 1H), 7.17 (d, *J* = 7.7 Hz, 1H), 6.36–6.29 (m, 1H), 5.22–5.18 (m, 2H), 4.31 (d, *J* = 9.8 Hz, 1H), 3.53 (s, 3H), 3.21 (ddd, *J* = 17.2, 12.3, 4.7 Hz, 1H), 2.91 (ddd, *J* = 17.5, 4.9, 2.7 Hz, 1H), 2.60 (ddd, *J* = 13.5, 4.7, 2.8 Hz, 1H), 2.17 (ddd, *J* = 13.4, 12.3, 4.9 Hz, 1H); ¹³C NMR (126 MHz, CDCl₃) δ 193.3, 170.0, 150.9, 147.9, 142.9, 138.4, 136.0, 135.5, 133.9, 132.5, 128.8, 128.4, 126.9, 123.3, 119.2, 62.4, 52.7, 52.5, 29.7, 26.5; IR (Neat Film, NaCl) 3029, 2950, 2848, 1732, 1687, 1599, 1573, 1479, 1454, 1429, 1356, 1295, 1274, 1241, 1216, 1171, 1122, 1077, 1025, 999, 979, 926, 807, 749, 716 cm⁻¹; HRMS (MM: ESI-APCI+) *m/z* calc'd for C₂₀H₂₀NO₃ [M+H]⁺: 322.1438, found 322.1442; HPLC conditions: 10% IPA, 1.0 mL/min, Chiralpak AD-H column, λ = 254 nm, *t_R* (min): minor = 13.45, major = 15.72.

(R)-methyl 1-oxo-2-((R)-1-(thiophen-2-yl)allyl)-1,2,3,4-tetrahydronaphthalene-2-carboxylate (100f)



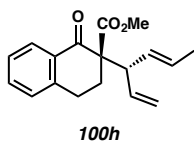
Ketoester **100f** was isolated by silica gel chromatography (gradient elution, 0→3% EtOAc in hexanes) as a white solid. 95% ee, $[\alpha]_D^{25} -14.2$ (*c* 0.86, CHCl₃); $R_f = 0.4$ (5% EtOAc in hexanes); ¹H NMR (500 MHz, CDCl₃) δ 8.08 (dd, *J* = 7.9, 1.2 Hz, 1H), 7.44 (td, *J* = 7.5, 1.4 Hz, 1H), 7.29 (t, *J* = 7.6 Hz, 1H), 7.17 (d, *J* = 7.7 Hz, 1H), 7.14 (dd, *J* = 5.1, 1.2 Hz, 1H), 6.93 (ddd, *J* = 3.6, 1.2, 0.7 Hz, 1H), 6.88 (dd, *J* = 5.1, 3.5 Hz, 1H), 6.23 (dt, *J* = 16.8, 10.0 Hz, 1H), 5.26–5.12 (m, 2H), 4.76 (d, *J* = 10.0 Hz, 1H), 3.59 (s, 3H), 3.25 (ddd, *J* = 17.2, 12.0, 4.8 Hz, 1H), 2.89 (ddd, *J* = 17.5, 5.0, 3.1 Hz, 1H), 2.55 (ddd, *J* = 13.7, 4.8, 3.1 Hz, 1H), 2.12 (ddd, *J* = 13.6, 12.0, 5.0 Hz, 1H); ¹³C NMR (126 MHz, CDCl₃) δ 193.2, 169.7, 143.2, 142.3, 135.9, 133.8, 132.3, 128.9, 128.4, 126.9, 126.8, 126.4, 124.9, 118.3, 62.9, 52.7, 49.5, 28.0, 26.2; IR (Neat Film, NaCl) 3071, 2949, 2925, 2853, 1731, 1686, 1639, 1599, 1484, 1453, 1433, 1354, 1293, 1272, 1240, 1214, 1170, 1119, 1078, 1032, 979, 924, 891, 853, 807, 749 cm⁻¹; HRMS (MM: ESI-APCI+) *m/z* calc'd for C₁₉H₁₉SO₃ [M+H]⁺: 327.1049, found 327.1048; SFC conditions: 10% IPA, 4.0 mL/min, Chiralcel OJ-H column, λ = 254 nm, *t_R* (min): major = 2.96, minor = 3.63.

(R)-methyl 2-((R)-1-(furan-2-yl)allyl)-1-oxo-1,2,3,4-tetrahydronaphthalene-2-carboxylate (100g)



Ketoester **100g** was isolated by silica gel chromatography (gradient elution, 0→3% EtOAc in hexanes) as a colorless oil. 95% ee, $[\alpha]_D^{25} +22.5$ (c 1.17, CHCl_3); $R_f = 0.4$ (5% EtOAc in hexanes); $^1\text{H NMR}$ (500 MHz, CDCl_3) δ 8.06 (dd, $J = 8.0, 1.4$ Hz, 1H), 7.45 (td, $J = 7.5, 1.5$ Hz, 1H), 7.28 (t, $J = 7.6$ Hz, 1H), 7.25 (dd, $J = 1.9, 0.9$ Hz, 1H), 7.17 (d, $J = 7.7$ Hz, 1H), 6.25 (dd, $J = 3.2, 1.8$ Hz, 1H), 6.19–6.09 (m, 2H), 5.26–5.18 (m, 2H), 4.63 (d, $J = 9.8$ Hz, 1H), 3.63 (s, 3H), 3.24 (ddd, $J = 17.3, 12.2, 4.8$ Hz, 1H), 2.88 (ddd, $J = 17.5, 4.9, 3.1$ Hz, 1H), 2.57 (ddd, $J = 13.8, 4.8, 3.1$ Hz, 1H), 1.99 (ddd, $J = 13.8, 12.1, 5.0$ Hz, 1H); $^{13}\text{C NMR}$ (126 MHz, CDCl_3) δ 192.7, 169.7, 153.4, 143.3, 141.6, 133.7, 133.6, 132.1, 128.9, 128.4, 126.7, 119.2, 110.3, 108.4, 62.2, 52.7, 47.9, 28.1, 26.1; IR (Neat Film, NaCl) 3116, 3075, 3024, 2950, 2848, 1734, 1731, 1689, 1639, 1600, 1500, 1485, 1453, 1433, 1356, 1293, 1271, 1243, 1216, 1172, 1155, 1120, 1110, 1078, 1012, 981, 965, 928, 905, 892, 806, 745, 736 cm^{-1} ; HRMS (ESI+) m/z calc'd for $\text{C}_{19}\text{H}_{19}\text{O}_4$ $[\text{M}+\text{H}]^+$: 311.1278, found 311.1275; SFC conditions: 10% IPA, 2.5 mL/min, Chiralpak AD-H column, $\lambda = 254$ nm, t_R (min): major = 5.21, minor = 6.03.

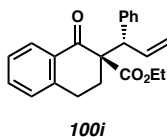
(R)-methyl 2-((S,E)-hexa-1,4-dien-3-yl)-1-oxo-1,2,3,4-tetrahydronaphthalene-2-carboxylate (100h)



Ketoester **100h** was isolated by silica gel chromatography (gradient elution, 0→2% EtOAc in hexanes) as a colorless oil. 90% ee, $[\alpha]_D^{25} +46.4$ (c 1.02, CHCl_3); $R_f = 0.5$ (5% EtOAc in hexanes); $^1\text{H NMR}$ (500 MHz, CDCl_3) δ 8.05 (dd, $J = 7.9, 1.2$ Hz, 1H), 7.45 (td, $J = 7.5, 1.5$ Hz, 1H), 7.30 (t, $J = 7.6$ Hz, 1H), 7.19 (d, $J = 7.7$ Hz, 1H), 5.98–5.87 (m, 1H), 5.74 (ddd, $J = 15.3, 8.0, 1.6$ Hz, 1H), 5.57–5.48 (m, 1H), 5.08–5.03 (m, 2H), 3.61 (s, 3H), 3.47 (t, $J = 8.4$ Hz, 1H), 3.12 (ddd, $J = 17.0, 12.0, 4.7$ Hz, 1H), 2.91 (dt, $J = 17.4, 4.1$ Hz, 1H), 2.45 (ddd, $J = 13.7, 4.7, 3.3$ Hz, 1H), 2.25 (ddd, $J = 13.7, 11.9, 4.9$ Hz, 1H), 1.65 (ddd, $J = 6.4, 1.7, 0.7$ Hz, 3H); $^{13}\text{C NMR}$ (126 MHz, CDCl_3) δ 194.2, 171.0, 143.1, 136.7, 133.6, 132.8, 129.8, 128.8, 128.2, 128.2, 126.8, 117.6, 62.0, 53.2, 52.4, 29.5, 26.5, 18.2; IR (Neat Film, NaCl) 3075, 3028, 2951, 2854, 1732, 1688, 1600, 1454, 1438, 1356, 1300, 1272, 1235, 1214, 1169, 1122, 1090, 999, 974, 917, 890, 803, 747 cm^{-1} ; HRMS (ESI+) m/z calc'd for $\text{C}_{18}\text{H}_{21}\text{O}_3$ $[\text{M}+\text{H}]^+$: 288.1485, found 288.1489; SFC conditions: 2% MeOH, 2.5 mL/min, Chiralpak IC column, $\lambda = 254$ nm, t_R (min): minor = 8.23, major = 8.87.

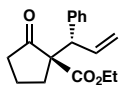
(R)-ethyl 1-oxo-2-((S)-1-phenylallyl)-1,2,3,4-tetrahydronaphthalene-2-carboxylate

(100i)



Ketoester **100i** was isolated by silica gel chromatography (gradient elution, 0→5% EtOAc in hexanes) as a white solid, >99% ee, $[\alpha]_D^{25} +42.7$ (c 1.09, CHCl_3); $R_f = 0.3$ (5% EtOAc in hexanes); $^1\text{H NMR}$ (500 MHz, CDCl_3) δ 8.03 (dd, $J = 7.9, 1.4$ Hz, 1H), 7.46–7.39 (m, 3H), 7.29–7.23 (m, 3H), 7.20–7.12 (m, 2H), 6.37 (dt, $J = 16.8, 10.0$ Hz, 1H), 5.20–5.07 (m, 2H), 4.40 (d, $J = 9.9$ Hz, 1H), 4.07–3.94 (m, 2H), 3.22 (ddd, $J = 17.3, 12.2, 4.8$ Hz, 1H), 2.88 (ddd, $J = 17.5, 5.0, 2.9$ Hz, 1H), 2.58 (ddd, $J = 13.6, 4.7, 3.0$ Hz, 1H), 2.12 (ddd, $J = 13.6, 12.1, 5.0$ Hz, 1H), 1.06 (t, $J = 7.1$ Hz, 3H); $^{13}\text{C NMR}$ (126 MHz, CDCl_3) δ 193.4, 169.7, 143.0, 140.0, 136.7, 133.5, 132.7, 130.3, 128.7, 128.3, 128.1, 126.9, 126.7, 117.9, 62.3, 61.6, 54.1, 29.2, 26.4, 14.0; IR (Neat Film, NaCl) 3063, 3027, 2978, 2934, 1727, 1699, 1689, 1685, 1599, 1490, 1452, 1363, 1298, 1282, 1235, 1212, 1157, 1107, 1080, 1018, 926, 899, 787, 773, 743 cm^{-1} ; HRMS (MM: ESI-APCI+) m/z calc'd for $\text{C}_{22}\text{H}_{23}\text{O}_3$ $[\text{M}+\text{H}]^+$: 335.1642, found 335.1651; SFC conditions: 5% IPA, 2.5 mL/min, Chiralpak AD-H column, $\lambda = 254$ nm, t_R (min): minor = 13.82, major = 16.53.

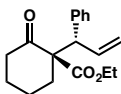
(R)-ethyl 2-oxo-1-((S)-1-phenylallyl)cyclopentanecarboxylate (103a)



103a

Ketoester **103a** was isolated by silica gel chromatography (gradient elution, 0→5% EtOAc in hexanes) as a colorless oil. 99% ee, $[\alpha]_D^{25} -52.5$ (*c* 1.04, CHCl₃); $R_f = 0.3$ (5% EtOAc in hexanes); ¹H NMR (500 MHz, CDCl₃) δ 7.31–7.15 (m, 5H), 6.14–6.03 (m, 1H), 5.20–5.10 (m, 2H), 4.37 (d, *J* = 8.9 Hz, 1H), 4.22–4.09 (m, 2H), 2.67 (dddd, *J* = 13.4, 7.1, 3.5, 1.7 Hz, 1H), 2.24–2.14 (m, 1H), 2.13–2.02 (m, 1H), 1.84–1.71 (m, 1H), 1.69–1.59 (m, 1H), 1.59–1.49 (m, 1H), 1.24 (t, *J* = 7.1 Hz, 3H); ¹³C NMR (126 MHz, CDCl₃) δ 213.4, 169.2, 139.3, 136.3, 129.9, 128.4, 127.1, 117.8, 65.9, 61.9, 52.8, 38.9, 28.5, 19.7, 14.2; IR (Neat Film, NaCl) 3083, 3062, 3030, 2979, 2891, 1752, 1719, 1639, 1601, 1493, 1465, 1452, 1405, 1365, 1315, 1223, 1138, 1105, 1026, 1003, 923, 864, 826, 757, 707 cm⁻¹; HRMS (MM: ESI-APCI+) *m/z* calc'd for C₁₇H₂₁O₃ [M+H]⁺: 273.1485, found 273.1483; HPLC conditions: 2% IPA, 0.6 mL/min, Chiralcel OD-H column, $\lambda = 210$ nm, t_R (min): major = 11.23, minor = 12.73.

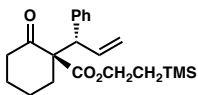
(R)-ethyl 2-oxo-1-((S)-1-phenylallyl)cyclohexanecarboxylate (103b)



103b

Ketoester **103b** was isolated by silica gel chromatography (gradient elution, 0→5% EtOAc in hexanes) as a white solid. 98% ee, $[\alpha]_D^{25} +140.6$ (c 1.25, CHCl_3); $R_f = 0.4$ (5% EtOAc in hexanes); ^1H NMR (500 MHz, CDCl_3) δ 7.36–7.30 (m, 2H), 7.29–7.22 (m, 2H), 7.21–7.15 (m, 1H), 6.33 (ddd, $J = 16.9, 10.2, 9.2$ Hz, 1H), 5.13–4.99 (m, 2H), 4.11–3.96 (m, 2H), 3.93 (d, $J = 9.2$ Hz, 1H), 2.47–2.39 (m, 2H), 2.36–2.29 (m, 1H), 1.92 (dddd, $J = 9.5, 4.8, 2.7, 1.5$ Hz, 1H), 1.79–1.47 (m, 3H), 1.12 (t, $J = 7.1$ Hz, 3H); ^{13}C NMR (126 MHz, CDCl_3) δ 206.7, 170.8, 140.0, 137.5, 130.3, 128.0, 126.8, 117.4, 65.5, 61.4, 54.6, 42.1, 35.0, 27.2, 22.8, 14.0; IR (Neat Film, NaCl) 3077, 3028, 2977, 2939, 2865, 1714, 1635, 1600, 1491, 1452, 1388, 1365, 1340, 1309, 1262, 1231, 1204, 1133, 1085, 1020, 1002, 919, 854, 756, 704 cm^{-1} ; HRMS (MM: ESI-APCI+) m/z calc'd for $\text{C}_{18}\text{H}_{23}\text{O}_3$ $[\text{M}+\text{H}]^+$: 287.1642, found 287.1639; SFC conditions: 10% IPA, 4.0 mL/min, Chiralpak IC column, $\lambda = 210$ nm, t_R (min): minor = 1.69, major = 1.94.

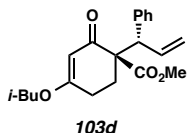
(R)-2-(trimethylsilyl)ethyl 2-oxo-1-((S)-1-phenylallyl)cyclohexanecarboxylate (103c)



103c

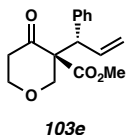
Ketoester **103c** was isolated by silica gel chromatography (gradient elution, 0→2% *i*-BuOAc in hexanes) as a colorless oil. >99% ee, $[\alpha]_D^{25} +91.6$ (*c* 0.45, CHCl₃); $R_f = 0.4$ (10% EtOAc in hexanes); ¹H NMR (500 MHz, CDCl₃) δ 7.37–7.32 (m, 2H), 7.24 (ddd, *J* = 8.2, 6.9, 1.4 Hz, 2H), 7.21–7.15 (m, 1H), 6.34 (ddd, *J* = 16.9, 10.2, 9.2 Hz, 1H), 5.21–4.86 (m, 2H), 4.05 (dddd, *J* = 58.0, 11.8, 10.8, 5.9 Hz, 2H), 3.92 (d, *J* = 9.2 Hz, 1H), 2.46–2.40 (m, 2H), 2.38–2.28 (m, 1H), 1.98–1.87 (m, 1H), 1.80–1.71 (m, 1H), 1.72–1.47 (m, 3H), 0.82 (qdd, *J* = 13.6, 11.7, 5.7 Hz, 2H), 0.01 (s, 9H); ¹³C NMR (126 MHz, CDCl₃) δ 206.6, 170.9, 139.9, 137.4, 130.2, 127.9, 126.7, 117.3, 65.4, 63.7, 54.5, 42.0, 34.9, 27.0, 22.7, 17.2, –1.6; IR (Neat Film, NaCl) 2950, 1712, 1452, 1250, 1231, 1133, 921, 859, 837 cm⁻¹; HRMS (MM: ESI-APCI+) *m/z* calc'd for C₂₁H₃₀NaO₃Si [M+Na]⁺: 381.1856, found 381.1865; SFC conditions: 3% IPA, 2.5 mL/min, Chiralcel OJ–H column, λ = 210 nm, *t_R* (min): minor = 1.93, major = 2.24.

(R)-methyl 4-isobutoxy-2-oxo-1-((S)-1-phenylallyl)cyclohex-3-enecarboxylate (103d)



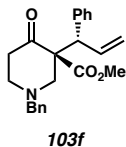
Ketoester **103d** was isolated by silica gel chromatography (gradient elution, 0→10% EtOAc in hexanes) as a colorless oil. $>99\%$ ee, $[\alpha]_D^{25} +31.5$ (c 1.88, CHCl_3); $R_f = 0.4$ (10% EtOAc in hexanes); $^1\text{H NMR}$ (500 MHz, CDCl_3) δ 7.34–7.29 (m, 2H), 7.27–7.20 (m, 2H), 7.20–7.13 (m, 1H), 6.24 (dt, $J = 16.7, 10.2$ Hz, 1H), 5.28 (s, 1H), 5.18 (ddd, $J = 16.8, 1.9, 0.8$ Hz, 1H), 5.12 (dd, $J = 10.0, 1.8$ Hz, 1H), 4.62 (d, $J = 10.4$ Hz, 1H), 3.64 (s, 3H), 3.53–3.45 (m, 2H), 2.79 (dddd, $J = 18.3, 11.8, 5.1, 1.6$ Hz, 1H), 2.43 (ddd, $J = 13.4, 5.1, 2.4$ Hz, 1H), 2.26 (ddd, $J = 18.2, 5.5, 2.4$ Hz, 1H), 1.94 (dt, $J = 13.3, 6.7$ Hz, 1H), 1.83 (ddd, $J = 13.4, 11.8, 5.5$ Hz, 1H), 0.91 (d, $J = 6.8$ Hz, 6H); $^{13}\text{C NMR}$ (126 MHz, CDCl_3) δ 192.8, 177.2, 170.0, 139.7, 136.1, 130.2, 128.1, 126.8, 118.0, 102.9, 74.9, 61.1, 52.6, 52.1, 27.7, 26.7, 25.2, 19.11, 19.08; IR (Neat Film, NaCl) 3073, 3029, 2958, 2874, 1727, 1664, 1607, 1582, 1491, 1470, 1452, 1443, 1431, 1406, 1384, 1369, 1316, 1298, 1231, 1193, 1177, 1140, 1116, 1079, 1012, 987, 921, 903, 844, 817, 788, 764, 724 cm^{-1} ; HRMS (MM: ESI-APCI+) m/z calc'd for $\text{C}_{21}\text{H}_{27}\text{O}_4$ $[\text{M}+\text{H}]^+$: 343.1904, found 343.1905; SFC conditions: 10% IPA, 2.5 mL/min, Chiralcel OD-H column, $\lambda = 254$ nm, t_R (min): major = 3.71, minor = 6.24.

(S)-methyl 4-oxo-3-((S)-1-phenylallyl)tetrahydro-2H-pyran-3-carboxylate (103e)



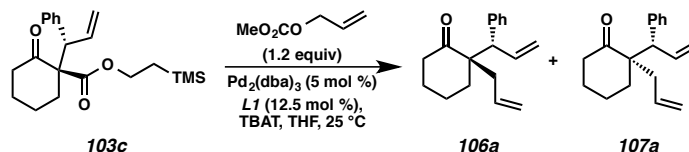
Ketoester **103e** was isolated by silica gel chromatography (gradient elution, 5→10% EtOAc in hexanes) as a colorless oil. 98% ee, $[\alpha]_D^{25} +71.1$ (c 0.88, CHCl_3); $R_f = 0.2$ (10% EtOAc in hexanes); ^1H NMR (500 MHz, CDCl_3) δ 7.35–7.30 (m, 2H), 7.31–7.25 (m, 2H), 7.24–7.19 (m, 1H), 6.43 (ddd, $J = 16.9, 10.2, 9.4$ Hz, 1H), 5.19–5.03 (m, 2H), 4.28 (dd, $J = 11.9, 1.2$ Hz, 1H), 4.03 (dddd, $J = 11.1, 6.2, 4.9, 1.3$ Hz, 1H), 3.98 (d, $J = 9.4$ Hz, 1H), 3.82 (dddd, $J = 11.3, 9.0, 4.5, 0.6$ Hz, 1H), 3.67 (d, $J = 11.8$ Hz, 1H), 3.61 (s, 3H), 2.70 (ddd, $J = 14.5, 8.9, 6.2$ Hz, 1H), 2.57 (dt, $J = 14.5, 4.7$ Hz, 1H); ^{13}C NMR (126 MHz, CDCl_3) δ 202.8, 169.7, 138.6, 136.7, 129.8, 128.4, 127.4, 118.0, 73.2, 68.6, 67.1, 52.4, 51.6, 41.9; IR (Neat Film, NaCl) 3063, 3029, 2973, 2951, 2863, 1746, 1716, 1635, 1600, 1492, 1472, 1454, 1433, 1378, 1360, 1310, 1290, 1229, 1212, 1176, 1140, 1112, 1085, 1033, 1001, 978, 925, 826, 763, 741 cm^{-1} ; HRMS (ESI+) m/z calc'd for $\text{C}_{16}\text{H}_{19}\text{O}_4$ $[\text{M}+\text{H}]^+$: 275.1278, found 275.1282; SFC conditions: 5% IPA, 2.5 mL/min, Chiralpak AD-H column, $\lambda = 210$ nm, t_R (min): minor = 4.65, major = 4.95.

(S)-methyl 1-benzyl-4-oxo-3-((S)-1-phenylallyl)piperidine-3-carboxylate (103f)



Ketoester **103f** was isolated by silica gel chromatography (gradient elution, 5→10% EtOAc in hexanes) as a colorless oil. 97% ee, $[\alpha]_D^{25} +34.3$ (c 0.87, CHCl_3); $R_f = 0.3$ (10% EtOAc in hexanes); ^1H NMR (500 MHz, CDCl_3) δ 7.39–7.29 (m, 5H), 7.28–7.24 (m, 2H), 7.24–7.14 (m, 3H), 6.44 (ddd, $J = 16.9, 10.2, 9.3$ Hz, 1H), 5.12–5.04 (m, 2H), 4.03 (d, $J = 9.4$ Hz, 1H), 3.59 (s, 3H), 3.64–3.54 (m, 2H), 3.15 (dd, $J = 11.9, 2.0$ Hz, 1H), 2.82–2.75 (m, 1H), 2.71 (ddd, $J = 14.1, 8.5, 5.7$ Hz, 1H), 2.65–2.56 (m, 2H), 2.53 (ddd, $J = 13.9, 5.4, 4.3$ Hz, 1H); ^{13}C NMR (126 MHz, CDCl_3) δ 205.3, 170.6, 139.4, 138.0, 137.4, 129.9, 129.2, 128.5, 128.2, 127.5, 127.1, 117.6, 66.1, 62.0, 60.2, 53.4, 53.0, 52.0, 40.9; IR (Neat Film, NaCl) 3060, 3027, 2949, 2811, 2765, 1718, 1631, 1600, 1584, 1493, 1468, 1452, 1432, 1364, 1345, 1310, 1286, 1228, 1194, 1138, 1073, 1047, 1028, 1001, 973, 922, 821, 740 cm^{-1} ; HRMS (MM: ESI-APCI+) m/z calc'd for $\text{C}_{23}\text{H}_{26}\text{NO}_3$ $[\text{M}+\text{H}]^+$: 364.1907, found 364.1908; SFC conditions: 10% IPA, 4.0 mL/min, Chiralpak AD-H column, $\lambda = 210$ nm, t_R (min): major = 2.49, minor = 2.94.

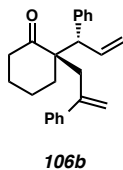
3.6.5. General procedure for Pd-catalyzed allylic alkylation



(R)-2-allyl-2-((S)-1-phenylallyl)cyclohexanone (106a). To a 0.5 dram scintillation vial equipped with a magnetic stir bar were added $\text{Pd}_2(\text{dba})_3$ (1.3 mg, 0.0014 mmol), **L8** (1.2 mg, 0.0035 mmol), TBAT (16.6 mg, 0.031 mmol) and THF (0.9 mL) in a nitrogen-filled glove box. The dark purple mixture was stirred at ambient glove box temperature (ca. 30 °C) for 35 minutes at which point the mixture had become red-orange. Ketoester **103c** (10.0 mg, 0.028 mmol) and allyl methylcarbonate (4.1 mg, 0.035 mmol) were then added neat to the reaction mixture. The resulting yellow-green reaction mixture was stirred at 20 °C until full conversion of the starting material was indicated by TLC analysis (reaction times typically ranged from 24 to 36 hours). The vial was removed from the glove box, uncapped and diluted with 2 ml of hexanes. Filtration through a celite pad afforded the crude residue, which was concentrated *in vacuo* and analyzed by ^1H NMR to determine the diastereomeric ratio of **106a** and **107a** (2:1). The residue was purified by silica gel flash chromatography (gradient elution, 0→2% EtOAc in hexanes) to afford **106a** and **107a** (6.5 mg, 91% combined yield) as a colorless oil. 99% ee (The enantiomeric excesses of the products **106a** and **107a** are inferred from the corresponding Ir-catalyzed allylic alkylation products (**103c**)). Spectroscopic data for compound **106a** is as follows: $[\alpha]_{\text{D}}^{25} -1.9$ (*c* 0.48, CHCl_3); $R_f = 0.3$ (0.4% EtOAc in hexanes); ^1H NMR (300 MHz, CDCl_3) δ 7.33–7.28 (m, 2H), 7.25–7.20 (m, 3H), 6.20 (dt, $J = 16.8, 10.1$ Hz, 1H),

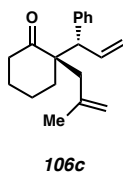
5.68 (dddd, $J = 17.1, 10.1, 8.8, 5.4$ Hz, 1H), 5.09 (ddd, $J = 10.1, 1.6, 0.4$ Hz, 1H), 5.08 (ddd, $J = 16.7, 1.7, 0.8$ Hz, 1H), 4.98 (dddd, $J = 10.2, 2.3, 1.3, 0.7$ Hz, 1H), 4.92–4.86 (m, 1H), 3.92 (d, $J = 9.9$ Hz, 1H), 2.75 (dd, $J = 13.7, 5.4$ Hz, 1H), 2.56–2.10 (m, 2H), 2.11–1.59 (m, 7H); ^{13}C NMR (126 MHz, CDCl_3) δ 212.9, 140.1, 136.3, 134.9, 130.0, 128.1, 126.8, 117.9, 117.4, 55.7, 52.8, 40.5, 37.6, 31.9, 26.2, 21.1; IR (Neat Film, NaCl) 3073, 3028, 2937, 2864, 1833, 1701, 1636, 1600, 1452, 1432, 1313, 1219, 1125, 1056, 1002, 916, 849, 787, 765 cm^{-1} ; HRMS (MM: ESI-APCI+) m/z calc'd for $\text{C}_{18}\text{H}_{23}\text{O}$ $[\text{M}+\text{H}]^+$: 255.1754; found 255.1743. Spectroscopic data for compound **107a** is as follows: $[\alpha]_{\text{D}}^{25} +6.1$ (c 0.75, CHCl_3); $R_f = 0.3$ (0.4% EtOAc in hexanes); ^1H NMR (300 MHz, CDCl_3) δ 7.33–7.28 (m, 2H), 7.25–7.20 (m, 3H), 6.19 (dt, $J = 16.8, 10.1$ Hz, 1H), 5.65 (dddd, $J = 17.1, 10.1, 8.8, 5.4$ Hz, 1H), 5.17 (dd, $J = 1.7, 1.0$, 1H), 5.15 (dd, $J = 1.7, 1.0$, 1H) 5.07–5.02 (m, 2H) 3.95 (d, $J = 8.5$, 1H), 2.75 (dd, $J = 13.7, 5.4$ Hz, 1H), 2.56–2.10 (m, 2H), 2.11–1.59 (m, 7H); ^{13}C NMR (126 MHz, CDCl_3) δ 213.2, 140.3, 138.0, 134.1, 129.8, 128.3, 126.8, 118.0, 117.8, 55.6, 53.4, 40.6, 38.6, 32.2, 25.6, 20.8; IR (Neat Film, NaCl) 3073, 3028, 2937, 2864, 1833, 1701, 1636, 1600, 1452, 1432, 1313, 1219, 1125, 1056, 1002, 916, 849, 787, 765 cm^{-1} ; HRMS (MM: ESI-APCI+) m/z calc'd for $\text{C}_{18}\text{H}_{23}\text{O}$ $[\text{M}+\text{H}]^+$: 255.1754; found 255.1750.

(R)-2-((S)-1-phenylallyl)-2-(2-phenylallyl)cyclohexanone (106b)



Ketone **106b** was isolated by silica gel chromatography (gradient elution, 0→1% Et₂O in hexanes) as a colorless oil. $[\alpha]_D^{25}$ -50.9 (c 0.22, CHCl₃); R_f = 0.5 (10% EtOAc in hexanes); ¹H NMR (500 MHz, CDCl₃) δ 7.32–7.13 (m, 10H), 6.24 (dt, J = 16.8, 10.1 Hz, 1H), 5.29 (d, J = 1.8 Hz, 1H), 5.22–5.02 (m, 3H), 3.92 (d, J = 10.0 Hz, 1H), 2.95 (ddd, J = 377.8, 13.8, 0.9 Hz, 2H), 2.15–2.00 (m, 2H), 1.76–1.57 (m, 4H), 1.54–1.43 (m, 2H); ¹³C NMR (126 MHz, CDCl₃) δ 212.8, 145.6, 142.8, 140.3, 136.2, 129.9, 128.1, 128.0, 127.0, 126.7, 126.5, 118.2, 117.7, 56.6, 54.4, 40.6, 37.6, 30.6, 24.8, 21.4; IR (Neat Film, NaCl) 2937, 2859, 1701, 1624, 1597, 1451, 1310, 1256, 1207, 1125 910, 779 cm⁻¹; HRMS (MM: ESI-APCI+) m/z calc'd for C₂₄H₂₆O [M+H]⁺: 331.2056, found 331.2065.

(R)-2-(2-methylallyl)-2-((S)-1-phenylallyl)cyclohexanone (106c)

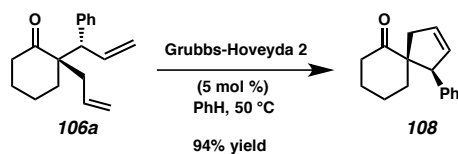


Ketone **106c** was isolated by silica gel chromatography (gradient elution, 0→2% EtOAc in hexanes) as a colorless oil. $[\alpha]_D^{25}$ -41.7 (c 0.46, CHCl₃); R_f = 0.4 (5% EtOAc in hexanes); ¹H NMR (500 MHz, CDCl₃) δ 7.33–7.28 (m, 2H), 7.25–7.19 (m, 3H), 6.19 (dt,

$J = 16.8, 10.1$ Hz, 1H), 5.08 (dd, $J = 10.2, 1.6$ Hz, 1H), 5.03 (ddd, $J = 16.8, 1.6, 0.8$ Hz, 1H), 4.74 (ddt, $J = 2.7, 1.8, 0.9$ Hz, 1H), 4.52 (ddt, $J = 2.4, 1.6, 0.9$ Hz, 1H), 3.86 (d, $J = 10.0$ Hz, 1H), 2.90 (d, $J = 13.1$ Hz, 1H), 2.37 (dtd, $J = 16.2, 4.9, 1.6$ Hz, 1H), 2.25 (ddd, $J = 15.9, 11.3, 6.0$ Hz, 1H), 2.00 (d, $J = 13.7$ Hz, 1H), 1.93–1.78 (m, 2H), 1.74–1.63 (m, 4H), 1.59 (dt, $J = 1.4, 0.7$ Hz, 3H); ^{13}C NMR (126 MHz, CDCl_3) δ 212.8, 143.0, 140.3, 136.5, 130.1, 128.2, 126.9, 117.4, 115.3, 55.5, 54.2, 40.7, 40.2, 30.8, 25.5, 25.1, 21.4; IR (Neat Film, NaCl) 3071, 3030, 2940, 2865, 1704, 1637, 1599, 1452, 1375, 1314, 1209, 1124, 994, 916, 893, 756 cm^{-1} ; HRMS (MM: ESI-APCI+) m/z calc'd for $\text{C}_{19}\text{H}_{25}\text{O}$ $[\text{M}+\text{H}]^+$: 269.1920; found 269.1920.

3.6.6. Determination of the relative configuration of compound **106a**

The relative configuration of compound **106a** was determined via NOE analysis of the corresponding spirocycle, **108**, obtained via ring-closing metathesis. The experimental procedure by which **108** was generated is as follows:



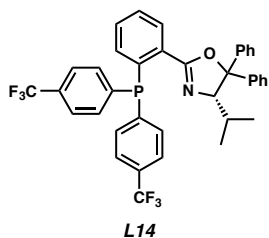
(1S,5R)-1-phenylspiro[4.5]dec-2-en-6-one (108). To a flask charged with Grubbs-Hoveyda second generation catalyst (1.85 mg, 0.0030 mmol) under an atmosphere of argon was added a solution of cyclohexanone **106a** (15.0 mg, 0.059 mmol) in 6 mL benzene. The reaction mixture was heated to 50 °C and stirred for 4 hours, at which point the reaction was determined to be complete by TLC analysis. The reaction vessel was

cooled to 25 °C and 0.5 mL of ethyl vinyl ether was added. After 30 minutes of stirring, the crude mixture was purified directly by silica gel chromatography (gradient elution, 0→3% EtOAc in hexanes) to afford spirocycle **108** (12.7 mg, 0.056 mmol, 94% yield) as a colorless oil. $[\alpha]_D^{25} -133.6$ (c 0.25, CHCl_3); $R_f = 0.5$ (10% EtOAc in hexanes); ^1H NMR (500 MHz, CDCl_3) δ 7.32–7.24 (m, 2H), 7.24–7.18 (m, 1H), 7.18–7.12 (m, 2H), 6.01–5.52 (m, 1H), 4.75 (p, $J = 2.1$ Hz, 1H), 2.66–2.56 (m, 2H), 2.56–2.44 (m, 2H), 1.95–1.85 (m, 1H), 1.64–1.49 (m, 3H), 1.42 (dtd, $J = 14.66, 3.6, 2.3$ Hz, 1H), 1.35–0.72 (m, 1H), 1.01 (ddd, $J = 13.9, 11.3, 4.5$ Hz, 1H); ^{13}C NMR (126 MHz, CDCl_3) δ 212.9, 140.6, 133.8, 129.3, 128.0, 127.4, 126.4, 59.8, 53.7, 42.8, 39.6, 35.5, 26.8, 22.2; IR (Neat Film, NaCl) 3944, 3693, 3053, 2986, 2941, 2866, 2685, 2305, 1698, 1422, 1264, 1129, 896, 756 cm^{-1} ; HRMS (MM: ESI-APCI+) m/z calc'd for $\text{C}_{16}\text{H}_{19}\text{O}$ $[\text{M}+\text{H}]^+$: 227.1430; found 227.1431.

3.6.7. Spectroscopic data for new phosphinoxazoline ligands

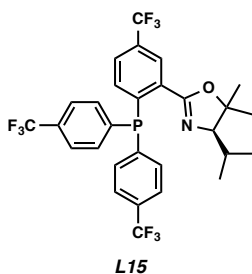
Phosphinoxazoline ligands **L14** and **L15** employed in these studies were generously donated by Dr. Robert A. Craig. They were generated following the method reported by McDougal and Stoltz. Comprehensive preparatory detail can be found in the Thesis of Dr. Craig.

(S)-2-(2-(bis(4-(trifluoromethyl)phenyl)phosphino)phenyl)-4-isopropyl-5,5-diphenyl-4,5-dihydrooxazole (L14)



$[\alpha]_D^{25}$ -163.33 (c 0.75, CHCl_3); $R_f = 0.3$ (4:1 hexanes in dichloromethane); ^1H NMR (500 MHz, C_6D_6) δ 8.22 (ddd, $J = 7.8, 3.9, 1.4$ Hz, 1H), 7.29 (ddd, $J = 49.4, 8.4, 1.4$ Hz, 4H), 7.21–7.14 (m, 5H), 7.10–7.02 (m, 7H), 7.02–6.94 (m, 3H), 6.89 (td, $J = 7.6, 1.4$ Hz, 1H), 6.81 (ddd, $J = 7.9, 3.4, 1.3$ Hz, 1H), 4.66 (d, $J = 4.5$ Hz, 1H), 1.74 (td, $J = 6.6, 4.6$ Hz, 1H), 0.83 (d, $J = 6.7$ Hz, 3H), 0.59 (d, $J = 6.5$ Hz, 3H); ^{13}C NMR (126 MHz, C_6D_6) δ 160.1 (d, $J_{\text{CP}} = 3.2$ Hz), 145.8, 144.4–143.9 (m) 141.2, 137.9 (d, $J_{\text{CP}} = 27.4$ Hz), 134.9, 134.5 (dd, $J_{\text{CP}} = 70.9, 20.8$ Hz), 132.6 (d, $J_{\text{CP}} = 21.4$ Hz), 131.3, 130.6 (dd, $J_{\text{CP}} = 32.3, 18.4$ Hz), 130.3 (d, $J_{\text{CP}} = 3.2$ Hz), 129.1, 127.5 (d, $J_{\text{CF}} = 11.2$ Hz), 126.8, 125.3 (ddt, $J_{\text{CF}} = 14.7, 7.6, 3.8$ Hz), 124.8 (d, $J_{\text{CF}} = 273.5$ Hz), 93.1, 81.1 (d $J_{\text{CP}} = 2.0$ Hz), 30.60, 22.0; ^{19}F NMR (282 MHz, C_6D_6) δ $-62.44, -62.53$; ^{31}P NMR (121 MHz, C_6D_6) δ -7.59 ; IR (Neat Film, NaCl) 3060, 2961, 1654, 1605, 1493, 1470, 1448, 1396, 1323, 1166, 1127, 1060, 1016, 954, 832, 756 cm^{-1} ; HRMS (MM: ESI-APCI+) m/z calc'd for $\text{C}_{28}\text{H}_{30}^{19}\text{F}_6\text{NOP}$ $[\text{M}+\text{H}]^+$: 662.2042, found 662.2080.

(R)-2-(2-(bis(4-(trifluoromethyl)phenyl)phosphino)-5-(trifluoromethyl)phenyl)-4-isopropyl-5,5-dimethyl-4,5-dihydrooxazole (L15)



$[\alpha]_D^{25} +9.45$ (c 3.20, CHCl_3); $R_f = 0.3$ (4:1 hexanes in dichloromethane); $^1\text{H NMR}$ (500 MHz, C_6D_6) δ 8.57 (dd, $J = 3.3, 2.0$ Hz, 1H), 7.41–7.36 (m, 4H), 7.21–7.15 (m, 4H), 7.10 (dd, $J = 8.2, 2.0$ Hz, 1H), 6.78 (dd, $J = 8.0, 3.0$ Hz, 1H), 3.22 (d, $J = 8.4$ Hz, 1H), 1.55 (ddt, $J = 13.0, 8.3, 6.5$ Hz, 1H), 1.21 (s, 3H), 1.08 (s, 3H), 0.99 (d, $J = 6.5$ Hz, 3H), 0.75 (d, $J = 6.5$ Hz, 3H); $^{13}\text{C NMR}$ (126 MHz, C_6D_6) δ 159.1 (d, $J_{\text{CP}} = 4.0$ Hz), 143.5 (t, $J_{\text{CP}} = 14.8$ Hz), 142.7 (d, $J_{\text{CP}} = 30.6$ Hz), 134.5 (dd, $J_{\text{CP}} = 21.3, 15.7$ Hz), 133.7 (d, $J_{\text{CP}} = 19.5$ Hz), 131.1 (q, $J_{\text{CF}} = 3.6$ Hz), 126.4–126.1 (m), 125.9 (d, $J_{\text{CF}} = 3.2$ Hz), 126.5–125.0 (m), 123.8 (d, $J_{\text{CF}} = 3.3$ Hz), 123.3, 87.2, 81.7 (d, $J_{\text{CP}} = 1.5$ Hz), 29.1, 28.8, 21.1, 20.8, 20.8 (d, $J_{\text{CP}} = 1.8$ Hz); $^{19}\text{F NMR}$ (282 MHz, C_6D_6) δ -62.63, -62.85; $^{31}\text{P NMR}$ (121 MHz, C_6D_6) δ -7.10; IR (Neat Film, NaCl) 2974, 1652, 1397, 1323, 1165, 1128, 1060, 1017, 832, 756 cm^{-1} ; HRMS (FAB+) m/z calc'd for $\text{C}_{29}\text{H}_{26}\text{O}^{19}\text{F}_9\text{NP}$ $[\text{M}+\text{H}]^+$: 606.1608, found 606.1585.

3.6.8 Determination of enantiomeric excess

Table 3.6.8.1. Determination of enantiomeric excess

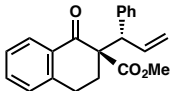
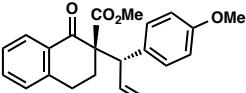
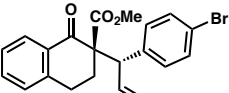
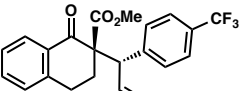
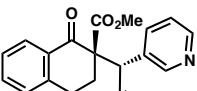
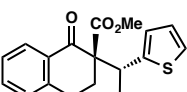
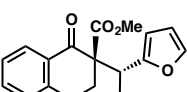
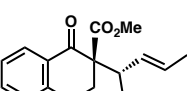
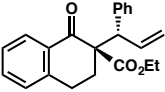
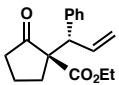
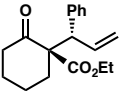
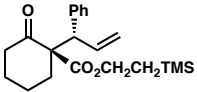
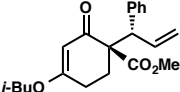
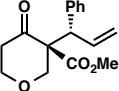
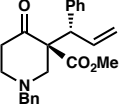
entry	compound	analytic conditions	ee (%)
1		HPLC Chiralcel OD-H, $\epsilon = 254$ nm 2% IPA/hexanes, 0.6 mL/min t_R (min): major 13.80, minor 17.89	>99
2		HPLC Chiralpak AD-H, $\epsilon = 254$ nm 2% IPA/hexanes, 0.6 mL/min t_R (min): minor 27.44, major 37.29	>99
3		HPLC Chiralpak AD-H, $\epsilon = 254$ nm 2% IPA/hexanes, 0.6 mL/min t_R (min): minor 19.71, major 23.59	99
4		SFC Chiralpak AD-H, $\epsilon = 254$ nm 5% IPA/CO ₂ , 4.0 mL/min t_R (min): minor 3.38, major 3.91	>99
5		HPLC Chiralpak AD-H, $\epsilon = 254$ nm 90% IPA/hexanes, 1.0 mL/min t_R (min): minor 13.45, major 15.72	98
6		SFC Chiralcel OJ-H, $\epsilon = 254$ nm 10% IPA/CO ₂ , 4.0 mL/min, t_R (min): major 2.96, minor 3.63	95
7		SFC Chiralpak AD-H, $\epsilon = 254$ nm 10% IPA/CO ₂ , 2.5 mL/min, t_R (min): major 5.21, minor 6.03	95
8		SFC Chiralpak IC, $\epsilon = 254$ nm 2% MeOH/CO ₂ , 2.5 mL/min, t_R (min): minor 8.23, major 8.87	90

Table 3.6.8.2 Determination of enantiomeric excess continued

entry	compound	analytic conditions	ee (%)
9		SFC Chiralpak AD-H, $\epsilon = 254$ nm 5% IPA/CO ₂ , 2.5 mL/min, t_R (min): minor 13.82, major 16.53	>99
10		HPLC Chiralcel OD-H, $\epsilon = 220$ nm 2% IPA/hexanes, 0.6 mL/min t_R (min): major 11.23, minor 12.73	99
11		SFC Chiralpak IC, $\epsilon = 210$ nm 10% IPA/CO ₂ , 4.0 mL/min t_R (min): minor 1.69, major 1.94	98
12		SFC Chiralcel OJ-H, $\epsilon = 210$ nm 3% IPA/CO ₂ , 2.5 mL/min t_R (min): minor 1.93, major 2.24	>99
13		SFC Chiralcel OD-H, $\epsilon = 254$ nm 10% IPA/CO ₂ , 2.5 mL/min t_R (min): major 3.71, minor 6.24	>99
14		SFC Chiralpak AD-H, $\epsilon = 210$ nm 5% IPA/CO ₂ , 2.5 mL/min t_R (min): minor 4.65, major 4.95	98
15		SFC Chiralpak AD-H, $\epsilon = 210$ nm 10% IPA/CO ₂ , 4.0 mL/min t_R (min): major 2.49, minor 2.94	97

3.7 REFERENCES AND NOTES

- (69) For selected reviews, see: (a) Douglas, C. J.; Overman, L. E. *Proc. Natl. Acad. Sci. U.S.A.* **2004**, *101*, 5363. (b) Christoffers, J.; Baro, A. Quaternary Stereocenters: Challenges and Solutions for Organic Synthesis, Wiley-VCH: Weinheim, 2005. (c) Trost, B. M.; Jiang, C. *Synthesis* **2006**, 369.
- (70) For reviews, see: (a) Krause, N.; Hoffmann-Röder, A. *Synthesis* **2001**, 171. (b) Christoffers, J.; Koripelly, G.; Rosiak, A.; Rössle, M. *Synthesis* **2007**, 1279. Selected examples, see: (c) Barnes, D. M.; Ji, J.; Fickes, M. G.; Fitzgerald, M. A.; King, S. A.; Morton, H. E.; Plagge, F. A.; Preskill, M.; Wagaw, S. H.; Wittenberger, S. J.; Zang, J. *J. Am. Chem. Soc.* **2002**, *124*, 13097. (d) Taylor, M. S.; Jacobsen, E. N. *J. Am. Chem. Soc.* **2003**, *125*, 11204. (e) Mase, N.; Thayumanavan, R.; Tanaka, F.; Barbas, C. F. III *Org. Lett.* **2004**, *6*, 2527. (f) Li, H.; Wang, Y.; Tang, L.; Wu, F.; Liu, X.; Guo, C.; Foxman, B. M.; Deng, L. *Angew. Chem., Int. Ed.* **2005**, *44*, 105. (g) Bencivenni, G.; Wu, L.-Y.; Mazzanti, A.; Giannichi, B.; Pesciaioli, F.; Song, M.-P.; Bartoli, G.; Melchiorre, P. *Angew. Chem., Int. Ed.* **2009**, *48*, 7200. (h) Ding, M.; Zhou, F.; Liu, Y.-L.; Wang, C.-H.; Zhao, X.-L.; Zhou, J. *Chem. Sci.* **2011**, *2*, 2035. (i) Chauhan, P.; Chimni, S. S. *Adv. Synth. Catal.* **2011**, *353*, 3203.

- (71) For reviews, see: (a) Ito, H.; Taguchi, T. *Chem. Soc. Rev.* **1999**, 28, 43. (b) Martín Castro, A. M. *Chem. Rev.* **2004**, 104, 2939. (c) Ilardi, E. A.; Stivala, C. E.; Zakarian, A. *Chem. Soc. Rev.* **2009**, 38, 3133. For selected communication, see: (d) Yoon, T. P.; MacMillan, D. W. C. *J. Am. Chem. Soc.* **2001**, 123, 2911. (e) Helmboldt, H.; Hiersemann, M. *Tetrahedron* **2003**, 59, 4031. (f) Abraham, L.; Körner, M.; Schwab, P.; Hiersemann, M. *Adv. Synth. Catal.* **2004**, 346, 1281. (g) Linton, E. C.; Kozlowski, M. C. *J. Am. Chem. Soc.* **2008**, 130, 16162. (h) Uyeda, C.; Jacobsen, E. N. *J. Am. Chem. Soc.* **2008**, 130, 9228. (i) Uyeda, C.; Rötheli, A. R.; Jacobsen, E. N. *Angew. Chem., Int. Ed.* **2010**, 49, 9753.
- (72) Streuff, J.; White, D. E.; Virgil, S. C.; Stoltz, B. M. *Nature Chem.* **2010**, 2, 192.
- (73) (a) Doyle, A. G.; Jacobsen, E. N. *Angew. Chem., Int. Ed.* **2007**, 46, 3701. (b) Trost, B. M.; Cramer, N.; Silverman, S. M. *J. Am. Chem. Soc.* **2007**, 129, 12396. (c) Trost, B. M.; Zhang, Y. *J. Am. Chem. Soc.* **2007**, 129, 14548. (d) Trost, B. M.; Miller, J. R.; Hoffman, C. M., Jr. *J. Am. Chem. Soc.* **2011**, 133, 8165. (e) Trost, B. M.; Silverman, S. M.; Stambuli, J. P. *J. Am. Chem. Soc.* **2011**, 133, 19483. (f) Tan, J.; Cheon, C.-H.; Yamamoto, H. *Angew. Chem., Int. Ed.* **2012**, 51, 8264.
- (74) See reference 55d and: Helmchen, G.; Kazmaier, U.; Fröster, S. In *Catalytic Asymmetric Synthesis*. Ojima, I. Ed; 3rd ed. Wiley, New Jersey, 2010, p. 497.

- (75) For the first example: Takeuchi, R.; Kashio, M. *Angew. Chem., Int. Ed. Engl.* **1997**, *36*, 263.
- (76) For recent reviews, see: (a) Helmchen, G.; Dahnz, A.; Dübon, P.; Schelwies, M.; Weihofen, R. *Chem. Commun.* **2007**, 675. (b) Helmchen, G. In *Iridium Complexes in Organic Synthesis*; Oro, L. A.; Claver, C. Eds.; Wiley-VCH: Weinheim, Germany, 2009; p. 211. (c) Hartwig, J. F.; Pouy, M. J. *Top. Organomet. Chem.* **2011**, *34*, 169. (d) Tosatti, P.; Nelson, A.; Marsden, S. P. *Org. Biomol. Chem.* **2012**, *10*, 3147. (e) Liu, W.-B.; Xia, J.-B.; You, S.-L. *Top. Organomet. Chem.* **2012**, *38*, 155.
- (77) Janssen, J. P.; Helmchen, G. *Tetrahedron Lett.* **1997**, *38*, 8025.
- (78) Ohmura, T.; Hartwig, J. F. *J. Am. Chem. Soc.* **2002**, *124*, 15164.
- (79) For mechanistic studies, see: (a) Kiener, C. A.; Shu, C.; Incarvito, C.; Hartwig, J. F. *J. Am. Chem. Soc.* **2003**, *125*, 14272. (b) Madrahimov, S. T.; Markovic, D.; Hartwig, J. F. *J. Am. Chem. Soc.* **2009**, *131*, 7228. (c) Spiess, S.; Raskatov, J. A.; Gnamm, C.; Brödner, K.; Helmchen, G. *Chem. Eur. J.* **2009**, *15*, 11087. (d) Raskatov, J. A.; Spiess, S.; Gnamm, C.; Brödner, K.; Rominger, F.; Helmchen, G. *Chem. Eur. J.* **2010**, *16*, 6601. (e) Madrahimov, S. T.; Hartwig, J. F. *J. Am. Chem. Soc.* **2012**, *134*, 8136. (f) Raskatov, J. A.; Jäkel, M.; Straub, B. F.; Rominger, F.;

- Helmchen, G. *Chem. Eur. J.* **2012**, *18*, 14314. (g) Leitner, A.; Shu, C.; and Hartwig, J. F. *Proc. Natl. Acad. Sci. U. S. A.* **2004**, *101*, 5830. (h) Leitner, A.; Shekhar, S.; Pouy, M. J.; Hartwig, J. F. *J. Am. Chem. Soc.* **2005**, *127*, 15506. For a review: (g) Hartwig, J. F.; Stanley, L. M. *Acc. Chem. Res.* **2010**, *43*, 1461.
- (80) Selected examples, see: (a) Lipowsky, G.; Miller, N.; Helmchen, G. *Angew. Chem., Int. Ed.* **2004**, *43*, 4595. (b) Alexakis, A.; Polet, D. *Org. Lett.* **2004**, *6*, 3529. (c) Graening, T.; Hartwig, J. F. *J. Am. Chem. Soc.* **2005**, *127*, 17192. (d) Weix, D. J.; Hartwig, J. F. *J. Am. Chem. Soc.* **2007**, *129*, 7720. (e) He, H.; Zheng, X.-J.; Li, Y.; Dai, L.-X.; You, S.-L. *Org. Lett.* **2007**, *9*, 4339. (f) Spiess, S.; Welter, C.; Franck, G.; Taquet, J.-P.; Helmchen, G. *Angew. Chem., Int. Ed.* **2008**, *47*, 7652. (g) Liu, W.-B.; He, H.; Dai, L.-X.; You, S.-L. *Org. Lett.* **2008**, *10*, 1815. (h) Chen, W.; Hartwig, J. F. *J. Am. Chem. Soc.* **2012**, *134*, 15249. (i) Hamilton, J. Y.; Sarlah, D.; Carreira, E. M. *J. Am. Chem. Soc.* **2013**, *135*, 994. (j) Bartels, B.; Helmchen, G. *Chem. Commun.* 1999, 741, and references therein.
- (81) (a) Dahnz, A.; Helmchen, G. *Synlett*, **2006**, 697. (b) Polet, D.; Alexakis, A.; Tissot-Croset, K.; Corminboeuf, C.; Ditrich, K. *Chem. Eur. J.* **2006**, *12*, 3596. (c) Xu, Q.-L.; Dai, L.-X.; You, S.-L. *Adv. Synth. Catal.* **2012**, *354*, 2275.

- (82) (a) Kanayama, T.; Yoshida, K.; Miyabe, H.; Takemoto, Y. *Angew. Chem., Int. Ed.* **2003**, *42*, 2054. (b) Chen, W.; Hartwig, J. F. *J. Am. Chem. Soc.* **2013**, *135*, 2068.
- (83) At the time these studies were conducted, a diastereoselective allylic alkylation of aldehydes was reported: Krautwald, S.; Sarlah, D.; Schafroth, M. A.; Carreira, E. *M. Science*, **2013**, *340*, 1065.
- (84) The Ir-phosphoramidite complex was generated *in situ* by treatment of [Ir(cod)Cl]₂ and ligand with TBD, see: (a) Welter, C.; Koch, O.; Lipowsky, G.; Helmchen, G. *Chem. Commun.* **2004**, 896. (b) Shu, C.; Leitner, A.; Hartwig, J. F. *Angew. Chem., Int. Ed.* **2004**, *43*, 4797, and reference 87b below.
- (85) Methyl 2-oxocyclohexanecarboxylate was previously employed in Ir-catalyzed allylation with 95% ee and 1:1 dr, see ref 81b for detail.
- (86) For a review of the use of phosphoramidite ligands in asymmetric catalysis, see: Teichert, J. F.; Feringa, B. L. *Angew. Chem., Int. Ed.* **2010**, *49*, 2486.
- (87) (a) Liu, W.-B.; He, H.; Dai, L.-X.; You, S.-L. *Synthesis* **2009**, 2076. (b) Liu, W.-B.; Zheng, C.; Zhuo, C.-X.; Dai, L.-X.; You, S.-L. *J. Am. Chem. Soc.* **2012**, *134*, 4812.

- (88) (a) Wu, Q.-F.; He, H.; Liu, W.-B.; You, S.-L. *J. Am. Chem. Soc.* **2010**, *132*, 11418. (b) Zhuo, C.-X.; Liu, W.-B.; Wu, Q.-F.; You, S.-L. *Chem. Sci.* **2012**, *3*, 205. (c) Wu, Q.-F.; Zheng, C.; You, S.-L. *Angew. Chem., Int. Ed.* **2012**, *51*, 1680. For an example using Ir-complex/Lewis acid: (d) Schafroth, M. A.; Sarlah, D.; Krautwald, S.; Carreira, E. M. *J. Am. Chem. Soc.* **2012**, *134*, 20276.
- (89) Poor regioselectivity was observed when aliphatic allyl carbonates, such as crotyl carbonate, were employed.
- (90) See Appendix A4 for details.
- (91) We and others have extensively investigated the enantioselective decarboxylative allylic alkylation of cyclic systems, see references 3, 9, 10, 15, 16a, 16d, 25 and: Burger, E. C.; Barron, B. R.; Tunge, J. A. *Synlett* **2006**, 2824.
- (92) Attempts to establish a single-vessel diallylation protocol have, thus far, proved unsuccessful. Subjecting allyl 2-oxocyclohexanecarboxylate to the optimized reaction conditions resulted in nonstereoselective decarboxylative allylic alkylation. Sequential addition of all reaction components also failed.

(93) See experimental section for the determination of the relative configuration.

Error! Bookmark not defined.

(94) McDougal, N. T.; Streuff, J.; Mukherjee, H.; Virgil, S. C.; Stoltz, B. M. *Tetrahedron Lett.* **2010**, *51*, 5550.

(95) (a) Wuts, P. G. M.; Ashford, S. W.; Anderson, A. M.; Atkins, J. R. *Org. Lett.* **2003**, *5*, 1483. (b) Malkov, A. V.; Gouriou, L.; Lloyd-Jones, G. C.; Starý, I.; Langer, V.; Spoor, P.; Vinader, V.; Kočovský, P. *Chem. Eur. J.* **2006**, *12*, 6910.

(96) (a) Mander, L. N.; Sethi, S. P. *Tetrahedron Lett.* **1983**, *24*, 5425. (b) Brown, D. S.; Marples, B. A.; Smith, P.; Walton, L. *Tetrahedron* **1995**, *51*, 3587.

APPENDIX 3

Spectra Related to Chapter 3:

*Construction of Vicinal Tertiary and All-Carbon Quaternary
Stereocenters via Ir-Catalyzed Regio-, Diastereo-, and Enantioselective
Allylic Alkylation and Applications in Sequential Pd-Catalysis*

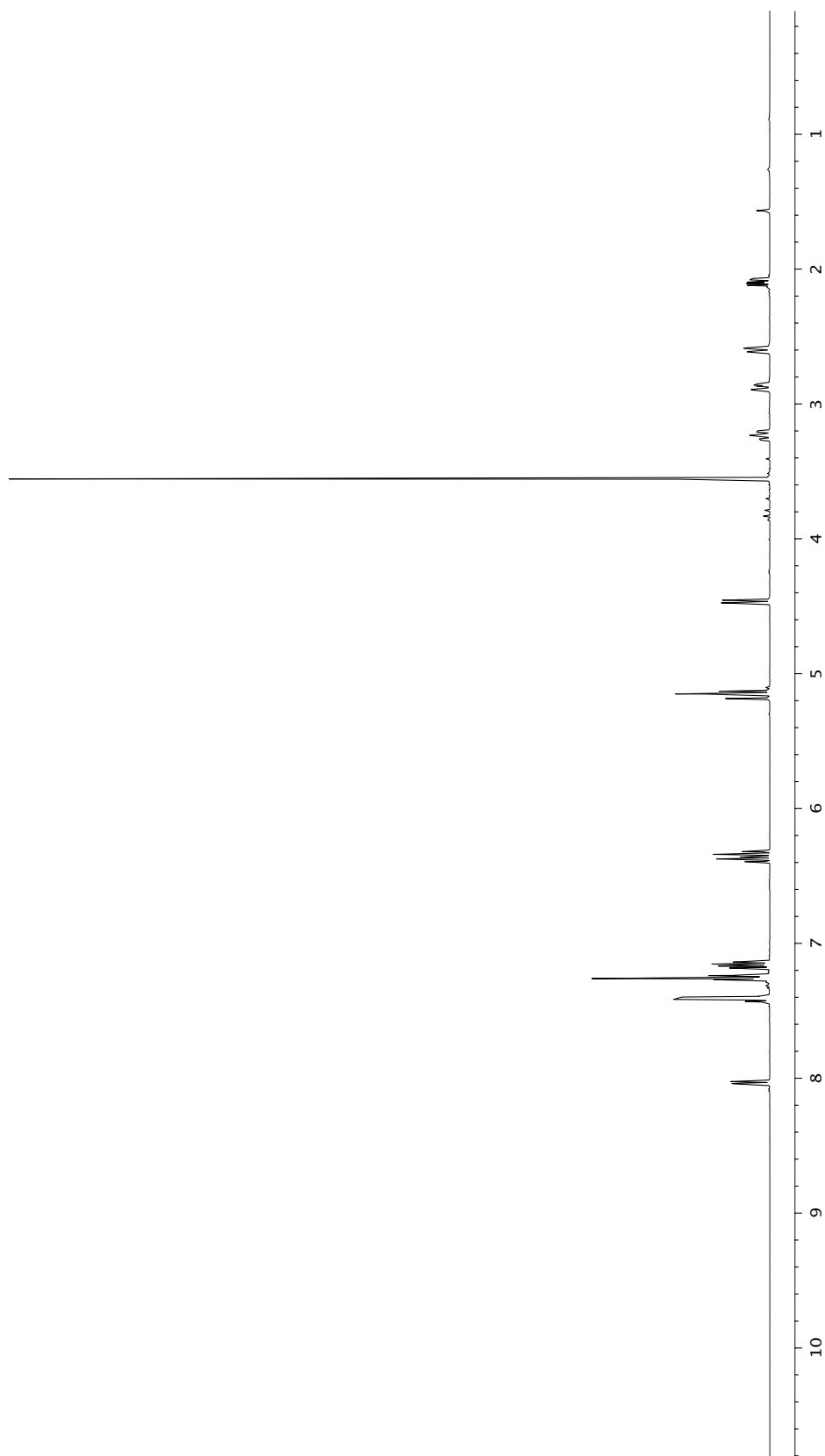
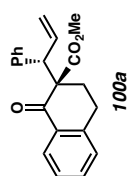


Figure A3.1 ¹H NMR (500 MHz, CDCl₃) of compound **100a**.

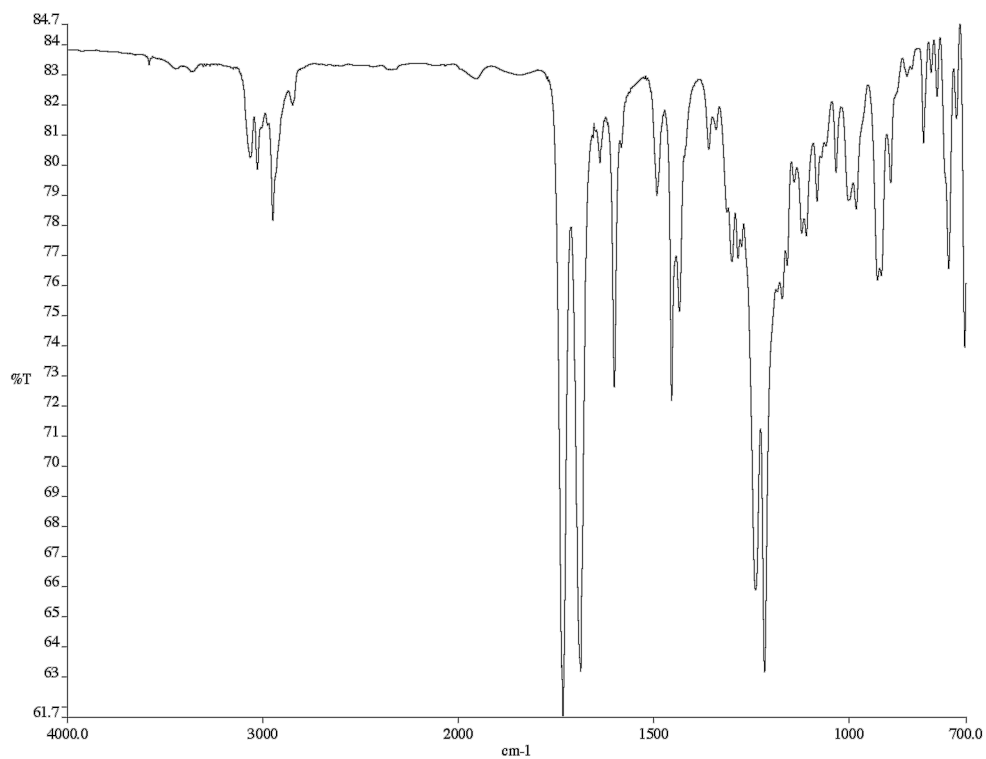


Figure A3.2 Infrared spectrum (thin film/NaCl) of compound **100a**.

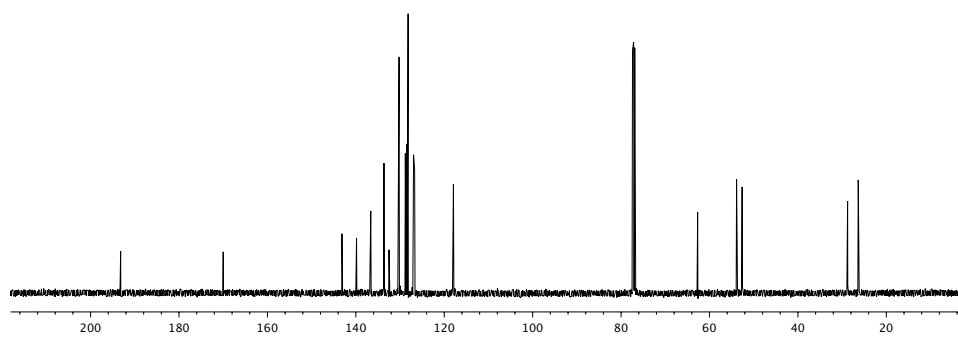


Figure A3.3 ¹³C NMR (125 MHz, CDCl₃) of compound **100a**.

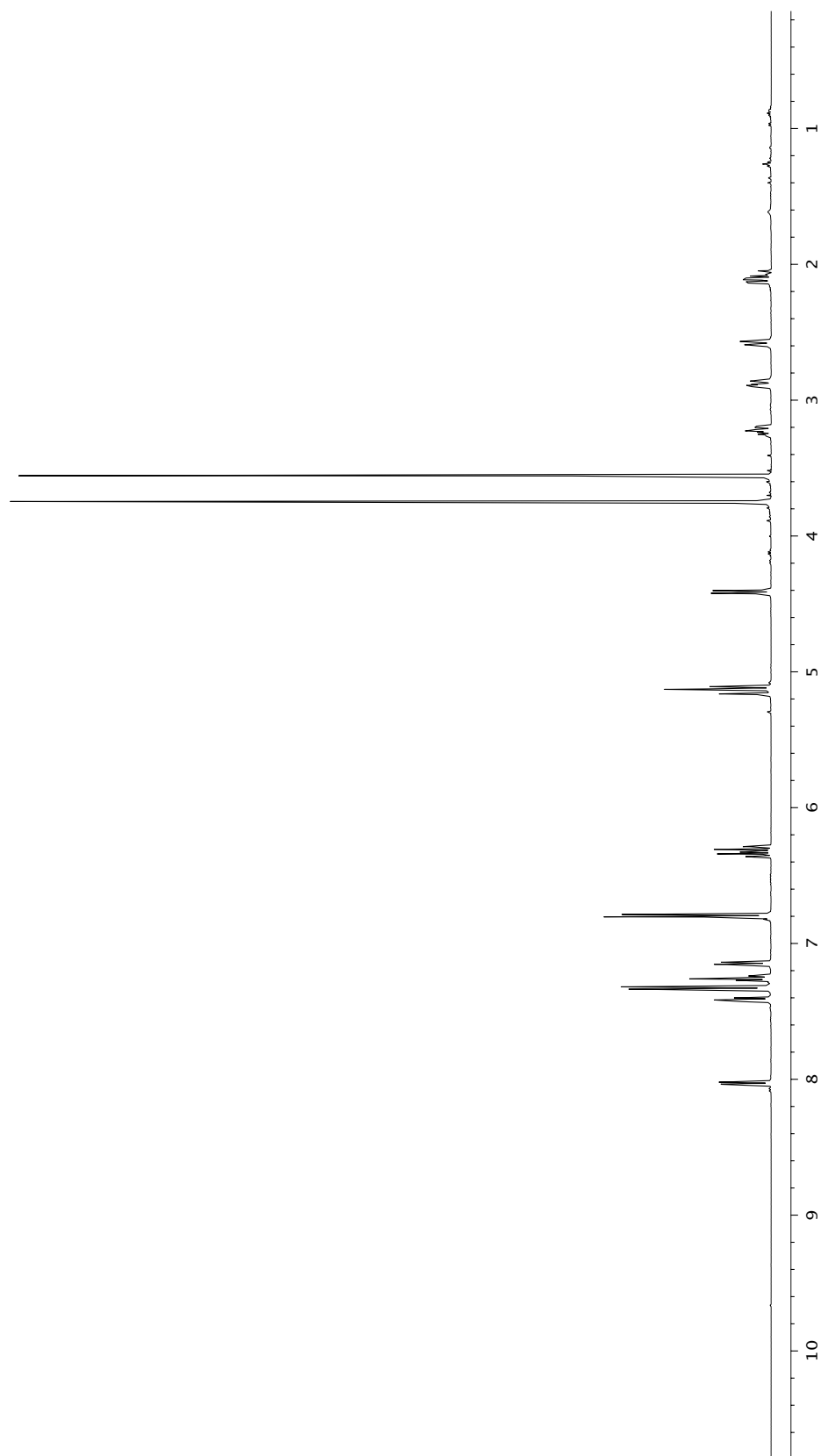
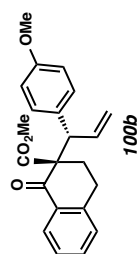


Figure A3.4 ¹H NMR (500 MHz, CDCl₃) of compound **100b**.

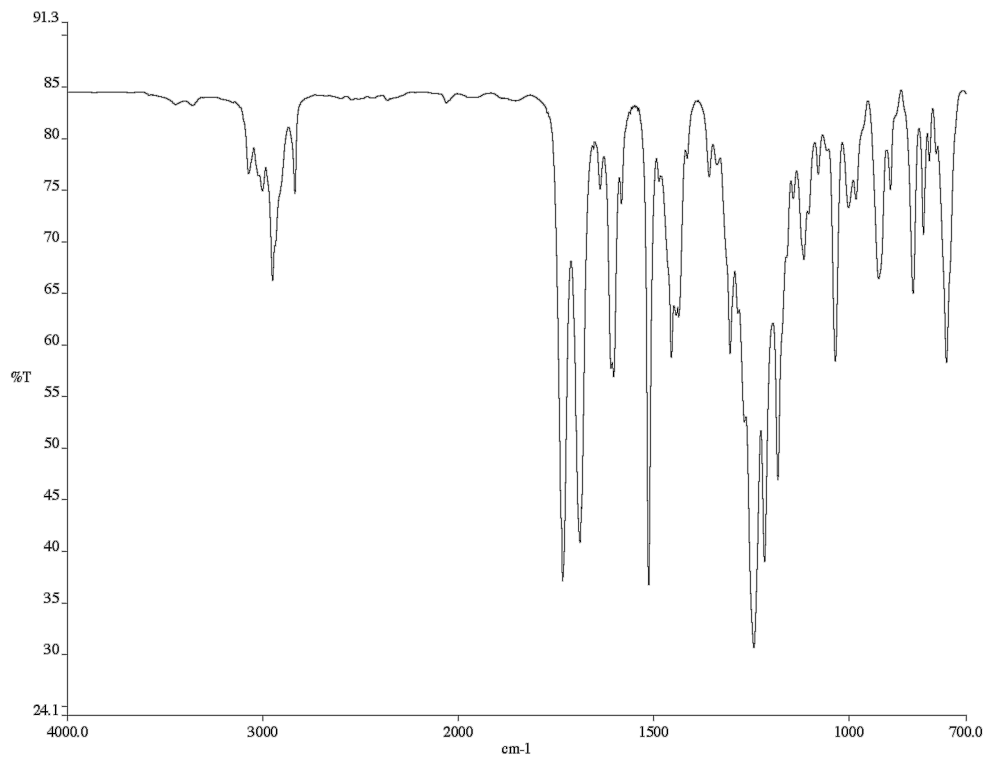


Figure A3.6 Infrared spectrum (thin film/NaCl) of compound **100b**.

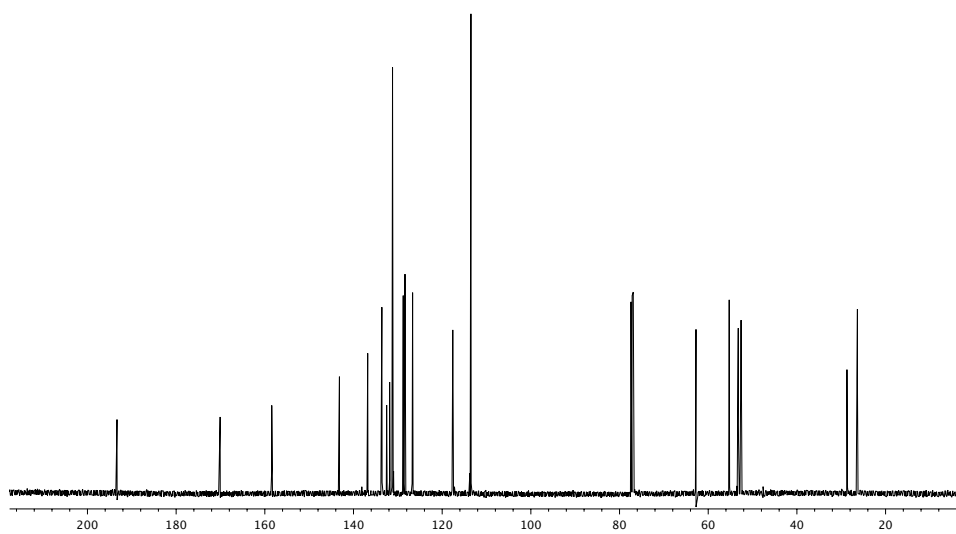


Figure A3.6 ¹³C NMR (125 MHz, CDCl₃) of compound **100b**.

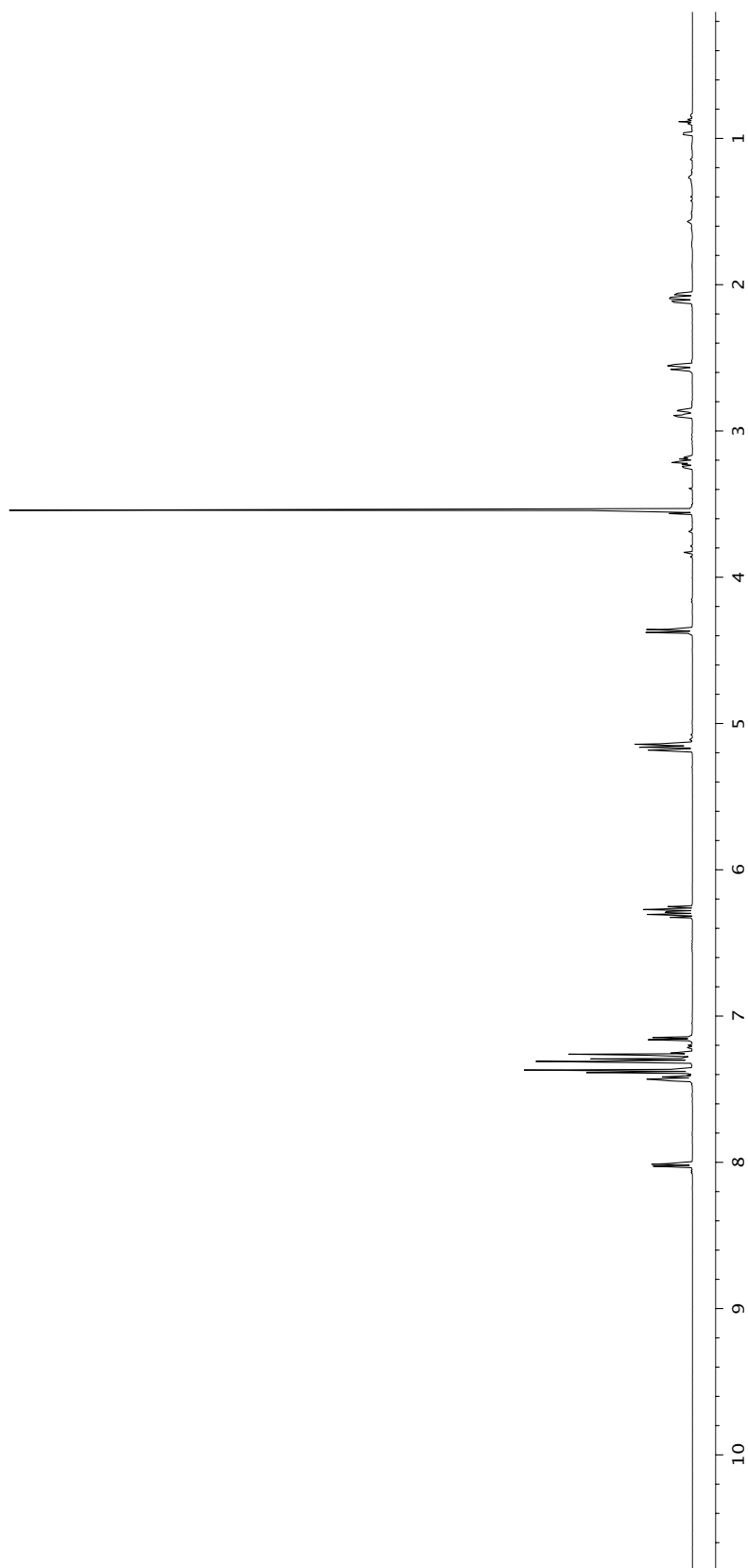
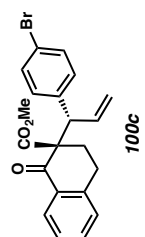


Figure A3.7 ^1H NMR (500 MHz, CDCl_3) of compound **100c**.

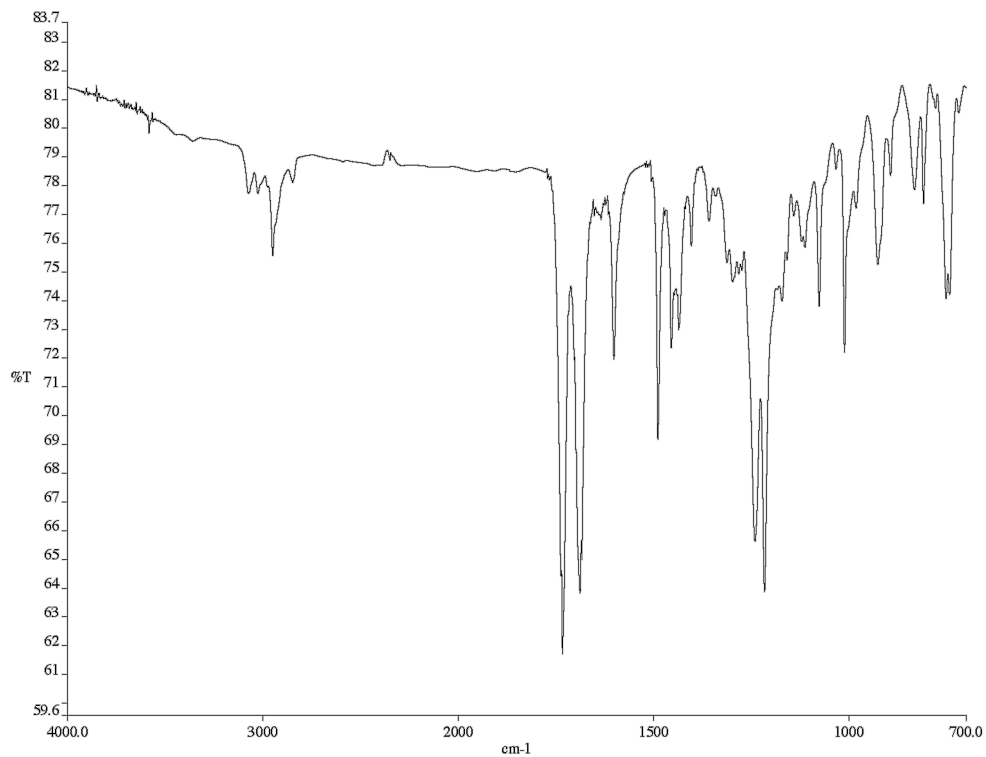


Figure A3.8 Infrared spectrum (thin film/NaCl) of compound **100c**.

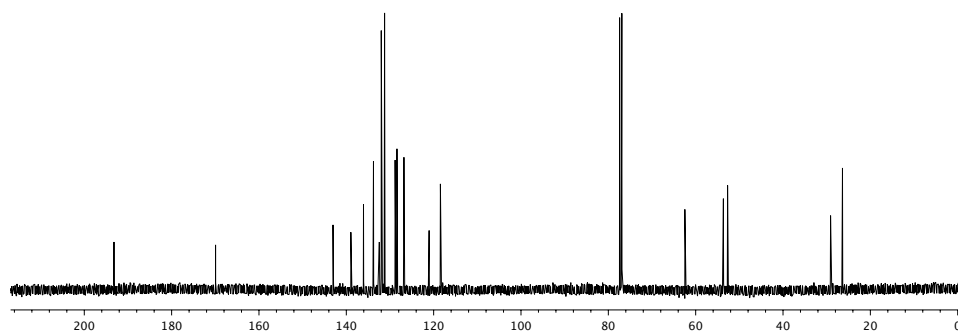


Figure A3.9 ¹³C NMR (125 MHz, CDCl₃) of compound **100c**.

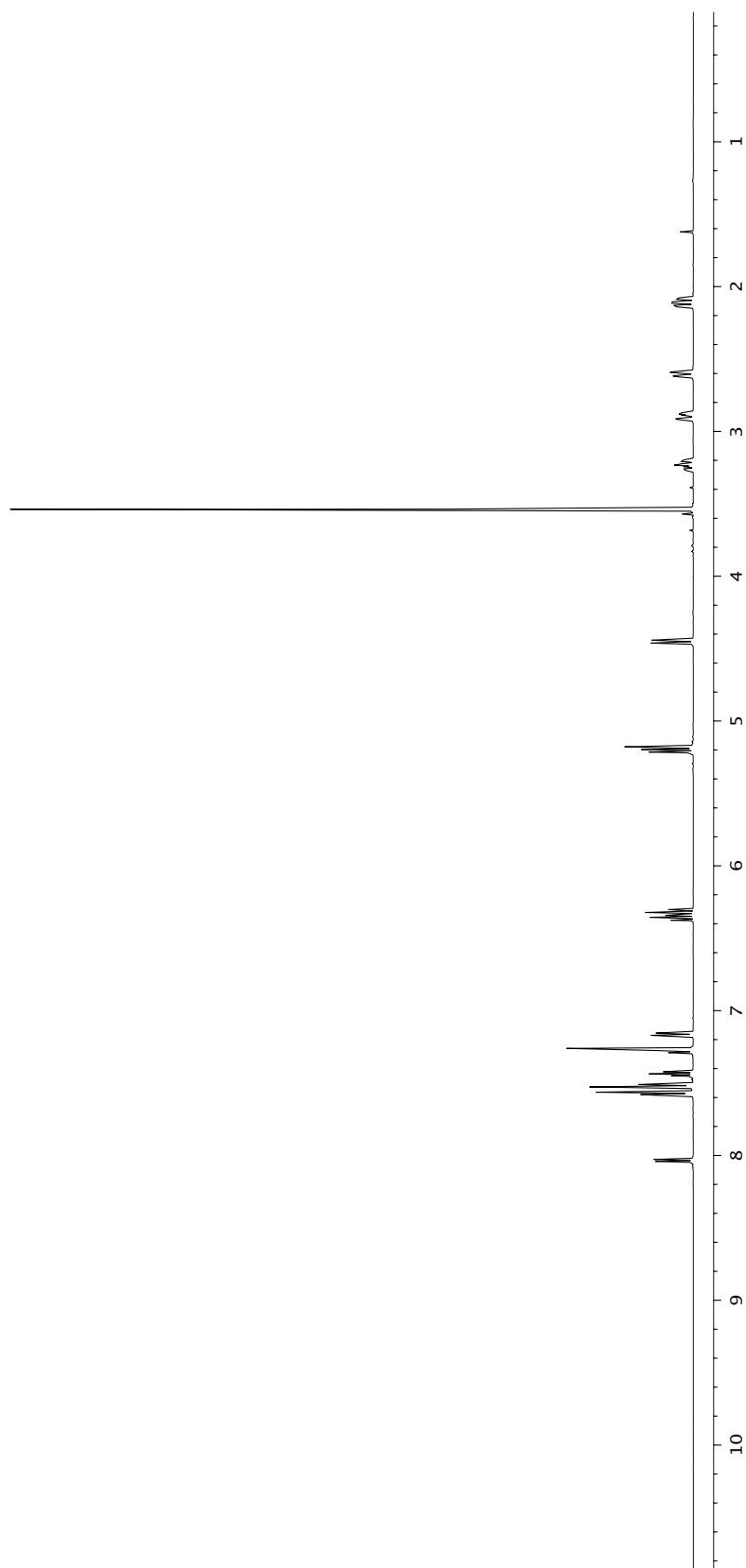
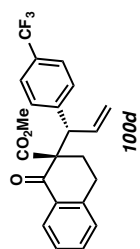


Figure A3.10 ¹H NMR (500 MHz, CDCl₃) of compound **100d**.

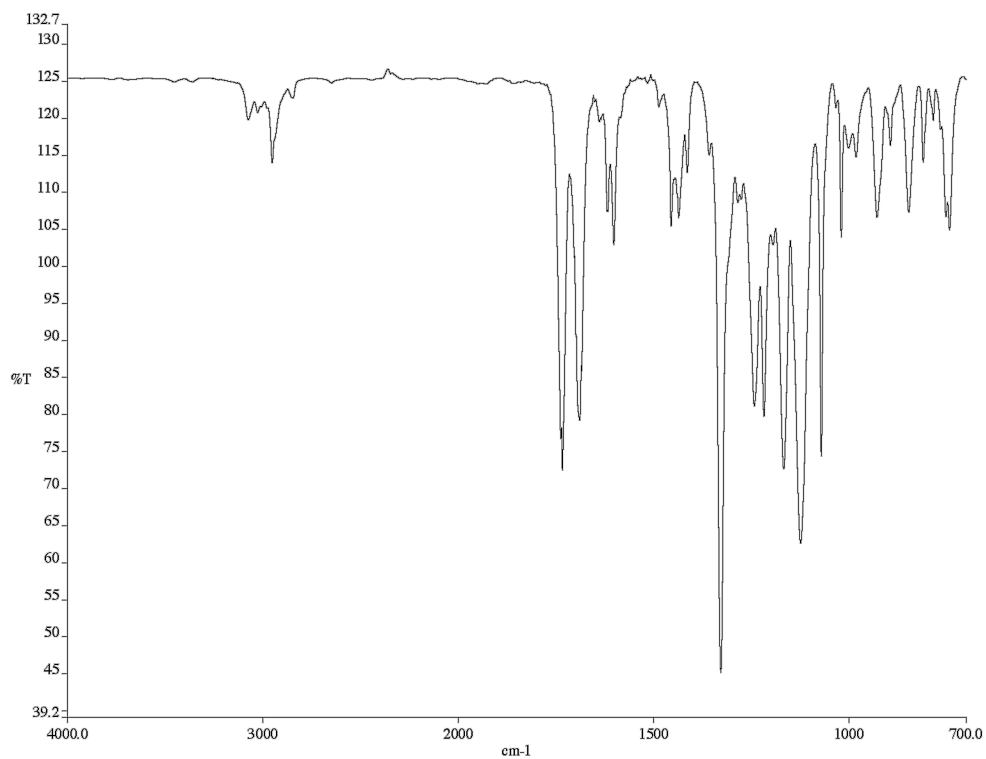


Figure A3.11 Infrared spectrum (thin film/NaCl) of compound **100d**.

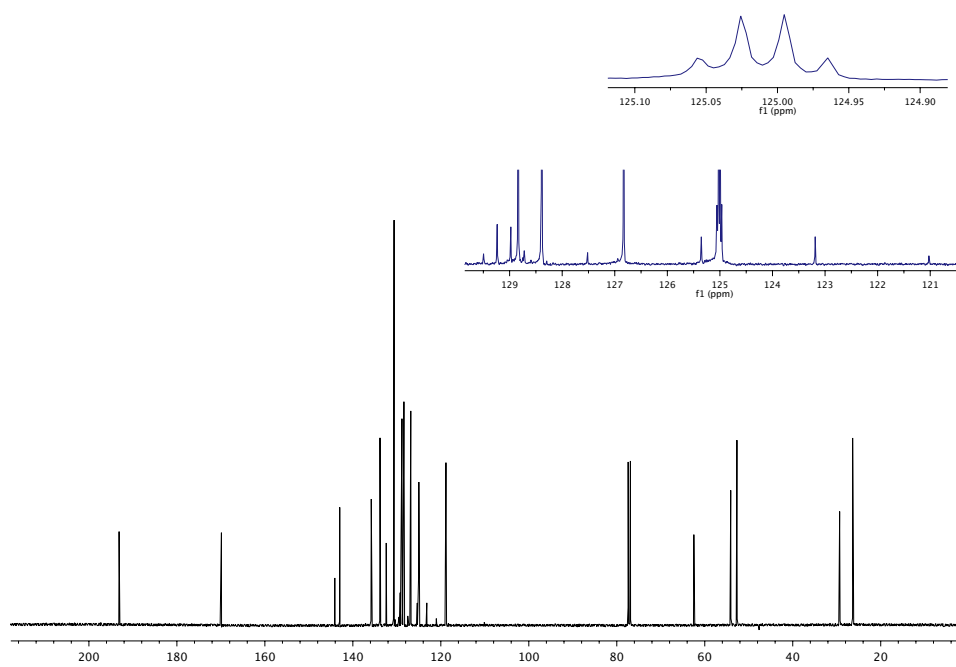


Figure A3.12 ¹³C NMR (125 MHz, CDCl₃) of compound **100d**.

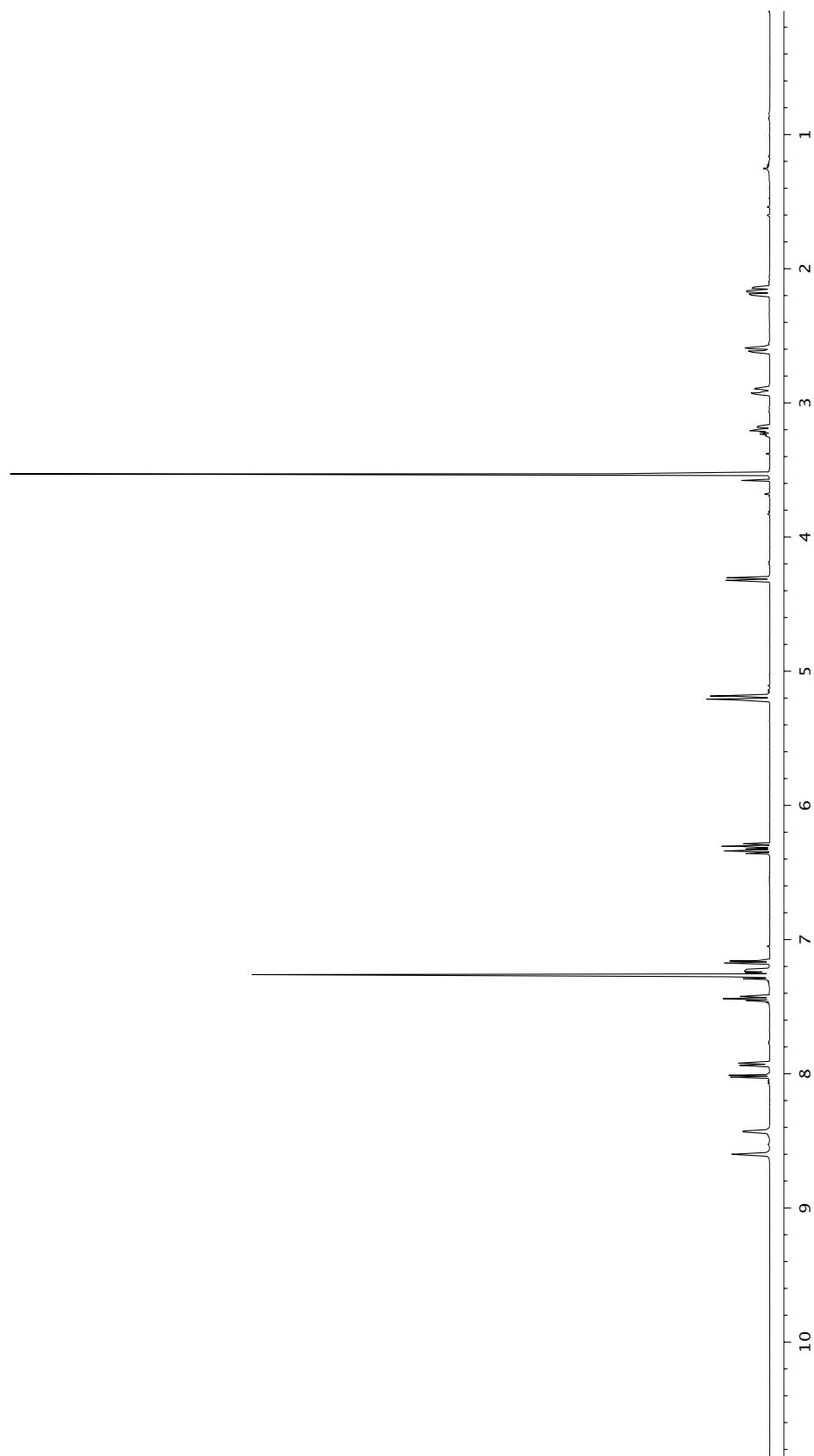
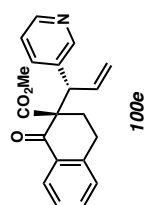


Figure A3.13 ^1H NMR (500 MHz, CDCl_3) of compound **100e**.

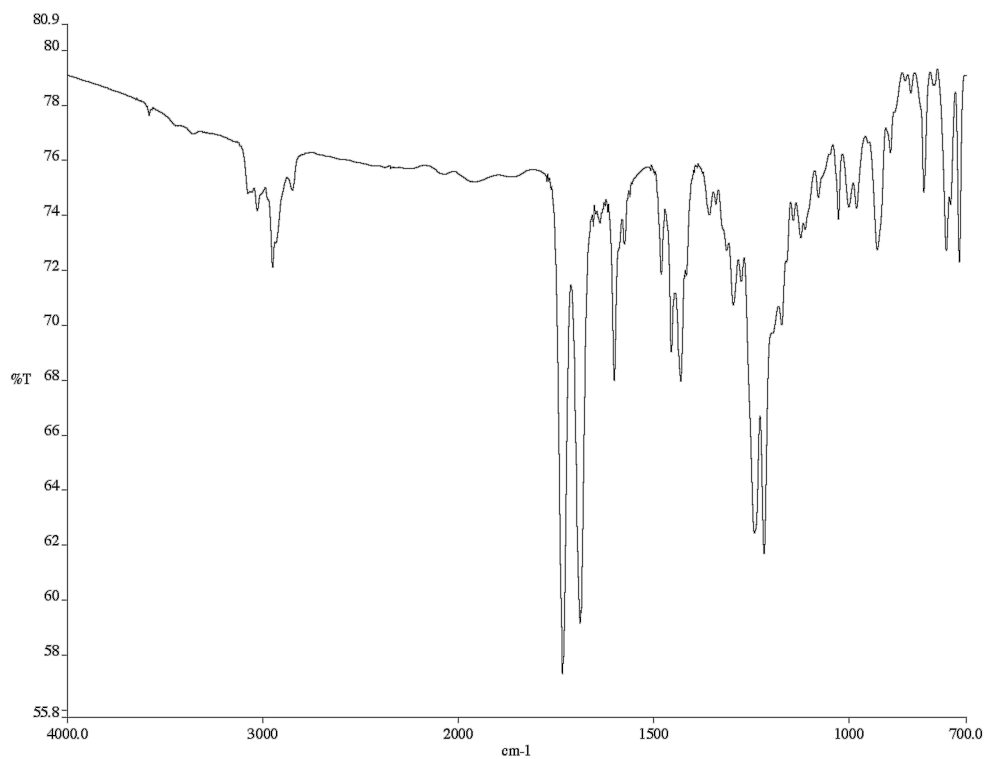


Figure A3.14 Infrared spectrum (thin film/NaCl) of compound **100e**.

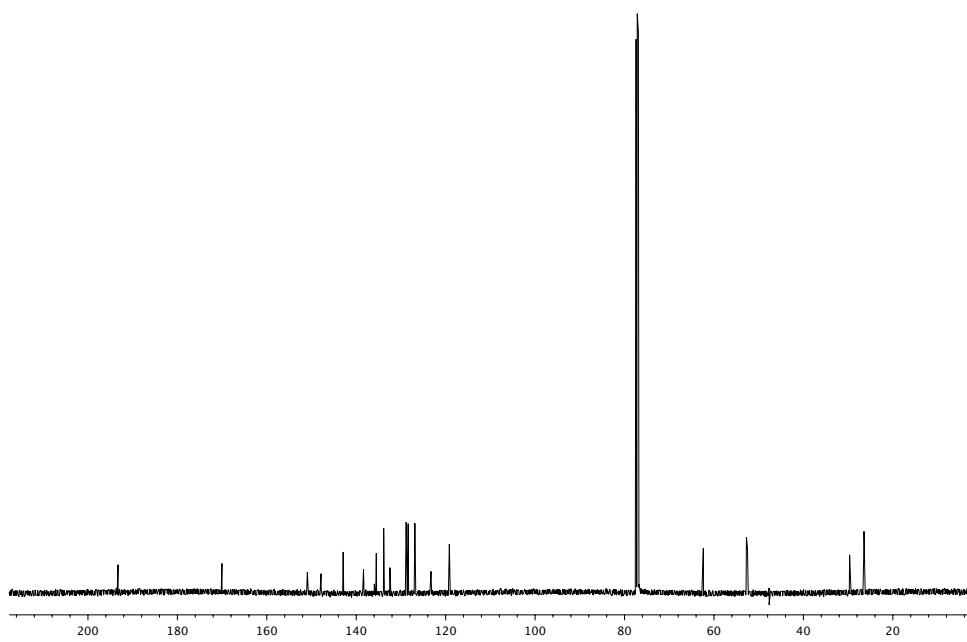


Figure A3.15 ¹³C NMR (125 MHz, CDCl₃) of compound **100e**.

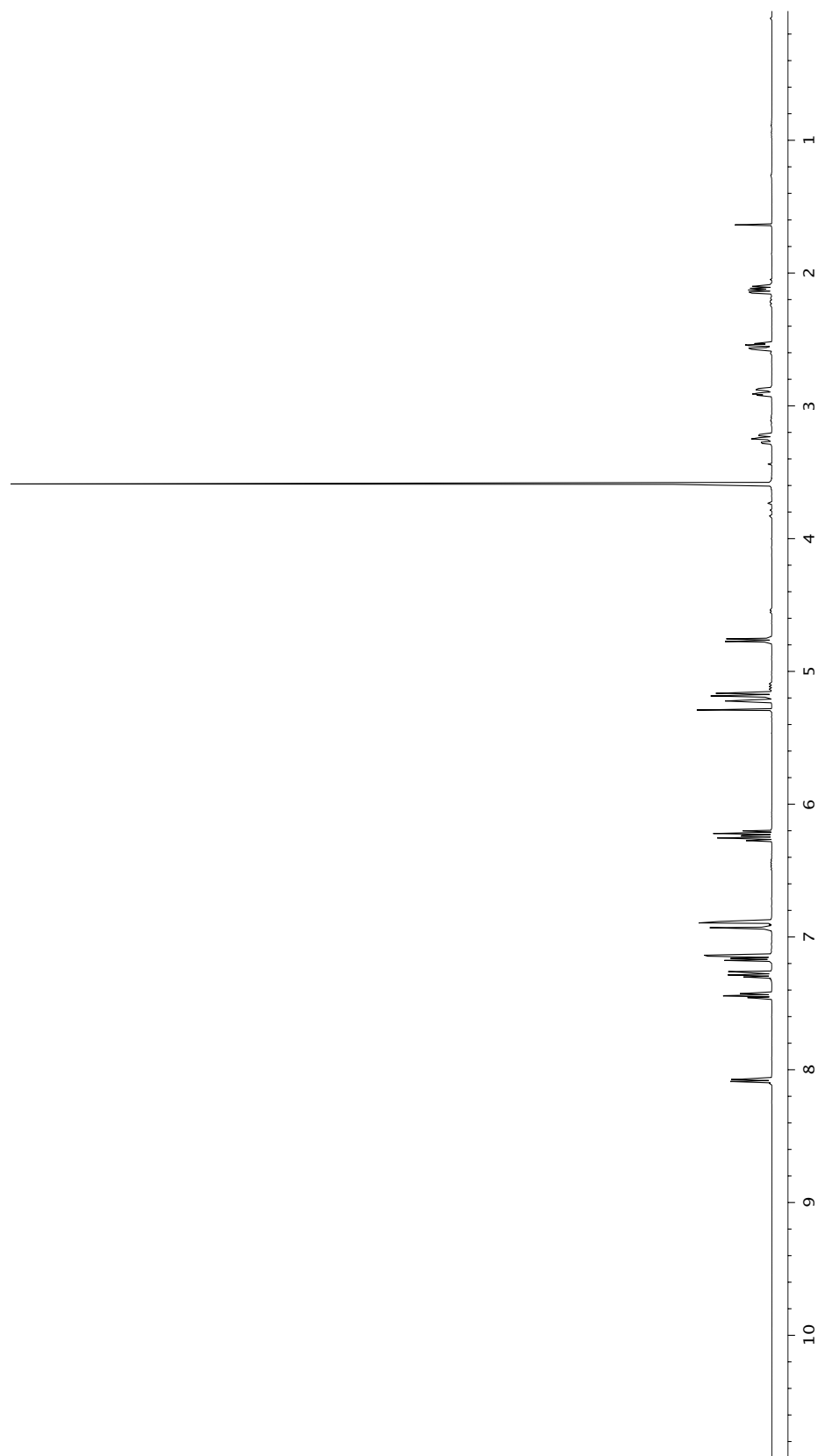
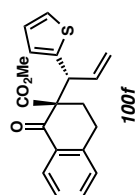


Figure A3.16 ¹H NMR (500 MHz, CDCl₃) of compound **100f**.

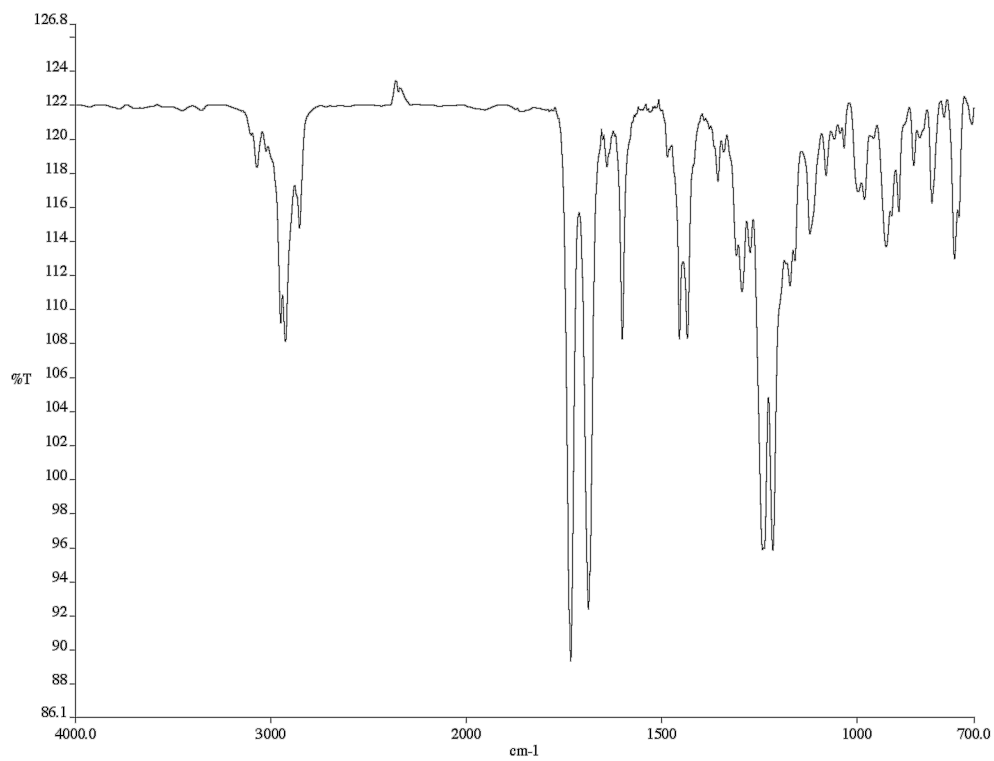


Figure A3.17 Infrared spectrum (thin film/NaCl) of compound **100f**.

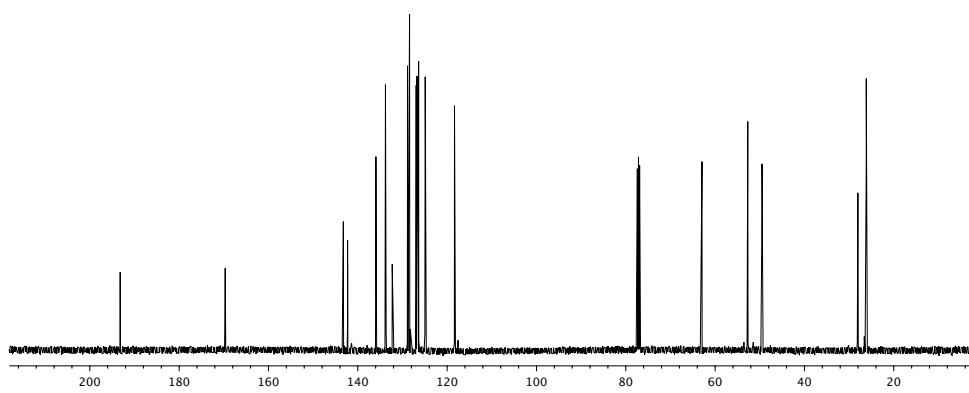


Figure A3.18 ¹³C NMR (125 MHz, CDCl₃) of compound **100f**.

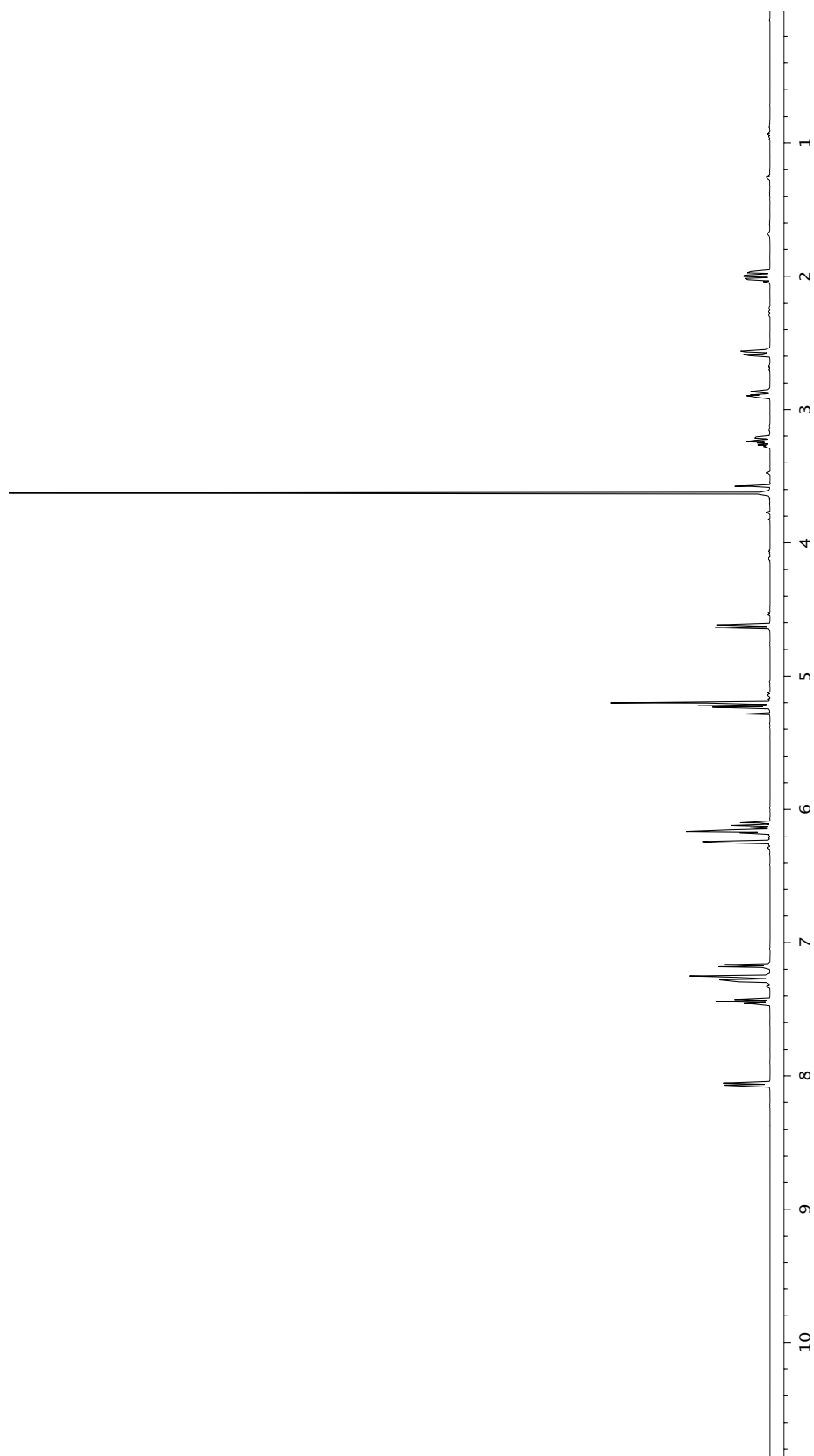
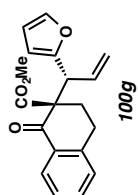


Figure A3.19 ¹H NMR (500 MHz, CDCl₃) of compound 100g.

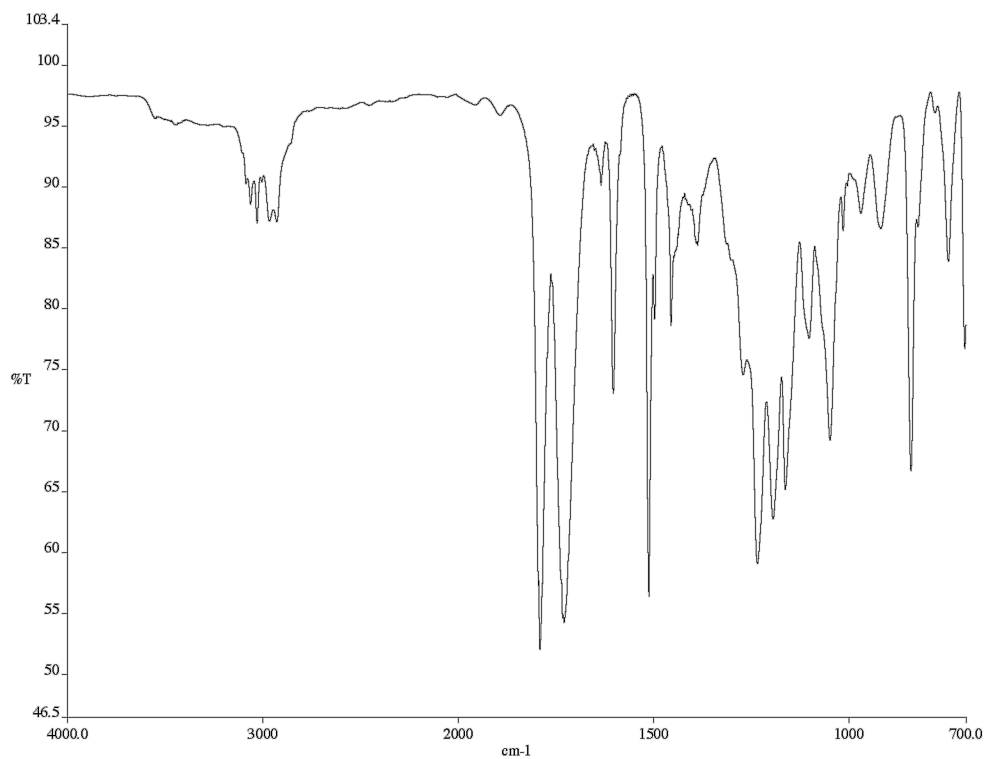


Figure A3.20 Infrared spectrum (thin film/NaCl) of compound **100g**.

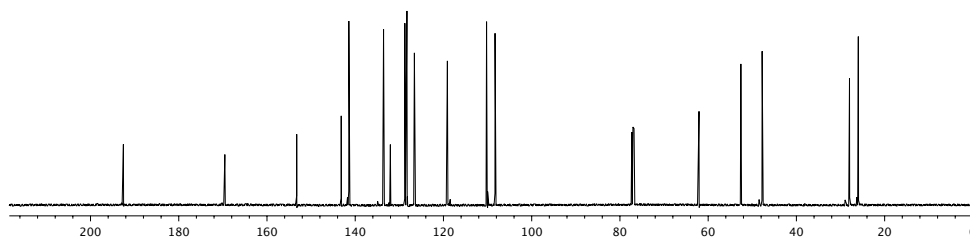


Figure A3.21 ¹³C NMR (125 MHz, CDCl₃) of compound **100g**.

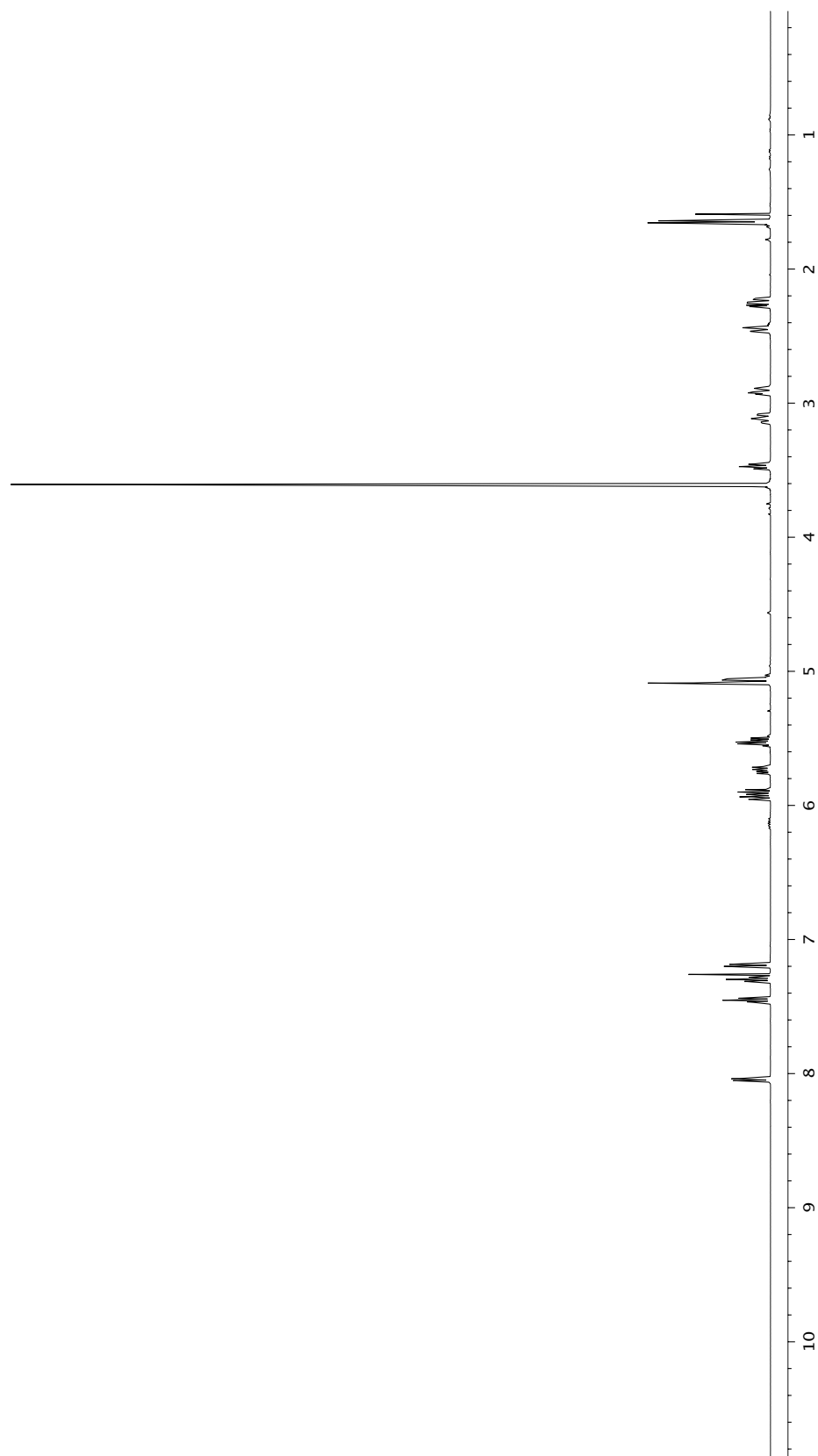
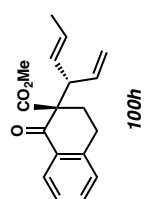


Figure A3.22 ¹H NMR (500 MHz, CDCl₃) of compound 100h.

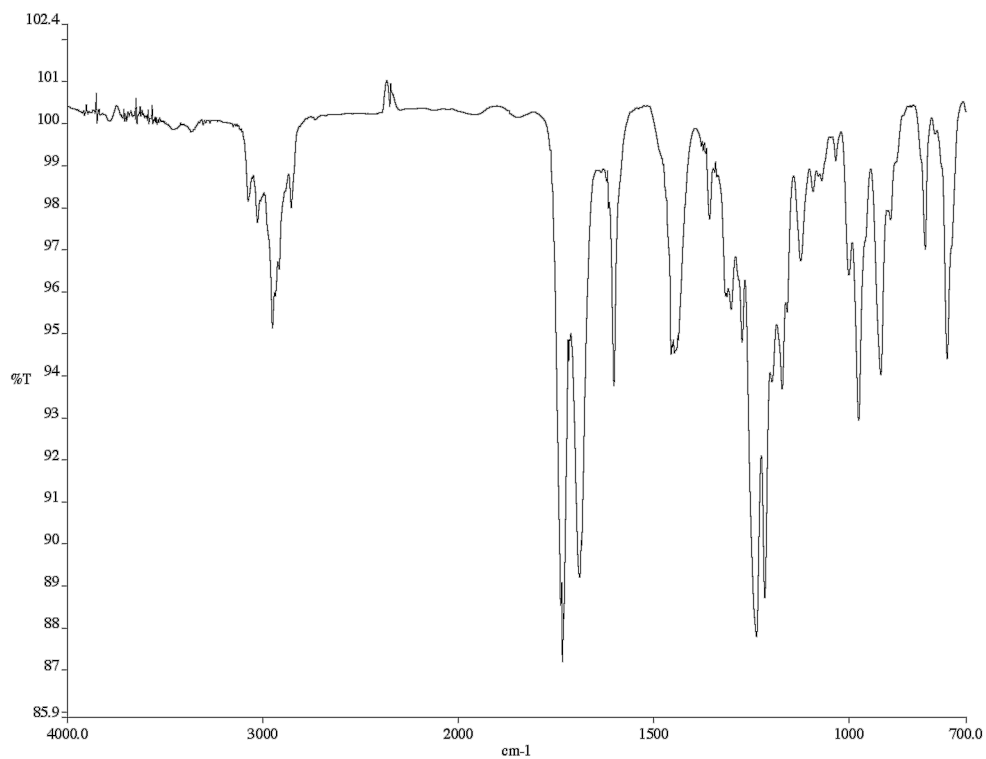


Figure A3.23 Infrared spectrum (thin film/NaCl) of compound **100h**.

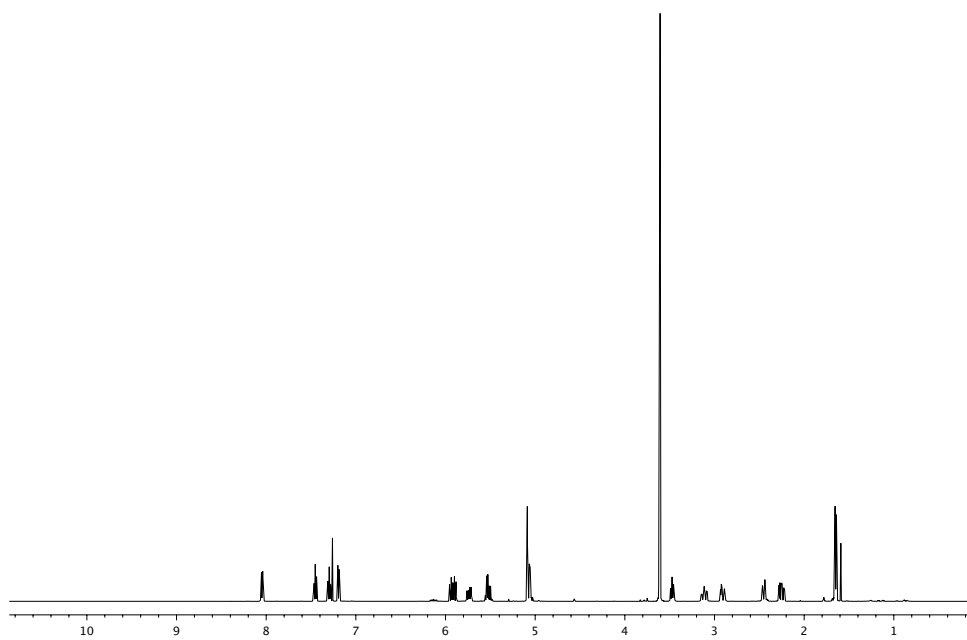


Figure A3.24 ¹³C NMR (125 MHz, CDCl₃) of compound **100h**.

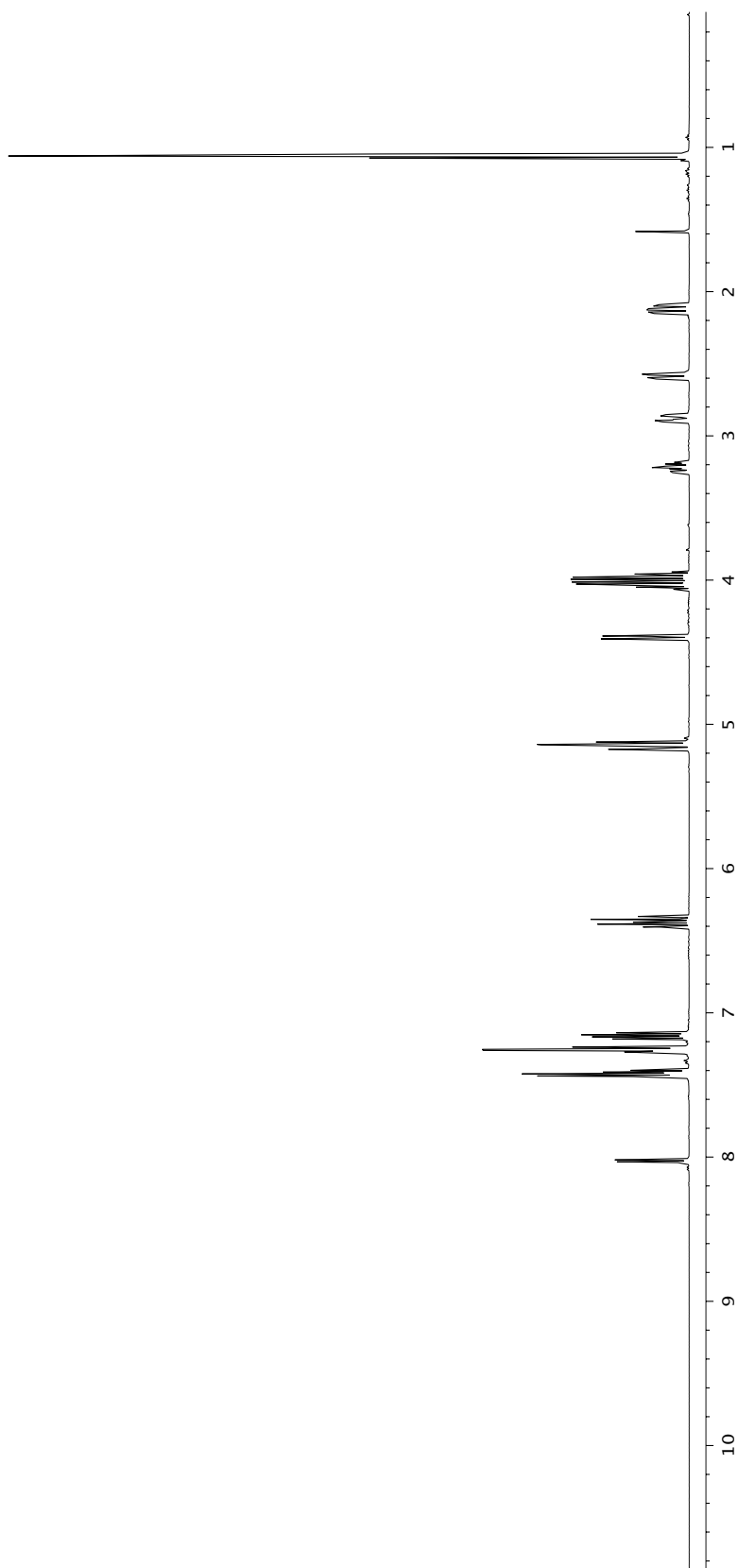
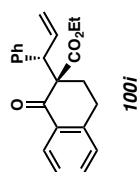


Figure A3.25 ¹H NMR (500 MHz, CDCl₃) of compound **100i**.

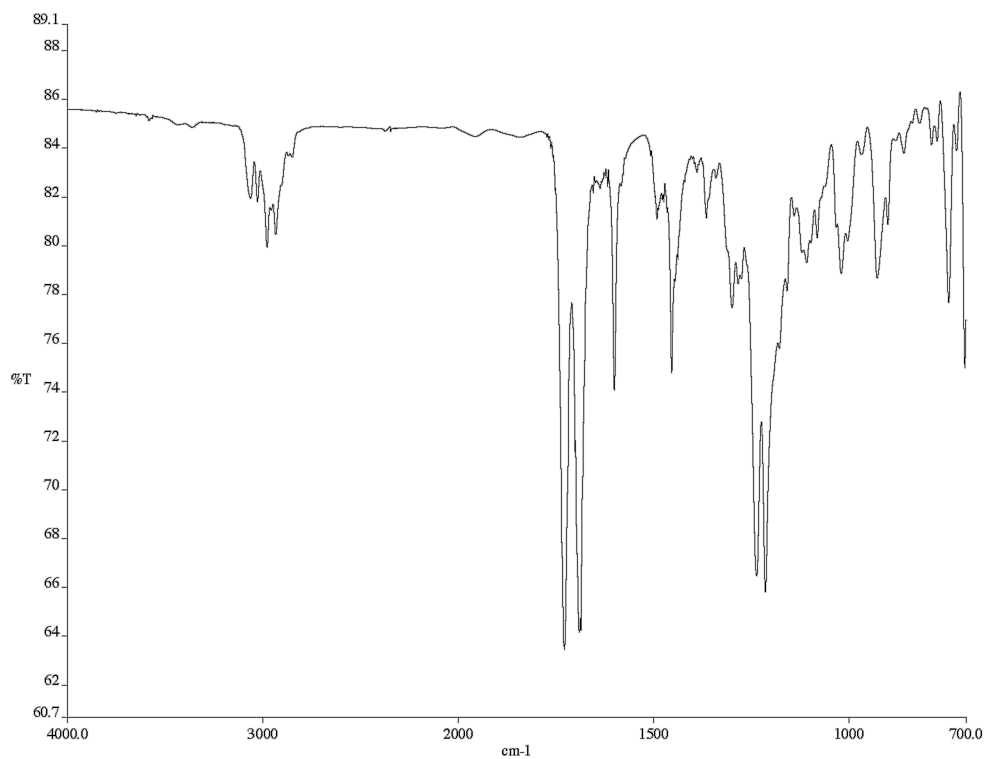


Figure A3.26 Infrared spectrum (thin film/NaCl) of compound **100i**.

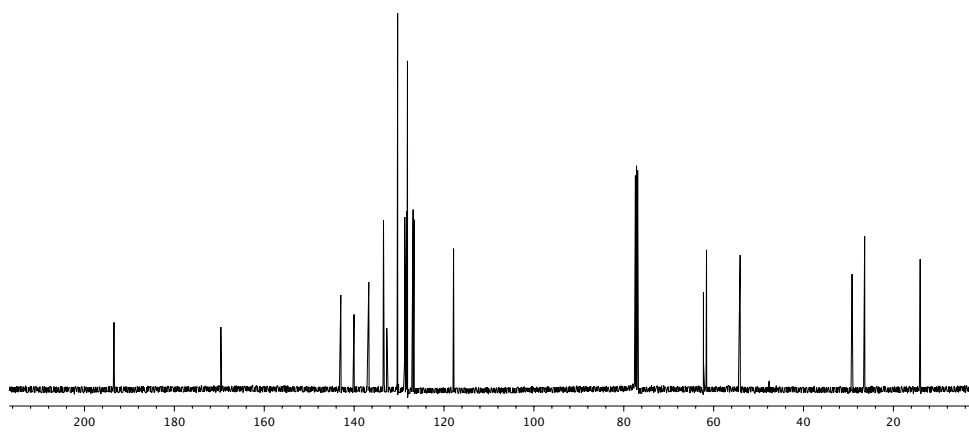


Figure A3.27 ¹³C NMR (125 MHz, CDCl₃) of compound **100i**.

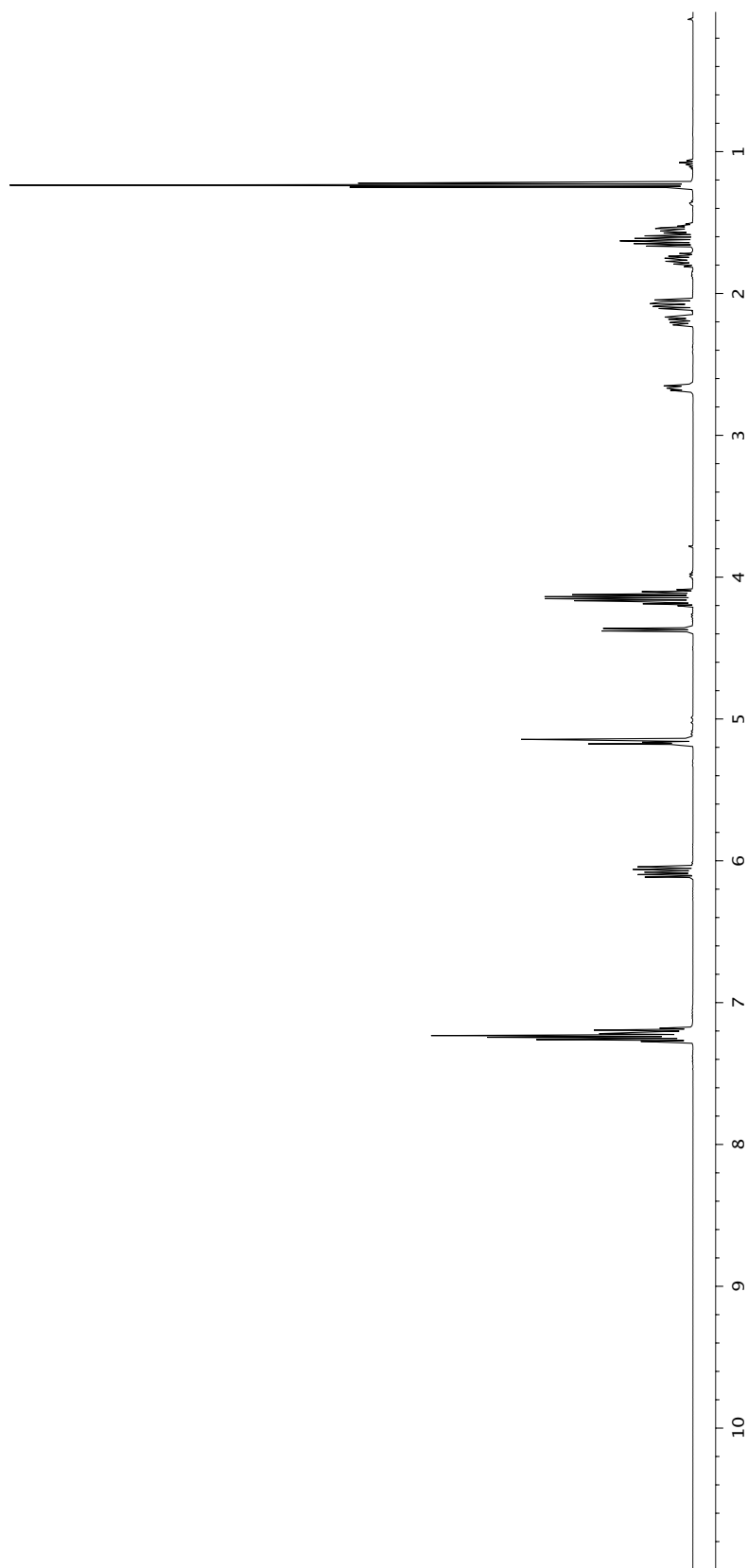
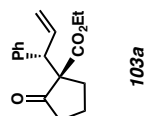


Figure A3.28 ¹H NMR (500 MHz, CDCl₃) of compound **103a**.

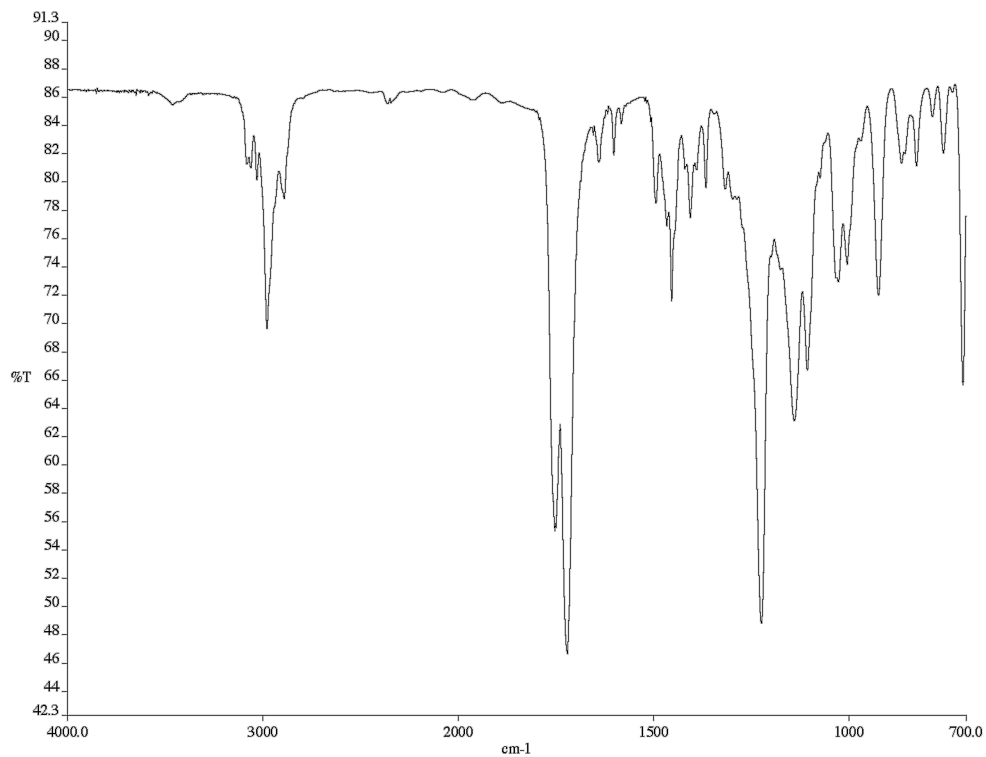


Figure A3.29 Infrared spectrum (thin film/NaCl) of compound **103a**.

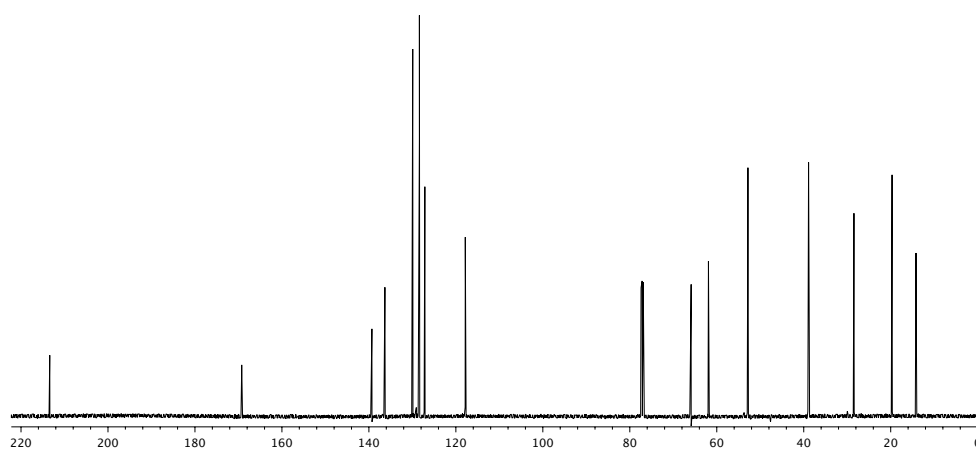


Figure A3.30 ¹³C NMR (125 MHz, CDCl₃) of compound **103a**.

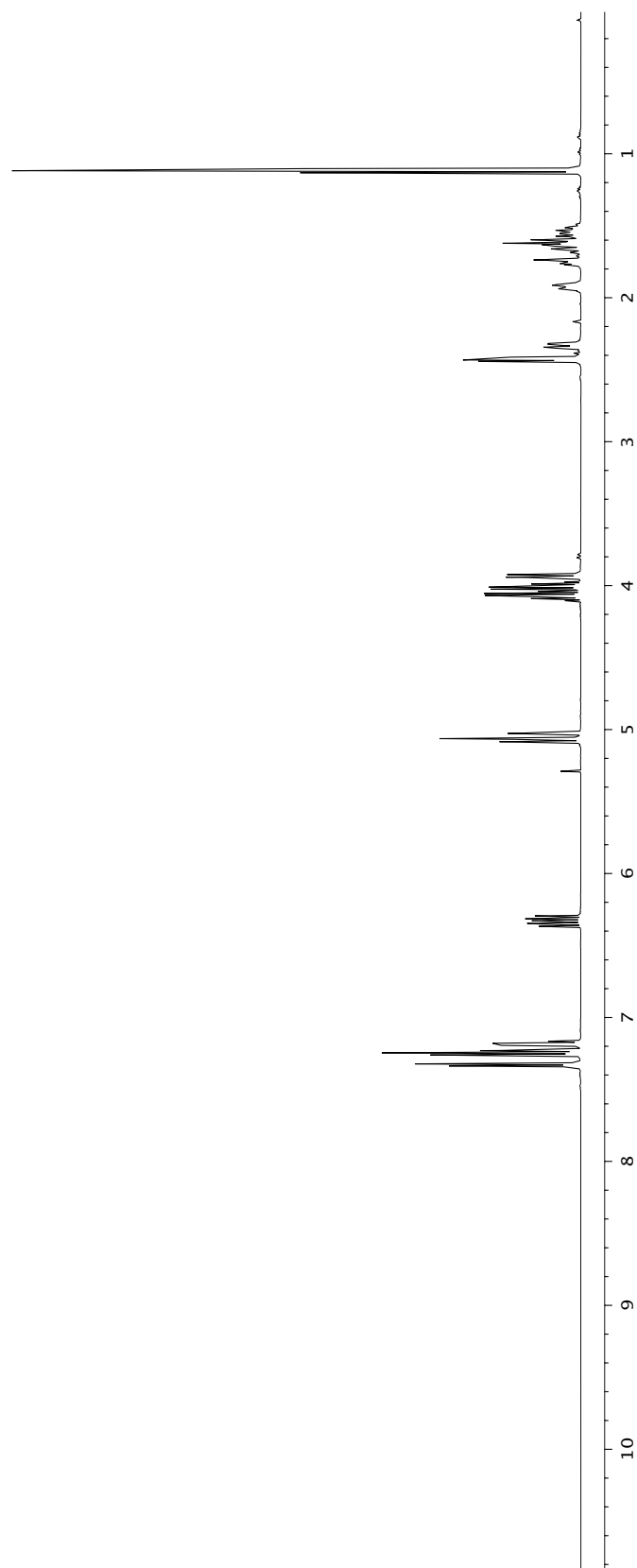
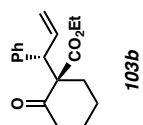


Figure A3.31 ¹H NMR (500 MHz, CDCl₃) of compound **103b**.

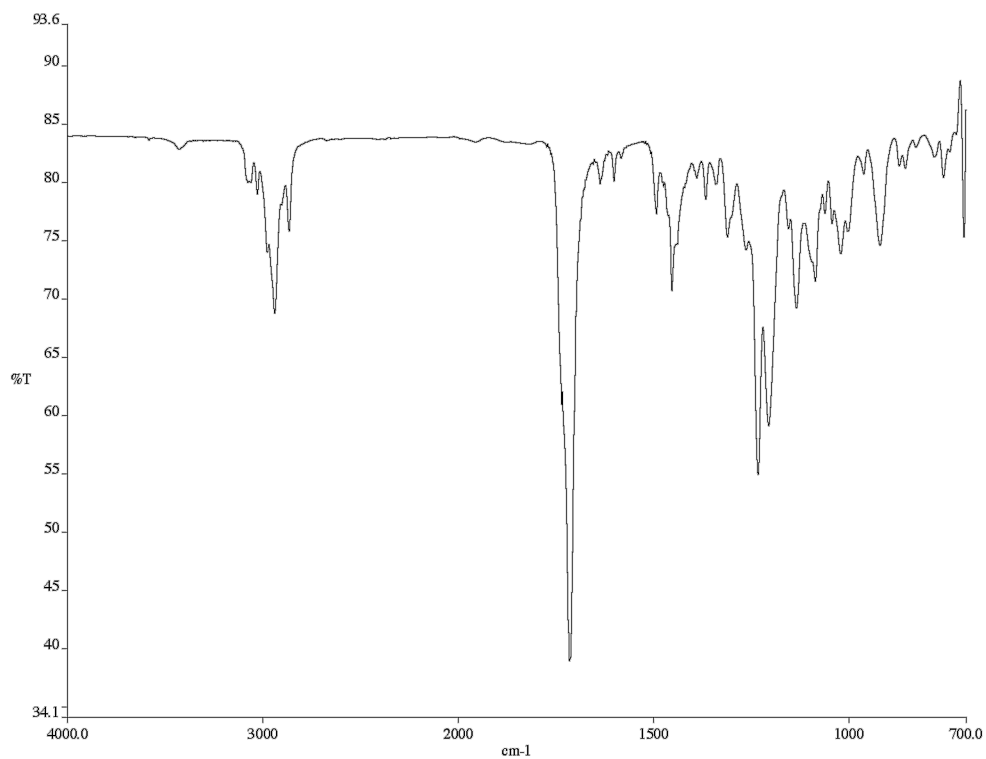


Figure A3.32 Infrared spectrum (thin film/NaCl) of compound **103b**.

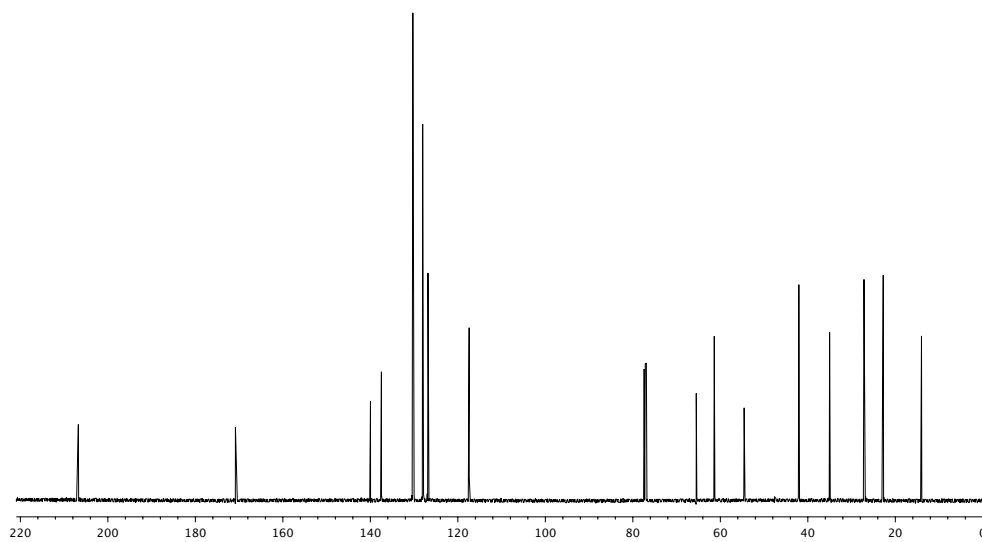


Figure A3.33 ¹³C NMR (125 MHz, CDCl₃) of compound **103b**.

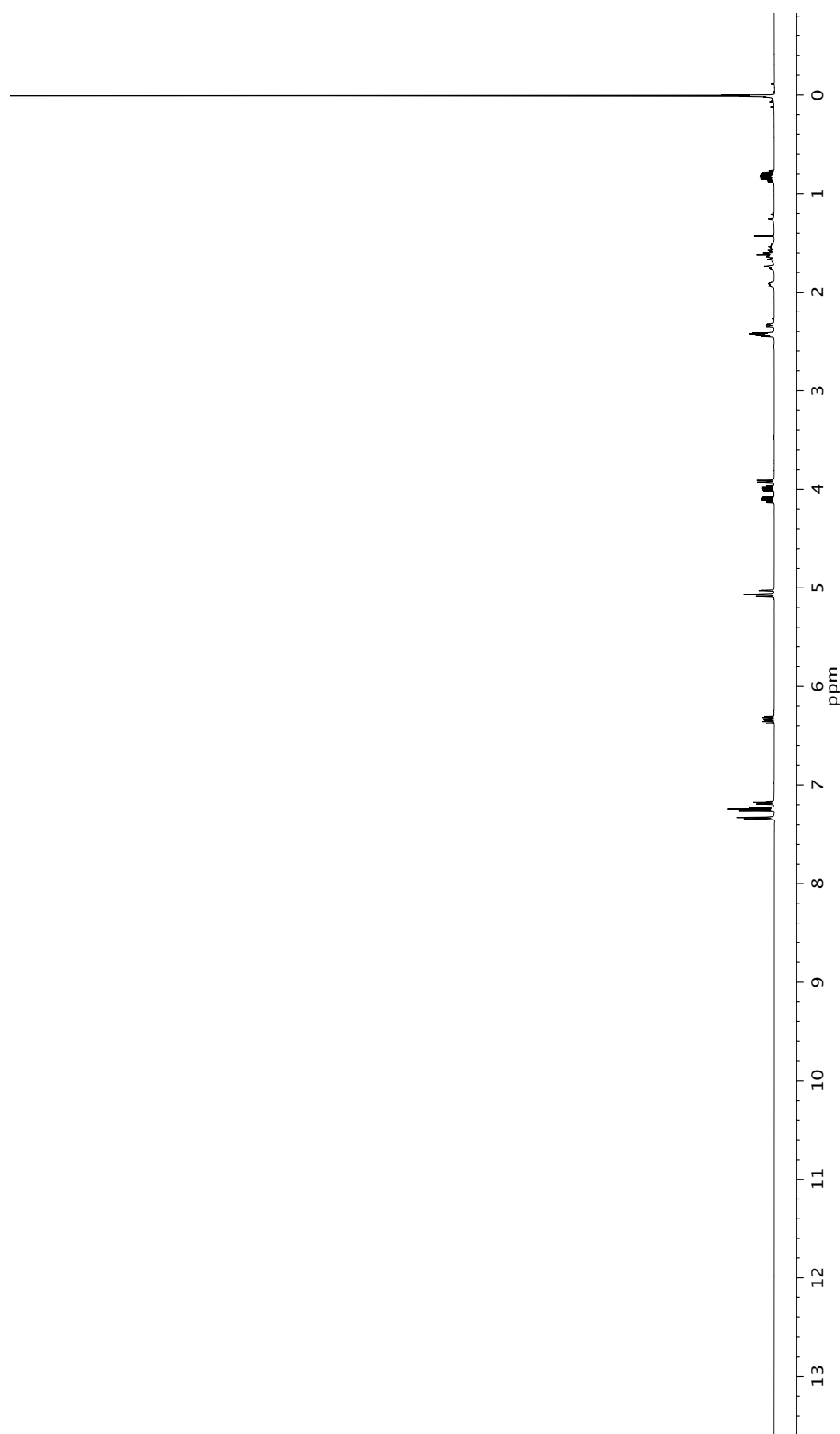
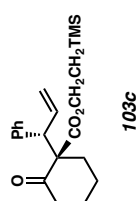


Figure A3.34 ¹H NMR (500 MHz, CDCl₃) of compound **103c**.

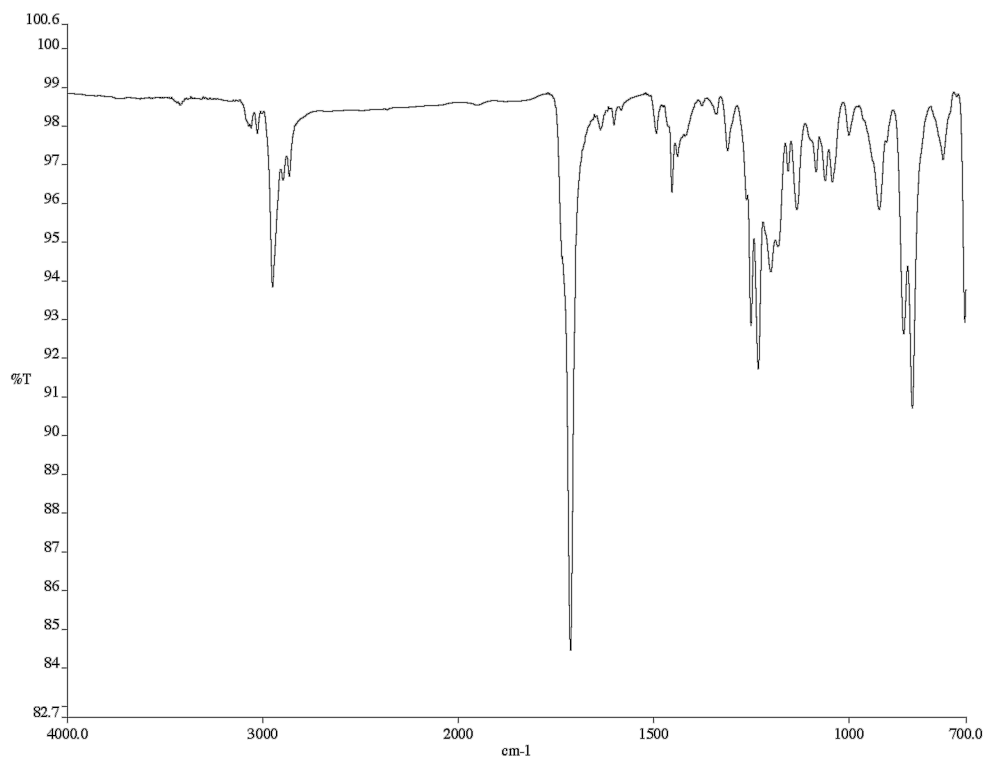


Figure A3.35 Infrared spectrum (thin film/NaCl) of compound **103c**.

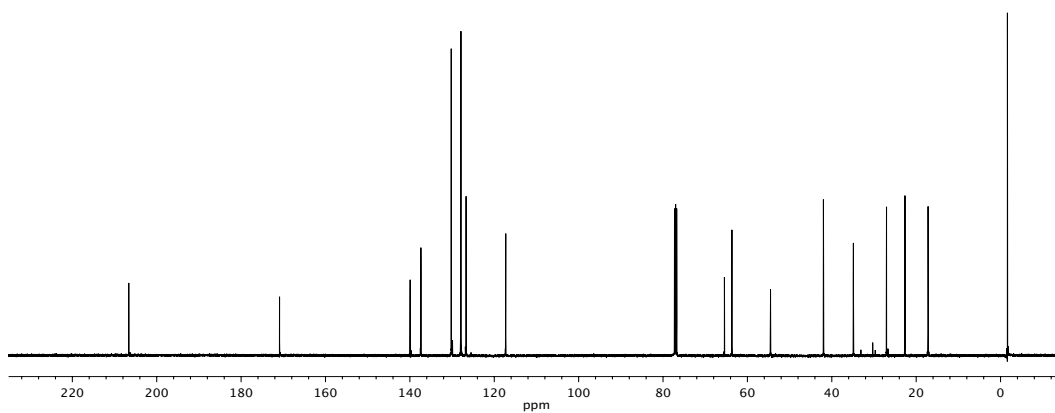


Figure A3.36 ¹³C NMR (125 MHz, CDCl₃) of compound **103c**.

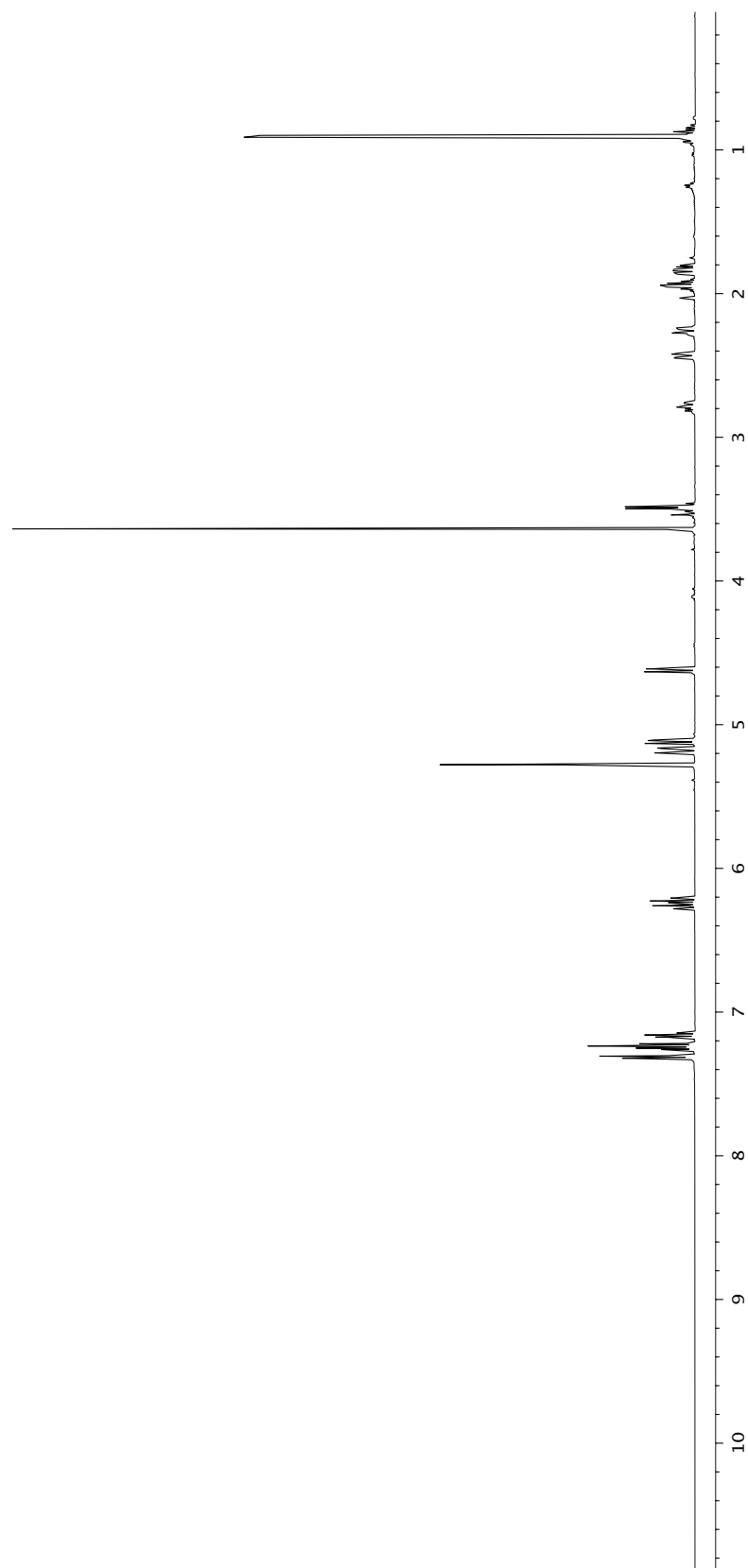
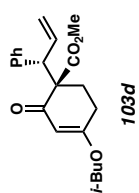


Figure A3.7 ¹H NMR (500 MHz, CDCl₃) of compound **103d**.

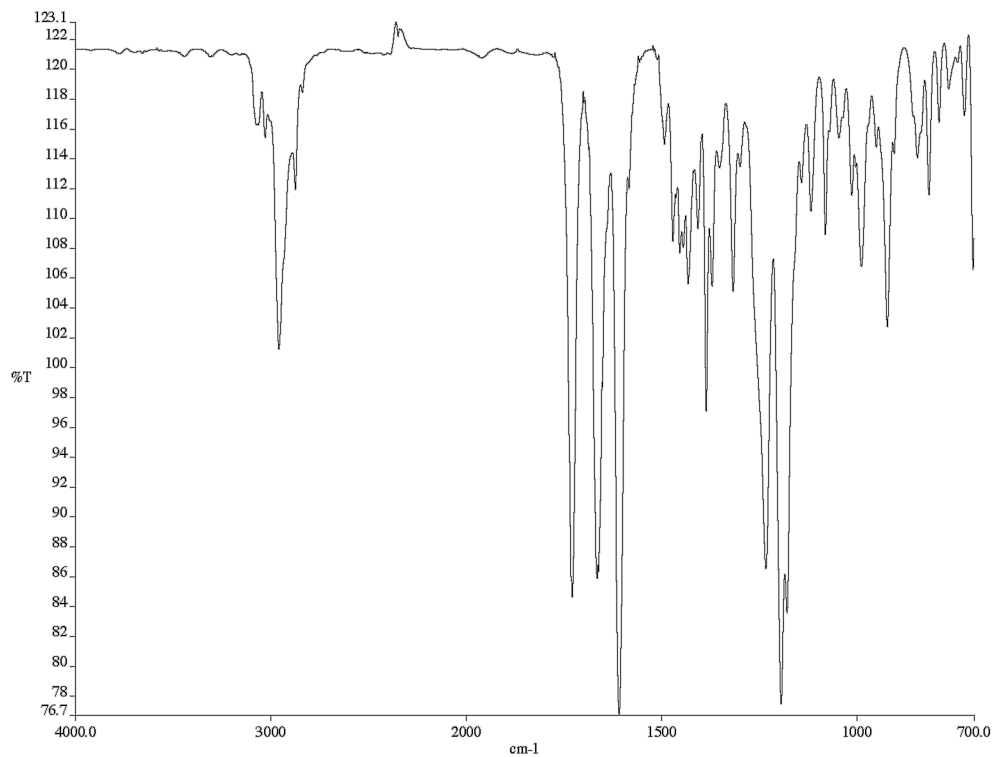


Figure A3.38 Infrared spectrum (thin film/NaCl) of compound **103d**.

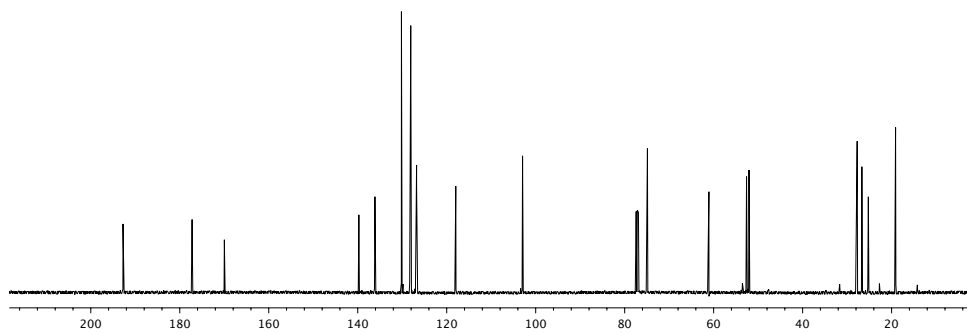


Figure A3.39 ^{13}C NMR (125 MHz, CDCl_3) of compound **103d**.

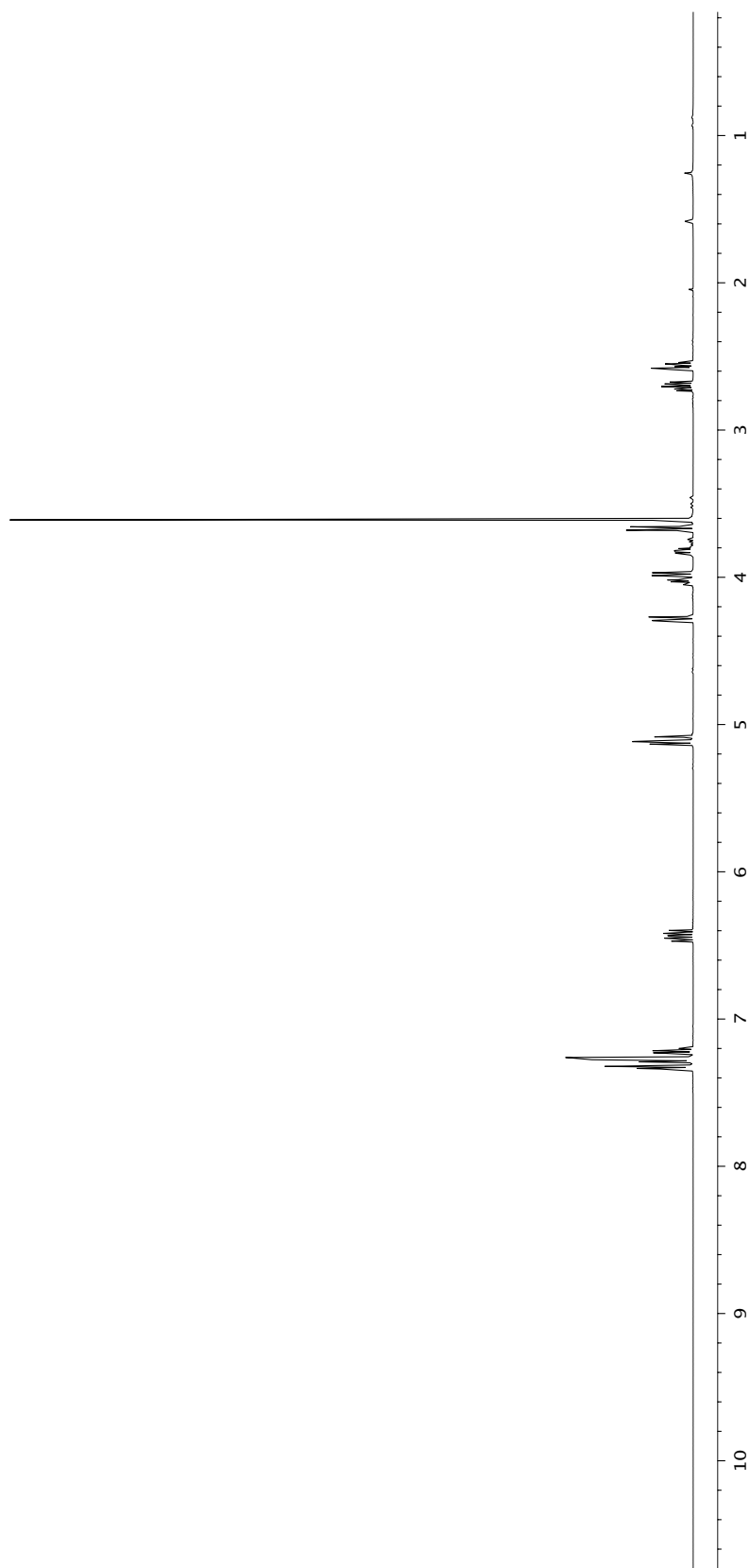
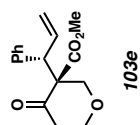


Figure A3.40 ¹H NMR (500 MHz, CDCl₃) of compound **103e**.

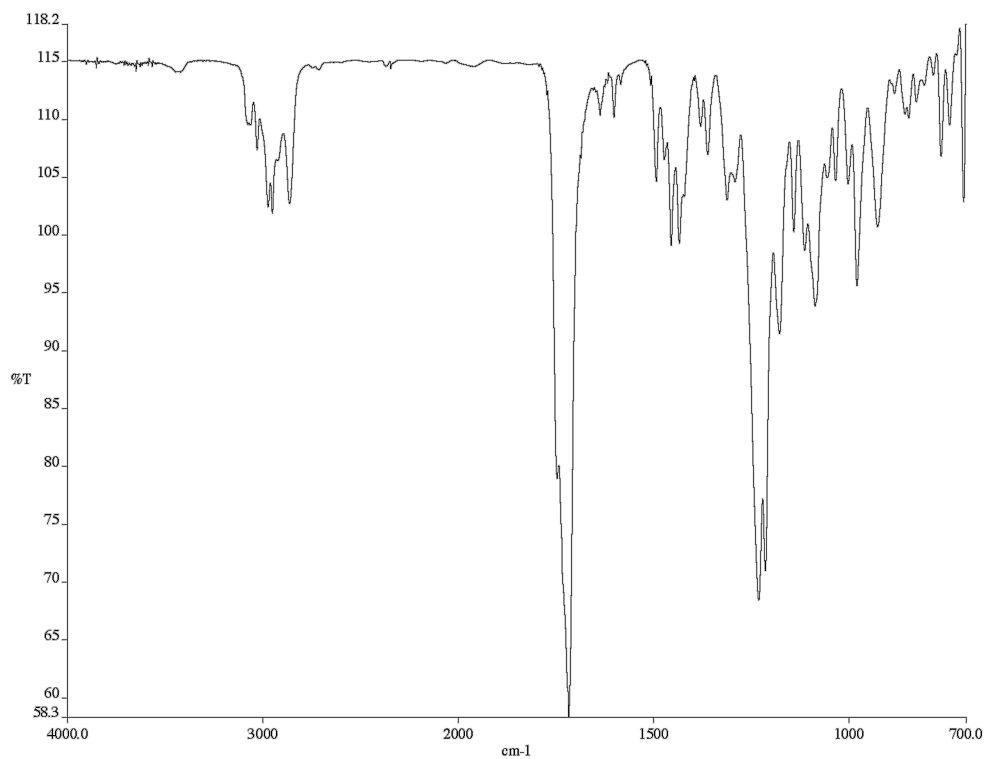


Figure A3.41 Infrared spectrum (thin film/NaCl) of compound **103e**.

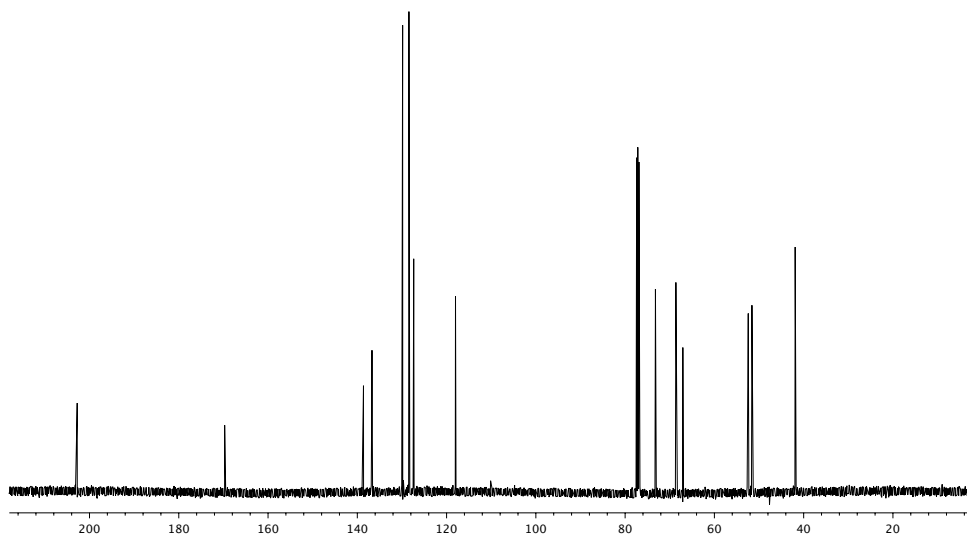


Figure A3.42 ¹³C NMR (125 MHz, CDCl₃) of compound **103e**.

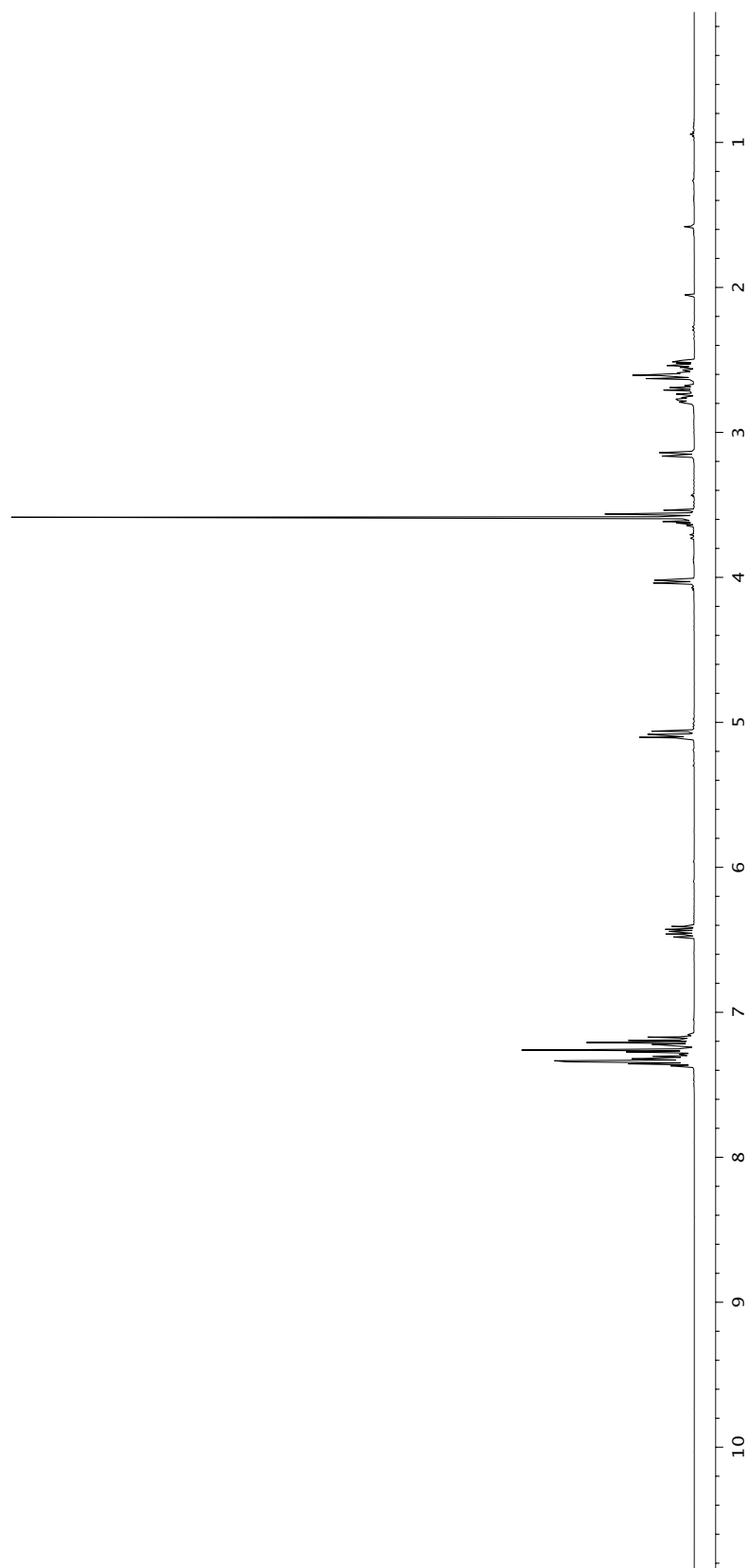
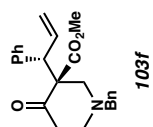


Figure A3.43 ¹H NMR (500 MHz, CDCl₃) of compound **103f**.

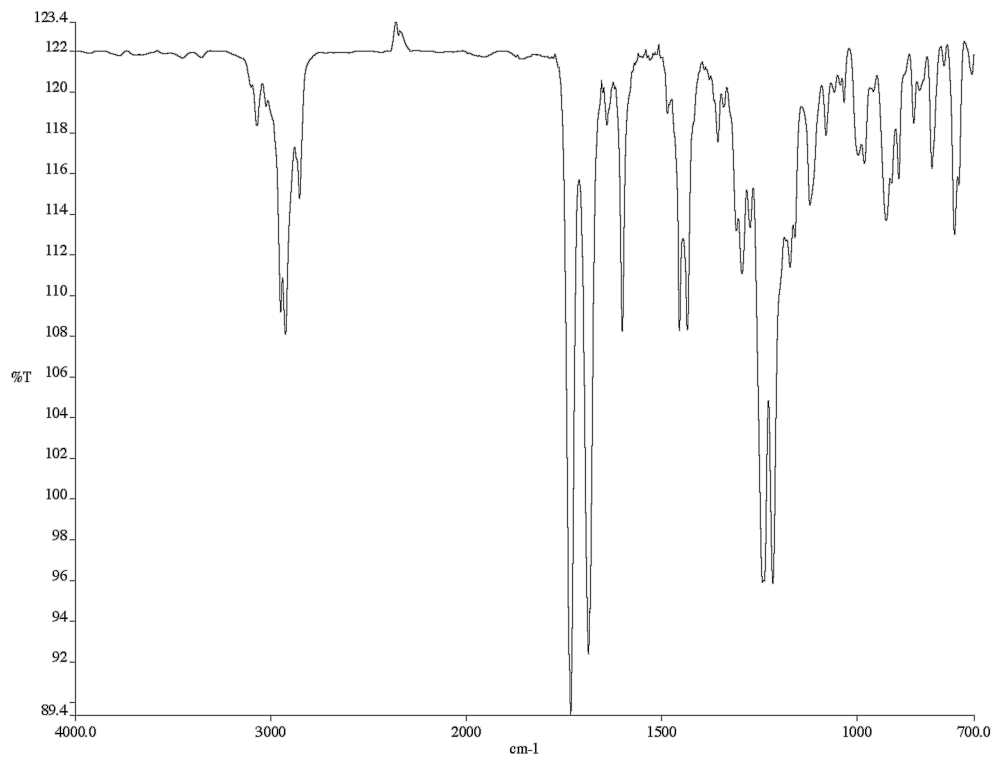


Figure A3.44 Infrared spectrum (thin film/NaCl) of compound **103f**.

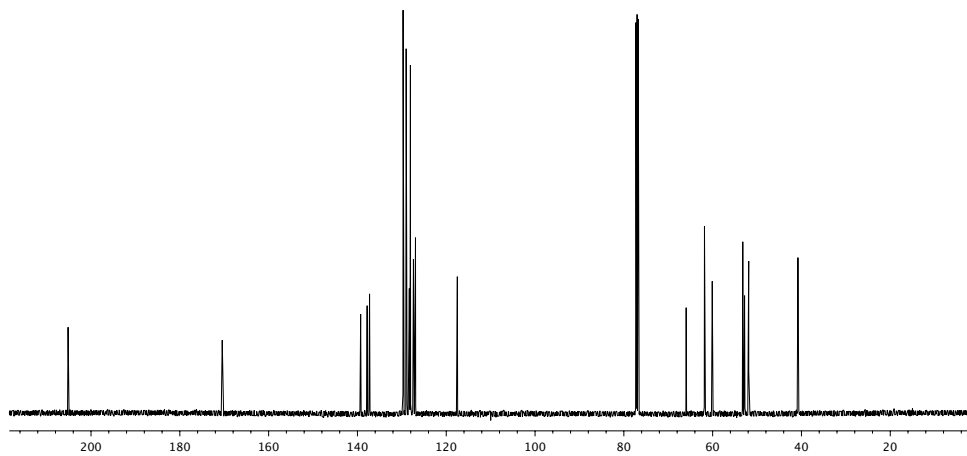


Figure A3.44 ¹³C NMR (125 MHz, CDCl₃) of compound **103f**.

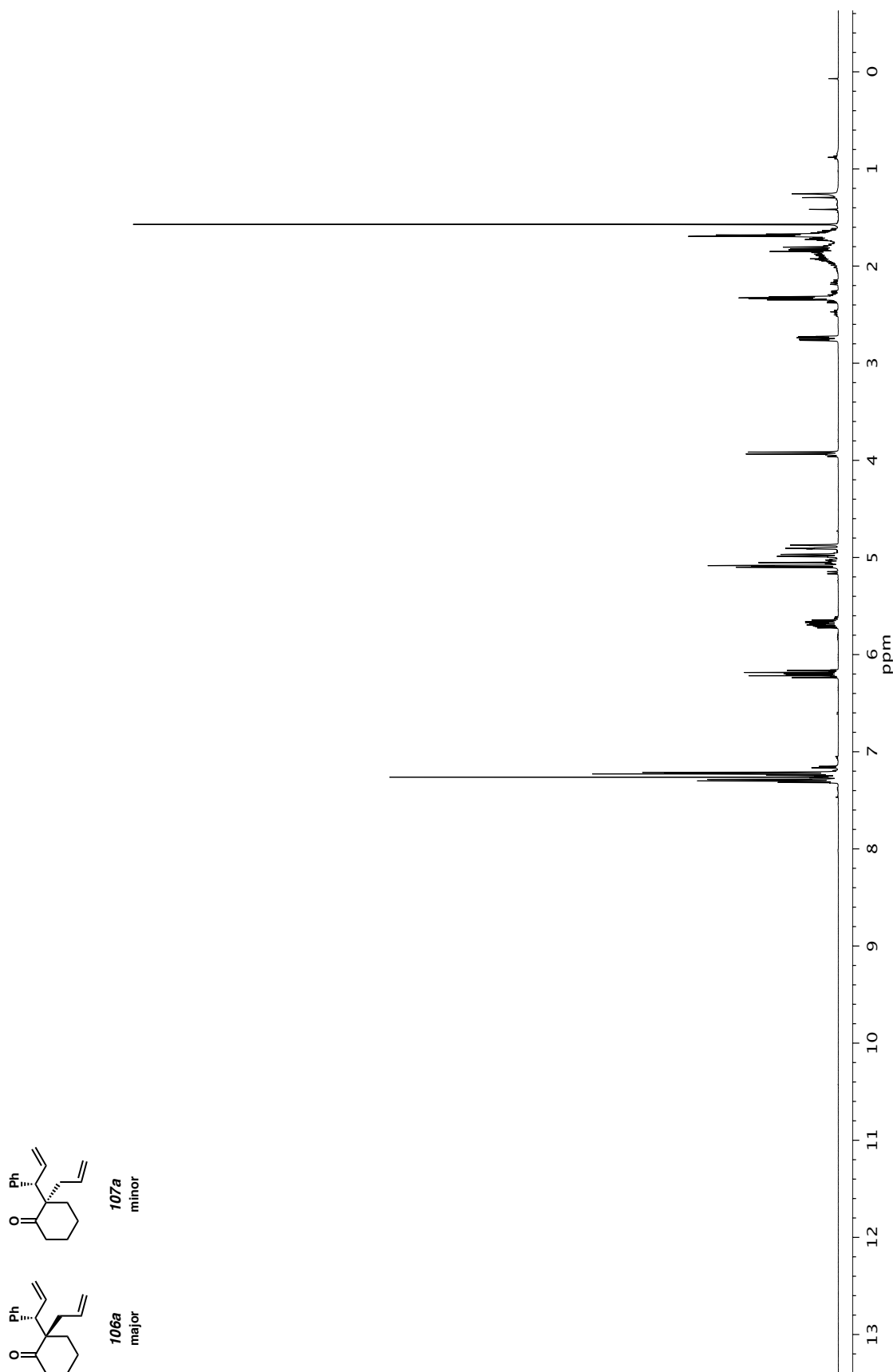


Figure A3.46 ¹H NMR (500 MHz, CDCl₃) of compound **106a** and **107a**.

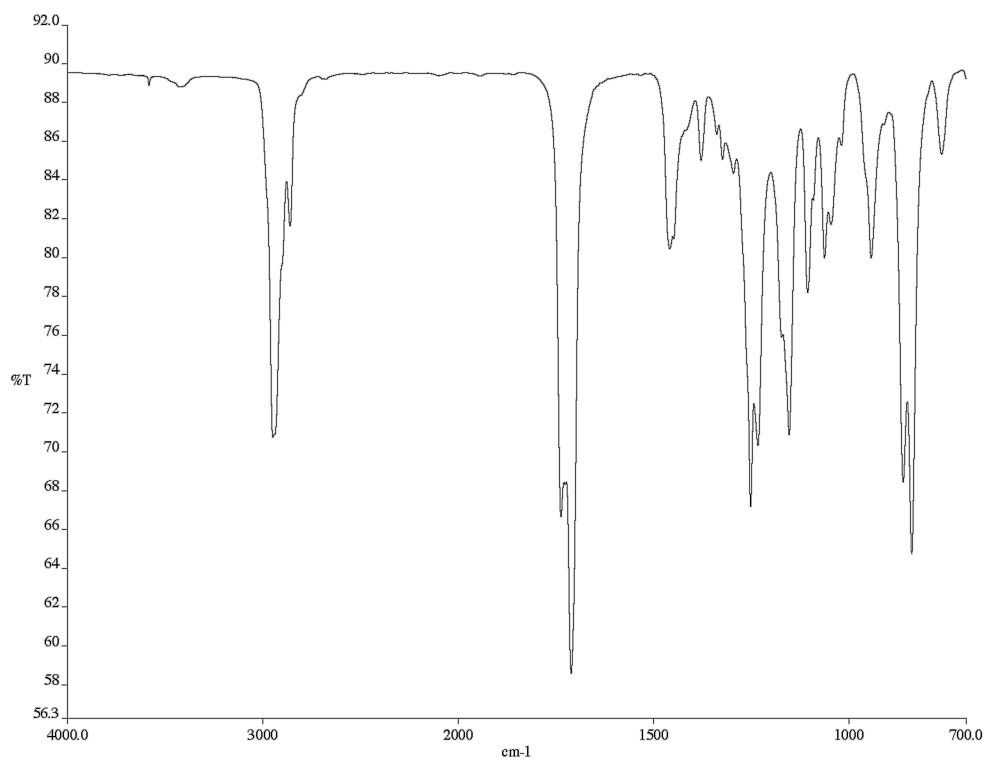


Figure A3.47 Infrared spectrum (thin film/NaCl) of compound **106a** and **107a**.

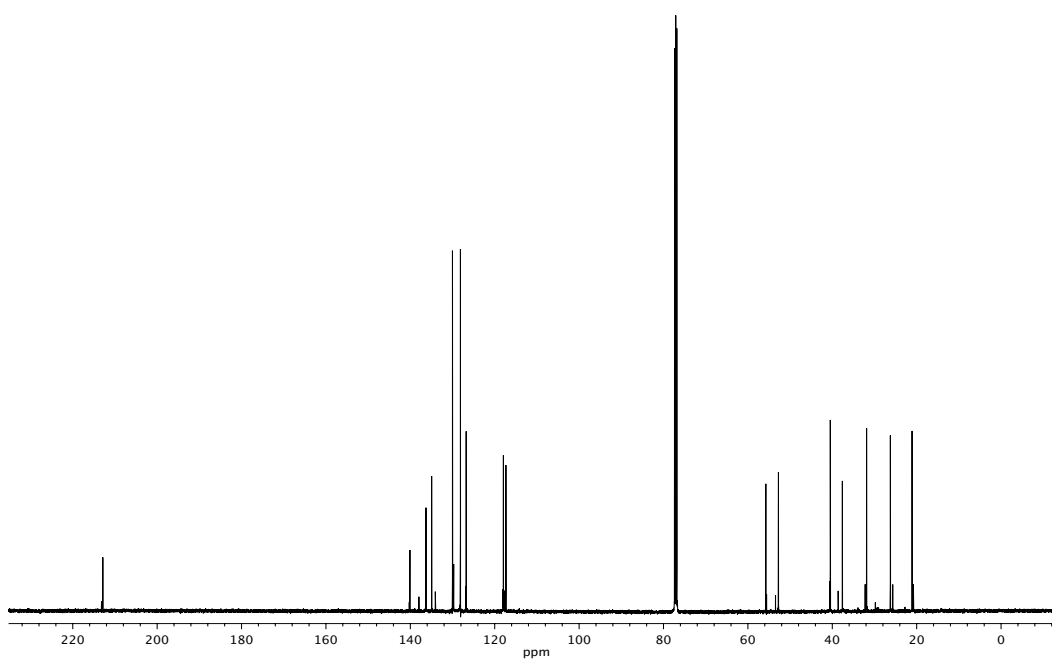


Figure A3.48 ¹³C NMR (125 MHz, CDCl₃) of compound **106a** and **107a**.

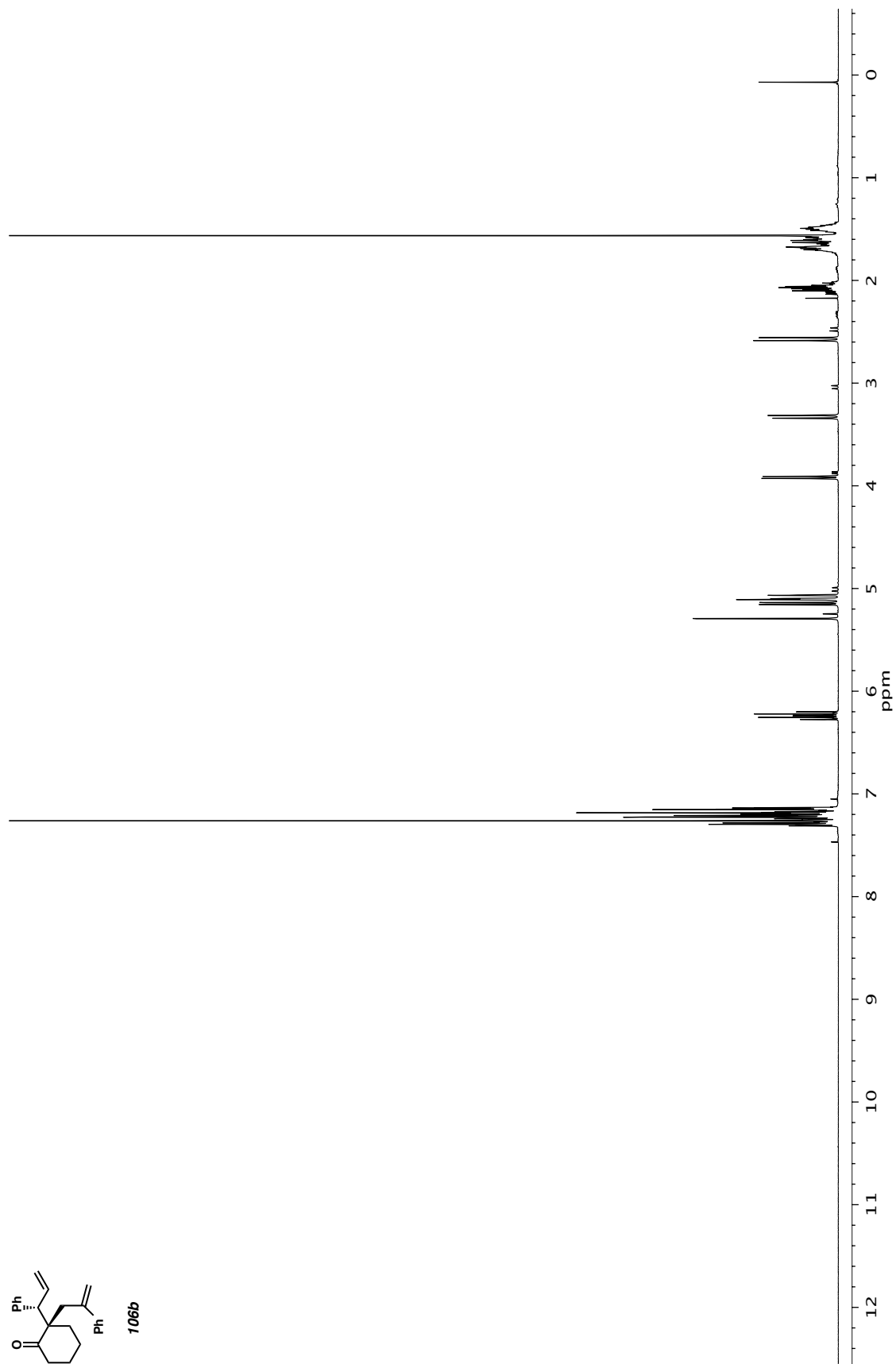
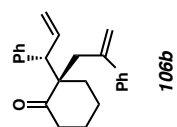


Figure A3.49 ¹H NMR (500 MHz, CDCl₃) of compound **106b**.

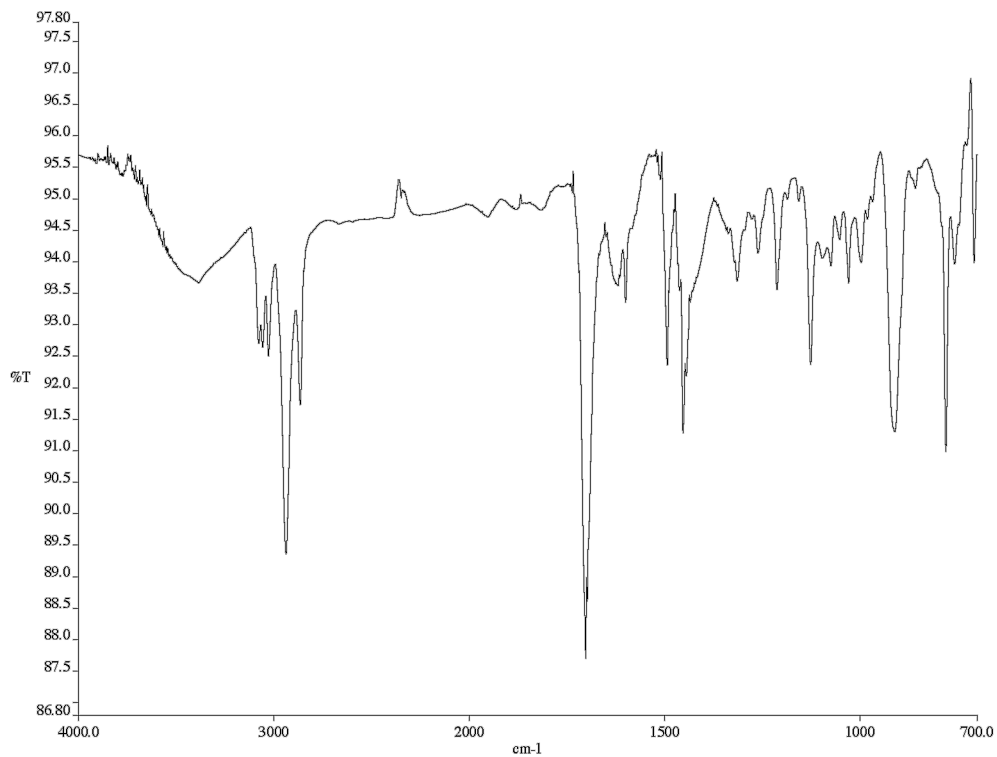


Figure A3.50 Infrared spectrum (thin film/NaCl) of compound **106b**.

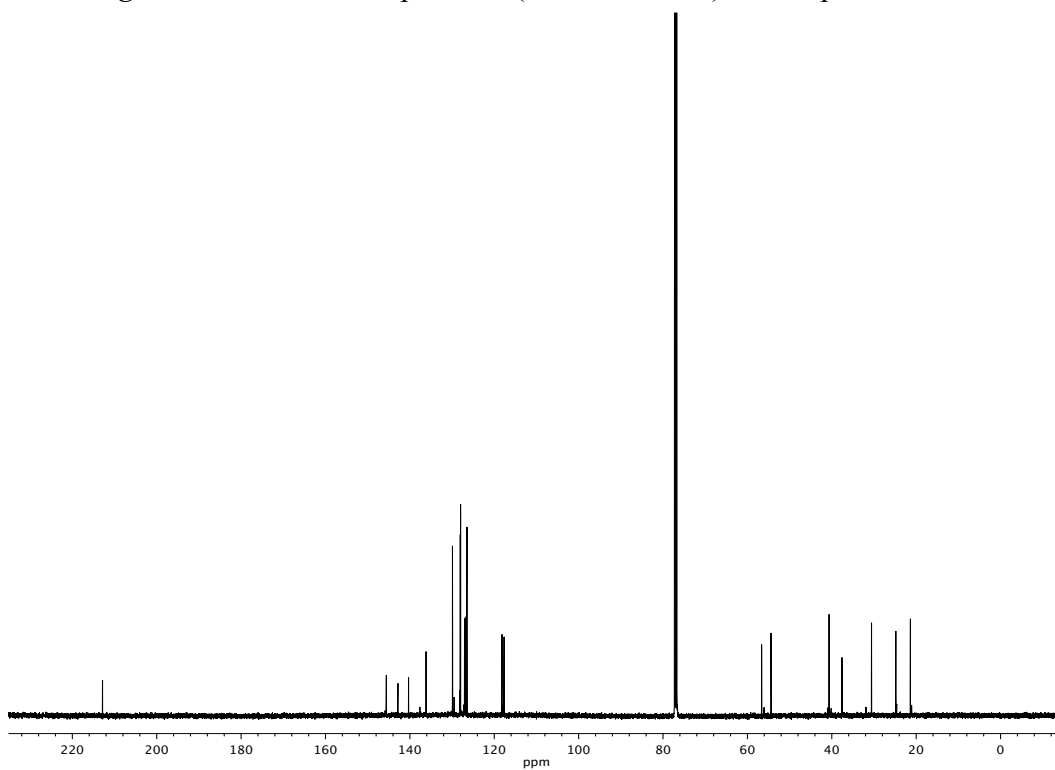


Figure A3.51 ¹³C NMR (125 MHz, CDCl₃) of compound **106b**.

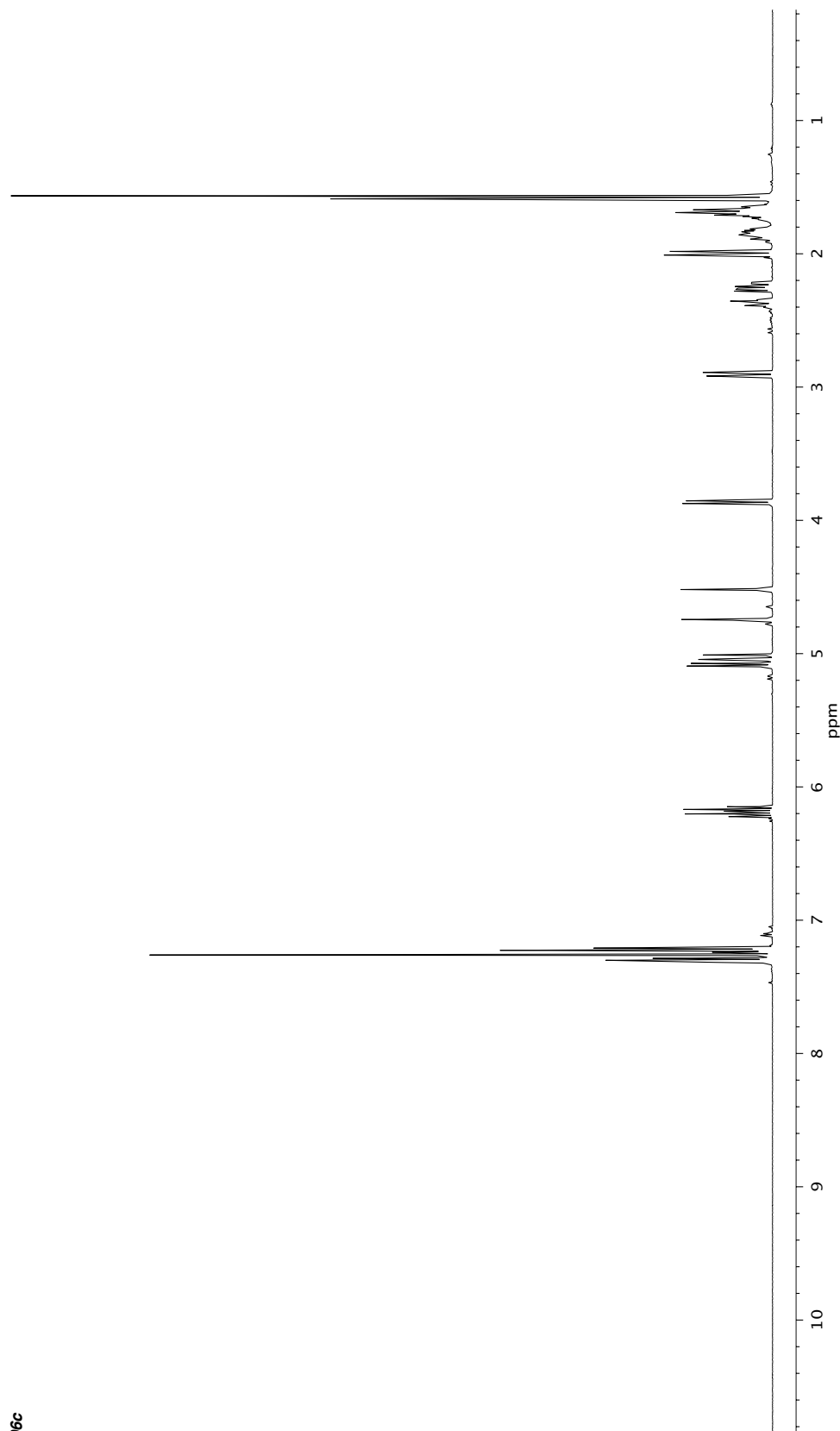
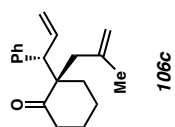


Figure A3.52 ¹H NMR (500 MHz, CDCl₃) of compound **106c**.

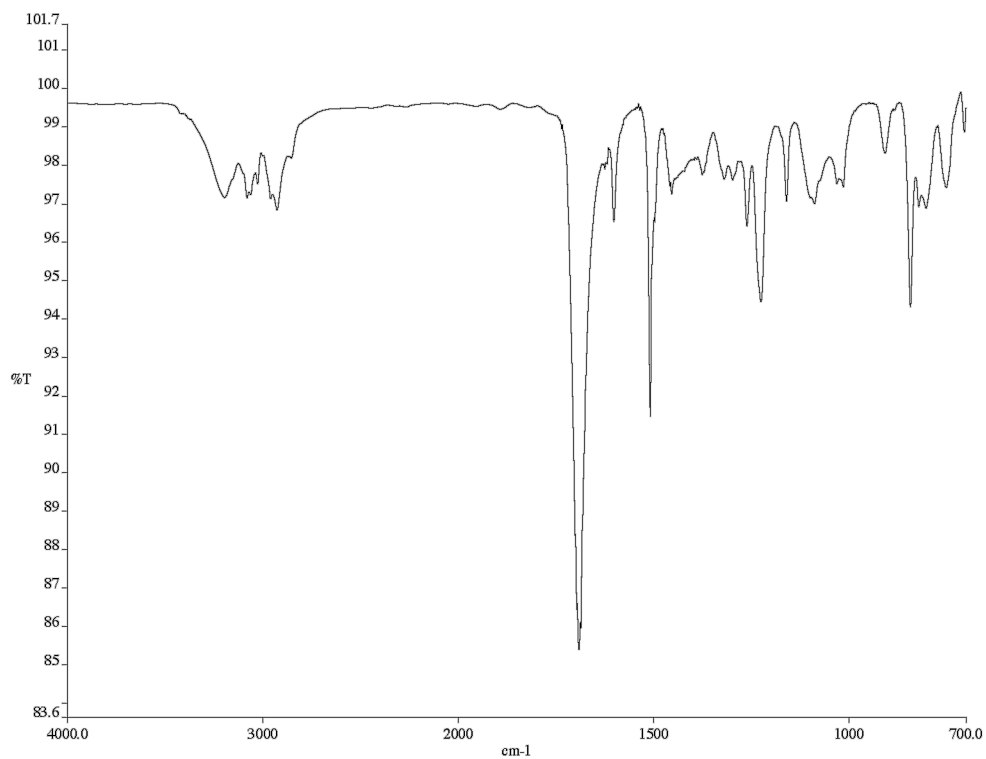


Figure A3.53 Infrared spectrum (thin film/NaCl) of compound **106c**.

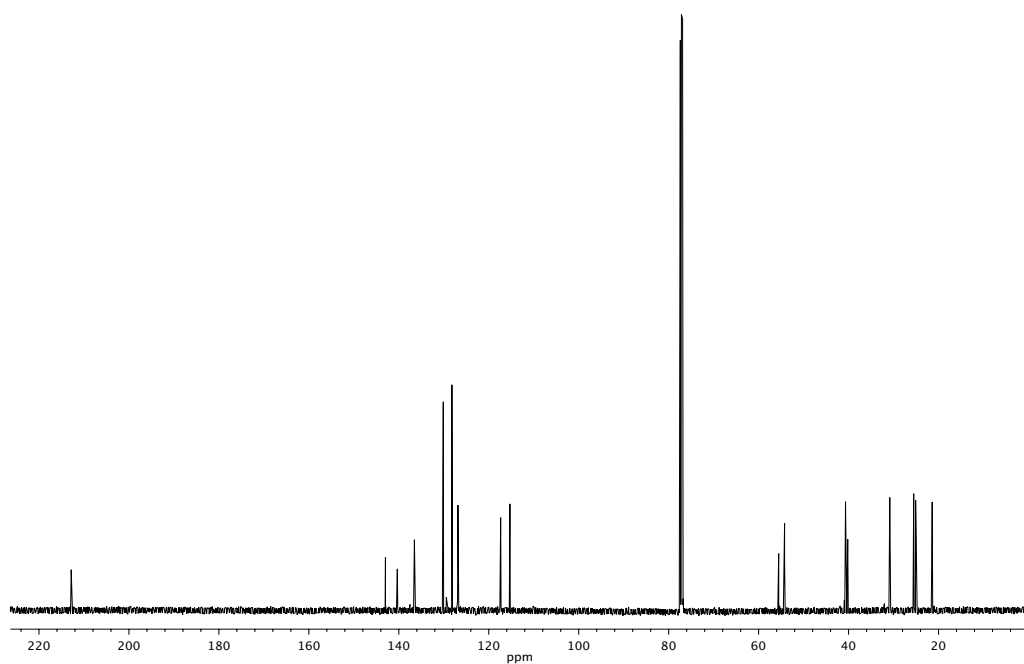


Figure A3.54 ^{13}C NMR (125 MHz, CDCl_3) of compound **106c**.

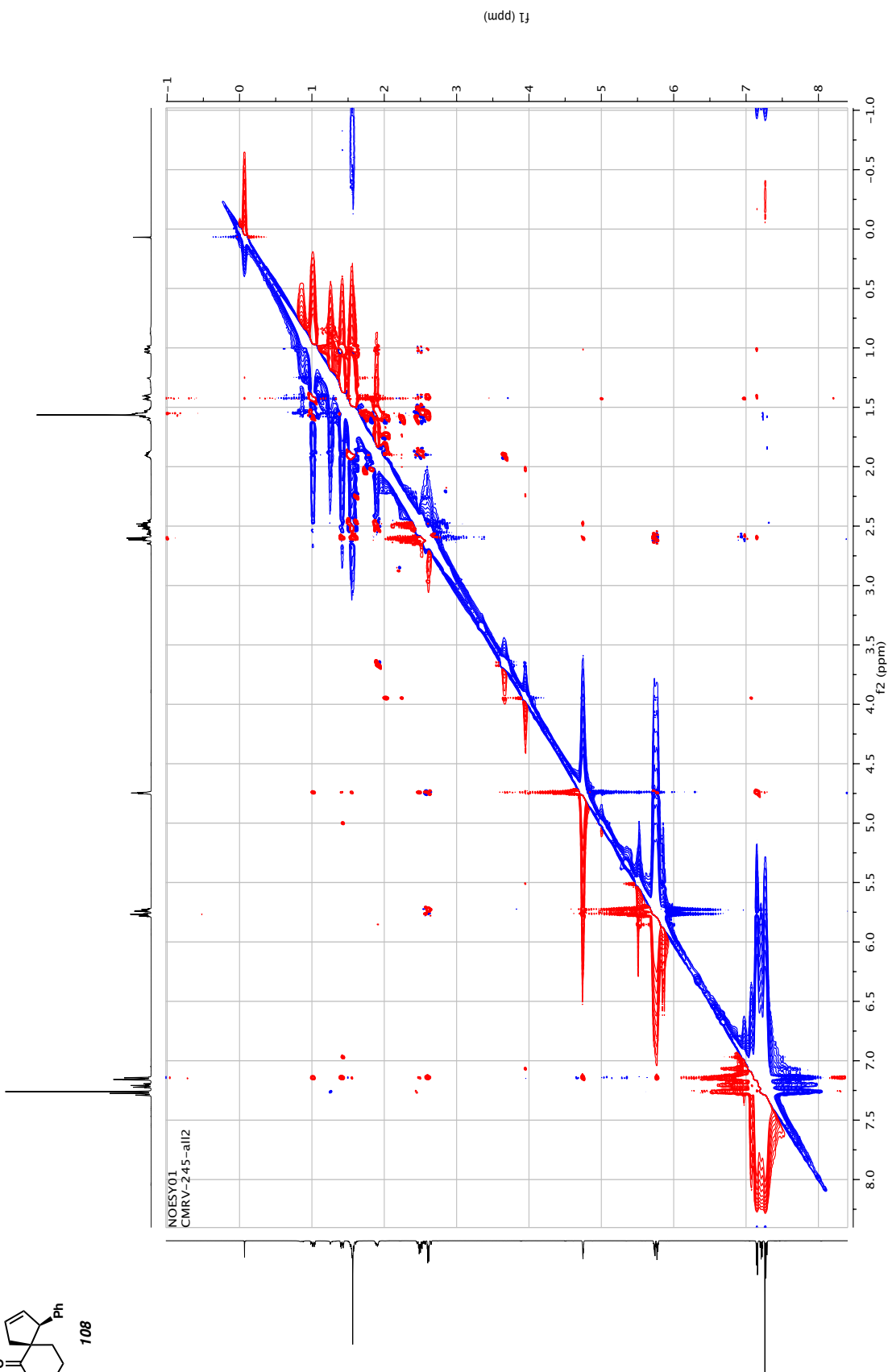
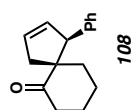


Figure A3.55 ¹H NOSEY NMR (600 MHz, CDCl₃) of compound **108**.

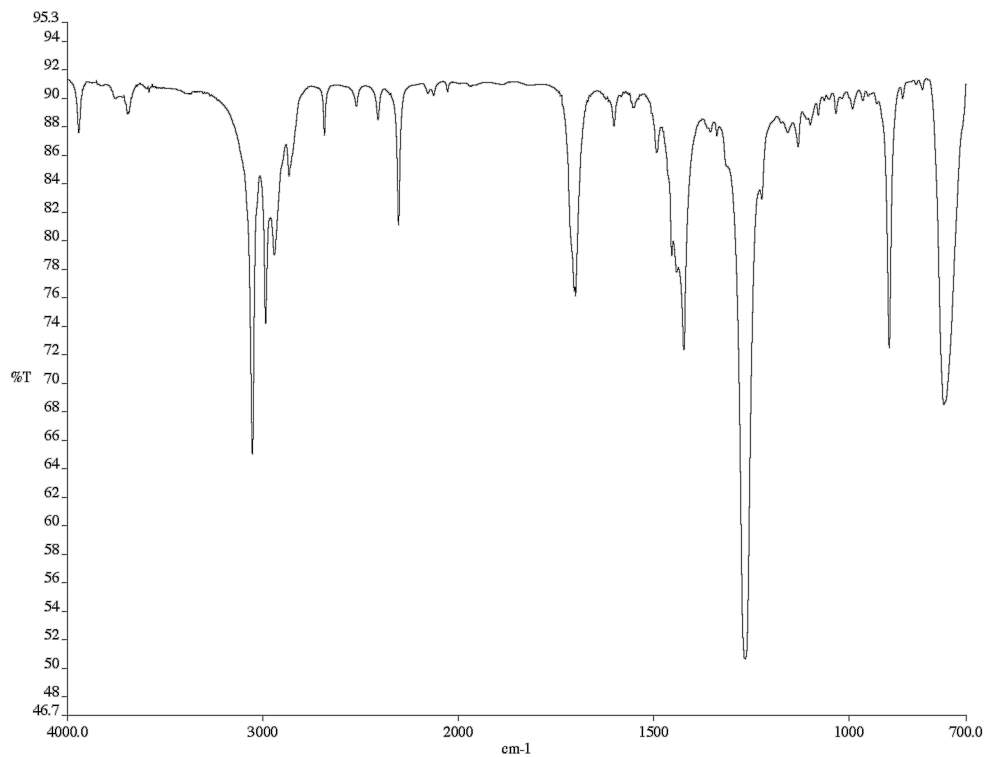


Figure A3.56 Infrared spectrum (thin film/NaCl) of compound **108**.

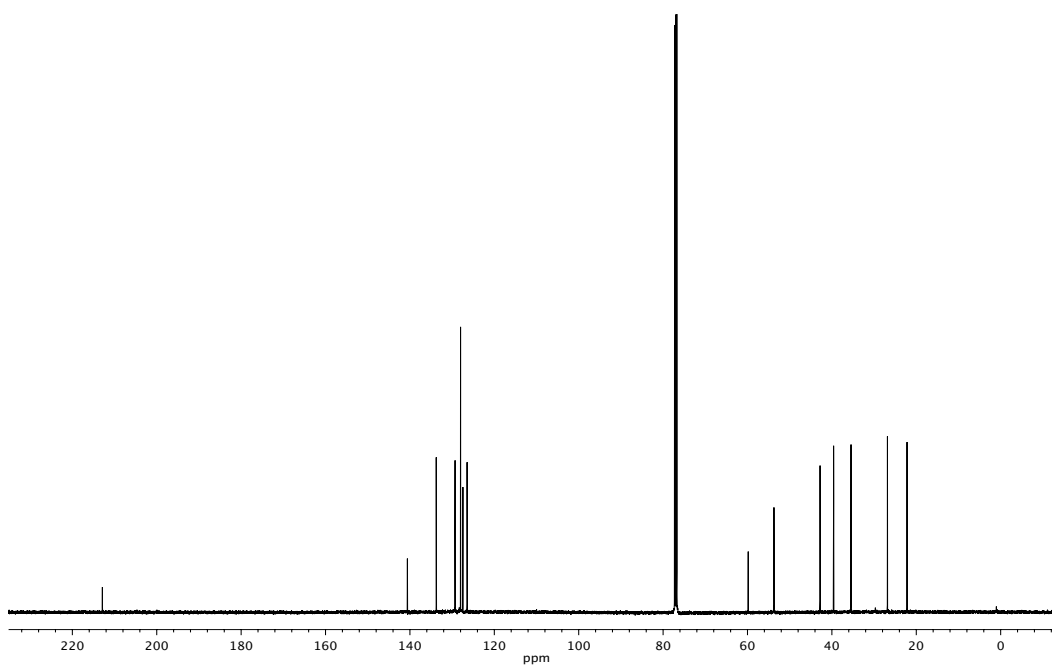


Figure A3.57 ¹³C NMR (125 MHz, CDCl₃) of compound **108**.

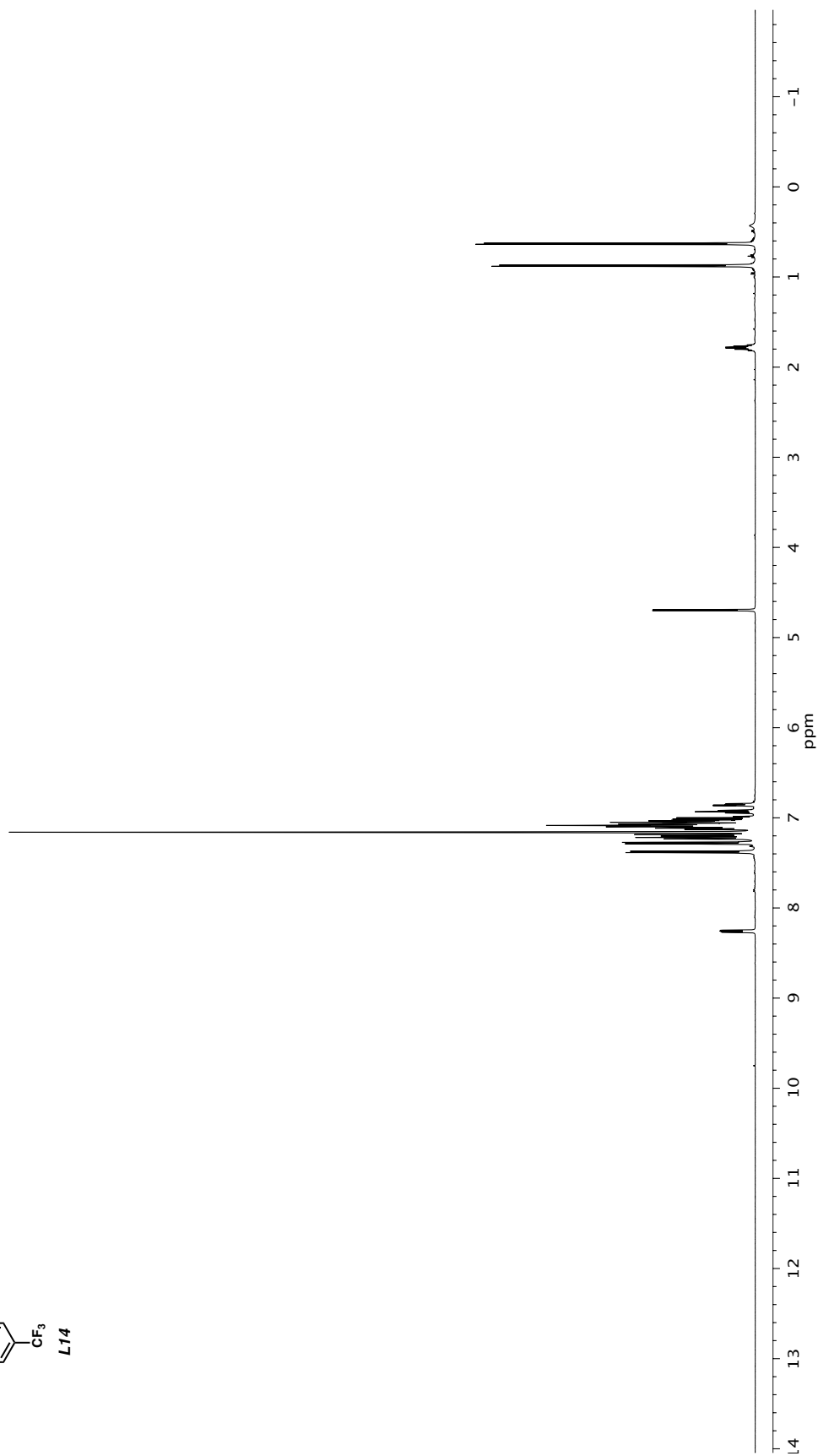
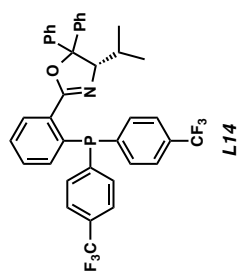


Figure A3.58 ¹H NMR (500 MHz, C₆D₆) of compound L14.

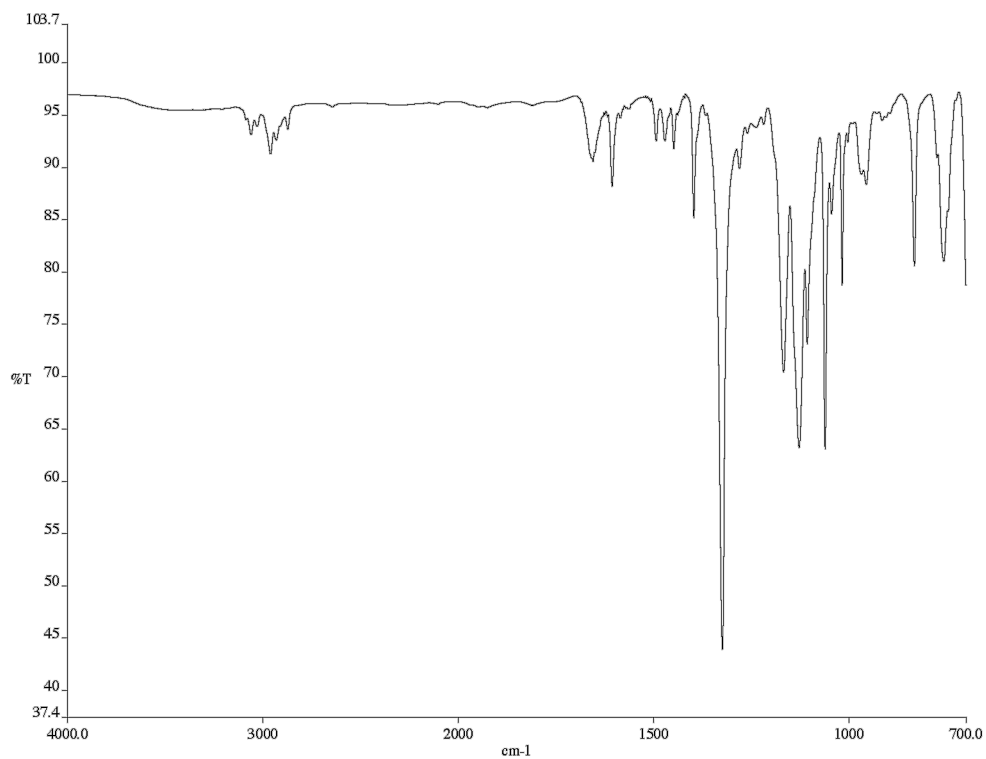


Figure A3.59 Infrared spectrum (thin film/NaCl) of compound **L14**.

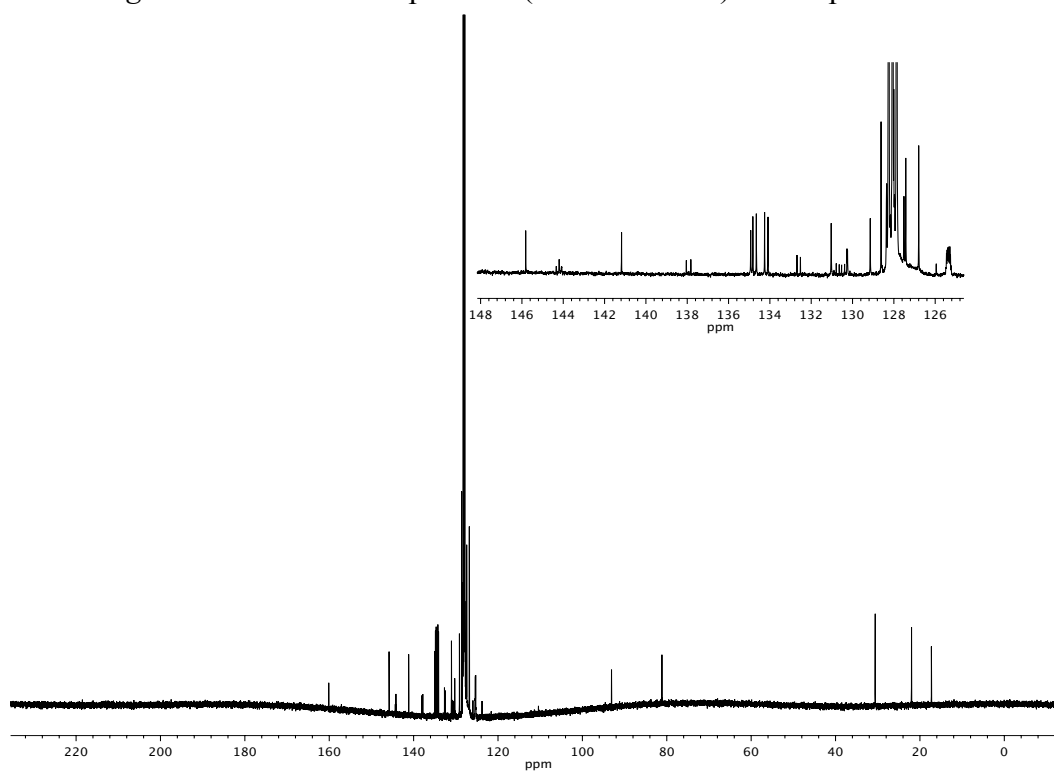


Figure A3.60 ¹³C NMR (125 MHz, C₆D₆) of compound **L14**.

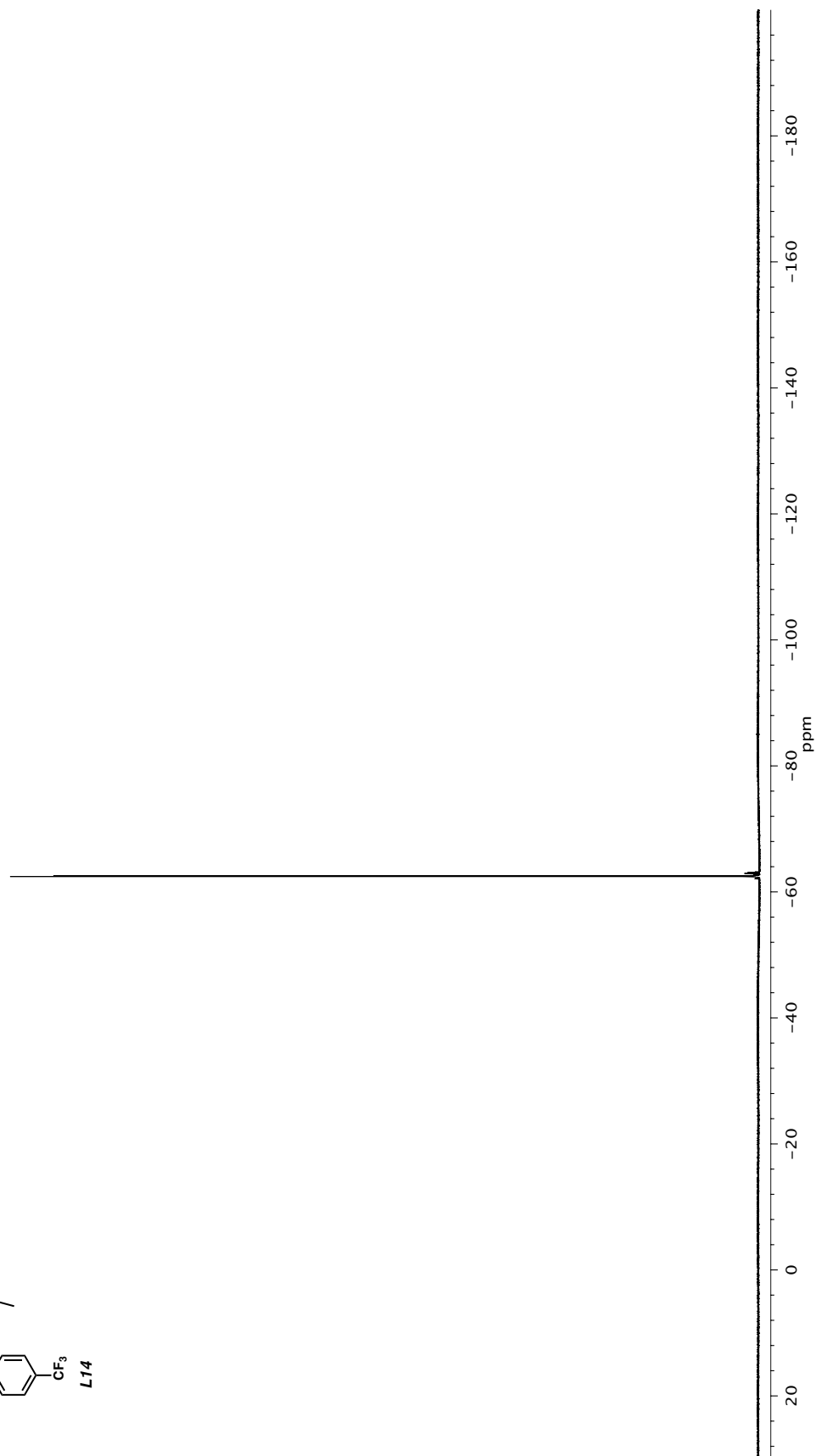
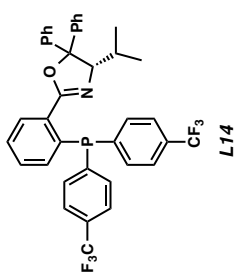


Figure A3.61 ¹⁹F NMR (282 MHz, C₆D₆) of compound L14.

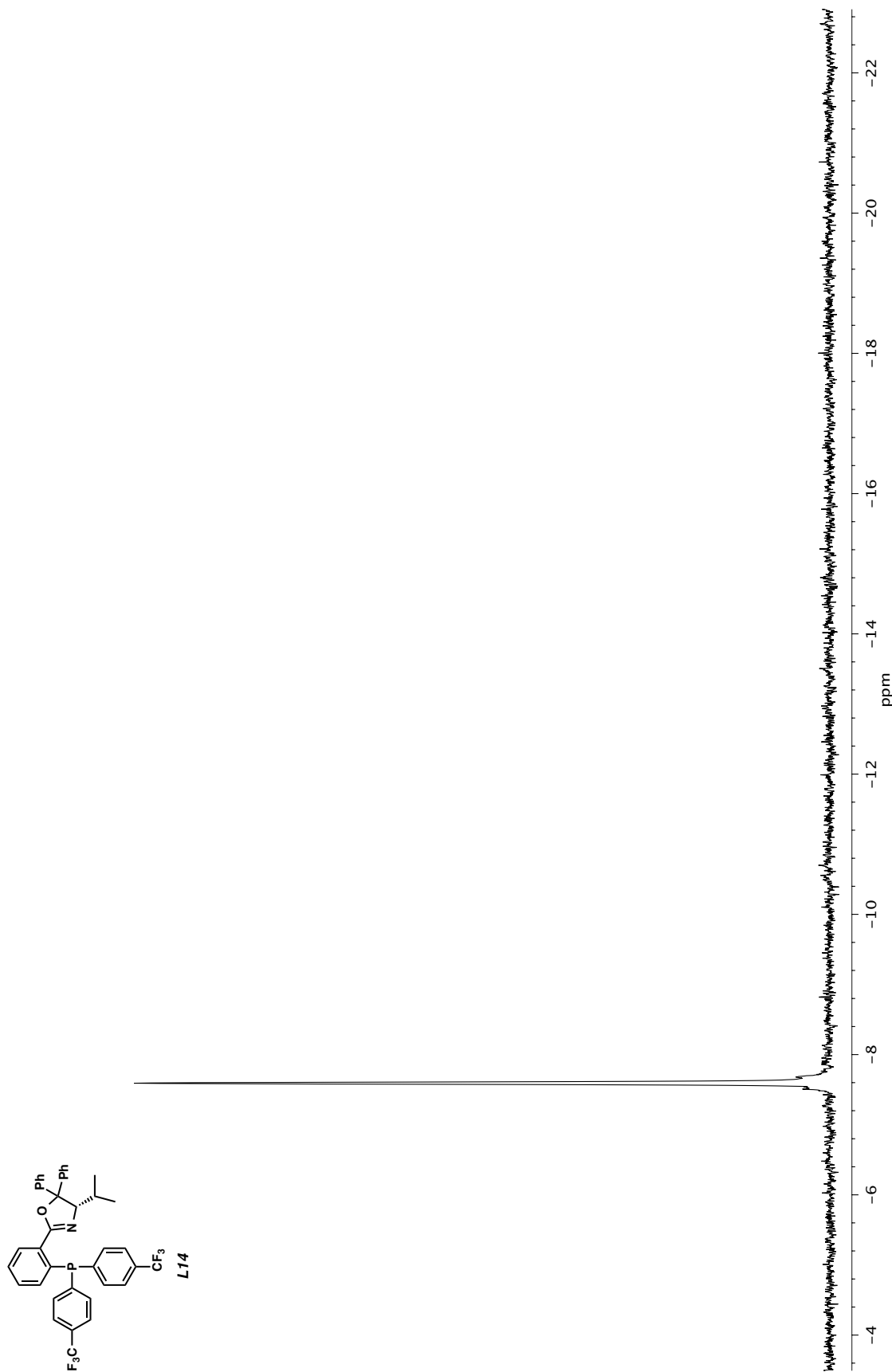


Figure A3.62 ^{31}P NMR (121 MHz, C_6D_6) of compound L14.

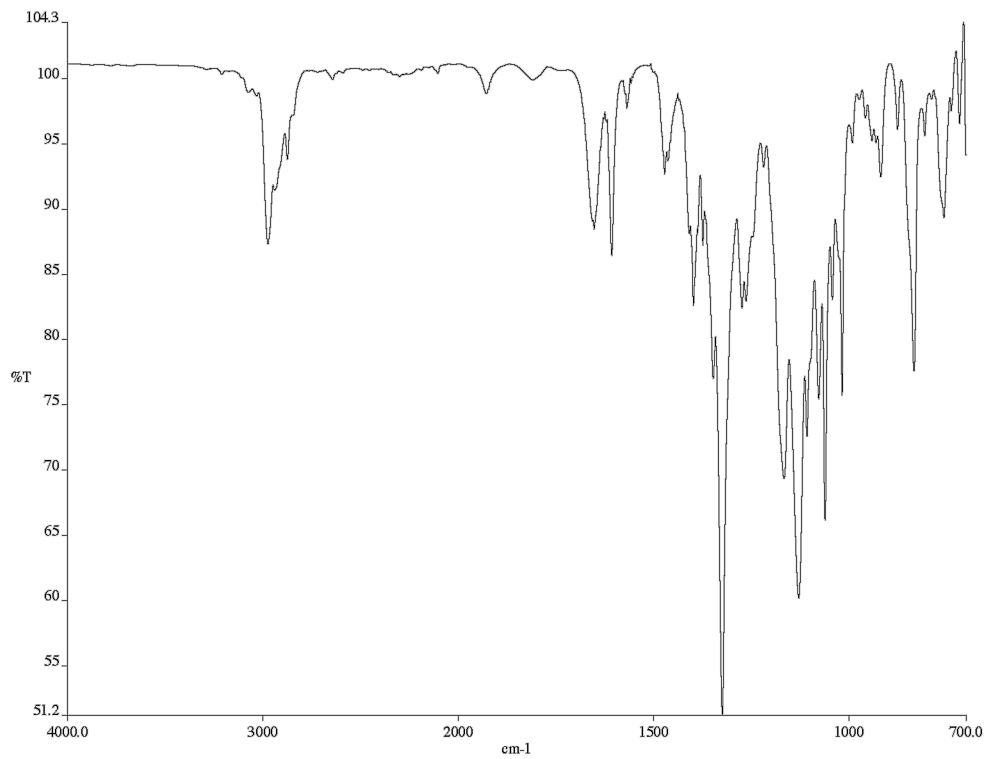


Figure A3.64 Infrared spectrum (thin film/NaCl) of compound **L15**.

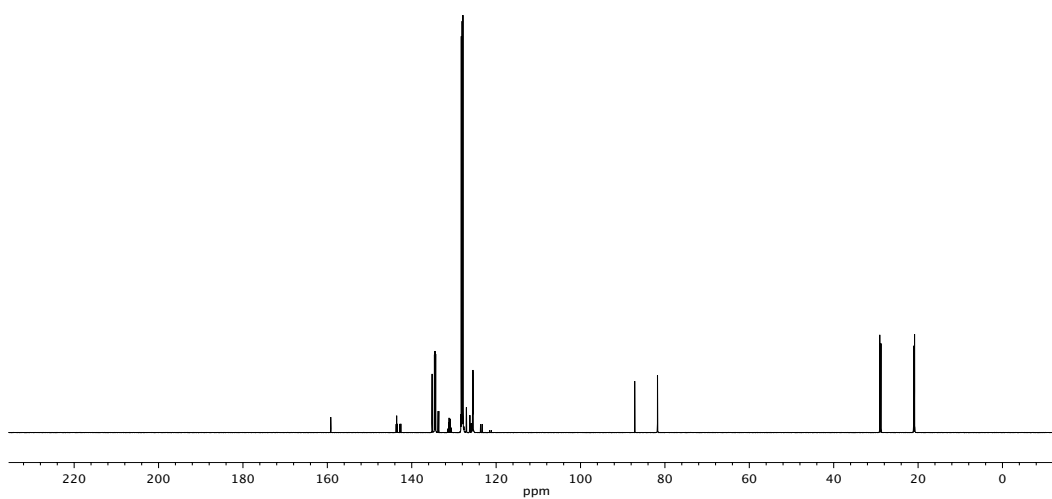


Figure A3.65 ¹³C NMR (125 MHz, C₆D₆) of compound **L15**.

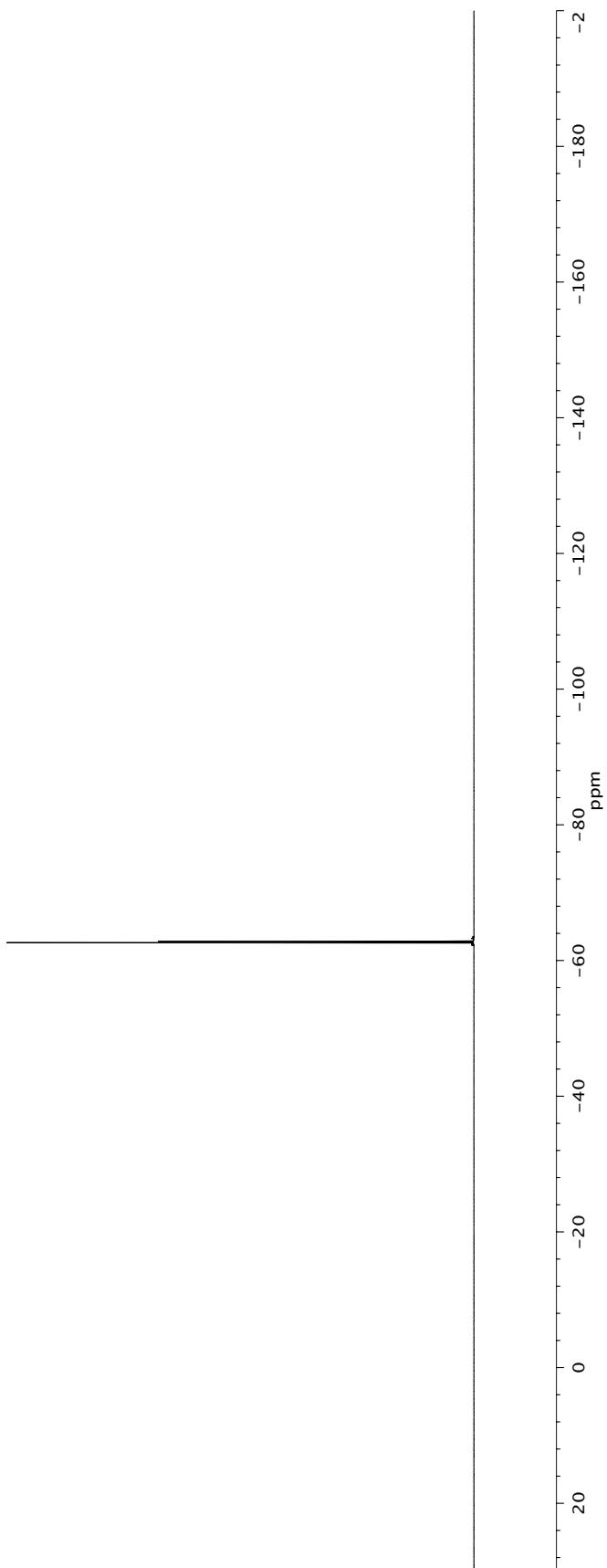
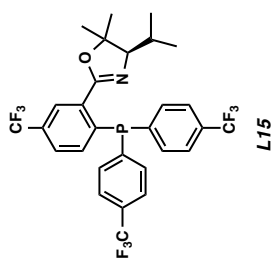


Figure A3.66 ^{19}F NMR (282 MHz, C_6D_6) of compound **L8**.

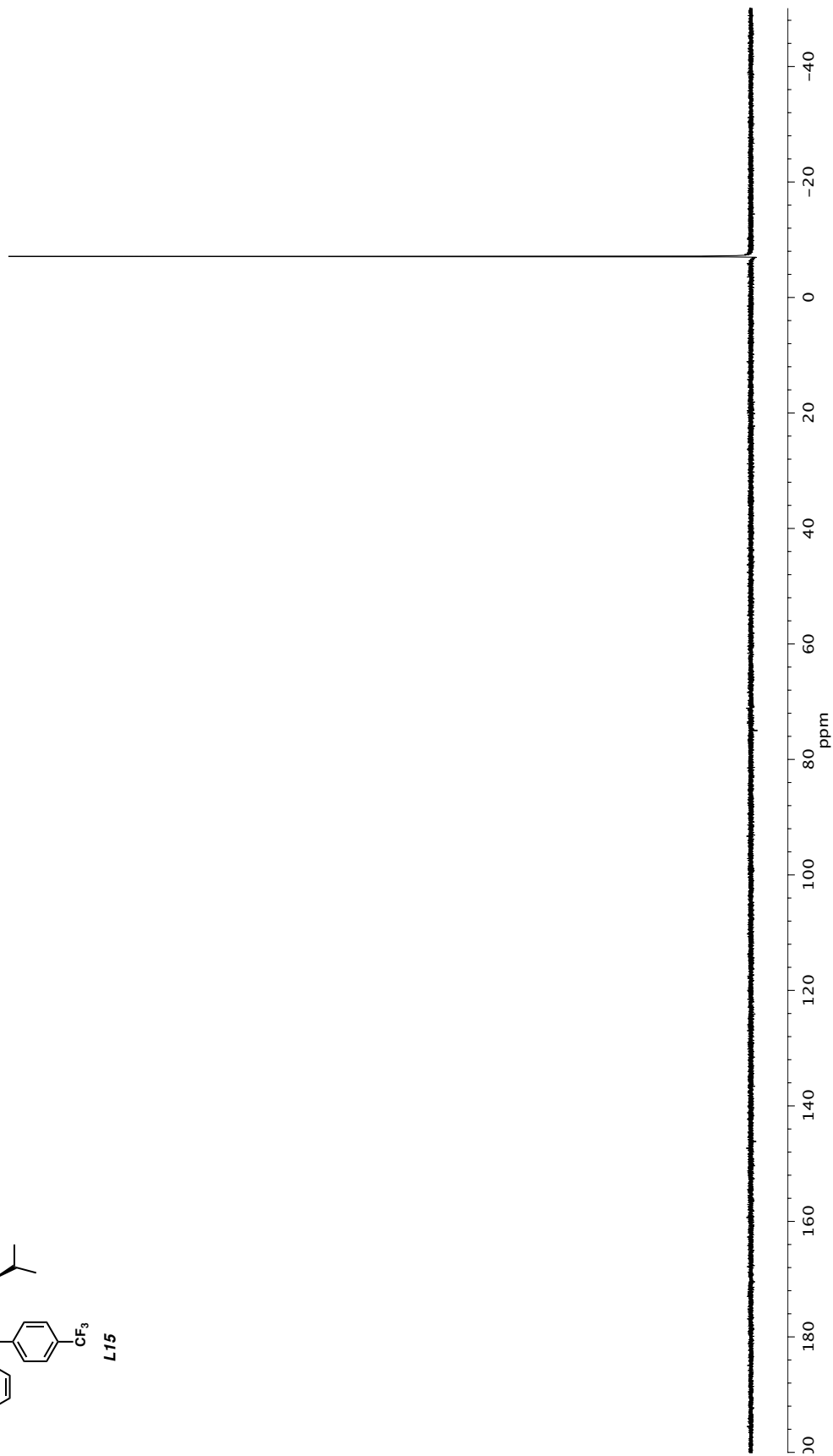
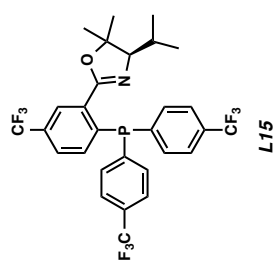


Figure A3.67 ^{31}P NMR (121 MHz, C_6D_6) of compound L15.

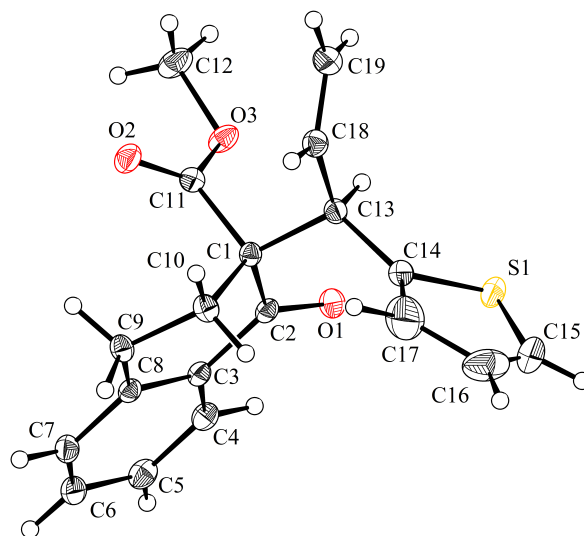
APPENDIX 4

X-ray Crystallography Reports

Relevant to Chapter 3

A4.1 CRYSTAL STRUCTURE ANALYSIS FOR COMPOUND 100f

Ketoester **100f** (>99% ee) was recrystallized from *i*-PrOH/hexanes (liquid/liquid diffusion) to provide suitable crystals for X-ray analysis, mp = 98-99 °C. NOTE: *Crystallographic data have been deposited in the Cambridge Database (CCDC), 12 Union Road, Cambridge CB2 1EZ, UK, and copies can be obtained on request, free of charge, by quoting the publication citation and the deposition number CCDC 939243.*

Figure A4.1.1. ORTEP drawing of **100f**.**Table A4.1.** Crystal Data and Structure Analysis Details for allylation ketoester **100f**.

Empirical formula	C ₁₉ H ₁₈ O ₃ S
Formula weight	326.39
Crystallization solvent	<i>i</i> -PrOH/hexanes
Crystal shape	block
Crystal color	colourless
Crystal size	0.13 x 0.23 x 0.29 mm

Data Collection

Preliminary photograph(s)	rotation
Type of diffractometer	Bruker SMART 1000 ccd
Wavelength	0.71073 Å MoK
Data collection temperature	100 K
Theta range for 9849 reflections used in lattice determination	2.30 to 30.92°
Unit cell dimensions	a = 8.4853(3) Å a = 90°

	b = 10.8613(4) Å	b = 90°
	c = 17.6979(6) Å	g = 90°
Volume	1631.06(10) Å ³	
Z	4	
Crystal system	orthorhombic	
Space group	P 21 21 21 (# 19)	
Density (calculated)	1.329 g/cm ³	
F(000)	688	
Theta range for data collection	2.2 to 36.7°	
Completeness to theta = 25.000°	99.9%	
Index ranges	-14 ≤ h ≤ 14, -18 ≤ k ≤ 18, -29 ≤ l ≤ 29	
Data collection scan type	and scans	
Reflections collected	49310	
Independent reflections	7841 [R _{int} = 0.0476]	
Reflections > 2s(I)	6228	
Average s(I)/(net I)	0.0436	
Absorption coefficient	0.21 mm ⁻¹	
Absorption correction	Semi-empirical from equivalents	
Max. and min. transmission	1.0000 and 0.9025	

Structure Solution and Refinement

Primary solution method	dual
Secondary solution method	?
Hydrogen placement	difmap
Refinement method	Full-matrix least-squares on F ²
Data / restraints / parameters	7841 / 0 / 303
Treatment of hydrogen atoms	refall
Goodness-of-fit on F ²	1.55
Final R indices [I > 2s(I), 6228 reflections]	R1 = 0.0483, wR2 = 0.0806
R indices (all data)	R1 = 0.0694, wR2 = 0.0846
Type of weighting scheme used	calc
Weighting scheme used	
Max shift/error	0.000
Average shift/error	0.000
Absolute structure parameter	0.01(3)
Extinction coefficient	n/a

Largest diff. peak and hole 0.37 and -0.24 e·Å⁻³

_refine_ls_abs_structure_details;

Flack x determined using 2400 quotients [(I+)-(I-)]/[(I+)+(I-)];

(Parsons and Flack (2004), Acta Cryst. A60, s61).

_refine_ls_abs_structure_Flack 0.01(3)

_refine_ls_abs_structure_Hoof 0.02(3)

Programs Used

Cell refinement	SAINT V8.27B (Bruker-AXS, 2007)
Data collection	Bruker SMART v5.054 (Bruker-AXS, 2007)
Data reduction	SAINT V8.27B (Bruker-AXS, 2007)
Structure solution	SHELXT (Sheldrick, 2012)
Structure refinement	SHELXL-2013/2 (Sheldrick, 2013)
Graphics	DIAMOND 3 (Crystal Impact, 1999)

Table A4.2. Atomic coordinates ($\times 10^4$) and equivalent isotropic displacement parameters ($\text{Å}^2 \times 10^3$) for **100f**. $U(\text{eq})$ is defined as one third of the trace of the orthogonalized U^{ij} tensor.

	x	y	z	U_{eq}
S(1)	9499(4)	3027(2)	9424(2)	26(1)
S(1A)	7396(4)	1194(2)	8920(1)	26(1)
O(1)	10909(1)	3864(1)	7769(1)	20(1)
O(2)	6712(1)	3819(1)	6298(1)	22(1)
O(3)	8198(1)	5196(1)	6915(1)	20(1)
C(1)	8415(2)	3108(1)	7316(1)	14(1)
C(2)	10216(2)	3266(1)	7292(1)	14(1)
C(3)	11064(2)	2667(1)	6651(1)	14(1)
C(4)	12665(2)	2961(1)	6537(1)	18(1)
C(5)	13491(2)	2453(2)	5941(1)	21(1)
C(6)	12737(2)	1641(2)	5451(1)	21(1)

C(7)	11165(2)	1346(1)	5556(1)	18(1)
C(8)	10300(2)	1842(1)	6161(1)	14(1)
C(9)	8605(2)	1477(1)	6273(1)	16(1)
C(10)	7999(2)	1793(1)	7062(1)	17(1)
C(11)	7676(2)	4054(1)	6775(1)	15(1)
C(12)	7433(2)	6145(2)	6468(1)	27(1)
C(13)	7740(2)	3432(1)	8120(1)	16(1)
C(14)	8255(2)	2565(1)	8741(1)	19(1)
C(15)	9443(3)	1759(2)	9876(1)	44(1)
C(16)	8455(3)	892(2)	9630(1)	42(1)
C(17)	7757(14)	1354(11)	8921(7)	51(4)
C(17A)	9366(19)	2793(11)	9301(7)	45(3)
C(18)	5962(2)	3506(2)	8090(1)	18(1)
C(19)	5128(2)	4517(2)	8192(1)	25(1)

Table A4.3. Bond lengths [\AA] and angles [$^\circ$] for **100f**.

S(1)-C(14)	1.681(3)
S(1)-C(15)	1.594(4)
S(1A)-C(14)	1.688(3)
S(1A)-C(16)	1.579(3)
O(1)-C(2)	1.2177(17)
O(2)-C(11)	1.2030(18)
O(3)-C(11)	1.3403(17)
O(3)-C(12)	1.452(2)
C(1)-C(2)	1.538(2)
C(1)-C(10)	1.539(2)
C(1)-C(11)	1.539(2)
C(1)-C(13)	1.5733(19)
C(2)-C(3)	1.492(2)
C(3)-C(4)	1.409(2)
C(3)-C(8)	1.406(2)
C(4)-H(4)	0.967(17)
C(4)-C(5)	1.380(2)
C(5)-H(5)	0.950(19)

C(5)-C(6)	1.394(2)
C(6)-H(6)	0.958(18)
C(6)-C(7)	1.385(2)
C(7)-H(7)	0.963(16)
C(7)-C(8)	1.405(2)
C(8)-C(9)	1.505(2)
C(9)-H(9A)	0.942(17)
C(9)-H(9B)	1.013(17)
C(9)-C(10)	1.527(2)
C(10)-H(10A)	0.977(17)
C(10)-H(10B)	0.966(18)
C(12)-H(12A)	0.96(2)
C(12)-H(12B)	1.03(2)
C(12)-H(12C)	1.02(2)
C(13)-H(13)	0.996(18)
C(13)-C(14)	1.511(2)
C(13)-C(18)	1.511(2)
C(14)-C(17)	1.418(11)
C(14)-C(17A)	1.391(12)
C(15)-H(15)	0.90(3)
C(15)-C(16)	1.334(3)
C(15)-C(17A)	1.517(15)
C(16)-H(16)	0.98(3)
C(16)-C(17)	1.476(12)
C(17)-H(17)	1.04(4)
C(17A)-H(17A)	0.97(5)
C(18)-H(18)	0.950(18)
C(18)-C(19)	1.319(2)
C(19)-H(19A)	0.97(2)
C(19)-H(19B)	1.01(2)
C(15)-S(1)-C(14)	94.87(18)
C(16)-S(1A)-C(14)	95.02(18)
C(11)-O(3)-C(12)	114.07(12)
C(2)-C(1)-C(10)	108.86(12)
C(2)-C(1)-C(11)	108.20(11)
C(2)-C(1)-C(13)	111.27(11)

C(10)-C(1)-C(13)	112.89(12)
C(11)-C(1)-C(10)	110.12(12)
C(11)-C(1)-C(13)	105.36(11)
O(1)-C(2)-C(1)	121.30(13)
O(1)-C(2)-C(3)	121.79(13)
C(3)-C(2)-C(1)	116.91(12)
C(4)-C(3)-C(2)	118.41(13)
C(8)-C(3)-C(2)	121.60(13)
C(8)-C(3)-C(4)	119.98(13)
C(3)-C(4)-H(4)	118.7(10)
C(5)-C(4)-C(3)	120.59(14)
C(5)-C(4)-H(4)	120.7(10)
C(4)-C(5)-H(5)	120.4(11)
C(4)-C(5)-C(6)	119.70(15)
C(6)-C(5)-H(5)	119.9(11)
C(5)-C(6)-H(6)	119.0(11)
C(7)-C(6)-C(5)	120.27(15)
C(7)-C(6)-H(6)	120.7(11)
C(6)-C(7)-H(7)	121.4(10)
C(6)-C(7)-C(8)	121.19(15)
C(8)-C(7)-H(7)	117.4(10)
C(3)-C(8)-C(9)	121.84(13)
C(7)-C(8)-C(3)	118.25(13)
C(7)-C(8)-C(9)	119.90(13)
C(8)-C(9)-H(9A)	108.3(10)
C(8)-C(9)-H(9B)	109.8(10)
C(8)-C(9)-C(10)	112.49(12)
H(9A)-C(9)-H(9B)	104.7(14)
C(10)-C(9)-H(9A)	108.8(10)
C(10)-C(9)-H(9B)	112.4(9)
C(1)-C(10)-H(10A)	107.6(10)
C(1)-C(10)-H(10B)	109.6(10)
C(9)-C(10)-C(1)	113.53(12)
C(9)-C(10)-H(10A)	109.2(10)
C(9)-C(10)-H(10B)	109.8(10)
H(10A)-C(10)-H(10B)	106.8(14)
O(2)-C(11)-O(3)	123.43(13)

O(2)-C(11)-C(1)	124.93(13)
O(3)-C(11)-C(1)	111.60(12)
O(3)-C(12)-H(12A)	113.2(14)
O(3)-C(12)-H(12B)	106.2(11)
O(3)-C(12)-H(12C)	110.2(11)
H(12A)-C(12)-H(12B)	109.9(18)
H(12A)-C(12)-H(12C)	106.8(18)
H(12B)-C(12)-H(12C)	110.5(16)
C(1)-C(13)-H(13)	106.6(10)
C(14)-C(13)-C(1)	114.33(12)
C(14)-C(13)-H(13)	107.1(10)
C(18)-C(13)-C(1)	110.12(12)
C(18)-C(13)-H(13)	108.2(10)
C(18)-C(13)-C(14)	110.28(13)
C(13)-C(14)-S(1)	121.21(15)
C(13)-C(14)-S(1A)	124.16(14)
C(17)-C(14)-S(1)	107.6(5)
C(17)-C(14)-C(13)	131.0(5)
C(17A)-C(14)-S(1A)	108.4(6)
C(17A)-C(14)-C(13)	127.1(6)
S(1)-C(15)-H(15)	120.9(19)
C(16)-C(15)-S(1)	117.68(19)
C(16)-C(15)-H(15)	121.4(19)
C(16)-C(15)-C(17A)	106.1(5)
C(17A)-C(15)-H(15)	132(2)
S(1A)-C(16)-H(16)	113.9(17)
C(15)-C(16)-S(1A)	118.07(19)
C(15)-C(16)-H(16)	128.0(17)
C(15)-C(16)-C(17)	106.8(5)
C(17)-C(16)-H(16)	125.0(17)
C(14)-C(17)-C(16)	112.8(8)
C(14)-C(17)-H(17)	116(2)
C(16)-C(17)-H(17)	131(2)
C(14)-C(17A)-C(15)	112.1(9)
C(14)-C(17A)-H(17A)	124(3)
C(15)-C(17A)-H(17A)	124(3)
C(13)-C(18)-H(18)	118.4(11)

C(19)-C(18)-C(13)	125.07(16)
C(19)-C(18)-H(18)	116.5(11)
C(18)-C(19)-H(19A)	121.1(14)
C(18)-C(19)-H(19B)	119.8(11)
H(19A)-C(19)-H(19B)	119.1(17)

Symmetry transformations used to generate equivalent atoms:

Table A4.4. Anisotropic displacement parameters ($\text{\AA}^2 \times 10^4$) for **100f**. The anisotropic displacement factor exponent takes the form: $-2p^2 [h^2 a^{*2} U^{11} + \dots + 2hk a^* b^* U^{12}]$

	U ¹¹	U ²²	U ³³	U ²³	U ¹³	U ¹²
S(1)	360(9)	243(10)	173(5)	5(6)	-83(5)	58(8)
S(1A)	335(10)	229(6)	231(7)	93(6)	-46(6)	-2(6)
O(1)	198(5)	189(5)	197(5)	-39(4)	-40(4)	-28(4)
O(2)	242(6)	202(5)	213(5)	-7(4)	-87(5)	5(4)
O(3)	220(6)	136(5)	253(6)	36(4)	-82(5)	-16(4)
C(1)	145(6)	132(6)	130(6)	-2(5)	-6(5)	-11(5)
C(2)	168(7)	127(6)	140(6)	26(5)	-27(5)	-4(5)
C(3)	151(6)	139(6)	138(6)	19(5)	-17(5)	-6(5)
C(4)	166(7)	188(7)	188(7)	24(5)	-23(6)	-20(6)
C(5)	160(7)	267(8)	204(7)	46(6)	-2(6)	-6(6)
C(6)	232(8)	258(8)	146(7)	24(6)	23(6)	39(6)
C(7)	223(8)	188(7)	143(6)	4(5)	-6(6)	3(6)
C(8)	168(7)	131(6)	136(6)	23(5)	-18(5)	4(5)
C(9)	185(7)	142(6)	153(6)	-24(5)	-2(5)	-32(5)
C(10)	191(7)	139(7)	170(7)	-10(5)	10(5)	-36(5)
C(11)	149(7)	150(6)	157(6)	4(5)	14(5)	-6(5)
C(12)	330(10)	151(7)	333(9)	58(7)	-107(8)	5(7)
C(13)	197(7)	140(6)	136(6)	-6(5)	-7(5)	4(5)
C(14)	215(7)	198(7)	152(7)	4(5)	7(6)	34(6)
C(15)	537(14)	571(14)	214(9)	-26(9)	-113(9)	224(12)
C(16)	451(13)	329(11)	469(12)	186(9)	150(10)	127(10)
C(17)	480(60)	540(60)	500(50)	-210(40)	-180(40)	20(40)

C(17A)	510(50)	330(50)	510(70)	90(40)	70(50)	-90(40)
C(18)	185(7)	194(7)	163(7)	6(6)	6(6)	-3(6)
C(19)	262(9)	251(9)	244(8)	-56(7)	-34(7)	49(7)

Table A4.5. Hydrogen coordinates ($\times 10^3$) and isotropic displacement parameters ($\text{\AA}^2 \times 10^3$) for **100f**.

	x	y	z	U _{iso}
H(4)	1318(2)	350(2)	689(1)	11(4)
H(5)	1457(2)	265(2)	587(1)	23(5)
H(6)	1331(2)	131(2)	503(1)	18(4)
H(7)	1063(2)	79(1)	522(1)	12(4)
H(9A)	852(2)	62(2)	620(1)	14(4)
H(9B)	793(2)	185(2)	586(1)	14(4)
H(10A)	846(2)	122(2)	743(1)	14(4)
H(10B)	687(2)	168(2)	708(1)	17(4)
H(12A)	766(3)	608(2)	594(1)	44(6)
H(12B)	784(2)	697(2)	667(1)	32(5)
H(12C)	624(3)	608(2)	652(1)	32(5)
H(13)	815(2)	426(2)	825(1)	17(4)
H(15)	1003(3)	165(3)	1030(2)	72(8)
H(16)	827(3)	7(3)	985(2)	80(9)
H(17)	689(4)	98(3)	857(2)	10(8)
H(17A)	1003(5)	352(4)	932(2)	9(11)
H(18)	539(2)	277(2)	799(1)	20(4)
H(19A)	564(3)	531(2)	828(1)	40(6)
H(19B)	394(2)	448(2)	818(1)	27(5)

Table A4.6. Hydrogen bonds for **100f** [\AA and $^\circ$].

D-H...A	d(D-H)	d(H...A)	d(D...A)	<(DHA)
C(12)-H(12B)...O(1)#1	1.03(2)	2.52(2)	3.539(2)	173.4(16)

Symmetry transformations used to generate equivalent atoms:

#1 $-x+2, y+1/2, -z+3/2$

CHAPTER 4

Enantio-, Diastereo- and Regioselective Iridium-Catalyzed Asymmetric Allylic Alkylation of Acyclic β -Ketoesters¹

4.1 INTRODUCTION

4.1.1 State of the art in the asymmetric construction of vicinal quaternary and tertiary carbon centers

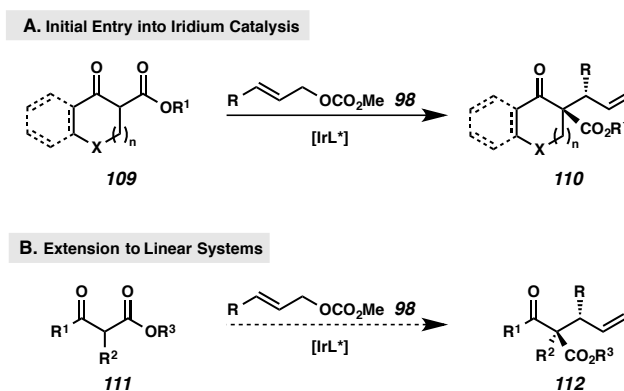
As outlined in Chapter 3 (vide supra), the generation of enantioenriched all-carbon quaternary centers is complicated by the presence of vicinal tertiary stereocenters due to increased steric demands and the introduction of requisite diastereocontrol. Modern strategies for accessing these highly-congested stereochemical dyads have relied primarily on transition-metal catalysis, notably Pd-catalyzed enolate alkylation cascades,³⁰ Pd-catalyzed trimethylenemethane cycloadditions,^{73b,e} Cu-catalyzed asymmetric Claisen rearrangements,^{73f} and Mo-^{73c,d} and Ir-catalyzed⁸³ allylic alkylations. Common to the majority of these reports is the constraint that the nascent quaternary center be formed at a cyclic nucleophile. At the outset of our studies in this area, only two groups had reported success in employing linear nucleophiles to produce vicinal

¹ This work was performed in collaboration with Wen-Bo Lui, postdoctoral researcher in the Stoltz group. This work has been published. See: Liu, W. -B.; Reeves, C. M.; Stoltz, B. M. *J. Am. Chem. Soc.* **2013**, *135*, 17298.

quaternary/tertiary arrays. Namely, Trost's communication on the molybdenum-catalyzed allylic alkylation of β -cyanoesters^{73d} and Carreira's recent report on the allylic alkylation of aldehydes using stereodivergent dual catalysis.⁸³ To address these limitations, we initiated studies investigating the asymmetric allylic alkylation of linear β -ketoesters.

As described above, we have shown iridium-*N*-arylphosphoramidite catalysis⁸⁷ to be a powerful tool for accessing vicinal all-carbon quaternary and tertiary stereocenters. The success of our protocol for the regio-, diastereo- and enantioselective asymmetric allylic alkylation of cyclic β -ketoesters (Figure 4.1.1.A)^{82, 88, 97} combined with the virtual absence of reports describing the application of this transformation to acyclic β -ketoesters encouraged our further exploration of iridium catalysts in the domain of this important substrate class. In this chapter, we detail the development of the first highly regio-, diastereo- and enantioselective allylic alkylation of acyclic β -ketoesters to forge vicinal tertiary, quaternary centers (Figure 4.1.1.B).

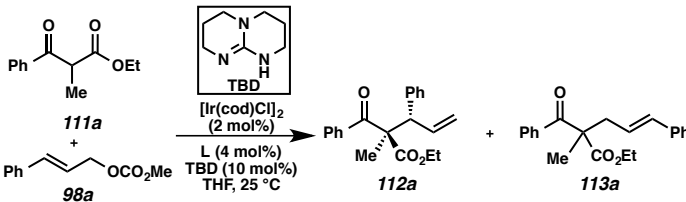
Figure 4.1.1.1. Representative Ir-catalyzed asymmetric allylic alkylation



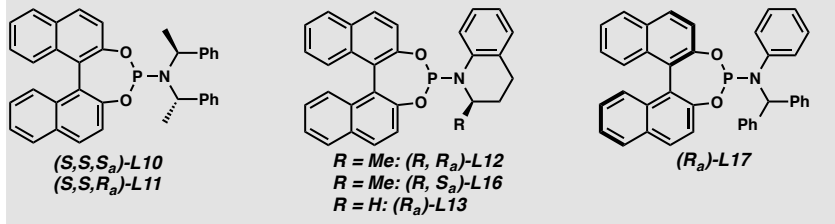
4.2 DEVELOPMENT AND OPTIMIZATION OF AN Iridium-CATALYZED ALLYLIC ALKYLATION OF LINEAR β -KETOESTERS

Our initial investigations in the domain of Ir-catalyzed allylic alkylation of linear β -ketoesters focused on identifying conditions that would afford both reaction efficiency and selectivity. We chose ethyl 2-methyl-3-oxo-3-phenylpropanoate (**111a**) and cinnamyl carbonate (**98a**) as standard coupling partners, and investigated several iridacycle complexes⁸⁴ at the outset of our studies. The result of these studies are shown in Table 4.2.1 (entries 1–6). We found that exposure of standard coupling components (**111a**) and (**98a**) to a combination of catalytic phosphoramidite ligand **L10**•[Ir(cod)Cl]₂ complex⁸⁶ and two equivalents of NaH in THF at ambient temperature afforded the desired product with good conversion, ee and regioselectivity, but low levels of diastereoselectivity (1:2) (entry 1). Use of either **L11** or **L16** under these conditions favored instead the reaction pathway yielding the undesired, linear allylic alkylation product (**113a**) in only modest conversion (entries 2 and 4). Ligands **L13** and **L17**^{87,98} gave the desired branched product in good conversion but with diminished diastereoselectivity and enantioselectivity and protracted reaction times (entries 5 and 6). We were pleased to find that tetrahydroquinoline based ligand **L12**⁸⁷ rapidly furnished the desired α -quaternary β -ketoester (**112a**) in greater than 95% conversion, 95:5 regioselectivity, 13:1 dr and 99% enantiomeric excess (entry 3). Previous reports demonstrating the marked effect of metal cations over regio-⁹⁹ and diastereoselectivity¹⁰⁰ in iridium-catalyzed allylic alkylations prompted further investigation of both bases and additives (entries 7–15). Contrary to our previous findings (vide infra, Chapter 3), a

sluggish reaction was observed when LiBr was used in place of NaH (entry 7), presumably due to the decreased α -acidity of acyclic β -ketoesters relative to cyclic substrates. While amine and organic bases did not perform well in the chemistry, the use of alkoxide bases resulted in considerably reduced reaction times (entries 8–9). Ultimately, it was found that the use of LiOt-Bu as base was optimal, delivering β -ketoester **112a** with an exceptional branched to linear ratio (93:7), >20:1 diastereoselectivity, and 98% enantioselectivity in only two hours (entry 8).

Table 4.2.1. Optimization of the Ir-catalyzed asymmetric allylic alkylation^a


entry	L	base/additive (x equiv)	time (h)	conv. (%) ^b	yield (%) ^c	112a:113a ^b	dr of 112a ^b	ee of 112 (%) ^d
1	L10	NaH (2)	22	91	–	89:11	1:1.8	81(97)
2	L11	NaH (2)	48	46	–	17:83	1:1	–
3	L12	NaH (2)	22	>95	64	95:5	13:1	99
4	L16	NaH (2)	48	34	–	42:58	3.5:1	–
5	L13	NaH (2)	72	>95	–	71:29	2:1	76
6	L17	NaH (2)	72	>95	–	93:7	7.3:1	72
7	L12	LiBr (1)	32	>95	91	95:5	>20:1	>99
8	L12	LiOt-Bu (2)	2	>95	97	93:7	>20:1	98
9	L12	KOt-Bu (2)	4	>95	–	93:7	2:1	94(87)
10	L12	Cs ₂ CO ₃ (2)	4	>95	–	83:17	1:2.2	87(94)
11	L12	DABCO (2)	24	>95	–	81:19	1:2.7	64(82)
12	L12	proton sponge (2)	4	>95	–	90:10	1:1	87(93)
13	L12	DMAP (2)	4	>95	–	83:17	1:1.4	91(93)
14	L12	Bu ₄ NBr (1)	3	>95	–	88:12	1:2.6	87(93)
15	L12	BnMe ₃ NBr (1)	4	>95	–	86:14	1:1	91(95)



(*S,S,S_a*)-L10
(*S,S,R_a*)-L11

R = Me: (*R, R_a*)-L12
R = Me: (*R, S_a*)-L16
R = H: (*R_a*)-L13

(*R_a*)-L17

^a Reactions performed with 0.1 mmol of **98a**, 0.2 mmol of **111a** at 0.1 M in THF at 20 °C. ^b Determined by ¹H NMR and UHPLC-MS analysis of the crude mixture. ^c Determined by chiral SFC analysis; parenthetical value is the ee of the alternate diastereomer. ^d Not determined.

4.3 EXPLORATION OF THE REACTION SCOPE AND SUBSTITUENT EFFECTS

4.3.1 Exploration of the iridium-catalyzed allylic alkylation of linear β -ketoesters with respect to allyl electrophile

With optimized conditions identified, the scope of the reaction with respect to the electrophile was next explored. A highly selective reaction was observed between β -

ketoester **111a** and various cinnamyl carbonate-derived electrophiles (**98**) bearing electron-donating substituents about the aryl group, R (Table 4.3.1.1, entries 2–4). 4-Me- (**98i**), 4-MeO- (**98b**), and 3-MeO-substitutions (**98j**) about the aryl ring gave the corresponding α -quaternary β -ketoesters (products **112b-112d**) in good to excellent yield, dr, ee and branched to linear ratio (Table 4.3.1.1). Electron deficient aryl substituents at the allyl group (entries 5–7) were also well tolerated, delivering the branched products **112e-112g**¹⁰¹ in good to excellent yield, outstanding ee and dr, and with only slightly diminished regioselectivities. Interestingly, (4-nitro)-aryl substitution at the allyl carbonate (entry 8, substrate **98l**) led to loss of regioselectivity in the reaction, giving equal amounts of products **112h** (14:1 dr, 93% ee) and **113h** (23% ee). We were pleased to discover, however, that heteroaryl-substituted allyl carbonates (substrates **98j** and **98g**) resulted in smooth reactions and delivered the alkylated products **112i** and **112j** with excellent yield, ee and regioselectivity and with good to excellent dr (entries 9–10). Finally, we found that sorbyl carbonate **98h** was also a suitable participant in the reaction, giving the corresponding β -ketoester product (**112k**) in good yield and dr and with excellent regio- and enantioselectivities (entry 11).

Table 4.3.1.1. Exploration of the reaction scope with respect to allyl electrophile^a

entry	98	product (112)	yield (%) ^b	112:113 ^c	dr of 112 ^c	ee of 112 (%) ^d	
1	98a		112a: R = H	97	93:7	>20:1	98
2	98i		112b: R = Me	97	95:5	20:1	>99
3 ^e	98b		112c: R = MeO	85	99:1	>20:1	>99
4	98j		112d: R = MeO	99	90:10	17:1	>99
5	98k		112e: R = Cl	98	84:16	19:1	99
6	98c		112f: R = Br	98	86:14	14:1	>99
7	98d		112g: R = CF ₃	86	78:22	16:1	99
8	98l		112h: R = NO ₂	78	50:50 ^f	14:1	93
9	98f		112i: X = S	99	97:3	8:1	95
10	98g		112j: X = O	93	95:5	13:1	>99
11	98h		112k	76	95:5	6:1	91

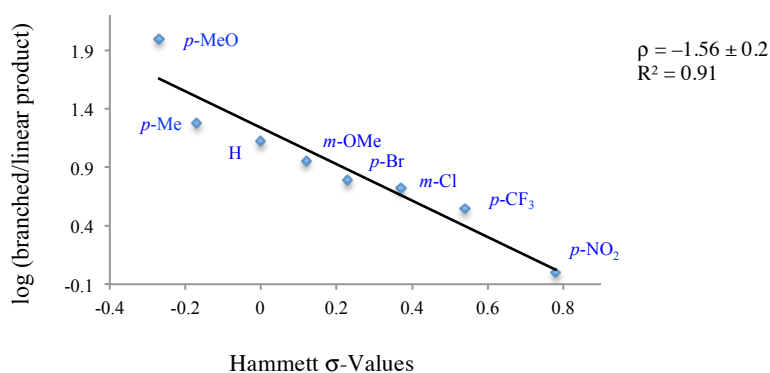
^a Reactions performed under the conditions of Table 1, entry 8. ^b Combined isolated yield of **112** and **113**. ^c Determined by ¹H NMR analysis of the crude mixture. ^d Determined by chiral SFC analysis of the major diastereomer. ^e Conditions of Table 1, entry 7. ^f 23% ee for the linear product.

4.3.2 Investigation of allyl electrophile substituent effects on reaction selectivity

During the course of this investigation, a trend relating regioselectivity and electrophile electron deficiency began to emerge. Specifically, the regioselectivity of the reaction diminished as the electron deficiency of the allyl substituent increased. In order to identify the linear free energy relationship governing the reaction, we performed a

Hammett analysis relating the log of the ratio of branched to linear products, which is proportional to the relative rates of product formation, to the corresponding Hammett σ -values. The negative ρ value observed from this plot suggests that as the magnitude of electropositive charge generated at the putative allyl-Ir intermediate^{8b} increases, the reaction pathway yielding the branched allylation product becomes more favorable. This analysis can be extended to account, in part, for the poor regioselectivity observed in the case of *p*-nitro substituted allyl component **98**.

Figure 4.3.2.1. Hammett plot of the log of product ratios (**112**:**113**) from Table 2 versus Hammett σ -values



4.3.3 Exploration of the iridium-catalyzed allylic alkylation of linear β -ketoesters with respect to β -ketoester nucleophile

Having investigated reaction substrate scope with respect to the allyl electrophile, we next examined the diversity of nucleophilic coupling partners permitted in the chemistry (Table 4.3.3.1). β -Ketoesters (**111**) bearing either electron-donating or electron-withdrawing aryl substituents (R^1) at the ketone fared very well in the reaction,

delivering products **112l** and **112m** in excellent yield, dr, ee and branched to linear ratio (entries 1 and 2). Gratifyingly, a wide variety of functional groups are readily permitted at the α -position (R^2), including alkyl, benzyl, allyl, propargyl, heteroaryl and keto groups (substrates **111d–111i**, entries 3–8, respectively). The products of these reactions (products **112n–112s**, respectively) were obtained with excellent ee and regioselectivities, and in good to excellent dr and yield. To the best of our knowledge, substrate **111g** represents the first example of a terminal propargyl-substituted nucleophile to undergo Ir-catalyzed allylic substitutions.¹⁰² Nitrile-containing substituents were tolerated in the reaction as well (substrate **111j**), and α -quaternary β -ketoester **112t** was furnished in excellent yield, ee and regioselectivity, albeit with a diminished dr of 3:1. We were pleased to learn that use of certain of α -halogenated nucleophiles (substrates **111k** and **111l**) also resulted in an efficient and selective reaction as α -fluoro and α -chloro β -ketoesters **112u** and **112v** were obtained in excellent yields, dr, ee and regioselectivity. In addition to aryl ketones, cyclohexenyl β -ketoester **111m** was found to deliver the corresponding product **112w** in excellent yield, dr, ee and branched to linear ratio with no detectable products resulting from competitive bimolecular Michael addition. Although the use of alkyl β -ketoesters **111n** and **111o** provided the desired products (**112x** and **112y**, respectively) with excellent yields, ee's and regioselectivities, we were disappointed to find that the diastereoselectivities were diminished considerably. Lastly, we found that the use of a sterically-hindered ester moiety (substrate **111p**) gave an efficient and highly enantioselective reaction but with a concurrent loss in regio- and diastereoselectivity (entry 15).

Table 4.3.3.1. Exploration of the reaction scope with respect to β -ketoester nucleophile^a

entry	111	product (112)	yield (%) ^b	112:113 ^c	dr of 112 ^c	ee of 112 (%) ^d
1	111b		93	93:7	17:1	99
2	111c		92	92:8	17:1	>99
3	111d	112n: R ² = Et	94	90:10	>20:1	>99
4	111e	112o: R ² = Bn	99	90:10	13:1	>99
5	111f	112p: R ² = allyl	98	95:5	>20:1	>99
6 ^e	111g	112q: R ² = propargyl	84	81:19	13:1	>99
7 ^f	111h	112r: R ² = (CH ₂) ₂ COMe	98	93:7	20:1	99
8	111i	112s: R ² =	88	95:5	7:1	>99
9	111j	112t: R ² = CH ₂ CH ₂ CN	99	95:5	3:1	>99 (>99) ^g
10	111k	112u: R ² = F	92	96:4	13:1	95
11	111l	112v: R ² = Cl	96	96:4	>20:1	>99
12	111m	112w	85	90:10	12:1	99
13	111n	112x: R ¹ = Cy R ² = Me	92	92:8	4:1	96
14	111o	112y: R ¹ = Me R ² = Et	90	93:7	1.5:1	90 (91) ^g
15	111p	112z	95	70:30	6:1	>99

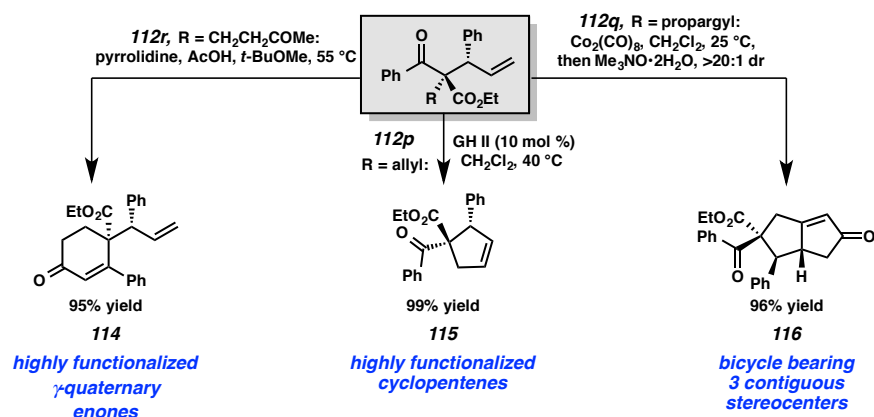
^a Reactions performed under the conditions of Table 1, entry 8. ^b Combined isolated yield of **112** and **113**. ^c Determined by ¹H NMR analysis of the crude mixture. ^d Determined by chiral SFC analysis of the major diastereomer. ^e 4 mol % of [Ir(cod)Cl]₂ and 8 mol % of **L12** were used. ^f The reaction was run at 0.5 mmol scale. ^g ee for the minor diastereomer.

4.4 ELABORATION OF THE ALLYLIC ALKYLATION PRODUCTS

In order to exhibit the utility of our method for generating interesting and useful chiral building blocks, a number of selective transformations were carried out on

products obtained in the course of our studies (Scheme 4.4.1). Aldol condensation of β -ketoester **112r** gave γ -quaternary cyclohexenone **114** in excellent yield. Ring-closing metathesis of diallyl β -ketoester **112p** cleanly furnished cyclohexene **115** in excellent yield. Finally, Pauson–Khand cyclization of propargyl-substituted β -ketoester **112q** smoothly delivered bicycle **116** in outstanding 99% yield.

Scheme 4.4.1. Rapid generation of molecular and stereochemical complexity employing allylic alkylation products



4.5 CONCLUDING REMARKS

In summary, the first enantioselective catalytic allylic alkylation of linear β -ketoesters to generate vicinal quaternary and tertiary stereocenters in high yield, dr, ee and regioselectivity has been developed. The process hinges on the use of an Ir•*N*-aryl-phosphoramidite catalyst (**L12**). A variety of substitution patterns at the allyl electrophile and β -ketoester are well tolerated in the chemistry. A number of transformations were carried out on reaction products to demonstrate the value this method holds for the rapid

generation of highly functionalized chiral building blocks. Studies utilizing this method toward the synthesis of complex biologically active natural products are underway in our laboratory and will serve to showcase the utility of the method in synthetic setting. Moreover, studies to extend the scope of functionality tolerated about the electrophile in the chemistry, in particular non-aromatic substituents, should greatly expand the potential applications of this method to total synthesis.

4.6 EXPERIMENTAL SECTION

4.6.1 Materials and Methods

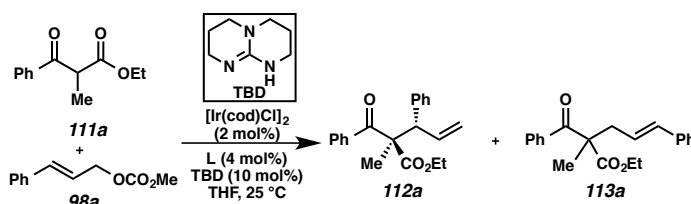
Unless otherwise stated, reactions were performed in flame-dried glassware under an argon or nitrogen atmosphere using dry, deoxygenated solvents. Solvents were dried by passage through an activated alumina column under argon.⁶¹ Reaction progress was monitored by thin-layer chromatography (TLC) or Agilent 1290 UHPLC-MS. TLC was performed using E. Merck silica gel 60 F254 precoated glass plates (0.25 mm) and visualized by UV fluorescence quenching, *p*-anisaldehyde, or KMnO₄ staining. Silicycle SiliaFlash® P60 Academic Silica gel (particle size 40–63 nm) was used for flash chromatography. ¹H NMR spectra were recorded on Varian Inova 500 MHz and 600 MHz spectrometers and are reported relative to residual CHCl₃ (δ 7.26 ppm) or C₆HD₅ (δ 7.16 ppm). ¹³C NMR spectra were recorded on a Varian Inova 500 MHz spectrometer (125 MHz) and are reported relative to CHCl₃ (δ 77.16 ppm) or C₆HD₅ (δ 128.06 ppm). ³¹P and ¹⁹F NMR spectra were recorded on a Varian Mercury 300 MHz (at 121 MHz and 282 MHz, respectively). ¹⁹F NMR spectra were reported relative to CFCl₃ (δ 0.0 ppm). ³¹P NMR spectra were reported relative to external H₃PO₄ (δ 0.0 ppm). Data for ¹H NMR

are reported as follows: chemical shift (δ ppm) (multiplicity, coupling constant (Hz), integration). Multiplicities are reported as follows: s = singlet, d = doublet, t = triplet, q = quartet, p = pentet, sept = septuplet, m = multiplet, br s = broad singlet, br d = broad doublet, app = apparent. Data for ^{13}C NMR are reported in terms of chemical shifts (δ ppm). IR spectra were obtained by use of a Perkin Elmer Spectrum BXII spectrometer or Nicolet 6700 FTIR spectrometer using thin films deposited on NaCl plates and reported in frequency of absorption (cm^{-1}). Optical rotations were measured with a Jasco P-2000 polarimeter operating on the sodium D-line (589 nm), using a 100 mm path-length cell and are reported as: $[\alpha]_{\text{D}}^{\text{T}}$ (concentration in g/100 mL, solvent). Analytical HPLC was performed with an Agilent 1100 Series HPLC utilizing a Chiralpak (AD-H or AS) or Chiralcel (OD-H, OJ-H, or OB-H) columns (4.6 mm x 25 cm) obtained from Daicel Chemical Industries, Ltd. Analytical SFC was performed with a Mettler SFC supercritical CO_2 analytical chromatography system utilizing Chiralpak (AD-H, AS-H or IC) or Chiralcel (OD-H, OJ-H, or OB-H) columns (4.6 mm x 25 cm) obtained from Daicel Chemical Industries, Ltd. High resolution mass spectra (HRMS) were obtained from Agilent 6200 Series TOF with an Agilent G1978A Multimode source in electrospray ionization (ESI+), atmospheric pressure chemical ionization (APCI+), or mixed ionization mode (MM: ESI-APCI+).

Reagents were purchased from Sigma-Aldrich, Acros Organics, Strem, or Alfa Aesar and used as received unless otherwise stated. Ligands **L12**, **L13**, **L16** and **L17**⁸⁷ allyl carbonates **98**,⁹⁵ and β -ketoesters **111**¹⁰³ were prepared by known methods.

4.6.2 Optimization of reaction parameters

Table 4.6.2.1 Optimization of reaction parameters



entry	L	base/additive (x equiv)	time (h)	conv. (%) ^b	yield (%) ^c	112a:113a ^b	dr of 112a ^b	ee of 112 (%) ^d
1	L10	NaH (2)	22	91	–	89:11	1:1.8	81(97)
2	L11	NaH (2)	48	46	–	17:83	1:1	–
3	L12	NaH (2)	22	>95	64	95:5	13:1	99
4	L16	NaH (2)	48	34	–	42:58	3.5:1	–
5	L13	NaH (2)	72	>95	–	71:29	2:1	76
6	L17	NaH (2)	72	>95	–	93:7	7.3:1	72
7	L12	LiBr (1)	32	>95	91	95:5	>20:1	>99
8	L12	LiOt-Bu (2)	2	>95	97	93:7	>20:1	98
9	L12	KOt-Bu (2)	4	>95	–	93:7	2:1	94(87)
10	L12	Cs ₂ CO ₃ (2)	4	>95	–	83:17	1:2.2	87(94)
11	L12	DABCO (2)	24	>95	–	81:19	1:2.7	64(82)
12	L12	proton sponge (2)	4	>95	–	90:10	1:1	87(93)
13	L12	DMAP (2)	4	>95	–	83:17	1:1.4	91(93)
14	L12	Bu ₄ NBr (1)	3	>95	–	88:12	1:2.6	87(93)
15	L12	BnMe ₃ NBr (1)	4	>95	–	86:14	1:1	91(95)

^a Reactions performed with 0.1 mmol of **98a**, 0.2 mmol of **111a** in 1 mL of THF. ^b Determined by ¹H NMR or UHPLC-MS analysis of the crude reaction mixture. ^c Isolated yield. ^d (ee) of the alternative diastereomer.

General Procedure for Optimization Reaction (Table 4.6.2.1): All experiments were performed in a nitrogen-filled glove box.

Procedure A (for entries 1-9): [Ir(cod)Cl]₂ (1.4 mg, 0.002 mmol, 2 mol%), ligand L (0.004 mmol, 4 mol%), and TBD (1.4 mg, 0.01 mmol, 10 mol%) were added to a 2 dram scintillation vial (vial A) equipped with a magnetic stirring bar. The vial was then charged with THF (0.5 mL) and stirred at 25 °C for 10 min, generating an orange solution. To another 2 dram scintillation vial (vial B) was added base (0.2 mmol, 2 equiv), 0.5 mL of THF and β -ketoester **111a** (41.2 mg, 0.2 mmol, 2.0 equiv). After

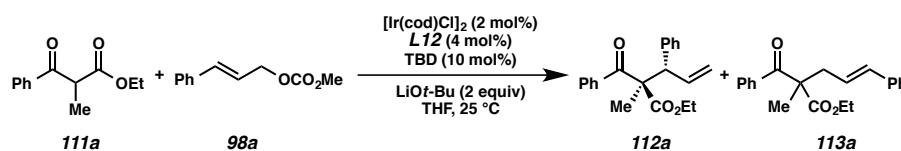
stirring for 10 min at 25 °C, the pre-formed catalyst solution (vial A) was transferred to vial B, and cinnamyl carbonate (**98a**) (19.2 mg, 0.1 mmol, 1.0 equiv) was added. The vial was sealed and stirred at 25 °C until allylic carbonate **98a** was fully consumed, as indicated by UHPLC-MS analysis. Upon completion of the reaction the vial was removed from the glove-box and uncapped. Saturated NH₄Cl aqueous solution was added and the mixture was extracted with CH₂Cl₂ (10 mL x 3), the combined organic phase was washed with brine, dried over Mg₂SO₄, filtered and concentrated *in vacuo*. The regioselectivity (branched product to linear product, b:l) and diastereoselectivity (dr) were determined by ¹H NMR. The residue was purified by silica gel flash chromatography (gradient elution, 0→1→2% EtOAc in hexanes) to afford the desired product.

Procedure B (for entries 10-15): [Ir(cod)Cl]₂ (1.4 mg, 0.002 mmol, 2 mol%), ligand **L** (0.004 mmol, 4 mol%), and TBD (1.4 mg, 0.01 mmol, 10 mol%) were added to a 2 dram scintillation vial equipped with a magnetic stirring bar. The vial was then charged with THF (0.5 mL) and stirred at 25 °C for 10 min, generating an orange solution. Cinnamyl carbonate (**98a**) (19.2 mg, 0.1 mmol, 1.0 equiv), β -ketoester **111a** (41.2 mg, 0.2 mmol, 2.0 equiv), base (0.2 mmol, 2 equiv) or additive (0.1 mmol, 1.0 equiv) and an additional 0.5 mL of THF were added. The vial was sealed and stirred at 25 °C until allylic carbonate **98a** was fully consumed, as indicated by UHPLC-MS analysis. Upon completion of the reaction the vial was removed from the glove-box and uncapped and THF evaporated under reduced pressure. Et₂O was added to the crude mixture and the resulting precipitate was filtered through a celite pad, rinsed with Et₂O and the filtrate was concentrated under reduced pressure. The regioselectivity (branched

product to linear product: b:l) and diastereoselectivity (dr) were determined by ^1H NMR. The residue was purified by silica gel flash chromatography (gradient elution, 0 \rightarrow 1 \rightarrow 2% EtOAc in hexanes) to afford the desired product.

4.6.3. General procedure for the Ir-catalyzed asymmetric allylic alkylation of acyclic β -ketoesters

*Note that the absolute configuration was determined only for compound **112f** via X-ray analysis of its derivative (vide infra). The absolute configuration for all other products **3** has been inferred by analogy. Isolated yields are reported in Tables 2 and 3 (see manuscript). For respective SFC conditions, please refer to Table 4.6.8.1. The relative configuration of product derivative **116** was determined by 2D NMR studies, see appendix A6 for details. The relative configurations of all other products determined by analogy.*



In a nitrogen-filled glove box, $[\text{Ir}(\text{cod})\text{Cl}]_2$ (1.4 mg, 0.002 mmol, 2 mol%), ligand **L12** (1.8 mg, 0.004 mmol, 4 mol%), and TBD (1.4 mg, 0.01 mmol, 10 mol%) were added to a 2 dram scintillation vial equipped with a magnetic stirring bar. The vial was then charged with THF (0.5 mL) and stirred at 25 °C for 10 min, generating an orange solution. To another 2 dram scintillation vial was added $\text{LiO}t\text{-Bu}$ (16.0 mg, 0.2 mmol, 2

equiv) and 0.5 mL of THF, then β -ketoester **111a** (41.2 mg, 0.2 mmol, 2.0 equiv) was added. After stirring for 10 min, the above pre-formed catalyst solution was transferred to this vial, followed by cinnamyl carbonate (**98a**) (19.2 mg, 0.1 mmol, 1.0 equiv). The vial was sealed and stirred at 25 °C until allylic carbonate **98a** was fully consumed, as indicated by UHPLC-MS analysis. Upon completion of the reaction the vial was removed from the glove-box and uncapped and saturated NH_4Cl aqueous solution was added. The mixture was extracted with CH_2Cl_2 (10 mL x 3), the combined organic layers washed with brine, dried over Mg_2SO_4 , filtered and concentrated under reduced pressure. The regioselectivity (branched product to linear product: b:l = 93:7) and diastereoselectivity (dr >20:1) were determined by ^1H NMR of the crude reaction mixture. The residue was purified by silica gel flash chromatography (gradient elution, 0→1→2% EtOAc in hexanes) to afford product (31.2 mg, 97% yield) as a colorless oil.

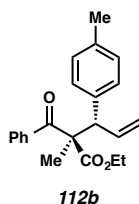
Ethyl-(2R,3S)-2-benzoyl-2-methyl-3-phenylpent-4-enoate (112a).

Ketoester **112a** was isolated by silica gel chromatography (gradient elution, 0→1→2% EtOAc in hexanes) as a colorless oil. >99% ee, $[\alpha]_{\text{D}}^{25} +76.6$ (*c* 0.77, CHCl_3); $R_f = 0.4$ (5% EtOAc in hexanes); ^1H NMR (500 MHz, CDCl_3) δ 7.69–7.60 (m, 2H), 7.52–7.43 (m, 1H), 7.38–7.33 (m, 2H), 7.26–7.15 (m, 5H), 6.35 (ddd, *J* = 17.0, 10.3, 8.3 Hz, 1H), 5.13 (ddd, *J* = 10.2, 1.7, 0.9 Hz, 1H), 5.07 (ddd, *J* = 17.0, 1.8, 1.2 Hz, 1H), 4.39 (dd, *J* = 8.3, 1.1 Hz, 1H), 4.09 (qd, *J* = 7.2, 0.6 Hz, 2H), 1.53 (s, 3H), 1.04 (t, *J* = 7.1 Hz, 3H); ^{13}C NMR (126 MHz, CDCl_3) δ 198.0, 173.0, 139.5, 137.8, 137.2, 132.3, 130.1, 128.4, 128.20, 128.17, 127.1, 117.5, 61.8, 61.6, 54.8, 21.0, 13.8; IR (Neat Film, NaCl) 3062, 3028, 2981, 2939, 2902, 1731, 1686, 1682, 1597, 1582, 1493, 1452, 1446, 1377, 1311,

1243, 1218, 1186, 1096, 1018, 1001, 962, 920, 860, 758 cm^{-1} ; HRMS (ESI+) m/z calc'd for $\text{C}_{21}\text{H}_{23}\text{O}_3$ $[\text{M}+\text{H}]^+$: 323.1642, found 323.1647; SFC conditions: 5% IPA, 2.5 mL/min, Chiralpak IC column, $\lambda = 254$ nm, t_R (min): major = 4.12, minor = 6.14.

4.6.4. Spectroscopic data for Ir-catalyzed allylic alkylation products

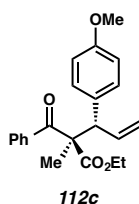
Ethyl (2*R*,3*S*)-2-benzoyl-2-methyl-3-(*p*-tolyl)pent-4-enoate (**112b**).



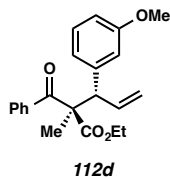
Ketoester **112b** was isolated by silica gel chromatography (gradient elution, 0→1→2% EtOAc in hexanes) as a colorless oil. 99% ee, $[\alpha]_D^{25} +80.4$ (c 1.82, CHCl_3); $R_f = 0.4$ (5% EtOAc in hexanes); ^1H NMR (500 MHz, CDCl_3) δ 7.69–7.65 (m, 2H), 7.47 (ddt, $J = 8.6, 7.0, 1.3$ Hz, 1H), 7.39–7.33 (m, 2H), 7.11–7.02 (m, 4H), 6.33 (ddd, $J = 16.9, 10.2, 8.3$ Hz, 1H), 5.11 (ddd, $J = 10.3, 1.8, 1.0$ Hz, 1H), 5.07 (ddd, $J = 17.0, 1.9, 1.2$ Hz, 1H), 4.38 (dd, $J = 8.3, 1.2$ Hz, 1H), 4.09 (qd, $J = 7.1, 2.6$ Hz, 2H), 2.29 (s, 3H), 1.54 (s, 3H), 1.05 (t, $J = 7.1$ Hz, 3H); ^{13}C NMR (126 MHz, CDCl_3) δ 198.1, 173.0, 137.9, 137.2, 136.6, 136.4, 132.3, 129.9, 128.9, 128.4, 128.2, 117.3, 61.8, 61.5, 54.3, 21.1, 20.9, 13.8; IR (Neat Film, NaCl) 3058, 3023, 2981, 2938, 1736, 1732, 1682, 1687, 1636, 1597, 1580, 1513, 1446, 1376, 1310, 1243, 1219, 1186, 1115, 1104, 1021, 1001, 963, 919, 820, 793 cm^{-1} ; HRMS (MM: ESI-APCI+) m/z calc'd for $\text{C}_{22}\text{H}_{25}\text{O}_3$ $[\text{M}+\text{H}]^+$: 337.1798, found 337.1805; SFC

conditions: 5% IPA, 2.5 mL/min, Chiralpak IC column, $\lambda = 254$ nm, t_R (min): major = 6.71, minor = 9.45.

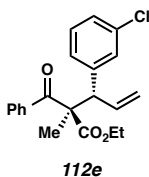
Ethyl (2*R*,3*S*)-2-benzoyl-3-(4-methoxyphenyl)-2-methylpent-4-enoate (112c).



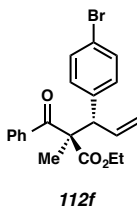
Ketoester **112c** was isolated by silica gel chromatography (gradient elution, 2→5% EtOAc in hexanes) as a colorless oil. $>99\%$ ee, $[\alpha]_D^{25} +81.5$ (c 2.02, CHCl_3); $R_f = 0.2$ (5% EtOAc in hexanes); $^1\text{H NMR}$ (500 MHz, CDCl_3) δ 7.70–7.63 (m, 2H), 7.52–7.43 (m, 1H), 7.38–7.32 (m, 2H), 7.15–7.08 (m, 2H), 6.85–6.74 (m, 2H), 6.32 (ddd, $J = 17.0, 10.3, 8.2$ Hz, 1H), 5.11 (ddd, $J = 10.3, 1.8, 1.0$ Hz, 1H), 5.05 (ddd, $J = 17.0, 1.8, 1.2$ Hz, 1H), 4.37 (d, $J = 8.2$ Hz, 1H), 4.09 (qd, $J = 7.1, 0.9$ Hz, 2H), 3.76 (s, 3H), 1.51 (s, 3H), 1.05 (t, $J = 7.1$ Hz, 3H); $^{13}\text{C NMR}$ (126 MHz, CDCl_3) δ 198.1, 173.0, 158.5, 138.0, 137.3, 132.3, 131.4, 131.1, 128.4, 128.2, 117.2, 113.5, 61.9, 61.5, 55.3, 53.9, 20.8, 13.9; IR (Neat Film, NaCl) 3067, 2981, 2937, 2904, 2835, 1731, 1686, 1682, 1610, 1597, 1581, 1511, 1446, 1376, 1302, 1245, 1218, 1181, 1114, 1101, 1034, 963, 922, 830 cm^{-1} ; HRMS (ESI+) m/z calc'd for fragment $\text{C}_{10}\text{H}_{11}\text{O}$ $[\text{M}-\text{C}_{11}\text{H}_{12}\text{O}_3+\text{H}]^+$: 147.0804, found 147.0808; SFC conditions: 5% IPA, 2.5 mL/min, Chiralpak AD-H column, $\lambda = 254$ nm, t_R (min): minor = 11.17, major = 12.67.

Ethyl (2*R*,3*S*)-2-benzoyl-3-(4-methoxyphenyl)-2-methylpent-4-enoate (112d).

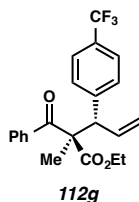
Ketoester **112d** was isolated by silica gel chromatography (gradient elution, 0→1→2% EtOAc in hexanes) as a colorless oil. $>99\%$ ee, $[\alpha]_D^{25} +85.1$ (c 1.21, CHCl_3); $R_f = 0.3$ (5% EtOAc in hexanes); $^1\text{H NMR}$ (500 MHz, CDCl_3) δ 7.70–7.63 (m, 2H), 7.52–7.43 (m, 1H), 7.42–7.32 (m, 2H), 7.23–7.11 (m, 1H), 6.82–6.71 (m, 3H), 6.32 (ddd, $J = 16.9, 10.3, 8.3$ Hz, 1H), 5.13 (ddd, $J = 10.3, 1.8, 0.9$ Hz, 1H), 5.09 (ddd, $J = 17.0, 1.8, 1.2$ Hz, 1H), 4.37 (dt, $J = 8.3, 1.1$ Hz, 1H), 4.09 (qd, $J = 7.2, 1.3$ Hz, 2H), 3.74 (s, 3H), 1.53 (s, 3H), 1.05 (t, $J = 7.1$ Hz, 3H); $^{13}\text{C NMR}$ (126 MHz, CDCl_3) δ 198.0, 172.9, 159.3, 141.0, 137.6, 137.3, 132.3, 129.1, 128.4, 128.2, 122.4, 117.6, 116.0, 112.4, 61.8, 61.6, 55.2, 54.8, 21.0, 13.8; IR (Neat Film, NaCl) 3078, 2982, 2940, 2835, 1731, 1683, 1598, 1583, 1488, 1454, 1377, 1315, 1245, 1217, 1186, 1162, 1096, 1049, 1019, 1001, 963, 922, 861, 781 cm^{-1} ; HRMS (ESI+) m/z calc'd for $\text{C}_{22}\text{H}_{25}\text{O}_4$ $[\text{M}+\text{H}]^+$: 353.1747, found 353.1761; SFC conditions: 2% MeOH, 2.5 mL/min, Chiralpak IC column, $\lambda = 254$ nm, t_R (min): major = 12.24, minor = 13.50.

Ethyl (2*R*,3*S*)-2-benzoyl-3-(3-chlorophenyl)-2-methylpent-4-enoate (112e).

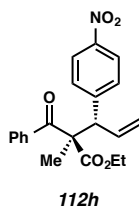
Ketoester **112e** was isolated by silica gel chromatography (gradient elution, 0→1→2% EtOAc in hexanes) as a colorless oil. 99% ee, $[\alpha]_D^{25} +99.1$ (c 1.13, CHCl_3); $R_f = 0.3$ (5% EtOAc in hexanes); $^1\text{H NMR}$ (500 MHz, CDCl_3) δ 7.70–7.63 (m, 2H), 7.48 (ddt, $J = 7.8, 6.9, 1.2$ Hz, 1H), 7.41–7.33 (m, 2H), 7.22–7.19 (m, 1H), 7.19–7.14 (m, 2H), 7.14–7.08 (m, 1H), 6.30 (ddd, $J = 17.0, 10.2, 8.4$ Hz, 1H), 5.15 (ddd, $J = 10.3, 1.6, 0.9$ Hz, 1H), 5.07 (dt, $J = 17.0, 1.4$ Hz, 1H), 4.34 (d, $J = 8.4$ Hz, 1H), 4.10 (q, $J = 7.2$ Hz, 2H), 1.52 (s, 3H), 1.06 (t, $J = 7.1$ Hz, 3H); $^{13}\text{C NMR}$ (126 MHz, CDCl_3) δ 197.6, 172.6, 141.7, 137.0, 136.9, 133.9, 132.5, 130.3, 129.3, 128.5, 128.4, 128.3, 127.2, 118.1, 61.7, 61.7, 54.5, 20.9, 13.8; IR (Neat Film, NaCl) 3068, 2982, 2943, 1732, 1682, 1595, 1574, 1475, 1446, 1378, 1301, 1245, 1218, 1194, 1095, 1018, 1001, 963, 924, 784 cm^{-1} ; HRMS (MM: ESI-APCI+) m/z calc'd for $\text{C}_{21}\text{H}_{22}\text{ClO}_3$ $[\text{M}+\text{H}]^+$: 357.1252, found 357.1260; SFC conditions: 10% IPA, 4.0 mL/min, Chiralpak IC column, $\lambda = 254$ nm, t_R (min): major = 1.59, minor = 1.77.

Ethyl (2*R*,3*S*)-2-benzoyl-3-(4-bromophenyl)-2-methylpent-4-enoate (112f).

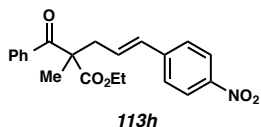
Ketoester **112f** was isolated by silica gel chromatography (gradient elution, 0→1→2% EtOAc in hexanes) as a colorless oil. $>99\%$ ee, $[\alpha]_D^{25} +89.0$ (c 1.42, CHCl_3); $R_f = 0.3$ (5% EtOAc in hexanes); $^1\text{H NMR}$ (500 MHz, CDCl_3) δ 7.70–7.63 (m, 2H), 7.50–7.45 (m, 1H), 7.40–7.33 (m, 4H), 7.13–7.08 (m, 2H), 6.29 (ddd, $J = 16.9, 10.2, 8.2$ Hz, 1H), 5.16–5.11 (m, 1H), 5.05 (dt, $J = 17.0, 1.4$ Hz, 1H), 4.36 (d, $J = 8.2$ Hz, 1H), 4.08 (q, $J = 7.1$ Hz, 2H), 1.51 (s, 3H), 1.05 (t, $J = 7.1$ Hz, 3H); $^{13}\text{C NMR}$ (126 MHz, CDCl_3) δ 197.6, 172.7, 138.6, 137.2, 136.9, 132.5, 131.9, 131.2, 128.5, 128.3, 121.1, 117.9, 61.7, 61.6, 54.1, 20.8, 13.8; IR (Neat Film, NaCl) 3077, 2981, 2938, 1728, 1683, 1597, 1488, 1446, 1377, 1305, 1243, 1217, 1186, 1099, 1076, 1010, 963, 922, 822, 802, 716 cm^{-1} ; HRMS (MM: ESI-APCI+) m/z calc'd for $\text{C}_{21}\text{H}_{22}\text{BrO}_3$ $[\text{M}+\text{H}]^+$: 401.0747, found 401.0754; SFC conditions: 10% IPA, 4.0 mL/min, Chiralpak AD-H column, $\lambda = 210$ nm, t_R (min): minor = 2.95, major = 3.47.

Ethyl (2*R*,3*S*)-2-benzoyl-2-methyl-3-(4-(trifluoromethyl)phenyl)pent-4-enoate (112g).

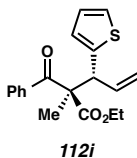
Ketoester **112g** was isolated by silica gel chromatography (gradient elution, 0→1→2% EtOAc in hexanes) as a colorless oil. $>99\%$ ee, $[\alpha]_D^{25} +77.4$ (c 0.94, CHCl_3); $R_f = 0.3$ (5% EtOAc in hexanes); $^1\text{H NMR}$ (500 MHz, CDCl_3) δ 7.69–7.63 (m, 2H), 7.53–7.45 (m, 3H), 7.39–7.35 (m, 4H), 6.33 (ddd, $J = 16.9, 10.2, 8.4$ Hz, 1H), 5.16 (ddd, $J = 10.2, 1.6, 0.9$ Hz, 1H), 5.07 (dt, $J = 17.0, 1.4$ Hz, 1H), 4.44 (d, $J = 8.4$ Hz, 1H), 4.09 (q, $J = 7.1$ Hz, 2H), 1.53 (s, 3H), 1.04 (t, $J = 7.1$ Hz, 3H); $^{13}\text{C NMR}$ (126 MHz, CDCl_3) δ 197.5, 172.6, 143.9, 136.9, 136.8, 132.6, 130.6, 129.2 (q, $J = 32.4$ Hz), 128.5, 128.3, 125.0 (q, $J = 3.7$ Hz), 124.3 (d, $J = 271.8$ Hz), 118.3, 61.8, 61.6, 54.6, 20.8, 13.8; IR (Neat Film, NaCl) 3070, 2984, 2941, 1732, 1687, 1682, 1617, 1597, 1581, 1446, 1413, 1379, 1327, 1245, 1220, 1166, 1123, 1069, 1018, 964, 924, 846 cm^{-1} ; HRMS (ESI+) m/z calc'd for $\text{C}_{22}\text{H}_{22}\text{F}_3\text{O}_3$ $[\text{M}+\text{H}]^+$: 391.1516, found 391.1517; SFC conditions: 2% IPA, 2.5 mL/min, Chiralpak AD-H column, $\lambda = 254$ nm, t_R (min): minor = 5.20, major = 6.68.

Ethyl (2*R*,3*S*)-2-benzoyl-2-methyl-3-(4-nitrophenyl)pent-4-enoate (112h).

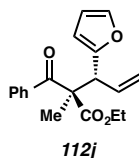
Ketoester **112h** was isolated by silica gel chromatography (5% EtOAc in hexanes) as a colorless oil. 93% ee, $[\alpha]_D^{25} +96.8$ (c 0.64, CHCl_3); $R_f = 0.3$ (10% EtOAc in hexanes); ^1H NMR (500 MHz, CDCl_3) δ 8.13–8.09 (m, 2H), 7.70–7.63 (m, 2H), 7.52–7.48 (m, 1H), 7.46–7.43 (m, 2H), 7.40–7.35 (m, 2H), 6.31 (ddd, $J = 16.9, 10.2, 8.5$ Hz, 1H), 5.23–5.16 (m, 1H), 5.08 (dt, $J = 17.0, 1.3$ Hz, 1H), 4.50 (d, $J = 8.5$ Hz, 1H), 4.10 (qd, $J = 7.1, 2.4$ Hz, 2H), 1.54 (s, 3H), 1.05 (t, $J = 7.1$ Hz, 3H); ^{13}C NMR (126 MHz, CDCl_3) δ 197.0, 172.3, 147.4, 146.8, 136.3, 136.1, 132.6, 131.0, 128.4, 128.2, 123.1, 118.8, 61.8, 61.4, 54.3, 20.5, 13.7; IR (Neat Film, NaCl) 3080, 2982, 2942, 1731, 1686, 1682, 1597, 1523, 1519, 1446, 1379, 1346, 1245, 1219, 1111, 1001, 1015, 964, 926, 853 cm^{-1} ; HRMS (MM: ESI-APCI+) m/z calc'd for $\text{C}_{21}\text{H}_{22}\text{O}_5\text{N}$ $[\text{M}+\text{H}]^+$: 368.1492, found 368.1508; SFC conditions: 5% MeOH, 3.0 mL/min, Chiralpak AD-H column, $\lambda = 254$ nm, t_R (min): minor = 4.47, major = 5.71.

Ethyl (*E*)-2-benzoyl-2-methyl-5-(4-nitrophenyl)pent-4-enoate (113h**).**

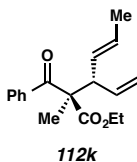
Ketoester **113h** was isolated by silica gel chromatography (5% EtOAc in hexanes) as a yellow solid. 23% ee, $[\alpha]_D^{25} +4.7$ (c 0.96, CHCl_3); $R_f = 0.3$ (10% EtOAc in hexanes); ^1H NMR (500 MHz, CDCl_3) δ 8.15 (dt, $J = 9.0, 2.5$ Hz, 2H), 7.86 (dt, $J = 8.5, 2.0$ Hz, 2H), 7.59–7.49 (m, 1H), 7.47–7.40 (m, 4H), 6.45 (dt, $J = 15.9, 1.2$ Hz, 1H), 6.32 (dt, $J = 15.7, 7.5$ Hz, 1H), 4.12 (qd, $J = 7.2, 1.1$ Hz, 2H), 3.00 (ddd, $J = 14.2, 7.3, 1.3$ Hz, 1H), 2.90 (ddd, $J = 14.2, 7.7, 1.2$ Hz, 1H), 1.58 (s, 3H), 1.05 (t, $J = 7.1$ Hz, 3H); ^{13}C NMR (126 MHz, CDCl_3) δ 197.0, 173.6, 146.9, 143.6, 135.4, 133.1, 132.1, 130.0, 128.7, 126.8, 124.1, 61.7, 57.3, 40.6, 21.6, 14.0; IR (Neat Film, NaCl) 2981, 2936, 1732, 1686, 1682, 1596, 1519, 1515, 1446, 1342, 1298, 1267, 1239, 1184, 1108, 973, 857 cm^{-1} ; HRMS (MM: ESI-APCI+) m/z calc'd for $\text{C}_{21}\text{H}_{22}\text{O}_5\text{N}$ $[\text{M}+\text{H}]^+$: 368.1492, found 368.1499; SFC conditions: 10% MeOH, 3.0 mL/min, Chiralpak AD-H column, $\lambda = 254$ nm, t_R (min): major = 7.13, minor = 8.06.

Ethyl (2*R*,3*R*)-2-benzoyl-2-methyl-3-(thiophen-2-yl)pent-4-enoate (112i).

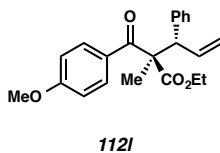
Ketoester **112i** was isolated by silica gel chromatography (gradient elution, 0→1→2% EtOAc in hexanes) as a colorless oil. 95% ee, $[\alpha]_D^{25} +53.0$ (c 1.63, CHCl_3); $R_f = 0.4$ (5% EtOAc in hexanes); $^1\text{H NMR}$ (500 MHz, CDCl_3) δ 7.74–7.68 (m, 2H), 7.51–7.47 (m, 1H), 7.42–7.35 (m, 2H), 7.16 (dd, $J = 5.1, 1.2$ Hz, 1H), 6.89 (dd, $J = 5.1, 3.5$ Hz, 1H), 6.84 (ddd, $J = 3.5, 1.2, 0.7$ Hz, 1H), 6.23 (ddd, $J = 16.4, 10.6, 9.0$ Hz, 1H), 5.23–5.16 (m, 2H), 4.77 (d, $J = 9.0$ Hz, 1H), 4.11 (q, $J = 7.1$ Hz, 2H), 1.52 (s, 3H), 1.09 (t, $J = 7.2$ Hz, 3H); $^{13}\text{C NMR}$ (126 MHz, CDCl_3) δ 197.5, 172.3, 142.1, 136.8, 136.6, 132.5, 128.5, 128.4, 126.9, 126.2, 124.9, 118.2, 62.2, 61.9, 49.8, 19.4, 13.9; IR (Neat Film, NaCl) 3069, 2981, 2937, 1732, 1687, 1682, 1597, 1580, 1446, 1383, 1298, 1246, 1221, 1107, 1018, 1001, 968, 924, 851, 795, 747 cm^{-1} ; HRMS (ESI+) m/z calc'd for $\text{C}_{19}\text{H}_{21}\text{O}_3\text{S}$ $[\text{M}+\text{H}]^+$: 329.1206, found 329.1214; SFC conditions: 5% IPA, 2.5 mL/min, Chiralpak IC column, $\lambda = 254$ nm, t_R (min): major = 7.92, minor = 11.24.

Ethyl (2*R*,3*R*)-2-benzoyl-3-(furan-2-yl)-2-methylpent-4-enoate (112j).

Ketoester **112j** was isolated by silica gel chromatography (gradient elution, 0→1→2% EtOAc in hexanes) as a colorless oil. $>99\%$ ee, $[\alpha]_D^{25} +67.3$ (c 1.34, CHCl_3); $R_f = 0.4$ (5% EtOAc in hexanes); ^1H NMR (500 MHz, CDCl_3) δ 7.73–7.67 (m, 2H), 7.52–7.45 (m, 1H), 7.40–7.35 (m, 2H), 7.27 (dd, $J = 1.8, 0.9$ Hz, 1H), 6.25 (dd, $J = 3.3, 1.8$ Hz, 1H), 6.17 (ddd, $J = 17.0, 10.2, 8.5$ Hz, 1H), 6.11 (dt, $J = 3.3, 0.7$ Hz, 1H), 5.19 (ddd, $J = 10.2, 1.7, 0.8$ Hz, 1H), 5.14 (ddd, $J = 17.0, 1.7, 1.1$ Hz, 1H), 4.62 (dd, $J = 8.5, 0.9$ Hz, 1H), 4.12 (q, $J = 7.1$ Hz, 2H), 1.52 (s, 3H), 1.10 (t, $J = 7.1$ Hz, 3H); ^{13}C NMR (126 MHz, CDCl_3) δ 196.9, 172.1, 152.9, 141.5, 136.6, 134.4, 132.2, 128.3, 128.2, 118.3, 110.1, 108.7, 61.6, 61.4, 47.9, 19.3, 13.8; IR (Neat Film, NaCl) 3081, 2983, 2941, 2904, 1732, 1686, 1597, 1581, 1501, 1446, 1378, 1301, 1246, 1222, 1149, 1096, 1013, 968, 926, 885, 860, 797, 736 cm^{-1} ; HRMS (MM: ESI-APCI+) m/z calc'd for $\text{C}_{19}\text{H}_{21}\text{O}_4$ $[\text{M}+\text{H}]^+$: 313.1431, found 313.1438; SFC conditions: 5% IPA, 2.5 mL/min, Chiralpak IC column, $\lambda = 254$ nm, t_R (min): major = 5.09, minor = 9.14.

Ethyl (2*R*,3*S*,*E*)-2-benzoyl-2-methyl-3-vinylhex-4-enoate (112k).

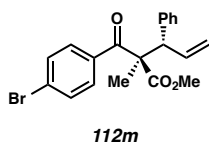
Ketoester **112k** was isolated by silica gel chromatography (gradient elution, 0→1→2% EtOAc in hexanes) as a colorless oil. 91% ee, $[\alpha]_D^{25} +43.5$ (c 1.86, CHCl_3); $R_f = 0.4$ (5% EtOAc in hexanes); $^1\text{H NMR}$ (500 MHz, CDCl_3) δ 7.80–7.71 (m, 2H), 7.52–7.46 (m, 1H), 7.42–7.36 (m, 2H), 5.98 (ddd, $J = 16.9, 10.5, 7.5$ Hz, 1H), 5.47–5.27 (m, 2H), 5.15–5.00 (m, 2H), 4.09 (qd, $J = 7.1, 1.5$ Hz, 2H), 3.73–3.69 (m, 1H), 1.65–1.58 (m, 3H), 1.48 (s, 3H), 1.07 (t, $J = 7.1$ Hz, 3H); $^{13}\text{C NMR}$ (126 MHz, CDCl_3) δ 197.4, 173.0, 137.2, 136.8, 132.4, 129.0, 128.5, 128.4, 128.3, 117.1, 61.4, 60.5, 51.6, 19.2, 18.2, 14.0; IR (Neat Film, NaCl) 3077, 2981, 2939, 2913, 1732, 1687, 1682, 1597, 1580, 1446, 1377, 1299, 1245, 1221, 1100, 1018, 1001, 970, 921, 859 cm^{-1} ; HRMS (ESI+) m/z calc'd for $\text{C}_{18}\text{H}_{23}\text{O}_3$ $[\text{M}+\text{H}]^+$: 287.1642, found 287.1654; SFC conditions: 2% IPA, 2.5 mL/min, Chiralpak AD-H column, $\lambda = 210$ nm, t_R (min): minor = 4.40, major = 5.52.

Ethyl (2*R*,3*S*)-2-(4-methoxybenzoyl)-2-methyl-3-phenylpent-4-enoate (112l).

Ketoester **112l** was isolated by silica gel chromatography (4% EtOAc in hexanes) as a colorless oil. 99% ee, $[\alpha]_D^{25} +53.9$ (c 1.51, CHCl_3); $R_f = 0.3$ (10% EtOAc in hexanes);

^1H NMR (500 MHz, CDCl_3) δ 7.76–7.69 (m, 2H), 7.25–7.17 (m, 5H), 6.87–6.82 (m, 2H), 6.36 (ddd, $J = 17.0, 10.3, 8.1$ Hz, 1H), 5.12 (ddd, $J = 10.3, 1.8, 1.0$ Hz, 1H), 5.05 (ddd, $J = 17.0, 1.8, 1.2$ Hz, 1H), 4.39 (dt, $J = 8.1, 1.2$ Hz, 1H), 4.10 (q, $J = 7.1$ Hz, 2H), 3.84 (s, 3H), 1.53 (s, 3H), 1.07 (t, $J = 7.1$ Hz, 3H); ^{13}C NMR (126 MHz, CDCl_3) δ 195.8, 173.4, 162.9, 139.6, 138.0, 130.8, 130.2, 129.5, 128.1, 127.0, 117.3, 113.6, 61.5, 61.3, 55.5, 54.7, 21.0, 13.9; IR (Neat Film, NaCl) 3083, 2981, 2940, 2842, 1727, 1677, 1600, 1576, 1513, 1454, 1417, 1376, 1310, 1247, 1221, 1176, 1118, 1031, 964, 842 cm^{-1} ; HRMS (ESI+) m/z calc'd for $\text{C}_{22}\text{H}_{25}\text{O}_4$ $[\text{M}+\text{H}]^+$: 353.1747, found 353.1752; SFC conditions: 10% IPA, 4.0 mL/min, Chiralpak IC column, $\lambda = 254$ nm, t_{R} (min): major = 2.67, minor = 3.51.

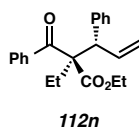
Methyl (2*R*,3*S*)-2-(4-bromobenzoyl)-2-methyl-3-phenylpent-4-enoate (112*m*).



Ketoester **112*m*** was isolated by silica gel chromatography (gradient elution, 1→2 Et_2O in hexanes) as a colorless oil. $>99\%$ ee, $[\alpha]_{\text{D}}^{25} +65.9$ (c 0.50, CHCl_3); $R_f = 0.3$ (10% EtOAc in hexanes); ^1H NMR (500 MHz, CDCl_3) δ 7.51–7.48 (m, 4H), 7.29–7.09 (m, 5H), 6.31 (ddd, $J = 16.9, 10.3, 8.4$ Hz, 1H), 5.21–4.96 (m, 2H), 4.37 (d, $J = 8.5$ Hz, 1H), 3.62 (s, 3H), 1.51 (s, 3H); ^{13}C NMR (126 MHz, CDCl_3) δ 196.6, 173.3, 139.1, 137.3, 135.7, 131.7, 130.0, 129.7, 128.2, 127.5, 127.1, 117.7, 61.8, 54.7, 52.5, 20.8; IR (Neat Film, NaCl) 3355, 3028, 2997, 2948, 1735, 1685, 1584, 1484, 1452, 1395, 1245, 1221, 1117, 1073, 966, 922, 841, 756 cm^{-1} ; HRMS (ESI+) m/z calc'd for $\text{C}_{20}\text{H}_{20}\text{BrO}_3$ $[\text{M}+\text{H}]^+$:

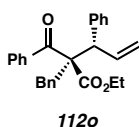
387.0590, found 387.0612; SFC conditions: 5% IPA, 2.5 mL/min, Chiralpak AD-H column, $\lambda = 254$ nm, t_R (min): major = 5.35, minor = 5.88.

Ethyl (2*R*,3*S*)-2-benzoyl-2-ethyl-3-phenylpent-4-enoate (112n).



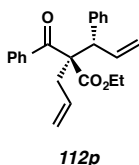
Ketoester **112n** was isolated by silica gel chromatography (gradient elution, 0→2 Et₂O in hexanes) as a colorless oil. >99% ee, $[\alpha]_D^{25} +77.4$ (*c* 0.25, CHCl₃); $R_f = 0.4$ (10% EtOAc in hexanes); ¹H NMR (500 MHz, CDCl₃) δ 7.61–7.51 (m, 2H), 7.48–7.38 (m, 1H), 7.35–7.11 (m, 7H), 6.33 (ddd, *J* = 17.0, 10.3, 7.8 Hz, 1H), 5.07 (ddd, *J* = 10.3, 1.8, 1.1 Hz, 1H), 4.96 (dt, *J* = 17.1, 1.5 Hz, 1H), 4.38 (dd, *J* = 7.9, 1.4 Hz, 1H), 4.06 (qd, *J* = 7.2, 3.3 Hz, 2H), 2.15 (dq, *J* = 15.0, 7.5 Hz, 1H), 1.89 (dq, *J* = 14.9, 7.5 Hz, 1H), 0.99 (t, *J* = 7.1 Hz, 3H), 0.78 (t, *J* = 7.5 Hz, 3H); ¹³C NMR (126 MHz, CDCl₃) δ 198.1, 172.9, 139.5, 138.4, 137.9, 132.0, 129.8, 128.2, 128.1, 127.9, 127.0, 116.6, 65.2, 61.0, 52.2, 27.6, 13.6, 8.5; IR (Neat Film, NaCl) 3061, 3028, 2980, 1729, 1679, 1597, 1446, 1386, 1303, 1228, 1208, 1097, 1028, 993, 917, 759 cm⁻¹; HRMS (ESI+) *m/z* calc'd for C₂₂H₂₅O₃ [M+H]⁺: 337.1798, found 337.1813; SFC conditions: 5% MeOH, 2.5 mL/min, Chiralpak AD-H column, $\lambda = 254$ nm, t_R (min): major = 2.48, minor = 2.20.

Ethyl (2*R*,3*S*)-2-benzoyl-2-benzyl-3-phenylpent-4-enoate (112o).



Ketoester **112o** was isolated by silica gel chromatography (gradient elution, 1→2 EtOAc in hexanes) as a white solid. >99% ee, $[\alpha]_D^{25} +37.1$ (*c* 1.29, CHCl₃); $R_f = 0.4$ (5% EtOAc in hexanes); ¹H NMR (500 MHz, CDCl₃) δ 7.33–7.29 (m, 1H), 7.29–7.21 (m, 4H), 7.17–7.10 (m, 8H), 7.04–7.00 (m, 2H), 6.37 (ddd, *J* = 17.0, 10.3, 8.1 Hz, 1H), 5.13 (ddd, *J* = 10.2, 1.8, 1.0 Hz, 1H), 5.02 (dt, *J* = 17.0, 1.5 Hz, 1H), 4.42 (d, *J* = 7.9 Hz, 1H), 3.99 (dq, *J* = 10.7, 7.1 Hz, 1H), 3.80 (dq, *J* = 10.7, 7.1 Hz, 1H), 3.28 (AB, *J* = 15.5, 13.5 Hz, 2H), 0.82 (t, *J* = 7.2 Hz, 3H); ¹³C NMR (126 MHz, CDCl₃) δ 200.5, 172.0, 139.7, 139.3, 138.3, 136.8, 131.4, 131.2, 130.0, 128.4, 128.1, 127.7, 127.6, 127.4, 126.9, 117.6, 67.5, 61.0, 56.8, 42.1, 13.4; IR (Neat Film, NaCl) 3063, 3029, 2982, 2929, 1729, 1673, 1600, 1582, 1496, 1448, 1367, 1299, 1241, 1209, 1082, 1066, 1025, 925, 757 cm⁻¹; HRMS (ESI+) *m/z* calc'd for C₂₇H₂₇O₃ [M+H]⁺: 399.1955, found 399.1956; SFC conditions: 4% IPA, 4.0 mL/min, Chiralpak AD-H column, $\lambda = 254$ nm, *t*_R (min): major = 5.06, minor = 8.94.

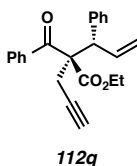
Ethyl (2*R*,3*S*)-2-allyl-2-benzoyl-3-phenylpent-4-enoate (112p).



Ketoester **112p** was isolated by silica gel chromatography (2% EtOAc in hexanes) as a colorless oil. >99% ee, $[\alpha]_D^{25} +80.7$ (*c* 0.31, CHCl₃); $R_f = 0.4$ (5% EtOAc in hexanes); ¹H NMR (500 MHz, CDCl₃) δ 7.54–7.49 (m, 2H), 7.43 (ddt, *J* = 7.7, 7.0, 1.2 Hz, 1H),

7.33–7.27 (m, 2H), 7.25–7.19 (m, 3H), 7.18–7.13 (m, 2H), 6.36 (ddd, $J = 17.0, 10.3, 8.0$ Hz, 1H), 5.71 (dddd, $J = 17.0, 10.2, 7.8, 7.0$ Hz, 1H), 5.10 (ddd, $J = 10.3, 1.8, 1.1$ Hz, 1H), 5.03 (ddt, $J = 10.2, 2.1, 1.0$ Hz, 1H), 4.99 (ddd, $J = 17.0, 1.8, 1.2$ Hz, 1H), 4.92 (dq, $J = 17.1, 1.7$ Hz, 1H), 4.35 (dt, $J = 8.0, 1.2$ Hz, 1H), 4.14–3.96 (m, 2H), 2.86 (ddt, $J = 14.6, 7.0, 1.3$ Hz, 1H), 2.63 (ddt, $J = 14.6, 7.7, 1.2$ Hz, 1H), 0.99 (t, $J = 7.2$ Hz, 3H); ^{13}C NMR (126 MHz, CDCl_3) δ 198.0, 172.4, 139.4, 138.3, 138.2, 132.5, 132.1, 130.1, 128.3, 128.14, 128.12, 127.2, 119.5, 117.2, 65.2, 61.2, 53.4, 39.4, 13.7; IR (Neat Film, NaCl) 3079, 3029, 2981, 2933, 1728, 1679, 1638, 1597, 1581, 1493, 1446, 1367, 1257, 1216, 1181, 1144, 1045, 1023, 1001, 921, 758 cm^{-1} ; HRMS (MM: ESI-APCI+) m/z calc'd for $\text{C}_{23}\text{H}_{25}\text{O}_3$ $[\text{M}+\text{H}]^+$: 349.1808, found 349.1808; SFC conditions: 3% IPA, 4.0 mL/min, Chiralpak IC column, $\lambda = 254$ nm, t_{R} (min): major = 7.16, minor = 8.60.

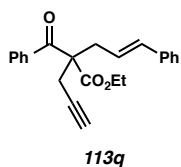
Ethyl (2*R*,3*S*)-2-benzoyl-3-phenyl-2-(prop-2-yn-1-yl)pent-4-enoate (112q).



Ketoester **112q** was isolated by silica gel chromatography (2% EtOAc in hexanes) as a colorless oil. $>99\%$ ee, $[\alpha]_{\text{D}}^{25} +57.7$ (c 0.94, CHCl_3); $R_f = 0.3$ (5% EtOAc in hexanes); ^1H NMR (500 MHz, CDCl_3) δ 7.62–7.55 (m, 2H), 7.46 (ddt, $J = 8.6, 7.0, 1.2$ Hz, 1H), 7.35–7.29 (m, 2H), 7.25–7.23 (m, 5H), 6.37 (ddd, $J = 17.0, 10.3, 7.8$ Hz, 1H), 5.15 (ddd, $J = 10.3, 1.8, 1.2$ Hz, 1H), 5.09 (dt, $J = 17.0, 1.5$ Hz, 1H), 4.58 (dt, $J = 7.8, 1.3$ Hz, 1H), 4.19–4.05 (m, 2H), 2.97 (dd, $J = 17.4, 2.7$ Hz, 1H), 2.69 (dd, $J = 17.4, 2.7$ Hz, 1H), 2.09

(t, $J = 2.7$ Hz, 1H), 1.05 (t, $J = 7.1$ Hz, 3H); ^{13}C NMR (126 MHz, CDCl_3) δ 196.0, 171.4, 138.9, 137.6, 137.3, 132.5, 130.1, 128.4, 128.32, 128.27, 127.4, 117.6, 79.3, 72.9, 64.0, 61.7, 52.5, 25.7, 13.8; IR (Neat Film, NaCl) 3288, 3060, 3030, 2981, 1728, 1682, 1597, 1580, 1446, 1255, 1213, 1183, 1046, 1001, 925 cm^{-1} ; HRMS (ESI+) m/z calc'd for $\text{C}_{23}\text{H}_{23}\text{O}_3$ $[\text{M}+\text{H}]^+$: 347.1642, found 347.1647; SFC conditions: 5% IPA, 2.5 mL/min, Chiralcel OD-H column, $\lambda = 254$ nm, t_{R} (min): minor = 5.67, major = 6.44.

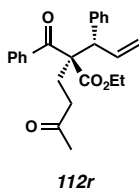
Ethyl (*E*)-2-benzoyl-5-phenyl-2-(prop-2-yn-1-yl)pent-4-enoate (113q**).**



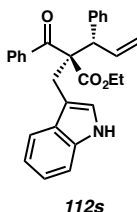
Ketoester **113q** was isolated by silica gel chromatography (2% EtOAc in hexanes) as a colorless oil. 34% ee, $[\alpha]_{\text{D}}^{25}$ -23.4 (c 0.42, CHCl_3); $R_f = 0.3$ (5% EtOAc in hexanes); ^1H NMR (500 MHz, CDCl_3) δ 7.88–7.85 (m, 2H), 7.59–7.54 (m, 1H), 7.48–7.42 (m, 2H), 7.30–7.24 (m, 4H), 7.21 (ddd, $J = 8.7, 4.9, 3.8$ Hz, 1H), 6.43 (dt, $J = 15.6, 1.3$ Hz, 1H), 5.90 (dt, $J = 15.5, 7.7$ Hz, 1H), 4.20 (qq, $J = 7.1, 3.6$ Hz, 2H), 3.19 (ddd, $J = 14.5, 7.9, 1.3$ Hz, 1H), 3.11 (ddd, $J = 14.5, 7.5, 1.4$ Hz, 1H), 2.98 (d, $J = 2.7$ Hz, 2H), 2.07 (t, $J = 2.7$ Hz, 1H), 1.13 (t, $J = 7.1$ Hz, 3H); ^{13}C NMR (126 MHz, CDCl_3) δ 195.2, 171.7, 137.1, 135.7, 134.9, 133.2, 128.8, 128.60, 128.57, 127.6, 126.4, 122.9, 79.0, 72.4, 62.1, 60.6, 36.5, 23.9, 14.1; IR (Neat Film, NaCl) 3287, 3059, 3026, 2979, 2933, 1729, 1679, 1596, 1580, 1446, 1367, 1285, 1270, 1239, 1192, 1180, 1094, 1064, 1023, 966, 937 cm^{-1} ; HRMS (ESI+) m/z calc'd for $\text{C}_{23}\text{H}_{23}\text{O}_3$ $[\text{M}+\text{H}]^+$: 347.1642, found 347.1651; SFC

conditions: 5% IPA, 2.5 mL/min, Chiralpak IC column, $\lambda = 254$ nm, t_R (min): minor = 9.81, major = 10.67.

Ethyl (*R*)-2-benzoyl-5-oxo-2-((*S*)-1-phenylallyl)hexanoate (112r**).**



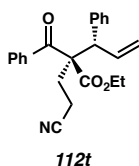
Ketoester **112r** was isolated by silica gel chromatography (gradient elution, 5→10% EtOAc in hexanes) as a colorless oil. 99% ee, $[\alpha]_D^{25} +66.8$ (c 1.20, CHCl_3); $R_f = 0.4$ (25% EtOAc in hexanes); ^1H NMR (500 MHz, CDCl_3) δ 7.59–7.55 (m, 2H), 7.48–7.43 (m, 1H), 7.37–7.30 (m, 2H), 7.26–7.14 (m, 5H), 6.34 (ddd, $J = 17.0, 10.3, 8.1$ Hz, 1H), 5.09 (ddd, $J = 10.3, 1.7, 1.0$ Hz, 1H), 4.97 (ddd, $J = 17.0, 1.7, 1.2$ Hz, 1H), 4.36–4.32 (m, 1H), 4.13–3.99 (m, 2H), 2.46–2.38 (m, 1H), 2.34–2.29 (m, 2H), 2.25–2.17 (m, 1H), 1.99 (s, 3H), 1.00 (t, $J = 7.2$ Hz, 3H); ^{13}C NMR (126 MHz, CDCl_3) δ 206.9, 198.0, 172.4, 139.1, 137.9, 137.8, 132.4, 129.7, 128.4, 128.3, 128.0, 127.3, 117.2, 64.2, 61.3, 53.2, 38.3, 29.9, 28.0, 13.7; IR (Neat Film, NaCl) 3063, 3030, 2981, 2905, 1733, 1717, 1681, 1637, 1596, 1582, 1495, 1446, 1419, 1367, 1243, 1214, 1137, 1093, 1029, 1002, 925, 860, 761 cm^{-1} ; HRMS (ESI+) m/z calc'd for $\text{C}_{24}\text{H}_{27}\text{O}_3$ $[\text{M}+\text{H}]^+$: 379.1904, found 379.1911; SFC conditions: 5% IPA, 2.5 mL/min, Chiralcel OD-H column, $\lambda = 254$ nm, t_R (min): minor = 8.00, major = 10.08.

Ethyl (2*R*,3*S*)-2-((1*H*-indol-3-yl)methyl)-2-benzoyl-3-phenylpent-4-enoate (112s).

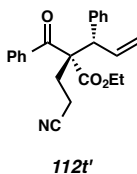
Ketoester **112s** was isolated by silica gel chromatography (gradient elution, 5→10% EtOAc in hexanes) as a colorless oil. >99% ee, $[\alpha]_D^{25} -7.7$ (*c* 1.60, CHCl₃); $R_f = 0.4$ (25% EtOAc in hexanes); ¹H NMR (300 MHz, C₆D₆) δ 7.70–7.65 (m, 1H), 7.36 (dd, *J* = 7.2, 1.8 Hz, 2H), 7.24–7.16 (m, 2H), 7.08–6.93 (m, 5H), 6.90–6.63 (m, 6H), 6.56 (br s, 1H), 5.17–5.12 (m, 1H), 5.10 (t, *J* = 1.0 Hz, 1H), 4.82 (d, *J* = 7.8 Hz, 1H), 3.82–3.63 (m, 3H), 3.62–3.45 (m, 1H), 0.40 (td, *J* = 6.7, 1.3 Hz, 3H); ¹³C NMR (126 MHz, C₆D₆) δ 199.7, 172.2, 139.7, 139.6, 138.9, 135.5, 130.8, 130.2, 128.4, 128.1, 127.9, 127.8, 127.6, 126.9, 124.3, 121.6, 119.7, 119.2, 116.9, 110.5, 66.6, 60.4, 56.0, 31.9, 12.9; IR (Neat Film, NaCl) 3411, 3060, 1724, 1673, 1456, 1241, 1216, 1096, 1012, 923, 747 cm⁻¹; HRMS (ESI+) *m/z* calc'd for C₂₉H₂₈NO₃ [M+H]⁺: 438.2064, found 438.2070; SFC conditions: 10% MeOH, 2.5 mL/min, Chiralpak IC column, $\lambda = 254$ nm, t_R (min): minor = 8.26, major = 9.30.

Ethyl (2*R*,3*S*)-2-benzoyl-2-(2-cyanoethyl)-3-phenylpent-4-enoate (112t) and ethyl (2*S*,3*S*)-2-benzoyl-2-(2-cyanoethyl)-3-phenylpent-4-enoate (112t').

Products **112t** and **112t'** were isolated by silica gel chromatography (5% EtOAc in hexanes) as a mixture of diastereomers (3:1), which were separated by preparative HPLC (20% EtOAc in hexanes).

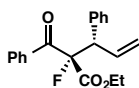


The major diastereomer **112t** was isolated as a white solid, >99% ee, $[\alpha]_D^{25} +59.1$ (*c* 1.81, CHCl₃); $R_f = 0.2$ (10% EtOAc in hexanes); ¹H NMR (500 MHz, CDCl₃) δ 7.52–7.44 (m, 3H), 7.36–7.30 (m, 2H), 7.26–7.20 (m, 3H), 7.15–7.11 (m, 2H), 6.33 (ddd, *J* = 17.0, 10.2, 8.2 Hz, 1H), 5.14 (ddd, *J* = 10.2, 1.6, 1.0 Hz, 1H), 5.01 (dt, *J* = 17.0, 1.3 Hz, 1H), 4.32 (dt, *J* = 8.0, 1.0 Hz, 1H), 4.15–4.06 (m, 2H), 2.50–2.36 (m, 2H), 2.28 (td, *J* = 8.0, 0.8 Hz, 2H), 1.01 (t, *J* = 7.2 Hz, 3H); ¹³C NMR (126 MHz, CDCl₃) δ 197.2, 171.8, 138.3, 137.5, 137.1, 132.8, 129.7, 128.7, 128.5, 128.1, 127.7, 119.1, 118.1, 64.0, 61.9, 53.6, 30.6, 13.7, 13.1; IR (Neat Film, NaCl) 3061, 3027, 2981, 2248, 1729, 1675, 1596, 1580, 1446, 1243, 1214, 1185, 1085, 1017, 971, 924, 757 cm⁻¹; HRMS (MM: ESI-APCI+) *m/z* calc'd for C₂₃H₂₄NO₃ [M+H]⁺: 362.1751, found 362.1766; SFC conditions: 5% IPA, 2.5 mL/min, Chiralpak AD-H column, $\lambda = 254$ nm, *t*_R (min): major = 9.77, minor = 11.61.



The minor diastereomer was isolated as a white solid, >99% ee, $[\alpha]_D^{25} +22.3$ (c 0.11, CHCl_3); $R_f = 0.2$ (10% EtOAc in hexanes); $^1\text{H NMR}$ (500 MHz, CDCl_3) δ 7.69–7.63 (m, 2H), 7.55–7.47 (m, 1H), 7.41–7.32 (m, 2H), 7.31–7.22 (m, 4H), 7.22–7.16 (m, 1H), 6.29 (dt, $J = 16.8, 10.2$ Hz, 1H), 5.21–5.11 (m, 2H), 4.35 (d, $J = 10.3$ Hz, 1H), 4.03 (dq, $J = 10.8, 7.2$ Hz, 1H), 3.84 (dq, $J = 10.8, 7.2$ Hz, 1H), 2.74–2.63 (m, 1H), 2.46–2.28 (m, 2H), 2.14–2.02 (m, 1H), 0.81 (t, $J = 7.2$ Hz, 3H); $^{13}\text{C NMR}$ (126 MHz, CDCl_3) δ 196.0, 171.3, 139.7, 136.7, 136.0, 133.0, 129.7, 128.7, 128.5, 128.3, 127.4, 119.2, 118.9, 63.8, 61.7, 53.0, 30.7, 13.3, 12.9; IR (Neat Film, NaCl) 3062, 3029, 2982, 2248, 1728, 1678, 1596, 1580, 1494, 1446, 1367, 1275, 1242, 1215, 1093, 1018, 972, 928, 757 cm^{-1} ; HRMS (MM: ESI-APCI+) m/z calc'd for $\text{C}_{23}\text{H}_{24}\text{NO}_3$ $[\text{M}+\text{H}]^+$: 362.1751, found 362.1757; SFC conditions: 5% IPA, 2.5 mL/min, Chiralpak AD-H column, $\lambda = 254$ nm, t_R (min): major = 10.65, minor = 12.02.

Ethyl (2*S*,3*S*)-2-benzoyl-2-fluoro-3-phenylpent-4-enoate (**112u**).

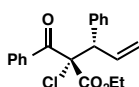


112u

Ketoester **112u** was isolated by silica gel chromatography (gradient elution, 1→2% EtOAc in hexanes) as a colorless oil. 95% ee, $[\alpha]_D^{25} +82.0$ (c 1.19, CHCl_3); $R_f = 0.4$ (5% EtOAc in hexanes); $^1\text{H NMR}$ (500 MHz, CDCl_3) δ 7.77 (ddt, $J = 7.6, 2.0, 1.2$ Hz, 2H), 7.49 (ddt, $J = 7.7, 7.0, 1.3$ Hz, 1H), 7.38–7.30 (m, 4H), 7.31–7.14 (m, 3H), 6.20 (ddd, $J = 17.0, 10.2, 9.4$ Hz, 1H), 5.27 (ddt, $J = 17.0, 1.5, 0.8$ Hz, 1H), 5.23 (ddd, $J = 10.1, 1.5, 0.6$

Hz, 1H), 4.65 (dd, $J = 33.3$ (J_{H-F}), 9.4 Hz, 1H), 4.31 (ddq, $J = 39.5, 10.8, 7.2$ Hz, 2H), 1.30 (t, $J = 7.1$ Hz, 3H); ^{13}C NMR (126 MHz, CDCl_3) δ 192.6 (d, $J = 27.1$ Hz), 166.3 (d, $J = 26.4$ Hz), 137.4, 134.9 (d, $J = 3.5$ Hz), 134.5 (d, $J = 4.0$ Hz), 133.6, 129.9 (d, $J = 2.6$ Hz), 129.5 (d, $J = 6.7$ Hz), 128.5, 128.4, 127.4, 119.1, 103.1 (d, $J = 208.4$ Hz), 63.1, 54.4 (d, $J = 18.3$ Hz), 14.2; ^{19}F NMR (282 MHz, CDCl_3) δ -169.39 (d, $J = 33.2$ Hz); IR (Neat Film, NaCl) 3062, 3030, 2982, 2934, 1749, 1694, 1597, 1454, 1447, 1367, 1230, 1187, 1129, 1038, 929, 856, 743 cm^{-1} ; HRMS (ESI+) m/z calc'd for $\text{C}_{20}\text{H}_{20}\text{FO}_3$ $[\text{M}+\text{H}]^+$: 327.1391, found 327.1401; SFC conditions: 5% IPA, 4.0 mL/min, Chiralpak IC column, $\lambda = 254$ nm, t_{R} (min): major = 2.02, minor = 3.18.

Ethyl (2*S*,3*S*)-2-benzoyl-2-chloro-3-phenylpent-4-enoate (**112v**).

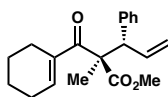


112v

Ketoester **112v** was isolated by silica gel chromatography (gradient elution, 2→3% EtOAc in hexanes) as a colorless oil. >99% ee, $[\alpha]_{\text{D}}^{25} +93.8$ (c 1.43, CHCl_3); $R_f = 0.4$ (5% EtOAc in hexanes); ^1H NMR (500 MHz, CDCl_3) δ 7.84–7.78 (m, 2H), 7.54–7.47 (m, 1H), 7.47–7.40 (m, 2H), 7.40–7.33 (m, 2H), 7.33–7.18 (m, 3H), 6.36 (ddd, $J = 16.9, 10.2, 8.7$ Hz, 1H), 5.20 (ddd, $J = 10.2, 1.5, 0.8$ Hz, 1H), 5.15 (ddd, $J = 16.9, 1.6, 1.0$ Hz, 1H), 4.66 (d, $J = 8.6$ Hz, 1H), 4.18 (q, $J = 7.1$ Hz, 2H), 1.12 (t, $J = 7.1$ Hz, 3H); ^{13}C NMR (126 MHz, CDCl_3) δ 189.8, 167.3, 138.0, 135.9, 134.8, 133.1, 130.7, 129.3, 128.3, 128.0, 127.5, 118.7, 77.3, 63.4, 55.8, 13.8; IR (Neat Film, NaCl) 3062, 3029, 2982, 1754, 1696,

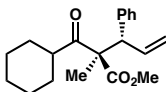
1597, 1581, 1446, 1367, 1299, 1239, 1207, 1186, 1094, 1075, 1025, 1007, 928, 749 cm^{-1} ;
HRMS (ESI+) m/z calc'd for $\text{C}_{20}\text{H}_{20}\text{ClO}_3$ $[\text{M}+\text{H}]^+$: 343.1095, found 343.1099; SFC
conditions: 10% MeOH, 2.5 mL/min, Chiralpak IC column, $\lambda = 254$ nm, t_{R} (min): major
= 2.52, minor = 2.77.

Ethyl (2*R*,3*S*)-2-(cyclohex-1-ene-1-carbonyl)-2-methyl-3-phenylpent-4-enoate (112w).



112w

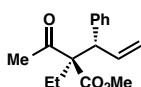
Ketoester **112w** was isolated by silica gel chromatography (1% EtOAc in hexanes) as a colorless oil. 99% ee, $[\alpha]_{\text{D}}^{25} +80.8$ (c 1.00, CHCl_3); $R_f = 0.3$ (10% EtOAc in hexanes); ^1H NMR (500 MHz, CDCl_3) δ 7.33–7.13 (m, 5H), 6.47 (td, $J = 3.9, 2.0$ Hz, 1H), 6.25 (ddd, $J = 16.8, 10.3, 8.0$ Hz, 1H), 5.09 (dt, $J = 10.2, 1.4$ Hz, 1H), 5.00 (dt, $J = 16.9, 1.4$ Hz, 1H), 4.29 (dd, $J = 8.0, 1.4$ Hz, 1H), 3.68 (d, $J = 0.8$ Hz, 3H), 2.24–2.03 (m, 3H), 1.97–1.81 (m, 1H), 1.55 (tq, $J = 7.0, 4.0, 2.3$ Hz, 4H), 1.43 (s, 3H); ^{13}C NMR (126 MHz, CDCl_3) δ 198.1, 173.8, 139.4, 138.3, 137.9, 137.2, 130.0, 128.0, 126.8, 117.1, 61.1, 54.5, 52.2, 25.9, 24.3, 22.0, 21.3, 20.7; IR (Neat Film, NaCl) 2938, 1732, 1671, 1636, 1452, 1433, 1234, 1113, 984, 917, 703 cm^{-1} ; HRMS (ESI+) m/z calc'd for $\text{C}_{20}\text{H}_{25}\text{O}_3$ $[\text{M}+\text{H}]^+$: 313.1798, found 313.1785; SFC conditions: 5% MeOH, 4.0 mL/min, Chiralpak IC column, $\lambda = 254$ nm, t_{R} (min): minor = 5.83, major = 6.55.

Methyl (2R,3S)-2-(cyclohexanecarbonyl)-2-methyl-3-phenylpent-4-enoate (112x).**112x**

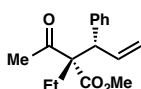
Ketoester **112x** was isolated by silica gel chromatography (5% EtOAc in hexanes) as a mixture of diastereomers (4:1 dr). *For the major isomer*: 96% ee, $[\alpha]_D^{25} +57.7$ (*c* 1.54, CHCl₃, measured with 4:1 dr mixture); $R_f = 0.3$ (5% EtOAc in hexanes); ¹H NMR (500 MHz, CDCl₃) δ 7.29–7.18 (m, 5H), 6.26 (ddd, *J* = 17.0, 10.2, 8.5 Hz, 1H), 5.08 (ddd, *J* = 10.2, 1.8, 0.9 Hz, 1H), 5.00 (ddd, *J* = 17.0, 1.8, 1.1 Hz, 1H), 4.18 (dt, *J* = 8.5, 1.0 Hz, 1H), 3.71 (s, 3H), 2.50 (tt, *J* = 11.4, 3.2 Hz, 1H), 1.79–1.56 (m, 5H), 1.53–1.46 (m, 1H), 1.33 (s, 3H), 1.32–1.11 (m, 4H); ¹³C NMR (126 MHz, CDCl₃) δ 210.3, 172.4, 139.6, 137.8, 129.9, 128.3, 127.0, 117.4, 64.7, 54.1, 52.2, 48.4, 30.3, 29.6, 25.8, 25.73, 25.71, 18.7; IR (Neat Film, NaCl) 2933, 2854, 1729, 1708, 1635, 1495, 1453, 1432, 1380, 1315, 1228, 1144, 1101, 989, 919 cm⁻¹; HRMS (ESI+) *m/z* calc'd for C₂₀H₂₆O₃ [M+H]⁺: 315.1955, found 315.1955; SFC conditions: 100% CO₂, 4.0 mL/min, Chiralcel OJ-H column, $\lambda = 210$ nm, *t_R* (min): minor = 7.28, major = 7.96.

Methyl (2R,3S)-2-acetyl-2-ethyl-3-phenylpent-4-enoate (112y) and methyl (2S,3S)-2-acetyl-2-ethyl-3-phenylpent-4-enoate (112y').

Ketoesters **112y** and **112y'** were isolated by silica gel chromatography (gradient elution, 0→4% EtOAc in hexanes) as mixture of two diastereomers (1.5:1 dr). The diastereomers were separated by preparative HPLC (gradient elution, 60→70% MeCN in H₂O).

**112y**

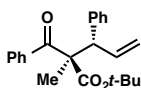
The major diastereomer **112y** was isolated as a colorless oil. 90% ee, $[\alpha]_D^{25} +72.7$ (c 0.60, CHCl_3); $R_f = 0.4$ (5% EtOAc in hexanes); ^1H NMR (500 MHz, CDCl_3) δ 7.32–7.25 (m, 2H), 7.25–7.18 (m, 1H), 7.17–7.07 (m, 2H), 6.28 (ddd, $J = 17.0, 10.2, 8.4$ Hz, 1H), 5.08 (ddd, $J = 10.2, 1.7, 0.9$ Hz, 1H), 4.97 (ddd, $J = 17.0, 1.7, 1.1$ Hz, 1H), 4.03 (d, $J = 8.5$ Hz, 1H), 3.76 (s, 3H), 2.06 (s, 3H), 1.86–1.68 (m, 2H), 0.77 (t, $J = 7.5$ Hz, 3H); ^{13}C NMR (126 MHz, CDCl_3) δ 205.8, 172.4, 139.5, 137.7, 129.3, 128.4, 127.3, 117.3, 68.2, 53.5, 51.9, 29.8, 27.4, 9.1; IR (Neat Film, NaCl) 3083, 3029, 2978, 2950, 2883, 1709, 1601, 1494, 1434, 1385, 1353, 1301, 1220, 1116, 1029, 993, 919, 755 cm^{-1} ; HRMS (MM: ESI-APCI+) m/z calc'd for $\text{C}_{16}\text{H}_{21}\text{O}_3$ $[\text{M}+\text{H}]^+$: 261.1485, found 261.1492; SFC conditions: 0.5% IPA, 2.5 mL/min, Chiralcel OJ-H column, $\lambda = 210$ nm, t_R (min): minor = 4.79, major = 7.02.

**112y'**

The minor diastereomer **112y'** was isolated as a colorless oil. 91% ee, $[\alpha]_D^{25} +25.3$ (c 0.26, CHCl_3); $R_f = 0.4$ (5% EtOAc in hexanes); ^1H NMR (500 MHz, CDCl_3) δ 7.26–7.23 (m, 2H), 7.21–7.17 (m, 1H), 7.17–7.13 (m, 2H), 6.31 (ddd, $J = 16.9, 10.2, 9.3$ Hz, 1H), 5.15 (ddd, $J = 10.2, 1.6, 0.7$ Hz, 1H), 5.10 (ddd, $J = 17.0, 1.7, 1.0$ Hz, 1H), 4.11 (d, $J = 9.4$ Hz, 1H), 3.63 (s, 3H), 2.12 (s, 3H), 2.09–1.98 (m, 1H), 1.80 (dq, $J = 14.8, 7.5$ Hz, 1H), 0.77 (t, $J = 7.5$ Hz, 3H); ^{13}C NMR (126 MHz, CDCl_3) δ 205.3, 172.3, 140.1, 137.3,

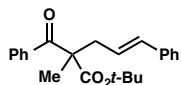
129.4, 128.2, 127.0, 117.6, 68.0, 52.5, 51.9, 30.1, 26.9, 8.8; IR (Neat Film, NaCl) 3063, 3030, 2962, 2925, 2850, 1710, 1600, 1446, 1354, 1286, 1260, 1223, 1182, 1118, 1095, 1023, 921, 864, 801 cm^{-1} ; HRMS (MM: ESI-APCI+) m/z calc'd for $\text{C}_{16}\text{H}_{21}\text{O}_3$ $[\text{M}+\text{H}]^+$: 261.1485, found 261.1494; SFC conditions: 0.5% IPA, 2.5 mL/min, Chiralcel OJ-H column, $\lambda = 210$ nm, t_R (min): minor = 6.29, major = 7.02.

***tert*-Butyl (2*R*,3*S*)-2-benzoyl-2-methyl-3-phenylpent-4-enoate (**112z**).**



112z

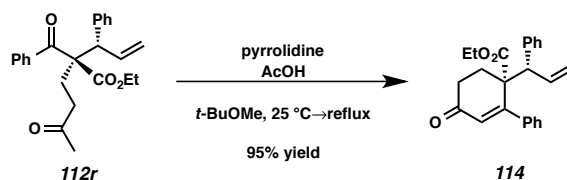
Ketoester **112z** was isolated by silica gel chromatography (gradient elution, 0→2→5% EtOAc in hexanes) as a colorless oil. >99% ee, $[\alpha]_D^{25} +67.4$ (c 1.54, CHCl_3); $R_f = 0.4$ (5% EtOAc in hexanes); ^1H NMR (500 MHz, CDCl_3) δ 7.74–7.70 (m, 2H), 7.49–7.46 (m, 1H), 7.39–7.34 (m, 2H), 7.25–7.16 (m, 5H), 6.34 (ddd, $J = 17.0, 10.3, 7.9$ Hz, 1H), 5.12 (ddd, $J = 10.3, 1.8, 1.1$ Hz, 1H), 5.03 (dt, $J = 17.0, 1.6$ Hz, 1H), 4.42 (dt, $J = 7.9, 1.2$ Hz, 1H), 1.50 (s, 3H), 1.29 (s, 9H); ^{13}C NMR (126 MHz, CDCl_3) δ 198.1, 171.8, 139.7, 138.1, 137.3, 132.2, 130.4, 128.5, 128.3, 128.1, 126.9, 117.1, 82.6, 62.1, 54.6, 27.8, 21.0; IR (Neat Film, NaCl) 3061, 3027, 2978, 2934, 1728, 1716, 1687, 1682, 1598, 1454, 1446, 1251, 1155, 1115, 961, 918, 844 cm^{-1} ; HRMS (ESI+) m/z calc'd for $\text{C}_{23}\text{H}_{27}\text{O}_3$ $[\text{M}+\text{H}]^+$: 351.1955, found 351.1955; SFC conditions: 5% IPA, 2.5 mL/min, Chiralpak IC column, $\lambda = 254$ nm, t_R (min): major = 4.14, minor = 5.80.

***tert*-Butyl (*E*)-2-benzoyl-2-methyl-5-phenylpent-4-enoate (**113z**).****113z**

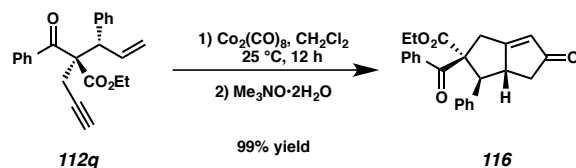
Ketoester **113z** was isolated by silica gel chromatography (gradient elution, 0→2→5% EtOAc in hexanes) as a colorless oil. 38% ee, $[\alpha]_{\text{D}}^{25} +3.9$ (c 0.74, CHCl_3); $R_f = 0.4$ (5% EtOAc in hexanes); $^1\text{H NMR}$ (500 MHz, CDCl_3) δ 7.92–7.89 (m, 2H), 7.56–7.51 (m, 1H), 7.46–7.41 (m, 2H), 7.33–7.27 (m, 4H), 7.23–7.18 (m, 1H), 6.39 (dt, $J = 15.8, 1.3$ Hz, 1H), 6.16–6.06 (m, 1H), 2.93 (ddd, $J = 14.2, 7.5, 1.4$ Hz, 1H), 2.84 (ddd, $J = 14.2, 7.7, 1.3$ Hz, 1H), 1.55 (s, 3H), 1.28 (s, 9H); $^{13}\text{C NMR}$ (126 MHz, CDCl_3) δ 197.8, 172.8, 137.3, 135.9, 133.9, 132.7, 128.8, 128.6, 128.5, 127.4, 126.3, 124.7, 82.2, 58.0, 40.7, 27.8, 21.5; IR (Neat Film, NaCl) 3058, 3026, 2977, 2933, 1728, 1686, 1682, 1597, 1579, 1447, 1368, 1249, 1212, 1152, 1111, 970, 845 cm^{-1} ; HRMS (ESI+) m/z calc'd for $\text{C}_{23}\text{H}_{27}\text{O}_3$ $[\text{M}+\text{H}]^+$: 351.1955, found 351.1949; SFC conditions: 5% IPA, 2.5 mL/min, Chiralpak IC column, $\lambda = 254$ nm, t_{R} (min): major = 9.88, minor = 8.48.

4.6.5 Procedures for derivatization of allylic alkylation products and spectroscopic data of derivatives

Synthesis of cyclohexenone **114**:



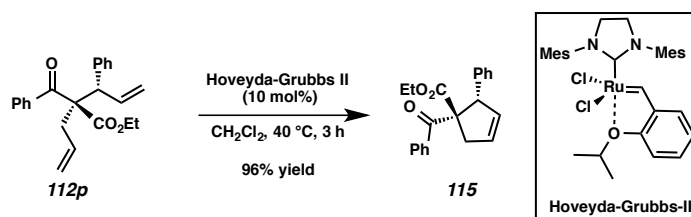
To a solution of ketoester **112r** (60.4 mg, 0.6 mmol) in *t*-BuOMe (2 mL) was added pyrrolidine (13.7 mg, 0.19 mmol) and AcOH (11.6 mg, 0.19 mmol). The mixture was stirred for 12 h at 25 °C then heated to reflux for 4 h. The solvent was removed under reduced pressure and the residue was subjected to column chromatography on silica gel (gradient elution, 10→25% EtOAc in hexanes) to give cyclohexenone **114** (55.1 mg, 95% yield) as a colorless oil. $[\alpha]_D^{25} +151.4$ (*c* 1.19, CHCl₃); $R_f = 0.5$ (25% EtOAc in hexanes); ¹H NMR (500 MHz, CDCl₃) δ 7.34–7.28 (m, 1H), 7.25–7.19 (m, 2H), 7.13–7.04 (m, 3H), 7.04–6.97 (m, 2H), 6.69–6.63 (m, 2H), 6.33 (ddd, *J* = 16.9, 10.2, 7.8 Hz, 1H), 6.07 (s, 1H), 5.10 (ddd, *J* = 10.2, 1.6, 1.0 Hz, 1H), 4.87 (dt, *J* = 17.0, 1.5 Hz, 1H), 4.31 (q, *J* = 7.1 Hz, 2H), 4.26 (dt, *J* = 7.5, 1.5 Hz, 1H), 2.91–2.77 (m, 1H), 2.62–2.53 (m, 3H), 1.32 (t, *J* = 7.1 Hz, 3H); ¹³C NMR (126 MHz, CDCl₃) δ 198.5, 173.2, 161.6, 139.5, 139.2, 138.0, 131.9, 129.8, 128.7, 128.2, 128.1, 128.0, 126.7, 118.1, 62.0, 54.0, 53.8, 34.7, 30.9, 14.3; IR (Neat Film, NaCl) 3058, 3030, 2981, 1725, 1673, 1602, 1492, 1444, 1326, 1240, 1214, 1170, 1016, 921, 882 cm⁻¹; HRMS (ESI+) *m/z* calc'd for C₂₄H₂₅O₃ [M+H]⁺: 361.1798, found 361.1798.

Synthesis of bicyclic enone 116:

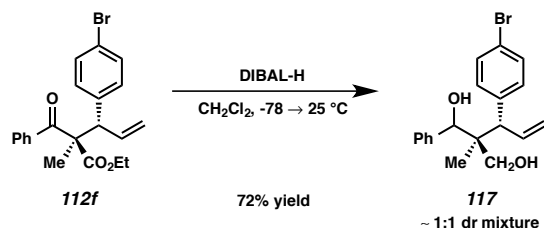
A dried flask was charged with a solution of enyne **112q** (8.6 mg, 0.025 mmol) and $\text{Co}_2(\text{CO})_8$ (11.8 mg, 0.034 mmol) in CH_2Cl_2 (2 mL) and the mixture was stirred at room temperature for 12 h under an atmosphere of argon. After full consumption of **112q** was observed by TLC analysis, $\text{Me}_3\text{NO}\cdot 2\text{H}_2\text{O}$ (7.6 mg, 0.068 mmol) was added. The mixture was stirred for 20 min and an additional portion of $\text{Me}_3\text{NO}\cdot 2\text{H}_2\text{O}$ (30.1 mg, 0.27 mmol) was added. Stirring was continued until complete consumption of the cobalt-alkyne complex was observed by TLC analysis (about 4 h). The mixture was filtered through a celite pad, washed with CH_2Cl_2 , the solvent removed under reduced pressure, and the residue subjected to column chromatography on silica gel (25% EtOAc in hexanes) to give the bicyclic enone **116** (9.3 mg, 99% yield) as a colorless oil. The relative stereochemistry of **116** was assigned by 2D-NOESY. $[\alpha]_{\text{D}}^{25} -178.8$ (c 0.79, CHCl_3); $R_f = 0.3$ (25% EtOAc in hexanes); ^1H NMR (500 MHz, CDCl_3) δ 7.33–7.26 (m, 1H), 7.26–7.18 (m, 4H), 7.13–7.02 (m, 5H), 6.03 (td, $J = 2.2, 1.1$ Hz, 1H), 4.11–3.91 (m, 3H), 3.82 (d, $J = 12.3$ Hz, 1H), 3.73–3.63 (m, 1H), 3.01 (dq, $J = 18.2, 1.1$ Hz, 1H), 2.54 (ddd, $J = 18.0, 6.4, 0.8$ Hz, 1H), 2.14 (ddd, $J = 18.0, 2.5, 1.7$ Hz, 1H), 0.86 (t, $J = 7.1$ Hz, 3H); ^{13}C NMR (126 MHz, CDCl_3) δ 209.3, 197.1, 183.8, 173.3, 137.1, 136.7, 132.4, 129.5, 128.5, 128.3, 127.9, 127.8, 126.1, 68.6, 62.0, 55.8, 50.4, 41.7, 39.2, 13.6; IR (Neat Film, NaCl) 3034, 2979, 2927, 1733, 1714, 1668, 1636, 1600, 1583, 1449, 1409, 1255, 1211, 1183,

1071, 1043, 927, 914, 819 cm^{-1} ; HRMS (MM: ESI-APCI+) m/z calc'd for $\text{C}_{24}\text{H}_{23}\text{O}_4$ $[\text{M}+\text{H}]^+$: 375.1596, found 375.1592.

Synthesis of compound **115**:



To a flame-dried Schlenk flask was added a solution of **112p** (20.8 mg, 0.06 mmol in 1.5 mL of CH_2Cl_2) and Hoveyda-Grubbs II catalyst (3.7 mg, 10 mol%). The reaction mixture was stirred for 3 h at 40 °C, filtered through a short silica pad and purified by silica gel chromatography (gradient elution, 1→5% EtOAc in hexanes) to give ketoester **115** (18.3 mg, 96% yield) as a white solid. $[\alpha]_{\text{D}}^{25}$ -613.7 (c 0.94, CHCl_3); R_f = 0.4 (5% EtOAc in hexanes); ^1H NMR (500 MHz, CDCl_3) δ 7.61–7.55 (m, 2H), 7.38 (ddt, J = 8.6, 7.1, 1.2 Hz, 1H), 7.28–7.21 (m, 2H), 6.97–6.93 (m, 3H), 6.89–6.83 (m, 2H), 5.90 (ddt, J = 6.1, 2.6, 1.8 Hz, 1H), 5.75 (dtd, J = 5.5, 2.6, 1.5 Hz, 1H), 4.92 (q, J = 2.3 Hz, 1H), 4.11 (q, J = 7.1 Hz, 2H), 4.03 (dtd, J = 18.0, 2.6, 1.9 Hz, 1H), 2.73 (ddd, J = 18.0, 2.6, 1.6 Hz, 1H), 1.00 (t, J = 7.1 Hz, 3H); ^{13}C NMR (126 MHz, CDCl_3) δ 194.2, 174.4, 138.4, 136.6, 133.8, 132.5, 129.5, 128.5, 128.1, 128.0, 127.4, 127.0, 68.3, 61.9, 58.0, 41.5, 13.8; IR (Neat Film, NaCl) 3060, 3028, 2959, 2932, 2871, 1736, 1732, 1686, 1682, 1598, 1582, 1492, 1447, 1365, 1258, 1243, 1220, 1157, 1087, 1048, 1004, 966, 922, 876, 761 cm^{-1} ; HRMS (MM: ESI-APCI+) m/z calc'd for $\text{C}_{21}\text{H}_{21}\text{O}_3$ $[\text{M}+\text{H}]^+$: 321.1485, found 321.1489.

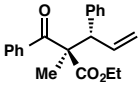
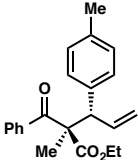
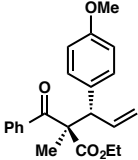
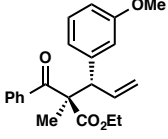
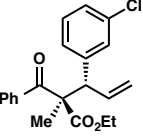
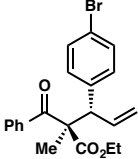
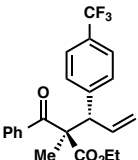
4.6.6 Determination of the absolute confirmation of compound 112f

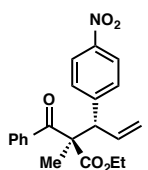
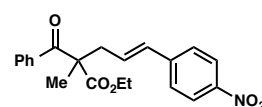
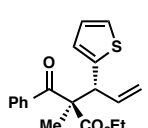
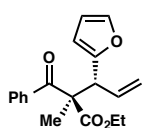
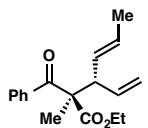
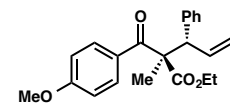
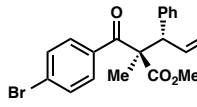
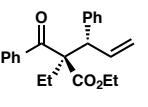
To a flame-dried flask was added **112f** (98% ee, 62.1 mg, 0.16 mmol), CH_2Cl_2 (5 mL) and this solution was cooled to -78°C . DIBAL-H (0.62 mL, 1.0 M solution in hexane) was added dropwise by syringe. The mixture was stirred for 2 h at -78°C , then allowed to warm to 25°C and stirred for an additional 12 h. The reaction was then cooled to 0°C , and another 0.62 mL of DIBAL-H solution was added, followed by stirring at 25°C for 3 h. The reaction mixture was then quenched with saturated aqueous Rochelle's salt (20 mL) and stirred for another 3 h. The aqueous layer was partitioned with a total of 100 mL of CH_2Cl_2 and the combined organic phases washed with brine, dried over MgSO_4 , filtered and concentrated under reduced pressure. The crude product was purified by silica gel chromatography (gradient elution, 5 \rightarrow 20% EtOAc in hexanes) to give 40.2 mg (72% yield) of **117** as white solid mixture (1:1 dr). The diastereomers were separated by preparative HPLC (gradient elution, 60 \rightarrow 90% MeCN in H_2O). *For isomer a*: white solid, $[\alpha]_{\text{D}}^{25} +58.9$ (c 0.47, CHCl_3); $R_f = 0.4$ (25% EtOAc in hexanes); ^1H NMR (500 MHz, CDCl_3) δ 7.46–7.39 (m, 4H), 7.36–7.31 (m, 2H), 7.31–7.27 (m, 1H), 7.27–7.23 (m, 2H), 6.79 (dt, $J = 16.9, 10.1$ Hz, 1H), 5.20–5.10 (m, 2H), 5.07 (s, 1H), 3.67 (d, $J = 10.1$ Hz, 1H), 3.34 (d, $J = 11.2$ Hz, 1H), 3.11 (dd, $J = 11.1, 0.7$ Hz, 1H), 1.56 (br s, 2H), 0.72 (s, 3H); ^{13}C NMR (126 MHz, CDCl_3) δ 141.5, 141.0, 140.4, 131.6, 131.4, 128.04, 128.79,

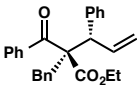
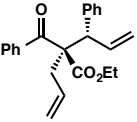
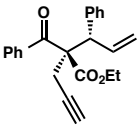
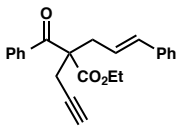
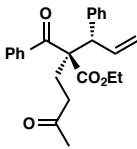
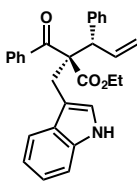
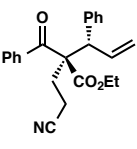
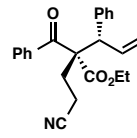
127.8, 120.5, 116.5, 76.0, 66.6, 55.8, 46.2, 15.3; IR (Neat Film, NaCl) 3423, 3070, 2969, 2923, 1486, 1452, 1403, 1342, 1074, 1012, 916, 827 cm^{-1} ; HRMS (ESI+) m/z calc'd for fragment $\text{C}_{19}\text{H}_{18}\text{Br} [\text{M}-\text{H}_4\text{O}_2+\text{H}]^+$: 325.0586, found 325.0585. *For isomer b*: white solid, $[\alpha]_{\text{D}}^{25} +53.4$ (c 0.43, CHCl_3); $R_f = 0.4$ (24% EtOAc in hexanes); ^1H NMR (500 MHz, CDCl_3) δ 7.50–7.45 (m, 2H), 7.35–7.27 (m, 5H), 7.25–7.20 (m, 2H), 6.30 (dt, $J = 16.8, 10.0$ Hz, 1H), 5.35 (ddd, $J = 16.8, 1.9, 0.8$ Hz, 1H), 5.24 (ddd, $J = 10.0, 1.9, 0.5$ Hz, 1H), 4.39 (d, $J = 10.0$ Hz, 1H), 4.26 (s, 1H), 3.64 (d, $J = 11.6$ Hz, 1H), 3.51 (dd, $J = 11.6, 1.8$ Hz, 1H), 1.58 (br s, 2H), 0.48 (s, 3H); ^{13}C NMR (126 MHz, CDCl_3) δ 141.0, 140.2, 137.2, 131.7, 131.3, 128.02, 127.97, 127.8, 120.6, 118.3, 80.0, 65.6, 49.7, 44.5, 15.5; IR (Neat Film, NaCl) 3372, 2973, 2938, 2888, 1637, 1486, 1473, 1454, 1402, 1348, 1266, 1203, 1101, 1077, 1024, 1010, 921, 894, 831, 782 cm^{-1} ; HRMS (ESI+) m/z calc'd for fragment $\text{C}_{19}\text{H}_{18}\text{Br} [\text{M}-\text{H}_4\text{O}_2+\text{H}]^+$: 325.0586, found 325.0588.

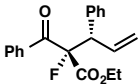
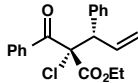
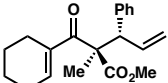
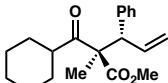
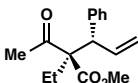
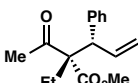
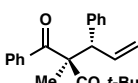
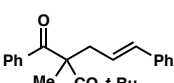
4.6.7 Determination of enantiomeric excess

Table 4.6.7.1. Determination of enantiomeric excess

entry	compound	SFC analytic conditions	ee (%)
1	 112a	Chiralpak IC, $\lambda = 254$ nm 5% IPA/CO ₂ , 2.5 mL/min t_R (min): major 4.12, minor 6.14	98
2	 112b	Chiralpak IC, $\lambda = 254$ nm 5% IPA/CO ₂ , 2.5 mL/min t_R (min): major 6.71, minor 9.45	>99
3	 112c	Chiralcel OJ-H, $\lambda = 254$ nm 4% IPA/CO ₂ , 2.5 mL/min t_R (min): minor 5.64, major 6.84	>99
4	 112d	Chiralpak IC, $\lambda = 254$ nm 2% MeOH/CO ₂ , 2.5 mL/min t_R (min): major 12.24, minor 13.50	>99
5	 112e	Chiralpak IC, $\lambda = 254$ nm 10% IPA/CO ₂ , 4.0 mL/min t_R (min): major 1.59, minor 1.77	99
6	 112f	Chiralpak AD-H, $\lambda = 254$ nm 10% IPA/CO ₂ , 4.0 mL/min t_R (min): minor 2.95, major 3.17	>99
7	 112g	Chiralpak AD-H, $\lambda = 254$ nm 2% IPA/CO ₂ , 2.5 mL/min t_R (min): minor 5.20, major 6.68	>99

entry	compound	SFC analytic conditions	ee (%)
8	 <p>112h</p>	Chiralpak AD-H, $\lambda = 254$ nm 5% MeOH/CO ₂ , 3.0 mL/min t_R (min): minor 4.47, major 5.71	93
9	 <p>113h</p>	Chiralpak AD-H, $\lambda = 254$ nm 10% MeOH/CO ₂ , 3.0 mL/min t_R (min): major 7.13, minor 8.06	23
10	 <p>112i</p>	Chiralpak IC, $\lambda = 254$ nm 5% IPA/CO ₂ , 2.5 mL/min t_R (min): major 7.92, minor 11.24	95
11	 <p>112j</p>	Chiralpak IC, $\lambda = 254$ nm 5% IPA/CO ₂ , 2.5 mL/min t_R (min): major 5.09, minor 9.14	>99
12	 <p>112k</p>	Chiralpak AD-H, $\lambda = 210$ nm 2% IPA/CO ₂ , 2.5 mL/min t_R (min): minor 4.40, major 5.52	91
13	 <p>112l</p>	Chiralpak IC, $\lambda = 254$ nm 10% IPA/CO ₂ , 4.0 mL/min t_R (min): major 2.67, minor 3.51	99
14	 <p>112m</p>	Chiralpak AD-H, $\lambda = 254$ nm 5% IPA/CO ₂ , 2.5 mL/min t_R (min): major 5.35, minor = 5.88	>99
15	 <p>112n</p>	Chiralpak AD-H, $\lambda = 254$ nm, 5% MeOH/CO ₂ , 2.5 mL/min, t_R (min): major = 2.48, minor = 2.20	>99

entry	compound	SFC analytic conditions	ee (%)
16	 <p>112o</p>	Chiralpak AD-H, $\lambda = 254$ nm 4% MeOH/CO ₂ , 4.0 mL/min t_R (min): major 5.06, minor 8.94	>99
17	 <p>112p</p>	Chiralpak IC, $\lambda = 254$ nm 3% IPA/CO ₂ , 4.0 mL/min t_R (min): major 7.16, minor 8.60	>99
18	 <p>112q</p>	Chiralcel OD-H, $\lambda = 254$ nm 5% IPA/CO ₂ , 2.5 mL/min t_R (min): minor 5.67, major 6.44	>99
19	 <p>113q</p>	Chiralpak IC, $\lambda = 254$ nm 5% IPA/CO ₂ , 2.5 mL/min t_R (min): major 10.67, minor 9.81	34
20	 <p>112r</p>	Chiralcel OD-H, $\lambda = 254$ nm 5% IPA/CO ₂ , 2.5 mL/min t_R (min): minor 10.8, major 8.0	99
21	 <p>112s</p>	Chiralpak IC, $\lambda = 254$ nm 10% MeOH/CO ₂ , 2.5 mL/min t_R (min): major 8.26, minor 9.30	>99
22	 <p>112t</p>	Chiralpak AD-H, $\lambda = 254$ nm 5% IPA/CO ₂ , 2.5 mL/min t_R (min): major 9.77, minor 11.60	>99
23	 <p>112t'</p>	Chiralpak AD-H, $\lambda = 254$ nm 5% IPA/CO ₂ , 2.5 mL/min t_R (min): major 10.65, minor 12.00	>99

entry	compound	SFC analytic conditions	ee (%)
24	 112u	Chiralpak IC, $\lambda = 254$ nm 5% IPA/CO ₂ , 4.0 mL/min t_R (min): major 2.02, minor 3.18	95
25	 112v	Chiralpak IC, $\lambda = 254$ nm 10% IPA/CO ₂ , 2.5 mL/min t_R (min): major 2.52, minor 2.76	>99
26	 112w	Chiralpak IC, $\lambda = 254$ nm 5% MeOH/CO ₂ , 4 mL/min t_R (min): major 6.56, minor 5.83	99
27	 112x	Chiralcel OJ-H, $\lambda = 210$ nm 100% CO ₂ , 4.0 mL/min t_R (min): minor 7.28, major 7.96	96
28	 112y	Chiralcel OJ-H, $\lambda = 210$ nm 0.5% IPA/CO ₂ , 2.5 mL/min t_R (min): minor 4.79, major 5.33	90
29	 112y'	Chiralcel OJ-H, $\lambda = 210$ nm 0.5% IPA/CO ₂ , 2.5 mL/min t_R (min): minor 6.29, major 7.02	91
30	 112z	Chiralpak IC, $\lambda = 254$ nm 5% IPA/CO ₂ , 2.5 mL/min t_R (min): major 4.14, minor 5.80	>99
31	 113z	Chiralpak IC, $\lambda = 254$ nm 5% IPA/CO ₂ , 2.5 mL/min t_R (min): major 9.88, minor 8.48	38

4.7 REFERENCES AND NOTES

- (97) For the first example see reference 75; for reviews see references 76.
- (98) Zhuo, C.-X.; Wu, Q.-F.; Zhao, Q.; Xu, Q.-L.; You, S.-L. *J. Am. Chem. Soc.* **2013**, *135*, 8169.
- (99) See references 80, 81 and: Bartels, B.; García-Yebra, C.; Helmchen, G. *Eur. J. Org. Chem.* **2003**, 1097.
- (100) Chen, W.; Chen, M.; Hartwig, J. F. *J. Am. Chem. Soc.* **2014**, *136*, 15825.
- (101) Absolute configuration of product **112f** determined by x-ray analysis of a derivative structure, see appendix A7 for detail. Absolute configuration of all other products determined by analogy. Relative configuration of product derivative **116** was determined by 2D NMR studies, see SI below and appendix A6 for details. The relative configurations of all other products determined by analogy.
- (102) (a) Xia, J.-B.; Liu, W.-B.; Wang, T.-M.; You, S.-L. *Chem. Eur. J.* **2010**, *16*, 6442.
(b) Farwick, A.; Engelhart, J. U.; Tverskoy, O.; Welter, C.; Umlauf, Q. A.; Rominger, F.; Kerr, W. J.; Helmchen, G. *Adv. Synth. Catal.* **2011**, *353*, 349.

- (103) (a) González, D. F.; Brand, J. P.; Waser, J. *Chem. Eur. J.* **2010**, *16*, 9457. (b) Bartoli, G.; Bosco, M.; Bellucci, M. C.; Marcantoni, E.; Sambri, L.; Torregiani, E. *Eur. J. Org. Chem.* **1999**, 617. (c) Stavber, G.; Zupan, M.; Stavber, S. *Tetrahedron Lett.* **2007**, *48*, 2671. (d) Meshram, H. M.; Reddy, P. N.; Sadashiv, K.; Yadav, J. S. *Tetrahedron Lett.* **2005**, *46*, 623. (e) Turner, J. A.; Jacks, W. S. *J. Org. Chem.* **1989**, *54*, 4229.
-

APPENDIX 5

Stereochemical Model and Mechanistic Discussion for Iridium-Catalyzed Allylic Alkylation

A5.1 INTRODUCTION

Following the first reports of iridium-catalyzed allylic alkylation⁷⁵ and amination⁷⁸ nearly two decades ago, myriad studies investigating the underlying mechanism of regio- and enantioselectivity in iridium-catalyzed allylic substitutions, and the nature of role of Ir-phosphoramidite complexes in these processes, have been conducted.⁷⁹ Seminal contributions from Hartwig and Helmchen⁷⁹ confirmed evidence that active species in Ir-phosphoramidite catalyzed allylic substitution processes are *in situ* generated iridacycles, formed by C–H insertion into the amidite domain of a Feringa type ligand.^{79a} Moreover, Hartwig and coworkers went on the show that only the stereocenter β to the metal center is crucial in affecting enantioinduction and that only one such center is requisite for stereocontrol.^{79g, 79h}

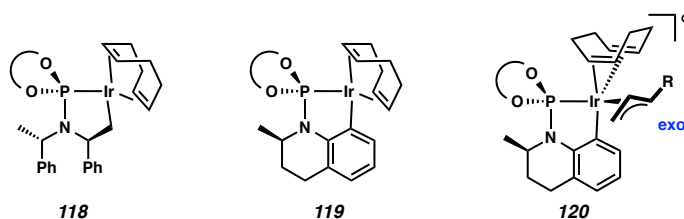
Comparatively less investigation has been undertaken to unearth the source of diastereoselectivity in iridium-catalyzed allylic substitution processes, in part due to the lack of reports describing such findings. Herein, we speculate as to the source of

diastereoselectivity in our iridium catalyzed regio-, diastereo- and enantioselective allylic alkylation, and present a plausible catalytic cycle.

A5.2 STEREOCHEMICAL MODEL FOR DIASTEREOSELECTIVITY IN IRIDIUM-CATALYZED ALLYLIC ALKYLATION

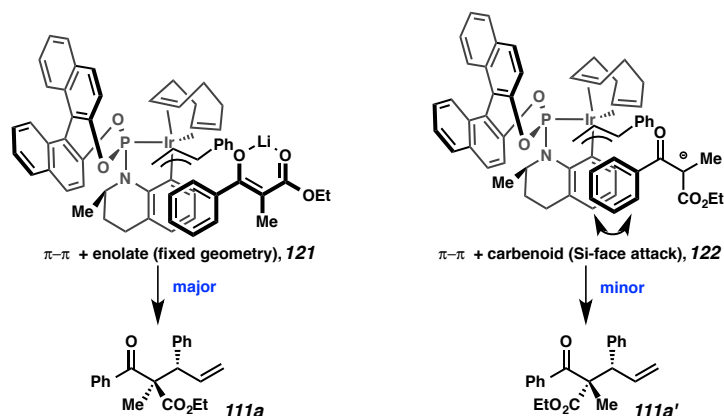
Feringa-type phosphoramidite ligands have been shown to form iridacycles via iridium(I) insertion into the C(sp³)–H bond (**118**, Figure A5.2.1). Investigations by You and coworkers⁸⁷ led to the development and N-arylphosphoramidite ligand **L12**, which was then shown to form an active iridacycle via transition metal insertion into the C(sp²)–H bond of the aryl group (**119**, Figure A5.2.1). DFT studies and single crystal X-ray diffraction analysis conducted by the You group⁸⁷ revealed that the (π-allyl)-Ir complex formed upon oxidative addition of iridium(I) into cinnamyl derived allyl carbonates is predominately the *exo* isomer¹⁰⁴ (**120**, Figure A5.2.1). This is at odds from what is observed with Feringa ligand-derived iridacycles. We speculate that both the ligand structure, in particular the aromatic amine moiety, and the unique allyl orientation may play a role in imparting **L12** its selectivity profile.

Figure A5.2.1. Selected iridium-phosphoramidite complexes: **118** Feringa type; **119** N-arylphosphoramidite (or You) type; **120** (π-allyl)-Ir complex with You type ligand.



In the course of our studies in iridium-catalyzed allylic alkylation, we were able to recrystallize β -Ketoester **112f** from *i*-PrOH/hexanes such that crystals suitable for X-ray analysis were obtained. Via single crystal X-ray diffraction studies, we were able to unambiguously assign the absolute stereochemistry of the products generated in studies presented in Chapter 4 (see Appendix 5 *vide infra* for detail). With this data in hand, and with knowledge of the spatial orientation of (π -allyl)-Ir complex **120**, we are able to begin speculation as to the origin of stereoselectivity in our allylic alkylation reaction.

What we believe to be the two most likely approaches of linear enolate nucleophiles prior to the bond-forming event are depicted in Figure A5.2.2 (**121** and **122**). In this depiction, the diene ligand, BINOL backbone of the ligand and protruding tetrahydroquinoline methyl create a steric environment around the metal center in which approach of the nucleophile is necessarily via the bottom-right quadrant. Our finding that aliphatic ketone substrates fare poorly with respect to diastereoselectivity leads us to hypothesize a potential π - π stacking interaction between the tetrahydroquinoline and ketone aryl group may be important in orienting the nucleophile. Our finding that lithium is a crucial component of the reaction mixture leads us to suppose that rigidly enforced enolate geometry is also essential with respect to diastereomeric outcome. Given these data, we believe that the approach shown to the left (**121**) is most plausible, in that both a π -stacking interaction is possible and enolate geometry is enforced.

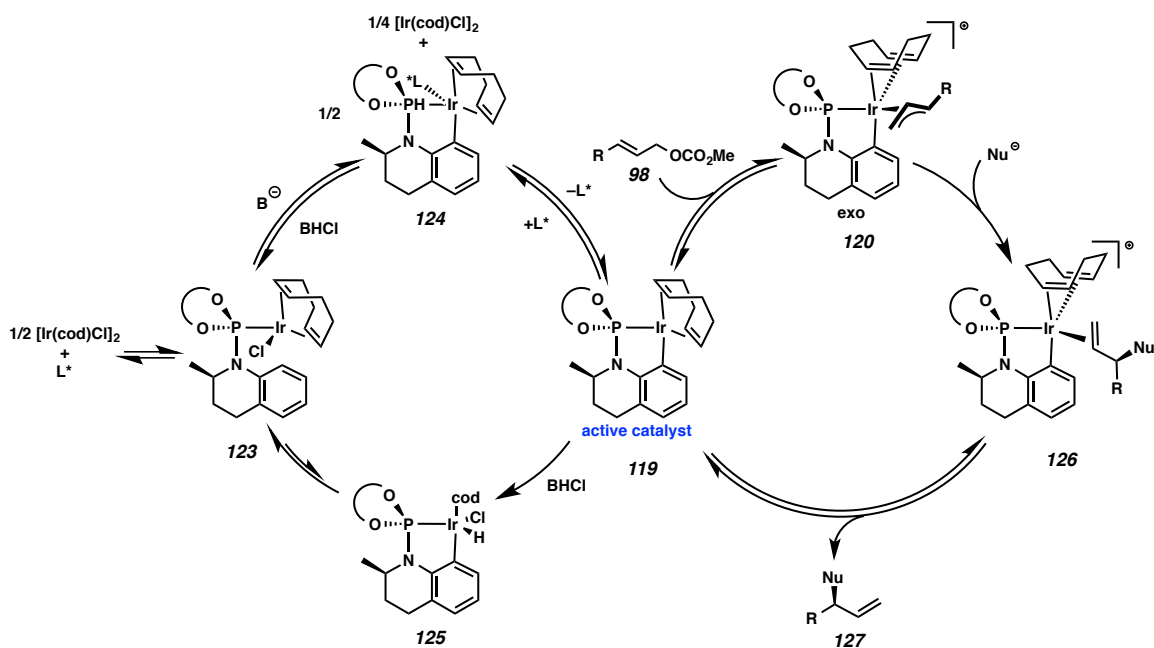
Figure A5.2.2. Approach of the enolate nucleophile in the Ir-catalyzed allylic alkylation.

The catalytic cycle we propose to be operative is depicted below in Figure A5.2.3. Beginning with dissociation of the precatalyst dimer, and association of an equivalent of iridium with ligand, we arrive at species **123**. Base promoted C–H insertion followed by loss of an associated ligand delivers the active catalyst species (**119**).¹⁰⁵ This complex may then undergo oxidative addition into cinnamyl carbonate **98** to deliver *exo* (π -allyl)-iridium complex **120**, which may then be attacked by an enolate nucleophile to give olefin-bound iridium complex **126**. Finally, dissociation of the olefin gives the allylated product and regenerates the active catalyst species.

While the cycle presented below is plausible, and is in line with what is known in the literature⁷⁹ it is also conjecture. More evidence is needed to confirm or support a variety of discreet steps; for example the reversibility of C–H insertion (i.e., **125** \rightarrow **123**, **124** \rightarrow **123**). Moreover, the discreet steps in such a cycle may change depending on the particular precatalyst, base and ligand that are employed.^{76d} As such, further investigations to elucidate the mechanism of this iridium-catalyzed allylic alkylation are

warranted, and should serve to inform the development of new modes of reactivity for these iridium complexes.

Figure A5.2.3. Proposed catalytic cycle for iridium-*N*-arylphosphoramidite complex-catalyzed allylic alkylation



A5.3 REFERENCES AND NOTES

- (104) The *exo* complex is defined as having the C2–H bond of the allylic moiety pointing toward diene, whereas the *endo* isomer places the C2–H bond of the allylic moiety pointing toward the amine part of the ligand.

- (105) While this has been shown to be the case for Feringa type ligands, unpublished work by the You group indicate that in the case of N-aryl phosphoramidite ligands, the iridacycle does not coordinate a second equivalent of ligand.

APPENDIX 6

Spectra Related to Chapter 4:

Enantio-, Diastereo- and Regioselective Iridium-Catalyzed

Asymmetric Allylic Alkylation of Acyclic β -Ketoesters

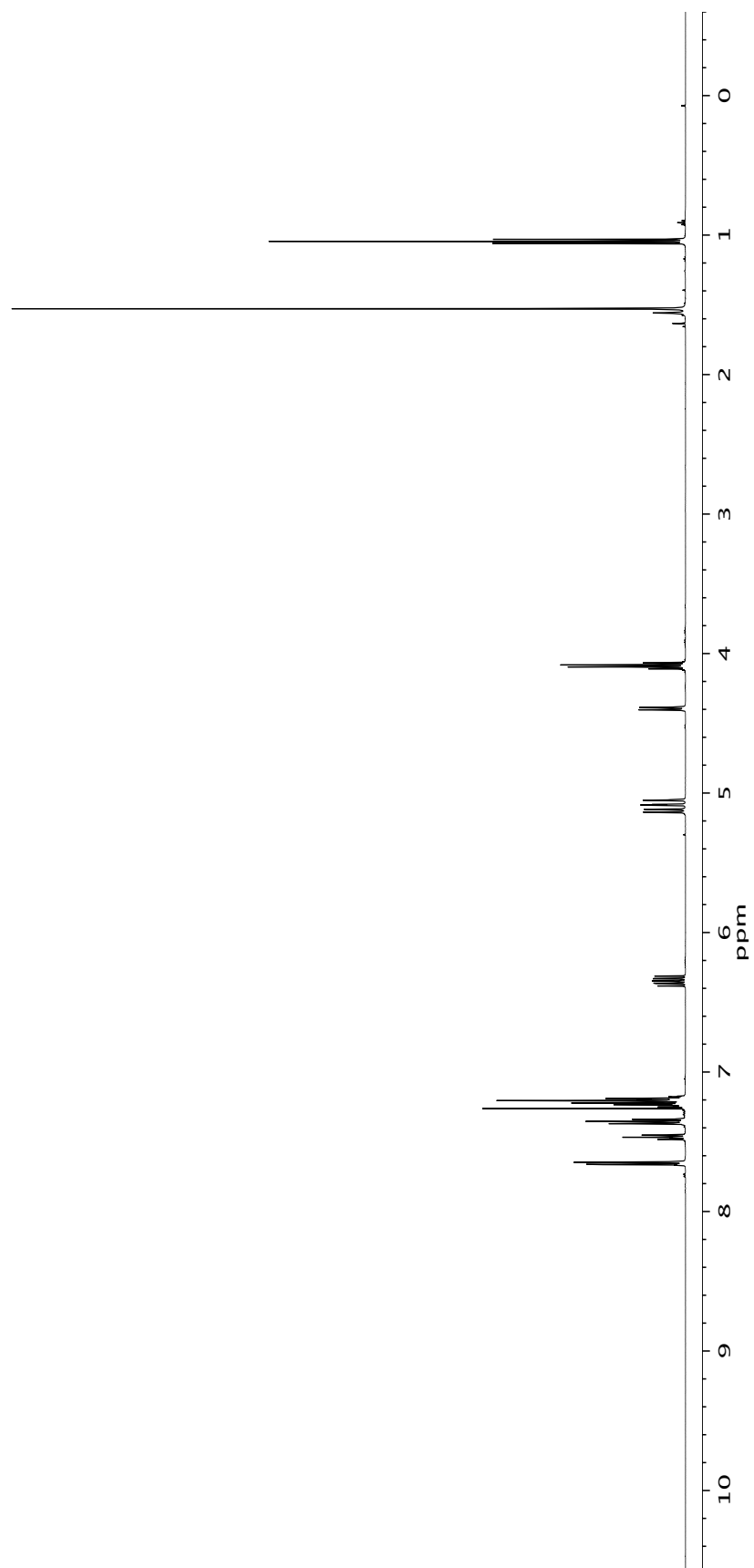
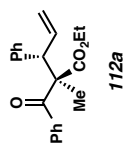


Figure A6.1 ¹H NMR (500 MHz, CDCl₃) of compound 112a.

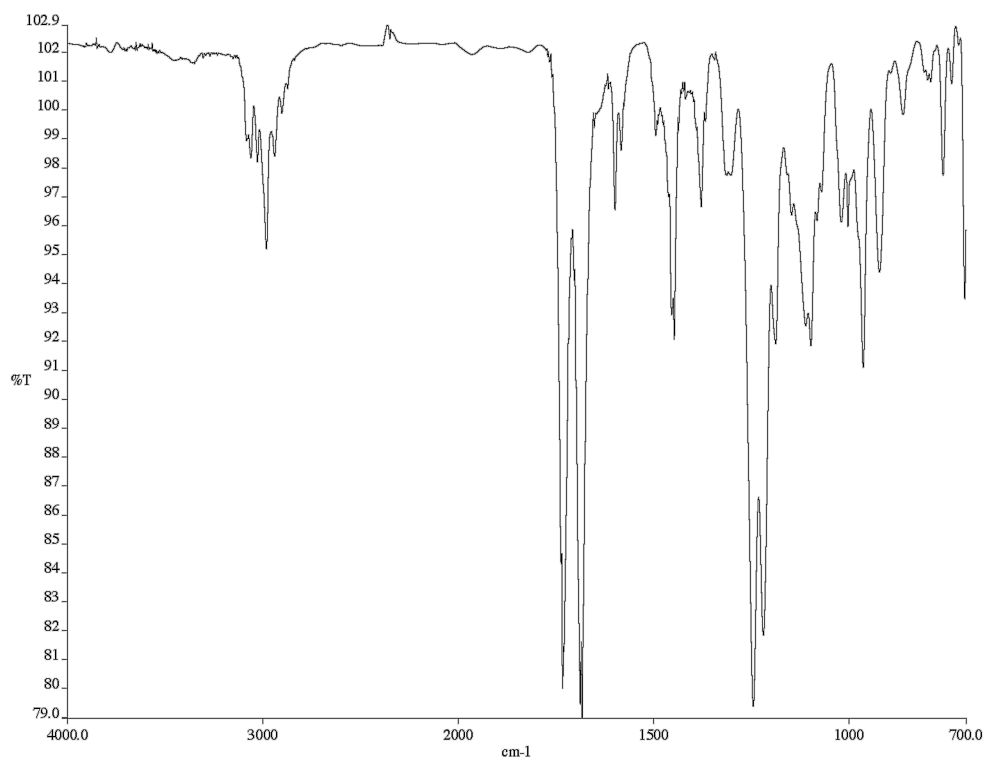


Figure A6.2 Infrared spectrum (thin film/NaCl) of compound **112a**.

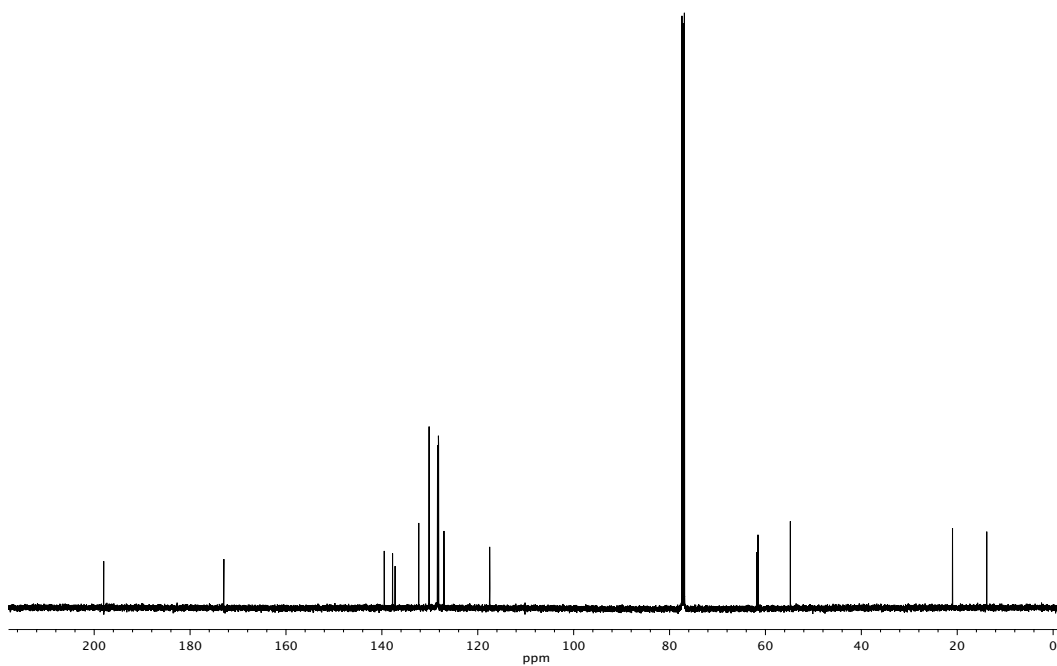


Figure A6.3 ¹³C NMR (125 MHz, CDCl₃) of compound **112a**.

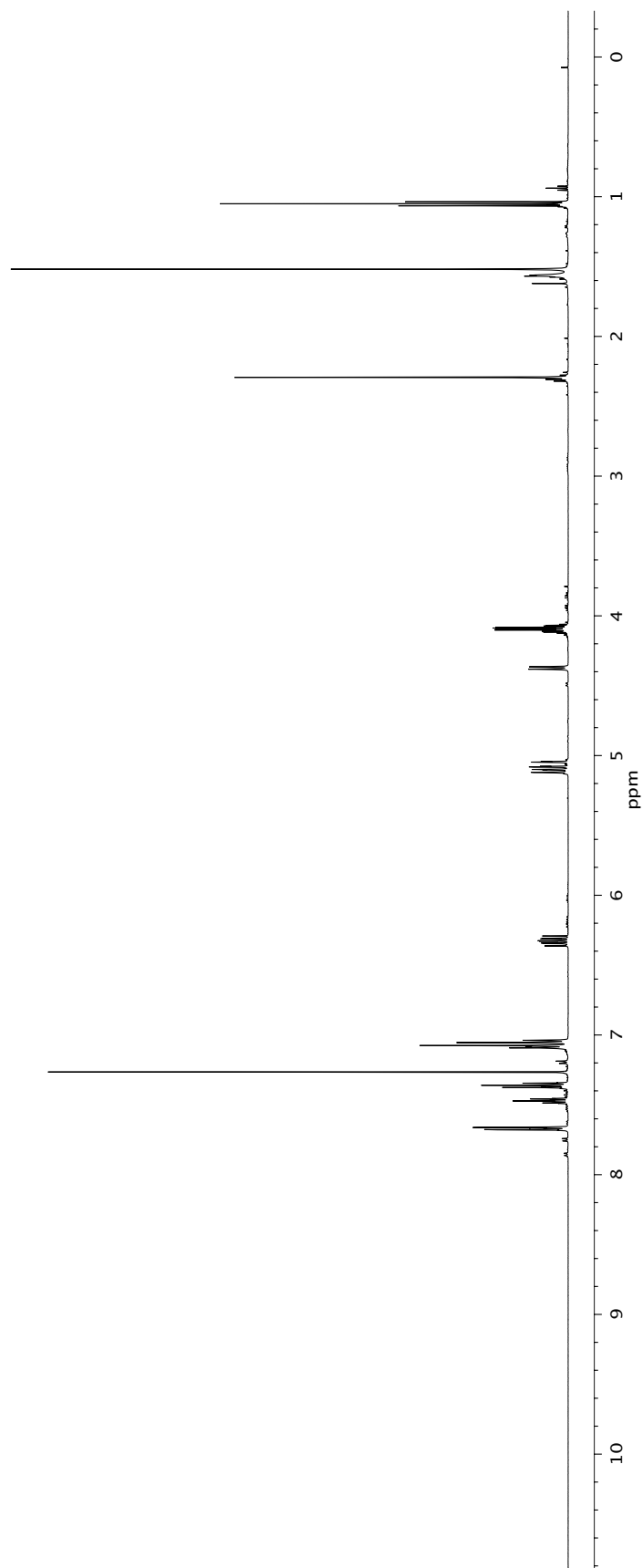
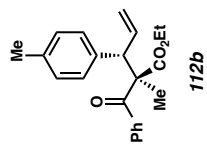


Figure A6.4 ¹H NMR (500 MHz, CDCl₃) of compound **112b**.

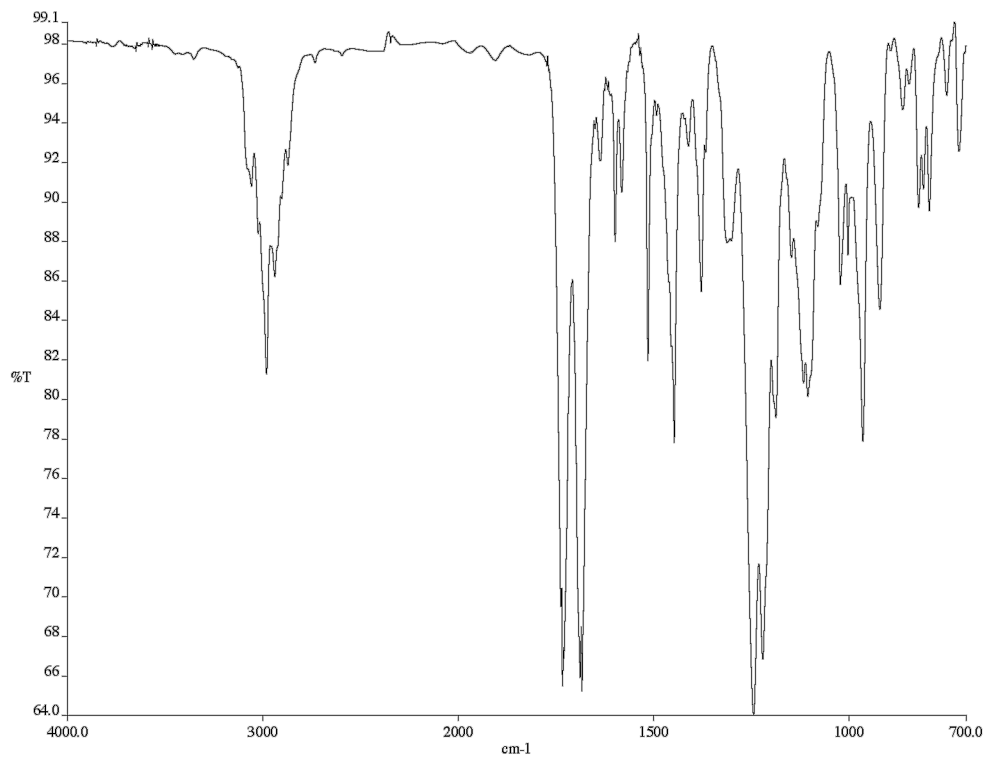


Figure A6.5 Infrared spectrum (thin film/NaCl) of compound **112b**.

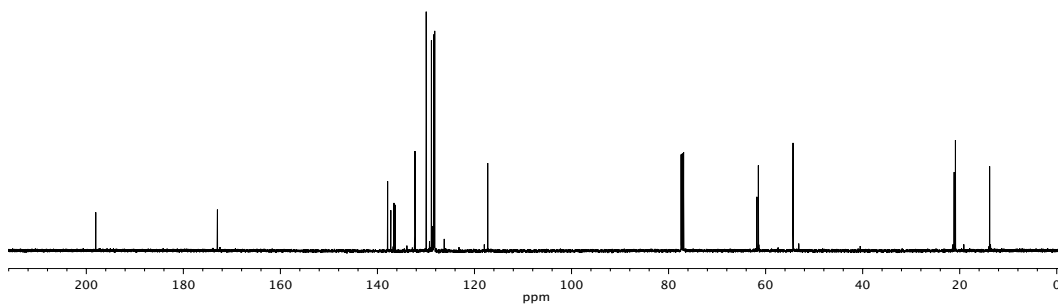


Figure A6.6 ¹³C NMR (125 MHz, CDCl₃) of compound **112b**.

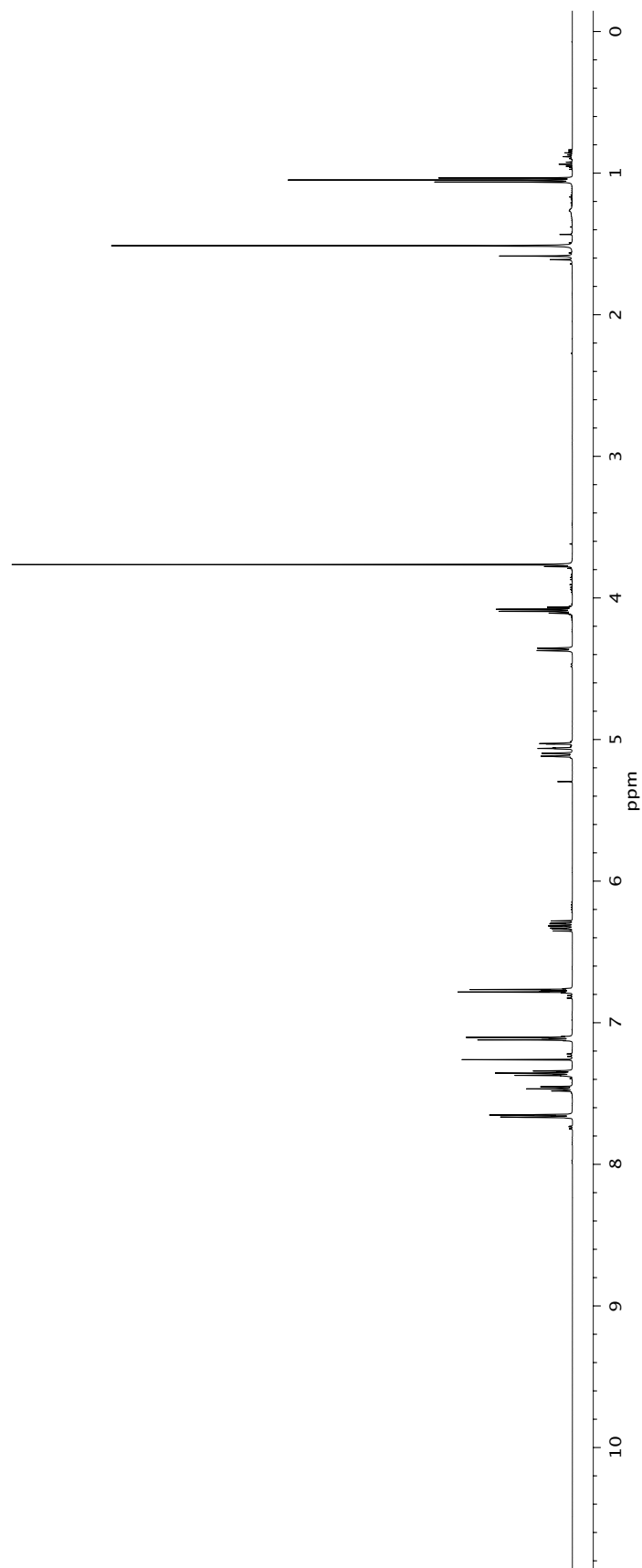
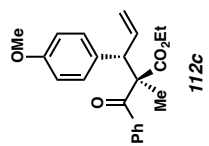


Figure A6.7 ¹H NMR (500 MHz, CDCl₃) of compound **112c**.

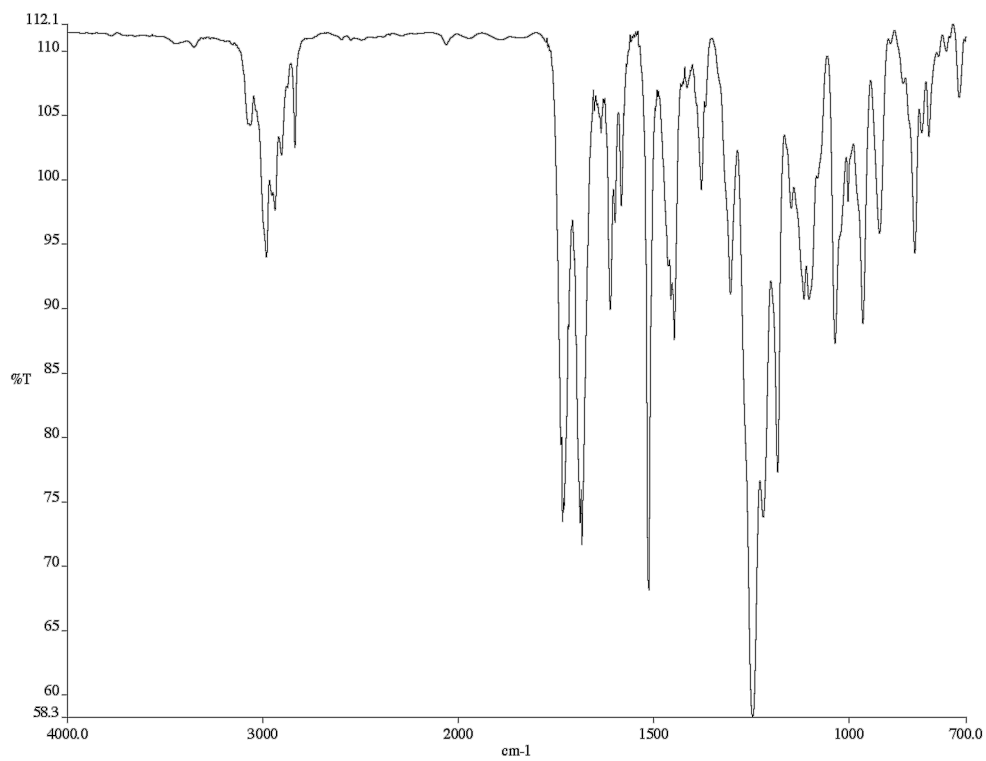


Figure A6.8 Infrared spectrum (thin film/NaCl) of compound **112c**.

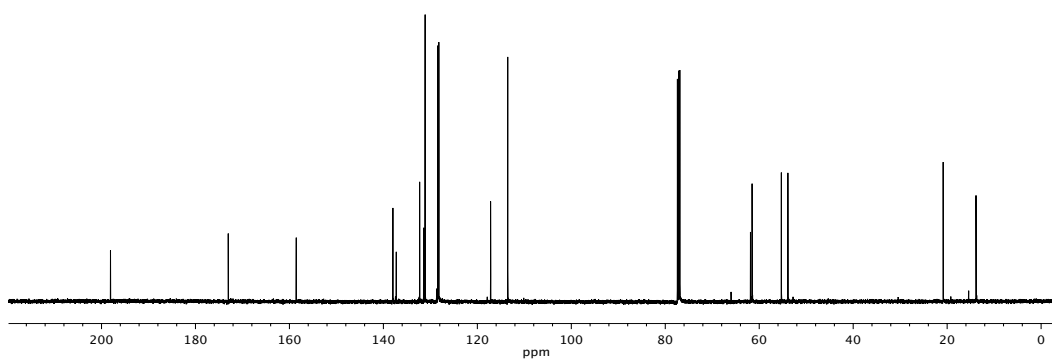


Figure A6.9 ¹³C NMR (125 MHz, CDCl₃) of compound **112c**.

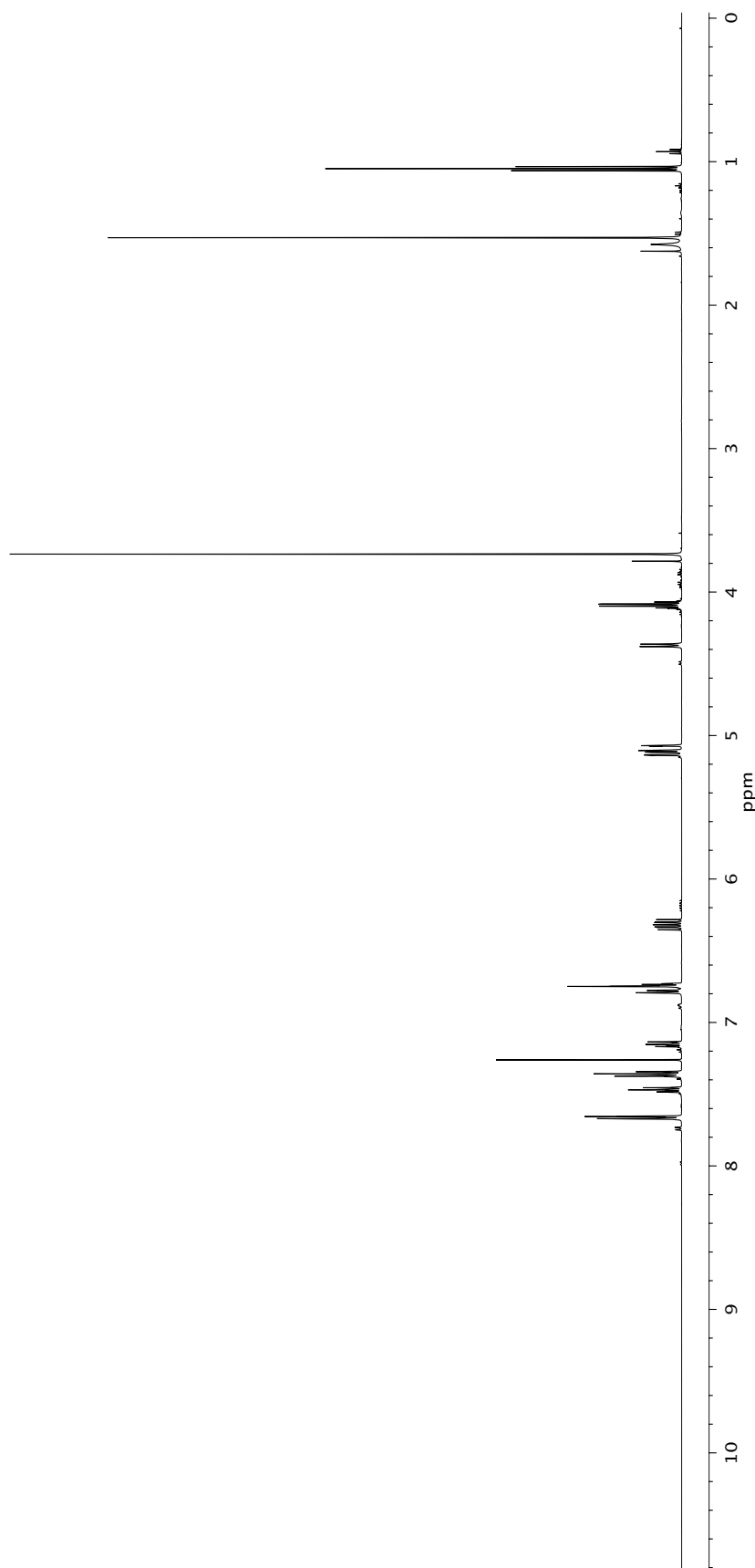
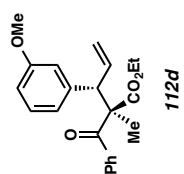


Figure A6.10 ¹H NMR (500 MHz, CDCl₃) of compound **112d**.

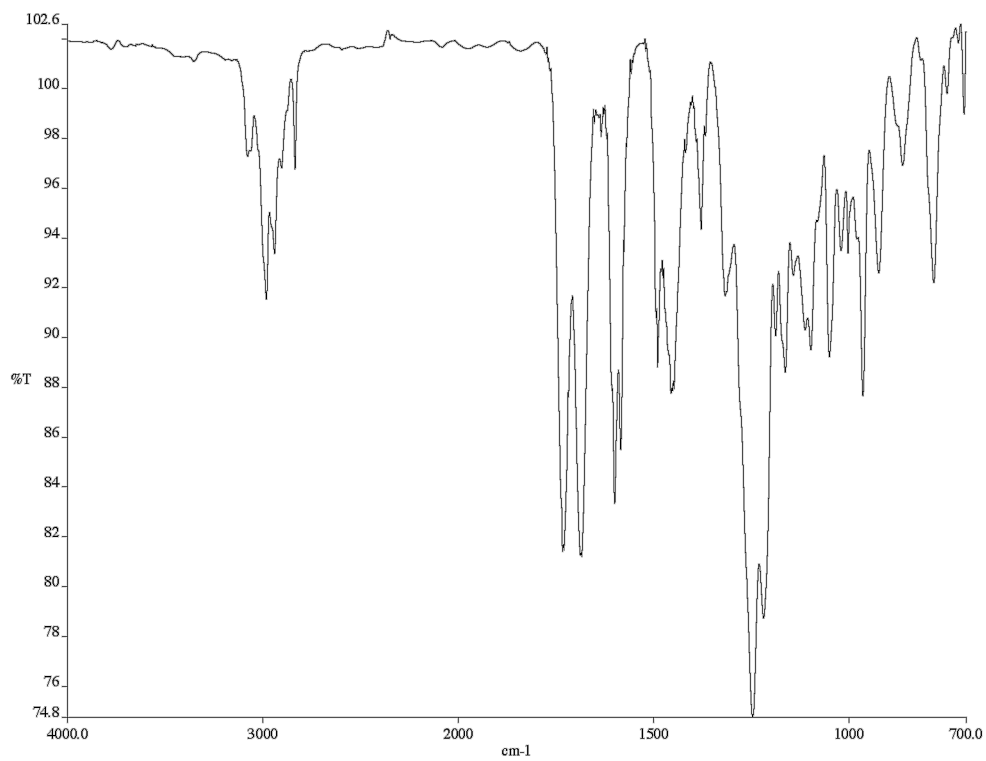


Figure A6.11 Infrared spectrum (thin film/NaCl) of compound **112d**.

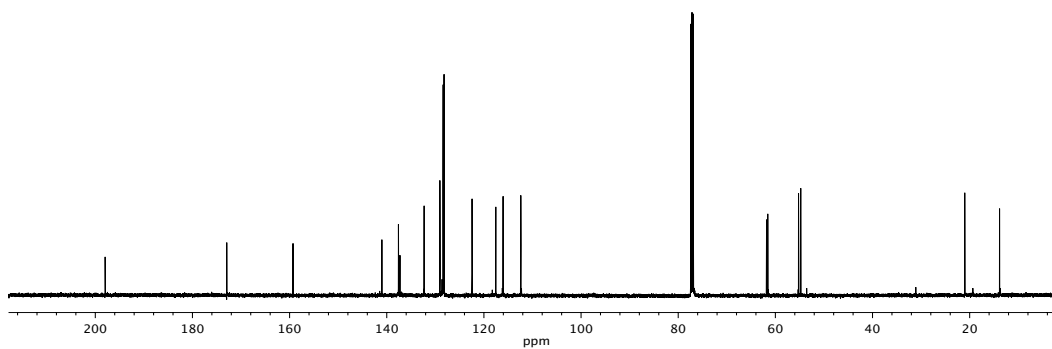


Figure A6.12 ¹³C NMR (125 MHz, CDCl₃) of compound **112d**.

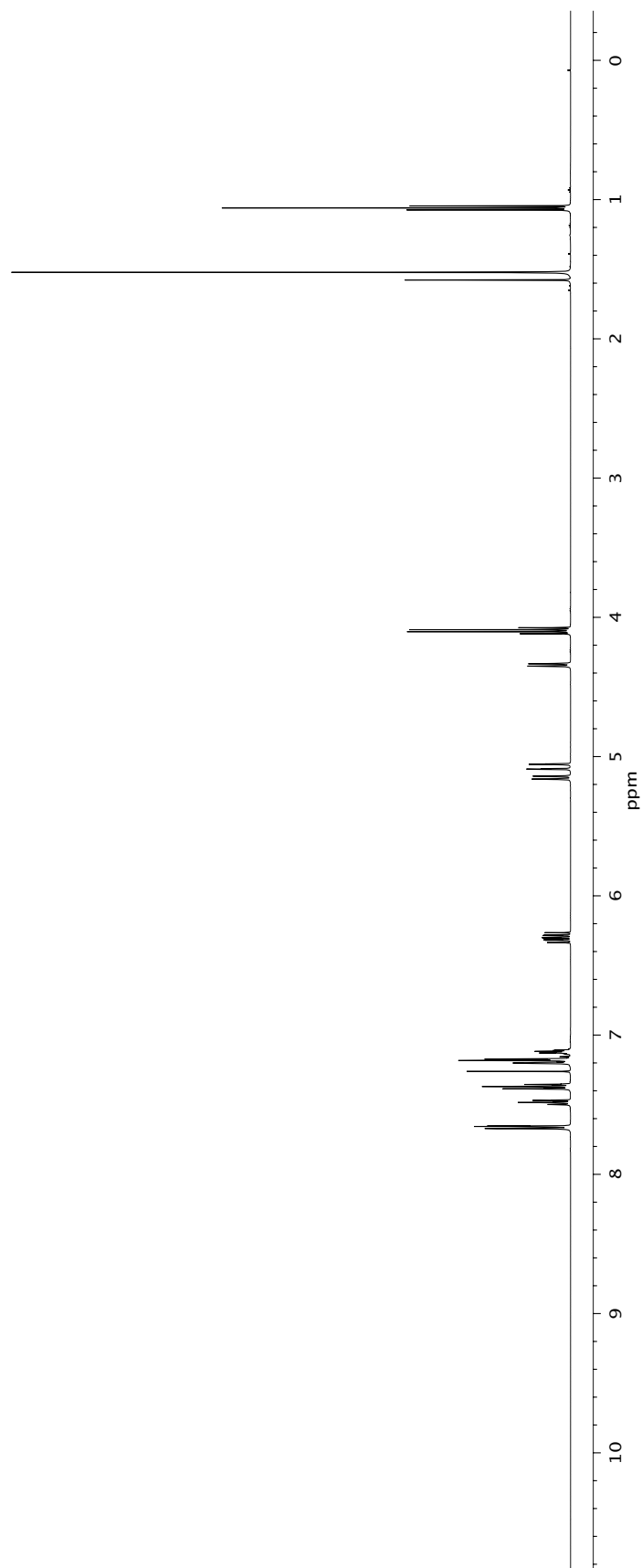
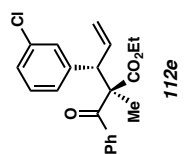


Figure A6.13 ¹H NMR (500 MHz, CDCl₃) of compound **112e**.

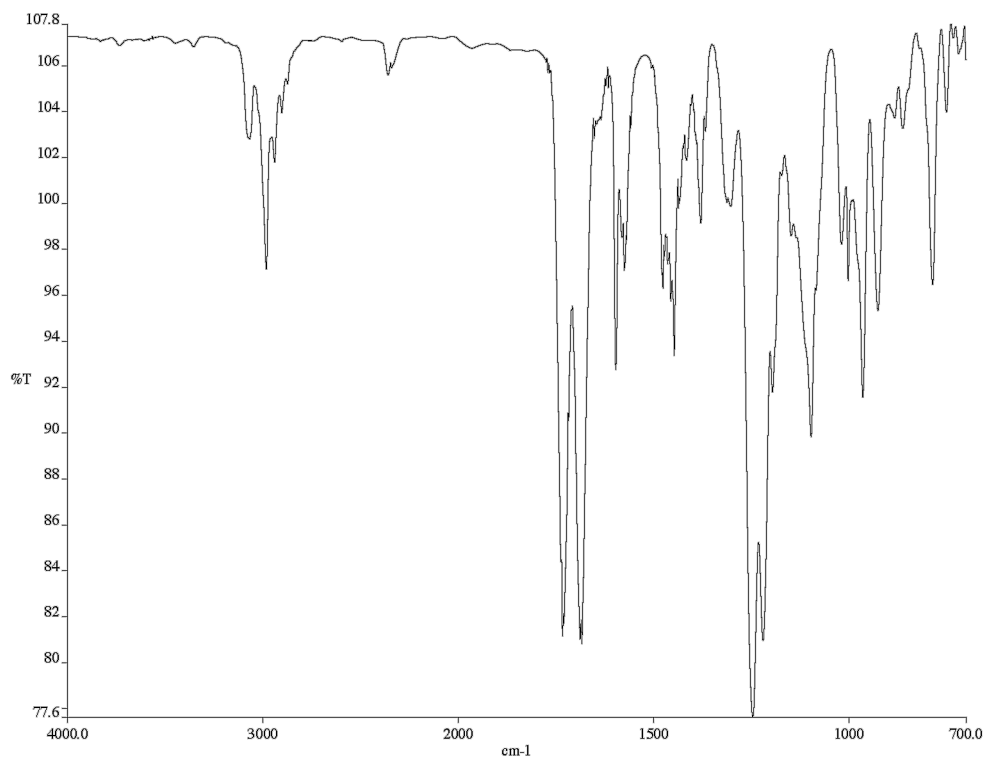


Figure A6.14 Infrared spectrum (thin film/NaCl) of compound **112e**.

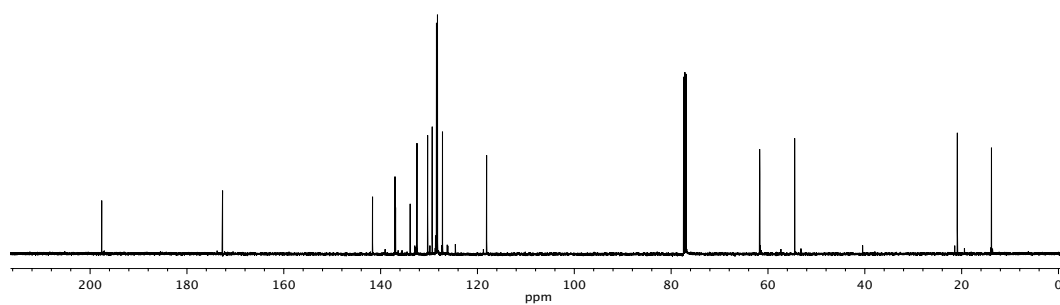


Figure A6.15 ¹³C NMR (125 MHz, CDCl₃) of compound **112e**.

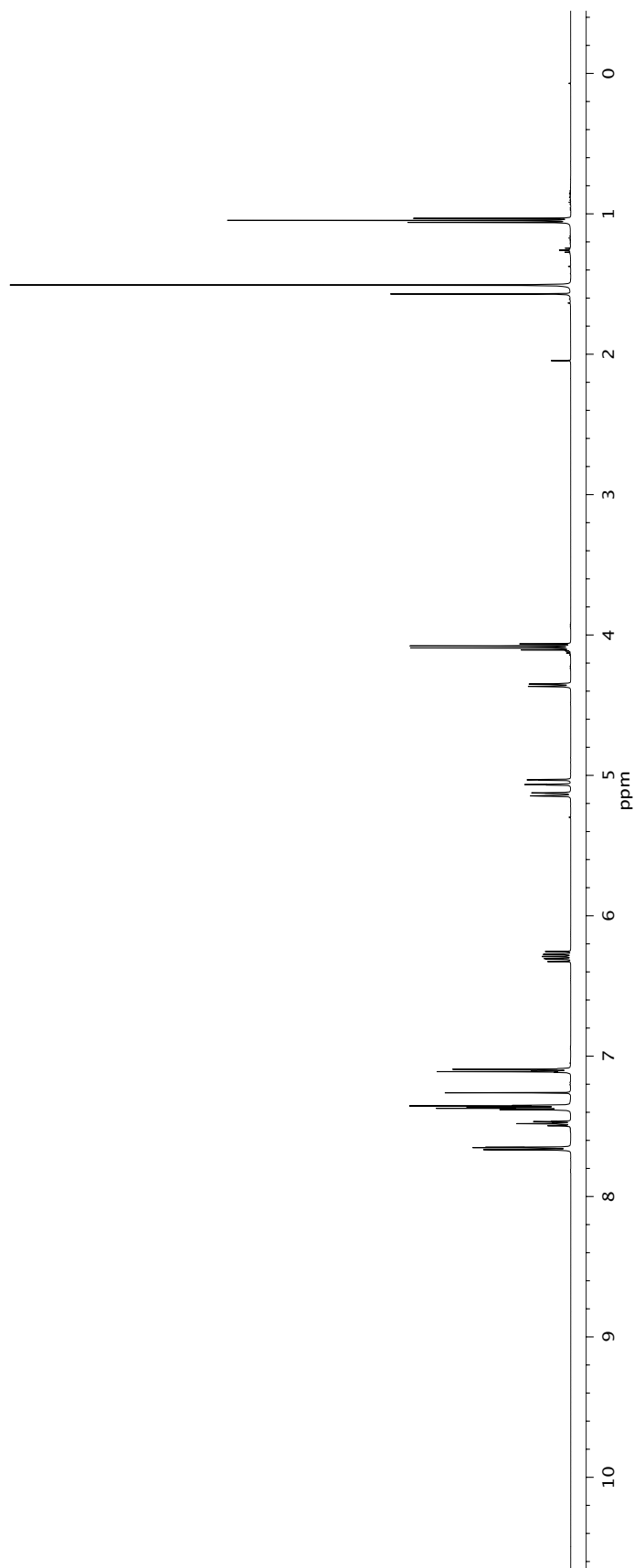
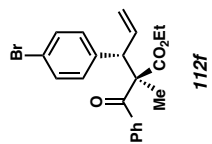


Figure A6.16 ¹H NMR (500 MHz, CDCl₃) of compound **112f**.

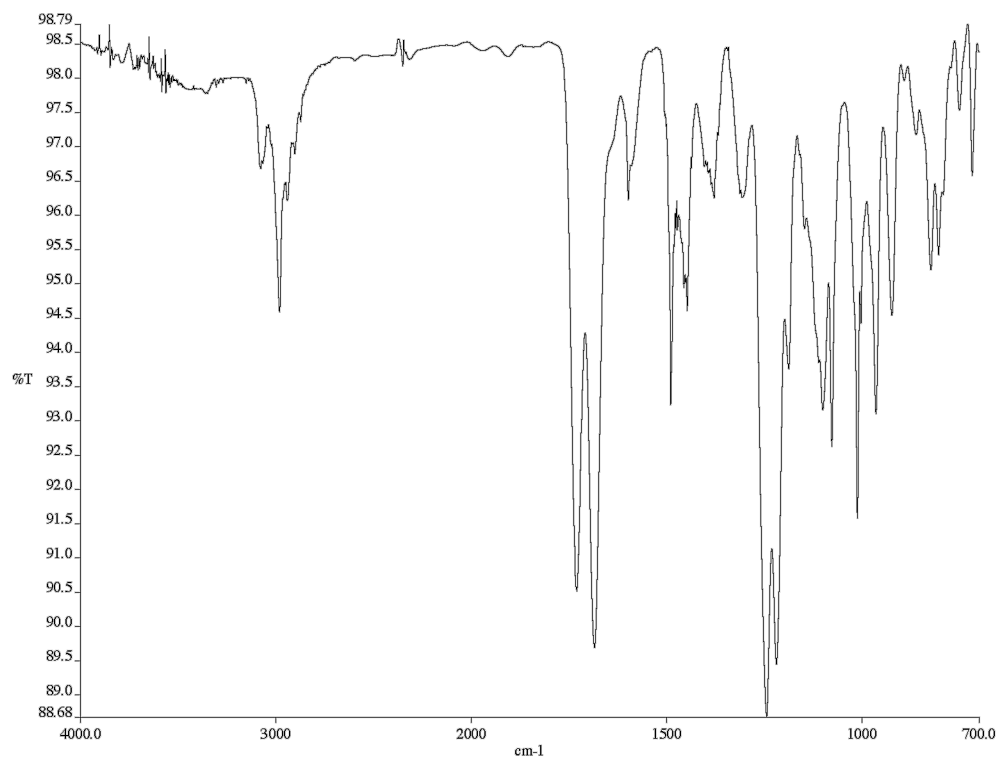


Figure A6.17 Infrared spectrum (thin film/NaCl) of compound **112f**.

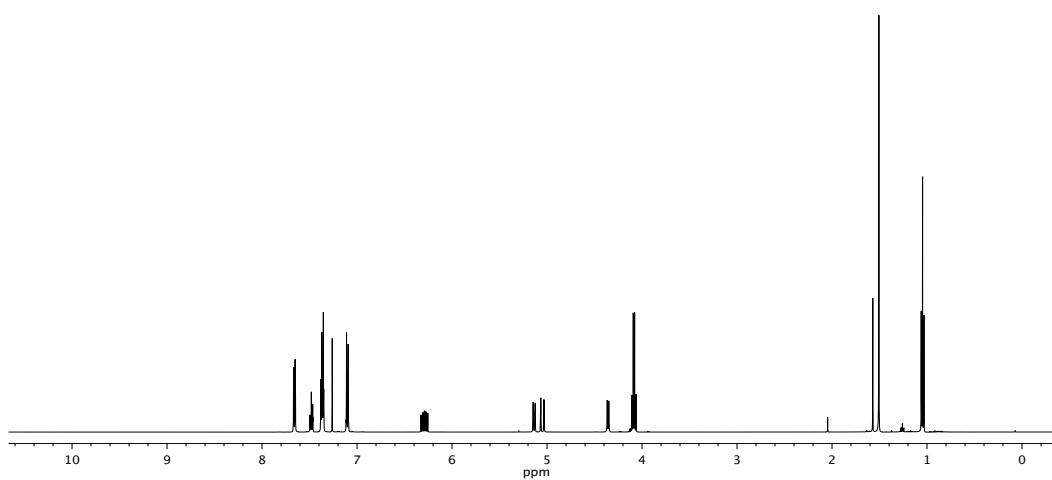


Figure A6.18 ¹³C NMR (125 MHz, CDCl₃) of compound **112f**.

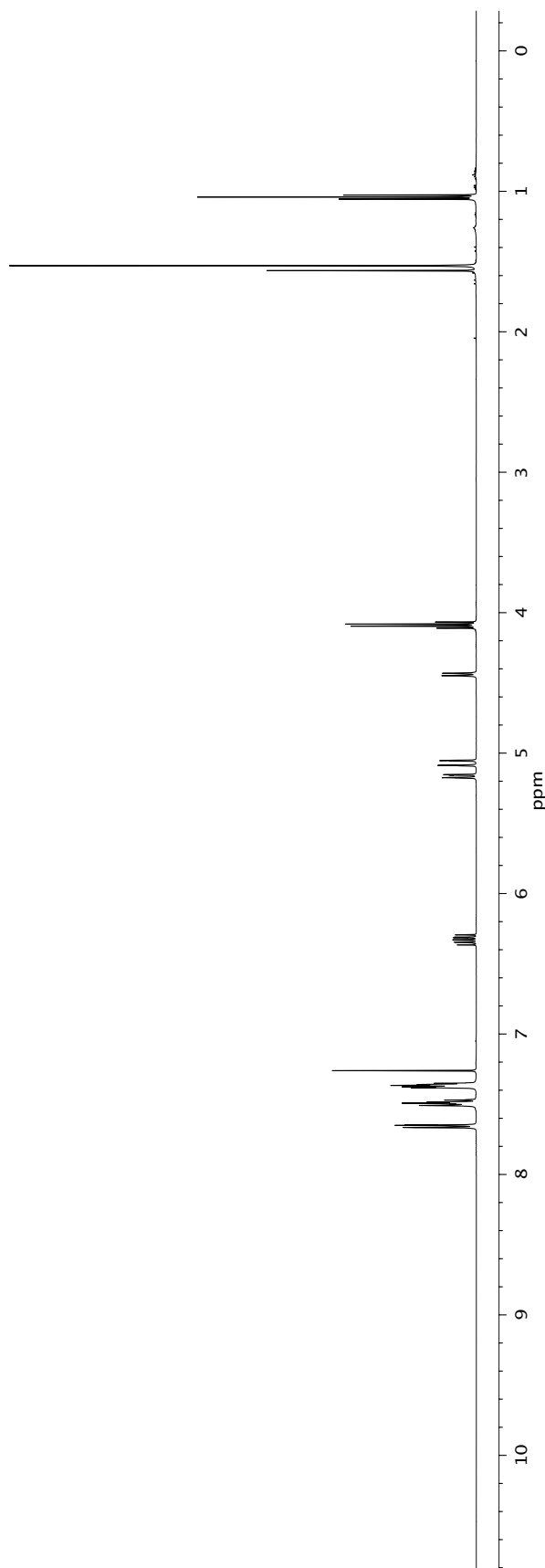
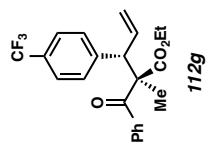


Figure A6.19 ¹H NMR (500 MHz, CDCl₃) of compound **112g**.

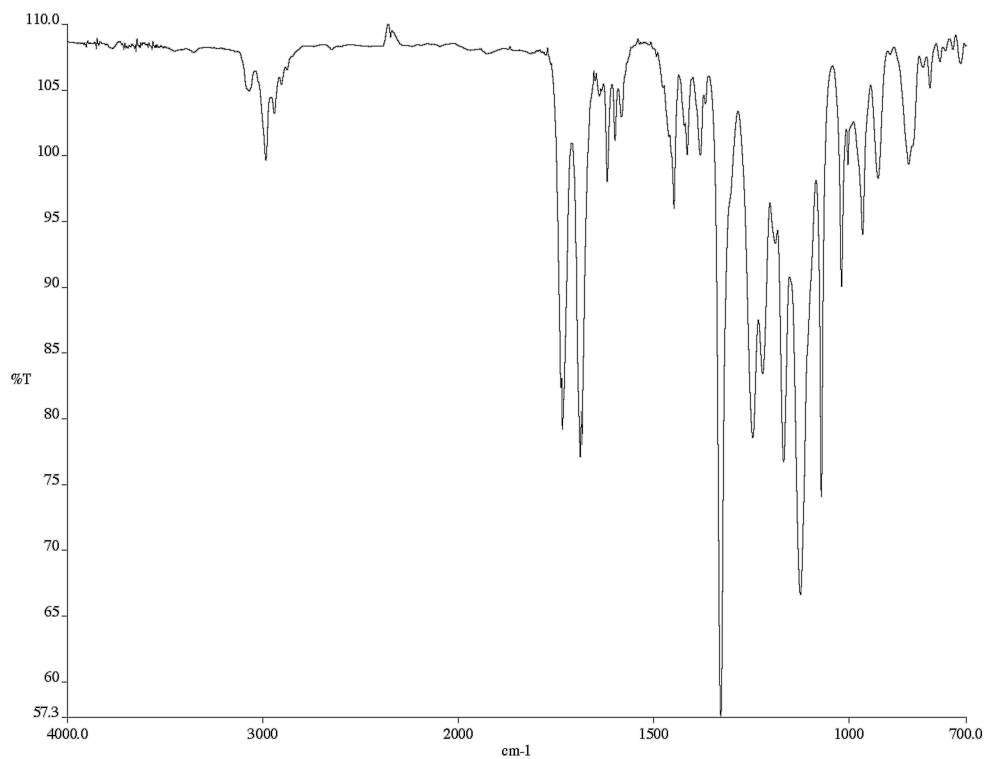


Figure A6.20 Infrared spectrum (thin film/NaCl) of compound **112g**.

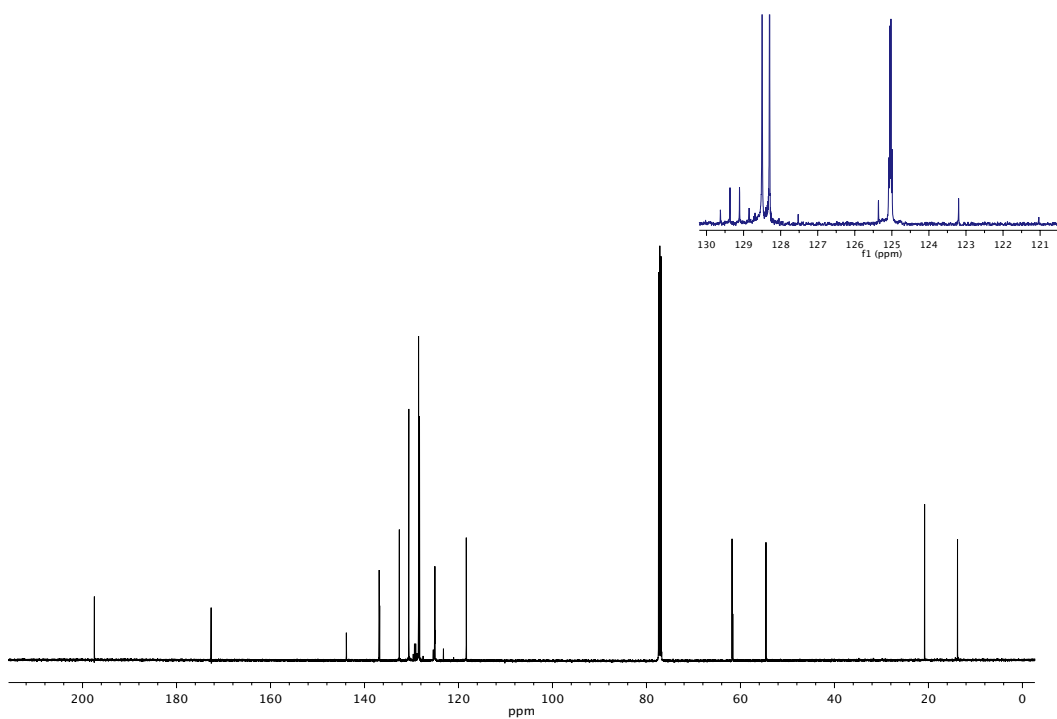


Figure A6.21 ^{13}C NMR (125 MHz, CDCl_3) of compound **112g**.

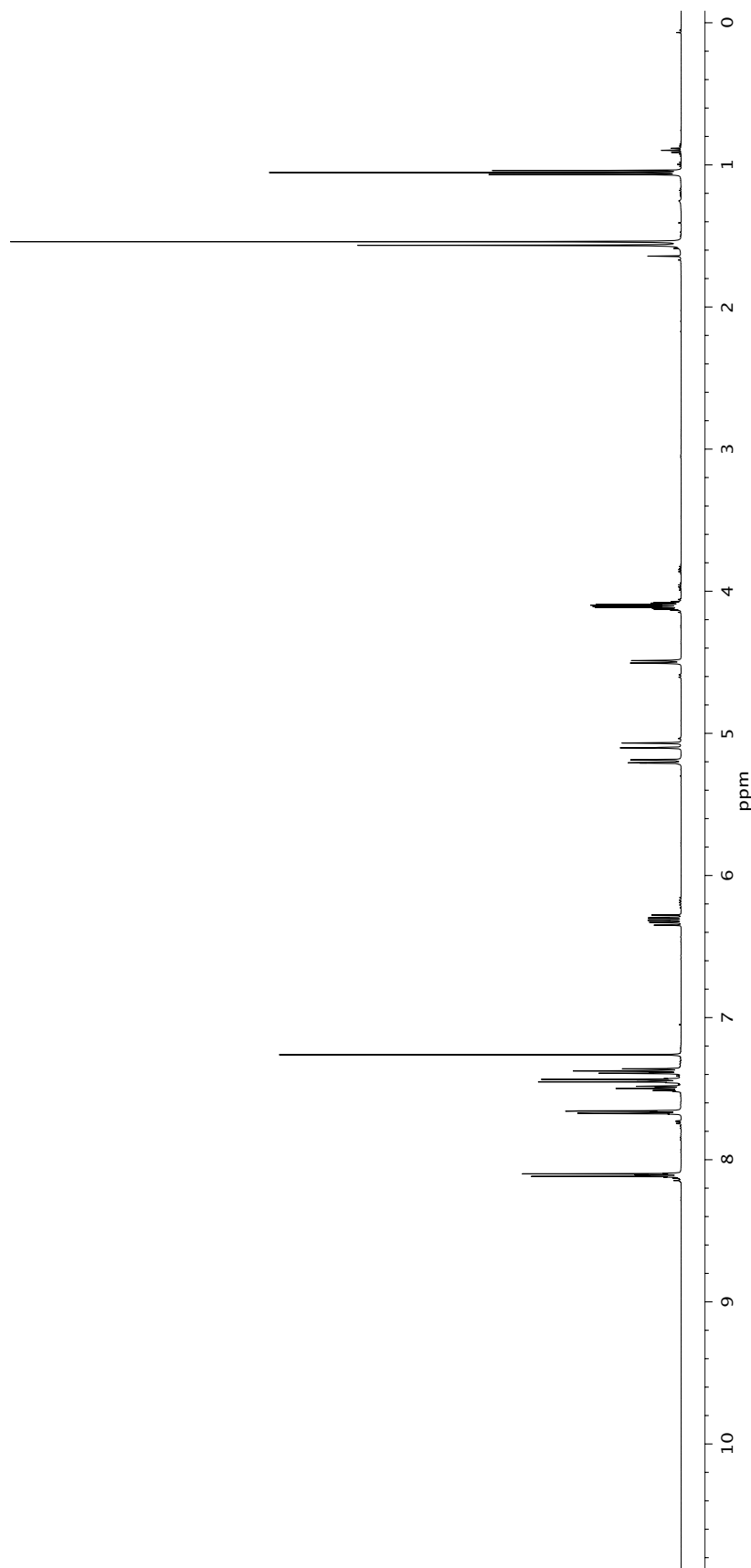
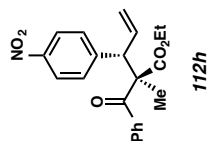


Figure A6.22 ¹H NMR (500 MHz, CDCl₃) of compound **112h**.

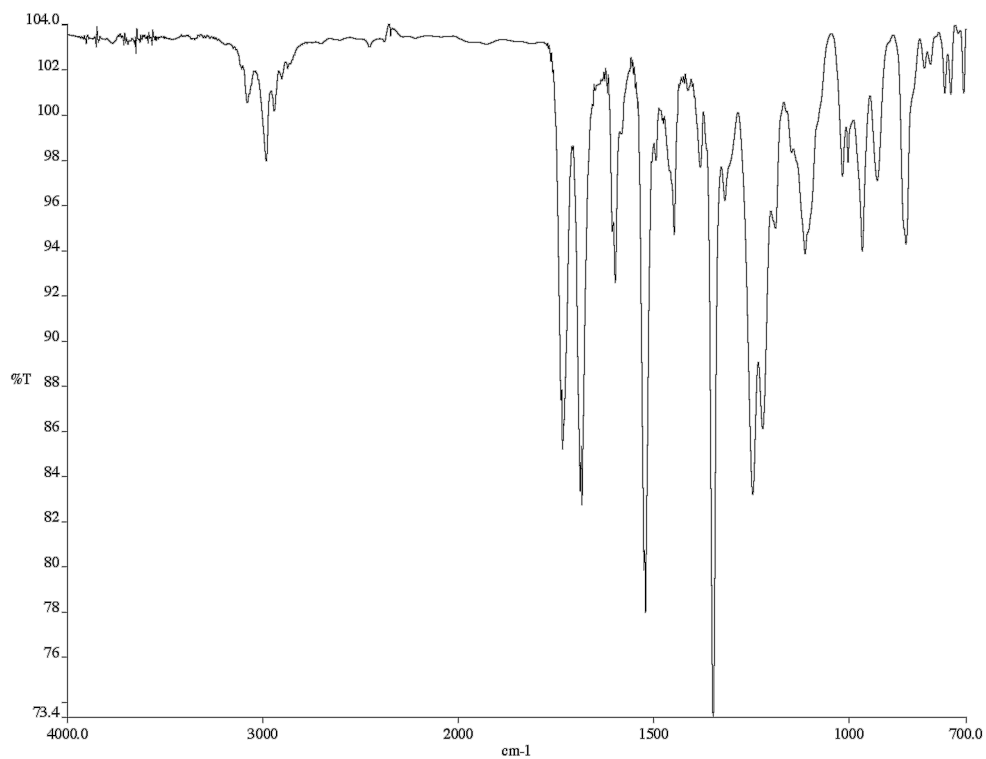


Figure A6.23 Infrared spectrum (thin film/NaCl) of compound **112h**.

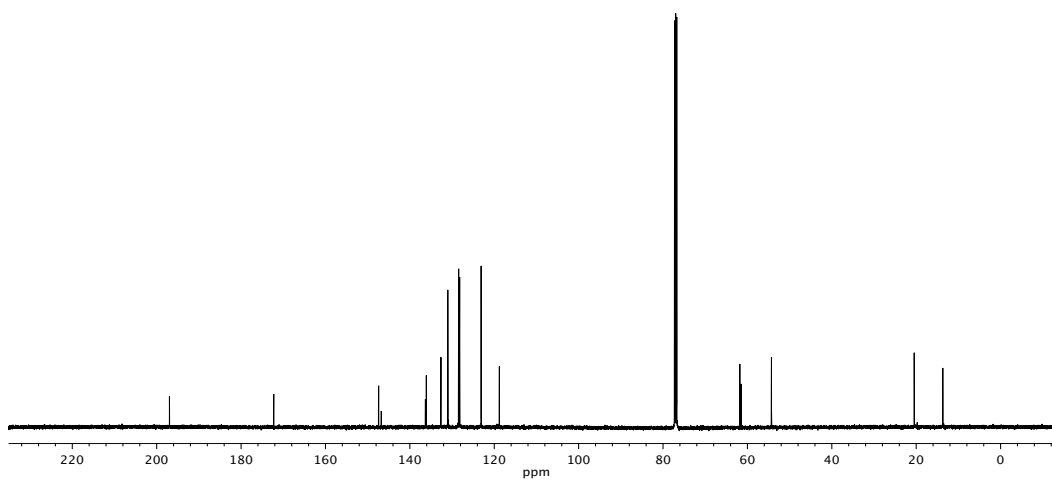


Figure A6.24 ¹³C NMR (125 MHz, CDCl₃) of compound **112h**.

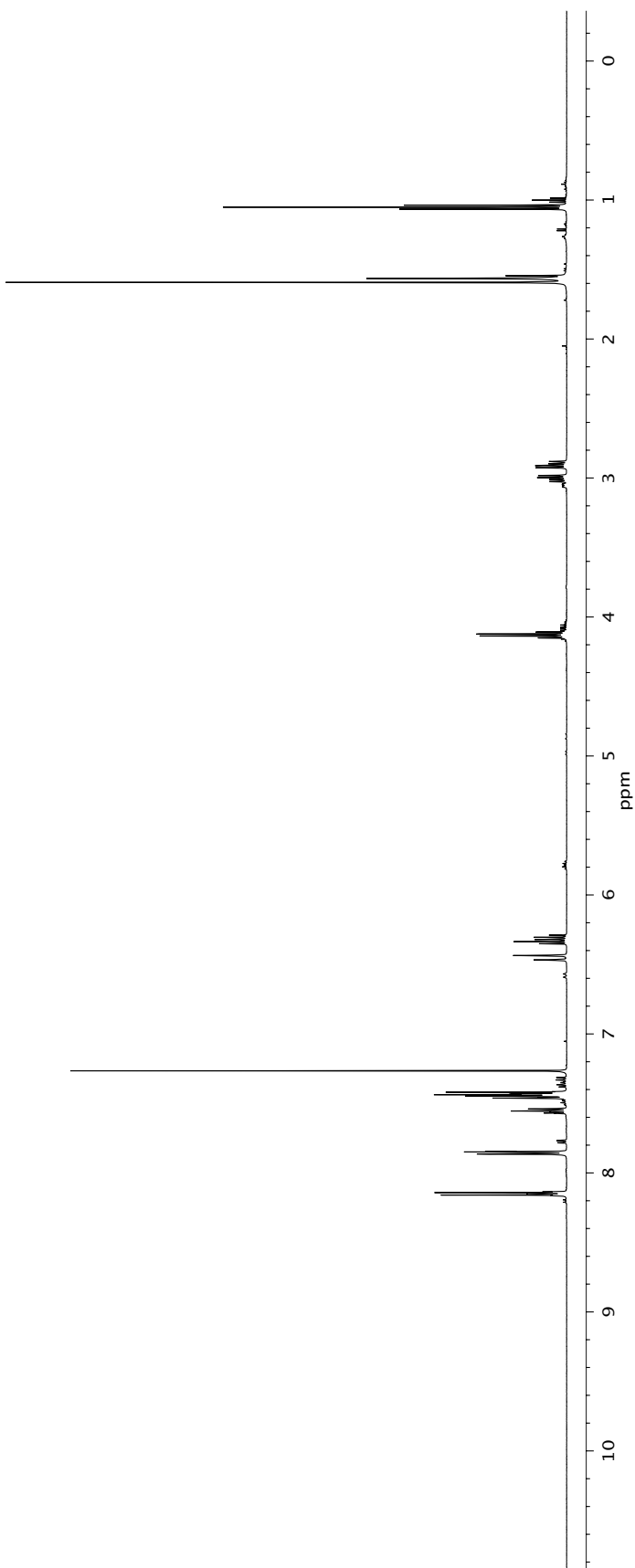
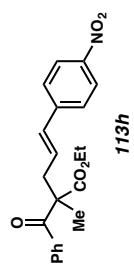


Figure A6.25 ¹H NMR (500 MHz, CDCl₃) of compound **113h**.

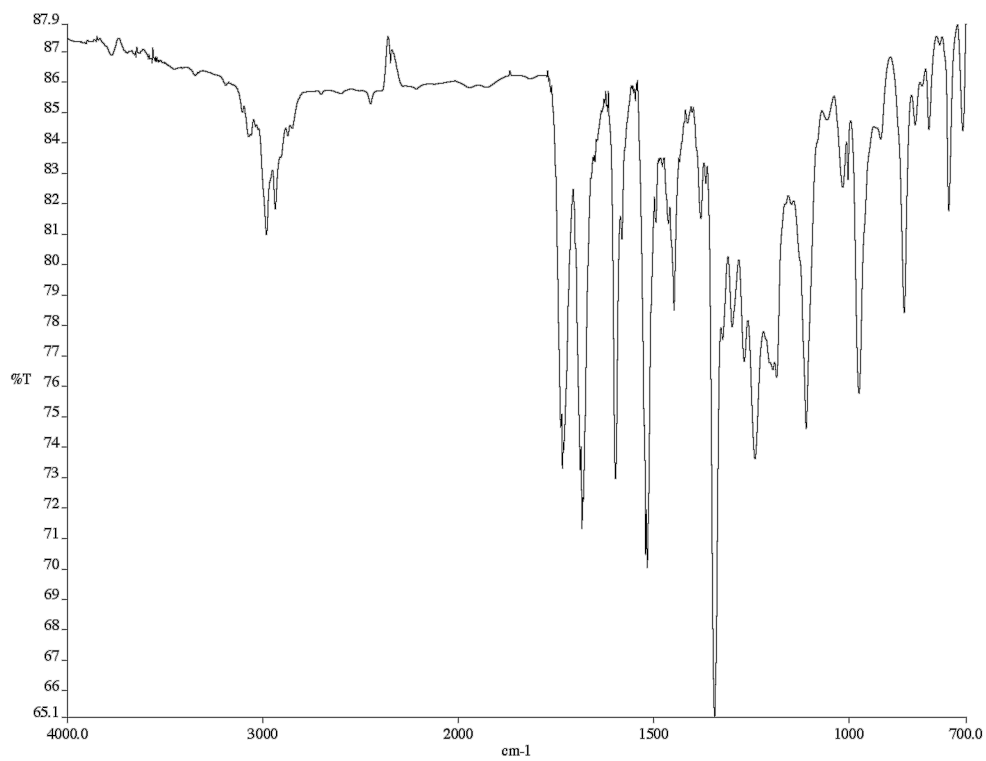


Figure A6.26 Infrared spectrum (thin film/NaCl) of compound **113h**.

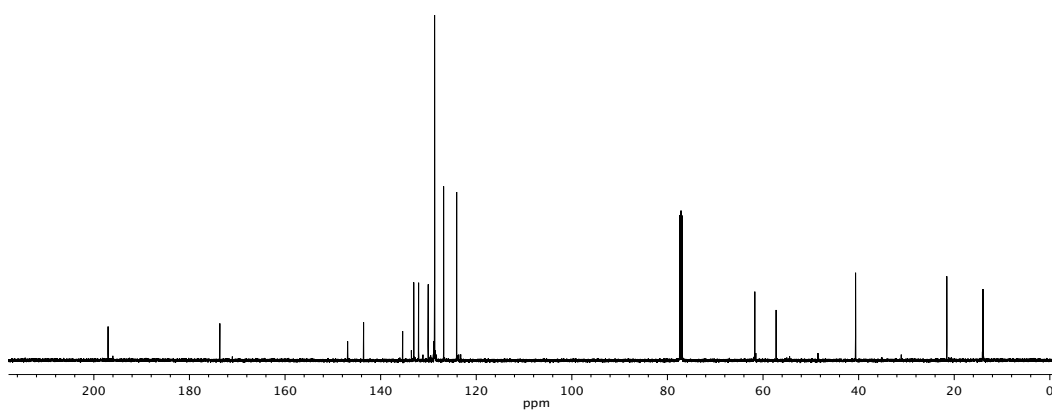


Figure A6.27 ¹³C NMR (125 MHz, CDCl₃) of compound **113h**.

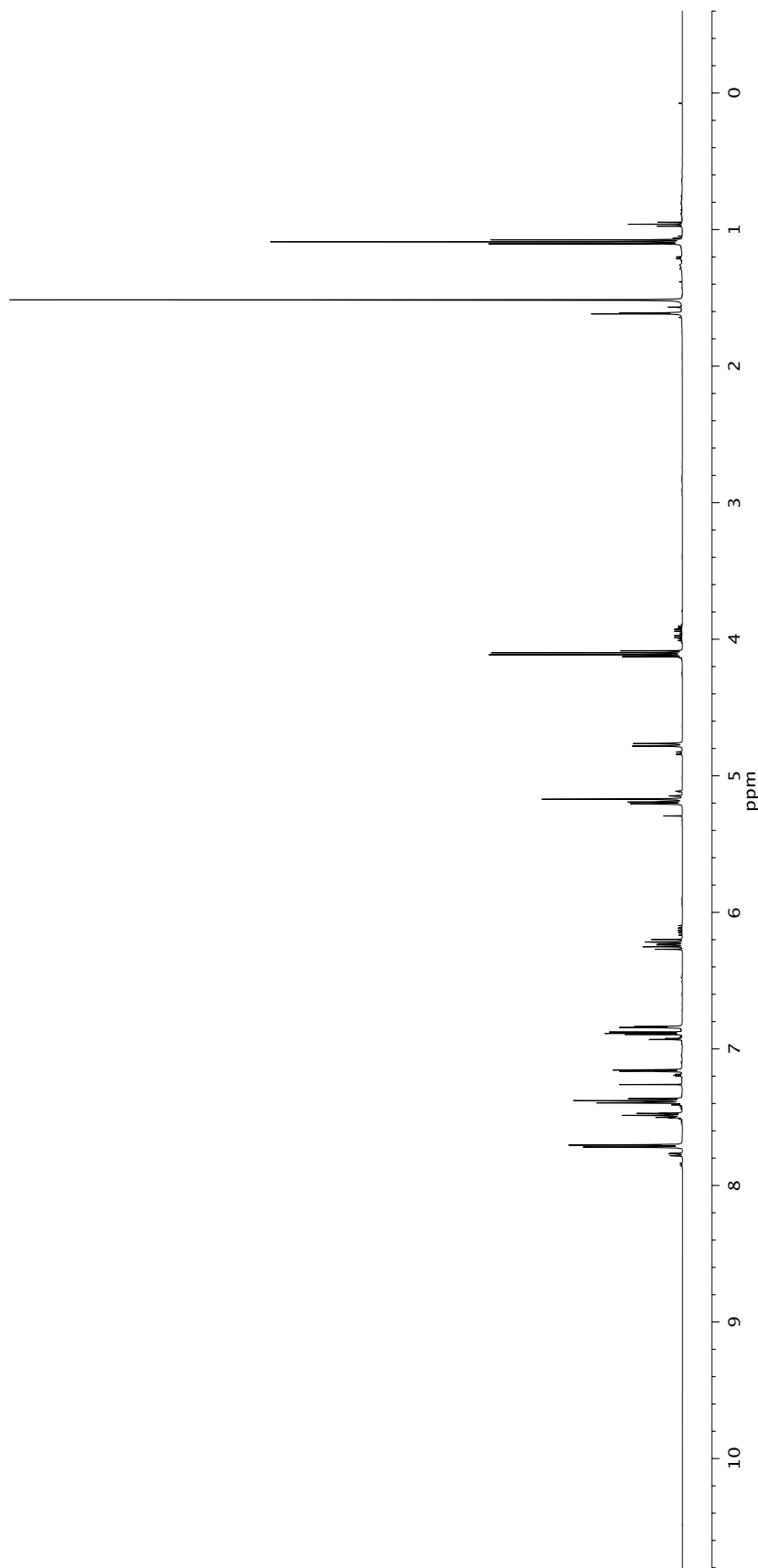
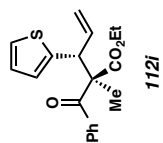


Figure A6.28 ¹H NMR (500 MHz, CDCl₃) of compound **112i**.

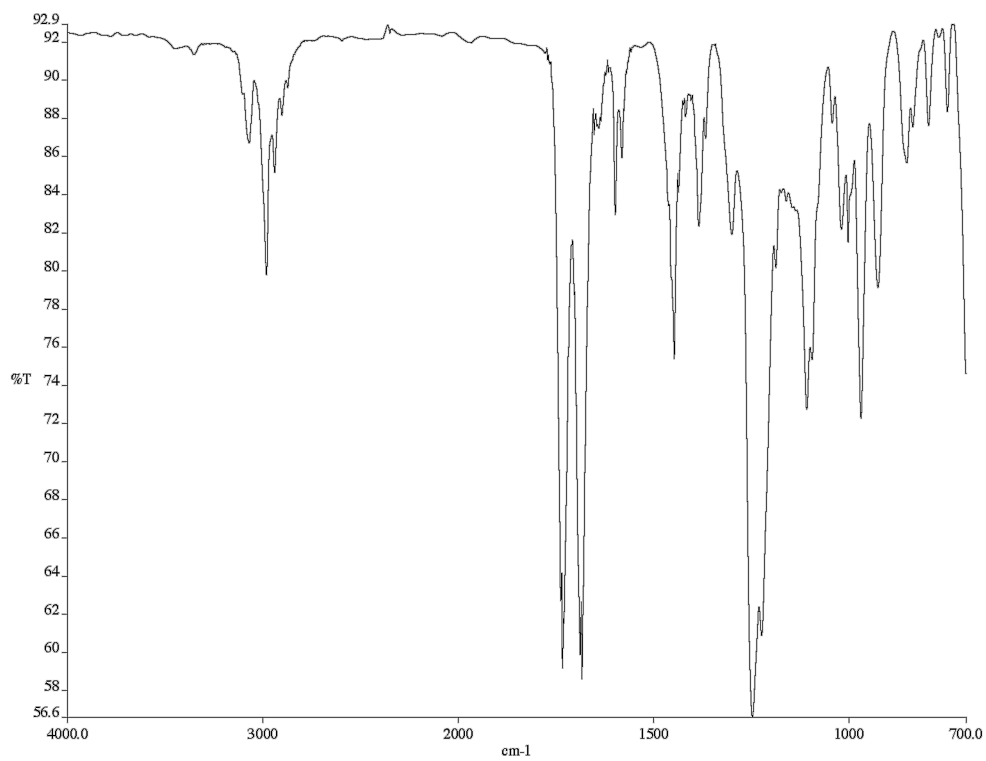


Figure A6.29 Infrared spectrum (thin film/NaCl) of compound **112i**.

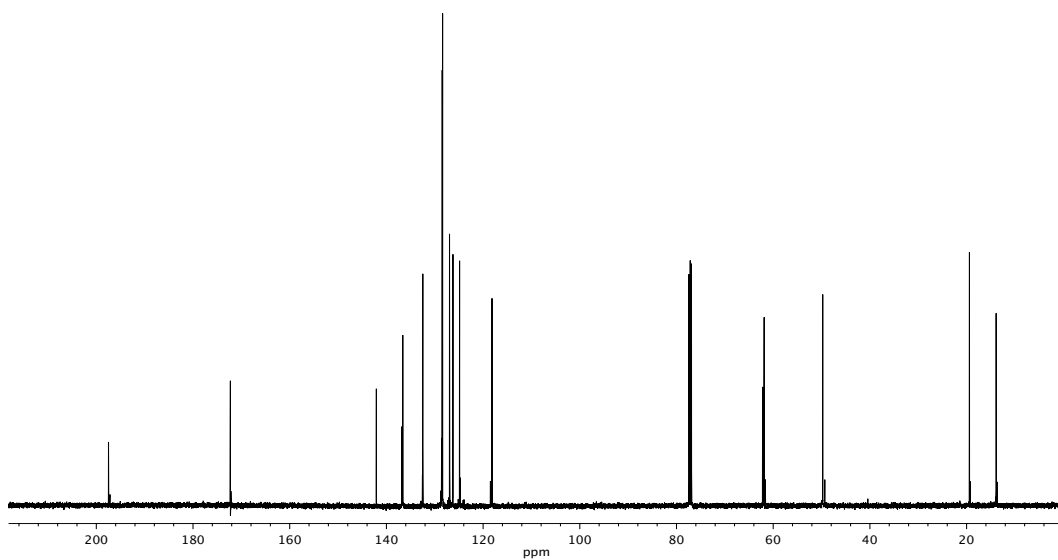


Figure A6.30 ¹³C NMR (125 MHz, CDCl₃) of compound **112i**.

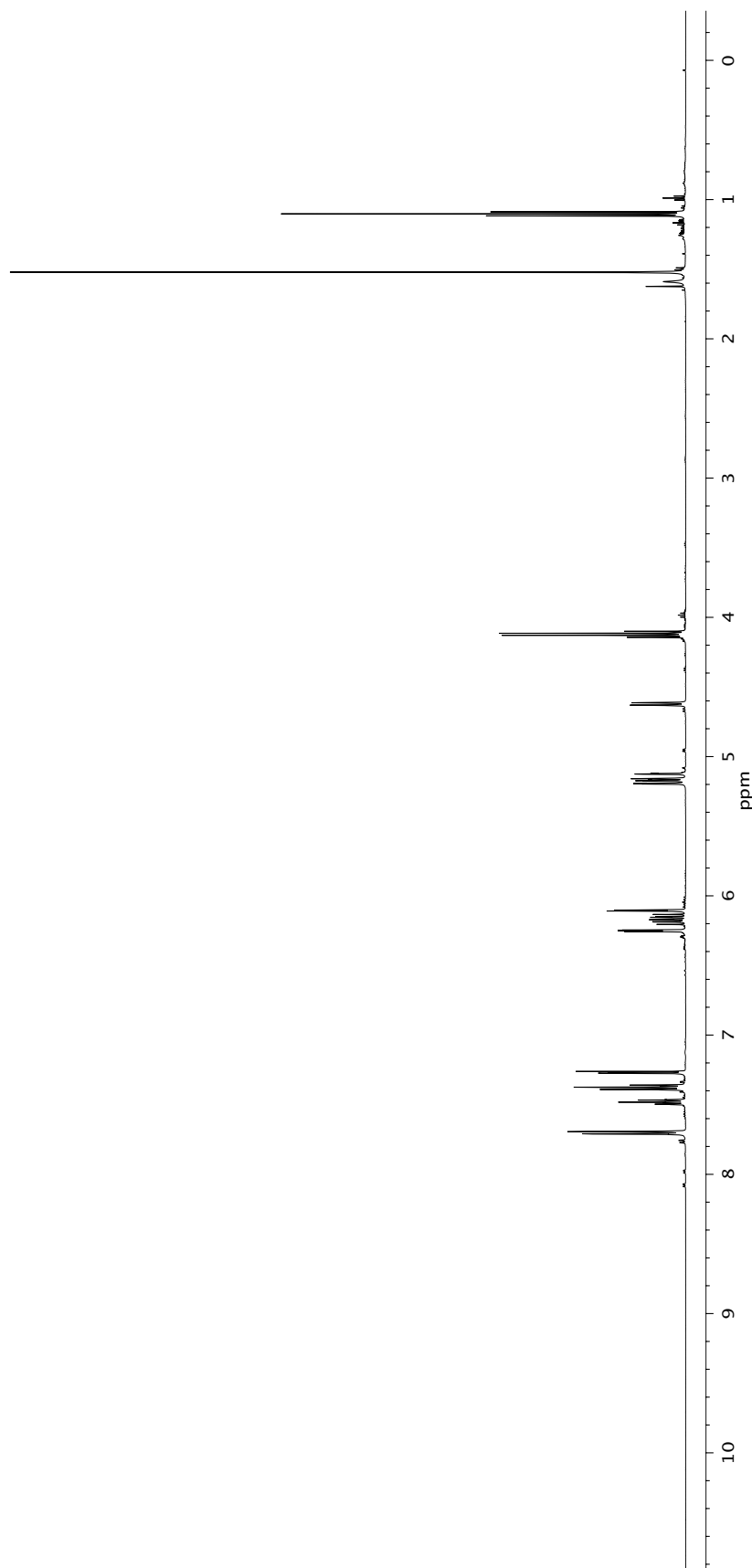
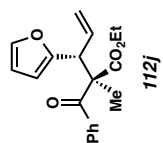


Figure A6.31 ¹H NMR (500 MHz, CDCl₃) of compound **112j**.

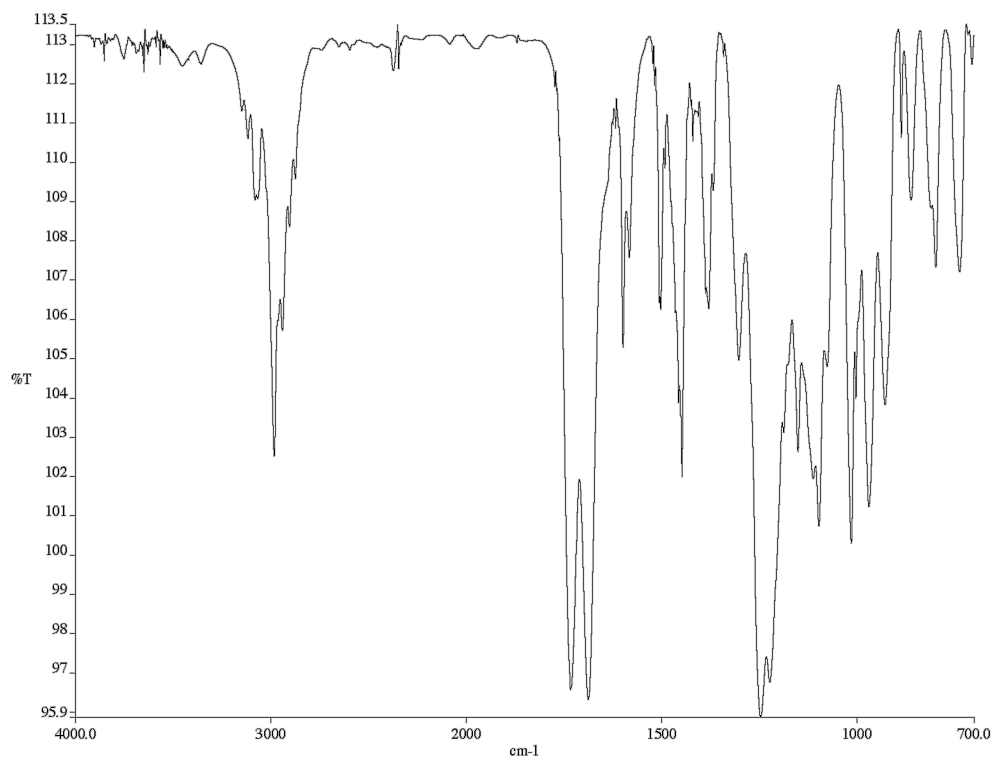


Figure A6.32 Infrared spectrum (thin film/NaCl) of compound **112j**.

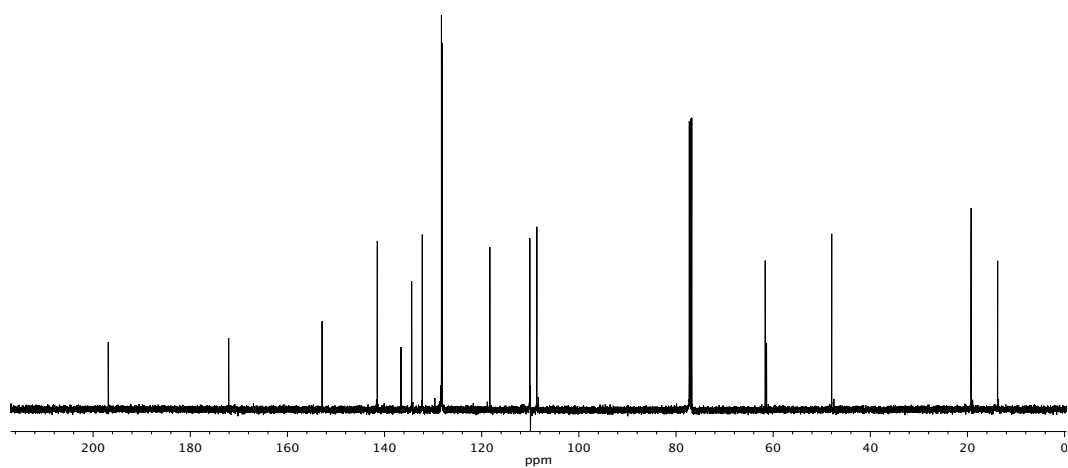


Figure A6.33 ¹³C NMR (125 MHz, CDCl₃) of compound **112j**.

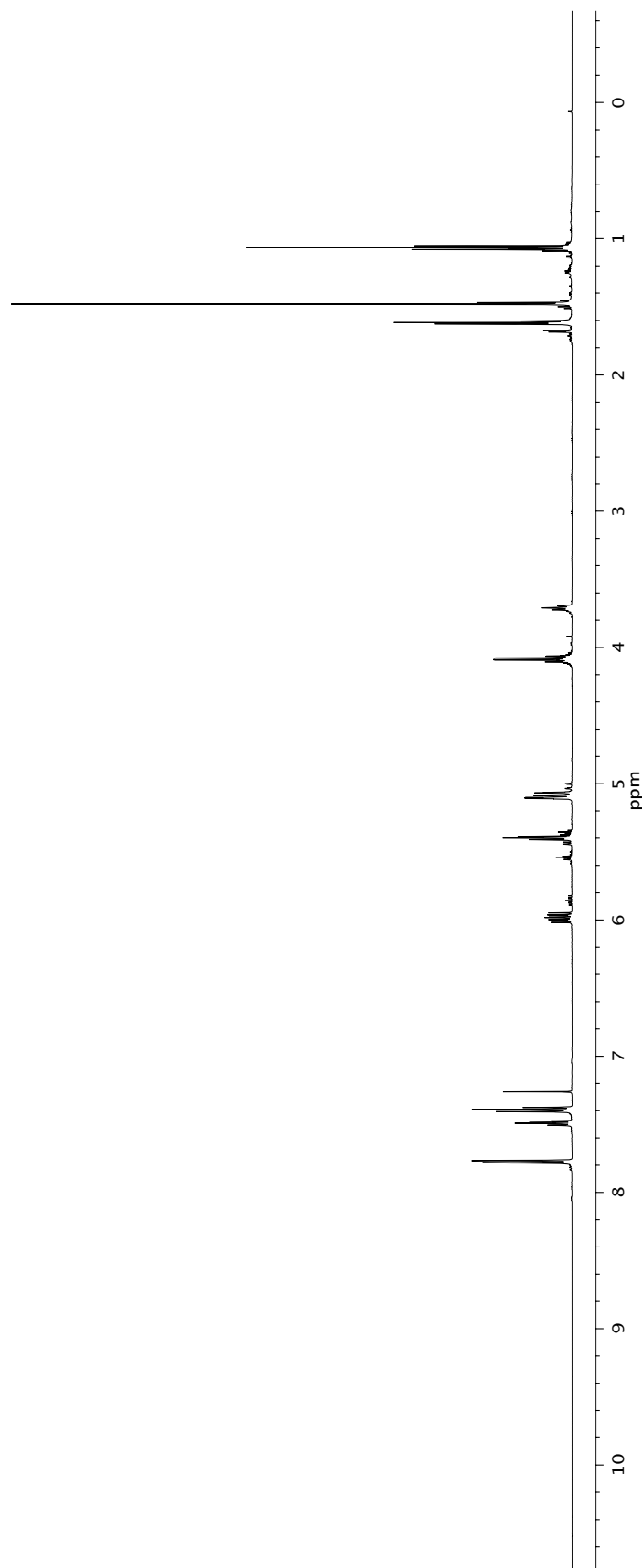
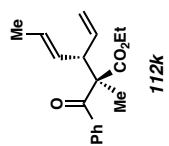


Figure A6.34 ¹H NMR (500 MHz, CDCl₃) of compound **112k**.

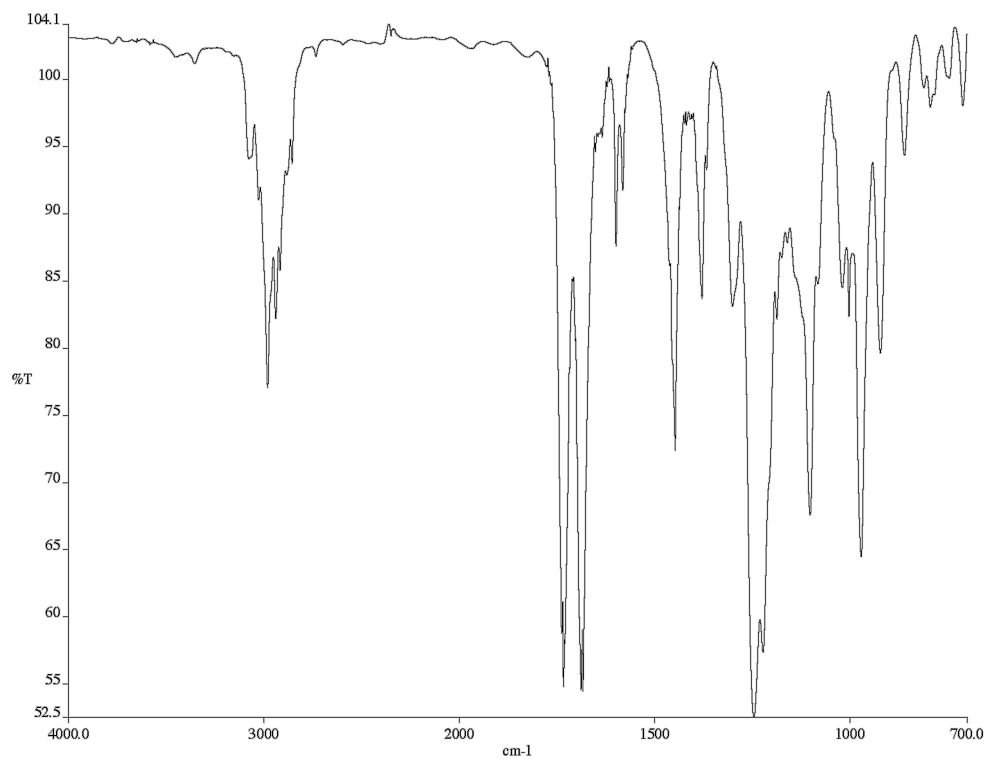


Figure A6.35 Infrared spectrum (thin film/NaCl) of compound **112k**.

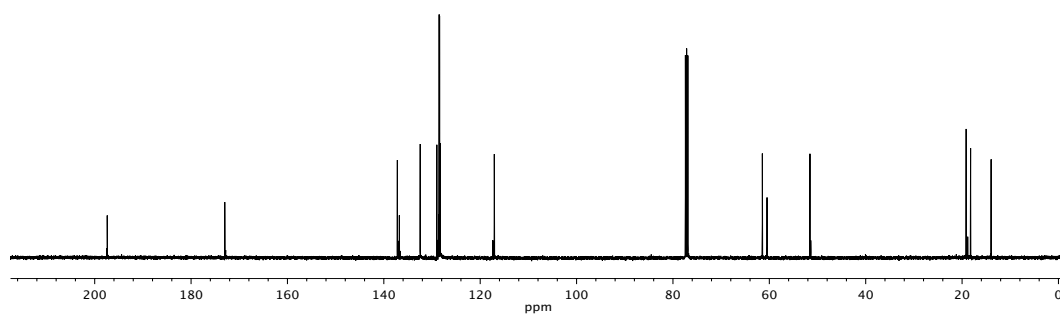
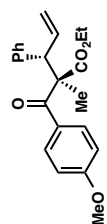
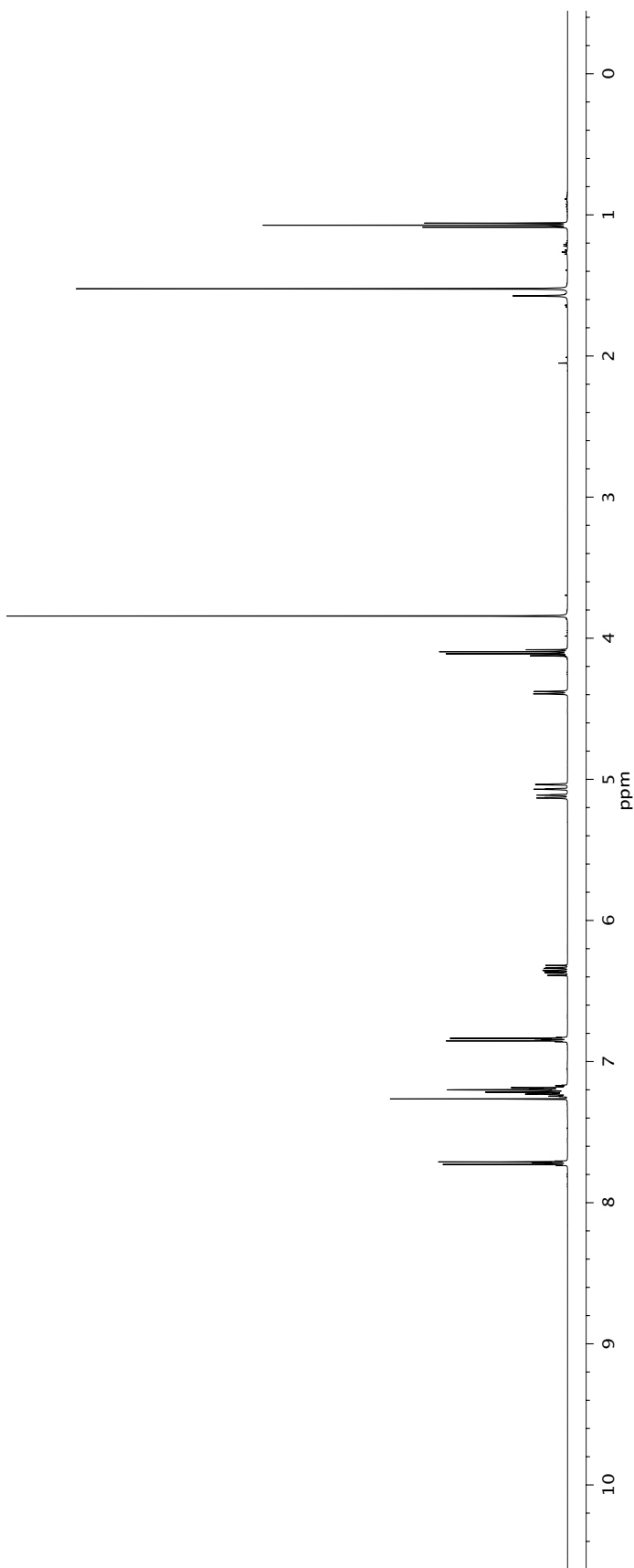


Figure A6.36 ¹³C NMR (125 MHz, CDCl₃) of compound **112k**.



112I

Figure A6.37 ¹H NMR (500 MHz, CDCl₃) of compound 112I.

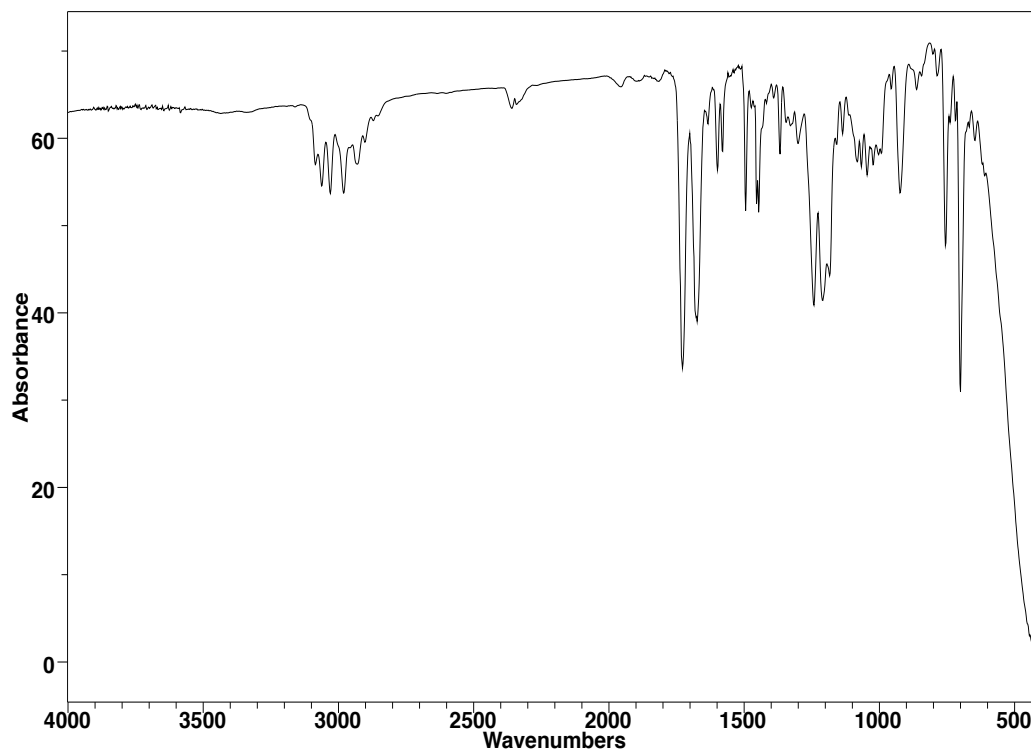


Figure A6.38 Infrared spectrum (thin film/NaCl) of compound **112I**.

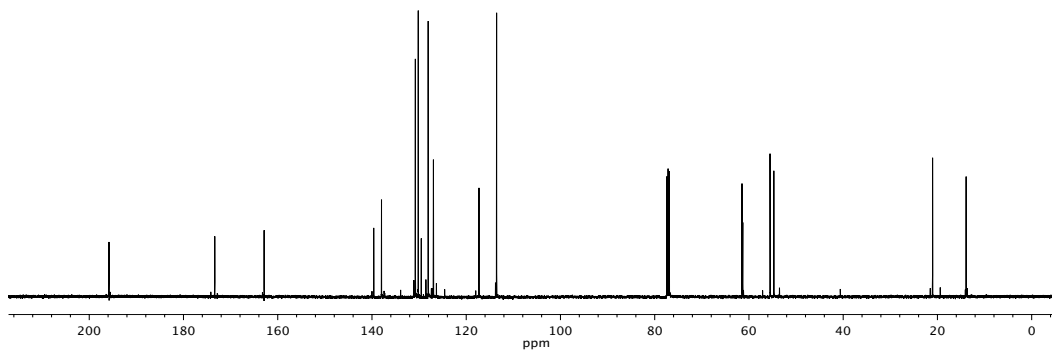


Figure A6.39 ¹³C NMR (125 MHz, CDCl₃) of compound **112I**.

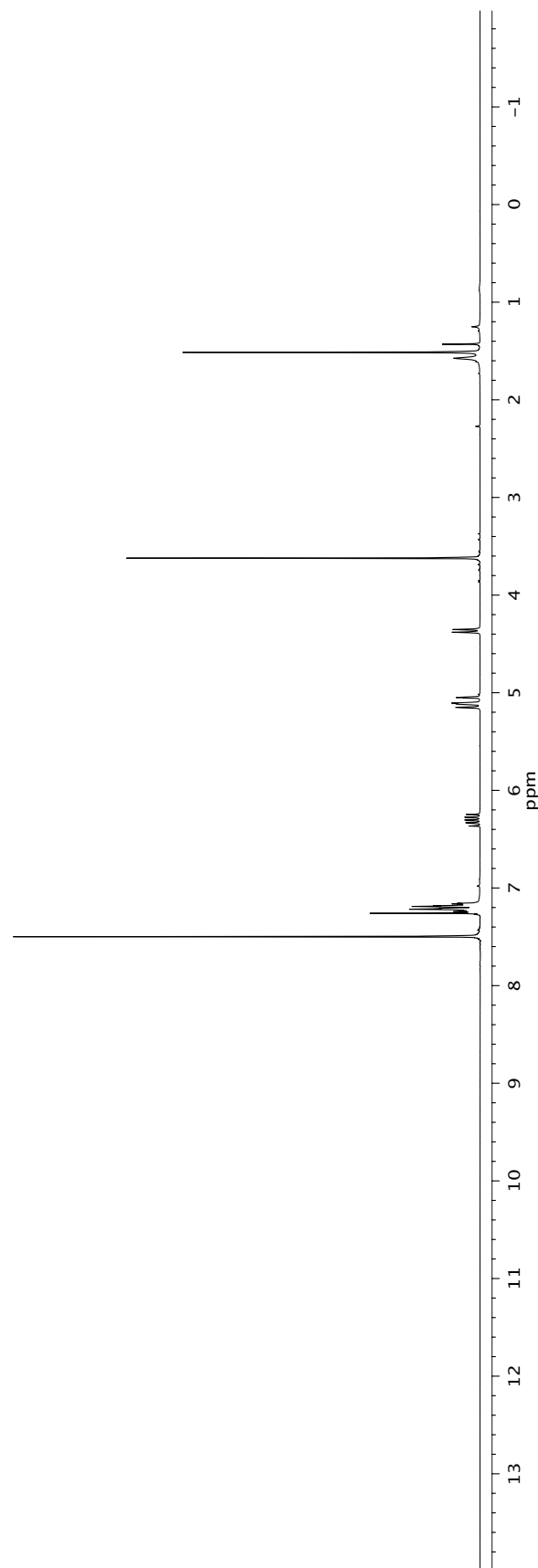
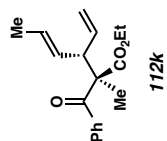


Figure A6.40 ¹H NMR (500 MHz, CDCl₃) of compound 112m.

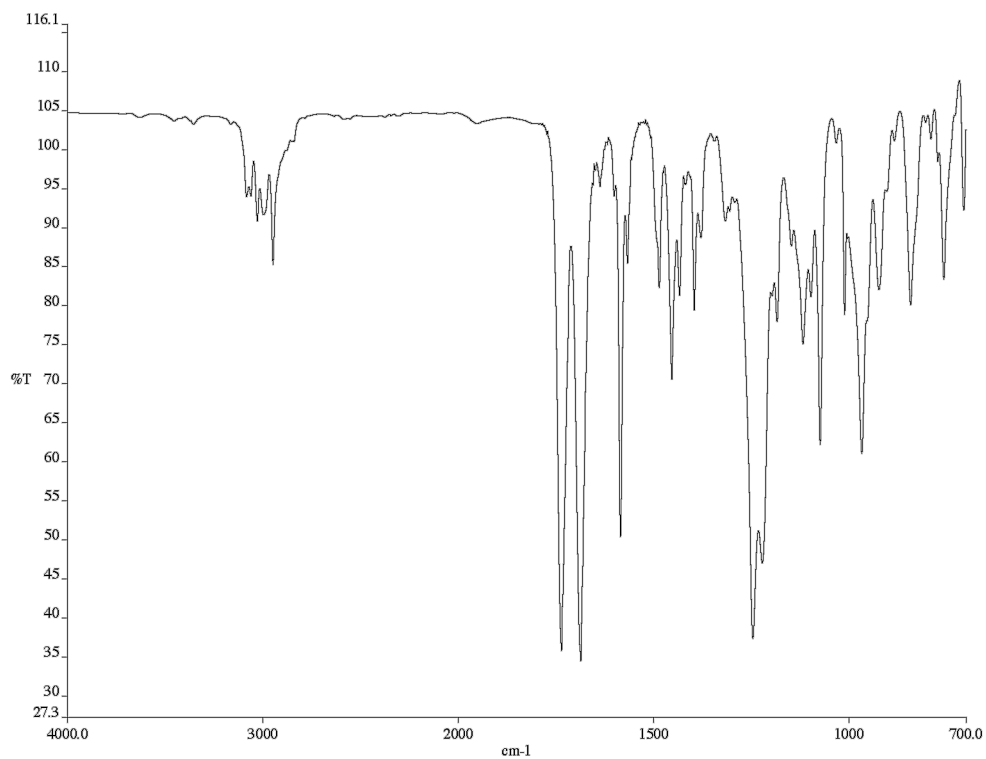


Figure A6.41 Infrared spectrum (thin film/NaCl) of compound **112m**.

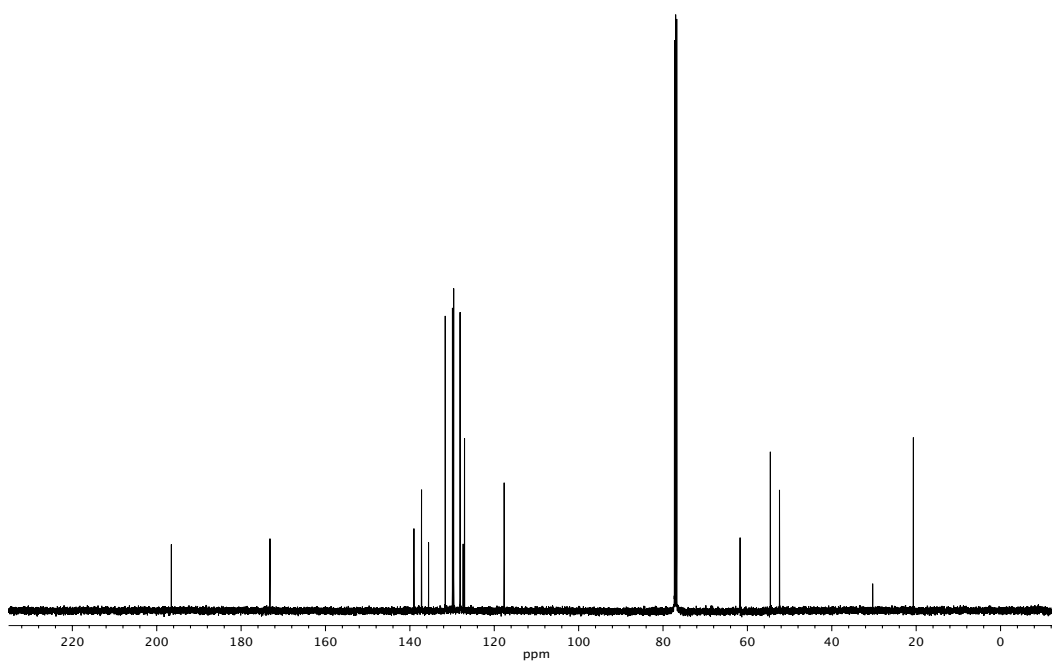


Figure A6.42 ¹³C NMR (125 MHz, CDCl₃) of compound **112m**.

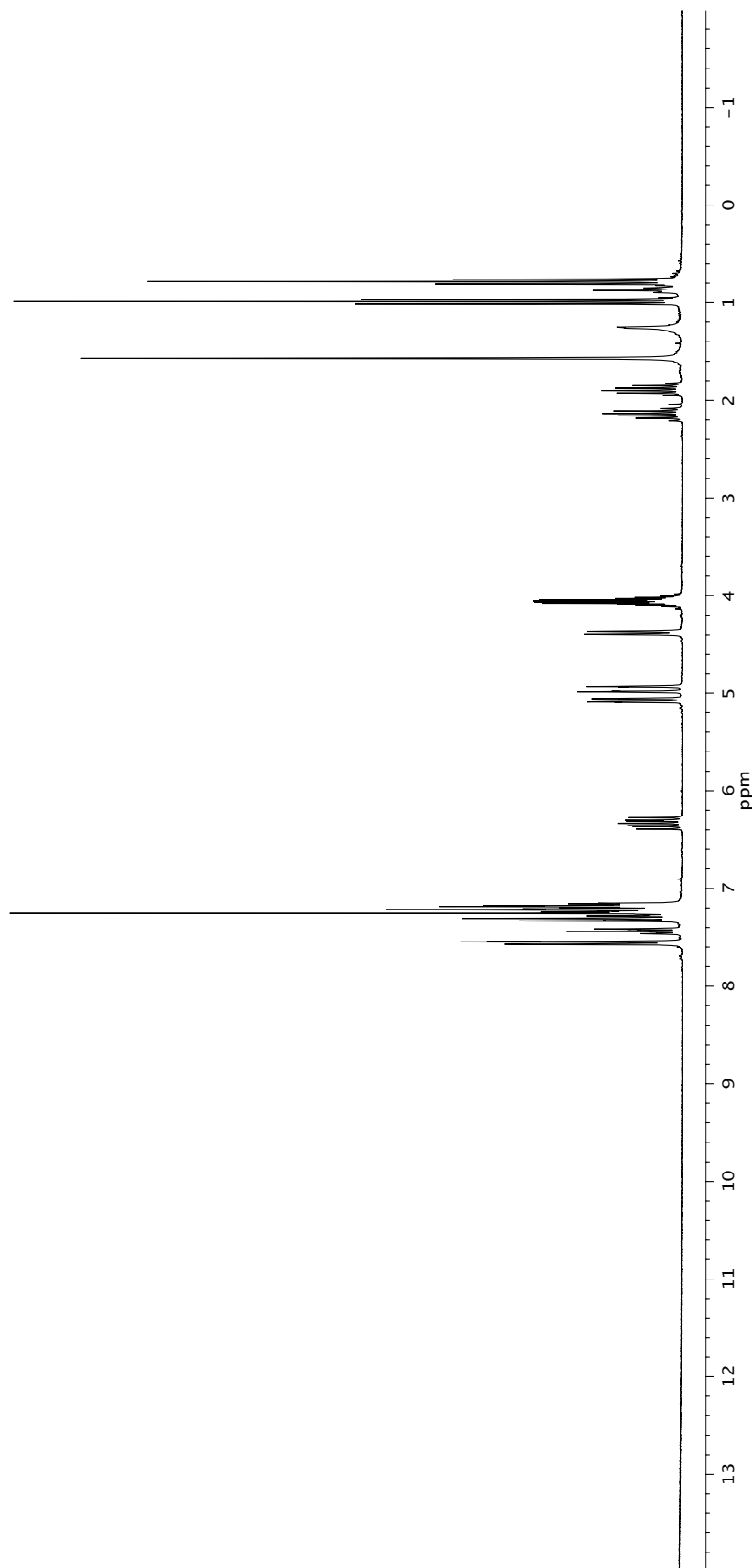
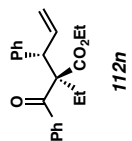


Figure A6.43 ¹H NMR (500 MHz, CDCl₃) of compound **112n**.

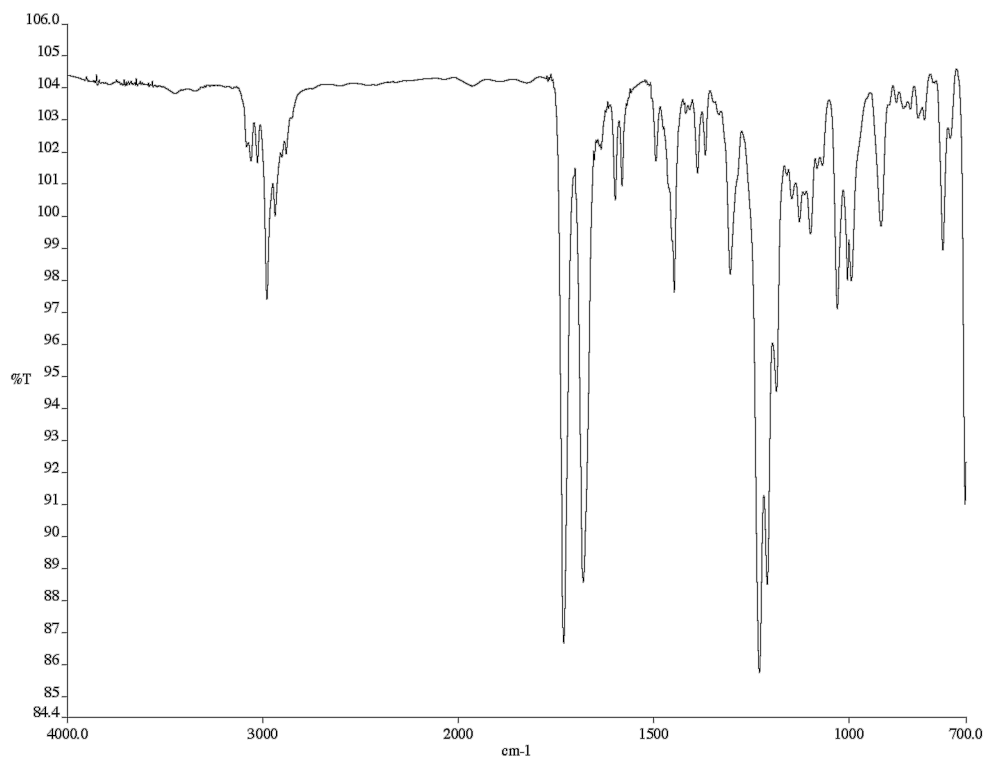


Figure A6.44 Infrared spectrum (thin film/NaCl) of compound **112n**.

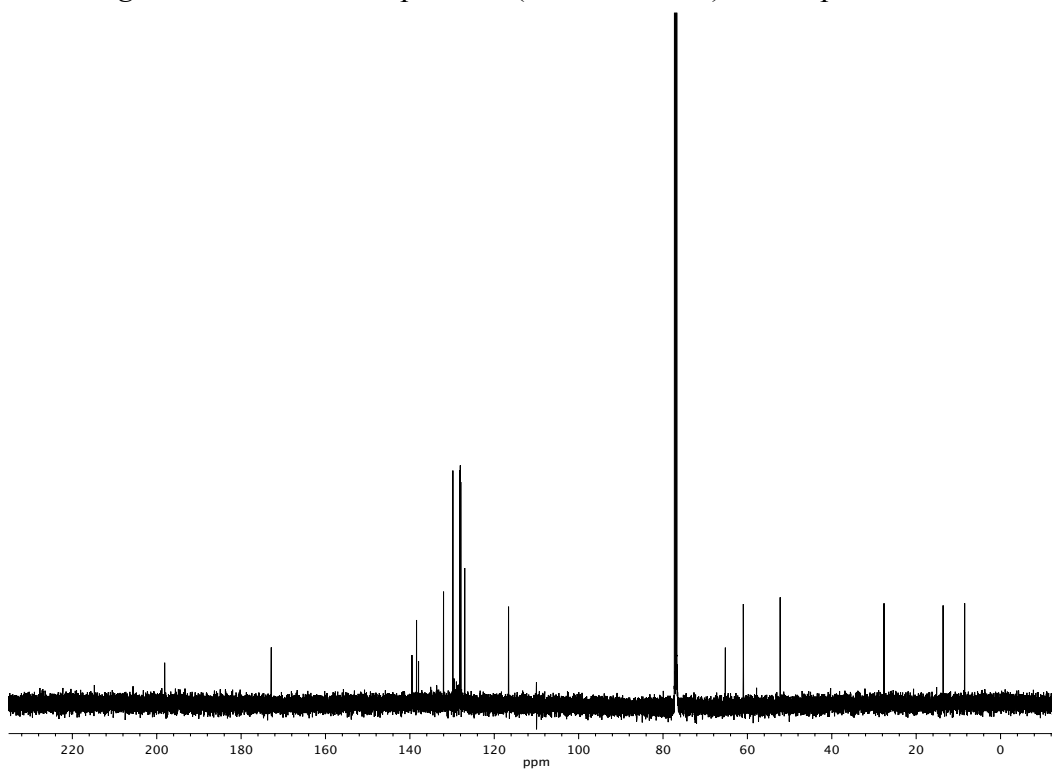


Figure A6.45 ¹³C NMR (125 MHz, CDCl₃) of compound **112n**.

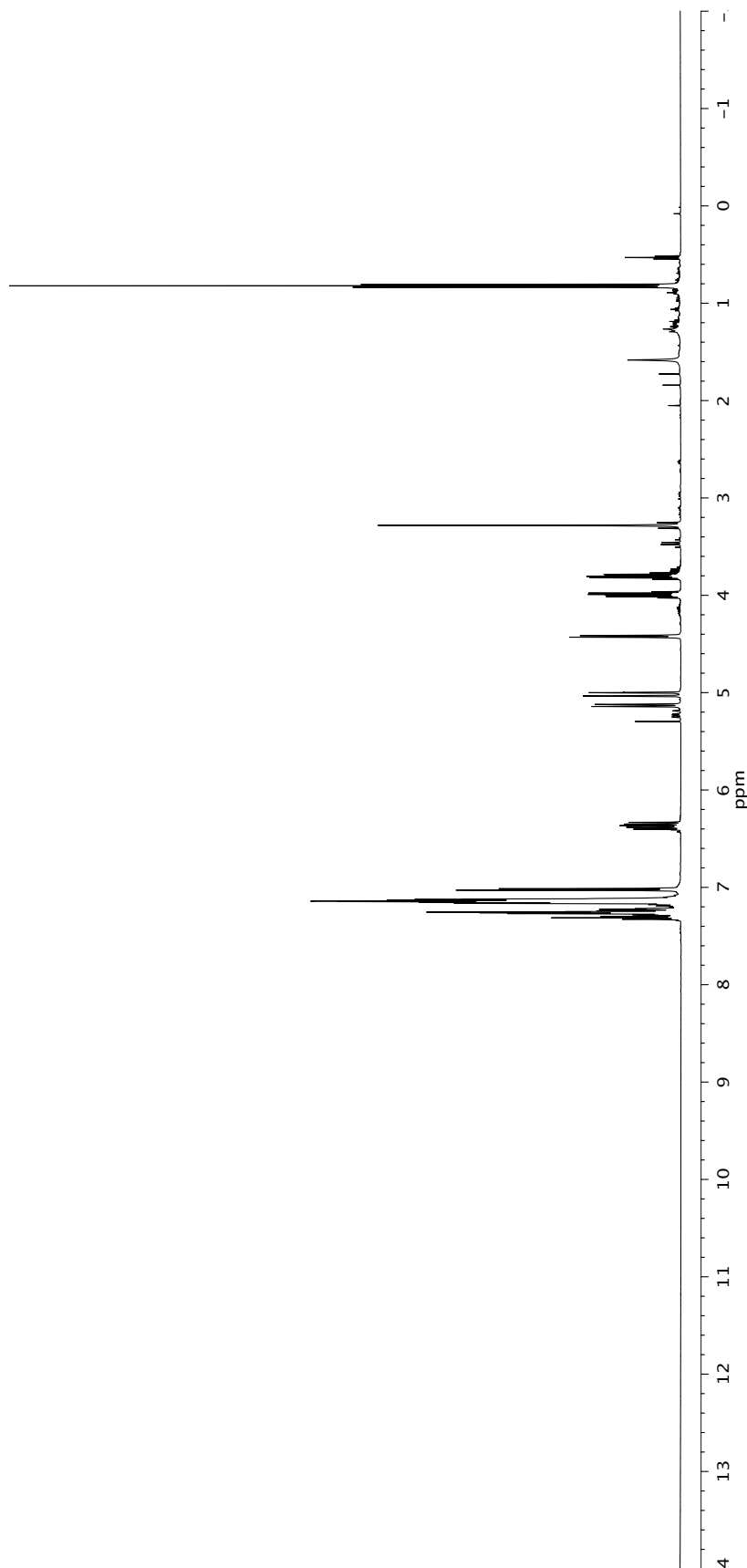
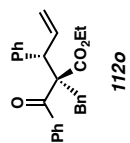


Figure A6.46 ¹H NMR (500 MHz, CDCl₃) of compound **1120**.

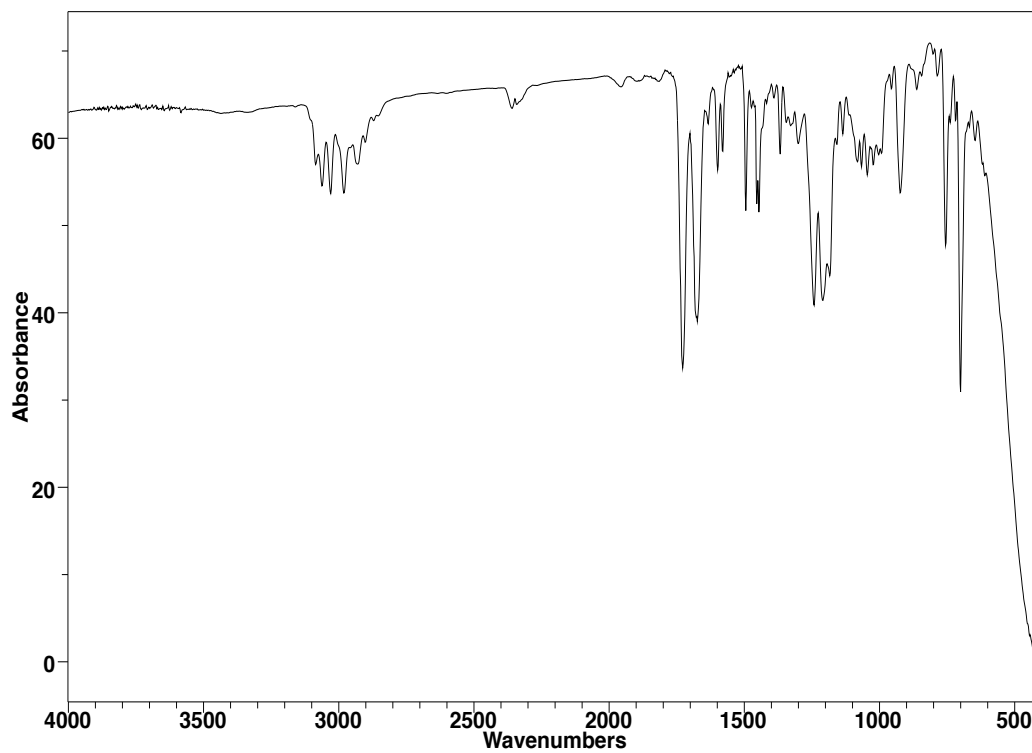


Figure A6.47 Infrared spectrum (thin film/NaCl) of compound **112o**.

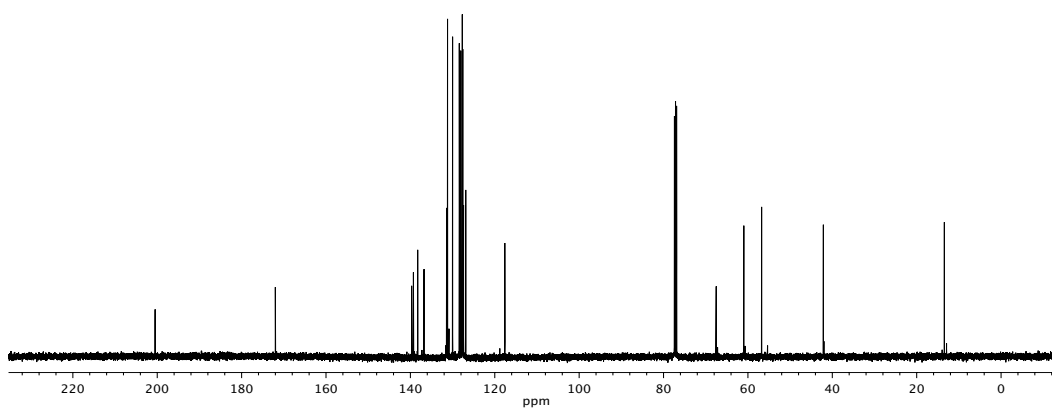


Figure A6.48 ¹³C NMR (125 MHz, CDCl₃) of compound **112o**.

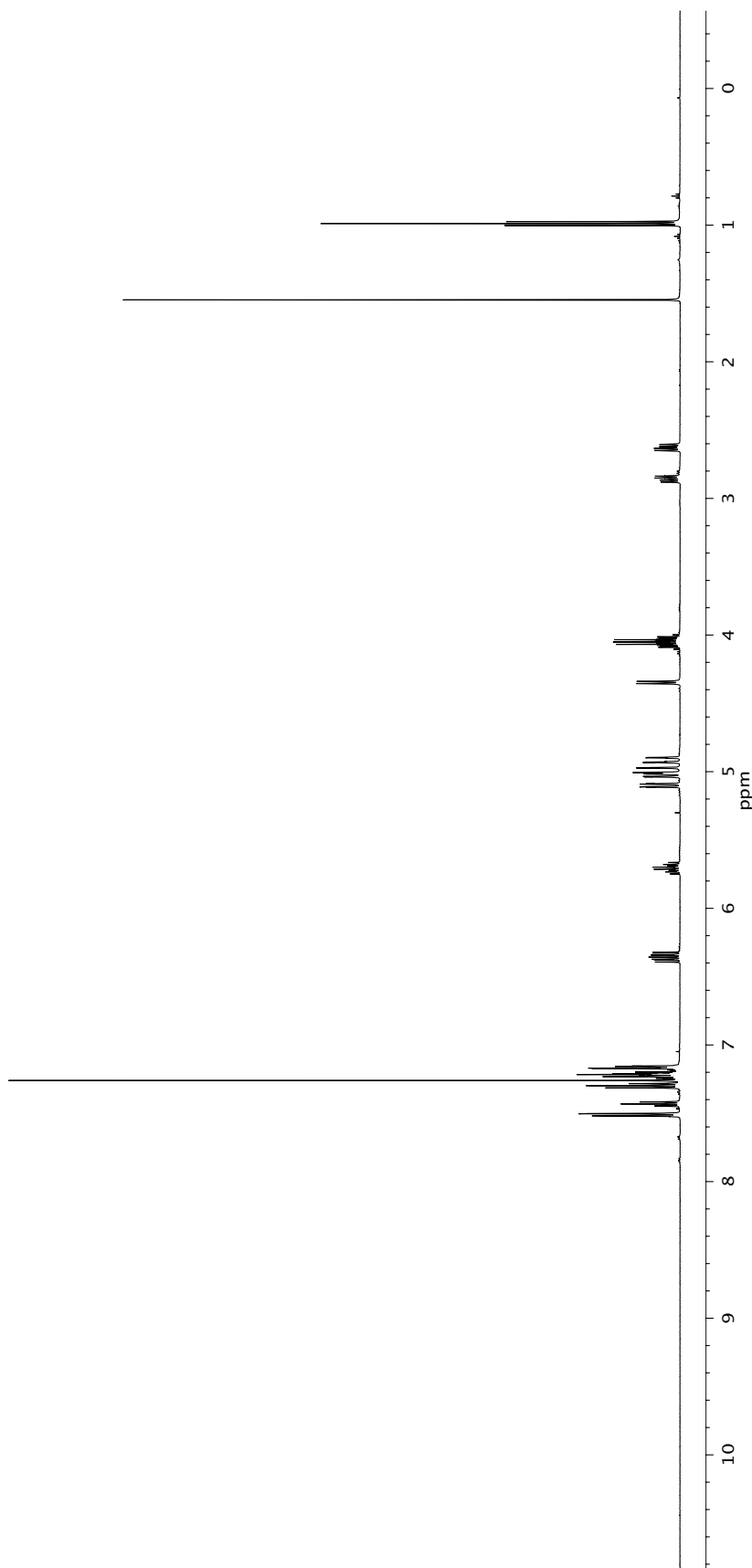
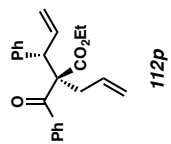


Figure A6.49 ¹H NMR (500 MHz, CDCl₃) of compound **112p**.

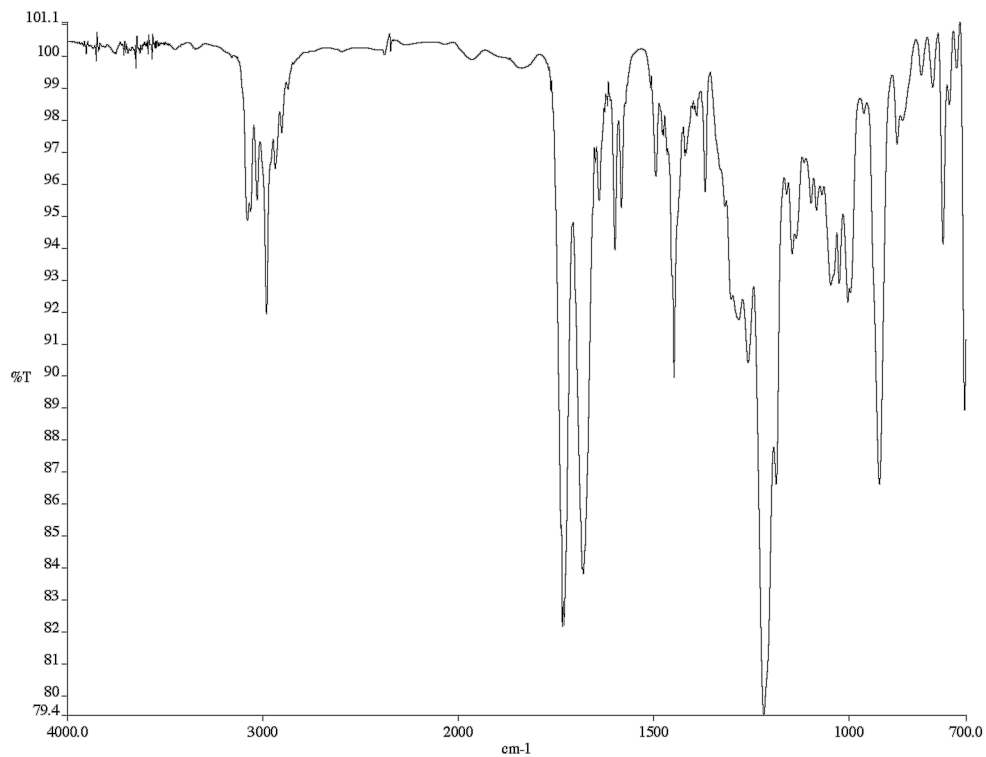


Figure A6.50 Infrared spectrum (thin film/NaCl) of compound **112p**.

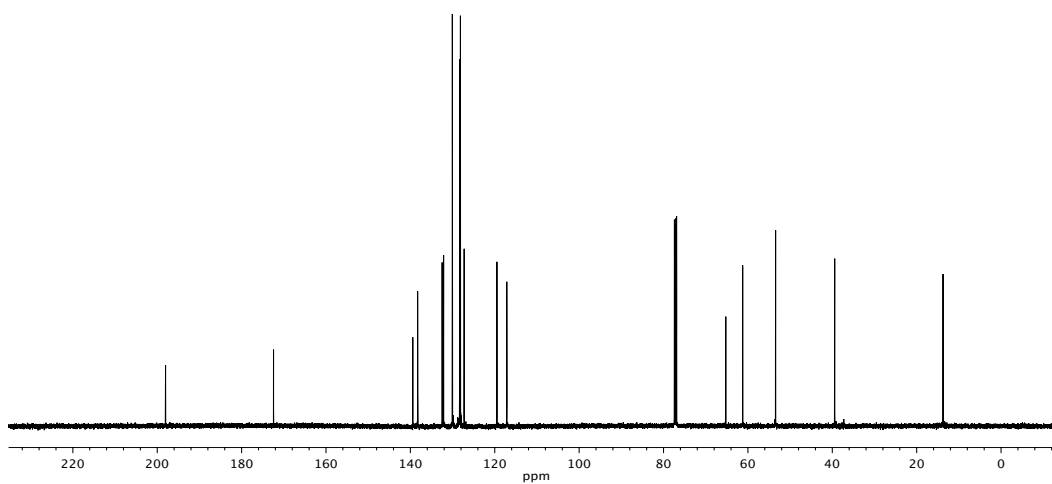


Figure A6.51 ¹³C NMR (125 MHz, CDCl₃) of compound **112p**.

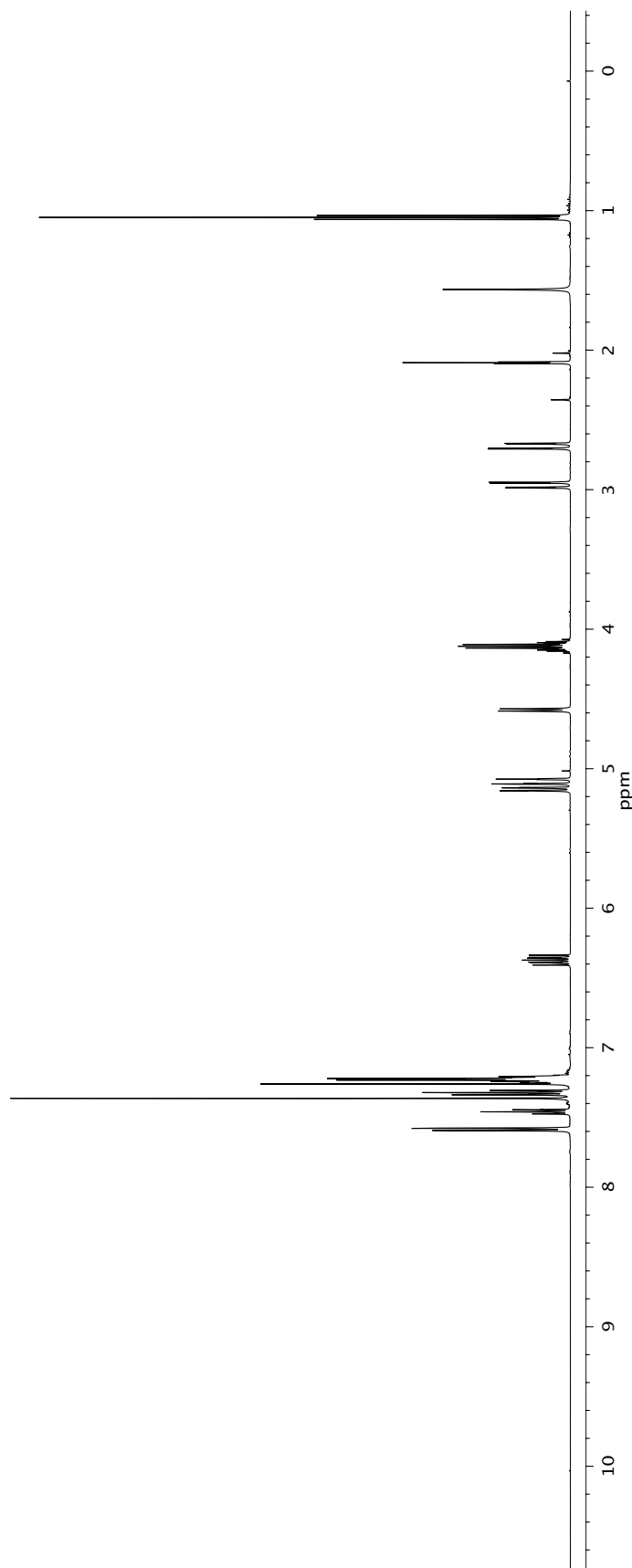
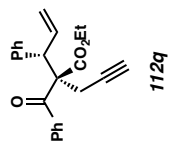


Figure A6.52 ¹H NMR (500 MHz, CDCl₃) of compound **112q**.

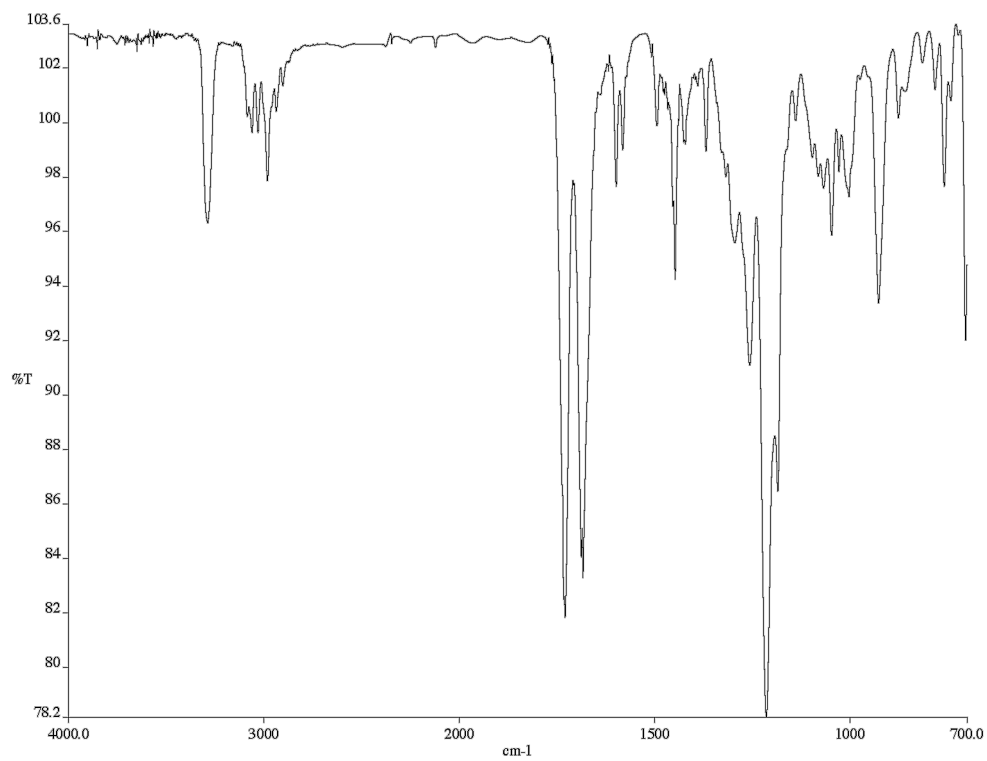


Figure A6.53 Infrared spectrum (thin film/NaCl) of compound **112q**.

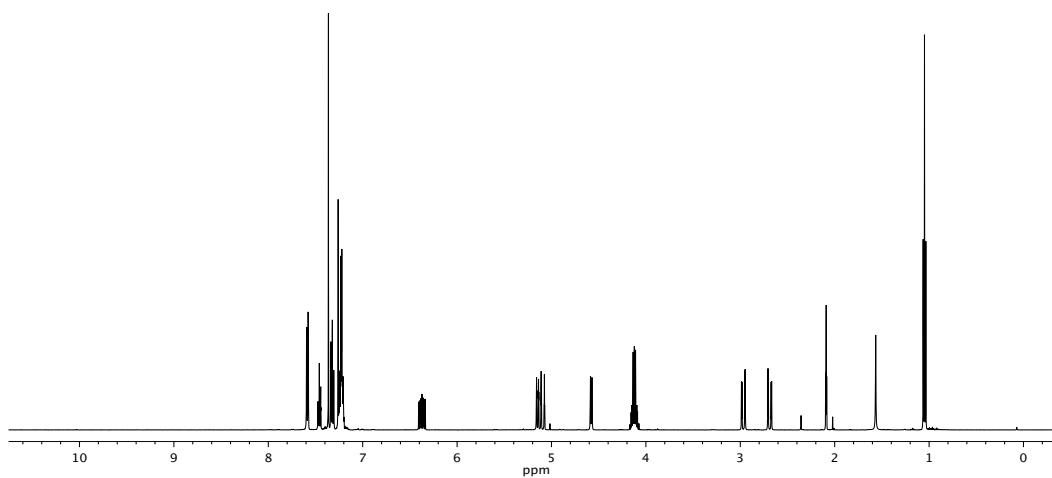


Figure A6.54 ¹³C NMR (125 MHz, CDCl₃) of compound **112q**.

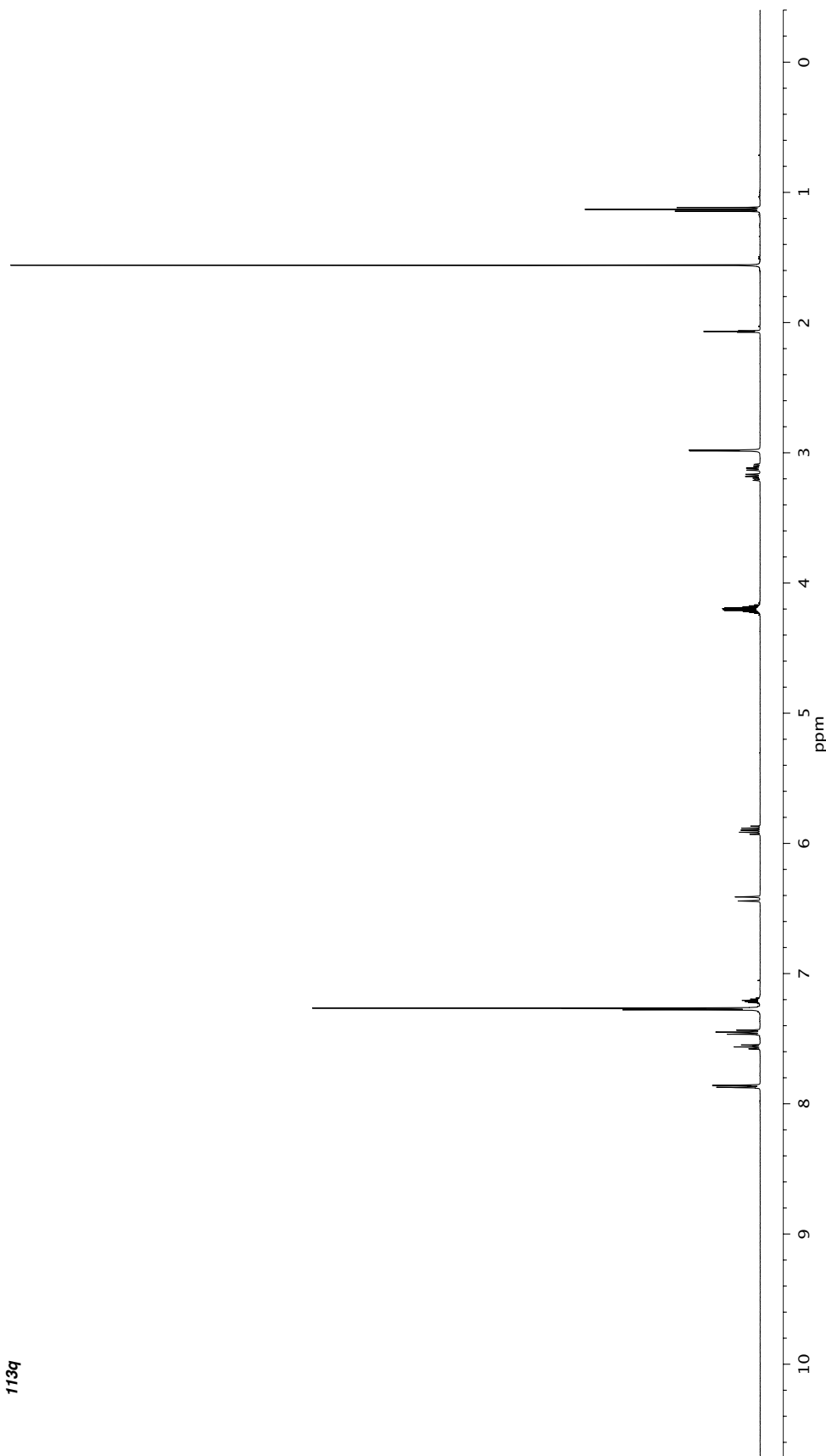
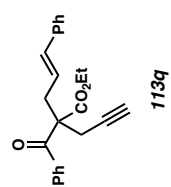


Figure A6.55 ¹H NMR (500 MHz, CDCl₃) of compound **113q**.

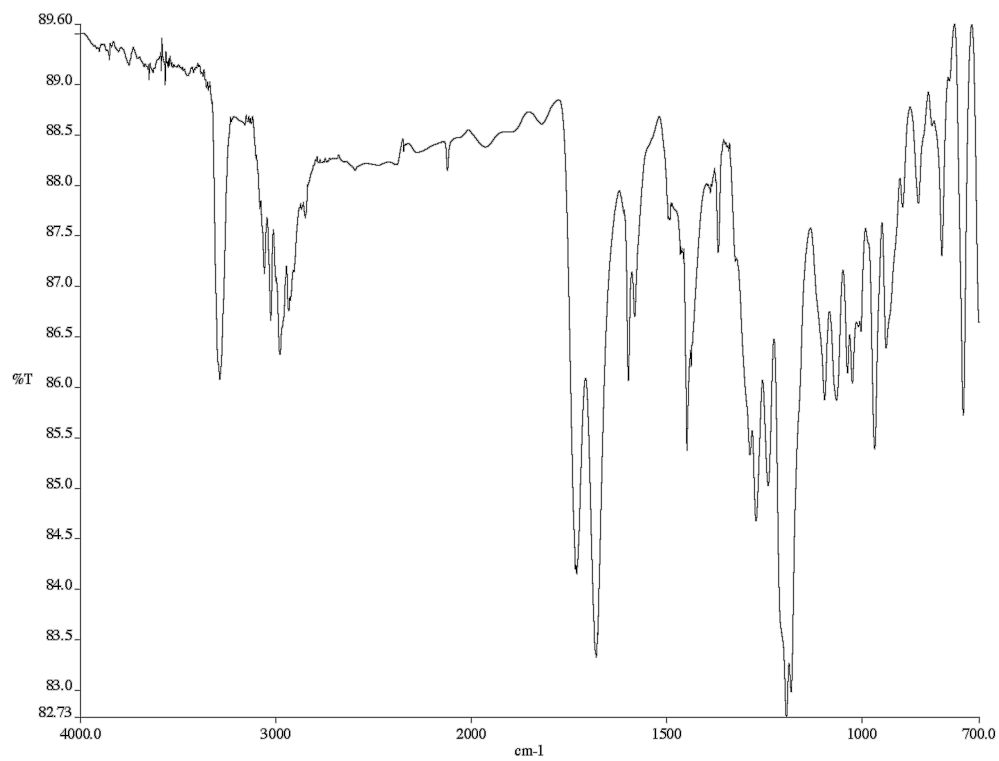


Figure A6.56 Infrared spectrum (thin film/NaCl) of compound **113q**.

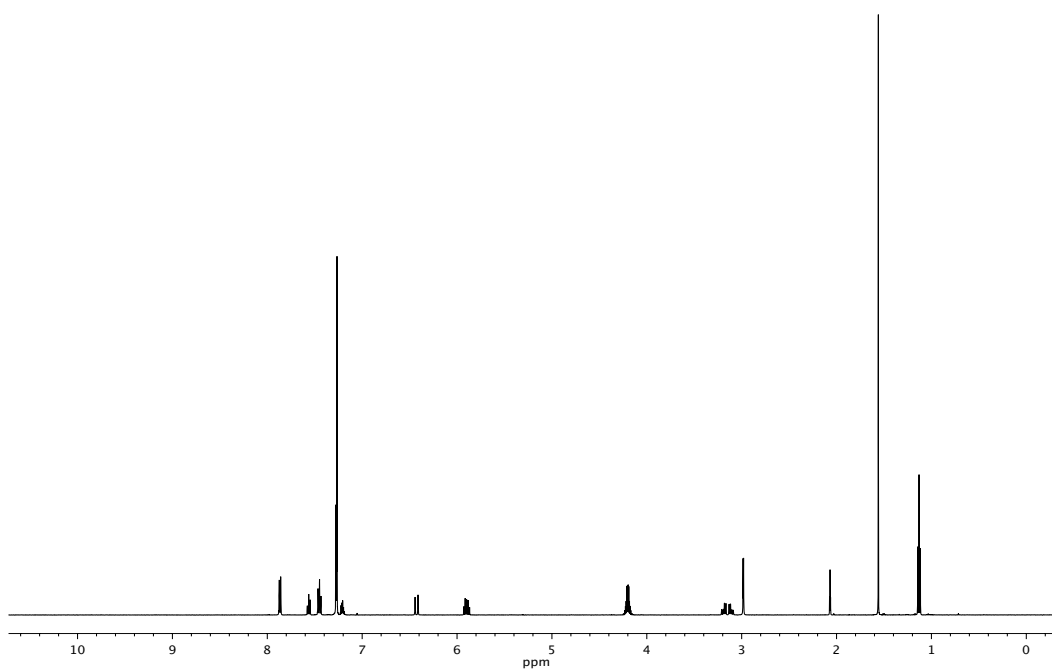


Figure A6.57 ¹³C NMR (125 MHz, CDCl₃) of compound **113q**.

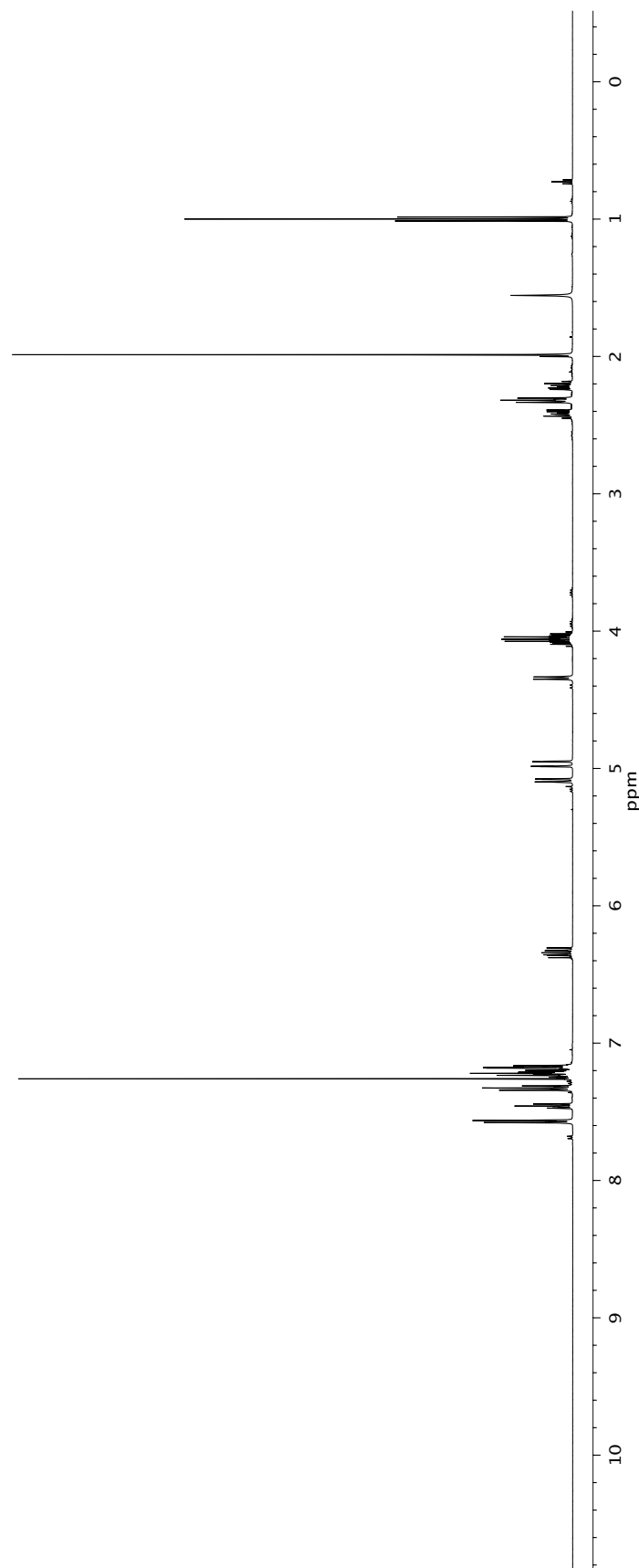
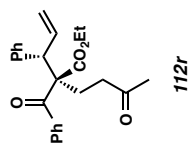


Figure A6.58 ¹H NMR (500 MHz, CDCl₃) of compound **112r**.

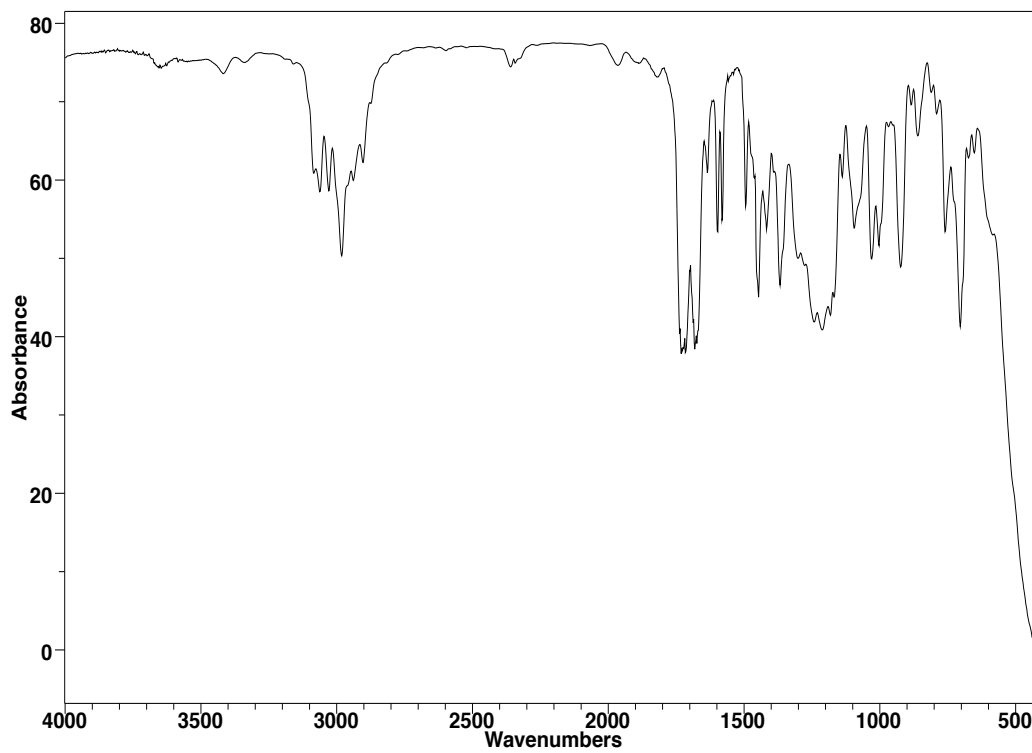


Figure A6.59 Infrared spectrum (thin film/NaCl) of compound **112r**.

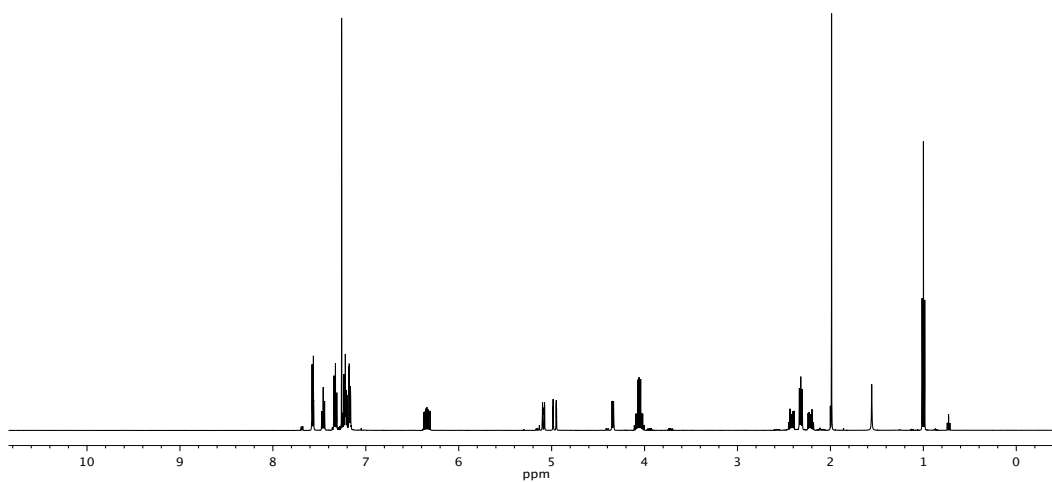


Figure A6.60 ¹³C NMR (125 MHz, CDCl₃) of compound **112r**.

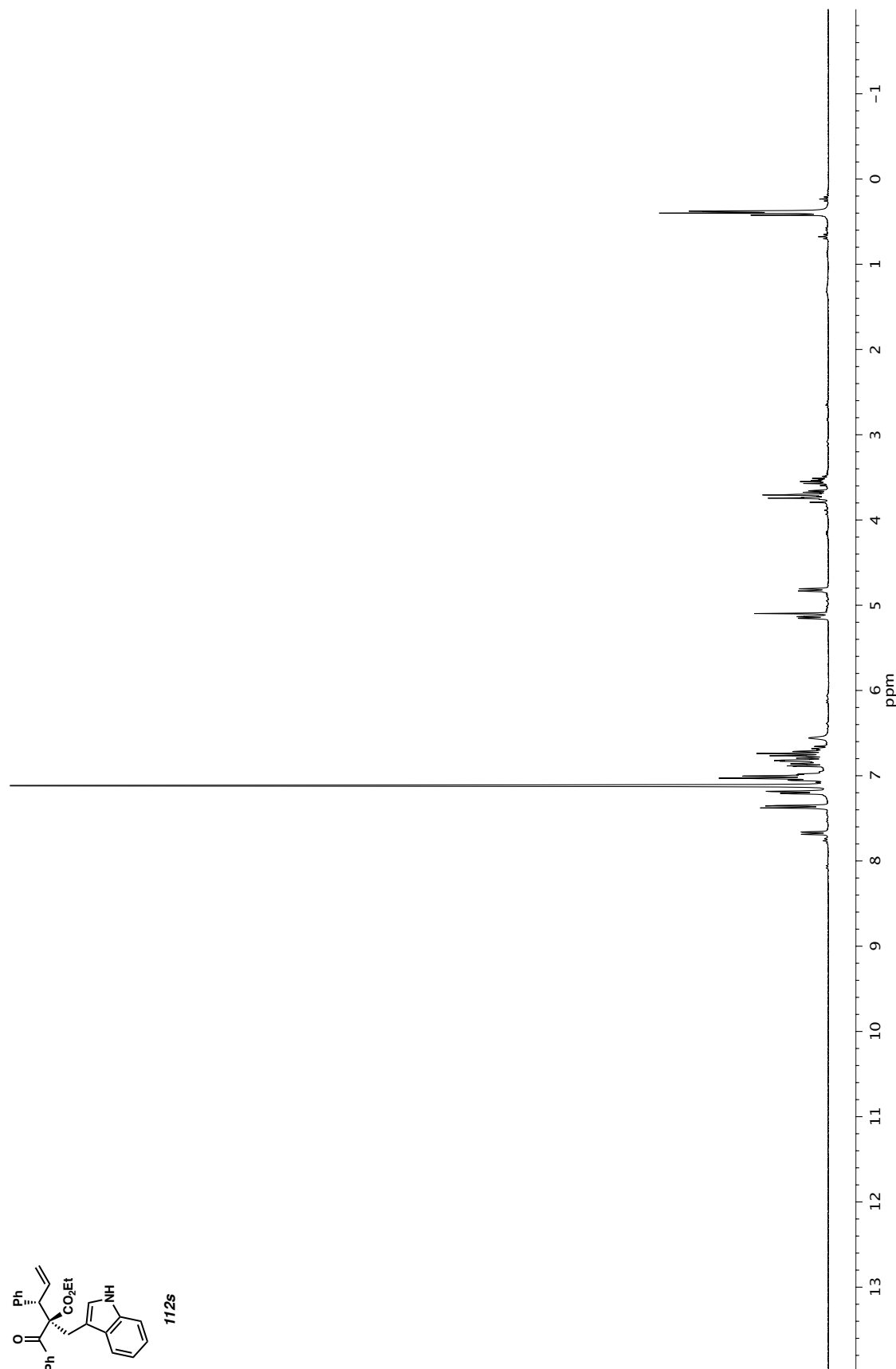
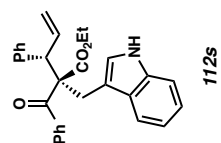


Figure A6.61 ¹H NMR (500 MHz, CDCl₃) of compound **112s**.

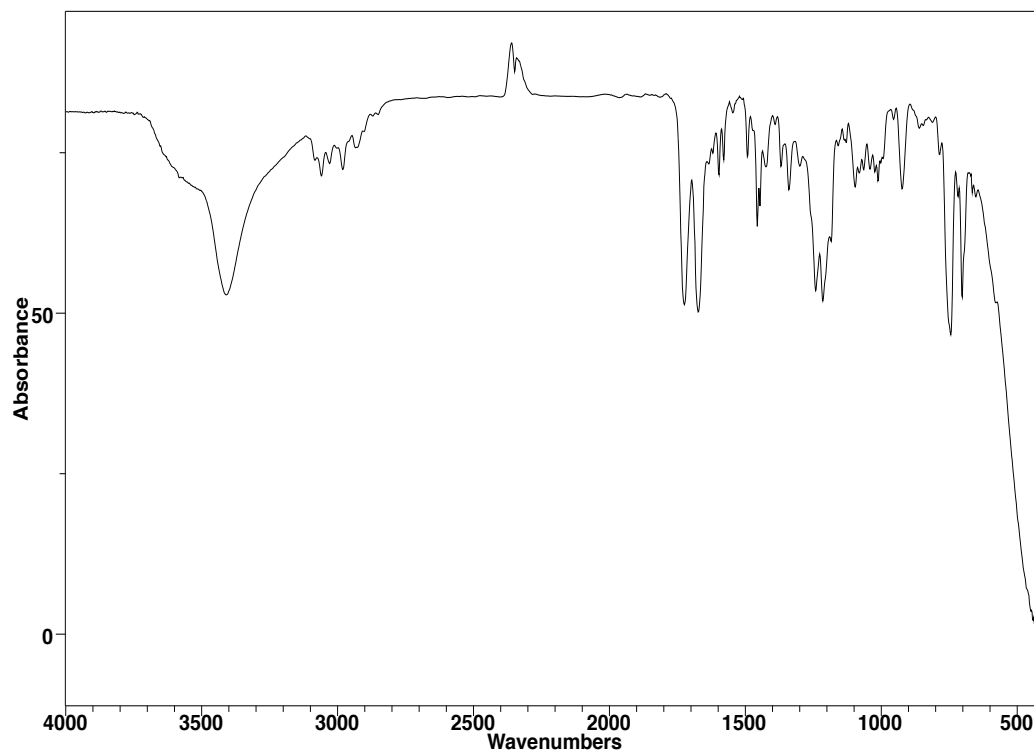


Figure A6.62 Infrared spectrum (thin film/NaCl) of compound **112s**.

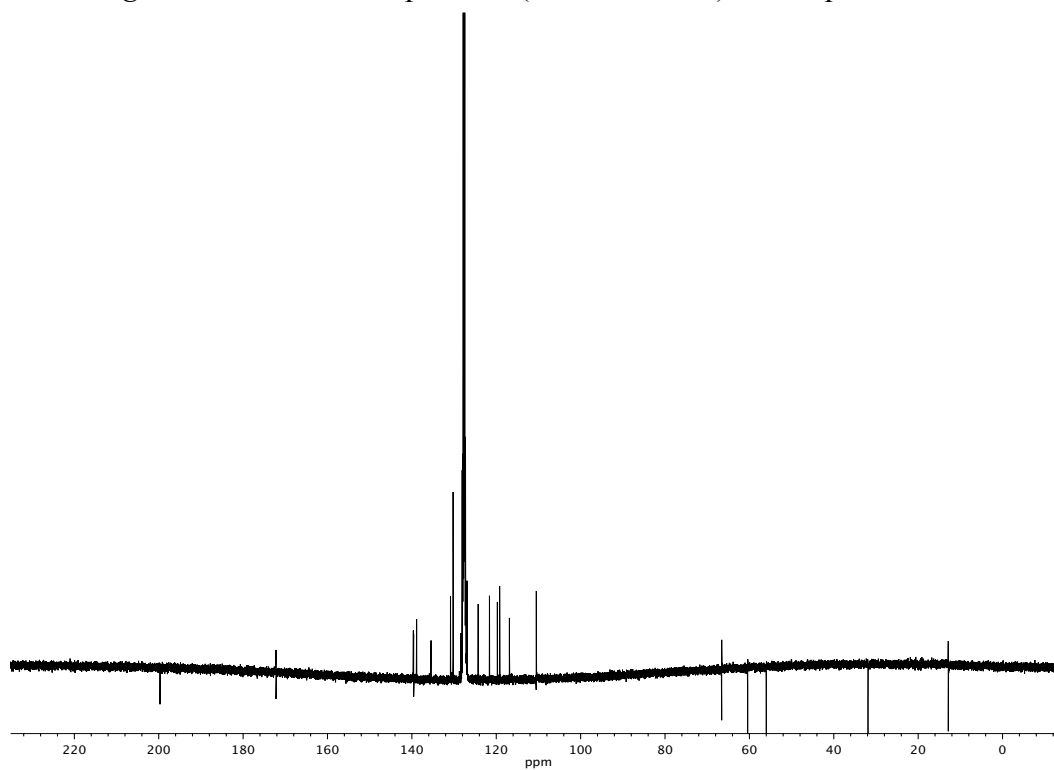


Figure A6.63 ¹³C NMR (125 MHz, CDCl₃) of compound **112s**.

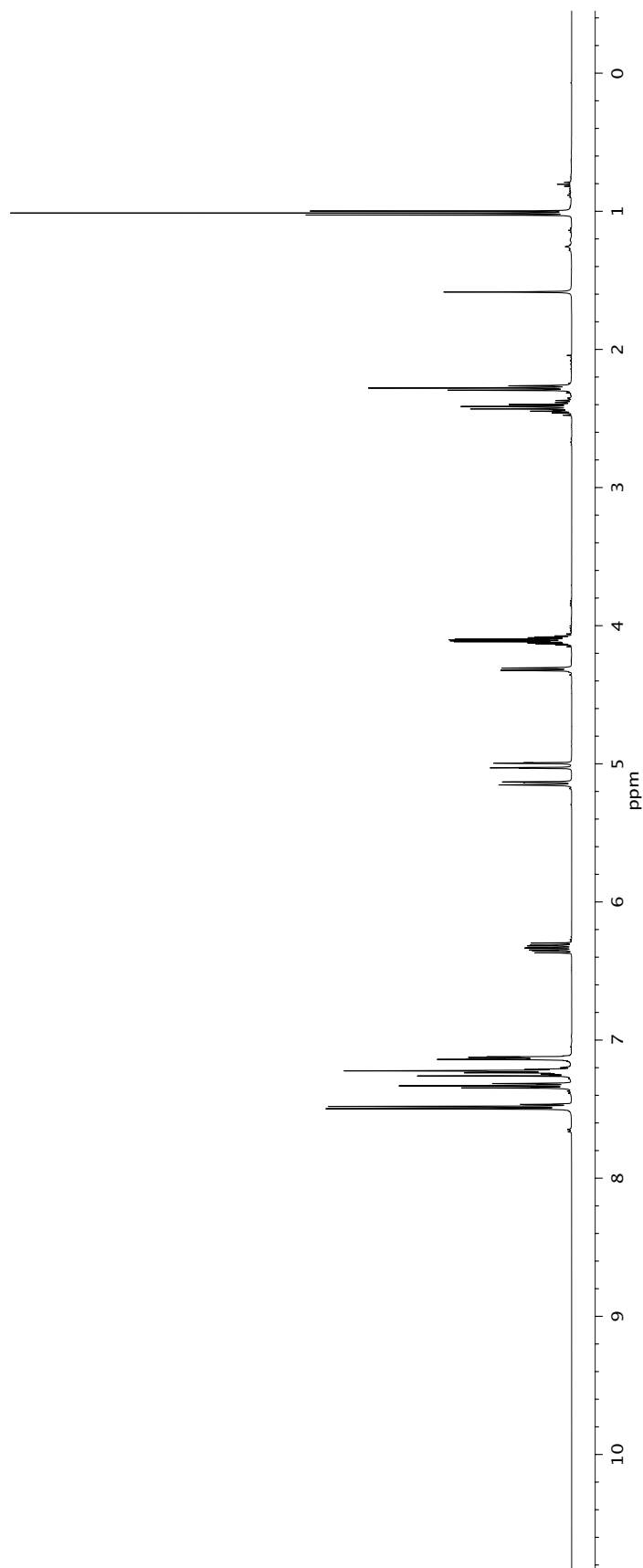
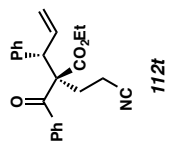


Figure A6.64 ¹H NMR (500 MHz, CDCl₃) of compound **112t**.

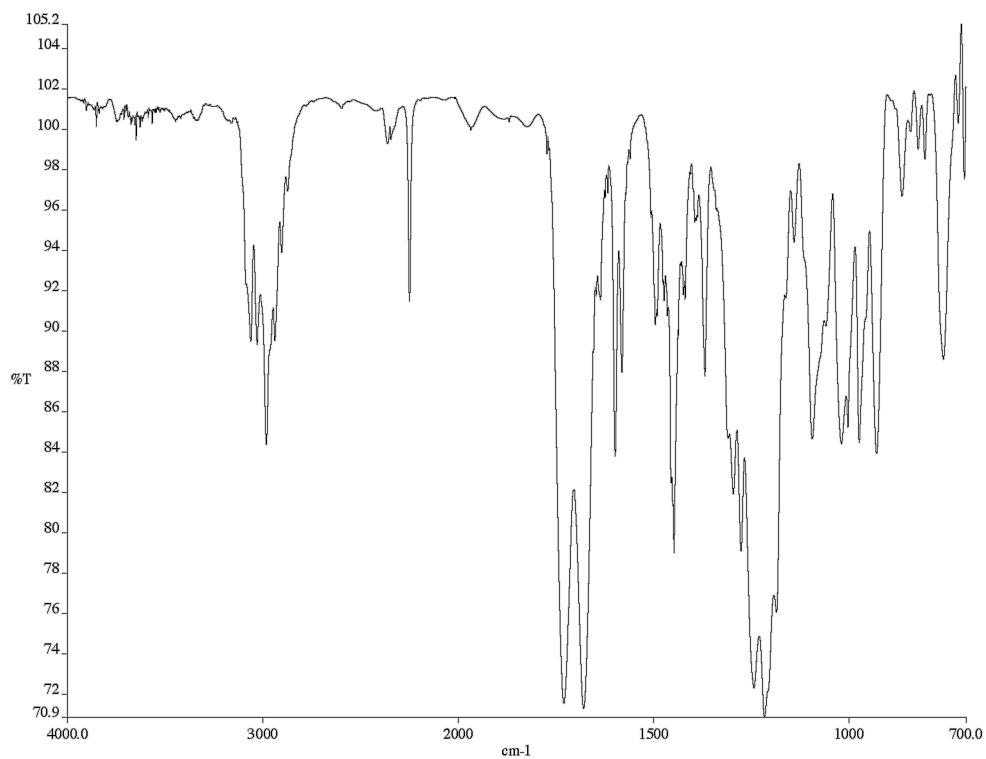


Figure A6.65 Infrared spectrum (thin film/NaCl) of compound **112t**.

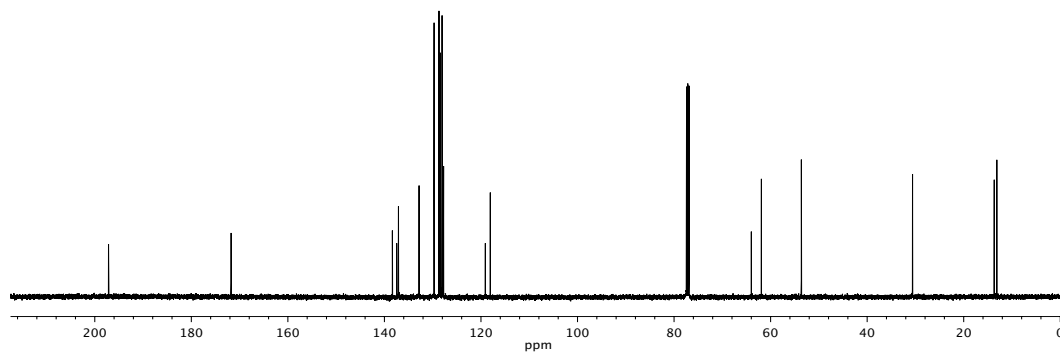


Figure A6.66 ¹³C NMR (125 MHz, CDCl₃) of compound **112t**.

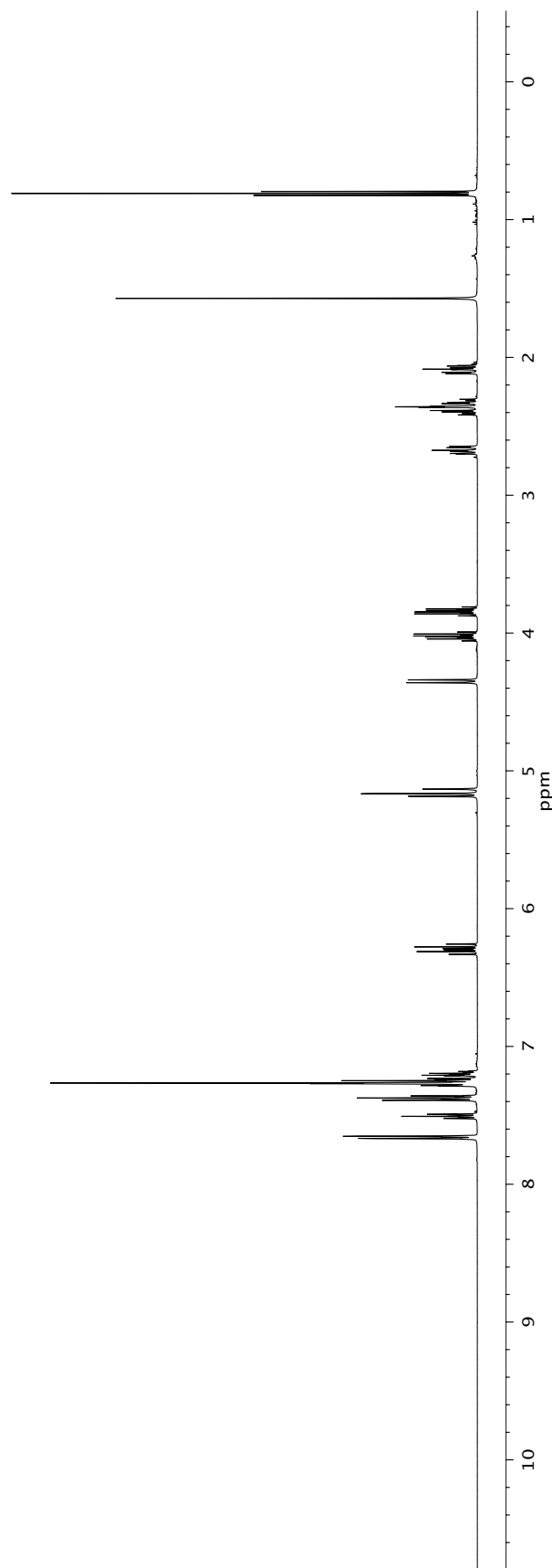
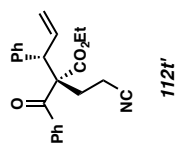


Figure A6.67 ¹H NMR (500 MHz, CDCl₃) of compound **112t'**.

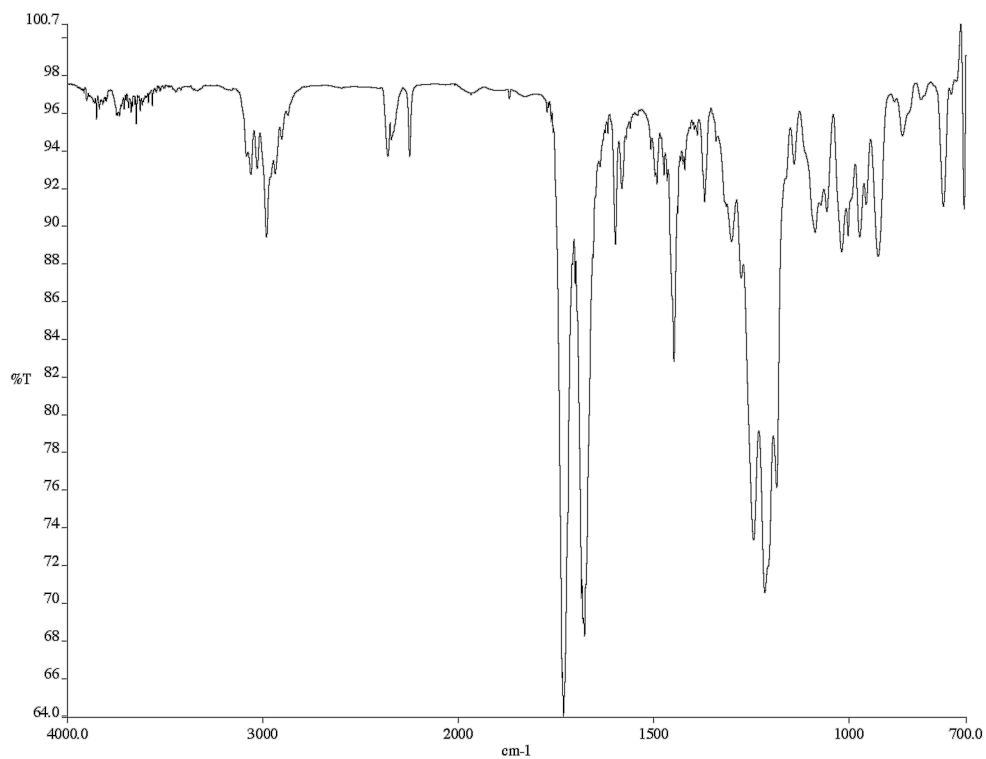


Figure A6.68 Infrared spectrum (thin film/NaCl) of compound **112t'**.

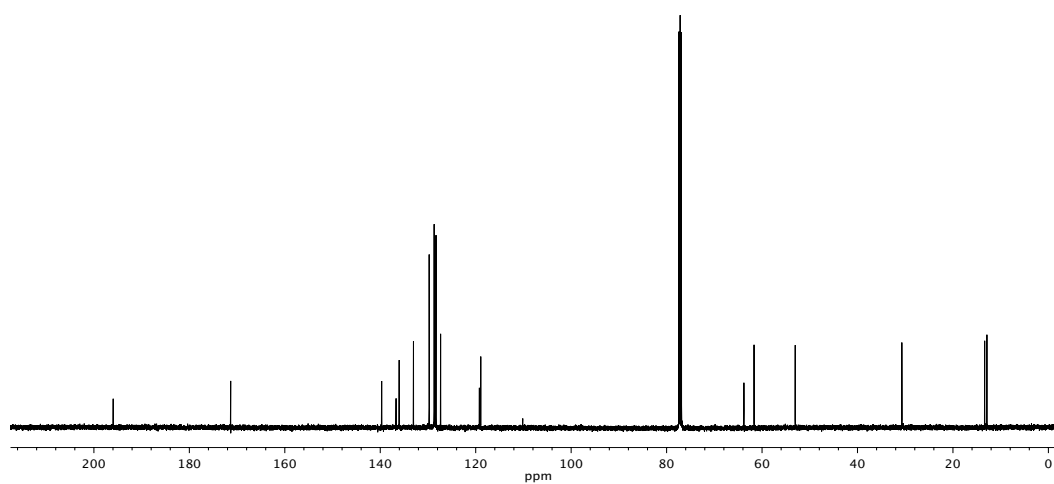


Figure A6.69 ^{13}C NMR (125 MHz, CDCl_3) of compound **112t'**.

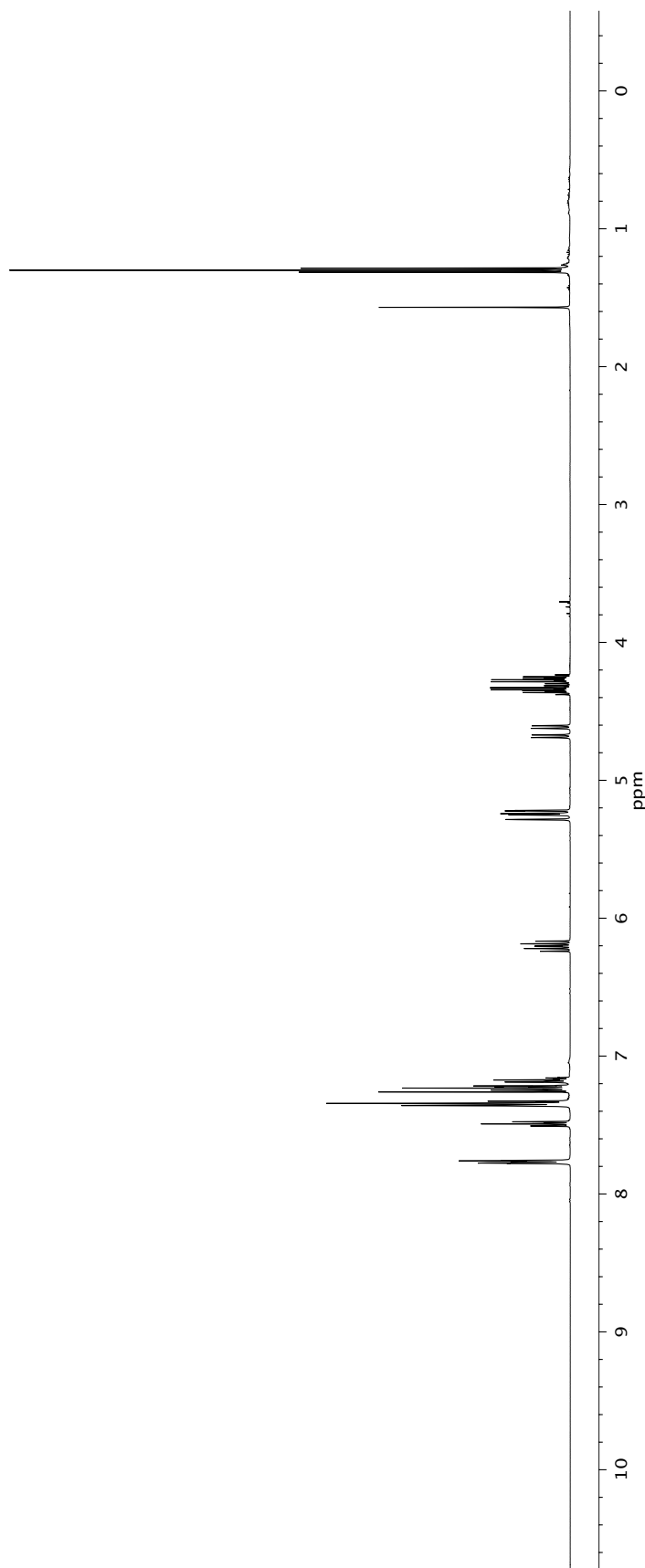
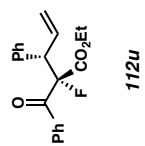


Figure A6.70 ¹H NMR (500 MHz, CDCl₃) of compound **112u**.

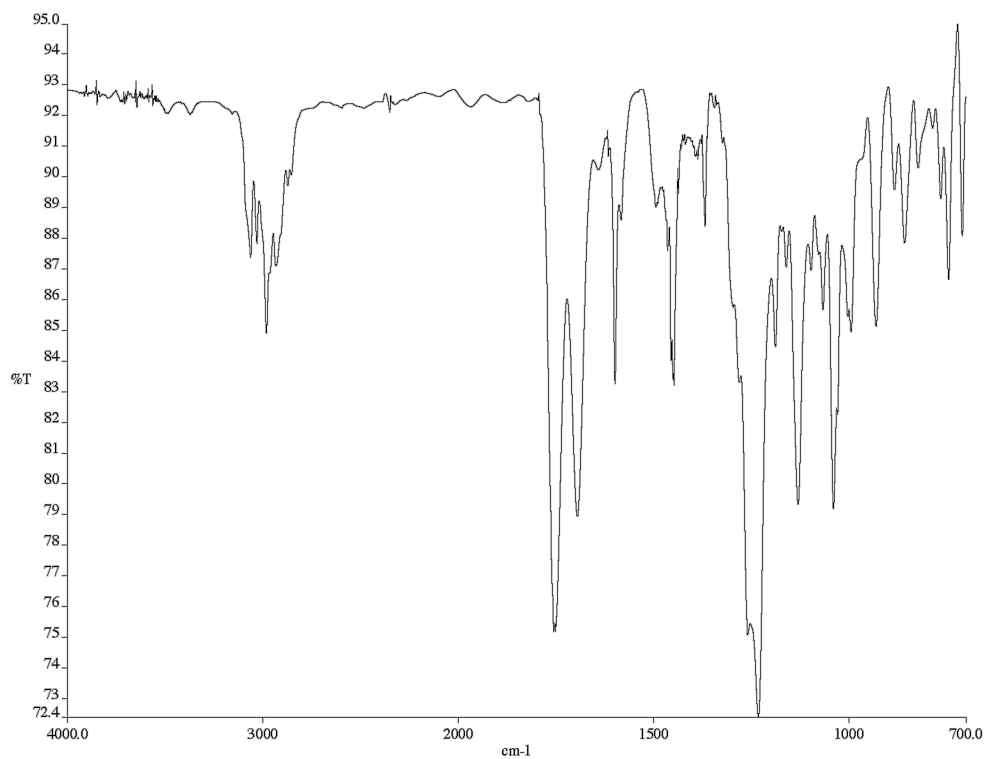


Figure A6.71 Infrared spectrum (thin film/NaCl) of compound **112u**.

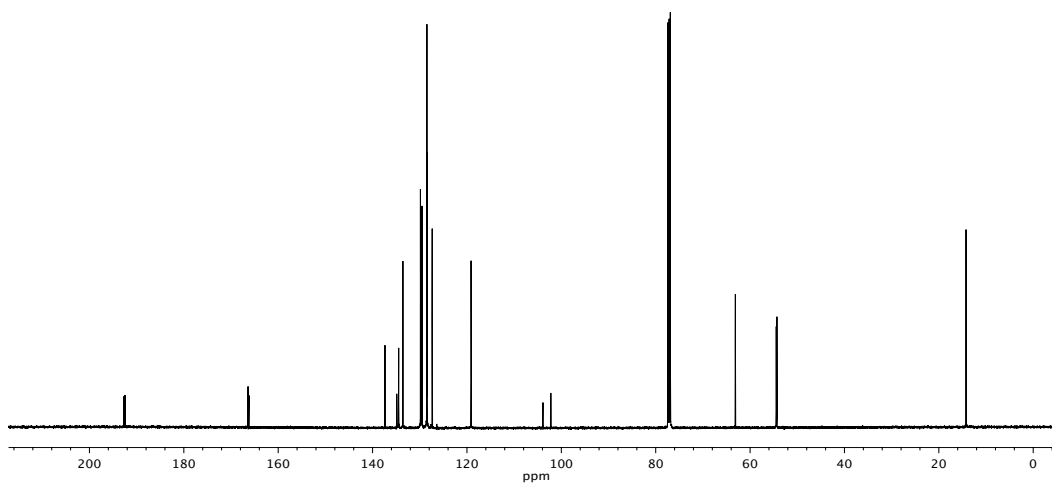


Figure A6.72 ¹³C NMR (125 MHz, CDCl₃) of compound **112u**.

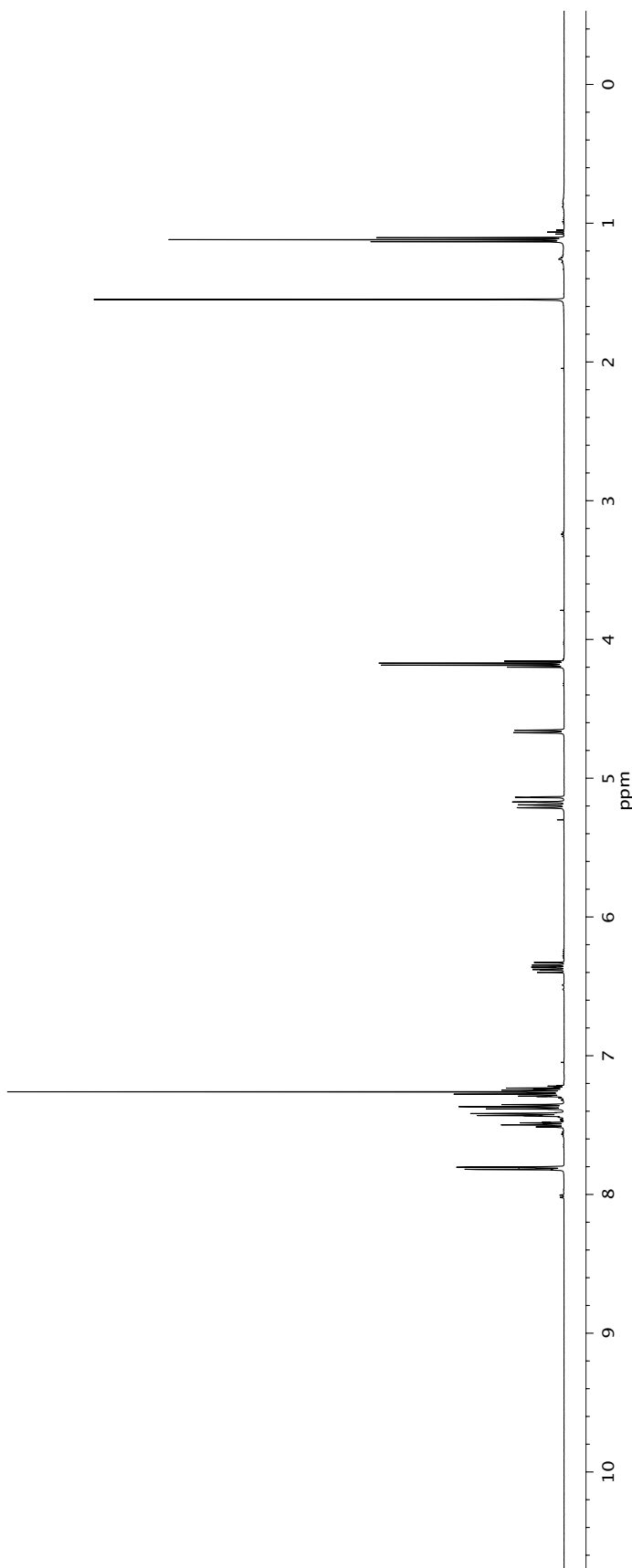
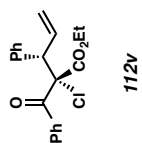


Figure A6.73 ¹H NMR (500 MHz, CDCl₃) of compound **112v**.

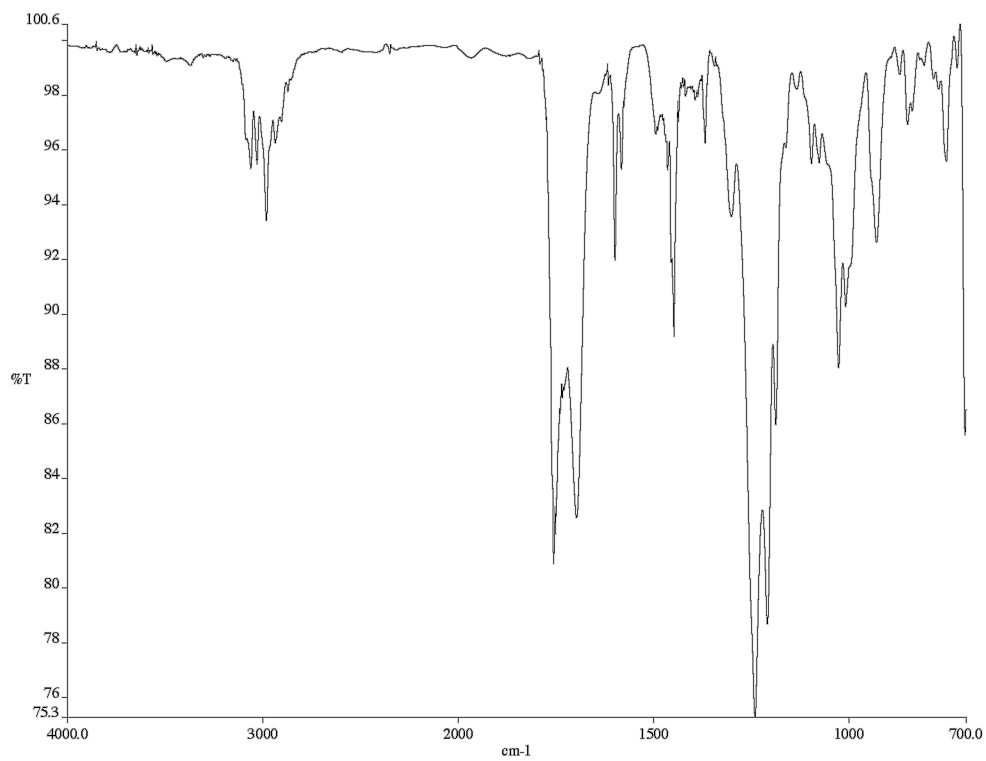


Figure A6.74 Infrared spectrum (thin film/NaCl) of compound **112v**.

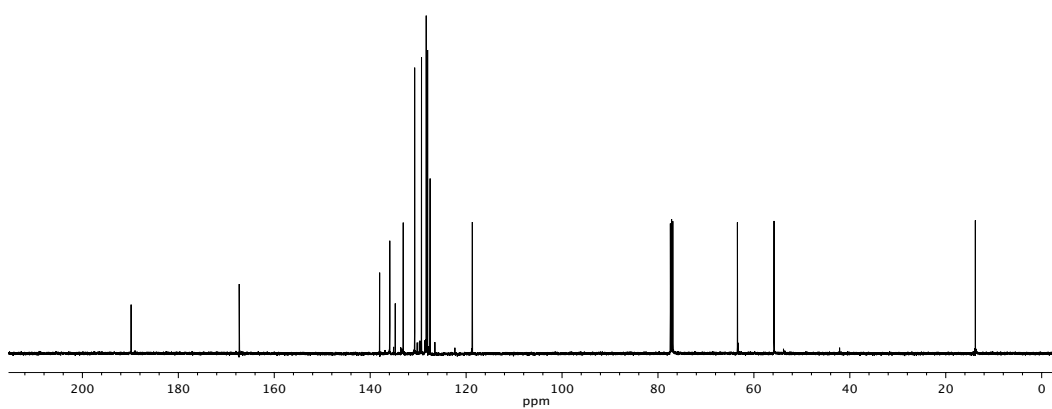
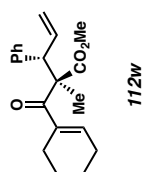


Figure A6.75 ¹³C NMR (125 MHz, CDCl₃) of compound **112v**.



112w

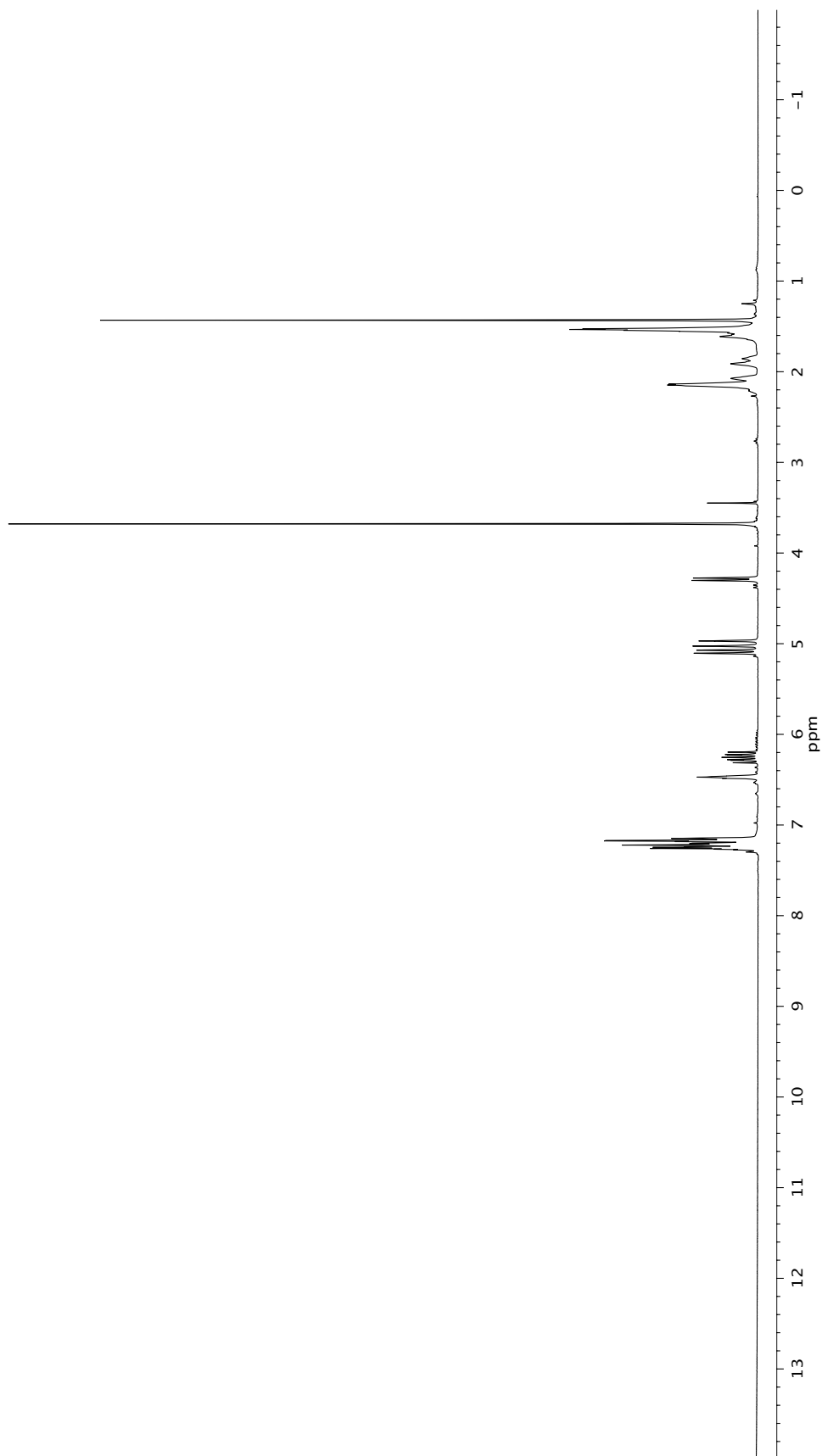


Figure A6.76 ¹H NMR (500 MHz, CDCl₃) of compound 112w.

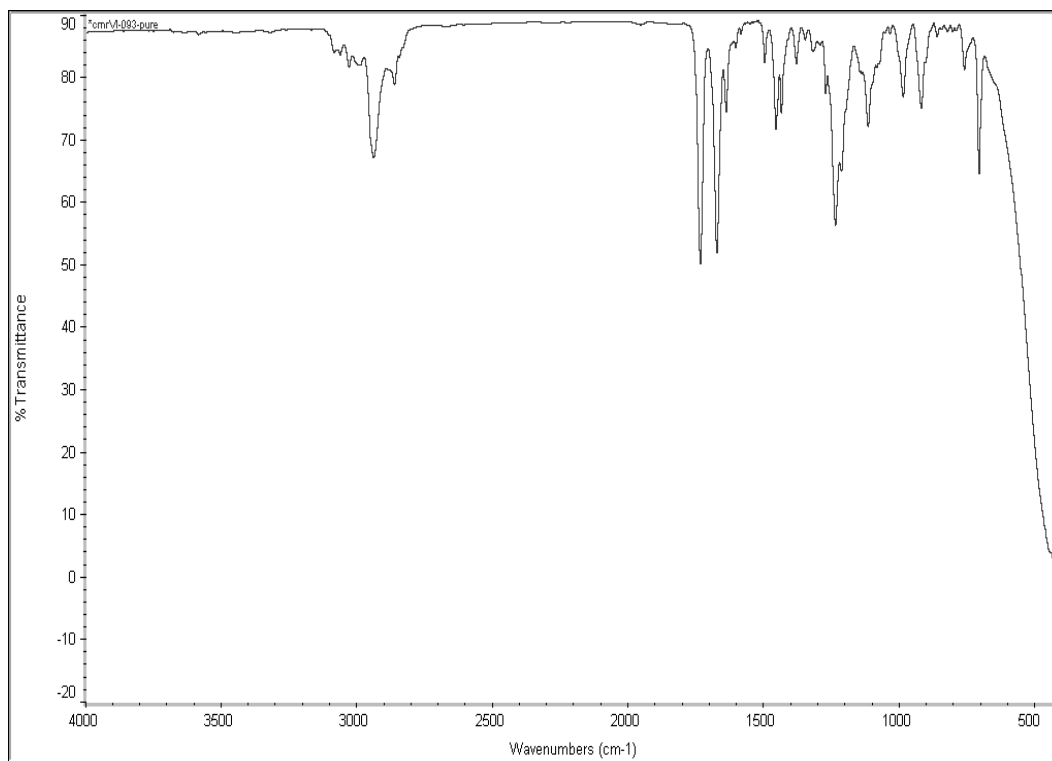


Figure A6.77 Infrared spectrum (thin film/NaCl) of compound **112w**.

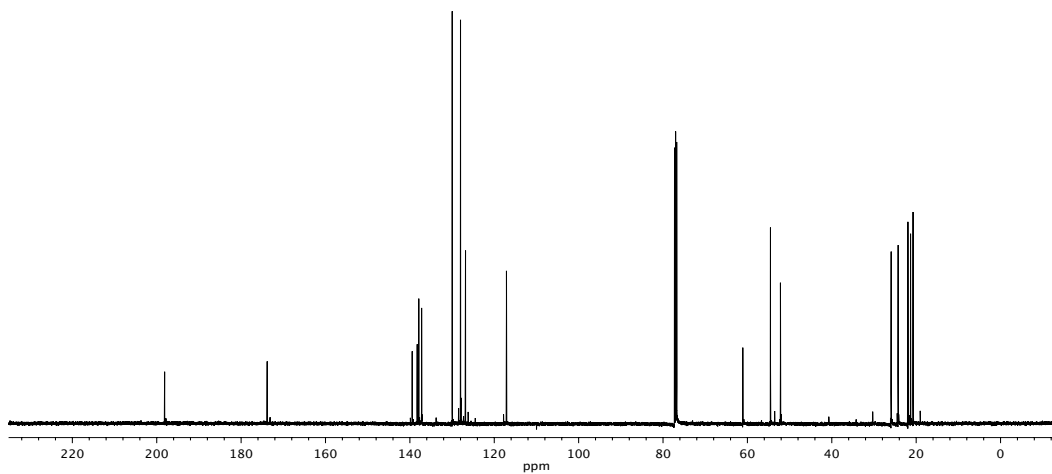


Figure A6.78 ^{13}C NMR (125 MHz, CDCl_3) of compound **112w**.

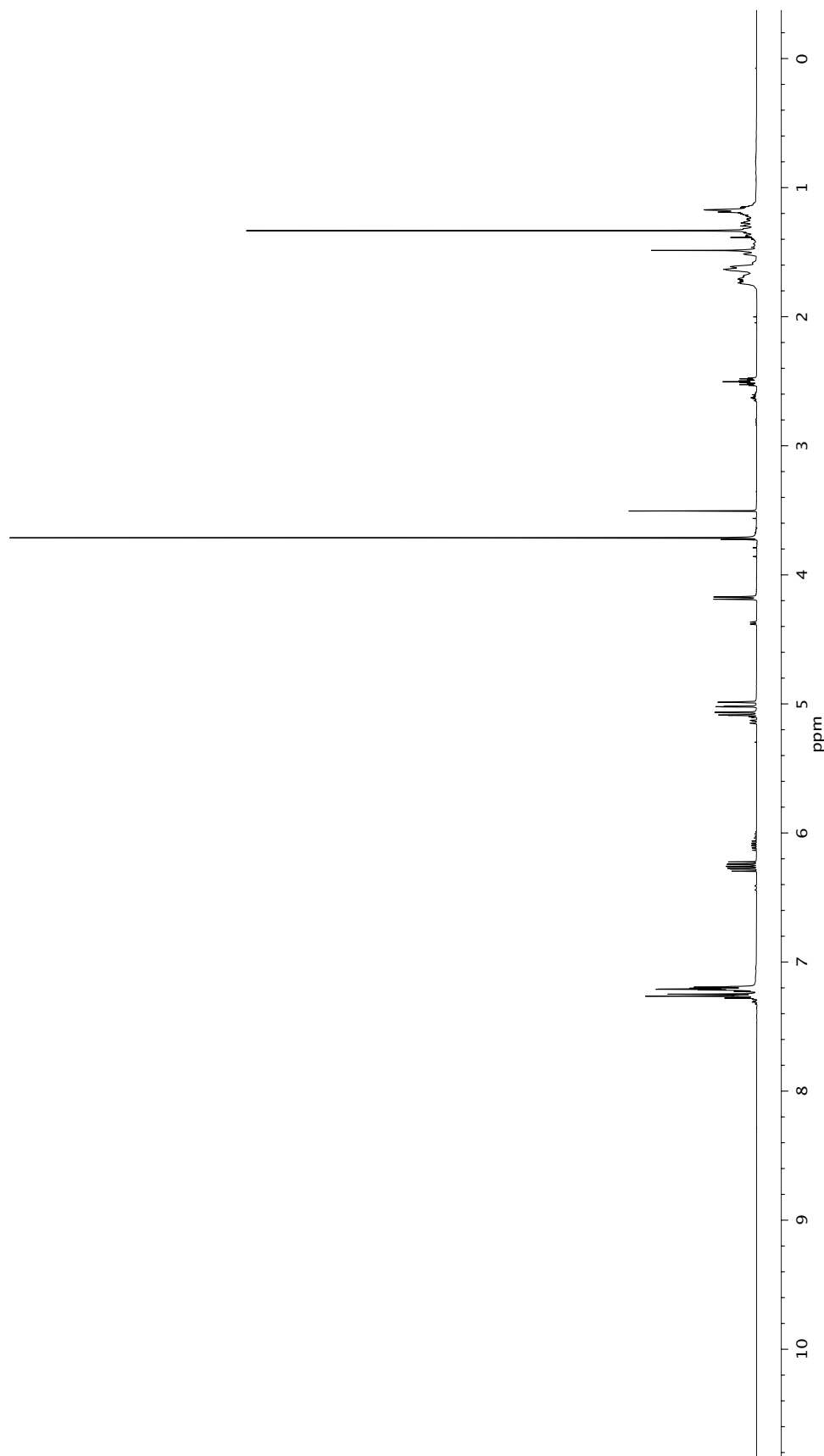
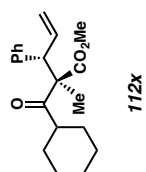


Figure A6.79 ¹H NMR (500 MHz, CDCl₃) of compound **112x**.

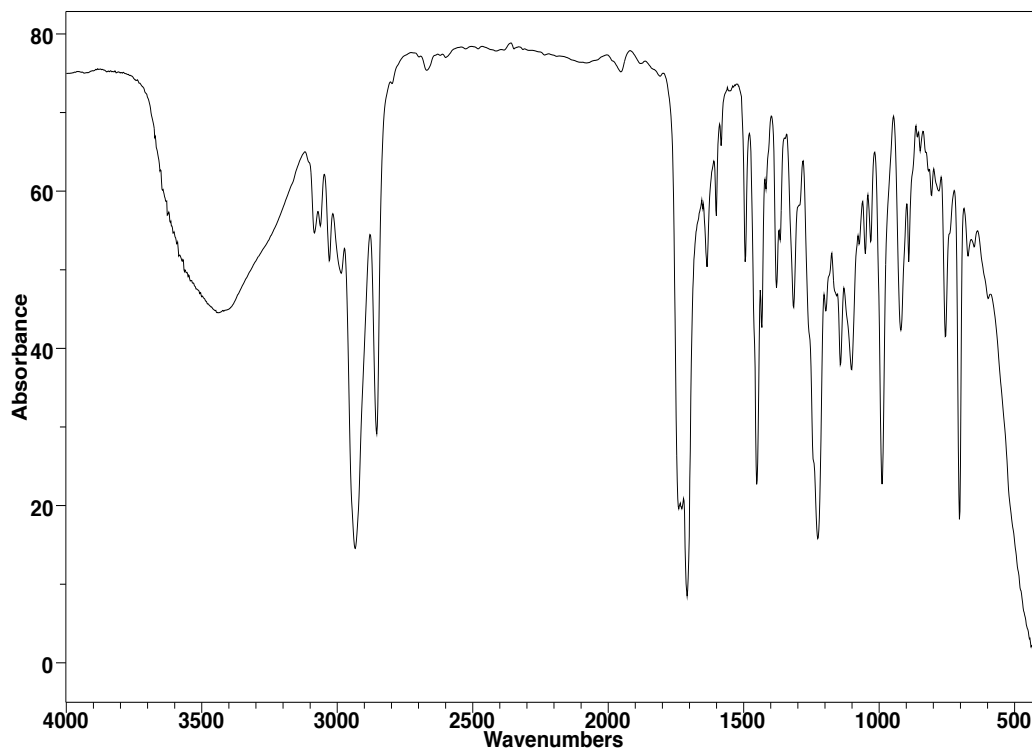


Figure A6.80 Infrared spectrum (thin film/NaCl) of compound **112x**.

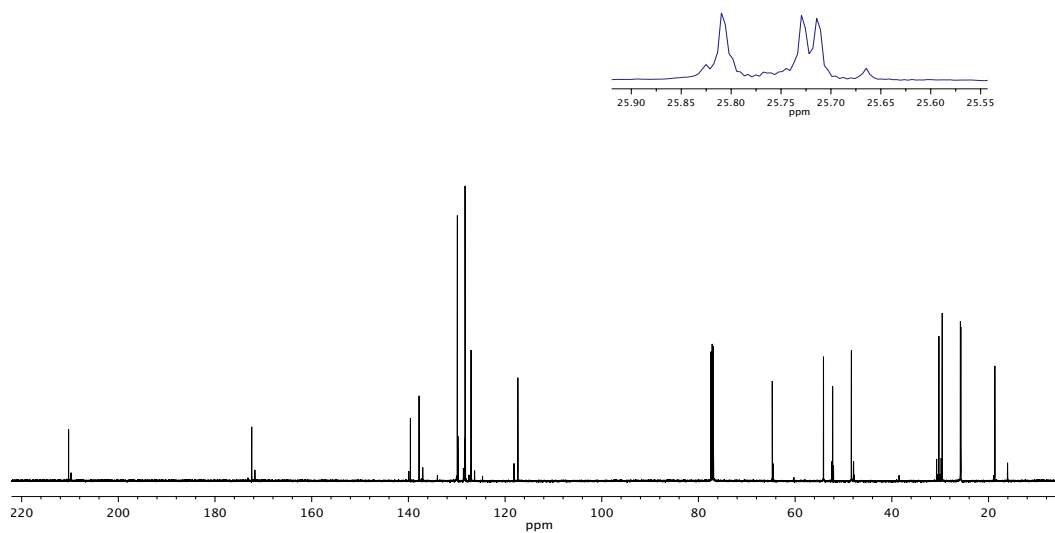


Figure A6.81 ¹³C NMR (125 MHz, CDCl₃) of compound **112x**.

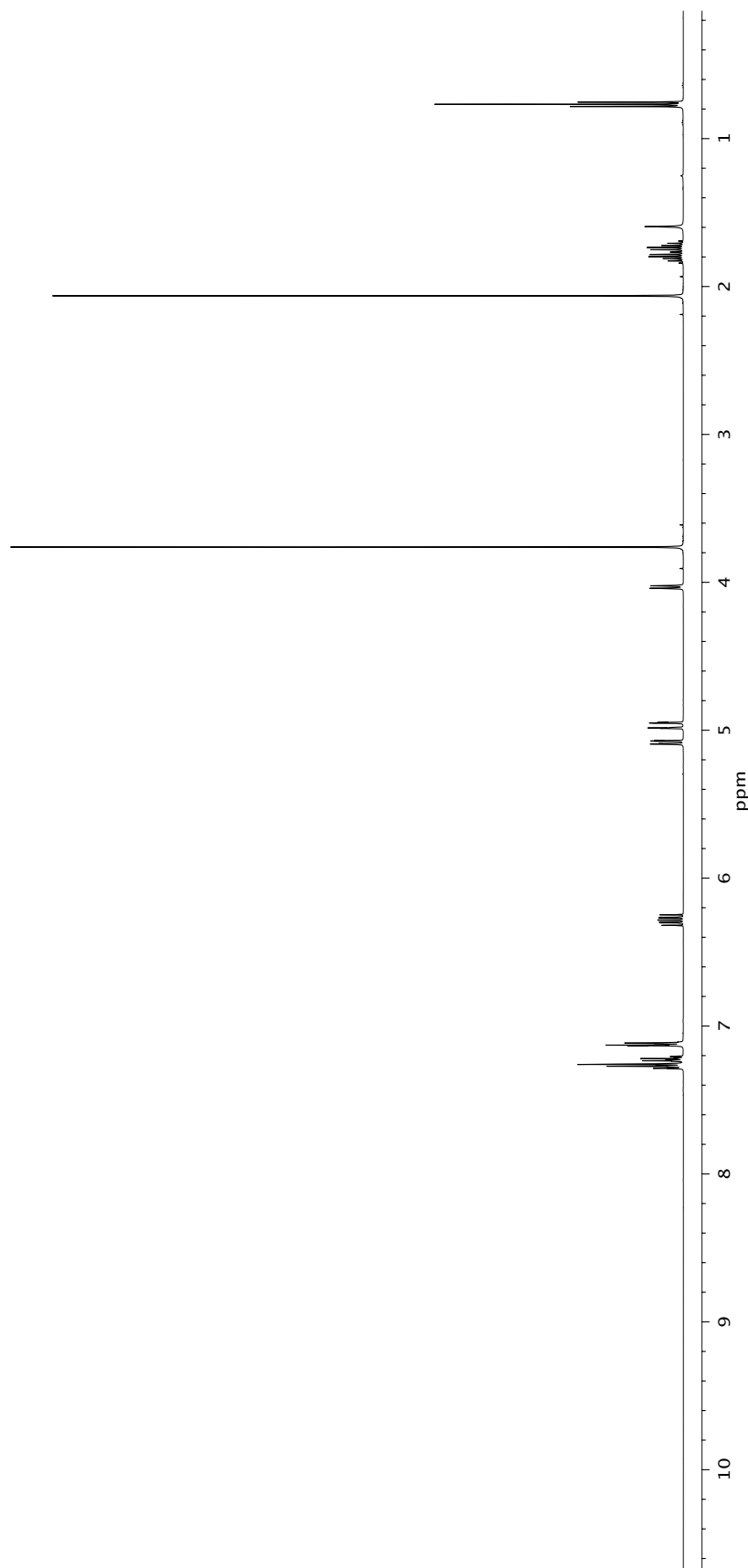
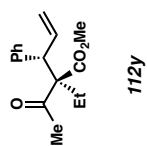


Figure A6.82 ¹H NMR (500 MHz, CDCl₃) of compound 112y.

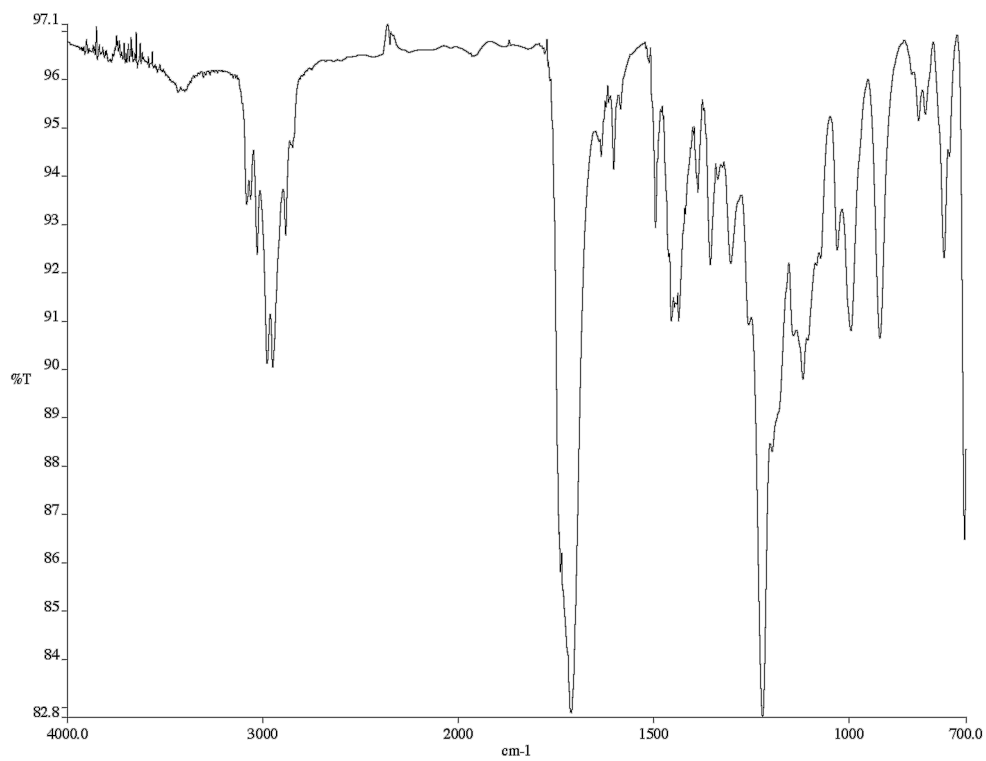


Figure A6.83 Infrared spectrum (thin film/NaCl) of compound **112y**.

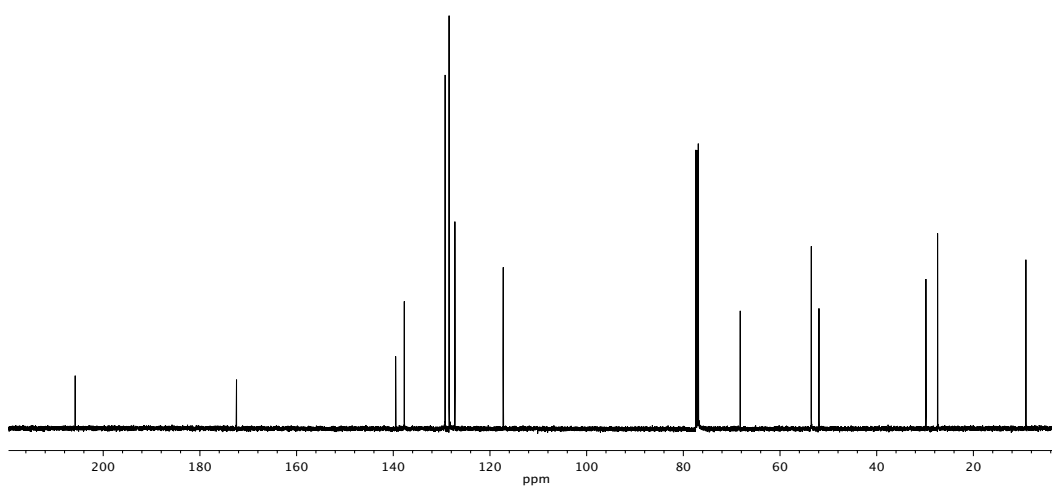


Figure A6.84 ¹³C NMR (125 MHz, CDCl₃) of compound **112y**.

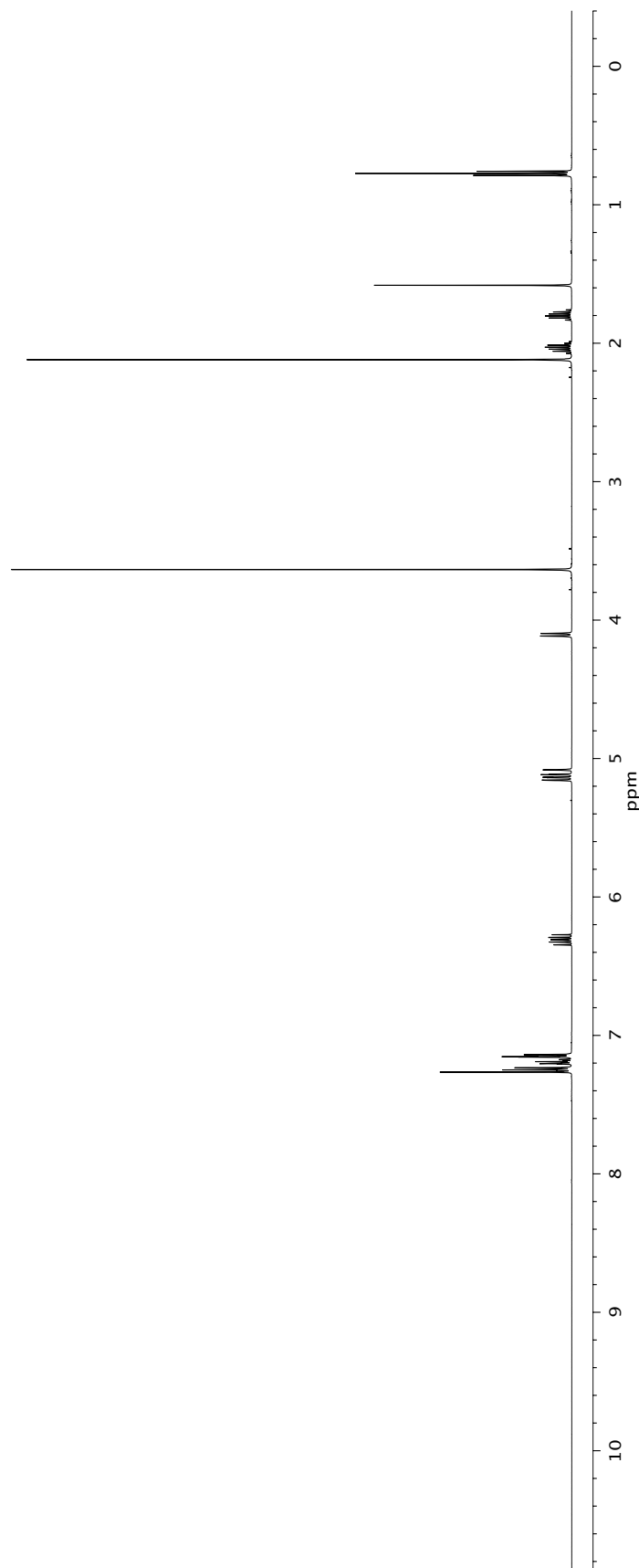
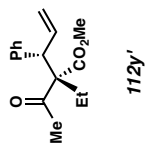


Figure A6.85 ¹H NMR (500 MHz, CDCl₃) of compound **112y**.

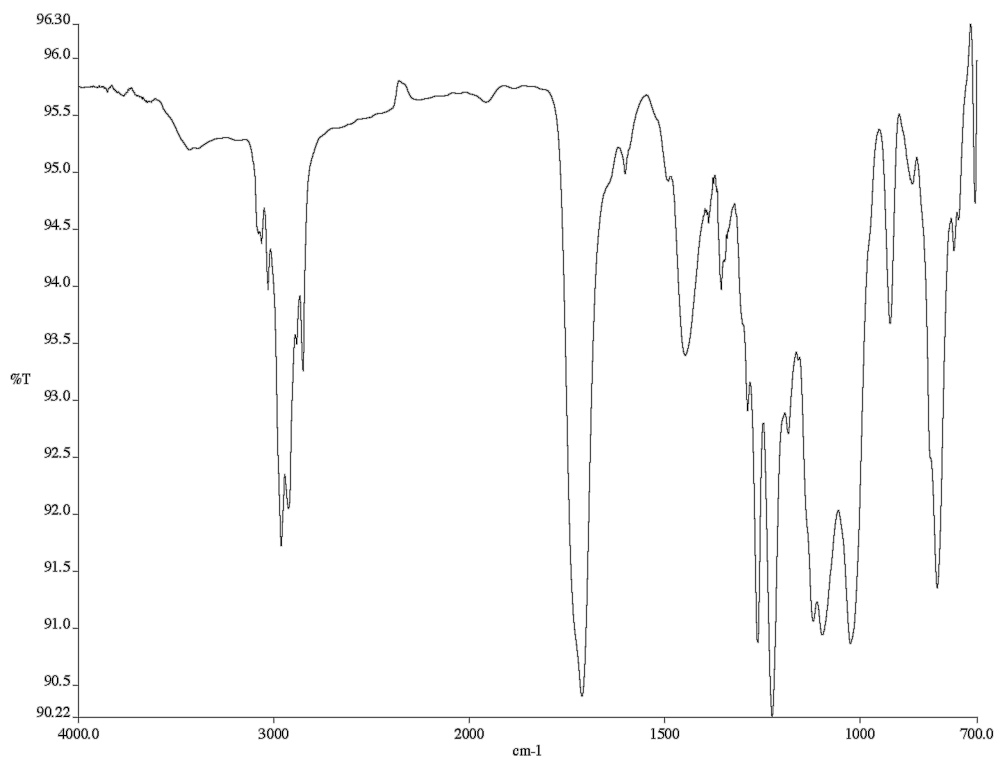


Figure A6.86 Infrared spectrum (thin film/NaCl) of compound **112y'**.

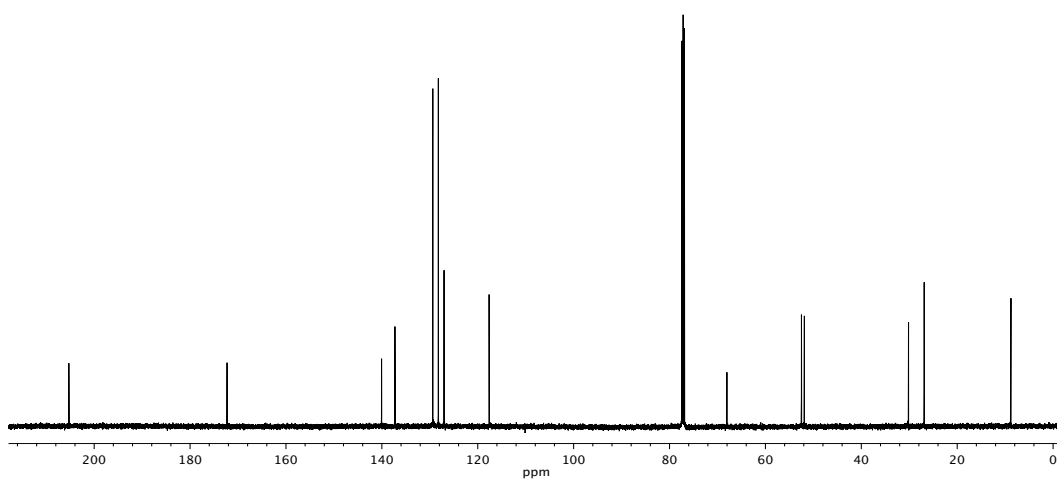


Figure A6.87 ^{13}C NMR (125 MHz, CDCl_3) of compound **112y'**.

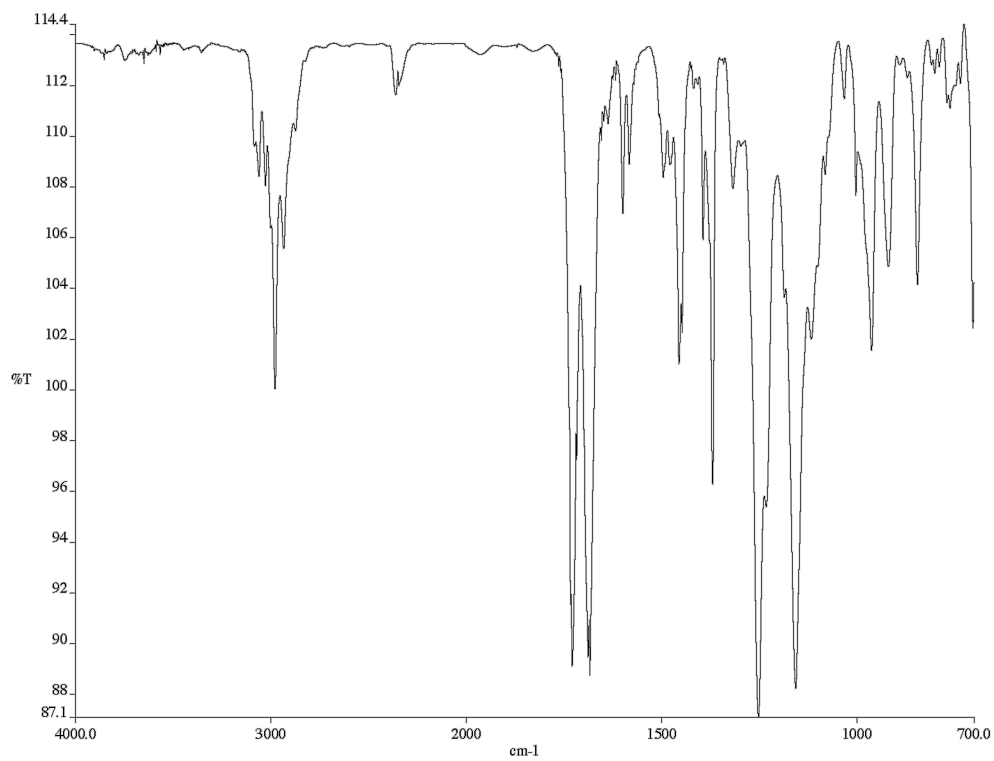


Figure A6.89 Infrared spectrum (thin film/NaCl) of compound **112z**.

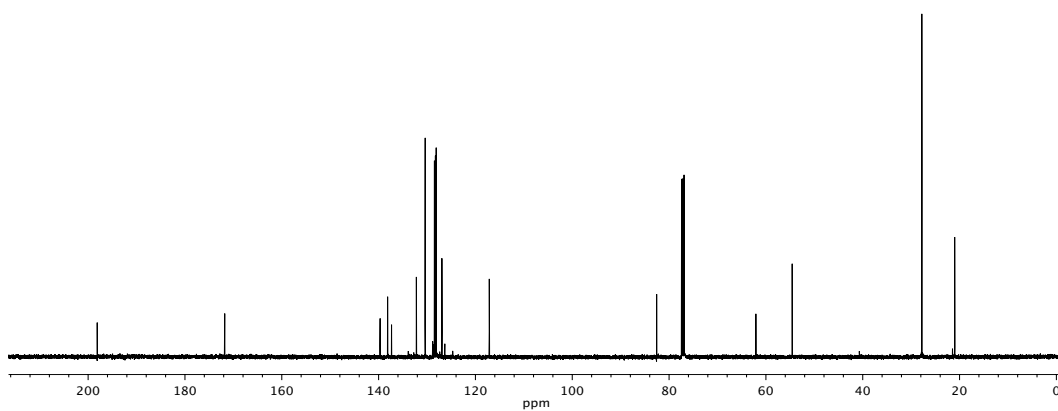


Figure A6.90 ¹³C NMR (125 MHz, CDCl₃) of compound **112z**.

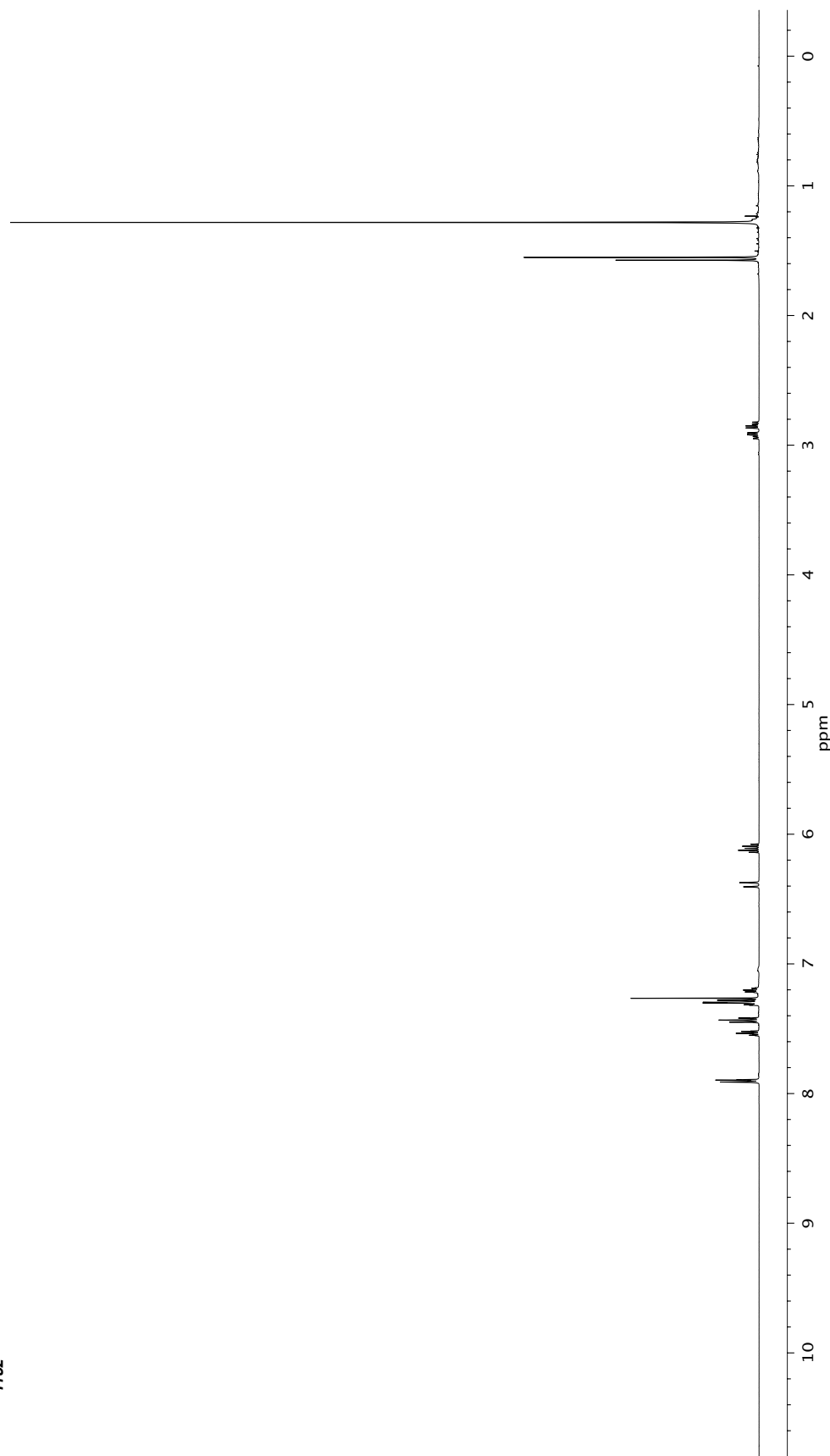
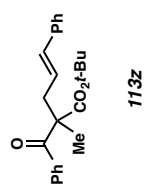


Figure A6.91 ¹H NMR (500 MHz, CDCl₃) of compound **113z**.

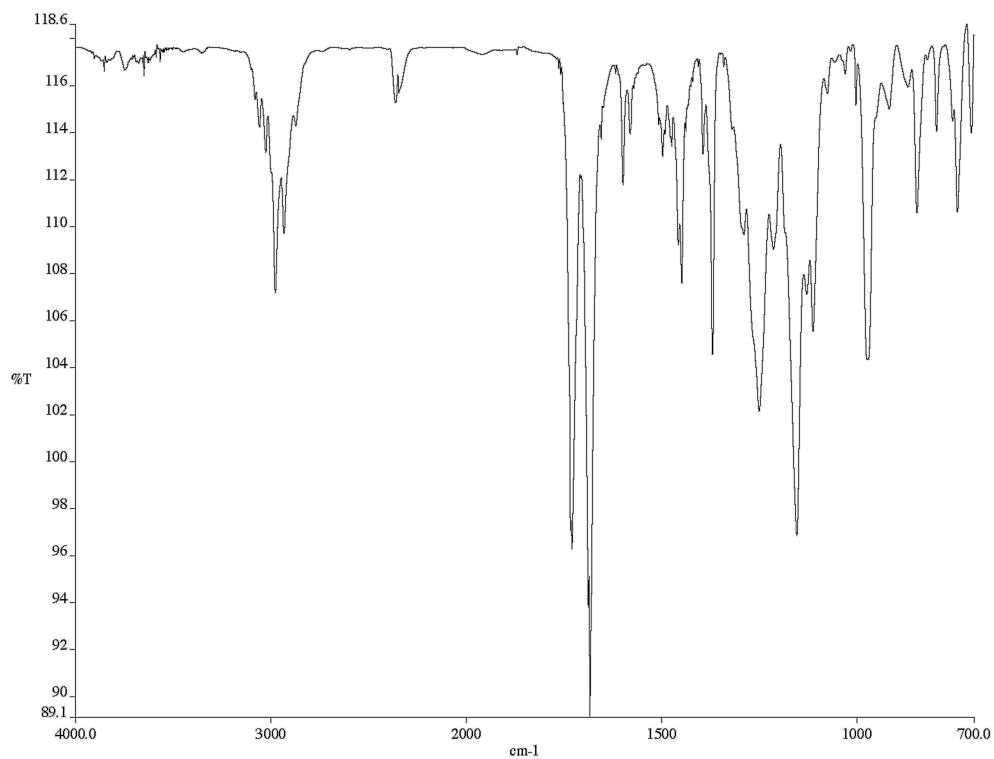


Figure A6.92 Infrared spectrum (thin film/NaCl) of compound **113z**.

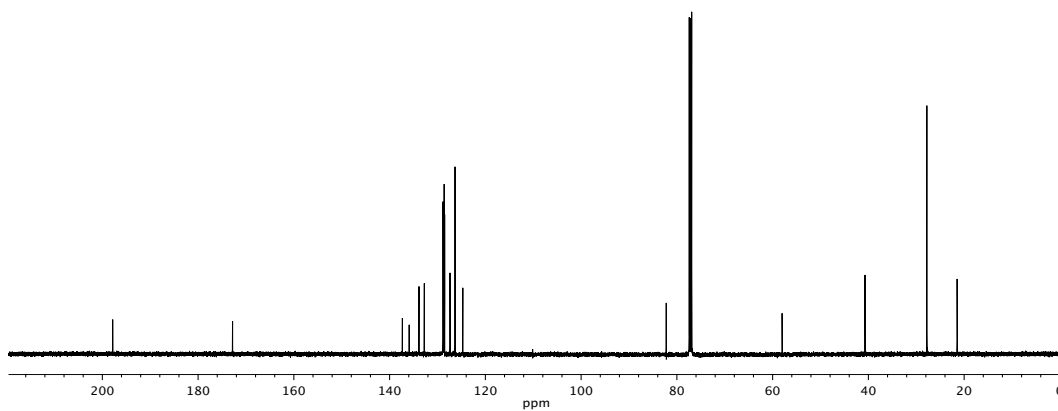


Figure A6.93 ¹³C NMR (125 MHz, CDCl₃) of compound **113z**.

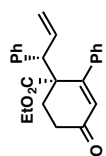
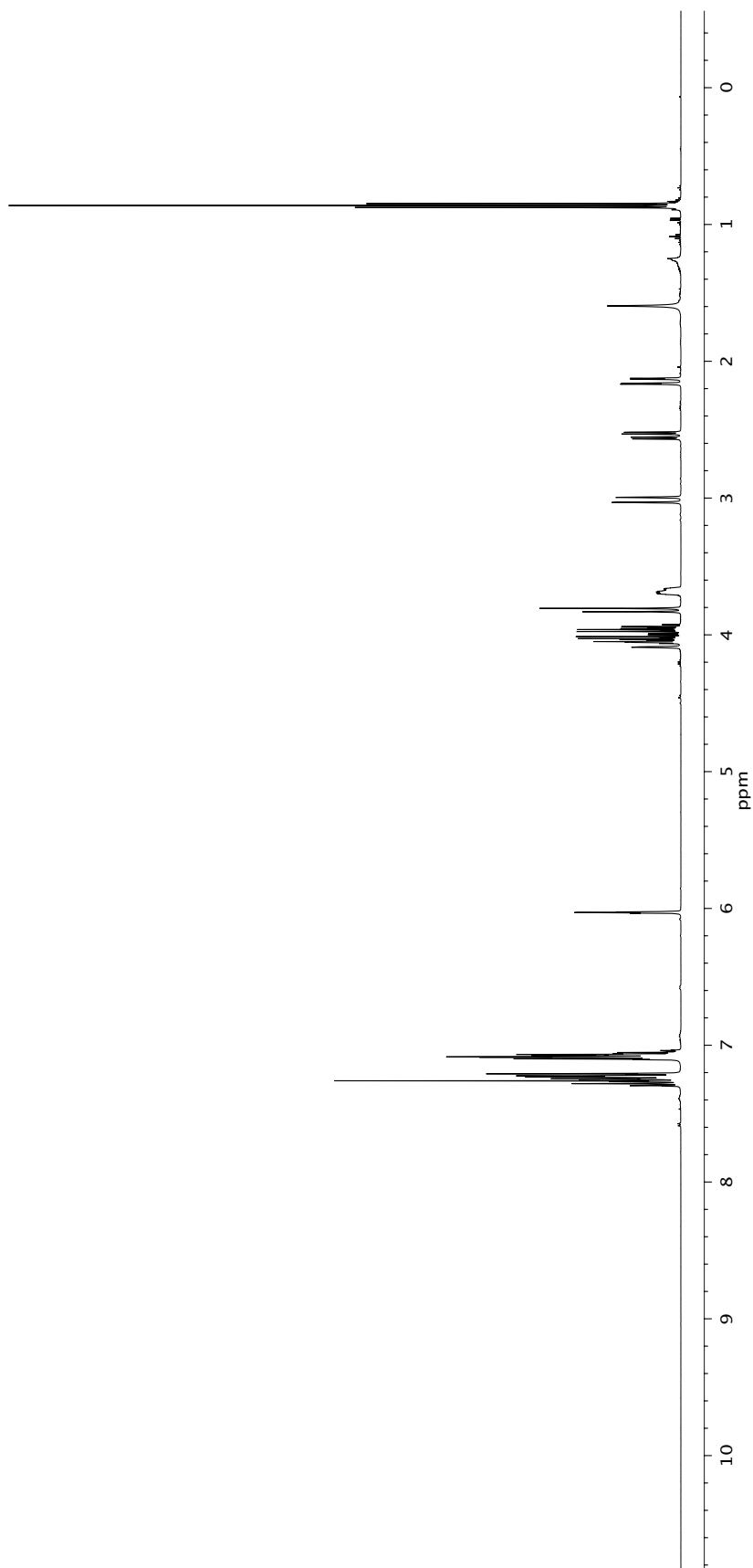
**114**

Figure A6.94 ¹H NMR (500 MHz, CDCl₃) of compound **114**.

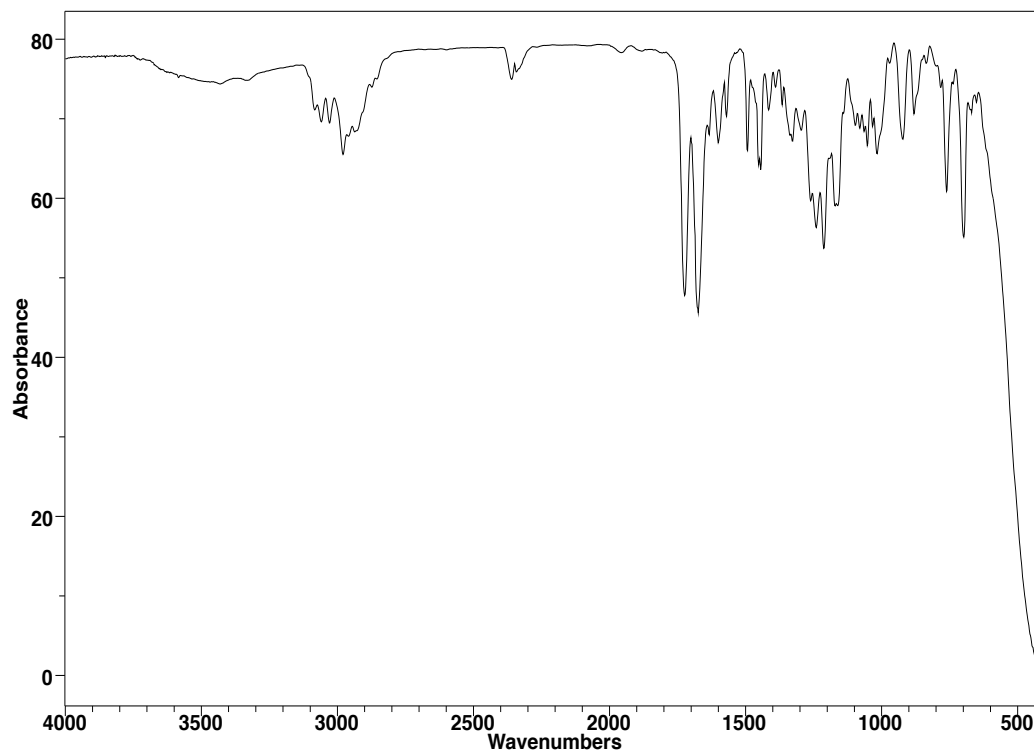


Figure A6.95 Infrared spectrum (thin film/NaCl) of compound **114**.

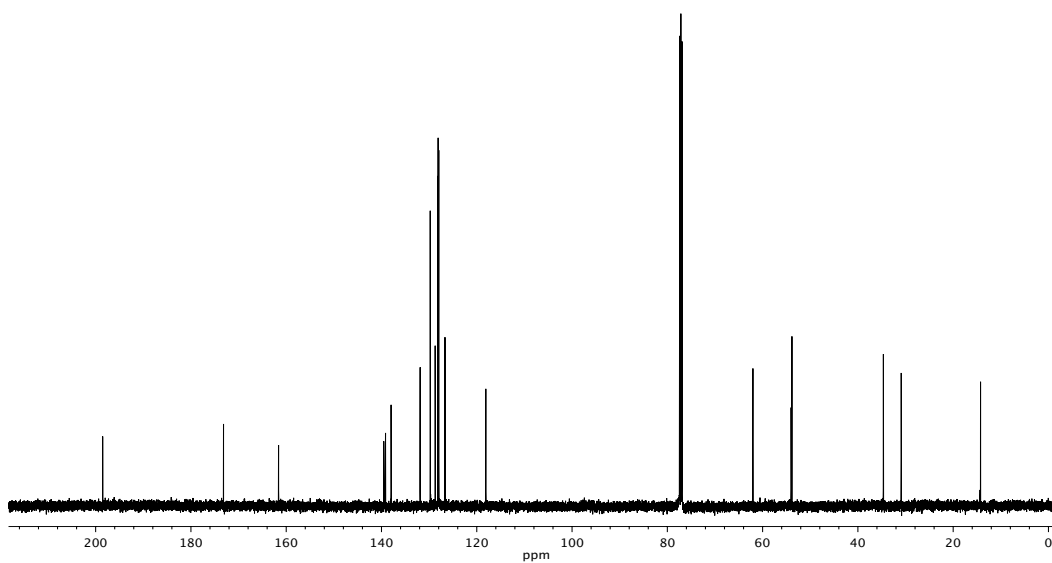
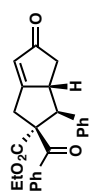
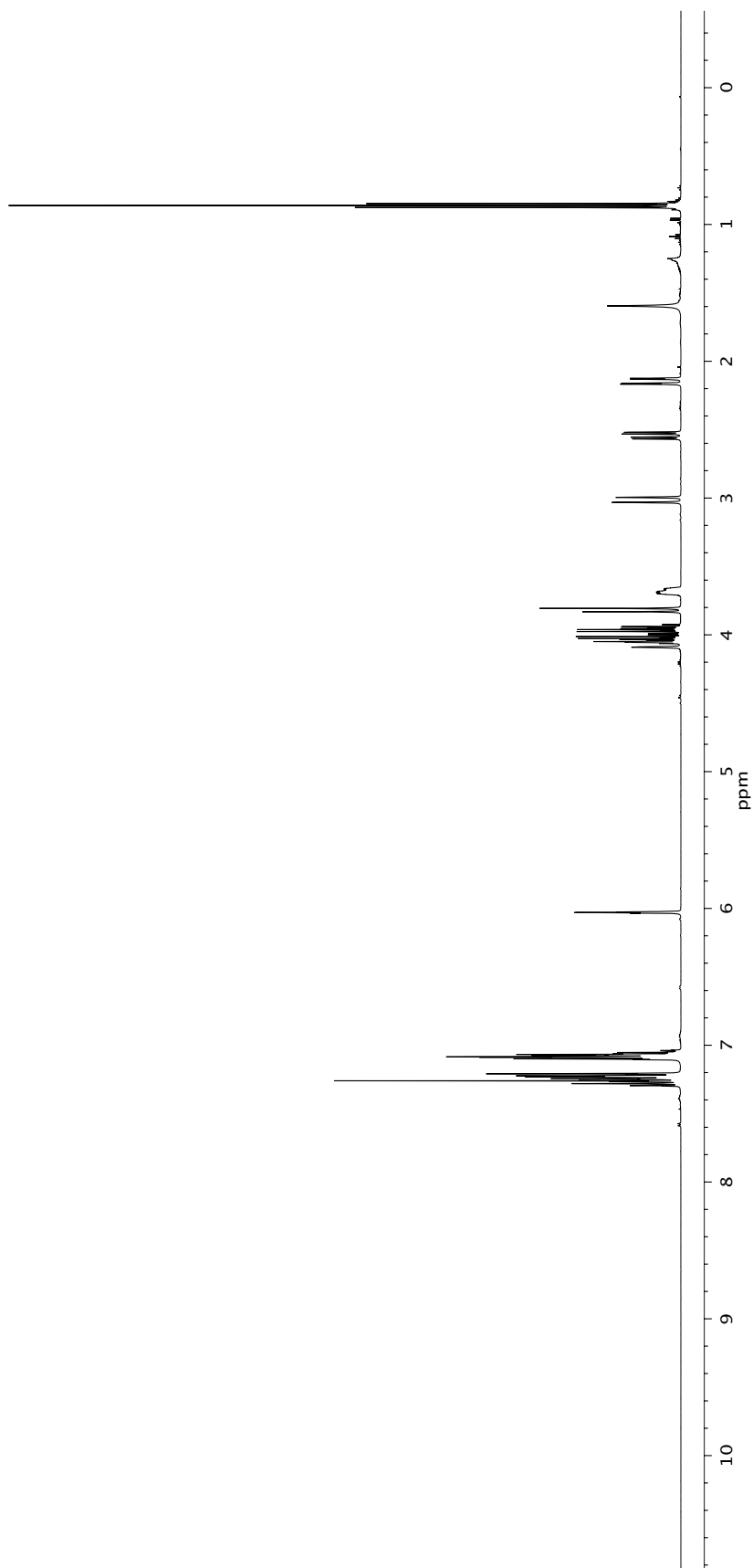


Figure A6.96 ¹³C NMR (125 MHz, CDCl₃) of compound **114**.



116

Figure A6.97 ¹H NMR (500 MHz, CDCl₃) of compound **116**.

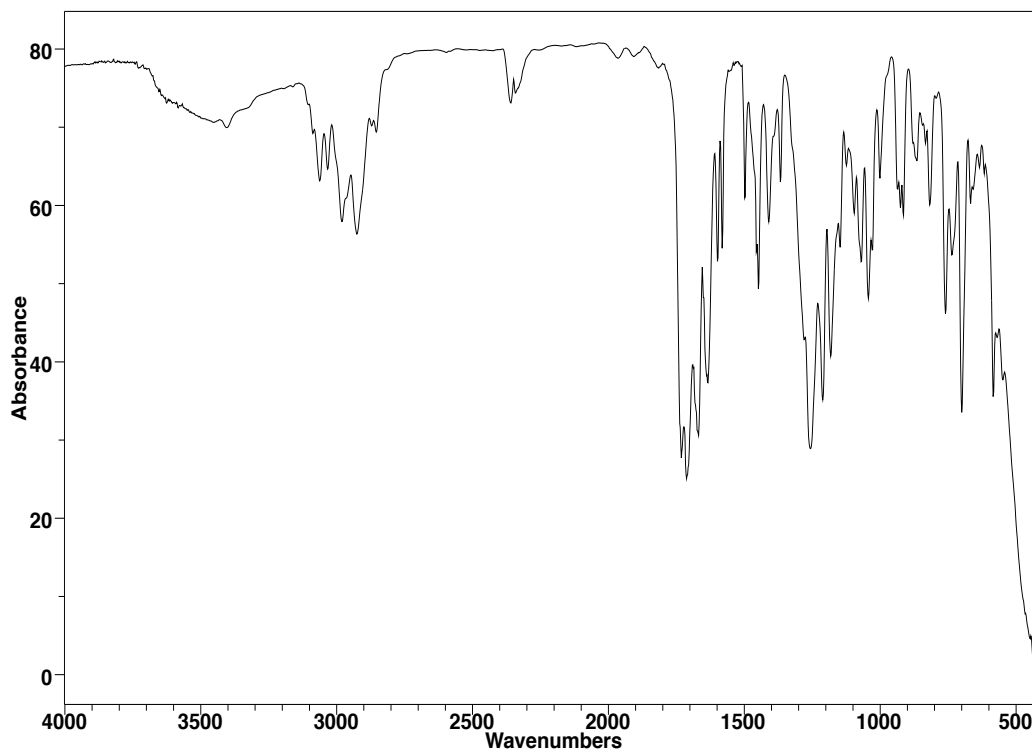


Figure A6.98 Infrared spectrum (thin film/NaCl) of compound **116**.

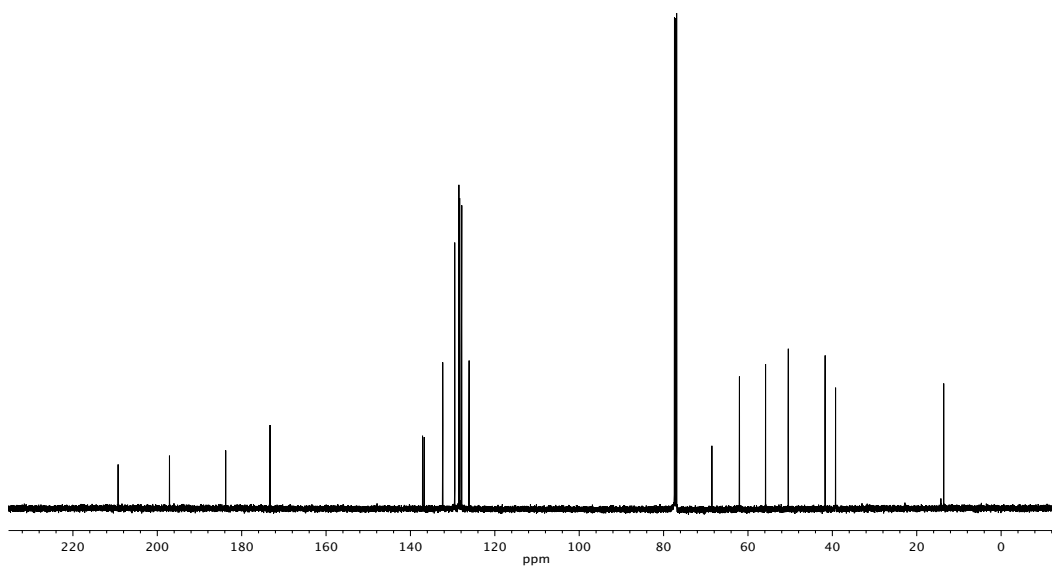
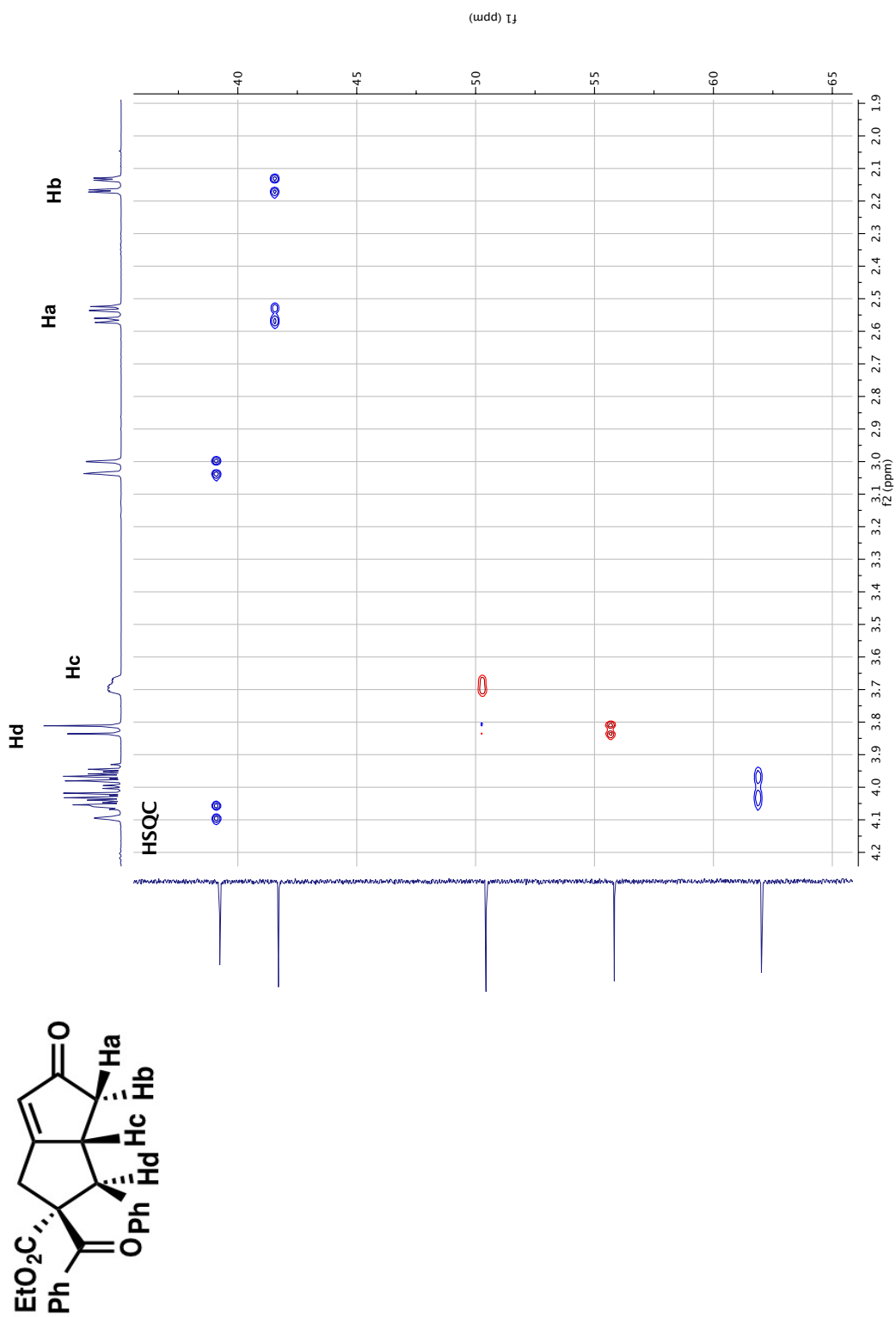
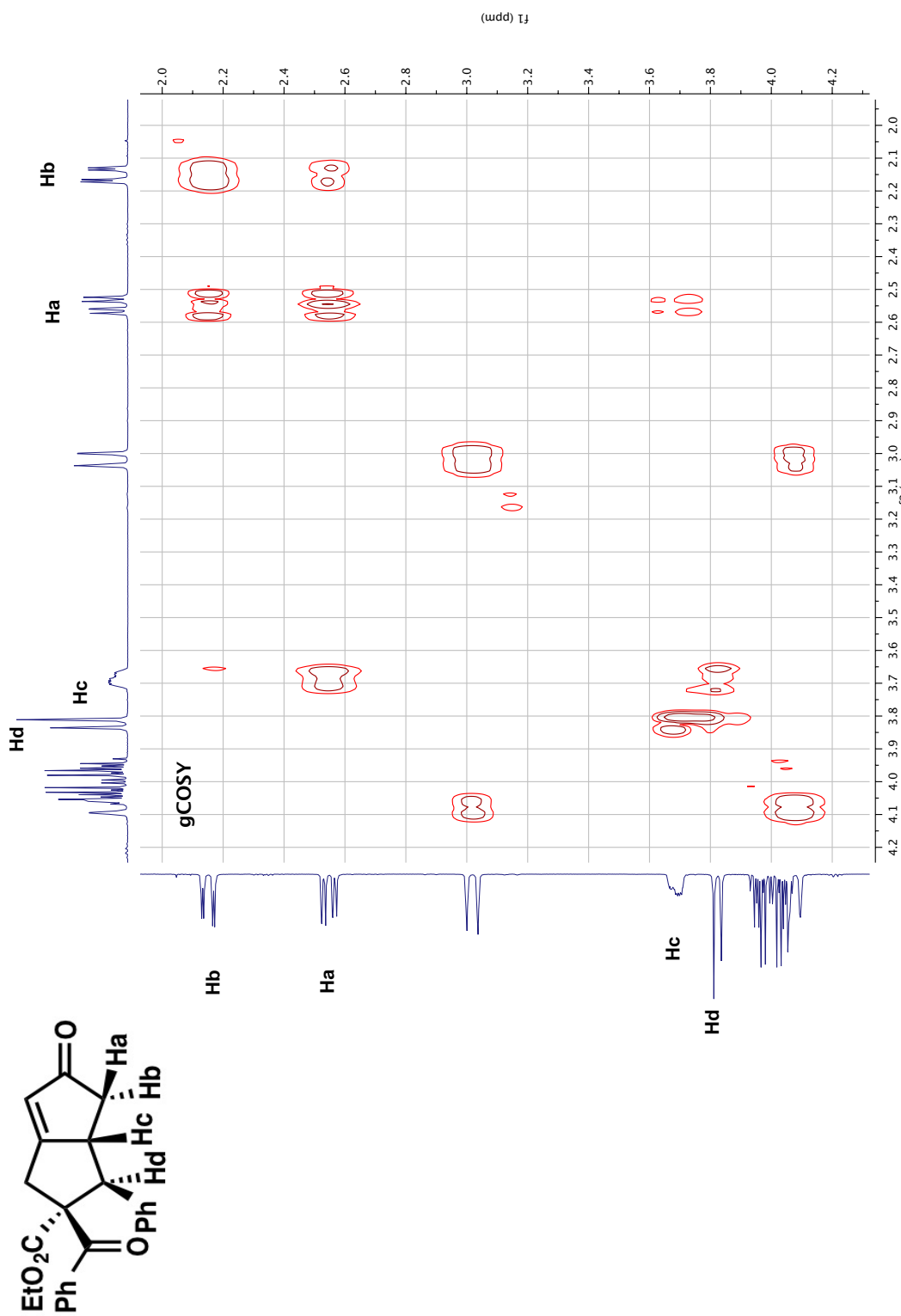
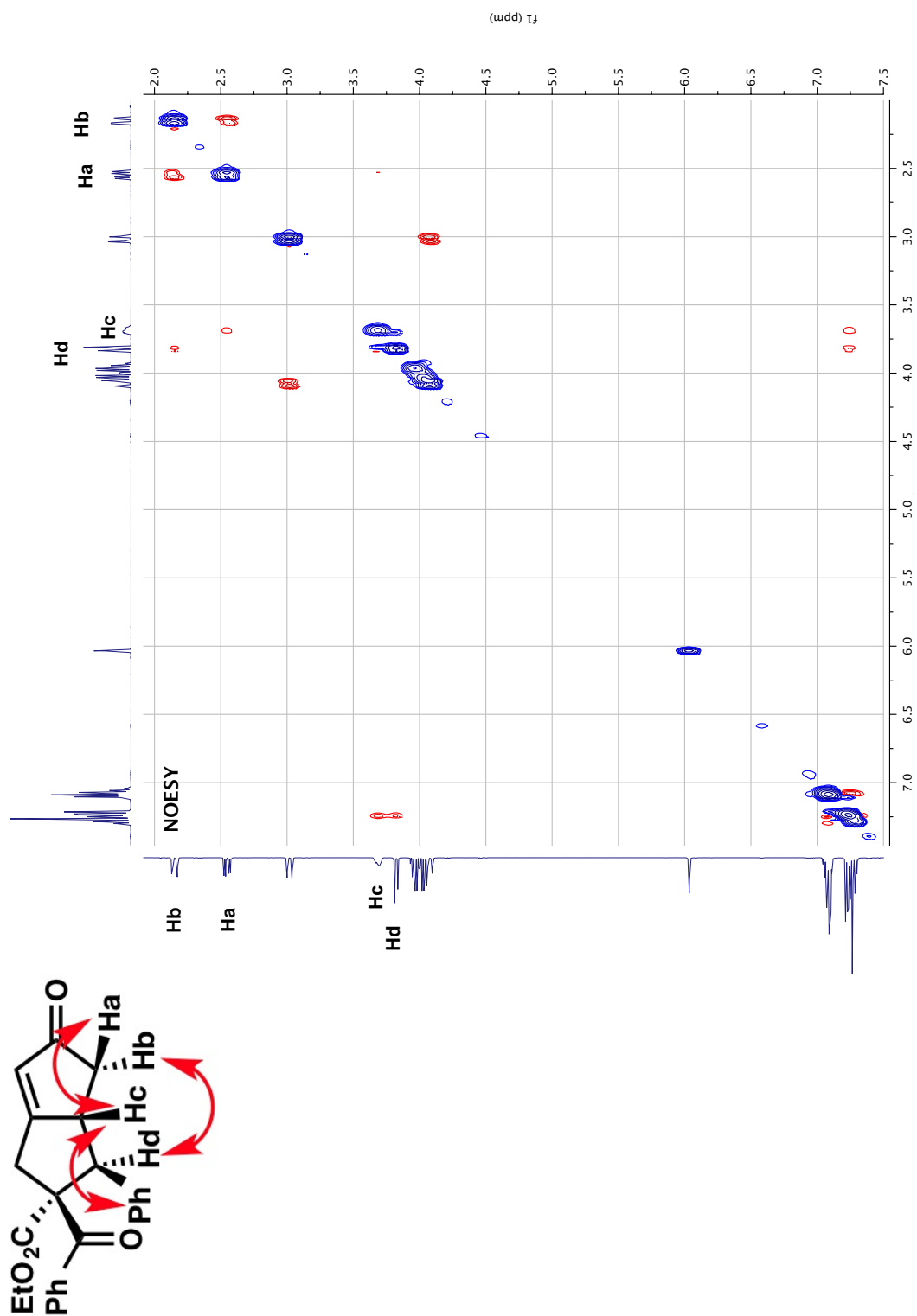


Figure A6.99 ¹³C NMR (125 MHz, CDCl₃) of compound **116**.

Figure A6.100 HSQC NMR (500 MHz, CDCl₃) of compound 116.

Figure A6.101 gCOSY NMR (500 MHz, CDCl₃) of compound 116.

Figure A6.102 NOESY NMR (500 MHz, CDCl₃) of compound 116.

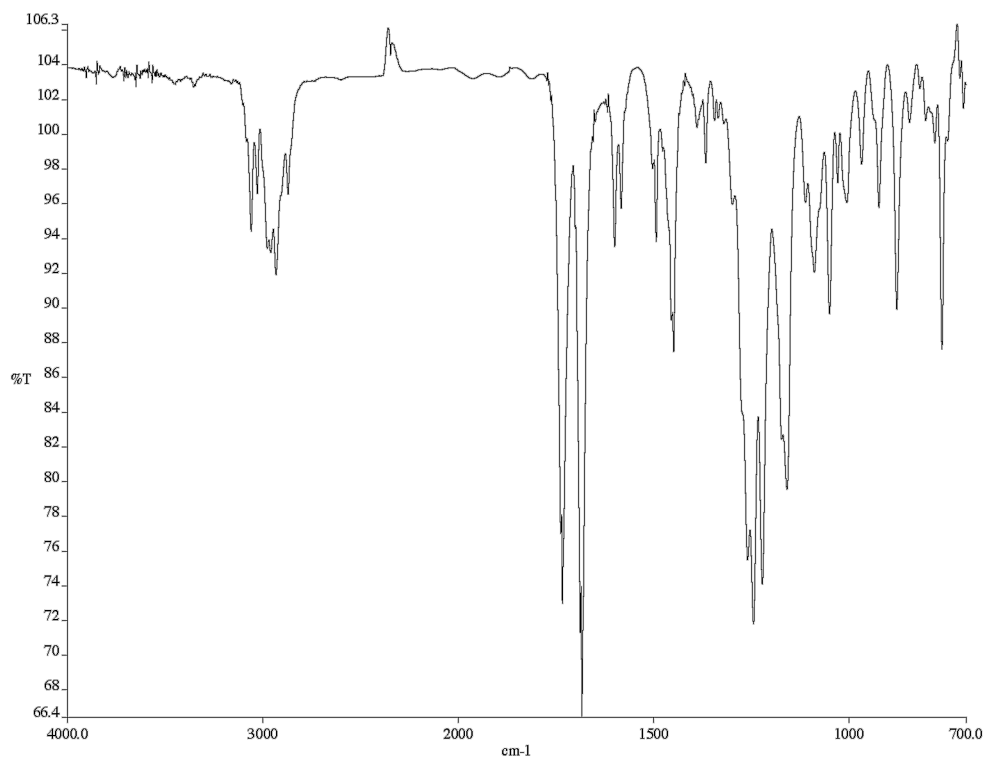


Figure A6.104 Infrared spectrum (thin film/NaCl) of compound **115**.

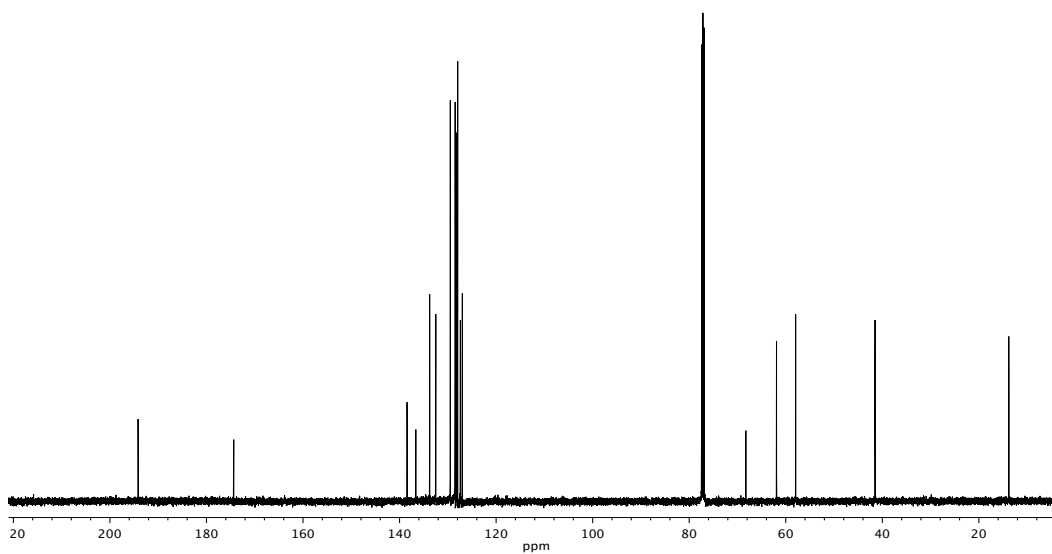


Figure A6.105 ¹³C NMR (125 MHz, CDCl₃) of compound **115**.

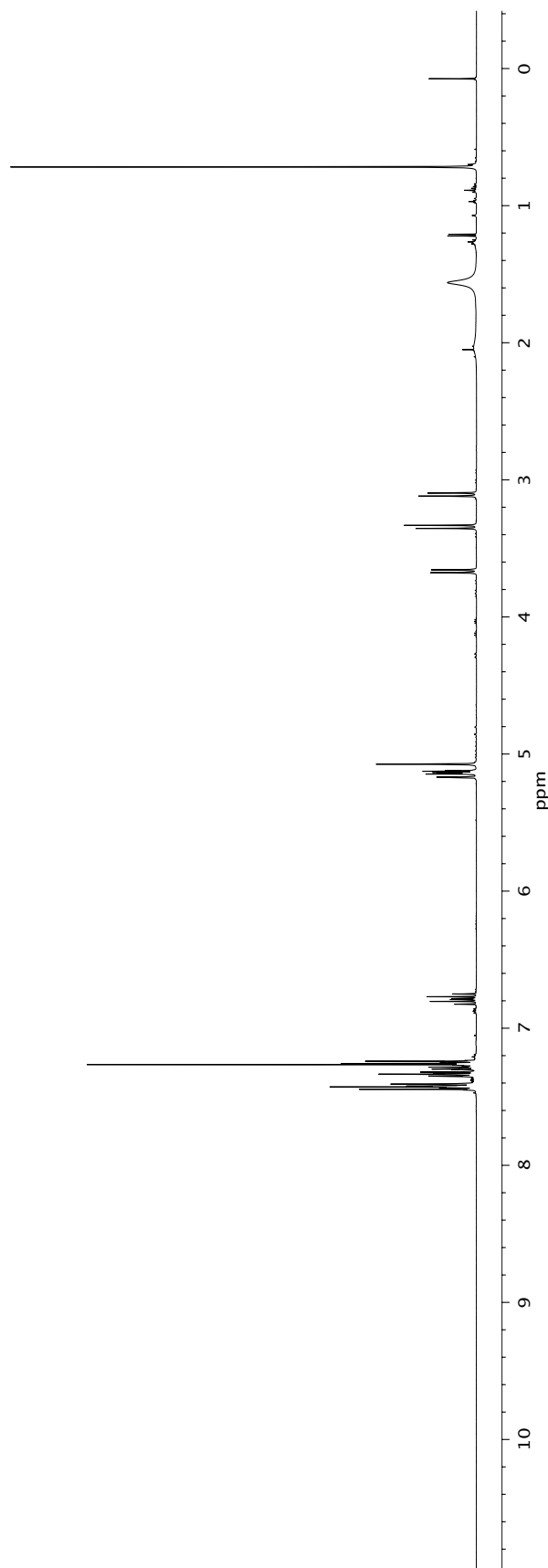
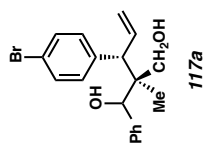


Figure A6.106 ¹H NMR (500 MHz, CDCl₃) of compound **117a**.

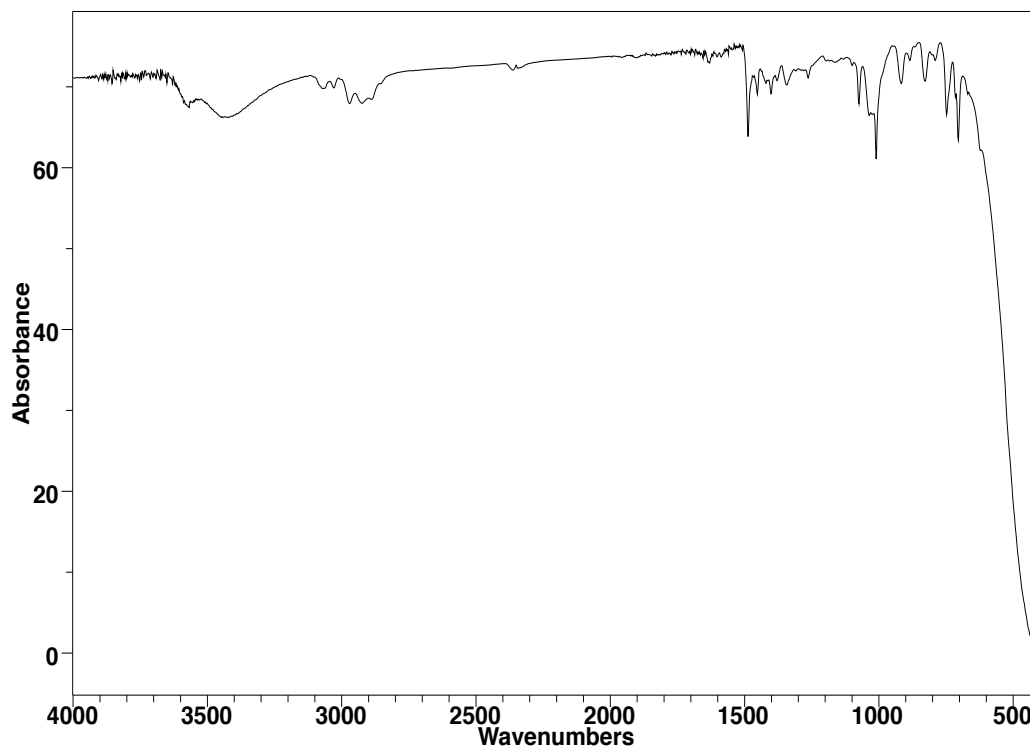


Figure A6.107 Infrared spectrum (thin film/NaCl) of compound **117a**.

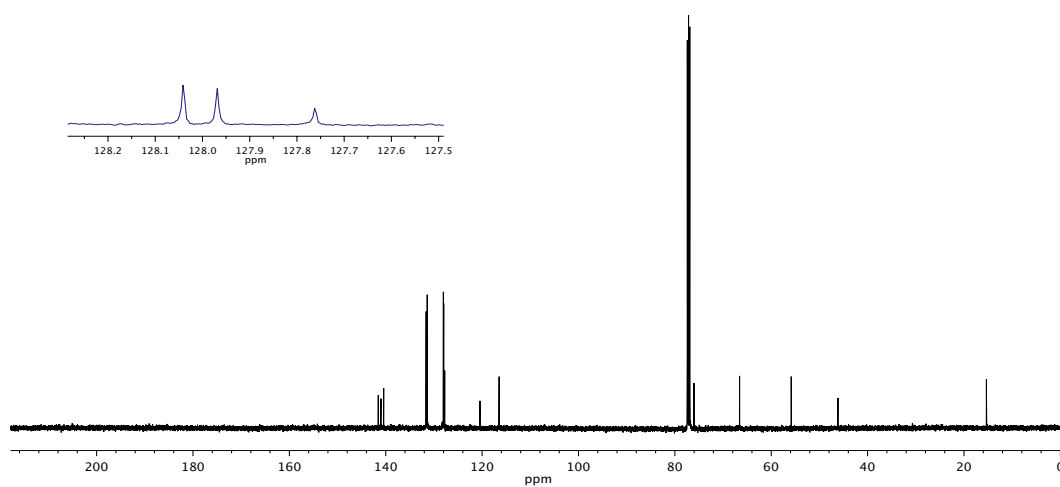


Figure A6.108 ¹³C NMR (125 MHz, CDCl₃) of compound **117a**.

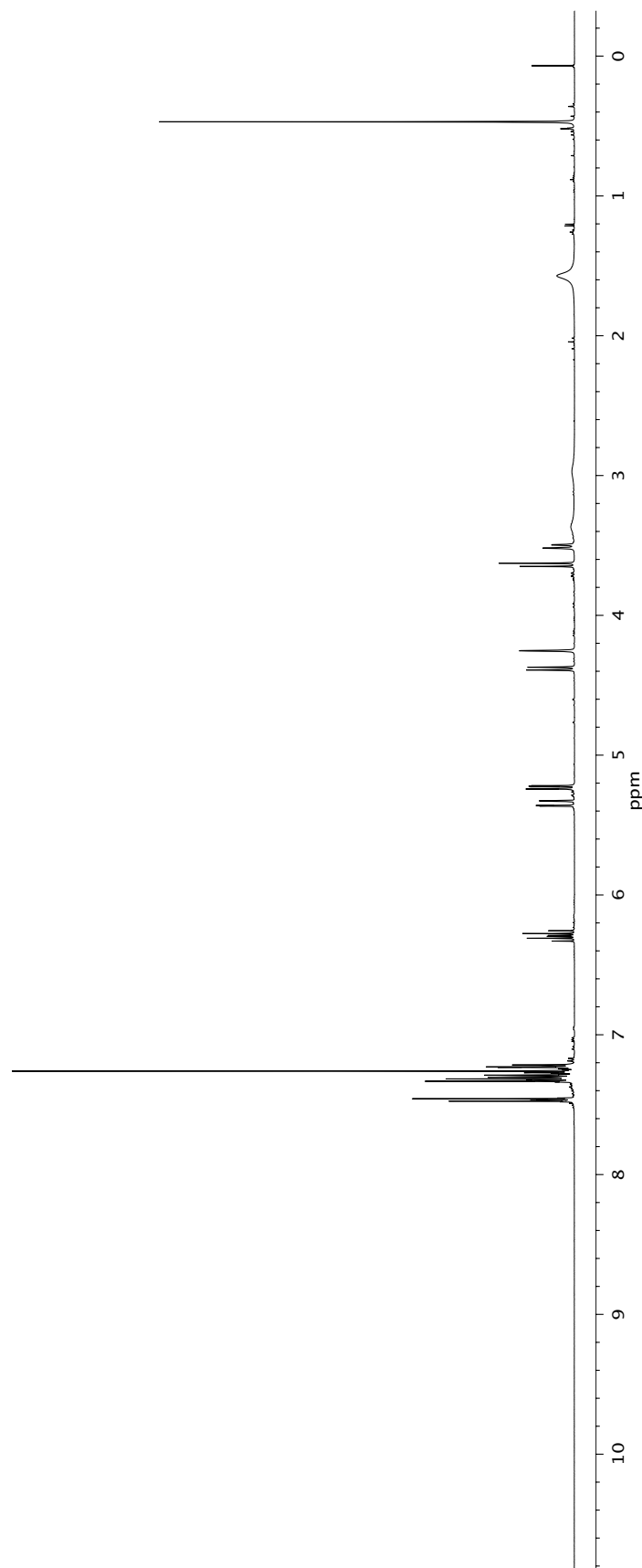
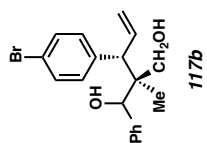


Figure A6.109 ¹H NMR (500 MHz, CDCl₃) of compound **117b**.

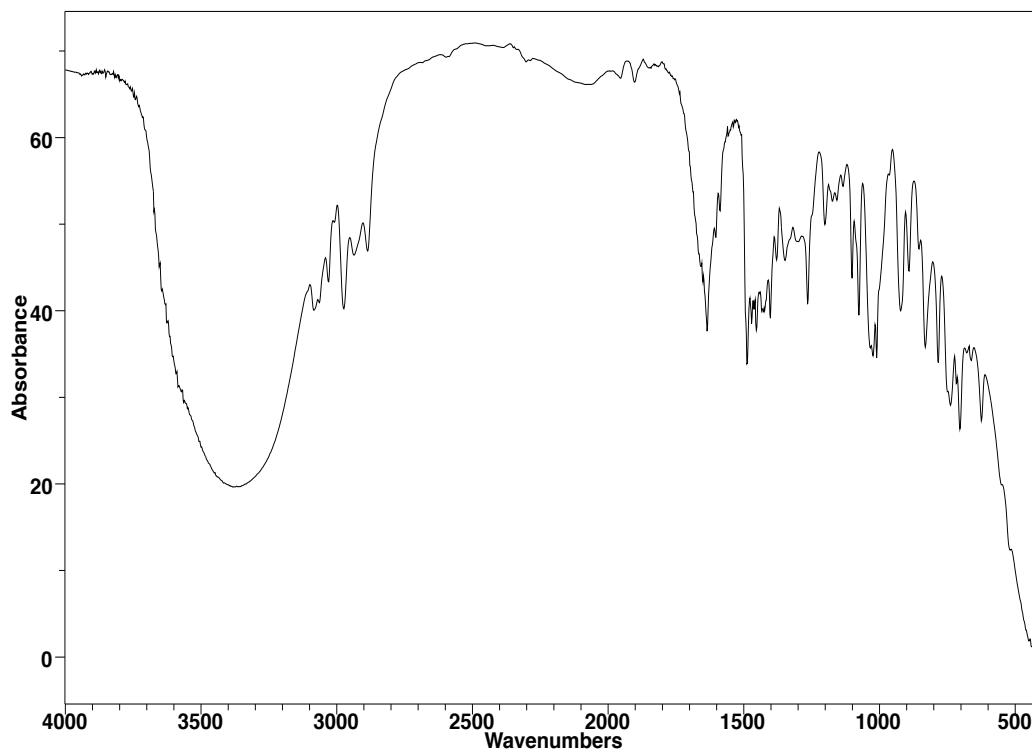


Figure A6.110 Infrared spectrum (thin film/NaCl) of compound **117b**.

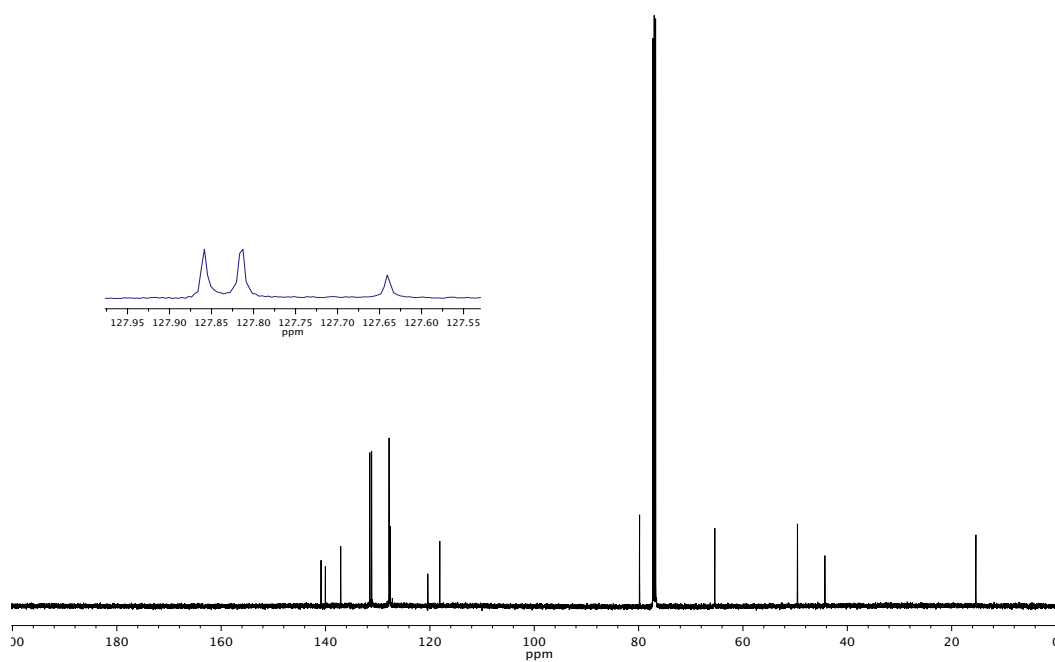


Figure A6.111 ¹³C NMR (125 MHz, CDCl₃) of compound **117b**.

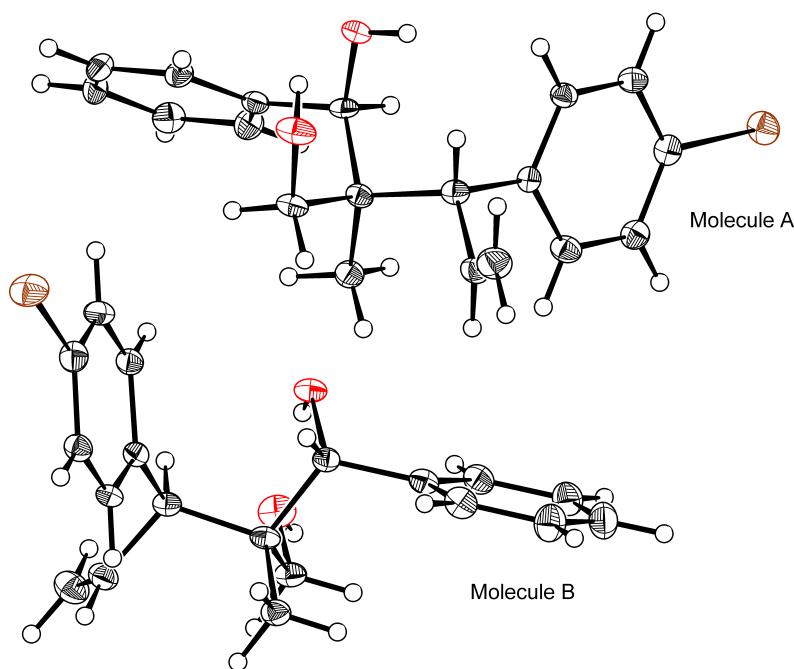
APPENDIX 7

X-ray Crystallography Reports

Relevant to Chapter 4

A7.1 CRYSTAL STRUCTURE ANALYSIS FOR COMPOUND 117

The *mixture of diastereomers 117* were recrystallized from *i*-PrOH/heptane (liquid/liquid diffusion) to provide crystals suitable for X-ray analysis. NOTE: *Crystallographic data have been deposited in the Cambridge Database (CCDC), 12 Union Road, Cambridge CB2 1EZ, UK, and copies can be obtained on request, free of charge, by quoting the publication citation and the deposition number CCDC 959511.*

Figure A7.1.1. ORTEP drawing of **117**.**Table A7.1.** Crystal Data and Structure Analysis Details for diol **117**.

Empirical formula	C ₁₉ H ₂₁ Br O ₂
Formula weight	361.27
Crystallization solvent	<i>i</i> -PrOH/heptane
Crystal shape	plate
Crystal color	colourless
Crystal size	0.06 x 0.16 x 0.45 mm

Data Collection

Preliminary photograph(s)	rotation	
Type of diffractometer	Bruker APEX-II CCD	
Wavelength	0.71073 Å MoK	
Data collection temperature	100 K	
Theta range for 9925 reflections used in lattice determination	2.31 to 24.19°	
Unit cell dimensions	a = 11.871(3) Å	∠ = 90°
	b = 13.179(3) Å	⊕ = 90°
	c = 21.761(5) Å	⊙ = 90°
Volume	3404.5(13) Å ³	

Z	8
Crystal system	orthorhombic
Space group	P 21 21 21 (# 19)
Density (calculated)	1.410 g/cm ³
F(000)	1488
Theta range for data collection	1.8 to 32.3°
Completeness to theta = 25.000°	99.8%
Index ranges	-17 " h " 17, -19 " k " 19, -32 " l " 32
Data collection scan type	and scans
Reflections collected	88198
Independent reflections	11569 [R _{int} = 0.1174]
Reflections > 2 σ (I)	8213
Average σ (I)/(net I)	0.0905
Absorption coefficient	2.42 mm ⁻¹
Absorption correction	Semi-empirical from equivalents
Max. and min. transmission	1.0000 and 0.6406

Structure Solution and Refinement

Primary solution method	dual
Secondary solution method	?
Hydrogen placement	geom
Refinement method	Full-matrix least-squares on F ²
Data / restraints / parameters	11569 / 0 / 403
Treatment of hydrogen atoms	constr
Goodness-of-fit on F ²	1.31
Final R indices [I > 2 σ (I), 8213 reflections]	R1 = 0.0549, wR2 = 0.1052
R indices (all data)	R1 = 0.0967, wR2 = 0.1137
Type of weighting scheme used	calc
Weighting scheme used	$w = 1 / [\sigma^2(F_o^2) + (0.0300P)^2]$ where
$P = (F_o^2 + 2F_c^2) / 3$	
Max shift/error	0.000
Average shift/error	0.000
Absolute structure parameter	0.032(5)
Extinction coefficient	n/a
Largest diff. peak and hole	1.70 and -0.98 e ⁻ Å ⁻³

Programs Used

Cell refinement	SAINT V8.32B (Bruker-AXS, 2007)
Data collection	APEX2 2013.6-2 (Bruker-AXS, 2007)
Data reduction	SAINT V8.32B (Bruker-AXS, 2007)
Structure solution	SHELXT (Sheldrick, 2012)
Structure refinement	SHELXL-2013/2 (Sheldrick, 2013)
Graphics	DIAMOND 3 (Crystal Impact, 1999)

Table A7.2. Atomic coordinates ($\times 10^4$) and equivalent isotropic displacement parameters ($\text{\AA}^2 \times 10^3$) for **117**. $U(\text{eq})$ is defined as one third of the trace of the orthogonalized U^{ij} tensor.

	x	y	z	U_{eq}
Br(1)	6018(1)	702(1)	2623(1)	24(1)
Br(1B)	2988(1)	6376(1)	6793(1)	29(1)
O(1)	2594(3)	2303(2)	5173(1)	17(1)
O(1B)	7801(3)	4619(2)	5244(2)	18(1)
O(2B)	9886(3)	5315(3)	5428(2)	24(1)
O(2)	1686(3)	4120(3)	5230(2)	24(1)
C(12)	4092(4)	2845(3)	5863(2)	16(1)
C(18)	2777(4)	4578(3)	5206(2)	18(1)
C(9)	3015(5)	4701(4)	3852(2)	18(1)
C(18B)	9487(4)	6230(4)	5137(2)	19(1)
C(8B)	6117(4)	7301(3)	6134(2)	17(1)
C(2B)	8002(4)	6397(4)	5956(2)	15(1)
C(1B)	8221(4)	6404(4)	5243(2)	16(1)
C(1)	3608(4)	3879(3)	4879(2)	15(1)
C(15)	4893(5)	2837(4)	7069(2)	24(1)
C(14)	3765(4)	3049(4)	6953(2)	22(1)
C(11)	3668(4)	2816(4)	5202(2)	16(1)
C(6)	5187(4)	1642(4)	3110(2)	18(1)
C(17)	5219(4)	2643(4)	5991(2)	21(1)
C(2)	3195(4)	3711(4)	4194(2)	16(1)
C(7B)	4982(4)	7302(4)	6324(2)	18(1)
C(8)	4928(4)	3307(4)	3522(2)	20(1)
C(3)	3933(4)	2995(3)	3819(2)	14(1)
C(13)	3366(4)	3055(4)	6356(2)	17(1)
C(19B)	7923(4)	7429(4)	4952(2)	19(1)
C(12B)	7652(4)	5450(4)	4243(2)	18(1)
C(6B)	4508(4)	6393(4)	6517(2)	21(1)
C(19)	4775(4)	4374(4)	4898(2)	20(1)
C(16)	5615(4)	2644(4)	6592(2)	22(1)
C(11B)	7514(4)	5552(3)	4936(2)	15(1)
C(4)	3595(4)	1989(4)	3747(2)	16(1)
C(5)	4218(4)	1308(4)	3397(2)	19(1)
C(3B)	6758(4)	6422(4)	6135(2)	15(1)
C(9B)	8651(4)	7213(4)	6288(2)	21(1)

C(7)	5550(4)	2637(4)	3168(2)	19(1)
C(13B)	8529(4)	4866(4)	3986(2)	22(1)
C(14B)	8635(5)	4779(4)	3355(2)	25(1)
C(4B)	6236(4)	5523(4)	6338(2)	18(1)
C(10B)	9604(4)	7033(4)	6590(2)	27(1)
C(10)	2036(5)	4974(4)	3618(2)	27(1)
C(15B)	7867(5)	5270(4)	2970(2)	28(1)
C(17B)	6896(4)	5927(4)	3852(2)	22(1)
C(5B)	5122(4)	5503(4)	6526(2)	21(1)
C(16B)	7008(5)	5844(4)	3217(2)	28(1)

Table A7.3. Bond lengths [\AA] and angles [$^\circ$] for **117**.

Br(1)-C(6)	1.906(5)
Br(1B)-C(6B)	1.902(5)
O(1)-H(1)	0.8400
O(1)-C(11)	1.445(5)
O(1B)-H(1B)	0.8400
O(1B)-C(11B)	1.443(5)
O(2B)-H(2B)	0.8400
O(2B)-C(18B)	1.442(6)
O(2)-H(2)	0.8400
O(2)-C(18)	1.430(5)
C(12)-C(11)	1.525(6)
C(12)-C(17)	1.391(7)
C(12)-C(13)	1.404(6)
C(18)-H(18A)	0.9900
C(18)-H(18B)	0.9900
C(18)-C(1)	1.527(6)
C(9)-H(9)	0.9500
C(9)-C(2)	1.517(6)
C(9)-C(10)	1.319(7)
C(18B)-H(18C)	0.9900
C(18B)-H(18D)	0.9900
C(18B)-C(1B)	1.538(6)
C(8B)-H(8B)	0.9500
C(8B)-C(7B)	1.409(7)
C(8B)-C(3B)	1.386(7)
C(2B)-H(2BA)	1.0000
C(2B)-C(1B)	1.574(6)
C(2B)-C(3B)	1.527(6)
C(2B)-C(9B)	1.507(7)
C(1B)-C(19B)	1.532(6)
C(1B)-C(11B)	1.553(6)
C(1)-C(11)	1.568(6)
C(1)-C(2)	1.585(6)
C(1)-C(19)	1.531(6)
C(15)-H(15)	0.9500
C(15)-C(14)	1.391(7)
C(15)-C(16)	1.369(7)
C(14)-H(14)	0.9500

C(14)-C(13)	1.382(7)
C(11)-H(11)	1.0000
C(6)-C(5)	1.381(7)
C(6)-C(7)	1.386(7)
C(17)-H(17)	0.9500
C(17)-C(16)	1.391(6)
C(2)-H(2A)	1.0000
C(2)-C(3)	1.524(6)
C(7B)-H(7B)	0.9500
C(7B)-C(6B)	1.389(7)
C(8)-H(8)	0.9500
C(8)-C(3)	1.408(6)
C(8)-C(7)	1.385(7)
C(3)-C(4)	1.394(7)
C(13)-H(13)	0.9500
C(19B)-H(19D)	0.9800
C(19B)-H(19E)	0.9800
C(19B)-H(19F)	0.9800
C(12B)-C(11B)	1.522(6)
C(12B)-C(13B)	1.411(7)
C(12B)-C(17B)	1.387(7)
C(6B)-C(5B)	1.381(7)
C(19)-H(19A)	0.9800
C(19)-H(19B)	0.9800
C(19)-H(19C)	0.9800
C(16)-H(16)	0.9500
C(11B)-H(11B)	1.0000
C(4)-H(4)	0.9500
C(4)-C(5)	1.391(7)
C(5)-H(5)	0.9500
C(3B)-C(4B)	1.408(7)
C(9B)-H(9B)	0.9500
C(9B)-C(10B)	1.329(7)
C(7)-H(7)	0.9500
C(13B)-H(13B)	0.9500
C(13B)-C(14B)	1.384(7)
C(14B)-H(14B)	0.9500
C(14B)-C(15B)	1.398(8)
C(4B)-H(4B)	0.9500
C(4B)-C(5B)	1.385(7)
C(10B)-H(10C)	0.9500
C(10B)-H(10D)	0.9500
C(10)-H(10A)	0.9500
C(10)-H(10B)	0.9500
C(15B)-H(15B)	0.9500
C(15B)-C(16B)	1.379(8)
C(17B)-H(17B)	0.9500
C(17B)-C(16B)	1.392(7)
C(5B)-H(5B)	0.9500
C(16B)-H(16B)	0.9500
C(11)-O(1)-H(1)	109.5

C(11B)-O(1B)-H(1B)	109.5
C(18B)-O(2B)-H(2B)	109.5
C(18)-O(2)-H(2)	109.5
C(17)-C(12)-C(11)	120.1(4)
C(17)-C(12)-C(13)	118.4(4)
C(13)-C(12)-C(11)	121.5(4)
O(2)-C(18)-H(18A)	109.6
O(2)-C(18)-H(18B)	109.6
O(2)-C(18)-C(1)	110.3(4)
H(18A)-C(18)-H(18B)	108.1
C(1)-C(18)-H(18A)	109.6
C(1)-C(18)-H(18B)	109.6
C(2)-C(9)-H(9)	118.4
C(10)-C(9)-H(9)	118.4
C(10)-C(9)-C(2)	123.3(5)
O(2B)-C(18B)-H(18C)	109.1
O(2B)-C(18B)-H(18D)	109.1
O(2B)-C(18B)-C(1B)	112.3(4)
H(18C)-C(18B)-H(18D)	107.9
C(1B)-C(18B)-H(18C)	109.1
C(1B)-C(18B)-H(18D)	109.1
C(7B)-C(8B)-H(8B)	119.2
C(3B)-C(8B)-H(8B)	119.2
C(3B)-C(8B)-C(7B)	121.7(4)
C(1B)-C(2B)-H(2BA)	106.1
C(3B)-C(2B)-H(2BA)	106.1
C(3B)-C(2B)-C(1B)	114.3(3)
C(9B)-C(2B)-H(2BA)	106.1
C(9B)-C(2B)-C(1B)	112.5(4)
C(9B)-C(2B)-C(3B)	110.9(4)
C(18B)-C(1B)-C(2B)	108.0(4)
C(18B)-C(1B)-C(11B)	110.8(4)
C(19B)-C(1B)-C(18B)	107.2(4)
C(19B)-C(1B)-C(2B)	112.0(4)
C(19B)-C(1B)-C(11B)	109.6(4)
C(11B)-C(1B)-C(2B)	109.3(4)
C(18)-C(1)-C(11)	111.0(4)
C(18)-C(1)-C(2)	108.8(4)
C(18)-C(1)-C(19)	108.3(4)
C(11)-C(1)-C(2)	108.1(4)
C(19)-C(1)-C(11)	109.2(4)
C(19)-C(1)-C(2)	111.4(4)
C(14)-C(15)-H(15)	119.9
C(16)-C(15)-H(15)	119.9
C(16)-C(15)-C(14)	120.2(4)
C(15)-C(14)-H(14)	120.0
C(13)-C(14)-C(15)	120.1(4)
C(13)-C(14)-H(14)	120.0
O(1)-C(11)-C(12)	110.2(4)
O(1)-C(11)-C(1)	111.0(3)
O(1)-C(11)-H(11)	106.9
C(12)-C(11)-C(1)	114.5(4)

C(12)-C(11)-H(11)	106.9
C(1)-C(11)-H(11)	106.9
C(5)-C(6)-Br(1)	118.3(4)
C(5)-C(6)-C(7)	121.3(4)
C(7)-C(6)-Br(1)	120.4(4)
C(12)-C(17)-H(17)	119.6
C(12)-C(17)-C(16)	120.8(4)
C(16)-C(17)-H(17)	119.6
C(9)-C(2)-C(1)	112.6(4)
C(9)-C(2)-H(2A)	106.2
C(9)-C(2)-C(3)	110.5(4)
C(1)-C(2)-H(2A)	106.2
C(3)-C(2)-C(1)	114.3(4)
C(3)-C(2)-H(2A)	106.2
C(8B)-C(7B)-H(7B)	120.8
C(6B)-C(7B)-C(8B)	118.4(4)
C(6B)-C(7B)-H(7B)	120.8
C(3)-C(8)-H(8)	119.4
C(7)-C(8)-H(8)	119.4
C(7)-C(8)-C(3)	121.1(4)
C(8)-C(3)-C(2)	123.2(4)
C(4)-C(3)-C(2)	118.9(4)
C(4)-C(3)-C(8)	117.8(4)
C(12)-C(13)-H(13)	119.8
C(14)-C(13)-C(12)	120.4(4)
C(14)-C(13)-H(13)	119.8
C(1B)-C(19B)-H(19D)	109.5
C(1B)-C(19B)-H(19E)	109.5
C(1B)-C(19B)-H(19F)	109.5
H(19D)-C(19B)-H(19E)	109.5
H(19D)-C(19B)-H(19F)	109.5
H(19E)-C(19B)-H(19F)	109.5
C(13B)-C(12B)-C(11B)	121.4(4)
C(17B)-C(12B)-C(11B)	119.9(4)
C(17B)-C(12B)-C(13B)	118.8(4)
C(7B)-C(6B)-Br(1B)	119.3(4)
C(5B)-C(6B)-Br(1B)	119.1(4)
C(5B)-C(6B)-C(7B)	121.6(4)
C(1)-C(19)-H(19A)	109.5
C(1)-C(19)-H(19B)	109.5
C(1)-C(19)-H(19C)	109.5
H(19A)-C(19)-H(19B)	109.5
H(19A)-C(19)-H(19C)	109.5
H(19B)-C(19)-H(19C)	109.5
C(15)-C(16)-C(17)	120.1(5)
C(15)-C(16)-H(16)	120.0
C(17)-C(16)-H(16)	120.0
O(1B)-C(11B)-C(1B)	106.8(3)
O(1B)-C(11B)-C(12B)	111.1(4)
O(1B)-C(11B)-H(11B)	107.7
C(1B)-C(11B)-H(11B)	107.7
C(12B)-C(11B)-C(1B)	115.5(4)

C(12B)-C(11B)-H(11B)	107.7
C(3)-C(4)-H(4)	119.2
C(5)-C(4)-C(3)	121.5(4)
C(5)-C(4)-H(4)	119.2
C(6)-C(5)-C(4)	119.0(5)
C(6)-C(5)-H(5)	120.5
C(4)-C(5)-H(5)	120.5
C(8B)-C(3B)-C(2B)	123.3(4)
C(8B)-C(3B)-C(4B)	117.5(4)
C(4B)-C(3B)-C(2B)	119.2(4)
C(2B)-C(9B)-H(9B)	118.5
C(10B)-C(9B)-C(2B)	123.0(5)
C(10B)-C(9B)-H(9B)	118.5
C(6)-C(7)-H(7)	120.4
C(8)-C(7)-C(6)	119.2(4)
C(8)-C(7)-H(7)	120.4
C(12B)-C(13B)-H(13B)	119.8
C(14B)-C(13B)-C(12B)	120.4(5)
C(14B)-C(13B)-H(13B)	119.8
C(13B)-C(14B)-H(14B)	120.1
C(13B)-C(14B)-C(15B)	119.8(5)
C(15B)-C(14B)-H(14B)	120.1
C(3B)-C(4B)-H(4B)	119.0
C(5B)-C(4B)-C(3B)	122.0(4)
C(5B)-C(4B)-H(4B)	119.0
C(9B)-C(10B)-H(10C)	120.0
C(9B)-C(10B)-H(10D)	120.0
H(10C)-C(10B)-H(10D)	120.0
C(9)-C(10)-H(10A)	120.0
C(9)-C(10)-H(10B)	120.0
H(10A)-C(10)-H(10B)	120.0
C(14B)-C(15B)-H(15B)	119.9
C(16B)-C(15B)-C(14B)	120.2(5)
C(16B)-C(15B)-H(15B)	119.9
C(12B)-C(17B)-H(17B)	119.6
C(12B)-C(17B)-C(16B)	120.8(5)
C(16B)-C(17B)-H(17B)	119.6
C(6B)-C(5B)-C(4B)	118.9(5)
C(6B)-C(5B)-H(5B)	120.6
C(4B)-C(5B)-H(5B)	120.6
C(15B)-C(16B)-C(17B)	120.1(5)
C(15B)-C(16B)-H(16B)	120.0
C(17B)-C(16B)-H(16B)	120.0

Symmetry transformations used to generate equivalent atoms:

Table A7.4. Anisotropic displacement parameters ($\text{\AA}^2 \times 10^4$) for **117**. The anisotropic displacement factor exponent takes the form

$$-2\pi^2 [h^2 a^{*2} U^{11} + \dots + 2 h k a^* b^* U^{12}]$$

U^{11}

U^{22}

U^{33}

U^{23}

U^{13}

U^{12}

Br(1)	216(2)	209(2)	285(2)	-37(2)	36(2)	57(2)
Br(1B)	176(2)	307(3)	382(3)	10(2)	76(2)	-18(2)
O(1)	164(16)	123(16)	218(17)	-4(14)	-13(13)	-28(13)
O(1B)	158(17)	130(16)	254(17)	27(13)	-4(14)	-4(13)
O(2B)	144(17)	223(19)	340(20)	29(15)	19(15)	75(15)
O(2)	149(16)	138(18)	430(20)	-13(16)	45(15)	28(13)
C(12)	160(20)	120(20)	190(20)	-7(17)	17(18)	-13(19)
C(18)	140(20)	120(20)	260(20)	-3(18)	8(18)	-9(17)
C(9)	240(20)	120(20)	200(20)	-3(17)	-10(20)	0(20)
C(18B)	160(20)	150(20)	260(20)	20(20)	33(18)	-3(19)
C(8B)	200(20)	110(20)	190(20)	-5(17)	5(19)	-20(20)
C(2B)	131(19)	120(20)	200(20)	15(18)	-1(18)	20(20)
C(1B)	150(20)	110(20)	220(20)	21(19)	-13(17)	0(18)
C(1)	150(20)	120(20)	190(20)	-8(17)	0(17)	8(17)
C(15)	360(30)	220(30)	130(20)	13(19)	-30(20)	-30(20)
C(14)	270(30)	200(20)	170(20)	11(18)	60(19)	-20(20)
C(11)	120(20)	130(20)	210(20)	20(18)	20(17)	-36(17)
C(6)	170(20)	190(20)	180(20)	10(18)	-5(18)	56(18)
C(17)	180(20)	240(30)	210(20)	10(20)	16(19)	10(20)
C(2)	140(20)	140(20)	200(20)	10(18)	6(17)	13(18)
C(7B)	180(20)	150(20)	210(20)	-17(18)	11(19)	20(20)
C(8)	150(20)	190(20)	250(20)	-13(19)	-1(19)	-20(19)
C(3)	140(20)	150(20)	136(19)	-1(16)	-2(17)	15(19)
C(13)	140(20)	190(20)	200(20)	5(19)	37(18)	-7(19)
C(19B)	200(20)	140(20)	230(20)	-3(18)	40(20)	10(20)
C(12B)	180(20)	140(20)	220(20)	5(18)	-18(18)	-6(18)
C(6B)	170(20)	250(30)	200(20)	-10(20)	3(18)	0(20)
C(19)	170(20)	240(30)	200(20)	0(20)	-18(17)	-60(20)
C(16)	200(20)	230(30)	240(30)	30(20)	-33(19)	10(20)
C(11B)	150(20)	130(20)	170(20)	20(17)	-14(17)	10(18)
C(4)	150(20)	160(20)	180(20)	0(18)	-5(17)	-22(18)
C(5)	210(20)	140(20)	210(20)	21(18)	0(17)	0(20)
C(3B)	150(20)	140(20)	160(20)	-4(18)	-8(16)	-5(18)
C(9B)	190(20)	190(20)	240(20)	-40(20)	31(19)	-40(20)
C(7)	150(20)	220(20)	200(20)	0(20)	13(19)	3(19)
C(13B)	230(30)	170(20)	240(30)	-20(20)	0(20)	20(20)
C(14B)	260(30)	220(30)	260(30)	-50(20)	40(20)	40(20)
C(4B)	210(30)	140(20)	180(20)	2(17)	0(18)	10(19)
C(10B)	210(30)	260(30)	330(30)	-50(20)	-10(20)	-20(20)
C(10)	330(30)	200(30)	280(30)	40(20)	-30(20)	20(30)
C(15B)	310(30)	330(30)	220(20)	-50(20)	20(20)	-10(30)
C(17B)	190(20)	200(30)	270(20)	-9(19)	-20(20)	40(20)
C(5B)	230(30)	160(30)	240(20)	0(19)	30(20)	-50(20)
C(16B)	280(30)	310(30)	230(20)	10(20)	-30(20)	40(20)

Table A7.5. Hydrogen coordinates ($\times 10^3$) and isotropic displacement parameters ($\text{\AA}^2 \times 10^3$) for 117.

	x	y	z	U_{iso}
--	---	---	---	------------------

H(1)	239	225	480	25
H(1B)	849	462	533	27
H(2B)	1057	523	535	36
H(2)	175	351	533	36
H(18A)	304	472	563	21
H(18B)	273	523	498	21
H(9)	364	515	380	22
H(18C)	963	619	469	23
H(18D)	991	682	530	23
H(8B)	645	792	600	20
H(2BA)	830	574	611	18
H(15)	516	283	748	28
H(14)	327	319	728	26
H(11)	422	240	496	19
H(17)	572	250	566	25
H(2A)	244	338	422	19
H(7B)	455	791	632	22
H(8)	518	399	356	24
H(13)	260	320	628	21
H(19D)	838	796	514	29
H(19E)	712	757	502	29
H(19F)	808	740	451	29
H(19A)	476	502	467	30
H(19B)	533	392	471	30
H(19C)	499	451	533	30
H(16)	639	251	667	27
H(11B)	670	570	502	18
H(4)	292	176	394	20
H(5)	398	62	336	23
H(9B)	837	789	628	25
H(7)	622	286	297	23
H(13B)	905	453	425	26
H(14B)	923	439	318	30
H(4B)	666	491	635	21
H(10C)	990	637	660	32
H(10D)	998	757	679	32
H(10A)	140	454	366	32
H(10B)	197	560	341	32
H(15B)	794	521	254	34
H(17B)	630	632	402	26
H(5B)	479	489	666	25
H(16B)	649	618	295	33

Table A7.6. Hydrogen bonds for **117** [\AA and $^\circ$].

D-H...A	d(D-H)	d(H...A)	d(D...A)	$\angle(\text{DHA})$
O(1B)-H(1B)...O(2B)	0.84	1.91	2.669(5)	150.6
O(2B)-H(2B)...O(2)#1	0.84	1.99	2.689(5)	140.2

O(2)-H(2)...O(1)	0.84	1.91	2.629(5)	142.7
------------------	------	------	----------	-------

Symmetry transformations used to generate equivalent atoms:

#1 $x+1,y,z$

Table A7.7. Torsion angles [°] for **117**.

Br(1)-C(6)-C(5)-C(4)	-179.3(3)
Br(1)-C(6)-C(7)-C(8)	179.6(3)
Br(1B)-C(6B)-C(5B)-C(4B)	-178.6(3)
O(2B)-C(18B)-C(1B)-C(2B)	55.2(5)
O(2B)-C(18B)-C(1B)-C(19B)	176.0(4)
O(2B)-C(18B)-C(1B)-C(11B)	-64.4(5)
O(2)-C(18)-C(1)-C(11)	-57.0(5)
O(2)-C(18)-C(1)-C(2)	61.9(5)
O(2)-C(18)-C(1)-C(19)	-176.9(4)
C(12)-C(17)-C(16)-C(15)	0.5(8)
C(18)-C(1)-C(11)-O(1)	63.0(5)
C(18)-C(1)-C(11)-C(12)	-62.6(5)
C(18)-C(1)-C(2)-C(9)	54.6(5)
C(18)-C(1)-C(2)-C(3)	-178.1(4)
C(9)-C(2)-C(3)-C(8)	45.4(6)
C(9)-C(2)-C(3)-C(4)	-132.4(4)
C(18B)-C(1B)-C(11B)-O(1B)	64.1(5)
C(18B)-C(1B)-C(11B)-C(12B)	-60.1(5)
C(8B)-C(7B)-C(6B)-Br(1B)	178.6(3)
C(8B)-C(7B)-C(6B)-C(5B)	0.0(7)
C(8B)-C(3B)-C(4B)-C(5B)	0.6(7)
C(2B)-C(1B)-C(11B)-O(1B)	-54.8(5)
C(2B)-C(1B)-C(11B)-C(12B)	-179.0(4)
C(2B)-C(3B)-C(4B)-C(5B)	177.8(4)
C(1B)-C(2B)-C(3B)-C(8B)	-79.4(5)
C(1B)-C(2B)-C(3B)-C(4B)	103.6(5)
C(1B)-C(2B)-C(9B)-C(10B)	-100.3(5)
C(1)-C(2)-C(3)-C(8)	-83.0(5)
C(1)-C(2)-C(3)-C(4)	99.3(5)
C(15)-C(14)-C(13)-C(12)	0.1(7)
C(14)-C(15)-C(16)-C(17)	-1.0(8)
C(11)-C(12)-C(17)-C(16)	-178.5(4)
C(11)-C(12)-C(13)-C(14)	178.2(4)
C(11)-C(1)-C(2)-C(9)	175.3(4)
C(11)-C(1)-C(2)-C(3)	-57.4(5)
C(17)-C(12)-C(11)-O(1)	137.1(4)
C(17)-C(12)-C(11)-C(1)	-97.0(5)
C(17)-C(12)-C(13)-C(14)	-0.6(7)
C(2)-C(1)-C(11)-O(1)	-56.4(5)
C(2)-C(1)-C(11)-C(12)	178.1(4)
C(2)-C(3)-C(4)-C(5)	178.2(4)
C(7B)-C(8B)-C(3B)-C(2B)	-177.6(4)
C(7B)-C(8B)-C(3B)-C(4B)	-0.6(6)
C(7B)-C(6B)-C(5B)-C(4B)	0.0(7)
C(8)-C(3)-C(4)-C(5)	0.3(7)
C(3)-C(8)-C(7)-C(6)	-0.2(7)
C(3)-C(4)-C(5)-C(6)	-0.6(7)
C(13)-C(12)-C(11)-O(1)	-41.8(6)
C(13)-C(12)-C(11)-C(1)	84.2(5)
C(13)-C(12)-C(17)-C(16)	0.3(7)

C(19B)-C(1B)-C(11B)-O(1B)	-177.8(3)
C(19B)-C(1B)-C(11B)-C(12B)	58.0(5)
C(12B)-C(13B)-C(14B)-C(15B)	-0.1(8)
C(12B)-C(17B)-C(16B)-C(15B)	1.0(8)
C(19)-C(1)-C(11)-O(1)	-177.7(4)
C(19)-C(1)-C(11)-C(12)	56.8(5)
C(19)-C(1)-C(2)-C(9)	-64.8(5)
C(19)-C(1)-C(2)-C(3)	62.5(5)
C(16)-C(15)-C(14)-C(13)	0.7(8)
C(11B)-C(12B)-C(13B)-C(14B)	179.6(5)
C(11B)-C(12B)-C(17B)-C(16B)	180.0(5)
C(5)-C(6)-C(7)-C(8)	0.0(7)
C(3B)-C(8B)-C(7B)-C(6B)	0.3(7)
C(3B)-C(2B)-C(1B)-C(18B)	-172.3(4)
C(3B)-C(2B)-C(1B)-C(19B)	69.9(5)
C(3B)-C(2B)-C(1B)-C(11B)	-51.7(5)
C(3B)-C(2B)-C(9B)-C(10B)	130.2(5)
C(3B)-C(4B)-C(5B)-C(6B)	-0.3(7)
C(9B)-C(2B)-C(1B)-C(18B)	60.0(5)
C(9B)-C(2B)-C(1B)-C(19B)	-57.8(5)
C(9B)-C(2B)-C(1B)-C(11B)	-179.4(4)
C(9B)-C(2B)-C(3B)-C(8B)	49.2(6)
C(9B)-C(2B)-C(3B)-C(4B)	-127.9(4)
C(7)-C(6)-C(5)-C(4)	0.4(7)
C(7)-C(8)-C(3)-C(2)	-177.7(4)
C(7)-C(8)-C(3)-C(4)	0.0(7)
C(13B)-C(12B)-C(11B)-O(1B)	-36.2(6)
C(13B)-C(12B)-C(11B)-C(1B)	85.7(5)
C(13B)-C(12B)-C(17B)-C(16B)	-0.9(7)
C(13B)-C(14B)-C(15B)-C(16B)	0.2(8)
C(14B)-C(15B)-C(16B)-C(17B)	-0.7(8)
C(10)-C(9)-C(2)-C(1)	-120.1(5)
C(10)-C(9)-C(2)-C(3)	110.7(5)
C(17B)-C(12B)-C(11B)-O(1B)	142.9(4)
C(17B)-C(12B)-C(11B)-C(1B)	-95.2(5)
C(17B)-C(12B)-C(13B)-C(14B)	0.5(7)

Symmetry transformations used to generate equivalent atoms:

APPENDIX 8

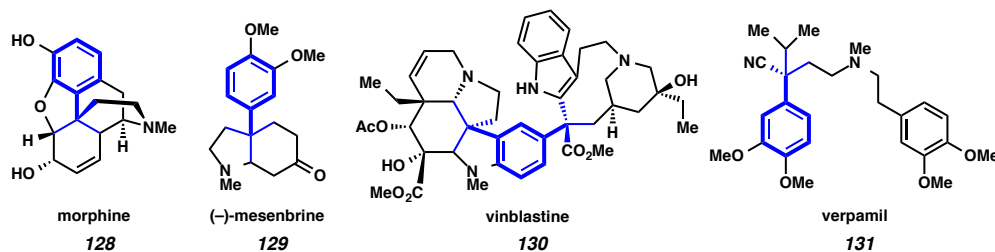
Development of an α -Arylation Reaction of TMSE β -Ketoesters

A8.1 INTRODUCTION

A8.1.1 Background and state of the art in the α -arylation of cyclic ketones

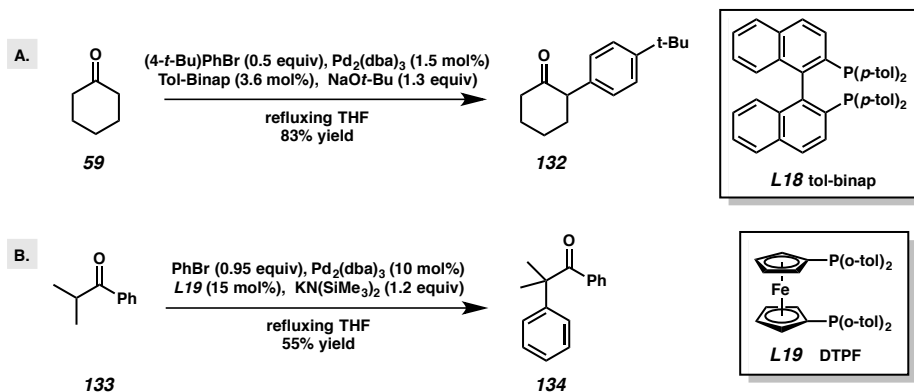
The ubiquity of all-carbon quaternary stereocenters in natural products and other compounds that possess antibiotic, antimicrobial, antifungal, anti-tumor and other therapeutic properties provides a strong impetus for researchers to continue to seek out new methods for the construction of this important motif.¹⁰⁶ Within this domain, benzylic quaternary ketones have received a significant amount of attention, owing in part to the presence of an excellent functional group handle (i.e. the carbonyl) as well as the prevalence of arylated quaternary centers in medicinally important compounds¹⁰⁷ (Figure A8.1.1).

Figure A8.1.1.1. Natural products containing benzylic quaternary stereocenters



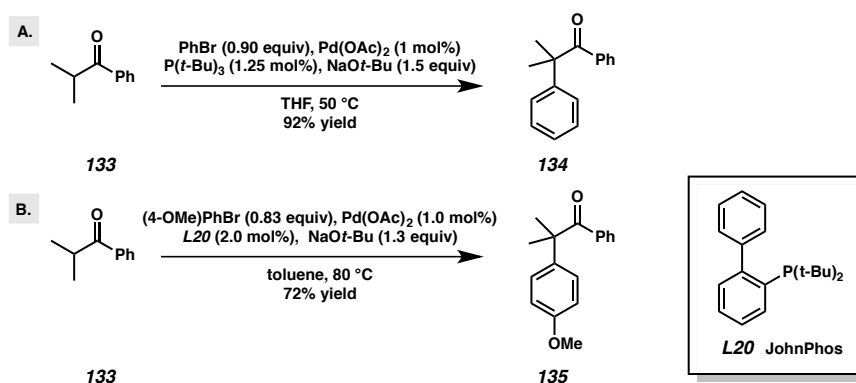
The development of methods for the preparation of arylated quaternary centers via the α -arylation of nonstabilized ketones has been a subject of intense research for the past two decades.¹⁰⁸ Early reports of transition-metal catalysis in this reaction focused on the use of palladium catalysts bound by sterically encumbered, electron-rich phosphine ligands. A milestone publication by Buchwald¹⁰⁹ and coworkers demonstrated that $\text{Pd}_2(\text{dba})_3$, bound with *p*-tol-Binap (**L18**) as ligand, serves as an efficient catalyst for the direct arylation of ketone enolates (Scheme A8.1.1.A). Concurrent this to publication, Hartwig¹¹⁰ disclosed a report describing the use of a 1,1'-Bis(di-*o*-tolylphosphino)ferrocene (**L19**, DTPF)/ $\text{Pd}_2(\text{dba})_3$ catalyst system for α -arylation that capably provided α -arylated α -quaternary ketones (Scheme A8.1.1.B). These two publications represent the first examples of direct catalytic α -arylations of nonstabilized ketones.

Scheme A8.1.1.1. Initial Reports of Direct α -Arylation of Ketones by Buchwald (A) and Hartwig (B)



Ensuing reports from a number of research groups, following these initial communications, revealed the superiority of extremely sterically bulky phosphine ligands in the formation of quaternary centers via this transformation.¹¹¹ The Hartwig and Buchwald groups have remained at the forefront of these developments. The reported improvements to their respective catalytic systems constitute the most successful α -arylation of nonstabilized enolates in the absence of blocking groups to date (Scheme A8.1.1.2, A¹¹² and B¹¹³).

Scheme A8.1.1.2. Improved Catalyst Systems for α -Arylation by Hartwig (A) and Buchwald (B)



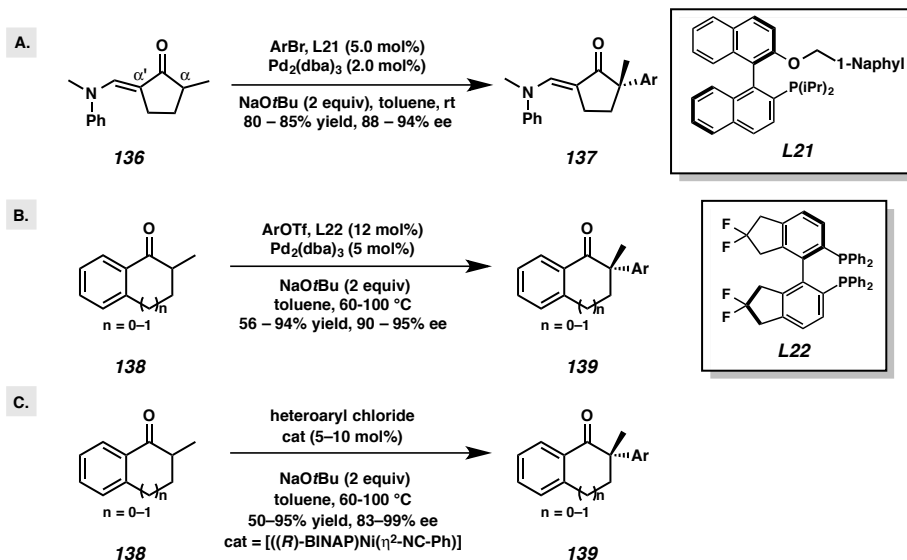
A8.1.2 State of the art in the asymmetric α -arylation of cyclic ketones

The current state of the art in the catalytic asymmetric α -arylation of ketones to form all-carbon quaternary centers is exemplified, again, by the research efforts of the Hartwig and Buchwald groups. Studies by Buchwald and co-workers have focused on the use of α' blocked α -methylcyclopentanone derivatives (**136**) as substrates (Scheme A8.1.2.1A).¹¹⁴ Sterically encumbered mono-phosphine ligand (**L20**) has been shown to efficiently catalyze the transformation (Scheme A8.1.2.1A) in good yields and excellent

enantiomeric excess. Unfortunately, the tolerance of the transformation to substrate variability has been highly limited and even seemingly innocuous adjustments to the substrate, such as employing the corresponding 6-membered α' -blocked α -methylcyclohexanone derivative, results in substantially diminished selectivity with ee's no higher than 70%. All attempts by Buchwald and coworkers, thus far, to generalize this reaction have proven nonviable.

Hartwig and co-workers obviated the need for an α' -blocking group by focusing their studies exclusively on substrates which inherently lack more than one enolizable proton, namely tetralone and indanone derivatives (**138**). Their work has shown that the use of chiral phosphine difluorophos (**L22**) under palladium catalysis is highly effective in promoting the α -arylation of tetralone and indanone substrates, delivering the corresponding α -quaternary ketone products (**139**) in moderate to excellent yields and uniformly excellent ee's (Scheme A8.1.2.1B). More recently, Hartwig and co-workers have also shown pre-formed nickel complex $[(R)\text{-BINAP}]\text{Ni}(\eta^2\text{-NC-Ph})$ to be an effective metal source for the heteroarylation of tetralone and indanone substrates (Scheme A8.1.2.1C).

Scheme A8.1.2.1. Current State of the Art in Catalytic Asymmetric α -Arylation to Form α -Quaternary Ketones



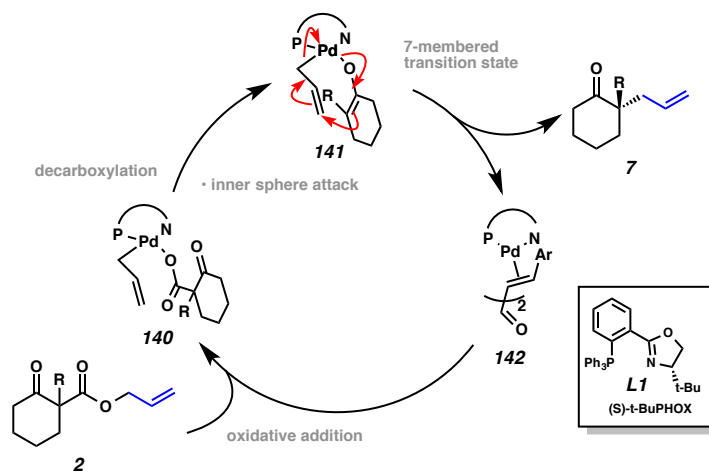
Although existing asymmetric α -arylation methods are outstanding, considerable deficiency remains in the scope of compatible substrates. Indeed, catalytic asymmetric means to access the deceptively simple looking 2-alkyl-2-arylcyclohexanone (**149**) shown in Figure A8.2.2.1 (R = alkyl) are not known. We believe that the use of prochiral enolates generated *in situ*, in the absence of exogenous base will be crucial in identifying a solution to this problem.

A8.2 BACKGROUND: EXTENSION OF CARBOXYLATE-PROTECTED ENOLATE CROSS-COUPLING STRATEGY TO α -ARYLATION

A8.2.1 Use of allyl β -ketoester-protected enolates in non-allylic alkylation processes

Considerable investigation by the Stoltz group has been devoted to advancing and extending the palladium-catalyzed asymmetric allylic alkylation methodology described in Chapters 1 and 2.¹⁵ Beginning with work by Behenna and Stoltz, it was shown that a variety of enolate precursors, including allyl enol carbonates (**1**), allyl β -ketoesters (**2**) and silyl enol ethers (**3**), are all amenable to asymmetric catalysis through the use of a chiral phosphinooxazoline ligand ((S)-*t*-BuPHOX, **L1**).⁹ All three of these substrate classes function well in the chemistry, to provide α -quaternary ketones (**7**) in good to excellent yields and enantioselectivities.¹⁰ The striking uniformity in enantiomeric excess between these substrate classes suggested to us the possibility of a common mechanistic pathway; studies to elucidate the catalytic cycle of this reaction led by members of the Stoltz group resulted in an intriguing mechanistic picture (Scheme 5.2.1.1).³⁵

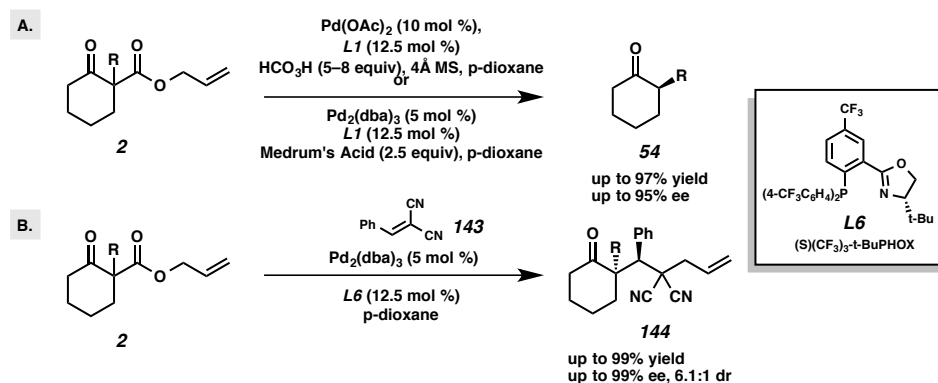
The catalytic cycle begins with the oxidative addition of a palladium(0) species into an allyl fragment (**2**) to generate an η^1 -palladium allyl species, which is also bound to the carboxylate in what has been shown to be the catalytic resting state species (**140**, Scheme A8.5.2.1.1).^{35a} Decarboxylation may then occur, to give Pd-bound prochiral enolate species (**141**). The resulting complex may then undergo an alkylation event via a 7-membered inner-sphere transition state to deliver the α -allylated product (**7**) and regenerate the catalyst (**142**).

Scheme A8.2.1.1. Proposed catalytic cycle of asymmetric allylic alkylation

With this mechanistic picture in mind, we became intrigued by the idea that we might intercept the palladium enolate species (**141**) with an alternative electrophile prior to the allylic alkylation event. Initial studies to test this hypothesis were conducted by employing a proton as an alternative to the allyl fragment electrophile. Work by Mohr and Stoltz showed that by subjecting allyl β -ketoesters substrates to reaction conditions similar to those developed for our allylic alkylation, but in the presence of a proton donor, chiral α -tertiary cyclic ketones (**54**) could be obtained in good yields and high enantioselectivities (Scheme A8.2.1.2A).⁵⁶ Expanding on these results, we sought to use alternative carbon-based electrophiles: work by Streuff and Stoltz demonstrated the viability of this approach. In this research, we found that by subjecting β -ketoesters substrates to palladium catalysis in the presence of a stabilized conjugate acceptors, such as benzylidene malononitrile (**143**), we could affect a sequential alkylation–allylation reaction, which resulted in two new C–C bonds and the generation of adjacent quaternary

and tertiary stereocenters in excellent yields and good to excellent enantioselectivities (Scheme A8.2.1.2B).^{30a}

Scheme A8.2.1.2. A. Asymmetric protonation of allyl β -ketoesters; B. Stereoselective conjugate addition–allylation cascade reaction.

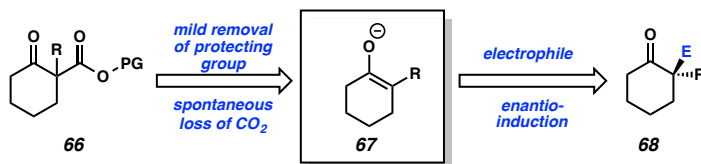


A8.2.2 New pathways into catalysis via a carboxylate-protected prochiral enolate strategy

The ability to use alternative electrophiles such as protons, or carbon-based conjugate acceptors, served as crucial proof of principle experiments for new catalytic reactions involving prochiral enolates. However, in both of these examples the presence of an allyl fragment, pendant to the palladium enolate, held sway over the reaction outcome. In the protonation case, allylic alkylation was an alternative reaction pathway, and the excess of proton source needed to shut down this pathway led to diminished enantioinduction. In the conjugate addition case, the anion intermediate resulting from conjugate addition is trapped by the palladium-allyl species present.

We reasoned that by eliminating allyl from the reaction mixture, we would obviate the problem of competing reaction pathways, and greatly expand the repertoire of *in situ* generated enolates of this type. We envisioned that our TMSE β -ketoester substrate (see Chapter 2) would be an ideal candidate to enable an investigation of this hypothesis. Specifically, we believed that electrophilic trapping of the enolate species (**67**) generated upon treatment of TMSE β -ketoester (**66**) with fluoride in the presence of a chiral catalyst may give rise to enantioenriched α -quaternary carbonyl products (**68**).

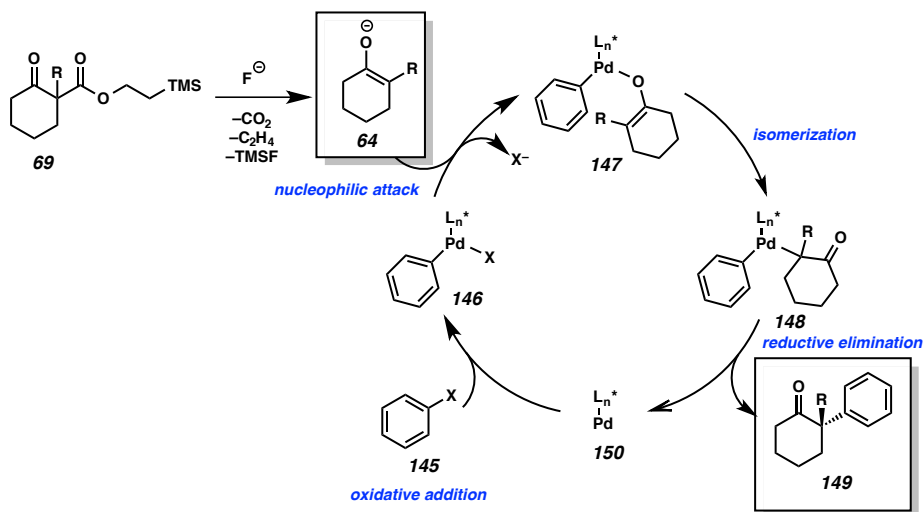
Figure A8.2.2.1. Proposed catalytic cycle for the α -arylation of cyclic ketones using *in situ* generated enolates



The first area in which investigation of this hypothesis began was in the α -arylation of TMSE β -ketoester (**69**). A proposed catalytic cycle for this transformation is depicted below in Scheme A8.2.2.2. Our proposed catalytic cycle begins with the oxidative addition of a palladium(0) species into an aryl–X bond to generate arylated palladium(II) species **146**. Upon unveiling of our prochiral enolate by treatment of β -ketoester **69** with fluoride, we envision that the nascent tetrasubstituted enolate (**64**) will displace the metal bound X group to deliver palladium enolate (**147**). Reductive elimination via the C-bound palladium enolate (**148**) would then complete the catalytic

cycle and furnish the desired α -quaternary ketone product (**149**) and regenerate palladium (0) intermediate **150**.

Figure A8.2.2.2. Proposed catalytic cycle for the α -arylation of cyclic ketones using *in situ* generated enolates



A8.3 INITIAL EVALUATION OF TMSE β -KETOESTER IN α -ARYLATION

A8.3.1 Symyx assisted reaction development: early experiments

Having demonstrated the ability of our (2-TMS)ethyl β -ketoester substrate to participate in palladium catalysis (*vide supra*, Chapter 2), we set out to identify conditions to affect the desired palladium-catalyzed α -arylation reaction. Broad screening of a variety of ligand classes, solvents and temperatures were conducted at the outset, and were assisted by the use of the Symyx automation system in collaboration with the Caltech Center for Catalysis and Chemical Synthesis. The basic transformation and parameters to be investigated are shown in Figure A8.3.1.1, below. In all cases,

$\text{Pd}_2(\text{dba})_3$ was used as the metal source, an equivalent of TBAT served to activate our substrate for deprotection and a slight molar excess of phenyl bromide was supplied as the aryl coupling partner. In our first such screen, a variety of phosphine ligands were employed at several temperatures against a number of solvents ranging broadly in polarity, dielectric constant and σ -donor ability. As this screening approach is combinatorial, the number of reactions per screen is easily calculated by multiplying the number of variables: in the case of Scheme A8.3.1.1, the product of 6 ligands, 4 solvents and 3 temperatures gives 72 reactions total. The best results for these experiments were obtained for reactions held at 60 °C, and the data for that screen are shown in Figure A8.3.1.1.

As can be seen in the Figure A8.3.1.1, very modest yields were seen in the first screen. While most reactions resulted in deprotection and protonation of starting β -ketoester **74** the combination of DMF as solvent and tricyclohexylphosphine ($\text{P}(\text{Cy})_3$) yielded the best result – a 5% yield of the desired α -quaternary ketone **149a**. These results indicated to us the importance of highly polar solvents and electron-rich phosphine ligands.

Scheme A8.3.1.1. Initial screens for α -arylation reactivity

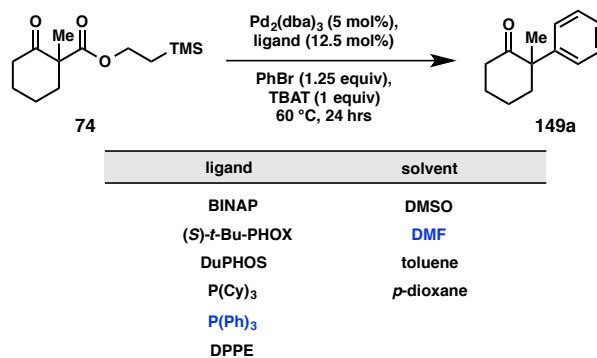
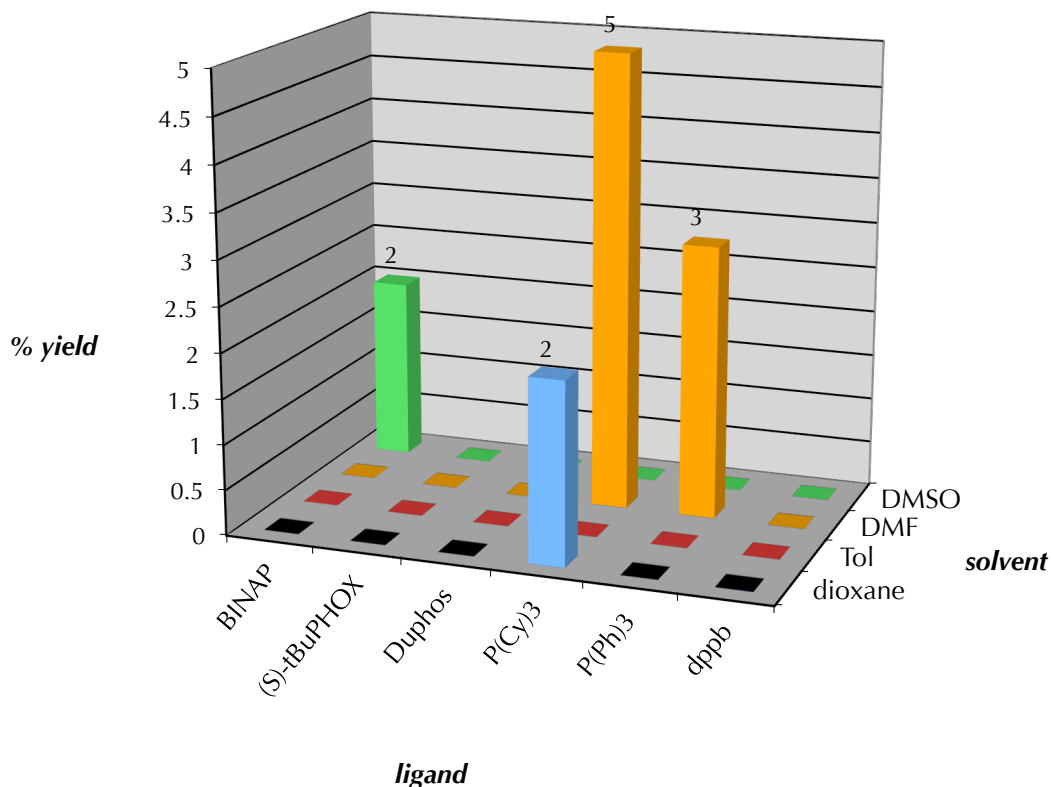


Figure A8.3.1.1. Summarized results^a of screen 1 at 60 °C

a. yield determined by GC analysis of tridecane internal standard

A8.3.2 Symyx assisted reaction development: beyond the initial experiments

With our first screen results in mind, we constructed a second screen with a focus on the use of more polar solvent, in particular those similar to DMF, and sterically bulky, electron rich-phosphine ligands. Again, we selected the same standard reaction parameters of β -ketoester **74**, Pd₂(dba)₃ as the metal source, an equivalent of TBAT to activate our substrate and bromobenzene as the aryl source (Scheme A8.3.2.1). In this case, we observed modest, yet encouraging, results with around 40% yield observed for the combination of DMF as solvent and P(*t*-Bu)₃ as ligand (Figure A8.3.2.1 depicts the results of the screen conducted at 60 °C). These results corroborate our initial findings

that sterically bulky, electron-rich phosphine ligand and polar solvents perform well in the reaction.

Scheme A8.3.2.1. Revised screens for α -arylation reactivity

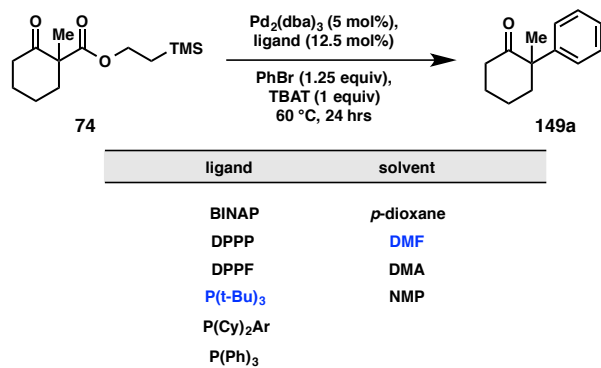
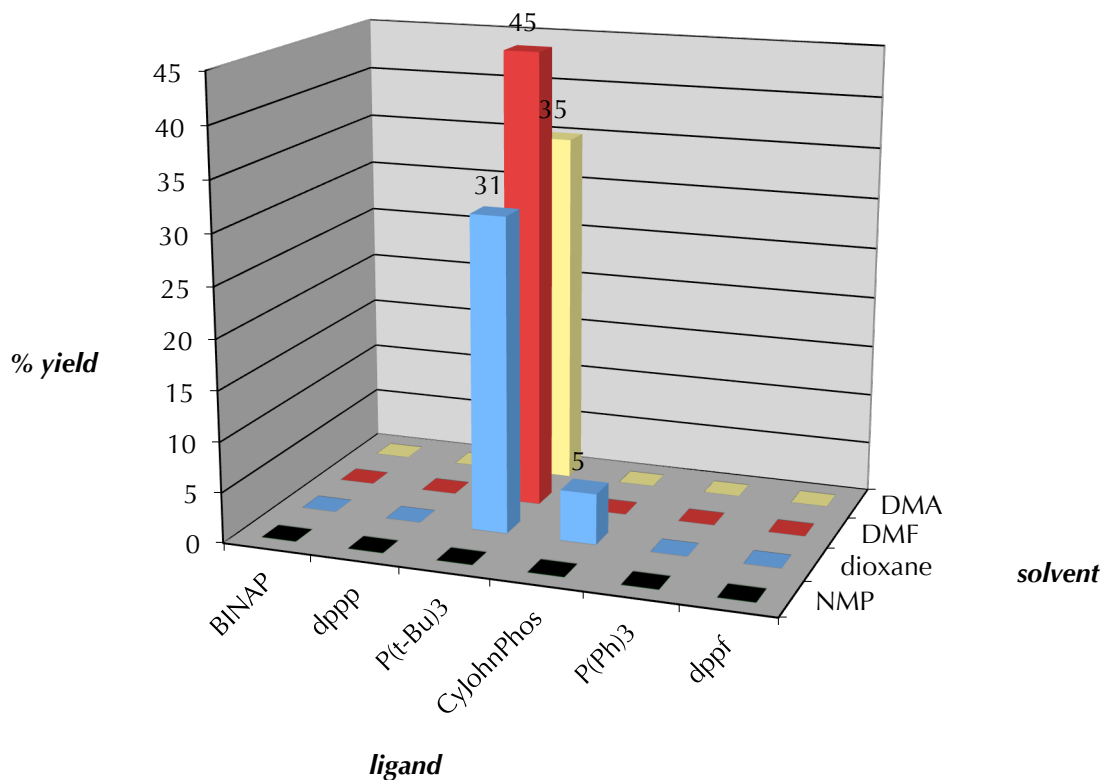


Figure A8.3.2.1. Summarized results^a of screen 2 at 60 °C

a. yield determined by GC analysis of tridecane internal standard

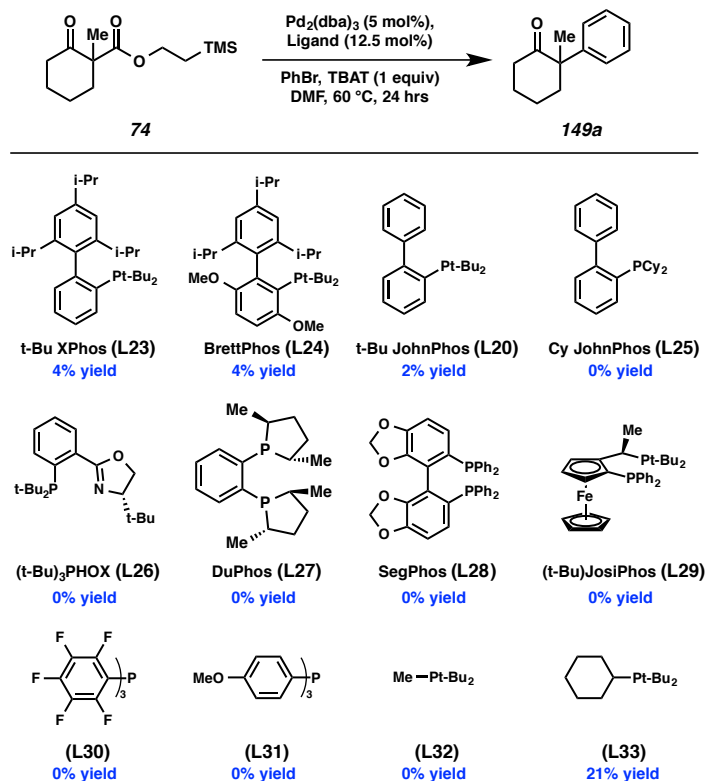
A8.4 OPTIMIZATION OF THE PALLADIUM-CATALYZED α -ARYLATION OF TMSE β -KETOESTERS

While we were pleased with the results of our initial reaction screening efforts, a considerable amount of further investigation was required to develop an α -arylation reaction that is synthetically useful.

We examined a wide array of phosphine ligands (**L23–L33**) while holding constant reaction parameters found to be optimal in our initial experiments (i.e., palladium source, solvent, fluoride source; Figure A8.3.2.1). The results of these

experiments were uniformly disappointing, with poor yields observed in the best cases. Ligands that Buchwald and coworkers have shown to be effective in palladium catalyzed α -arylation chemistry, such as the Brett-, John- and XPhos ligands (**L23–L25**), as well as *t*-Bu-JosiPhos (**L29**), delivered minimal amounts of the desired product.¹¹⁴ Likewise, ligands that Hartwig and coworkers have employed in the α -arylation of tetralone derivatives, such as SegPhos (**L28**) also failed to deliver the desired product.¹¹² In addition to mono- and bisphosphine ligands, P,N type phosphinooxazoline ligands were also explored to no fruitful end.

To tease out the relative importance of sterics and electronics in the ligand scaffold, a series of mono-phosphine of varying polarity and steric encumbrance were investigated. The observation that tripentafluorophenylphosphine (**L30**), which is both electron-poor and sterically large, possessing a ligand cone angle¹¹⁵ of greater than 180°, was not a proficient ligand suggests that excess electron density about palladium is a prerequisite feature of successful catalyst systems for this transformation. Steric hindrance about the ligand also proved to be essential to reaction efficiency, inasmuch as substituting one phosphine *tert*-butyl substituent with a cyclohexyl (i.e., ligand **L33**) resulted in a halving of the best previously observed yield.

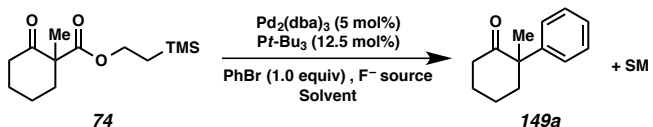
Figure A8.4.1. Elaborated ligand search^a

a. yield determined by GC analysis of tridecane internal standard

Given these dissatisfactory results, we reasoned that attempts to first improve reaction efficiency by optimizing other reaction parameters might lead us to conditions that would tolerate alternative ligand scaffolds, while retaining optimal conversions. Therefore, we set about to identify conditions capable of delivering synthetically useful yields, beginning with a screen of alternative fluoride sources, temperature, and reaction times (Figure A8.4.2). Unfortunately, we were met again with disappointing results. Alternative fluoride sources, such as CsF, a combination of KF in 18-crown-6, tris(dimethylamino)sulfonium difluorotrimethylsilicate (TASF), and sodium hexafluorosilicate all proved to be less optimal relative to TBAT. Variation in reaction

time and temperature, as well, only served to demonstrate that the conditions that we had previously identified worked best in the chemistry.

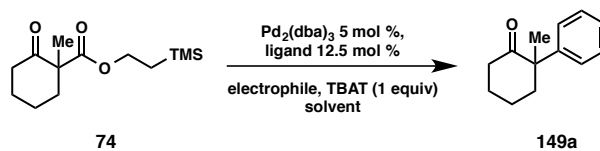
Figure A8.4.2. Optimization of fluoride donor, reaction time and temperature



entry	solvent	F ⁻ source	time (h)	temp (°C)	% yield ^a
1	DMF	18c6/KF	24	60	29
2	dioxane	18c6/KF	24	60	0
3	DMF	Na ₂ SiF ₆	24	60	2
4	MeCN	CsF	24	60	0
5	DMF	TAS-F	24	60	9
6	dioxane	TAS-F	24	60	6
8	DMF	TBAT	24	60	46 ^b
9	DMF	TBAT	48	60	45
10	DMF	TBAT	72	60	45
11	DMF	TBAT	24	25	2
12	DMF	TBAT	24	40	38
13	DMF	TBAT	24	80	33
14	DMF	TBAT	24	110	23

a. yield determined by GC analysis of tridecane internal standard; b. isolated yield.

In addition to the experiments detailed in Figure A8.4.2, alternative electrophiles (including phenyl iodide, phenyl chloride, phenyl triflate and biaryl iodonium triflates), molar ratio of phenyl bromide to substrate, molar ratio of TBAT to substrate, catalyst loading, alternative palladium sources (Pd(OAc)₂, Pd(PPh₃)₄), and alternative metals (nickel and copper) were investigated. Unfortunately, through all of these experiments, in no case did we observe reaction yields improved over the original system (Figure A8.4.2, entry 8). Selected results from these experiments are shown below in Figures A8.4.3 and A8.4.4.

Figure A8.4.3. Further optimization of ligand, solvent and temperature

entry	ligand	solvent	temp (°C)	electrophile/ equiv	time (hrs)	mol% cat.	%yield ^a (XX)
1	Segphos	DMF	70	PhBr/ 1.05	24	5	0
2	Segphos	dioxane	70	PhBr/ 1.05	24	5	0
3	Segphos	toluene	70	PhBr/ 1.05	24	5	0
4	Segphos	DMF	80	PhBr/ 1.05	24	5	0
5	Segphos	dioxane	80	PhBr/ 1.05	24	5	0
6	Segphos	toluene	80	PhBr/ 1.05	24	5	0
7	Segphos	DMF	110	PhBr/ 1.05	24	5	0
8	Segphos	dioxane	110	PhBr/ 1.05	24	5	0
9	Segphos	toluene	110	PhBr/ 1.05	24	5	0
10	<i>t</i> -Bu ₃ P	DMF	80	PhBr/ 1.05	48	5	17
11	<i>t</i> -Bu ₃ P	DMF	110	PhBr/ 1.05	48	5	17
12	<i>t</i> -Bu ₃ P	DMF	80	PhI/ 1.05	48	5	18
13	<i>t</i> -Bu ₃ P	DMF	110	PhI/ 1.05	48	5	19
14	<i>t</i> -Bu ₃ P	DMF	110	PhI/ 1.05	72	5	21
15	none	DMF	60	PhBr/ 1.05	24	5	0
16	(F ₅ C ₆) ₃ P	DMF	60	PhBr/ 1.05	24	5	0
17	<i>t</i> -BuJosiphos	DMF	60	PhBr/ 1.05	24	5	0.2
18	CyJosiphos	DMF	60	PhBr/ 1.05	24	5	0
19	<i>t</i> -Bu ³ PHOX	DMF	60	PhBr/ 1.05	24	5	0
20	none	DMA	60	PhBr/ 1.05	24	5	0
21	(F ₅ C ₆) ₃ P	dioxane	60	PhBr/ 1.05	24	5	0
22	<i>t</i> -BuJosiphos	dioxane	60	PhBr/ 1.05	24	5	0
23	CyJosiphos	dioxane	60	PhBr/ 1.05	24	5	0

a. yield determined by GC analysis of tridecane internal standard

Figure A8.4.4. Further optimization of ligand, solvent and temperature

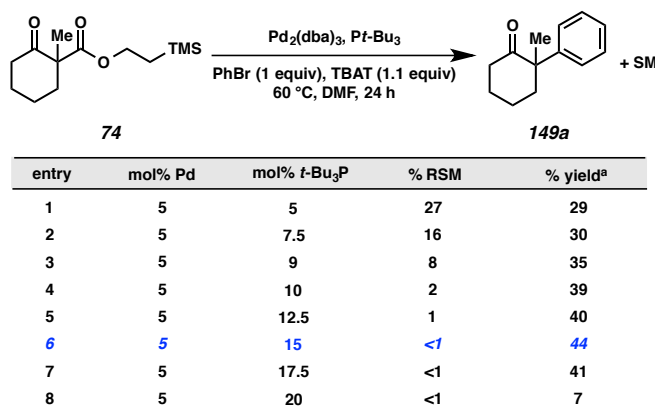
entry	ligand	solvent	temp (°C)	electrophile/ equiv	time (h)	mol% cat.	%yield ^a
1	<i>t</i> -Bu ₃ P	dioxane	80	PhBr/ 1.05	24	2.5	4.8
2	<i>t</i> -Bu ₃ P	dioxane	60	PhBr/ 1.05	24	5.0	31.1
3	<i>t</i> -Bu ₃ P	dioxane	80	PhBr/ 1.05	24	5.0	20.6
4	<i>t</i> -Bu ₃ P	DMF	60	PhBr/ 1.05	24	5.0	64.0
5	<i>t</i> -Bu ₃ P	DMF	80	PhBr/ 1.05	24	5.0	44.5
6	<i>t</i> -Bu ₃ P	DMF	80	PhBr/ 2.0	24	5.0	34.7
7	<i>t</i> -Bu ₃ P	DMF	80	PhBr/ 3.0	24	5.0	44.1
8	<i>t</i> -Bu ₃ P	THF	60	PhBr/ 1.05	24	5.0	12.6
9	<i>t</i> -Bu ₃ P	THF	80	PhBr/ 1.05	24	5.0	3.8
10	<i>t</i> -Bu ₃ P	DMF	60	PhCl/ 1.05	24	5.0	1.5
11	<i>t</i> -Bu ₃ P	DMF	80	PhCl/ 1.05	24	5.0	4.6
12	<i>t</i> -Bu ₃ P	dioxane	60	PhCl/ 1.05	24	5.0	--
13	<i>t</i> -Bu ₃ P	dioxane	80	PhCl/ 1.05	24	5.0	0.4
14	<i>t</i> -Bu ₃ P	toluene	80	PhCl/ 1.05	24	5.0	0.4
15	<i>t</i> -Bu ₃ P	DMF	25	PhI/ 1.05	12	5.0	1.9
16	<i>t</i> -Bu ₃ P	DMF	40	PhI/ 1.05	12	5.0	37.9
17	<i>t</i> -Bu ₃ P	DMF	60	PhI/ 1.05	12	5.0	45.9
18	<i>t</i> -Bu ₃ P	dioxane	60	PhI/ 1.05	12	5.0	--
19	<i>t</i> -Bu ₃ P	dioxane	80	PhI/ 1.05	12	5.0	18.8
20	<i>t</i> -Bu ₃ P	toluene	25, 40, 60	PhI/ 1.05	12	5.0	--
21	<i>t</i> -Bu ₂ MeP	DMF	25, 40, 60	PhBr/ 1.05	24	5.0	--
22	<i>i</i> -PrJohnPhos	DMF	60	PhBr/ 1.05	24	5.0	3.7
23	<i>i</i> -PrJohnPhos	DMF	80	PhBr/ 1.05	24	5.0	1.3
24	<i>i</i> -PrJohnPhos	DMF	110	PhBr/ 1.05	24	5.0	4.2
25	<i>i</i> -PrJohnPhos	dioxane	60	PhBr/ 1.05	24	5.0	3.5
26	<i>i</i> -PrJohnPhos	dioxane	60	PhBr/ 1.05	24	5.0	1.6
27	<i>i</i> -PrJohnPhos	toluene	25, 40, 60	PhBr/ 1.05	24	5.0	--

a. yield determined by GC analysis of tridecane internal standard

One screen that produced results meriting discussion was that which explored reaction efficiency with respect to varying ratios of ligand and metal source (Figure A8.4.5). Interestingly, when the ratio of P(*t*-Bu)₃ to palladium was 1:1, a considerable amount of starting material remain in the product mixture, even in the presence of excess fluoride source (Figure A8.4.5, entry 1). As we increased the ligand loading, we

observed a sharp decline in the amount of starting material remaining until the ratio of palladium to ligand surpassed 2:1. Noting the stability of the palladium carboxylate species formed in our allylic alkylation reaction, we believe it is plausible that the correct stoichiometry of palladium and ligand is needed for the formation of a catalyst complex capable of chelating the β -dicarbonyl, which in turn may be required to activate our (2-TMS)ethyl β -ketoester substrate for deprotection by TBAT.

Figure A8.4.5. Importance of metal source to ligand ratio



a. yield determined by GC analysis of tridecane internal standard

A8.5 OUTLOOK AND FUTURE DIRECTIONS FOR CARBOXYLATE PROTECTED ENOLATES IN α -ARYLATION

A8.5.1 Hypotheses that remain to be tested in α -arylation of TMSE β -ketoesters

We have, at this point, a number of unanswered questions regarding our catalyst system and reaction as developed thus far. For example, we would like to determine the role of our catalyst in promoting the deprotection of our substrate. We would like to

devise a method to determine the particular mode of reductive elimination operative in our reaction. Our inability to make direct comparisons between the reaction we have developed and existing methods for α -arylation, due to the nature of our substrate, is an unfortunate limitation of the TMSE β -ketoester substrate class, elimination of which we believe would help to answer a number of our questions. For instance, every example of asymmetric α -arylation published to date employs toluene as solvent; however, TBAT is insoluble in toluene to the point of being completely ineffectual. In view of work by Rawal¹¹⁶ and others,¹¹⁷ demonstrating the importance of the presence or absence of metal salts in determining α -arylation reaction outcomes, we would like to examine the efficiency of our reaction in the absence of fluoride salts. However, successful solvents for our reaction, DMF and 1,4-dioxane in particular, also ensure that salts generated in the course of the reaction remain soluble. We believe that the use of an alternative substrate may afford us the opportunity to better dissect our reaction and determine the relative importance of the factors enumerated above. In particular, we envision that substrates that follow a deacylative pathway into catalysis may be highly valuable in this regard.

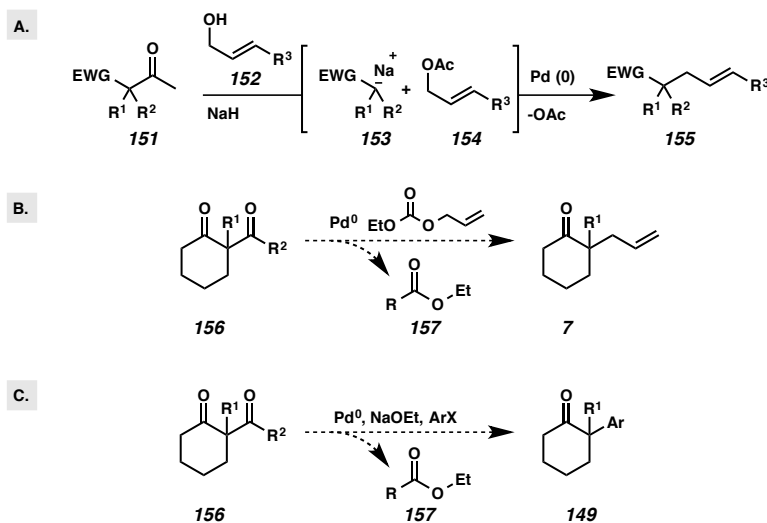
A8.5.2 Deacylative in situ access to prochiral enolates

Recent reports by Tunge and co-workers¹¹⁸ inspired us to consider a deacylative pathway into catalysis. Tunge has shown that treatment of α -electron withdrawing acetyl compounds (Scheme A8.5.2.1, **151**) with sodium allyloxide produces a molecule of allyl acetate (**153**) and generates the α -stabilized carbanion (**152**). In the presence of a palladium catalyst, an equivalent of acetate ion is liberated in the formation of a

palladium π -allyl species, which are labile to attack by **152**, and results in allylic alkylation to generate an α -quaternary carbon stereocenter (**7**).

We envisioned a deacylative allylic alkylation scenario (Scheme A8.5.2.1) in which to test our substrate. Upon combining catalytic palladium (0) and an alkyl allyl carbonate, the co-catalytic amount of alkoxide generated would attack substrate **156** and generate the desired prochiral enolate and byproduct ester **157**. Trapping of the enolate with an allyl palladium species would complete the catalytic cycle to deliver **7** (Scheme A8.5.2.1B). In the case of α -arylation, we imagined that subjecting substrate **156** to a nucleophile like sodium ethoxide would provide access to a prochiral enolate, which could subsequently participate in palladium catalysis and afford α -arylated products (**149**, Scheme A8.5.2.1C).

Scheme A8.5.2.1. Conceptual schemes for deacylative enolate formation: A. previous research by Tunge and coworkers; B. proposed allylic alkylation via deacylative pathway; C. proposed α -arylation via deacylative pathway



A number of potential benefits are inherent in this substrate class. The commercial starting materials needed to make derivatives of **156** (e.g., acetic anhydride, trichloroacetyl chloride or trifluoroethyl acetate) all cost less than one dollar per gram, whereas the 2-TMS-ethanol needed to make our (2-TMS)ethyl β -ketoester substrate is priced at nine dollars per gram. Furthermore, these substrates will allow us to investigate the conditions we have developed in a broader range of solvents, such as toluene, in the absence of fluoride salts and explore a catalytic cycle in which the decarboxylation step is absent. However, synthesis of substrate **156** has thus far proven challenging, and our attempts to make any such substrate following the procedure of Tunge and coworkers have failed.

A8.6 CONCLUDING REMARKS

This appendix details our development of an α -arylation reaction of carboxylate-protected enolates, which makes use of the TMSE β -ketoester substrate class that we have developed. The best observed results for this transformation occurred with a combination of Pd₂(dba)₃ as metal source and P(*t*-Bu)₃ as ligand, phenyl bromide the aryl source, TBAT the fluoride source, DMF as solvent, and at 60 °C, with a 45% isolated yield of the racemic desired product. Notably, arylation occurs strictly at the site of deprotection to afford α -quaternary arylated compounds, despite the presence of other enolizable protons. This constitutes a significant inroad to a highly challenging, unsolved problem—the efficient and enantioselective α -arylation of carbonyl compounds bearing more than one enolizable proton. Given this promising beginning, it is our hope that further investigation of alternative ligand (for example N-heterocarbene ligands),

alternative metal sources (including an exhaustive investigation of nickel catalysts) and alternative substrate classes (such as the 1,3-diketones discussed above) will reveal conditions that confer synthetic utility to this potentially valuable transformation.

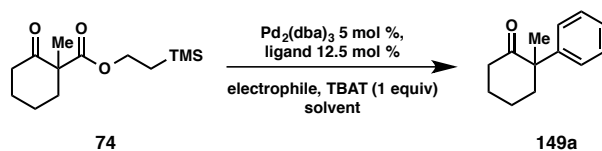
A8.7 EXPERIMENTAL SECTION

A8.7.1 Materials and Methods

Unless otherwise stated, reactions were performed in flame-dried glassware under an argon or nitrogen atmosphere using dry, deoxygenated solvents. Solvents were dried by passage through an activated alumina column under argon.⁶¹ Reaction progress was monitored by thin-layer chromatography (TLC) or Agilent 1290 UHPLC-MS. TLC was performed using E. Merck silica gel 60 F254 precoated glass plates (0.25 mm) and visualized by UV fluorescence quenching, *p*-anisaldehyde, or KMnO₄ staining. Silicycle SiliaFlash® P60 Academic Silica gel (particle size 40–63 nm) was used for flash chromatography. All reagents were purchased from Sigma-Aldrich, Acros Organics, Strem, or Alfa Aesar and used as received unless otherwise stated. Reaction temperatures were controlled by an IKAmag temperature modulator unless otherwise indicated. Stirring was accomplished with Teflon® coated magnetic stir bars. Glove-box manipulations were performed under a N₂ atmosphere. ¹H NMR spectra were recorded on Varian Inova 500 MHz and 600 MHz spectrometers and evaluated relative to residual CHCl₃ (δ 7.26 ppm) or C₆HD₅ (δ 7.16 ppm). ¹³C NMR spectra were recorded on a Varian Inova 500 MHz spectrometer (125 MHz) and evaluated relative to CHCl₃ (δ 77.16 ppm) or C₆HD₅ (δ 128.06 ppm). Analytical chiral GC analysis was performed with an

Agilent 6850 GC using a GT-A column (0.25 m \times 30.00 m) employing a 130 °C isotherm and a flow rate of 1.0 mL/min.

A8.6.2 Procedure for Symyx assisted screening of α -arylation



This description will use the screen described in Scheme A8.3.1.1 as a representative example. All Symyx reaction screenings were conducted in a nitrogen-filled glove-box at the Caltech Center for Catalysis and Chemical Synthesis using solvents that were degassed with nitrogen after passage through an activated alumina column under argon. Overall screen design was predicated by the desired individual reaction volume (in the case at hand 0.33 mL with a 0.1 M substrate concentration), and by the number of reactions to be conducted. All stock solutions were prepared in ca. 1.5 times excess to the exact amount of compound required for screening.

First, a stock solution of $\text{Pd}_2(\text{dba})_3$ was prepared by combining 0.1448 g of $\text{Pd}_2(\text{dba})_3$ with 20 mL of THF in a 20 mL scintillation vial.¹¹⁹ The Symyx robot arm was then used to dispense 0.208 mL of this stock solution into each of the 72 half-dram reaction vials. Using the Symyx Automation Studios program a sequence for the robot arm was loaded, the arm was initialized and flushed with 7 mL of the backing solvent, THF. Multi-dispense mode was used and a 10 μL airgap, source overshoot of 5%, draw speed of 20 $\mu\text{L}/\text{second}$ (lowered from the normal draw speed due to viscosity), dispense speed of 150 $\mu\text{L}/\text{second}$ (again, due to viscosity), 1 mm draw distance from bottom

(calibrated prior to each screen) and 1 mL rinse of backing solvent prior to each draw were employed. Upon completion of the addition, the dispense needle was flushed with an additional 5 mL of THF. The 72 reaction vials were then separated onto 2 36 reaction well plates and stripped of solvent by vacuum centrifugation using a Thermo Electro Corporation SDP 121P vacuum centrifuge until a pressure of 1.5 torr was reached (ca. 1 h under vacuum). Thus, each vial then contained 1.51 mg (0.00165 mmol) of Pd₂(dba)₃.

Stock solutions for all other compounds were prepared according to the amount of volume to be dispensed and the number of reactions planned. For example, for the screen at hand, 8.5 mg of TMSE β -ketoester substrate (**74**, 0.033 mmol) were to be dispensed in 0.08325 mL of solvent to each reaction vessel. Total masses to be used in each stock solution were calculated by multiplying (mass per reaction) x (total number of planned reactions per solvent) x 1.5; in the present case, 0.0085 g x 18 x 1.5 = 0.23 g of **74** per stock solution. Stock solutions of **74** were prepared thusly by combining 0.1956 g, 0.2126 g, 0.2275 g and 0.2313 g of **74** with 1.916 mL, 2.080 mL, 2.228 mL and 2.265 mL of dioxane, toluene, DMF and DMSO, respectively. For each of these stock solutions, 0.08325 mL of solution contains 8.5 mg of compound. TBAT stock solutions were then prepared in the same fashion, such that TBAT could be dispensed in 0.1665 mL of solvent. Finally, ligand stock solutions were prepared in the same fashion, such that the ligand could be dispensed in 0.08325 mL of solvent. Phenyl bromide and tridecane (internal standard) would be added neat, and their volumes considered negligible. Therefore, each reaction vessel would contain 0.33 mL of solvent total (0.08325 mL + 0.08325 mL + 0.1665 mL) once all reaction components had been added to the reaction vessel. As the Symyx robot is only capable of dispensing homogenous

liquid solutions, and some of the reaction components are only sparingly soluble in the desired solvents, some compounds had to be added manually, by hand. This proved to be the case for BINAP, as BINAP is minimally soluble in all solvents other than THF.

Once all of the stock solutions were prepared and compounds for which stock solutions could not be prepared had been added manually, the reactions were split evenly onto 3 plates (24 reactions per plate). For bookkeeping, the reactions were each given a number according to the position on the plate, and organized accordingly. For example, reactions contained in the plate held at 60 °C are given the following designations:

	dioxane	toluene	DMF	DMSO
rac-BINAP	1	2	3	4
<i>t</i>-BuPHOX	5	6	7	8
DuPhos	9	10	11	12
PCy₃	13	14	15	16
PPh₃	17	18	19	20
dppe	21	22	23	24

In a similar fashion, number values are assigned to all other reactions in increasing order, such that a similar chart depicting plate number 3 (held at 110 °C) would put reaction number 72 in the bottom right hand corner.

The robot arm was then used to dispense compounds to the individual reaction vials. Using the same sequence, the robot arm was again initialized and flushed with 5 mL of the backing solvent, THF. Multi-dispense mode was used and a 10 μ L airgap, source overshoot of 5%, draw speed of 20 μ L/second (lowered from the normal draw speed of 50 μ L, due to viscosity), dispense speed of 150 μ L/second (again, due to viscosity), 1 mm draw distance from bottom (calibrated prior to each screen) and 1 mL

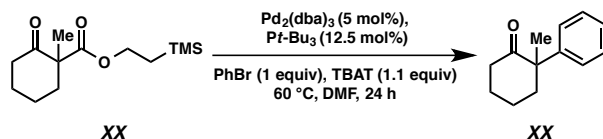
rinse of backing solvent prior to each draw were employed. The compounds were then added in the following order: ligand (solution), substrate (**74**, solution), bromobenzene (neat), TBAT (solution), tridecane (neat). Teflon® coated magnetic stirring bars were then added to each vial and each vial was fitted with a Teflon® lined screw cap. The plates were then set into heated stirring wells set to 60, 80 and 110 °C, and stirred at a rate of 400 rpm.

After stirring at the indicated temperatures for 24 hours the reactions were removed from the glovebox, and processed manually. The workup procedure for reactions run in dioxane and toluene is as follows: each reaction is diluted to a total volume of 2 mL with hexanes and then pushed through a plug of silica with compressed air and collected in a 20 mL scintillation vial. Silica plugs were made by crushing one fourth of a Watman fiberglass pad (1" diameter) into a 6" pipette and then filling the pipette with ca. 1 mL of silica. After passing the reaction solution through the pipette plug, it was rinsed with 3 mL of hexanes and the collected eluents diluted further with hexanes until 10 mL total volume was reached. 1.5 mL of this solution is then used to prepare a sample for GC analysis. For reactions run in DMF or DMSO, each reaction was first transferred to a 20 mL scintillation vial, diluted with 5 mL hexanes, washed thoroughly with water, extracted and then passed through a pipette plug of silica. These samples were diluted with hexanes to 10 mL volume total and analytical samples prepared by taking ca. 1.5 mL of this solution.

GC analysis of the analytical samples was then carried out. Retention time (t_R) for tridecane – 3.31 min, t_R for **74** – 27.04, 27.79 min, t_R for **149a** – 17.097, 17.33

min. All other screening experiments discussed in the text that were carried using the Symyx automation system, were conducted by adaptation of the above procedure.

A8.6.3 Procedure for manual screening of α -arylation



To a 2 mL scintillation vial with a stir bar were added $\text{Pd}_2(\text{dba})_3$ (16.4 mg, 0.015 mmol), $\text{P}(t\text{-Bu})_3$ (21.9 mg, 0.037 mmol) and DMF (9 mL) in a nitrogen-filled glove-box. The dark purple mixture was stirred at ambient glove-box temperature (ca. $30\text{ }^\circ\text{C}$) for 35 minutes at which point the mixture had become red-orange. TBAT (80.0 mg, 0.31 mmol) was added to the reaction mixture, followed by phenyl bromide (80.0 mg, 0.31 mmol) and tridecane (80.0 mg, 0.31 mmol). Finally, TMSE β -ketoester **74** (80.0 mg, 0.31 mmol) was added as a solution in DMF (x.x M). The resulting yellow-green reaction mixture was stirred at $60\text{ }^\circ\text{C}$ until full conversion of the starting material was indicated by TLC analysis (reaction times typically ranged 18 to 36 hours). The vial was removed from the glove-box, diluted with 3 mL of Et_2O , extracted with 3 mL H_2O (x3), dried over Mg_2SO_4 directly purified by flash column chromatography (SiO_2 , 2% EtOAc in hexanes to 10% EtOAc in hexanes) afforded **149a** (41 mg, 45% yield) as colorless oil. $R_f = 0.3$ (15% Et_2O in pentane); Spectroscopic data for this compound matched that reported in the literature.

A8.7 REFERENCES AND NOTES

- (106) Martin, S. F. *Tetrahedron*, **1980**, 36, 419.
- (107) Burtoloso, A. C. B. *Synlett*, **2009**, 2, 320.
- (108) (a) Culkin, D. A.; Hartwig, J. F. *Acc. Chem. Res.* **2003**, 36, 234. (b) Johansson, C. C. C.; Colacot, T. J. *Angew. Chem., Int. Ed.* **2010**, 49, 676. (c) Novak, P.; Martin, R. *Curr. Org. Chem.* **2011**, 15, 3233.
- (109) Palucki, M.; Buchwald, S. L. *J. Am. Chem. Soc.* **1997**, 119, 11108.
- (110) Hamann, B. C.; Hartwig, J. F. *J. Am. Chem. Soc.* **1997**, 119, 12382.
- (111) (a) Viciu, M. S.; Germaneau, R. F.; Nolan, S. P. *Org. Lett.* **2002**, 4, 4053. (b) Grasa, G. A.; Colacot, T. J. *Org. Lett.* **2007**, 9, 5489. (c) Matsubara, K.; Ueno, K.; Koga, Y.; Hara, K. *J. Org. Chem.* **2007**, 72, 5069. (d) Ehrentraut, A.; Zapf, A.; Beller, M. *Adv. Synth. Catal.* **2002**, 344, 209. (e) Adjabeng, G.; Brenstrum, T.; Frampton, C. S.; Robertson, A. J.; Hillhouse, J.; McNulty, J.; Capretta, A. *J. Org. Chem.* **2004**, 69, 5082. (f) Matsubara, K.; Ueno, K.; Koga, Y.; Hara, K. *J. Org. Chem.* **2007**, 72, 5069. (g) Cao, C.; Wang, L.; Cai, Z.; Zhang, L.; Guo, J.; Pang, G.; Shi, Y. *Eur. J. Org. Chem.* **2011**, 1570.

- (112) (a) Kawatsura, M.; Hartwig, J. F. *J. Am. Chem. Soc.* **1999**, *121*, 1473. (b) Hama, T.; Culkin, D. A.; Hartwig, J. F. *J. Am. Chem. Soc.* **2006**, *128*, 4976.
- (113) Fox, J. M.; Huang, X.; Chieffi, A.; Buchwald, S. L. *J. Am. Chem. Soc.* **2000**, *122*, 1360.
- (114) (a) Åhman, J.; Wolfe, J. P.; Troutman, M. V.; Palucki, M.; Buchwald, S. L. *J. Am. Chem. Soc.* **1998**, *120*, 1918. . (b) Hamada, T.; Chieffi, A.; Åhman, J.; Buchwald, S. L. *J. Am. Chem. Soc.* **2002**, *124*, 1261.
- (115) Tolman, C. A. *Chem. Rev.* **1977**, *77*, 313.
- (116) Iwama, T.; Rawal, V. H. *Organic Letters* **2006**, *8*, 5725.
- (117) (a) Kuwajima, I.; Urabe, H. *J. Am. Chem. Soc.* **1982**, *104*, 6831. (b) Hennings, D. D.; Iwasa, S.; Rawal, V. H. *Tetrahedron Lett.* **1997**, *38*, 6379. (c) Liu, X.; Hartwig, J. F. *J. Am. Chem. Soc.* **2004**, *126*, 5182.
- (118) (a) Grenning, A. J.; Tunge, J. A. *J. Am. Chem. Soc.* **2011**, *133*, 14785. (b) Grenning, A. J.; Tunge, J. A. *Angewandte Chemie International Edition* **2011**, *50*, 1688.
- (119) This amount of Pd₂(dba)₃ is ca. at the solubility limit in 20 mL of THF.

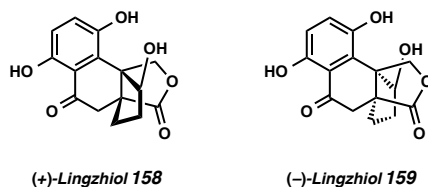
APPENDIX 9

Studies Toward the Enantioselective Total Synthesis of (+)-Lingzhiol

A9.1 INTRODUCTION

A9.1.1 Isolation studies of the lingzhiols

The *Ganoderma* genus of mushrooms is native to southern China and contains around 80 species of mushrooms, many of which have long been used in traditional eastern medicine for ailments of the kidneys.¹²⁰ Recently, investigation into this genus led to the isolation of (+)-lingzhiol (**158**) and (–)-lingzhiol (**159**) from the *Ganoderma lucidum* mushroom (commonly called the Lingzhi mushroom) (Figure A9.1.1.1).¹²¹ (+)-Lingzhiol (**158**) and (–)-lingzhiol (**159**) are a pair of enantiomeric meroterpenoids, or natural products bearing both polyketide and terpenoid sub-units. Vicinal all-carbon quaternary stereocenters (C-3'–C-7') define a common axis about which three of the four rings in the novel 5/5/6/6 rotor-like structure of the lingzhiols hinge. Extensive NMR studies and single crystal X-ray diffraction studies of **158** and **159** enabled the unambiguous assignment of the stereochemistry of the compounds.¹²¹ To date, only one total synthesis of lingzhiol has been reported.¹²²

Figure A9.1.1.1. The structures of (+)-lingzhiol and (–)-lingzhiol

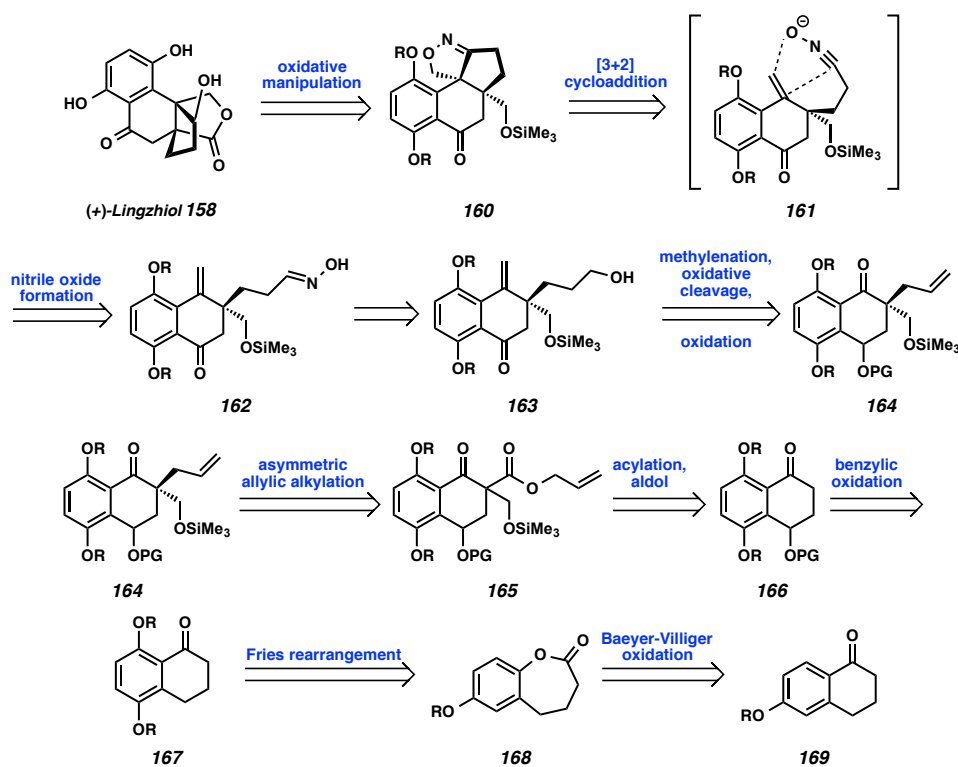
A9.1.2 Biological studies on and bioactivity profile of lingzhiol

Studies conducted subsequent to the isolation lingzhiol have shown it to possess a swath of biological activity against pathogenesis in diabetic nephropathy and renal fibrosis. Diabetic nephropathy and renal fibrosis are prevalent complications that arise in longstanding cases of diabetes and may lead to liver failure, which is usually life-threatening.¹²³ Pathogenic factors contributing to diabetic nephropathy and renal fibrosis include oxidative stress,¹²⁴ extra cellular matrix (ECM) buildup, chronic inflammation and associated disorder of the TGF- β /Smads signaling pathways.¹²⁵ Lingzhiol has been shown to both inhibit ROS directly and to induce nuclear factor erythroid 2-related factor 2 (Nrf2), which up-regulates the production of protective antioxidant species in instances of high oxidative stress.¹²⁶ Chronic inflammation and buildup of ECM in chronic kidney disease have been linked to the deregulation of TGF- β /Smad signaling pathway; in particular, the hyper-phosphorylation of Smad2/3 and loss of Smad 7 have been implicated in the renal scar formation, diabetic nephropathy and renal fibrosis.¹²⁷ Lingzhiol has been shown to selectively inhibit Smad3 phosphorylation, while allowing Smad 2 phosphorylation, which, when taken alone, may have a renal protective role.¹²¹

This striking biological profile has prompted our investigation into the total synthesis of lingzhiol.

A9.2 RETROSYNTHETIC ANALYSIS OF (+)-LINGZHIOL

Retrosynthetically, we envisioned that (+)-lingzhiol (**158**) could originate from tetracycle **160** via oxidative manipulation. Tetracycle **160** could arise from the intramolecular (3+2) dipolar cycloaddition of a pendant nitrile oxide across the exocyclic olefin borne by tetralone derivative **161**. The oxime precursor to tetralone derivative **161**, **162**, would then be obtained by simple condensation subsequent to oxidation of alcohol **163**. Alcohol **163**, in turn, would arise from elaboration of α -quaternary ketone **164**. α -Quaternary ketone **164** would be derived in enantioselective fashion from the decarboxylative allylic alkylation of β -ketoester **165**, which may be prepared by the acylation and aldol reaction of tetralone derivative **166**. Bicycle **166** would be generated via benzylic oxidation of known tetralone derivative **167**, which may be prepared from Fries rearrangement of benzannulated lactone **168**. Finally, lactone **168** may be prepared via the Baeyer-Villiger oxidation of commercially available 7-methoxy tetralone **169**.

Scheme A9.2.1. First-generation retrosynthetic analysis for (+)-lingzhiol

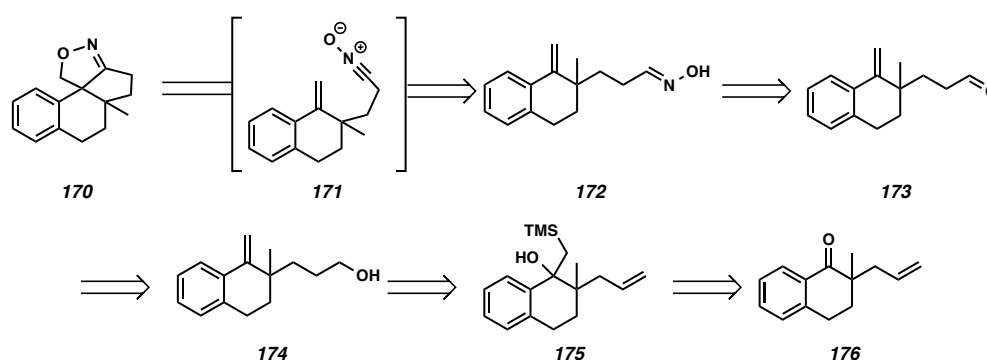
A9.3 MODEL STUDIES TO INVESTIGATE KEY (3+2) CYCLOADDITION IN THE SYNTHESIS (+)-LINGZHIOL

A9.3.1 Retrosynthetic plan for lingzhiol model system

In order to rapidly evaluate the viability of our proposed key (3 + 2) cycloadditions, we began our investigation into the total synthesis of (+)-lingzhiol in the context of a somewhat simplified model system. We reasoned that by eliminating much of the oxidation about the core of lingzhiol we could streamline access to the carbocyclic core (**170**) and, thereby, rapidly arrive at a capable (3+2) cycloaddition substrate such as nitrile oxide **171** (Figure A9.3.1.1). Oxime **172** could arise from the condensation of hydroxylamine onto aldehyde **173**, which could be accessed via the oxidation of primary

alcohol **174**. Carefully orchestrated hydroboration/oxidation and Grignard addition/elimination sequences of known tetralone derivative **176** were planned to access styrenyl alcohol **175**. Tetralone derivative **176** could then be delivered via a palladium catalyzed allylic alkylation.

Scheme A9.3.1.1. First-generation retrosynthetic analysis for (+)-lingzhiol model system

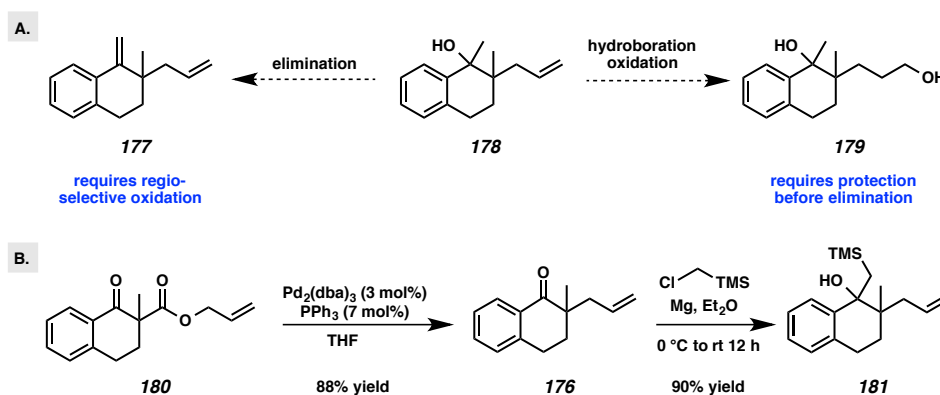


A9.3.2 Synthesis of lingzhiol model system and testing of key (3+2) cycloaddition

Known α -quaternary ketone was accessed in a racemic fashion via the palladium-catalyzed allylic alkylation of allyl β -ketoester **176** (see Chapter 1, *vide infra*). Although ketone to olefin transposition is known to proceed via methyl Grignard addition/elimination, we decided to first explore a Peterson olefination as opposed to something less exotic: our reasoning was twofold (Figure A9.3.2.1A). On one hand, we believed that simple methyl Grignard addition to α -quaternary ketone **176** followed by elimination would give diene **177** and require a subsequent regioselective hydroboration/oxidation. On the other hand, if hydroboration oxidation was carried out prior to methyl Grignard addition, elimination of the tertiary alcohol would be

complicated by the presence of the primary alcohol, **179**, and require an additional protection/deprotection sequence. Peterson olefination, however, would obviate these issues, and allow for simultaneous olefin formation and oxidation. After some optimization we found that the desired tertiary alcohol **181** could be prepared in 90% yield from addition of the Grignard of (chloromethyl)trimethylsilane to ketone **176** (Figure A9.3.2.1B).

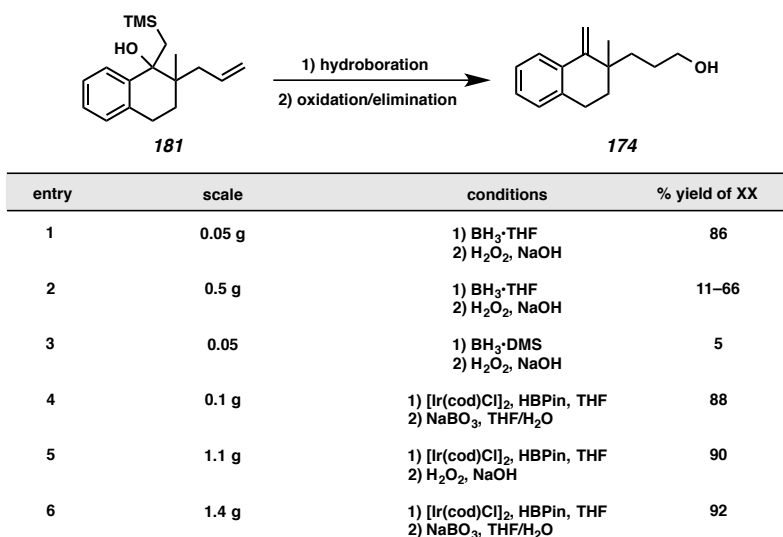
Scheme A9.3.2.1 A. Foreseeable difficulties in advancing methyl Grignard addition to ketone **176**;
B. Synthesis of olefin **181**



With tertiary alcohol **181** in hand, we began studies to identify effective hydroboration/oxidation conditions to access primary alcohol **174**. We were encouraged to find that treatment of olefin **181** with $\text{BH}_3 \cdot \text{THF}$ complex, followed by aqueous hydrogen peroxide and sodium hydroxide, delivered the primary alcohol with concurrent elimination of trimethylsilyl alcohol to afford the desired styrenyl alcohol in 86% yield, when performed on 0.05 g scale (Scheme A9.3.2.2, entry 1). Unfortunately, this result proved difficult to replicate when carried out on larger scale, or when newly purchased reagents were employed (entry 2). Similarly, $\text{BH}_3 \cdot \text{DMS}$ complex proved to be less

efficient than the THF complex. To our delight, we discovered that conditions for the iridium-catalyzed regioselective hydroboration/oxidation developed by Crudden and coworkers,¹²⁸ delivered the desired product in excellent and consistent yields irrespective of reaction scale (entries 4–6).

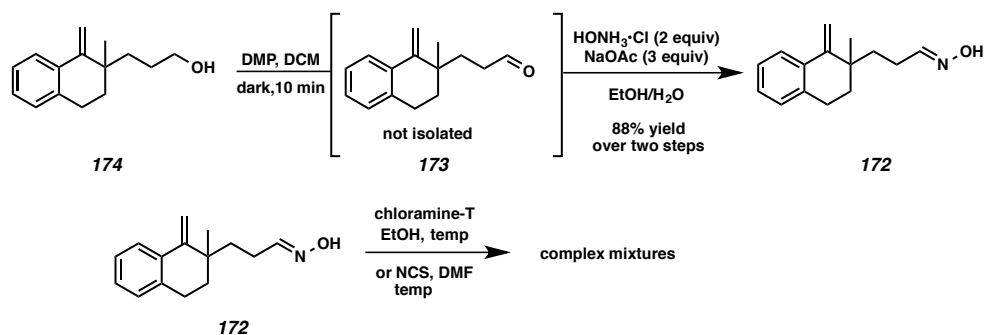
Scheme A9.3.2.2. Optimization studies for the tandem hydroboration/oxidation elimination of **181**



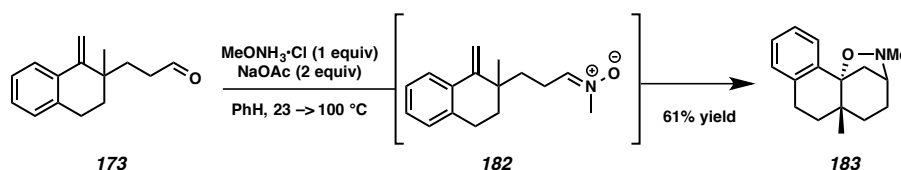
Dess-Martin periodinane (DMP) oxidation of primary alcohol **174** proceeded smoothly, to give aldehyde **173**, which was observed by ¹H NMR, and without rigorous isolation subjected conditions for oxime formation (Scheme A9.3.2.3). When crude aldehyde **173** was treated with hydroxylamine hydrochloride (5 equiv), pyridine (15 equiv), in EtOH a 25% yield (over 2 steps) of oxime **172** was observed. However, by changing the base employed to sodium acetate and reducing the equivalents of hydroxylamine hydrochloride (below, Scheme A9.3.2.3), an 88% yield was observed for the formation of oxime **172**. Pleased with these results, we next attempted to affect our

key (3+2) cycloaddition addition reaction, via the *in situ* formation of the corresponding nitrile oxide.¹²⁹ Attempts using chloramine-T¹³⁰ in ethanol at a variety of temperature failed to deliver anything other than complex mixtures. Likewise, attempts at nitrile oxide formation/(3+2) cycloaddition using N-chlorosuccinamide (NCS) and other oxidants¹³¹ also delivered complex mixtures of products, none of which appeared to be the desired tetracycle.

Scheme A9.3.2.3. Synthesis of oxime **172** and attempts at (3+2) cycloaddition



While we were discouraged by these results, we reasoned that the styrene functionality of oxime **172** may be unstable, and that attempting a (3+2) cycloaddition via the corresponding nitron might be less harsh and limit the degree of undesired reactivity observed. We therefore subjected aldehyde **173** to N-methylhydroxylamine hydrochloride and sodium acetate in benzene at increasing temperature and, finally, observed a (3+2) cycloaddition in 61% yield. Unfortunately, the regioselectivity by which the cycloaddition proceeded afforded the undesired, albeit interesting bridged product (**183**, Scheme A9.3.2.4).

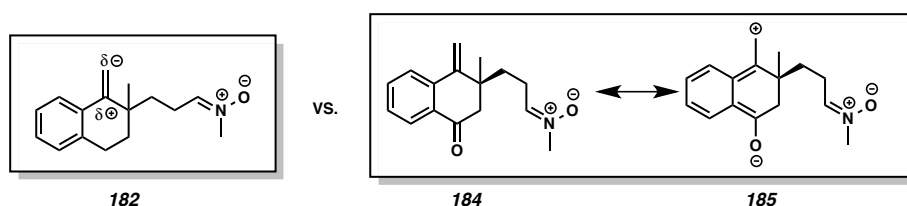
Scheme A9.3.2.4. The intramolecular (3+2) cycloaddition of nitron **182** to form tetracycle **183**

^a Unless otherwise noted, full characterization data for compounds depicted in this scheme have not been collected.

A9.4 REVISED MODEL STUDIES TO INVESTIGATE KEY (3+2) CYCLOADDITION IN THE SYNTHESIS (+)-LINGZHIOL

A9.4.1 Rationale and revised plan for (+)-lingzhiol model system

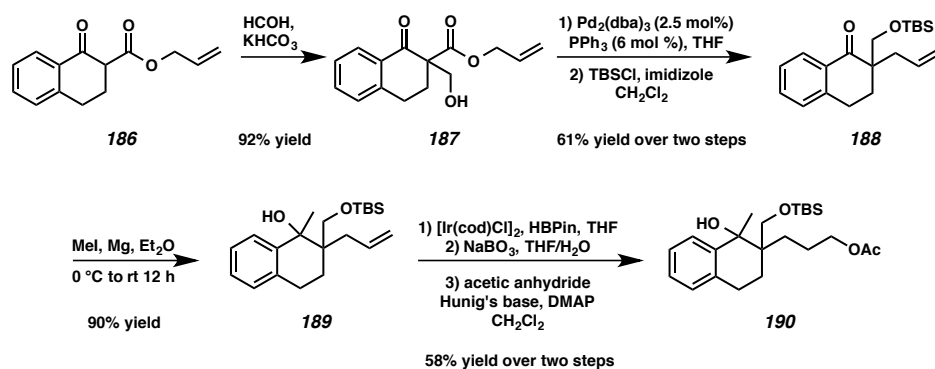
With the disappointing results described in Section A9.3 in mind, we returned to our model system with the goal of biasing the electronics of the styrene olefin, such that we could invert the regioselectivity observed in the (3+2) cycloaddition. We believe that, due to inductive donation from the aryl group, a partial positive charge is present at the terminal position of the exocyclic olefin and that this was, in part, the source of regioselectivity we observed in the intramolecular cycloaddition of nitron **182** (Figure A9.4.1.1). We reasoned that by introducing the ketone present in the natural product at an earlier stage, the benzylogous enolate resonance contributor might serve to invert the electronics of the exocyclic olefin in **184** (Figure A9.4.1.1). By this rationale, we hypothesized that we might affect an inversion in the regioselectivity of the (3+2) cycloaddition in favor of the desired pathway. Therefore, we set about constructing a new model compound with which we would test our key cycloaddition.

Figure A9.4.1.1. A hypothesis regarding the electronics of exocyclic olefin **182**

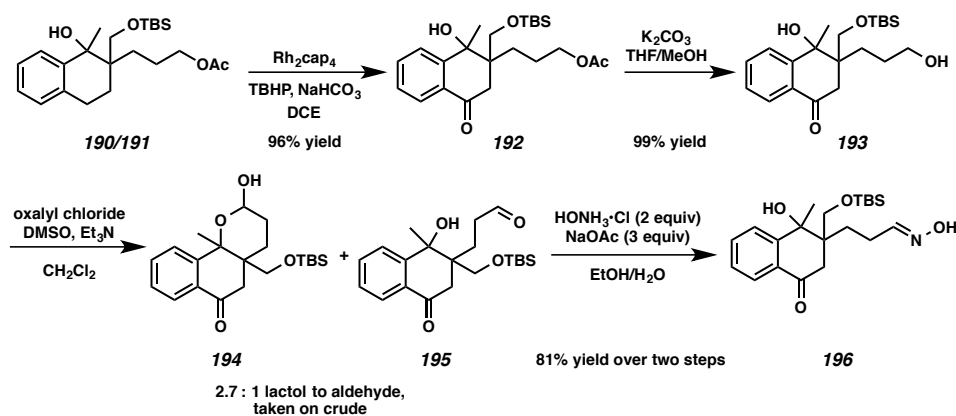
A9.4.2 Synthesis of the revised model system for (+)-lingzhiol

As we wished to install the requisite ketone via late stage benzylic oxidation, our early experiments towards a revised model system involved attempts to directly oxidize substrates generated in our previous model system. However, as most benzylic oxidation processes involve the formation of a benzylic radical, the presence of an exocyclic styrenyl olefin or allyl group in the benzylic oxidation substrate proved troublesome. As a consequence of this, a new route in which formation of the styrenyl olefin and hydroboration were reordered was required.

Ultimately we chose to pursue the route shown below in Scheme A9.4.2.1. Beginning with acylated tetralone derivative **186**, aldol reaction with formaldehyde, palladium catalyzed allylic alkylation, and silyl protection of the primary alcohol proceeded smoothly to give silyl ether **188** in 56% yield over the three steps. The reaction of ketone **188** with methyl Grignard reagent furnished tertiary alcohol **189** in 90% yield. This alcohol was then elaborated to bicycle **190** by iridium-catalyzed hydroboration, oxidation with sodium perborate and, finally, acetate protection, all of which proceeded in 58% yield overall.

Scheme A9.4.2.1. Synthesis of revised model for (3+2) cycloaddition studies

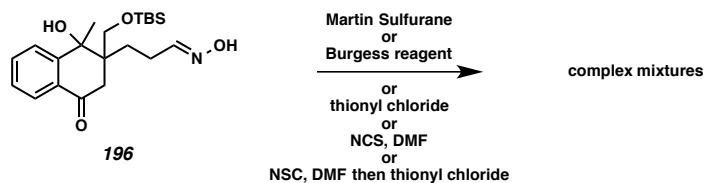
With acetate **190** in hand, we were poised to explore benzylic oxidation strategies. After numerous failed attempts to first brominate and then affect a Kornblum-type oxidation, we turned to a report from Doyle and co-workers,¹³² in which benzylic oxidation is catalyzed by dirhodium tetracaprolactamate. This strategy proved successful in the event, and we were pleased to isolate benzylic ketone **192** in 96% yield in just a single step from bicycle **191** (Scheme A9.4.2.2). An uneventful deprotection of the primary acetate under standard conditions liberated primary alcohol **193**, which was oxidized to a 2.7:1 mixture of lactol **194** and aldehyde **195** and via Swern oxidation. This mixture was then subjected directly to the conditions for oxime formation with which we had previous success. In the present case, these conditions furnished oxime **196** in 81% yield overall from primary alcohol **193**.

Scheme A9.4.2.2. Synthesis of revised model for (3+2) cycloaddition studies

With a reliable route to access oxime **196** in place, we set about attempting to affect the formation of our desired (3+2) cycloaddition precursor. Concerned over the stability of the pendant oxime, we began our investigation by employing relatively mild dehydrating agents such as Martin sulfurane¹³³ and Burgess reagent.¹³⁴ Unfortunately, neither of these experiments nor experiments employing harsher reagents such as thionyl chloride proved fruitful, and in all cases resulted in complex mixtures of products, none of which were believed to be the desired styrene (Scheme A9.4.2.3). We believe these disappointing results may be, in part, accounted for by the incompatibility of an electrophilic styrene moiety and nucleophilic oxime oxygen both present in the desired product. Efforts to first form the α -chloro oxime using NCS¹²⁹ and subsequently affect simultaneous olefin and nitrile oxide formation were also met with failure. Noting the relative instability of the oxime moiety to the conditions required for dehydration, we attempted to preclude these difficulties by dehydrating at an earlier point in the synthesis. However, efforts to advance styrenyl compounds in which the protected alcohol had yet

to be oxidized were met with what we believe to be hetero-Michael addition processes by the alcohol oxygen into the styrene olefin.

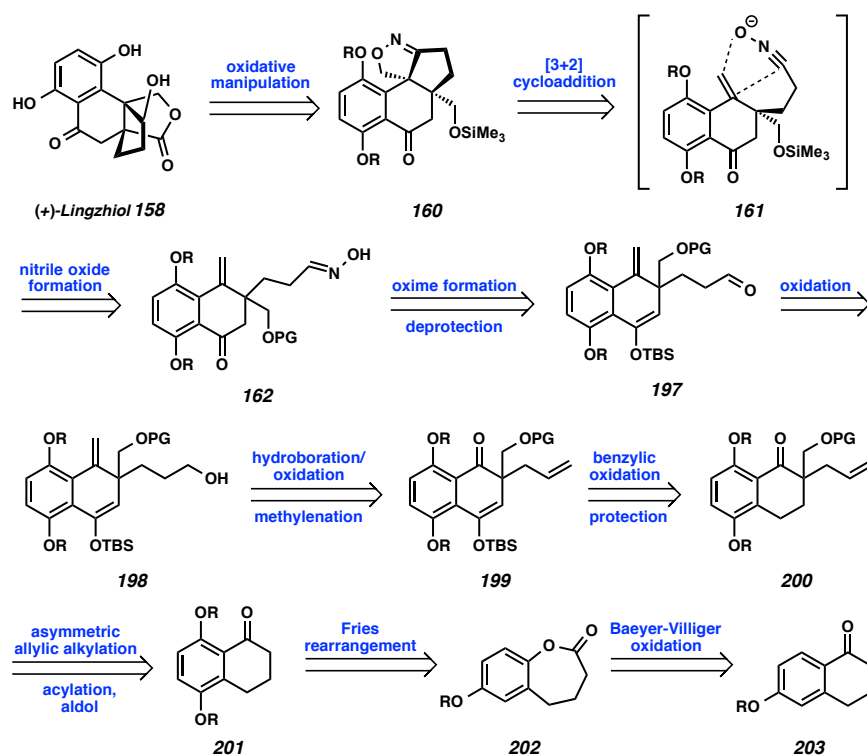
Scheme A9.4.2.3. Studies toward the dehydration of tertiary alcohol **196**



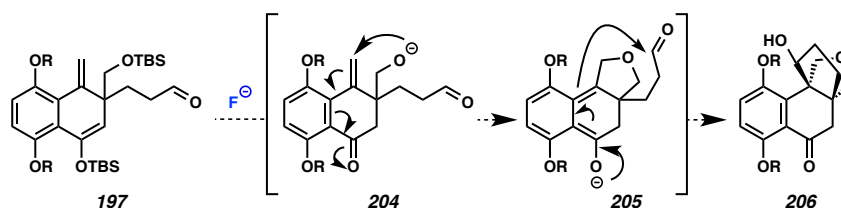
A9.5 REVISED STRATEGY FOR THE SYNTHESIS OF (+)-LINGZHIOL

Disappointed with the failure of our model system, we sought to take advantage of the lessons learned in our attempts to model (+)-lingzhiol in a revised overall strategy. One thing that became apparent over the course of our revised model system studies was the high electrophilicity of the styrene moiety once the benzylic ketone was in place. Indeed, this system could also aptly be described as a benzylogous enone. We believe that this reactivity can be exploited and efforts toward a new route to do so are underway. A revised retrosynthetic analysis detailing how such reactivity may be harnessed is depicted below in Scheme A9.5.1.

While much of our initial retrosynthesis (Scheme A9.1.1.2, *vide infra*) is survived in the revised version shown below, the benzylogous enone moiety (i.e., **162**) is unveiled later in the synthesis, such that oxidative manipulation of the primary alcohol formed from hydroboration/oxidation (**198**) of the allyl fragment is already complete (Scheme A9.5.1). We believe this reordering to be crucial to the success of the route.

Scheme A9.5.1. Second-generation retrosynthetic analysis toward the synthesis of (+)-lingzhiol

An additional benefit inherent to the revised synthetic plan is that it will enable our exploration of alternative endgame strategies that exploit the high electrophilicity of the benzylogous enone moiety. In particular, we believe that by simultaneously deprotecting both the silyl enol ether and primary silyl (PG = SiR₃) in bicycle **197**, we may be able to affect a conjugate addition/aldol cascade, wherein alkoxide **204** acts as a nucleophile and undergoes intramolecular conjugate addition to afford benzylogous enolate **205** (Scheme A9.5.2). Intramolecular aldol addition of the benzylogous enolate **205** to the pendent aldehyde may then take place to furnish tetracycle **206**. Tetracycle **206** may then undergo oxidative manipulation to furnish the natural product.

Scheme A9.5.2. Second-generation retrosynthetic analysis toward the synthesis of (+)-lingzhiol

A9.6 CONCLUDING REMARKS

Described herein is our progress toward the asymmetric total synthesis of marine natural product (+)-lingzhiol. Two iterations of model systems were explored in order to evaluate the feasibility of a proposed key intramolecular (3+2) cycloaddition, which would furnish vicinal quaternary carbons and two rings in a single step. Key discoveries uncovered in our model systems include the use of interrupted Peterson olefination to install a sterically-hindered exocyclic olefin and the successful employment of dirhodium tetracaprolactamate catalysis to affect the benzylic oxidation of highly functionalized intermediate **191**. Finally, a new retrosynthetic analysis, which makes use of information gained in our model studies, is presented.

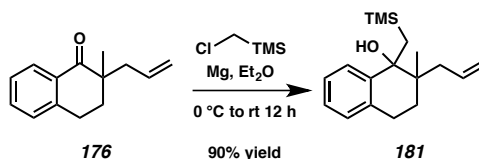
A9.7 EXPERIMENTAL SECTION

A9.7.1 Materials and Methods

Unless otherwise stated, reactions were performed in flame-dried glassware under an argon or nitrogen atmosphere using dry, deoxygenated solvents. Solvents were dried by passage through an activated alumina column under argon.⁶¹ Reaction progress was monitored by thin-layer chromatography (TLC). TLC was performed using E. Merck

silica gel 60 F254 precoated glass plates (0.25 mm) and visualized by UV fluorescence quenching, *p*-anisaldehyde, or KMnO₄ staining. Silicycle SiliaFlash® P60 Academic Silica gel (particle size 40–63 nm) was used for flash chromatography. ¹H NMR spectra were recorded on Varian Inova 300 MHz and 500 MHz spectrometers and are reported relative to residual CHCl₃ (δ 7.26 ppm) or C₆HD₅ (δ 7.16 ppm). ¹³C NMR spectra were recorded on a Varian Inova 500 MHz spectrometer (125 MHz) and are reported relative to CHCl₃ (δ 77.16 ppm) or C₆HD₅ (δ 128.06 ppm). Data for ¹H NMR are reported as follows: chemical shift (δ ppm) (multiplicity, coupling constant (Hz), integration). Multiplicities are reported as follows: s = singlet, d = doublet, t = triplet, q = quartet, p = pentet, sept = septuplet, m = multiplet, br s = broad singlet, br d = broad doublet, app = apparent. Data for ¹³C NMR are reported in terms of chemical shifts (δ ppm). IR spectra were obtained by use of a Perkin Elmer Spectrum BXII spectrometer or Nicolet 6700 FTIR spectrometer using thin films deposited on NaCl plates and reported in frequency of absorption (cm⁻¹). Reagents were purchased from Sigma-Aldrich, Gelest, Strem, or Alfa Aesar and used as received unless otherwise stated.

A9.7.2 Procedures for the preparation of and spectroscopic data for compounds in scheme A9.3.2.1

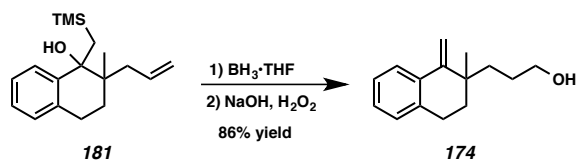


To a 25 mL 3-neck round bottom flask was added 0.122 g (5.0 mmol) of magnesium turnings. The central neck of the flask was fitted with a reflux condenser, which was fitted with a rubber septum, and the remaining two necks of the flask were

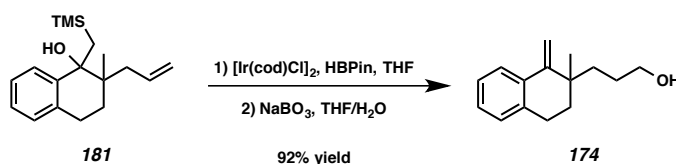
also capped rubber septa. The flask was put under vacuum and vigorously flame dried for ca. 5 min. The flask was allowed to cool under vacuum for 15 min, at which point it was back filled with Ar₂ (x3). 0.05 mL of 1,2-dibromoethane was added, along with a minimal amount of Et₂O, ca. 0.5 mL. A syringe containing 2.5 mL of Et₂O was fitted through one septum where it remained until the addition of reagents was complete. A second syringe containing 0.7 mL (chloromethyl)trimethylsilane (5.0 mmol) was fitted through another septum and added in a drop-wise fashion until an exotherm was perceptible by touching the bottom of the flask. Shortly after the generation of heat had become perceptible, the reaction mixture began to boil. Additional (chloromethyl)trimethylsilane was added to the flask at a rate that maintained a gentle reflux. If ever the exotherm went beyond that of a gentle boil, additional Et₂O was added to slow the exotherm. This process was continued until the addition of (chloromethyl)trimethylsilane was complete, at which point the reaction was heated to 40 °C via oil bath and allowed to stir for 2 hours. At this point only trace magnesium turnings remained in the reaction mixture. The reaction vessel was removed from the oil bath, and placed in a water ice bath and an additional 2 mL of Et₂O were added. Finally, 0.10 g of α -quaternary ketone **176** (0.5 mmol) in 0.5 mL of Et₂O was added drop-wise and the reaction was allowed to warm to 25 °C and stirred for an hour. The reaction was then judged to be complete by TLC analysis and then carefully quenched with saturated aqueous NH₄Cl, acidified to pH 5 by the addition of 1 N aqueous HCl, and extracted with EtOAc (10 mL x3). The combined organic washings were dried over MgSO₄, filtered and concentrated *in vacuo*. 0.13 g of tertiary alcohol **181** (0.4 mmol) in a 6:1 ratio of diastereomers was then isolated by flash column chromatography (SiO₂, 5% EtOAc in

hexanes to 15% EtOAc in hexanes) as a colorless oil. 90% yield. $R_f = 0.4$ (10% EtOAc in hexanes); ^1H NMR for minor diastereomer (300 MHz, CDCl_3) δ 8.05 (dd, $J = 7.8, 1.4$ Hz, 1H), 7.46 (td, $J = 7.4, 1.4$ Hz, 1H), 7.34–7.28 (m, 1H), 7.23 (d, $J = 7.7$ Hz, 1H), 5.79 (ddt, $J = 15.2, 10.8, 7.4$ Hz, 1H), 5.13 (d, $J = 9.9$ Hz, 1H), 5.09–5.06 (m, 1H), 2.99 (q, $J = 5.7$ Hz, 2H), 2.28 (dd, $J = 13.9, 7.6$ Hz, 1H), 2.13–2.08 (m, 1H), 1.96–1.90 (m, 1H), 1.73–1.69 (m, 1H), 1.20 (s, 3H), -0.12 (s, 17H); ^1H NMR for major diastereomer (300 MHz, CDCl_3) δ 7.63 (dd, $J = 7.6, 1.7$ Hz, 1H), 7.20–7.10 (m, 2H), 7.07–7.00 (m, 1H), 6.06–5.87 (m, 1H), 5.10 (td, $J = 4.9, 3.7, 1.8$ Hz, 1H), 5.04–4.86 (m, 1H), 2.79 (td, $J = 8.8, 4.6$ Hz, 2H), 2.27 (ddd, $J = 207.5, 13.6, 7.8$ Hz, 1H), 1.86 (ddd, $J = 14.4, 9.0, 5.9$ Hz, 2H), 1.74–1.62 (m, 2H), 1.37 (dd, $J = 14.9, 1.3$ Hz, 1H), 1.10 (s, 2H), 1.05 (dd, $J = 14.9, 1.3$ Hz, 1H), 0.81 (s, 1H), -0.11 (d, $J = 2.2$ Hz, 9H); ^{13}C NMR for minor diastereomer (75 MHz, CDCl_3) δ 144.6, 136.3, 134.7, 128.3, 126.3, 125.7, 125.6, 117.2, 41.4, 41.1, 33.3, 30.6, 28.5, 25.2, 21.9, 18.9, 0.3; ^{13}C NMR for major diastereomer (75 MHz, CDCl_3) δ 144.7, 136.6, 135.0, 128.4, 126.3, 125.6, 125.4, 117.4, 41.4, 41.2, 39.0, 30.2, 29.4, 24.9, 20.2, 0.3.

A9.7.3 Procedures for the preparation of and spectroscopic data for compounds in scheme A9.3.2.2



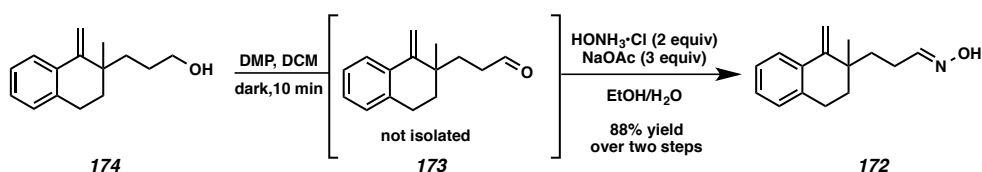
General procedure for the hydroboration/oxidation of tertiary alcohol **181** by borane•THF complex: To a solution of 0.05 g of tertiary alcohol **181** (0.173 mmol) in 1.7 mL of Et₂O was added 0.21 mL of 1 M BH₃•THF complex solution (0.21 mmol, 1.2 equiv) in a drop-wise fashion over 5 min at 25 °C. The reaction mixture was then allowed to stir for an additional 2 hours, at which point 0.020 mL of H₂O₂ (34% aqueous solution, 0.21 mmol, 1.2 equiv) and 0.692 mL of 1 N aqueous NaOH (0.692 mmol, 0.4 equiv) were added sequentially. This mixture was allowed to stir for 12 hours, at which point it was poured into 5 mL of H₂O, acidified to pH 7 with 1 N aqueous HCl, and extracted with Et₂O (5 mL x 4). The combined organic fractions were dried over MgSO₄, and concentrated *in vacuo*. 0.032 g of primary alcohol **174** (0.4 mmol) was then isolated by flash column chromatography (SiO₂, 1% EtOAc in hexanes to 25% EtOAc in hexanes) as a colorless oil. 86% yield. *R*_f = 0.3 (25% EtOAc in hexanes); ¹H NMR (300 MHz, CDCl₃) δ 7.56 (dd, *J* = 7.3, 2.0 Hz, 1H), 7.22–7.12 (m, 2H), 7.12–7.01 (m, 1H), 5.49 (s, 1H), 5.03 (s, 1H), 3.60–3.50 (m, 2H), 2.99–2.71 (m, 2H), 1.80–1.66 (m, 2H), 1.65–1.37 (m, 5H), 1.30–1.20 (m, 2H), 1.19 (s, 3H).



The general procedure for the hydroboration/oxidation of tertiary alcohol **181** by iridium catalysis was adapted from a procedure reported by Crudden and coworkers: In a nitrogen-filled glove box, a previously flame dried 50 mL round bottom flask charged with magnetic stirring bar was charged with 0.062 g of [Ir(cod)Cl]₂ (0.093 mmol, 0.025 equiv), and 0.08 g of 1,4-bis(diphenylphosphino)butane (0.186 mmol, 0.05 equiv) and

dissolved in 4 mL of THF. To this solution, 1.07 g of tertiary alcohol **181** (3.71 mmol, 1 equiv) in 6 mL of THF was added and the mixture was allowed to stir at 25 °C for 15 min. 0.63 g of pinacolborane (4.34 mmol, 1.2 equiv) was then added, the reaction vessel capped with a rubber septum and the mixture allowed to stir for an additional 24 hours. At this point the reaction mixture was removed from the glove-box and concentrated *in vacuo*. The crude reaction mixture was subject then taken up in 17 mL of THF, and combined with 17 mL of H₂O, 1.58 g of NaBO₃·4H₂O (10.3 mmol, 3 equiv) and stirred for an additional 12 hours. This mixture was then extracted with EtOAc (10 mL x 3), the combined organic fractions were dried over MgSO₄, and concentrated *in vacuo*. 0.74 g of primary alcohol **174** (0.4 mmol) was then isolated by flash column chromatography (SiO₂, 10% EtOAc in hexanes to 25% EtOAc in hexanes) as a colorless oil. 92% yield.

A9.7.4 Procedures for the preparation of and spectroscopic data for compounds in scheme A9.3.2.3

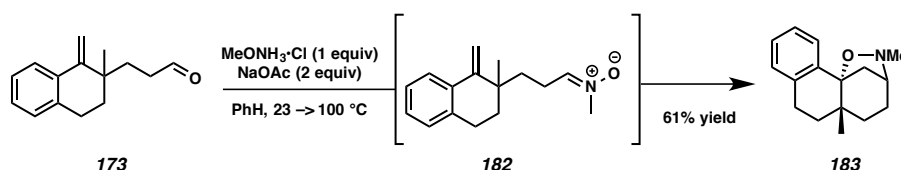


Dess-Martin periodinane (DMP) was prepared following literature procedure.¹³⁵ 0.185 g of primary alcohol **174** (0.856 mmol, 1 equiv) was transferred to a 25 mL round bottom flask with 0.93 mL of CH₂Cl₂ containing 0.417 g of DMP (0.984 mmol, 1.15 equiv) in 2.5 mL of CH₂Cl₂. The reaction was judged to be complete in 10 min, at which point the reaction mixture was poured into 7 mL of saturated aqueous NaHCO₃

containing 10 weight % Na₂S₂O₃ (1.85 g), and this mixture stirred for 5 min. The mixture was then extracted with 7 mL of Et₂O, and the organic fraction was washed with 3 mL of saturated aqueous NaHCO₃, dried over MgSO₄, filtered and concentrated *in vacuo*. The crude reaction mixture was >95% pure by ¹H NMR, and taken on without further purification. ¹H NMR for aldehyde **173** (300 MHz, CDCl₃) δ 9.78–9.51 (m, 1H), 7.55 (dd, *J* = 7.0, 2.2 Hz, 1H), 7.24–7.02 (m, 3H), 5.53 (s, 1H), 5.03 (s, 1H), 3.06–2.71 (m, 3H), 2.55–2.25 (m, 2H), 2.01–1.60 (m, 5H), 1.18 (s, 3H).

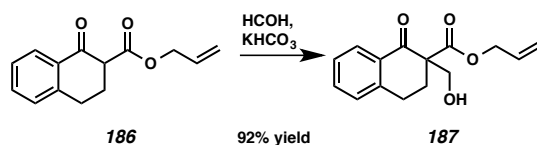
To 0.055 g of freshly prepared aldehyde **173** (0.259 mmol, 1 equiv), in 1.7 mL of H₂O and 3.3 mL of EtOH was added 0.036 g of H₃NO•HCl (0.518 mmol, 2 equiv), and the reaction mixture was cooled to 0 °C using an ice water bath. To the cooled reaction mixture, 0.064 g of NaOAc (0.777 mmol, 3 equiv) was added portion-wise over 15 min and the mixture was allowed to warm to room temperature and stir for 12 hours, at which point the reaction was judged to be complete by TLC analysis. The EtOH was removed *in vacuo* and the remaining aqueous mixture was extracted with EtOAc (5 mL x 3). The combined organic fractions were dried over MgSO₄, concentrated *in vacuo*, and the resulting crude oil was purified by flash column chromatography (SiO₂, 3% EtOAc in hexanes to 4% EtOAc in hexanes) to give 0.052 g of oxime **172** as a colorless oil. 88% yield over two steps. *R*_f = 0.5 (25% EtOAc in hexanes); ¹H NMR (300 MHz, CDCl₃) δ 7.56 (dd, *J* = 7.3, 2.0 Hz, 1H), 7.34 (t, *J* = 5.9 Hz, 1H), 7.21–7.13 (m, 2H), 7.09 (ddd, *J* = 6.3, 2.7, 0.9 Hz, 1H), 6.78 (s, 1H), 5.51 (s, 1H), 5.03 (s, 1H), 2.99–2.74 (m, 2H), 2.31–1.98 (m, 2H), 1.84–1.70 (m, 2H), 1.68–1.58 (m, 1H), 1.20 (s, 3H); ¹³C NMR (75 MHz, CDCl₃) δ 152.7, 150.4, 135.9, 135.0, 128.7, 127.5, 126.1, 125.5, 108.2, 37.4, 35.4, 34.2, 25.9, 25.6, 24.8.

A9.7.5 Procedures for the preparation of and spectroscopic data for compounds in scheme A9.3.2.4

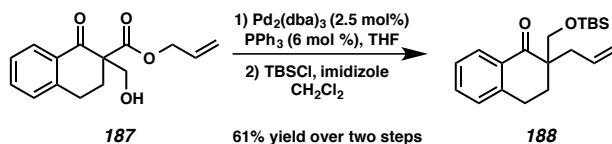


To a flame dried 5 mL microwave vial was charged 0.015 g of crude aldehyde **172** (0.07 mmol, 1 equiv), 0.006 g of MeH₂NOH•HCl (0.07 mmol, 1 equiv), 0.0193 g of K₂CO₃ (0.14 mmol, 2 equiv), and 1 mL of benzene. The microwave vial was capped with a rubber septum and stirred for 6 hours at room temperature, at which point all starting materials had been consumed by TLC analysis. The reaction mixture was then heated to 100 °C for 24 hours. The mixture was then concentrated *in vacuo*, and the crude oil was purified directly by flash column chromatography (SiO₂, 12% EtOAc in hexanes to 60% EtOAc in hexanes) to give 0.0103 g of tetracycle **183** as a colorless oil. 61% yield. $R_f = 0.3$ (25% EtOAc in hexanes); ¹H NMR (300 MHz, CDCl₃) δ 7.50 (dd, $J = 7.3, 1.9$ Hz, 1H), 7.24–7.17 (m, 2H), 7.13–7.09 (m, 1H), 3.44 (t, $J = 4.7$ Hz, 1H), 2.93–2.82 (m, 1H), 2.81 (s, 3H), 2.79–2.66 (m, 2H), 2.17 (d, $J = 12.2$ Hz, 1H), 2.07 (td, $J = 13.2, 5.8$ Hz, 1H), 1.92–1.79 (m, 2H), 1.78–1.68 (m, 1H), 1.37–1.29 (m, 2H), 0.95 (t, $J = 0.7$ Hz, 3H); ¹³C NMR (75 MHz, CDCl₃) 138.9, 133.7, 129.7, 127.7, 127.1, 126.3, 66.0, 64.8, 53.6, 47.7, 36.9, 34.5, 33.7, 32.9, 28.3, 25.9.

A9.7.6 Procedures for the preparation of and spectroscopic data for compounds in scheme A9.4.2.1



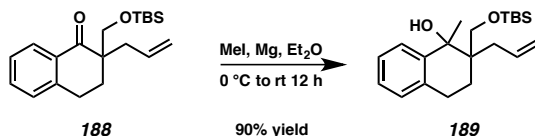
To a 100 mL round bottom flask containing a magnetic stirring bar was added 3.8 g of β -ketoester **186** (16.5 mmol, 1 equiv), 4.95 g of KHCO_3 (49.5 mmol, 3 equiv) and 47 mL of THF. The mixture was cooled to 0 °C via an ice water bath, and 9.24 mL of 37 wt. % formaldehyde in H_2O (113.9 mmol, 6.9 equiv) was added slowly over 5 min. The mixture was then allowed to warm to room temperature and stirred for 12 hours, at which point the reaction was judged to be complete by TLC analysis. The crude reaction mixture was diluted with H_2O (50 mL), and CH_2Cl_2 (100 mL) and extracted with CH_2Cl_2 (30 mL x 4). The combined organic fractions were dried over MgSO_4 , filtered and concentrated *in vacuo*. The crude oil was then purified by flash column chromatography (SiO_2 , 20% EtOAc in hexanes to 25% EtOAc in hexanes) to give 3.96 g of alcohol **187** as a colorless oil. 92% yield. $R_f = 0.2$ (33% EtOAc in hexanes); ^1H NMR (300 MHz, CDCl_3) δ 8.07 (ddd, $J = 7.9, 1.6, 0.5$, 1H), 7.51 (td, $J = 7.5, 1.5$, 1H), 7.34 (dddd, $J = 8.0, 7.3, 1.4, 0.7$, 1H), 7.24 (dd, $J = 7.2, 1.2$, 1H), 5.80 (ddt, $J = 17.5, 10.2, 5.5$, 1H), 5.21–5.15 (m, 1H), 5.14–5.10 (m, 1H), 4.68–4.57 (m, 2H), 4.06–3.85 (m, 2H), 3.42–3.25 (m, 1H), 3.00 (dt, $J = 9.6, 4.8$, 2H), 2.46 (dt, $J = 13.6, 4.5$, 1H), 2.18 (ddd, $J = 13.6, 10.6, 5.6$, 1H).



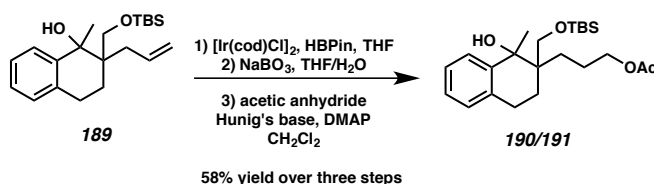
In a nitrogen-filled glove-box at 27 °C, a 250 mL round bottom flask containing a magnetic stirring bar was charged with 0.156 g of Pd₂(dba)₃ (0.171 mmol, 0.025 equiv), 0.107 g of PPh₃ (0.41 mmol, 0.06 equiv) and 100 mL of THF, and allowed to stir for 30 min. To this mixture was added 1.78 g of β-ketoester **187** as a solution in 35 mL THF, the flask was capped with a rubber septum, the lip of the septum sealed with electrical tape, and the flask removed from the glove-box. After stirring for 12 hours, the reaction was judged to be complete by TLC analysis. The crude reaction mixture was concentrated *in vacuo* and the resulting oil was passed through a silica plug (SiO₂, 20% EtOAc in hexanes to 30% EtOAc in hexanes), to give 1.47 g of crude product. This oil was then taken on without further purification. $R_f = 0.2$ (25% EtOAc in hexanes).

To a 200 mL round bottom flask containing a magnetic stirring bar was added 1.47 of the crude ketone, 1.54 g of TBSCl (10.25 mmol, 1.5 equiv based on previous reaction), 2.32 g of imidazole (34.15 mmol, 5 equiv based on previous reaction), and 70 mL of CH₂Cl₂, at 25 °C and the reaction mixture was allowed to stir for 12 hours, at which point the reaction was judged to be complete by TLC analysis. The crude reaction mixture was poured into 100 mL of H₂O and extracted with CH₂Cl₂ (50 mL x 4), washed with saturated aqueous NH₄Cl (50 mL), washed with brine (50 mL), and then concentrated *in vacuo*. The crude oil was then purified by flash column chromatography (SiO₂, 3% EtOAc in hexanes to 10% EtOAc in hexanes) to give 1.38 g of silyl ether **188** (4.18 mmol) as a colorless oil. 61% yield over two steps. $R_f = 0.4$ (10% EtOAc in hexanes); ¹H NMR data for the precursor alcohol **188'** (300 MHz, CDCl₃) δ δ 8.01 (dd, *J*

= 7.9, 1.4 Hz, 1H), 7.48 (td, $J = 7.5, 1.4$ Hz, 1H), 7.35–7.27 (m, 1H), 7.26–7.22 (m, 1H), 5.95–5.66 (m, 1H), 5.25–5.14 (m, 1H), 5.13 (q, $J = 1.1$ Hz, 1H), 3.70 (qd, $J = 11.5, 1.0$ Hz, 2H), 3.24–3.03 (m, 1H), 2.94 (t, $J = 4.6$ Hz, 1H), 2.88 (t, $J = 4.6$ Hz, 1H), 2.58–2.26 (m, 2H), 2.14–1.98 (m, 1H), 1.98–1.84 (m, 1H).



Tertiary alcohol **188** was prepared following the same procedure as that which was employed to prepare tertiary alcohol **181** (vide supra). Compound **189** was isolated by flash column chromatography (SiO₂, 5% EtOAc in hexanes to 10% EtOAc in hexanes) as a colorless oil. 90% yield. $R_f = 0.4$ (10% EtOAc in hexanes); ¹H NMR (300 MHz, CDCl₃) δ 7.74 (dd, $J = 7.6, 1.6$ Hz, 1H), 7.65 (dd, $J = 7.8, 1.5$ Hz, 2H), 6.01–5.71 (m, 2H), 5.23–5.03 (m, 5H), 4.15 (s, 2H), 3.69–3.65 (m, 3H), 3.61 (d, $J = 10.3$ Hz, 1H), 3.54–3.50 (m, 2H), 3.47 (t, $J = 7.0$ Hz, 4H), 3.06–2.50 (m, 9H), 2.16 (dd, $J = 13.7, 7.3$ Hz, 1H), 1.96 (dd, $J = 14.7, 6.9$ Hz, 2H), 1.82–1.65 (m, 2H), 1.53 (s, 5H), 1.48–1.40 (m, 2H), 1.37 (s, 3H), 1.21 (t, $J = 7.0$ Hz, 8H), 0.96 (s, 15H), 0.81 (s, 9H), 0.13 (d, $J = 5.6$ Hz, 10H), -0.11 (d, $J = 31.4$ Hz, 6H).



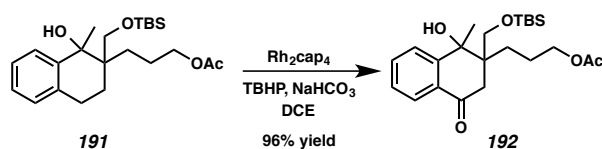
Hydroboration and oxidation of olefin **189** was accomplished following the general procedure detailed above for the synthesis of alcohol **174** (vide supra), beginning

with 1.3 g of olefin **189**. The crude reaction mixture was extracted with EtOAc, the combined organic fractions were dried over MgSO₄, and concentrated *in vacuo* to give 1.35 g of the intermediate diol as a colorless oil. $R_f = 0.4$ (10% EtOAc in hexanes); ¹H NMR for diastereomer 1 of boronate intermediate (300 MHz, CDCl₃) δ 7.63 (dd, $J = 7.7$, 1.5 Hz, 1H), 7.18 (ddd, $J = 8.8$, 7.5, 1.4 Hz, 1H), 7.10 (td, $J = 7.3$, 1.5 Hz, 1H), 7.03–6.98 (m, 1H), 4.13 (s, 1H), 3.69 (s, 2H), 2.91 (dt, $J = 18.6$, 9.7 Hz, 1H), 2.69 (dt, $J = 17.5$, 3.9 Hz, 1H), 1.92 (ddd, $J = 14.0$, 11.3, 5.6 Hz, 1H), 1.58 (d, $J = 5.3$ Hz, 1H), 1.52 (s, 3H), 1.50–1.42 (m, 2H), 1.41–1.31 (m, 1H), 1.29–1.17 (m, 3H), 1.13 (d, $J = 6.8$ Hz, 12H), 0.94 (s, 9H), 0.85 (d, $J = 19.9$ Hz, 1H), 0.77–0.65 (m, 1H), 0.13 (d, $J = 4.1$ Hz, 5H). ¹H NMR for diastereomer 2 of boronate intermediate (300 MHz, CDCl₃) δ 7.72 (dd, $J = 7.7$, 1.6 Hz, 1H), 7.15 (dtd, $J = 18.9$, 7.3, 1.7 Hz, 2H), 7.03–6.96 (m, 1H), 4.79 (s, 1H), 3.62 (s, 2H), 2.90–2.61 (m, 2H), 2.06–1.91 (m, 1H), 1.89–1.78 (m, 1H), 1.77–1.65 (m, 1H), 1.58 (dd, $J = 7.6$, 3.6 Hz, 1H), 1.54–1.38 (m, 2H), 1.35 (s, 3H), 1.23 (s, 12H), 1.14 (d, $J = 4.7$ Hz, 2H), 0.92 (s, 1H), 0.81 (s, 10H), 0.13 (s, 1H), -0.09 (d, $J = 32.0$ Hz, 6H).

A 25 mL round bottom flask was charged with 1.35 g of the crude diol, 0.77 g of Hunig's base (4.44 mmol, 1.2 equiv based on previous reactions), 0.045 g of DMAP (0.37 mmol, 0.1 equiv based on previous reactions), and 5.3 mL of CH₂Cl₂, and cooled to 0 °C. 0.378 mL of acetic anhydride was then added drop-wise to the cooled solution and the mixture was stirred for 3 hours, at which point the reaction was judged to be complete by TLC analysis. The crude reaction mixture was quenched with 5 wt. % HCl in H₂O, neutralized with 1 N NaOH (ca. 5 mL) and washed with brine. The organic fraction was dried over MgSO₄ and then concentrated *in vacuo*. The crude oil was then purified by flash column chromatography (SiO₂, 5% EtOAc in hexanes to 10% EtOAc in

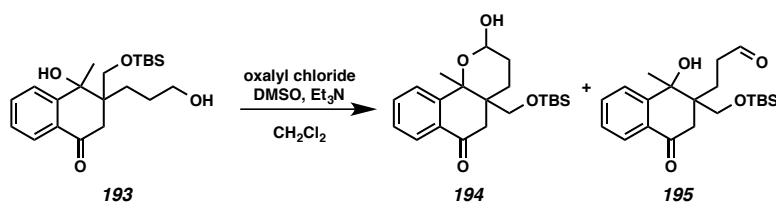
hexanes) and the diastereomers separated. 0.5 g of diastereomer A (**190**) and 0.380 g of diastereomer B (**191**) were isolated as colorless oils. 58% yield over three steps. $R_f = 0.3$ (10% EtOAc in hexanes); ^1H NMR for diastereomer 1 (**190**) (300 MHz, CDCl_3) δ 7.73–7.59 (m, 1H), 7.23–7.09 (m, 2H), 7.08–7.00 (m, 1H), 2.91–2.64 (m, 3H), 1.74 (ddd, $J = 8.1, 6.7, 2.8$ Hz, 2H), 1.58 (d, $J = 3.6$ Hz, 3H), 1.44 (d, $J = 1.2$ Hz, 3H), 1.41–1.18 (m, 3H), 1.01 (d, $J = 0.5$ Hz, 2H), 0.98–0.92 (m, 2H), 0.91–0.86 (m, 2H).; ^1H NMR for diastereomer 2 (**191**) (300 MHz, CDCl_3) δ 7.74 (dd, $J = 7.7, 1.6$ Hz, 1H), 7.25–7.07 (m, 2H), 7.07–6.95 (m, 1H), 4.61 (s, 1H), 4.19–4.03 (m, 2H), 3.69–3.49 (m, 2H), 2.90–2.60 (m, 2H), 2.23–2.09 (m, 1H), 2.05 (d, $J = 0.6$ Hz, 3H), 1.70 (dddd, $J = 15.4, 12.0, 8.1, 5.0$ Hz, 4H), 1.48–1.36 (m, 1H), 1.34 (s, 3H), 1.28–1.24 (m, 3H), 0.98–0.84 (m, 3H), 0.81 (d, $J = 0.6$ Hz, 9H), -0.10 (d, $J = 34.0$ Hz, 5H); ^{13}C NMR for diastereomer 2 (**191**) (75 MHz, CDCl_3) δ 171.2, 145.3, 133.6, 127.8, 126.3, 126.3, 126.1, 126.1, 125.5, 66.2, 65.4, 65.2, 41.4, 27.4, 27.0, 26.7, 26.0, 25.9, 25.8, 25.8, 25.7, 25.6, 24.6, 23.2, 21.0, 17.9, -6.0, -6.1

A9.7.7 Procedures for the preparation of and spectroscopic data for compounds in scheme A9.4.2.2



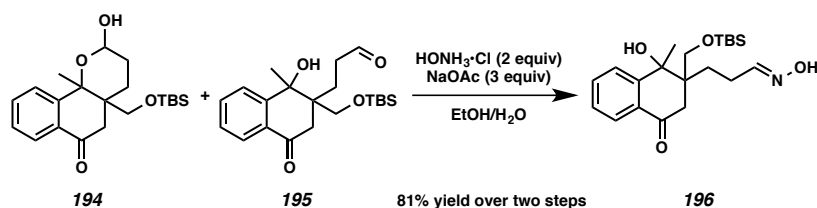
To a 1 mL microwave vial containing a magnetic stirring bar 25 °C, was charged with 0.05 g of diastereomer A of tertiary alcohol **191** (0.123 mmol, 1 equiv), 0.0004 g or $\text{Rh}_2(\text{cap})_4$ (0.0006 mmol, 0.005 equiv), 0.005 g of NaHCO_3 (0.0615 mmol, 0.5 equiv) and 0.5 mL of DCE. This mixture was then allowed to stir for 30 min until all of tertiary

^1H NMR for diastereomer 1 (500 MHz, CDCl_3) δ 7.90 (d, $J = 7.8$ Hz, 1H), 7.74 (d, $J = 7.9$ Hz, 1H), 7.58 (t, $J = 7.7$ Hz, 1H), 7.30 (t, $J = 7.6$ Hz, 1H), 3.87 (d, $J = 10.4$ Hz, 1H), 3.61 (d, $J = 10.4$ Hz, 1H), 3.43 (t, $J = 6.7$ Hz, 2H), 2.43 (d, $J = 17.3$ Hz, 1H), 2.32 (d, $J = 17.4$ Hz, 1H), 1.99 (ddd, $J = 14.3, 12.2, 4.8$ Hz, 1H), 1.61 (s, 3H), 1.48–1.32 (m, 2H), 1.28–1.18 (m, 1H), 0.93 (d, $J = 1.6$ Hz, 9H), 0.14 (d, $J = 13.7$ Hz, 5H); ^{13}C NMR for diastereomer 1 (75 MHz, CDCl_3) δ 195.5, 149.9, 134.6, 129.7, 127.0, 125.9, 125.8, 76.1, 65.9, 63.0, 45.3, 41.5, 28.5, 27.1, 25.7, 18.0, -5.7, -5.8; ^1H NMR for diastereomer 2 (**193**) (500 MHz, CDCl_3) δ 7.91 (dddd, $J = 13.3, 8.0, 1.4, 0.6$ Hz, 2H), 7.64 (ddd, $J = 7.8, 7.3, 1.4$ Hz, 1H), 7.38 (td, $J = 7.5, 1.2$ Hz, 1H), 5.09 (s, 1H), 3.80–3.70 (m, 2H), 3.70–3.59 (m, 2H), 2.61 (d, $J = 18.6$ Hz, 1H), 2.50 (d, $J = 18.6$ Hz, 1H), 2.29–2.19 (m, 1H), 1.60 (dddd, $J = 15.7, 12.2, 8.6, 6.2$ Hz, 3H), 1.46 (s, 3H), 0.81 (s, 9H), -0.10 (d, $J = 64.7$ Hz, 5H); ^{13}C NMR for diastereomer 2 (**193**) (75 MHz, CDCl_3) δ 196.1, 151.1, 134.5, 130.1, 127.2, 126.3, 125.4, 66.7, 63.4, 44.5, 44.0, 27.2, 26.8, 26.6, 25.5, 17.8, -6.0, -6.2.



To a septum capped 1 mL microwave vial containing a magnetic stirring bar was added 5.43 μL of oxalyl chloride (0.06 mmol, 1.48 equiv) in 0.25 mL of CH_2Cl_2 . The mixture was cooled to -78 $^\circ\text{C}$ and 7.5 μL of DMSO (0.1056 mmol, 2 equiv) in 0.25 mL CH_2Cl_2 was added drop-wise over 20 min and the mixture was stirred for an additional 30 min. 0.02 g of diastereomer 1 of primary alcohol **193** (0.053 mmol, 1 equiv) in 0.5 mL CH_2Cl_2 was then added drop-wise over 45 min and the mixture was stirred for an

additional 30 min. 30.0 μL of Et_3N was then added neat over 1 minute, and the mixture was stirred vigorously for 30 min as it was allowed to warm to $0\text{ }^\circ\text{C}$. 1 mL of H_2O was then added, the mixture was washed with 0.5 M HCl (1 mL), H_2O (1 mL), saturated aqueous NaHCO_3 (1 mL) and brine (1 mL). The organic fraction was dried over MgSO_4 , and concentrated *in vacuo* to give 0.0197 g of lactol **194** and aldehyde **195** as a 2.7:1 mixture. Lactol **194** and aldehyde **195** were taken on without further purification. ^1H NMR for lactol **194** (300 MHz, CDCl_3) δ 8.08–7.93 (m, 1H), 7.67–7.52 (m, 2H), 7.38 (ddd, $J = 7.8, 6.5, 2.0$ Hz, 1H), 6.37 (ddd, $J = 6.2, 2.4, 1.5$ Hz, 1H), 4.56 (td, $J = 5.6, 5.0, 2.2$ Hz, 1H), 3.87–3.61 (m, 2H), 2.81 (d, $J = 2.1$ Hz, 2H), 2.10 (ddd, $J = 17.9, 5.1, 1.5$ Hz, 1H), 1.69–1.58 (m, 2H), 1.54 (s, 3H), 0.89 (s, 11H), 0.05 (d, $J = 3.8$ Hz, 6H); ^1H NMR for aldehyde **195** (300 MHz, CDCl_3) δ 8.01 (ddd, $J = 7.9, 1.4, 0.6$ Hz, 1H), 7.74–7.61 (m, 2H), 7.50–7.40 (m, 1H), 3.91–3.71 (m, 2H), 2.79 (d, $J = 3.2$ Hz, 2H), 2.53 (dt, $J = 18.1, 8.9$ Hz, 1H), 2.21 (ddd, $J = 18.5, 8.5, 3.6$ Hz, 1H), 2.07–1.94 (m, 1H), 1.75 (dt, $J = 14.3, 8.9$ Hz, 1H), 1.67 (d, $J = 0.6$ Hz, 3H), 0.91 (d, $J = 0.6$ Hz, 10H), 0.10 (d, $J = 2.3$ Hz, 6H); ^{13}C NMR for aldehyde **195** (75 MHz, CDCl_3) δ 194.9, 170.5, 147.0, 135.3, 129.7, 128.5, 126.8, 125.6, 84.4, 64.6, 44.7, 27.1, 26.4, 25.8, 24.8, 18.2, -5.6, -5.7.



0.01 g of the mixture of crude diastereomer 2 of lactol **194** and diastereomer 2 of aldehyde **195** were combined with 0.0037 g of $\text{HONH}_2\cdot\text{HCl}$ (0.053 mmol, 2 equiv from previous reaction), 0.0065 g NaOAc (0.0797 mmol, 3 equiv), 0.18 mL H_2O and 0.35 mL

EtOH in a 1 mL microwave containing a magnetic stirring bar and stirred at 25 °C for 12 hours. The crude reaction mixture was adsorbed into 0.1 g SiO₂ by concentration *in vacuo* and the resulting fine particulate was then purified by flash column chromatography (SiO₂, 10% EtOAc in hexanes to 40% EtOAc in hexanes), to give 0.085 g of a mixture of *E* and *Z* oximes **196** as a colorless oil. 81% yield over two steps. $R_f = 0.2$ (33% EtOAc in hexanes); ¹H NMR (300 MHz, CDCl₃) δ 7.99–7.82 (m, 2H), 7.64 (td, $J = 7.6, 1.5$ Hz, 1H), 7.49 (t, $J = 5.7$ Hz, 0H), 7.45–7.31 (m, 1H), 6.82 (s, 1H), 5.06 (s, 1H), 3.75–3.54 (m, 2H), 3.53–3.43 (m, 0H), 2.66 (d, $J = 3.2$ Hz, 0H), 2.60 (d, $J = 3.1$ Hz, 1H), 2.51 (d, $J = 7.4$ Hz, 1H), 2.48–2.41 (m, 1H), 2.33–2.23 (m, 1H), 2.10 (s, 1H), 2.04 (s, 1H), 1.84–1.63 (m, 1H), 1.44 (s, 3H), 1.33–1.13 (m, 2H), 0.96–0.85 (m, 0H), 0.80 (d, $J = 0.8$ Hz, 9H), -0.05 (d, $J = 1.1$ Hz, 3H), -0.19 (s, 3H).

A9.8 REFERENCES AND NOTES

- (120) Qu, L.; Wang, X. S.; Cao, A. G. *Gansu J. Tradit. Chin. Med.* **2011**, *24*, 28.
- (121) Yan, Y.-M.; Ai, J.; Zhou, L. L.; Chung, A. C. K.; Li, R.; Nie, J.; Fang, P.; Wang, X.-L.; Luo, J.; Hu, Q.; Hou, F.-F.; Cheng, Y.-X. *Org. Lett.* **2013**, *15*, 5488.
- (122) Long, R.; Huang, J.; Shao, W.; Liu, S.; Lan, Y.; Gong, J.; Yang, Z. *Nat. Commun.* **2014**, *5*.
- (123) Lewis, A.; Steadman, R.; Manley, P.; Craig, K.; de la Motte C.; Hascall, V.; Phillips, A. O. *Histol Histopathol.* **2008**, *23*, 731.

- (124) Brownlee, M. *Nature* **2001**, *414*, 813.
- (125) Lan, H. Y. *Clin. Exp. Pharmacol. Physiol.* **2012**, *39*, 731.
- (126) Itoh, K.; Tong, K. I.; Yamamoto, M. *Free Radic. Biol. Med.* **2004**, *36*, 1208.
- (127) Lan, H. Y. *Kidney Res. Clin. Pract.* **2012**, *31*, 4.
- (128) Crudden, C. M.; Hleba, Y. B.; Chen, A. C. *J. Am. Chem. Soc.* **2004**, *126*, 9200.
- (129) Liu, K.-C.; Shelton, B. R.; Howe, R. K. *J. Org. Chem.* **1980**, *45*, 3916.
- (130) A. Hassner and K. Rai, *Synthesis* **1989**, *1*, 57
- (131) Lee, G. A. *Synthesis* **1982**, *6*, 508.
- (132) Catino, A. J.; Nichols, J. M.; Choi, H.; Gottipamula, S.; Doyle, M. P. *Org. Lett.* **2005**, *7*, 5167.
- (133) Arhart, R.J.; Martin, J.C. *J. Am. Chem. Soc.* **1972**, *94*, 5003.
- (134) Atkins, G. M.; Burgess, E. M. *J. Am. Chem. Soc.* **1968**, *17*, 4744

(135) Ireland, R. E.; Liu, L. *J. Org. Chem.* **1993**, 58, 2899.

APPENDIX 10

Spectra Related to Appendix 9:

Studies Toward the Enantioselective Total Synthesis of (+)-Lingzhiol

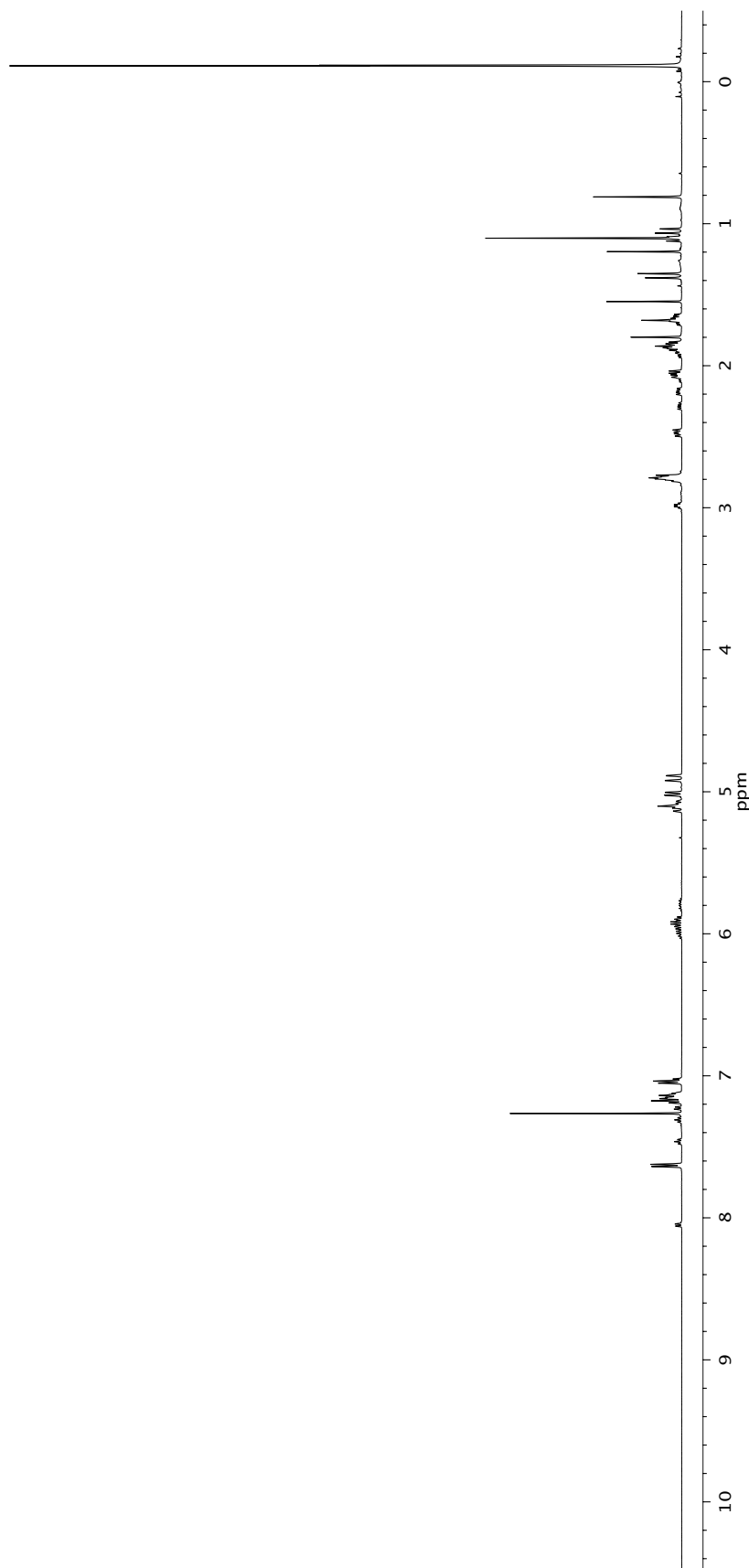
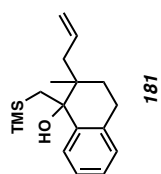


Figure A10.1 ¹H NMR (500 MHz, CDCl₃) of compound **181**.

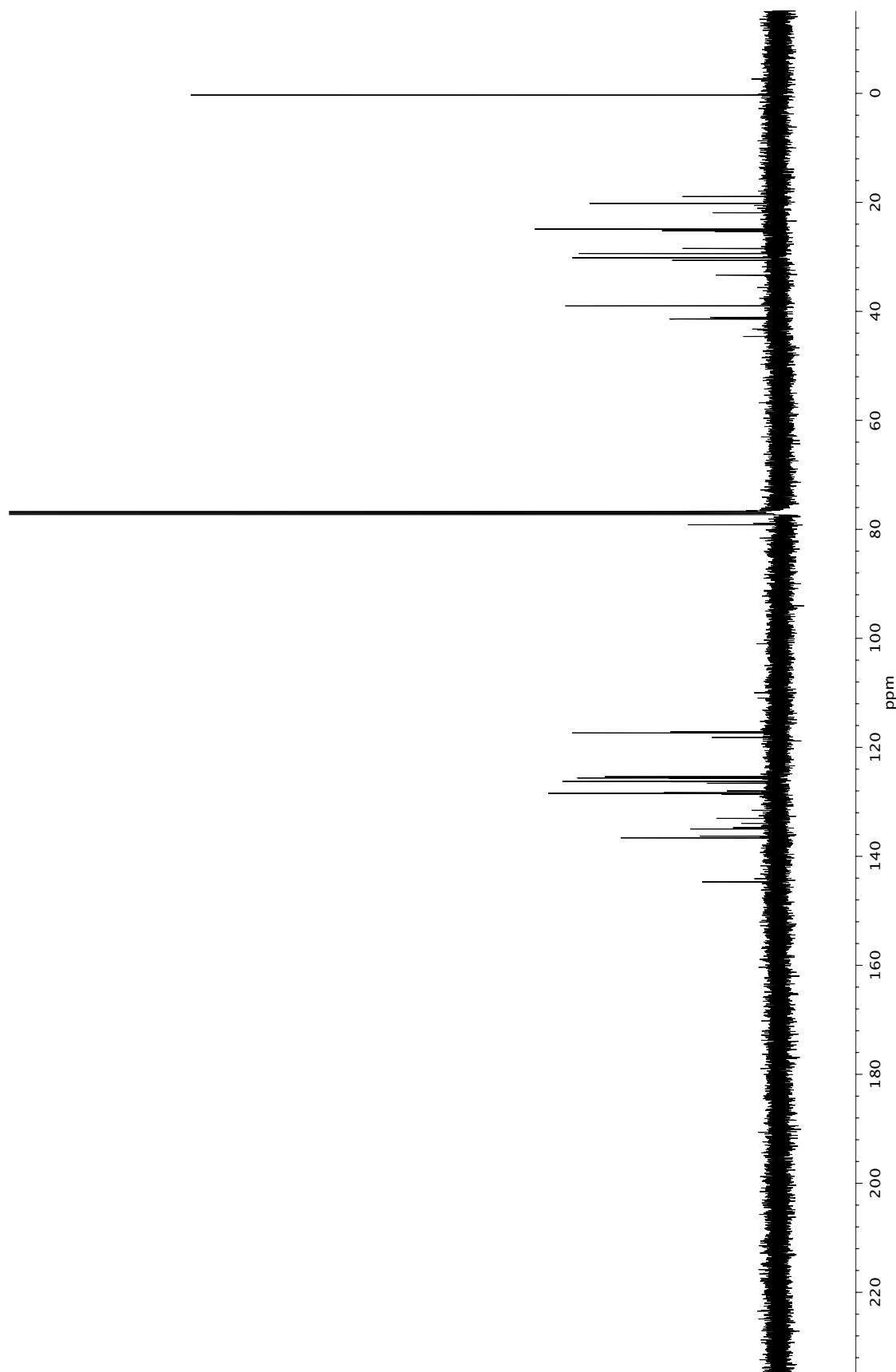


Figure A10.2 ^{13}C NMR (500 MHz, CDCl_3) of compound **181**.

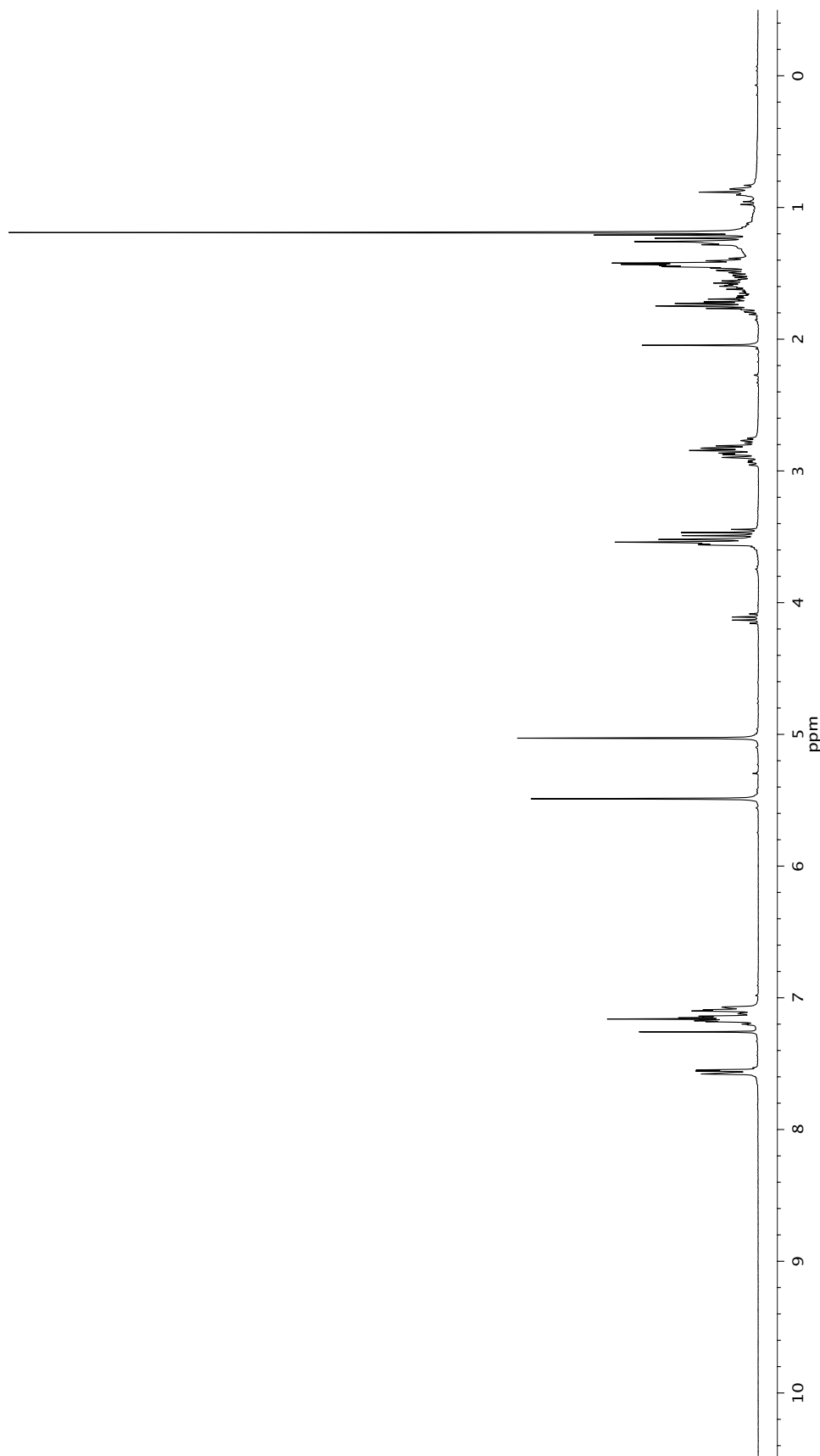
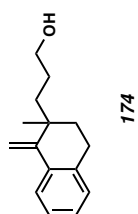
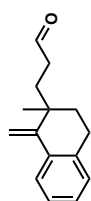


Figure A10.3 ¹H NMR (500 MHz, CDCl₃) of compound 174.



173

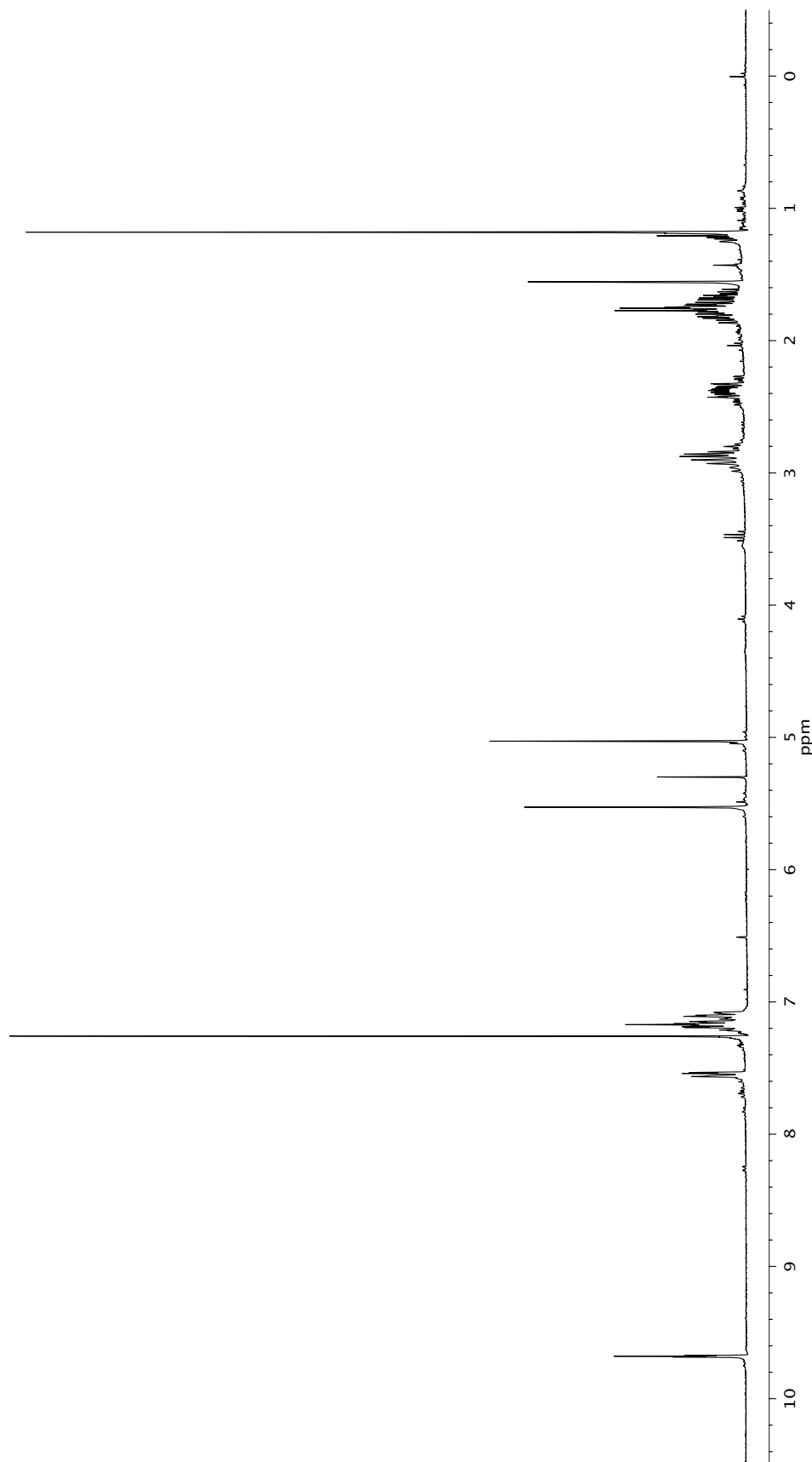
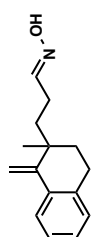


Figure A10.4 ^1H NMR (300 MHz, CDCl_3) of compound 173.



172

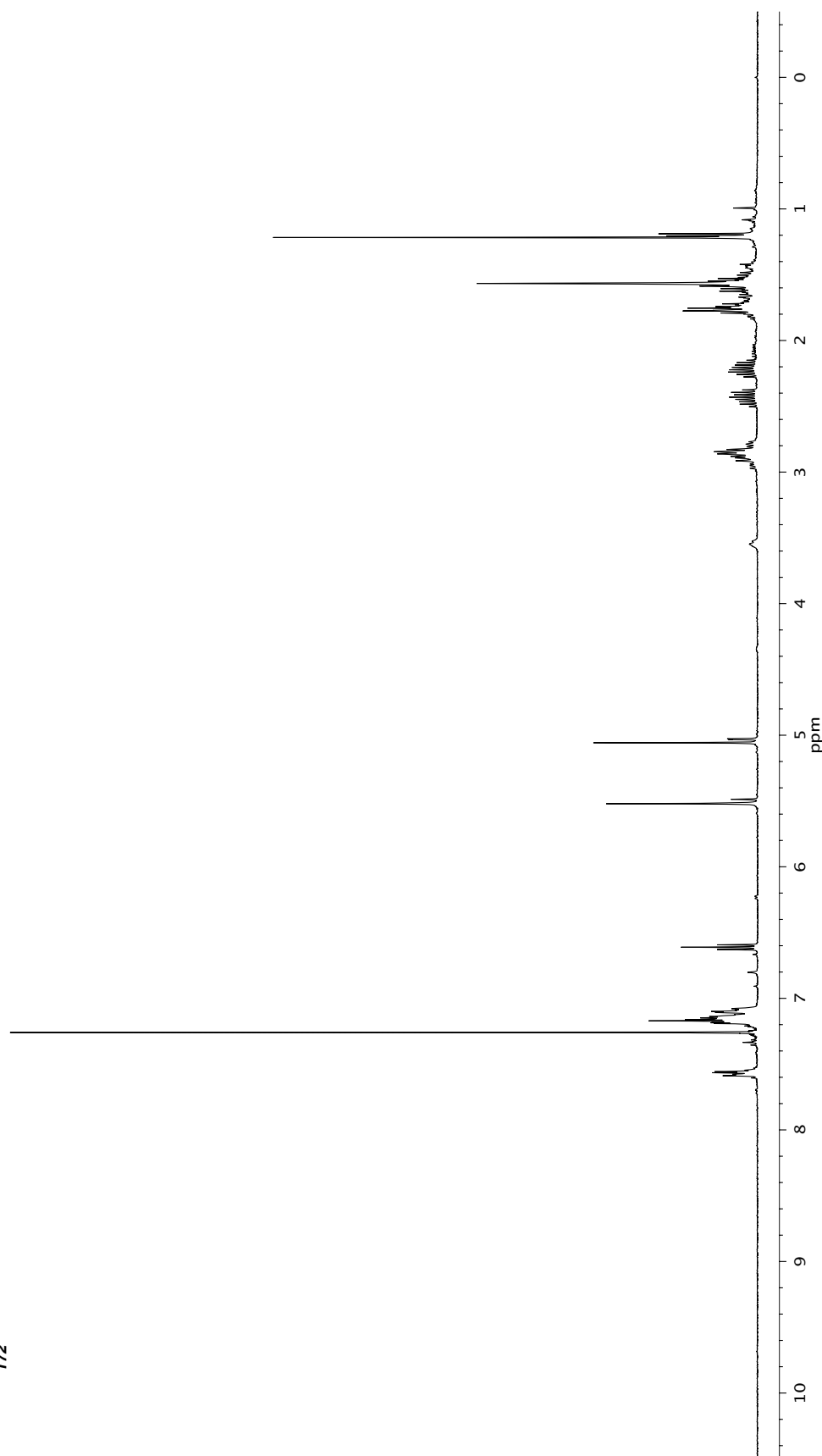


Figure A10.5 ^1H NMR (300 MHz, CDCl_3) of compound 172.

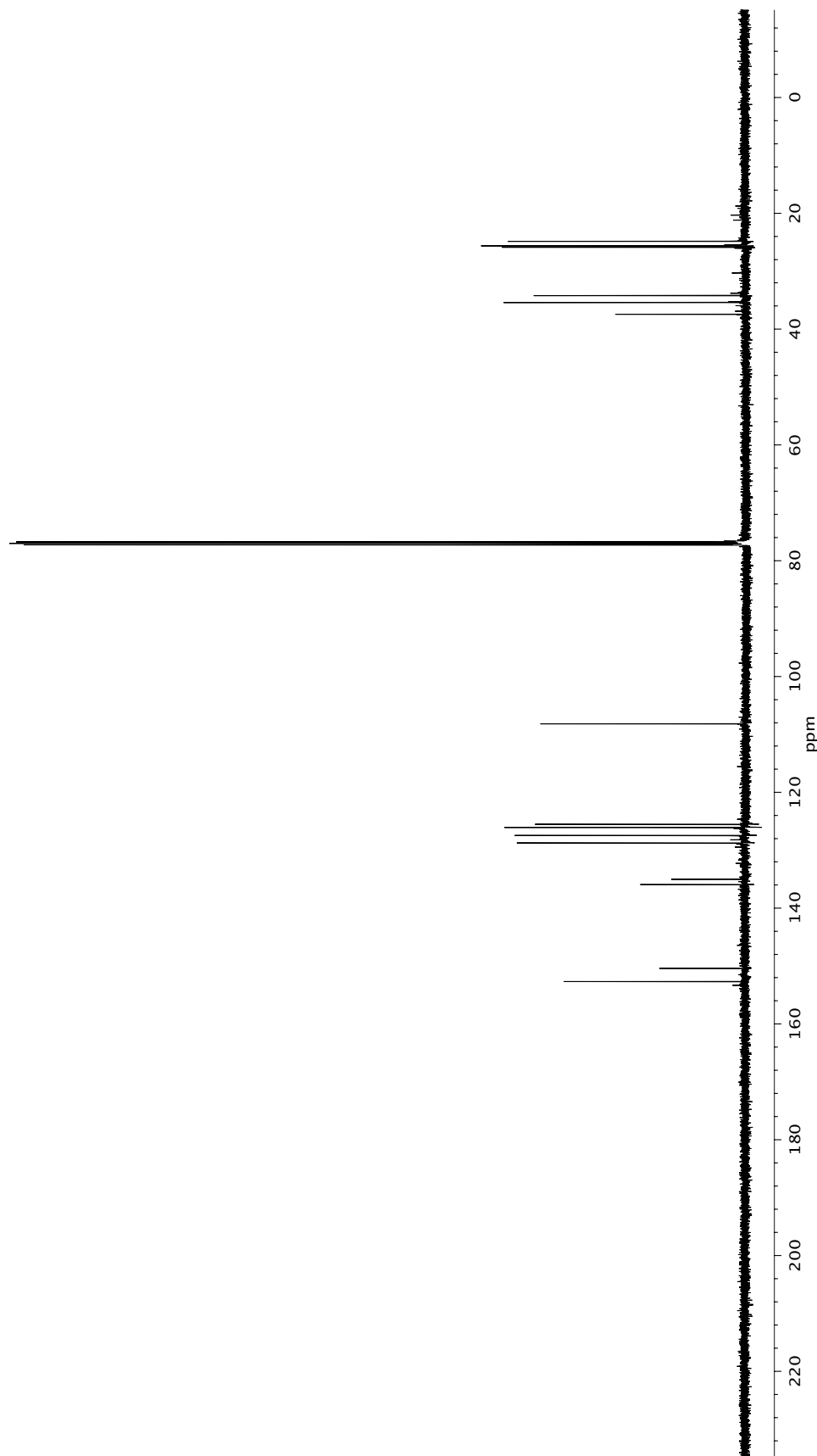


Figure A10.6 ^{13}C NMR (500 MHz, CDCl₃) of compound 172.

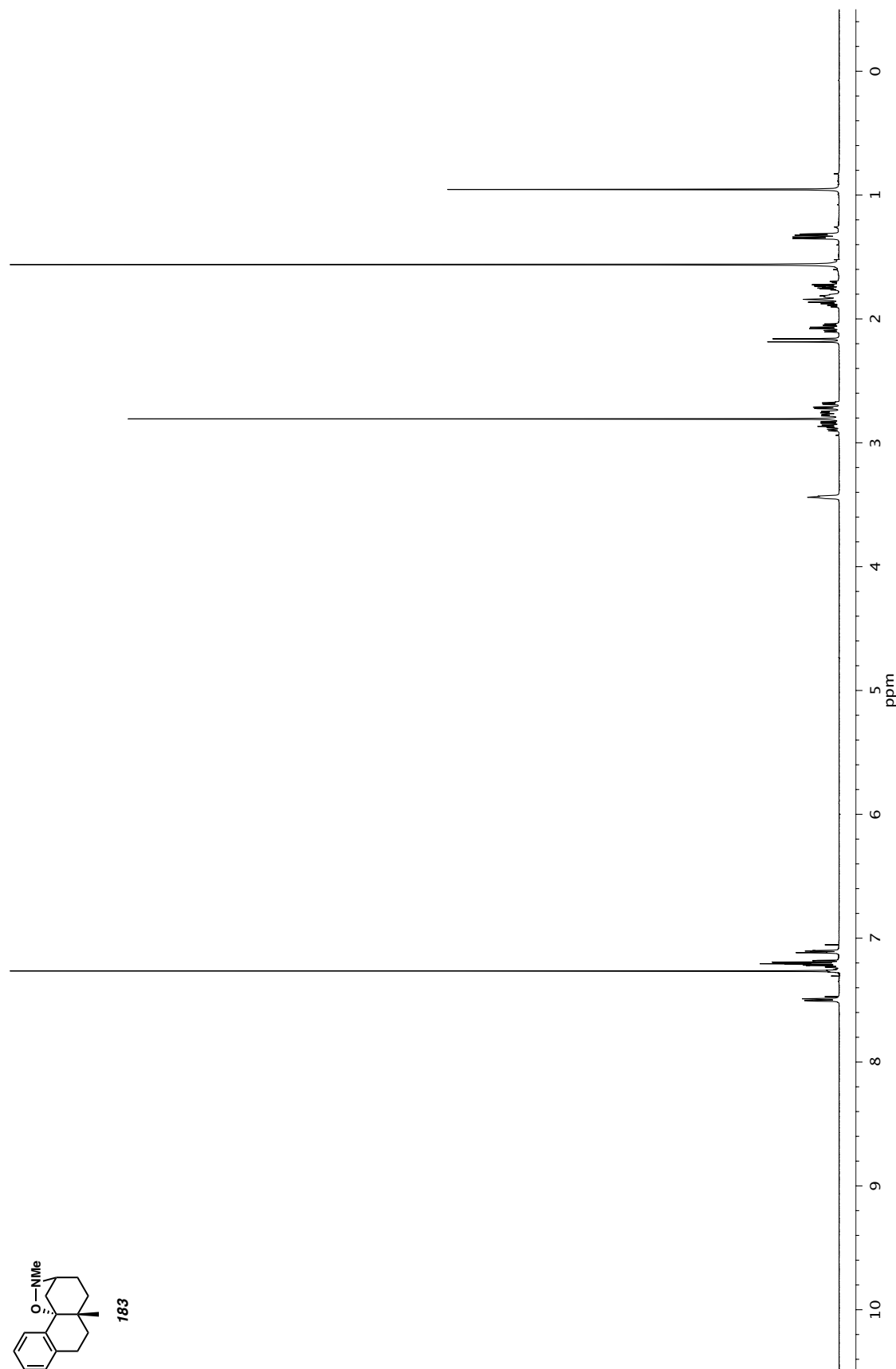
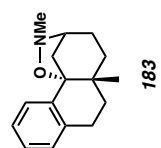


Figure A10.7 ¹H NMR (500 MHz, CDCl₃) of compound 183.

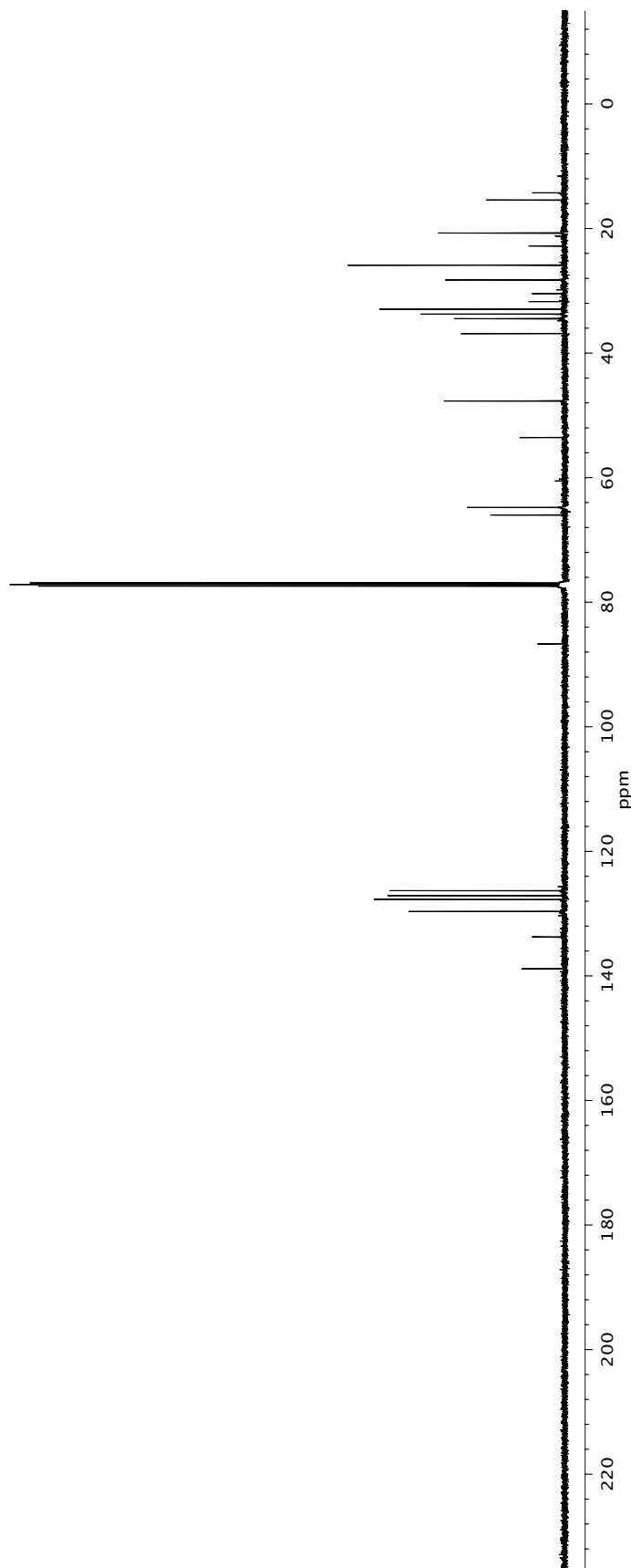


Figure A10.8 ^{13}C NMR (500 MHz, CDCl_3) of compound 183.

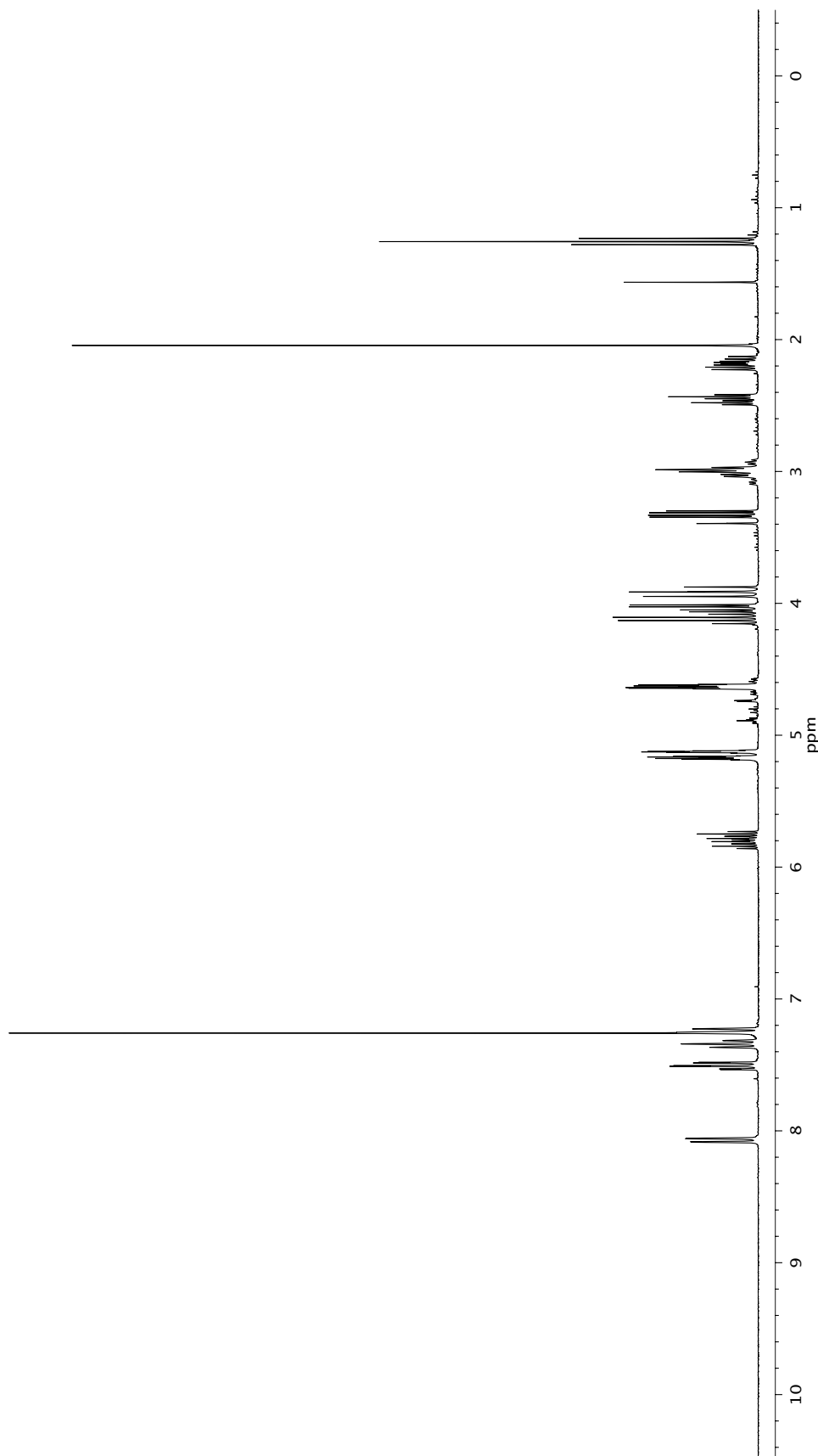
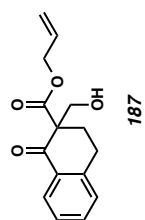


Figure A10.8 ¹H NMR (300 MHz, CDCl₃) of compound **187**.

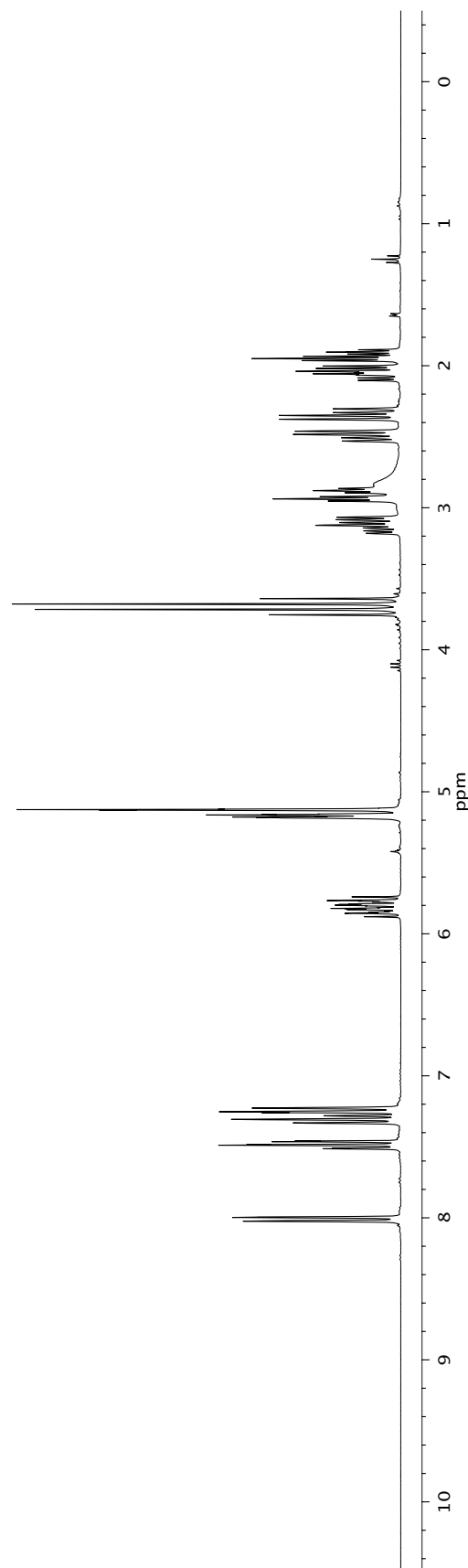
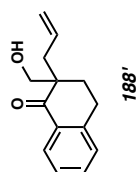


Figure A10.9 ¹H NMR (300 MHz, CDCl₃) of compound **188**.

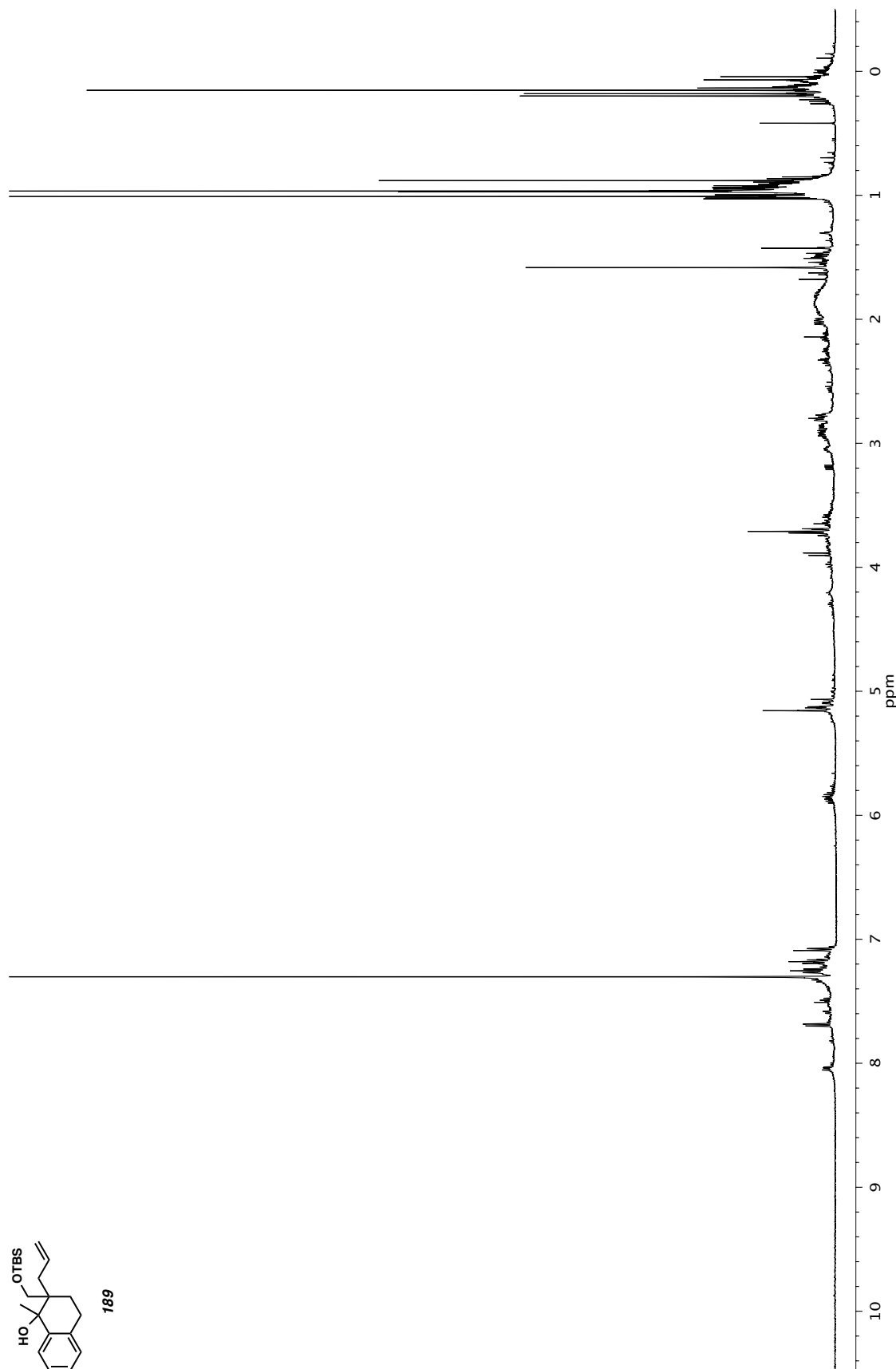
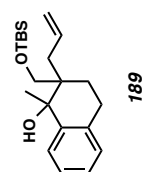


Figure A10.10 ¹H NMR (500 MHz, CDCl₃) of compound 189.

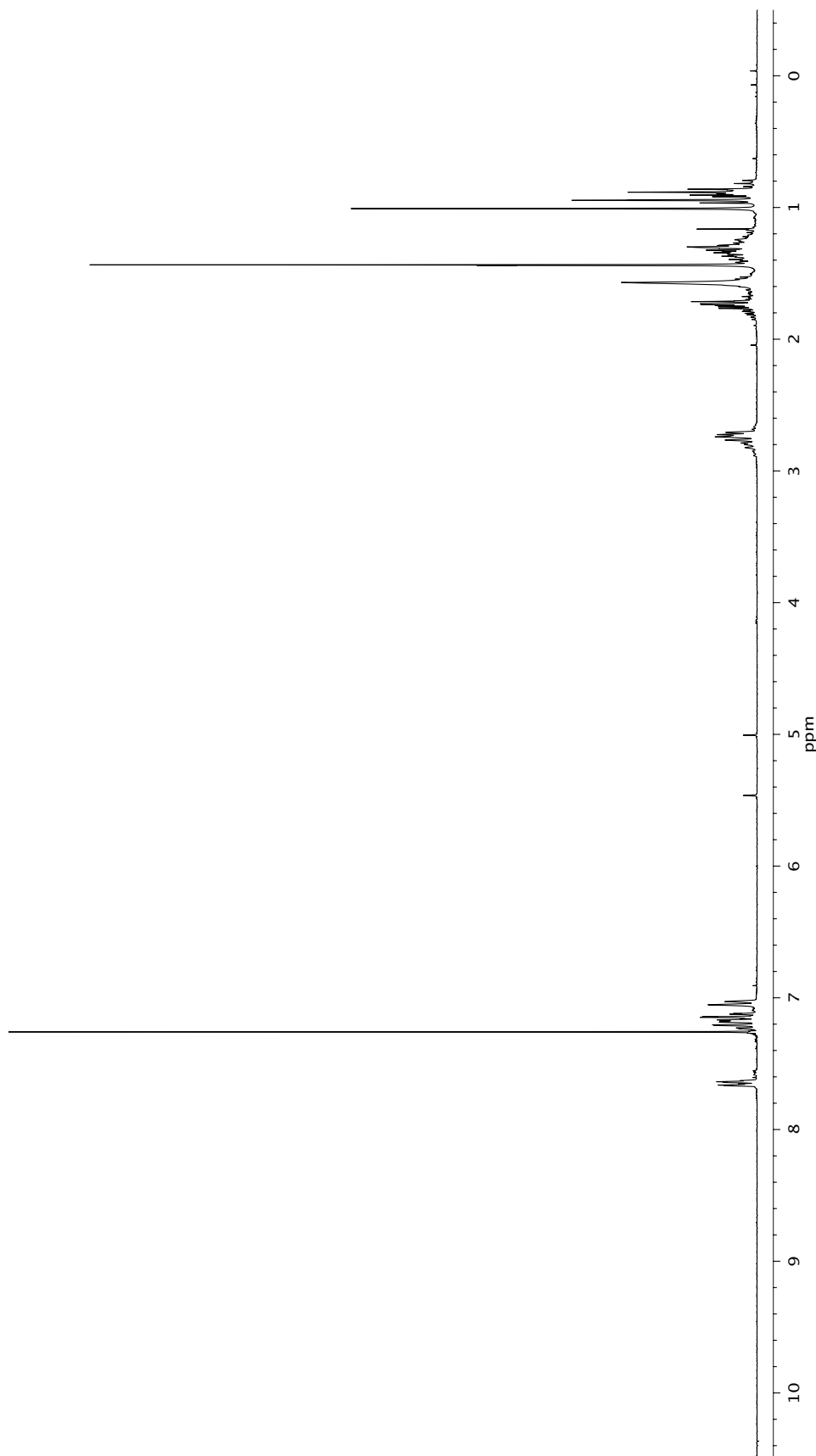
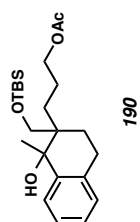


Figure A10.11 ¹H NMR (500 MHz, CDCl₃) of compound **190**.

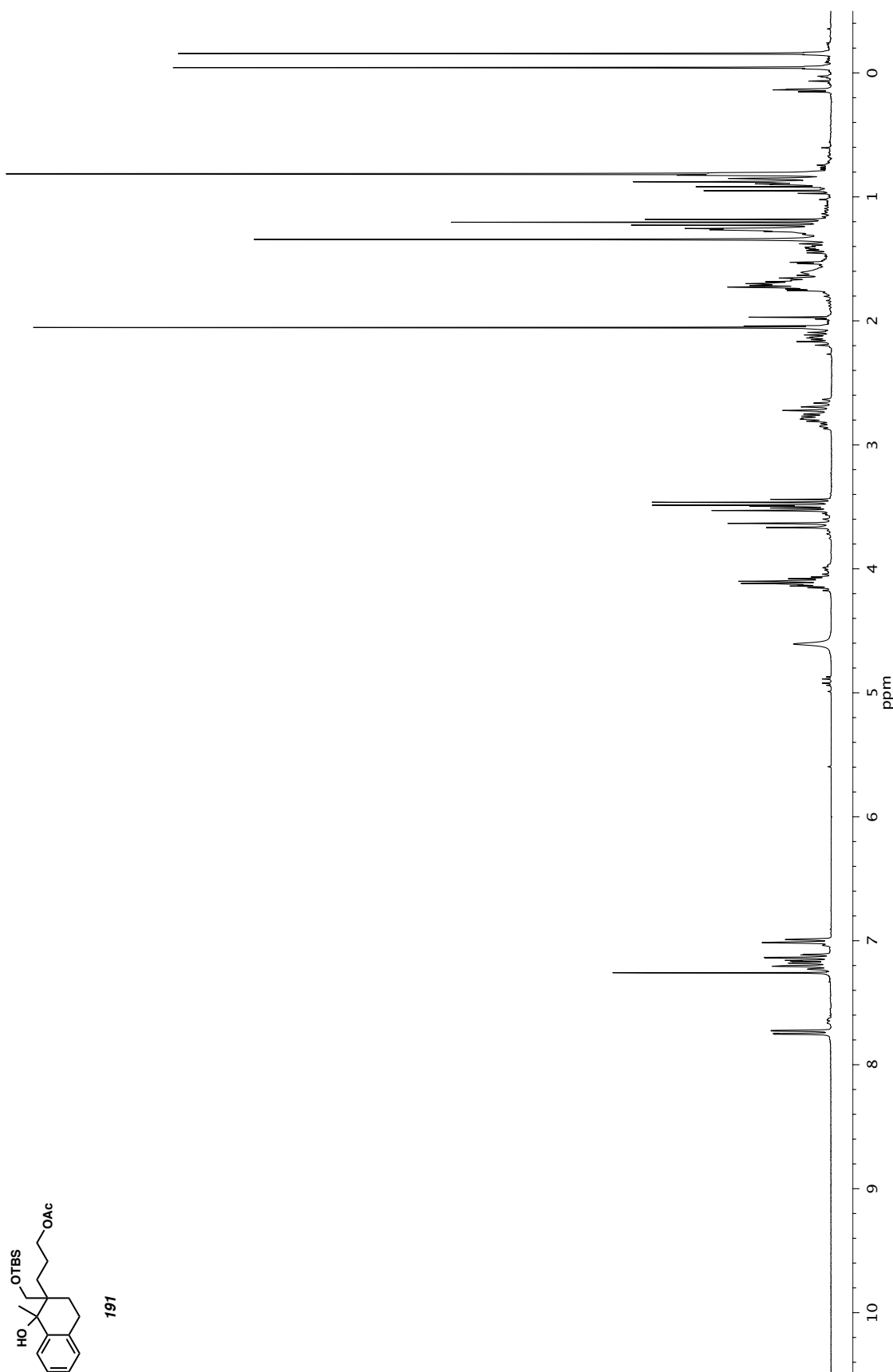


Figure A10.12 ¹H NMR (500 MHz, CDCl₃) of compound 191.

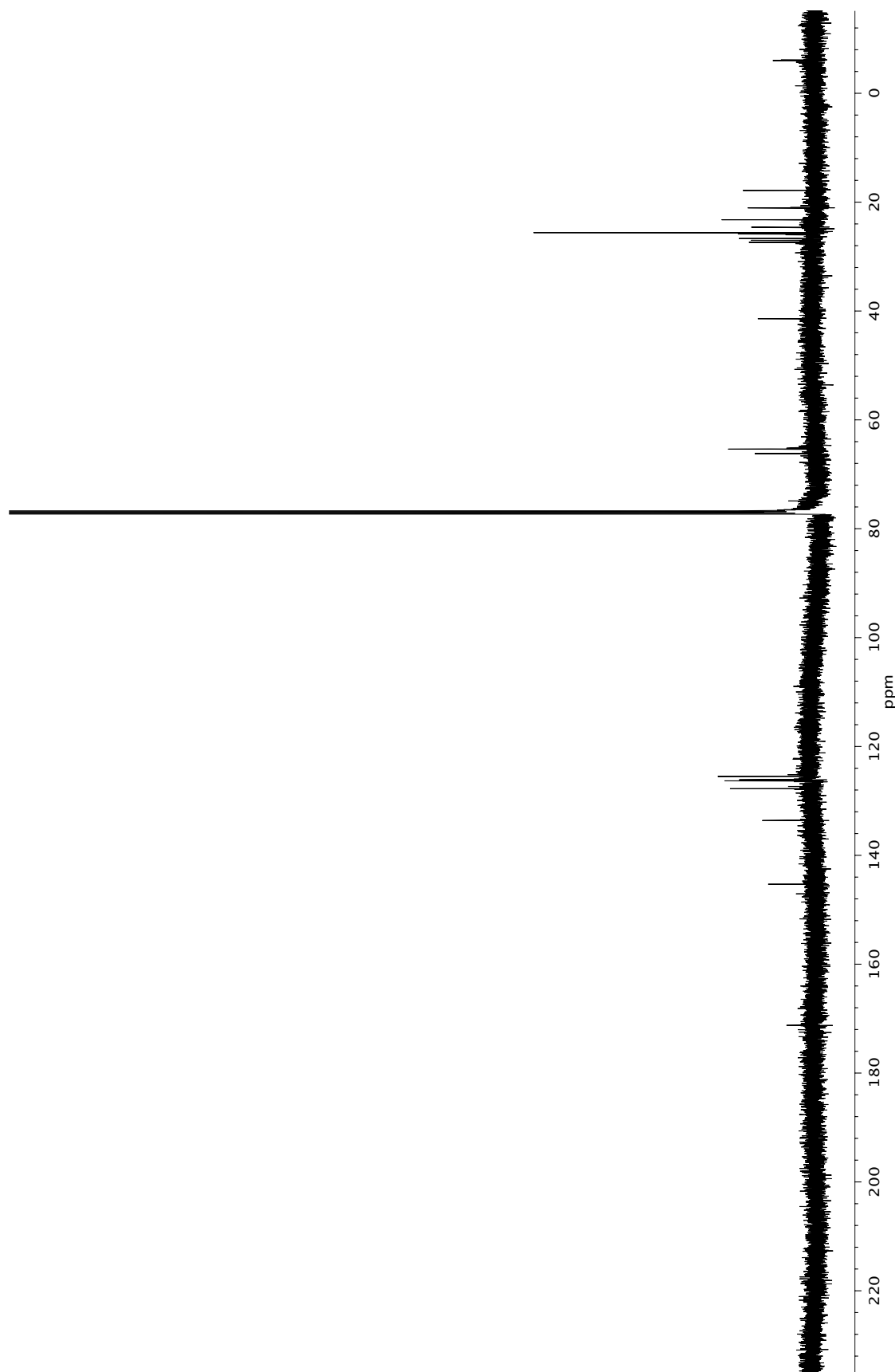


Figure A10.13 ^{13}C NMR (125 MHz, CDCl_3) of compound 191.

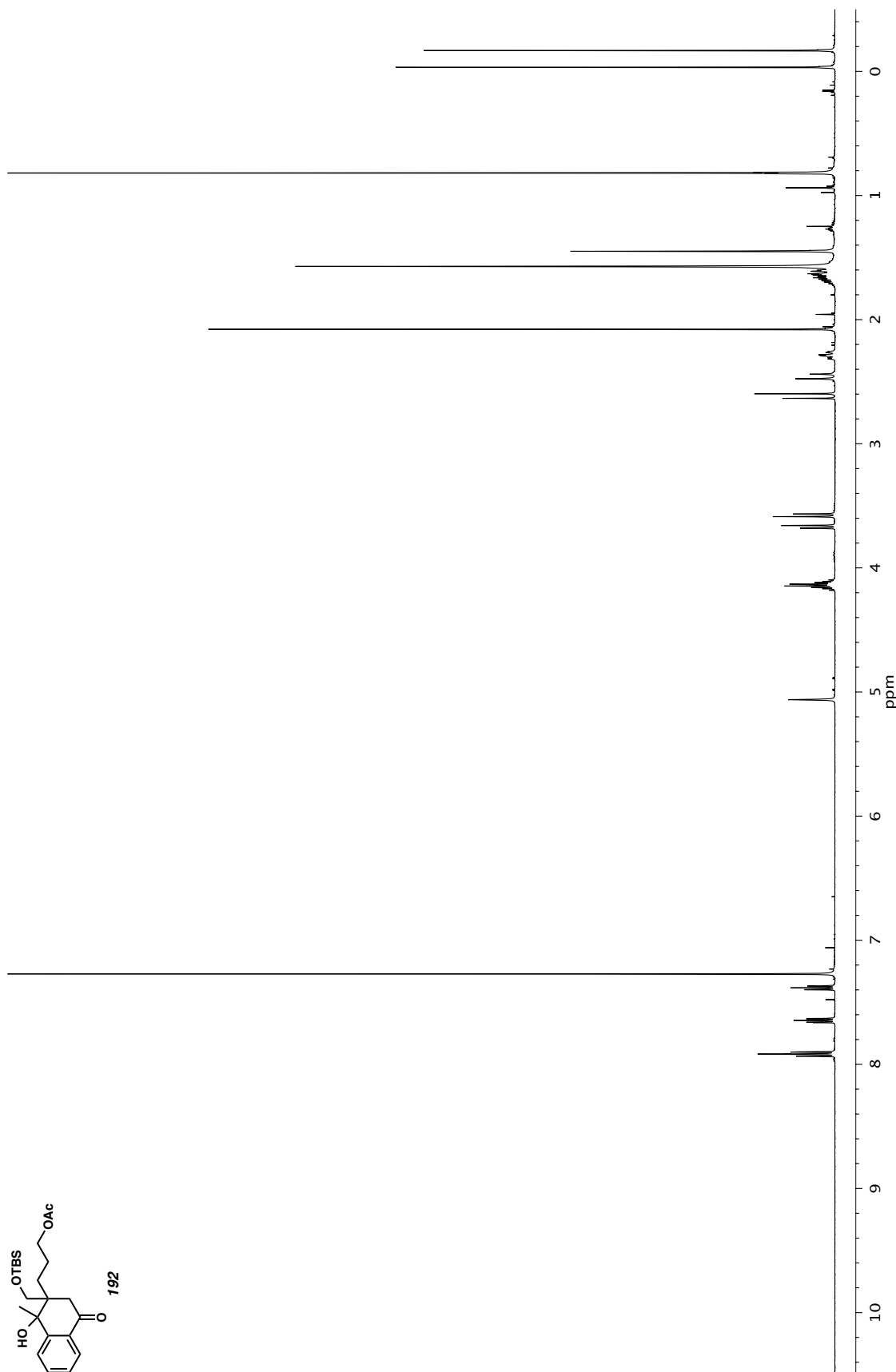


Figure A10.14 ^1H NMR (500 MHz, CDCl_3) of compound **192**.

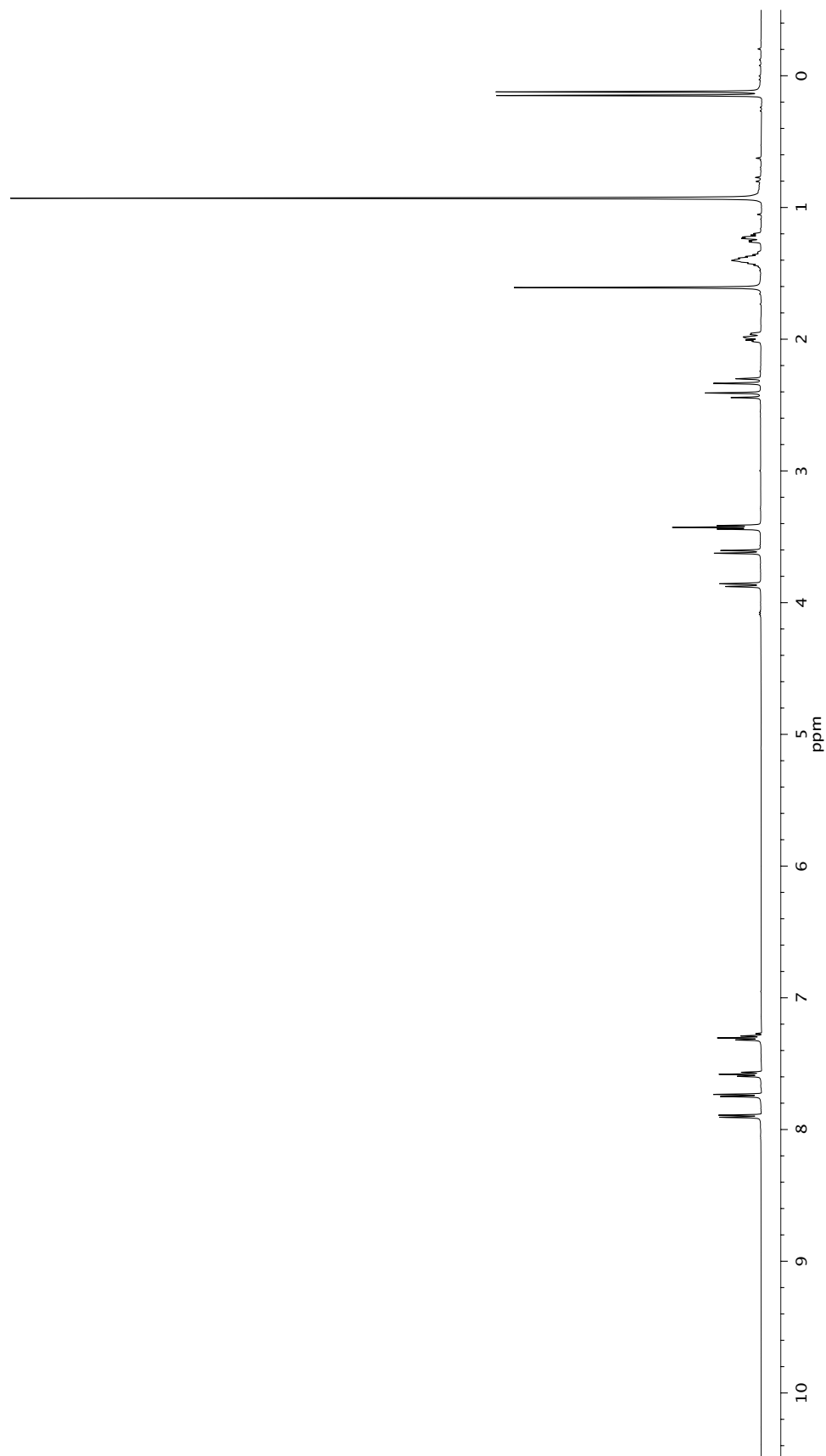
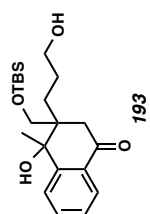


Figure A10.15 ¹H NMR (500 MHz, CDCl₃) of compound 193.

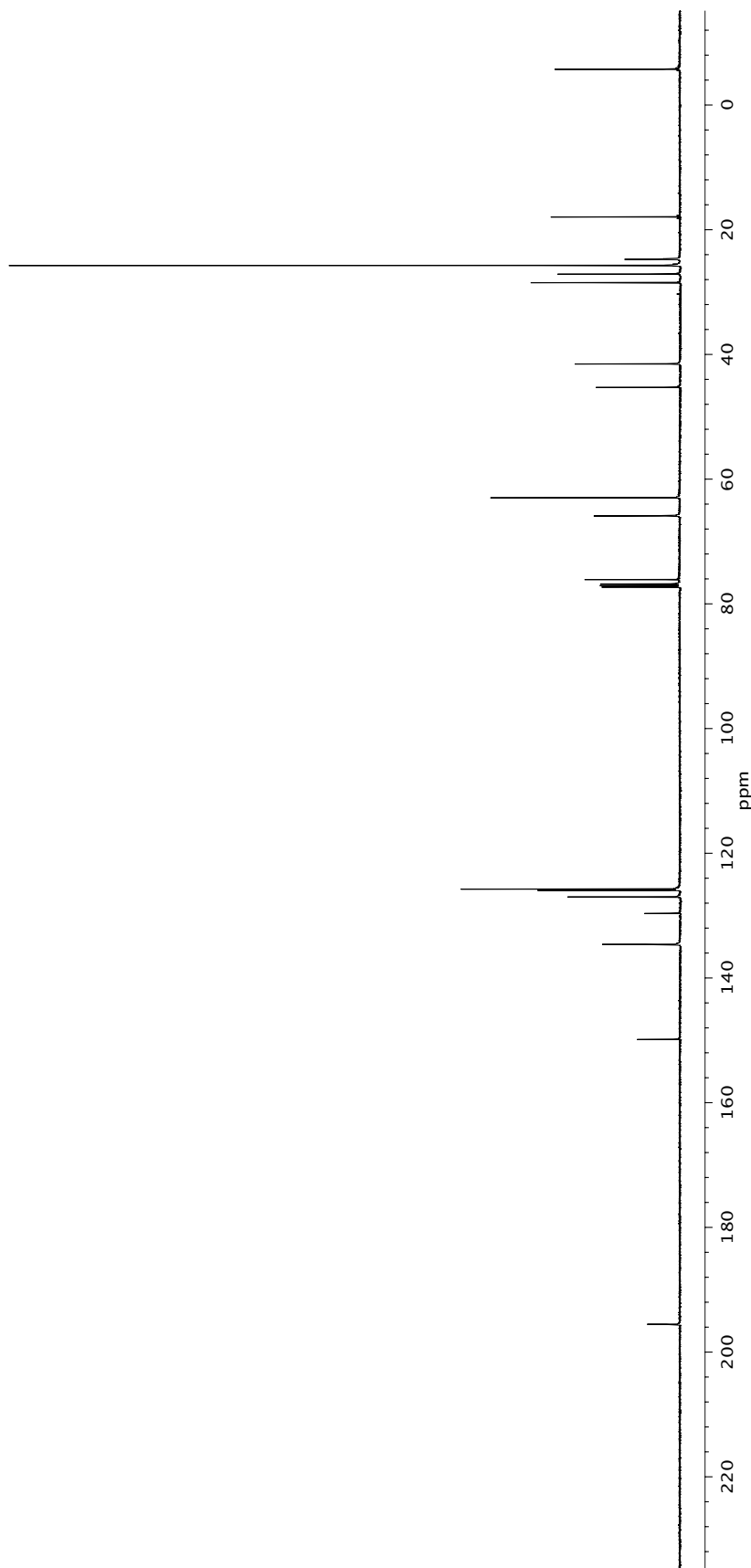


Figure A10.16 ^{13}C NMR (125 MHz, CDCl_3) of compound 193.

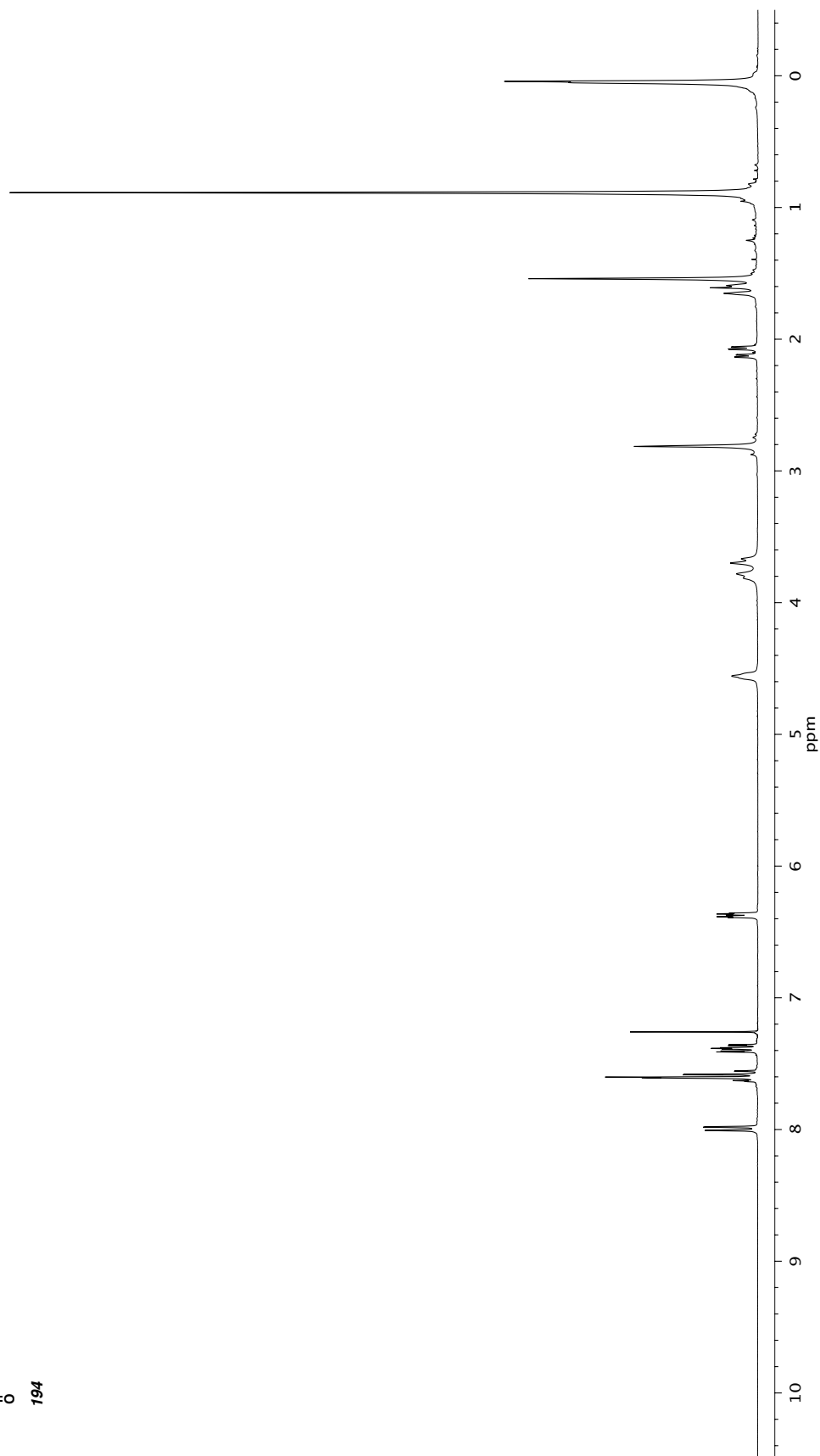
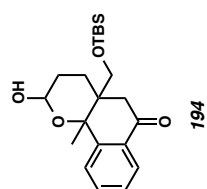


Figure A10.19 ¹H NMR (500 MHz, CDCl₃) of compound **194**.

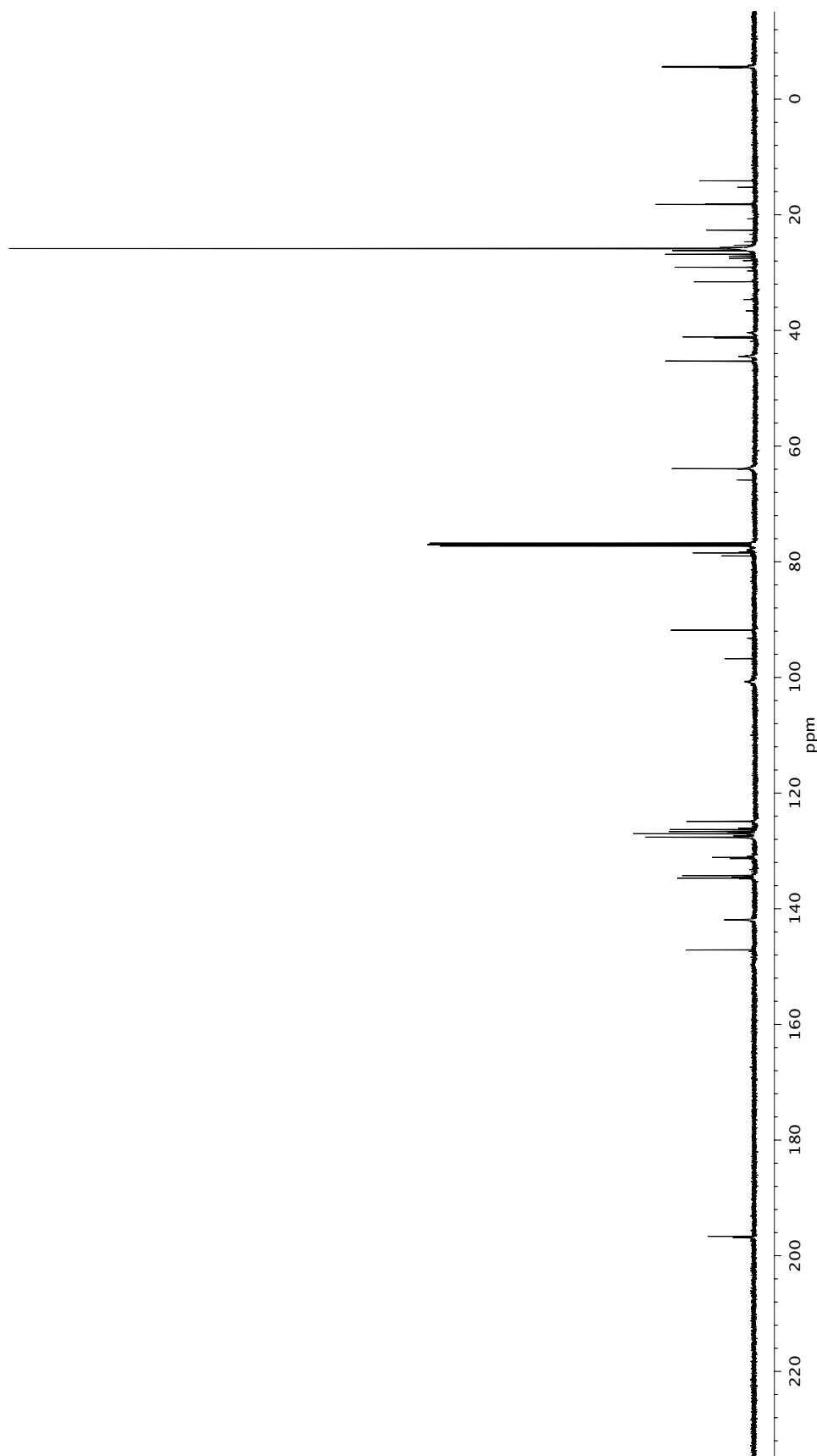


Figure A10.20 ^{13}C NMR (125 MHz, CDCl_3) of compound 194.

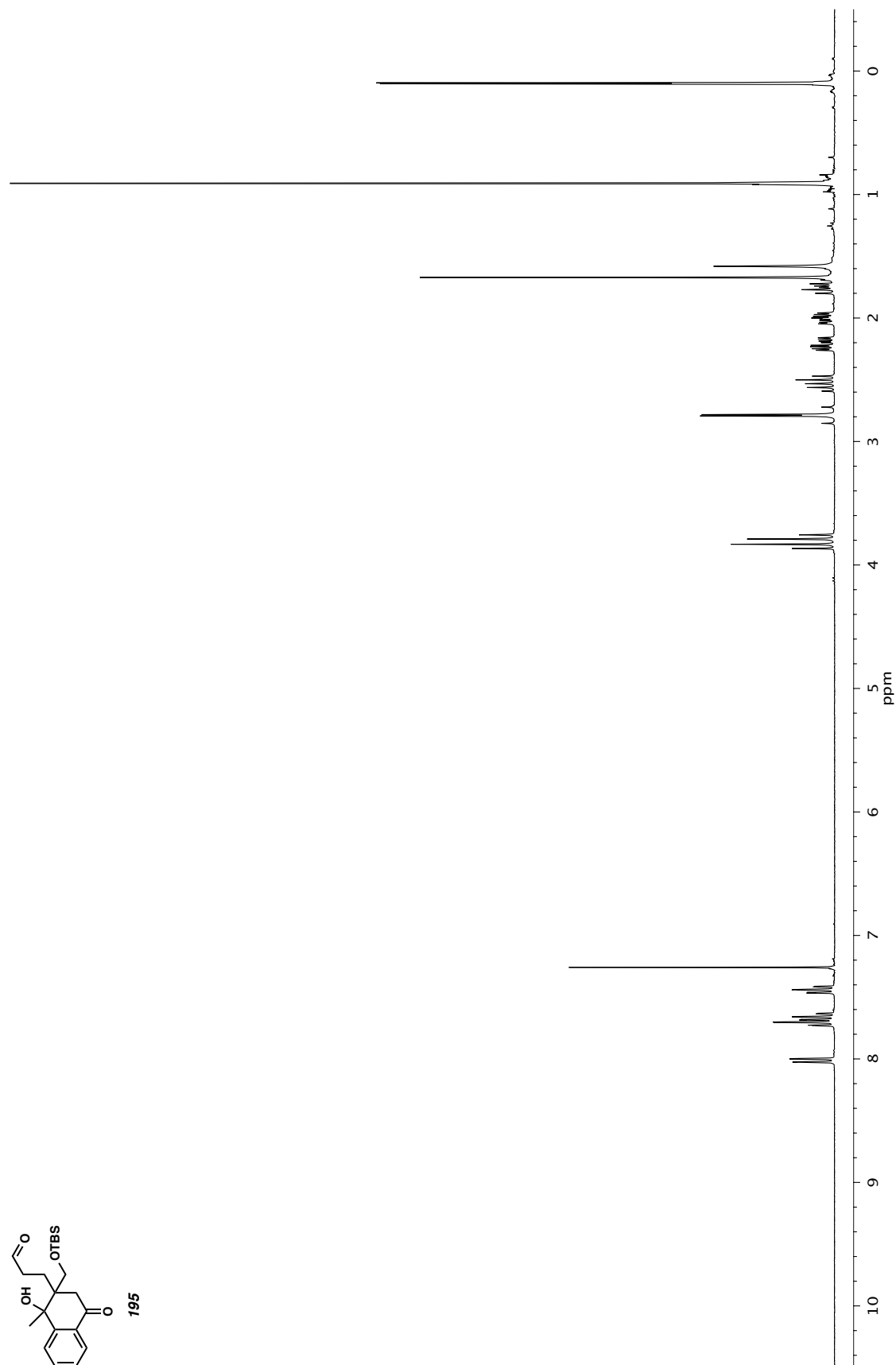
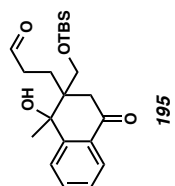


Figure A10.17 ¹H NMR (500 MHz, CDCl₃) of compound 195.

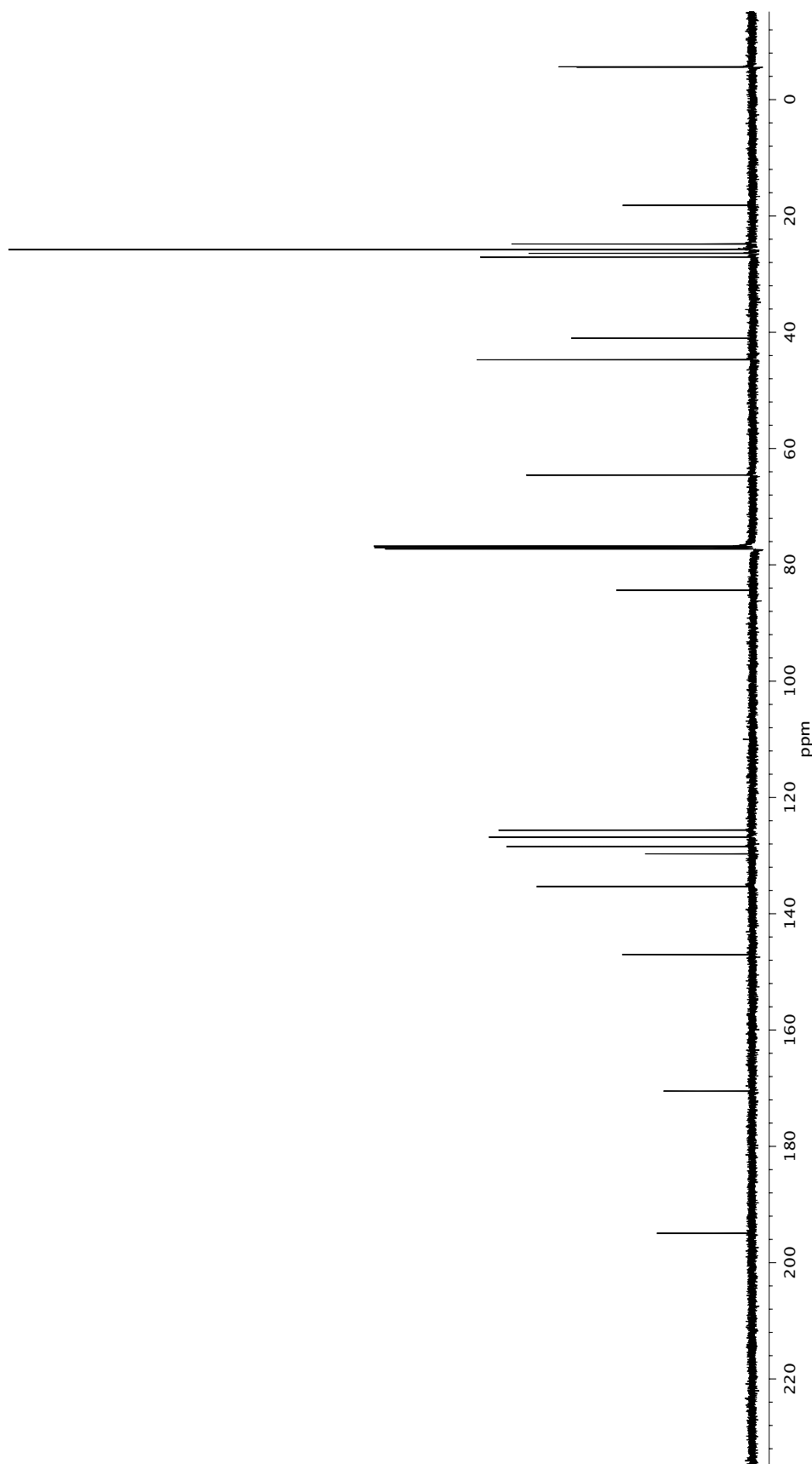
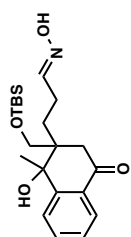
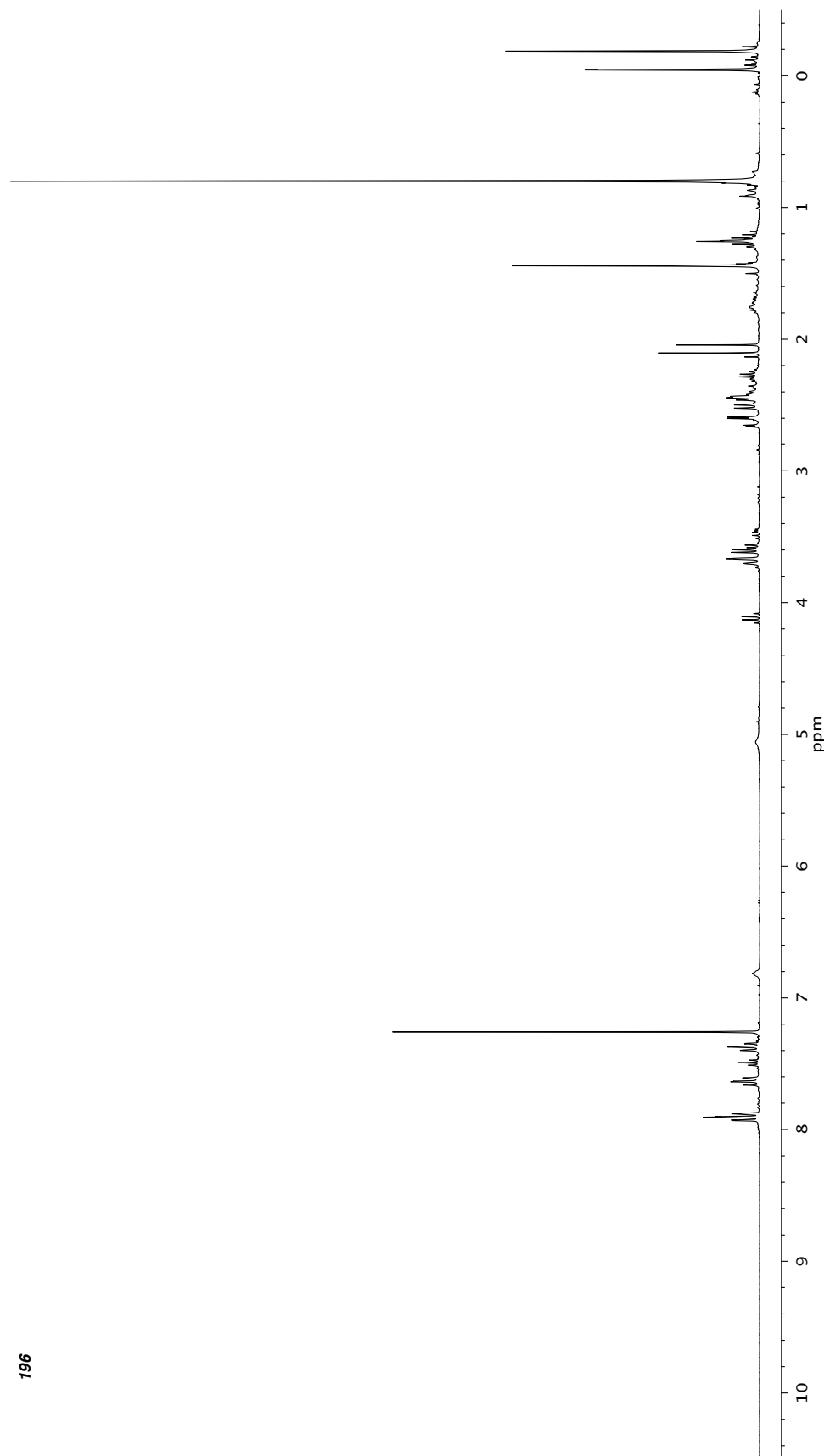


Figure A10.18 ^{13}C NMR (125 MHz, CDCl_3) of compound 195.

**196***Figure A10.21* ¹H NMR (300 MHz, CDCl₃) of compound **196**.

COMPREHENSIVE BIBLIOGRAPHY

A. Hassner and K. Rai, *Synthesis* **1989**, *1*, 57

Abraham, L.; Körner, M.; Schwab, P.; Hiersemann, M. *Adv. Synth. Catal.* **2004**, *346*, 1281.

Adjabeng, G.; Brenstrum, T.; Frampton, C. S.; Robertson, A. J.; Hillhouse, J.; McNulty, J.; Capretta, A. *J. Org. Chem.* **2004**, *69*, 5082.

Åhman, J.; Wolfe, J. P.; Troutman, M. V.; Palucki, M.; Buchwald, S. L. *J. Am. Chem. Soc.* **1998**, *120*, 1918.

Alexakis, A.; Polet, D. *Org. Lett.* **2004**, *6*, 3529.

Arhart, R.J.; Martin, J.C. *J. Am. Chem. Soc.* **1972**, *94*, 5003.

Atkins, G. M.; Burgess, E. M. *J. Am. Chem. Soc.* **1968**, *17*, 4744

Back, T. G.; Wulff, J. E. *Angew. Chem., Int. Ed.* **2004**, *43*, 6993.

Barnes, D. M.; Ji, J.; Fickes, M. G.; Fitzgerald, M. A.; King, S. A.; Morton, H. E.; Plagge, F. A.; Preskill, M.; Wagaw, S. H.; Wittenberger, S. J.; Zang, J. *J. Am. Chem. Soc.* **2002**, *124*, 13097.

Bartels, B.; García-Yebra, C.; Helmchen, G. *Eur. J. Org. Chem.* **2003**, 1097.

- Bartels, B.; Helmchen, G. *Chem. Commun.* **1999**, 741.
- Bartoli, G.; Bosco, M.; Bellucci, M. C.; Marcantoni, E.; Sambri, L.; Torregiani, E.
Eur. J. Org. Chem. **1999**, 617.
- Bauld, N. L.; J. Cessac, R. L. Holloway, *J. Am. Chem. Soc.* **1977**, *99*, 8140.
- Baum, J. S.; Shook, D. A.; Davies, H. M. L.; Smith, H. D. *Synth. Commun.* **1987**,
14, 1709.
- Bauzá, A.; D. Quiñonero, P. M. Deyà, A. Frontera, *Chem. Phys. Lett.* **2012**, *536*,
166.
- Behenna, D. C.; J. T. Mohr, N. H. Sherden, S. C. Marinescu, A. M. Harned, K.
Tani, M. Seto, S. Ma, Z. Novák, M. R. Krout, R. M. McFadden, J. L.
Roizen, J. A. Enquist Jr., D. E. White, S. R. Levine, K. V. Petrova, A.
Iwashita, S. C. Virgil, B. M. Stoltz, *Chem.—Eur. J.* **2011**, *17*, 14199.
- Behenna, D. C.; Stoltz, B. M. *J. Am. Chem. Soc.* **2004**, *126*, 15044.
- Behenna, D. C.; Y. Liu, T. Yurino, J. Kim, D. E. White, S. C. Virgil, B. M. Stoltz,
Nature Chem. **2012**, *4*, 130.
- Bélanger, É.; Cantin, K.; Messe, O.; Tremblay, M.; Paquin, J.-F. *J. Am. Chem. Soc.*
2007, *129*, 1034.
- Belluš, D.; B. Ernst, *Angew. Chem. Int. Ed. Engl.* **1988**, *27*, 797.

Bencivenni, G.; Wu, L.-Y.; Mazzanti, A.; Giannichi, B.; Pesciaioli, F.; Song, M.-P.; Bartoli, G.; Melchiorre, P. *Angew. Chem., Int. Ed.* **2009**, *48*, 7200.

Berg, U. in *Patai Series: the Chemistry of Functional Groups* (Eds.: Z. Rappoport, J. F. Liebman, S. Patai) John Wiley & Sons, Ltd, Chichester, UK, **2005**. pp. 83-131.

Brownlee, M. *Nature* **2001**, *414*, 813.

Burger, E. C.; Barron, B. R.; Tunge, J. A. *Synlett* **2006**, 2824.

Burtoloso, A. C. B. *Synlett*, **2009**, 2, 320.

Caine, D. Alkylation and Related Reactions of Ketones and Aldehydes via Metal Enolates. In *Carbon-Carbon Bond Formation*; Augustine, R. L., Ed.; Marcel Dekker: New York, 1979; Vol. 1, pp 85–250.

Caine, D.; Alkylation of Enols and Enolates. In *Comprehensive Organic Synthesis*, Trost, B. M.; Fleming, I, Eds.; Pergamon Press: Oxford, 1991, Vol. 3, pp. 1-63.

Cao, C.; Wang, L.; Cai, Z.; Zhang, L.; Guo, J.; Pang, G.; Shi, Y. *Eur. J. Org. Chem.* **2011**, 1570.

Carbon-carbon s-bond formation. In *Comprehensive Organic Synthesis*; Trost, B.M., Fleming, I., Eds.; Pergamon Press: New York, 1991; Vol. 3.

- Carroll, M. P.; Guiry, P. J. *Chem. Soc. Rev.* **2014**, *43*, 819.
- Catino, A. J.; Nichols, J. M.; Choi, H.; Gottipamula, S.; Doyle, M. P. *Org. Lett.* **2005**, *7*, 5167.
- Cazeau, P.; Duboudin, F.; Moulines, F.; Babot, O.; Dunogues, J. *Tetrahedron* **1987**, *43*, 2075.
- Cazeau, P.; Duboudin, F.; Moulines, F.; Babot, O.; Dunogues, J. *Tetrahedron*, **1987**, *43*, 2089.
- Chauhan, P.; Chimni, S. S. *Adv. Synth. Catal.* **2011**, *353*, 3203.
- Chaumontet, M.; R. Piccardi, N. Audic, J. Hitce, J.-L. Peglion, E. Clot, O. Baudoin, *J. Am. Chem. Soc.* **2008**, *130*, 15157.
- Chen, W.; Chen, M.; Hartwig, J. F. *J. Am. Chem. Soc.* **2014**, *136*, 15825.
- Chen, W.; Hartwig, J. F. *J. Am. Chem. Soc.* **2012**, *134*, 15249.
- Chen, W.; Hartwig, J. F. *J. Am. Chem. Soc.* **2013**, *135*, 2068.
- Cheon, H. C.; Yamamoto, H. *J. Am. Chem. Soc.* **2008**, *130*, 9246.
- Christoffers, J.; Baro, A. *Quaternary Stereocenters: Challenges and Solutions for Organic Synthesis*, Wiley-VCH: Weinheim, 2005.
- Christoffers, J.; Koripelly, G.; Rosiak, A.; Rössle, M. *Synthesis* **2007**, 1279.

- Crudden, C. M.; Hleba, Y. B.; Chen, A. C. *J. Am. Chem. Soc.* **2004**, *126*, 9200.
- Culkin, D. A.; Hartwig, J. F. *Acc. Chem. Res.* **2003**, *36*, 234.
- Dahnz, A.; Helmchen, G. *Synlett*, **2006**, 697.
- Dai, Y.; Wu, F.; Zang, Z.; You, H.; Gong, H. *Chem. –Eur. J.* **2012**, *18*, 808.
- Davies, H. M. L.; Cantrell, Jr., W. R.; Romines, K. R.; Baum, J. S. *Org. Syn.* **1992**, *70*, 93.
- Dembitsky, V. M.; *J. Nat. Med.* **2008**, *62*, 1.
- Ding, M.; Zhou, F.; Liu, Y.-L.; Wang, C.-H.; Zhao, X.-L.; Zhou, J. *Chem. Sci.* **2011**, *2*, 2035.
- Dolling, U.-H.; Davis, P.; Grabowski, E. J. J. *J. Am. Chem. Soc.* **1984**, *106*, 446.
- Douglas, C. J.; Overman, L. E. *Proc. Natl. Acad. Sci. U.S.A.* **2004**, *101*, 5363.
- Doyle, A. G.; Jacobsen, E. N. *Angew. Chem., Int. Ed.* **2007**, *46*, 3701.
- Doyle, A. G.; Jacobsen, E. N. *J. Am. Chem. Soc.* **2005**, *127*, 62.
- Ehrentraut, A.; Zapf, A.; Beller, M. *Adv. Synth. Catal.* **2002**, *344*, 209.
- F. Kleinbeck, F. D. Toste, *J. Am. Chem. Soc.* **2009**, *131*, 9178.
- Fairlamb, I. J. S.; Kapdi, A. R.; Lee, A. F. *Org. Lett.* **2004**, *6*, 4435.

Falciola, C. A.; Alexakis, A. *Eur. J. Org. Chem.* **2008**, 3765.

Farwick, A.; Engelhart, J. U.; Tverskoy, O.; Welter, C.; Umlauf, Q. A.; Rominger, F.; Kerr, W. J.; Helmchen, G. *Adv. Synth. Catal.* **2011**, 353, 349.

Fitjer, L. in *Methods of Organic Chemistry Vol. E17e* (Ed.: A. De Meijere), Georg Thieme Verlag: Stuttgart, **1997**, pp 251-316.

Flegelová, Z.; Pátek, M. *J. Org. Chem.* **1996**, 61, 6735.

Fox, J. M.; Huang, X.; Chieffi, A.; Buchwald, S. L. *J. Am. Chem. Soc.* **2000**, 122, 1360.

Fu, N.-Y.; S.-H. Chan, H. N. C. Wong in *Patai Series: the Chemistry of Functional Groups* (Eds.: Z. Rappoport, J. F. Liebman, S. Patai) John Wiley & Sons, Ltd, Chichester, UK, **2005**, pp. 357–440.

González, D. F.; Brand, J. P.; Waser, J. *Chem. Eur. J.* **2010**, 16, 9457.

Graening, T.; Hartwig, J. F. *J. Am. Chem. Soc.* **2005**, 127, 17192.

Grasa, G. A.; Colacot, T. J. *Org. Lett.* **2007**, 9, 5489.

Grenning, A. J.; Tunge, J. A. *Angewandte Chemie International Edition* **2011**, 50, 1688.

Grenning, A. J.; Tunge, J. A. *J. Am. Chem. Soc.* **2011**, 133, 14785.

- Grenning, A. J.; Tunge, J. A. *J. Am. Chem. Soc.* **2011**, *133*, 14785.
- Grenning, A. J.; Van Allen, C. K.; Maji, T.; Lang, S. B.; Tunge, J. A. *J. Org. Chem.* **2013**, *78*, 7281.
- Hale, K.J.; Grabski, M.; Flasz, J.T. *Org. Lett.*, **2013**, *15*, 370.
- Hama, T.; Culkin, D. A.; Hartwig, J. F. *J. Am. Chem. Soc.* **2006**, *128*, 4976.
- Hamada, T.; Chieffi, A.; Åhman, J.; Buchwald, S. L. *J. Am. Chem. Soc.* **2002**, *124*, 1261.
- Hamann, B. C.; Hartwig, J. F. *J. Am. Chem. Soc.* **1997**, *119*, 12382.
- Hamilton, J. Y.; Sarlah, D.; Carreira, E. M. *J. Am. Chem. Soc.* **2013**, *135*, 994.
- Hartwig, J. F.; Pouy, M. J. *Top. Organomet. Chem.* **2011**, *34*, 169.
- Hartwig, J. F.; Stanley, L. M. *Acc. Chem. Res.* **2010**, *43*, 1461.
- He, H.; Zheng, X.-J.; Li, Y.; Dai, L.-X.; You, S.-L. *Org. Lett.* **2007**, *9*, 4339.
- Hehn, J. P.; C. Mueller, T. Bach in *Handbook of Synthetic Photochemistry* (Eds.: A. Albini, M. Fagnoni), Wiley-VCH, Weinheim, **2010**, pp. 171–215.
- Helmboldt, H.; Hiersemann, M. *Tetrahedron* **2003**, *59*, 4031.
- Helmchen, G. In *Iridium Complexes in Organic Synthesis*; Oro, L. A.; Claver, C. Eds.; Wiley-VCH: Weinheim, Germany, 2009; p. 211.

- Helmchen, G.; Dahnz, A.; Dübon, P.; Schelwies, M.; Weihofen, R. *Chem. Commun.* **2007**, 675.
- Helmchen, G.; Kazmaier, U.; Fröster, S. In *Catalytic Asymmetric Synthesis*. Ojima, I. Ed; 3rd ed. Wiley, New Jersey, 2010, p. 497.
- Helmchen, G.; Pfaltz, A. *Acc. Chem. Res.* **2000**, *33*, 336.
- Hennings, D. D.; Iwasa, S.; Rawal, V. H. *Tetrahedron Lett.* **1997**, *38*, 6379.
- Hollingworth, C.; Hazari, A.; Hopkinson, M. N.; Tredwell, M.; Benedetto, E.; Huiban, M.; Gee, A. D.; Brown, J. M.; Gouverneur, V. *Angew. Chem. Int. Ed.* **2011**, *50*, 2613.
- Hong, A. Y.; Stoltz, B. M. *Angew. Chem., Int. Ed.* **2012**, *51*, 9674.
- Hughes, D. L. Alkylation of Enolates. In *Comprehensive Asymmetric Catalysis*; Jacobsen, E. N., Pfaltz, A., Yamamoto, H., Eds.; Springer: Berlin, 1999; Vol. 2, pp 1273–1294.
- Hughes, D. L. Alkylation of Enolates. In *Comprehensive Asymmetric Catalysis*; Jacobsen, E. N., Pfaltz, A., Yamamoto, H., Eds.; Springer: Berlin, 2004; Supplement 1, pp161.
- Igarashi, J.; Kobayashi, Y. *Tetrahedron Lett.* **2005**, *46*, 6381.
- Ilardi, E. A.; Stivala, C. E.; Zakarian, A. *Chem. Soc. Rev.* **2009**, *38*, 3133.

- Ireland, R. E.; Liu, L. *J. Org. Chem.* **1993**, *58*, 2899.
- Ito, H.; Taguchi, T. *Chem. Soc. Rev.* **1999**, *28*, 43.
- Itoh, K.; Tong, K. I.; Yamamoto, M. *Free Radic. Biol. Med.* **2004**, *36*, 1208.
- Iwama, T.; Rawal, V. H. *Organic Letters* **2006**, *8*, 5725.
- Janssen, J. P.; Helmchen, G. *Tetrahedron Lett.* **1997**, *38*, 8025.
- Jiang, B.; J. Qiao, Y. Yang, Y. Lu, *J. Cell. Biochem.* **2012**, *113*, 2560.
- Johansson, C. C. C.; Colacot, T. J. *Angew. Chem., Int. Ed.* **2010**, *49*, 676.
- Kanayama, T.; Yoshida, K.; Miyabe, H.; Takemoto, Y. *Angew. Chem., Int. Ed.* **2003**, *42*, 2054.
- Kawatsura, M.; Hartwig, J. F. *J. Am. Chem. Soc.* **1999**, *121*, 1473.
- Keith, J. A.; D. C. Behenna, N. Sherden, J. T. Mohr, S. Ma, S. C. Marinescu, R. J. Nielsen, J. Oxgaard, B. M. Stoltz, W. A. Goddard, III. *J. Am. Chem. Soc.* **2012**, *134*, 19050.
- Kiener, C. A.; Shu, C.; Incarvito, C.; Hartwig, J. F. *J. Am. Chem. Soc.* **2003**, *125*, 14272.
- Knobloch, E.; Brückner, R. *Synthesis* **2008**, *14*, 2229.
- Kobayashi, S.; Manabe, K.; Ishitani, H.; Matsuo, J. –I. In *Science of Synthesis*,

Houben-Weyl Methods of Molecular Transformations, Bellus, D.; Ley, S. V.; Noyori, R.; Regitz, M.; Schauman, E.; Shinkai, I.; Thomas, E. J.; Trost, B. M. Eds.; Georg Thieme Verlag: Stuttgart, 2002, Vol. 4, pp. 317–369.

Krause, N.; Hoffmann-Röder, A. *Synthesis* **2001**, 171.

Krautwald, S.; Sarlah, D.; Schafroth, M. A.; Carreira, E. M. *Science*, **2013**, *340*, 1065.

Krout, M. R.; Mohr, J. T.; Stoltz, B. M. *Org. Synth.* **2009**, *86*, 181.

Kuwajima, I.; Urabe, H. *J. Am. Chem. Soc.* **1982**, *104*, 6831.

Lan, H. Y. *Clin. Exp. Pharmacol. Physiol.* **2012**, *39*, 731.

Lan, H. Y. *Kidney Res. Clin. Pract.* **2012**, *31*, 4.

Lee-Ruff, E. in *Methods of Organic Chemistry, Vol. E17e* (Ed.: A. De Meijere), Georg Thieme Verlag, Stuttgart, **1997**, pp 179–187.

Lee-Ruff, E. in *Patai Series: the Chemistry of Functional Groups* (Eds.: Z. Rappoport, J. F. Liebman, S. Patai) John Wiley & Sons, Ltd, Chichester, UK, **2005**, pp. 281–355.

Lee-Ruff, E.; G. Mladenova, *Chem. Rev.* **2003**, *103*, 1449.

Lee, G. A. *Synthesis* **1982**, *6*, 508.

- Levine, S. R.; Krout, M. R.; Stoltz, B. M. *Org. Lett.* **2009**, *11*, 289.
- Lewis, A.; Steadman, R.; Manley, P.; Craig, K.; de la Motte C.; Hascall, V.; Phillips, A. O. *Histol Histopathol.* **2008**, *23*, 731.
- Li, H.; Wang, Y.; Tang, L.; Wu, F.; Liu, X.; Guo, C.; Foxman, B. M.; Deng, L. *Angew. Chem., Int. Ed.* **2005**, *44*, 105.
- Li, Y.-S.; K. Matsunaga, M. Ishibashi, Y. Ohizumi, *J. Org. Chem.* **2001**, *66*, 2165.
- Linton, E. C.; Kozlowski, M. C. *J. Am. Chem. Soc.* **2008**, *130*, 16162.
- Lipowsky, G.; Miller, N.; Helmchen, G. *Angew. Chem., Int. Ed.* **2004**, *43*, 4595.
- Liu, K.-C.; Shelton, B. R.; Howe, R. K. *J. Org. Chem.* **1980**, *45*, 3916.
- Liu, W.-B.; He, H.; Dai, L.-X.; You, S.-L. *Org. Lett.* **2008**, *10*, 1815.
- Liu, W.-B.; He, H.; Dai, L.-X.; You, S.-L. *Synthesis*, **2009**, 2076.
- Liu, W.-B.; Xia, J.-B.; You, S.-L. *Top. Organomet. Chem.* **2012**, *38*, 155.
- Liu, W.-B.; Zheng, C.; Zhuo, C.-X.; Dai, L.-X.; You, S.-L. *J. Am. Chem. Soc.* **2012**, *134*, 4812.
- Liu, X.; Hartwig, J. F. *J. Am. Chem. Soc.* **2004**, *126*, 5182.
- Long, R.; Huang, J.; Shao, W.; Liu, S.; Lan, Y.; Gong, J.; Yang, Z. *Nat. Commun.* **2014**, *5*.

- López-Carrillo, V.; A. M. Echavarren, *J. Am. Chem. Soc.* **2010**, *132*, 9292.
- Lu, Z.; Ma, S. *Angew. Chem.* **2008**, *120*, 264; *Angew. Chem., Int. Ed.* **2008**, *47*, 258.
- Madrahimov, S. T.; Hartwig, J. F. *J. Am. Chem. Soc.* **2012**, *134*, 8136.
- Madrahimov, S. T.; Markovic, D.; Hartwig, J. F. *J. Am. Chem. Soc.* **2009**, *131*, 7228.
- Mailhol, D.; Duque, M. d. M. S.; Raimondi, W.; Bonne, D.; Constantieux, T.; Coquerel, Y.; Rodriguez, J. *Adv. Synth. & Catal.* **2012**, *354*, 3523.
- Markham, J. P.; S. T. Staben, F. D. Toste, *J. Am. Chem. Soc.* **2005**, *127*, 9708.
- Marrero, J.; A. D. Rodríguez, P. Baran, R. G. Raptis, J. A. Sánchez, E. Ortega-Barria, T. L. Capson, *Org. Lett.* **2004**, *6*, 1661.
- Martín Castro, A. M. *Chem. Rev.* **2004**, *104*, 2939.
- Martin, S. F. *Tetrahedron*, **1980**, *36*, 419.
- Mase, N.; Thayumanavan, R.; Tanaka, F.; Barbas, C. F. III *Org. Lett.* **2004**, *6*, 2527.
- Matsubara, K.; Ueno, K.; Koga, Y.; Hara, K. *J. Org. Chem.* **2007**, *72*, 5069.
- Matsubara, K.; Ueno, K.; Koga, Y.; Hara, K. *J. Org. Chem.* **2007**, *72*, 5069.

- Matsuda, T.; Makino, M.; Murakami, M. *Angew. Chem.* **2005**, *117*, 4684; *Angew. Chem. Int. Ed.* **2005**, *44*, 4608.
- Matsuda, T.; Makino, M.; Murakami, M. *Bull. Chem. Soc. Jpn.* **2005**, *78*, 1528.
- Matsuda, T.; Makino, M.; Murakami, M. *Org. Lett.* **2004**, *6*, 1257.
- Matsuda, T.; Shigeno, M.; Murakami, M. *J. Am. Chem. Soc.* **2007**, *129*, 12086.
- Matsuo, K.; Arase, T.; Ishida, S.; Sakaguchi, Y. *Heterocycles*, **1996**, *43*, 1287.
- McDougal, N. T.; Streuff, J.; Mukherjee, H.; Virgil, S. C.; Stoltz, B. M. *Tetrahedron Lett.* **2010**, *51*, 5550.
- McDougal, N. T.; Virgil, S. C.; Stoltz, B. M. *Synlett* **2010**, 1712.
- Meshram, H. M.; Reddy, P. N.; Sadashiv, K.; Yadav, J. S. *Tetrahedron Lett.* **2005**, *46*, 623.
- Mohr, J. T.; Behenna, D. C.; Harned, A. M.; Stoltz, B. M. *Angew. Chem. Int. Ed.* **2005**, *44*, 6924
- Mohr, J. T.; Krout, M. R.; Stoltz, B. M. *Org. Synth.* **2009**, *86*, 194.
- Mohr, J. T.; Nishimata, T.; Behenna, D. C.; Stoltz, B. M. *J. Am. Chem. Soc.* **2006**, *128*, 11348.
- Mohr, J. T.; Stoltz, B. M. *Chem.–Asian J.* **2007**, *2*, 1476.

Moustafa, M. M. A. R.; Pagenkopf, B. L. *Org. Lett.* **2010**, *12*, 4732.

Moustafa, M. M. A. R.; Stevens, A. C.; Machin, B. P.; Pagenkopf, B. L. *Org. Lett.* **2010**, *12*, 4736.

Murakami, M.; Amii, H.; Shigeto, K.; Ito, Y. *J. Am. Chem. Soc.* **1996**, *118*, 8285.

N. Hoffmann in *Handbook of Synthetic Photochemistry* (Eds.: A. Albini, M. Fagnoni), Wiley-VCH, Weinheim, **2010**, pp. 137–169.

Nahra, F.; Macé, Y.; Lambin, D.; Riant, O. *Angew. Chem., Int. Ed.* **2013**, *52*, 3208.

Nakamura, M.; Hajra, A.; Endo, K.; Nakamura, E. *Angew. Chem.* **2005**, *117*, 7414;
Angew. Chem., Int. Ed. 2005, *44*, 7248.

Nemoto, H.; H. Ishibashi, M. Nagamochi, K. Fukumoto, *J. Org. Chem.* **1992**, *57*,
1707.

Neuhaus, C. M.; Liniger, M.; Stieger, M.; Altmann, K. -H. *Angew. Chem., Int. Ed.* **2013**, *52*, 5866.

Nishimura, T.; Ohe, K.; Uemura, S. *J. Am. Chem. Soc.* **1999**, *121*, 2645.

Novak, P.; Martin, R. *Curr. Org. Chem.* **2011**, *15*, 3233.

O'Brien, J. M.; Kingsbury, J. S. *J. Org. Chem.* **2011**, *76*, 1662.

Ohmura, T.; Hartwig, J. F. *J. Am. Chem. Soc.* **2002**, *124*, 15164.

- Palucki, M.; Buchwald, S. L. *J. Am. Chem. Soc.* **1997**, *119*, 11108.
- Pangborn, A. M.; Giardello, M. A.; Grubbs, R. H.; Rosen, R. K.; Timmers, F. J. *Organometallics*, **1996**, *15*, 1518.
- Pete, J.-P. *Advances in Photochemistry*, John Wiley & Sons, Inc., Hoboken, NJ, USA, **1996**.
- Polet, D.; Alexakis, A. *Chim. Oggi* **2007**, *25*, 31.
- Polet, D.; Alexakis, A.; Tissot-Croset, K.; Corminboeuf, C.; Ditrich, K. *Chem. Eur. J.* **2006**, *12*, 3596.
- Presset, M.; Coquerel, Y.; Rodriguez, J. *J. Org. Chem.* **2009**, *74*, 415.
- Presset, M.; Mailhol, D.; Coquerel, Y.; Rodriguez, J. *Synthesis* **2011**, 2549.
- Qu, L.; Wang, X. S.; Cao, A. G. *Gansu J. Tradit. Chin. Med.* **2011**, *24*, 28.
- Raskatov, J. A.; Jäkel, M.; Straub, B. F.; Rominger, F.; Helmchen, G. *Chem. Eur. J.* **2012**, *18*, 14314.
- Raskatov, J. A.; Spiess, S.; Gnam, C.; Brödner, K.; Rominger, F.; Helmchen, G. *Chem. Eur. J.* **2010**, *16*, 6601.
- Rasmussen, J. K. *Synthesis* **1977**, 91.
- Schafroth, M. A.; Sarlah, D.; Krautwald, S.; Carreira, E. M. *J. Am. Chem. Soc.*

2012, 134, 20276.

Schleicher, K. D.; Jamison, T. F. *Beilstein J. Org. Chem.* **2013**, 9, 1533.

Seebach, D. *Angew. Chem., Int. Ed. Engl.* **1988**, 27, 1624.

Seiser, T.; T. Saget, D. N. Tran, N. Cramer, *Angew. Chem.* **2011**, 123, 7884;
Angew. Chem. Int. Ed. **2011**, 50, 7740.

Sergeiko, A.; V. V. Poroikov, L. O. Hanus, V. M. Dembitsky, *Open Med. Chem. J.*
2008, 2, 26.

Seto, M.; Roizen, J. L.; Stoltz, B. M. *Angew. Chem. Int. Ed.* **2008**, 47, 6873.

Sherden, N. H.; D. C. Behenna, S. C. Virgil, B. M. Stoltz, *Angew. Chem. Int.*
Ed. **2009**, 48, 6840.

Shigeno, M.; Yamamoto, T.; Murakami, M. *Chem.–Eur. J.* **2009**, 15, 12929.

Shimizu, I.; T. Yamada, J. Tsuji, *Tet. Lett.* **1980**, 21, 3199.

Shu, C.; Leitner, A.; Hartwig, J. F. *Angew. Chem., Int. Ed.* **2004**, 43, 4797.

Spiess, S.; Raskatov, J. A.; Gnam, C.; Brödner, K.; Helmchen, G. *Chem. Eur. J.*
2009, 15, 11087.

Spiess, S.; Welter, C.; Franck, G.; Taquet, J.-P.; Helmchen, G. *Angew. Chem., Int.*
Ed. **2008**, 47, 7652.

- Stavber, G.; Zupan, M.; Stavber, S. *Tetrahedron Lett.* **2007**, *48*, 2671.
- Stevens, S. J.; Bérubé, A.; Wood, J. L. *Tetrahedron* **2011**, *67*, 6479.
- Streuff, J.; D. E. White, S. C. Virgil, B. M. Stoltz, *Nature Chem.* **2010**, *2*, 192.
- Sun, C. -S.; Lin, Y. -S.; Hou, D. -R. *J. Org. Chem.* **2008**, *73*, 6877.
- Takeuchi, R.; Kashio, M. *Angew. Chem., Int. Ed. Engl.* **1997**, *36*, 263.
- Tan, J.; Cheon, C.-H.; Yamamoto, H. *Angew. Chem., Int. Ed.* **2012**, *51*, 8264.
- Tanaka, N.; M. Okasaka, Y. Ishimaru, Y. Takaishi, M. Sato, M. Okamoto, T. Oshikawa, S. U. Ahmed, L. M. Consentino, K.-H. Lee, *Org. Lett.* **2005**, *7*, 2997.
- Tani, K.; Behenna, D. C.; McFadden, R. M.; Stoltz, B. M. *Org. Lett.* **2007**, *9*, 2529.
- Taylor, M. S.; Jacobsen, E. N. *J. Am. Chem. Soc.* **2003**, *125*, 11204.
- Teichert, J. F.; Feringa, B. L. *Angew. Chem., Int. Ed.* **2010**, *49*, 2486.
- Tolman, C. A. *Chem. Rev.* **1977**, *77*, 313.
- Tosatti, P.; Nelson, A.; Marsden, S. P. *Org. Biomol. Chem.* **2012**, *10*, 3147.
- Trost, B. M. *Chem. Pharm. Bull.* **2002**, *50*, 1.
- Trost, B. M. *Org. Process Res. Dev.* **2012**, *16*, 185.

- Trost, B. M.; Bream, R. N.; Xu, J. *Angew. Chem. Int. Ed.* **2006**, *45*, 3109.
- Trost, B. M.; Cramer, N.; Silverman, S. M. *J. Am. Chem. Soc.* **2007**, *129*, 12396.
- Trost, B. M.; Crawley, M. L. *Chem. Rev.* **2003**, *103*, 2921.
- Trost, B. M.; Jiang, C. *Synthesis* **2006**, 369.
- Trost, B. M.; Miller, J. R.; Hoffman, C. M., Jr. *J. Am. Chem. Soc.* **2011**, *133*, 8165.
- Trost, B. M.; Silverman, S. M.; Stambuli, J. P. *J. Am. Chem. Soc.* **2011**, *133*, 19483.
- Trost, B. M.; Strege, P. E. *J. Am. Chem. Soc.* **1977**, *99*, 1649.
- Trost, B. M.; T. Yasukata, *J. Am. Chem. Soc.* **2001**, *123*, 7162.
- Trost, B. M.; Xu, J. *J. Am. Chem. Soc.* **2005**, *127*, 17180.
- Trost, B. M.; Xu, J.; Schmidt, T. *J. Am. Chem. Soc.* **2009**, *131*, 18343.
- Trost, B. M.; Zhang, Y. *J. Am. Chem. Soc.* **2007**, *129*, 14548.
- Tsuji, J.; Takahashi, H.; Morikawa, M. *Tetrahedron Lett.* **1965**, *49*, 4387.
- Tsuji, J.; I. Minami, I. Shimizu *Tet. Lett.* **1983**, *24*, 1793.
- Tsuji, J.; I. Minami, I. Shimizu, *Chem. Lett.* **1983**, 1325.
- Tsuji, J.; Minami, I. *Acc. Chem. Res.* **1987**, *20*, 140.

- Turner, J. A.; Jacks, W. S. *J. Org. Chem.* **1989**, *54*, 4229.
- Ukai, T.; Kawazura, H.; Ishii, Y.; Bonnet, J. J.; Ibers, J. A. *J. Organometallic Chem.* **1999**, *65*, 253.
- Uyeda, C.; Jacobsen, E. N. *J. Am. Chem. Soc.* **2008**, *130*, 9228.
- Uyeda, C.; Rötheli, A. R.; Jacobsen, E. N. *Angew. Chem., Int. Ed.* **2010**, *49*, 9753.
- Viciu, M. S.; Germaneau, R. F.; Nolan, S. P. *Org. Lett.* **2002**, *4*, 4053.
- Weix, D. J.; Hartwig, J. F. *J. Am. Chem. Soc.* **2007**, *129*, 7720.
- Welter, C.; Koch, O.; Lipowsky, G.; Helmchen, G. *Chem. Commun.* **2004**, 896.
- White, D. E.; Stewart, I. C.; Grubbs, R. H.; Stoltz, B. M. *J. Am. Chem. Soc.* **2008**, *130*, 810.
- Wiberg, K. B. in *Patai Series: the Chemistry of Functional Groups* (Eds.: Z. Rappoport, J. F. Liebman, S. Patai), John Wiley & Sons, Ltd, Chichester, UK, **2005**. pp. 1–15.
- Williams, P.; Albericio, F.; Giralt, E. Chemical approaches to the synthesis of peptides and proteins. Boca Raton: CRC Press, 1997, pp.116–119.
- Wood, J. L.; Thompson, B. D.; Yusuff, N.; Pflum, D. A.; Matthäus, M. S. P. *J. Am. Chem. Soc.* **2001**, *123*, 2097.

- Wu, Q.-F.; He, H.; Liu, W.-B.; You, S.-L. *J. Am. Chem. Soc.* **2010**, *132*, 11418.
- Wu, Q.-F.; Zheng, C.; You, S.-L. *Angew. Chem., Int. Ed.* **2012**, *51*, 1680.
- Xia, J.-B.; Liu, W.-B.; Wang, T.-M.; You, S.-L. *Chem. Eur. J.* **2010**, *16*, 6442.
- Xu, Q.-L.; Dai, L.-X.; You, S.-L. *Adv. Synth. Catal.* **2012**, *354*, 2275.
- Xuan, M.; Paterson, I.; Dalby, S. M. *Org. Lett.* **2012**, *14*, 5492.
- Yamashita, Y.; Odashima, K.; Koga, K. *Tetrahedron Lett.* **1999**, *40*, 2803.
- Yan, Y.-M.; Ai, J.; Zhou, L. L.; Chung, A. C. K.; Li, R.; Nie, J.; Fang, P.; Wang, X.-L.; Luo, J.; Hu, Q.; Hou, F.-F.; Cheng, Y.-X. *Org. Lett.* **2013**, *15*, 5488.
- Yoon, T. P.; MacMillan, D. W. C. *J. Am. Chem. Soc.* **2001**, *123*, 2911.
- Yoshikawa, K.; A. Kaneko, Y. Matsumoto, H. Hama, S. Arihara, *J. Nat. Prod.* **2006**, *69*, 1267.
- Zhuo, C.-X.; Liu, W.-B.; Wu, Q.-F.; You, S.-L. *Chem. Sci.* **2012**, *3*, 205.
- Zhuo, C.-X.; Wu, Q.-F.; Zhao, Q.; Xu, Q.-L.; You, S.-L. *J. Am. Chem. Soc.* **2013**, *135*, 8169.

INDEX

A

- acylation..... 150, 513
- allylic alkylation ... 1, 2, 3, 4, 5, 8, 9, 10, 11, 13, 138, 139, 140, 141, 143, 144, 145, 146, 148, 149, 151, 152, 227, 228, 230, 232, 233, 234, 235, 236, 330, 331, 332, 334, 337, 338, 340, 485, 486, 487, 499, 501, 513, 515, 520
- asymmetric ... 1, 2, 3, 4, 5, 7, 12, 13, 14, 32, 52, 140, 152, 226, 230, 330, 331, 334, 335, 482, 484, 485, 486, 487, 500, 525

B

- Baeyer-Villiger oxidation 14, 513
- Beckmann rearrangement 14
- benzylic oxidation 513, 520, 521, 525
- biological activity 512

C

- carbonate..... 143, 144, 147, 148, 149, 150, 151, 228, 232, 235, 236, 332, 335, 334, 336, 501
- carboxylate 2, 138, 139, 140, 485, 487, 499
- catalysis.....6, 10, 15, 139, 142, 226, 234, 235, 330, 481, 483, 485, 486, 487, 489, 500, 501, 482, 525, 515
- catalytic cycle..... 2, 9, 138, 485, 486, 488, 489, 501, 502
- cycloaddition..... 6, 14
- cyclobutanone 6, 7, 9, 15
- cyclobutene 5
- cycloaddition..... 513, 514, 515, 518, 519, 521, 522, 525

D

- diastereoselective..... 151, 236

diabetes	512
diabetic nephropathy	512
E	
enantioselective	1, 2, 3, 4, 15, 137, 141, 145, 226, 227, 228, 229, 331, 338, 340, 502, 511, 513
enol carbonate	1, 3, 137, 485
ester	2, 137, 139, 146, 151, 145, 146, 147, 151, 233, 338, 501
F	
fluoride	145, 148, 149, 234, 488, 493, 495, 496, 498, 500, 502
Fries rearrangement	513
G	
Grignard	515, 516, 520
H	
hydroboration oxidation	515
I	
iridium	228, 331, 515
K	
ketone	2, 3, 141, 143, 146, 148, 150, 151, 227, 234, 248, 337, 481, 483, 489, 490, 513, 515, 516, 519, 520, 521, 523, 513, 520, 524
L	
lactam	15, 141, 147
lingzhiol	511, 512, 513, 514, 515, 519, 520, 523, 524, 525
M	
mechanism	9
O	
optimization	9, 10, 11, 143, 144, 153, 228, 230, 229, 332, 334, 493, 496, 497, 498, 516, 517

orthogonal	152
oxidative addition	1, 138, 485, 488
P	
palladium	1, 2, 5, 10, 11, 15, 138, 481, 483, 485, 486, 487, 488, 489, 493, 494, 496, 498, 500, 501, 515, 520
Peterson olefination	515, 525
phosphine.....	235, 481, 482, 483, 490, 491, 493, 494
phosphinooxazoline	3, 8, 231, 250, 485, 494
phosphoramidite.....	227, 228, 229, 332
Q	
quaternary center.....	1, 7, 8, 13, 228, 236, 330, 331, 480, 481, 482
R	
reductive elimination	488, 500
regioselectivity.....	137, 231, 332, 335, 336, 338, 340, 518, 519
retrosynthetic analysis.....	514, 515, 523, 524, 525
ring-closing metathesis.....	15, 249
S	
silyl enol ether	2, 3, 137, 138, 485, 524
substrate synthesis.....	7, 139, 140, 141, 142, 150
T	
total synthesis	237, 341, 511, 513, 514, 525
transition metal	6, 7, 14, 15, 138, 139, 226, 330, 481
W	
Wolff rearrangement.....	8

ABOUT THE AUTHOR

Corey M. Reeves was born in Santa Monica, CA, USA. Corey obtained a BS in Chemistry and BA in Sociology from Columbia University in New York City in 2010. During this time, he completed undergraduate research under the guidance of Prof. Tristan Lambert.

In 2010, he began doctoral studies at the California Institute of Technology, working in the laboratory of Prof. Brian Stoltz in the field of synthetic methods development. During his time in the Stoltz laboratory, Corey's work in reaction methodology began with the development of a palladium-catalyzed allylic alkylation reaction of cyclobutanones. Following this he helped to develop an iridium-catalyzed regio-, diastereo-, and enantioselective allylic alkylation of cyclic and acyclic β -ketoester. Corey went on to develop a novel class of carboxylate protected enolate, and demonstrated their application in palladium catalyzed allylic alkylation and arylation. This compound class was also used in sequence with the iridium catalyzed allylic alkylation to afford control over nascent vicinal stereocenters. Lastly, Corey worked on the total synthesis of the natural product lingzhiol.

Upon completion of his doctoral research in the summer of 2015, Corey will begin work in the medicinal chemistry division of Amgen Pharmaceuticals in Thousand Oaks, CA.